

Edited by

Imre Blank, Matthias Wüst, Chahan Yeretian

Expression of Multidisciplinary Flavour Science

Proceedings of the 12th Weurman Symposium
Interlaken, Switzerland, 2008



Institut of Chemistry and Biological Chemistry
Zürich University of Applied Sciences
Wädenswil, Switzerland

Zürich University
of Applied Sciences

**zh
aw**

Life Sciences and
Facility Management

Institute of Chemistry and
Biological Chemistry

Edited by

Imre Blank, Matthias Wüst, Chahan Yeretjian

Expression of Multidisciplinary Flavour Science

Proceedings of the 12th Weurman Symposium

Institut Für Chemie und Biologische Chemie
Department für Life Science und Facility Management
**ZHAW Zürcher Hochschule
für Angewandte Wissenschaften**

Expression of Multidisciplinary Flavour Science
Edited by
Imre Blank, Matthias Wüst, Chahan Yeretjian

Zürcher Hochschule für Angewandte Wissenschaften
Institut Für Chemie und Biologische Chemie
ISBN-10:
ISBN-13: 978-3-905745-19-1

Alle Rechte vorbehalten
© Zürcher Hochschule für Angewandte 2010
Wissenschaften, Winterthur

Institut für Chemie und Biologische Chemie (ICBC)
www.icbc.zhaw.ch

Preface

The Weurman Flavour Research Symposium, one of the most renowned international meetings on flavour science, takes place every 3 years in Europe. The 1st meeting was held in 1975 in The Netherlands dedicated in memory of Cornelius Weurman, a pioneer of flavour research. Since then this symposium series has become the reference for flavour scientists as a unique platform addressing both the width and depth of flavour science. Participants from academia and industry from all five continents meet to discuss advances and trends in flavour science in an informal and open atmosphere. Traditionally, many young scientists can present their work, some of them sponsored by the Weurman symposium, and exchange views and experiences with well-known experts in the area.

In July 2008, the 12th Weurman Flavour Research Symposium was organized in Interlaken, Switzerland, by Prof. Renato Amadò and Prof. Felix Escher from the ETH Zurich. The symposium was held in the Casino-Kursaal Interlaken, a stylish conference centre with long tradition. Interlaken is situated in the centre of Switzerland and Europe, between the Lakes of Thun and Brienz and at the foot of the famous trio of peaks, the Eiger, the Mönch and the Jungfrau.

About 230 participants from 34 countries contributed with 177 lectures and posters to the wealth of flavour-related knowledge. The contributions were grouped in 8 sessions, i.e. biology, retention & release, psychophysics, quality, thermal generation, bioflavors, impact molecules, and analytics. Emerging topics were discussed in 3 workshops dealing with flavour and health, in-vivo flavour research, and flavour metabolomics. Highlights of the 12th Weurman symposium were published in a special issue of the Journal of Agricultural and Food Chemistry in 2009.

The 12th Weurman Flavour Research Symposium has been the most impressive *Expression of Multidisciplinary Flavour Science*. It has offered an excellent forum for passionate exchange of recent results, obtained by traditional and emerging methods in flavour research. We believe that these proceedings will fructify and propel the development of flavour science and become an important reference to the field. Enjoy!

This could only be achieved with the help of an organisation committee, composed of Renato Amadò, Imre Blank, Felix Escher, Jeannette Nuessli, and Heidi Sigrist, fully dedicated to make this symposium successful. They were assisted by students of the University of Applied Sciences in Sion, namely Brice Christen, Carole Constantin, and Valerie Möckli, whose engagement was greatly appreciated.

The expert contribution of the Scientific Committee is acknowledged for selecting and reviewing of the contributions as well as proof-reading of the manuscripts. The members of the Scientific Committee were:

Renato Amadò (Institute of Food Science and Nutrition, ETH Zurich)

Imre Blank (Nestlé Product Technology Center, Orbe)

Christoph Cerny (Firmenich, Geneva)

Felix Escher (Institute of Food Science and Nutrition, ETH Zurich)

Klaus Gassenmeier (Givaudan, Dübendorf)

Johannes Le-Coutre (Nestle Research Center, Lausanne)

Thomas Münch (Givaudan, Dübendorf)

Jeannette Nuessli (Institute of Food Science and Nutrition, ETH Zurich)

Hedwig Schlichtherle-Cerny (Agroscope Liebefeld-Posieux Research Station, Bern)

Matthias Wüst (University of Applied Sciences, Sion)

Chahan Yeretzian (University of Applied Sciences, Wädenswil)

Finally, the 12th Weurman Flavour Research Symposium was generously sponsored by Firmenich, Givaudan, Nestle, Pepsico, Philip Morris International, and Unilever.

The next Weurman Flavour Research Symposium will be held in 2011 in Saragossa, Spain, organised by Prof. Vicente Ferreira.

See you there and looking forward to further outstanding breakthroughs in Flavour Science !

Imre BLANK

Nestle PTC Orbe

Matthias WÜST

University of Bonn

Chahan YERETZIAN

*Zurich University
of Applied Sciences*

Table of Content

1. Receptors and Physiological Effects in Chemosensation	1
Human taste receptors3 <i>Wolfgang Meyerhof</i>	3
hTAS2R38 Receptor genotypes predict sensitivity to bitterness of thiourea compounds in solution and in selected vegetables13 <i>Mari Sandell, Paul Breslin</i>	13
Agonist activation of bitter taste receptors16 <i>Anne Brockhoff, Maik Behrens, Giovanni Appendino, Christina Kuhn, Bernd Bufe, Wolfgang Meyerhof</i>	16
N-Glycosylation is required for bitter taste receptor function20 <i>Claudia Reichling, Wolfgang Meyerhof, Maik Behrens</i>	20
Involvement of the epithelial sodium channel in human salt taste perception24 <i>Frauke Stähler, Katja Riedel, Stefanie Demgensky, Andreas Dunkel, Alexander Täubert, Thomas Hofmann, Wolfgang Meyerhof</i>	24
3D-Quantitative structure-activity relationships study of ligands for two human olfactory receptors29 <i>Anne Tromelin, Guenhaël Sanz, Loïc Briand, Jean-Claude Pernollet, Elisabeth Guichard</i>	29
Modelling the dynamics of odour transport in the olfactory epithelium33 <i>Andrew J. Taylor, Florian Wulfert, Oliver E. Jensen, Antoni Borysik, David J. Scott</i>	33
Workshop 1: Flavour, health & wellbeing - Balance between appetite and healthy diet37 <i>Wolfgang Langhans</i>	37
Novel approaches to induce satiation <i>via</i> aroma in foods41 <i>Rianne Maj Ruijschop, Alexandra E.M. Boelrijk, Maurits J.M. Burgering, Cees de Graaf, Margriet S. Westerterp-Planteng</i>	41
2. Psychophysics of Flavour Perception and Interactions	45
Effect of high-in-taste pulses on taste perception47 <i>Johanneke Busch, Janine Knoop, Carole Tournier, Gerrit Smit</i>	47
Salt enhancement by aroma compounds51 <i>Max Batenburg, Eric Landrieu, Rob van der Velden, Gerrit Smit</i>	51
CO ₂ perception and its influence on flavour55 <i>Bénédicte Le Calve, Hélène Goichon, Isabelle Cayeux</i>	55
Synergy in odour detection by humans59 <i>Toshio Miyazawa, Michelle Gallagher, George Preti, Katsuyuki Matumoto, Takashi Hamaguchi, Paul M. Wise</i>	59
Odorant mixture gestalt63 <i>Anne J. Kurtz, Harry T. Lawless, Terry E. Acree</i>	63

Comparing sensory profiles in logarithmically serial dilutions of coffee and soy sauce	68
<i>Tetsuo Aishima, Keiko Lizuka, Kae Morita</i>	
Correlation between sensory typicality and aromatic composition in Sauternes botrytized wines	72
<i>Elise Sarrazin, Takatoshi Tominaga, Philippe Darriet</i>	
Sensory evaluation of commercial apple juices and relation to selected key aroma compounds	76
<i>Martin Steinhaus, Sebastian Baer, Peter Schieberle</i>	
Do difference tests predict ecologic consumers' discrimination performance?	80
<i>Léri Morin-Audebrand, Claire Sulmont-Rossé, Sylvie Issanchou</i>	
Improving the palatability of oral nutritional supplements for elderly people aiming to increase intake	84
<i>Lisa Methven, Mia C. Bushell, Lauren Gray, Margot A. Gosney, Orla B. Kennedy, Donald S. Mottram</i>	
Sparse biplots for quantitative descriptive analysis	88
<i>Rudi van Doorn, Eduard P.P.A. Derks</i>	
3. In-Vivo Measurements in Flavour Release	93
Workshop 2: Characterisation of food perception - Tracing the chemosensations <i>in-vivo</i>	95
<i>Andrea Büttner</i>	
Flavour delivery from the oral cavity to the nose	101
<i>Robert S.T. Linforth, Andrew J. Taylor</i>	
How model cheese composition can influence salt and aroma compounds mobilities and their perception	105
<i>Clémentine Lauverjat, Anne Saint-Eve, Céline Magnan, Isabelle Déléris, Ioan Cristian Tréléa, Isabelle Souchon</i>	
Understanding physiological and physicochemical influences on in-mouth aroma release from yogurts using mechanistic modelling	109
<i>Isabelle Souchon, Samuel Atlan, Anne Saint-Eve, Isabelle Déléris, Etienne Sémon, Elisabeth Guichard, Ioan Cristian Tréléa</i>	
<i>In-vivo</i> aroma release of a low and a high fat semi-hard cheeses	113
<i>Christine Counet-Kersch, Wilma Wesselink, Anneke Hettinga, Loes Oeseburg, Hannemieke Luyten, Carina Ponne</i>	
Texture-aroma interactions in dairy products: Do <i>in-vivo</i> and <i>in-vitro</i> aroma release explain sensory perception?	117
<i>Elisabeth Guichard, Etienne Sémon, Isabelle Gierczynski, Carole Tournier, Anne Saint-Eve, Isabelle Souchon, Claire Sulmont-Rossé, Hélène Labouré</i>	
Chewing simulation, a way to understand the relationships between mastication, food breakdown and flavour release	121
<i>Claude Yven, Amparo Tarrega, Etienne Sémon, Sofiane Guessasma, Christian Salles</i>	

Influence of mouth model masticatory force on the release of limonene from orange fruit glucomannan jelly	125
<i>Sachiko Odake, Saskia van Ruth, Jacques P. Roozen, Takayuki Miura, Ryozo Akuzawa</i>	
Effect of antioxidant and saliva addition on the release of aromatic compounds from dry-fermented sausages in <i>in-vitro</i> model mouth system	129
<i>Mónica Flores, Alicia Olivares</i>	
The effect of saliva on the release of aroma volatiles in pork	133
<i>Lene Meinert, Anja Niehues Birch, Annette Schäfer, Susanne Støier, Margit Dall Aaslyng</i>	
4. Flavour Retention and Release in Food Systems	137
Flavour ingredient interactions in confections	139
<i>Alicia Holt, Rajesh V. Potineni, Devin G. Peterson</i>	
Aroma barrier properties of <i>iota</i> -carrageenan emulsion-based films used for encapsulation of active compounds	143
<i>Alicia Hambleton, Maria Jose Fabra, Frédéric Debeaufort, Andrée Voilley</i>	
Aroma barrier properties of sodium caseinate and <i>iota</i> -carrageenan edible films. Interaction between aroma compounds and edible films	147
<i>Maria Jose Fabra, Alicia Hambleton, Pau Talens, Frédéric Debeaufort, Amparo Chiralt, Andrée Voilley</i>	
Effect of gum base ingredients on release of specific compounds from strawberry flavour chewing gum	151
<i>Stine Kreuzmann, Kenneth Due Nielsen</i>	
Aroma release from encapsulation systems in chewing gum	154
<i>Kai Sostmann, Rajesh Potineni, Guillaume Blancher, Xiaomei Zhang, Marian Espinosa-Diaz, Robert N. Antenucci</i>	
Impact of milk fat composition on diffusion and perception of flavour compounds in yogurts	157
<i>Anne Saint-Eve, Isabelle Déléris, Anne Meynier, Isabelle Souchon</i>	
How flavour retention reflects the emulsifying properties of acacia gums	161
<i>G.Savary, N.Hucher, E.Bernadi, I.Jaouen, Catherine Malhiac, Michel Grisel</i>	
Behaviour of selected flavour compounds in dairy matrices: Stability and release	165
<i>Katja Buhr, Bernd Köhlnhofer, Andrej Heilig, Jörg Hinrichs, Peter Schieberle</i>	
Effect of flour, fiber and phytase on volatile extract composition and sensory perception of bread	169
<i>Pauline Poinot, Joëlle Grua-Priol, Gaëlle Arvisenet, Catherine Fillonneau, Alain Le-Bail, Carole Prost</i>	
Determination of aroma compounds diffusion properties in dairy gelled emulsions using mechanistic modelling	173
<i>Isabelle Deleris, Imen Zouid, Isabelle Souchon, Ioan Cristian Tréléa</i>	

Quantitative structure-property relationships approach of aroma compounds behaviour in polysaccharide gels	177
<i>Anne Tromelin, Yacine Merabtine, Isabelle Andriot, Samuel Lubbers, Elisabeth Guichard</i>	
Retention and release of carvacrol used as antimicrobial agent into soy proteins matrix based active packaging	181
<i>Pascale Chalier, Afef Ben Arfa, Valérie Guillard, Nathalie Gontard</i>	
Influence of ethanol on aroma compounds sorption into a polyethylene film	185
<i>Aurélie Peychès-Bach, Michel Moutounet, Stéphane Peyron, Pascale Chalier</i>	
5. Flavour Quality, Changes Upon Storage and Off-flavours	189
Quality: An important topic in the complex world of flavorings	191
<i>Gerhard E. Krammer, Franz-Josef Hammerschmidt, Gerd Lösing, Jan Förstner, Lars Meier, Jörg Osthaus, Bernhard Weckerle, Claus Oliver Schmidt, Stephan Trautzsch, Berthold Weber, Stefan Brennecke, Rüdiger Wittlake</i>	
Vanilla bean quality - A flavour industry view	203
<i>Klaus Gassenmeier, Eva Binggeli</i>	
Odour-active compounds of UFA/CLA enriched butter and conventional butter during storage	207
<i>Silvia Mallia, Felix Escher, C. Hartl, Peter Schieberle, Hedwig Schlichtherle-Cerny</i>	
Influence of ethylene-blocking action, harvest maturity and storage duration on aroma profile of apples (Ildrød pigeon) during storage	211
<i>Marta Popielarz, Mikael A. Petersen, Torben B. Toldam-Andersen</i>	
Changes in the key odour-active compounds and sensory profile of cashew apple juice during processing	215
<i>Deborah D.S. Garruti, Heliofábia V.D.V. Facundo, Manoel A.D.S. Neto, Roger Wagner</i>	
Strategies for minimising the influence of the barley crop year on beer flavour stability	219
<i>Andreas Stephan, Georg Stettner</i>	
HS-SPME GC-MS analysis of fresh and reconstituted orange juices	223
<i>Ann D. Winne, Patrick Dirinck</i>	
Fate of polyfunctional thiols in Sauternes wines through ageing	227
<i>Sabine Bailly, Sonia Collin</i>	
Aromatic profile of oxidised red wines	231
<i>Margarita Aznar, Tania Balboa, Teresa Arroyo, Juan M. Cabello</i>	
Inhibition of light-induced off-flavour development by singlet oxygen quenchers in cloudy apple juice	235
<i>Midori Hashizume, Michael H. Gordon, Donald S. Mottram</i>	
Earthy off-flavour in wine: Evaluation of remedial treatments for geosmin contamination	238
<i>Maria T. Lisanti, Paola Piombino, Angelita Gambuti, Alessandro Genovese, Luigi Moio</i>	

Identifying aroma components responsible for light-induced off-flavour in pasteurised milk	242
<i>Marty Martens, Marc Reekers, Wim Timmermans, Carina Ponne</i>	
Sensorial aspects of “brett character”: Re-evaluation of the olfactory perception threshold of volatile phenols in red wine	245
<i>Andrea Romano, Marie Claire Perello, Aline Lonvaud-Funel, Gilles de Revel</i>	
The olfactoscan: In-vivo screening for off-flavour solutions	249
<i>Kerstin M.M. Burseg, Catrienus D. Jong</i>	
Influence of modified atmosphere packaging on the aroma of cheese	253
<i>Isabelle van Leuven, Tim Van Caelenberg, Patrick Dirinck</i>	
Intense odorants of cardboard and their transfer to foods	257
<i>Michael Czerny</i>	
6. Flavour Generation by Thermal Processes	261
Effect of reaction conditions on the generation of 4-hydroxy-2,5-dimethyl-3(2H)-furanone from rhamnose	263
<i>Tomas Davidek, Silke Illmann, Elisabeth Gouézec, Andreas Rytz, Heike P. Schuchmann, Imre Blank</i>	
Basic and acidic sugars as flavour precursors in Maillard reaction	267
<i>Karin Kraehenbuehl, Tomas Davidek, Stéphanie Devaud, Olivier Mauroux</i>	
Quenching method, moisture content, and aroma stability of roast and ground coffee	271
<i>Juerg Baggenstoss, Felix Escher</i>	
Coffee flavour modulation – Reinforcing the formation of key odorants while mitigating undesirable compounds	275
<i>Luigi Poisson, Josef Kerler, Frank Schmalzried, Tomas Davidek, Imre Blank</i>	
Structures and sensory activity of mouth-coating taste compounds formed by ellagitannin transformation during oak wood toasting used in barrel manufacturing	280
<i>Arne Glabasnia, Thomas Hofmann</i>	
Modelling the generation of flavour in a real food system	284
<i>Dimitrios P. Balagiannis, Jane K. Parker, D. Leo Pyle, Neil Desforges, Donald S. Mottram</i>	
Formation of flavour precursors by the AMP pathway in chicken meat	288
<i>Michel Aliani, James T. Kennedy, Colin W. McRoberts, Linda J. Farmer</i>	
Meat flavour generation in Maillard complex model systems	293
<i>Sara I.F.S. Martins, Guillaume A. Desclaux, Annelies Leussink, Ed .A.E. Rosing, Lionel Jublot, Gerrit Smit</i>	
Hydroxycinnamic acid-Maillard reactions: Insights into flavour development of whole grain foods	297
<i>Deshou Jiang, Devin G. Peterson</i>	
Changes in the aroma components of pecans during roasting	301
<i>Keith R. Cadwallader, Hun Kim, Sirima Puangraphant, Yaowapa Lorjaroenphon</i>	

Aroma compounds in French fries from three potato varieties	305
<i>J. Stephen Elmore, Jodie A. Woolsgrove, Deng K. Wang, Andrew T. Dodson, Donald S. Mottram</i>	
Understanding the impact of conching on chocolate flavour using a combination of instrumental flavour analysis and tasting techniques	309
<i>Anja Fischer, Tahira Abubaker, Alexander Hässelbarth, Frank Ullrich</i>	
Flavour evolution investigations in a tobacco gene-to-smoke project	313
<i>Felix Frauendorfer, Monika Christlbauer, Jan Carlos Hufnagel, Jean-Pierre Schaller, Anneke Glabasnia, Ferruccio Gadani</i>	
7. Flavour Generation by Bio-Mediated Processes	317
White biotechnology: Sustainable options for the generation of natural volatile flavours ...	319
<i>Ralf G. Berger</i>	
Bioconversion of β -myrcene to perillene – Metabolites, pathways, and enzymes	328
<i>Ulrich Krings, Sven Krügener, Sascha Rinne, Ralf G. Berger</i>	
Biocatalysis based transformation of valencene into nootkatone	332
<i>Martina Djuris, Vladimir Stefuca, Mohammed Eghbaldar, Peter V. D. Schaft</i>	
Generation of norisoprenoid flavours from carotenoids by fungal peroxidases	336
<i>Kateryna Zelena, Björn Hardebusch, Bärbel Hülsdau, Ralf G. Berger, Holger Zorn</i>	
Biotransformations of secondary alcohols and their esters: Enantioselective esterification and hydrolysis	340
<i>Henk Strohm, Susanne Dold, Kathrin Pendzialek, Marcel Weiher, Karl-Heinz Engel</i>	
Integrated bioprocess for the production of the natural antimicrobial monoterpene R-(+)-perillic acid with <i>P. putida</i>	344
<i>Marco-Antonio Mirata, Jens Schrader</i>	
Linalool biotransformation with fungi	349
<i>Marco-Antonio Mirata, Matthias Wüst, Armin Mosandl, Jens Schrader</i>	
Production of methionol and 3-(methylthio)-propylacetate with yeasts	354
<i>Maria W. Etschmann, Peter Koetter, Wilfried Bluemke, Karl-Dieter Entian, Jens Schrader</i>	
β -Glucosidase production by non- <i>Saccharomyces</i> yeasts isolated from vineyard	359
<i>Teresa Arroyo, G. Cordero, A. Serrano, E. Valero</i>	
Assessment of aroma of chocolate produced from two Ghanaian cocoa fermentation types	363
<i>Margaret Owusu, Mikael A. Petersen, Hanne Heimdal</i>	
Aroma formation in a cheese model system by different <i>Lactobacillus helveticus</i> strains	367
<i>Mikael A. Petersen, Helle T. Kristensen, Mette Bakman, Camilla Varming, Marie P. Jensen, Ylva Ardö</i>	
Odorants in mild and traditional acidic yoghurts as determined by SPME-GC/O/MS	371
<i>Hedwig Schlichtherle-Cerny, David Oberholzer, Ulrich Zehntner</i>	

Flavour ingredients from fermented dairy streams	375
<i>Marie-Laure Delabre, Justin G. Bendall</i>	
Biosynthesis of vanillin via ferulic acid in <i>Vanilla planifolia</i>	379
<i>Osamu Negishi, Yukiko Negishi</i>	
Diversity of volatile patterns in a gene bank collection of parsley (<i>Petroselinum crispum</i> [Mill.] Nyman)	383
<i>D. Ulrich, H. Budahn, T. Struckmeyer, F. Marthe, H. Krüger, U. Lohwasser</i>	
Atmospheric carbon dioxide induces changes of aroma volatiles in <i>Brassicaceae</i>	387
<i>Angelika Krumbein, Monika Schreiner, Hans-Peter Kläring, Ilona Schonhof</i>	
8. Impact Aroma & Taste Molecules	391
Identification of β -alanyl dipeptides contributing to the thick-sour, white-meaty orosensation induced by chicken broth	393
<i>Andreas Dunkel, Thomas Hofmann</i>	
LC Taste® as a novel tool for the identification of flavour modifying compounds	397
<i>Katharina V. Reichelt, Regina Peter, Michael Roloff, Jakob P. Ley, Gerhard E. Krammer, Karl-Heinz Engel</i>	
Structural analogues of hispolon as flavour modifiers	402
<i>Jakob P. Ley, Susanne Paetz, Maria Blings, Petra Hoffmann-Lücke, Thomas Riess, Gerhard E. Krammer</i>	
Dihydromaltol (2,3-dihydro-5-hydroxy-6-methyl-4 <i>H</i> -pyran-4-one): Identification as a potent aroma compound in Ryazhenka kefir and sensory evaluation	406
<i>Martin Preininger, Ludmilla Gimelfarb, Hui-Chen Li, Benjamin E. Dias, Farid Fahmy, James White</i>	
Characterisation of compounds involved in specific fruity aromas of red wines	411
<i>Bénédicte Pineau, Jean-Christophe Barbe, Cornelis V. Leeuwen, Denis Dubourdieu, Philippe Darriet</i>	
Original indirect identification of 3-sulfanylhexas-1-ol dimer (3,3'-disulfanedihexan- 1-ol) in Sauternes botrytised wines	415
<i>Elise Sarrazin, Svitlana Shinkaruk, Cécile Thibon, Pierre Babin, Bernard Bennetau, Takatoshi Tominaga, Philippe Darriet</i>	
Key odorants of the typical aroma of sherry vinegar	419
<i>Raquel M. Callejón, M. Lourdes Morales, Ana M. Troncoso, A.C. Silva Ferreira</i>	
Novel key aroma components of galbanum oil	423
<i>Norio Miyazawa, Akira Nakanishi, Naomi Tomita, Yasutaka Ohkubo, Susumu Ishizaki, Tomoko Maeda</i>	
Aroma volatiles of mangaba (<i>Hancornia speciosa</i> Gomes)	427
<i>Lilia C. Oliveira, Filomena Valim, Narendra Narain, Russell L. Rouseff</i>	
Chemical and aroma profiles of different cultivars of Yuzu (<i>Citrus junos</i> Sieb. ex Tanaka) essential oil	431
<i>Masayoshi Sawamura, Nguyen T. Lan Phi</i>	

Volatile compounds and amino acids in cheese powders made from matured cheeses <i>Camilla Varming, Tove K. Beck, Mikael A. Petersen, Ylva Ardö</i>	435
First identification of two potent thiol compounds in ripened cheeses <i>Alain M. Sourabié, Sophie Landaud, Pascal Bonnarme, Anne Saint-Eve, Henry-Eric Spinnler</i>	439
Chemical and sensory analysis of cysteine-S-conjugates as flavour precursors <i>Christian Starkenmann, Bénédicte Le Calvé, Yvan Niclass, Isabelle Cayeux, Sabine Beccucci, Myriam Troccaz</i>	443
Grape odourless precursors of some relevant wine aromas <i>Ricardo Lopez, Natalia Loscos, Purificación Hernández-Orte, Juan Cacho, Vicente Ferreira</i>	447
Identification of volatile compounds responsible for prune aroma in prematurely aged red wines <i>Alexandre Pons, Valérie Lavigne, Eric Frérot, Philippe Darriet, Denis Dubourdiou</i>	451
Quantification of dimethyl tetrasulphide in onions by a newly developed stable isotope dilution assay <i>Michael Granvogl, Peter Schieberle</i>	455
Novel esters in thai green chilli <i>J. Stephen Elmore, Siriwan Srisajjalertwaja, Andrew T. Dodson, Arunee Apichartsarangkoon, Donald S. Mottram</i>	459
Volatile compounds important to the aroma of Italian type salami: Assessment by OSME and detection frequency techniques <i>Roger Wagner, Maria A.A.P. Da Silva, Maria Regina B. Franco</i>	463
Aroma compounds in eleven edible mushroom species: Relationship between volatile profile and sensorial characteristics <i>P. Guedes de Pinho, Bárbara Ribeiro, Rui F. Gonçalves, Paula Baptista, Patrícia Valentão, Rosa M. Seabra, Paula B. Andrade</i>	467
Development of high impact sulphur chemicals for mushroom flavours <i>Hans Colstee, Marc V. D. Ster, Lesly Braamer, Cor Niedevelde, Carolien Merlier</i>	472
2-Acetyl-2-thiazoline, a new character impact volatile in jasmine rice <i>Kanjana Mahattanatawee, Russell L. Rouseff</i>	475
Impact flavour compounds in cooked rice cultivars from the Camargue area (France) <i>Isabelle Maraval, Christian Mestres, Karine Pernin, Fabienne Ribeyre, Renaud Boulanger, Elisabeth Guichard, Ziya Gunata</i>	479
Spice up your life – The rotundone story <i>Claudia Wood, Tracey E. Siebert, Mango Parker, Dimitra L. Capone, Gordon M. Elsey, Alan P. Pollnitz, Marcus Eggers, Manfred Meier, Tobias Vössing, Sabine Widder, Gerhard E. Krammer, Mark A. Sefton, Markus J. Herderich</i>	483
The influence of chemical structure on odour qualities and odour potencies in chloro-organic substances <i>Andrea Strube, Andrea Buettner</i>	486

Aroma analysis of sea buckthorn berries by sensory evaluation, headspace SPME and GC-olfactometry	490
<i>Saara Lundén, Katja Tiitinen, Heikki Kallio</i>	
The analysis of volatiles and non-volatiles in Yerba maté tea (<i>Ilex paraguariensis</i>)	494
<i>Neil C. Da Costa, Ying Yang, Jerry Kowalczyk, Mauricio L. Poulsen</i>	
Cigarette smoke: GC-olfactometry analyses using two computer programs	498
<i>V.M.E. Cotte, S.K. Prasad, P.H.W. Wan, Robert S.T. Linforth, Andrew J. Taylor</i>	
9. Targeted and Holistic Approaches in Flavour Analysis	502
Opportunities for flavour analysis through hyphenation	504
<i>Philip J. Marriott, Graham T. Eyres, Jean-Pierre Dufour</i>	
Two-dimensional GC and nitrogen chemiluminescence detection to analyse volatile N-compounds in wine with and without off-flavour.....	513
<i>Doris Rauhut, Beata Beisert, Stefanie Fritsch, Helmut Kürbel</i>	
A fast and simple procedure for the selective isolation of polyfunctional mercaptans in a micro solid phase extraction cartridge	517
<i>Laura Mateo-Vivaracho, Juan Cacho, Vicente Ferreira</i>	
Solid-phase extraction as a routine method for comparing key aroma compounds in fruits	521
<i>Jane K. Parker, Evangelos Tsormpatsidis, J. Stephen Elmore, Alexandra Wagstaffe, Donald S. Mottram</i>	
Design of an artificial crushing finger device for rapid evaluation of essential oils from aromatic plants leaves	525
<i>Chaker El Kalamouni, Christine Raynaud, Thierry Talou</i>	
Analysis of limited substances in complex flavourings by direct thermal desorption and multidimensional gas chromatography - mass spectrometry	529
<i>Carlos Ibàñez, Josep Solà</i>	
Critical parameters in the performance of a dynamic purging system for the production of extracts for gas chromatography-olfactometry	533
<i>Felipe San Juan, Ana Escudero, Juan Cacho, Vicente Ferreira</i>	
Furaneol® and mesifuran in strawberries – An analytical challenge	537
<i>Barbara Siegmund, Kristina Bagdonaite, Erich Leitner</i>	
Absolute stereochemistry of flavour related 2-substituted-3(2 <i>H</i>)-furanones, 2,5-dimethyl-4-hydroxy-3(2 <i>H</i>)-furanone and analogues	541
<i>Makoto Emura, Yoshihiro Yaguchi, Daisuke Sugimoto, Atsufumi Nakahashi, Nobuaki Miura, Kenji Monde</i>	
Hydrophobic interactions between aroma compounds and β -lactoglobulin using NMR and a fluorescent probe	545
<i>Laurette Tavel, Céline Moreau, Eunice C.Y.Li-Chan, Elisabeth Guichard</i>	
Gas chromatography-pedestal olfactometer	549
<i>Fanny A. Parisot, Emeline Satre, Robert C. Williams, Anne J. Kurtz, Terry E. Acree</i>	

Improvement of sensitivity in quantitative GC-olfactometric measurements	553
<i>Ján Petka, Jana Sádecká, Ana Escudero, Kristína Kukurová, Vicente Ferreira</i>	
Number of panellists or number of replicates - How to receive most information from a GC-O-MS study	557
<i>Annette Schäfer, Margit D. Aaslyng, Lene Meinert</i>	
Analytical method for identification of odour-active compounds in polyolefins	561
<i>Helene Hopfer, Nina Haar, Erich Leitner</i>	
Assessment of ciders typicality characterisation through odorant volatile compounds	565
<i>Angélique Villiere, Gaëlle Arvisenet, Carole Prost, Thierry Sérot</i>	
Quantitation of sulphur aroma compounds in Maillard model reaction systems of different composition	569
<i>Lionel Jublot, Ed.A.E Rosing, Leon van den Blom, Guillaume Desclaux, Sara.I.F.S. Martins, A.Max Batenburg, Gerrit Smit</i>	
Workshop 3: Flavour metabolomics - Holistic versus targeted approaches in flavour research	573
<i>Ric C.H. de Vos, Yury Tikunov, Arnaud G. Bovy, Robert D. Hall</i>	
Coffee chemometrics as a new concept: Untargeted metabolic profiling of coffee	581
<i>Christian Lindinger, Ric C.H. de Vos, Charles Lambot, Philippe Pollien, Andreas Rytz, Elisabeth Voirol-Baliguet, René Fumeaux, Fabien Robert, Chahan Yeretjian, Imre Blank</i>	
Mass spectrometry-based electronic nose classification of commercial coffee blends	585
<i>Inge Dirinck, Ann D. Winne, Isabelle V. Leuven, Patrick Dirinck</i>	
Food pairing from the perspective of the 'Volatile Compounds in Food' database	589
<i>Miriam Kort, Ben Nijssen, Katja V. Ingen-Visscher, Jan Donders</i>	

Section 1

**Receptors and Physiological Effects
in Chemosensation**

HUMAN TASTE RECEPTORS

W. MEYERHOF

German Institute of Human Nutrition Potsdam-Rehbruecke, Department of Molecular Genetics, Arthur-Scheunert-Allee 114-116, 14558 Nuthetal, Germany

Abstract

Taste research has made large progress during the last decade. This article summarises the recent developments in the field of gustation with particular emphasis on those aspects that have attracted greatest attention, *i.e.*, the molecular biology of taste receptors, taste genetics and the functional organisation of taste buds.

Functional organisation of the taste bud

In order to produce a perception, taste stimuli must interact with oral taste receptor cells. These specialised epithelial cells assemble with other cell types into groups of ~50 to 100 cells, called taste bud (1). Several thousand of these small organs are embedded in the oral epithelium, yet on the tongue taste buds are organised in fungiform, foliate, or circumvallate papillae. Taste buds are innervated by afferent nerve fibers that convey gustatory information to the brain. Depending on their localisation on the anterior tongue, posterior tongue, and pharynx, taste buds are innervated by the 7th, 9th, and 10th cranial nerves, respectively. Tastants interact with taste receptor cells in the pore region that they form with their apical aspects, whereas their basolateral parts are shielded from external stimuli by tight junctions.

We can distinguish two principle cell types engaged in taste signaling. One has been referred to as type II cells (2,2a,3). Morphologically, this cell type is characterised by a large, electron-lucent nucleus and several short apical microvilli. Functionally, type II cells are characterised by the receptor proteins they contain. In a mutually exclusive manner type II cells express the receptors for sweet, bitter or umami compounds (4,4a,5); thus, they form at least three different subpopulations dedicated exclusively to the detection of sweet compounds, amino acids/ribonucleotides, or bitter substances. Evidence has been presented showing that receptor cells dedicated to bitter detection are not functionally equivalent but form a heterogeneous population of cells (6). This is due to the fact that they express, on average, only seven out of 25 bitter taste receptors. It remains to be elucidated whether this property of bitter taste cells allows us to discriminate among bitter stimuli. Type II cells also express a variety of downstream signaling molecules, including the $\gamma 13$ subunit of heterotrimeric G proteins, the G protein subunit α -gustducin, phospholipase C- $\beta 2$, type III inositol trisphosphate receptor, transient receptor potential channel M5 (Trpm5), pannexin 6 and connexin 30 (7). They lack however, voltage-gated calcium channels and other proteins engaged in synaptic release of neurotransmitter (3,8). In accordance with these observations, type II cells can only be excited by tastants but not by depolarisation with potassium chloride. Moreover, although type II cells are in close proximity to the afferent nerves they cannot form synapses. When excited, they release the neurotransmitter ATP through

so called hemichannels (9,10). Evidence shows that gustatory neurotransmission requires ionotropic P2X₂/P2X₃ ATP receptors be present on the afferent nerves (11).

The other principle type of taste signaling cells is the type III cell (2,2a,3). Morphological characteristics of type III cells are an elongated invaginated nucleus and a single large microvillus. These cells express a number of neuronal marker proteins such as neuronal cell adhesion molecule, protein gene product 9.5, synaptosome associated protein 25, and glutamate decarboxylase. Type III cells form synapses with the afferent nerves indicating that excitation of these cells induces gustatory nerve transmission. Type III cells cannot be activated by sweet, bitter or umami stimuli, they are, however, activated by potassium depolarization or the transmitter compound ATP. Functional and histochemical experiments indicate that activated type III cells release serotonin as transmitter substance (9). Type III cells also express the polycystic kidney disease gene 1L3 (PKD1L3) and the polycystic kidney disease gene 2L1 (PKD2L1) that encode transient receptor potential channels thought to act as heterodimers (7,12-14). Mice genetically ablated for PKD2L1 cells selectively lost their sensitivity to sour stimuli arguing that PKD2L1-expressing cells are dedicated to detecting acidic stimuli (14). Moreover, data from functional expression studies with PKD1L3/PKD2L1 in heterologous cells proposed, but by far did not prove, that these channels may be part of a sour transduction mechanism (13).

A population of cells dedicated to salt taste detection has not been precisely identified. However, electrophysiological data suggest that salt sensitive cells lack voltage-gated calcium channels and therefore do not belong to the population of type III cells (15). Based on their electrical response profile it has been proposed that the salt receptor cells belong to so called type I cells, a population of cells originally been thought of as supportive cells for the taste signaling cells (16).

The cellular organization of the taste bud raises questions about how taste stimulation is coupled to nerve excitation and how taste qualities are encoded. Originally, researchers assumed that the taste buds function unidirectionally, *i.e.* signal detection at the apical side is linked to neurotransmitter release at the basolateral side. Now, we learn that these small organs not only detect but also likely process gustatory information (2). Stimulation of type II cells by tastants could possibly be propagated to excitation of the afferent nerves *via* two pathways. In one, type II cells would directly stimulate afferent nerves through P2X₂/P2X₃ receptors. The other pathway would involve activation of type III cells through type II cells and the type III cells would finally excite the afferent fibers. At present, experimental data argue in support of both pathways. Future work will reveal the details of taste bud function and the rules that govern the innervation of taste buds.

Two hypotheses have been put forward to solve the longstanding question of how taste qualities are encoded (17). The labeled line theory proposes that the basic taste qualities are conveyed to the cerebral cortex by separate pathways, *i.e.* taste cells in the periphery and central gustatory neurons are dedicated to only one quality. In other words, these cells would respond either to sweet, umami, bitter, sour, or salty stimuli but never to two or more stimuli. In marked contrast, the pattern theory assumes that peripheral taste cells and central gustatory neurons respond variably to stimuli across modalities, *i.e.* they are excited by several different taste stimuli. In the pattern generated by a given taste stimulus, information is contained in excited neurons and in silent neurons alike. The generated patterns have to be decoded by the cerebral cortex. Neurophysiological and behavioural work with gene-targeted animals and data from calcium-imaging experiments using *ex vivo* taste bud

preparations clearly showed that the type II receptor cells are dedicated to only one taste quality (4,18). However, the latter experiments also demonstrated that presynaptic type III cells, which, as mentioned above, cannot respond directly to sweet, umami, and bitter stimuli, were activated by stimuli of different modalities. This led to the conclusion that type II cells converge on type III cells generating a pattern of activity. This activity pattern of taste bud cells is likely transmitted by a small number of afferent fibers to the gustatory neurons of the *nucleus tractus solitarius* (19), from where gustatory information is sent to the respective thalamic relay nuclei, and finally to the somatosensory cortex. This is supported by neurophysiological recordings that revealed similar activity patterns also in these regions (17).

Taste bud cells express an impressive number of hormones and/or hormone receptors. The list includes neuropeptide Y, cholecystokinin, glucagon-like peptide 1, and leptin (20-22). Data suggest that these hormones regulate signal processing within the taste buds and allow cross talk among the various taste bud cells. Another very attractive idea is that these hormones adapt taste signaling to metabolic requirements (21,22). This assumption is based on the well-known function of these hormones in appetite regulation or energy balance. For instance, it has been shown that sweet taste cells carry OBRB, the functional form of the leptin receptor and respond to leptin with reduced sensitivity to sweet stimulation (22). Thus, when satiation is reached sweets may be less attractive resulting in reduced consumption.

Receptors for salt stimuli

Minerals are essential for body fluid composition, cell physiology, and function of the nervous system. As land living animals, we continually excrete and thereby lose minerals. Salt taste is considered part of a homeostatic system that maintains appropriate mineral levels in the body (23). It functions as a mineral sensor that governs the intake of minerals, in particular sodium, and in this manner compensates for the loss of salts in sweat, urine and feces. Humans have a taste for various salts, but only sodium chloride possesses a pure salty taste. The taste of almost all other mineral ions is associated with numerous other descriptors.

Two salt transduction pathways have been described in rodents. One is sensitive to the drug amiloride and specific for sodium ions. Various lines of evidence suggest that the epithelial sodium channel, ENaC, likely composed of two alpha, one beta, and one gamma subunit, is a *bona fide* rodent "receptor" candidate for tasting sodium ions (23). In humans, we found that alpha, beta, and gamma-ENaC subunits are expressed in taste bud cells (24). We also found the delta-ENaC subunit, for which a gene is missing in the rodent genome, is expressed in human taste buds. This subunit is exclusively seen in taste pores, the site at which taste stimuli contact the receptor cells, whereas the other three subunits are found at the basolateral part of taste bud cells. When alpha-, beta-, gamma-ENaC or delta-, beta-, gamma ENaC were functionally expressed in *Xenopus laevis* oocytes, we found that several substances that enhanced saltiness of sodium chloride solutions in sensory experiments with human subjects increased ENaC-mediated sodium membrane currents in an amiloride-sensitive manner. Together, the data suggest that ENaC may have a role in taste, particularly the delta- subunit. This channel may even play a role in salt taste, although final proof is missing. The data also raise questions about the subunit composition of lingual ENaC. Based on the histochemical staining pattern of the delta-subunit that resembles that of tight junction proteins (25), it may also be that the delta subunit either alone or in association with other proteins allows sodium

ions to access the intragemmal fluid, while α -, β -, γ ENaC could mediate sodium influx through the basolateral membrane of taste cells. Future work will reveal these details.

The other salt transduction pathway is insensitive to amiloride and not specific for sodium ions. This transduction pathway is sensitive to cetylpyridinium chloride (26). It has been proposed that a variant of the transient receptor potential channel V1 is involved in this pathway (27). In humans, such a pathway has not been identified yet.

Sour transduction

Sour taste detects acids. Strong sourness is aversive and potentially associated with the rejection of unripe or spoiled food. Mild sourness, however, is considered to be interesting, fully consistent with the fact that most of our beverages are slightly acidic (23). Sourness is only loosely correlated to the pH of the extracellular fluid (2, 28). This is evident, for instance, from the observation that the strong inorganic acid, HCl, elicits almost no sour taste at pH 2, whereas weak organic acid such as acetic acid or citric acid taste already sour at higher pH values. Sourness correlates much better to the concentration of the protonated acids. Recently, Lyall et al. showed that intracellular acidification is the proximate sour stimulus (29). The undissociated organic acids readily diffuse through the plasma membrane into the cytosol and then dissociate leading to intracellular acidification. At high concentrations also protons permeate to limited extent through ion channels or transport systems into the cytosol explaining the slight sourness of inorganic acids at very low pH (2). Recently, Roper and colleagues showed that presynaptic type III taste cells responded with calcium influx and release of the neurotransmitter serotonin to exposure with acetic acid (30). In line with the finding that intracellular acidification is the proximate sour stimulus these authors further demonstrated that the response amplitudes were correlated with concentration changes of acetic acid at constant pH but not with acetic acid at a fixed concentration titrated to various pH values.

In the past, a number of transmembrane ion channels have been proposed to function as the sour sensors based on their gating properties by extracellular protons (2). The challenge now is to verify or falsify these candidates by proving or disproving that they are gated by intracellular acidification. Evidence for gating by intracellular protons is also missing for the PKD1L3-PKD2L1 channel that is expressed in taste cells dedicated to sour detection. Other candidates for a sour receptor are the two-pore domain potassium channels. Some of these channels are sensitive to intracellular acidification and are expressed in taste cells (31). However, their specific role in (sour) taste transduction still needs to be demonstrated.

Sweet and umami taste receptors

Both of these tastes are considered to function as detectors of nutritive calories in form of carbohydrates or meat (32). Consistent with this conjecture sweet taste is stimulated by mono- and disaccharides that may be released *in situ* by lingual amylase. However, a number of other substances taste sweet as well including but not limited to the amino acids L-glycine, L-alanine, and D-tryptophane, aliphatic alcohols such as glycerol, sorbitol, and xylitol, secondary plant metabolites such as stevioside, proteins of tropical plants such as monellin or thaumatin, the synthetic sulfonamide sweeteners saccharin and acesulfame-K, synthetic peptide sweeteners such as aspartame or alitame, metal salts of lead and beryllium, whereas

umami taste is elicited by amino acids and ribonucleotides. Sweet and umami taste are associated with attraction and promote ingestion of the respective food.

Three genes play a major role in umami and sweet taste, referred to as TAS1R1, TAS1R2 and TAS1R3 (4). The encoded polypeptides, also referred to as T1R1, T1R2, and T1R3, belong to the class C of G protein-coupled receptors characterised by large N-terminal ectodomains. Evidence suggests that they dimerize to form functional taste receptors. In heterologous expression assays T1R1-T1R3 responds to various L-amino acids (for the mouse form) and to L-glutamate (for the human form), the responses being enhanced by the simultaneous presence of ribonucleotides. This property makes this dimer a strong umami receptor candidate, although it should be mentioned that other glutamate receptors have also been implicated in the umami response.

Strong evidence from experiments with gene-targeted mice, heterologous expression assays, and human sensory studies, indicates that T1R2-T1R3 functions as a general sweet taste receptor. Numerous compounds known to taste sweet activate this heterodimer *in-vitro* (33). In addition, the T1R2-T1R2 and T1R3-T1R3 homodimers have been suggested to function as sweet taste receptors for perillartine or high concentrations of sucrose [Jay Slack, personal communication]. In fish, T1Rs have only been activated by amino acids but not by sugars (34) suggesting that these receptors originally functioned as amino acid sensors. Only later in evolution the T1R2 gene developed to encode sensors for sugars.

An important question that emerged is how sweet compounds bind to and activate their cognate receptor. Based on truncated receptor subunits that have been functionally expressed and analyzed it has been concluded that the T1R1 and T1R2 subunits of the dimeric sweet or umami receptors signal through G proteins. In addition, various efforts have been made to investigate how sweeteners interact with T1R2-T1R3 including biochemical and biophysical analysis of the recombinantly produced N-terminal ectodomains, functional expression of interspecies mixtures of T1R2 and T1R3 subunits, mutational analysis of heterologously expressed subunits and molecular modeling (33). The data that emerged from these studies indicated that the T1R2-T1R3 heterodimer contains several binding sites for sweeteners explaining the ability of mammals to sense so many structurally different sweet tasting chemicals with only one receptor (33). Based on homologies to other class C GPCRs, the ectodomains of T1Rs have been shown to form so called venus fly trap binding motifs. It appears that glucose, sucrose and the halogenated sucrose derivative sucralose binds to or at these motifs in both subunits, while the peptide sweeteners aspartame and neotame have been shown to bind the venus fly trap motif of T1R2 only. Brazzein, an intensely sweet tasting protein, binds to a cysteine-rich region in T1R3 that connects the ectodomain to the heptahelical part of the receptor subunit. Finally, the sweet substances cyclamate and neohesperidin dihydrochalcone bind to sites formed within the transmembrane segments of T1R3. Interestingly, the sweet taste inhibitor lactisole also binds to this site. Mutational analyses clearly showed that the three chemicals interacted with an overlapping set of amino acids of T1R3's transmembrane domains. Consistent with this finding is the observation that lactisole inhibited T1R2-T1R3 activation by cyclamate or neohesperidin dihydrochalcone competitively, whereas it allosterically blocked T1R2-T1R3 activation by aspartame, a compound that binds, as mentioned above, to the venus fly trap motif of T1R2.

Bitter taste receptor genes

Bitter compounds are even more numerous and more chemically diverse than sweet molecules. Estimates go into thousands (35). Usually, bitter substances elicit aversion leading to rejection of bitter food. It has been argued that bitter taste prevents us from ingesting potentially harmful or poisonous compounds. In fact, many bitter compounds, including food-borne substances, are toxic, although a relation of bitterness and toxicity has not been established. Moreover, certain toxins, such as α -amanitin, do not taste bitter at all, whereas some compounds, such as salicin, a compound that has successfully been used in human medicine for several thousand years, exhibit an offending bitter taste. Bitter taste is innate and the rejection response is particularly prominent in neonates and children, *i.e.* at times when our other defense systems are not fully developed. Later in life with aging, we accept and even appreciate a moderate bitterness of some compounds in our food and beverages. The reasons for and the mechanisms underlying this change are unknown. However, it is not correlated to altered bitterness sensitivity measured as threshold values of recognizing bitter compounds (36). It could be that the reduced bitterness rejection reflects only learned eating behaviours. Alternatively, in light of the fact that plants use bitter compounds as protective agents against infections, oxidative stress, etc., it could also be that uptake of certain bitter chemicals with our food transfers chemical protection to our own bodies – particularly at ages when we are beginning to suffer again from greater vulnerability. The fact that health beneficial effects have been assigned to various bitter compounds supports this assumption.

In vertebrates, bitter compounds are detected by means of a family of specific receptors, the TAS2Rs. However, the number of genes in different species varies enormously. In the chicken genome, researchers found only three TAS2R genes, whereas they surprisingly discovered 49 genes in frogs. These findings are difficult to explain. Possibly chicken feed very selectively on few non-toxic items making a defense system based on the bitterness of fed-contained chemicals superfluous. Frogs which predominantly feed on insects are apparently exposed to astonishingly numerous bitter toxins. Insects may frequently use bitter chemicals as weapons against predators or for hunting prey. Another property of TAS2R genes is that they fall into subgroups (37). One subgroup shows a clear one-to-one orthology among species as most other genes do. The other displays lineage-specific expansions. It has been argued that the former allows animals to detect chemicals present in common food whereas the latter allows recognition of potentially harmful substances in food encountered specifically by only one species.

Lessons from functional expression of TAS2R genes

The human genome contains 25 TAS2R genes at four *loci* on chromosomes 5, 7, and 12 (35). Based on a lack of sequence conservation with other G protein-coupled receptor genes they encode an own subfamily of G protein-coupled receptors. These receptors are glycosylated at a strictly conserved Asn-linked glycosylation sites in the second extracellular loop (38). During biosynthesis TAS2Rs interact with various chaperones (39). Both phenomena, glycosylation and interaction with auxiliary proteins, are required for functional cell surface expression of TAS2Rs.

For the majority of TAS2Rs cognate compounds have been identified by functional expression of TAS2Rs in heterologous cells (40). Intriguingly, all compounds that activate TAS2Rs taste bitter. This observation suggests that all members of the TAS2R family serve as oral bitter receptors, although they likely

have additional functions based on the observation that the TAS2R genes are expressed at various extra-oral sites. Various TAS2Rs show quite specific agonist-profiles, in a sense that the agonists have certain chemical substructures in common. Prototypical receptors are TAS2R16 and TAS2R38 (41,42). TAS2R16 is activated by β -gluco, and mannopyranosides with small hydrophobic aliphatic or phenolic aglycons. TAS2R16 does, however, not respond to galactosides. Increasing sizes and hydrophilicity of the aglycons renders compounds less potent to stimulate TAS2R16. Good agonists are the above mentioned substance salicin and the toxin of bitter almonds amygdalin. As estimates count some ten thousand plant species that produce toxic glycosides the number of chemicals to which TAS2R16 responds is numerous and could be in the range of hundreds to thousand. Similarly, TAS2R38 is sensitive to numerous chemicals that contain $-N=C=S$ groups. In marked contrast, some TAS2Rs are very broadly tuned to chemicals that do not necessarily share common substructures. For instance, TAS2R14 was activated in heterologous expression systems by a quarter of all bitter compounds tested (43). Another example is given by TAS2R46, a receptor, sensitive to sesquiterpene lactones, clerodane and labdane diterpenoids, strychnine, sucrose octaacetate, and denatonium benzoate (44). The data indicate that the broad tuning of TAS2Rs fully explains the ability of humans to recognize Thousands of compounds as bitter with only 25 receptors. Other mechanisms may not or not substantially contribute.

Bitter taste and nutrition

An important issue that emerges is whether bitter taste sensitivity is related to intake behaviour and eventually with health and disease risk. Previous studies conducted before the TAS2Rs have been cloned were biased by the facts that (i) subjects have only phenotypically been classified based on their tasting abilities and that (ii) only bitterness in general has been studied. Now the challenge is to design studies with defined genotyped cohorts to be tested with specific cognate bitter compounds for known TAS2Rs.

The threshold values of activation of TAS2Rs determined in functional expression assays agreed well with the recognition threshold values for the same compounds determined in sensory studies with human subjects (41,42,45). In some cases the threshold values measured for the recombinant receptor in cell lines were somewhat lower than those recorded in sensory studies. These differences have been explained by the fact that the cellular assays use chimeric G proteins designed for specifically for that purpose (42), whereas TAS2R-G protein-coupling in taste receptor cell membranes involves natural G proteins, including α -gustducin, G β 1, G β 3, and G γ 13 (35). From these studies it has been concluded that the biochemical properties of taste receptors determine our sensitivity of tasting bitter compounds.

Above conclusion is further supported by the genetics of bitter taste. Recently, the genetic basis has been uncovered for perceiving the bitterness of $-N=C=S$ compounds, such as phenyl thiocarbamide and propyl thiouracil, or not (46). Three non-synonymous single nucleotide polymorphisms in the TAS2R38 gene define two major haplotypes that are referred to as PAV or AVI depending on the amino acid residues encoded by the affected triplets. When the two variants are expressed in heterologous cells the PAV variant of TAS2R38 was sensitive to low concentrations of compounds with the $-N=C=S$ group, whereas the AVI variant did not respond at all (42). Moreover, subjects homozygous for the PAV haplotype readily taste low concentrations of $-N=C=S$ compounds whereas subjects homozygous for the AVI haplotype are taste "blind" for these compounds. A linkage of genotype, receptor

properties and sensitivity for bitterness has also been demonstrated for the TAS2R43 and TAS2R44 genes and their agonists aloin and saccharin (47). Based on the observation of the pronounced genetic variability among TAS2R genes we might expect that in the future additional genetically determined perceptual differences in the population will be uncovered. Many of the detected SNPs are not equally present in the genomes of the world populations suggesting that genetic variations in the TAS2R genes likely account for ethnic differences in bitter taste sensitivities as well (48).

Above data suggested that TAS2R gene sequences determine the biochemical properties of the encoded receptor, which, in turn, defines the sensitivity of subjects to taste certain bitter compounds. Moreover, they indicate that the sensitivity for bitter compounds varies in the population. This raises the question whether or not the genetically determined perceptual differences in the population cause individual likes or dislikes of food rich in such substances and eventually result in personal eating habits. Due to a lack of data, we do not have the answer yet. However, it is clear that, for instance, in the case of TAS2R38 cognate bitter compounds are present in various frequently consumed legumes in concentrations in the perceptual range of PAV-tasters and out of the perceptual range of AVI-non-tasters (49). Consequently, bitterness scores for edible plants containing –N=C=S compounds segregate according to TAS2R38 genotype of subjects, while bitterness scores for plants not containing –N=C=S compounds do not (50).

To date, we have only circumstantial evidence in support of impact of taste receptors on nutrition and health. One example stems from the molecular evolution of the *TAS2R16* gene (51). A mutation in this gene at a site corresponding to the putative agonist binding site occurred in the Paleolithic some 80,000 to 800,000 years ago. The novel allele encodes a receptor with higher potency for certain glycopyranosides, many of which are cyanogenic and therefore highly toxic. This allele shows many signs of positive selection. Therefore, the novel high-potency-allele became rapidly fixed in the genomes of our ancestors and, with the migration of humans out of Africa, distributed all over the planet. In contrast, the ancestral low-potency-variant survived in central Africa with a relatively low frequency of ~ 14%. This observation strongly suggests that carriers of the novel allele could establish healthier diets low in the content of toxic glycosides posing a selective advantage on them allowing them to more effectively reproduce and pass on their genes to the next generations. The ancestral gene variant shows a distribution similar to that of anti-malaria genes. Its survival may be explained by assuming that high threshold values for tasting glycosides, including cyanogenic glycosides, are causing elevated intake of plants containing such compounds, leading to chronic cyan intoxication. The resulting sickle cell anemia protects subjects from deadly Malaria infections. Thus the ancestral allele likely was of advantage for humans living in areas contaminated by mosquitoes infected with *Plasmodium falciparum*.

Another example that illustrates the connection of taste and nutrition comes from the animal kingdom. All kinds of cats from tigers to our domestic cats are indifferent to sweets. They cannot be trained through the awards of sugar lumps to perform certain tricks or stunts. This correlates to the fact that cats do not possess a functional sweet taste receptor due to various mutations in the gene encoding the T1R2 subunit of the sweet receptor (52). This distinguishes cats from other carnivores, including dogs and bears, which have a functional sweet receptor and are well-known to be attracted by sweets. These pieces of circumstantial evidence are in support of a strong impact of taste on nutrition and health and let us optimistically expect more direct evidence in the near future.

Acknowledgements

Original work carried out in the author's laboratory and referred to in the present article was supported by the German Science Foundation (Me 1024).

References

1. Miller I.J., Jr. (1995) In *Handbook of Olfaction and Gustation* (Doty, R.L., ed.), Dekker: New York, Basel, Hong Kong, pp 521-547.
2. Roper S.D. (2007) *Pflugers Arch* 454: 759-776.
- 2a. Clapp T.R., Yang R., Stoick C.L., Kinnamon S.C., Kinnamon J.C. (2004) *J. Comp. Neurol.* 468: 311-321.
3. DeFazio R.A., Dvoryanchikov G., Maruyama Y., Kim J.W., Pereira E., Roper S.D., Chaudhari, N. (2006) *J. Neurosci.* 26: 3971-3980.
4. Chandrashekar J. (2006) *Nature* 444: 288-294.
- 4a. Zhang Y., Hoon M.A., Chandrashekar J., Mueller K.L., Cook B., Wu D., Zuker C.S., Ryba N.J. (2003) *Cell* 112: 293-301.
5. Mueller K.L., Hoon M.A., Erlenbach I., Chandrashekar J., Zuker C.S., Ryba N.J.P. (2005) *Nature* 434: 225-229.
6. Behrens M., Foerster S., Staehler F., Raguse J.D., Meyerhof W. (2007) *J. Neurosci.* 27: 12630-12640.
7. Kataoka S., Yang R., Ishimaru Y., Matsunami H., Seigny J., Kinnamon J.C., Finger T.E. (2008) *Chem. Senses* 33: 243-254.
8. Clapp T.R., Medler K.F., Damak S., Margolskee R.F., Kinnamon S.C. (2006) *BMC Biol.* 4: 7.
9. Huang Y.J., Maruyama Y., Dvoryanchikov G., Pereira E., Chaudhari N., Roper S.D. (2007) *Proc. Natl Acad. Sci. U S A*, 104(15): 6436-6441.
10. Romanov R.A., Rogachevskaja O.A., Bystrova M.F., Jiang P., Margolskee R.F., Kolesnikov S.S. (2007) *Embo. J.* 26: 657-667.
11. Finger T.E., Danilova V., Barrows J., Bartel D.L., Vigers A.J., Stone L., Hellekant G., Kinnamon, S.C. (2005) *Science* 310: 1495-1499.
12. LopezJimenez N.D., Cavenagh M.M., Sainz E., Cruz-Ithier M.A., Battey J.F., Sullivan S.L. (2006) *J. Neurochem.* 98: 68-77.
13. Ishimaru Y., Inada H., Kubota M., Zhuang H., Tominaga M., Matsunami H. (2006) *Proc. Natl Acad. Sci. U S A* 103: 12569-12574.
14. Huang A.L., Chen X., Hoon M.A., Chandrashekar J., Guo W., Trankner D., Ryba N.J., Zuker C.S. (2006) *Nature* 442: 934-938.
15. Bigiani A., Cuoghi V. (2007) *J. Neurophysiol.* 98: 2483-2487.
16. Vandenbeuch A., Clapp T.R., Kinnamon S.C. (2008) *BMC Neurosci* 9, 1.
17. Simon S.A., de Araujo I.E., Gutierrez R., Nicolelis M.A. (2006) *Nat. Rev. Neurosci.* 7: 890-901.
18. Tomchik S.M., Berg S., Kim J.W., Chaudhari N., Roper S.D. (2007) *J. Neurosci.* 27: 10840-10848.
19. Zaidi F.N., Whitehead M.C. (2006) *J. Neurosci.* 26: 8243-53.
20. Zhao F.L., Shen T., Kaya N., Lu S.G., Cao Y., Herness S. (2005) *Proc. Natl Acad. Sci. U S A* 102: 11100-11105.
21. Shin Y.K., Martin B., Golden E., Dotson C.D., Maudsley S., Kim W., Jang H.J., Mattson M.P., Drucker D.J., Egan J.M., Munger S.D. (2008) *J. Neurochem* 106: 455-463.
22. Ninomiya Y., Shigemura N., Yasumatsu K., Ohta R., Sugimoto K., Nakashima K., Lindemann B. (2002) *Vitam Horm* 64: 221-248.
23. Lindemann B. (1996) *Physiol. Rev.* 76: 718-766.
24. Stähler F., Riedel K., Demgensky S., Neumann K., Dunkel A., Täubert A., Raab B., Behrens M., Raguse J.-D., Hofmann T., Meyerhof W. (2008) *Chemosensory Perception* 1: 78-90.
25. Michlig S., Damak S., Le Coutre J. (2007) *J. Comp. Neurol.* 502: 1003-1011.

26. DeSimone J.A., Lyall V., Heck G.L., Phan T.H., Alam R.I., Feldman G.M., Buch R.M. (2001) *J. Neurophysiol.* 86: 2638-2641.
27. Lyall V., Heck G.L., Vinnikova A.K., Ghosh S., Phan T.H., Alam R.I., Russell O.F., Malik S.A., Bigbee J.W., DeSimone J.A. (2004) *J. Physiol.* 558: 147-159.
28. Da Conceicao Neta E.R., Johanningsmeier S.D., McFeeters R.F. (2007) *J. Food Sci.* 72: R33-38.
29. Lyall V., Alam R.I., Phan D.Q., Ereso G.L., Phan T.H., Malik S.A., Montrose M.H., Chu S., Heck G.L., Feldman G.M., DeSimone J.A. (2001) *Am. J. Physiol. Cell. Physiol.* 281: C1005-1013.
30. Huang Y.A., Maruyama Y., Stimac R., Roper S.D. (2008) *J. Physiol., in press*
31. Richter T.A., Dvoryanchikov G.A., Chaudhari N., Roper S.D. (2004) *J. Neurophysiol.* 92: 1928-1936.
32. Breslin P.A., Spector A.C. (2008) *Curr. Biol.* 18: R148-155.
33. Max M., Shanker Y.G., Huang L., Rong M., Liu Z., Campagne F., Weinstein H., Damak S., Margolskee R.F. (2001) *Nat. Genet.* 28: 58-63.
34. Oike H., Nagai T., Furuyama A., Okada S., Aihara Y., Ishimaru Y., Marui T., Matsumoto I., Misaka T., Abe K. (2007) *J. Neurosci.* 27: 5584-5592.
35. Meyerhof W. (2005) *Rev. Physiol. Biochem. Pharmacol.* 154: 37-72.
36. Ganchrow J.M.J. (2203) In *Handbook of Olfaction and Gustation* (Dekker M., ed.), Doty: New York, pp 823-946.
37. Shi P., Zhang J., Yang H., Zhang Y.P. (2003) *Mol. Biol. Evol.* 20: 805-814.
38. Reichling C., Meyerhof W., Behrens M. (2008) *J. Neurochem.* 106(3):1138-1148.
39. Behrens M., Bartelt J., Reichling C., Winnig M., Kuhn C., Meyerhof W. (2006) *J. Biol. Chem.* 281: 20650-20659.
40. Behrens M.S., F.; Peng Shi.; Bufe B., Meyerhof W. (2007) In *Wiley Encyclopedia of Chemical Biology*, John Wiley & Sons (ed.).
41. Bufe B., Hofmann T., Krautwurst D., Raguse J.D., Meyerhof W. (2002) *Nat. Genet.* 32: 397-401.
42. Bufe B., Breslin P.A., Kuhn C., Reed D.R., Tharp C.D., Slack J.P., Kim U.K., Drayna D., Meyerhof W. (2005) *Curr. Biol.* 15: 322-327.
43. Behrens M., Brockhoff A., Kuhn C., Bufe B., Winnig M., Meyerhof W. (2004) *Biochem. Biophys. Res. Commun* 319: 479-485.
44. Brockhoff A., Behrens M., Massarotti A., Appendino G., Meyerhof W. (2007) *J. Agric. Food Chem.* 55: 6236-6243.
45. Kuhn C., Bufe B., Winnig M., Hofmann T., Frank O., Behrens M., Lewtschenko T., Slack J.P., Ward C.D., Meyerhof W. (2004) *J. Neurosci.* 24: 10260-10265.
46. Kim U.K., Jorgenson E., Coon H., Leppert M., Risch N., Drayna D. (2003) *Science* 299: 1221-1225.
47. Pronin A.N., Xu H., Tang H., Zhang L., Li Q., Li, X. (2007) *Curr. Biol.* 17: 1403-1408.
48. Kim U., Wooding S., Ricci D., Jorde L.B., Drayna D. (2005) *Hum. Mutat.* 26: 199-204.
49. Drewnowski A., Gomez-Carneros, C. (2000) *Am. J. Clin. Nutr.* 72: 1424-1435.
50. Sandell M.A., Breslin P.A. (2006) *Curr. Biol.* 16: R792-794.
51. Soranzo N., Bufe B., Sabeti P.C., Wilson J.F., Weale M.E., Marguerie R., Meyerhof W., Goldstein D.B. (2005) *Curr. Biol.* 15: 1257-1265.
52. Li X., Li W., Wang H., Bayley D.L., Cao J., Reed D.R., Bachmanov A.A., Huang L., Legrand-Defretin V., Beauchamp G.K., Brand J.G. (2006) *J. Nutr.* 136: 1932S-1934S.

hTAS2R38 RECEPTOR GENOTYPES PREDICT SENSITIVITY TO BITTERNESS OF THIOUREA COMPOUNDS IN SOLUTION AND IN SELECTED VEGETABLES

Mari SANDELL^{1,2} and Paul Breslin²

¹ *University of Turku, Functional Foods Forum, FI-20014 Turku, Finland*

² *Monell Chemical Senses Center, 3500 Market St, Philadelphia, PA-19104, USA*

Abstract

With twenty-five G-protein-coupled TAS2R receptors bitterness is the most complex taste sensation in terms of signal transduction. The objective of this sensory study was to investigate the effect of hTAS2R38 bitter receptor gene genotypes on intensity of bitterness of different N-C=S containing compounds. In addition, we studied the bitterness of vegetables that produce glucosinolates, which also contain thiourea groups. People homozygous for the PAV form of the hTAS2R38 gene were significantly more sensitive to N-C=S containing compounds than those homozygous for the AVI haplotype. However, PAV subjects were not more sensitive than AVI subjects for structurally unrelated bitter tasting compounds. In addition, PAV/PAV subjects rated the glucosinolate generating vegetables as 60% more bitter on average than did the AVI/AVI subjects. This shows that genetic variation in taste perception predictably determines the taste of vegetables.

Introduction

Flavour has a great impact on food choice and acceptability. Taste and Aroma are the foundation of flavour. Bitterness is known to be the most complex taste sensation with twenty-five taste receptors being members of G-protein-coupled TAS2R receptor family. Bitterness may be a principal reason for food rejection. Human's ability to taste bitter compounds that contain a thiourea (-N-C=S) structure, such as phenylthiocarbamide (PTC) and its chemical relative propylthiouracil (PROP), depends on their TAS2R38 bitter receptor genotype (1,2). Similarly, genetic approaches may be employed to determine sources of variability in the perception of complex chemical matrices such as in foods. Many nutritionally important compounds may contribute to unpleasant bitter taste. But individual differences in bitterness perception of these compounds might be significant. Yet, a receptive field for this receptor and its parallel in human bitterness sensitivity have not been mapped. Understanding of these genetic differences in humans is necessary for the study of food and specific food preferences.

The objective of this study was to investigate the effect of hTAS2R38 bitter receptor gene genotypes on intensity of bitterness of different N-C=S containing compounds. In addition, we studied the bitterness of vegetables that produce glucosinolates, which also contain thiourea groups (3). We hypothesised that people who possess one or two PAV alleles of hTAS2R38 would find these stimuli and vegetables bitterer than those who carried only the insensitivity alleles (AVI/AVI).

Experimental

All participating subjects (19-64 years) were genotyped for their hTAS2R38 genotypes and pre-screened for being homozygous sensitive (PAV) or homozygous insensitive (AVI) using allele-specific probes and primers (1). Subjects were recruited according to a protocol approved by the Office of Regulatory Affairs at University of Pennsylvania.

Thiourea compounds such as PTC, PROP, dimethylthiourea, diethylthiourea, diphenylthiourea, acetylthiourea, 2-mercaptobenzimidazole, sodium thiocyanate and methimazole were high quality (>99% purity) and commercially available. As control stimuli we used pure uracil, urea and QHCl.

The taste profiles of different N-C=S containing compounds were examined with a trained sensory panel (n= 24) at the sensory evaluation laboratory at Monell Chemical Senses Center. The subjects rated the intensity of bitterness on computer controlled gLMS scales. All the compounds were tasted in 1/2-log step solution series in three different sessions. In addition to N-C=S-compounds, the subjects evaluated also selected vegetables (3).

Results

Bitterness of N-C=S compounds. The mean ratings of PAV/PAV (n=13) and AVI/AVI (n= 11) genotypes for N-C=S containing compounds are shown in Figure 1. Results show that people possessing the PAV form of the hTAS2R38 gene were significantly more sensitive to N-C=S containing compounds than were those possessing the AVI haplotype. Plots for PTC and PROP were similar to other N-C=S compounds and also previous studies (1). However, in case of control compounds (QHCl, uracil and urea) without N-C=S the sensitive people (PAV/PAV) were not more sensitive than insensitive people (AVI/AVI). This result shows the power of N-C=S moiety on individual differences.

Bitterness of vegetables. To find out the effect of N-C=S also in vegetables the subjects tasted both glucosinolate generating and control vegetables (3). The vegetables that produce glucosinolates were perceived bitterer by people who possess sensitive PAV allele of hTAS2R38 gene. Overall, PAV/PAV subjects rated glucosinolate generating vegetables as 60% more bitter than AVI/AVI. However, these two genotype groups found the nonglucosinolate-generating vegetables equally bitter. This shows that, general bitterness of non-glucosinolate generating vegetables could not be explained by hTAS2R38 receptor genotype.

Conclusions

People homozygous for the PAV form of the hTAS2R38 gene were significantly more sensitive to N-C=S containing compounds than those homozygous for the AVI haplotype. However, PAV subjects were not more sensitive than AVI subjects for bitter tasting compounds structurally unrelated to N-C=S. In addition, PAV/PAV subjects rated the glucosinolate generating vegetables more bitter than did the AVI/AVI subjects. This shows that genetic variation in taste perception predictably determines the taste of vegetables. Moreover, this may also mediate preference and consumption of vegetables, which remains to be determined. The taste of foods has a large impact on food choice. Furthermore, the relationship between perception and the physical food properties is central to new food product development. There is a need to increase the knowledge on the taste and sensory quality of vegetables but also other healthful foods overall to improve their intake.

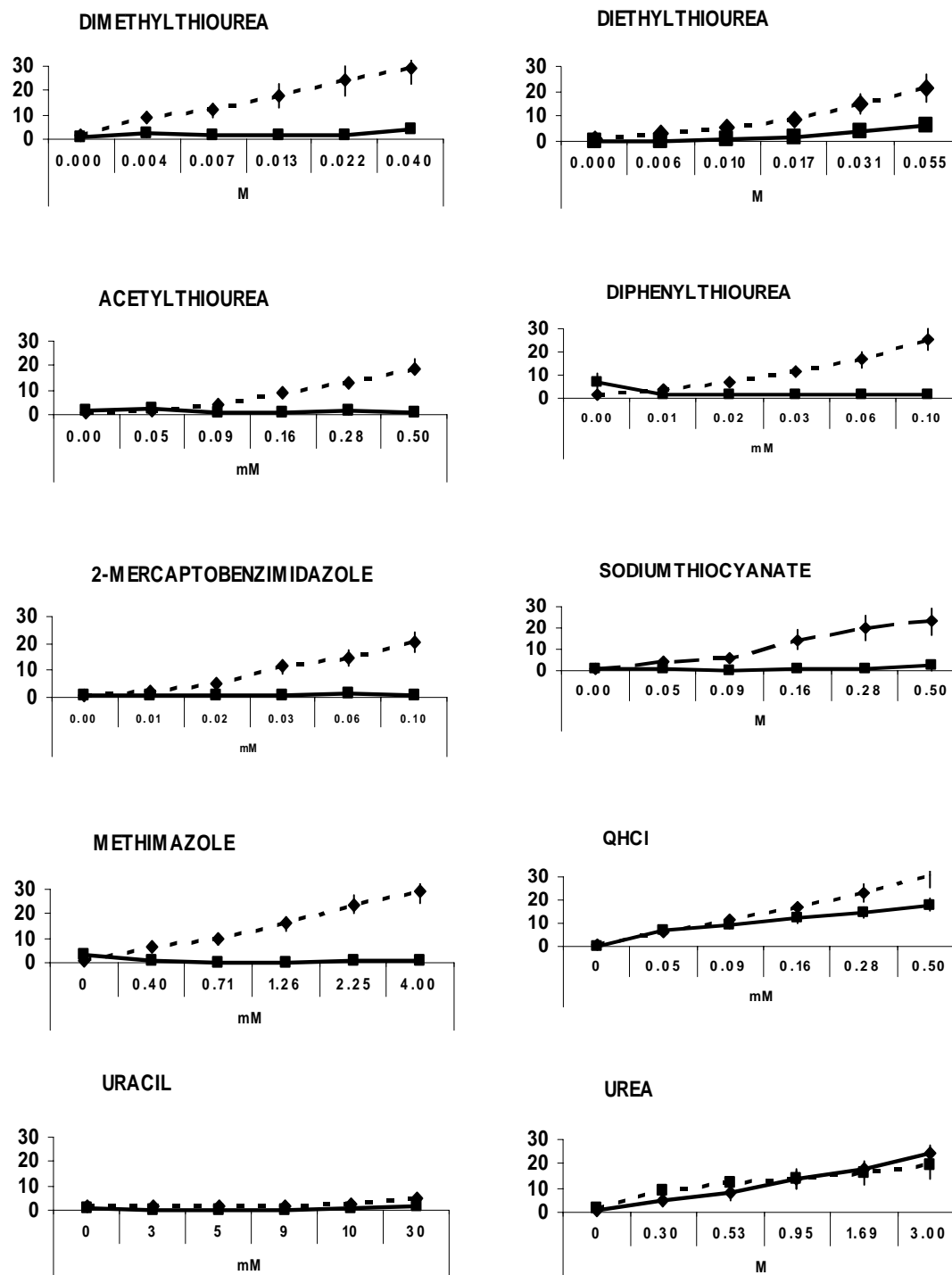


Figure 1. Mean intensities of bitterness of thiourea compounds and control stimuli. Panel consisted of 13 PAV/PAV (---◆---) and 11 AVI/AVI (---■---) subjects.

The study was funded by NIH DC02995 (PASB).

References

1. Bufe B., Breslin P.A.S., Kuhn C., Reed D., Tharp C., Slack J., Kim U.-K., Drayna D., Meyerhof W. (2005) *Current Biol.* 22: 322-327.
2. Kim U.-K., Breslin P.A.S., Reed D.R., Drayna D. (2004) *J. Dent. Res.* 83: 448-453.
3. Sandell M., Breslin, P.A.S. (2006) *Current Biol.* 16: R792-R794.

AGONIST ACTIVATION OF BITTER TASTE RECEPTORS

A. Brockhoff¹, M. Behrens¹, G. Appendino², C. Kuhn¹, B. Bufe¹, and W. MEYERHOF¹

¹ *Department of Molecular Genetics, German Institute of Human Nutrition Potsdam-Rehbruecke, Arthur-Scheunert-Allee 114-116, 14558 Nuthetal, Germany*

² *University of Eastern Piedmont, DISCAFF, Via Bivio 6, 28100 Novara, Italy*

Abstract

The human bitter taste receptor gene family (hTAS2R) consists of 25 members, which are responsible for the detection of thousands of bitter compounds. The identification of agonists for most of the hTAS2Rs demonstrated that each receptor recognises numerous substances, thus explaining how such few receptors may suffice for the detection of so many different bitter compounds. Compared to most other G protein-coupled receptors, which interact very specifically with single or few high affinity ligands, the agonist interaction mode of hTAS2Rs must be different. In order to elucidate the structure-function relationships of human bitter taste receptors, we focused on a subfamily of the closely related hTAS2R43-50 genes. Although the amino acid sequences of these receptors are highly similar, their agonist spectra vary considerably. By functional heterologous expression of chimeric and point-mutated receptors in mammalian cell lines we identified regions influencing interaction with agonists. Interestingly, a limited number of amino acid positions appear to determine agonist specificity profoundly.

Introduction

Human bitter taste is mediated by 25 G protein-coupled receptors of the hTAS2R gene family (for a recent review see [1]). Most of the hTAS2Rs are broadly tuned to the detection of many bitter compounds. This explains how only 25 receptors might allow for the detection of thousands of bitter compounds found in nature. Usually, the interaction of G protein-coupled receptors with their ligands involves the specific interaction between the side chains of particular amino acid residues and chemical groups of few or single high affinity ligands, as seen for e.g. peptide hormone receptors (for a review see [2]). For bitter taste receptors that are activated by numerous, structurally diverse low affinity agonists the organisation of their binding pockets is not understood. In general, two mutually exclusive binding modes are conceivable: (i) they could possess a binding pocket that loosely fits all the different agonists, where a number of side chains of amino acid residues make weak contacts to the bound chemicals, (ii) the binding pocket consists of few residues making rather stable contacts to bound agonists, analogous to the situation in peptide hormone receptors. By mutagenesis of residues forming the binding site within hTAS2Rs the two above described mechanisms should become experimentally accessible, because only in the second model receptors will likely respond to single amino acid exchanges with profound effects on their agonist profile.

In the present publication we describe the construction and functional characterization of human bitter taste receptor chimeras to identify regions critical for agonist activation. For this study we chose receptors of a subfamily of closely related receptors including hTAS2R43-50. Although highly similar in their peptide sequence,

the agonist activation profiles of these receptors differ considerably, thus allowing the identification of the regions involved in agonist selectivity. Further we performed *in-vitro* mutagenesis to pin-point those residues, which resided in regions discovered by receptor chimeras and are different among the studied receptors. Finally, all identified amino acid positions important for agonist activation in the receptor hTAS2R46 were incorporated in an *in silico* model to gain insight in the structure of the putative binding pocket.

Experimental

Generation of receptor constructs for functional expression analyses. All receptor constructs were cloned into the vector pcDNA5FRT (Invitrogen). To allow for high level cell surface expression and facilitate immunocytochemical detection the vector was modified with an sst3-tag [3] added to the amino-terminus and an hsv-epitope added to the carboxyl-terminus of cloned receptor constructs, respectively. Additionally, an endogenous EcoRI-site was removed to allow utilisation of the MCS-EcoRI site for cloning [4]. Subcloning of the different receptor constructs was done using the restriction endonucleases EcoR I and Not I leading to an in-frame fusion of the receptor coding region with sst3- and hsv-epitopes. Receptor chimeras and *in-vitro* mutagenesis were generated by PCR-mediated recombination [5].

Functional characterisation of receptor constructs. Heterologous expression of receptor constructs and calcium imaging was done as before [6]. Briefly, HEK 293T cells stably expressing the G protein chimera G α 16gust44 [7] were transiently transfected with receptor constructs and incubated overnight. For calcium imaging cells were loaded with Fluo4-am and analysed in a fluorimetric imaging plate reader (FLIPR, Molecular Devices). Changes in intracellular calcium were monitored and used to calculate dose-response relations with SigmaPlot 2000 (SPSS Inc.).

Homology modelling of hTAS2R46. An *in silico* model of the bitter taste receptor hTAS2R46 was build based on homology to the crystal structure of light-activated bovine rhodopsin [8] using the module "Prime" of the Schrodinger modelling software package.

Results and Discussion

In order to identify the receptor regions involved in the selective recognition of bitter agonists we constructed chimeras between hTAS2R46, a receptor that is activated by numerous sesquiterpene lactones, diterpenes, and other bitter substances including strychnine [6], and hTAS2R44, which is stimulated by the purely bitter compound aristolochic acid, as well as the artificial sweeteners saccharin and acesulfame K and others [9-11]. Although both receptors share 83% amino acid identity, their agonist activation patterns show no overlaps. Exchanging the extracellular loops 1-3 between both receptors abolishes or largely impairs their ability to respond to their corresponding agonists. Both receptor chimeras, hTAS2R44 carrying all extracellular loops of hTAS2R46, and hTAS2R46 with the extracellular loops of hTAS2R44, show residual responses to aristolochic acid and strychnine stimulation, respectively. This result suggests that extracellular loops and transmembrane domains are important for agonist interaction as already speculated by Pronin et al. [9]. The generation of chimeras with anchoring points within transmembrane domain 3 and intracellular loop 3, respectively, revealed that the ability of hTAS2R46 to be specifically activated by strychnine must reside within the region spanning part of the intracellular loop 3 until the carboxyl-terminus, including transmembrane domains 6 and 7 and the extracellular loop 3.

Of the few differing amino acids within this area, two positions within transmembrane domain 7 stuck out. Whereas hTAS2R46 has an acidic residue in position 265 (Glu265) and a small hydrophobic residue in position 268 (Ala268), hTAS2R44 has basic residues in positions 265 (Lys265) and 268 (Arg268), respectively. We therefore exchanged the amino acids at positions 265 and 268 of hTAS2R46 against the corresponding residues in hTAS2R44 and *vice versa*. By stimulation of the wild type and mutant receptors we observed that the mutated receptors underwent an agonist switch. Whereas the receptor mutant hTAS2R44 K265E R268A became responsive towards strychnine stimulation, the corresponding mutant hTAS2R46 E265K A268R was activated by aristolochic acid (Figure 1). Additionally, both mutants lost their responsiveness towards stimulation with the agonists of their parental receptors. This result indicates that specific amino acid residues in transmembrane helix 7 are involved in the selective interaction with agonists in different receptors.

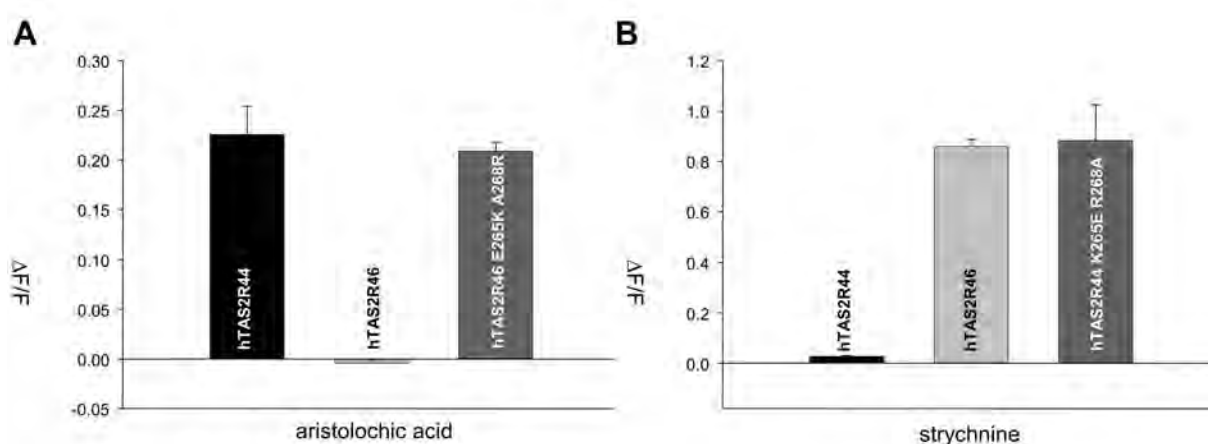


Figure 1. Exchange of two amino acid residues between hTAS2R44 and hTAS2R46 leads to a switch in agonist activation. Graphs A and B show the functional analyses of receptor constructs stimulated with aristolochic acid and strychnine, respectively. A) Calcium imaging experiment showing the responses of hTAS2R44, hTAS2R46, and hTAS2R46 E265K A268R upon stimulation with 10 μ M aristolochic acid. Note the pronounced response of the hTAS2R46 mutant to the hTAS2R44-specific agonist while the parental receptor, hTAS2R46, is not activated. B) Calcium imaging experiment showing the responses of hTAS2R46, hTAS2R44, and hTAS2R44 K265E R268A upon stimulation with 30 μ M strychnine. Note the pronounced response of the hTAS2R44 mutant to the hTAS2R46-specific agonist while the parental receptor, hTAS2R44, is not activated. $\Delta F/F$ = change in fluorescence after stimulation/basal fluorescence.

We reasoned that additional residues could be involved in the specific agonist interaction of the receptors studied that we might have missed just because of the high conservation of the peptide sequences. Therefore, we performed additional mutagenesis studies and extended the template receptors onto hTAS2R43 and hTAS2R50. Especially hTAS2R50 is considerably less related to hTAS2R46 and should therefore help to identify additional critical residues for the characterization of the putative agonist interaction pocket of hTAS2R46. By using the same approach as exemplified above, we identified in total 12 amino acid residues involved in the interaction of hTAS2R46 with strychnine. Transferring these residues in the receptor backbones of hTAS2R43, -44, and -50 does not only result in strychnine

responsiveness, but also induces responsiveness to additional selective hTAS2R46 agonists such as absinthin and denatonium suggesting that the exchanged residues are part of a common binding pocket shared, at least in part, by several of these bitter compounds. This fact is further supported by molecular modelling data (Figure 2). Most residues identified by our *in-vitro* mutagenesis experiments are located in close proximity to each other in a groove within the receptor hTAS2R46 that is formed by the upper part of several transmembrane domains and extracellular loops.

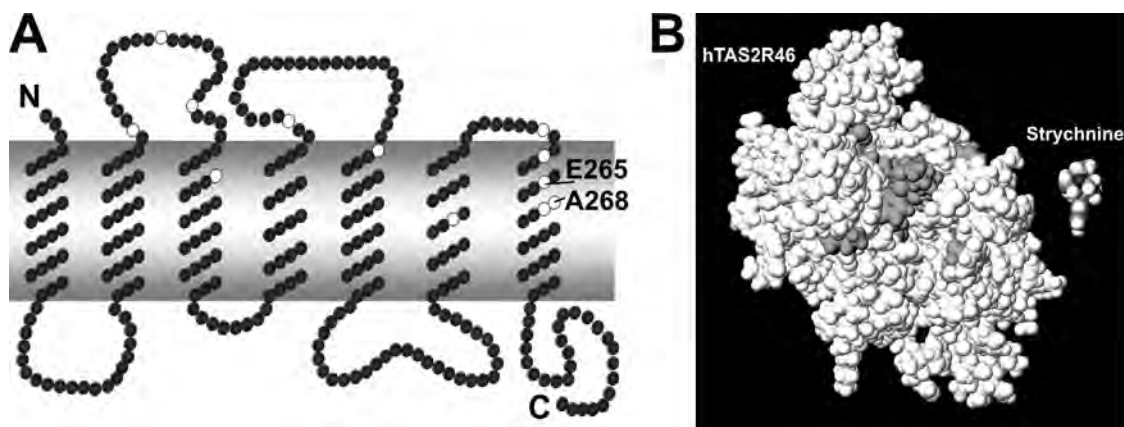


Figure 2. A) Snake diagram of the peptide sequence of hTAS2R46. Residues involved in activation by strychnine are indicated by white circles. The two residues discussed in the text, E265 and A268, are labelled. B) Homology modelling of the receptor hTAS2R46. Top view onto the receptor hTAS2R46 (from the extracellular side). The residues of the extracellular loop two have been removed to allow insight into the putative binding pocket of hTAS2R46. Amino acid positions identified to be involved in agonist activation by mutagenesis are highlighted in dark grey. The model was generated using the Schrodinger software modules “Prime” and “Maestro”.

References

1. Behrens M., Meyerhof W. (2006) *Cell. Mol. Life Sci.* 63: 1501-1509.
2. Wheatley M., Hawtin S.R., Wesley V.J., Howard H.C., Simms J., Miles A., McEwan K., Parslow R.A. (2003) *Biochem. Soc. Trans.* 31: 35-39.
3. Ammon C., Schafer J., Kreuzer O.J., Meyerhof W. (2002) *Arch. Physiol. Biochem.* 110: 137-145.
4. Bufe B., Hofmann T., Krautwurst D., Raguse J.D., Meyerhof W. (2002) *Nat. Genet.* 32: 397-401.
5. Fang G.W., Weiser B., Visosky A., Moran T., Burger H. (1999) *Nat. Med.* 5: 239-242.
6. Brockhoff A., Behrens M., Massarotti A., Appendino G., Meyerhof W. (2007) *J. Agric. Food Chem.* 55: 6236-6243.
7. Ueda T., Ugawa S., Yamamura H., Imaizumi Y., Shimada S. (2003) *J. Neurosci.* 23: 7376-7380.
8. Salom, D., Lodowski, D.T., Stenkamp, R.E., Le Trong, I., Golczak, M., Jastrzebska, B., Harris, T., Ballesteros, J.A., Palczewski, K. (2006) *Proc. Natl. Acad. Sci. USA* 103: 16123-16128.
9. Pronin, A.N., Tang, H., Connor, J., and Keung, W. (2004). *Chem. Senses* 29: 583-593.
10. Pronin, A.N., Xu, H., Tang, H., Zhang, L., Li, Q., Li, X. (2007) *Curr. Biol.* 17: 1403-1408.
11. Kuhn, C., Bufe, B., Winnig, M., Hofmann, T., Frank, O., Behrens, M., Lewtschenko, T., Slack, J.P., Ward, C.D., Meyerhof, W. (2004) *J. Neurosci.* 24: 10260-10265.

N-GLYCOSYLATION IS REQUIRED FOR BITTER TASTE RECEPTOR FUNCTION

C. Reichling, W. Meyerhof, and M. BEHRENS

Department of Molecular Genetics, German Institute of Human Nutrition Potsdam-Rehbruecke, Arthur-Scheunert-Allee 114-116, 14558 Nuthetal, Germany

Abstract

Human bitter taste is mediated by ~25 bitter taste receptors (hTAS2Rs), which recognize an enormous number of structurally diverse, toxic and non-toxic bitter substances. Heterologous expression in mammalian cells is a useful tool to investigate interactions between these receptors and their agonists. However, many bitter taste receptors are poorly expressed at the cell surface of heterologous cells requiring the addition of plasma membrane export-tags to the hTAS2R proteins. Currently, nothing is known about amino acid motifs or other receptor-intrinsic features of hTAS2Rs affecting plasma membrane association. In the present study, we investigated the Asn-linked glycosylation of hTAS2Rs. We show that all hTAS2Rs contain a conserved N-glycosylation site in the 2nd extracellular loop. For two receptors we demonstrated that this consensus site is utilised in mammalian cells. The almost complete loss of function caused by mutation of all receptors we investigated demonstrates the significance of glycosylation.

Introduction

Humans possess ~25 genes encoding putative TAS2R bitter taste receptors, which are all expressed in taste receptor cells on the tongue. It is generally believed that the taste of bitter substances is a warning mechanism against the ingestion of toxic food compounds. Therefore, the bitterness of food stuff influences our daily diet. To learn more about hTAS2Rs one has to functionally characterise receptor/agonist interactions. Usually, this is achieved by heterologous expression and functional analysis of such receptors (for a recent review, see [1]. Like many other chemoreceptors, including odorant receptors (ORs) [2], and pheromone receptors of the V2R gene family [3], hTAS2Rs are difficult to express in heterologous systems because plasma membrane export is insufficient. This problem is usually circumvented by the addition of “export-tags”, like the amino terminal 45 amino acids of the rat sst3 receptor [4], to the receptor proteins. In recent studies special emphasis was put on the identification of proteins involved in chemoreceptor cell surface targeting (see e.g. [5,6]). For some hTAS2Rs receptor transporting protein (RTP) 3 and 4, have been already identified to promote the functional expression [7]. However, analyses on the receptor proteins’ primary structure influencing subcellular targeting are scarce.

N-linked glycosylation is the most common posttranslational modification of GPCRs and occurs exclusively at the consensus sequence NXS/T. N-glycosylation is initiated in the ER and is completed during transport through the Golgi (for a recent review, see [8]). The roles of N-linked glycosylation in modulating GPCR targeting to the cell surface differ among GPCRs. For some proteins N-linked glycosylation was

shown to be associated with cell surface export [9], whereas for others efficient plasma membrane targeting is independent of glycosylation [10].

In the present study, we investigated if heterologously expressed human bitter taste receptors are glycosylated at conserved consensus sites for Asn-linked glycosylation. By *in-vitro* mutagenesis of the consensus sequences we changed the glycosylation status of the investigated hTAS2Rs. Functional consequences of experimentally induced hypoglycosylation were investigated by recombinant expression of mutant constructs in human embryonic kidney 293 cells (HEK 293T).

Experimental

Generation of receptor constructs and mutational analysis. Fusion constructs coding for hTAS2R16 and hTAS2R46 open reading frames and carboxy-terminal FLAG epitopes were cloned into the pcDNA5/FRT/TO vector (Invitrogen). Site-directed mutagenesis was performed according to the QuikChange protocol (Stratagene).

Calcium imaging. HEK 293T cells stably expressing the G protein chimera G α 16gust44 were transfected with taste receptor constructs. After 24 h, the cells were loaded for 1 h with the calcium-sensitive dye Fluo4-AM (Molecular Probes), were washed three times in bath solution, and stimulated with the corresponding agonists. Then changes in fluorescence were monitored, and dose–response curves were calculated as before [7].

Results and Discussion

In a previous study we recognized that hTAS2Rs with their native amino termini, to which no export tag has been attached, behaved differently, if expressed in heterologous cells. With respect to their function some receptors seemed to be independent from the addition of amino-terminal export-tags, others required the co-expression of auxiliary factors, whereas another group of receptors showed no function upon stimulation with their agonists without sst3-tag added to their amino-termini [7]. We hypothesized that the reason for the observed individuality in functional experiments must reside in the peptide sequence of hTAS2Rs. An alignment of the amino acid sequence of the 25 hTAS2Rs revealed a positionally conserved consensus sequence for Asn-linked glycosylation (N X S/T) in the 2nd extracellular loops of all receptors [11] (Figure 1).

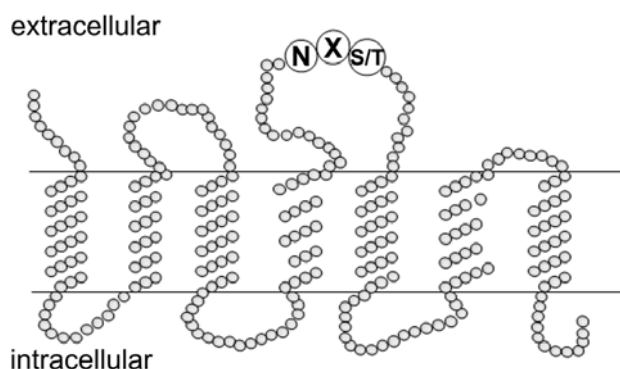


Figure 1. Snake diagram of hTAS2Rs. Based on an alignment of the amino acid sequences of all 25 human TAS2Rs a positionally conserved consensus site for Asn-linked glycosylation was identified. The consensus sequence, Asn (N)-X-Ser(S)/Thr(T), is centered in the extracellular loop two of the receptor proteins.

By suppressing N-glycosylation through treatment with the inhibitor tunicamycin or by the generation of receptor mutants with defective consensus sequences in the 2nd extracellular loop we confirmed experimentally the utilization of this site (not shown).

Subsequent calcium imaging experiments of HEK 293T cells demonstrated that the function of the analyzed bitter taste receptors upon agonist stimulation critically depended on the presence of glycans added to their peptide chain. In one set of experiments the glycosylation of hTAS2Rs was inhibited by using increasing concentrations of the inhibitor tunicamycin, ranging from 0 ng/ml as a negative control to 1 µg/ml culture medium, during the culture period prior to the functional assays (not shown). Another set of experiments was performed using hTAS2R constructs in which the consensus sequence within the extracellular loop was destroyed by a point mutation resulting in an exchange of Asn by Gln. As observed for the tunicamycin-treated hTAS2Rs, only minor residual activation of hTAS2Rs by stimulation with the corresponding bitter agonist was observed. Whereas the dose-response relationship observed for the receptor hTAS2R16 shows a clear stimulation by its agonist salicin [4] at concentrations of 3 mM and higher, the hypoglycosylated mutant hTAS2R16 N163Q is non-functional (Figure 2).

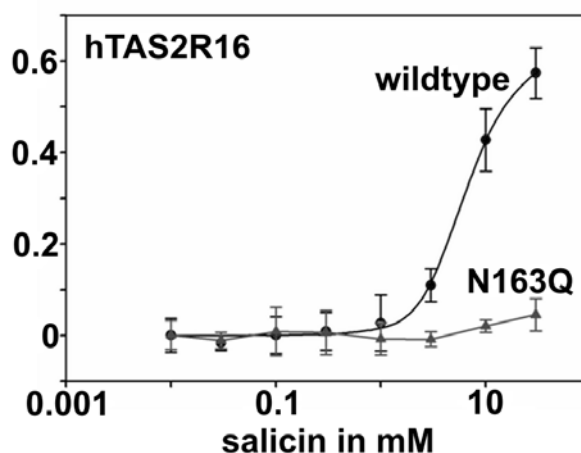


Figure 2. Dose response curves of glycosylated and non-glycosylated hTAS2R16. For functional analyses both, the hTAS2R16 and the glycosylation-deficient hTAS2R16 N163Q were transiently expressed in HEK 293T cells stably expressing the G protein chimera *Gα16gust44*. After ~24 h of incubation, cells were washed, loaded with the calcium-sensitive dye, Fluo4-AM, and stimulated with different concentrations of the agonist salicin. Changes in fluorescence induced by agonist stimulation were monitored using a Fluorometric Imaging Plate Reader (FLIPR, Molecular Devices) and plotted onto the y-axis $\Delta F/F$.

Similar observations were made using the glycosylated receptor hTAS2R46 and its corresponding non-glycosylated mutant hTAS2R46 N161Q. In case of the hTAS2R46 dose-response relationships were monitored (not shown) with two of its cognate and structurally very different bitter agonists, absinthin and strychnine [12], indicating that the glycan structures may not be directly involved in agonist recognition, but rather play a role during the biosynthetic pathway of hTAS2Rs. Further experiments (not shown) indicated that the lack of function observed for the non-glycosylated receptor hTAS2R16 might be, at least in part, due to a reduced number of receptors present at the cell surface and/ a reduced association with the

ER-resident chaperone calnexin along its biosynthetic pathway [11]. A persistent glycosylation, however, is not required for the function of hTAS2R16 in heterologous cells, as indicated by the fact that the responsiveness of the mutant hTAS2R16 N163Q to salicin stimulation could be enhanced by the co-expression of the auxiliary factors RTP3 and RTP4 [7,11].

References

1. Behrens M., Meyerhof W. (2006) *Cell. Mol. Life Sci.* 63: 1501-1509.
2. Gimelbrant A.A., Stoss T.D., Landers T.M., McClintock T.S. (1999) *J. Neurochem.* 72: 2301-2311.
3. Loconto J., Papes F., Chang E., Stowers L., Jones E.P., Takada T., Kumanovics A., Fischer Lindahl K., Dulac C. (2003) *Cell.* 112: 607-618.
4. Bufe B., Hofmann T., Krautwurst D., Raguse J.D., Meyerhof W. (2002) *Nat. Genet.* 32: 397-401.
5. Dwyer N.D., Troemel E.R., Sengupta P., Bargmann C.I. (1998) *Cell.* 93: 455-466.
6. Saito H., Kubota M., Roberts R.W., Chi Q., Matsunami H. (2004) *Cell.* 119: 679-691.
7. Behrens M., Bartelt J., Reichling C., Winnig M., Kuhn C., Meyerhof W. (2006) *J. Biol. Chem.* 281: 20650-20659.
8. Hebert D.N., Garman S.C., Molinari M. (2005) *Trends Cell. Biol.* 15: 364-370.
9. Rands E., Candelore M.R., Cheung A.H., Hill W.S., Strader C.D., Dixon R.A. (1990) *J. Biol. Chem.* 265: 10759-10764.
10. van Koppen C.J., Nathanson N.M. (1990) *J. Biol. Chem.* 265: 20887-20892.
11. Reichling C., Meyerhof W., Behrens M. (2008) *J. Neurochem.* 106:1138-1148.
12. Brockhoff A., Behrens M., Massarotti A., Appendino G., Meyerhof W. (2007) *J. Agric. Food Chem.* 55: 6236-6243.

INVOLVEMENT OF THE EPITHELIAL SODIUM CHANNEL IN HUMAN SALT TASTE PERCEPTION

F. STÄHLER¹, K. Riedel¹, S. Demgensky¹, A. Dunkel², A. Täubert², T. Hofmann², and W. Meyerhof¹

¹ *German Institute of Human Nutrition Potsdam-Rehbruecke, Department of Molecular Genetics, Arthur-Schneunert-Allee 114-116, 14558 Nuthetal, Germany*

² *Technical University of Munich, Chair of Food Chemistry und Molecular Sensory Science, Lise-Meitner-Str. 34, 85354 Freising, Germany*

Abstract

Sodium is an essential mineral for all vertebrates regulating electrolyte-homeostasis. The sense of taste promotes the intake of salt in order to compensate for the permanent loss of sodium through excretion. In rodents, salt taste is thought to involve several transduction pathways. One is elicited by various cations and cetylpyridinium-chloride-sensitive, whereas another is selectively stimulated by Na⁺ and inhibited by amiloride. The latter is supposed to involve the epithelial sodium channel (ENaC). The molecular mechanisms of human salt taste transduction remained elusive so far. In this report, we demonstrate by RT-PCR studies that all ENaC-subunits are expressed in fungiform and circumvallate (CV) papillae as well as in non-chemosensory lingual tissues, with the following rank order: $\alpha \sim \beta > \gamma \gg \delta$. All four subunits were also identified in CV taste buds by immunohistochemistry with specific antisera, whereas α -ENaC was not detected in fungiform taste buds. Interestingly, δ -ENaC was only found in taste pores, strongly suggesting a prominent role in taste transduction. L-arginine enhanced both, saltiness of Na⁺-containing test solutions in subjects and amiloride-sensitive sodium membrane-currents in $\alpha\beta\gamma$ - or $\delta\beta\gamma$ -ENaC expressing oocytes. No stimulating effect was observed in control experiments for L-glutamine in either system. Taken together, ENaC is possibly involved in taste transduction, however further research is needed to identify its specific function.

Introduction

Sodium is an essential mineral, as it is involved in nerve conductance, osmotic pressure, water homeostasis and pH regulation (1). As sodium is crucial for the physiology of organisms, mechanisms evolved to detect sodium and other mineral ions in the environment. In vertebrates, this mechanism is provided by the sense of taste (2). In humans, sodium taste is perceived as a unique taste quality, salty. Although other minerals possess a salty taste as well, other descriptors are usually being used to fully describe the taste of these salts. The detailed transduction mechanisms of salt taste have not yet been worked out; however, ion channels appear intimately involved. Species-specific differences of salt transduction have been observed. For instance, humans and rodents perceive saltiness of NaCl and KCl, yet only in rodents is the taste of NaCl substantially blocked by the diuretic agent amiloride whereas the block is modestly, if at all, present in humans (3-7). Nerve recordings performed in rodents pointed to the involvement of several transduction mechanisms for salt taste. They demonstrated that responses, elicited

by Na⁺, of the glossopharyngeal nerve innervating the posterior part of the tongue, were sensitive to amiloride (8-12) whereas this drug blocked such responses in the chorda tympani nerve, which innervates the anterior part of the tongue (8-14). Taken together, these data demonstrated that, at least in rodents, salt taste is perceived via amiloride-sensitive and amiloride-insensitive pathways. Based on its selectivity for Na⁺ ions and its sensitivity to amiloride, the epithelial sodium channel (ENaC) has been suggested to function as a salt taste receptor (15-17). In rodents, ENaC is a non-voltage-gated, sodium permeable, heteromeric ion channel composed of α -, β - and γ - subunits. Expression studies in rodents demonstrated that all ENaC subunits are present in fungiform papillae, while in vallate and foliate papillae only α -ENaC could easily be found (18-20). Nothing was known about the expression of ENaC subunits in human taste tissue.

Experimental

General procedures for RT-PCR, immunohistochemistry, sensory studies and two-electrode-voltage clamp measurements have been described previously (21).

Results and Discussion

To elucidate whether ENaC is involved in human salt taste transduction, RT-PCR studies on human circumvallate and fungiform papillae were performed. Non-chemosensory lingual tissue was included as a control. We amplified fragments of the predicted size for α -, β -, and γ -ENaC subunits using non-chemosensory lingual tissue and taste papillae (Figure 1). An additional ENaC subunit, δ -ENaC, is expressed in humans; rodents do not possess a gene for δ -ENaC. This δ -subunit was also included in the PCR analyses. Like the other three ENaC subunits, δ -ENaC could be amplified using cDNA from non-chemosensory lingual tissue and taste papillae (Figure 1). However, in the case of circumvallate papillae, an additional PCR amplification was necessary for δ -ENaC in order to obtain visible bands after agarose gel electrophoresis suggesting low δ -ENaC mRNA levels in taste tissue.

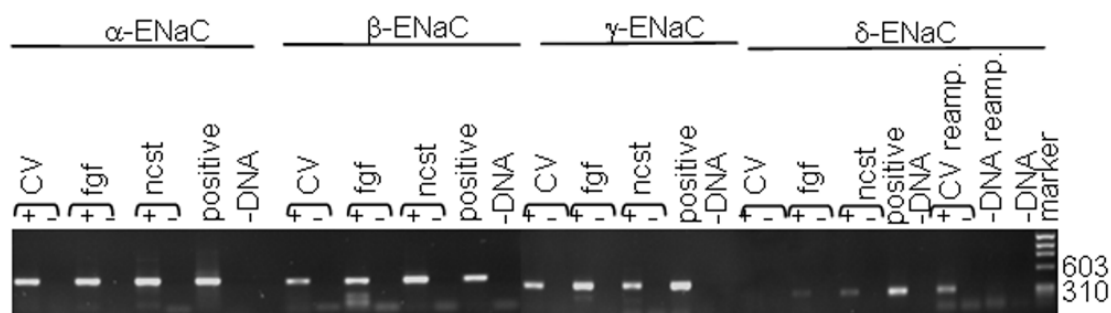


Figure 1. PCR amplification of ENaC fragments. Fragments have been amplified with gene-specific primers using RNA from human circumvallate papillae (CV), fungiform papillae (fgf) and non-chemosensory lingual tissue (ncst) previously transcribed into cDNA (+) or not (-) by reverse transcriptase. We used cDNA from lung as positive control for α -, β - and γ -ENaC mRNAs and from brain for δ -ENaC. The negative control (-DNA) contains all reagents except template DNA.

In order to measure the expression levels of ENaC subunits, quantitative RT-PCR studies were performed. The expression levels of all ENaC subunits were higher in non-chemosensory lingual tissues than in taste tissues (data not shown). In taste

tissues, the following rank order was found for the abundance of ENaC subunit mRNAs: $\alpha \sim \beta > \gamma \gg \delta$. These RT-PCR data demonstrated that all ENaC subunits are expressed in non-chemosensory lingual tissues and in taste tissues. However, these experiments did not reveal the cell types that express ENaC subunits. To clarify which cells express ENaC subunits, we performed localization studies with specific antisera and human circumvallate and fungiform papillae. We determined that all four ENaC subunits are present in taste bud cells of circumvallate papillae (Figure 2). Whereas α - and γ -subunits were readily detected at the basolateral part of taste bud cells, β -ENaC-like immunoreactivity was weak and only present in few cells. Delta-ENaC was exclusively found in all pore regions examined. All ENaC antisera stained also epithelial cells surrounding the taste buds (Figure 2 arrows). No staining was observed in the control experiments in which we omitted the primary antibody or pre-absorbed the primary antibody with its respective blocking peptide (data not shown).

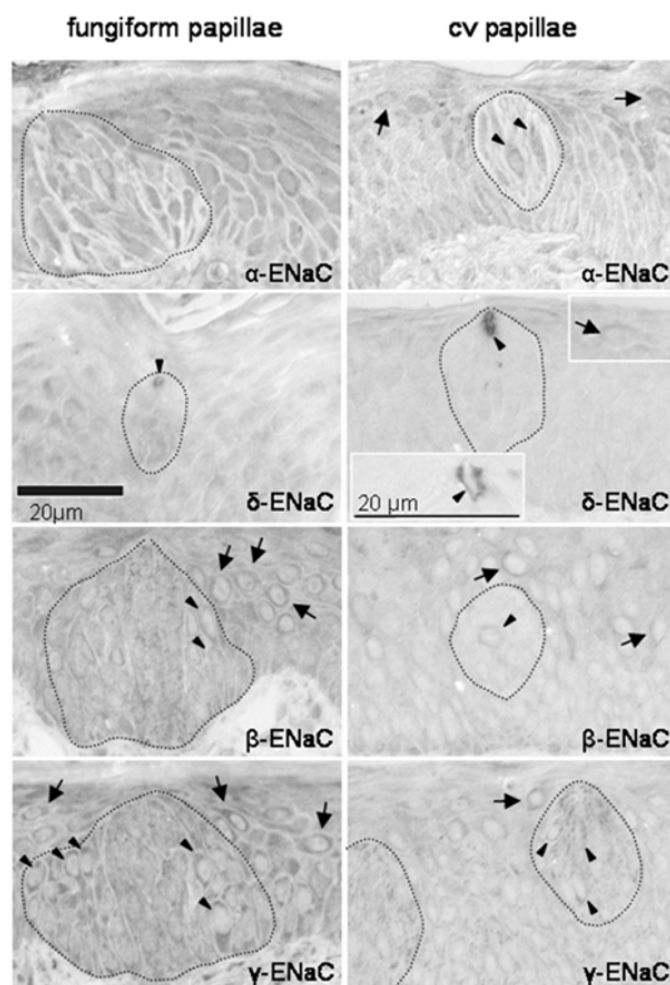


Figure 2. Indirect immunohistochemistry for α -, β -, γ - or δ -ENaC subunits. The polypeptides were detected with specific primary antisera and peroxidase-conjugated secondary antibodies on 2- μ m sections of paraffin-embedded human circumvallate and fungiform papillae. The inset in the upper right corner of the panel showing localization of δ -ENaC in circumvallate papillae depicts a stained keratinocyte of the non-chemosensory tissue. The inset on the lower left corner presents a taste pore stained for δ -ENaC immunoreactivity at higher magnification. Arrowheads indicate labeled taste bud cells; arrows indicate labeled cells outside taste buds.

For human fungiform papillae, β - and γ -ENaC immune-like reactivity was observed in the basolateral aspect of taste bud cells. The anti- α -ENaC antiserum did not specifically label any cells at all. Interestingly, the δ -ENaC antiserum stained all visible taste pores. Taken together, all ENaC subunit are located in taste bud cells and could form functional channels participating in taste transduction. A possible role in taste transduction is particularly probable for the δ -subunit based on its exclusive location in pore regions, *i.e.*, the sites where tastants can interact with their receptor molecules. Our data also suggest that the subunit compositions of ENaC may vary among the type of papillae.

To further investigate ENaC's role in human taste transduction, we employed a combination of human sensory studies with heterologous expression experiments in oocytes. If ENaC is crucial for salt transduction in humans, we predict that compounds which enhance the saltiness of solutions containing Na^+ ions in human subjects also enhance sodium membrane-currents in frog oocytes expressing recombinant human ENaC. A salt taste stimulating activity has recently been reported for L-arginine (22). Therefore, we tested this amino acid and, as control, L-glutamine in both experimental settings. Firstly, iso-intensity measurements were carried out with test solutions containing 30 mM NaCl and the respective amino acid at concentrations of 10 or 40 mM. Trained panellists compared the saltiness of the test solutions to a row of solutions with increasing Na^+ concentrations. They reported that the saltiness of the test solutions containing L-arginine were similar to the saltiness of solutions containing 43 or 48 mM Na^+ (Figure 3A). Presence of L-glutamine in the test solution was without effect (Figure 3A).

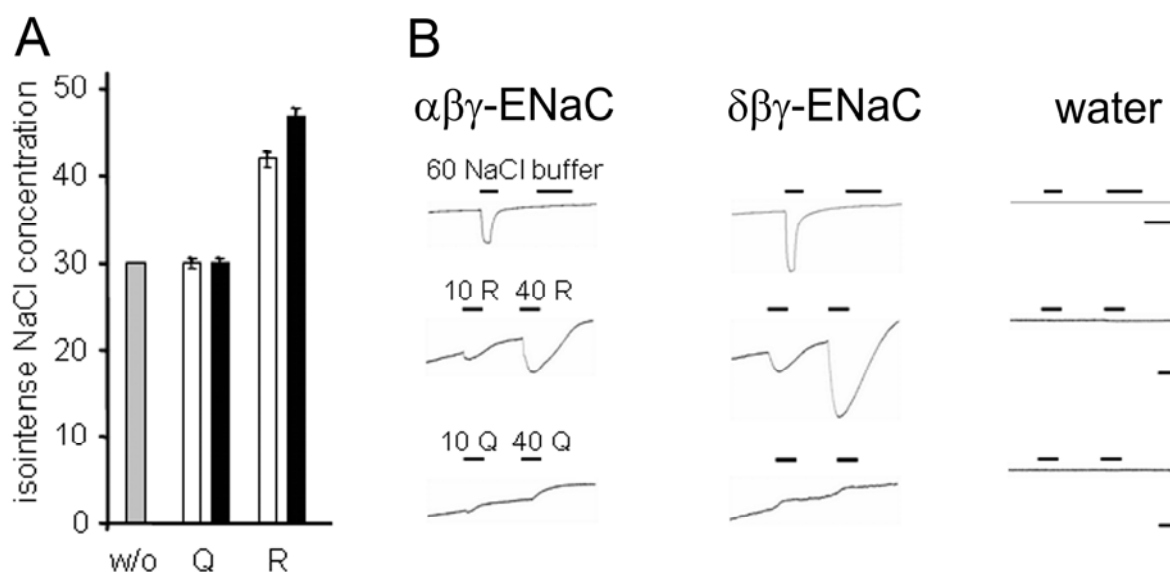


Figure 3. Enhancement of saltiness and ENaC-mediated membrane sodium currents by L-arginine. **(A)** To measure increases in saltiness by L-arginine, test solutions were compared to reference solutions with increasing concentrations of NaCl. The test solutions contained 30 mM NaCl (grey) and 30 mM NaCl plus 10 mM (white) or plus 40 mM (black) L-arginine (R) or L-glutamine (Q). **(B)** Two-electrode voltage clamp recordings were performed in a perfusion solution containing 30 mM NaCl in oocytes previously microinjected with cRNA for $\alpha\beta\gamma$ -ENaC or $\delta\beta\gamma$ -ENaC. Horizontal bars indicate the application scheme of the test compounds in mM. Scale bars: horizontal 1 min, vertical, 0.5 μA .

Secondly, we injected *Xenopus laevis* oocytes with cRNAs for α -, β -, and γ -ENaC subunits or δ -, β -, and γ -ENaC subunits. As a control we also injected oocytes with H₂O. Two days later the membrane current responses of ENaC-injected oocytes to application of test compounds were recorded in the presence of 30 mM Na⁺ by two-electrode voltage-clamp measurements. Increasing the Na⁺ concentration from 30 to 60 mM enhanced the inward membrane current in ENaC expressing oocytes, whereas no current changes was observed for H₂O-injected oocytes. In line with published data, these results suggest that both $\alpha\beta\gamma$ - and $\delta\beta\gamma$ -ENaC are functional in this system (Figure 3B) (23). Administration of L-arginine to $\alpha\beta\gamma$ - or $\delta\beta\gamma$ -ENaC-expressing oocytes increased the sodium membrane inward currents in a concentration dependent manner (Figure 3B). These current changes were sensitive to amiloride (data not shown). No current changes were observed after L-glutamine application in $\alpha\beta\gamma$ - or $\delta\beta\gamma$ -ENaC-expressing oocytes. Mock-injected oocytes did not respond to either stimulus (Figure 3B). Thus, the data obtained with the recombinant ENaC in oocytes correspond well with those from the sensory studies. This correspondence argues for a role of ENaC in human salt taste perception. In conclusion, ENaC appears to be an interesting molecule possibly involved in taste, yet its precise role still needs to be determined.

References

1. Denton D. (1982) *Springer-Verlag*, Berlin-Heidelberg-New York.
2. McCaughey S. A., Scott T.R. (1998) *Neurosci. Biobehav Rev.* 22:663-676.
3. Schiffman S.S., Lockhead, E., Maes F.W. (1983) *Proc. Natl Acad. Sci. USA* 80:6136-6140.
4. Avenet P., Lindemann B. (1988) *J. Membr. Biol.* 105:245-255.
5. Tennissen A. M. (1992) *Physiol. Behav.* 51:1061-1068.
6. Smith D.V., Ossebaard C.A. (1995) *Physiol. Behav.* 57:773-777.
7. Halpern B.P., Darlington R.B. (1998) *Chem. Senses* 23:501-511.
8. Doolin R.E., Gilbertson T.A. (1996) *J. Gen. Physiol.* 107:545-554.
9. Gilbertson T.A., Fontenot D.T. (1998) *Chem. Senses* 23:495-499.
10. Formaker B.K, Hill D.L. (1991) *Physiol. Behav.* 50:765-976.
11. Kitada Y., Mitoh Y., Hill D.L. (1998) *Physiol. Behav.* 63:945-949.
12. Ninomiya Y. (1998) *Proc. Natl. Acad. Sci. USA* 95:5347-50.
13. Brand J.G, Teeter. J.H., Silver W.L. (1985) *Brain Res.* 334:207-214.
14. Sollars S.I., Bernstein I.L. (1994) *Behav. Neurosci.* 108:981-987.
15. Gilbertson T.A., Kinnamon S.C. (1996) *Chem. Biol.* 3:233-237.
16. Lindemann B. (1996) *Taste reception. Physiol. Rev.* 76:718-766.
17. Boughter J.D. Jr., Gilbertson T.A. (1999) *Neuron.* 22:213-215.
18. Kretz O., Barbry P., Bock R., Lindemann B. (1999) *J Histochem Cytochem* 47:51-64.
19. Lin W., Finger T.E., Rossier B.C., Kinnamon S.C. (1999) *J Comp Neurol* 405:406-420.
20. Shigemura N., Islam A.A., Sadamitsu C., Yoshida R., Yasumatsu K., Ninomiya Y. (2005) *Chem Senses* 30:531-538.
21. Stähler R.K., Demgensky S, Neumann K, Dunkel A, Täubert A, Raab B, Behrens M, Raguse J.D, Hofmann T., Meyerhof W. (2008) *Chem. Percept.* 1:78-90.
22. Ogawa T., Nakamura T., Tsuji E., Miyanaga Y., Nakagawa H., Hirabayashi H., Uchida T. (2004) *Chem Pharm Bull (Tokyo)* 52:172-177.
23. Waldmann R., Champigny G., Bassilana F., Voilley N., Lazdunski M. (1995) *J Biol Chem* 270: 27411-27414.

3D-QUANTITATIVE STRUCTURE-ACTIVITY RELATIONSHIPS STUDY OF LIGANDS FOR TWO HUMAN OLFACTORY RECEPTORS

A. TROMELIN^{1,2,3}, G. Sanz^{4,5}, L. Briand^{1,2,3}, J.C. Pernellet^{4,5} and E. Guichard^{1,2,3}

¹ INRA, UMR 1129 FLAVIC, F-21000 Dijon, France

² ENESAD, UMR 1129 FLAVIC, F-21000 Dijon, France

³ Université de Bourgogne, UMR 1129 FLAVIC, F-21000 Dijon, France

⁴ INRA, UMR 1197 NOPA, F-78352 Jouy-en-Josas, France

⁵ Université Paris XI, UMR 1197 NOPA, F-78352 Jouy-en-Josas, France

Abstract

The perception of thousands of odours by about 380 human olfactory receptors (ORs) results from a combinatorial coding, in which one OR recognizes multiple odorants and odorants are recognised by different combinations of ORs. We used data of 95 odorant molecules tested on two human ORs, OR1G1 (class II) and OR52D1 (class I), to perform a 3D molecular modelling study of ligands using Catalyst/HypoGen software. The sorting-out procedure previously used for OR1G1 ligands was transposed to OR52D1 ligands. The 3D-QSAR models obtained for OR1G1 and OR52D1 ligands essentially differ by distance between their features. This result suggests a path to decipher the odotopes of OR1G1 and OR52D1 agonists in order to investigate the role of ORs in olfactory coding.

Introduction

Mammals are able to detect and discriminate myriads of structurally diverse odorants through their interaction with hundreds of olfactory receptors (ORs) (1). It is commonly accepted that the perception of thousands of odours by about 380 human ORs results from a combinatorial coding, in which one OR recognises multiple odorants and different odorants are recognized by different combinations of ORs (2-5). Until now, only a few human ORs have been essayed for several individually tested odorants (6, 7). In a previous study (8), the functional characterisation on two human ORs, named OR1G1 (class II) and OR52D1 (class I) have been performed using 95 odorant molecules.

We used these functional data (8) to perform a molecular modelling study of ligands using Catalyst/HypoGen software (Accelrys Inc.). Catalyst/HypoGen takes into account molecular flexibility by considering each compound as a collection of conformers. It generates models, named 'hypotheses', which describe ligands as sets of chemical functions. These models should be able to predict the activities of different compounds having the same receptor binding behaviour. In a previous study we obtained an alignment model of OR1G1 ligands, which satisfactorily explained the experimental activities, and permitted to predict novel agonists for OR1G1 (9, 10). These agonists have been validated experimentally. In the present work, we applied the same approach to activity data of OR52D1 ligands and compared the best significant hypothesis models obtained for both OR1G1 and OR52D1 ligands. Our goal was to decipher the odotopes of OR1G1 and OR52D1 agonists in order to investigate the role of ORs in olfactory coding.

Experimental

Biological assays. Odorants were purchased from Sigma-Aldrich, Fluka or Acros Organics (Noisy-le-Grand, France) and prepared in 100% MeOH (Spectroscopic grade, Sigma). HEK293 cells (Human Embryo Kidney cells) were stably transfected with the $G_{\alpha 16}$ protein and the human ORs (OR1G1 or OR52D1). HEK293 derivative cells were seeded onto a poly-L-lysine-coated 96-well plate. Twenty-four hours later, cells were loaded with the Ca^{2+} -sensitive dye Fluo-4 (Molecular Probes). Calcium imaging was carried out as previously described, stimulating cells with different OR agonists applied as vapour phase (8). Data were expressed as number of responding cells (8).

Compounds and physicochemical data. We used activity data previously reported for the interaction of 95 compounds with OR1G1 or OR52D1 (8).

Computational methods. The 95 compounds were built with Catalyst/HypoGen software (Catalyst version 4.11, Accelrys Inc., San Diego, 2004, running on a Pentium IV computer with the Linux Red Hat Enterprise 2.1 OS). The conformers of each compound were generated using Catalyst/COMPARE module (11). HypoGen module (12) was used to perform automated hypothesis generation. HypoGen automatically generated the simplest hypotheses that best correlate estimated and experimental affinities. The statistical relevance of the various hypotheses was therefore assessed on the basis of their cost relative to the null hypothesis and the fixed hypothesis (the total costs should be as close as possible to the fixed cost) (13). According to Catalyst calculation, we used percent of non-responding cells normalised to responding cells as activity values.

Results and Discussion

Concerning OR1G1 ligands, we use the 35-ligands set previously identified to perform a hypothesis generation run, and we obtained a model similar to thus obtained with Catalyst running on SG-O2 workstation (10). Two hydrophobic features and one hydrogen bond acceptor constitute the best significant hypothesis (correl= 0.93, total cost= 165, fixed cost= 67, null cost= 727). This model was validated by randomisation at 99% confidence level.

The first hypothesis generation performed on the entire set using OR52D1 activity data did not lead to a significant model and we performed an iterative procedure as used in our previous study of OR1G1 ligands. In this way, the subset finally obtained contains 16 compounds and the best significant hypothesis is formed by one hydrophobic, one hydrophobic aliphatic and two hydrogen bond features (correl= 0.99, total cost= 53, fixed cost= 51, null cost= 195). The model was validated by randomisation at 95% confidence level. Interestingly, it was impossible to obtain a hypothesis generation result using a spacing value higher than 200 pm. Distances between features are reported in (Figure 1).

The models obtained for OR1G1 and OR52D1 ligands essentially differ by distance between their features. Indeed, the features of OR1G1 ligand model are located according a triangle (larger angle= 104.5 deg), and distance between features are at least around 5 Å. Conversely, OR52D1 ligand model features are quasi-linearly situated, (large angle= 149.6 deg) and the distance between the two hydrophobic features is lower than 3 Å.

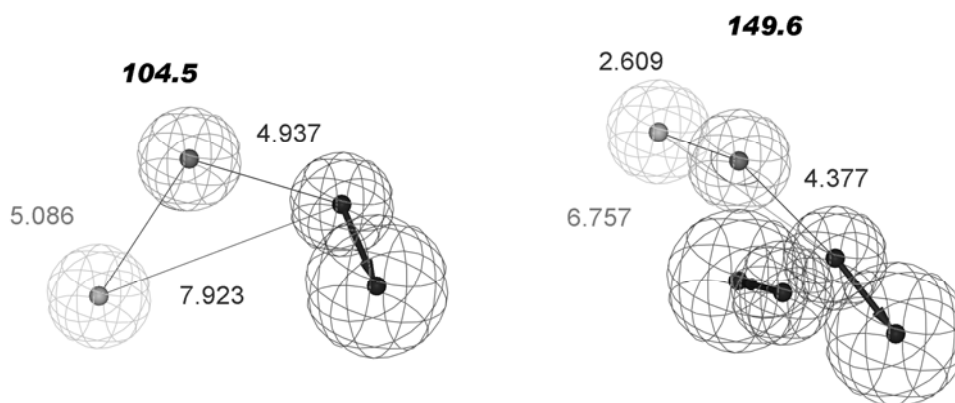


Figure 1. Hypothesis models for OR1G1 (left) and OR52D1 (right). In light grey and medium grey: hydrophobic and hydrophobic aliphatic features of ligands, corresponding to hydrophobic sites on the receptor. In dark grey: Hydrogen Bond Acceptor features of ligands, constituted by a small sphere corresponding to the centre of hydrogen bond acceptor, and a large sphere that is the projection sphere corresponding to a Hydrogen Bond Donor on the receptor site. Distance values are in Å, angle values (bold character) in degree.

Comparison of 36cmpds-OR1G1 and 17cmpds-OR52D1 subsets shows that 12 compounds are common to the two groups. The distribution of their activity values are reported in (Figure 2).

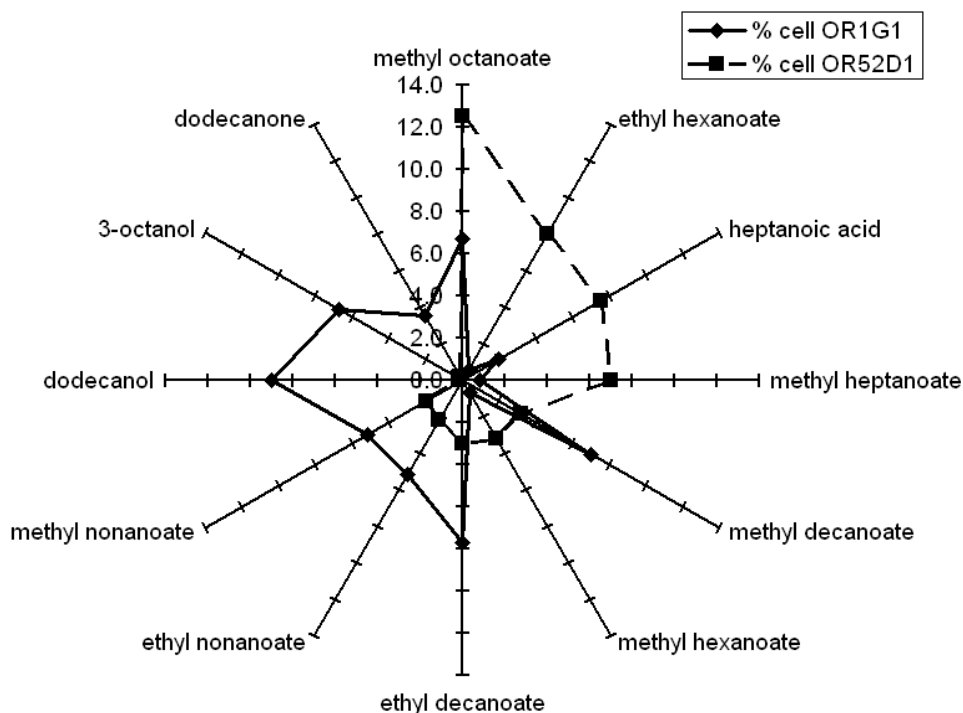


Figure 2. Activity values of ligands belonging to both OR1G1 and OR52D1 models. The activity values are reported as percent of responding cells.

The compounds used for model generation, belonging to both OR1G1 and OR52D1 training sets, exhibit different activity on OR1G1 and OR52D1. We focused on methyl octanoate that is the most active compound for 17cmpds-OR52D1 set and has a medium activity on OR1G1. Conformational spaces adopted by methyl

octanoate according mapping on OR1G1 and OR52D1 hypothesis models are presented in (Figure 3). The methyl octanoate appears to be in a more extended conformation on OR52D1 model than on OR1G1 model.

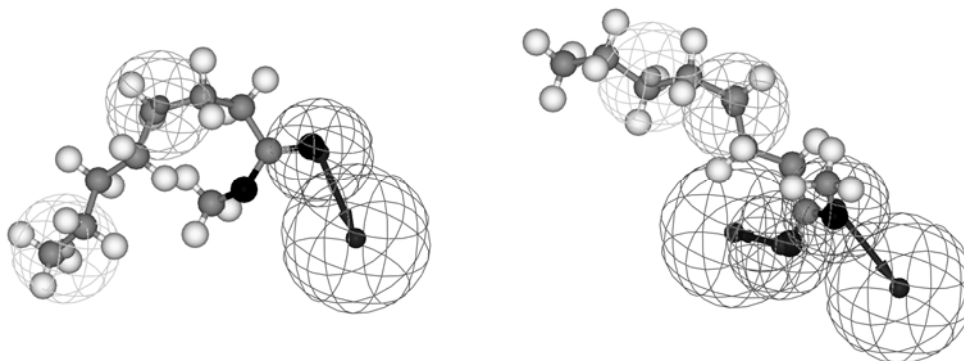


Figure 3. Methyl octanoate mapped on OR1G1 hypothesis model (left) and OR52D1 hypothesis model (right). Carbon atoms are in light grey, hydrogen in white, oxygen in black.

This approach allowed showing how the same molecule could adopt different conformations according to the bonded OR, and this behaviour may be linked to different component of their odour quality. This result suggests a path to decipher the odotopes of OR1G1 and OR52D1 agonists in order to investigate the role of ORs in olfactory coding.

Acknowledgments

This work was supported by INRA-04-PRA-001-SIFOOD and ANR-05-PNRA-002 AROMALIM.

References

1. Buck L., Axel R. (1991) *Cell* 65: 175-187.
2. Duchamp-Viret P., Chapu, M.A., Duchamp A. (1999) *Science* 284: 2171-2174.
3. Malnic B., Hirono J., Sato T., Buck L.B. (1999) *Cell* 96: 713-723.
4. Niimura Y., Nei M. (2007) *PLoS ONE* 2:e708.
5. Araneda R.C., Kini A.D., Firestein S. (2000) *Nat. Neurosci.* 3: 1248-1255.
6. Shirokova E., Schmiedeberg K., Bedner P., Niessen H., Willecke K., Raguse J.D., Meyerhof W., Krautwurst D. (2005) *J. Biol. Chem.* 280: 11807-11815.
7. Jacquier V., Pick H., Vogel H. (2006) *J. Neurochem.* 97: 537-544.
8. Sanz G., Schlegel C., Pernollet J.C., Briand L. (2005) *Chem. Senses* 30: 69-80.
9. Tromelin A., Sanz G., Briand L., Pernollet J.C., Guichard E. (2006) *11th Weurman Flavour Research Symposium, Comwell Roskilde, Denmark*
10. Sanz G., Thomas-Danguin T., Hamdani E.H., Briand L., Pernollet J.C., Guichard, E., Tromelin A. (2008) *Chem. Senses* 33: 639-653.
11. Smellie A., Teig S.L., Tobwin P. (1995) *J. Comput. Chem.* 16: 171-187.
12. Li H., Sutter J., Hoffman R. (2000) In *Pharmacophore perception, Development and Use in Drug Design* (Güner, O.F., ed.); *IUL Biotechnology Ser.*, pp 171-189.
13. Kurogi Y., Guner O.F. (2001) *Curr. Med. Chem.* 8: 1035-1055.

MODELLING THE DYNAMICS OF ODOUR TRANSPORT IN THE OLFACTORY EPITHELIUM

A.J. TAYLOR¹, F. Wulfert¹, O.E. Jensen², A. Borysik¹, and D.J. Scott¹

¹ School of Biosciences, University of Nottingham, Sutton Bonington Campus, LE12 5RD, UK;

² School of Mathematical Sciences, University of Nottingham, University Park, Nottingham NG7 2RD, UK

Abstract

The role of Odour Binding Protein (OBP) in the mammalian olfaction process is not entirely clear. The binding behaviour of odorants with OBP has been studied, mainly over long time periods and under equilibrium conditions. However, little is known about the dynamics of odour transport from the nasal gas phase to the odour receptors (and vice versa). Direct measurement is technically difficult due to the micro scale of the liquid mucus phase and the small amounts of volatiles involved. Using data from the literature, the physico-chemical mechanisms, length scales and timing of odour mass transfer can be inferred and a theoretical mass transfer model of the process built. Hypotheses can then be tested with the model to determine mass transfer behaviour in the system and, from the results, the contribution of the different factors that drive odour uptake from the gas phase to the receptor, can be assessed.

Introduction

OBPs are found in the olfactory mucus layer of many species [1]. The proteins bind a wide range of hydrophobic odour compounds and the mechanism of binding has been studied using techniques like X-ray crystallography data [2] and molecular dynamics [3]. The exact role of OBP in transferring odour from the gas phase to the receptors is the subject of some debate and both passive and active modes have been proposed [3]. The passive mode assumes OBP simply acts as an agent to help hydrophobic aroma molecules solubilise in the mucus phase and access the Olfactory Receptors (ORs). In the active mode, it is hypothesised that OBP binds with an odour ligand and then the complex interacts with the OR. Recently, we proposed a mechanism where OBP serves to maintain the odour signal to the ORs which has the potential benefit of amplifying the signal as well as prolonging its duration [4]. The proposed scheme is shown in (Figure 1).

Experiments to test this hypothesis are difficult to formulate. Most experiments to study OBP-odour binding are based on liquid *in-vitro* systems and are often carried out over long time periods using equilibrium or displacement techniques to obtain information on fundamental biophysical processes like dissociation constants (K_d). Dynamic measurements in our laboratory have provided data on the dynamic competition between odorants, the extent of binding and the time to load and unload OBP, although the length scales were much greater (several hundred μm) than those found *in-vivo* [4]. Direct measurement of odour transport in a system that recreates the length- and time-scales found in the olfactory epithelium is difficult. Mass transfer in the olfactory epithelium occurs across very thin films (several μm thick) and over

very short (about 5 second) time scales. These factors create sensitivity and speed issues for most analytical techniques and there is no readily available approach which might provide useful data for odour molecules. Instead, a simple mathematical model was developed to determine the effect of the different rate constants on the mass transfer of odorants (Figure 1). Existing mass transfer models for odorants in the nose [5, 6] do not include an OBP factor and, thus, a model, relating only to the scheme shown in Figure 1, was developed.

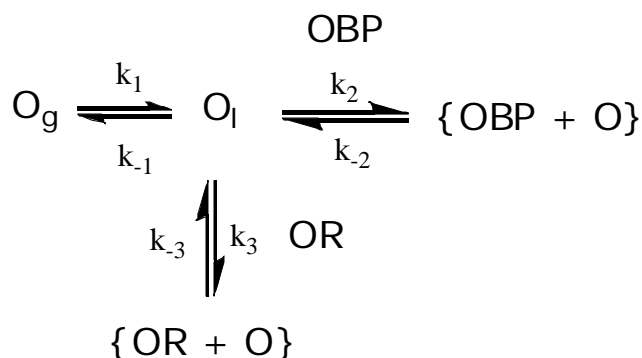


Figure 1. Scheme showing the transport of odours from the gas phase (O_g) into the liquid phase (O_l) with binding to OR or OBP. The on and off rate constants are denoted by k and $-k$ respectively.

Experimental

Standard mass transfer equations were used to build a model based on well-established interfacial mass transfer principles [7]. The model was hosted in Matlab and accessed through a user interface to allow values to be input. The key principles were: gas-liquid mass transfer across the interface is driven by partition; mass transfer in the liquid layer is entirely through diffusion, binding to OBP follows the known patterns from *in-vitro* systems, binding to OR is assumed to follow general ligand binding (and release) behaviour. The system was set up so that the rate constants could be input as dimensionless numbers to study the relative influence of each factor.

Results

Effect of air-water partition (K_{gl}) on mass transfer. To test the model, the input values (the k values in Figure 1) were all set to zero except for k_1 and $-k_1$ which were set to give ratios typical of K_{gl} values for odours (10^{-2} to 10^{-5}) and the odour input was set to sinusoidal to mimic the breathing cycle in humans. Figure 2 shows the effect of K_{gl} where values around 10^{-1} produce fluctuations of odour concentration in the liquid layer which are offset from the input sinusoidal gas patterns due to the time taken for mass transfer. As K_{gl} changes towards 10^{-4} , the mass transfer is driven more towards the liquid phase and the odour is rapidly and almost completely removed from the gas phase. The gas phase trace is the lower one in each box and changes from a clear “up and down” sinusoidal trace ($K_{gl} 10^{-1}$) to a flat line trace ($K_{gl} 10^{-4}$). Thus partition coefficient is one of the potential factors determining the rate and extent of odour mass transfer as typical values lie between 10^{-2} and 10^{-5} .

Expression of Multidisciplinary Flavour Science

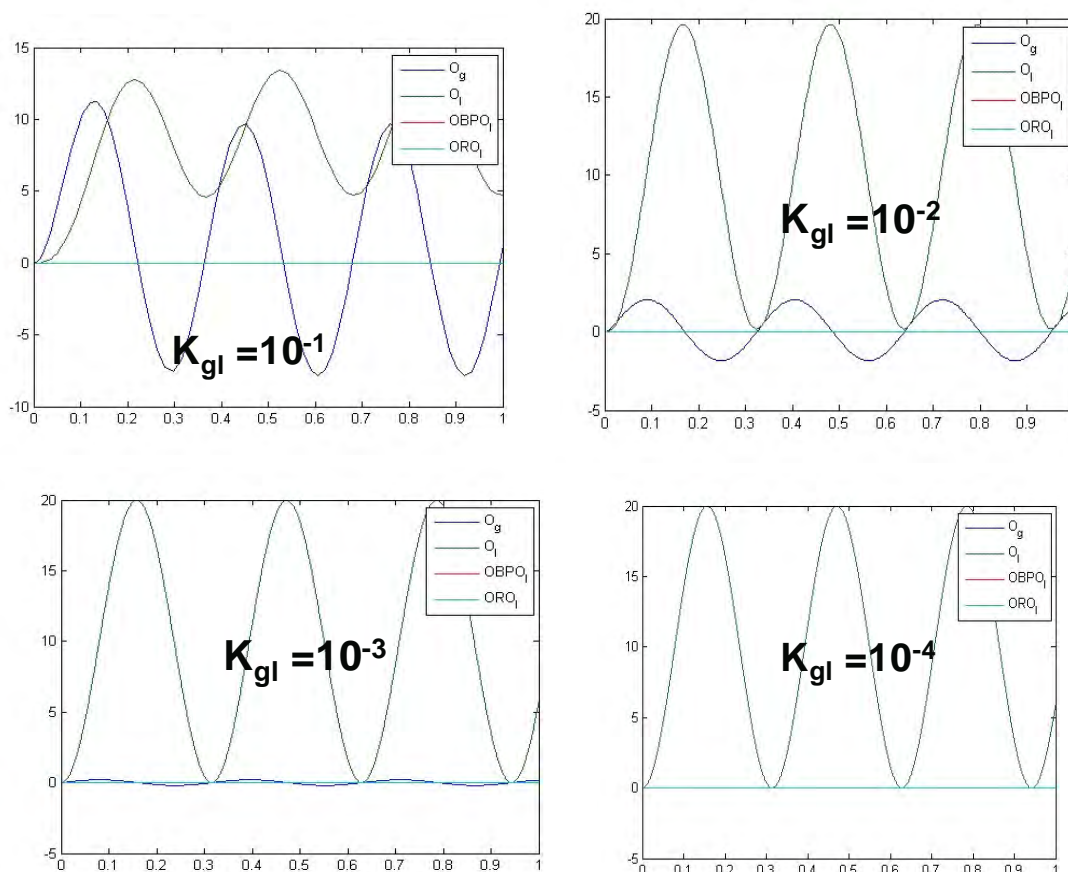


Figure 2. Odour concentrations in the gas and liquid phases as a function of K_{gl} values. X axis; time, Y axis; concentration, both in arbitrary units.

Factors favouring prolongation of the odour signal in the liquid phase. The model was then used to determine which of the various rate constants were key in prolonging the concentration of an odour ($K_{gl} 10^{-4}$) to the ORs. A range of values were input into the model to produce the sort of trace shown in Figure 3, where the change in concentration of OBP complexes and the gas and liquid distribution of odour can be plotted as a function of time. In this case, the values of the rate constants were modified to optimise the concentration of the {OR+O} form as the hypothesis in Figure 1 suggests this is the form which will produce the greatest odour signal. This concept is based on the results of experiments which describe that, prolonging the stimulus to a receptor can amplify the signal output, as well as increasing the signal duration [8, 9]. For example, Firestein [8], demonstrated in salamander, that increasing the duration of an odour stimulus from 0.5 s to 1.2 s not only increased the duration of the output signal from the olfactory system but also increased the signal intensity by a factor of 5. From the mass transfer model, the key factor in prolonging the signal to the ORs was found to be the off rate of odours from OBP (k_{-2}) and the task now is to measure the on and off rates of odours onto OBP experimentally to determine whether the values are related to those found in the theoretical modelling studies. If the model outputs are useful and related to the olfactory events, then a revised version of the model is planned where the values can be input as real concentrations of odours and OBP along with their associated diffusion coefficients, and can be adjusted for temperature and the presence of mucus, to give a more sophisticated model. Data can then be compared with observed data from the literature to determine whether the model is robust.

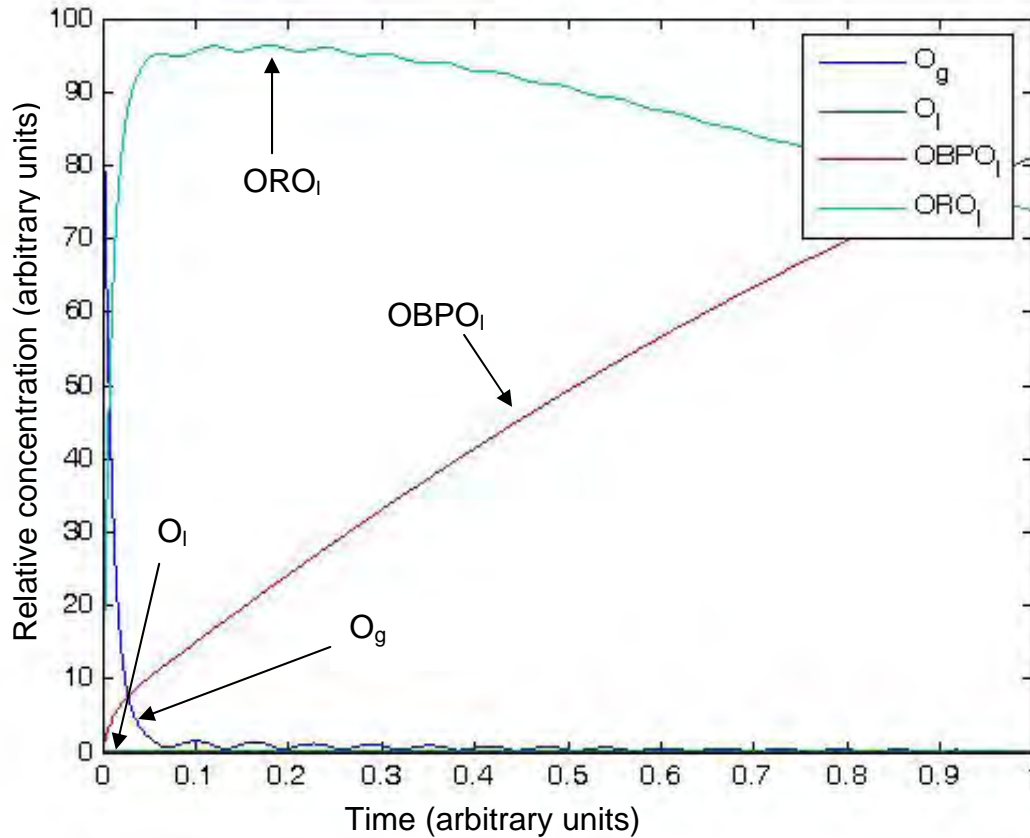


Figure 3. Optimisation of input values to prolong stimulation of the ORs by maximising the ORO_l complex levels over time.

References

1. Hildebrand J.G., Shepherd G.M. (1997) *Ann. Rev. Neurosci.* 20: 595-631.
2. Golebiowski J., Antonczak S., Fiorucci S., Cabrol-Bass D. (2007) *Proteins-Structure Function and Bioinformatics* 67: 448-458.
3. Hajjar E., Perahia D., Debat H., Nespoulous C., Robert C.H. (2006) *J. Biol. Chem.* 281: 29929-29937.
4. Taylor A.J., Cook D.J., Scott D.J. (2008) *Chemosens. Percep.* 1: 153-162.
5. Hahn I., Scherer P.W., Mozell M.M. (1994) *J. Theoret. Biol.* 167: 115-128.
6. Keyhani K., Scherer P.W., Mozell M.M. (1997) *J. Theoret. Biol.* 186: 279-301.
7. Scherer P.W., Keyhani K., Mozell M.M. (1994) *Inhal. Toxicol.* 6: 85-97.
8. Firestein S., Picco C., Menini A. (1993) *J. Physiol. (London)* 468: 1-10.
9. Hummel T., Kobal G. (2002) In *Methods in Chemosensory Research*, Simon, S.A., Nicolelis, M.A.L., Editors., CRC Press: Boca Raton.

FLAVOUR, HEALTH AND WELLBEING: BALANCE BETWEEN APPETITE AND HEALTHY DIET

W. LANGHANS

Physiology and Behaviour Group, Dept. of Agricultural and Food Sciences, ETH Zurich, Schorenstrasse 16, 8603 Schwerzenbach, Switzerland

Abstract

Flavour determines the hedonic value of food, which is positively related to the amount eaten. The almost constant and ubiquitous availability of good-tasting food in our affluent societies may therefore promote overeating and contribute to the development of obesity with all its health risks. But flavour stimuli are also beneficial for health. They trigger the release of digestive enzymes and gastrointestinal (GI) peptides through activating cephalic reflexes and by acting on taste receptors on enteroendocrine cells. GI peptides are essential for postingestive nutrient handling because they control gastrointestinal function and metabolism. GI peptides also affect food intake, and some are promising therapeutic substances for the treatment of type-2-diabetes. Moreover, flavour stimuli can modulate the immune system. The balance between these positive and negative effects of flavour stimuli determines the effects of flavour on health and well-being.

Introduction

Obesity increases the risk of cardiovascular disease, type-2-diabetes, non alcoholic fatty liver disease, some cancers, and many other chronic diseases. Superficially, the causes of obesity are simple – we eat too much and exercise too little; but why do we eat too much? The answer to this question is not that simple. Clearly, we eat (1) for pleasure, which often provides the strongest motivation to eat, and (2) because of homeostatic needs, which are physiologically important, but often secondary in our current environment. Also, external cues can trigger eating through conditioned reflexes, and, not surprisingly, learning plays a major role, *i.e.* we eat what we like based on previous experience. Flavour stimuli form the basis for this associative learning by providing the stimuli for food discrimination and hedonic experience [1]. As a result, flavour stimuli can cause overeating and may thus contribute to the development of obesity. But flavour stimuli also have effects that are beneficial for health. They help us learn to avoid what could make us sick, and they trigger the release of digestive enzymes and gastrointestinal (GI) peptides by activating cephalic reflexes or by direct action on enteroendocrine cells (EEC). These secretions are necessary for the adequate handling of ingested nutrients. Finally, flavour stimuli have an immune-modulating effect. Below I will briefly describe these seemingly opposite effects of flavour stimuli on health.

Flavour preference and avoidance learning

Flavour determines palatability, *i.e.* the hedonic value of food, and palatability influences how much we eat in the short- and in the long-term [2]. Palatability drives eating especially early in a meal, but it decreases with eating and is gradually

counteracted by negative feedback arising from the presence of food in the GI tract. As a result, meal size increases when palatability is high [3, 4]. As the prandial decrease in palatability contributes to meal termination and is specific for the sensory properties of the food eaten, it is called sensory-specific satiety [SSS] [5]. Because of this specificity, other available food may still be consumed. Thus, flavour variety in a meal also increases the amount eaten, that is why we can still eat dessert after an opulent meal. Also, flavour variety in a diet chronically increases food intake and body weight [6], suggesting that the constant and ubiquitous availability of different, good-tasting foods in our affluent societies promotes overeating and weight gain, thus contributing to the obesity epidemic with its deleterious consequences for health. SSS can also be shown at the neurophysiological level: Single unit recordings from orbitofrontal cortex (OFC) neurons revealed that feeding monkeys a glucose solution to satiety reduced the response of particular OFC neurons to ingested glucose, whereas these same neurons' response to blackcurrant juice remained unchanged [7].

Flavour stimuli are essential for food discrimination and food selection. Interestingly, only the initial preference for sweet and the avoidance of bitter and to some extent sour taste are innate, whereas all other responses to flavours are learned [1]. Even the innate preference and avoidance reactions can be modulated by powerful learning mechanisms. Some of this learning is psychologically based, such as the “mere exposure effect”, *i.e.* the increase in preference observed with repeated, unreinforced exposure to a particular food [1]. More efficient, physiologically based, preference learning is related to the positive consequences of food ingestion [1]. For instance, the energy content of food has a powerful reinforcing effect in animals and humans [1, 8]. Context-related factors such as social settings, ideas of appropriateness etc., which are associated with a flavour, can also increase the preference for a particular food [9]. On the other hand, animals and humans quickly learn to avoid foods that have been associated with disturbed well-being or illness. The acquisition of flavour aversions can occur after a single exposure, *i.e.* it is rapid, potent, long-lasting, and positively related to the salience and the novelty of the sensory stimulus [10]. Aversion learning is also modulated by external factors. The convergence of taste and smell pathways in parts of the basal ganglia including the amygdala, in cortical areas such as the caudate nucleus, the globus pallidus and the OFC, and in the hypothalamus form the neuroanatomical and neurophysiological basis for flavour-related learning. Activation of these brain areas in response to flavour stimuli, and even discrimination of pleasant and unpleasant stimuli, can be shown by functional magnetic resonance imaging [7]. Interestingly, palatability is processed in the same brain areas as other natural (*e.g.* sex) and unnatural (*e.g.* drugs of abuse) rewards, and several neurotransmitters such as dopamine, endogenous opioids, GABA, serotonin, and endocannabinoids are involved in central reward processing [11]. Finally, extensive, bidirectional interactions of reward and homeostatic systems are essential for an adequate control of eating [12, 13], and flavour perception is modulated by interoceptive signals derived from nutritional state, metabolism, and even body weight [14].

Flavour effects on GI peptide release

In addition to serving as stimuli for “unhealthy” and “healthy” associations as described above, flavour stimuli have effects on health and well-being that are related to their stimulatory effects on digestive enzyme and GI peptide release (Figure 1). Visual, olfactory and gustatory cues rapidly stimulate exocrine (digestive enzymes) and endocrine (gut peptide) secretory responses [15] through vagal

efferent signaling. These responses help the organism to better digest, absorb, and metabolize the ingested nutrients. Their health relevance is documented by the disturbances of digestion, absorption and metabolism that occur when food is directly administered into the GI tract [15].

Flavour stimuli can also act directly on EEC. Intestinal EEC are remarkably similar to taste cells in the oral cavity in that they express taste receptors and α -gustducin [16-18]. Also, some EEC express smell receptors [19] or the transient receptor potential ankyrin-1 (TRPA-1) channel [20] that is targeted by several spices [21]. Tastants, odourants, and spices can therefore stimulate the release of GI peptides or serotonin by direct activation of these EEC receptors. GI peptides affect food intake, GI function and metabolism, and some of them are promising therapeutic substances for the treatment of obesity or type 2 diabetes [22]. Serotonin is released from a special group of EEC [23, 24] that has recently been shown to express smell receptors [19]. Serotonin is involved in control of gut motility and secretion. By triggering the release of GI peptides and serotonin from EEC, flavour stimuli can have beneficial effects on health.

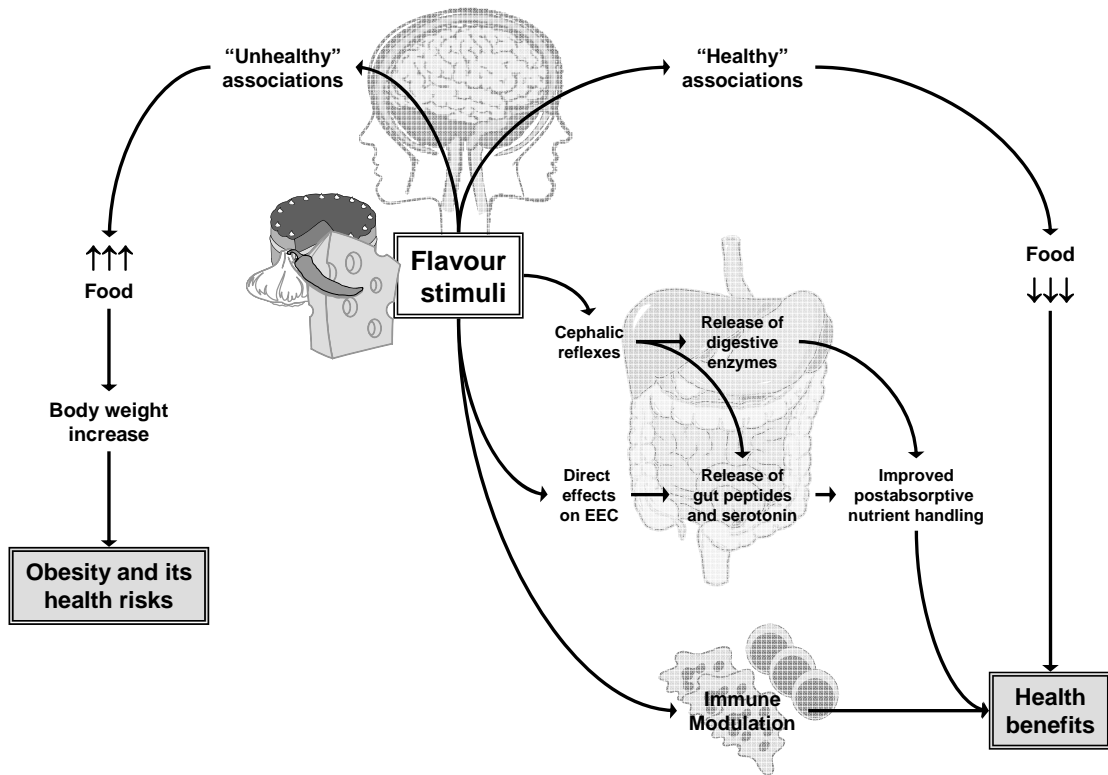


Figure 1: Potentially negative and positive effects of flavour stimuli on health. See text for further details.

Flavour effects on the immune system

Spices (usually the dried aromatic parts) and herbs (mostly from the leaves and stem) of plants [25] can alter various immune functions. Some immune-modulatory effects of herbs and spices are based on their antioxidant capacity; others are related to their effects on biotransformation enzyme activities [25], their function as nitric oxide and peroxynitrite scavengers [26, 27], or their antibacterial, antiviral, and anti-inflammatory effects [25, 28, 29]. Some evidence suggests that herbs and spices may also counteract the inflammatory reactions that accompany obesity and contribute substantially to the deterioration of insulin sensitivity with increasing body weight.

Synopsis

All in all, flavour stimulates appetite by increasing the hedonic value of the food we consume. In our modern world this may contribute to weight gain and obesity with all its health risks, because the mechanisms that control food intake are not designed to protect us from overeating [30]. On the other hand, flavour can modulate immune functions directly and help to initiate a plethora of GI peptide-related mechanisms of satiation and efficient post-absorptive nutrient handling. The balance between these different actions ultimately determines the effects of flavour on health and wellbeing.

References

1. Gibson E.L., Brunstrom J.M. (2007) In *Appetite and Body Weight: Integrative Systems and the Development of Anti-obesity Drugs* (Kirkham T.C., Cooper S.C., eds.), Academic Press, Elsevier: Amsterdam, pp 271-300.
2. Yeomans M.R. (2007) In *Appetite and Body Weight: Integrative Systems and the Development of Anti-obesity Drugs* (Kirkham, T.C., Cooper, S.C., eds.), Academic Press, Elsevier: Amsterdam, pp 247-269.
3. de Castro J.M., Bellisle F., Dalix A.M., Pearcey S.M. (2000) *Physiol. Behav.* 70: 343-350.
4. de Castro J.M., Bellisle F., Dalix A.M. (2000) *Physiol. Behav.* 68: 271-277.
5. Rolls B.J. (1986) *Nutr. Rev.* 44: 93-101.
6. Rolls B.J., van Duijvenvoorde P.M., Rowe E.A. (1983) *Physiol. Behav.* 31: 21-27.
7. Rolls E.T. (2006) *Phil. Trans. Royal Soc. B-Biol. Sci.* 361: 1123-1136.
8. Sclafani A. (1997) *Appetite* 29: 153-158.
9. Rozin P., Vollmecke, T.A. (1986) *Annu. Rev. Nutr.* 6: 433-456.
10. Garcia J., Lasiter P.S., Bermudez-Rattoni F., Deems D.A. (1985) *Ann. NY Acad. Sci.* 443: 8-21.
11. Berridge K.C. (2007) In *Appetite and Body Weight: Integrative Systems and the Development of Anti-obesity Drugs* (Kirkham T.C., Cooper S.C., eds.), Academic Press/Elsevier: Amsterdam, pp. 191-215.
12. Berthoud H.R., Morrison C. (2008) *Annu. Rev. Psychol.* 59: 55-92.
13. Kelley A.E., Baldo B.A., Pratt W.E., Will M.J. (2005) *Physiol. Behav.* 86: 773-795.
14. Figlewicz D.P., MacDonald N.A., Sipols A.J. (2007) *Physiol. Behav.* 91: 473-478.
15. Zafra M.A., Molina F., Puerto A. (2006) *Neurosci. Biobehav. Rev.* 30: 1032-1044.
16. Dyer J., Salmon K.S., Zibrik L., Shirazi-Beechey S.P. (2005) *Biochem. Soc. Trans.* 33: 302-305.
17. Hofer D., Puschel B., Drenckhahn D. (1996) *Proc. Natl. Acad. Sci. USA* 93: 6631-6634.
18. Wu S.V., Rozengurt N., Yang M., Young S.H., Sinnott-Smith J., Rozengurt E. (2002) *Proc. Natl. Acad. Sci. USA* 99: 2392-2397.
19. Braun T., Volland P., Kunz L., Prinz C., Gratzl M. (2007) *Gastroenterology* 132: 1890-1901.
20. Purhonen A.K., Louhivuori L.M., Kiehne K., Kerman K.E., Herzig K.H. (2008) *FEBS Lett.* 582: 229-232.
21. Dhaka A., Viswanath V., Patapoutian A. (2006) *Annu. Rev. Neurosci.* 29: 135-161.
22. Brubaker P.L. (2007) *Trends Endocrinol. Metab.* 18: 240-245.
23. Grube D. (1986) *Anat. Embryol. (Berl.)* 175: 151-162.
24. Schonhoff S.E., Giel-Moloney M., Leiter A.B. (2004) *Endocrinology* 145: 2639-2644.
25. Lampe J.W. (2003) *Am. J. Clin. Nutr.* 78: 579S-583S.
26. Ho S.C., Tsai T.H., Tsai P.J., Lin C.C. (2008) *Food Chem. Toxicol.* 46: 920-928.
27. Tsai P.J., Tsai T.H., Yu C.H., Ho S.C. (2007) *Food Chem. Toxicol.* 45: 440-447.
28. Jagetia G.C., Aggarwal B.B. (2007) *J. Clin. Immunol.* 27: 19-35.
29. Woo H.M., Kang J.H., Kawada T., Yoo H., Sung M.K., Yu R. (2007) *Life Sci.* 80: 926-931.
30. Speakman J.R. (2004) *J. Nutr.* 134(8, Suppl.): 2090S-2105S.

NOVEL APPROACHES TO INDUCE SATIATION VIA AROMA IN FOODS

R.M. RUIJSCHOP¹, A.E.M. Boelrijk², M.J.M. Burgering¹, C. de Graaf³, and M.S. Westerterp-Plantenga⁴

¹ NIZO food research, Kernhemseweg 2, PO Box 20, 6710 BA Ede, The Netherlands

² Danone Research Medical Nutrition, Bosrandweg 20, PO Box 7005, 6700 CA Wageningen, The Netherlands

³ Division of Human Nutrition, Department of Agrotechnology and Food Sciences, Wageningen University, Bomenweg 2, PO Box 8129, 6700 EV, Wageningen, The Netherlands

⁴ Department of Human Biology, Maastricht University, Universiteitssingel 50, PO Box 616, 6200 MD Maastricht, The Netherlands

Abstract

The food industry currently is looking for new food products that combine liking with limited food intake due to enhanced satiety signals. Sensory satiation is probably one of the most important factors in meal termination, and aromas play part in it. Using a computer-controlled stimulator based on air dilution olfactometry, aroma stimuli can be administered separately from other stimuli, such as different ingredients, textures and tastes. Hence, the relative importance of aroma stimuli apart from other stimuli on satiation mechanisms can be investigated. Our studies showed that satiation can be influenced making use of differences in retro-nasal aroma release profiles. Complexity of the aroma stimulus and ingredient-related aroma cues are other aspects of aroma, which might affect appetite regulation. In view of obesity, these are interesting concepts for the food industry, to develop products, which decrease food intake without compromising on palatability.

Introduction

During the consumption of a meal, aroma molecules reach the olfactory epithelium retro-nasally (perceived as arising from the mouth). The brain response, *i.e.* neural brain activation to a retro-nasally sensed food odour is signalling the perception of food and is hypothesized to be related to satiation (1), *i.e.* sensory-related satiation. Ultimately, retro-nasal aroma stimulation inhibits the process of eating, contributing to meal termination. There are indications that not all food types result in the same quality or quantity of retro-nasal aroma stimulation (2). Additionally, interpersonal differences in retro-nasal aroma stimulation are of importance as well (3). It is hypothesized that difference in the extent of retro-nasal aroma stimulation can be linked to interpersonal or food product differences in sensory satiation and food intake behaviour.

Experimental

Tailored olfactometer equipment has been developed, which is able to deliver specific well-defined aroma profiles to the subjects. The ability to administer aroma stimuli separately from other stimuli (such as different ingredients, textures and

tastes) enables investigating the relative importance of aroma stimuli for satiation. As already described by Visschers *et al.* (4), delivering food-related aroma stimuli via an olfactometer to subjects involves a variety of parameters and matching the aroma stimuli to such a level that can be genuinely related to food is a complex process. The approach used is based on the knowledge of measuring aroma release *in-vivo* in real time, using atmospheric pressure chemical ionization-mass spectrometry (APCI-MS) (5, 6). It has been demonstrated that indeed the aroma profile that is generated with the olfactometer closely resembles the concentration of volatiles in the nose space measured for an individual subject eating or drinking a specific product. This enables the design of complete aroma release profiles that mimic those obtained by *in-vivo* experiments during the consumption of foods (4).

Results

Using APci-MS, *in-vivo* real-time retro-nasal aroma release was determined for 30 subjects consuming 9 different food products, varying in physical structure (*i.e.* (semi)-liquid, and solid food products) (7). Absolute differences were observed in retro-nasal aroma release profiles for (semi)-liquid compared to solid food products, likely due to differences in intensity and duration of oral processing (Figure 1) (7).

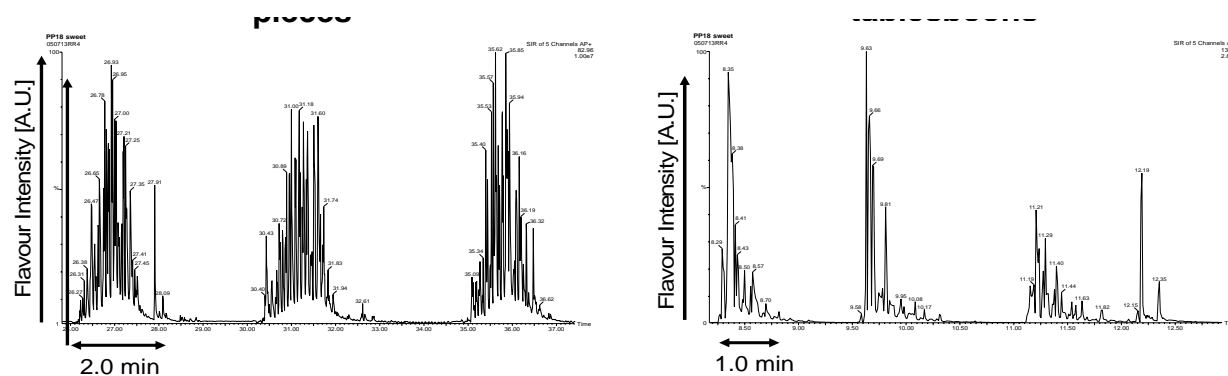


Figure 1. Example of one subject, taken from reference 7, illustrating the differences in the extent of retro-nasal aroma stimulation between (left) the consumption of three times one mouthful (on average 5 g per mouthful) of winegum candy ((soft) solid food) and (right) three times one mouthful (on average 19 g per tablespoon) of custard (liquid food), measured by APci-MS technology (5, 8).

The differences in food characteristics related to the extent of retro-nasal aroma release they evoke, were used to study whether a beverage becomes more satiating when the retro-nasal aroma release profile coincides with the profile of a (soft) solid food (9). In a double-blind, placebo-controlled, randomized, cross-over full factorial design, twenty-seven healthy subjects were administered aroma profiles by a computer-controlled stimulator based on air dilution olfactometry. Profile A consisted of a profile that is obtained during consumption of normal beverages. Profile B is normally observed during consumption of (soft) solids. The quality of the stimulus was strawberry aroma, and this was administered in a retro-nasal fashion, while the subjects consumed a sweetened milk drink. Before, during and after the sensory stimulation, appetite profile measurements were performed. A significant difference was demonstrated in perceived satiation during the aroma delivery matching a normal beverage aroma profile, compared to the aroma delivery matching a soft solid aroma profile (Figure 2). During aroma stimulation subjects felt significantly more

satiated if they were longer aroma stimulated ($F= 4.24$; $P= 0.04$). Despite changes in perceived satiation, there was no impact on *ad libitum* amount consumed (9).

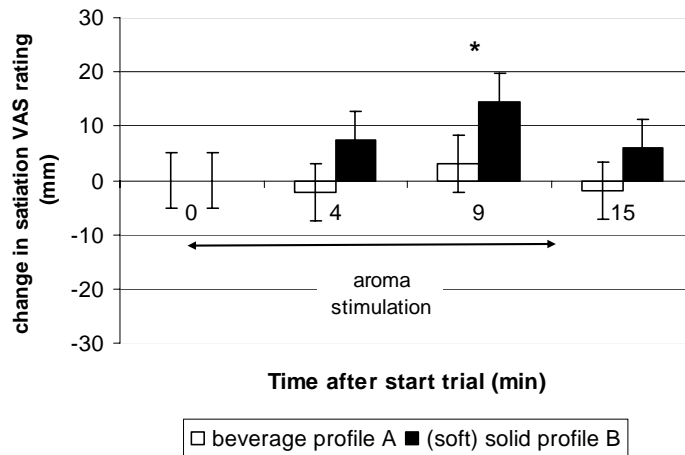


Figure 2. Change in satiation VAS rating after stimulation with aroma profile A vs. aroma profile B. Data are means with their standard errors represented by vertical bars. * denotes effect of type of aroma stimulation (profile A or B) on change in satiation VAS rating with $p < 0.05$ (8, 9).

This study suggests that the contribution of aroma in inducing satiation seems promising and appealing. While active ingredients may induce satiety at later stages in the food intake cycle, sensory triggers operating at early stages have a consumer benefit that is immediately noticeable. (Figure 3) gives an overview of some features, which are suggested to have an important contribution to the extent of retro-nasal aroma stimulation and sensory satiation, both from consumer and food product point of view.

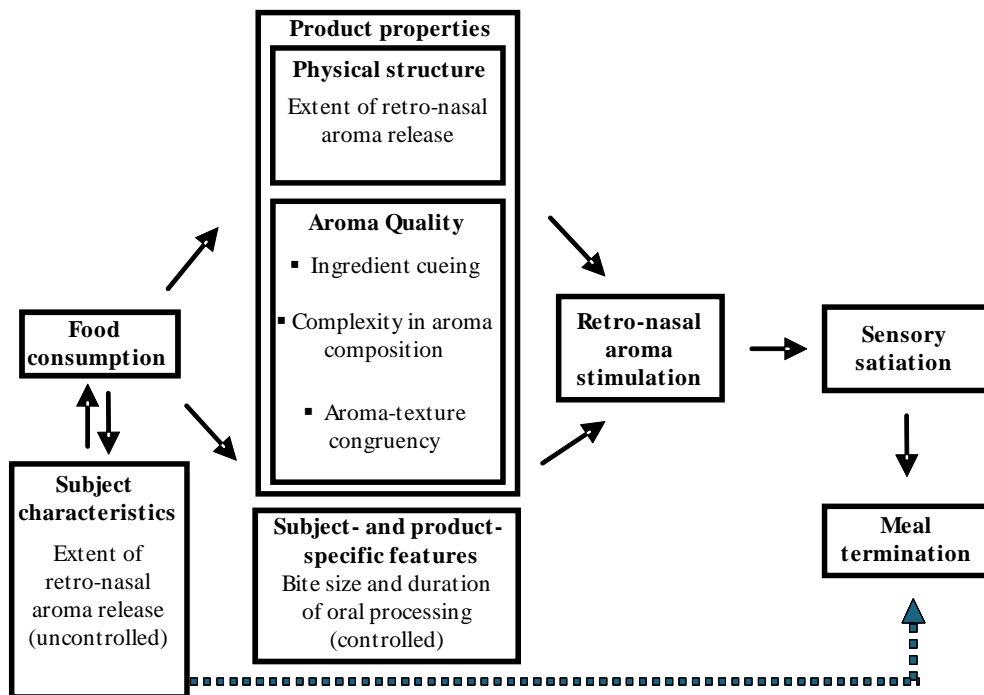


Figure 3. Schematic representation of features that are suggested to contribute to the extent of retro-nasal aroma stimulation and sensory satiation, from both the subject and food product point of view.

The subject's extent of *in-vivo* retro-nasal aroma release is an uncontrolled characteristic that is suggested to vary across individuals (7). Additionally, the physical structure of a food product and the oral processing it evokes (7), and the aroma quality (e.g. ingredient-related aroma cues (10), complexity in aroma composition (11) and congruency in aroma and texture (12) are more food product related properties with respect to the extent of retro-nasal aroma stimulation. Moreover, bite size and duration of oral processing (13) have been suggested to be of importance for the extent of retro-nasal aroma stimulation, from both the subject and food product point of view. Tailoring these features may lead to a higher quality and/or quantity of retro-nasal aroma stimulation, which in turn may lead to enhanced feelings of satiation and ultimately contribute to a decrease in food intake.

Acknowledgments

Supported by DiOGenes and Dutch Dairy Organization. DiOGenes is the acronym of the project 'Diet, Obesity and Genes' supported by the European Community (Contract no. FOOD-CT-2005-513946), The Parties of the project are listed on the web-site of the project, (<http://www.diogenes-eu.org/>).

References

1. Small D.M., Gerber J.C., Mak Y.E., Hummel T. (2005) *Neuron* 47: 593-605.
2. Vickers Z., Holton E.A. (1998) *J. Sensory Stud.* 13: 199-212.
3. Buettner A., Beer A., Hanning C., Settles M., Schieberle P. (2002) *Food Qual. Pref.* 13: 497-504.
4. Visschers R.W., Jacobs M.A., Frasnelli J., Hummel, T., Burgering M., Boelrijk A.E.M. (2006) *J. Agric. Food Chem.* 54: 5509-5515.
5. Weel K.G.C., Boelrijk A.E.M., Burger J.J., Gruppen H., Voragen A.G.J., Smit G. (2003) *J. Food Sci.* 68: 1123-1128.
6. de Kok P.M.T., Boelrijk A.E.M., de Jong C., Burgering M.J.M., Jacobs M.A. (2006) In: *Developments in Food Science; Flavour Science, Recent Advances and Trends* (Bredie, W., Petersen, M.A., Eds.); Elsevier, pp. 585-599.
7. Ruijschop R.M.A.J., Burgering M.J.M., Jacobs M.A., Boelrijk A.E.M. (2009) Retro-nasal aroma release depends on both subject and product differences: A link to food intake regulation? *Chem. Senses* 34: 395-403.
8. Ruijschop R.M.A.J., Burgering M.J.M. (2007) *Agro Food Industry Hi-Tech* 18: 37-39.
9. Ruijschop R.M.A.J., Boelrijk A.E.M., de Ru J.A., de Graaf C., Westerterp-Plantenga, M.S. (2008) *Br. J. Nutr.* 99: 1140-1148.
10. Ruijschop R.M.A.J., Boelrijk A.E.M., Burgering M.J.M., de Graaf C., Westerterp-Plantenga M.S. (2009) Effects of ingredient-related aroma cues on satiation and food intake. *Food Qual. Pref.*, submitted for publication.
11. Ruijschop R.M.A.J., Boelrijk A.E.M., Burgering M.J.M., de Graaf C., Westerterp-Plantenga M.S. (2009) Acute effects of complexity in aroma composition on satiation and food intake. *Chem. Senses* 34: in press.
12. Harthoorn L.F., Ruijschop R.M.A.J., Weinbreck F., Burgering M.J.M., de Wijk R.A., Ponne C.T., Bult J.H.F. (2008) *Food Qual. Pref.* 19:644- 650.
13. Ruijschop R.M.A.J., Zijlstra N., Boelrijk A.E.M., Dijkstra A., Burgering M.J.M., de Graaf C., Westerterp-Plantenga M.S. (2009) Effects of bite size and duration of oral processing on retro-nasal aroma release – features contributing to meal termination. *Physiol. Behav.*, submitted for publication.

Section 2

Psychophysics of Flavour Perception and Interactions

EFFECT OF HIGH-IN-TASTE PULSES ON TASTE PERCEPTION

J. BUSCH¹, J. Knoop^{1,2}, C. Tournier¹, and G. Smit¹

¹ *Unilever Food & Health Research Institute, Unilever R&D Vlaardingen, Olivier van Noortlaan 120, 3133 AT Vlaardingen, The Netherlands*

² *Current address: TI Food and Nutrition, NIZO food research B.V., P.O. Box 20, 6710 BA Ede, The Netherlands*

Abstract

There is an increased urgency, advocated by the WHO, to reduce the sodium content in food products. A significant lower sodium intake of the world population should lead to reduced incidences of high blood pressure and associated cardiovascular diseases. A number of approaches can be taken to reduce sodium: via adaptation, salt substitutes, multisensory principles and salt boosters. Other ways to enhance perception were explored as a means to reduce sodium, by building further on the generic principle of receptors as contrast detectors. The increase of saltiness perception was investigated via controlled delivery of 'high-in-salt pulses' into the mouth of assessors using a gustometer. A significant effect on saltiness perception for 2 second 'high-in-salt pulses' was shown, as compared to constant salt delivery. These results suggest that saltiness perception may be modified by changing the salt delivery profile.

Introduction

There is a growing body of scientific evidence regarding the link between high sodium intake and high blood pressure, and the associated risk with cardiovascular disease (1). Considering the significant reductions that the WHO is recommending (daily intake of 5 g of salt (NaCl) per day (2000 mg sodium), instead of current typical daily intakes of 9-12 g of salt), there is a need for solutions for sodium reduction (2). The key challenge is maintaining the same taste with lower sodium content.

There are a number of approaches that can be taken to reduce sodium:

Adaptation. By reducing sodium in products in small steps a preference for lower salt products can be induced (3). This approach is most successful when it is conducted across industry, to prevent that consumers will switch to high-salt alternatives.

Salt substitutes. Traditionally, salt substitutes are used to replace NaCl. Composites of this group are primarily mineral salts, typically KCl, often in combination with different types of bitter maskers, in order to mask the bitter and metallic off-taste of this mineral salt (2, 4).

Multisensory principles. It is well established that the different senses can influence each other (e.g. 5). Therefore, in order to enhance saltiness perception, other modalities may be modified (e.g. aroma, colour, texture). Few examples have been reported on increasing saltiness by aroma (4, 6). see also Batenburg et al., elsewhere in these proceedings.

Salt boosters. The toolbox for salt reduction might be extended with new ingredients that can trigger or boost the sodium channel receptor (potentially

enabling >30 % sodium reduction). Approaches to find such ingredients (using cellular receptor assays) are currently scoped by specialized food and ingredient companies.

What else? We have focused on other ways to enhance perception, by building further on the generic principle of receptors as contrast detectors, e.g. (7). It was investigated whether contrast in taste delivery can increase perception. More specifically, it was tested whether short high-in-taste pulses can increase taste perception as compared with constant stimulation using the same overall tastant content. We used salt solutions as a model system. With sip-wise sample delivery a minimum sample frequency rate of about 15 seconds can be reached. In order to increase the frequency rate we used a gustometer (8). The use of the gustometer as a method for delivering different concentrations in continuous flow to the mouth of the panellist has been validated by comparison with similar conditions delivered via cups (9). This paper investigates the increase of saltiness perception via controlled delivery of high-in-salt pulses, as a means to reduce the sodium content in products.

Experimental

A gustometer (8) was used under conditions that were optimized for continuous flow mode. Four different delivery designs were used (Figure 1A). Each design delivered the same average NaCl concentration of 6.3 g/L during 60 seconds. The flow rate was 40 mL/min. Design 1 consisted of a constant delivery of 6.3 g/L NaCl. In design 2 the concentration was changed every 5 seconds, with a concentration difference of 10 % (5.95 and 6.65 g/L NaCl, respectively), starting with the lower concentration. Design 3 was similar to design 2, except that the concentration difference was 20 % (5.6 and 7.0 g/L NaCl). In design 4 the lower concentration (5.6 g/L NaCl) was delivered for 8 seconds, followed by a high concentration pulse of 2 seconds (9.1 g/L NaCl) (38 % concentration difference); this was repeated six times. The total flow rate during the 2 second pulses was 48 mL/min. The change in the flow rate was not perceivable by the panel. Eleven subjects (20-47 year) were recruited for this experiment. The sensory evaluation via time intensity and data analysis (Anova of area under the curve (AUC)) are described in detail in (9).

Results

The average time-intensity profiles as produced by the panel are presented in (Figure 1B). It can be seen that the profile resulting from the constant concentration delivery reaches maximum saltiness after 15 seconds (a score of about 75), followed by a slight decrease in saltiness (around 70). The saltiness score is then relatively stable until the salt delivery is ended. Finally, a rapid decrease in perceived saltiness corresponds to the beginning of the aftertaste part.

The other 3 delivery profiles display similar features to each other. These profiles consist of 6 peaks that correspond to the varied saltiness delivery repeated every 10 seconds. The amplitude of the peaks is globally similar for each of the three delivery profiles: although the salt differences for the three profiles are different, the average salt content delivered into the mouth is the same. While the two 5 second profiles show a slight decline with time of the peak maximums and minimums, the peaks resulting from the 2 second pulses appear to increase slightly throughout their delivery.

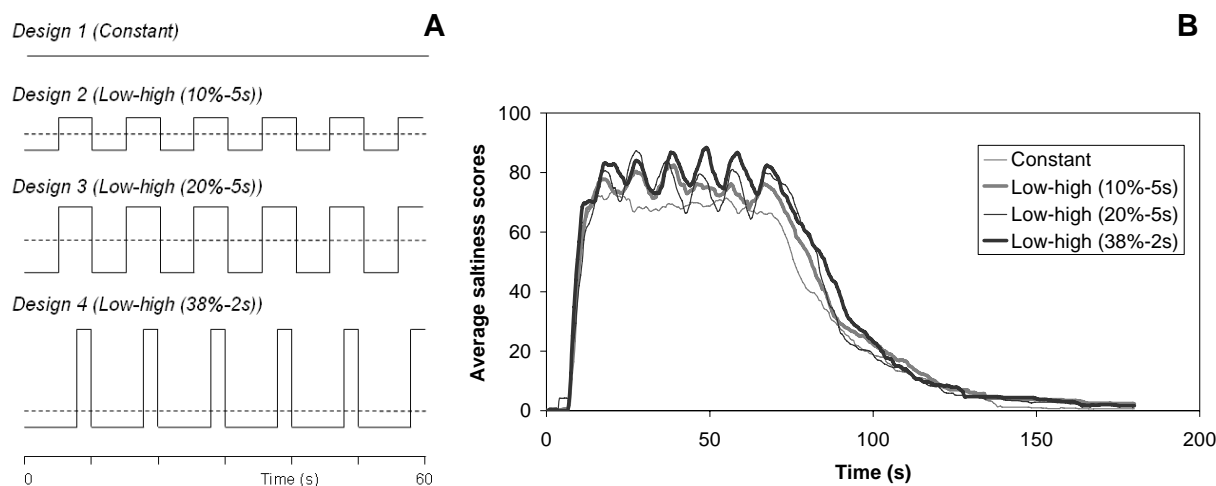


Figure 1. A. Schematic overview of salt delivery designs. Salt concentration and frequency as delivered via a gustometer is indicated. Dashed line (---) indicates average salt concentration of 6.3 g/L for all conditions. See Material and methods for further details. B. Average TI curves. Average salt concentration is 6.3 g/L

The analysis of variance of the average area under the curves revealed a significant stimulus effect for the parameters Total taste ($F= 3.29$, $p= 0.034$), a tendency for the Taste ($F= 2.82$, $p= 0.056$), but no effect for the parameter Aftertaste ($F= 2.09$, $p> 0.1$) (Figure 2A). From the Student-Newman-Keuls tests it can be concluded that the 2 second pulse profile has been rated significantly more salty than the constant stimulus over the whole rating time (Total taste) and to a lower extent during the stimulus delivery in the mouth (= Taste parameter). The two other (5 second) profiles were not perceived as significantly different from the other designs.

All three designs with varied saltiness delivery were offered in the same sequence of 'Low-high' concentration. In other experiments that involved both 'Low-high' and 'High-low' sequences a significantly higher AUC was obtained for the aftertaste of the 'Low-high' sequence, which appeared to be directly proportional to the last concentration of the sequence (9). In order to exclude effects that are directly due to the impact on the aftertaste the same concentration can be delivered for a fixed interval at the end of each design. Furthermore, as the 2 s delivery profile had a higher flow rate than the other conditions, this condition should be tested with the same flow rate as the other designs. These adaptations have been incorporated in further experiments (9).

We have explored the implication of these findings for product design. Therefore a chicken cream soup product with high-in-salt (chicken) particulates was tested (Figure 2B). The original soup contains unsalted particulates (A and B), while the adapted soup (C) comprises high-in-salt particulates. The high-in-salt particulates deliver a contrast in saltiness during consumption of the soup, reflecting the high-in-salt pulses as delivered by the gustometer. Furthermore, during consumption the particulates are being chewed and therefore the residence time of these particulates in the mouth, and the salt released during chewing, can be expected to be higher than that of salt present in the liquid soup itself.

The impact on saltiness perception of these soups was tested with a group of 60 consumers. Consumers received two of the three chicken cream soups on two consecutive days (one soup on each day, in random order). Consumers had to

answer various questions, including a question on the saltiness of the soup. The soup with the salty particulates (C) was scored significantly higher in saltiness than the soup with the same sodium content and unsalted particulates (B) (Figure 2B). The saltiness of Soup A was not significantly different from the two other soups. Thus using high-in-salt particulates the perceived saltiness of the soup was increased (4, 10). It can be envisaged that several parameters will affect the (enhanced) perception of such a soup with high-in-salt particulates, such as the size and number of particulates, diffusivity of salt from the particulates, and the salt differences between particulates and soup.

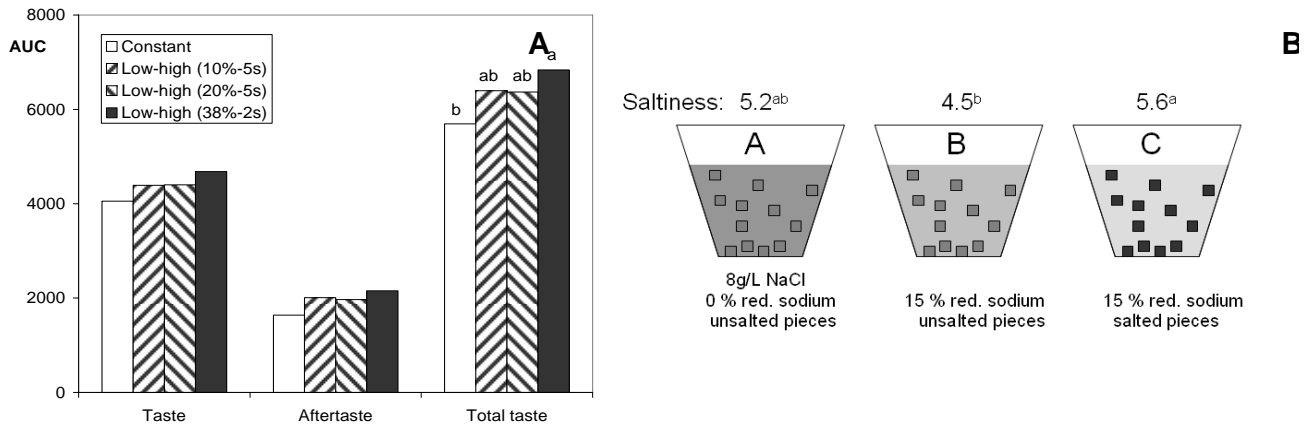


Figure 2. A. Areas under the curve. B. Sodium distribution in soups. Darker shading reflects higher sodium content. The saltiness of the soups as determined with consumers is indicated. Mean values associated with the same letter are not significantly different ($\alpha=0.05$).

References

1. World Health Organisation (2007) *Report of a WHO Forum and Technical Meeting*. WHO Document Production Services.
2. Kilcast D., Angus F. (Eds.) (2007) *Reducing salt in foods: practical strategies*. Woodhead Publishing Limited.
3. Bertino M., Beauchamp G.K., Engelman K. (1982) *Am. J. Clin. Nutr.* 36: 1134-1144.
4. Dötsch M., Busch J.L.H.C., Batenburg A.M., Liem G., Tareilus E., Mueller R., Meijer G. (2008) *Submitted for publication*.
5. Delwiche J. (2004) *Food Qual. Pref.* 15: 137-146.
6. Djordjevic J., Zatorre R.J., Jones-Gotman M. (2004) *Exp. Brain Res.* 159: 405-408.
7. Baek I., Linforth R.S.T., Blake A., Taylor A.J. (1999) *Chem. Sens.* 24: 155-160.
8. Bult J.H.F., de Wijk R.A., Hummel T. (2007) *Neurosci. Lett.* 411: 6-10.
9. Busch J.L.H.C., Tournier C., Knoop J.E., Kooyman G., Smit G. (2009) *Chem. Senses* 34: 341-348.
10. Busch J.L.H.C., Keulemans C., van den Oever G.J., Reckweg F. (2008) WO 2008/074606.

SALT ENHANCEMENT BY AROMA COMPOUNDS

M. BATENBURG, E. Landrieu, R. van der Velden, and G. Smit

Unilever Food & Health Research Institute, Unilever R&D Vlaardingen, Olivier van Noortlaan 120, 3133 AT Vlaardingen, The Netherlands

Abstract

It is shown that multi-sensory interaction between aroma and taste can be employed to compensate the lower salt levels of healthy food products. The demonstrated saltiness enhancement by complex flavourings was unraveled by experiments with 'salt-congruent' single compounds, using trained and naïve panels. Several savoury compounds, but especially sotolon (4,5-dimethyl-3-hydroxy-2(5H)-furanone), have a significant impact on perceived saltiness. As expected, a naïve panel is more suitable to demonstrate multi-sensory interaction than a trained panel. The results were confirmed by consumer tests. A combination of KCl-based salt replacer and extra aroma was found to compensate approximately 30% sodium reduction without significant change of the flavour profile.

Introduction

High dietary sodium has been shown to cause hypertension and hence increase the risk of developing cardiovascular diseases. In fact there is even epidemiologic evidence of a direct correlation between stroke incidence and salt consumption (1). As 75% of sodium intake in industrialized countries is from processed and restaurant foods, the food industry is urged by national and international authorities to reduce sodium levels in their products. However, reduction of salt without affecting taste is a major challenge. Reducing the salt content in food products obviously leads to a loss of saltiness, but also to a decrease of overall flavour intensity. It is known that people can adapt to lower salt levels for instance in bread (2), but this approach will only work if it is done industry-wide in a concerted way, which is difficult to organise. Most approaches therefore are based on some kind of compensation, using salt replacers or salt boosters. These usually contain potassium chloride, which is definitely salty, but also bitter and metallic. Other minerals and specific amino acids may also be used in replacer mixes, but the salt reduction that can be compensated in savoury products like soups and sauces remains limited to approximately 15-20%.

Besides the salt-contrast concept discussed in one of the oral presentations (3), a further compensation of the effects of low salt content might be derived from the exploitation of multi-sensory integration. As stated before salt functions as (savory) flavour enhancer. It can be envisioned that this interaction is mutual, and that extra added aroma will not only restore the aroma attributes, but also the perceived saltiness. For sweet flavour the enhancing effect of taste on aroma, and vice versa, has clearly been shown (4-6). The interaction takes place at the cognitive level (7). Relatively few publications deal with salt-aroma interactions. Only one study reports an enhancement of saltiness by a 'congruent' aroma, namely that of soy sauce (8). The aroma here, however, is administered orthonasally, and findings can not easily be exploited in real-life food products.

The present work was aimed to show that the principle can be used in a very practical way: flavourings were selected that, when added to a salt-reduced bouillon or soup, could compensate the effects of the low salt level, without significantly changing the flavour profile of the product. In first instance the savoury flavourings used in the recipe were simply increased in level. The second part is a systematic study of the impact of various types of potentially congruent, savoury aroma compounds on perceived saltiness in the context of an industrial bouillon. The selection of the single compounds is based on the known key aroma composition of meat flavour, encompassing 'brothy', 'meaty', and 'roasted' notes. The aim of the study was to identify which of the mentioned flavour directions and compounds is most effective in saltiness boosting.

Earlier studies indicated that the magnitude of multisensory interaction between taste and aroma varies between individuals, and especially trained panelists appeared insensitive and capable of separating aroma from basic taste (9). This indicates that cross-modal interactions to a large extent are not "hard-wired", but rather based on learned associations, and hence can be unlearned by training. In line with this, instructions to panelists strongly influence the results obtained (10). For that reason products were evaluated with an untrained and a trained panel, as well as with naïve consumers.

Experimental

All aroma chemicals were from Aldrich, food-grade KCl and NH₄Cl were from Merck and Riedel-de Haan respectively. Regular dry bouillon ingredients were from Unilever-Germany. Bouillons were prepared in advance and served at ~60°C in a 50ml medicinal cup.

The naïve panel (or 'untrained panel') was composed of ~12 untrained subjects. All panelists were tested on taste sensitivity, mainly focused on salt. Taste sessions took place in a sensory room with individual booths. The sessions were held once every two weeks in order to limit exposure and avoid training. Samples were served at 60 °C, and attributes were scored on a 12-points scale using bouillons of two different salt levels as references. To reduce the dumping effect (a salt enhancement effect only due to the response bias), it was decided to score on two attributes: the "salt intensity" and the "overall flavour intensity". Only salt intensity data are shown.

The trained (descriptive) panel was composed of 10-12 external people and was selected and trained to characterise savoury products in terms of perceived attributes and intensities. The used Spectrum training procedure is an extension of the QDA descriptive analysis technique (standardised lexicon of terms, all scales standardised on the same basis and anchored with multiple reference points). Assessors scored the products in booths in a comparative way, per attribute instead of per product to increase sensitivity.

In the consumer study (with up to 60 subjects) individuals were subjected to either a 2-AFC test, simply answering the question 'which of the two samples is most salty', or a 'multi-attribute-scale' test. The latter paired-comparison test avoids dumping effect by using a 2-step approach and open questions rather than forced choice. First it was asked if any difference is tasted, and if the answer was yes, individuals were asked in step 2 whether a difference was tasted on 6 attributes (bitter, sweet, salt, sour, aroma, and thickness) and if so, which sample was most intense on the attribute in question.

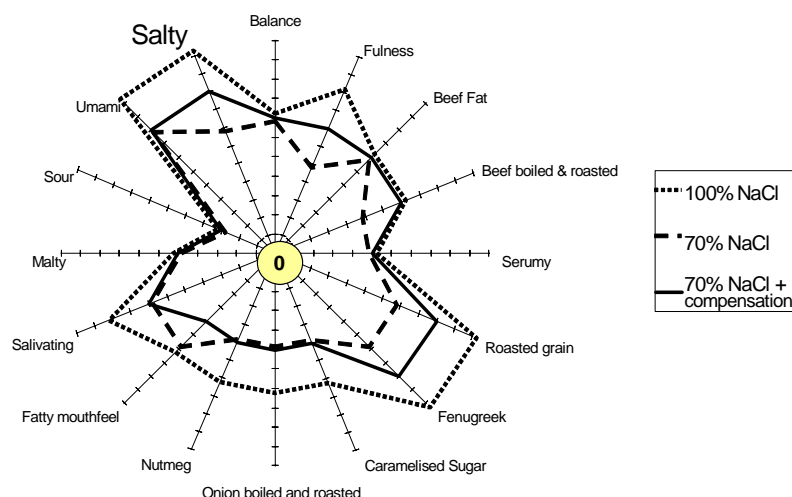


Figure 1. Sensory effect of salt reduction in beef bouillon, and subsequent compensation by extra aroma.

Results

Figure 1 clearly shows the flavour enhancing effect of sodium chloride in beef bouillon in a descriptive panel. Upon reduction of the sodium level with 30% not only the perceived saltiness is reduced, but in fact the rating on most other attributes is lowered as well, also on those primarily related to aroma, like ‘beef’, ‘fenugreek’, etc. Reduction of salt apparently leads to a bland, tasteless product. It is shown that the flavour profile could indeed be partially restored by addition of extra flavouring. For most of the attributes, about half of the flavour loss is compensated. Most remarkably this also holds for attribute ‘salty’. This effect was solely due to the aroma, since we made sure that the salt added via the flavouring was compensated.

Higher levels of aroma did not add to the compensation, and instead led to unbalance in the flavour profile. Combining the extra flavour with a mixture of potassium- and ammonium chloride, however, a close match of the original flavour profile could be obtained. Compensation on the basis of solely these minerals at higher levels led to improved saltiness, but also to a bitter off-note not perceived in the combination with flavour. Similar results were obtained with chicken bouillon and various types of dry soups (data not shown). Generalizing it can be stated that about 15% sodium reduction can be compensated by extra aroma without significant change of the flavour profile, and 30% in combination with KCl-based salt replacers (not shown).

For further unraveling of the effect of these cross-modal interactions in terms of key enhancing compounds, we have made use of three categories of subjects: untrained panellists, trained panellists and naïve consumers. A commercial chicken bouillon was used for these studies. Using the naïve panellists we found that several ‘congruent’ single compounds significantly enhanced salt perception. ‘Seasoning’ or ‘brothy’ compounds, esp. sotolon (4,5-dimethyl-3-hydroxy-2(5*H*)-furanone), had the largest impact (Figure 2). Significant salt enhancement was also found for several sulphur-containing ‘meaty’ and ‘roasted’ components. The trained panel did not demonstrate a statistically significant effect on saltiness, in line with its analytical way of tasting and due to its training, which leads to unlearning of the associations on which multi-sensory interactions are based (10).

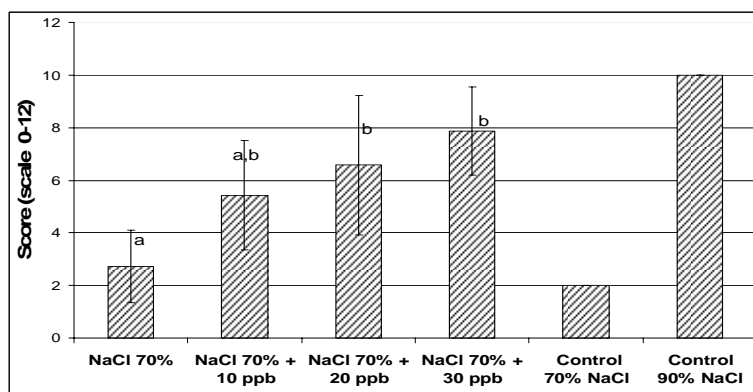


Figure 2. Saltiness enhancement in 30% salt-reduced bouillon by increasing doses (10, 20, and 30 ppb) of sotolon, assessed by the untrained panel. The letters refer to significance of differences ($p < 0.05$).

When tested with naive consumers (data not shown) the effect of single aroma compounds could only be noticed when subjects were focused on saltiness perception by means of a 2-AFC forced comparison test. This approach bears the risk that any difference, e.g. in flavour intensity, is dumped on the single attribute 'saltiness', and cannot be used as conclusive evidence for saltiness enhancement. For a complex flavouring, in contrast, saltiness enhancement could be demonstrated in a convincing way using open questions, hence not biased by a 'dumping' effect. The difference in perceived saltiness here was clearly significant.

The data provided show that indeed aroma-taste multi-sensory interaction can be employed to compensate salt reductions. Further analysis showed that several classes of potentially congruent aroma compounds, giving 'brothy', 'meaty' and 'roasted notes', contribute to the salt enhancement effect. In line with earlier studies of multi-sensory interactions the set-up of the sensory experiments (trained vs. naïve panel, forced choice vs. open questions) determines to a large extent the results. Trained descriptive panels, due to their analytical way of tasting, are not very suitable instruments to assess multimodal interaction, but can be used to check for undesired changes in the flavour pattern.

References

1. Perry I.J., Beevers, D.G. (1992) *J. Human Hypertension* 6: 23-25.
2. Girgis S., Neal B., Prescott J., Prendergast J., Dumbrell S., Turner C., Woodward M. (2003) *Eur. J. Clin. Nutr.* 57: 616-20.
3. Busch J., Knoop J., Tournier C., Smit G. (2009) In *Proceedings of the 12th Weurman Flavour Research Symposium, Interlaken, Switzerland* (I. Blank, M. Wüst, C. Yeretian, eds.), pp 47-50.
4. Noble A.C. (1996) *Trends Food Sci. Technol.* 7: 439-44.
5. Stevenson R.J., Prescott J., Boakes R.A. (1999) *Chem. Senses* 24: 627-35.
6. Prescott J., Johnstone V., Francis J. (2004) *Chem. Senses* 29: 331-40.
7. Davidson J.M., Linforth R.S., Hollowood T.A., Taylor A.J. (1999) *J. Agric. Food Chem.* 47: 4336-40.
8. Djordjevic R., Zatorre R.J., Jones-Gotman M. (2004) *Chem. Senses* 29: 199-206.
9. Hort J., Hollowood T.A. (2004) *J. Agric. Food Chem.* 52: 4834-4843.
10. Frank R.A., van der Klaauw N.J., Schifferstein H.N. (1993) *Percept. Psychophys.* 54: 343-354.

CO₂ PERCEPTION AND ITS INFLUENCE ON FLAVOUR

B. LE CALVÉ, H. Goichon, and I. Cayeux

Firmenich SA, Route des Jeunes 1, P.O. Box 239, CH-1211 Geneva 8

Abstract

The oral perception of CO₂ dissolved alone in water and in a model beverage was studied. The dose-response curve showed that a slight increase of CO₂ resulted in a significant increase in the perception of sparkling intensity (selected attribute to describe CO₂ perception). The average detection threshold of dissolved CO₂ in water was measured at 0.26 g/L. The sensation perceived by panellists at threshold level was not only sparklingness, but also saltiness. Neither sensitisation nor desensitisation was observed with carbon dioxide under adaptative experiments. Taste-taste interactions as well as taste-smell interactions were observed with carbonated beverages. The sparkling intensity was influenced by a congruent taste such as sourness. Trigeminal-trigeminal interactions also occur between temperature and sparkling intensity.

Introduction

Drinking a glass of still champagne certainly reveals how important CO₂ is in certain beverages perception. Carbonated drinks simultaneously stimulate the olfactory, gustatory and somesthetic senses. Although interactions between taste and smell are well documented (1-3) less information is available on the influence of trigeminal stimuli on flavour perception (4). The aim of this study was to better understand (a) CO₂ perception when dissolved alone in water and (b) how it interacts with other sensory modalities in carbonated beverages.

Experimental

Tap water was carbonated using a carbonator (Loop Aqua device, IMI Cornelius). Different concentrations of CO₂ were obtained by mixing different volumes of carbonated and still water. Samples were prepared the day before the sensory and carbonation measurements were made and stored at 6°C.

Flavoured samples were prepared as follows: a base of 200 mL containing sucrose syrup, citric acid and a lemon flavour dissolved in still water added with 800 mL of water (100% still water, 50% still water mixed with 50% carbonated water or 100% carbonated water). Two liters of each sample were prepared; one for sensory test and the other for carbonation measurement. CO₂ gas concentration was measured by thermal conductivity (Orbisphere 3658 device, HachUltra). Each CO₂ gas value was registered with its corresponding temperature.

For sensory tests, samples (30 mL) were served at a temperature between 9°C and 12°C in three digit random coded cups. Special care was taken to serve samples in order to minimize the loss of CO₂: pouring was done by series of 6 samples; cups were closed and stored at 6°C for no longer than 15 minutes prior to service.

30 subjects participated to each test, except for the threshold determination which was done with 42 subjects. Panellists were all Firmenich employees and were familiar with the use of linear scale to rate their perceptions. Subjects were asked to sip the sample, keep it for 5 seconds in their mouth and then swallow it. They rinsed their mouth with room temperature water between each sample.

Dose response curve. Five concentrations of CO₂ and a replicate were tested (6.3, 3.7, 3.1 (repeated), 1.5 and 0 g/L corresponding to 100%, 75%, 50%, 25% and 0% of carbonated water in still water). Sparkling intensity was evaluated on linear scale from “not at all” (= 0) to “very intense” (= 10). At the beginning of the study subjects tasted the most carbonated sample to best estimate the highest possible level.

Threshold measurement. The standard ASTM method of the best estimate threshold was applied (ASTM-E679). Six three-alternative forced choice (3AFC) tests were performed with the ascending range of CO₂ concentrations (0.05, 0.09, 0.19, 0.37, 0.74, 1.49 g/L). For each test, subjects had to determine the odd sample among three, two samples containing still water and one containing carbonated water. They were also asked to indicate the attributes of the different sample from the list: sour, bitter, sparkling, temperature, salty or “by chance”.

Adaptation test. Seven identical samples (6.3 g/L of CO₂) were served (30 mL). Subjects were asked to sip and swallow samples. The seven samples were tested following the same protocol with ten seconds between each and without any mouth rinsing. Sparkling intensity was rated on a linear scale. A warm up sample was presented one minute before the test.

Study of interactions between taste, smell and trigeminal perceptions. Five parameters with different levels were chosen: sucrose concentration (100 g/L, 40 g/L or 0 g/L), CO₂ gas concentration (4.5 g/L, 3 g/L or 0 g/L), citric acid (1.5 g/L or 0 g/L), lemon flavour concentration (1.3 mL/L or 0 mL/L) and temperature (8.5°C or 11.5°C). The 72 samples of the factorial experimental plan were split into 12 sessions of 6 samples. The sample containing 3 g/L CO₂, 4 g/L sucrose, 1.5 g/L citric acid and 1.3 mL/L lemon flavour was rated in each session in order to control the repeatability of the panel. Subjects were asked to evaluate sparkling, sweetness, sourness and lemon flavour intensities on a linear scale.

Results & Discussion

Dose-response curve. Below 3.7 g/L, the dose response plot appears rather steep, which means that a slight increase of CO₂ concentration (2 g/L) results in a significant increase of perceived sparkling intensity (Figure 1). This shape of dose response curve fits with published data on CO₂ nasal perception (5). According to ANOVA and means comparison test (Duncan’s test), each level of CO₂ concentration tested corresponded to a specific level of sparkling intensity.

Detection threshold. The individual detection threshold was calculated as soon as the subject found the odd sample for at least the two highest concentrations. The average detection threshold was the geometric mean of all the individual values (ASTM-E679). The detection threshold of dissolved CO₂ in water was measured at 0.26 g/L. This value is comparable to values measured in pasteurized milk (6) and in yogurt (7).

Around threshold, the subjects rated the odd sample not only as sparkling. Most subjects who found the odd sample at 0.19 g/L and 0.37 g/L described it as being salty (Figure 2). Subjects who failed the test mostly answered “by chance”.

Expression of Multidisciplinary Flavour Science

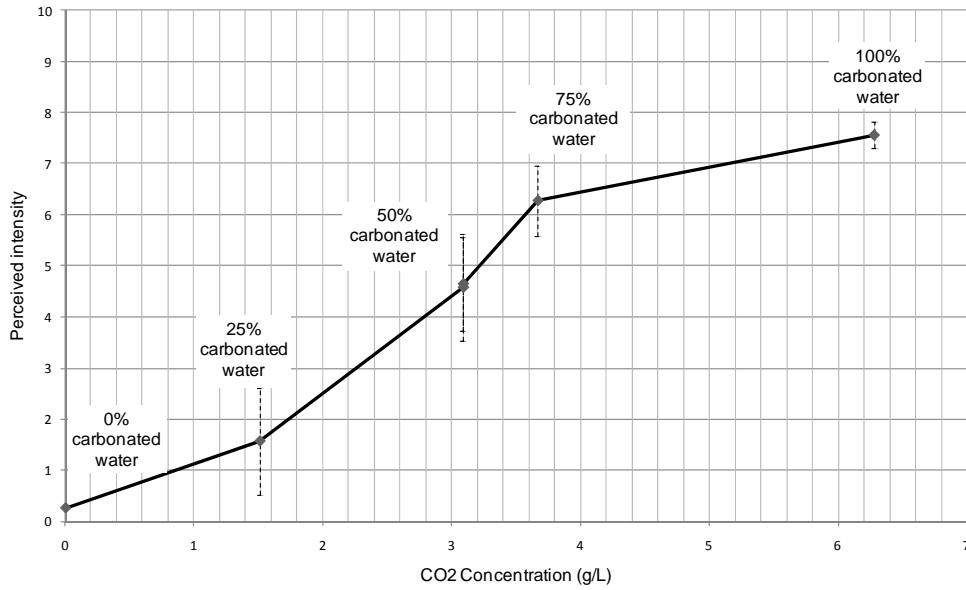


Figure 1. Dose response curve of CO₂ in water.

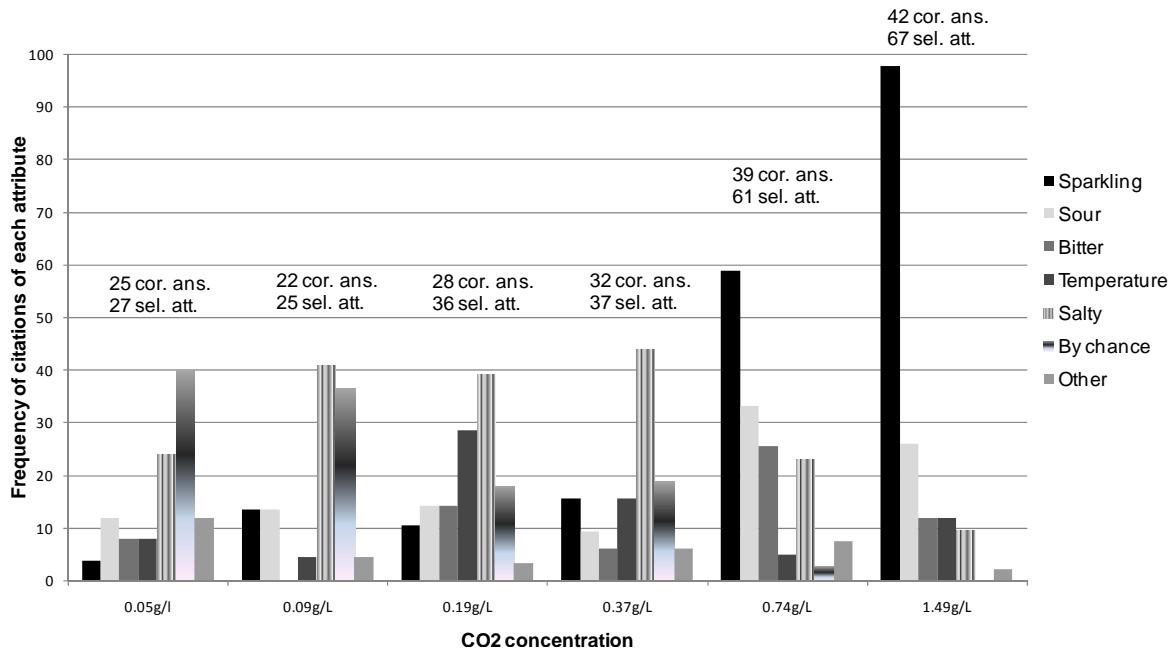


Figure 2. Frequency of citations of each attribute selected by subjects who find the odd sample. For each concentration, number of correct answers (cor. ans.) and total number of selected attributes (sel. att.) are indicated.

Adaptation test. Inter-individual differences were observed in terms of the use of the scale. But, for 26 subjects among 30 the successive tasting of 7 carbonated samples demonstrated neither an increase nor a decrease of the sparkling intensity. Study of interactions between taste, smell and trigeminal perceptions. For each sensory response ANOVA was done with each physical parameter as factor. All significant effects of each factor on sensory response are summarized in Table 1. Results obtained for the sample repeated in each session were not significantly different according to ANOVA (for sparkling intensity: $F= 1.27$, $p= 0.24$, for sweetness: $F= 0.35$, $p= 0.97$, for sourness: $F= 0.48$, $p= 0.91$ and for flavour intensity: $F= 1.32$, $p= 0.21$).

Table 1. Significant effect of an increase of each main factor on each sensory response.

Perception	Factors				
	CO ₂ Quantity	Sucrose	Citric acid	Lemon Flavour	Temperature
Sparkling intensity	↗		↗		↘
Sweetness	↘	↗	↘	↗	
Sourness	↗	↘	↗	↗	
Lemon Flavour		↗	↗	↗	

As expected, each sensory response was impacted by its corresponding physical parameter. Sparkling intensity increased with CO₂ quantity ($F= 850.4$; $p \leq 0.0001$), in presence of citric acid ($F= 73.6$, $p \leq 0.0001$) and for colder samples ($F= 35.5$, $p \leq 0.0001$). Sweetness decreased when the quantity of CO₂ increased ($F= 24.5$, $p < 0.0001$) or citric acid was added ($F= 143.9$, $p < 0.0001$). It increased with the sucrose concentration ($F= 4890.8$, $p < 0.0001$) as expected but also when lemon flavour was added ($F= 18.6$, $p < 0.0001$). Sourness increased with CO₂ quantity ($F= 80.44$; $p < 0.0001$), citric acid ($F= 1354.61$, $p < 0.0001$) and lemon flavour addition ($F= 12.86$, $p = 0.001$) but decreased when sucrose concentration increased ($F= 158.31$; $p < 0.0001$). Lemon flavour intensity increased with sucrose ($F= 27.07$, $p < 0.0001$), citric acid ($F= 155.94$, $p < 0.0001$) and lemon flavour concentration ($F= 924.14$, $p < 0.0001$).

Conclusion

Taste-taste and taste-smell interactions already demonstrated in non carbonated samples occur also in carbonated. In the context of carbonated soft drinks lemon flavour, citric acid and sucrose are congruent. This congruence seems to enhance these interactions (8). The reduction of sweetness and sourness observed with increasing CO₂ could be explained by a physical effect: the pH of the solutions decreases when CO₂ quantity increases. Conversely, samples with or without citric acid, at low or high temperature contain the same quantity of CO₂. Sparkling intensity increases observed for colder samples or with citric acid demonstrate that trigeminal-trigeminal and taste-trigeminal interactions do occur in carbonated beverages.

References

1. Noble A.C. (1996) Trends Food Sci. Techn. 7: 439-444.
2. Delwiche J.F. (2004) Food Qual. Pref. 15: 137-146.
3. Valentin D., Chrea C., Nguyen N. (2006) In Optimising Sweet Taste in Foods (W.J. Spillane, ed), pp. 66-84.
4. Cowart B.J. (1998) Chem. Senses 23: 397-402.
5. Wise, P. M., Wysocki, C.J., Radil, T. (2003) Chem. Senses 28: 751-760.
6. Hotchkiss, J. H., Chen, J.H., Lawless, H. T. (1999) J. Dairy Sci. 82: 690-695.
7. Wright A.O., Ogden L.V., Eggett D.L. (2003) J. Food Sci. 68: 378-381.
8. Schifferstein H.N.J., Verlegh P.W.J. (1996) Acta Psychologica 94: 87-105.

SYNERGY IN ODOUR DETECTION BY HUMANS

T. MIYAZAZWA^{1,2}, M. Gallagher², G. Preti^{2,3}, K. Matumoto¹, T. Hamaguchi¹, and P.M. Wise²

¹ *Flavor System & Technology Laboratory, R&D Control Division, Ogawa & Co., Ltd., 15-7 Chidori, Urayashu-shi, Chiba 279-0032, Japan*

² *Monell Chemical Senses Center, 3500 Market Street, Philadelphia, Pennsylvania 19104, U.S.A.*

³ *Department of Dermatology, School of Medicine, University of Pennsylvania, 3451 Walnut Street, Philadelphia, Pennsylvania 19104, U.S.A.*

Abstract

This study investigated whether low levels of added carboxylic acids affect the perception of maple lactone (ML), a common flavour in coffee. Sub-threshold concentrations of acetic (C₂) and butyric acid (C₄) were added to peri-threshold concentrations of ML that ranged from just above chance (guessing) level to a level that subjects could almost always detect. Psychometric functions were measured for both pure compounds and binary mixtures. Mixture interactions were compared to response-addition (independent processing of mixture-components). Overall, mixture-detection exceeded additivity, *i.e.* synergy occurred. The study showed that sub-threshold concentrations of carboxylic acids can have a statistically significant impact on the detection of a common coffee aroma.

Introduction

In studies of odour-odour interactions, approximate additivity (at threshold level) or mutual suppression (at the supra-threshold level) are most common (1, 2). Hints of synergy, *i.e.* sensory impact of a mixture that exceeds the sum of the impacts of the unmixed components, have been rare, but do occur. For example, the addition of a sub-threshold odour can produce a small but measurable increase in the perceived intensity of supra-threshold beverage aromas and the sweetness of supra-threshold sucrose solutions (3, 4). These results support reports of professionals, *e.g.* chefs, flavourists, and perfumers, who suggest that adding seemingly insignificant amounts of key ingredients can sometimes have a substantial impact on aroma, taste or flavour.

Experimental

Subjects. Seventeen healthy adults (10 female) participated. Ages ranged from 22 to 47 (average = 31.1). All had served in previous experiments using the same method to examine thresholds for carboxylic acids. All subjects were screened for general anosmia and for specific hyposmia to the test compounds, and provided written informed consent on forms approved by the IRB of the University of Pennsylvania.

Materials. Subjects received a six-step dilution series of each unmixed compound (C₂, C₄, and ML, Figure 1). Successive concentration-steps differed by a factor of about 2.2. Mixtures included all six steps of ML plus two fixed, sub-threshold concentrations of C₂, and all levels of ML+ two sub-threshold levels of C₄.

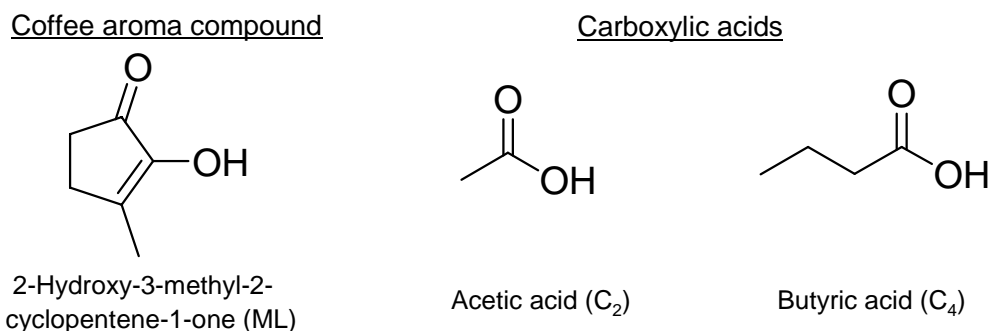


Figure 1. Chemical structures of the stimulus materials.

Procedure. Detection was measured using a two-out-of-five, forced-choice procedure. Each session included six presentations of each concentration of a stimulus. In each session, the subject contributed six trials per concentration. In addition, each stimulus was tested in two sessions. The stimulus could be either a pure compound or binary mixture, *i.e.* a fixed concentration of carboxylic acid added to ML. Psychometric functions of carboxylic acids were measured first to determine appropriate concentrations to add to ML. The concentration of each carboxylic acid fell at least one or two dilution-steps below (-1,-2) the each subject's measured threshold.

Apparatus. An air dilution olfactometer (Figure 2) delivered stimuli of constant and known vapour-phase concentration. This device precisely controlled both concentration and duration of stimuli.

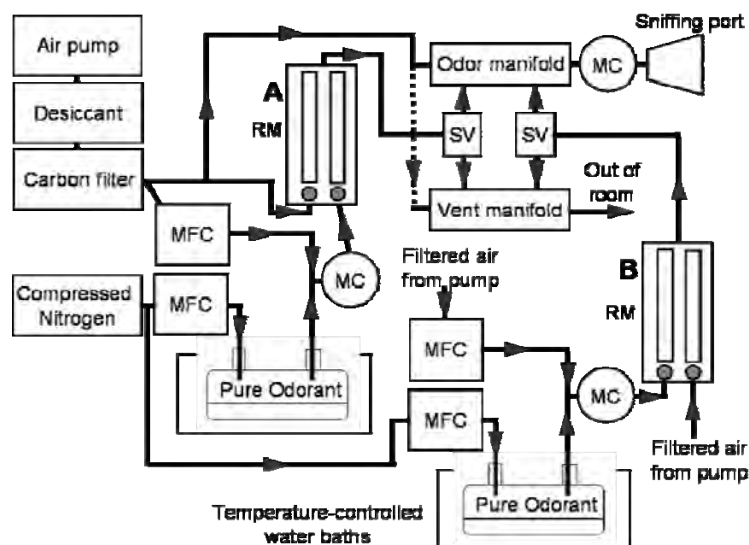


Figure 2. A schematic of the olfactometer. MC = mixing chamber, MFC = mass flow controller, RM = rotameter, and SV = solenoid valve.

Calibration. Samples were collected at the output of the olfactometer in Tedlar bags. Concentrations of samples were measured using solid-phase micro extraction to collect odorants and GC/MS to separate and quantify odorants (Table 1). Standard curves were created by measuring MS response to gas standards of known concentration.

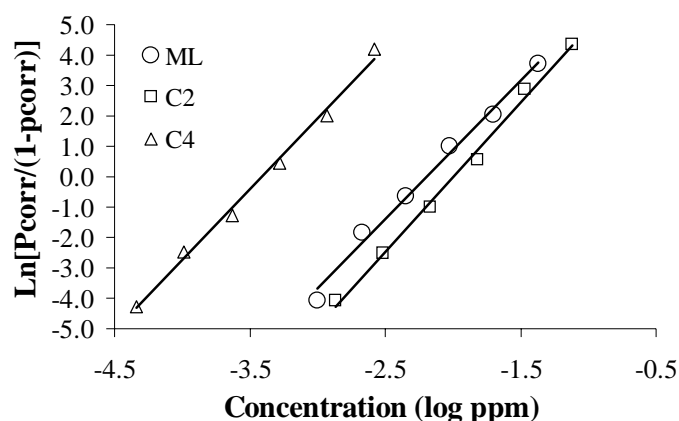
Table 1. Odorant concentrations (log ppm). Values in parentheses were estimated based on extrapolation of linear fits.

Step	ML	C ₂	C ₄
1	(-3.40)	(-3.55)	(-4.86)
2	-3.08	-3.20	-4.51
3	-2.75	-2.85	-4.15
4	-2.43	-2.50	-3.80
5	-2.10	-2.15	-3.45
6	-1.78	-1.80	-3.10

Data analysis. The basic data consisted of psychometric functions, *i.e.* proportion correct detection plotted against log stimulus-concentration. ANOVA models were used to compare dose-response relationships across mixtures. Before statistical analysis, proportion correct was corrected for chance-level and a log-odds ratio transform was applied to make functions approximately linear. Mixture detection was also compared to response-addition. According to response-addition, processing of the components of mixtures is statistically independent. Response-addition is computed as: $p(AB) = p(A) + p(B) - p(A)p(B)$, where $p(AB)$ represents the probability of detecting the mixture, $p(A)$ represents the probability of detecting component A, and $p(B)$ represents the probability of detecting component B. According to the model, if detection of the mixture matches response-addition, the components do not interact. Mixture detection that falls below response-addition indicates suppression relative to statistical independence. Mixture detection that exceeds response-addition indicates some form of mutual enhancement, or synergy.

Results

Psychometric functions for individual components. According to A 3(Odorant) X 6(Concentration-step) ANOVA, detection performance increased monotonically with stimulus concentration, and the slopes of the functions were quite similar across compounds (Figure 3). Fitted psychometric functions were used to generate the predictions of response-addition for detection of binary mixtures.

**Figure 3.** Psychometric functions for individual components.

Psychometric functions for binary mixtures. Psychometric functions with added carboxylic acids showed significant differences from corresponding functions for pure ML (Data not shown). According to A 3(Stimulus-condition) X 6(Concentration-step),

repeated-measures ANOVA, the effect of added acid reached significance for both C₂, $F(2,32) = 22.19$, $p < .001$, and C₄, $F(2,32) = 106.41$, $p < .001$. These results suggest that the addition of relatively low concentrations of carboxylic acids significantly enhanced detection relative to that of pure ML.

Mixture interactions with respect to response-addition. A comparison between psychometric functions for mixtures and the predictions of response-addition also suggest that mixture-detection exceeded additivity, except at the lowest and highest concentration (Figure 4). Data for mixtures that included C₂ and C₄ were submitted to separate 3-way ANOVAs: Model comparison (mixture-detection vs. response-addition) X Level added (-1 and -2) X Concentration-step (six levels). The main effect of Model-comparison reached significance for both C₂, $F(1,16) = 17.38$, $p < .01$, and C₄, $F(1,16) = 43.87$, $p < .01$. Overall, these results provide evidence for detection that exceeds independence, *i.e.* synergy.

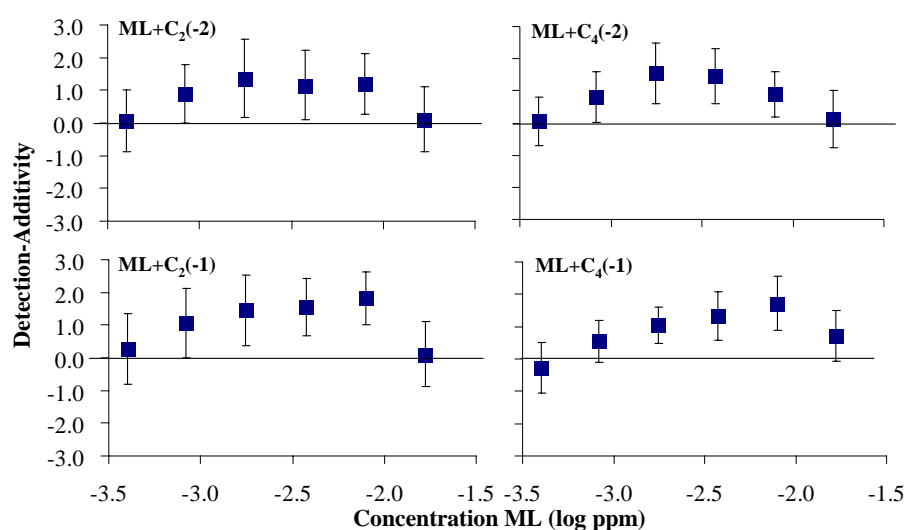


Figure 4. A difference between measured detection performance for binary mixtures and predictions of response-addition. Error bars represent 95% confidence intervals of difference scores. Positive values indicate synergy, 0 indicates perfect additivity, and negative values indicate suppression.

Discussion

Mixture-detection exceeded additivity, *i.e.* synergy occurred. These results provide a clear demonstration of synergy in odour detection, perhaps the first to combine rigorous stimulus control, vapour-phase calibration of stimuli, measurement of full detection functions, and a clear statistical definition of synergy. Accordingly, chemicals with little individual impact might combine with other compounds to have a measurable impact. Future studies can determine if these results are particular to the compounds studied. One long-term goal is to build a predictive, structure-activity model of interactions. Such a model might suggest promising candidates for synergistic or suppressive combinations.

References

1. Cometto-Muñiz J.E., Cain W.S., Abraham M.H. (2005) *Behav. Brain Res.* 156: 115-123.
2. Wise P.M., Miyazawa T., Gallagher M., Preti G. (2007) *Chem. Senses* 32: 475-482.
3. Ito Y., Kubota K. (2005) *Mol. Nutr. Food Res.* 49: 61-68.
4. Labbe D., Rytz C., Morgenegg S., Ali S., Martin N. (2007) *Chem. Senses* 32: 205-214.

ODORANT MIXTURE GESTALT

A.J. Kurtz¹, H.T. Lawless², T.E. ACREE¹

¹ *Food Science & Technology, Cornell University, Geneva NY 14456, USA*

² *Food Science, Cornell University, Ithaca NY 14850, USA*

Abstract

Octanal (C₈) and hexanal (C₆) exhibit two distinct qualia, the quale of C₈ is citrus and the quale of C₆ is green. This paper examines figure-ground perception of C₆-C₈ binary mixtures using an odour reference matching task while varying concentration ratios within the binary mixtures. Three perceptible concentrations of C₆ and C₈ (low (**L**), medium (**M**), and high (**H**)) were determined. Panellists were trained to properly match individual component odours to the corresponding reference. The reference odour is the “figure” while the other odorant within the mixture is the “ground”. Upon completion of the training task, panellists were presented with a series of odour mixture matching tasks. Both C₆ and C₈ matching tasks were tested, the figure odorant is indicated in **bold**, and ground odorant is not bolded. Stimuli for the C₆ matching tasks were: **6L**-8M, **6M**-8L, **6M**-8M, **6M**-8H, and **6H**-8M. Stimuli for the C₈ matching task were: **8L**-6M, **8M**-6L, **8M**-6M, **8M**-6H, **8H**-6M. When the figure odorant was of equal or lower intensity than the ground odour (C₆ matching task: **6L**-8M, **6M**-8M, **6M**-8H; and C₈ matching task: **8L**-6M, **8M**-6M, **8M**-6H), panellists matched these mixtures to references of lesser intensity. When the figure odorant was of greater intensity than the ground (for C₆ matching tasks: **6M**-8L and **6H**-8M; for C₈ matching tasks: **8M**-6L and **8H**-6M) mixtures matched to the proper reference. When the figure and ground are similar intensity the perception is suppressed. The Gestalt interpretation of figure-ground phenomena in vision may be applicable to odour-mixture perception and determine how flavour is predicted from chemistry.

Introduction

With experience humans perceive single odours in a single sniff easily and accurately. Although the process of perceiving an odour is quite rapid, as the number of components within the mixture increases, identification of odorants within the mixture decreases. Detection of odorants in mixtures is dependent on several factors including odorant ratio intensity, similar/ dissimilar odour quality, training, and time.

Elemental processing of odour mixtures states that components within a mixture are perceptible parts of a whole (1). Combinatorial odour processing states that components within a mixture create a novel odour different from the components (2). A qualia (percept) is formed when an odorant (ligand) binds to an olfactory receptor (OR). More than a single ligand can activate an OR, although the activation may be strongest to a particular set of ligands (3). Zhao et. al. (3) identified the first ligand-receptor pair in rats as octanal (C₈)-OR-I7. However, OR-I7 elicited little to no response when exposed to the single carbon homologue C₆. Kittel (4) examined a series of straight chain aldehydes ranging in length from 6-12 carbons using free choice profiling illustrating C₆ as grassy/ green in character while aldehydes C₇-C₁₂

were citrus. Thus, C₆ and C₈ have dissimilar odour qualities as well as dissimilar OR binding properties.

Dissimilar odorants are more easily perceived in odour mixtures (5). Depending on the intensities of odorants in binary mixtures, the perceptions of the mixture change due to mixture suppression and odorant quality (6). Training, odour quality, and intensity can influence the ability to detect odours within a mixture. Dissimilar odours are more easily perceived within mixtures, but it is unclear how odours are perceived when odorants are at equal intensities.

Rubin (1921), studied figure-ground gestalt theory using ambiguous images. Rubin's vase, one of the most famous ambiguous images presents the viewer with two separate images simultaneously where the viewer sees only one at a time (Figure 1) (7). The ability to perceive these forms in the ambiguous images is the result of the gestalt effect. Our brains recognize figures within an image instead of the lines and curves that create it. Rubin reached several conclusions concerning the properties of visual gestalt which demonstrated that context is extremely important to image formation and distinct properties of an image such as colour can influence the distinctions made for figure and ground assignments (7).

The ability to smell a component of a mixture is similar to the detection of a figure in vision. Several studies have demonstrated the ability to distinguish a component (figure) from the remaining mixture (ground) (5, 8). The purpose of this study is to examine binary mixtures of C₆ and C₈, odorants with dissimilar odour quality and OR binding.



Figure 1. Rubin's vase, the contours of the vase create the image of two faces.

Experimental

Panellists. Six panellists, five women and one man, non-smokers with normal olfactory function and mean age of 28.2 (S.D. 3.2) years, volunteered to participate. Experimental protocol was reviewed and approved by the Committee on Human panellists of Cornell University.

Stimuli. Straight chain aliphatic aldehydes C₆ and C₈, were obtained from Sigma-Aldrich (ST. Louis, MO). All odorants were dissolved in poly(ethylene glycol) (PEG). Low (L), medium (M), and high (H) intensity dilutions were made for both odorants. C₆ concentrations were 4.1 mM (6L), 20.3 mM (6M), 244 mM (6H) and C₈ were 1.0 mM (8L), 4.0 mM (8M), and 64.0 mM (8H). Odorants were presented in 250 mL polyethylene squeeze modified with 0.5 inch Teflon ball fitted around the neck of the bottle for nasal comfort, and labelled with a random three-digit code. Binary mixtures are illustrated in Table 1. Stimuli were presented on perfumer's blotters dipped in the

stimuli to 1 cm, placed in the plastic squeeze bottles, and left to equilibrate for one hour prior to testing. All bottles contained two perfumer's strips. For single odorants, one strip was dipped in odorant and the other in solvent (PEG).

Training. Panellists learned to distinguish L, M, and H intensities of each odour using a reference-matching task (ABC-X) for both C₆ and C₈. Panellists were trained in individual sessions for odorants C₆ and C₈. The AB-X sensory test asks panellists to match stimulus X to either reference A or B (29). Panellists examined references A (L), B (M), and C (H), and were presented with bottles containing L, M, and H intensities of the odorants. Panellists were asked to match the stimuli to the appropriate reference (Figure 2). A 30-second break occurred between each judgment. Panellists were required to receive a score of 100% on the odour reference-matching task before evaluating mixtures. During each session two sets of seven odorant bottles were presented, where between each set there was a five-minute break.

Mixture sorting task. Panellists were presented with references of single odorants as in the training session; however, binary mixtures of C₆ and C₈ were added to the sorting task. There were a total of eight mixture reference task sessions. A 30-second inter-stimulus interval occurred between each odour intensity determination with a five-minute break in between the presentation of a new set of odorants.

Table 1. All mixture stimuli presented during testing. The figure odorant is in bold.

C6	6L -8M	6M -8L	6M -8M	6M -8H	6H -8M
C8	8L -6M	8M -6L	8M -6M	8M -6H	8H -6M

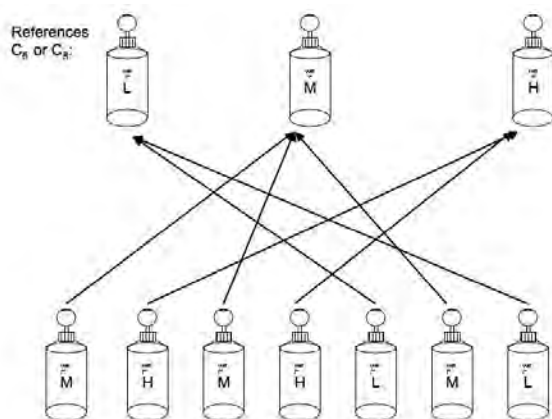


Figure 2. Example of either C₆ or C₈ training task for odour matching task. Odorants must be successfully matched to the corresponding reference.

Results

Odorants in mixtures often display mixture suppression. Panellists were asked to determine the intensity of a single odorant within a binary mixture and match the odorant for intensity to a specific reference. The reference odour in the mixture is defined as the figure odorant, while the other odorant present within the mixture is defined as ground. An example of increasing ground intensity in a C₈ matching task would be **8M**-6L, **8M**-6M, **8M**-6H. As the intensity of the ground odour increases (in

this example C_6) demonstrated figure suppression, where the panellist's ability to determine the figure's (C_8) intensity decreased with increasing ground intensity. Panellists also demonstrated poor discrimination of C_8 for mixtures **8L-6M**. However, panellists were able to accurately distinguish the figure when figure intensity was greater than ground intensity (**8M-6L** and **8H-6M**). The same results were found for C_6 matching tasks. When the intensity of the figure is diminished by the intensity of the ground, the panellist must decide the degree to which the figure intensity has decreased (9).

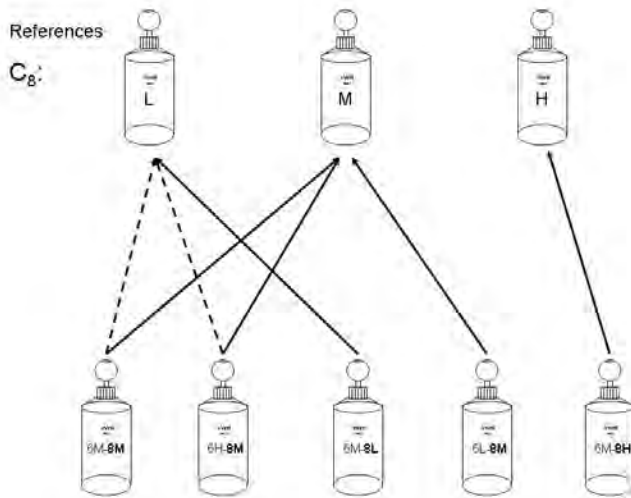


Figure 3. Figure suppression, as indicated by the dashed line, for both C_6 and C_8 mixture matching tasks, as the ground intensity of the mixture increases, the figure intensity is suppressed due to the ground intensity concealing the figure.

Mixture suppression is most evident in mixtures **6M-8L**, **8M-6H**, and **6M-8H**; however, in a separate study examining cross-adaptation of odorants C_6 , C_8 , C_{10} , and C_{11} , C_6 did not cross-adapt with C_8 , C_{10} , or C_{11} (10). The inability to cross-adapt C_6 and C_8 , inability to excite OR-17, and difference in free-choice profiling, suggests these two odorants excite different OR families. However, these two odorants display mixture suppression, suggesting that mixture suppression is a cross-adaptation that occurs through different neural mechanisms.

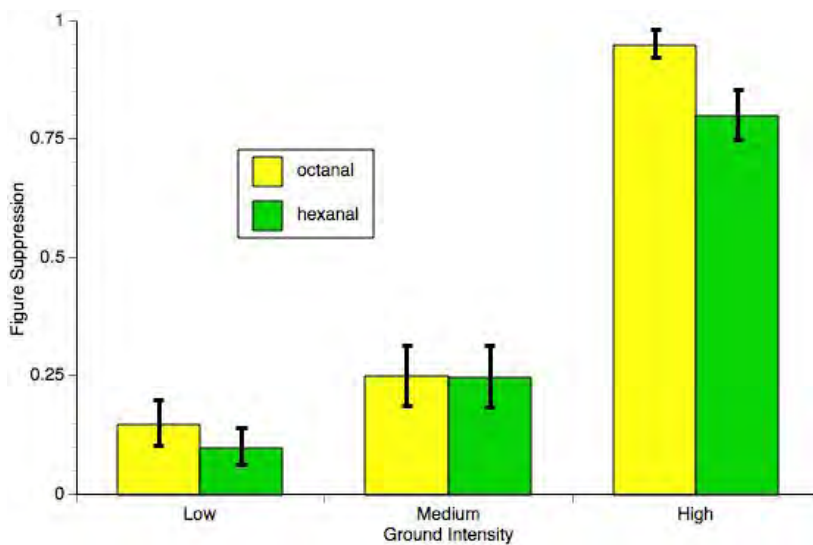


Figure 4. Figure suppression for both C_6 and C_8 mixture matching tasks, as the ground intensity of the mixture increases, the figure intensity is suppressed due to the ground intensity concealing the figure.

References

1. Laing D.G., Willcox M.E. (1983) Perception of components in binary odor mixtures. *Chemical Senses* 7: 249-264.
2. Zou Z., Buck L.-B. (2006) *Science* 311: 1477-1781.
3. Zhao H., Ivic L., Otaki J.-M., Hashimoto M., Mikoshiba K., Firestein S. (1998) *Science* 279: 237-242.
4. Kittel K.M., Barnard J., Kurtz A.J., Acree T.E. (2008) Free-choice profiling of OR-I7 agonists and homologues using GC-O. *Chemosensory Perception*, in press.
5. Gottfried J.A., Winston J.S., Dolan R.J. (2006) *Neuron* 49: 467-479.
6. Cain, W. S. & Drexler, M. (1974) *Ann N.Y. Acad. Sci.* 237: 427-439.
7. Yantis, S., Ed. (2001) *Visual Perception: Essential Readings*. Philadelphia, PA: Psychology Press.
8. Kadohisa M., Wilson D.A. (2006) *J. Neurophysiology* 95:1888-1896.
9. Kurtz A.J., Lawless H.T., Acree T.E. (2008) Reference matching of dissimilar binary odor mixtures. *Chemosensory Perception*, in press.
10. Kurtz A.J., Lawless H.T., Acree T.E. (2008) Cross-adaptation between OR-I7 agonists and homologues. *Chemosensory Perception*, in press.

COMPARING SENSORY PROFILES IN LOGARITHMICALLY SERIAL DILUTIONS OF COFFEE AND SOY SAUCE

T. AISHIMA, K. Iizuka, and K. Morita

Chemometrics and Sensometrics Laboratory, 1-197 Sengen cho, Omiya-ku, Saitama 330-0842, Japan

Abstract

We applied the serial dilution sensory analysis to coffee and soy sauce in order to quantify the relative importance of individual sensory attributes in diluted samples. Sensory scores in all attributes exponentially decreased according to dilution values. However, score percentages calculated for individual sensory attributes based on their total in every dilution suggested noticeable changes. In coffee, percentages of *burnt* and *coffee aroma* decreased drastically according to dilution values but those of *sweet aroma*, *green* and *dusty* notes increased inversely. In soy sauce, percentages of *alcoholic* and *burnt* notes decreased but those of *fruity* and *sweet aroma* increased by dilution. PLS regression analysis revealed positive and negative effects of individual attributes to *coffee aroma* and *soy sauce aroma*, respectively.

Introduction

Today the Aroma Extract Dilution Analysis (AEDA) is widely used as an essential technique for aroma research since this analysis can quantify the intensity of individual aroma components (1). However, our nose does not detect aroma components individually, but rather it simultaneously senses a mixture of several aroma notes derived from numerous volatile chemicals, where complicated mutual interactions may take place. As it is widely known, when diluted with water, not only the aroma strength of beverage or liquid food becomes weaker but also the aroma note itself changes or deteriorates. This suggests that a balance or harmony of whole sensory attributes is essential for generating a specific food aroma. Further, while changes in strengths of certain sensory attributes may give critical effects on the aroma note, those of others may not. The descriptive sensory analysis (2) can quantify individual sensory attributes in food by fully taking account of interactive effects of all attributes. Therefore, we attempted to examine the significance of individual sensory attributes for generating unique aroma notes of coffee and soy sauce by applying the serial dilution sensory analysis (SDSA).

Experimental

A marketed canned coffee "Black" (UCC Ueshima Coffee, Kobe, Japan) and deep-coloured type soy sauce (Kikkoman, Tokyo Japan) were diluted 1, 10, 31.6, 100, 316, 562, 1,000, 3,162 and 10,000 folds, *i.e.* logarithms: 0, 1, 1.5, 2, 2.5, 2.75, 3, 3.5 and 4, with purified water. In the whole steps of SDSA, 40 ml of each sample ca. at 25°C was served to the sensory panel in the descending order of dilution values. Strengths of attributes identified commonly in all dilutions in preliminary sessions were quantified by 7 panellists using a line scale. Obtained sensory scores for each

attributes in every dilution were transformed into percentage proportions for individual attributes based on their total in sensory categories, *i.e.* aroma, taste and flavour, to qualitatively compare their profiles. Sensory data were analysed by principal component analysis (PCA) and partial least squares regression (PLSR) analysis using Unscrambler ver. 9.7 (CAMO Software AS, Oslo, Norway).

Results

Coffee. Although we had not supplied any information on the sample property to the sensory panel, they unambiguously identified the *coffee aroma* note even in the thinnest solution. Fifteen attributes, 9 for aroma including *coffee aroma*, 3 for taste and 3 for flavour, have been commonly identified in all dilutions in the preliminary sessions. Sensory scores in all attributes exponentially decreased in accordance with dilution values. However, sensory profiles of percentage proportions for individual attributes for each dilution clearly illustrated significant difference in their aroma quality (Figure 1). As the dilution value increased, percentages of *burnt* and *coffee aroma* decreased drastically but those of *sweet*, *green* and *dusty* notes increased contrarily. Sensory attributes showing larger percentages in highly diluted samples may be derived from highly active compounds (3) but may not necessarily contribute to the *coffee aroma* itself.

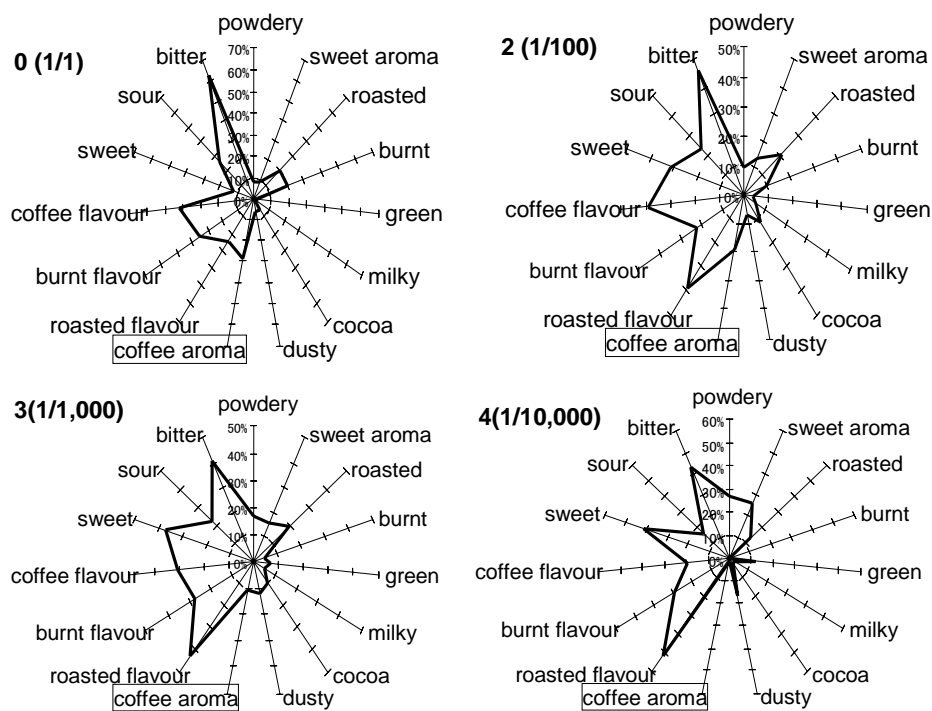


Figure 1. Profiles of sensory attribute proportions (%) in undiluted coffee and its serial dilutions.

Soy sauce. In the preliminary sessions, the sensory panel detected the unique aroma note of soy sauce, even in the thinnest solution. 21 sensory attributes, 11 for aroma including *soy sauce aroma*, 5 for taste and 5 for flavour, were identified in these sessions. As diluted thinner, proportions of *alcoholic* and *burnt* notes decreased rapidly but those of *fruity* and *sweet* notes increased contrarily (Figure 2). On the other hand, some attributes, *i.e.* *yoghurt* and *miso* or soybean paste, initially increased but started decreasing afterwards. In fermented soy products, *i.e.* soy

sauce and *miso*, a very sweet smelling furanone derivative was identified in soy sauce and proposed to be a key aroma compound (4), but increase in the percentage of *sweet aroma* in diluted soy sauce makes the *soy sauce aroma* weaker.

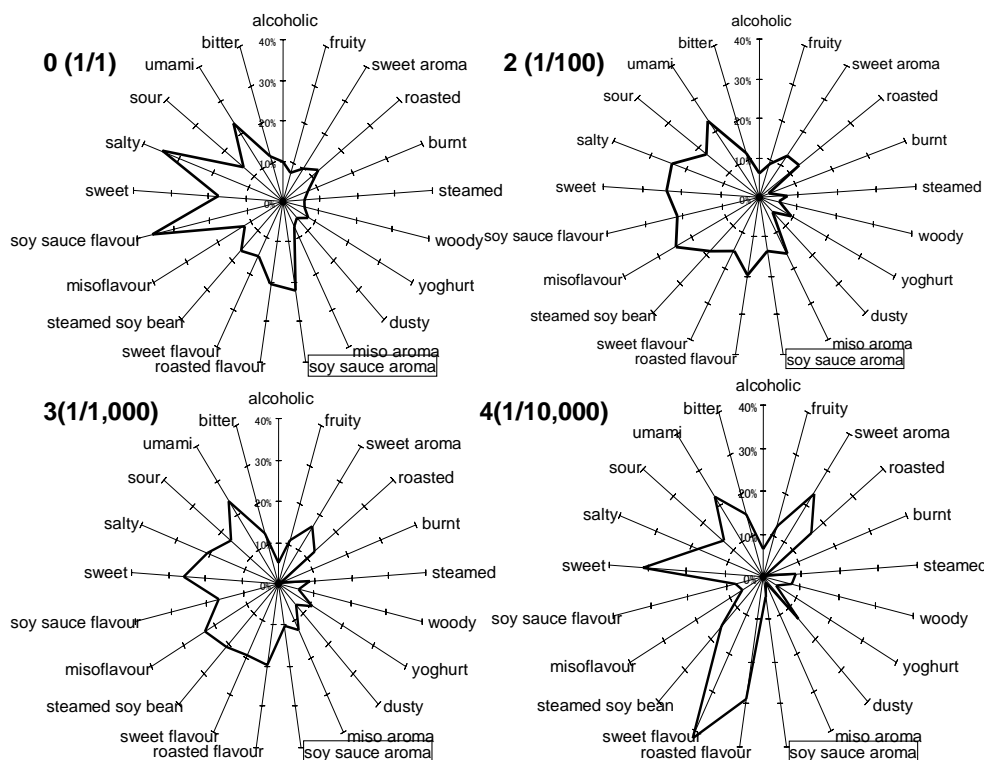


Figure 2. Profiles of sensory attribute proportions (%) in undiluted soy sauce and its serial dilutions.

Chemometric data analysis PCA biplots shown in Figure 3 suggest that whole sensory qualities have changed continuously in accordance with dilution values in both coffee and soy sauce. Against our expectation, however, the closest attribute to undiluted coffee was *burnt flavour* but instead *coffee aroma* located closely to the 10folds dilution (Figure 3A). On the other hand, *sweet* and *green* notes located nearby highly diluted coffee. Similarly, *alcoholic* aroma was situated in the vicinity of undiluted soy sauce but *soy sauce aroma* itself was placed adjacent to the 10folds dilution (Figure 3B).

PLSR models highly predictive for *coffee aroma* ($R^2 = 0.991$) and *soy sauce aroma* ($R^2 = 0.989$) were calculated using other 8 and 10 aroma attributes as predictors, respectively. PLS loading plots clearly suggest high contribution of *burnt* and *roasted* notes to *coffee aroma* (Figure 4A) and *burnt* and *alcoholic* notes to *soy sauce aroma* (Figure 4B), respectively. However, these attributes indicated their significant contribution to *coffee aroma* and *soy sauce aroma* do not necessarily occupy larger proportions in sensory profiles shown in (Figures 1) and (Figure 2), respectively.

High contribution of *burnt* and *roasted* notes to the *coffee aroma* strongly support the importance of roasting process in coffee manufacturing. In soy sauce, *alcoholic* and *burnt* aroma notes derived from yeast fermentation in the *moromi* or mash period and from pasteurization process of raw soy sauce, respectively, demonstrates the significance of these two processes for brewing quality soy sauce, as it has been widely recognized by soy sauce manufacturers in Japan.

Expression of Multidisciplinary Flavour Science

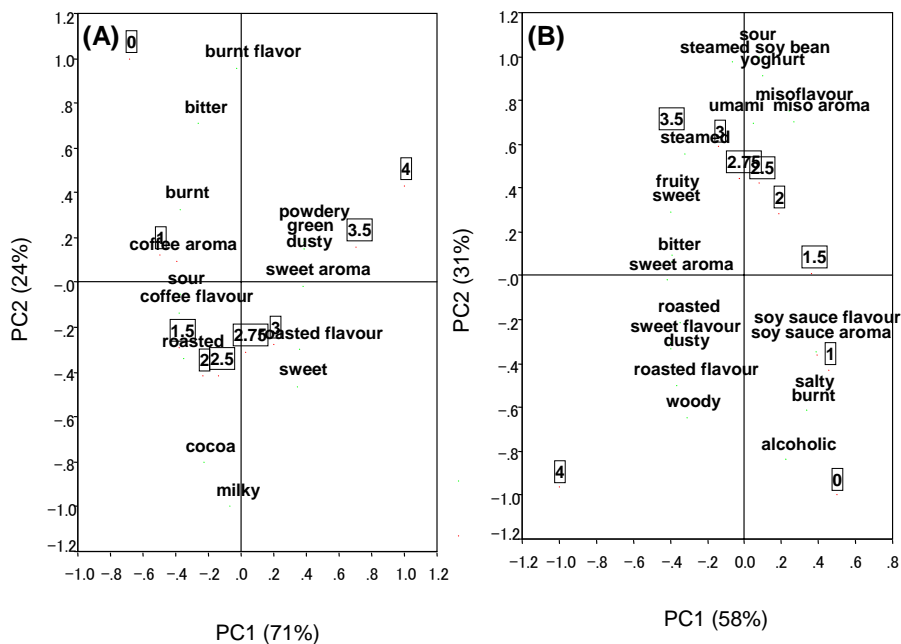


Figure 3. PCA biplots for coffee (A) and soy sauce (B).

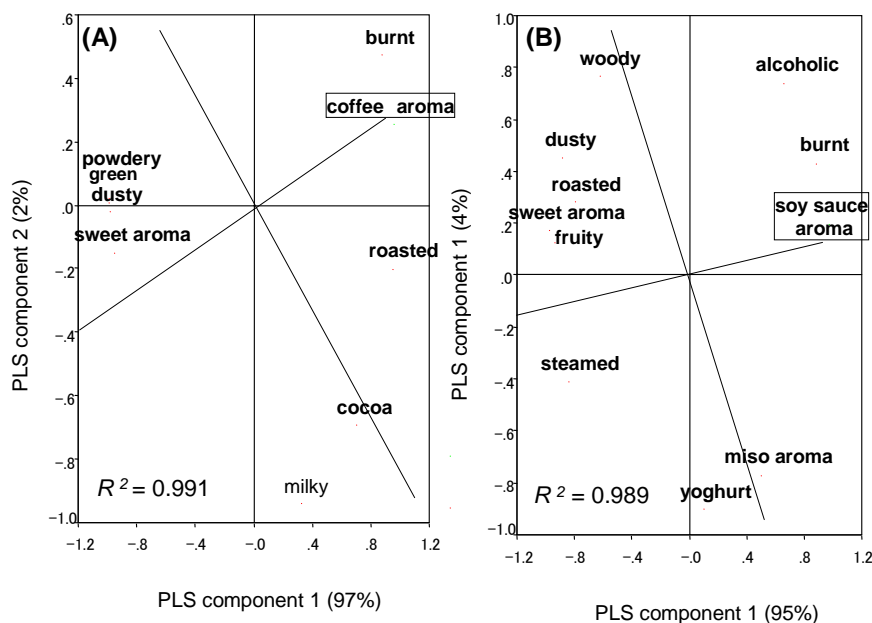


Figure 4. PLS loading plots for coffee (A) and soy sauce (B).

References

1. Ullrich F., Grosch W. (1987) *Z. Lebensm. Unters. Forsch.* 184: 277-282.
2. Stone H., Sidel J., Oliver S., Woolsey A., Singleton R.C. (1974) *Food Technol.* 28(11): 24-34.
3. Semmelroch P. and Grosch W. (1996) *J. Agric. Food Chem.* 44: 537-543.
4. Nunomura N., Sasaki M., Yokotsuka T. (1980) *Agric. Biol. Chem.* 44: 339-351.

CORRELATION BETWEEN SENSORY TYPICALITY AND AROMATIC COMPOSITION IN SAUTERNES BOTRYTISED WINES

E. Sarrazin, T. Tominaga, and PH. DARRIET

Faculté d'Œnologie, Institut des Sciences de la Vigne et du Vin, UMR 1219, INRA, Université Bordeaux II, 351 cours de la Libération, F-33405 Talence Cedex, FRANCE

Abstract

Sauternes botrytised wines are famous for their complex aromas. However, little research has been performed on the odorants that contribute to their distinctive flavour. In the first step of this work, the Sauternes wine sensory concept was studied. Thirty wines were evaluated by a 13-expert panel focusing on Sauternes typicality. This made it possible to validate the existence of a specific Sauternes wine aroma, which differs from dry white wines and from other sweet wines. In a second step, 18 odorants recently characterised in Sauternes wines, were quantified in 20 wines to investigate relationships with typicality. According to their chemical composition, the best Sauternes examples were clearly distinguished from dry white wines and from other sweet wines. This supported that sensory differences between botrytised and dry white wines are mainly due to aromatic composition changes.

Introduction

Sauternes botrytised wines are well-known for their exceptional range of aromas evoking citrus, honey and dried fruits. Recently, some key-odorants have been identified in Sauternes wines (1, 2). However, most of these compounds are also present in dry white wines made from the same grape varieties (*i.e.* Sémillon and Sauvignon blanc). Therefore, their correlation with Sauternes typicality needed to be investigated. In the first step of this work, the existence of a Sauternes wine concept was studied. Then, 18 odorants were quantified in numerous wines to assess their relationships with Sauternes typicality.

Experimental section

Validation of the Sauternes sensory wine concept. The existence of a Sauternes wine concept was studied using the method developed by Ballester *et al.* (3). Thirty commercially available wines were presented to the sensory panel (Table 1). The jury consisted in 13 subjects (11 men, 2 women) with an extensive experience of Sauternes wines (*e.g.* enologists, winemakers). For each wine, judges were asked to assess the degree of typicality on an 11-point structured scale, according to their own Sauternes wine concept, (0: very bad example of Sauternes wine; 10: very good example). Wines were presented in dark coded glasses and were evaluated only orthonasally (sniffing after swirling).

Quantitative assays of odorants. Twenty wines were selected among the 30 evaluated by the expert panel. They consisted in 13 Sauternes botrytised wines (best

and worst examples), 3 Bordeaux dry white wines, and 4 sweet wines from other French regions.

Furaneol[®], homofuraneol, norfuraneol, methional, phenylacetaldehyde, phenylacetic acid, phenylethyl acetate, ethyl levulinate, and ethyl caproate were quantified using the method described by Sarrazin *et al.* (1). 4-Methyl-4-sulfanylpentan-2-one (4M4SP), 3-sulfanylhexan-1-ol (3SH), 3-sulfanylpentan-1-ol (3SP), 3-sulfanylheptan-1-ol (3SHp), and 2-methyl-3-sulfanylbutan-1-ol (2M3SB) were quantified according to Sarrazin *et al.* (2). Lactones were assayed following the method proposed by Ferreira *et al.* (4).

For each odorant, correlation coefficients were calculated between quantitative assays and typicality mean values. Pearson-Kendall tables were used to investigate relationships with Sauternes typicality.

Table 1. Wines selected for sensory analysis (origin, grape varieties, vintages, and abbreviations used on Figures 1 and 2).

	Number of samples	Grape varieties	Vintages	Abbreviation
Sauternes botrytized wines	23	Sémillon Sauvignon blanc	1996 (1) 2001 (9) 2004 (13)	<i>Liq</i>
Bordeaux dry white wines	3	Sémillon Sauvignon blanc	2005	<i>Sec</i>
Other French sweet wines	4	Chenin or Petit Manseng	1997 (1) 2003 (1) 2004 (2)	<i>CL-97</i> <i>CL-03</i> <i>Ju-04 and Pa-04</i>

Results and Discussion

Validation of the Sauternes sensory wine concept. In a first step, Sauternes wine typicality was studied as proposed by Ballester *et al.* (2005) (3). To represent wines according to their sensory differences, a principal component analysis (PCA) was performed on the scores of the experts. As shown in (Figure 1), the first two axes represented 59% of the original variability. The 13 judges (represented by black segments) were all situated on the positive side of F1 axis that demonstrated a good agreement among panellists. Moreover, PCA made it possible to isolate the best Sauternes examples from the non-Sauternes samples. As wines were only assessed orthonasally in dark glasses, these results validated the existence of a typical Sauternes wine aroma, which differs from dry white wines and from other sweet wines.

Quantitative assays of odorants. In a second step, 18 volatiles recently characterized in Sauternes wines (1, 2), were assayed in 20 wines to investigate relationships with Sauternes typicality. Pearson-Kendall coefficients were determined from the quantitative assays of each odorant and the typicality mean values of the 20 wines (Table 2). Volatile thiols (4M4SP, 3SH, 3SP, 3SHp, and 2M3SB) were shown to make a positive correlation with sensory representativeness. The same was true for phenylacetaldehyde, phenylacetic acid, methional, ethyl levulinate, γ -nonalactone, and massoia lactone, as well as for whisky lactones (*cis* and *trans*), which are extracted from oak wood during ageing.

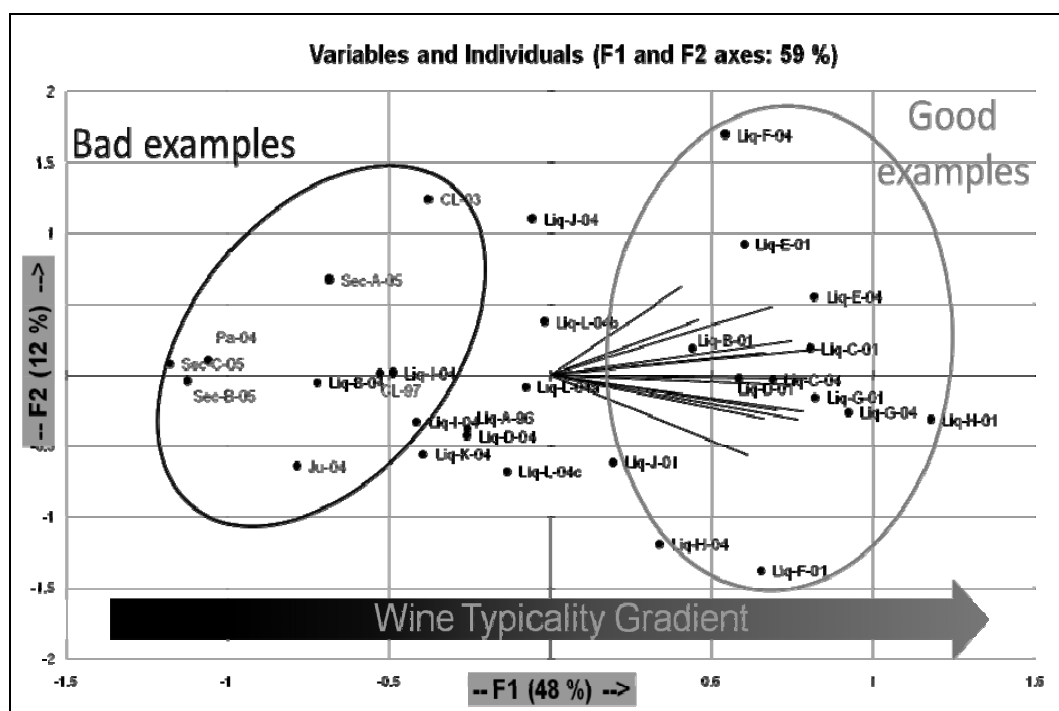


Figure 1. PCA obtained from the scores of the 13 judges for the 30 wines. Isolation of the best Sauternes examples according to their olfactory profile.

Table 2. Correlation between sensory typicality and odorant assays of wines.

Compounds	Correlation with Sauternes typicality	
4M4SP, 3SH, 3SP, 3SHp, 2M3SB	$p < 0.01$	+
Methional	$p < 0.10$	+
Phenylacetaldehyde	$p < 0.05$	+
Phenylacetic acid	$p < 0.02$	+
Furaneol®, Homofuraneol, Norfuraneol	Non significant	+
γ -nonalactone	$p < 0.01$	+
Massioa lactone	$p < 0.10$	+
Whisky lactones (<i>cis</i> and <i>trans</i>)	$p < 0.01$	+
Ethyl levulinate	$p < 0.01$	+
Ethyl caproate	$p < 0.01$	-
Phenylethyl acetate	$p < 0.05$	-

On the contrary, fermentative esters, such as ethyl caproate or phenylethyl acetate, showed negative correlations with the level of typicality. This result was in agreement with previous work showing the hydrolysis of fermentative esters by *Botrytis cinerea* esterase (5).

Concerning furanones, no significant correlation was demonstrated. Actually, the levels of furaneol®, homofuraneol, and norfuraneol were high in Sauternes wines, as well as in the other sweet wines.

To compare samples according to their chemical composition, a second PCA was performed using odorant concentrations as variables. This statistical processing gave a plan where the axes F1 and F3 showed 70% of the total variation. As shown in (Figure 2), this clearly isolated the best Sauternes examples from dry white wines and from other sweet wines. Therefore, these results validated the role of the odorants in the typical Sauternes aroma. In addition, this supported that sensory differences between botrytised and dry white wines were mainly due to aromatic composition changes.

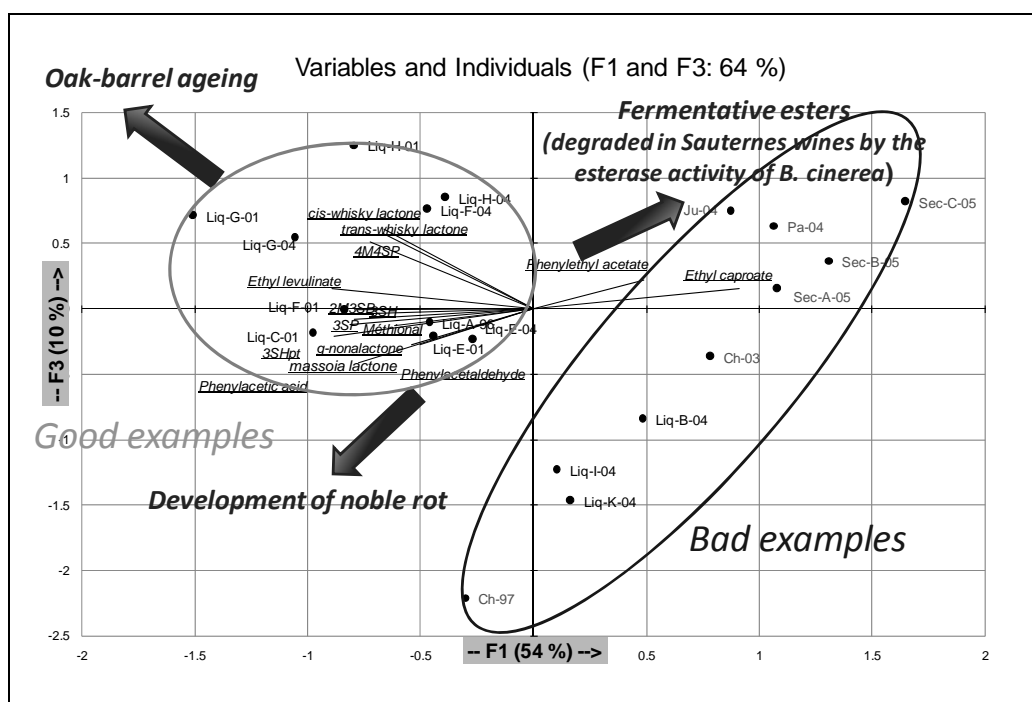


Figure 2. PCA obtained from the odorant concentrations of 20 wines and wine typicality mean values. Isolation of the best Sauternes examples according to their chemical composition.

Conclusion

These results validated the existence of a typical Sauternes wine aroma that differs from other sweet wines and from dry white wines. Moreover, this study established a correlation between Sauternes typicality and 15 odorants already identified. Reconstitution tests must now be performed to evaluate the sensory contribution of the volatile compounds.

References

1. Sarrazin E., Dubourdieu D., Darriet P. (2007) *Food Chem.* 103: 536-545.
2. Sarrazin E., Shinkaruk S., Tominaga T., Bennetau B., Frérot E., Dubourdieu D. (2007) *J. Agric. Food Chem.* 55: 1437-1444.
3. Ballester J., Dacremont C., Le Fur Y., Etiévant P. (2005) *Food Qual. Pref.* 16: 351-359.
4. Ferreira V., Jarauta I., Ortega L., Cacho J. (2003) *J. Chrom. A* 1025: 147-156.
5. Dubourdieu D., Ribéreau-Gayon P. (1985) *Bull OIV*, 648-649.

SENSORY EVALUATION OF COMMERCIAL APPLE JUICES AND RELATION TO SELECTED KEY AROMA COMPOUNDS

M. STEINHAUS, S. Baer, and P. Schieberle

Deutsche Forschungsanstalt für Lebensmittelchemie, Lichtenbergstraße 4, D-85748 Garching, Germany

Abstract

Commercial apple juice samples of 23 different brands were analysed for their hedonic value as well as for the concentrations of four selected key aroma compounds ((E)- β -damascenone, hexanal, (E)-2-hexenal, dimethyl sulphide). Results showed that juices with good hedonic values were rather high in (E)-2-hexenal and hexanal and low in dimethyl sulphide, whereas juices with poor sensory scores were either low in hexanal and (E)-2-hexenal or high in dimethyl sulphide. Throughout all samples, naturally cloudy juices showed higher concentrations of cooked apple-like smelling (E)- β -damascenone than filtrated samples.

Introduction

The consumption of fruit juices in Europe amounts to approximately 25 L per capita and year (1). In addition to orange juice, apple juice makes up a major part of it, particularly in Germany, the world's leading country in fruit juice consumption (40 L per capita and year).

Our recent research on the key aroma compounds of apple juice (2) revealed cooked apple-like smelling (E)- β -damascenone and grassy smelling hexanal as the odorants with the highest odor activity values. Omission tests applied on an apple juice reconstitute containing 15 odorants, namely (E)- β -damascenone, hexanal, diacetyl, acetaldehyde, dimethyl sulphide, (Z)-1,5-octadien-3-one, (E)-2-hexenal, (Z)-3-hexenal, ethyl 2-methylbutanoate, methional, 1-octene-3-one, 1-butanol, methyl 2-methylbutanoate, 1-hexanol, and linalool, additionally showed the major importance of apple-like smelling (E)-2-hexenal for the overall flavour of apple juice. On the other hand, dimethyl sulphide, exhibiting an asparagus-like smell, may cause an undesired vegetable-like off-flavour in apple juice when present in higher concentrations.

The aim of the following work was to assess the hedonic values of commercial apple juices in the market by sensory evaluations and compare the results to the concentrations of the key odorants (E)- β -damascenone, hexanal, (E)-2-hexenal, and dimethyl sulphide.

Experimental

Apple juice samples of 23 different brands were purchased from local supermarkets in the Munich area (Germany). Samples included clear and cloudy juices, juices from concentrate and NFC-juices, as well as conventionally produced ones and those with bio-label. Prices ranged from 0.55 to 3.73 €/L.

Hedonic scoring was performed by 16 trained panelists using a scale adopted from German school marks ranging from 1 to 6 with 1 = very good, 2 = good, 3 = satisfactory, 4 = fair, 5 = poor, 6 = unsatisfactory.

Concentrations of (E)- β -damascenone, hexanal, (E)-2-hexenal and dimethyl sulphide were determined by stable isotope dilution analyses using [$^2\text{H}_6$]- (E)- β -damascenone, [$^2\text{H}_4$]-hexanal, [$^2\text{H}_2$]- (E)-2-hexenal, and [$^2\text{H}_6$]-dimethyl sulphide as internal standards. Standards were added to the juice samples before work-up. Determination of dimethyl sulphide was achieved by headspace-SPME in combination with a GC-GC-MS-system (3). Using the same GC-GC-MS-system, (E)- β -damascenone, hexanal and (E)-2-hexenal were quantified after solvent extraction, isolation of volatiles by SAFE distillation (4), and liquid injection.

Results

Hedonic scores (Figure 1) ranged from 2.1 (good) to 4.9 (poor). Naturally cloudy juices showed greater variance in the hedonic value (2.1 - 4.9) than clear juices (3.3 - 4.1). Concentrations of (E)- β -damascenone, hexanal, (E)-2-hexenal and dimethyl sulphide (Figure 2) were highly variable among the 23 apple juices analysed.

A direct correlation of hedonic scores to the concentrations of any individual aroma compound was not observed. But, juices with good hedonic values predominantly showed rather high concentrations of (E)-2-hexenal and hexanal and low concentrations of dimethyl sulphide, whereas most juices with rather bad sensory scores were either low in hexanal and (E)-2-hexenal or high in dimethyl sulphide. However, samples not following that rule (e.g. 7, 17) indicate that further aroma-active compounds have an additional influence on the overall hedonic value.

A clear correlation was found between filtration and (E)- β -damascenone concentration (Figure 2, topmost diagram). Naturally cloudy apple juices showed considerably higher concentration values (9-17 $\mu\text{g/L}$) than clear samples (1-6 $\mu\text{g/L}$). Since (E)- β -damascenone is not present in raw apple juices, but formed during juice pasteurization (5), this observation indicates that a major part of its precursors is removed during the filtration process.

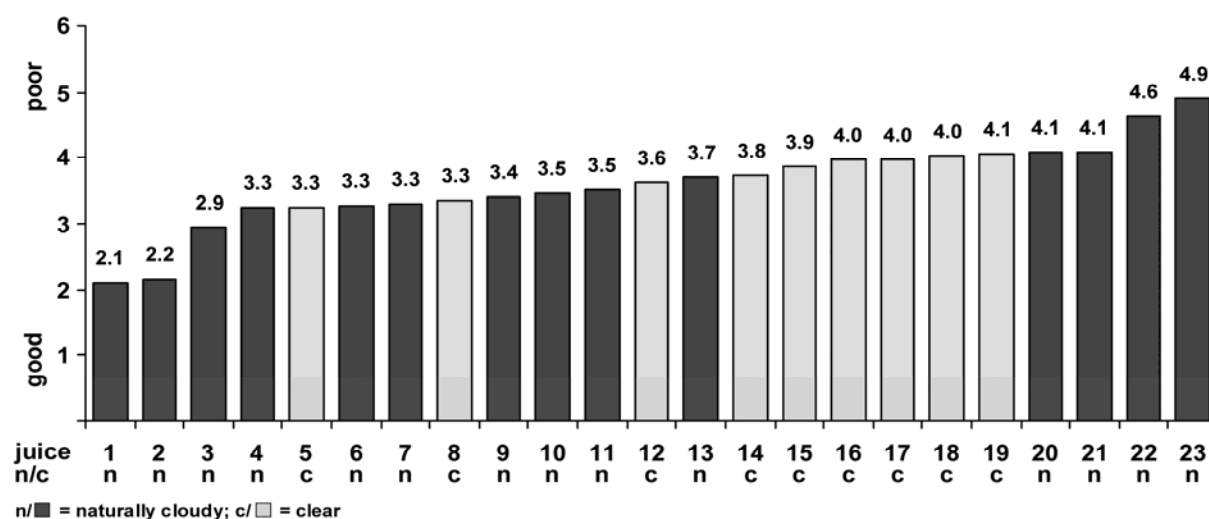


Figure 1. Sensory evaluation of the hedonic value of 23 commercial apple juices.

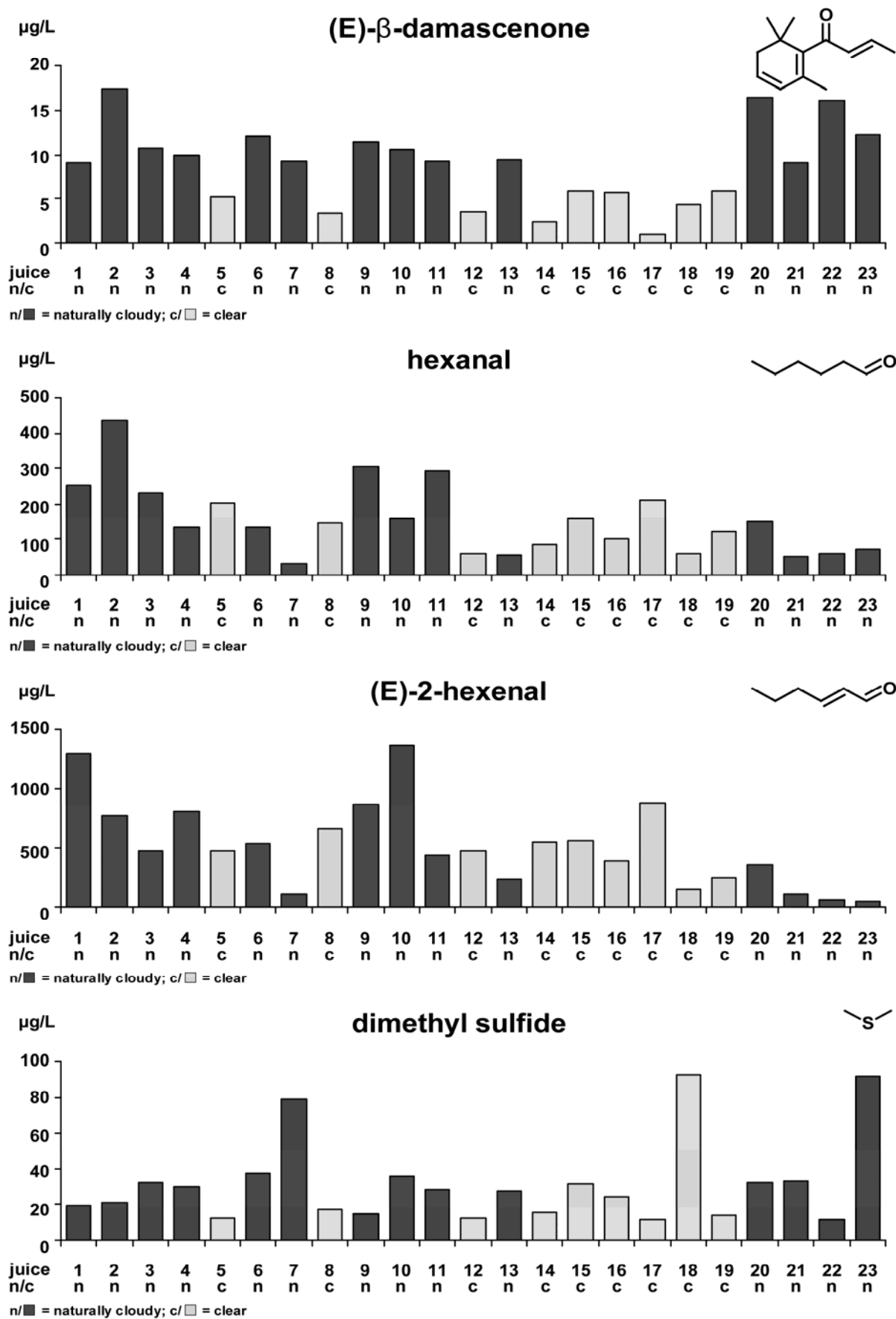


Figure 2. Concentrations of selected key odorants in 23 commercial apple juices.

References

1. Verband der Deutschen Fruchtsaft-Industrie. www.fruchtsaft.net.
2. Steinhaus M., Bogen J., Schieberle P. (2005) *Lebensmittelchemie* 59: 91.
3. Steinhaus M., Fritsch H.T., Schieberle P. (2003) *J. Agric. Food Chem.* 51: 7100-7105.
4. Engel W., Bahr W., Schieberle P. (1999) *Eur. Food Res. Technol.* 11: 237-241.
5. Steinhaus M., Bogen J., Schieberle P. (2008) In *Recent Highlights in Flavour Chemistry & Biology*. Proceedings of the 8th Wartburg Symposium (Hofmann T., Meyerhof W., Schieberle P., eds.); *Deutsche Forschungsanstalt für Lebensmittelchemie*, Garching, pp. 123-128.

DO DIFFERENCE TESTS PREDICT ECOLOGIC CONSUMERS' DISCRIMINATION PERFORMANCE?

L. MORIN-AUDEBRAND^{1,2}, C. Sulmont-Rossé¹, and S. Issanchou¹

¹ INRA, UMR 1129 FLAVIC, F-21000 Dijon, France

² HES-SO Wallis, Rte du Rawyl 47, CH-1951 Sion, Switzerland

Abstract

This study investigates participants' ability to discriminate between a drink they regularly consume and slightly varied versions of this drink. Two kinds of tests are compared: a difference test ("Is the product that I am tasting identical to or different from the reference given by the experimenter?"), classically used to test discrimination between an "old" product and a one produced with a new process or recipe, and a memory test ("Is the product that I am tasting identical to or different from the one I regularly consume?"), much more close to consumers' natural situation of comparison of a new product with an "old" one. This study revealed that difference test results do not predict discrimination ability that occurs in a much more natural context of decision such as memory test, suggesting that memory tests could be preferred to classic difference tests when producers want to check if consumers discriminate between an old and a new formula of a product.

Introduction

When food producers want to change ingredients or process while keeping unchanged sensory perception of the product, they classically conduct difference tests such as duo-trio, triangle test, A-NonA..., where both the 'old' version and the new version are presented conjointly and compared. However in a real life situation, such comparison rarely occurs, but the perception induced by the tasted product is compared to memorized information from previous experience involving the same or similar foods.

The present study intended to compare consumers' ability to discriminate a regularly consumed soft drink (the target of the study) from slightly varied versions of this drink in two situations: first, participants were asked to discriminate distractors from a remembered target (memory test); second, participants were asked to discriminate distractors from a physically presented target (difference test). While difference tests are often used in sensory evaluation to maximise the chance to reveal a difference between products ("Is the product that I am tasting identical to or different from the reference given by the experimenter?"), a memory test is much closer to what happens in daily life ("Is the product that I am tasting identical to or different from the one I regularly consume?"). In fact, difference test implies intentional (voluntary) learning and short-term cognitive processes while memory test implies incidental (involuntary) learning and long-term cognitive processes.

Experimental

The market leader brand of non-sparkling soft drinks was chosen as target for the study. Six distractors were produced by varying the concentration of either a sweet or sour or flavour compound. The just noticeable differences (JNDs) were used as common unit of variation to ensure that variation was slight but perceptible. A preliminary experiment was carried out with a separate group of 16 young adults to estimate the JNDs of each compound in the target drink, according to the procedure described by Köster et al. (1). The varied compounds were the same as those actually used in the production of the target drink.

Ninety-five regular consumers of the target drink were recruited (41 men, 54 women; 18 to 30 years old). Twenty-three percent consumed only the target brand for this type of soft drink (exclusive consumers). The others consumed several such brands, but mostly the target brand (non-exclusive consumers). Fifty-three percent consumed the target several times a week (weekly consumers). The others consumed the target between once and four times a month (monthly consumers).

In a first session, the participants performed a memory test, consisting in a recognition test. They received a monadic random series of ten samples, consisting of four samples of the target and one sample of each of the six distractors. They were asked to taste each sample and to answer the question “Is this sample identical to or different from your regular drink?”.

In a second session, the participants performed a difference test, consisting in an A-NonA test. They received a monadic series of ten pairs, each consisting of a reference sample, identical to the target, and an experimental sample. The 10 experimental samples comprised four samples of the target and one sample of each of the six distractors. For each pair, participants were asked to taste the reference sample and then the experimental sample and to answer the question “Is this sample identical to or different from the presented reference?”.

The sessions were conducted in a sensory room under red light. Samples were coded with three-digit numbers that varied between tests. Presentation order was systematically varied between participants and tests, with a limiting principle of never having more than two successive targets. After each sample (memory test) or pair (difference test), participants were asked to take a break of one minute and to rinse their mouth with crackers and water.

Concerning data analysis, for each participant and each test, four categories of answers were determined (2): the number of hits (saying “Identical to my favourite drink / to the reference” to a target sample), and its complement, the number of misses (saying “Different from my favourite drink / from the reference” to a target sample), and the number of false alarms FA (saying “Identical to my favourite drink / to the reference” to a distractor sample) and its complement, the number of correct rejections CR (saying “Different from my favourite drink / from the reference” to a distractor sample). Then, an index Z was calculated as follows to evaluate participants' ability to discriminate between target and distractors for each test: $Z = \log((\text{hits} + 0.5) / (\text{misses} + 0.5)) - \log((\text{FA} + 0.5) / (\text{CR} + 0.5))$. A Z index higher than zero indicated that participants were able to discriminate between target and distractors, *i.e.* they recognized the target among the distractors in the memory test or they differentiated the target and the distractors in the difference test.

Results

An ANOVA performed on Z value, with test (discrimination; memory), consumption frequency (weekly; monthly), consumption exclusivity (exclusive; non-exclusive) and their interactions as fixed factors, and participant as random factor, showed a significant effect of test on Z ($F(1, 91) = 10.35, p < 0.01$). In fact, participants were not able to discriminate the target from the distractors during the memory test ($Z = -0.08, SE = 0.14, t(94) = -0.59, p > 0.05$) but were able to perceive a difference between the target and the distractors during the difference test ($Z = 0.74, SE = 0.13, t(94) = 5.56, p < 0.001$). Nevertheless, the observation of the individual Z values revealed that 40 participants out of the 95 obtained a Z index higher than zero in memory test and 64 in difference test, with values ranging from -2.8 to +3.5 in both cases. The ANOVA did not reveal any significant effect of consumption frequency or consumption exclusivity on the Z index, whatever the test (no significant interaction).

In order to check the link between performance on the difference test and on the memory test at an individual level, correlation between Z values of both tests was calculated and appeared to be non significant. ($r^2 = 0.002$). In other words, participants with high memory performance did not necessarily obtain high difference performance and vice versa (Figure 1).

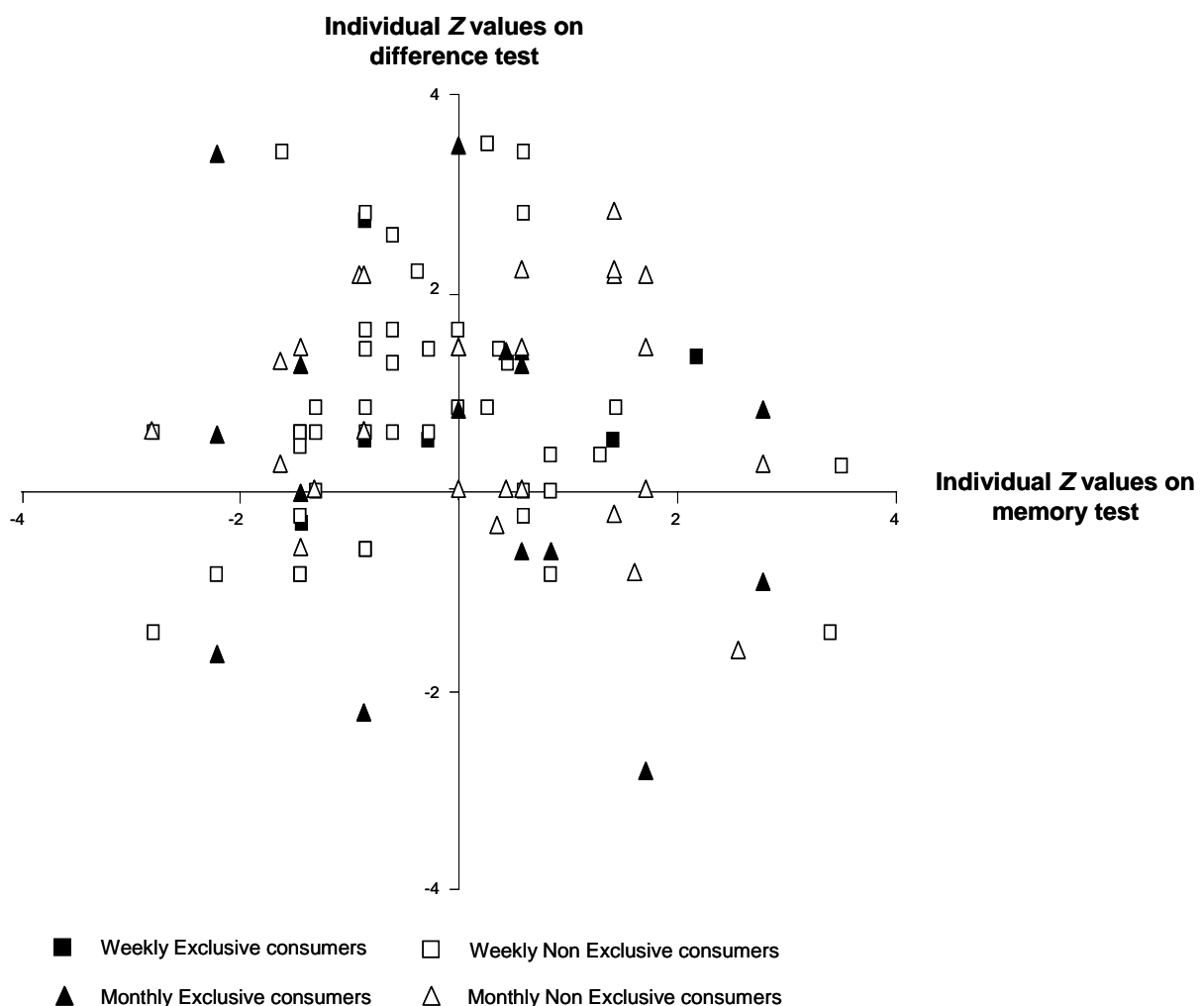


Figure 1. Individual Z values on memory test plotted against individual Z values on difference test. Each point corresponds to a participant.

Discussion

This study investigated participants' ability to discriminate between a target drink and slightly varied versions of this drink (distractors), through two kinds of tests: first, a memory test, in which participants were asked to compare some target samples (identical to the drink they regularly consumed in their daily life) and distractor samples to a remembered target; second, a difference test, in which they were asked to compare some target and distractor samples to a physically presented target. Surprisingly, analysis of results for the whole group revealed that participants were not able to discriminate their usual drink from distractors in the memory test, even though they were able to distinguish between this drink and distractors in the difference test.

The observation of results at an individual level revealed that there was no correlation between individual discrimination performance on the difference test and on the memory test. It is interesting to mention that in a previous study performed on memory for custard dessert, three kinds of distractors were produced from the target by slightly varying thickness intensity (thickness distractors), aroma intensity (aroma distractors) or sweetness intensity (sweetness distractors). Results showed that, on one hand, participants did not discriminate the aroma distractors from the target during the memory test, even if they significantly rated these distractors as different from the target during an attribute intensity rating test, but that, on the other hand, a significant memory effect occurred for sweetness even if participants did not significantly rate the sweetness distractors as different from the target during the attribute intensity rating test (3).

In conclusion, significant discrimination during a difference test does not necessarily predict that significant discrimination will occur in a much more natural context of decision of novelty of a product, not based on a direct comparison, but on recollection of information from previously eaten foods. Conversely, memory test could sometimes be more acute to discriminate between products than classic sensory tests. Thus, these results suggest that memory tests could be preferred to classic difference tests when producers want to check if consumers discriminate between an old and a new formula of a product.

Acknowledgements

This work was funded by the Regional Council of Burgundy.

References

1. Köster M.A., Prescott J., Köster E.P. (2004) Incidental learning and memory for three basic tastes in food. *Chem. Sens.* 29: 441-453.
2. Macmillan N., Creelman C. (2005) *Detection theory: A user's guide*. Lawrence Erlbaum Associates, Mahwah, NJ.
3. Morin-Audebrand L., Laureati M., Sulmont-Rossé C., Issanchou S., Köster E.P., Mojet J. (2007) Different sensory aspects of a food are not remembered with equal acuity. *Food Qual. Pref.* 20: 92-99.

IMPROVING THE PALATABILITY OF ORAL NUTRITIONAL SUPPLEMENTS FOR ELDERLY PEOPLE AIMING TO INCREASE INTAKE

L. METHVEN¹, M.C. Bushell¹, L. Gray¹, M.A. Gosney², O.B. Kennedy¹, and D.S. Mottram¹

¹ *Department of Food Biosciences, University of Reading, Whiteknights, Reading RG6 6AP, UK*

² *Institute of Health Sciences, University of Reading, London Road, Reading RG1 5AQ, UK*

Abstract

Oral nutritional supplements are beverages designed for people known to have, or to be at risk of, malnutrition. They can lead to increase in body weight and nutritional status, however the products are frequently wasted due to unacceptable taste or sweetness. The hypothesis of this study was that reduction in sweetness would alter older people's perception and preference of the products. Replacement of sucrose with palatinose™ and reduction of serving temperature (from 21°C to 6°C and -13 °C) both significantly reduced perceived sweetness by trained sensory panel and by older consumers (n= 25 to 29, age range 65-84). Clusters of consumers preferred the less sweet variants, although there was no significant difference in mean preference.

Introduction

There is a high prevalence of malnutrition in elderly people; in the UK it can be as high as 60% of hospitalised patients (1). Oral nutritional supplements (ONS) are used to treat malnutrition in elderly people. They can have beneficial effects on body composition (2), however, the benefits can only be delivered if the older patients consume the products. The wastage of ONS is high and can be due to dislike of taste and sweetness (3).

This study reports on sweetness modification of ONS, aiming to improve acceptability of the products and improve consumption compliance. Palatinose™ (α -D-glucopyranosyl-1,6-fructose) has the same calorific value as sucrose, however the rate of absorption is slower than sucrose (4) and it is 50% less sweet than sugar. Low dextrose equivalent (DE) maltodextrin, like glucose syrup, is manufactured by the partial hydrolysis of maize starch; however it has a higher proportion of polysaccharide and a lower level of glucose and, hence a lower relative sweetness. Anecdotal evidence suggests that the temperature of serving affects the acceptability of the products (5). Lower temperature affects taste and flavour, either by suppressing flavour release or due to a numbing effect on the palate.

Experimental

Manufacture of UHT ONS modifications. ONS samples were manufactured on a pilot scale ultra heat treatment (UHT) plant, at 142°C for 4 seconds. The control formulation consisted, per 100g, of glucose syrup (18.7g), sodium caseinate (3.8 g),

sucrose (2.2g), oil blend (4.9g), milk protein concentrate (2g), soy protein isolate (1.4 g) and a commercial blend of emulsifier, vanilla flavour, vitamins and minerals. In a palatinose™ modification, all sucrose was replaced with palatinose™. In a low DE maltodextrin modification, the sucrose was replaced with palatinose™ and 25 % of the glucose syrup (22 DE) was replaced with the maltodextrin (5 DE). The total solids content of all products, as measured by refractometer, was 32 %. pH ranged from 6.6 to 6.8. Density ranged from 1.05 and 1.09 g/ml. The control and palatinose™ formulations had viscosities (Brookfield synchro-lectric viscometer) of 0.11 Pascal seconds (Pa-s), whereas the low DE maltodextrin formulation was more viscous at 0.31 Pa-s.

Manufacture of ice cream. The formulation for ice cream, per 100 g consisted of commercial ONS (Ensure Plus, Vanilla) (94.7g), sucrose (4.5g) and stabiliser (0.8g; mixture of guar, locust bean and carrageen gum). The sucrose was in order to lower the freezing point and produce a sufficiently soft ice cream. Ice cream was manufactured using a batch pasteuriser (80°C) and horizontal freezer. Air incorporation calculated as the percentage change in density, or overrun, was 70 %.

Sensory panel. Twelve screened and trained assessors (age 21-27) developed a sensory vocabulary to characterise Vanilla ONS using two commercial vanilla ONS products. A consensus vocabulary was reached on 20 attributes. Quantitative sensory assessment took place in individual sensory booths. Each sample (20 g) was given a 3-digit code, assessed twice with a randomised presentation order. Data was acquired using TASTE software (Reading Scientific Services Ltd., Reading, UK). Intensity was scored using 100-point unstructured line scales. To compare sweetness modifications, products were served at room temperature. To compare temperature, the commercial vanilla products was served at room temperature (21°C), chilled (6°C) and as ice cream (-13 °C).

Consumer panel. An older healthy adult cohort (n=25-29, age 65-84) preference tested products using a 9 point hedonic scale (extremely dislike, 1, to extremely like, 9). Sweetness intensities were scored using a 100-point unstructured line scale. Sample were 3-digit coded, presentation order was randomised.

Statistical analysis. Parametric testing of quantitative data and non-parametric testing of preference data were carried out using SenpaQ (Qi Statistics) and XLSTAT (version 2008.3.01).

Results and Discussion

Replacement of sucrose with palatinose™ resulted in a profile of reduced sweetness ($p < 0.001$) and dairy flavour ($p = 0.05$). Changing 25% glucose syrup for low DE maltodextrin further reduced sweetness, but significantly increased viscosity ($p = 0.007$) (Figure 1).

Older consumers perceived the reduction in sweetness ($p < 0.0001$). Preference was split between consumers who preferred less sweet variants, and those who preferred the sweeter control (Figure 2), there was no difference in mean preference. The viscosity of the maltodextrin modification was not liked.

Regarding temperature, the analytical panel found ice cream to be significantly lower in odour than the room temperature product ($p < 0.05$ for 3 odours) and sweet taste to be significantly lower in the chilled drink compared to the room temperature drink ($p = 0.06$). Older consumers found significant difference in sweetness between serving temperatures ($p = 0.001$). Clusters of consumers preferred chilled and ice cream products over the standard room temperature product (Figure 3).

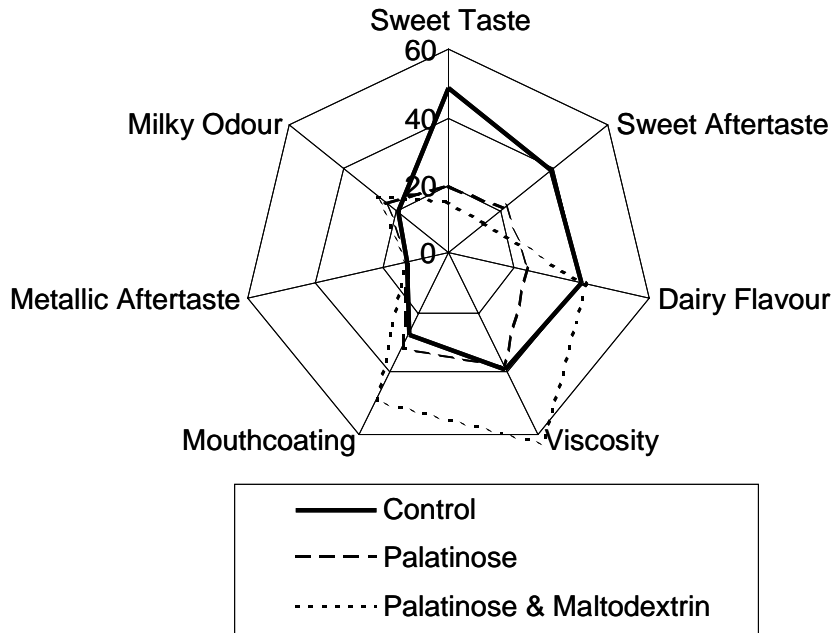


Figure 1. Effect of Saccharide on profile of ONS.

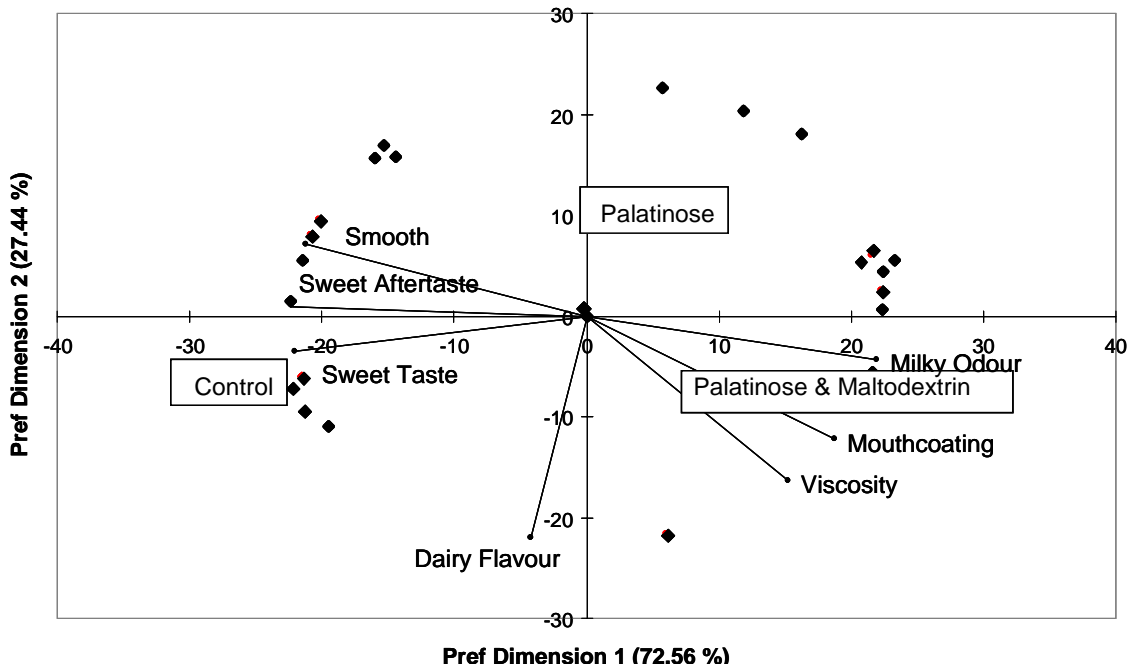


Figure 2. Preference Map of ONS Vanilla Modifications (Diamond = consumer liking position; Text box = sample position; Line and attribute = sensory driver).

Conclusions

Sweetness of ONS was successfully reduced by replacing sucrose with palatinose™, and by reducing serving temperature. Reducing sweetness did increase acceptability of products for some older consumers, but not for all. Further work is needed to establish the effect of repeat consumption on preference, and to establish the effect of reduced sweetness on preference of other flavour variants.

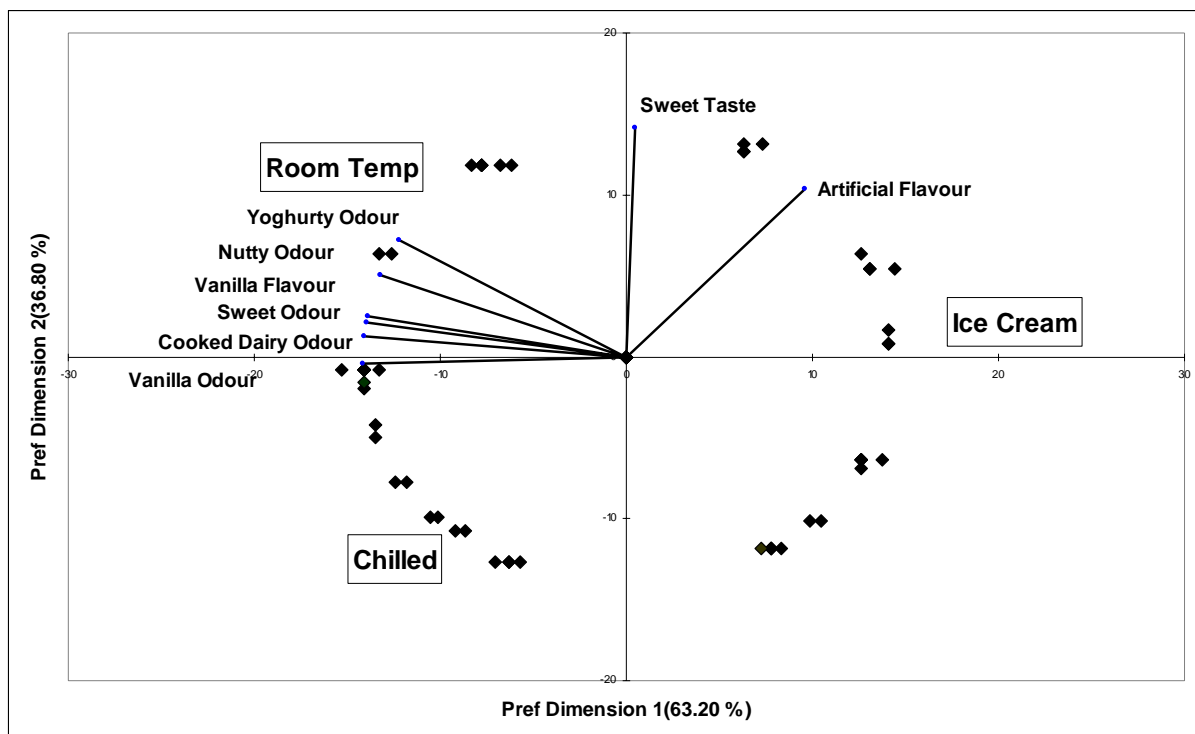


Figure 3. Preference map of ONS products at different temperatures (Diamond = consumer liking; Text box = sample position; Line and attribute = sensory driver).

Acknowledgments

This work has been supported by Research into Ageing, a UK Charity. Abbott Nutrition is thanked for supply of ingredients and for advice.

References

1. Age Concern (2006) In *Hungry to be Heard; the scandal of malnourished older people in hospital*. Age Concern, London.
2. Lauque S., Arnud-Battandier F., Mansourian R. (2000) *Age Aging* 29: 51-56.
3. Gosney M (2003) *J. Adv. Nurs.* 43: 275-280.
4. Kawai K., Yoshikawa H., Murayama Y. (1989) *Horm. Metab. Res.* 21 (6): 338-340.
5. Nolan A. (1999) *J. Hum. Nutr. Diet.* 12: 453-458.

SPARSE BIPLOTS FOR QUANTITATIVE DESCRIPTIVE ANALYSIS

R. van Doorn and E.P.P.A. DERKS

DSM Food Specialties, Department Sensory Research, P.O. Box 1, 2600 MA Delft, The Netherlands

Abstract

Sparse Principal Components Analysis was applied to data from industrial practice to demonstrate its abilities to reduce complexity and enhance the readability of PCA-biplots from sensory descriptive analysis. Sparse PCA can be considered as a combination of subset-selection (like in least angle regression) and Principal Component Analysis (PCA) and aims to compute a sparse low-dimensional representation of the high-dimensional data, explaining maximum variance. In this work, the Sparse PCA algorithm of Zou and coworkers was applied to study the sensory effects of natural and accelerated aging of caseine containing beverage formulations from industrial practice. It is discussed how Sparse PCA can be used to establish a simple scatter-plot based on maximum explained variance and sparseness criteria and to facilitate improved key-results communication.

Introduction

Principal Component Analysis (PCA) [1, 2, 3] has become a standard tool in sensory analysis to create low dimensional summaries of high-dimensional quantitative descriptive analysis (QDA) data. However, the interpretation of these summarizers (*i.e.* principal components) is often cumbersome as they comprise a linear combination of all sensory attributes which are all together displayed in the PCA-biplots. Consequently, for large descriptor lists, the bi-plots become very crowded and difficult to interpret. Viable ways to simplify the bi-plots have been reported in the literature. McCabe [4] proposed a subset selection method which computes 'principal variables'. Cadima et al [5] discussed the approach of ignoring small magnitude loadings. Vines [6] introduced 'Simple Principle Components' by restricting the loadings. Ledauphin et al [7] tried to simplify the bi-plot by assessing the significance of the loadings. Joliffe et al [8] applied a shrinkage method 'Least Absolute Shrinkage and Selection Operator (LASSO). LASSO acts like a variable subset selection algorithm by shrinking noisy correlated small-magnitude loadings towards zero. Zou et al [9, 10, 11] proposed the 'elastic net' and 'Least Angle Regression' (LARS) to produce modified principal components with sparse loadings. The algorithm from Zou et. al [12] was used in this paper.

Theory

Principal Component Analysis. PCA aims to minimize the following objective function

$$\min(\|\mathbf{X} - t\mathbf{p}\|^2) \quad (1)$$

decomposing matrix \mathbf{X} (products x attributes) into scores t (products) and loadings p (attributes) for each principal component restricted by $p'p=1$ or $\mathbf{P}'\mathbf{P}=\mathbf{I}$ for all components simultaneously. The scores \mathbf{T} (products x number of components) provide a low dimensional summary of the products in the full sensory space (products x attributes) whereas the loadings provide the required information about the sensory directions (in terms of descriptive attributes) in which the product may differ. A PCA-biplot is a joined low dimensional representation of scores and loadings, providing a good visual summary of the high dimensional sensory data.

Sparse Principal Component Analysis. Sparse PCA extends the PCA-objective function with an additional term which penalizes for the number and size of descriptive attributes.

$$\min(\|\mathbf{X} - t\mathbf{p}'\|^2 + \lambda \sum_i |p_i|) \quad (2)$$

Low (near zero) values for λ will have a negligible effect on the PCA-biplot and the percentage of explained variance whereas increased λ 's tend to shrink the small and co-varying loadings to zero, obtaining sparse loadings at the cost of reduced explained variance. The parameter λ needs to find the best balance between model simplicity (sparseness) and descriptive ability in terms of explained variance. The Sparse PCA algorithm from Zou et al. [11] was compared to conventional PCA (*i.e.* $\lambda=0$) using complex time resolved data from industrial practice.

Experimental

Caseine containing beverage formulations were subjected to natural and accelerated aging (*i.e.* 20°C and 35°C) (Table 1) and evaluated by means of Quantitative Descriptive Analysis (N= 12). Variance component models were used to estimate the mean profile for each product. Sparse PCA was applied to the mean-centred profiles for increasing lambda's.

Table 1. *Treatments of the caseine containing beverage formulations (temperature x time).*

Nr	Temperature (°C)	Time (months)	Code
1	0	12	0
2	20	1	m1-20
3	20	3	m3-20
4	20	6	m6-20
5	20	9	m9-20
6	20	12	m12-20
7	35	1	m1-35
8	35	3	m3-35
9	35	6	m6-35
10	35	9	m9-35
11	35	12	m12-35

Results

Table 2 shows the amount of explained variance for each principle component. It can be observed that λ gradually changes the Sparse PCA algorithm from a linear summarizer (PCA) into a subset-selector as the sensory attributes are ‘assigned’ to the principal components (see Figure 2). Consequently, compared to PCA, the sparse principal components are easier to interpret (*i.e.* the sensory attributes are aligned to the principle components, providing them with a sensory meaning). The amount of explained variance for the first two principal components gradually decreases as a function of lambda, which merely is a consequence of adding a restriction. This effect appears less deteriorative when successive sparse components are included as the variance in the data is now partially explained by the successive PC’s (see Table 3).

Table 2. Explained variance as a function of lambda, for PC1 ... PC4.

λ	PC1(%)	PC2(%)	PC3(%)	PC4(%)
0	55	15	2	<1
0.0001	40	14	6	2
0.1	22	12	10	7

Table 3. Sparse loadings as a function of lambda, for PC1 & PC2.

Attributes	$\lambda = 0$		$\lambda = 0.0001$		$\lambda = 0.1$	
	PC1(55%)	PC2(15%)	PC1(40%)	PC2(14%)	PC1(22%)	PC2(12%)
<i>intensity.fl</i>	-0.29	-0.08	-0.40	0.00	-0.21	0.00
<i>fruity.fl</i>	0.27	0.18	0.26	0.15	0.01	0.00
<i>artificial.fl</i>	-0.26	0.26	-0.19	0.24	-0.14	0.00
<i>fermentation.fl****</i>	-0.35	0.01	-0.22	0.00	-0.20	0.00
<i>astringent.fl***</i>	-0.30	0.04	-0.21	0.01	-0.03	0.00
<i>sweet.fl</i>	0.14	0.54	0.00	0.60	0.00	0.72
<i>sour.fl</i>	-0.05	0.30	0.00	0.26	0.00	0.23
<i>bitter.fl</i>	-0.32	0.01	-0.19	-0.02	0.00	0.00
<i>fermentation.at****</i>	-0.35	-0.01	-0.72	0.00	-0.88	0.00
<i>lengthAT.at</i>	-0.23	0.40	-0.06	0.34	-0.09	0.09
<i>sour.at</i>	-0.11	0.28	-0.09	0.29	0.00	0.32
<i>whey.at</i>	-0.33	-0.07	-0.27	0.00	0.00	0.00
<i>astringent.at*</i>	-0.35	0.03	-0.10	0.00	-0.34	0.00
<i>sweet.at</i>	0.11	0.51	0.01	0.55	0.00	0.57

Figure 1 shows a conventional PCA-biplot ($\lambda= 0$). It can be observed that accelerated aging at 35°C caused significant movements in the direction of 'fermented (taste & aftertaste)', 'astringent aftertaste'. On the other hand, the samples stored at 20°C were hardly affected by aging, which implies good shelf-life properties at 'normal' storage conditions.

Figure 2 shows a sparse PCA-biplot ($\lambda= 0.1$). It is clear that most variation in the data is explained by PC1 (22%) which is predominantly about accelerated aging (*i.e.* at 35°C). PC2 explains variance (*i.e.* 12%) in the opposite direction (*i.e.* sweet and sour taste & aftertaste). The attribute 'length-aftertaste' points in the diagonal direction between sweet/sour and fermented (even at $\lambda= 0.1$) which indicates that the

aftertaste attribute could have been perceived as a combination of PC1 (sweet/sour) and PC2 (fermented) and could even comprise most variation in a successive principal component.

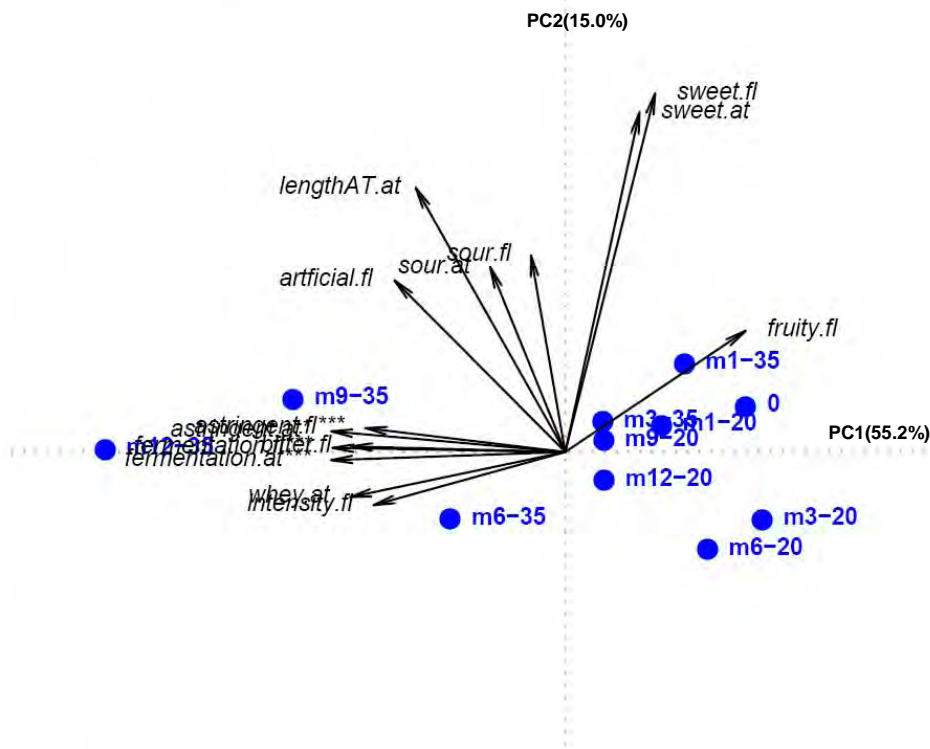


Figure 1. PCA-biplot ($\lambda=0$).

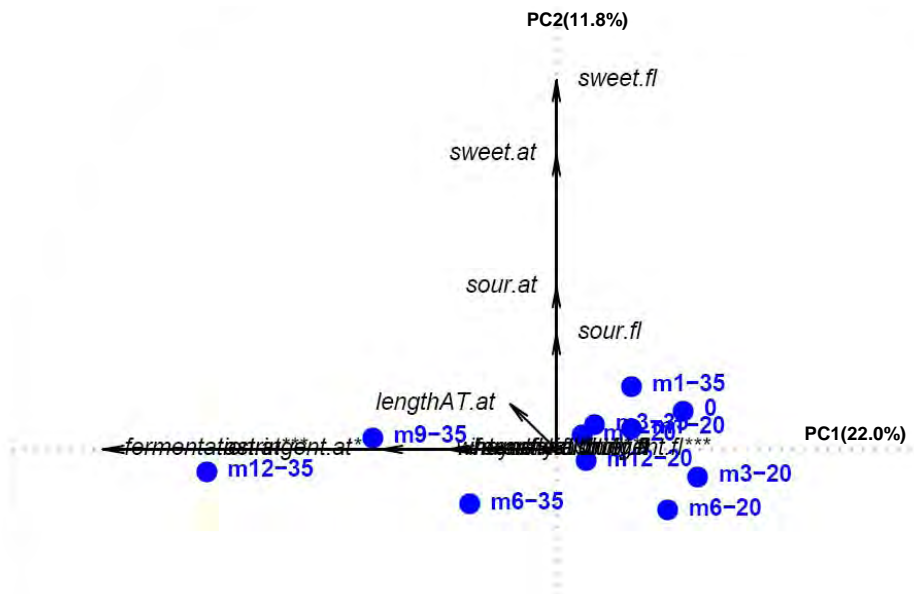


Figure 2. Sparse PCA-biplot ($\lambda=0.1$).

It can be observed from Figure 2 that lambda aligns the sensory attributes with the first two principal components without major changes in the structure of the scores (positions of the products in the sensory space). Consequently, the major variance structures in this dataset can be subdivided in the sensory effects (astringent (after)taste, fermented (after)taste and bitter) due to accelerated aging at elevated temperatures) and the sensory effects sour & sweet (after)taste) due to

natural aging. As can be expected, the effects of artificial aging are very different and much more deteriorative compared to aging at room temperature and below.

Conclusion and Discussion

In this paper, Sparse PCA was introduced as a tool to enhance the interpretability of QDA-biplots which are generally densely loaded with sensory attributes and therefore difficult to interpret. It has been argued that these biplots can be simplified into simple scatterplots in which the axes have a true sensory meaning which non-technical (without a statistical background) can easily understand. It needs to be noted that the added restriction (let's call it a 'complexity penalty') suppresses the amount of explained variance in the first principal components. Consequently, compared to PCA, it is likely that more variance is explained at higher principal components. One of the drawbacks of Sparse PCA is that there is limited control on the effect of the complexity penalty on highly correlated sensory attributes and it might happen that business-critical sensory attributes simply disappear whereas other correlated less important attributes are displayed in the sparse bi-plot. A viable solution is to rename this component with a sensible name, representing all correlated variables. Another more pragmatic solution is to use prior knowledge about the sensory attributes which definitely should be retained (for reasons of business communications or prior knowledge). This heuristic control can conveniently be applied by assigning weights for each attribute to control the effect of lambda.

References

1. Wold S., Esbensen K., Geladi P. (1987) In *Chemometrics and Intelligent Laboratory Systems* 2, pp 37-52.
2. Jolliffe I.T. (1986) *Principal Component Analysis*. Springer-Verlag.
3. Jackson J.E. (1991) *A User's Guide to Principal Components*. 1st ed. Wiley-Interscience, New York.
4. McGabe G.P. (1984) *Technometrics* 26: 137-144.
5. Cadima J, Jolliffe I.T. (1995) *J. Appl. Statist.* 22: 203-214.
6. Vines S.K. (2000) *Appl. Statistics* 29: 441-451.
7. Ledauphin S., Hanafi M., Qannari E.M. (2004) *Chemometrics and Intelligent Laboratory Systems* 74: 277-281.
8. Jolliffe I.T., Trendafilov N.T., Uddin M. (2003) *Journal of Computational and Graphical Statistics* 12: 531-547.
9. Efron B., Hastie T., Johnstone I., Tibshirani R. (2004) *Ann. Statist.* 32: 407-499.
10. Zou H., Hastie, T. (2005) *J. Royal. Statist. Soc. B.* 67: 301-320.
11. Zou H., Hastie T., Tibshirani, R. (2006). *Journal of Computational and Graphical Statistics* 15: 265-286.
12. Zou H., Hastie T. (2007) *Elasticnet: Elastic Net Regularization and Variable Selection*. R-Package version 1.0-4.

Section 3

***In-Vivo* Measurements in Flavour Release**

CHARACTERISATION OF FOOD PERCEPTION: TRACING THE CHEMOSENSATIONS *IN-VIVO*

A. BUETTNER^{1,2}

¹ *Institute of Pharmacy and Food Chemistry, University Erlangen-Nürnberg, Schuhstrasse 19, 91052 Erlangen, Germany*

² *Fraunhofer-Institute for Process Engineering and Packaging, Giggenhauser Strasse 35, 85354 Freising, Germany*

Abstract

Over the last decades, analytical tools have been developed for *in-vivo* monitoring of chemosensorically active compounds such as food odorants and tastants, and their release phenomena during eating under physiological conditions. This review discusses methodologies that target at tracing the paths of chemosensorically active compounds, from their liberation within the oral cavity to their interaction with human physiology. These techniques include on-line mass spectrometric breath analysis methods and trapping procedures. Physio-analytical studies that have formed our current understanding of the influence of chewing, salivation, breath flow and swallowing are also presented. Furthermore, experimental mimicking instruments are examined and systems are reconsidered on the basis of current knowledge on perceptual phenomena and the specific chemosensory impressions of humans. Finally, analytical limitations and open questions in "*In-vivo flavour research*" are discussed.

Introduction

The flavour of a food comprises taste impressions as well as texture and other sensations such as temperature, astringency, stinging, tingling, and burning. A key modulator for food consumption and food preference is retronasal aroma perception. Odorants are released in the oral cavity during mastication, and proceed to the receptors in the nasal cavity. Several factors such as saliva, mucosal effects, masticatory forces and tongue movements, as well as metabolic processes, have been considered important for flavour release and perception phenomena. Accordingly, it is nowadays agreed that the overall flavour composition, *i.e.* the headspace profile of food, does not directly correlate with the specific sensations during the course of eating, thus making both *in-vivo* and *in-vitro* studies indispensable.

Instruments and developments for *in-vivo* flavour monitoring: Breath analysis

A first attempt to understand *in-vivo* flavour release was the collection of breath volatiles during consumption, which was carried out either by cryo-focussing with liquid N₂ or by adsorption on materials such as Tenax™ (1-5). Mostly, breath samples were pooled, either over the entire eating sequence or over several chewing or breathing cycles, or trapped for defined periods. Subsequent analysis of the trapped volatiles was performed using GC-FID or GC-MS.

In developing this analytical process further, “oral vapour gas phase-chromatography” was designed. In this procedure, air is sampled directly from the oral cavities of the taste panellists (6,51) to directly trace the oral release of characteristic compounds during consumption, which is then correlated with flavour perception. A similar approach was used, for example, in the “buccal headspace” technique to follow flavour release from hard cheese (3,4). Breath volatile concentrations from the nose (“nosepace”) have also been studied during consumption of diverse foods (7-10) by trapping volatiles on Tenax™ at defined intervals and analyzing compounds by conventional GC-MS. In a similar set-up, the Exhaled Odorant Measurement (EXOM) approach combines Tenax™ trapping or cryo-focussing with GC-Olfactometry (GC-O) and GC-SIDA, thereby achieving high selectivity and sensitivity for odorant identification and quantification (11,12).

For several foods, nosepace profiles have been compared with corresponding headspace samples, while sensory perception was evaluated according to Time-Intensity procedures. Following these studies it became clear that volatile release during eating is a highly dynamic process, with continuous intensity changes of the released volatiles. Accordingly, profiles either from the mouth or the nose were investigated and found to exhibit considerable differences when compared with those derived from conventional headspace analysis (1,7). In general, high variations between panellists of total quantities and dynamics of volatiles released were observed. To overcome this problem, investigators replaced analyses of specific individuals with assessments of large numbers of panellists. By subjecting the data to comprehensive algorithms the wide range of variation between individuals could be smoothed out.

The main advantage of trapping is that the compounds can be enriched from large volumes of breath, with separation and purification prior to analysis. A drawback, however, is a generally poor temporal resolution. The need for short response times in breath analysis led to the development of mass spectrometric techniques that allowed direct analysis of breath samples, e.g. utilising membrane separators or fibre interfaces (13-15,46). However, the main analytical disadvantages of the membrane systems were discrimination of compounds according to their affinity for the membranes, and non-optimum volatile diffusion rates and response times.

Overcoming this limitation, the research group of A.J. Taylor developed the *MS Nose™* technique, which utilises atmospheric pressure ionisation MS (API-MS) for convenient direct breath analysis. A specific venturi inlet in this system allows continuous flow sampling of limited gas volumes into the API-MS source through a minimised inlet aperture (16-18). Linearity, fragmentation patterns and detection thresholds of this system have been investigated (18-23), with variations and improvements made: e.g. the flavourspace technique utilises a simple glass tube inlet system to draw samples directly into the ionisation chamber (24).

Another technique is proton transfer reaction MS (PTR-MS) (25-30). As in API-MS, H_3O^+ ions are used as the ionising agents. The key difference, compared to API-MS, is that PTR-MS has two distinct chambers; the hollow cathode ion source, where H_3O^+ ions are generated, and the drift tube (reaction chamber) with temperature and pressure control, which contains air as the reaction buffer gas. Here, the analytes collide with H_3O^+ ions from the ions source and undergo PTR. Chewing experiments with PTR-MS breath analysis have been performed, for example, on coffee beverage and red kidney beans (27,31). A variant chemical ionisation technique is selected ion flow tube MS (SIFT-MS) (32,33), but its application in food research, especially *in-vivo* aroma analysis, has so far been limited.

By connecting the API or PTR to a time of flight (TOF) MS, compound differentiation via accurate mass determination has been applied to overcome analytical limitations in selectivity (52). In other studies, a venturi inlet, as used with MS Nose™, has been combined with a LCQ-API-MS system (34) to increase the moisture level in the reaction chamber so that sensitivity could be increased and fragmentation decreased.

Physiological facts and mimicking of human physiological conditions

Due to the complexity of the human physiology and the impossibility of distinguishing between individual effects, researchers quickly aimed to model *in-vivo* situations via *in-vitro* studies. It has been generally agreed that temperature, salivation, mastication and breathing patterns likely play an important role in aroma release and perception (35-37). From simple systems (“stirring cells”) to complex model mouth systems, the underlying principle, the oral cavity and its functional properties, has been mimicked (38-47). In a typical set-up, a certain amount of food or model is placed in a defined – usually temperature-controlled – vessel. Chewing actions are simulated by up/down motions, grinding movements of pestles, or by stirring. Scaled-up systems have also been applied in order to increase sensitivity. Often (artificial) saliva is introduced and (humidified) gas flow simulates breathing (36). Even oral mucosa has been simulated by adherently growing epithelial tissue cells of a human cervix carcinoma line within the respective release devices (45). Analysis is usually carried out by headspace sampling, e.g. via gas tight syringes or by purging N₂ through the food, followed by Tenax™ trapping, cryo-focussing, or by direct on-line MS analysis such as API-MS or PTR-MS (27,48,49). In some studies, collection at defined time intervals has been controlled using valves (39,50) or computerised systems (44,45).

Model mouth systems and their release patterns have been compared with each other and with those of conventional headspace techniques (e.g. 38,39,51,52), as well as with breath analyses from human subjects to verify the validity of the model mouth equipment and its performance (e.g. 43). Volatile release from the model mouth systems has been, in numerous cases, reported to closely resemble those profiles which are obtained from *in-vivo* measurements (e.g. 38,47), either from exhaled breath from the nose (“nose space”), or from the oral cavity (“oral vapour” or “mouth space”) (53,54). This would indicate that the intra-oral release patterns show high correlation with those obtained from the air phase expired from the nose.

On the other hand, swallowing effects as mentioned above are not taken into account by these systems. Therefore, an artificial throat system was developed to mimic dynamic pharyngeal release from liquid and semi-liquid foods (55). This system consisted of a temperature-controlled vertical glass tube with an intermediate Viton rubber section that could be closed and opened by a clamp to simulate swallowing, and a unidirectional air-flow applied via an upward orientated gas inlet to mimic exhalation. Liquids were administered, with or without the addition of artificial saliva, and subsequently “swallowed” by opening the clamp. The investigation primarily focussed on the initial exhalation immediately after swallowing, but also on release effects from food material adsorbed to the inner pharynx walls. Due to extensive spreading of the coating layer on the mucosal tissue and exposure to a relatively high gas stream during exhalation, the release of odorants from this coating is considered to be more or less instantaneous. Considerable agreement for release patterns obtained from the artificial throat and from *in-vivo* release has been reported, as well as clear deviations compared to those from a mouth model system. In conclusion, the model mouth “chews” but does not “swallow”, while the opposite is

true for the model pharynx. To date, no system incorporating both principles has been realised, and it is not entirely clear which physiological part plays the major role for which type of food system.

Intra-oral and metabolic studies

An initial attempt to elucidate residual flavour in aftertaste within the oral cavity was undertaken by Hussein *et al.* (56). Based on these observations, the Spit-Off Odorant Measurement (SOOM) was developed in order to quantify odorants retained by the oral mucosa (57,58). Summarising the approach, SOOM is a means of indirectly determining the amounts of odorants being “lost” within the oral cavity by quantifying the remaining amounts of odorants after oral application and expectoration in the spit-off material. However, it was not discernible whether odorants are really “lost” due to adsorption or also resorption by the oral mucosa. Therefore, release from oral mucosa was examined using the buccal odor screening system (BOSS), while odorant metabolism in the presence of saliva was monitored in specific assays (59).

Perceptual phenomena and analysis: how can we objectify the subjective?

Apart from oral, pharyngeal or nasal effects, several studies highlighted that interactions between different modalities such as taste and aroma can considerably influence the subjective sensory rating of aroma (*e.g.* 60,61). Recently, the phenomenon of interaction between different sensory modalities has been increasingly discussed with regard to either enhancement or reduction of sensory impressions. “Congruency” resulting in mutual enhancement has been reported, for example, for a fruity or savoury aroma in the presence of a sweet or salty taste, and for sensations such as texture (60,62,63). For instance, authors have reported a higher sensory correlation of mint-flavour perception with sucrose release rather than menthone release during consumption. The same effect occurred when tastants were reduced in their sensory perceptibility, for example due to thickener addition above c^* (point of random coil overlap), while their real sample concentration remained the same (64). Regarding texture, Weel *et al.* reported that the texture of gels, rather than the in-nose concentration, determines the perception of flavour intensity (62). Similarly, the effect of “mouthfeel” sensations on the perception of taste and aroma has been noted (65).

Future *in-vivo* flavour research: Analytical limitations and open questions

The following topics and open questions were addressed during the workshop as most promising for future research:

- Do we know all physiological factors and their impacts on flavour perception? Do we know, for instance, about the kinetics of odorant transfer (*e.g.* OBPs) from nasal air phase to receptors?
- How complete do present model systems mimic human parameters? Do we need combined systems that can, for example, both chew and swallow?
- Do we know all metabolic factors involved in flavour perception, and all “chemical” release processes? Do we understand metabolism of odorants in the nose (66)?
- Limited data on taste modalities, their interactions, and their interactions with other flavour parameters was regarded as one key bottleneck in the understanding of flavour perception.
- What are the physiological processes behind sensory interaction phenomena and how can we monitor or influence these?

- Limited data on the impact of hedonics, emotions, expectations, “human” factors on sensory perceptions was addressed as key drawback, as well as
- limitations in our descriptive and lingual resources to address and describe sensory phenomena, and to compare between different individuals.

References

1. Linforth R., Taylor A.J. (1993) *Food Chem.* 48: 115-120.
2. White J., Croasmun W., Leland J. (1996) Kraft Foods, Inc.; U.S. Patent 5,479,815.
3. Delahunty C., Piggott J., Conner J., Paterson A. (1995) In *Bioflavour 95* (Etievant P.; Schreier P.; eds.); INRA, Dijon, pp 45-53.
4. Delahunty C., Piggott J., Conner J., Paterson A. (1996) *J. Sci. Food Agric.* 71: 273-281.
5. Ruiz R., Hartman T., Karmas K., Lech J., Rosen R. (1994) In *Food phytochemicals for Cancer Prevention I*. ACS Symp. Ser. 546 (Huang M.-T., Osawa T., Ho C.-T., Rosen R., eds.); pp 102-119.
6. Roozen J., Legger-Huysman A. (1995) In *Aroma perception, formulation, evaluation* (Rothe M., Kruse H., eds); DIfE, Potsdam-Rehbrücke, Germany, pp 627-632.
7. Linforth R., Savary I., Taylor A. (1994) In *Trends in flavor research* (Maarse H., van der Heij D., eds); Elsevier Science, Amsterdam, pp 65-68.
8. Ingham K., Linforth R., Taylor A. (1995) *Flavour Fragr. J.* 10: 15-24.
9. Ingham K., Taylor A., Chevance F., Farmer L. (1996) In *Flavour Science: recent developments* (Taylor A., Mottram D.; eds.); Royal Soc. Chem., London, pp 386-391.
10. Linforth R.S.T., Ingham K.E., Taylor A.J. (1996) In *Flavour science: recent developments* (Taylor A.J., Mottram D.S.; eds.); Royal Soc. Chem., London, pp 361-368.
11. Buettner, A., Schieberle, P. (2000) *Food Sci. Technol.* 33: 553-559.
12. Buettner A., Griess M. (2005) In *State-of-the-Art in Flavour Chemistry and Biology* (T. Hofmann, T. Rothe, P. Schieberle, eds.); DFA, Garching, Germany, pp 381-386.
13. Wigaeus E., Löf A., Nordqvist M. (1982) *Scand. J. Work Environ. Health* 8: 121-128.
14. Soeting W., Heidema J. (1988) *Chem. Senses* 13: 607-612.
15. Haring P. (1990) In *Flavour Science and Technology*, Wiley, Chichester, pp. 351-354.
16. Linforth R., Taylor A. (1998) European Patent, EP 0819 937 A2.
17. Taylor A., Linforth R. (1997) In *Flavor perception, aroma, evaluation* (Kruse H.-P., Rothe M., eds.); DIfE, Potsdam, pp 131-142.
18. Taylor A., Linforth R., Harvey B., Blake A. (2000) *Food Chem.* 71: 327-338.
19. Taylor A., Linforth R. (2000) In *Flavour Release* (Roberts D., Taylor A., eds.); ACS Symp. Ser. 763, Oxford University Press, Washington, pp 8-21.
20. Buffo R., Zehentbauer G., Reineccius G. (2005) *J. Agric. Food Chem.* 53: 702-707.
21. Sunner J., Nicol G., Kebarle P. (1988) *Anal. Chem.* 60: 1300-1307.
22. Sunner J., Ikonomou M.G., Kebarle P. (1988) *Anal. Chem.* 60: 1308-1313.
23. Taylor A., Besnard S., Puaud M., Linforth R. (2001) *Biomol. Eng.* 17: 143-150.
24. Grab W., Gfeller H. (2000) In *Frontiers of flavour science* (Schieberle P., Engel K.H., eds.); DFA, Garching, Germany, pp 261-270.
25. Lindinger W., Hansel A., Jordan A. (1998) *Chem. Soc. Rev.* 27: 347-354.
26. Gasperi F., Gallerani G., Boschetti A., Biasiolo F., Monetti A., Boscaini E., Jordan A., Lindinger W., Iannotta S. (2001) *J. Sci. Food Agric.* 81: 357-363.
27. Graus M., Yeretziyan C., Jordan A., Lindinger W. (2002) Book of abstracts, XIIIth symposium on atomic, cluster and surface physics, pp 298-302.
28. Boscaini E., van Ruth S., Biasiolo F., Gasperi F., Märk T. (2003) *J. Agric. Food Chem.* 51: 1782-1790.
29. Boschetti A., Biasiolo F., van Opbergen M., Warneke C., Jordan A., Holzinger R., Prazeller P., Karl T., Hansel A., Lindinger W., Iannotta S. (1999) *Postharvest Biol. Technol.* 17: 143-151.

30. Boamfa E., Steeghs M., Cristescu S., Harren F. (2004) *Int. J. Mass Spectrom.* 239: 193-201.
31. van Ruth S., Dings L., Buhr K., Posthumus M.A. (2004) *Food Res. Int.* 37: 785-791.
32. Spanel P., Smith D. (1999) *Rapid Commun. Mass Spectrom.* 13: 585-596.
33. Davis B., Senthilmohan S., Wilson P., McEwan M. (2005) *Rapid Commun. Mass Spectrom.* 19: 2272-2278.
34. Zehentbauer G., Krick T., Reineccius G. (2000) *J. Agric. Food Chem.* 48: 5389-5395.
35. Burdach K., Doty R. (1987) *Physiol. Behavior* 41: 353-356.
36. de Roos K., Wolswinkel K. (1994) In *Trends in Flavor Research* (Maarse H., van der Heij D., eds.); Elsevier Science, Amsterdam, pp 15-32.
37. Land D. (1994) In *Flavor-Food Interactions* (McGorin R.J., Leland J., eds.); ACS Symp. Ser. 633, Washington, pp 2-11.
38. van Ruth S., Roozen J., Cozijnsen J. (1994) In *Trends in flavor research* (Maarse H., van der Heij D., eds.); Elsevier Science, Amsterdam, pp 59-64.
39. Roberts D., Acree T. (1995) *J. Agric. Food Chem.* 43: 2179-2186.
40. Nassl K., Kropf F., Klostermeyer H.Z. (1995) *Lebensm.-Unters. -Forsch.* 201: 62-68.
41. Odake S., Roozen J., Burger J. (2000) In *Frontiers of Flavour Science* (Schieberle P., Engel K.-H., eds.); DFA, Garching, Germany, pp 287-291.
42. van Ruth S., O'Connor C., Delahunty C. (2000) *Food Chem.* 71: 393-399.
43. Deibler K., Lavin E., Linforth R., Taylor A., Acree T. (2001) *J. Agric. Food Chem.* 49: 1388-1393.
44. Rabe S., Krings U., Banavara D., Berger R. (2002) *J. Agric. Food Chem.* 50: 6440-6447.
45. Rabe S., Krings U., Berger R. (2004) *Chem. Senses* 29: 153-162.
46. Springett M., Rozier V., Bakker J. (1999) *J. Agric. Food Chem.* 47: 1125-1131.
47. Piggott J., Schaschke C. (2001) *Biomol. Engineer.* 17: 129-136.
48. van Ruth S., Buhr K. (2004) *Int. J. Mass Spectrom.* 239: 187-192.
49. Boland A., Buhr K., Giannouli P., van Ruth S. (2004) *Food Chem.* 86: 401-411.
50. Roberts D., Acree T. (1996) In *Flavor-Food Interactions* (McGorin R., Leland J., eds.); ACS Symp. Ser. 633, Washington, pp 179-187.
51. Legger A., Roozen J. (1994) In *Trends in Flavor Research* (Maarse H., van der Heij D., eds.) Elsevier Science, Amsterdam, pp 287-291.
52. van Ruth S., Boscaini E., Mayr D., Pugh J., Posthumus M. (2003) *Int. J. Mass Spectr.* 223-224: 55-65.
53. van Ruth S., Roozen J. (2000) *Talanta* 52: 253-259.
54. Margomenou L., Birkmyre L., Piggott J., Paterson A. (2000) *J. Inst. Brewing* 106: 101-105.
55. Weel K., Boelrijk A., Burger J., Verschueren M., Gruppen H., Voragen A., Smit G. (2004) *J. Agric. Food Chem.* 52: 6564-6571
56. Hussein M., Kachikian R., Pidel A. (1983) *J. Food Sci.* 48: 1884-1885.
57. Buettner A., Schieberle P. (2000) In *Flavor release* (Roberts D., Taylor A., eds.); ACS symp. ser. 763, New Orleans, pp 87-98.
58. Buettner A., Schieberle P. (2000) *Food Chem.* 71: 347-354.
59. Buettner A. (2007) *Aroma release and perception during consumption of food taking into account physiological aspects.* Verlag Dr. Hut, Germany, ISBN 978-3-89963-559-1.
60. Davidson J., Linforth R., Hollowood T., Taylor A. (1999) *J. Agric. Food Chem.* 47: 4336-4340.
61. Dalton P., Doolittle N., Nagata H., Breslin P. (2000) *Nat. Neurosci.* 3: 431-432.
62. Weel K., Boelrijk A., Altling A., van Milt P., Burger J., Gruppen H., Voragen A., Smit G. (2002) *J. Agric. Food Chem.* 50: 5149-5155.
63. Hort J., Hollowood T. (2004) *J. Agric. Food Chem.* 52: 4834-4843.
64. Hollowood T., Linforth R., Taylor A. (2002) *Chem. Senses* 27: 583-591.
65. Pangborn R.M., Trabue I.M., Szczesniak A.S. (1973) *J. Texture Stud.* 4: 224-241.
66. Schilling B. (2006) Odorant metabolism in the human nose. AChemS 28th Annual meeting, April 2006, Sarasota, Florida.

FLAVOUR DELIVERY FROM THE ORAL CAVITY TO THE NOSE

R. LINFORTH and A.J. Taylor

Food Sciences, School of Biosciences, Sutton Bonington Campus, University of Nottingham. LE12 5RD. UK

Abstract

The oral and nasal breath volatile content was studied whilst panellists consumed chewing gum or boiled sweets. Consumption of chewing gum produced approximately equal amounts of volatile in oral and nasal breath, consistent with the exhalation of pulses of air from the oral cavity entering the pharynx with each chewing cycle. In contrast, sucking the boiled sweet resulted in an oral breath concentration six times greater than that of nasal breath following swallowing. This suggests that the air in the mouth was not efficiently delivered to the upper airway during swallowing. This may be caused by the differences in mouth movements during chewing and swallowing. Chewing decreases the oral volume and ejects air, which is carried away by tidal breath flow before air enters the mouth as the jaw is lowered. In contrast, during swallowing, the jaw is raised and lowered before exhalation commences, potentially drawing air from the pharynx back into the mouth, reducing the availability of volatile laden air for exhalation.

Introduction

Much is known about the effects of human physiology and the physicochemical characteristics of compounds on mass transfer in-vivo [1]. One of the key features is the potential for isolation of the oral cavity from the pharynx by the velum. Main eating events such as chewing and swallowing are recognized as important for causing the velum to open, allowing air from the mouth to pass into the upper airway and transferring volatile compounds to the nose and olfactory epithelium during exhalation.

There is little quantitative data on the relative efficiency of chewing or swallowing on gaseous volatile transmission. Early studies showed that in-mouth helium was transferred to the nose under conditions where mouth movements were greater [2]. However, the data did not allow a quantitative assessment of efficiency and was qualitative in nature. Videofluoroscopy studies have clearly shown movements in the velum which have the potential for the transfer of volatiles to the upper airway [2], although the exact extent of gaseous transfer cannot be established with such techniques.

Direct measurement of aroma compounds in the breath has shown that chewing tends to result in pulses of aroma in the breath with each chewing cycle typically resulting in an aroma pulse [3, 4]. The less frequent swallowing action can also result in pulses of aroma in the breath. It is the balance between mouth movements and an individual's physiology that are most likely to determine the overall frequency of gaseous aroma transfer from mouth to nose.

To investigate the impact of swallowing and chewing on gaseous aroma transfer, samples of food typically chewed (chewing gum) and sucked (boiled sweets) were

eaten, and breath sampled from both the mouth and nose. Chewing gum typically produces regular chewing related pulses of aroma in the breath, whilst aroma delivery for the boiled sweet is often associated with the swallowing action [4]. This would show the relative concentrations of oral gaseous aroma and that exhaled nasally under the two processes.

Experimental

Mint and fruit flavoured boiled sweets and chewing gum were purchased from a local supermarket. Menthone release was monitored as a marker for mint flavour and ethyl butyrate was monitored for the fruity samples.

The breath menthone or ethyl butyrate content was measured by sampling breath (30 ml/min) into an Atmospheric Pressure Chemical Ionisation source of a Platform II mass spectrometer (Micromass, Manchester UK) [5]. Both compounds were detected as the protonated molecular ion, in selected ion mode (4kV positive ionisation).

The breath inlet consisted of a heated (120 °C) deactivated fused silica tube (1 m x 0.53 mm ID) which ran from the source to the panellist. For nasal breath sampling, the panellist consumed the samples, exhaled and inhaled, whilst resting their nose on a tube inserted into a "T" piece on the end of the transfer line. For oral breath sampling the panellist inhaled nasally, inserted a tube mounted on the "T" between their lips and exhaled through the mouth. Each panellist sampled their oral and nasal breath four times for each sample. The peak heights for the peaks observed following each exhalation were recorded for comparison.

Results

The transfer of volatile compounds from the oral cavity to the nose during eating will depend on a number of factors including the opening of the velum at the back of the mouth, breathing patterns and movement of the jaw which affects oral volume. During chewing, the jaw rises, the cheeks move in and the tongue presses against the roof of the mouth decreasing the oral volume, this forces air from the mouth into the throat where it meets the tidal breath air flow. If the flow is to the lungs, the volatiles are absorbed and lost to the large epithelial surface, consequently they are not observed in the subsequent exhalation (data not shown). Flow to the nose, carries volatile compounds to the olfactory epithelium and the atmosphere. The air flow rate in the upper airway is fast enough to carry the volatile laden air away from the pharynx, before the lowering of the jaw at the end of the chewing cycle draws air into the mouth from the pharynx.

Consequently, when chewing gum is consumed, the chewing action results in regular pulses of aroma in the exhaled nasal breath [3] due to air passing from throat-to-mouth around 100 times per minute. This represents a highly dynamic gas flow environment. It might be expected that this would result in an oral gas phase volatile concentration similar to that of the nasally exhaled breath.

When the fruity chewing gum was consumed, the maximum ethyl butyrate oral and nasal concentrations were virtually identical for both panellists (Table 1). The in-mouth gas phase was representative of that exhaled nasally and is consistent with air from the mouth passing into the throat during chewing which is then exhaled without much loss or absorption. The menthone signal showed a two fold difference between the concentration in the mouth and that exhaled nasally. This could be due to absorption in the nasal cavity decreasing the breath volatile content, a direct result of

its lower air/water partition coefficient [6]. Therefore, chewing can draw air from the pharynx into the mouth to where volatile compounds can partition into it and this air is then pumped back into the throat later in the chewing cycle where it can be exhaled.

Table 1. Average peak heights (and standard deviations SD) for volatiles in the breath of panellists consuming mint (menthone) or fruity (ethyl butyrate) chewing gum. Breath was sampled from either the mouth (oral) or nose (nasal). Values are arbitrary peak height units $\times 10^{-6}$.

	Panellist 1				Panellist 2			
	Oral		Nasal		Oral		Nasal	
	mean	SD	mean	SD	Mean	SD	mean	SD
Menthone	7.2	1.3	4.1	0.2	7.2	1.4	4.0	3.8
Ethyl butyrate	12.7	6.6	13.2	9.4	14.4	12.7	16.0	9.7

It also appears from Table 1 that the menthone data was generally more consistent (see also Table 2) than the ethyl butyrate data (relatively smaller standard deviations). This has been observed as a common feature of in-vivo release, where compounds with higher air/water partition coefficients (such as ethyl butyrate) show poor mass transfer relative to their thermodynamic equilibrium and hence have the potential for high variability. Low air/water partition coefficient compounds have a more stable, efficient mass transfer, even if it is lower in absolute terms.

In the case of boiled sweets, the main release events have often been observed at the point of swallowing, with mouth movements between swallowing events insufficient to transfer significant amounts of gas from the oral cavity to the upper airway [4]. There is consequently a longer time period available for equilibration between the gas and liquid phases in the mouth between release events, compared with when samples are chewed. It might be anticipated that this style of oral processing would simply result in a reduction in the standard deviations observed for the ethyl butyrate data, with nasal and oral volatile concentrations showing the same ratios seen in Table 1.

However, it is clear from Table 2 that both panellists had a much higher oral volatile concentration than that seen for the nasal breath. It is widely believed that swallowing delivers air from the mouth to the pharynx and that this air is subsequently exhaled (in an analogous way to the shorter pulse formed during chewing). If this were the case, the two gas phase volatile concentrations should be more similar.

An explanation for these findings might be found in the swallowing event itself. During swallowing, breath flow in the upper airway ceases, to allow the safe transfer of solids and liquids from the mouth to the oesophagus [3]. At this time the oral cavity decreases its volume, but in a different pattern to that of chewing. Rather than focusing on compression or shearing of the bolus the objective is to remove part or all of it. The tongue rises to meet the palate at the front of the oral cavity and then the tongue contacts the palate further and further back in the oral cavity forcing the sample (and oral gas phase) to be swallowed. Once the bolus has been transferred through the pharynx into the oesophagus the lower jaw is lowered prior to exhalation. This will draw some air from the pharynx back into the mouth. This may be some of the volatile laden air originally forced from the mouth, reducing the amount available for nasal exhalation. In this low gas flow environment, there is also a potential for mixing-induced dilution prior to the exhalation of the gases. Consequently, during

swallowing, the transfer of volatiles from mouth to nose may not reflect the oral gas phase concentration.

Table 2. Average peak heights (and standard deviations SD) for volatiles in the breath of panellists consuming mint (menthone) or fruity (ethyl butyrate) boiled sweets. Breath was sampled from either the mouth (oral) or nose (nasal). Values are arbitrary peak height units $\times 10^6$.

	Panellist 1				Panellist 2			
	Oral		Nasal		Oral		Nasal	
	mean	SD	mean	SD	Mean	SD	mean	SD
Menthone	18.3	2.1	6.9	2.0	28.0	2.6	3.9	1.4
Ethyl butyrate	7.4	3.4	0.9	1.2	6.6	0.9	1.2	0.2

Modern confectionery has given us the extremes of foodstuffs that are almost exclusively either chewed or sucked for long periods of time, far longer than most typical eating experiences. These appear to highlight differences in gas phase transfer during the processes of chewing or swallowing. It is, however, important to remember that these are atypical examples of foodstuffs in general. The majority of foods result in a complex pattern of chewing and swallowing, delivering aroma over the eating time course with minimal potential for long phases of in-mouth, saliva/air volatile equilibration.

References

1. Linforth R.S.T., Taylor A.J. (2006) In *Flavour in Food* (Voilley A., Etievant P.X., eds.); *Woodhead Publishing Ltd.*, pp: 287-307.
2. Buettner A., Beer A., Hannig C., Settles M. (2001) *Chem. Senses*. 26: 1211-1219.
3. Hodgson M., Linforth R.S.T., Taylor A.J. (2003) *J. Agric. Food Chem.* 51: 5052-5057.
4. Linforth R.S.T., Hodgson M., Taylor A.J. (2003) In *Flavour Research at the dawn of the Twenty-first Century* (LeQuere J.-L., Etievant P.X., eds.); *Lavoisier*, pp: 143-147.
5. Linforth R.S.T., Taylor A.J. (2003) *Int. J. Mass Spec.* 223-224: 179-191.
6. Keyhani K., Scherer P.W., Mozell M.M. (1997) *J. Theor. Biol.* 186: 279-301.

HOW MODEL CHEESE COMPOSITION CAN INFLUENCE SALT AND AROMA COMPOUNDS MOBILITIES AND THEIR PERCEPTION

C. Lauerjat, A. Saint-Eve, C. Magnan, I. Délérís, I.C. Tréléa, and I. SOUCHON

UMR 782 Génie et microbiologie des procédés alimentaires, AgroParisTech – INRA, F-78850 Thiverval-Grignon, France

Abstract

The aim of our study was to identify properties (partition or/and diffusion coefficients) and mechanisms explaining mass transfer and release of salt and aroma compounds in model cheeses with different compositions and textures, in order to better understand kinetic of available quantity of stimuli during eating in relation to perception. The systematic study enabled to quantify the impact of fat, dry matter and salt on physicochemical properties and on perception. As expected the level of fat and of dry matter affected the retention of the aroma compounds. However, neither the mobility of the flavour compounds nor salt mobility in model cheeses was significantly modified by any of the studied composition factors. In-nose measurements of aroma release during eating highlighted the importance of chewing behaviour on release and perception. All these results bring some quantitative information to better understand what are the main mechanisms involved in aroma and salt release and how they could explain or not perception.

Introduction

The daily consumption of salt in developed countries is too high and may lead to health issues like hypertension, coronary diseases and strokes. Consequently, there is an increasing interest for the production of low-sodium food products. However, as salt perception interact with aroma perception [1], the reduction of salt in food product without modifications of organoleptic properties needs a better understanding of the effects of food structure and composition on aroma and salt release and perceptions. Different studies have observed that texture influences salt and aroma release during consumption [2, 3] but, to our knowledge, it was scarcely related to mechanisms of release as the stimuli mobility in food matrix or breakdown in mouth. In this context, the aim of the present study was to determine the physicochemical properties as partition and diffusion coefficients for salt and aroma compounds in model cheeses with different textures and compositions to explain release and perception.

Experimental

Product preparation. The model cheeses varied in dry matter content (DM: 370 – 440 g/kg), fat content (F: 20 – 40%, dry basis) and salt content (S: 0.5 – 1.5%) leading to product with different composition and structure. Model cheeses were flavoured with three aroma compounds (ethyl hexanoate, 2-heptanone, and diacetyl).

Determination of diffusion and partition coefficient of aroma compounds. 25g of flavored product were introduced in a 250mL vial and equilibrated at 13°C during 24h. The headspace was purged during 12 min with a constant air flow and analysed

by proton transfer reaction – mass spectrometry (PTR–MS), leading to air stripping kinetics. The PTR-MS instrument drift tube was thermally controlled (60°C) and operated at 2.0 mbar with a voltage set to 600 V. Measurements were performed with a dwell time per mass of 0.1s. The mass fragments for the studied compounds were as follows: $m/z= 87$ (diacetyl), $m/z= 115$ (heptan-2-one) and $m/z= 145$ (ethyl hexanoate). A mass transfer analysis, similar to the approach developed by Juteau-Vigier *et al.* [4] was performed to determinate from air stripping kinetics, partition and diffusion coefficients.

Determination of diffusion and partition coefficient of salt. Adaptation of the PRV method [5] allowed the determination of water/product partition coefficient of salt. Different quantities of model cheese (10 to 40g) were introduced in 250 mL bottles and different volumes of deionised water (40 to 150 mL) were added in order to get different water/product ratios. The bottles were kept in a water bath at 13°C during 48h to reach thermodynamic equilibrium. The NaCl concentration was determined using a calibrated conductivity probe coupled with a control sample without salt. A non-linear regression, similar to the one developed by Atlan *et al.* [6] led to the determination of the partition coefficient.

To obtain salt release kinetics, 40g of product were gelled in a 10 cm diameter beaker and 500 mL of deionised water was poured and placed under agitation at 13°C. The salt release was recorded during 48h with a calibrated conductivity probe. Diffusion coefficient was determined adjusting a mathematical model based on the second Fick's law to the experimental data.

In nose measurement of aroma compounds release. The breath of 4 panelists consuming the flavored model cheeses was analysed using a PTR–MS during 10 minutes. No special instructions were given to the assessors regarding how to consume the product. The same ions as for *in-vitro* measurements were monitored. Thanks to software developed in the laboratory, several parameters were extracted from the raw data including maximal intensities (I_{max}), area under the curve (AUC) before and after swallowing.

Sensory analysis. A quantitative analysis was performed with 10 trained panelists on the products to study texture, taste and olfactory perceptions.

Data analyses. Analysis of variance was performed using SAS software package, version 9.1.

Results and Discussion

Influence of texture and composition on aroma compounds and salt mobilities. The adjustment of the mathematical model lead to the determination of both partition and diffusion coefficients of each of the 3 studied aroma compounds (Figure 1). The analysis of variance showed differences in air/product partition coefficients between products. An increase in fat content led to a decrease in partition and diffusion coefficients for hydrophobic compounds (2-heptanone and ethyl hexanoate). Whatever the volatile compounds, an increase in dry matter led to a decrease of partition and diffusion coefficients. Salt content increase induced an increase of partition and diffusion coefficients of ethyl hexanoate only. These results established the existence of interactions between the product composition and the flavor compounds.

The values of water/product partition coefficient of salt measured by the PRV method were below 1, meaning that salt was partially retained by the product but the composition of the matrix did not influence this retention. Concerning salt diffusion, a

slight increase of the diffusion coefficient when fat content increases was observed. Salt content increase induced an increase of salt diffusion. The known effect of dry matter was highlighted as diffusion coefficient was twice higher in the product presenting the lower dry matter (Figure 2).

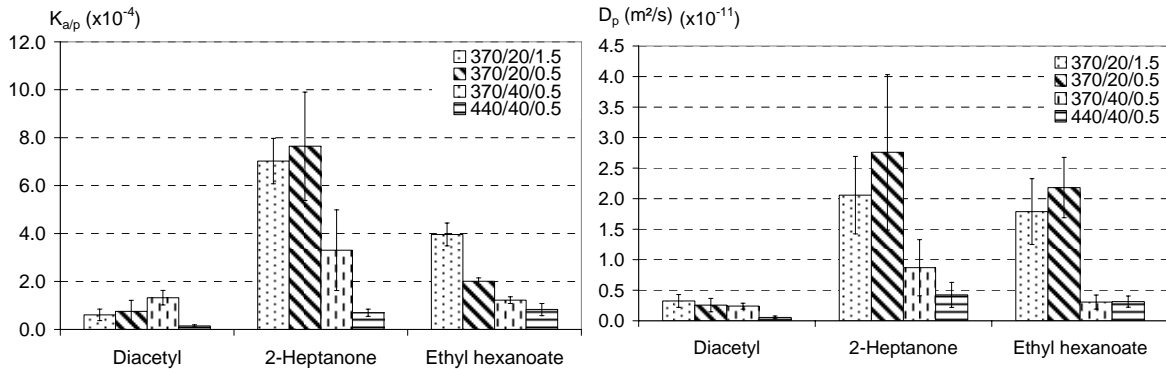


Figure 1. Air/product partition ($K_{a/p}$) and diffusion coefficients of aroma compounds (D_p) in model cheeses at 13°C (Product code: Dry Matter (g/kg) / Fat Content (%) / Salt (%))

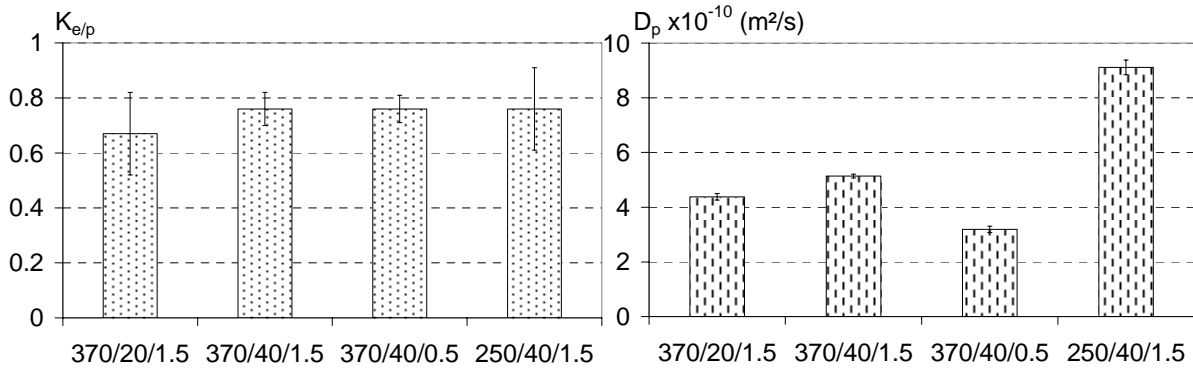


Figure 2. Water/product partition ($K_{w/p}$) and diffusion coefficients (D_p) of salt in the model cheeses at 13°C (Product code: Dry Matter (g/kg) / Fat Content (%) / salt (%))

Influence of texture and composition on in-vivo aroma compounds release. The analysis of variance showed that fat and dry matter variations led to differences in flavor release during consumption contrary to salt content which did not influence flavor release. As expected when fat content increased, the amount of released hydrophobic aroma after swallowing decreased. On the contrary when dry matter increased the amount of released aroma increased before swallowing (Figure 3). This result could be explained by the chewing duration. Indeed as shown in

Figure 4, the chewing time slightly increased when model cheeses firmness increased, leading to an increase in aroma release. This result is in agreement with other authors like Boland et al. [2].

Influence of texture and composition on aroma compounds and salt perception. The quantitative analysis showed a significant decrease in “blue cheese” perception and butter perception when fat content and salt increased respectively. On the contrary, overall odor intensity increased when salt content increased. No significant difference was observed according to dry matter. Also, texture and composition of the model cheeses did not influence salty perception.

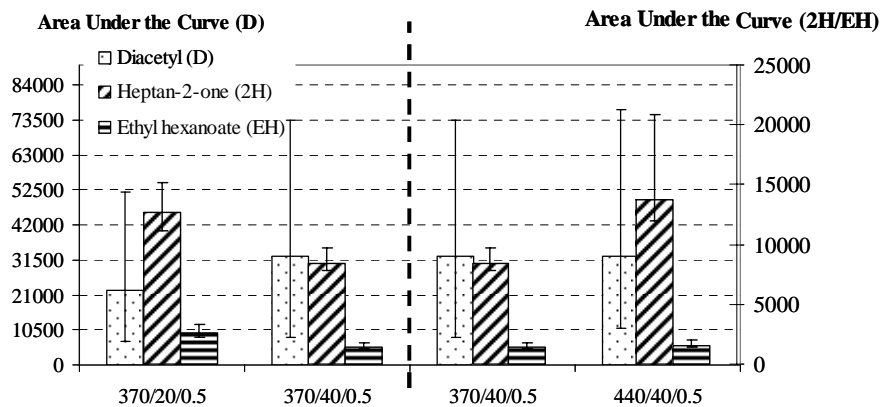


Figure 3. Influence of fat and dry matter on the amount of released aroma before swallowing (Product code: Dry Matter (g/kg) / Fat Content (%) / salt (%))

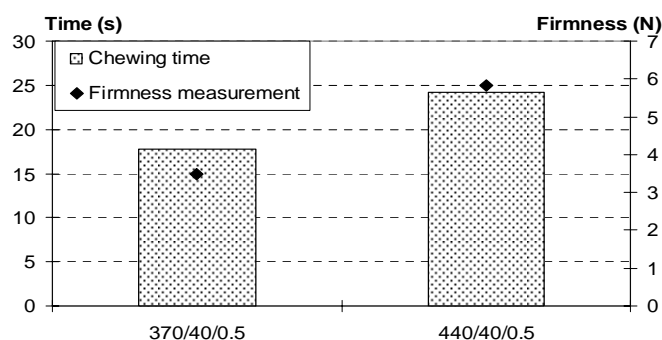


Figure 4. Chewing duration according firmness of the model cheeses (Product code: Dry Matter (g/kg) / Fat Content (%) / salt (%)).

In conclusion, variations in composition and texture of the studied model cheeses did not highly influence salt and aroma compounds mobility, but physicochemical interactions between aroma compounds and matrices were highlighted. The physicochemical interactions are in agreement with aroma release, but food breakdown during eating seems to have more influence on aroma release than physicochemical properties. Salty perception was not influenced by texture and composition, but cognitive interactions between aroma perception and salty perception could exist and could represent an interesting way to reduce salt content without a loss of the organoleptic qualities.

References

1. Djordjevic J., Zatorre R.J., Jones-Gotman M. (2004) *Exp. Brain Res.*, 159: 405-408.
2. Boland A.B., Delahunty C.M., van Ruth S.M. (2006) *Food Chem.*, 96: 452-460.
3. Phan V.A., Yven C., Lawrence G., Chabanet C., Reparet J.M., Salles C. (2008) *Int. Dairy. J.*, 18: 956-963.
4. Juteau-Vigier A., Atlan S., Deleris I., Guichard E., Souchon I., Trelea I.C. (2007) *J. Agric. Food Chem.*, 55: 3577-3584.
5. Ettre L.S., Welter C., Kolb B. (1993) *Chromatographia*, 35: 73-84.
6. Atlan S., Trelea I.C., Saint-Eve A., Souchon I., Latrille E. (2006) *J. Chromatogr. A*, 1110: 146-155.

UNDERSTANDING PHYSIOLOGICAL AND PHYSICOCHEMICAL INFLUENCES ON IN-MOUTH AROMA RELEASE FROM YOGURTS USING MECHANISTIC MODELLING

I. SOUCHON, S. Atlan, A. Saint-Eve, I. Déléris, E. Sémon, E. Guichard, and I.C. Tréléa

UMR 782 Génie et Microbiologie des Procédés Alimentaires, INRA - AgroParisTech, 1 av. Lucien Brétignières, F-78850 Thiverval-Grignon, France

UMR1129 Flaveur, Vision et Comportement du Consommateur (FLAVIC), INRA – ENESAD - Université de Bourgogne, 17 rue Sully, BP 86510, F-21065 Dijon, France

Abstract

On the basis of a first mechanistic model predicting aroma release in the oropharynx during food consumption, the aim of the present work was to improve its accuracy and to use it to identify the main mechanisms responsible for in-mouth aroma release. Comparison between predicted release kinetics and the ones measured by APCI-MS in the nasal cavity of subjects eating flavoured yogurt highlighted the reasonably accurate time predictions of the relative aroma concentration in the nasal cavity and the model ability to simulate successive swallowing events as well as partial velopharyngeal closure. Parameters identified as the most influent for *in-vivo* aroma release were related to either physico-chemistry (equilibrium air/product partition coefficient, mass transfer coefficient in the product), physiology (the volume of the nasal cavity, breath airflow rate) or interaction between both (the amount of residual product in the pharynx, air/product contact area).

Introduction

Consumer choices and preferences clearly depend on food organoleptic properties. Yet, the relationship that exists between aroma release during eating and perception is quite complex and not well understood because of the existence of perceptual interactions and possibly of other poorly known mechanisms (1). Few studies developed an integrated modelling approach taking the whole physiological, physicochemical and kinetic phenomena into account (2-4). Recently, a mechanistic mathematical model describing aroma release in the nasal cavity during the consumption of semi-solid (gelled) product was build, considering retronasal aroma intensity as a function of volatility and transfer properties of aroma compounds in food matrices and physiological characteristics of consumers (5).

The first aim of the present work was to improve the previous model accuracy, notably by taking the inter-individual variability of physiological behaviour into account. The second objective was to use this model to identify the main mechanisms responsible for in-mouth aroma release and to better understand how the characteristics of products (composition, structure) and/or individuals (physiological parameters, individual experience) could explain sensory differences.

Results and Discussion

Description of the mechanistic model. As illustrated in Figure 1, the model we developed is based on a physiological representation of (a) the upper respiratory tract, described as five interconnected reactors (oral and nasal cavities, pharynx, oesophagus and trachea), with time-varying volume and containing an air phase and possibly a flavoured product; (b) the swallowing process, divided into four main steps: product conservation in mouth, the contraction of the oral cavity, product swallowing (contraction of the pharynx) and finally the relaxation of both the pharynx and the oral cavity. Volatile release is quantitatively described using tools from chemical engineering. Detailed mass balances are written for each step in each compartment. Mass balances include volatile release at air-product interface and, when appropriate, bulk flows for product and air (5).

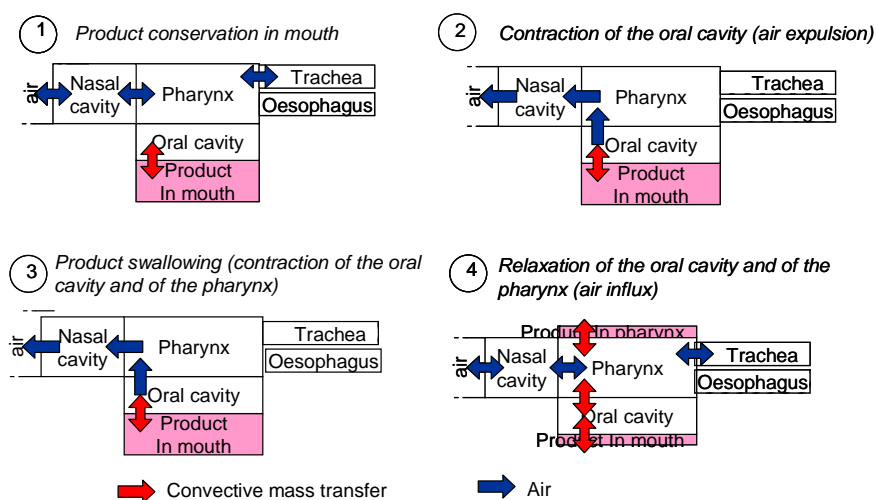


Figure 5. Schematic representation of the different steps of the mechanistic model of consumption.

Model validation. Predictions of the release kinetic of aroma compound in the nasal cavity during yogurt consumption were compared to gaseous concentration measured by atmospheric pressure chemical ionisation mass spectrometry (APCI-MS). As illustrated on (Figure 6), agreement with the measured nose-space concentration is reasonably good, taking the simplifying modelling assumptions versus the complexity of the oropharynx anatomy and of the swallowing physiology into account. This fair adequacy was observed for 3 aroma compounds having different physicochemical properties in the case of 2 stirred yogurt consumed by 3 panellists. This release kinetic confirmed the major importance of the first swallowing event for aroma release as gaseous concentration is very low before and increased drastically just after (6).

Velopharynx closure while keeping the product in the mouth can be more or less tight, depending on experiments, on individuals, and on product texture (6). Imperfect closure can result in an additional aroma release from the oral cavity as illustrated in (Figure 7) for a panellist (symbols) but was not correctly predicted by our initial model (perfect velopharynx closure, Figure 7a). Imperfect closure was represented in the model by a nonzero contact area between the oral cavity and the pharynx. This model extension led to a more accurate prediction of aroma release for partial velopharynx closure (Figure 7b).

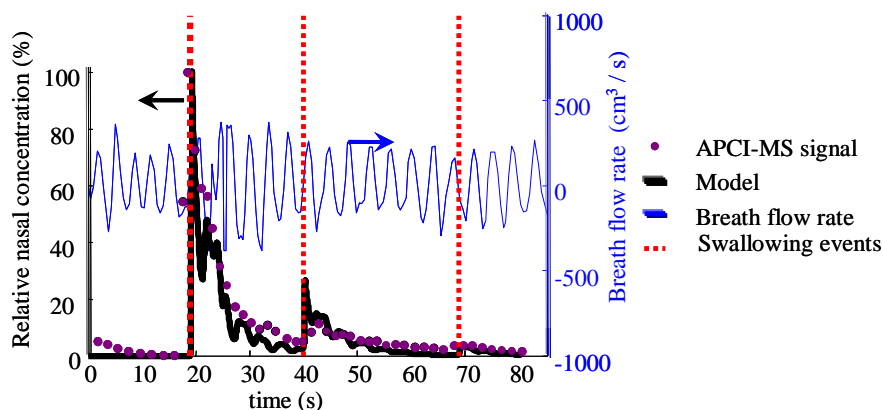


Figure 6. Release of ethyl acetate in the nasal cavity of a panellist during the consumption of a yogurt. Measured (symbols) and simulated (bold line) relative aroma compound concentration in the nasal cavity, breath flow rate (thin line) and deglutition events (dashed line).

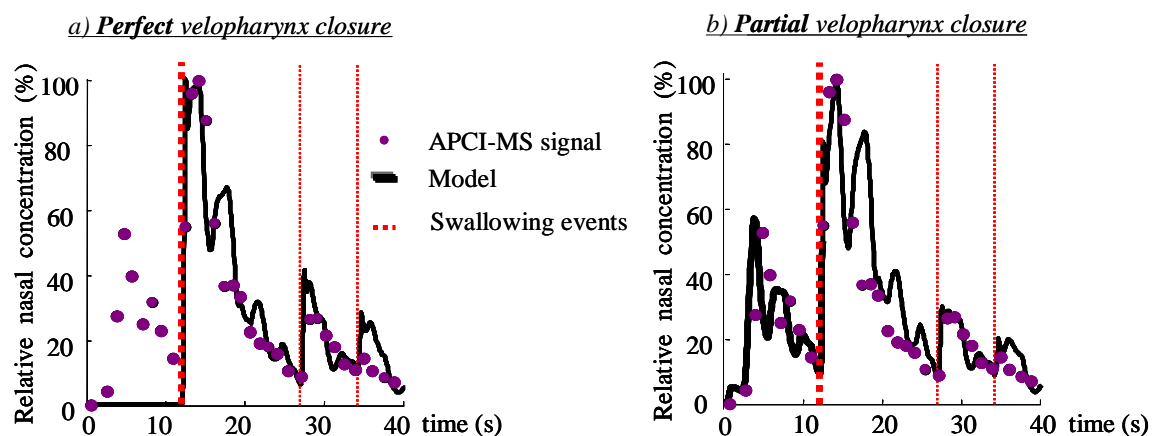


Figure 7. Measured (symbols) and simulated (bold lines) relative aroma compound concentration in the nasal cavity of one panellist during the consumption of a yogurt and deglutition events (dashed line). Prediction of aroma release with a (a) perfect or (b) partial velopharynx closure while the product is kept in the mouth.

Identification of critical model parameters. As the presented mechanistic model contains a large number of parameters, some of which are poorly known, difficult to measure experimentally and/or subject to significant interindividual variability. The goal was to determine those on which future experimental effort should be concentrated in order to improve prediction accuracy and those for which order of magnitude estimations would be sufficient.

Among all the physicochemical parameters of the aroma/product couple, the most significant effect is obtained for variations in the equilibrium air/product partition coefficient, which represents the volatility of the compound in the matrix being studied (Figure 8a). A 2-fold increase in the air/product partition coefficient induced a roughly 1.5-fold increase in the aroma concentration in the nasal cavity, whereas a 2-fold decrease has a symmetrically opposite effect. Similar, but somewhat smallest effects (1.3-fold increase or decrease) were observed and for the mass transfer coefficient in the product (not shown). The volume of the product introduced in the mouth was also found to have a moderate effect, as already noted by Linforth *et al.*

(7). Concerning physiological parameters, variation of the breath flow rate has a strong effect, as could be expected: the lowest the breath flow rate, the highest the aroma persistence (Figure 8b).

Finally, some parameters, dependent on interaction between physico-chemistry and physiology, were identified as influent on aroma release: the contact area between the air and the product in the pharynx (Figure 8c), which is related to the residual amount of product in the pharynx and to its mechanical behaviour and adhesiveness on mucosa.

All other model parameters, as for example, the contact area between the air and the product in the oral cavity or the mass transfer coefficient in the air, have negligible effect on the simulated nasal aroma concentration, indicating that their accurate knowledge is not essential for running the model. It should be emphasised, however, that these observations are valid for the product, the experimental protocol, the volatile compounds, and the mathematical representation used in this paper.

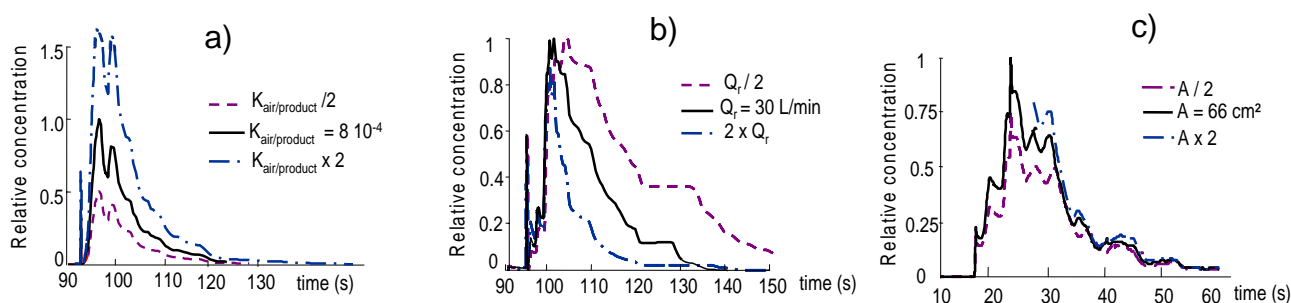


Figure 8. Effect of some of the most sensitive model parameters on the simulated aroma compound concentration in the nasal cavity. Evolution with time of the measured relative ethyl hexanoate concentration in the nasal cavity of one panellist during the consumption of yogurt. Variation of the air/product equilibrium partition coefficient $K_{air/product}$ (a), of the respiration flow rate Q_R (b) and of the air/product contact area in the pharynx A (c).

Conclusions

This mechanistic and quantitative analysis of aroma release enables to better describe the influence of physiological, anatomical and physicochemical parameters and interaction that can exist between these factors. Perspectives concern a better understanding of product breakdown in mouth and application of a similar approach to sapid compounds. Possible applications include computer-aided product formulation, considering the retronasal aroma intensity as a function of aroma compound properties in food matrices and anatomico-physiological characteristics of the consumers.

References

1. Bult J.H.F., de Wijk R.A., Hummel T. (2007) *Neuroscience Letters* 411 (1): 6-10.
2. Wright K.M., Sprunt J., Smith A.C., Hills B.P. (2003) *Int. J. Food Sci. Tech.* 38: 351-360.
3. Lian G., Malone M.E., Houan J.E., Norton I.A. (2004) *J. Control. Rel.* 98: 139-155.
4. Normand V., Avison S., Parker A. (2004) *Chem. Senses* 29: 235-245.
5. Trelea C., Atlan S., Déléris I., Saint-Eve A., Martin M., Souchon I. (2008) *Chem. Senses* 33: 181-192.
6. Buettner A., Beer A., Hannig C., Settles M., Schieberle P. (2002) *Food Quality Prefer.* 13: 497-504.
7. Linforth R.S.T., Blissett A., Taylor A.J. (2005) *J. Agric. Food Chem.* 53:7217-7221.

IN-VIVO AROMA RELEASE OF LOW AND HIGH FAT SEMI-HARD CHEESES

C. COUNET-KERSCH, W. Wesselink, A. Hettinga, L. Oeseburg, H. Luyten and C. Ponne

Friesland Foods Corporate Research, Harderwijkerstraat 41006, 7418BA Deventer, The Netherlands

Abstract

In this study, the EXOM method (EXhaled Odorant Measurement) was modified and specifically adapted to dairy products. We were able, for the first time, to follow the *in-vivo* aromas during the eating of high and low fat hard cheeses. A total of 9 important key aromas were followed using gas chromatography – mass spectrometry: 2,3-butanedione, 3- and 2-methylbutanoic acids, ethyl butanoate, 2-heptanone, 3-methylbutanol, 3-methylbutanal, methional, and 2-butanone. We observed, for instance, that during the consumption of the high-fat cheese, more ethyl butanoate (sweet) was released while the dominant aroma in low-fat cheese was 3-methylbutanol (solvent-like). The swallowing event appeared to play a central role for the release of the aromas of cheese. Time-intensity sensory analysis confirmed also the importance of swallowing. The comparison of the *in-vivo* aroma release with the aroma concentration was used to determine whether the release observed was due to an effect of concentration or an effect of the specific texture of the cheese.

Introduction

Low-fat cheese is known to have a flavor and texture different from that of high fat cheese. In order to optimise the flavor, a better understanding is needed of what happens during consumption. The objective of this work was to understand the *in-vivo* aroma release of low-fat and high fat cheese. The *in-vivo* data were linked to sensory analysis of the cheeses (Time-Intensity, TI) and to analytical data (concentration of aromas in the cheese).

Experimental

The existing EXOM method (EXhaled Odorant Measurement) (1) was not sensitive enough to analyse the low concentration of aromas that are present in cheese (2). This study modified and specifically adapted this method to dairy products. The amount of water collected in the Tenax tube was limited and, consequently, the aroma detection was improved. A specific cooling element was added before the Tenax tube and the tube was gently dried before analysis at 35°C for 5 min. Three subjects were served the 2 cheeses in duplicate. The samples were eaten at 1 chew/second. The low-fat cheese and the high fat cheese were swallowed after 20s and 11s, respectively. *In-vivo* samples were collected from the mouth after intervals of 1s, 4s, 7s, 11s for the high fat cheese and 1s, 4s, 7s, 13s or 20s for the low-fat cheese. A further sample was also collected 5s after the swallowing of the cheese. A control

sample was collected for each subject in duplicate. A control of the sampling time was done using a webcam and the time was for some subjects corrected (± 2 s). *In-vivo* samples (Tenax tube) were analysed by GC-Trace MS. The aroma concentration of each cheese was determined by GC-MS-TOF and the standard addition method. A time-intensity (TI) analysis of overall flavor intensity was carried out by 10 trained panelists (including the 3 “*in-vivo*” subjects) in triplicate. The polarity of an aroma was estimated on the basis of its experimental log P (from our flavor database).

Results

Our *in-vivo* release method gave reproducible results for the low and high fat cheeses (Figure 1). The release profiles were also similar for the 3 panelists. In high fat cheese, more ethyl butanoate (*sweet, fruity*) and 2-heptanone (*fruity, sweet, herbal*) were released. In low-fat cheese, 4 aromas were dominant: 3-methylbutanoic acid (*rancid-cheese, sweaty socks*), 2-methylbutanoic acid (*fruity, waxy, sweaty-fatty acid*), 3-methylbutanol (*solvent-like, fruity, alcohol*), and diacetyl (*buttery*).

It can be seen from (Figure 1) that aroma concentrations were higher after the swallowing event. For 2-heptanone (data not shown), the release only occurred during the swallowing. This phenomenon was not a surprise since during swallowing the velum (3) opens and probably creates a coating of cheese in the throat (4) leading to a higher release of aromas. For almost all compounds, the release profile was similar for high and low fat cheese. However, clear differences were seen in the height of the peak.

To investigate whether the aroma release curves result from differences in concentrations of aromas in the cheese, we measured the concentrations of the aromas in the cheese and recalculated the *in-vivo* curves on the basis of equal starting concentrations.

An effect of concentration of the cheese was observed for the release of ethyl butanoate (Figure 2a) and 2-heptanone. These compounds, deriving from fat, were found in higher concentration in the high fat cheese. The effect of the specific texture-composition of the cheese can explain the differences between the two cheeses if no effect of concentration was present. An effect of the specific texture-composition of the cheese was observed for the release of 3-methylbutanol (Figure 2b), 3-methylbutanal and 3-methylbutanoic acid. The first two compounds are polar and then more release from the high fat cheese which contained less water. It is still unclear why the 3-methylbutanoic acid, a polar compound, was more released for the low-fat cheese.

The TI results (Table 1) shows that the high fat cheese has more total flavor (I_{max} and Area significantly higher for high fat cheese). The total flavor was perceived at its highest level at a later point in time for low-fat cheese than for high fat cheese. There were no significant differences in the duration of the plateau for the low-fat and high fat cheeses (difference TSPI-TEPI). The higher value of a TI total flavor, as well as the higher point of the *in-vivo* aroma release, corresponds to the swallowing time event.

In conclusion, a method to monitor the *in-vivo* release of aromas during the eating of high and low fat hard cheeses was presented. During the consumption of the high-fat cheese, more ethyl butanoate and 2-heptanone were released while the dominant aromas in low-fat cheese were 3-methylbutanol, 3(and 2)-methylbutanoic acids and diacetyl. The swallowing event appeared to play a central role for the release of the aromas of cheese. TI sensory analysis confirmed the importance of swallowing. The comparison of the *in-vivo* aroma release with the aroma concentration showed whether the observed release was due to an effect of concentration or to an effect of

the specific texture-composition of the cheese. The use of *in-vivo* methods using real cheese is potentially very useful to improve the flavour of low-fat cheeses.

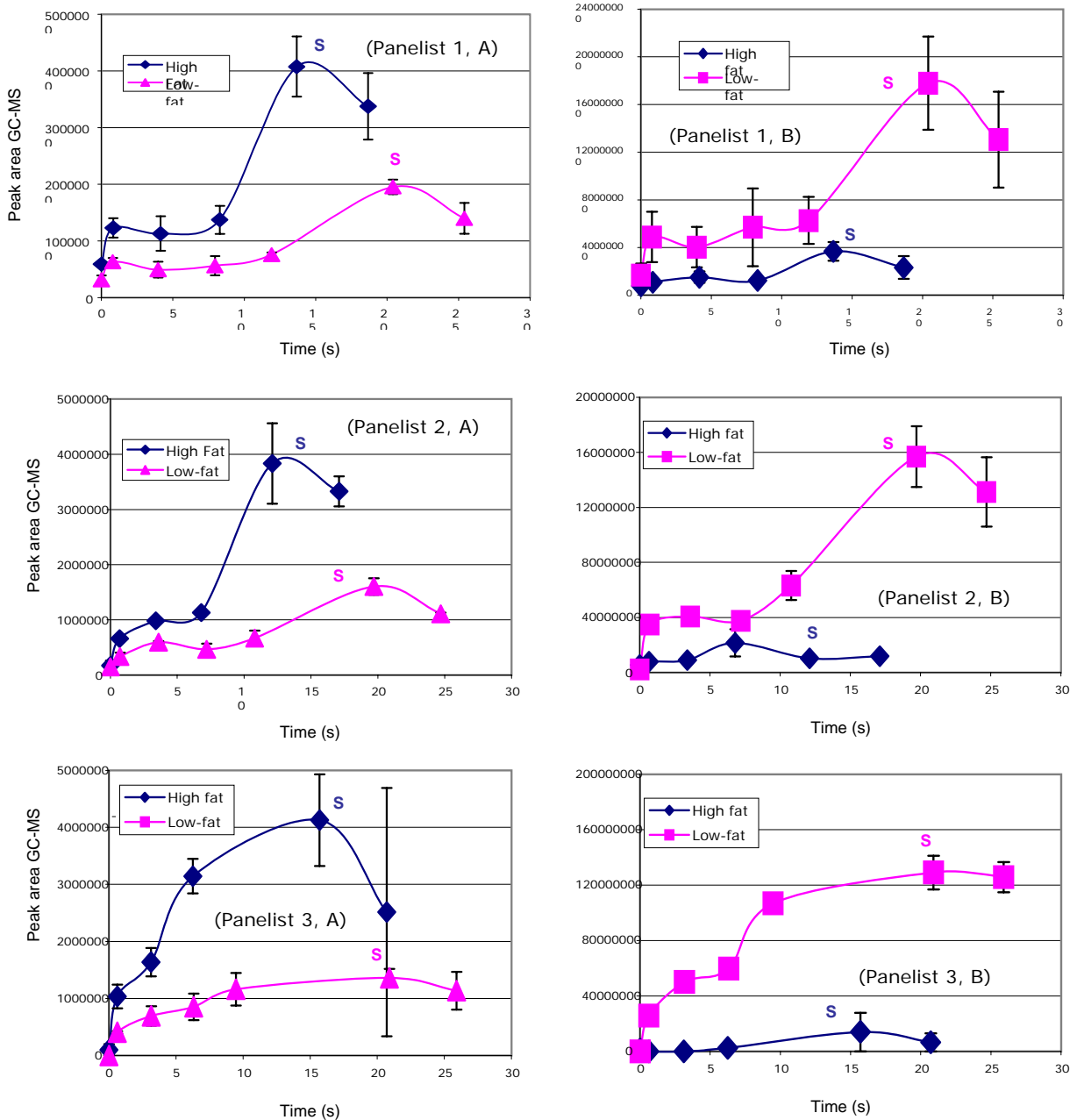


Figure 1. Release of ethyl butanoate (A) and 3-methylbutanol (B) in function of the time (s). SW = swallowing time.

Table 1. Parameters of the time-intensity (TI) test (total flavor).

Parameter	High fat	Low-fat
Imax ^a	75	64
AREA ^b	3002	2503
TSPI ^c	19	26
TEPI ^d	26	34

^a Imax = maximum intensity of the curve, ^b AREA = total area under the TI curve, ^c TSPI = start time of the plateau, ^d TEPI = end time of the plateau. The values in the table are significantly different from each other.

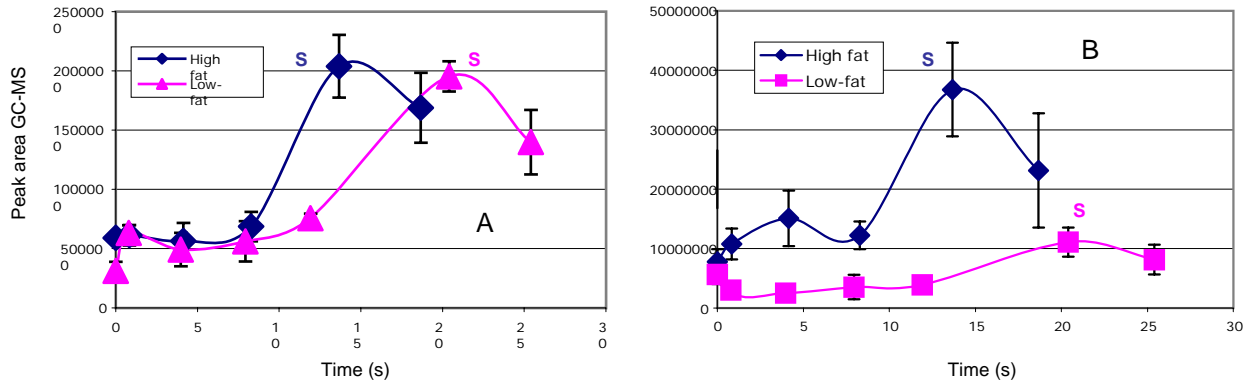


Figure 2. Release of ethyl butanoate (A) and 3-methylbutanol (B) in function of the time (s) - Curves recalculated in function of the concentration (panelist 1). SW = swallowing time.

References

1. Buettner A., Schieberle P. (2000) *Lebensm. Wiss. Technol.* 33: 553-559.
2. Curioni P.M.G., Bosset J.O. (2002) *Internat. Dairy J.* 12: 959-984.
3. Buettner A., Beer A., Hannig C., Settles M. (2001) *Chem. Senses* 26: 1211-1219.
4. Buettner A., Beer A., Hannig C., Settles M., Schieberle P. (2002) *Food Qual. Pref.* 13: 497-504.

TEXTURE-AROMA INTERACTIONS IN DAIRY PRODUCTS: DO *IN-VIVO* AND *IN-VITRO* AROMA RELEASE EXPLAIN SENSORY PERCEPTION?

E. GUICHARD^{1,2,3}, E. Sémon^{1,2,3}, I. Gierczynski^{1,2,3}, C. Tournier^{1,2,3}, A. Saint-Eve⁴, I. Souchon⁴, C. Sulmont-Rossé^{1,2,3}, and H. Labouré^{1,2,3}

¹ INRA, UMR 1129 FLAVIC, F-21000 Dijon, France

² ENESAD, UMR 1129 FLAVIC, F-21000 Dijon, France

³ Université de Bourgogne, UMR 1129 FLAVIC, F-21000 Dijon, France

⁴ UMR 782 GMPA, AgroParisTech, INRA, F-78850 Grignon, France

Abstract

The influence of the texture on perceived aroma intensity and on *in-vivo* and *in-vitro* aroma release was investigated on three types of dairy products, prepared with different textures. Aroma release depends on in mouth breakdown of the product. The consequences of a textural modification on aroma perception were not the same for the different products. In the case of liquid to semi-liquid products (yogurt and custard dessert), *in-vivo* aroma release decreased when viscosity increased. For firm gels (model cheeses) *in-vivo* aroma release was found to increase when cheese hardness increased, but inverse results were obtained in *in-vitro* conditions. Thus, aroma release could explain perceived aroma intensity for yogurts but not for cheeses for which large inter-individual differences were observed. An adaptation of the chewing pattern was supposed *in-vivo* leading to high structural modifications.

Introduction

The molecules responsible for olfactive and gustative stimuli are released during food mastication and then reach the sensory receptors. Despite the new technical developments for measuring *in-vivo* release of molecules during food consumption, the origin of the differences observed in sensory perception between matrices with different structures are not well elucidated, suggesting a combined effect of physico-chemical and cognitive mechanisms. In the context of a French collaborative project (RARE-CANAL-ARLE), the Atmospheric Pressure Chemical Ionisation-Mass Spectrometry (APCI-MS) technique was used to follow *in-vivo* and *in-vitro* aroma release in different types of food matrices. For each type of dairy food, different textures were obtained in order to evaluate the influence of the texture on aroma release and to relate these data to sensory analyses of aroma and texture attributes.

Experimental.

Products. Two yogurts (22.5% dry matter, 4% fat, 5.4% protein) were prepared as already described (1) and only differed by their complex viscosity measured at a low shear stress of 0.1 Pa: thick yogurt (60 Pa·s) and liquid yogurt (25 Pa·s) .

Dairy desserts (skim milk containing 3.2% protein, 7% sucrose, 3% starch and 0.2% κ-carrageenan) were prepared with different apparent viscosities (measured at 50 s⁻¹): viscous dessert (2.51 Pa·s) and soft dessert (1.02 Pa·s). For both yogurts and

dairy desserts, texture was modified at constant composition by applying an additional mechanical treatment.

Model cheeses (10% protein, 4% lactose, 1% NaCl, 0.2% yeast extract) were prepared as already described (2). They differed in their hardness by addition of chymosin: hard cheese with 1% chymosin ($F_{\max} = 2.11$ N) and soft cheese ($F_{\max} = 0.53$ N) with 0% chymosin.

In-vivo aroma release. On-line *in-vivo* aroma release measurements were performed using APCI-MS (2). The following compounds were analysed: ethyl butanoate (MH^+ : m/z 117) in yogurts and cheeses and benzaldehyde (MH^+ : m/z 107) in dairy dessert. The samples were taken into the oral cavity, chewed while keeping the mouth closed, then swallowed.

In-vitro aroma release (example of cheeses). Samples of 60g were placed in a mouth simulator (3) (30°C) then stirred for 6 min at a same shear rate of 110 s^{-1} . Headspace was continuously drawn at 30 ml/min and led to the APCI-MS.

Sensory analysis. Sensory properties of texture, taste and aroma were evaluated by a trained panel or a panel of naive consumers (in the case of dairy dessert).

Results

In-vivo aroma release. For all food products aroma release in the nasal cavity reached its maximum concentration (I_{\max}) after swallowing. For yogurts (Figure 1 left), I_{\max} was the highest for the liquid sample. In dairy desserts (Figure 1 right), I_{\max} was higher and the time to reach I_{\max} tend to be shorter in the soft product. Concerning model fresh cheeses (Figure 2), the reverse situation was observed, with a higher I_{\max} for the harder cheese.

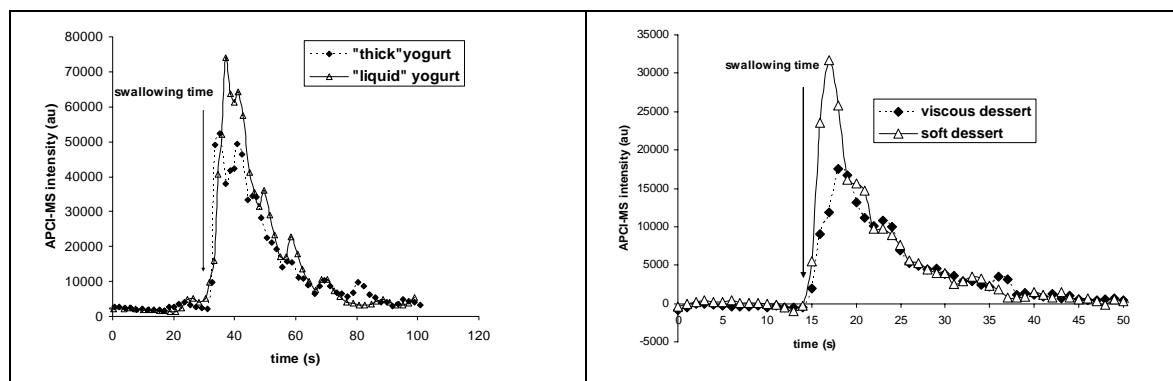


Figure 1. *In-vivo* APCI-MS release curves for ethyl butanoate from yogurt (left) with low mechanical treatment (thick yogurt) and with high mechanical treatment (liquid yogurt) and for benzaldehyde from dairy desserts (right) without mechanical treatment (viscous dessert) and with high mechanical treatment (soft dessert).

In the case of liquid or semi-liquid products (yogurt or dairy dessert), no or low release was observed before swallowing whereas for model cheeses two groups of subjects have been identified according to their *in-vivo* aroma release profiles: for group 1 aroma compounds are released in the nasal cavity before and after swallowing whereas for group 2 aroma compounds are detected mainly after swallowing. Moreover the shapes are similar for the 2 cheeses. These differences may be explained by physiological considerations (4, 5). During swallowing the velum

opens to allow the transfer of the bolus into the pharynx, thus allowing the aroma compounds to reach the nasal cavity. For subjects of group 1, the velum opens also during the chewing phase.

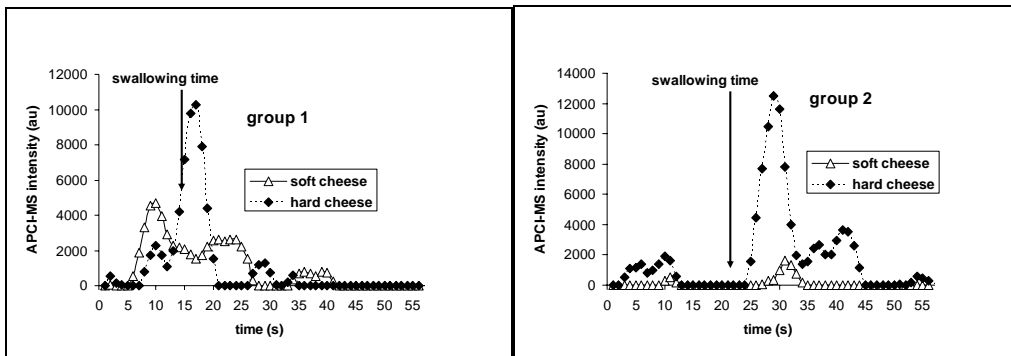


Figure 2. *In-vivo* APCI-MS release curves for ethyl butanoate from model cheeses varying in gel hardness, soft cheese without addition of chymosin (soft cheese), with addition of chymosin (hard cheese), example of 2 subjects with different behaviour (group1 and group 2).

In-vitro aroma release. In addition, *in-vitro* experiments were performed in order to avoid the impact of inter-individual differences and physiological parameters on aroma release. By applying the same stirring rate for the 2 cheeses differing in texture, no difference in the intensity of aroma release was observed, but a higher rate of release in the soft cheese (Figure 3 left). During the *in-vitro* experiments the soft cheese should be better mixed and the surface layers are renewed more rapidly which explains the higher rate of release. During *in-vivo* experiments, panelists may adapt their chewing pattern to the hardness and thus more structural modifications may occur for the hard gel. This result tends to confirm that *in-vivo* aroma release differences were due to an adaptation of the masticatory behaviour of the panelists to food texture rather than to a direct impact of the modification of the structure (2).

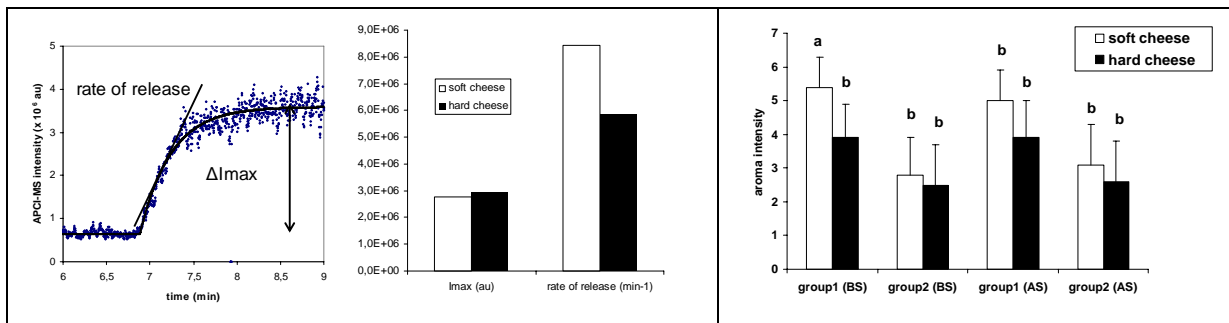


Figure 3. Left: *In-vitro* aroma release curve of ethyl butanoate from model cheeses by applying the same rate of stirring and values of rate of release and maximum intensity obtained for soft and hard cheeses. Right: Aroma perception for the 3 model cheeses before (BS) and after swallowing (AS): mean of aroma intensity for each group of subjects.

Sensory analysis: Texture and aroma. For all products the different textures were significantly discriminated by the panellists. However the consequences of a textural modification on aroma perception were dependant of the type of dairy products. For

yogurts, the liquid sample was perceived significantly higher in aroma intensity at persistence (6). For these products, *in-vivo* aroma release could explain sensory perception. For dairy dessert, no significant effect was observed (7). In the case of model cheeses, the soft cheese was perceived with slightly higher aroma intensity (8) whereas aroma release was less intense. These differences between aroma release and aroma perception could be explained by the fact that panellists paid more attention to texture attributes than to aroma attributes, or by taking taste - aroma interactions into account as the hardest cheese was also perceived with the lowest saltiness. By looking at the sensory results within each group of subjects (Figure 3 right), we noticed that the intensity of aroma perception was differently perceived: aroma intensity was perceived more intense for group 1 which presented a release before and after swallowing and a significant difference in aroma intensity between the 2 different cheeses was found only for group 1. These different behaviours could be explained by differences in physiology.

Conclusion

This paper points out the influence of in mouth food breakdown on aroma release and aroma perception. During food consumption liquid products can cover more extensively the mucus membranes of the mouth and the throat and consequently develop a greater exchange area for the mass transfer of aroma compounds from the product to the air flow of the breath leading to a higher aroma perception. In the case of liquid to semi-liquid products (yogurts), this effect was perceived by trained panelists. In the case of solid products panelists adapt their mastication with a more intense chewing for the harder product, which will induce a higher aroma release due to a higher exchange area between the broken product and the air flow. Perceptual interactions were also observed between texture and aroma for the solid products.

References

1. Saint-Eve A., Juteau A., Atlan S., Martin N., Souchon I. (2006) *J. Agric. Food Chem.* 54: 3997-4004.
2. Gierczynski I., Labouré H., Sémon E., Guichard E. (2007) *J. Agric. Food Chem.* 55: 3066-3073.
3. Decourcelle N., Lubbers S., Vallet N., Rondeau P., Guichard E. (2004) *Int. Dairy J.* 14: 783-789.
4. Buettner A., Beer A., Hannig C., Settles M. (2001) *Chem. Senses* 26: 1211-1219.
5. Mestres M., Kieffer R., Buettner A. (2006) *J. Agric. Food Chem.* 54: 1814-1821.
6. Saint-Eve A., Martin N., Guillemin H., Sémon E., Guichard E., Souchon I. (2006) *J. Agric. Food Chem.* 54: 7794-7803.
7. Tournier C., Sulmont-Rossé C., Sémon E., Issanchou S., Guichard E. (2009) *Int. Dairy J.* 19: 450-458.
8. Gierczynski I., Labouré H., Guichard E. (2007) *J. Agric. Food Chem.* 56: 1697-1703.

CHEWING SIMULATION, A WAY TO UNDERSTAND THE RELATIONSHIPS BETWEEN MASTICATION, FOOD BREAKDOWN AND FLAVOUR RELEASE

C. Yven¹, A. Tarrega¹, E. Sémon¹, S. Guessasma², and C. SALLES¹

¹ INRA, Unité Mixte de Recherches 1129 Flaveur, Vision, Comportement du consommateur, 17 rue Sully, BP86510, F-21065 Dijon Cédex, France

² INRA, UR1268 Biopolymères Interactions Assemblages, INRA, rue de la Géraudière, F-44300 Nantes, France

Abstract

Understanding in-mouth mechanisms is necessary to understand flavour release and perception phenomena. To overcome the limitations of *in-vivo* flavour release measurements, we developed a chewing simulator that faithfully reproduced many mouth functions. Using brittle foods, we showed that *in-vitro* food breakdown was very comparable to that obtained *in-vivo*. We also studied on model cheeses *in-vitro* flavour release by connecting on-line the chewing simulator to APCI-MS. Preliminary results are discussed.

Introduction

Mastication is a complex process involving many mouth functions [1]. The main consequences of this process are the food matrix breakdown and impregnation of food by saliva. This allows flavour compounds to be released in the mouth before reaching olfactory and taste receptors, inducing perception. During chewing and swallowing, flavour release is dependent upon food composition and texture, saliva and mastication parameters as well as the nature of the flavour compounds [2, 3]. It is an important issue in food science that has been extensively studied *in-vivo* these last years, using direct on-line analyses by connecting the subject's nose to an Atmospheric Pressure Chemical Ionization Mass Spectrometer (APCI-MS) [4]. This device also enables real-time monitoring of several aroma compounds released during chewing. Although temporal *in-vivo* studies enable the direct release-perception tests, numerous limitations are observed, such as major inter-individual differences and moderate intra-individual reproducibility. In addition, the food sample must be acceptable to panellists and only a limited number of samples can be evaluated daily. The use of a chewing simulator to perform *in-vitro* temporal analyses could overcome these difficulties. However, the functionalities of the existing devices already are low.

The aim of the present study was to develop a system reproducing as faithfully as possible the main phenomena occurring in mouth during eating such as compression and shearing forces and introduction of saliva, while allowing fluid sampling during the chewing time. We also present the first results obtained *in-vitro* on food breakdown and flavour release.

Experimental

Chewing simulator. The system is made of a mechanical part, an electronic control box and a computer to monitor and tune each parameter. It is fully detailed in reference [5].

Breakdown of hard and brittle food. Four volunteers were asked to eat three peanuts and, after 4 and 8 chews, to spit the sample which was rinsed and dried. For *in-vitro* measurements, the same procedure in terms of number of peanuts and chew cycles was applied. Different procedures were studied, varying in terms of the maximum bite force or the shearing angle value. Three replicates were performed for each procedure. The degree of fragmentation of both *in-vivo* and *in-vitro* chewed samples was studied by measuring the weight of masticated peanuts that could pass through both 4 mm and 2 mm aperture size sieves. Weight percentages were calculated for the 3 size fractions (> 4 mm, 4-2 mm, < 2mm).

Breakdown of airy and brittle food. The *in-vivo* and *in-vitro* experimentations are precisely described in [6]. Two cornflakes types, coded B (more cohesive and sticky) and K (more brittle and crackly), were used. One panellist was asked to eat 2 g of each product. Electromyography recording was done simultaneously. The bolus was collected after 3, 5, 7, 10, 15 chew cycles and just before swallowing and dried. Particle characteristics were determined by image analysis. Analogue experiments were made using the chewing simulator.

In-vitro flavour release. This experiment was carried out on flavoured lipoproteic matrices made by action of rennet on a mixture of milk powder, milk fat to which volatile compounds had been added (Figure 1), NaCl (1 %) and water (water/milk powder: 2.55). Bite force (250 and 350 N), salivary flow rate (1 and 3 mL/min) and ratio fat/proteins (0.5 and 1) were the considered variables. Shear angle remained constant at 3°. Artificial saliva was used [7] without alpha-amylase. Three replicates were considered for each variable. The chewing simulator was connected to an APCI-MS (mass spectrometer equipped with atmospheric pressure chemical ionisation source) apparatus. Air flow rate due to the venturi effect was 30 mL/min. The APCI-MS conditions were similar to that given in reference [8].

Results and Discussion

Breakdown of hard and brittle food under mastication conditions. High *in-vivo* interindividual variability in masticatory performance was observed at 4 and 8 bites for the 4 panellists (10). At a fixed number of peanuts and bites, the same particle distribution was approximately reproduced *in-vitro* by varying the biting force. Biting force and shearing angle were the parameters, which most affected the degree of peanut breakdown. Changes in the saliva flow rate did not modify the degree of peanut breakdown probably because of product hardness and high fat content.

In order to study the effect of bite force and shearing angle on the degree of breakdown, differences in the particle size distribution of fragmented peanuts obtained after 4 and 8 chews were studied. As expected, an increase in both shearing angle and bite force resulted in an increase in the degree of peanut breakdown with a significant interaction between the two factors. In general, the effect of bite force on particle size distribution was greater when no shearing was applied rather than when shearing angles of 3° and 6° were applied.

Breakdown of airy and brittle food in mastication conditions. The objective was to relate human mastication to food texture of brittle products in order to model fracture

mechanisms [6]. *In-vivo*, despite a high variability, the rate of average particle area significantly decreased for B whereas it was not significantly changed for K during chewing. In the case of product B, electromyography data depicted a large increase of the chewing force during the 5 first cycles. A cohesive bolus was obtained after 7 chewing cycles for B whereas it was observed later (after 10 chewing cycles) for K. These results suggested that the transition between the fragmentation and agglomeration mechanisms operated at different characteristic times depending on the nature of the airy product.

In-vitro, using the chewing simulator, the force increased continuously during the first cycle due to the reaction force exerted by the products when the mobile jaw of the system moved forward. Major fracturing events were observed between 200 N and 300N.

Product B exhibited a higher increase of the force compared to product K for up to 5 seconds. Note here that the duration of the chewing cycle duration was imposed to 10 s. As the force level reached about 300 N, complex fracture mechanisms lead to a decrease of the force in the case of product B in the first cycle from 300 to 200 N. Further increase of the force up to 350 N corresponded to the densification of the chewed particles. During the last two cycles, the force stabilised to a value lower than 200 N before an increase of the force which, was inferred to a spatial rearrangement of food fragments in the mouth. Such stabilisation of the force suggested that no further fractures occurred. In the case of product K, the chewing force increased continuously up to 350 N during all the chewing process and the continuous increase of the force was not altered by the chewing cycles. This means that particle breakdown was still operating for K.

In-vitro flavour release from solid matrices in mastication conditions. Superposition of the total ionic current obtained for 3 replicates made in the same conditions showed the good reproducibility of the *in-vitro* flavour release measurements obtained by coupling the chewing simulator directly to APCI-MS. The initial speed of release (initial slope) and maximum intensity were extracted for diacetyl (m/z 89) and 3-octanone (m/z 129) from the release curves for each detectable ion (Figure 1).

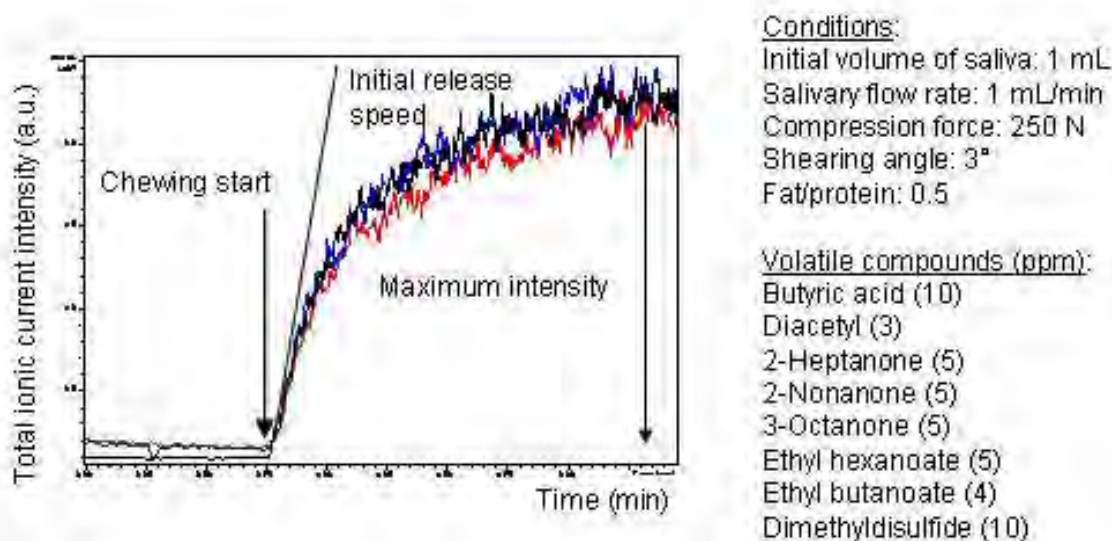


Figure 1. *In-vitro* flavour release from a flavoured lipoproteic matrix by direct coupling of the chewing simulator with APCI-MS apparatus (3 replicates).

For diacetyl, no significant effect of saliva flow rate and food composition (fat/protein ratio) on both initial speed of release and maximum intensity of released diacetyl was observed. The only observed effect was a negative effect of bite force on diacetyl release speed as the effect at 250 N was significantly more important than at 350 N. Concerning 3-octanone, a negative effect of bite force on maximum release intensity was observed, as for diacetyl, and at higher bite force, lower F/P ratio released less volatiles. The same results were obtained for initial release speed. These first results were rather surprising but explanations can be proposed. The negative effect of force could be due to higher agglomeration of particles after breakdown at higher forces, reducing the release phenomenon. The effect of fat could be explained by texture differences: as though fat is well known to retain apolar volatile compounds, the matrices containing higher quantity of fat had a lower hardness and were more easily broken down, leading to a more important release of compounds. That should be confirmed by further experiments.

In conclusion, this device allows getting food breakdown and flavour release results very comparable to *in-vivo* data. Compared to existing systems, its high level of functionalities (real teeth, both bite and shear forces) allows to faithfully mimicking human mouth process as each function can be independently programmed. It is an essential tool to identify the main physical or physiological phenomena explaining the active compound release and to validate the proposed assumptions to model *in silico* flavour release.

References

1. van der Bilt A., Engelen L., Pereira L.J., van der Glas H.W., Abbink J.H. (2006) Oral physiology and mastication. *Physiol. Behav.* 89: 22-27.
2. Tarrega A., Yven C., Semon E., Salles C. (2008) Aroma release and chewing activity during different model cheeses. *Int. Dairy J.* 18: 849-857.
3. Linforth R.S.T., Taylor A.J. (2006) The process of flavour release. In *Flavour in food* (A. Voilley and P. Etievant, Eds.), pp. 287-307. Woodhead Publishing Limited, Cambridge, UK.
4. Taylor A.J., Linforth R.S.T., Harvey B.A., Blake B. (2000) Atmospheric pressure chemical ionisation mass spectrometry for in vivo analysis of volatile flavour release. *Food Chem.* 71: 327-338
5. Salles C., Tarrega A., Mielle P., Maratray, J., Gorria P., Liaboeuf J., Liodenot J.J. (2007) Development of a chewing simulator for the analysis of *in vitro* flavor compounds release in a mouth environment. *J. Food Eng.* 82: 189-198.
6. Yven C., Guessasma S., Chaunier L., Della Valle G., Salles C. (2008) The role of mechanical properties of brittle airy foods on the masticatory performance. *J. Food Eng.*, submitted for publication.
7. Odake S., Roozen J.P., Burger J.J. (2000). Flavor release of diacetyl and 2-heptanone from cream style dressings in three mouth model systems. *Biosci. Biotech. Bioch.* 64: 2523-2529.
8. Savary G. (2006) Impact de la structure de gel composite à base de polyosides sur la liberation d'arôme: exemple des bases de fruits-sur-sucre. *PhD dissertation*. University of Burgundy, Dijon, France.

INFLUENCE OF MOUTH MODEL MASTICATORY FORCE ON THE RELEASE OF LIMONENE FROM ORANGE FRUIT GLUCOMANNAN JELLY

S. ODAKE¹, S. M. Van Ruth², J. P. Roozen², T. Miura¹, and R. Akuzawa¹

¹ *Nippon Veterinary and Life Science University*

² *Wageningen University & Research Center*

Abstract

The release of limonene during mimicked mastication of orange glucomannan jelly using two mouth models was positively correlated to masticatory force. Both models showed shear force effects with increasing masticatory force, and the amount of released limonene was significantly greater with shear effect than without in one model. It is clear that masticatory force is one of the important factors that influence the amount of retronasal volatile release, and work value determined the amount of released limonene.

Introduction

The release of volatiles during mastication evokes retronasal aroma sensations and determines the final palatability of food. There are many factors that influence the release of volatiles during mastication such as: mastication cycle, masticatory force, salivation, and breath flow. Many mouth models, mainly from the 1990's, have been used to investigate such factors (1), and new models, devised to break down foods under realistic conditions, have recently been reported (2-4). This study focused on the effect of masticatory force on volatile release during mimicked mastication of orange fruit glucomannan jelly using two mouth models.

Materials and Methods

Orange fruit glucomannan jelly (Konnyakubatake, Mannanlife Co. Ltd. Gunma, Japan), which can be stored at room temperature, was purchased from a local supermarket in Tokyo. A jelly sample was cut out with a cork poler (ø 2.0 cm) and then trimmed to a height of 2.0 cm. The average sample weight was 5.93 ± 0.17 g.

Mouth model A, the first apparatus utilizing two actions (5), mimicked mastication using a reciprocating vertical plunger with a rotating motion. A thin sensor sheet (Figure 1, 90-130 µm thickness, B201-L, Nitta Corporation, Osaka, Japan) was placed along the inside wall of the sample flask to set a sensing position between the plunger and sample jelly, and mastication force was measured using a computerized tactile sensor system (FlexiForce® ELF, 50-1014, Nitta Corporation).

Mouth model B (Figure 2) was designed to mimic mastication using both upper and lower artificial teeth, which could be moved vertically with a grinding angle of 60°. The interior dimensions of the mouth cavity were ø5.0 cm and a height of 5 cm. The applied force was monitored using a force load cell (VLS-10K of 98.07 N, Valcom, Osaka, Japan) equipped inside the upper teeth plate, and masticatory force was controlled by a feedback system.

Artificial saliva (3 mL) was added, and the headspace of the mouth system was flushed for 1 min at a rate of 100 mL purified nitrogen gas per min, and the released volatiles were trapped on Tenax TA. The peak area of limonene was determined by GC-MS volatile analysis, which was conducted using the method described by Otake. *et al.* (6). Measurements were replicated five times.

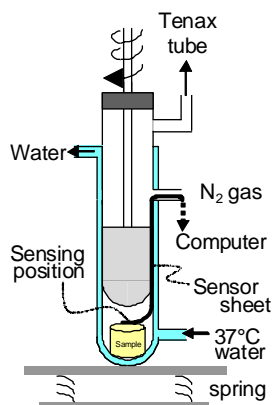


Figure 1. Mouth model A with a force sensor sheet.

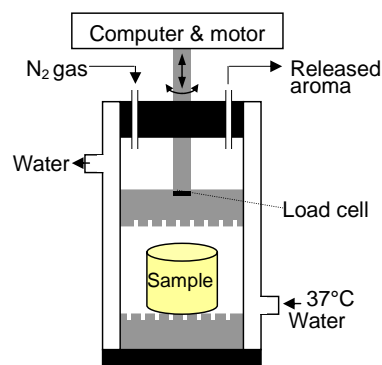


Figure 2. Mouth model B.

Results and Discussion

Comparison of mouth models. Mouth models A and B were operated at 1 Hz vertical motion with a stroke of 2.5 cm and at 86 rpm in A and with 60 ° grinding in B. In all tests, mastication force curves decreased with mastication time (Figures 3a/b and 4a/b), and samples were broken down to a sticky, limp consistency after mastication. The mastication results were different between models A and B. Since the spring foot system (7) absorbed some of the force applied by the plunger in model A, the maximal masticatory force was smaller than that of model B, regardless of the stroke force. In addition, force curves of model A were more irregular than those of B because the vibration caused by the plunger of model A made the sensing sheets unstable in the sample flask. The plunger of model A pressed samples gradually during the entire duration of mastication. In contrast, model B resulted in a larger stroke to the sample with the first bite, both with and without grinding, and the masticatory force changed drastically during a short period at the beginning of mastication. Therefore, samples masticated using model B became limp sooner than those using model A.

Both models showed that the shear effect increased masticatory force during mimic mastication of glucomannan jelly. Furthermore, the difference in force, with and without grinding effect, was greater in model A than in B. This is thought to be caused by differences in the mastication environment between pressing the sample gradually in model A and collapsing the sample in several strokes in model B. The sample height in model A was maintained for a longer period than in model B, and consequently the rotational shear force effect applied to the sample was maintained for the duration of mastication.

The amount of released limonene in model B was greater than in model A (Figure 3c and 4c). This is believed to be due to differences in sample surface area during mastication; with a larger sample surface area in model B as a result of quick sample collapse by the greater mastication force in the larger interior space than in model A. The amount of released limonene in model A with shear effect was significantly greater than that without (t-test, $p < 0.05$). However, no significant difference was

detected using model B (t-test). The difference in masticatory force, with and without shear effect, was more pronounced in model A, and this resulted in a significantly increased volatile release. The difference in shear effect in model B was not considered sufficient to produce a significant difference in the release of volatiles. The sample product in this study showed high elasticity, becoming flexible, sticky, and limp after mastication, and did not separate into particles. Salles (2) reported bigger shear effects on peanuts being the smaller particles during mimicked mastication. Arvisenet (7) showed that after mastication the smallest apple particles showed the highest volatile release. For comparative analysis, it would be interesting to masticate such particulate food samples using models A and B.

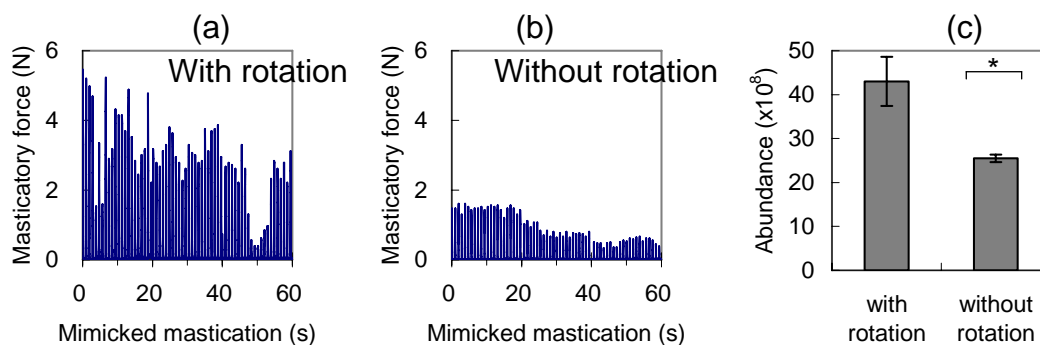


Figure 3. Mimicked mastication by mouth model A with and without rotation: (a) masticatory force with rotation, (b) without rotation, (c) released limonene.

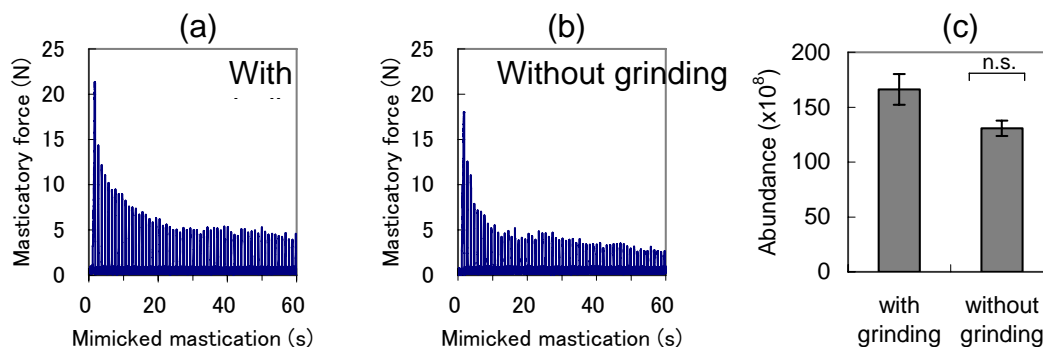


Figure 4. Mimicked mastication by mouth model B with and without grinding motion: (a) masticatory force with grinding, (b) without grinding, (c) released limonene.

Effect of mastication force on volatile release. Different patterns of mastication force (1.0 N, 5.0 N and 7.3 N) with the first bite were obtained by adjusting stroke and clearance in model B (Figure 5a, b, and c, respectively), which was operated at a 0.5 Hz cycle with grinding. The amount of limonene released increased with increasing first bite force (Figure 6a). This is believed to be caused by the larger displacement of the jelly matrix with higher forces. This phenomenon can be explained physically as follows. Work (joules), as shown in Figure 6b, was calculated as mastication force (N) multiplied by displacement (m). Displacement was calculated by the computer system of model B, which monitors the upper tooth position. Basal amounts of released limonene in the dynamic headspace without mastication were regarded as zero, and a linear equation $Y = 222.56 X$ ($r^2 = 0.9755$, $p < 0.05$) was obtained to approximate the relationship between masticatory work and the amount of released volatiles (Figure 6c).

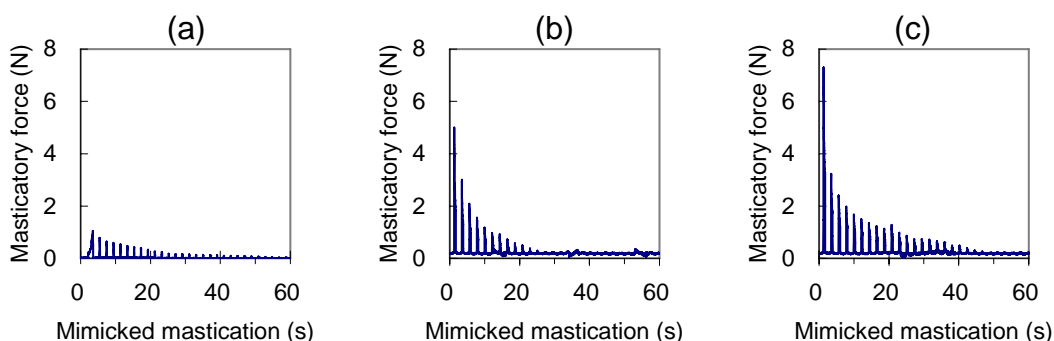


Figure 5. Masticatory force pattern with different first bite force.

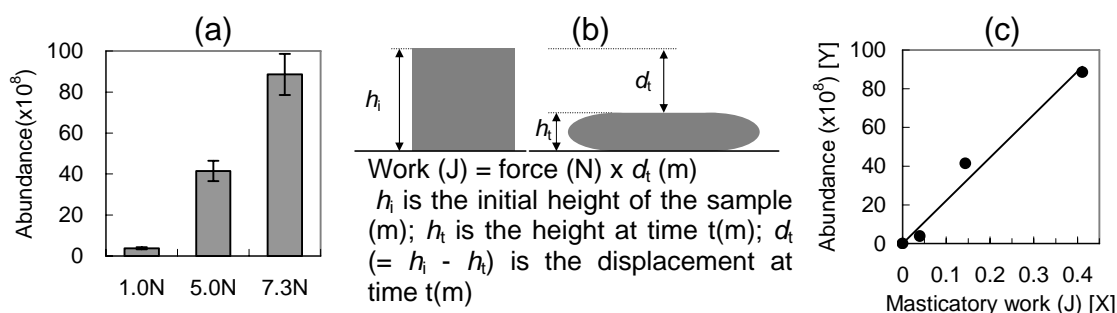


Figure 6. The amount of released limonene and masticatory work.

This research confirms that mastication force is an important factor in influencing the amount of released volatiles for retronasal perception (8). It is also shown that masticatory work, calculated using masticatory force and sample displacement, can be used to predict the amount of released volatiles. It can also be said that a new era has begun in the investigation of retronasal volatile release using the effective mouth model recently reported (2-4) and shown in this study.

Acknowledgements

This study was supported by a Grant-in-Aid for Scientific Research (B)No.20300241 from JSPS, Japan and High-Tech-Research Center Project (2004-2008) from MEXT, Japan. The authors are grateful to D. Hirai for his experimental assistance.

References

1. Piggott J.R., Schaschke C.J. (2001) *Biomolecular Engineering*, 17:129-136.
2. Arvisenet G. *et al.* (2006) In: *Flavour Science, Recent Advances and Trends* (Bredie W.L.P., Petersen M.A., eds.); *Elsevier Science B. V.*, pp 3456-468.
3. Arvisenet G. *et al.* (2008) *J. Agric. Food Chem.*, 56:3245-3253.
4. Salles C. *et al.* (2007) *J. Food Engineering*, 82:189-198.
5. van Ruth S.M. *et al.* (1994) In *Trends in Flavour Research* (Maarse H., van der Hij D.G., eds.); *Elsevier Science B. V.*, pp 59-64.
6. Otake S. *et al.* (2000) *Biosci. Biotechnol. Biochem.*, 64:2523-2529.
7. van Ruth S.M. (1995) Doctoral thesis, *Wageningen Agricultural University*, pp 30-31.
8. Brown W.E., Wilson C.E. (1996) In *Flavour Science, Recent Developments* (Taylor A.J., Mottram, D.S., eds.); *The Royal Society of Chemistry*, pp 451-455.

EFFECT OF ANTIOXIDANT AND SALIVA ADDITION ON THE RELEASE OF AROMATIC COMPOUNDS FROM DRY-FERMENTED SAUSAGES IN *IN-VITRO* MODEL MOUTH SYSTEM

M. FLORES and A. Olivares

Instituto de Agroquímica y Tecnología de Alimentos (CSIC), Apartado 73, 46100 Burjassot (Valencia), Spain

Abstract

The release of aroma compounds from dry fermented sausages was studied by extracting the headspace at different times using a solid phase micro-extraction device. The effect of the addition of an antioxidant and saliva on the release was determined. The compounds were analysed by gas chromatography using a flame ionization detector and identified by mass spectrometry. The addition of butylated hydroxytoluene to dry fermented sausages produced a significant reduction of the release of linear aldehydes indicating an oxidation process during sampling. The addition of water and saliva to the dry fermented sausages produced a higher release of pentanal, hexanal and octanal, while propanal and phenylethyl alcohol showed a lower rate of release.

Introduction

The typical aroma of dry-fermented sausages cannot be attributed to a single compound and is due to a mixture of volatile compounds in the appropriate amounts [1]. However, the aroma perception in meat products depends on the concentration and odor thresholds of volatile compounds and on their interactions with other food components that will affect its gas phase concentration. Hundreds of volatile compounds have been identified in dry fermented sausages [2-4] although only a few of them are the main odorants responsible for the dry-cured aroma [1].

Meat products have a very complex matrix that mainly contains proteins and lipids. In this sense, dry fermented sausages are composed by almost 30 % lipids that affect the aroma release. The flavour development in dry fermented sausages is mainly formed by lipid oxidation reactions and from bacterial metabolism [5]. Many studies have been focused on the lipid oxidation phenomenon during processing but there are not studies about the release of these volatile compounds from the meat matrix. However, the stability of these lipids is a major fact that should be previously controlled. Therefore, the aim of the present work was to study the effect of the addition of an antioxidant and water and saliva on the release of volatile compounds from dry fermented sausages.

Experimental

Dry fermented sausages were made with lean pork (80 %) and pork back fat (20 %) as described by Marco et al., [5]. At the end of the process (44 days), three sausages were sliced, vacuum packaged and stored frozen at -20°C until analysis.

Release of aromatic compounds from dry fermented sausages in in-vitro model system. The release was studied using a 10 ml HS vial, sealed with a PTFE faced silicone septum (Supelco, Bellefonte, PA, USA) containing three grams of minced sausage. The frozen sausage was minced using a Waring blender (Waring Commercial 8010, CT, USA). Three experimental conditions were analysed, sausage alone, sausage in the presence of water (3 ml) and sausage in the presence of saliva (3 ml) [6]. The addition of 10 mg butylated hydroxytoluene (BHT) during sausage mincing was also analysed. The extraction of volatile compounds from the vial was performed using a solid phase micro extraction (SPME) device (Supelco, Bellefonte, Pennsylvania, USA) with a 85 μm carboxen/polydimethylsiloxane fibre (CAR/PDMS stb). The released volatile compounds were extracted by exposing the SPME fibre for different times (0.5, 1, 2 and 3h) to the headspace maintained at 30° C. Each experimental point was done in triplicate. The compounds adsorbed by the fibre were quantified and identified by gas chromatography analysis.

Identification and quantification of volatile compounds. The identification was done in a gas chromatograph (GC HP 5890 series II, Hewlett Packard, Palo Alto, CA), with a HP 5972 mass selective detector, following the procedure described by Marco *et al.* [4]. The quantification of volatile compounds was done as described Gianelli, Flores and Toldrá [7]. The content of each of the volatile compounds in each experience was calculated from the FID area and expressed as area units.

Statistical analysis. The effect of the different experimental conditions and the addition of the antioxidant on the volatile compounds were tested by two-factor analysis of variance (ANOVA) using the statistic software Statgraphics plus (v 5.1).

Results

The rate of release for each volatile compound in each experience was determined through the calculation of the initial slope obtained from the linear regression of the compound area vs the extraction time (Figure 1). The initial slope was calculated from the two or three first points depending on the compound. This parameter has been previously used to measure the rate of flavor release [8-9].

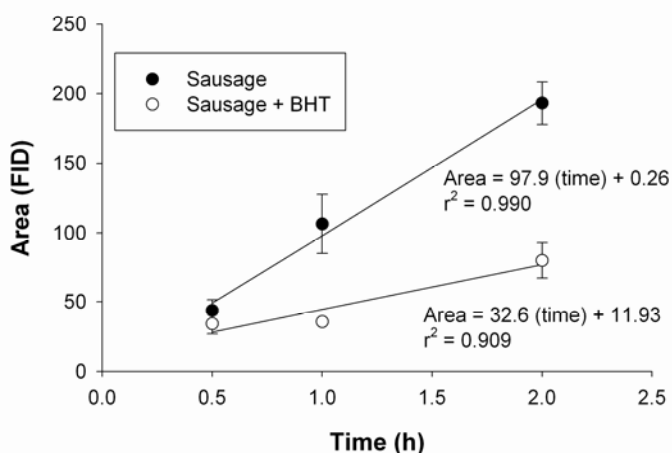


Figure 1. Release of nonanal from dry fermented sausage with or without BHT.

The volatile compounds were grouped according to their possible origin. Those coming from the lipid auto-oxidation process and those originated from the bacterial metabolism being this latest group divided in compounds coming from carbohydrate fermentation, amino acid catabolism, staphylococci esterase activity and lipid β -

oxidation. In Figure 2 are shown the initial slopes for the groups of volatile compounds and can be observed that in all cases the addition of BHT produced a significant decrease except for those compounds derived from the lipid β -oxidation process. Also, the different experimental conditions analysed affected the initial slope.

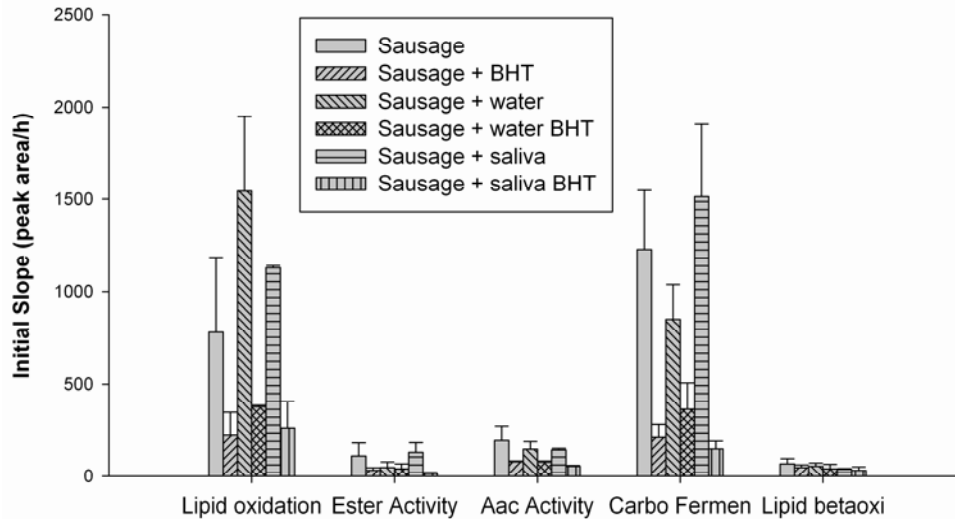


Figure 2. Slopes of the aroma compounds derived from the lipid auto-oxidation process; staphylococci esterase activity; carbohydrate fermentation; amino acid catabolism and lipid β -oxidation generated from dry fermented sausages in the presence of water, saliva and antioxidant.

In Figure 3 is shown the rate of release of the linear aldehydes and it was affected by the experimental conditions. Propanal showed a higher release in the sausage alone while the release of pentanal, hexanal and octanal was higher in the presence of water and saliva. Also, nonanal showed a higher release when saliva was added. In addition, the effect of BHT was significant for these compounds. BHT produced a reduction in the slopes therefore, BHT addition to meat products is necessary to avoid the oxidation of the lipid fraction during sampling.

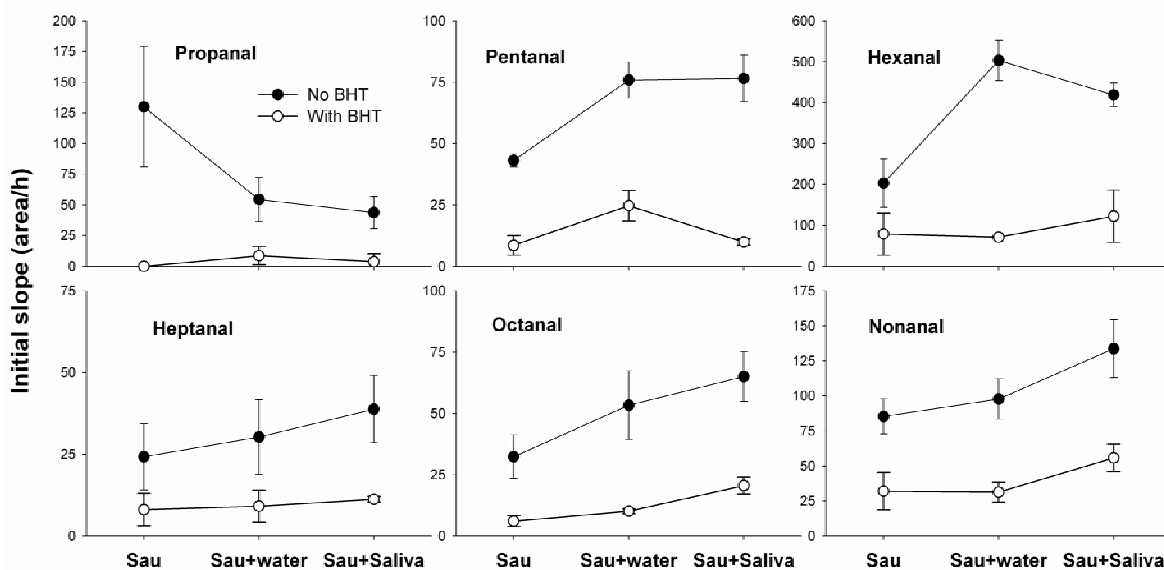


Figure 3. Slopes of linear aldehydes generated from dry fermented sausages in the presence of water, saliva and antioxidant.

The higher release of linear aldehydes in the presence of water and saliva is partially in accordance with the results obtained by van Ruth and Roozen [10] in the study of flavor release in mouth conditions from sunflower oil and its emulsion. During mouth conditions the addition of water increased hexanal release but with artificial saliva a decreased release was detected. The decrease in the release by the addition of saliva detected in both techniques was explained by the presence of proteins (mucin and alpha-amylase) in the artificial saliva responsible of the aroma binding [11].

Until now, there are a few studies about the binding ability of sarcoplasmic and myofibrillar proteins obtained from fresh pork muscle and dry-cured ham [12]. These authors reported the ability of sarcoplasmic and actomyosin proteins to bind several compounds including hexanal, although the binding was highly affected by the ionic strength and protein conformation. Therefore, the addition of water and saliva could have affected the binding of hexanal to proteins producing a release from the matrix.

The initial slopes of the compounds derived from amino acid catabolism are shown in Figure 4. Only a few of them were affected by the two factors studied. Phenylethyl alcohol showed a reduction in the rate of release with the addition of saliva and water. Moreover, BHT addition produced a significant reduction in the release rate of benzaldehyde.

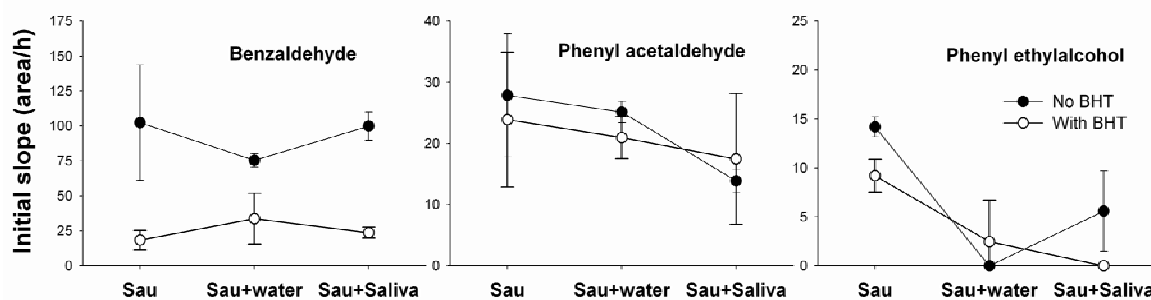


Figure 4. Slopes of compounds derived from amino acids and generated from dry fermented sausages in the presence of water, saliva and antioxidant.

Acknowledgements

Financial support from AGL2005-00713 (MEC, Spain) and FEDER and from GVA (Spain) to A. Olivares are fully acknowledged.

References

1. Marco A., Navarro J.L., Flores M. (2007) *J. Agric. Food Chem.* 55: 3058-3065.
2. Stahnke L.H. (1994) *Meat Sci.* 38: 39-53.
3. Marco A., Navarro J.L., Flores M. (2004) *Food Chem.* 84: 633-641.
4. Marco A., Navarro J.L., Flores M. (2006) *Meat Sci.* 73: 660-673.
5. Marco A., Navarro J.L., Flores M. (2008) *Eur Food Res Technol.* 226: 449-458.
6. van Ruth S.M., Roozen J.P., Legger-Huysman A. (1997) In: *Flavour Perception. Aroma evaluation* (H.P Kruse, M. Rotne, eds.) pp 143-151, Universitaet Postdam, Germany.
7. Gianelli M.P., Flores M. Toldrá, F. (2002) *J. Sci. Food Agric.* 82: 1703-1709.
8. Pozo-Bayón M.A., Ruíz-Rodríguez A., Pernin K., Cayot N. (2007) *J. Agric. Food Chem.* 55: 1418-1426.
9. Cayot N., Dury-Brun C., Karbowiak, T., Savary G., Voilley A. (2008) *Food Res. Int.* 41: 349-362.
10. van Ruth S.M., Roozen J.P. (2000) *Eur. Food Res. Tech.* 210: 258-262.
11. Kinsella J.E. (1990) *Inform.* 1: 215-226.
12. Pérez-Juan M., Flores M., Toldrá F. (2008) *Food Chem.* 108: 1226-1233.

THE EFFECT OF SALIVA ON THE RELEASE OF AROMA VOLATILES IN PORK

L. MEINERT, A.N. Birch, A. Schäfer, S. Støier, and M.D. Aaslyng

Danish Meat Research Institute, Maglegaardsvej 2, DK-4000 Roskilde, Denmark

Abstract

Saliva may affect the release of flavour volatiles in foods. In pork, hexanal, dimethyldisulphide and trimethylpyrazine are known flavour compounds. The aim of this study was to investigate the effect of added saliva (fresh versus heat-treated) on the release of the three volatiles from both authentic solutions and heated pork. Saliva was collected under standardised conditions from three test persons, but there was a clear variation in the saliva. Test person 2 had a significantly faster saliva secretion rate than test persons 1 and 3. The release of trimethylpyrazine was significantly higher when saliva from test person 3 was added compared with saliva from the other two test persons. The release of dimethyldisulphide and hexanal was not affected by the addition of saliva. In mixtures with hexanal and saliva from test persons 1 and 2, 1-hexanol was detected. The addition of saliva to heated pork did not affect the release of the three volatiles.

Introduction

People have very different perceptions and preferences regarding pork. Danish consumers have recently recognised fried flavour as one of the most important attributes of good eating quality of cooked pork (1). Many volatiles have been identified as being important for the overall flavour profile of heated pork. Among these are hexanal, dimethyldisulphide and trimethylpyrazine (2). Volatiles are released through chewing, during which mixing with saliva also affects flavour release (3). Previous investigations have shown that saliva changes the concentration of certain volatiles and that this might be due to enzymatic activity (4). However, the mechanisms behind this are not fully understood. The aim of this study was to investigate the effect of adding i) fresh saliva, ii) heat-treated saliva and iii) water (reference) to aqueous solutions of hexanal, dimethyldisulphide and trimethylpyrazine and to heated pork.

Experimental

Saliva collection. Saliva was collected under standardised conditions from three test persons, all healthy non-smoking and non-medicated young women aged between 23 and 30 years. Saliva was collected two hours after breakfast and tooth brushing. The test persons rinsed their mouths with water and were subsequently sat in a chair in a bent-forward position. One gram of paraffin wax was placed in the oral cavity of each test person in order to stimulate saliva production (5). The persons started chewing at time “zero” and spat out saliva every minute. The saliva was immediately weighed and frozen at -18°C. Some saliva (only from test person 1) was boiled for 2

min in a water bath prior to frozen storage. In a preliminary test in our lab, it was shown that short-term frozen storage did not alter the characteristics of the saliva.

Authentic volatiles. To 1 μL solution of each volatile (500 mg/L), 1 mL of saliva or water (reference) was added and mixed in a conical sample flask, which was immediately closed with a Dreschel head connected to a trap packed with Tenax/Carbograph. The solution mixtures were conditioned in a water bath (37°C) for 10 min followed by purging with nitrogen (60 mL/min) for 20 min.

Heat treatment of pork. A thin layer (1-2 mm) of minced pork (3 g) was smeared up the side of a conical sample flask. The flask was closed with a watch glass, and the meat was heated in an oven at 160°C for 10 min. Immediately after heating, the meat was scraped from the side of the flask to the bottom and mixed with 1 mL saliva or water (reference). The pork/saliva mixtures were conditioned in a water bath (37°C) for 10 min followed by purging with nitrogen (60 mL/min) for 20 min.

Aroma analysis. Desorption of volatiles was performed thermally using an ATD 400 automatic thermal desorption system (Perkin Elmer, Bucks, UK). The Tenax/Carbograph traps were thermally desorbed with helium (20 ml/min) at 240°C for 10 min. The volatiles were cryofocused in the ATD cold trap (-30°C) and subsequently desorbed from the cold trap at 250°C for 5 min with a helium flow of 20 ml/min and an outlet split ratio of 1:10. Separation was performed by GC-MS (Agilent Technologies, Palo Alto, USA) under the following conditions: column, Innowax (30 m x 0.25 mm, i.d. x 0.25 μm film thickness, J & W Scientific, USA); carrier gas, helium; oven programme: 35°C for 6 min, 10°C/min to 85°C, 2°C/min to 110°C, 10°C/min to 240°C, and holding for 5 min at 240°C. The mass selective detector was operated in the electron impact mode with an energy voltage of 70 eV and an emission current of 35 μA . The MS detector scanned from 33 m/z to 450 m/z at a rate of 1.9 scan/s.

Results and Discussion

The aroma profile of pure saliva did not show any content of hexanal, dimethyldisulphide or trimethylpyrazine. There was a clear difference in the rate of saliva secretion (Figure 1) and also in the consistency of the saliva from the three test persons.

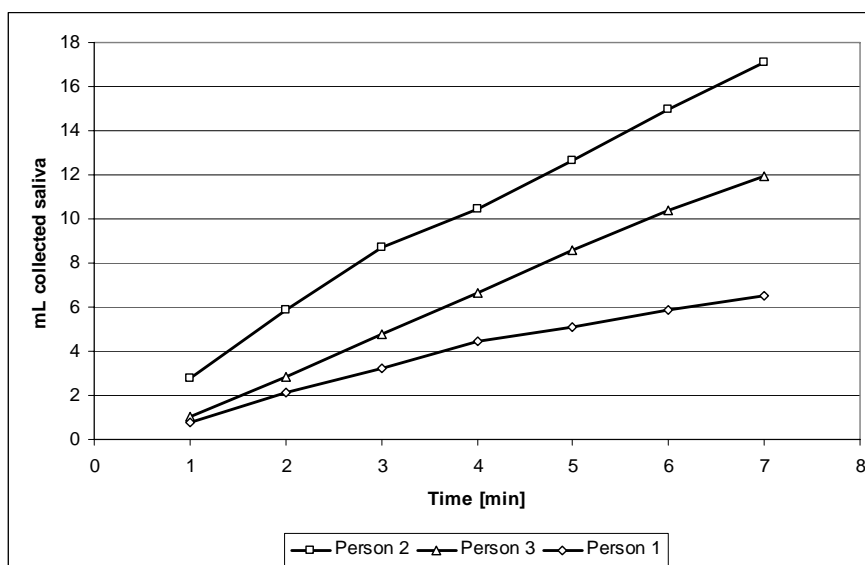


Figure 1. The secretion rate (mL saliva/min) of saliva from the three test persons.

Saliva from test person 3 was more viscous (visual observation). However, there was no correlation between the saliva secretion and saliva consistency, as saliva from test person 3 (intermediate secretion rate) was more viscous than saliva from test persons 1 and 2.

As the only volatile, the release of trimethylpyrazine was significantly higher ($P=0.0005$) when saliva from test person 3 was added to the authentic solution (Figure 2). However, the addition of saliva from test persons 1 and 2 did not influence the release of trimethylpyrazine. There was no difference in the release of trimethylpyrazine when mixed with fresh saliva compared with boiled saliva, both from test person 1. There was no significant difference in the release of hexanal when saliva was added (Figure 3).

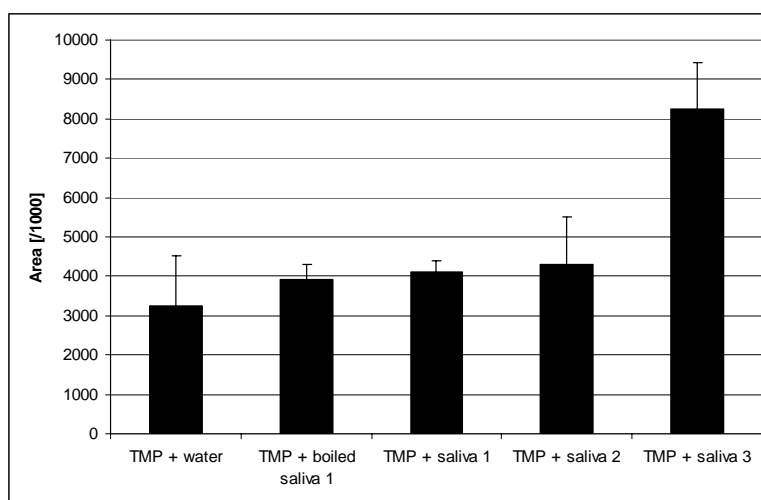


Figure 2. The release of trimethylpyrazine, TMP, (authentic solution) when mixed with water, heat-treated saliva from test person 1, fresh saliva from test persons 1, 2 and 3, respectively. The error bars represent standard deviation of three replicates.

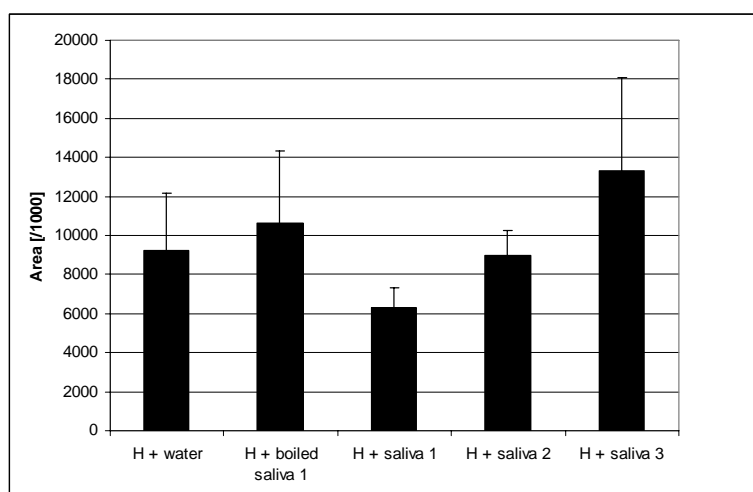


Figure 3. The release of hexanal, H, (authentic solution) when mixed with water, heat-treated saliva from test person 1, fresh saliva from test persons 1, 2 and 3, respectively. The error bars represent the standard deviation of three replicates.

There was, however, a tendency towards a lower release when saliva from test person 1 was added. Furthermore, a tendency towards a higher release of hexanal was observed when saliva from test person 1 was boiled compared with the fresh saliva. However, this was not significant.

The volatile 1-hexanol was identified in the mixtures of hexanal and saliva from test persons 1 and 2, but not in the mixtures containing saliva from test person 3, water or heat-treated saliva. Saliva had no influence on the release of dimethyldisulphide in the authentic solution. The addition of saliva had no effect on the release of hexanal, dimethyldisulphide or trimethylpyrazine from heated pork.

Discussion

The observed differences in saliva consistency between the three test persons may indicate differences in saliva composition. This was supported by the detection of 1-hexanol in the mixtures of hexanal and saliva from test persons 1 and 2, but not from test person 3. Furthermore, a significantly higher release of trimethylpyrazine was observed when the authentic solution was mixed with saliva from test person 3 compared with the other two test persons. In a previous study, Buettner (6) showed that hexanal (20 %) was reduced to 1-hexanol by the addition of saliva. This may be caused by the activity of enzymes in the saliva, as 1-hexanol was not detected in the mixture of hexanal and heat-treated saliva. Buettner (4, 6) also found large differences in the release of aroma volatiles between individuals.

The addition of saliva had no effect on the release of the three aroma volatiles in heated pork. One explanation could be the binding of volatiles in the meat matrix (7). It was expected that boiling the saliva would inactivate the enzymes, resulting in a general increase in volatile release. There were some indications of an inactivation of the enzyme reducing hexanal to 1-hexanol. However, no other effects were observed.

Conclusion

The saliva from the three test persons differed in terms of secretion rate and consistency, and indications of differences in saliva composition were also seen. The release of trimethylpyrazine, as the only volatile, was influenced by the addition of saliva. In some samples, hexanal was reduced to 1-hexanol. The release of volatiles from heated pork was not affected by the addition of saliva.

References

1. Aaslyng M.D., Oksama M., Olsen E.V., Bejerholm C., Baltzer M., Andersen G., Bredie, W.L.P., Byrne D.V., Gabrielsen G. (2007) *Meat Sci.* 76: 61-73.
2. Meinert L., Andersen L.T., Bredie W.L.P., Bjerregaard C., Aaslyng M.D. (2007) *Meat Sci.* 75: 229-242.
3. van Ruth S.M., Roozen J.P., Cozijnsen J.L. (1995) *Food Chem.* 53: 15-22.
4. Buettner A. (2002) *J. Agric. Food Chem.* 50: 3283-3289.
5. Nauntofte B. (2005) Personal comm. University of Copenhagen.
6. Buettner A. (2002) *J. Agric. Food Chem.* 50: 7105-7110.
7. Harrison M. (1998) *Proceedings of COST action 96*, Gothenborg, pp 91-96.

Section 4

**Flavour Retention and Release
in Food Systems**

FLAVOUR-INGREDIENT INTERACTIONS IN CONFECTIONS

Alicia Holt, Rajesh V. Potineni, and D.G. PETERSON

Department of Food Science, The Pennsylvania State University, 327 Food Science Building, University Park, PA 16802

Abstract

The influence of aroma compound structure and acidulants on the aroma release profile and the flavour perception of hard candy were investigated. In aqueous model systems, the addition of aroma compounds separately versus as a mixture resulted in an aroma release profile that was more rapid and higher in concentration; particularly for aroma compounds with a similar molecular structure. However, the addition of an acidulant to the models did suppress the aroma release for the separate flavour addition technique; although the release profile was still higher in concentration in comparison to the mixture flavour addition technique. Similarly, in hard candy, the aroma release monitored by breath analysis was higher in concentration and was perceived to be more intense by a sensory panel for the separate versus mixture flavour dosed sample formulated with malic acid. In summary, interactions between the flavour compounds themselves were reported to influence the flavour performance of hard candy.

Introduction

The flavour properties of confections are undoubtedly an important product attribute for consumption. Understanding key flavour-ingredient interactions in foods would help to better deliver flavour compounds during mastication that in turn impact flavour perception. The influence of different food ingredients either through binding/partitioning (protein, carbohydrate, and fat) or through texture/structure modifications (viscosity, emulsions) on flavour release have been studied in detail (1-3). However, in some foods such as confections, flavour compound-compound interactions can also play a role in flavour delivery.

In chewing gum, for example, aroma-sugar alcohol interactions have been reported to influence flavour delivery during mastication (4). Typical chewing gum composition consists of a water-insoluble gum base continuous phase and a water-soluble sugar or sugar alcohol discontinuous phase in a ratio of approximately 1:4 with a flavor load of 1%. Previous research by Harrison et al. (5) using stagnant layer theory and de Roos et al. (6) using non-equilibrium partition model emphasized the gum base as a major factor dictating the release kinetics of various flavor compounds based on hydrophobicity. Similarly, the release of flavor compounds from chewing gum has been predicted in the flavor/gum industry based on log P or log cP values. Contrary to the prediction models, Potineni and Peterson (4) reported that the release profile of cinnamaldehyde (log cP= 1.22) was correlated with sorbitol during chewing gum mastication. However for a similar hydrophobic compound, p-cresol (log cP= 1.02), this correlation was not observed. In contrast, breath analysis of a flavored gum base (no sorbitol) reported that release of cinnamaldehyde was similar to cresol, as predicted by Log cP values. Further investigation using tandem mass

spectrometry analysis indicated cinnamaldehyde reacted with sorbitol to generate transient hemiacetal products with increased polarity that reverted back to cinnamaldehyde in oral cavity (Figure 1). The increased polarity of these transient reaction products would result in a more rapid release of cinnamaldehyde from chewing gum during mastication than predicted by Log cP models. Therefore flavour release in chewing gum was controlled, in part, by aroma-sugar alcohol interactions.

In other confections, such as hard candy, interactions between the aroma compounds themselves have also been reported to influence flavour release and perception. The flavouring materials in hard candy exist as a discontinuous phase in the continuous glass sugar or sugar alcohol matrix. During candy mastication, the aroma compounds are released as a concentrated material in the oral cavity. The 'close' association of the aroma compounds during mastication would facilitate molecular interactions and potentially could alter compound volatility. Schober and Peterson (7) investigated flavour compound-compound interactions on flavour delivery by monitoring the release of menthol and 1,8-cineol during mastication by breath analysis using a binary flavoured candy (menthol and 1,8-cineol) prepared by two different flavour dosing techniques: (a) the flavour compounds were added as a mixture and (b) the flavour compounds were added separately during candy manufacture. Although both samples had equal flavour concentrations, the release profile of menthol and 1,8-cineol was approximately 2-fold higher during mastication for the separate flavour addition candy. A trained sensory panel also found the separate flavour addition dosed sample to have higher perceived flavour intensity (7).

This paper investigates in more detail the influence of molecular structure on aroma compound-compound interactions as well as the influence of aroma-acidulant interactions on aroma delivery and perception of hard candy.

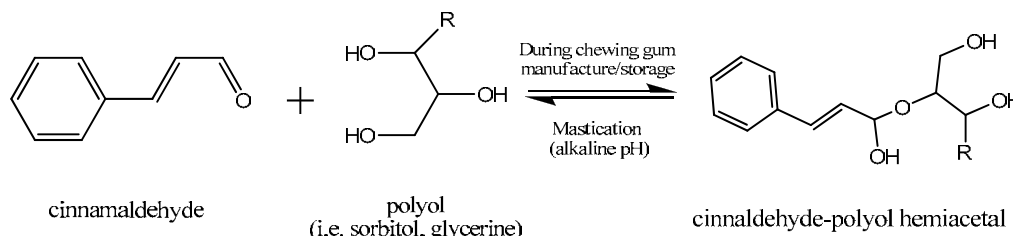


Figure 1. A proposed flavour delivery mechanism for cinnamaldehyde (aldehyde) in chewing gum; adapted from Potineni and Peterson (4).

Experimental

Hard candy sample preparation. Samples were prepared as previously described by Schober and Peterson (7). The fruit flavoured sample consisted of malic acid, *cis*-hexenol, benzaldehyde and ethyl hexanoate at 11, 0.03, 0.04 and 0.04 mg/g of candy respectively.

Aqueous model system: Flavour compound-compound interactions analysis. A custom 218-mL sealed water jacketed vessel fitted with Teflon cap interfaced with an atmospheric pressure chemical ionization – mass spectrometer (APCI-MS) was used to monitor the release of binary or tertiary aroma mixtures into the air from water in real time. Flavours were injected as a mixture or separately. For the binary mixture, benzaldehyde release was monitored in combination with octanol, octanal, ethyl hexanoate, 3-phenyl-1-propanal, 3-phenyl-1-propanol, or 2-phenylethyl formate. For the tertiary mixture, the release profile was determined for *cis*-3-hexenol, benzaldehyde and ethyl hexanoate (fruit model) added as a mixture or added separately into the aqueous model with and without malic acid.

Breath analysis. The volatile release from hard candy and chewing gum were measured using APci-MS as described by Schober and Peterson for hard candy (7).

Gas Chromatography (GC). Quantification of the volatile compounds from hard candy was analysed using a Agilent 6890 GC equipped with a split/splitless injector, flame ionization detector (FID), auto sampler (HP 7673) and a capillary column (DB-5 or DB-WAX) as previous reported (7).

Sensory analysis. Time-intensity analysis of the hard candy samples were conducted as previously described (7).

Results

To examine the role of molecular structure on the flavour release profile of a mixture versus separate flavour dosed candy, the release of benzaldehyde from a series of binary flavours from an aqueous model system was determined. Each binary flavour consisted of benzaldehyde and one other compound from two distinct structural groups (Set 1: octanol, octanal or ethyl hexanoate - aliphatic; Set 2: phenylpropanal, 3-phenyl-1-propanol or 2-phenylethyl formate - aromatic). Overall, a larger difference in the benzaldehyde release profile for the separate versus the mixture flavour addition technique was reported for the compounds in Set 2 compared to the compounds from Set 1. Benzaldehyde release when added as a mixture or added separately with octanol or 3-phenyl-1-propanol is shown in (Figure 2). The release of benzaldehyde was more rapid for both separate additions in comparison to the mixture addition techniques. The greatest suppression in release was observed for the 3-phenyl-1-propanol binary flavour. These results suggest that pi-pi interactions between benzaldehyde and the compounds from Set 2 may result in stronger compound interactions (i.e. enhanced colloidal interactions) formed during their injection into the aqueous phase which suppressed compound volatility and flavour delivery.

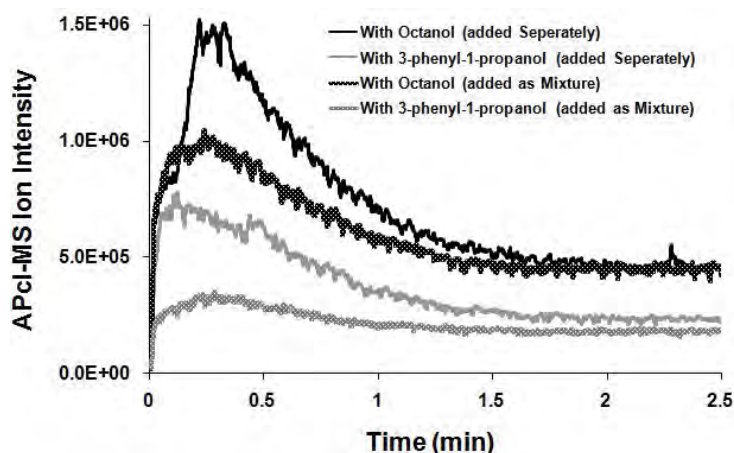


Figure 2. Release of benzaldehyde added separately or as a mixture with 3-phenyl-1-propanol or octanol from an aqueous model system.

In addition to aroma compounds, acidulants are common candy flavourings, particularly in fruit flavoured products. The influence malic acid on the release of *cis*-3-hexenol, benzaldehyde and ethyl hexanoate added by separate versus mixture addition was analysed using a model mouth and subsequently by breath and sensory analysis of a candy sample. Based on the model mouth, the addition of acidulant to the aqueous phase suppressed the release profiles of the separate flavour addition technique for these three aroma compounds; however, the separate addition still had a higher flavour release profile in comparison to the mixture addition analysis (data

not shown). In the hard candy, the results generally agreed with the model mouth analysis. The release of benzaldehyde during mastication for the mixture and separate flavour dosed samples are illustrated in Figure 3. The release of benzaldehyde was generally 2-fold higher during the first 1.5 min of mastication for the separate flavour addition candy; however negligible differences were reported after this time point. Similar results were reported for ethyl hexanoate, while for *cis*-3-hexenol the release was similar for both samples (data not shown). Perhaps, during mastication, the acidulant concentration increased in the oral cavity which increased aroma-acidulant interactions over time and for the separate flavour dosed sample ultimately further suppressed the aroma release profile. Sensory time-intensity analysis was in agreement with the analytical data. The separate flavour dosed sample had higher perceived fruit flavour intensity (data not shown).

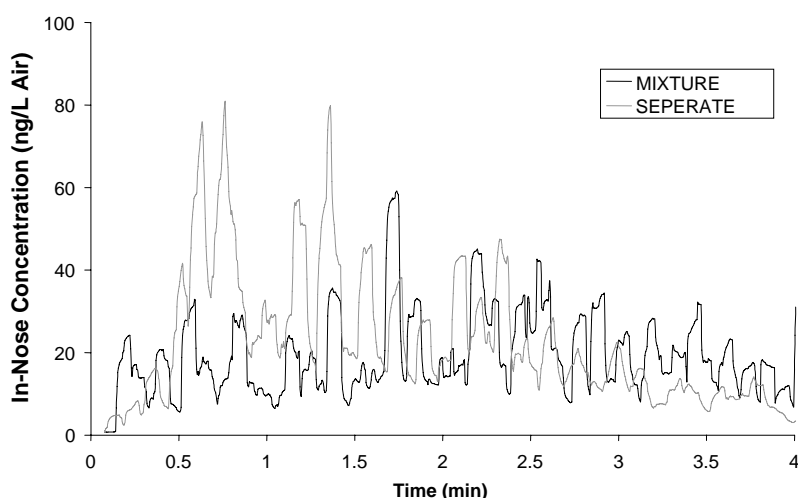


Figure 3. Breath analysis profile of benzaldehyde from hard candy with 1% malic acid comparing two techniques of flavour addition, flavour added as a 1) mixture or 2) separately with *cis*-3-hexenol and ethyl hexanoate; each aroma compound at equivalent concentrations. Each curve represents the mean of three replicates from one representative panellist subsequently smoothed by a 1.5-s moving average trend line.

In summary, aroma release and perception in hard candy can be enhanced by adding the aroma compounds separately as opposed to the conventional protocol of mixture addition during manufacture, particularly for aroma compounds with the similar chemical structure. However, the difference in the aroma release profile between the separate and the mixture dosed sample was suppressed by the addition of malic acid, indicating aroma-acidulant interactions also influence flavour aroma delivery in these products.

References

1. Bakker J. (1995) In *Ingredient Interactions-Effect on Food Quality* (Gaonkar A.G., ed.), Marcel Dekker., pp: 411-439.
2. Philippe E. (2003) *J. Agric. Food Chem.* 51, 1393-1398.
3. Kokini J.L. (1985) *Food Technol.* 39, 86-94.
4. Potineni R.V.; Peterson D.G. (2008) *J. Agric. Food Chem.* 56: 3260-3267.
5. Harrison M. (2000) In *Flavor Release* (Roberts D.D., Taylor A.J., eds.); Oxford University Press., Vol. 763, pp: 179-191.
6. de Roos K.B. (1994) In *Trends in Flavour Research* (Maarse H., van den Heij D.G., eds.); Elsevier., Vol. 35, pp: 15-31.
7. Schober A.L.; Peterson D.G. (2004) *J. Agric. Food Chem.* 52: 2623-2627.

AROMA BARRIER PROPERTIES OF IOTA-CARRAGEENAN EMULSION-BASED FILMS USED FOR ENCAPSULATION OF ACTIVE COMPOUNDS.

A. Hambleton¹, M.J. Fabra²; F. DEBEAUFORT^{1,3}, and A. Voilley¹

¹ ENSBANA-EMMA, Université de Bourgogne, 1 esplanade Erasme, 21000 Dijon, France

² Food Technology Department – Institute of Food Engineering for Development. Polytechnic University. Camino de Vera s/n. 46022. Valencia (Spain).

³ IUT-Génie Biologique, Boulevard Dr. Petitjean, B. P. 17867, 21078 Dijon Cedex, France

Abstract

The conservation of food products requires the maintenance of their initial properties while protecting them from the environment and in limiting the transfers and losses of matter. Edible films improve food quality by serving as barriers to moisture transfer, oxygen uptake and losses of volatile aroma compounds. Edible films made of *iota*-carrageenans display interesting advantages: good mechanical properties, stabilisation of emulsions and reduction of oxygen transfers. Moreover, the addition of lipid globules in emulsion-based films can be considered to encapsulate active molecules such as aroma compounds. It also enhances the barrier properties. The aim of this study was to better understand the influence of the composition and the structure of the films matrix on its aroma barrier properties and thus on its capacity to protect encapsulated active substances. The study of the aroma compound permeability of films with or without aroma compound and/or fat showed that interaction between aroma compound/*iota*-carrageenan and aroma compound/fat modifies the film structures and thus their permeability. This study brings new understanding on the role of the emulsion-based edible films as a matrix, on its capacity to protect encapsulated aroma compounds and on its aroma barrier properties.

Introduction

The conservation of food products requires the maintenance of their initial properties in protecting them from the environment and in limiting the transfers and losses of matter (1). Edible packaging are effective to control the transfers within composite food (2) and have been defined as "a packaging as a film, a coating or a thin protective layer which is an integral part of the food and/or can be eaten with". The edible films are obtained from: hydrocolloids (protein, polysaccharides) and showed good mechanical and structural properties but have low water barrier properties and/or lipids giving water impermeability but having poor mechanical properties. Emulsified films improved water barrier properties and they only need one step to be obtained (3). The interactions between hydrocolloids, lipids and aroma compounds are going to determine the film stability and properties (4). The use of microcapsules encapsulating aromas in hydrocolloid-based edible films gives them the status of active films. This encapsulation controls the release (or loss) of aroma compounds

which are organic molecules having high saturated vapour pressure. The main objective is to better understand the influence of the composition and the structure of *iota*-carrageenan emulsion-based edible films on its aroma barrier properties.

Experimental

Edible films ingredients. *iota*-Carrageenan was supplied by Cargill (95% purity, DTS, Baupre, France) and used as the main component of the film matrix. Anhydrous glycerol (98% purity, Fluka Chemical, Germany) acts as a plasticizer in order to improve the mechanical properties of carrageenan films. The fat used in this study, namely Grinsted Barrier System 2000 (GBS) is an acetic acid ester of mono and diglycerides blended with 20% w/w beeswax, having a melting point of 57°C (Danisco, Bradbrand, Denmark). Glycerol MonoStearate (GMS) is the emulsifier (99% purity, Merck Eurolab, France). The aroma compound *n*-hexanal (98% purity, Sigma-Aldrich, Germany) was used as a model encapsulated active molecule. It has a boiling point of 128°C, a log P 1.97, a saturated vapour pressure of 1420 Pa at 25°C, and its solubility in water is 3.81 mg/mL at 25°C

Carrageenan-based film preparation. A carrageenan film-forming solution was prepared by dispersing 6 g of *iota*-carrageenan powder in 200 mL of distilled water at 65°C for 15 minutes under magnetic stirring; 1.8g of glycerol was then added in the carrageenan solution also under magnetic stirring. The aroma compound was pre-solubilised (10 000ppm, in saturation) in 2.4g of melted fat before being dispersed in the film-forming solution. Then the mixture was homogenised at 24 000 rpm with an Ultra Turrax (T25 IKA) for 1 minute. The film-forming solution was poured onto smooth polymethylmethacrylate (Plexiglas®) plates.

In order to obtain a film, the water was removed by drying the film-forming solution in a ventilated climatic chamber (KBF 240 Binder, ODIL, France) for 8 hours with temperature and relative humidity fixed at $30 \pm 1^\circ\text{C}$ and $40 \pm 2\%$, respectively. Film thickness after drying was measured with an electronic gauge (Multichek FE SODEXIM, France) and was about $50 \mu\text{m} \pm 4\mu\text{m}$. The four types of films were: with or without aroma compound (wa or woa respectively) and with or without fat (wf or wof respectively).

Aroma compound vapour permeability. The basis of this dynamic method is the aroma compound transfer in the vapour phase through the film. Analyses were carried out on a Chrompack CP 9000 gas chromatograph with flame ionizing detector (FID) and a stainless steel Carbowax column of 20 m and 1/8" internal diameter. The permeation cell was composed of two chambers divided by the film to be studied. The film area exposed to transfer was 15.9 cm². Operating conditions were as follows: the two chambers were continuously swept by a 30 mL min⁻¹ nitrogen flow (carrier gas) in the downside chamber and aroma compound flow in the upperside chamber at 25°C. The FID detector temperature was 190°C. The volatile compounds passing across the film were swept by the carrier gas (N₂) and carried out to an automatic injection valve through a transfer line heated at 190°C to prevent adsorption. A total of 1 mL of the carrier gas was automatically injected at periodical time in the gas chromatograph.

Films were equilibrated at 30 % relative humidity at 25°C before permeability determinations. Three replicates were made for each permeability measurement. The aroma compounds selected for permeability measurements are typical flavours present in some food products and their physicochemical characteristics are summarised in (Table 1).

Table 1. Physicochemical characteristics of aroma compounds (Ambrose et al. (5)).

Characteristic	Ethyl Acetate	Ethyl butyrate	Ethyl hexanoate	2-Hexanone	1-Hexanol	cis-3 hexenol
Sensory note	Ether, pineapple	Fruit, pineapple	Fruity, banana pineapple	Like acetone but more pungent	Green grass	Green fresh grass
Chemical formula	C ₄ H ₈ O ₂	C ₆ H ₁₂ O ₂	C ₈ H ₁₆ O ₂	C ₆ H ₁₂ O	C ₆ H ₁₄ O	C ₆ H ₁₂ O
Molecular weight (g/mol)	88.1	116.2	144.2	100.1	102.18	100
Density at 25° (g/mL)	0.9	0.878	0.87	0.812	0.818	0.792
P _{vapour saturated} (Pa) at 25°	11356	1425	120	1550	10	139
log K	0.73	1.88	3.62	1.38	2.03	1.34
Solubility in water (g/L)	80.8	5.6	0.52	16.4	6.03	19.9

Results and Discussion

Figure 1 shows the permeability of two ethyl esters (ethyl butyrate and ethyl acetate) and 2-hexanone. The effect of lipid and encapsulated aroma compound (n-hexanal) presence on aroma permeability was assessed by a multifactor variance analysis.

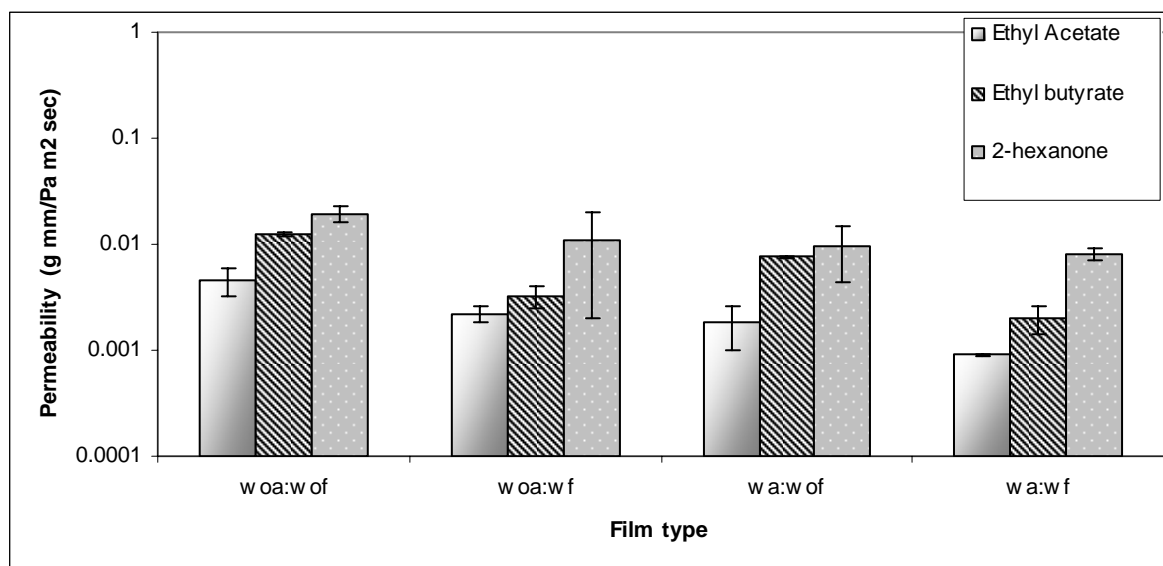


Figure 1. Aroma compound Permeability (g.mm/ Pa.m².sec).

In the case of ethyl acetate the results showed that aroma permeability was significantly different ($p < 0.05$) only between the control film (woa:wof) and the prepared films with n-hexanal and/or fat. As has been shown in previous works, the encapsulated n-hexanal probably interacts with CH₂OH and/or sulphated groups of *iota*-carrageenan lateral chains obtaining a lower permeability. In the case of ethyl butyrate, the results showed that aroma permeability was significantly different ($p < 0.05$) between the films with and without fat (wf and wof). This can be explained

by the log K of the ethyl butyrate (log K= 1.88) that limits their solubility in the hydrophilic *iota*-carrageenan film matrix and then promotes the interactions with the fat. For ethyl hexanoate, the higher hydrophobic character (log K= 3.62) limits its transfer through composite films due to the lower affinity for *iota*-carrageenan films. This hydrophobic character promotes probably strong interactions with fat where ethyl hexanoate is retained, and the permeability values were lower than the equipment threshold. In ethyl acetate and ethyl butyrate films with fat, there are no significant differences ($p>0.05$) for the films with fat despite the different log K. Nevertheless in films without fat, there are significant differences ($p<0.05$) of the butyrate permeability which is much higher. This is related to the saturated vapour pressure of the ethyl butyrate which is much lower than that of ethyl acetate as Quezada-Gallo *et al.* (1) explained. At lower saturated vapour pressure, the solubility increase induces an aroma permeability rise. The ethyl hexanoate behaviour is significantly different ($p<0.05$) to the other two esters, this is due to the higher hydrophobicity as we previously explained.

For the 2-hexanone, there was no significant difference ($p>0.05$) between the four types of films. This is probably because the ketone group interacts with the *iota*-carrageenan OH group as Quezada-Gallo *et al.* (1) has shown, and thus hiding the fat and n-hexanal effect on aroma compound permeability.

The n-hexanol and *cis*-3-hexenol permeability values were lower than the equipment threshold. The alcohol residue may interact with the lateral chains of *iota*-carrageenan and could form hydrogen bonds which limit the aroma compound permeability. When we compared the 6 carbon chain compounds the results were significantly different ($p<0.05$), even if their chains had the same carbon number. We observed that, for aroma compound permeability, not the chain length but the chemical nature of functional group is going to determine the transfer whatever the log K value (like in the case of 2-hexanone with the n-hexanol which have similar log K value).

Conclusions

This study brings new understanding on the role of emulsion-based edible films as a matrix, on its capacity to protect encapsulated aroma compounds and on its aroma barrier properties. The study of aroma compound permeability of films with or without n-hexanal and/or fat showed that an interaction between *iota*-carrageenan/n-hexanal/fat modifies the films structure and thus their permeability. So carrageenan based edible films could be for flavour encapsulation.

References

1. Quezada-Gallo A., Debeaufort F., Voilley A. (2000) In *Food Packaging: Testing Methods and Applications* (Risch, S.J. ed.). ACS Symposium Series 753, pp 125-140.
2. Kester J.J., Fennema O (1986). *Food Technol.*, 42, 47-59.
3. Hambleton A., Debeaufort F., Beney L., Karbowiak T., Voilley A. (2007). *Biomacromolecules*, 9, 1058–1063.
4. Karbowiak T., Hervet H., Leger L., Champion D., Debeaufort F., Voilley A. (2006). *Biomacromolecules*. 7, 2011-2019.
5. Ambrose D., Ellender J.H., Lees E.B., Sprake C.H., Townsend R.J. (1975). *J. Chem. Thermodynamics*, 13(8), 795-802.

AROMA BARRIER PROPERTIES OF SODIUM CASEINATE AND IOTA-CARRAGEENAN EDIBLE FILMS. INTERACTION BETWEEN AROMA COMPOUNDS AND EDIBLE FILMS

M.J. FABRA¹, A. Hambleton², P. Talens¹, F. Debeaufort^{2,3}, A. Chiralt¹ and A. Voilley²

¹ Food Technology Department – Institute of Food Engineering for Development. Polytechnic University. Camino de Vera s/n. 46022. Valencia (Spain).

² ENSBANA-EMMA, Université de Bourgogne, 1 esplanade Erasme, 21000 Dijon, France

³ IUT-Génie Biologique, Boulevard Dr. Petitjean, B.P. 17867, 21078 Dijon Cedex, France

Abstract

The mass transport of 3 different aroma compounds (ethyl acetate, ethyl butyrate and ethyl hexanoate) was studied through sodium caseinate and *iota*-carrageenan based films with different oleic acid (OA):beeswax (BW) ratios. Control films did not contain lipids. Aroma permeability of films depends on aroma physico-chemical properties and also on OA:BW ratio. The efficiency of sodium caseinate based- and *iota*-carrageenan based films to retain or limit transfers of aroma compounds is the highest when it has low affinity for volatile compounds and low diffusivity. *iota*-Carrageenan matrices have lower aroma permeability as compared to sodium caseinate due to polysaccharides with higher hydrophilic nature than proteins.

Introduction

Edible films and coatings have received increasing attention from researchers and industry as an interesting alternative to plastic food packaging (1-3). Many biomolecules including proteins, carbohydrates and lipids have been used to prepare edible barrier films. Functional properties of edible films strongly depend on their composition. Proteins and polysaccharides such as sodium caseinate and *iota*-carrageenan provide good mechanical properties. They are effective barriers to gases and aroma compounds but they have low water barrier efficiency (4-6).

Nevertheless, the transfer of aroma compounds into the packaging induces a modification of the organoleptic properties of foods during storage (7-8). The loss of volatile compounds diminishes flavour intensity, thus changing the aromatic note of the food product. The interactions between hydrocolloids, lipids and aroma compounds are going to determine the film stability and its properties (9). The loss of volatile compounds diminishes flavour intensity, thus changing the aromatic note of the food product. A reduction of food quality may result either from the oxidation of aroma compounds due to the ingress of oxygen, or from the loss of specific aroma compounds into the packaging material or environment. Thus, the permeability of volatile compounds is very important in storage and distribution.

Experimental

Materials. Two groups of edible films were prepared. For each group, Alanate 110 sodium caseinate (Llorella, S. A. Barcelona, Spain) or *iota*-carrageenan (Texturizing Solutions, Baupte, France) was used as a film-forming component of the hydrophilic

continuous phase for emulsion-based edible films. In both groups of films, lipid fraction was composed of oleic acid (OA) (Panreac quimica, Castellar Del Vallés, Barcelona, Spain) and beeswax (BW) (Brillocera, Valencia, Spain) in different OA:BW ratios (70:30, 50:50 and 30:70) and two of these films were prepared without lipid (control films). Glycerol (Panreac quimica, Castellar Del Vallés) was used as a plasticizer in 1:0.3 (hydrocolloid:glycerol ratio)

Sodium caseinate and iota-carrageenan film preparation. The film-forming aqueous dispersions of the control film, contained sodium caseinate or *iota*-carrageenan and the amount of plasticizer required to obtain the pre-determined hydrocolloid to plasticizer ratio. For films containing lipids, lipid fraction was composed of oleic acid (OA) and beeswax (BW) in different OA:BW ratios (70:30; 50:50; 30:70). After glycerol was added to aqueous dispersions of sodium caseinate or *iota*-carrageenan, the amount of beeswax required was melted in the hot solution and was also homogenized for 1 min at 13'500 rpm, followed by 1 min at 20'500 rpm. The homogenization temperature was 85°C. The emulsions were cooled at room temperature and oleic acid was added in the amount required for each film composition. Each emulsion was homogenized again with a vacuum high-shear probe mixer (Ultraturax T25, Janke & Kunkel, Germany) for 2 min at 20'500 rpm. The film-forming dispersions were degasified at room temperature with a vacuum pump. Films were prepared by weighing the amount of the degasified film-forming dispersion/emulsion on Teflon casting plate resting on a levelled surface. All of the films were dried in a ventilated chamber (KBF 20 Binder, ODIL, France) for about 24 h at 45% RH and 20° C. Dry films could be peeled intact from the casting surface.

Aroma compound vapour permeability. The basis of this dynamic method is the aroma compound transfer in the vapour phase through the film. Analyses were carried out on a Chrompack CP 9000 gas chromatograph with a flame ionizing detector (FID) and a stainless steel Carbowax column of 20 m and 1/8" internal diameter. The permeation cell was composed of two chambers divided by the film to be studied. The film area exposed to transfer was 15.9 cm². Operating conditions were as follows: the two chambers were continuously swept by a 30 mL/min nitrogen flow (carrier gas) in the downside chamber and aroma compound flow in the upper side chamber at 25°C. The FID detector temperature was 190°C. The volatile compounds passing across the film were swept by the carrier gas (N₂) and carried out to an automatic injection valve through a transfer line heated at 190°C to prevent adsorption. A total of 1 mL of the carrier gas was automatically injected at fixed time intervals in the gas chromatograph.

Films were equilibrated at 30% relative humidity at 25°C before permeability determinations. Three replicates were made for each permeability measurement. The aroma compounds selected for permeability measurements are typical flavours present in some food products and their physicochemical characteristics are summarised in (Table 1).

Results

The effectiveness of a polymer or edible films as an aroma barrier can be described by its diffusion, solubility, and then permeability coefficients. (Tables 2 and 3) show the permeability of three ethyl esters (ethyl butyrate, ethyl acetate and ethyl hexanoate) of sodium caseinate and *iota*-carrageenan based films. The effect of type of hydrocolloid, lipid presence and OA:BW ratios on aroma barrier properties are evaluated. Sodium caseinate based films are less efficient as aroma barrier than *iota*-carrageenan and these differences can be explained because of aroma compounds

are mainly hydrophobic and they are absorbed easily in sodium caseinate matrices. In general, proteins have higher hydrophobic nature of proteins as compared to polysaccharides. Moreover, in both types of matrices, the aroma barrier efficiency is significantly influenced ($p < 0.05$) by the type of lipid presence for the most of aroma compounds. While the oleic acid presence produces a sharp increase in aroma permeability values of sodium caseinate based films (the higher the OA content, the greater the permeability), ethyl acetate and ethyl butyrate permeability diminishes significantly for *iota*-carrageenan–lipid films. This effect can be attributed to aroma compounds that adsorb more easily in the composite films having polarity close to that of the aroma compound. The affinity of volatile compounds for the film matrix is the main factor controlling the permeability, due to the physicochemical interactions.

Table 1. Physicochemical characteristics of aroma compounds.

Characteristic	Ethyl Acetate	Ethyl butyrate	Ethyl Hexanoate
Odour	Ether, pineapple	fruit, pineapple	Fruit, banana pineapple
Chemical formula	$C_4H_8O_2$	$C_6H_{12}O_2$	$C_8H_{16}O_2$
molecular weight ($g\ mol^{-1}$)	88.1	116.2	144.2
density at 25° C ($g\ mL^{-1}$)	0.9	0.878	0.87
$P_{vapour\ saturate}$ (Pa) at 25°	11366	1425	120
log K	0.73	1.88	3.62

Table 2. Ethyl acetate, Ethyl butyrate and Ethyl hexanoate permeability of sodium caseinate based films.

OA:BW ratio	Ethyl Acetate permeability ($g\ mm/Pa\ m^2\ s$)	Ethyl Butyrate permeability ($g\ mm/Pa\ m^2\ s$)	Ethyl Hexanoate permeability ($g\ mm/Pa\ m^2\ s$)
Control	0.006 (0.001) ^a	0.19 (0.05) ^a	$<4.5 \cdot 10^{-4a}$
70:30	26 (7) ^{bc}	349 (17) ^c	657 (25) ^c
50:50	19 (2) ^c	239 (0.7) ^d	639 (9) ^c
30:70	0.13 (0.02) ^a	1.07 (0.15) ^a	$<4.5 \cdot 10^{-4a}$

Mean (standard deviation)

a-d: homogeneous groups, values having the same letter are not significantly different at p level < 0.05

However, aroma permeability decreases significantly with the beeswax content, though these differences are weak for ethyl acetate in *iota*-carrageenan based films. The higher efficiency of BW in controlling aroma permeability compared to oleic acid is based on the great hydrophobicity of its long chain fatty alcohols and alkanes and its high solid fat content. Indeed, lower physicochemical interactions could occur. Sorption and diffusion mechanisms can be easier through oleic acid due to its liquid state. On the contrary, beeswax is highly crystalline which limits the diffusion of aroma compound and the aroma sorption phenomena can only occur on the globule surface of the beeswax instead of occurring inside the crystalline structure of the wax. Indeed, in the case of crystals, only surface adsorption occurs and absorption never occurs within the crystalline structure (10).

Barrier efficiency against aroma transfer through an edible film depends mainly on both sorption and diffusion. While sorption mechanism affects the transfer of small molecules (maximum 5 carbon atoms) and without interactions, diffusion mechanism plays an important role into volatile molecule transfers with higher molar volume. So, ethyl acetate and ethyl butyrate transfers were mainly governed by the sorption

mechanism and the differences observed could be attributed to their different physico-chemical properties. The solubility of aroma compounds increases with their boiling point and when the saturated vapour pressures decreases, which is related to the increase in their molecular weight, thus making their adsorption easier on the edible films. On the contrary, the higher hydrophobic character of ethyl hexanoate ($\log k = 3.62$) limited its transfer through control films (without lipid) due to the lower affinity for this aroma compound to hydrocolloids. It may be noted that the ethyl hexanoate permeability of both sodium caseinate and *iota*-carrageenan films increases significantly for films containing lipids. The higher hydrophobic character of this aroma compound favours its solubilisation in lipid phase.

The results reveal that the efficiency of edible films to retain or limit transfers of aroma compounds is the highest when it has low affinity for volatile compounds and low diffusivity (the higher the affinity, the greater the permeability). So, the affinity of volatile compounds for sodium caseinate or *iota*-carrageenan-lipid films seems to be the main factor controlling aroma transfers.

Table 3. Ethyl acetate, Ethyl butyrate and Ethyl hexanoate permeability of *iota*-carrageenan based films.

OA:BW ratio	Ethyl Acetate permeability (g mm/Pa m ² s)	Ethyl Butyrate permeability (g mm/Pa m ² s)	Ethyl Hexanoate permeability (g mm/Pa m ² s)
Control	0.004 (0.002) ^a	0.012 (0.003) ^a	<1.4*10 ^{-4a}
70:30	0.00096 (0.00003) ^b	0.0017 (0.0003) ^b	0.009 (0.003) ^b
50:50	0.00073 (0.00008) ^b	0.0013 (0.0001) ^c	0.004 (0.002) ^{bc}
30:70	0.00083 (0.00001) ^b	0.001 (0.0001) ^d	0.002 (0.00) ^c

Mean (standard deviation)

a-d: homogeneous groups, values having the same letter are not significantly different at *p* level <0.05

Conclusion

Aroma barrier efficiency is dependent on oleic acid:beeswax ratio and physico-chemical properties of aroma compounds. The higher efficiency of beeswax in controlling aroma permeability compared to oleic acid is based on the great hydrophobicity of the long chain of fatty alcohols and alkanes and on its high solid fat content. Indeed, lower physico-chemical interactions could occur. The efficiency of Na-caseinate and *iota*-carrageenan based films to retain or limit aroma compounds transfers depends on the affinity of the volatile compound to the films which relates physicochemical interactions between the volatile compound and the film.

References

1. Debeaufort F., Quezada-Gallo J.A., Voilley A. (1998) *Cri. Rev. Food Sci.* 38: 299-313.
2. Tharanathan R. N. (2003) *Trends Food Sci. Technol.*, 14(3): 71-78.
3. Krochta J. M., Mulder-Johnston, C. (1997) *Food Tech.* 51: 61-74.
4. Miller K.S., Krochta J.M. (1997) *Trends Food Sci. Technol.* 8: 228-237.
5. Fabra M.J., Talens P., Chiralt A. (2008) *J. Food Eng.* 85: 393-400.
6. Hambleton A., Debeaufort F., Beney L., Karbowiak T., Voilley A. (2008) *Biomacromolecules* 9: 1058–1063.
7. Debeaufort F., Voilley A. (1994) *J. Agric. Food Chem.*, 42: 2871-2875.
8. Dury-Brun C., Chalier P., Desobry S., Voilley A. (2007) *Food Rev. Int.*, 23: 199-255.
9. Karbowiak T., Hervet H., Leger L., Champion D., Debeaufort F., Voilley A. (2006) *Biomacromolecules* 7: 2011-2019.
10. Fabra M.J., Hambleton A., Talens P., Debeaufort F., Chiralt A., Voilley A (2008) *Biomacromolecules* 9: 1406-1410.

EFFECT OF GUM BASE INGREDIENTS ON RELEASE OF SPECIFIC COMPOUNDS FROM STRAWBERRY FLAVOUR CHEWING GUM

S. KREUTZMANN¹ and K.D. Nielsen²

¹ *Department of Food Science, University of Copenhagen, Faculty of Life Sciences, Rolighedsvej 30, DK-1978 Frederikseberg C, Denmark*

² *Chew Tech I/S, Dandyvej 19, 7100 Vejle, Denmark*

Abstract

The aim of the present study was to evaluate correlations between the release of specific compounds from strawberry flavour chewing gum and the perceived intensity of the sensory attributes: flavour intensity, acidity and sweetness and to evaluate if this relationship is effected by different gum base ingredients (elastomer / resin types). Atmospheric-pressure-chemical-ionisation mass-spectrometry also called MS-nose technology provides a unique tool to measure in vivo flavour release profiles. Breath analysis from the MS nose was combined with data obtained from sensory analysis and correlations between the consumer perceptions during chewing and specific volatiles that are released from the gum were investigated. This information was then combined with the knowledge of the gum ingredients to clarify the impact of a single ingredient. No correlations between these specific volatile compounds and sensory perceived intensity, acidity and sweetness was found, which was unexpected. Further the result showed that the variations of gum base ingredients affected the release of the analysed flavour compounds.

Introduction

The demand for specialized chewing gum products is rapidly increasing as the differentiation in consumer preferences world wide becomes more and more pronounced. Since long lasting taste is the key parameter for chewing gum, knowledge about release of flavours needs to be provided. It is known that flavour release during chewing depends upon many factors such as composition, texture and rheological parameters of the matrix, strength of mastication and flow rate of saliva (1-2). Furthermore, release of flavours from chewing gum is often quite limited due to the fact that flavours are lipophilic and therefore retained in the gum base to a large extent (4). In order to further elucidate this process it is necessary to combine instrumental analysis of the release of volatile compounds from the food matrix with sensory evaluation of the food product. Therefore, to gain an insight into the kinetics of volatile release in vivo techniques have been developed which are capable of monitoring real-time volatile release. Atmospheric-pressure-chemical-ionisation mass-spectrometry (APCI-MS, MS-nose) is one of the most commonly used methods for this purpose. With these systems part of the participant's breath is continuously sampled, allowing for sensitive and fast monitoring of volatile release (1,3,4).

The aim of the present study was to investigate how changes in gum base ingredients (elastomer / resin types) influenced the release of strawberry volatiles in vivo and sensory perception. By combining the breath analysis from the MS nose with data obtained from sensory analysis correlations between the consumer

perceptions during chewing and specific volatiles that are released from the gum was investigated. This information was then combined with the knowledge of the gum ingredients to clarify the impact of a single ingredient.

Experimental

Samples. 17 different chewing gums based upon systematic variations of the elastomer (three different types) / resin (four different types) types were investigated.

In-vivo measurements by APCI-MS. Flavour release was measured in exhaled breath of two experienced assessors in duplicate. Assessors breathed in and out through the nose, with the entire nose placed in a glass mask. The end of the mask was connected to a T-piece allowing excess breath to exhaust from the mask. Sample air (breath) was drawn into the ionization source through a heated deactivated fused silica transfer line (1 m x 0.53 mm i.d., heated to 100 °C) at a constant flow of 80 mL min⁻¹. The APCI-MS was a Waters Micromass ZQ2000. Compounds entering the source, were ionized by a 4 kV positive corona pin discharge, and the ions formed were separated and detected according to their *m/z* ratio. The molecules measured were ethyl butanoate *m/z* 117, isopentyl acetate *m/z* 131, Limonene *m/z* 137, Methyl anthranilate *m/z* 152.

Sensory evaluation. Sensory evaluation of chewing gum were carried out by sensory panel consisting of nine members, who had been selected and trained according to guidelines in ISO/DIS 8596-1 and ASTM STP 758 (1993). The Time Intensity (TI) method was used to assess the changes on intensities in flavour, acidity, and sweetness in chewing gum. The panellists were asked to assess the intensities according to a TI procedure and the time of recording was 600 s. The assessors rinsed their mouths with tap water and neutralised their palates between samples by eating cucumbers and neutral biscuits.

Statistics. Principal Component Analysis (PCA) (The Unscrambler 9.2, CAMO ASA, Trondheim, Norway) was performed to describe the correlation between sensory quality and instrumental measurements of release of selected volatile compounds. Average sensory response values over replicates were used in data analysis. Results are presented by score and loading plots.

Results and Discussion

17 different chewing gums were developed, such that systematic variations of the elastomer (three different types) / resin (four different types) types could be investigated. Release curves were determined for each assessor for each of the compounds from the different gums. As example for the molecules measured with APCI-MS the release profile of ethyl butanoate is shown in (Figure 1).

The curve shows that ethyl butanoate has a fast initial release and reach maximum after approximately 1.5 min of mastication for most of the chewing gum samples. The samples having the highest intensity seems to be the samples containing high amount of the resin PVA

Using PCA the data showed that initially (after 30 sec. mastication, data not shown) the sensory attributes (sweetness, flavour intensity and acidity) and the compound ethyl butanoate were correlated (Figure 2). After 9.5 min mastication no correlations between specific volatile compounds (ethyl butanoate, isopentyl acetate, limonene and methyl anthranilate) and sensory perceived intensity, acidity and sweetness was found, which was unexpected.

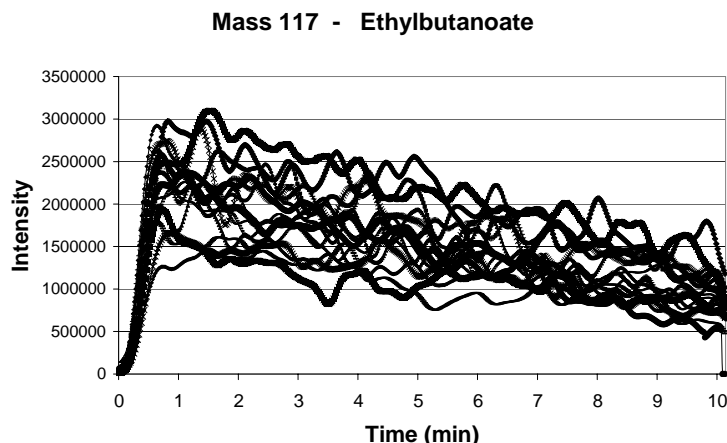


Figure 1. Flavour release profiles of ethyl butanoate for the 17 different chewing gum obtained by two subjects measured by APCI-MS.

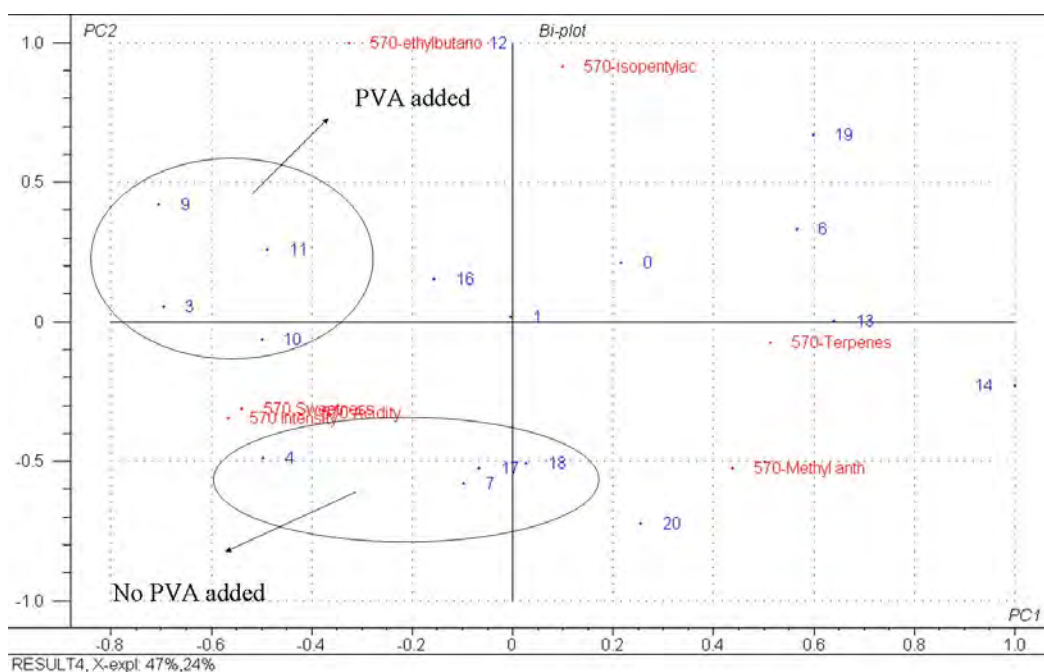


Figure 2. Variation in the 17 chewing gums, flavour content and sensory attributes analysed by principal component analysis (PCA bi-pot, PC1 vs. PC2). The PCA plot shows variation after 9.5 min (570 sec.).

The design of the elastomer / resin systems indicates that these ingredients influence the flavour release. Initially the chewing gums with high amount of the resin PVA are characterised by having higher intensities in the sensory attributes and in ethyl butanoate (e.g. sample 0, 3 & 19, data not shown). However, the different resins influence on flavour release after 9.5 min mastication is less predictable and needs further investigations.

References

1. Boland A.B., Delahunty C.M. van Ruth S.M. (2006) *Food Chem.* 96: 452-460.
2. Koliandris A., Lee A., Ferry A.-L., Hill S. Mitchell, J. (2008) *Food Hydrocol.* 22: 623-630
3. Haahr A.-M., Madsen H., Smedsgaard J., Bredie W.L.P., Stahnke L.H., Refsgaard H.H.F. (2003) *Anal. Chem.* 75: 655–662.
4. Taylor A.J., Linforth R.S.T., Harvey B.A., Blake A. (2000) *Food Chem.* 71: 327–338.

AROMA RELEASE FROM ENCAPSULATION SYSTEMS IN CHEWING GUM

K. SOSTMANN, R. Potineni, G. Blancher, X. Zhang, M. Espinosa-Diaz, R.N. Antenucci

Givaudan Flavors Corp.; 1199 Edison Drive, Cincinnati, OH-45216, USA.

Abstract

Proton-Transfer-Reaction Mass-Spectroscopy allows fast quantification of dynamic aroma compound release during consumption of food products. We applied this technique for *in-vivo* measurements of aroma release from chewing gum. Mint flavour was loaded into different encapsulation systems which were added separately into chewing gums. Menthol and menthone concentration in the exhaled air was monitored during 8 min of mastication. The different types of encapsulation systems generated significant differences in overall release, maximum intensity and time to reach maximum intensity. The analytical data was correlated to sensory studies of mint and sweetness perception. The results prove the ability of the tested encapsulation systems to create unique and distinguishable aroma release curves which are able to change the flavour perception during consumption of the respective food product.

Introduction

PTR-MS allows fast quantification of dynamic aroma release during consumption of food products (1-3). When chewing gum, consumers look for a product that tastes good and continuously releases a pleasant flavour sensation over a long period of time. To achieve this, the flavour industry needs to understand how aroma compounds are released during food consumption and develop flavours accordingly. With this knowledge, the flavour profile over time can be designed using different encapsulation systems (ES). In this study, we measured *in-vivo* flavour release from chewing gum using a PTR-MS. Our aim is to determine how the release of a mint flavour is affected by the type of encapsulation system used to flavour the gum.

Experimental

Materials. Non-coated chewing gums were prepared using gum base (140g), sorbitol (277g), maltitol syrup (50g), glycerine (25g), aspartame (0.2g), acesulfame K (0.2g), and triacetin (3g). The mint flavour was composed of menthol, menthone and menthyl acetate. Three different proprietary encapsulation systems (ES1, ES2, ES3) were used and a liquid flavour was used as reference.

PTR-MS measurements. Each gum was chewed and the exhalations were analysed using a PTR-MS (Ionicon Analytik GmbH, Austria). The experiments were performed by 3 panellists with 2 repetitions each. The panellists started with 5 blank exhalations to determine the breathing background. Then, they put the chewing gum in the mouth and chewed it during 8 min at one chew per second swallowing every 30 seconds. The time was controlled by a timer.

Sensory evaluation. Ten trained panellists (selected independently to the PTR-MS experiments) chewed the gums for 8 min and rated the mint intensity every 20 seconds using an unstructured intensity scale. They were trained to follow a protocol of discrete time-intensity recording the intensities of several descriptors. This article reports only the results on the mint flavour and sweetness descriptors.

Results

We obtained the menthol and menthone PTR-MS release curves from chewing gum using different encapsulation systems. Since both flavour compounds showed similar behaviour we will only mention the results for menthol. We compared the release curves of menthol to the time-intensity curves of mint sensory perception (Figure 1).

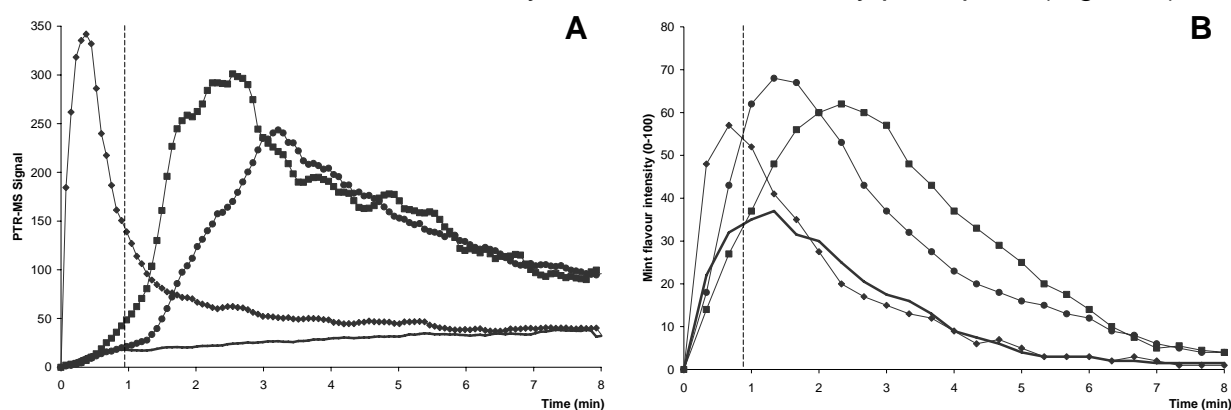


Figure 1. Comparison between menthol release curves of menthol (PTR-MS) (A) and mint sensory perception (B) using different encapsulation systems in chewing gum: (—) reference, (—○—) ES1, (—■—) ES2, and (—▲—) ES3. The dotted line at 0.92 min corresponds to the time at which maximum intensity of sweetness is perceived (average for all gums).

For all three encapsulation systems we observed a good correlation between the release curves of menthol measured by PTR-MS and the time-intensity curves of mint perception evaluated by sensory techniques: early maximum in menthol release corresponds to early maximum in mint perception and later maximum in menthol release corresponds to later maximum in mint perception. All encapsulation systems had a much higher overall release of menthol compared to liquid flavour which explains the higher perceived mint intensity.

The time-intensity parameters for menthol release and mint perception are shown in (Table 1).

Table 1. Mean time-intensity parameters determined by PTR-MS (menthol release) and sensory (mint perception).

Encapsulation system	t_{\max} (min) Sensory	t_{\max} (min) PTR-MS	I_{\max} Sensory	I_{\max} PTR-MS
Reference	1.08 ± 0.58	-	41	-
ES 1	0.87 ± 0.27	0.30 ± 0.13	63	358
ES 2	1.53 ± 0.39	2.37 ± 0.22	71	320
ES 3	2.18 ± 0.64	3.19 ± 0.19	68	253

The time to reach maximum mint intensity was significantly different for all encapsulation systems. While mint perception was delayed with ES3 compared to

liquid flavour (t_{\max} = 2.18 and 1.08 min respectively), it was accelerated with ES1 (t_{\max} = 0.87 min). The perceived mint intensity was about 60% higher for all encapsulation systems compared to liquid flavour.

While there is a clear maximum for mint perception at 1.08 min for the chewing gum with liquid flavour, no maximum menthol release was measured during the 8 min of mastication. These results can be perfectly explained by the influence of taste on the overall flavour perception (4, 5). This is shown by the similar time to reach maximum mint perception for the chewing gum containing liquid flavour and the time of maximum sweetness perception (dotted line at 0.92 min in Figure 1).

Moreover, sensory adaptation can have played a role. PTR-MS measurements show that the amount of menthol present in the breath is fairly constant over time for the chewing gum containing liquid flavour. In contrast, the perceived mint intensity decreases over time after the maximum is reached. The same tendency can be observed with ES1 after 2 min.

The influence of sweetness perception is also shown with the different encapsulation systems. In all three cases the time for maximum mint perception is shifted towards the time for maximum sweetness perception (at 0.92 min for all encapsulation systems). For ES1 the maximum mint perception is reached later than the time of maximum menthol release (0.87 compared to 0.30 min). For ES2 and ES3 the maximum mint perception happens earlier than the maximum menthol release (1.53 compared to 2.37 min, and 2.18 compared to 3.19 min, respectively). The time-intensity curves for mint perception can therefore be explained as a combination of the menthol release curves and the intensity curve of sweetness perception.

Conclusion

The release profile of the mint aroma was greatly affected by the type of encapsulation system, as measured by PTR-MS. The three studied encapsulation systems showed clear differences in terms of time to reach maximum intensity. A strong link was found between PTR-MS and sensory data. The effect of taste-flavour interactions was confirmed. We were able to demonstrate that the encapsulation systems are effective to accelerate or delay flavour release and perception even if the influence of taste compounds shifted the time of maximum mint perception towards the maximum of sweetness perception. These techniques will make it possible to modulate on demand the time-intensity sensory profile of the flavour in chewing gums by using different encapsulation systems with desired release profiles.

Acknowledgments

We want to thank Vincent Heijman for the preparation of the chewing gums and Chris Soper for providing the encapsulation systems.

References

1. Mei J.B., Reineccius G.A., Knighton W.B., Grimsrud E.P. (2004) *J. Agric. Food Chem.* 52: 6267-6270.
2. Van Ruth S., de Witte L., Uriarte A.R. (2004) *J. Agric. Food Chem.* 52: 8105-8110.
3. Mestres M., Moran N., Jordan A., Buettner A. (2005) *J. Agric. Food Chem.* 53: 403-409.
4. Davidson J.M., Linforth R.S.T., Hollowood T.A., Taylor A.J. (1999) *J. Agric. Food Chem.* 47: 4336-4340.
5. Potineni R.V., Peterson D.G. (2008) *J. Agric. Food Chem.* 56: 3254-3259.

IMPACT OF MILK FAT COMPOSITION ON DIFFUSION AND PERCEPTION OF FLAVOUR COMPOUNDS IN YOGURTS

A. SAINT-EVE¹, I. Déléris¹, A. Meynier², and I. Souchon¹

¹ UMR 782 Génie et microbiologie des procédés alimentaires, AgroParisTech - INRA, F-78850 Thiverval-Grignon, France

² UR 1268, Biopolymères Interactions Assemblages, INRA, BP 71627, F-44316 Nantes, France

Abstract

The aim of the present study was focused on the level of solid milk fat level in flavoured yogurt on their rheological properties, flavour release and diffusion in relation to their sensory properties. Whereas variation of solid fat level slightly influenced texture perception of yogurts, a large effect of solid fat level on flavour release and olfactory perception was highlighted. At 10°C, the odour of yogurt with the highest solid fat fraction (82%) was perceived more intense than yogurts with the lowest solid fat fractions (25% and 70%), in agreement with aroma release (for 10/17 flavour compounds). The diffusion of flavour compounds in the yogurt was slightly affected by the solid fat level. All these results demonstrated that it is not the total fat content that govern flavour release and perception but the uncrystalline or liquid fat content.

Introduction

Fat plays a major role in the determination of texture and flavour of complex food products and its quantitative impact was largely investigated in the past (1). In order to understand the physicochemical mechanisms responsible for olfactory perception during food eating, it seems necessary to take into account, not only the fat content in food, but also its structure and composition. The role of fat composition (animal or vegetable, or equilibrium of liquid-solid phase) on flavour release was previously investigated (2, 3). This last seems to be dependent on the physical state of fat (crystallised or liquid form) in model dairy foods (4, 5).

To our knowledge the study of the influence of solid fat level on a real flavoured product, as yogurt, has been limited in literature, particularly on their sensory impact. In this context, the aim of the present study was focused on the impact of fat composition (solid fat level) on both physicochemical properties (flavour release and diffusion) and sensory properties of yogurts.

Experimental

Product preparation. Three flavoured stirred yogurts (dry matter (22.5%), fat (4%) and proteins (5.4%)) varying in the anhydrous milk fat fraction (solid fat level at 10°C): LMF (Low Milk Fat) presented a solid fat level of 25%, AMF (Anhydrous Milk Fat) a solid fat level of 70% and HMF (High Milk Fat) a solid fat level of 82%. Yogurts were flavoured with a strawberry flavour containing 17 compounds (6).

Sensory evaluation. Sensory evaluation was carried out with 30 untrained panellists.

Discriminative tests. The effect of solid fat fraction was investigated by triangle tests i) on non flavoured yogurts in order to focus on differences on texture perception, and ii) on flavoured yogurts in order to focus on differences on flavour differences.

Descriptive tests. A comparative descriptive analysis of the three samples (LMF, AMF, HMF) was performed on three attributes: overall odour intensity (orthonasal attribute), thickness and overall flavour intensity (retronasal attribute).

Rheological properties. The rheological properties of the three yogurts were measured at 10°C in harmonic regime with a controlled-stress rheometer (model RS1, Haake, Germany). Three types of measures were conducted: frequency sweep test, complex viscosity by stress sweep, flow curve of yogurt by increasing the shear rate from 0 to 100 s⁻¹, followed by decreasing the shear rate from 100 to 0 s⁻¹.

Flavour compound release. Measurements of flavour release were performed at 10°C using a gas chromatograph equipped with a flame ionization detector and an automatic headspace sampler CombiPal: either in static conditions or in dynamic conditions. Flavour release in static conditions was determined by SPME method (6). Diffusion coefficients in yogurts were determined from experimental release kinetics obtained in a diffusion cell (7).

Data analyses. Data analyses were carried out using SAS software package, version 9.1. Analyses of variance were performed to reveal the sensory and release differences between yogurts.

Results and Discussion

Influence of solid fat level on texture perception and physical properties. Sensory results revealed differences on texture perception between the 2 products with extreme fat compositions. In particular LMF yogurt (25% of solid fat level) was perceived thicker than the two others.

Rheological properties study showed that the three yogurts are weak gels (storage modulus $G' >$ loss modulus G'' over the frequency range) as determined by frequency sweep test. The complex viscosities measured at low shear stress (0.1 Pa) did not significantly differ between the three yogurts (Table 1). Moreover, the thixotropic hysteresis loops of the three yogurts were not affected by the variation of solid fat level.

Table 1. Complex viscosity (Pa.s) for the three yogurts obtained at low shear stress (0.1Pa).

	Complex viscosity at 0.1 Pa (in Pa.s)	Standard deviation
AMF yogurt	38.85	5.87
LMF yogurt	42.31	9.75
HMF yogurt	37.64	10.54

In conclusion, only the yogurt with the lowest solid fat level (LMF yogurt) was perceived thicker than the others, but this was not related to its rheological properties. An assumption to explain this difference could be the formation of a higher fat layer on the tongue at the origin of mouth-coating perception. Indeed, LMF

yogurt contained the lowest percent of solid fat at 10°C and was perceived as being the thickest. We could also assume a higher coating of this yogurt in mucous tongue helped by its high quantity of liquid fat. A halo effect could be thus supposed: coating perception would be evaluated by panellists on thick perception scale.

Influence of solid fat level on olfactory perception and flavour release. Triangle tests performed by sniffing on flavoured yogurts showed a significant difference only between LMF and HMF yogurts ($p < 0.1\%$). Moreover, odour intensity evaluation on the three yogurts showed that HMF yogurt was perceived more intense (23-30 % of variation) in odour than the others ($p < 0.1\%$).

In static conditions, release of the majority of flavour compounds (10/17) was the highest from HMF yogurt and 8 flavour compounds were the least released from LMF yogurts (Figure 1). The AMF yogurt presented an intermediary behaviour. Quantitatively, these modifications were mainly noticeable for hydrophobic flavour compounds. For ethyl acetate, a hydrophilic flavour compound, a different behaviour was observed: this compound was more released from LMF yogurt than from the others. All these results seemed to highlight that interactions (solubilisation) between flavour compounds and fat occurred with the liquid fraction of fat, and not with the crystalline part of fat. Liquid lipids can solubilise flavour compounds and act as a reservoir for the aroma as shown on emulsions or model dairy gels (2,4,8). In addition, flavour release and flavour perception are in agreement, in particular in static conditions and for hydrophobic flavour compounds.

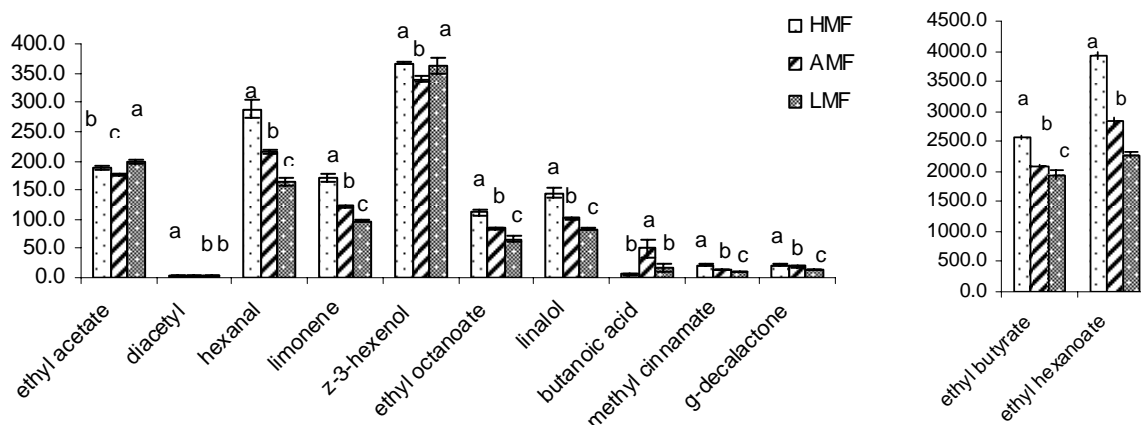


Figure 1. Flavour release measurements performed by static headspace method by Solid Phase MicroExtraction (PDMS fibre) for \square HMF, \square AMF and \square LMF.

Concerning diffusion coefficients, a significant effect of solid fat level was only observed for ethyl hexanoate, which was significantly higher in HMF yogurt than in others in accordance with olfactory perception (Figure 2). The diffusion of others aroma compounds was not significantly related to the solid fat level. Our study contributes thus to precise the mechanism involved in flavour perception during consumption. Mobility of aroma compounds (diffusion coefficient) would have only a weak impact on released flavour quantity in mouth, accentuated by the relatively short timescale of yogurt in mouth cavity when consumption.

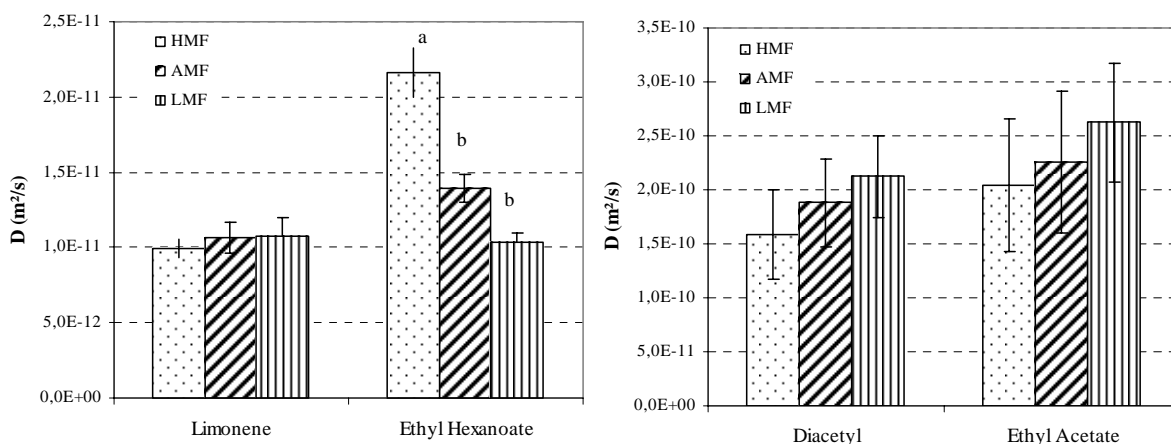


Figure 2: Diffusion coefficients D (m^2/s) of 4 flavour compounds between the 3 products for \square HMF, \square AMF and \square LMF.

Conclusion

In studied flavoured stirred yogurts, solid fat level induced a large effect on flavour release and perception, but not on texture and rheological properties. This work clearly suggests that the underlying molecular organisation, which depends on lipid composition, takes a great part in flavour behaviour, with consequences in olfactory perception. To reduce fat in food, it is also essential to better take fat structure into account as well as the evolution of its physical state during eating to control flavour release and perception.

References

1. De Roos K. B. (1997) *Food Technol. (Chicago)* 51(1): 60-62.
2. Roberts D.D., Pollien P., Watzke B. (2003) *J. Agric. Food Chem.* 51: 189-195.
3. Relkin P., Fabre M., Guichard E. (2004) *J. Agric. Food Chem.* 52: 6257-6263.
4. Bongard S., Meynier A., Riaublanc A., Genot C. (2006) In *Flavour Science*. W.L.P. Bredie and M.A. Peterson (eds.), Elsevier, pp. 399-402.
5. Roudnitzky N., Rondaut G., Guichard E. (2006) In *Food Lipids: Chemistry, Flavor, and Texture*. Vol. 920. pp. 191-204.
6. Saint-Eve A., Juteau A., Atlan S., Martin N., Souchon I. (2006) *J. Agric. Food Chem.* 54: 3997-4004.
7. Deleris I., Atlan S., Souchon I., Marin M., Trelea L.C. (2008) *J. Food Eng.* 85: 232-242.
8. Ghosh S., Peterson D.G., Coupland J.N. (2006) *J. Agric. Food Chem.* 54: 1829-1837.

HOW FLAVOUR RETENTION REFLECTS THE EMULSIFYING PROPERTIES OF ACACIA GUMS

G. SAVARY¹, N. Hucher¹, E. Bernadi¹, I. Jaouen², C. Malhiac¹, M. Grisel¹

¹ *Université du Havre, URCOM, EA3221, 25 rue P. LEBON, BP 540, F-76058 Le Havre cedex, France*

² *Alland & Robert, 125 Grande rue, F-27940 Port Mort, France*

Abstract

This work focuses on the study of the flavour release of two different hydrophobic aroma compounds from Acacia gum aqueous solutions. Retention was measured using the phase ratio variation method under equilibrium whereas diffusion was assessed by DOSY-NMR. This study established the relationship between the emulsifying ability of Acacia gum and the behaviour of aroma compounds in the corresponding solution. Better emulsifying ability of Acacia gum sample appears strongly correlated to an increase in flavour retention and a decrease in molecular mobility as the result of hydrophobic interactions.

Introduction

Acacia gum (GA) is a natural polysaccharide associated with a small amount of linked protein (2%, w/w). Three different fractions can be isolated:

- the Arabino-Galactan fraction (AG) (88% of the total gum - 20% total proteins)
- the Arabino-Galactan Protein fraction (AGP) (10% - 55% total proteins)
- the Glyco-Protein fraction (GP) (about 1% - 25% total proteins).

Because of its unique emulsifying and stabilising properties, acacia gum is commonly used in many food applications. In beverage flavoured with essential oil, for instance, the GA efficiently stabilises the flavour compounds in the aqueous phase. For industrial applications it is important to easily evaluate the emulsifying ability of gums. The emulsifying properties seem to be related to two important parameters: the molecular weight of the AGP fraction and the nature of the proteins (1-4). Gel permeation chromatography (GPC) coupled with a triple detection (MALLS, UV and RI) is currently used to characterise acacia gums, nevertheless most of the time analysis results are only slightly different in spite of significant differences in emulsifying abilities. In this work, we proposed an original way to evaluate the emulsifying potential of several acacia gums selected for their good emulsifying potential. First different samples of *Acacia Senegal* gums were selected and characterised using GPC. Then the behaviour of two aroma compounds in the solutions containing AG was analysed. Behaviour of these two probes was then compared and put in relation with the stability of corresponding emulsions; such a method made possible to determine whether flavour retention and diffusion measurements were efficient ways or not to evaluate the emulsifying ability of AG.

Experimental

Molecular characterisation. The AG, GP and AGP percentages were determined in a gel permeation chromatography (GPC) system equipped with a Superose 6 10/300 GL (GE Healthcare). A refractive index detector (Sopares, France), an UV detector (Series 1100 Helwett Packard, France) at 214 nm and a Dark V3 detector (Consenxus, Germany) operating at 532 nm were used. The mobile phase was 0.1 mol.L⁻¹ sodium chloride at a 0.4 ml min⁻¹ flow at ambient temperature. The injection volume was 50 µL. A value of 0.142 cm³ g⁻¹ was measured for the refractive index increment (dn/dc) in this mobile phase. The GA solution was prepared at 3 g L⁻¹ in mobile phase 24 h before analysis and filtered (0.45 µm) 1 h before injection.

Rheological characterisation of GA solutions. 5% GA solutions in ultra pure water were prepared 24 h before measurement. Apparent viscosities were then recorded at 20 °C using a Brookfield viscometer model LVT with the spindle no. 1 at 100 rpm.

Aroma diffusion measurement. 5% GA aqueous solutions were flavoured with α -terpineol (0.8 g.L⁻¹). DOSY-NMR experiments were performed at 298 K on a Bruker Advanced 300 equipped with a 5 mm gradient inverse probe. A stimulated echo sequence (STE) incorporating bipolar gradients (BP) with longitudinal eddy current delay (LED) of 5 ms was used. Duration of the magnetic field pulse gradient (δ) was 1 ms and a diffusion time (Δ) of 550 ms was applied to observe a complete signal decay with the maximum gradient strength. After Fournier transformation, phase and baseline corrections, the diffusion coefficient (D) was obtained using the xwinmr 3.5 software.

Aroma retention measurement. The retention of ethyl decanoate in the GA solutions was calculated according to Jouquand et al. (5) using the PRV method. 5% (w/w) solutions of AG were prepared 24 h before analysis. Solutions or water were flavoured with a solution of ethyl decanoate diluted in ethanol at a concentration of 2.76 g L⁻¹ to have a final concentration of 4.6 ppm in the solution. Increasing volumes (1, 2, 3 and 4 mL) of the flavoured solutions were placed into headspace vial (20.7 mL) and hermetically sealed. Once the equilibrium time reached (corresponding to 6 h at 30 °C), a 1 mL sample of headspace was injected into the GC by a gas syringe (30 °C) using a Combipal CTC analytics automatic headspace sampler. A Varian CP-3800 GC system with a flame ionization detector (FID) and a BP-1 column (0.25 mm \times 15 m \times 0.25 µm, SGE) was used. Oven temperature was programmed at 150 °C for 3 min. Detector and injector temperatures were 250 °C. Helium was used as carrier gas at a flow rate of 1 mL min⁻¹. Injection was performed with a 1/20 split.

Results

Characteristics of the GA samples. In this study, four samples of acacia gums were selected for their good emulsifying potential. The emulsifying property, the AGP and AG + GP fractions percentages and also the apparent viscosity (5% GA solutions) of each sample are given in (Table 1).

Table 1. Characteristics of the acacia gums (* data provided by Alland & Robert).

	Emulsifying properties*	Apparent viscosity (mPa.s)	% AGP	% AG + GP
GA1	+	27	9.3	90.7
GA2	+	25	11.3	88.7
GA3	+++	28	14.1	85.9
GA4	+++	34	14.7	85.3

GA1 and GA2 had a good potential whereas GA3 and GA4 were particularly efficient emulsifier. According to the gums composition reported, the gums GA3 and GA4 were composed of higher fraction of AGP than the two other gums GA1 and GA2. As a consequence, better emulsifying ability corresponds to higher AGP fraction, thus confirming the primary implication of the AGP fraction in the emulsifying properties (1-3). Finally, no significant difference in the apparent viscosity was observed when comparing the different samples of GA. Apparent viscosity of the solutions was notably measured to help understanding the behaviour of the flavour compounds in the GA solutions.

Flavour retention and diffusion. Two different aroma compounds were used: α -terpineol and ethyl decanoate (Table 2).

Table 2. Characteristics of the two aroma compounds.

	Solubility in water at 25 °C (g L ⁻¹)	log P	Odour characteristics
α -Terpineol	1.80	3.0	Sweet, floral, lilac
Ethyl decanoate	0.016	4.7	Sweet, fruit, dry fruits

These compounds, naturally found in several floral or fruity aroma fractions, are soluble in water in the concentration range used in this study and are enough lipophilic (log P) to be representative of compounds present in essential oils currently used to flavour beverages.

The gas/liquid partition coefficients of ethyl decanoate, as measured by the PRV method in water and in the four solutions of GA are reported on (Figure 1).

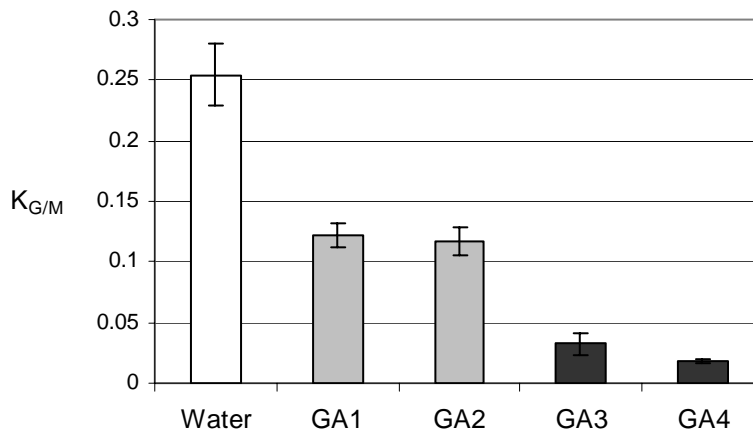


Figure 1. Gas/liquid partition coefficients of ethyl decanoate at 30 °C.

The partition coefficient of ethyl decanoate was lower in the GA solutions than in water. This indicates a significant retention of ethyl decanoate whatever the GA samples. Thus, interactions existed between ethyl decanoate and GA. Hydrophobic interaction appear the most probable type as the consequence of the lipophilic nature of this aroma compound. Moreover the decrease in the release of ethyl decanoate in the headspace depended on the GA sample. Two different tendencies were observed: $K_{G/L}$ of ethyl decanoate was similar for GA1 and GA2 solutions, and similar but much lower for GA3 and GA4 solutions. From these results, it is possible to calculate the percentages of retention (R) of ethyl decanoate in the solutions as compared to water. R was 52% and 54% for GA1 and GA2, respectively and 87% and 93% for the better emulsifiers GA3 and GA4, respectively. As a consequence,

the better the emulsifying power of the GA, the higher the retention. The retention of ethyl decanoate indicated the presence of hydrophobic interactions that reflected the quality of the acacia gum. The hydrophobic interactions could be put in relation with the gum's AGP content. The higher the AGP fraction, the higher the retention of ethyl decanoate. As a consequence, the role of the proteins of the AGP fraction was suggested in the establishment of bindings with lipophilic compounds, even if more experiments should be performed to confirm this result.

In a second step, DOSY NMR measurements were performed to obtain the diffusion coefficients of α -terpineol. (Figure 2) indicates the values obtained in water and in the 5% GA solutions.

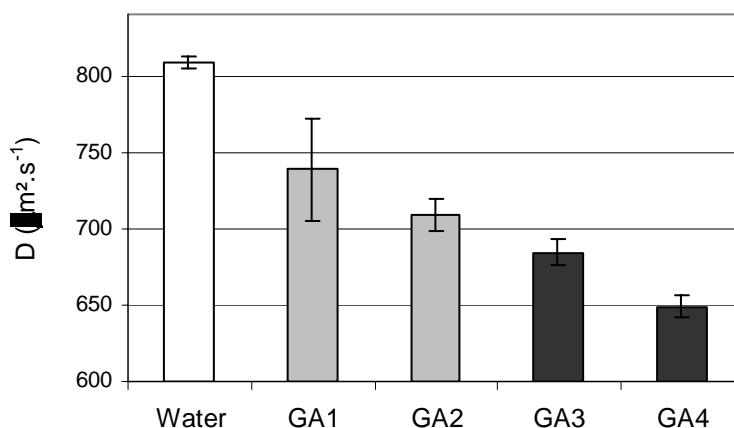


Figure 2. Diffusion coefficients of ethyl decanoate at 30 °C.

The diffusion coefficient (D) of α -terpineol decreased in the solution of GA as compared to the diffusion in water. This decrease strongly depended on the GA sample following the order: GA1 \ge GA2>GA3>GA4. The apparent viscosities of the solutions (Table 1) did not explain this evolution of D. As a result, the D decreasing was rather linked to the emulsifying properties of the gums and these results confirmed the conclusions drawn using the PRV method, a completely different tool based on the utilisation of another volatile probe molecule. The better the emulsifying power, the lower the diffusion coefficient.

Conclusions

This study demonstrated that good GA emulsifying properties induce hydrophobic interactions that sharply reduce the release and the mobility of aroma compounds in the GA solution even at low gum content. Moreover, not only flavour retention but also flavour diffusion correlated well with the emulsifying properties of GA as revealed by the DOSY NMR experiments. These results may be confirmed with samples of GA of wilder origins.

References

1. Randall R., Phillips G., Williams P. (1988) *Food Hydrocolloids* 2: 131-140.
2. Randall R., Phillips G., Williams P. (1989) *Food Hydrocolloids* 3: 65-75
3. Garti N., Leser M. (2001) *Polym. Adv. Technol.* 12: 123-135
4. Al-Assaf S., Phillips G., Williams P., (2006) *Food Hydrocolloids* 20: 369-377
5. Jouquand C., Aguni Y., Malhiac C., Grisel M. (2008) *Food Hydrocolloids* 22: 1097-107.

BEHAVIOUR OF SELECTED FLAVOUR COMPOUNDS IN DAIRY MATRICES: STABILITY AND RELEASE

K. BUHR^{1,3}, B. Köhlnhofer¹, A. Heilig², J. Hinrichs², and P. Schieberle^{1,3}

¹ *Deutsche Forschungsanstalt für Lebensmittelchemie (DFA), Lichtenbergstraße 4, D-85748 Garching, Germany*

² *Institut für Lebensmittelwissenschaft und Biotechnologie (LTH), Garbenstraße 21, D-70599 Stuttgart, Germany*

³ *Lehrstuhl für Lebensmittelchemie, Technische Universität München (TUM), Lichtenbergstraße 4, D-85748 Garching, Germany*

Abstract

Stability of ethyl hexanoate was found to be reduced in low fat dairy matrices. Release of limonene, ethyl hexanoate, diacetyl and 2-methylbutanoic acid from various dairy matrices and sunflower oil was measured by Proton Transfer Reaction - Mass Spectrometry and compared with orthonasal detection thresholds.

Introduction

Despite increasing knowledge on interaction between flavour compounds and various food matrices, it remains a challenge to adapt complex flavourings to dairy matrices. This is mainly due to the complexity and variability of these matrices. In this relation, numerous studies focused on individual aspects of flavour - dairy matrix interaction. For example, it was shown that milk proteins, especially bovine serum albumine and β -lactoglobuline, are able to specifically bind flavour compounds resulting in a reduced availability for perception [1-3]. Furthermore it was shown that higher fat contents lead to retention of lipophilic flavour compounds while the release of more polar compounds like diacetyl is hardly affected [4-6]. Additional influencing variables are different degrees of technological processing (heating, acidification or fermentation) as well as addition of polysaccharides [4] or sugars [6].

While most of the studies mentioned above focus on individual aspects of flavour - dairy matrix interaction and release, it is the objective of this study to perform a systematic investigation on flavour - dairy matrix interaction and release of selected aroma compounds by stepwise increasing the complexity of the matrix. The aroma compounds diacetyl, 2-methylbutanoic acid, methoxyfuraneol, ethyl hexanoate, limonene, δ -decalactone and vanillin were selected based on their industrial relevance and in order to account for a wide range of functional groups, lipophilicity and possible interaction mechanisms. Stepwise increase of the matrix complexity was achieved by studying the release of the same aroma compounds from water, sunflower oil as a replacement for milk fat, dispersions of whey protein, casein, milk permeate as well as various dairy product matrices by Proton Transfer Reaction - Mass Spectrometry (PTR-MS) [7]. Results were compared with orthonasal detection thresholds of the same aroma compounds determined by the triangle test approach. Additionally, the stability of the aroma compounds was investigated by Stable Isotope Dilution Assays [8].

Experimental

Stability of aroma compounds in yogurt matrices. For investigation of stability of aroma compounds in yogurt matrices, recovery of selected compounds from yogurt matrices with varying fat contents was determined by Stable Isotope Dilution Analysis according to [8].

Proton Transfer Reaction - Mass Spectrometry (PTR-MS). Aroma release from model solutions as well as dairy product matrices was studied by Proton Transfer Reaction - Mass Spectrometry (PTR-MS; Ionicon Analytik GmbH, Innsbruck, Austria) according to the method described by Lindinger et al. [7].

For headspace sampling, 5 g of flavoured yogurt or 100 mL of model solution or milk was placed in a 1 L Erlenmeyer flask, closed with a septum and left for 60 min at ambient temperature for equilibration. The heated nose of the instrument was pierced through the septum into the headspace of the flask. Additionally a disposable needle was pierced through the septum in order to allow for replacement of the air continuously sampled by the instrument at 170 mL/min. Analyses were performed at 120°C (inlet); 80°C (drift tube) and a drift voltage of 600 V.

The following mass fragments and dwell times were selected for monitoring the release of the selected aroma compounds: diacetyl (m/z 87, 0.2 s), 2-methylbutanoic acid (m/z 103, 0.2 s), ethyl hexanoate (m/z 117 and 145, 0.2 s), limonene (m/z 81 and 137, 0.2 s). Analyses of unflavoured matrices as well as fragmentation studies of individual compounds prove no significant overlaps in mass fragments for the selected aroma compounds. Due to their low volatilities, temporal release of vanillin, δ -decalactone and methoxyfuraneol could not be monitored under these conditions.

Results

Stability of aroma compounds in dairy matrices. Aroma release is first of all dependent on the quantities of aroma compounds present in the food matrix. Therefore, recovery of limonene, vanillin, diacetyl, 2-methylbutanoic acid, methoxyfuraneol, δ -decalactone, and ethyl hexanoate was determined by Stable Isotope Dilution Analysis [8] before and after acidification of yogurt matrices with varying fat contents. All aroma compounds except ethyl hexanoate showed excellent recovery rates close to 100% [data not shown]. As shown in (Table 1), recovery rates of ethyl hexanoate from yogurt matrices with max. 0.1% fat were 58% before and 45% after acidification.

Table 1. Recovery of 8 mg/kg ethyl hexanoate in various dairy matrices 48 h after sample preparation.

Fat content [g/100 g]	Recovery in non-acidified yogurt matrices [mg/kg]	Recovery in acidified yogurt matrices [mg/kg]
0.1	4.85 ± 0.59 (58.7%)	3.53 ± 0.05 (45.3%)
4	6.79 ± 0.05 (87.1%)	7.69 ± 0.03 (98.6%)
12	6.61 ± 0.37 (84.7%)	7.75 ± 0.30 (99.4%)
20	8.54 ± 0.12 (109.5%)	8.09 ± 0.13 (103.7%)

Low recovery rates were independent of microbial fermentation or acidification by glucono- δ -lactone. However, low stability of ethyl hexanoate may be compensated by higher release rates from low-fat dairy matrices as shown in the next section.

Aroma release from dairy matrices as measured by PTR-MS. Comparison with orthonasal detection thresholds. As shown in (Figure 1), fat has the most pronounced retention effect on the more lipophilic aroma compounds limonene and ethyl hexanoate. Although not as pronounced as measured by PTR-MS, this is mirrored by increased orthonasal threshold values. As shown in (Table 2), odour threshold values above solutions in sunflower oil increase by a factor of 70 in the case of limonene and a factor of 8 in the case of ethyl hexanoate compared to threshold values above aqueous solutions.

While limonene release from milk permeate, casein and whey protein dispersions shows reduced release rates as compared to water, the same differences are not present in the case of ethyl hexanoate. Interestingly, for both compounds retention from whole milk is much more pronounced than would be expected by addition of the retention effects from casein dispersion, whey protein dispersion, milk permeate, and sunflower oil as a semblance for milk fat.

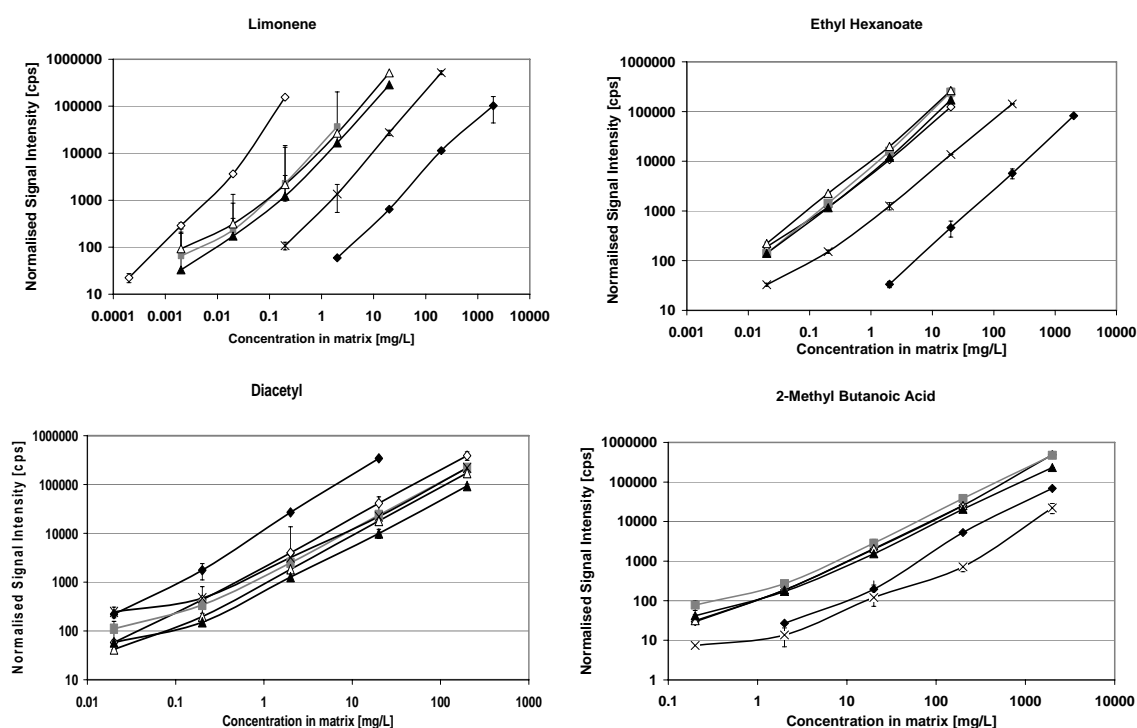


Figure 1. Release of selected aroma compounds from water (◇), sunflower oil (◆), milk permeate solution (■), casein dispersion (△), whey protein dispersion (▲) and whole milk (X) as measured by Proton Transfer Reaction - Mass Spectrometry (PTR-MS).

When comparing orthonasal detection thresholds as shown in (Table 2), the limonene threshold in whole milk (6.5 mg/L) corresponds with the PTR-MS measurements and is found to be between the thresholds above water (0.2 mg/L) and sunflower oil (14.7 mg/L). Although release rates of ethyl hexanoate from whole milk are significantly higher as compared to sunflower oil, the orthonasal detection thresholds of ethyl hexanoate in whole milk (0.3 mg/L) was found to be even higher than in sunflower oil (0.04 mg/L). This is indicating possible perceptual interactions with other volatile compounds from the milk matrix leading to a reduced sensitivity for the respective aroma compound.

Table 2. *Orthonasal detection thresholds and LogP-values [9] of limonene, ethyl hexanoate, diacetyl and 2-methylbutanoic acid above solutions in water, whole milk and sunflower oil.*

	Log P	Water [mg/L]	Whole milk [mg/L]	Sunflower oil [mg/L]
Limonene	3.61	0.2	6.5	14.7
Ethyl hexanoate	2.69	0.005	0.3	0.04
2-Methylbutanoic acid	1.18	0.5	10.3	0.1
Diacetyl	-0.60	0.015	0.050	0.010

2-Methylbutanoic acid does not show any significant differences in release from water, milk permeate, casein or whey protein dispersions while aroma retention is more pronounced in whole milk than in sunflower oil, which is mirrored by an increased orthonasal detection threshold above solutions of 2-methylbutanoic acid in whole milk.

Due to its ability to form dimers as well as hydrogen bonds in aqueous media, diacetyl release is enhanced in an aprotic medium like sunflower oil. However, as an original aroma compound in whole milk, its orthonasal detection threshold is increased by a factor of 3.3 compared to water.

Acknowledgement

This work is supported by the German Federal Ministry of Economy and Technology (BMWi/AIF) via Research Association of the German Food Industry (FEI), Project No. AIF-FV 15158 N.

References

1. Kühn J., Considine T., Singh H. (2006) *J. Food Sci.* 71: R72-R82.
2. Guth H., Fritzler R. (2004) *Chem. Biodiv.* 1 : 2001-2023.
3. Guichard E., Langourieux I. (2000) *Food Chem.* 71 : 301-308.
4. Gonzales-Tomas L., Bayarri S., Taylor A.J., Costell E. (2007) *Food Res. Int.* 40 : 520-528.
5. Miettinen S.A., Hyvönen L., Tuorila H. (2003) *J. Agric. Food Chem.* 51: 5437-5443.
6. Brauss M.S., Linforth R.S.T., Cayeux I., Harvey B., Linforth A.J. (1999) *J. Agric. Food Chem.* 47: 2055-2059.
7. Lindinger W., Hansel A., Jordan A. (1998) *Int. J. Mass Spectrom. Ion Process.* 173: 191-241.
8. Schieberle P., Grosch W. (1987) *J. Agric. Food Chem.* 35: 252-257.
9. <http://www.molinspiration.com/cgi-bin/properties>.

EFFECT OF FLOUR, FIBER, AND PHYTASE ON VOLATILE EXTRACT COMPOSITION AND SENSORY PERCEPTION OF BREAD

P. POINOT, J. Grua-Priol, G. Arvisenet, C. Fillonneau, A. Le-Bail, C. Prost

ENITIAA, UMR GEPEA CNRS 6144, Nantes Atlantiques Universités, Rue de la Géraudière, 44322 Nantes Cedex 3, France

Abstract

To be well accepted, bread with increased nutritional quality must be characterised by a good flavour. This work aimed at investigating the effect of nutritional ingredients like flour, inulin and phytase on the aromatic profile and the resulted aroma of bread. Flour had a significant impact on the volatiles formed in bread and consequently on its odour. Phytase did not modify odorant properties of breads, while inulin in white bread led to a modification of its odour linked to higher quantity of Maillard compounds formed when this fibre was added. Finally, inulin and phytase enriched breads were characterised by odorant properties close to the non-enriched breads. These breads could thus become good nutritional alternative, with the same organoleptic properties than conventional breads which are considered as acceptable by consumers.

Introduction

Being a source of proteins, dietary fibres, vitamins and micronutrients, bread is considered to be of global importance in nutritional equilibrium. As a response of public health problems (cancers, obesity, cardiovascular diseases and type II diabetes) innovative bread formulations have been in progress. Bread enriched with fibres were then formulated (1). Likewise, phytase enzyme has also been added in bread recipe to increase minerals intake by the consumers (2). This enzyme hydrolyses phosphomonoester bonds from phytate. This permits to make bio-available multivalent cations, which form insoluble complexes with phytate (2). This is particularly true for whole bread which contains more minerals than white bread, because whole flour is issued from the totality of the seed. Although the aroma of bread based on a standard recipe has been largely studied, to our knowledge none of the studies has focused on the aromatic profile of bread with added nutritional quality. However, it has been demonstrated that bread aroma was clearly influenced by the ingredients incorporated in the recipe (3). This work aimed at investigating the effect of flour (white flour and whole flour), fibre (inulin) and phytase on the odorant profile of bread and on its resulting odour.

Materials and Methods

Bread-making procedure. Eight different breads were formulated following a full experimental design. Each bread type was replicated four times. Dough formula consisted in white wheat flour (T55) or whole wheat flour (T150) (100%), fresh yeast (5%), salt (2%), improvers (1%), and water (58%). 3% (w/w) of inulin (1) and 0.25% (v/w) of phytase from *Aspergillus niger* (2) were incorporated in the recipe. When

inulin was added, 3% of flour were removed. Ingredients were mixed during 2 min at 100 rpm and 7 min at 200 rpm. Dough was then rested (15 min), divided (2100g), rested (10 min), and flattened with a roller. It was divided in 30 ball samples about 70g. Samples were then placed in a proofing cabinet for 60 min at 35°C, 95% relative humidity. Baking was done in a static sole oven during 20 min at 230°C with 0.5 L of steam at start baking.

Sensory analysis. Triangular tests were performed to assess the effect of flour, inulin and phytase on bread odour. Eight sessions were carried out to evaluate the effect of the incorporation of each of the three ingredients tested. Thirty minutes after the final baking, four breads per baking batch were crushed and homogenized. 6g of crushed bread were put in 100 mL brown flasks. These were hermetically closed and identified by a three-number code. Sessions were carried out 90 min after the samples preparation, in a sensory room where panellists were isolated from each other in cubicles. For each triangular test, samples were presented to 30 naive judges, aged from 20 to 50 years. A significant odorant difference for a risk of 5% between two breads was obtained when it was perceived by more than 15 judges.

Analysis of bread volatile compounds. Four breads per baking batch were used to carry out the experiments. The HS-SPME conditions (fibre type, extraction time and extraction temperature) were previously optimised (4). 30 min after baking, breads were entirely crushed (crust and crumb). Six grams of homogenized crushed bread and 5 µL of internal standard were placed in a 125 mL sealed flask, stirred and placed at 35°C. After 5 min equilibrium, a 75 µm Car/Pdms fibre was exposed to the sample headspace for 30 min. Four extractions of volatiles were carried out for each bread formulation. The identification and the quantification of volatile compounds were carried out by GC-MS/FID, following the procedure described by Poinot et al (2008) (3).

Results

Flour was found to have a significant impact on bread odorant perception (24 correct answers about 30 judges). To explain these results, volatile compounds extracted from the different formulations were identified and quantified. 49 different volatiles were identified in white breads, while 40 were identified in whole breads. Flour had a significant impact (at a risk of 5%) on the volatiles formed in breads which could then explain the difference of odour between white and whole breads. Whole breads contained higher quantity of most of volatiles issued from the fermentation and lipid oxidation, whereas Maillard volatiles were in higher quantity in white breads.

For white breads, 21 volatiles were influenced by one (or both) ingredient(s) (Table 1), while 9 compounds were influenced in whole breads (Table 2). Phytase in white breads had no effect on all compounds quantities, except for 1-pentanol. Its slight effect could explain the same odour for phytase enriched breads and non-enriched breads (shown by triangular test). As it was previously obtained by other authors (1), white breads enriched with inulin were perceived differently to the non-enriched breads. This could be explained by the higher amount of Maillard volatile compounds formed in it. It may be that the heating of inulin during the baking resulted in its degradation in mono or oligosaccharides which could then participate in Maillard reaction (5). Moreover, the higher quantity of some fermentative compounds in inulin enriched white bread might result from the fermentation by yeast of short chains of oligosaccharides present in inulin. Furthermore, it could be seen that some Maillard and acid volatiles quantities were reduced when phytase was added with

inulin. This could be the reason for the similar odour of inulin and phytase enriched breads and non-enriched breads.

Table 1. Volatile compounds of white breads which were influenced by the presence of inulin, phytase or both.

Volatile compounds issued from	Volatile compounds	LRI	Inulin effect	Phytase effect	Inulin-phytase effect
Fermentation	Ethanol	945	↗		
	2-Methyl-1-propanol	1116	↗↗		
	3-Methyl-1-butanol	1254	↗↗		
	3-Hydroxy-2-butanone	1323	↗		
	Acetic acid	1456	↗		↘
	Phenylethyl alcohol	1895			
Lipid oxidation	2-Butenal	1070	↘		
	1-Pentanol	1286		↘↘↘	
Maillard reaction	2-Ethylpyrazine	1377	↗		
	2,6-Dimethylpyrazine	1383	↗↗		↘
	2,3-Dimethylpyrazine	1397			↘
	2-Ethyl-6-methylpyrazine	1441	↗		↘
	2-Ethyl-5-methylpyrazine	1450	↗↗		
	2,3,5-Trimethylpyrazine	1473	↗↗		
	6-Methyl-2-vinylpyrazine	1478			↘
	2-Acetylfuran	1556			↘
	Dihydro-2(3H)-furanone	1722			↘
2-Acetylpyrrole	1890			↘	
Fermentation and Maillard reaction	2,3-Butanedione	985	↗		
Lipid oxidation and Maillard reaction	2-Pentylfuran	1227			↗
Undetermined origin	2,3-Butanediol	1592-1636	↗		

↗: significant increase with a confidence level of 90%; ↘: significant decrease with a confidence level of 90%; ↗↗: significant increase with a confidence level of 95%; ↘↘: significant decrease with a confidence level of 95%; ↗↗↗: significant increase with a confidence level of 99%; ↘↘↘: significant decrease with a confidence level of 99%. Compounds were identified by LRI: Linear Retention Index on DB-WAX column, MS: Identification based on standard MS spectra databases: Wiley 6 and STD: Identification based on standard injection.

Phytase had no effect on whole breads odorant perception. This was quite surprising as it induced a slight change in their volatile composition (Table 2). Indeed, it could be seen that these breads contained more volatiles issued from fermentation and/or lipid oxidation when phytase was added. The higher amount of fermentative compounds could be linked to the enhancement of α -amylase activity due to the release of calcium ions by phytate hydrolysis (2). The increase of volatiles issued from the lipid oxidation in these breads might also be linked to an improvement of lipooxygenase activity by minerals released from phytase action (6). This may then result in more volatiles issued from linoleic and linolenic acids oxidation. Inulin had no impact on whole breads odorant perception. This could be issued from the little change in their volatiles composition. Indeed, as whole breads have naturally high amount of fibres and proteins which could participate in Maillard reaction, the substitution of 3% of whole flour by inulin may not be sufficient to induce an increase of Maillard volatile quantities. Finally, opposite effects of inulin and phytase on some

volatiles of whole breads could be seen. This may be linked to the same odours for inulin and phytase enriched whole breads and that of the non-enriched breads.

Table 2. Volatile compounds of whole breads which were influenced by the presence of inulin, phytase or both.

Volatile compounds issued from	Volatile compounds	LRI	Inulin effect	Phytase effect	Inulin-phytase effect
Fermentation	2-Methyl-1-butanol	1245		↗	
	3-Methyl-1-butanol	1254		↗↗	
	3-Methylbutanoic acid	1691		↗↗	
Lipid oxidation	1-Hexanol	1389	↘	↗	
	1-Octen-3-ol	1469	↘	↗↗	
Maillard reaction	2-Acetylpyrrole	1890		↗↗	
Fermentation and lipid oxidation	1-Propanol	1050		↗	
	(E)-2-Heptenal	1385	↘↘		
	Hexanoic acid	1884	↘↘		

↗: significant increase with a confidence level of 90%; ↘: significant decrease with a confidence level of 90%; ↗↗: significant increase with a confidence level of 95%; ↘↘: significant decrease with a confidence level of 95%; ↗↗↗: significant increase with a confidence level of 99%; ↘↘↘: significant decrease with a confidence level of 99%. Compounds were identified by LRI: Linear Retention Index on DB-WAX column, MS: Identification based on standard MS spectra databases: Wiley 6 and STD: Identification based on standard injection.

Breads odorant properties were then not modified when inulin and phytase were added simultaneously. Inulin and phytase enriched breads could thus become good nutritional alternatives, with the same organoleptic properties of conventional breads which are considered as acceptable by consumers.

Acknowledgements

This study has been carried out with financial support from the Commission of the European Communities, FP6, Thematic Area "Food quality and safety", FOOD-2006-36302 EU-FRESH BAKE. It does not necessarily reflect its views and in no way anticipates the Commission's future policy in this area.

References

1. Wang J., Rosell C.M., Benedito de Barber C. (2002) *Food Chem.* 79: 221-226.
2. Haros M., Rosell C., Benedito C. (2001) *J. Agric. Food Chem.* 49: 5450-5454.
3. Poinot P., Arvisenet G., Grua-Priol J., Colas D., Fillonneau C., Le-Bail A., Prost C. (2008) *J. Cereal Sci* 48: 686-697.
4. Poinot P., Grua-Priol J., Arvisenet G., Rannou C., Semenou M., Le Bail A., Prost C. (2007) *Food Res. Int.* 40: 1170-1184.
5. De Gennaro S., Birch G.G., Parke S.A., Stancher B. (2000) *Food Chem.* 68: 179-183.
6. Marcelle R.D. (1991) *Biol. Tec.* 1: 101-109.

DETERMINATION OF AROMA COMPOUNDS DIFFUSION PROPERTIES IN DAIRY GELLED EMULSIONS USING MECHANISTIC MODELLING

I. DELERIS, I. Zouid, I. Souchon, and I.C. Tréléa

UMR 782 Génie et Microbiologie des Procédés Alimentaires, INRA - AgroParisTech, 1 av. Lucien Brétignières, F-78850 Thiverval-Grignon, France

Abstract

This paper describes a mechanistic mathematical model developed for the prediction of the release of aroma compounds from dairy emulsions and for the calculation of their apparent diffusion properties. The main implementation in regards with our previous work was to take the biphasic structure of the emulsion into account. The calculation of apparent diffusion properties only required to know fat content and the local physicochemical properties of aroma compounds within the different phases of the emulsion. Comparison with experimental diffusion properties of four aroma compounds within dairy gels with different fat contents demonstrated the validity and the accuracy of such a determination.

Introduction

In a context where the reduction of some food constituents (fat, sugar or salt) constitutes a challenge for food industries, a better understanding of aroma compound release from food products is of great interest to optimise food formulation and flavouring. Aroma compounds partition and diffusion properties are key parameters to explain their availability for their release into the gaseous phase (1-6). Because of food complexity (they are generally multiphase systems), this repartition is of major importance as it can change the perceived flavour during eating (7-8). Experimental determination of apparent diffusion properties can be difficult to perform. Modelling approach developed by several authors to predict transport properties in multiphase media on the basis of local physicochemical properties (9-11) provided a quite accurate determination of apparent diffusion properties but often relied on simplifications which must be unrealistic for true macroscopic emulsions. To better understand the main phenomena involved in aroma release, the objective of the present work was to develop mechanistic models describing the aroma release kinetics from emulsified dairy matrices and allowing the determination of apparent diffusion properties of aroma compounds.

Materials and Methods

Aroma compounds and products: This study concerned the diffusion properties of 4 aroma compounds presenting a wide range of volatility ($K_{\text{air/water}}$) and hydrophobicity ($\log P$) (diacetyl, ethyl acetate, ethyl hexanoate and linalool, Aldrich, Germany) (Table 1) within 3 unflavoured stirred yogurts with different fat contents (0, 2.0 or 4.0% w/w; anhydrous milk fat, Lactalis, Isigny, France) prepared as described by Délérís *et al.* (12) (dry matter: 22.5% w/w; total protein content: 5.4%; sugar: 50g/kg).

Experimental release kinetics of aroma compound from dairy matrices: The release kinetics of aroma compounds from dairy gels were determined at 8°C using a diffusion cell composed of 2 gaseous compartments separated by a product layer (13). The lower gaseous compartment contained a mix of pure molecules and provided a continuous source of aroma compounds. Products were not initially flavoured. The gaseous concentrations of aroma compounds above the product were obtained by regular sampling of the headspace and gas chromatography analysis. Two replicate experiments were performed for each product.

Table 1: Main physicochemical characteristics of the studied aroma compounds.

Compounds	Molecular mass (g/mol)	Hydrophobicity constant $\log P^a$	Air/water partition coefficient $K_{\text{air/water}} \times 10^{-3}$ at infinite dilution (dimensionless, 25°C)	Saturated vapour pressure $P_{\text{sat}, 25^\circ\text{C}}^d$ (Pa)
diacetyl	86.09	-1.34	0.547 ^b	7718.5
ethyl acetate	88.05	0.73	5.48 ^b	12108.1
ethyl hexanoate	144.2	2.83	29.5 ^{b, c}	225.1
linalool	154.2	2.97	0.879 ^b	27.27

^a: $\log P$ = logarithm of the ratio of the compound concentration in octanol and in water, calculated value (EPI, 2000, estimation Programs Interface V3,10: data base). ^b: (Voutsas *et al.*, 2001). ^c: (Athès *et al.*, 2004). ^d: calculated on the basis of the Antoine equation.

Mechanistic modelling: The mechanistic analysis we used is based on chemical engineering principles. Two models were developed.

Model 1 for the determination of apparent diffusion coefficient from release kinetics: a description of main mass transfer phenomena occurring within the compartments of the diffusion cell (upper and lower gaseous compartments and product compartment) was performed. Assuming local thermodynamic equilibrium at the interfaces and mass flux conservation through the interfaces at all times, mass balances for each phase were established, leading to a mathematical description of the system (13). The apparent diffusion coefficient D_P was determined by numerically fitting the mechanistic model to experimental release data using the Levenberg-Marquardt algorithm (least squares curve fitting). Confidence intervals were determined to evaluate the accuracy of the estimated apparent diffusion coefficients.

Model 2 for the prediction of aroma release kinetics taking product composition and structure into account: to go further in the understanding of the involved mechanisms and namely into the role of the fat in aroma release, this mechanistic model considered the product as a biphasic system composed of a continuous aqueous phase in which the lipid phase is dispersed in spherical fat globules (radius R of $0.5 \cdot 10^{-6}$ m). This approach proposed a more realistic and accurate description of mass transfer mechanisms within the system. Model resolution led to the prediction of aroma release kinetic provided that the fat content and the physicochemical properties of aroma compounds within the different phases of the product are known.

Results and Discussion

Comparison of experimental release kinetics with predicted ones. As shown on Figure 1, the predicted release kinetics of (a) ethyl hexanoate from a 2%-fat yogurt and (b) ethyl acetate from both 2% and 4%-fat yogurts were in agreement with

experimental data. Experimental and predicted kinetics had a similar shape whatever the mechanistic model used for calculation. Concerning hydrophobic compounds such as ethyl hexanoate (Figure 1a), the condition for a proper prediction of aroma release with model 2 was that only the liquid fat fraction was considered (36.3% at 8°C, determined by DSC measurements). This condition was not necessary for the prediction of ethyl acetate release (Figure 1b): this result is in agreement with the hydrophilic properties of this aroma compound.

Determination of apparent diffusion properties and effect of fat content. As experimental and predicted release kinetics were equivalent whatever the model, the calculation of diffusion properties from these kinetics using model 1 led to a similar estimation of the apparent diffusion coefficient of aroma compounds within dairy emulsions (Figure 2). Apparent diffusion properties of the studied aroma compounds depended on their physicochemical characteristics: ethyl acetate and diacetyl, which were the most hydrophilic and the smallest molecules, had apparent diffusion coefficients 2 to 12-fold higher than the two others molecules. No effect of fat content was observed on diffusion properties of ethyl acetate and diacetyl. The 3-fold decrease in linalool and ethyl hexanoate diffusion coefficients when fat was added confirmed the preponderant effect of fat on apparent diffusion for the most hydrophobic and the biggest molecules (14). Yet, no additional effect was observed for these molecules when fat content increased from 2 to 4%.

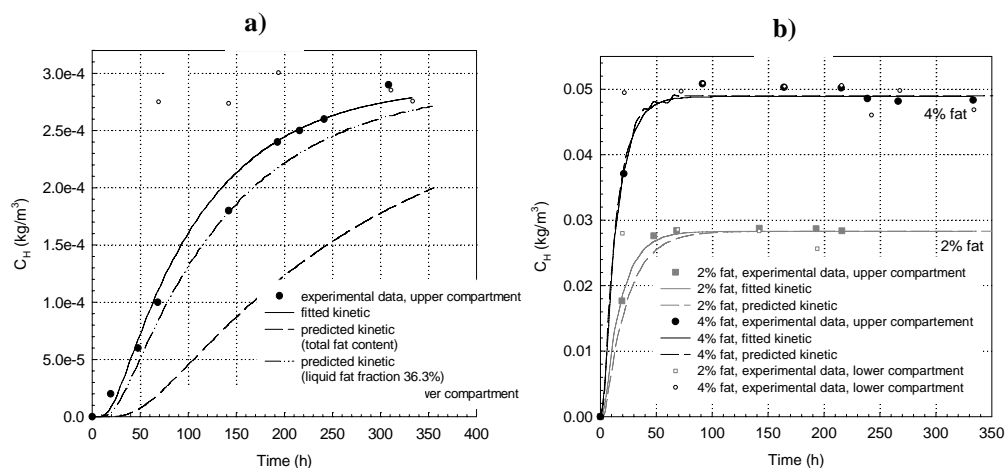


Figure 1. Evolution with time of the headspace concentration C_H (measured by GC-FID in the diffusion cell) at 8°C of **a)** ethyl hexanoate above 2%-fat yogurt and **b)** ethyl acetate above 2% or 4%-fat yogurts. Symbols: experimental gaseous concentration in the upper compartment of the diffusion cell; plain lines: simulated gaseous concentration from model 1 (fitted to experimental data); dashed lines: predicted data from model 2.

Identification of the main parameters influencing aroma release. Beyond the prediction, the interest of such a modelling approach is to evaluate the impact of parameters which can be difficult to modify or to measure experimentally. Thanks to model 2, we highlighted that, except the liquid fat fraction and partition properties between aqueous and lipid phase, parameters related to the lipid phase in the tested range (fat globule size varying from $0.5 \cdot 10^{-9}$ to $0.5 \cdot 10^{-5}$ m and 10-fold modification of the diffusion coefficient within the fat phase) were not limiting for aroma compound transport. Whatever the compounds and the fat content, no concentration gradient existed within fat globules. Thus, the main resistance to mass transfer was probably in the aqueous phase.

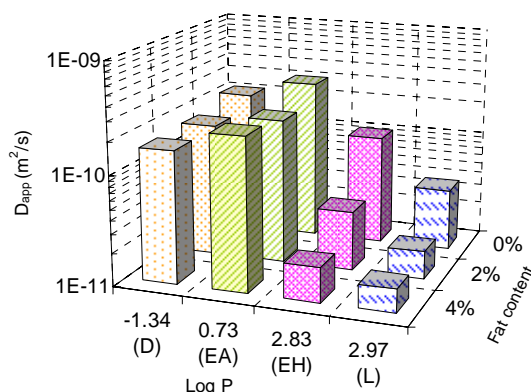


Figure 2. Apparent diffusion coefficients (D_{app}) of diacetyl (D), ethyl acetate (EA), ethyl hexanoate (EH) and linalool (L) in three dairy gels varying in their fat content (0, 2 and 4%) at 8°C. The determination was performed by fitting model 1 parameters to release kinetic.

Model parameters were modified to take the swallowing physiology into account and to get close to what happen in mouth during food eating (product initially flavoured, increase in the product/air volumetric ratio from $4.7 \cdot 10^{-2}$ to 10^{-1} , air/product contact area fixed to $6.6 \cdot 10^{-3} \text{ m}^2$ (pharynx surface) and air flow rate of $4 \cdot 10^{-4} \text{ m}^3 \text{ s}^{-1}$ representing the breath). Simulations, performed on short duration time (30s) highlighted the main effect of the breath flow rate and of the air/product contact area, parameters that depends on physiological conditions. We previously highlighted that the real structure of the product do not have to be necessarily considered to estimate properly apparent diffusion properties of aroma compounds within dairy emulsions. But, simulations illustrated the importance of product structure description to properly predict *in vivo* aroma release (predicted release kinetics were different depending on the way the product structure was described). Some improvements can still be performed, notably concerning the fat globule size and distribution within the aqueous phase, which were considered in this study as homogeneous. This will led to a useful tool to predict aroma release knowing fat content and physicochemical properties in each phase in order to optimise formulation step.

References

1. Landy P., Rogacheva S., Lorient D., Voilley A. (1998) *Coll. Surf. B: Biointerfaces* 12: 57-65.
2. Carey M.E., Asquith T., Linforth R.S.T., Taylor, A.J. (2002). *J. Agric. Food Chem.* 50: 1985-1990.
3. Philippe E., Seuvre A.M., Colas B., Langendorff V., Schippa C., Voilley A. (2003). *J. Agric. Food Chem.* 51: 1393-1398.
4. Rabe S., Krings U., Berger, R.G. (2004) *Food Chem.* 84: 117-125.
5. Meynier A., Lecoq C., Genot C. (2005) *Food Chem.* 93: 153-159.
6. Giroux H.J., Perreault V., Britten M. (2007). *J. Food Sci.* 72: S125-S129.
7. Guichard, E. (2002) *Food Rev. Intern.* 18: 49-70.
8. de Roos K.B. (2006) In *Food Lipids: Chemistry, Flavor and Texture*. ACS symposium series 920, pp. 145-158.
9. Yoon K.A., Burgess D.J. (1998) *J. Pharm. Pharmacol.* 50: 601-610.
10. Kalnin J.R., Kotomin E.A., Maier J. (2002) *J. Phys. Chem. Solids* 63: 449-456.
11. Vitrac O., Hayert M. (2006) *IUFoST 2006*, DOI:10.1051/IUFoST:20060999.
12. Délérís I., Zouid I., Souchon I., Tréléa, I.C. (2009). *J. Food Engin., submitted*.
13. Délérís I., Atlan S., Souchon I., Marin M., Tréléa I.C. (2008) *J. Food Engin.* 85: 232-242.
14. de Roos K.B. (2000) In *Flavor Release - ACS Symposium Series no. 763* (Roberts D, Taylor A.J., eds.), Chapter 11, pp 126-141.

QUANTITATIVE STRUCTURE-PROPERTY RELATIONSHIPS APPROACH OF AROMA COMPOUNDS BEHAVIOUR IN POLYSACCHARIDE GELS

A. TROMELIN^{1,2,3}, Y. Merabtine^{1,2,3}, I. Andriot^{1,2,3}, S. Lubbers^{1,2,3}, and E. Guichard^{1,2,3}

¹ INRA, UMR 1129 FLAVIC, F-21000 Dijon, France

² ENESAD, UMR 1129 FLAVIC, F-21000 Dijon, France

³ Université de Bourgogne, UMR 1129 FLAVIC, F-21000 Dijon, France

Abstract

Pectin and carrageenan are common used thickeners in fat free foods. The aim of this work was to study separately and to compare their respective effects on the aroma release, in order to investigate the nature of involved interactions. In this way, we studied the influence of the chemical structure of 13 aroma compounds on retention/release equilibrium between vapour phase and gels using QSPR tools. Six descriptors are involved in the best obtained QSPR equations, and three of them appeared to play a critical role in the behaviour of aroma compound. Our results put forward the role of polar effects on the retention of odorant molecules in both *iota*-carrageenan and pectin gels, indicating that *iota*-carrageenan polymer do not change the interaction between aroma compounds and water molecules, whereas pectin causes slightly different interaction involving positive charged surfaces areas in the retention phenomenon.

Introduction

The demand for fat free food products is constantly increasing, but the reduction of fat content in a food system induces changes in flavour release (1), flavour perception, appearance, mouth-feel, and structure (2). Fat and flavour are important factors in food acceptance and can affect the partitioning of hydrophobic flavour molecules (3). In order to retain the properties of a product when the fat is removed, fat-substitutes as starch, pectin and carrageenans are used. The retention/release equilibrium has been studied most frequently for inhomogeneous products (4; 5), than for thickeners separately (6). Pectin and carrageenan are common used thickeners, and the aim of this work was to study and to compare their respective effects on aroma release. In this way, the amount of 13 aroma compounds released in the headspace was quantified at equilibrium above pure water, *iota*-carrageenan and pectin gels. To evaluate the influence of the chemical structure of aroma compounds on retention/release equilibrium between vapour phase and gels, we used QSPR approach. QSPR methods attempt to find relationships between the properties of molecules and an experimental response; the assumption is that changes in molecular properties elicit different responses. The QSPR study is intended to represent a physico-chemical property into a simple mathematical relationship, the QSPR equation: $ER = f(p_1, p_2, p_3, \dots, p_n)$.

Our present aim consists first to propose a qualitative interpretation in order to investigate the nature of involved interactions by identifying some relevant structural properties related to the retention.

Experimental

All the flavour compounds used were obtained from Sigma-Aldrich (Saint Quentin Fallavier, France). Purity of flavour compounds was evaluated by GC-FID (> 95 %). *iota*-Carrageenan was kindly supplied by Rhodia Food (Aubervilliers, France). The low-methoxyl and low-amidated pectin 102-AS was purchased from CP Kelco (Denmark). The final aromatized gels are respectively composed of (i) 1 % *iota*-carrageenan, 0.3 % sodium chloride and 15 $\mu\text{L L}^{-1}$ for all aroma compounds in water and (ii) 0.36% pectin and 16 $\mu\text{L L}^{-1}$ for all aroma compounds in water.

The partition coefficient $PC = \frac{[\text{flavour compound}]_{\text{matrix}}}{[\text{flavour compound}]_{\text{vapour}}}$ was determined by PRV method, based on the influence of the volume of the sample on the concentration of volatile in the headspace (7). They established the following Eq. (1):

$$\frac{1}{A} = \frac{1}{f_i \times C_M} \times (PC + \beta) \quad \text{Eq. (1)}$$

where A is the chromatographic peak area at equilibrium, f_i is the proportional factor, C_M is the initial sample concentration in the matrix and β is the ratio $V_{\text{vapour}}/V_{\text{matrix}}$. High phase ratio β were used, from 207 to 3.16; each matrix was analysed in triplicate. Headspace analysis was performed after equilibration at 30 °C for at least 2 h 30 on a Trace (Thermoelectron, France) gas chromatograph using a flame ionization detector (FID), and the data were processed using software developed in our laboratory (8; 9).

The retention constant (K_{ret}) by the matrix is defined with the following Eq. (2) (10):

$$K_{\text{ret}} = \frac{[\text{flavour compound}]_{\text{matrix}} / 1}{[\text{flavour compound}]_{\text{vapour}} \times R \times T / 1} = \frac{[\text{flavour compound}]_{\text{matrix}}}{[\text{flavour compound}]_{\text{vapour}} \times RT} \quad \text{Eq. (2)}$$

where R is the perfect gas constant and T the temperature (K), and $K_{\text{ret-water}}$, $K_{\text{ret-GC}}$ and $K_{\text{ret-GP}}$ express the retention constant of flavour compounds between water solution, *iota*-carrageenan and pectin gels respectively; $\log K_{\text{ret}}$ values were used for regression calculations.

The three-dimensional molecular structures of the 13 aroma compounds were calculated using DS Viewer Pro 6.0 (Accelrys Inc.). The structures were then analysed with Cerius2 software (version 4.10; Accelrys Inc., San Diego, 2005) running on a Silicon Graphics workstation (SGI-O2). The equation generation was performed by GA statistical method available in Cerius2 package (10). Reliability and significance of the equations was estimated by r^2 CV- r^2 and Bootstrap- r^2 values. For equations obtained with 3 independent variables, validation was carried out by Y-randomization at 95% confidence level (19 randomized trials) and by means of a leave-one-out method.

Results and Discussion

The values of retention constant obtained for the different flavour compounds are reported in (Figure 3). Globally the retention constants are quite similar for water (W), *iota*-carrageenan (CG) and pectin (PG) gels. We found that the most retained compounds are aldehydes and ketones, and the most released in vapour phase are esters. However, ethyl *trans*-2-butenoate is more retained than 2-ethylbutanal,

showing that the whole structure has a greater importance than only the chemical function.

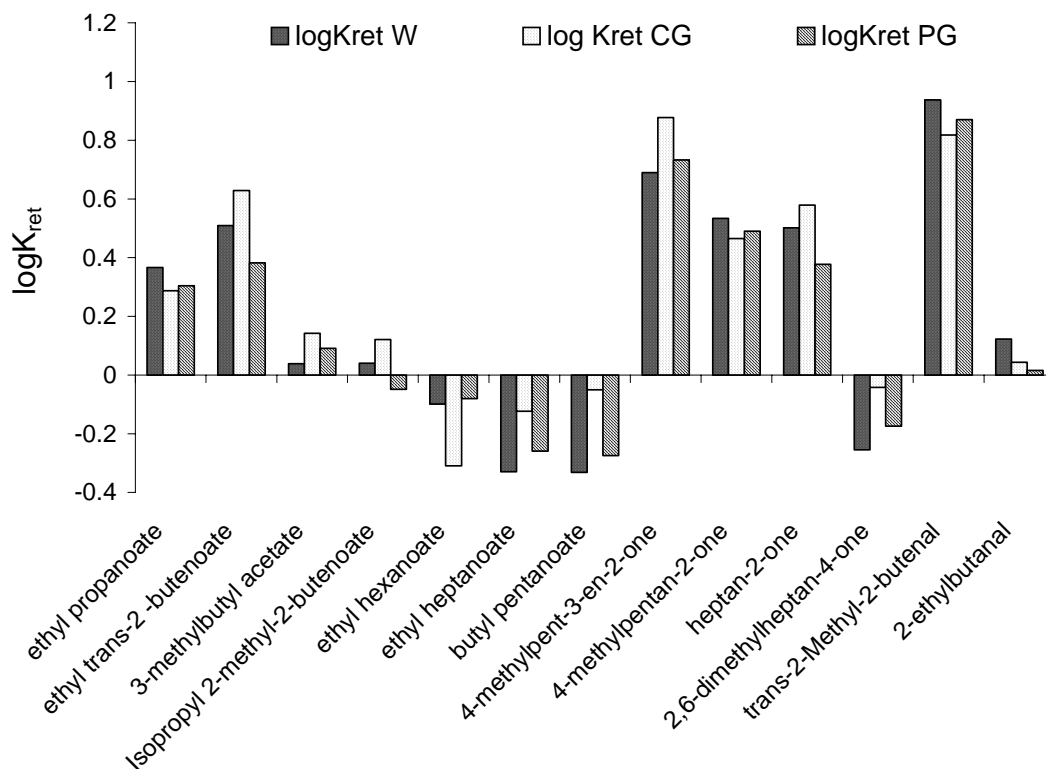


Figure 3. $\log K_{ret}$ values for the 13 aroma compounds.

Starting from descriptors belonging to the classical groups of descriptors (conformational, electronic, spatial, structural, thermodynamic and topological descriptors) and on the basis of the highest correlation with the property and the lowest between descriptors, we retained 10 descriptors to be used in the equation generation. All reported equations are generated without constant adding and the best obtained equations are reported in Table 2.

Table 2. Best obtained equations with 2 factors eqs. 3 to 5 and with 3 factors eqs. 6 to 8.

Eq	logK _{ret}	Factor 1	Factor 2	Factor 3	r ²	F	CV-r ²	BS-r ²
3	water	+ 0.015881 Jurs-WNSA-2	+ 0.01691 Jurs-PNSA-1		0.88	77	0.82	0.88
4	CG	+ 0.01285 Jurs-WNSA-2	+ 0.01523 Jurs-PNSA-1		0.74	29	0.67	0.79
5	PG	+ 3.80674 Jurs-RPSA	- 0.587947 CHI-V-3_P		0.87	71	0.76	0.87
6	water	+ 0.017198 Jurs-PNSA-1	- 0.192219 CHI-V-3_P	+ 0.012865 Jurs-WNSA-2	0.89	41	0.75	0.89
7	CG	+ 0.033951 Jurs-PNSA-1	+ 12.1295 Jurs-FNSA-3	+ 0.016598 Jurs-WNSA-2	0.81	22	0.67	0.82
8	PG	- 0.127817 Jurs-FPSA-2	- 0.367312 CHI-V-3_P	+ 3.94632 Jurs-RPSA	0.85	36	0.56	0.896

Meaning of the descriptors used in equations are reported in the Handbook of Molecular Descriptors (11). We found that Jurs-PNSA-1 and Jurs-WNSA-2 are involved in the two-variables equations obtained for both $\log K_{\text{ret}}\text{-W}$ and $\log K_{\text{ret}}\text{-CG}$. For Jurs-WNSA-2 value, the total solvent accessible surface area value weights the partial negative surface area; Jurs-WNSA-2 values are minimum for small molecules with small negative charged surface area (small aldehydes), and maximum for large molecules with large negative surface areas (large esters). In the three-variable equations, CHI-V-3_P and Jurs-FNSA-3 descriptors are added for $\log K_{\text{ret}}\text{ W}$ and $\log K_{\text{ret}}\text{ CG}$ respectively. The use of Jurs-FNSA-3 in $\log K_{\text{ret}}\text{-CG}$ equation should suggest that interactions with carrageenan gel are more sensible to negative charges.

The three descriptors involved in $\log K_{\text{ret}}\text{-PG}$ 3 variables equation are Jurs-RPSA, CHI-V-3_P and Jurs-FPSA-2. The best equation obtained with 2 variables involves Jurs-RPSA, CHI-V-3_P. Jurs-RPSA involves solvent-accessible polar surfaces areas of atoms with absolute value of partial charges greater or equal to 0.2, which represents both negatively and positively charged surfaces areas. Sign of Jurs-RPSA is positive in the $\log K_{\text{ret}}\text{-PG}$ equation, that suggest that both negatively and positively charged surfaces areas are involved in the retention interaction. The sign negative of terms CHI-V-3_P and Jurs-FPSA-2 in the 3 variable equations allows modulating the attractive effect by taking into account the repulsive effect due to carbon chain.

To conclude, we observed that *iota*-carrageenan polymer do not change the interaction of aroma compounds with water molecules, whereas pectin causes slightly different interaction involving positive charged surfaces areas in the retention phenomenon. Our results highlight the role of polar effects on the retention of odorant molecules and put forward that retention/release properties are not determined by the chemical classes, but by some chemical properties together. In this way, QSPR approach constitutes a promising tool for the characterisation of interactions involved in complex food matrices.

References

1. Forss D.A. (1969) *J. Agric. Food Chem.* 17: 681-85.
2. Wendin K., Solheim R., Alimere T., Johansson L. (1997) *Food. Qual. Prefer.* 8: 281-291.
3. Guichard E. (2002) *Food Rev. Int.* 18: 49-70.
4. De Roos K. (2003) *Int. Dairy J.* 13: 593-605.
5. Lubbers S., Decourcelle N., Martinez D., Guichard E., Tromelin A. (2007) *J. Agric. Food Chem.* 55: 4835-4841.
6. Hansson A., Leufven A., Pehrson K.B.S. (2002) *J. Agric. Food Chem.* 50: 3803-3809.
7. Ettre L.S., Kolb B. (1991) *Chromatographia* 32: 5-12.
8. Almanza R., Mielle P. (1990) *Deuxième journée de la mesure INRA*, Port-Leucate (FRA).
9. Almanza R., Couton Y., Mielle P., Nicolardot B. (1989) *Cahiers techniques de l'INRA* 20: 49-56.
10. Rogers D., Hopfinger A.J. (1994) *J. Chem. Inform. Comp. Sci.* 34: 854-866.
11. Todeschini R., Consonni V. (2000) In *Methods and Principles in Medicinal Chemistry* (Mannhold R., Kubinyi H., Timmerman H., eds.), Chapter 11, Wiley-VCH, Weinheim.

RETENTION AND RELEASE OF CARVACROL USED AS ANTIMICROBIAL AGENT INTO SOY PROTEINS MATRIX BASED ACTIVE PACKAGING

P. CHALIER, A. Ben Arfa, V. Guillard, and N. Gontard

UMR IATE, cc 023 Université Montpellier II; Pl. E. Bataillon, 34095 Montpellier cedex 5, France

Abstract

In this work, an antimicrobial paper packaging was designed by introducing carvacrol as antimicrobial agent into a soy protein matrix used as coated matrix of paper. The ability of the soy proteins matrix to retain carvacrol added at different ratio (10%, 30%, 60% w/w) was evaluated by measuring the aroma compound losses after process. The losses varied between 12 and 30% depending on the carvacrol load. The ability of the soy protein to release carvacrol was studied as a function of relative humidity (60, 80 and 100%) for three temperatures 5, 20 and 30°C. Increasing RH and temperature clearly increased carvacrol release. At 30°C and 100% RH, the total amount of carvacrol was released after 2 days of storage. Kinetic release could be modelled by second Fick's law and diffusivity coefficients evaluated. The control of relative humidity and temperature associated with high retention ability of soy proteins permits to limit the losses of antimicrobial agent during process and storage in adapted conditions and to favour the release of carvacrol in conditions of microbial growth, i.e. high temperature and relative humidity.

Introduction

Nowadays, there is an increasing interest in the possible use of aroma compounds to prevent microbial growth in the food items (1). The use of antimicrobial packaging appears as a promising way preventing microbial growth by the controlled release of an active agent and lowering its concentration in the product (2). Aroma compounds as volatile antimicrobial agents can act through the intra packaging atmosphere without direct contact with food product. In this purpose, an antimicrobial paper packaging was designed by introducing, as antimicrobial agent, an aroma compound into a soy protein solution used as the coated matrix of paper. Carvacrol, the major aroma compound of Oregano essential oil and an efficient inhibitor against a wide spectrum of micro-organisms (3) was selected to be incorporated into the soy proteins matrix based active packaging. The release rate of the volatile agent from the packaging system is an important parameter to control the antimicrobial efficiency. The present work aimed at studying the potentiality of soy proteins matrix to retain and to release carvacrol in controlled conditions of temperature and relative humidity.

Experimental

Preparation of carvacrol/SPI coated paper. Soy Proteins Isolates coated papers were prepared by the procedure previously described (4). SPI (10% w/v) from Seah

International, having 91.8 % proteins content, were dissolved in distilled water heated at 50°C by continuously stirring for 30 min at 500 rpm. Carvacrol (Sigma Aldrich) was added at a percentage of 10, 30 or 60% (w/w of SPI). Homogenisation was carried out with an Ultra-Turrax (T-25, IKA Labortechnik, Germany) at 8000 rpm for 10 min. The coating process was performed at 25°C: a support paper (provided by “Ahlstrom Research and Services”) was maintained on a perforated iron plate under partial vacuum and the coating solution was applied by an adjustable micrometer thin layer chromatography applicator. Then, coated papers were dried for 3 hours at $23 \pm 2^\circ\text{C}$ and at $50 \pm 5\%$ RH.

Kinetic release of carvacrol from SPI coated papers. Pieces of coated papers (3 cm x 3 cm) were put on tray in a controlled temperature incubator at the selected temperature and relative humidity. The incubator was maintained at the following temperatures: 30°C, 20°C, 5°C and for each temperature, the relative humidity (60%, 80% and 100%) were adjusted by humidified air and by the presence of saturated salts solutions. At prescribed time intervals, pieces of coated papers were removed for carvacrol extraction by water and n-pentane mixture (50/50 v/v). After internal standard addition (2-nonanol), the solution was shaken for 16 hours under magnetic agitation (300 min^{-1}). The removed organic phase was analysed by gas chromatography. Quantification of carvacrol was performed using the internal standard method and after extraction yield estimation ($87\% \pm 5\%$). For each condition, time, temperature and RH, the extraction was done in triplicate from two different coated papers.

Results

Carvacrol retention by SPI matrix after process. Retention of the antimicrobial compound by matrix is one of the most important features of the coating process. It depends on the total compound amount retained in the coating matrices after drying (at ambient temperature) compared to the initial compound quantity introduced in the coating solutions. Carvacrol retention was determined for different ratio of aroma compound/protein (10, 30, 60 % w/w) and losses ranged between 12 and 30% depending on the carvacrol load (Figure 1).

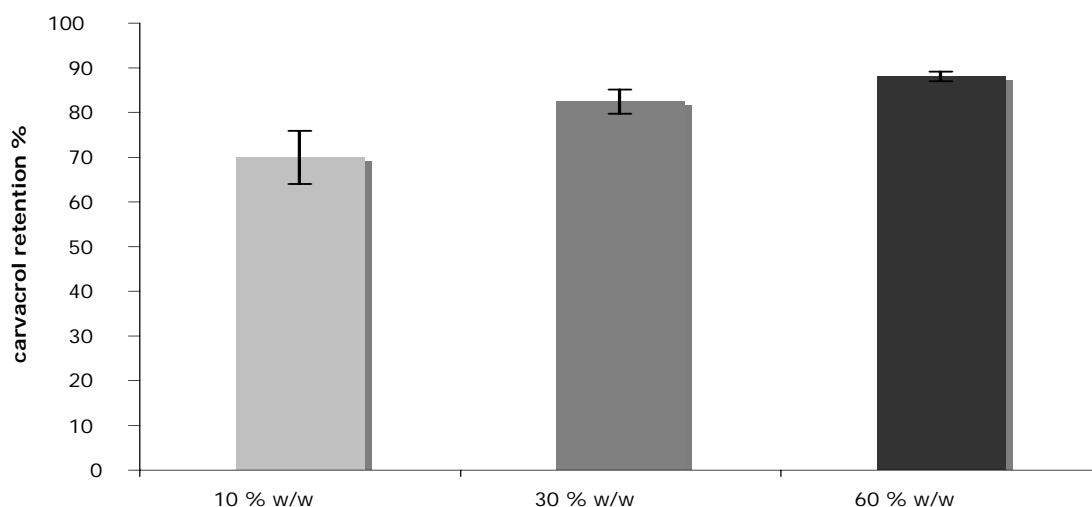


Figure 1. Effect of Carvacrol/SPI ratio on carvacrol retention by SPI matrix.

Weak losses were obtained for the highest carvacrol concentration showing the high ability of SPI matrix to retain carvacrol. The unexpected highest losses observed for the lowest 10% initial carvacrol concentration could be explained by the development of an important air/solution interface on the surface of the thin coating layer due to the foaming properties of soy protein, favouring the migration toward the surface of carvacrol. This amount, independently to the initial load, might easily be eliminated during the drying step. The hydrophobic nature of carvacrol with a $\log P$ of 3.52 suggested that hydrophobic interactions were preferentially involved. Soy proteins and particularly 11S globulin exhibit high capacity of retention for lipophilic molecules due to its specific quaternary structure characterised by hydrophobic cavity (5).

Carvacrol release from SPI matrix in controlled conditions. Carvacrol release from coated papers as a function of time was determined at 60, 80 and 100% of relative humidity (RH) and for three temperatures 5°C, 20°C and 30°C. Results are reported in Figure 2 (A, B, C).

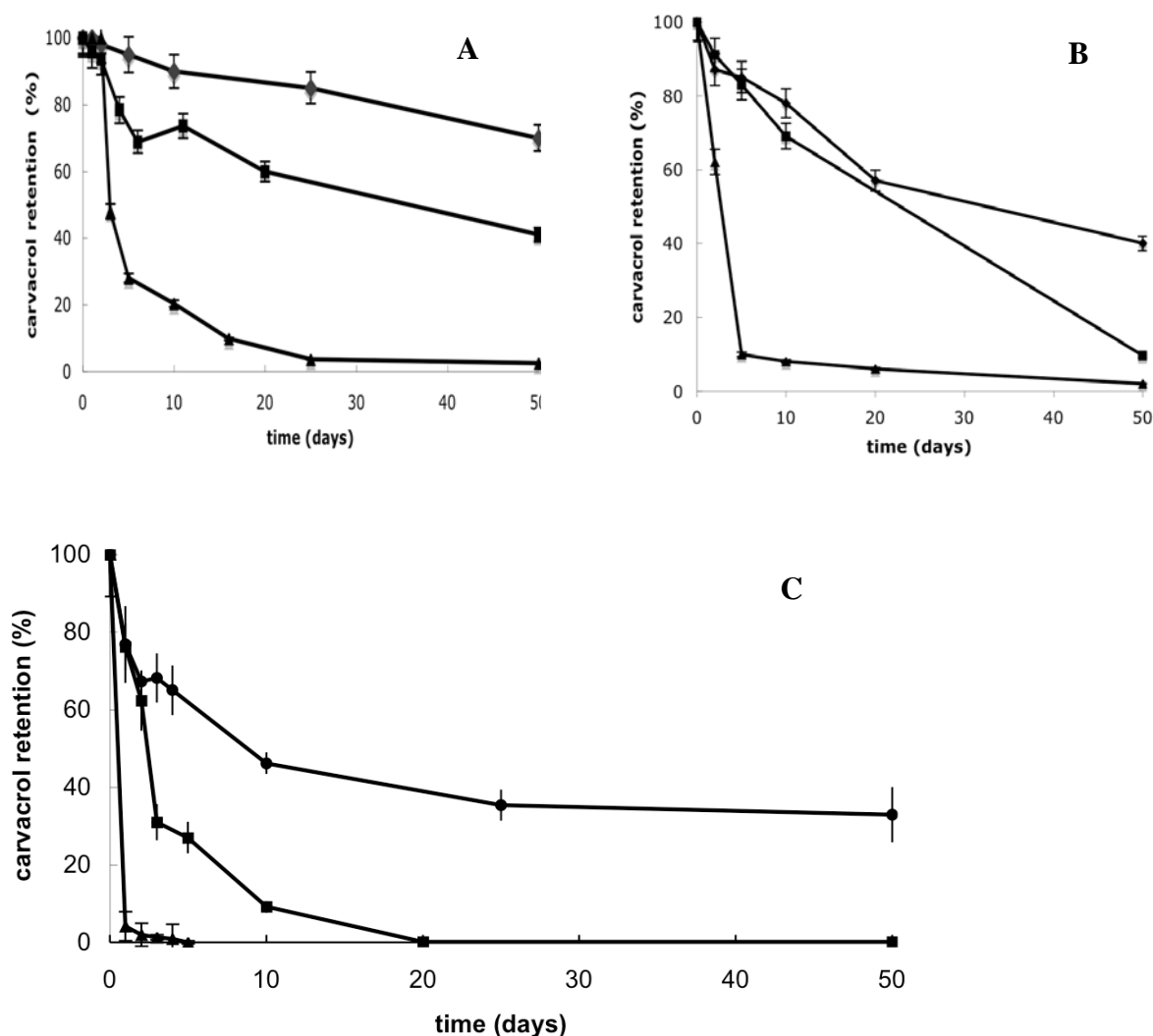


Figure 2. Kinetic of carvacrol release at different relative humidity (ν) 60%RH, (ν) 80% RH, (σ) 100 % RH and at **A**) 5°C, **B**) 20°C and **C**) 30°C.

When the SPI coated papers were stored at 5°C, 20°C or 30°C, carvacrol release clearly increased with the RH.

While after 50 days of storage at 5°C and 60% RH, the residual carvacrol in the matrix was about 75% of the quantity present at the beginning of the storage (Figure 2A), at 30°C and 100% RH carvacrol release was total within 1 day (Figure 2C). For a given relative humidity, the increase of temperature acted by fastening the carvacrol release from the coated paper.

Modelling of release kinetic using the Fick's second law can be realized to characterize the carvacrol transfer by diffusion coefficients. At 5°C and 60% RH, the value of diffusivity was found equal to $0.11 \cdot 10^{-16} \text{ m}^2 \text{ s}^{-1}$ while at 30°C and 100% RH, diffusivity was 100 times higher with a value of $138 \cdot 10^{-16} \text{ m}^2 \text{ s}^{-1}$. From the results, it can be concluded that the storage of coated papers at 5°C and 60% could be suitable to avoid losses of carvacrol. In contrast, a high release of carvacrol from SPI matrix occurs at the current micro-organism's growth conditions, i.e. at high temperature and relative humidity.

SPI matrix is promising as antimicrobial delivered support due to its high carvacrol retention ability and to its temperature and relative humidity reactivity permitting the controlled release of carvacrol, an efficient antimicrobial agent.

References

1. Burt S., (2004) *Intern. J. Food Microbiol.* 94: 223-253.
2. Appendini P., Hotchkiss J. H. (2002) *J. Appl. Polymer Sci.* 3: 113-126.
3. Ben Arfa A., Combes S., Preziosi-Belloy L., Gontard N., Chalier P. (2006) *Lett. Appl. Microbiol.* 43: 149-154.
4. Ben Arfa A., Chalier P., Preziosi-Belloy L., Gontard N. (2007) *J. Agric. Food Chem.* 55: 2155-2162.
5. Semenova M.G., Antipova A.S., Wasserman L.A., Misharina T.A., Golovnya (2002) *Food Hydrocol.* 16: 565-571.

INFLUENCE OF ETHANOL ON AROMA COMPOUNDS SORPTION INTO A POLYETHYLENE FILM

A. Peychès-Bach¹, M. Moutounet¹, S. Peyron², and P. CHALIER²

¹ UMR SPO, INRA, 2 pl Viala, 34060 Montpellier cedex 01, France

² UMR IATE, Université Montpellier II, cc 023; Pl. E. Bataillon, 34095 Montpellier cedex 05, France

Abstract

The effect of ethyl alcohol concentration on four aroma compounds sorption into a Polyethylene film was studied using partition coefficients ($K_{\text{polymer/solution}}$) determination. In aqueous solution without ethanol, a high sorption of hydrophobic esters (ethyl butanoate and hexanoate) into the apolar PE film was observed while the phenolic compounds, with high solubility in water, were weakly sorbed. Excepted for 4-ethyl phenol, sorption into the PE film was lower in the presence of ethanol than in water. The concentration of ethanol and the interactions between the matrix and each aroma compound appeared to influence the scalping rates. Moreover, higher partition coefficients, i.e. higher affinity for the PE was obtained when the aroma compounds were present in mixture comparatively to the flavour compound alone.

Introduction

Due to their good water and oxygen barrier properties, plastic materials are commonly used for food packaging. However, they can interact with the food itself, and particularly with aroma compounds causing the rejection of the product by consumers. Polyethylene (PE) film, which is one of the most common type food contact packaging, sorbs a wide range of flavour compounds (1-2) leading to an unbalanced aromatic profile (scalping). The interactions of aroma compounds with plastic films are more complex than interactions between packaging and gases or water molecules. Indeed, the aroma compounds characteristics, the properties of the polymer, the environmental conditions and the composition and structure of food matrices have an effect on the sorption and the transfer of aroma compounds (3).

For alcoholic beverages, the concentration of ethanol could influence the sorption phenomena. Hence, this work focused on the effect of ethanol concentration on the sorption of four aroma compounds into a PE film. The impact of the presence of other aroma compounds on the sorption behaviour was studied by comparing the sorption of each individual compound with that in mixture.

Experimental

Sorption experiment. The PE film was a commercial film with a thickness of 50 μm . Aroma compounds, ethyl butanoate (MW 116.16, $\log P= 1.9$), ethyl hexanoate (MW 144.21, $\log P= 2.8$), 4-ethyl phenol (MW 122.16, $\log P= 1.6$) and 2-phenyl ethyl alcohol (MW 122.16, $\log P= 2.6$) were purchased from Sigma-Aldrich and Fluka. The sorption of aroma compounds has been investigated in acidified water ($\text{pH}= 3.5$) and in acidified hydro-alcoholic solutions ($\text{pH}= 3.5$) with different concentrations of ethyl

alcohol: 10%, 12% and 15% (v/v). The concentration of the aroma compound in the solution was 40 ppm for 2-phenyl ethyl alcohol and 1 ppm for ethyl butanoate, ethyl hexanoate and 4-ethyl phenol respectively. Small pieces of film (9 cm²) were immersed in the different solutions containing the aroma compounds in mixture or alone. The experiments were realised in triplicate at 25°C, during 21 days. For this time, a constant amount of each volatile compound was reached and sorption coefficients (g m⁻³) could be determined.

Aroma extraction and K determination. The aroma compound amounts absorbed into the film were extracted using dichloromethane during 16h at 500 rpm. Internal standard was added to the organic phase and quantification was performed by gas chromatography analysis. The results were expressed by calculating the partition coefficients $K_{PE/solution}$ between material and solution. K is defined as the aroma compound concentration into the PE film in g m⁻³ related to the residual aroma compound concentration in g m⁻³ of the solution. The residual concentration was deducted by subtracting the amount absorbed into the film to the initial amount of aroma compound in solution at the beginning of experiment. The higher K was, the higher sorption in PE was.

Results

Partition coefficients in water. First, the partition coefficients of each aroma compound were determined when the PE was in contact of the mixture of compounds in acidified water (Table 1).

Table 1. Partition coefficients ($K_{PE/solution}$) of ethyl butanoate, ethyl hexanoate and phenyl-2-ethyl alcohol in water.

Aroma compound	Ethyl butanoate	Ethyl hexanoate	2- Phenyl-ethyl alcohol
$K_{PE/water}$	1158 ± 172	3769 ± 360	0.71 ± 0.07

The sorption of 4-ethyl phenol into PE was not detected and the sorption of 2-phenyl ethanol was very weak despite a concentration 40 times higher than 4-ethyl phenol. In contrast, the sorption of esters into PE was strong and particularly for the most apolar ester according to the apolar nature of the film. These results clearly showed the affinity of esters for PE comparatively to phenolic compounds in relation to their high water solubility.

Influence of ethanol concentration. In ethyl alcohol solutions, the sorption of 2-phenyl ethyl alcohol into PE film was not detected in spite of its high concentration. It may be due to its relative polar nature and its greater affinity for hydro alcoholic solution than for the PE film. In contrast, 4-ethyl phenol which was more apolar (logP= 2.6) than 2-phenyl ethanol (logP= 1.6), was highly sorbed by the PE film. Excepted for 4-ethyl phenol, sorption into the PE film was lower in the hydro-alcoholic solutions than in water (Figure 1). The presence of ethyl alcohol is known to favour the solubility of aroma compounds but the gain in solubility is function of the aroma compound. It was shown that for 4-ethyl phenol, the solubility was unchanged (4). It could be suggested that ethyl alcohol acted as a carrier in the sorption phenomena of 4-ethyl phenol. This hypothesis was confirmed by its increased sorption with the ethyl alcohol concentration and by the high sorption of ethanol (30Kg m⁻³) into the film.

For ethyl butanoate as for 4-ethyl phenol, maximal sorption was observed at 15% (v/v) of ethyl alcohol in solution. For ethyl hexanoate the maximal sorption was reached for 10% (v/v) ethanol solution. Subsequently, the sorption strikingly decreased. Fukamachi *et al.* (5) found partition coefficient values for ethyl butanoate and ethyl hexanoate in LDPE film equal to 2.1 and 30 respectively, i.e. inferior to the values obtained in this study, due certainly to different experimental procedure (20°C against 25°C) and PE physical characteristic. However, similar sorption behaviour was observed with a maximal sorption detected at 5%-10% (v/v) for ethyl hexanoate and followed by a decrease and the highest sorption for the most apolar ester. It is known that for a chemical family, the sorption in apolar films is the highest for the most hydrophobic compound. However, the impact of hydrophobicity was not relevant when ethyl hexanoate (log P= 2.8) sorption was compared to that of 4-ethyl phenol (log P= 2.6), leading to suppose the influence of chemical aroma nature in the sorption phenomena.

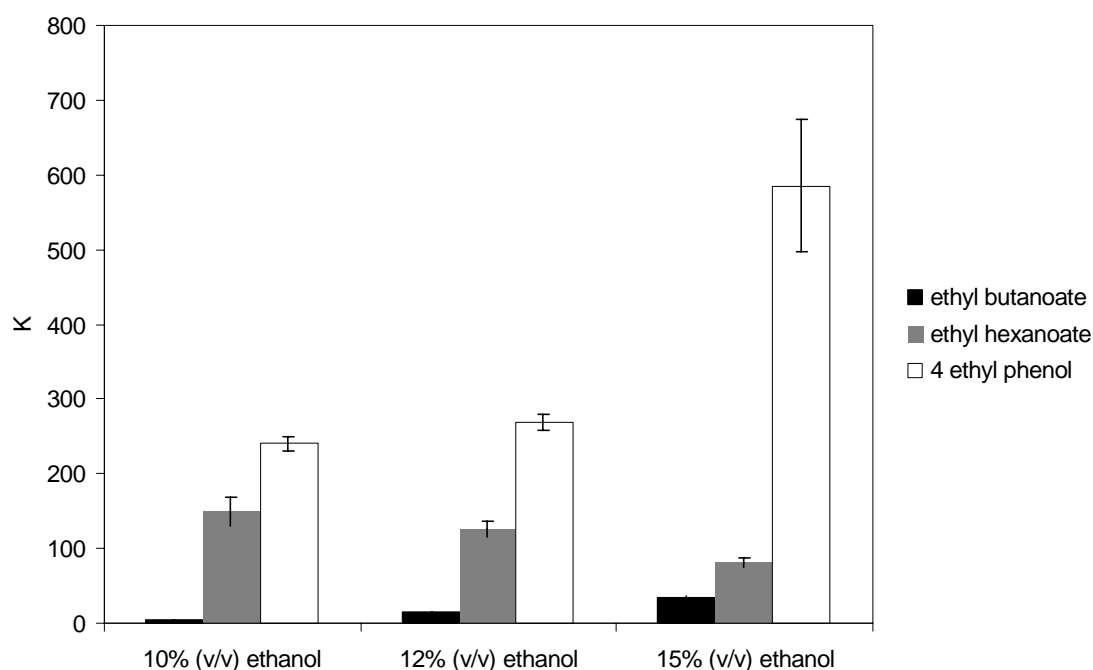


Figure 1. Partition coefficients ($K_{PE/solution}$) of ethyl butanoate, ethyl hexanoate and 4-ethyl phenol as a function of ethanol concentration.

Influence of the presence of other aroma compounds on PE sorption. Partition coefficients of aroma compounds obtained when they were in mixture, were compared to partition coefficients obtained when each aroma compound was alone, both in 12% (v/v) ethanol solution (Figure 2). As previously observed, 2-phenyl ethyl alcohol was not detected into the PE film. The sorption of ethyl butanoate was weakly modified. In contrast, for the most apolar compounds - ethyl hexanoate and 4-ethyl phenol - partition coefficients were found ~2 and 21 times respectively lower than when the aroma compounds were in mixture. This surprising behaviour could be explained by a stimulant effect of the other aroma compound favouring the sorption into the PE films.

Aroma compounds sorption was strongly affected by the presence of ethanol in solution but also by the presence of other aroma compounds. The sorption of aroma compound in PE film was not easily predictable since parameters other than polarity

and chemical nature must be taken account such as interactions with matrix and competition between aroma compounds.

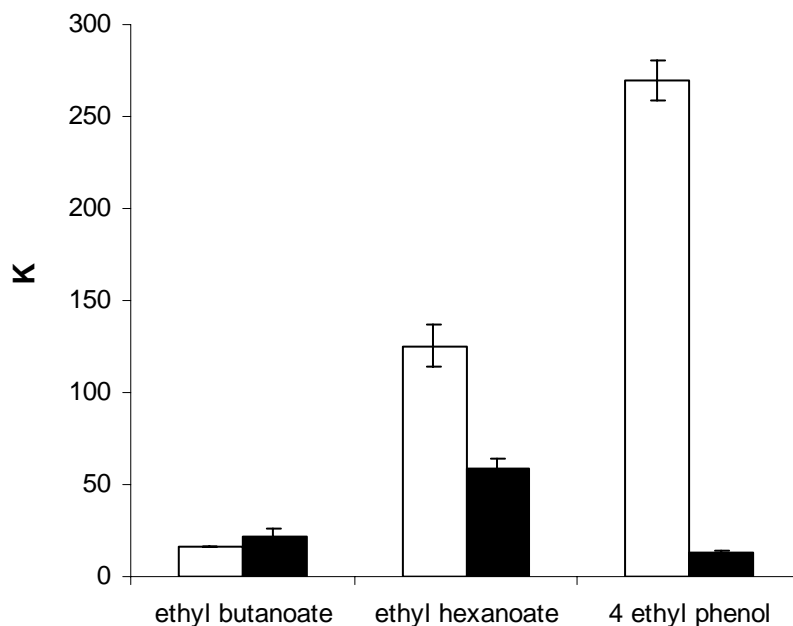


Figure 2. Partition coefficients K (PE/12% (v/v) ethanol solution) of ethyl butanoate, ethyl hexanoate and 4-ethyl phenol present in mixture (empty bar) or alone (full bar) in the hydro-alcoholic solution.

References

1. Johansson F., Leufven A. (1994) *J. Food Sci.* 59: 1328-1331.
2. Sajilata M.G., Savitha K., Singhal R.S., Kanetkar V.R. (2007) *Compreh. Rev. Food Sci. Food Safety* 6: 17-35.
3. Dury-Brun C., Chalier P., Desobry S., Voilley A. (2007) *Food Rev. Int.*, 23: 199-225.
4. Barrera-Garcia V.D., Gougeon R.D., Voilley A., Chassagne D. (2006) *J. Agric. Food Chem.* 54: 3982-3989.
5. Fukamachi M., Matsui T., Hwang Y.-H., Shimoda M., Osajima Y. (1996) *J. Agric. Food Chem.* 44: 2810-2813.

Section 5

Flavour Quality, Changes Upon Storage and Off-flavours

QUALITY: AN IMPORTANT TOPIC IN THE COMPLEX WORLD OF FLAVOURINGS

G.E. KRAMMER, F.-J. Hammerschmidt, G. Lösing, J. Förstner, L. Meier, J. Osthaus, B. Weckerle, C.O. Schmidt, S. Trautzsch, B. Weber, S. Brennecke, and R. Wittlake

Symrise GmbH & Co. KG, Flavor & Nutrition, Research & Innovation, P.O. Box 1253, D-37601 Holzminden, Germany

Abstract

Quality is the important topic in the complex world of flavourings. Increasing food safety standards, together with increasing food ethical requirements and massive changes in supply chain structures lead to a strong need for smart tools like a comprehensive analytical toolbox, rapid and robust methods and a systematic link of analytical methods, which is described in this publication. A new approach to global specifications supports the link of product properties and analytical methods and builds the basis for future challenges like contaminants from bio-magnification or nano-scale materials in food.

Introduction

The world of flavouring substances is becoming more and more complex. In the early days people used aromatic products like fruit juices or fruit juice concentrates which were relatively weak and still close to the related foodstuff. Later, with more knowledge of separation techniques, infusions, extracts, oleoresins and absolues ranging from weak to strong impact were used to impart aroma. Essential oils such as spice oils already have a very strong impact. Improved analytical technologies allowed the evaluation of the chemical compositions of extracts and essential oils, so that isolates either as powerful mixtures or even as single compounds could be obtained. Modern receptor research and converging scientific dynamics between chemistry, biology and medicine led to development of flavouring substances with flavour modifying properties, which recently found consideration in the codex definition of flavourings: "Flavourings are products that are added to food to impart, modify or enhance the flavor of food" (CCFA 39th Session in April 2007) (1). The quality of food and flavourings is built on the conformance to legal, technology related and business requirements. In the last years more and more the area of food ethical compliance referring to kosher, halal, vegetarian or organic is gaining importance. Especially for flavourings the quality of organoleptic properties and sensory are of highest importance and strongly support the understanding that quality is not negotiable.

Sensory

Sensory is the most important product property of flavourings and at the same time comprises a set of criteria, which are very difficult to be measured and monitored. Therefore a broad set of established testing methods has been developed to identify deviations of profiles, compare intensities and understand statistical correlations. On

the scientific side the integration of aroma and taste thresholds are the basis of the odour activity value concept (OAV) and the corresponding taste activity value concept (TAV). In addition the combination of human nose and tongue with modern separation technologies led to powerful tools for the evaluation of aroma and taste compounds from mixtures (GC-O, LC Taste[®]). These technologies require time and highly trained specialists. Therefore we still see a major difference between sensory testing methods applied in flavour research and modern QC, which is in many cases based on detailed in/out tests (Figure 1).

The standardization of natural flavouring complexes like recovery flavours from fruits implicates high level requirements for the sensorial and instrumental analysis and in addition also for the correlation of analytical and sensorial data (2), in order to ensure that the pattern of selected aroma substances is relevant of the sensorial quality of a product such as apple juice from concentrate. According to Annex 1 Nr. 1b of the European Fruit Juice Directive (3) juices from concentrate have to show the same organoleptic and analytical properties like direct juice. For direct juice from apples major variations because of origin, variety, seasonal changes and harvest conditions are leading to a highly complex data space. This situation is illustrated in (Figure 2), which shows flavour profiles of 16 direct juice qualities from apple sharing the strong variation of key ingredients like ethyl butyrate and 2(E)-hexenal in comparison to the described sensory profile. Therefore the quality assessment of this product category should be based on sensory supported by analytical measurements.

Stability

Modern food industry is confronted with the consumers' increased requirements concerning color, flavor, texture and sensory stability. This requires extensive knowledge in various fields, *i.e.*

- processing properties of the flavor
- the behavior of the flavor during the production of the food
- and the behavior of the flavor during the shelf-life of the food
- the interactions of flavor and foodstuff plus packaging

Apart from simple handling and easy dosage, a constant high-level product quality and a guaranteed shelf-life is absolutely essential. The stability of a food product is affected by a multiplicity of factors like process temperature and time, residual moisture, degree of browning, the physical and chemical constitution of ingredients. A further factor of crucial importance is the type and the quality of the packaging material (4). The execution of real time stability tests is essential for control purposes in the food industry. Storage conditions have to be adapted as realistically as possible based on the following criteria:

- original packaging, temperature and light conditions
- transport, storage and handling influences

In addition accelerated shelf-life testing helps to indicate possible degradation or interaction reactions (5). Figure 3 provides a condensed overview about possibilities between flavoring substances on one side and flavoring substances and the food matrix on the other side (6).

A good example for flavour food matrix interaction is given by the application of a cream flavour on an instant cappuccino drink base, which resulted in a strong off-

note formation during storage. The off-note was described as “green banana, tropical fruit-like“. Analyses via Solid Phase Micro Extraction (SPME) using GC/MS for the comparison of the volatile components of a fresh reference sample vs. a stored sample revealed the formation of trimethyloxazol, a compound with a strong green-fruity note. A detailed investigation of the reaction mechanism showed that diacetyl originating from the flavouring reacted with alanine from milk powder to yield trimethyloxazol (Figure 4), which was perceived as an off flavour.

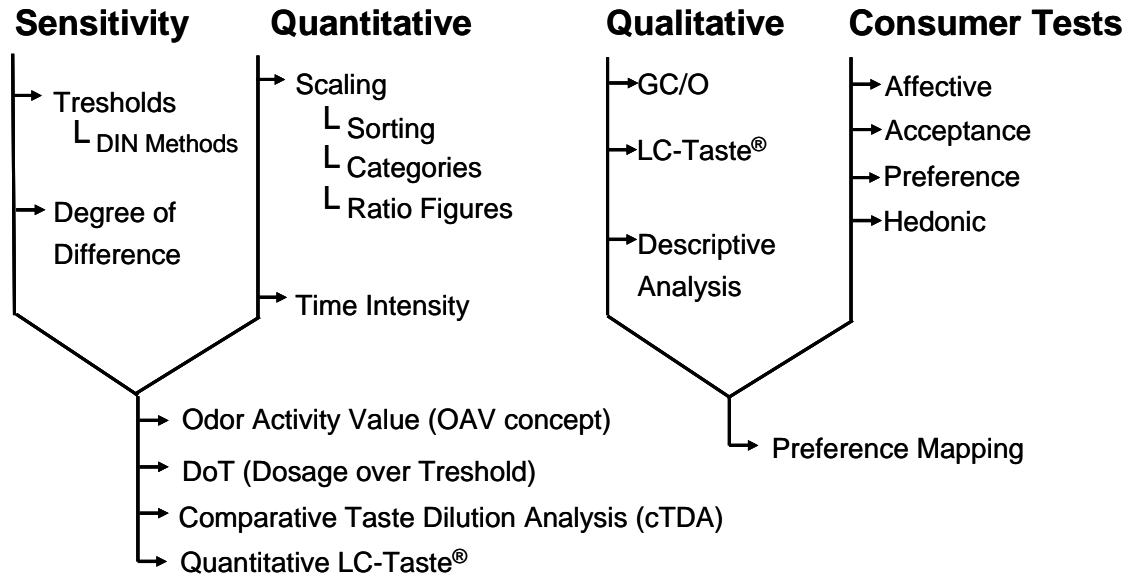


Figure 1. Overview of sensory testing methods including the coupling of liquid chromatography with on-line taste analysis (LC Taste®), taste dilution analysis (TDA) and qualitative descriptive analysis (QDA).

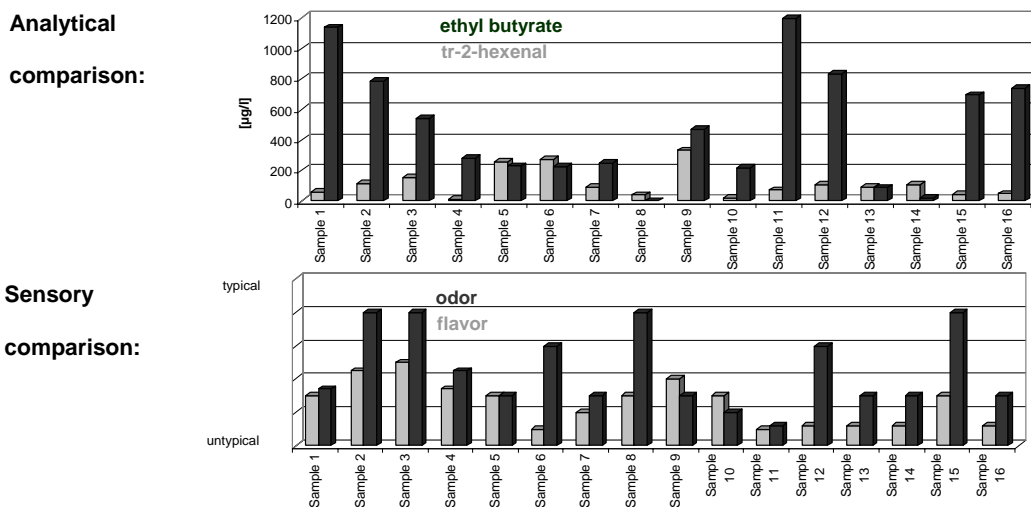


Figure 2. Comparison of the typical sensory profile of 16 apple direct juice samples from the German market in 2008 in correlation to the ethyl butyrate and the 2(E)-hexenal content (data from Symrise survey).

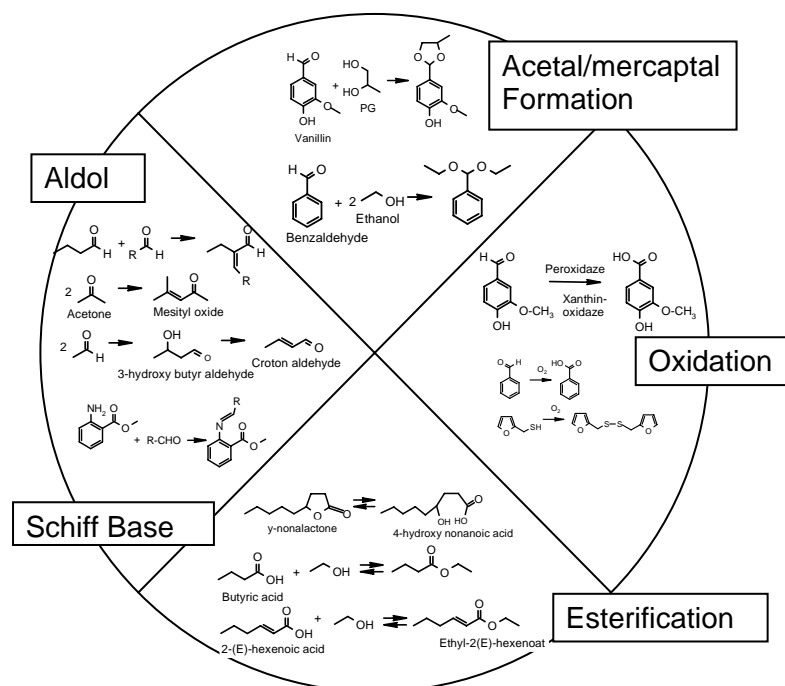


Figure 3. Possible chemical reactions of flavouring substances.

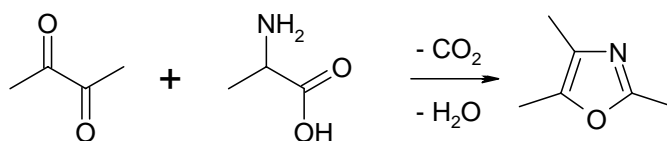


Figure 4. Formation of trimethyloxazol in a cappuccino base (5).

Authenticity

Besides GC/MS analysis, chiral separation of enantiomers (7) and isotope ratio mass spectrometry (IRMS) are getting increasing attention. The lactone chemistry of strawberries was subject to numerous studies. Starting with derivatization and non chiral column techniques, multidimensional gas chromatography equipped with chiral cyclodextrin GC columns enabled a rapid determination of enantiomeric excess data. The flavour analysis of raspberry water phase extracts after freeze-drying (Table 1) illustrate that the enantiomeric distribution of natural products and the analysis of chiral discrimination of individual marker substances for authenticity has to be investigated carefully with regard to the interpretation of the natural origin of flavouring substances. While γ -decalactone as a main ingredient is occurring in high enantiomeric purities homologous lactones such as γ -octa- and γ -nonalactone are occurring only in minor enantiomeric purity.

In particular modern IRMS methods are getting more important for the authenticity analysis of raw materials and the conformity of production technologies for natural flavouring substances (8). In the last years the supply of authentic garlic oils was subject to changes with regard to availability and price. As a consequence improved methods for authenticity control received a strong focus. Based on a dedicated SDE method garlic oils from Europe, China and Middle East were analysed via IRMS. For a detailed evaluation the $\delta^{13}\text{C}$ -data and $\delta^2\text{H}_{\text{V-SMOW}}$ data for synthetic and authentic

allylmethylsulphide, diallylsulphide, allylmethylsulphide, diallyldisulphide, allylmethyltrisulphide were compared. Figure 5 shows the pattern for natural, authentic material as well as for synthesis derived compounds.

Table 1. Enantiomeric distribution of 4-alkanolides in concentrated raspberry water Phase (6).

	R(+)	S(-)
δ -Octalactone	39.8 %	60.2 %
γ -Octalactone	64.6 %	35.4 %
γ -Nonalactone	57.0 %	43.0 %
δ -Decalactone	47.5 %	52.5 %
γ -Decalactone	98.1 %	1.9 %
δ -Dodecalactone	66.0 %	34.0 %
γ -Dodecalactone	99.5 %	0.5 %

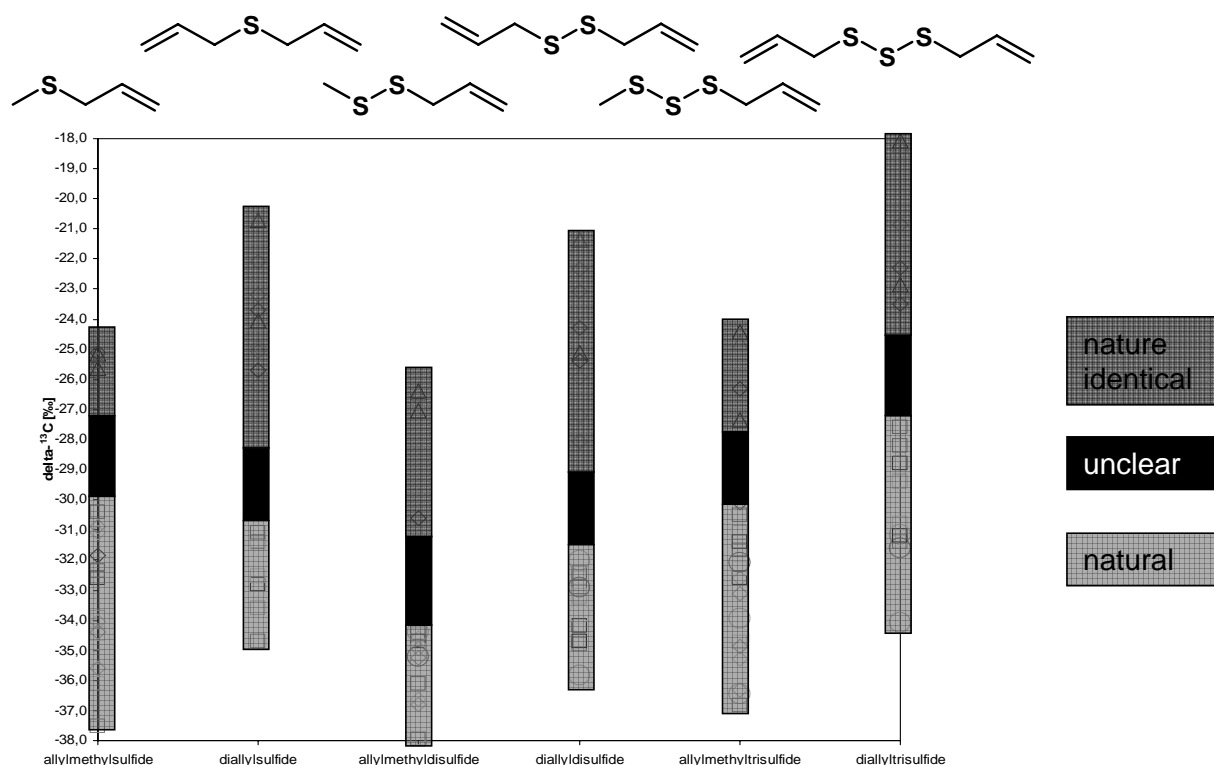


Figure 5. Data ranges for natural and synthesis derived selected compounds, (allylmethylsulphide, diallylsulphide, allylmethylsulphide, diallyldisulphide, allylmethyltrisulphide) from authentic garlic oils and from synthetic origin; (data from Symrise study).

Based on these findings a decision tree approach for garlic oils was developed which is shown in (Table 2).

Table 2. Decision tree approach for the authenticity analysis of garlic oils; data based on Symrise study.

Selected flavour compound	Data range for materials from natural sources
Allylmethylsulphide	$\delta^{13}\text{C}_{\text{V-PDB}} < -30,4\text{‰}$
Diallylsulphide	$\delta^{13}\text{C}_{\text{V-PDB}} < -31,1\text{‰}$
allylmethylsulphide	$\delta^{13}\text{C}_{\text{V-PDB}} < -34,4\text{‰}$
Diallyldisulphide	$\delta^{13}\text{C}_{\text{V-PDB}} < -32,0\text{‰}$ and $\delta^2\text{H}_{\text{V-SMOW}} < -90\text{‰}$
allylmethyltrisulphide	$\delta^{13}\text{C}_{\text{V-PDB}} < -30,5\text{‰}$ and $\delta^2\text{H}_{\text{V-SMOW}} < -140\text{‰}$
Diallyltrisulphide	$\delta^{13}\text{C}_{\text{V-PDB}} < -27,6\text{‰}$
Comparison of selected compounds	Difference of $\delta^{13}\text{C}$ data
allylmethylsulfide vs. diallylsulfide	$\Delta\delta^{13}\text{C}_{\text{V-PDB}} < -3,6\text{‰}$
allylmethyldisulfide vs. diallyldisulfide	$\Delta\delta^{13}\text{C}_{\text{V-PDB}} < -4,6\text{‰}$
allylmethyltrisulfide vs. diallyltrisulfide	$\Delta\delta^{13}\text{C}_{\text{V-PDB}} < -5,4\text{‰}$

For onion oils this decision tree approach needs to be based on the $\delta^{13}\text{C}$ -data and $\delta^2\text{H}_{\text{V-SMOW}}$ data for synthetic and authentic methylpropylsulphide, dipropylsulphide, methylpropylsulphide and dipropylsulphide. In addition the two marker compounds 2-hexyl-5-methyl-3(2H)-furanone (cepanon) and 2-octyl-5-methyl-3(2H)-furanone (norcepanon) need also to be considered, which lead to an amended decision tree approach for allium derived raw materials (Table 3).

Table 3. Amended decision tree approach for the authenticity analysis of onion oils using marker compounds from genuine origin (data based on Symrise study).

Selected flavour compound	Data range for materials from natural sources
Methylpropylsulphide	$-37,4\text{‰} < \delta^{13}\text{C}_{\text{V-PDB}} < -33,7\text{‰}$
Dipropylsulphide	$-34,8\text{‰} < \delta^{13}\text{C}_{\text{V-PDB}} < -31,1\text{‰}$
Methylpropylsulphide	$-37,9\text{‰} < \delta^{13}\text{C}_{\text{V-PDB}} < -33,4\text{‰}$
Dipropylsulphide	$-37,2\text{‰} < \delta^{13}\text{C}_{\text{V-PDB}} < -32,3\text{‰}$
all $\delta^2\text{H}_{\text{V-SMOW}}$ values	$< -200\text{‰}$
Comparison of selected compounds	Difference of $\delta^{13}\text{C}$ data
Methylpropylsulphide and dipropylsulphide	$\Delta\delta^{13}\text{C}_{\text{V-PDB}} < -4,2\text{‰}$
Methylpropyltrisulphide and dipropyltrisulphide	$\Delta\delta^{13}\text{C}_{\text{V-PDB}} < -4,0\text{‰}$
Marker substances	Presence in raw materials from natural origin
2-Hexyl-5-methyl-3(2H)-furanone „Norcepanon“	Present
2-Octyl-5-methyl-3(2H)-furanone “Cepanon”	Present

Essential oils are often showing high complexity, which requires the application of IRMS analysis combined with GC/MS and enantio-specific analysis in order to answer authenticity related questions. The aroma of laurel leaf oil is described with a fresh-green, strong, sweet-spicy, aromatic eucalyptus-like odor and a fresh, delicate spicy, camphor/eucalyptus-like taste. The key odorants of the leaves were characterized recently by means of aroma extract dilution analysis as (Z)-3-hexenal, eugenol, 1,8-cineole, and linalool (9). A main compound is α -terpinyl acetate, ranging between 5 to 15 %, which might originate from seasonal variations or from different geographical origins. Since these variations are able to generate problems in finished consumer goods, qualities are often pooled and sometimes standardized.

The chiro-specific analysis of laurel leaf oil hydro distillates from France and Turkey revealed a ratio 4S(-)- α -terpinyl acetate to 4R(+)- α -terpinyl acetate of 92.4 to 7.6 and 91.3 to 8.7, respectively. This finding was in contrast of two lots from a commercial oil originating from the Croatian/Dalmatian coast showing a 80:20 ratio (Table 4).

Since it is known that the enantiomers and the racemate occur in many essential oils (e.g. cardamom with about 40 %, Siberian pine-needle and cypress oils) a detailed analysis of these qualities is necessary. In α -terpinyl acetate various amounts of γ -terpinyl acetate as synthesis by-product are detected. In addition IRMS data based on $\delta^{13}\text{C}$, $\delta^2\text{H}_{\text{V-SMOW}}$ and $\delta^{18}\text{O}$ values have to be collected in order to get a complete picture (Table 5). This extended decision tree approach involves all levels of instrumental analysis: GC/MS, enantio-GC/MS as well as $\delta^{13}\text{C}$, $\delta^2\text{H}$ and $\delta^{18}\text{O}$ -IRMS (10).

Table 4. Chiro-specific analysis of α -terpinyl acetate based on GC and chiral GC. Relative concentration [%] of α - and γ -terpinyl acetate in GC/MS (10).

Samples	conc. GC/MS [%]			
	4S(-) α - Terpinyl acetate [%]	4R(+) α - Terpinyl acetate [%]	α -Terpinyl acetate	γ -Terpinyl acetate
Laurel leaf oil, com. A, Croatian/Dalmatian coast (pooled)	80.0	20.0	10.65	1.22
Laurel leaf oil, com. B, Croatian/Dalmatian coast (pooled)	80.0	20.0	10.48	1.22
Laurel leaf oil, hydro dist., France	92.4	7.6	10.55	-
Laurel leaf oil, hydro dist., Turkey	91.3	8.7	8.51	-
α -Terpinyl acetate, synth. ex <i>Pinus pinaster</i> , France	50.0	50.0	57.27	22.65
α -Terpinyl acetate, synth. ex <i>Pinus spec.</i> , USA	41.4	58.6	80.62	15.29

Table 5. GC/C-IRMS and GC/TC-IRMS data of natural and synthetic α -terpinyl acetate (10)

Sample	$\delta^{13}\text{C}_{\text{V-PDB}}$ [‰] s.d.: 0.3‰	$\delta^2\text{H}_{\text{V-SMOW}}$ [‰] s.d.: 10-20‰	$\delta^{18}\text{O}_{\text{V-SMOW}}$ [‰] s.d.: 1.0‰
ex Laurel leaf (France)	-31.8	-252	8.7
ex Laurel leaf (Turkey)	-30.0	-253	11.9
ex Laurel leaf oil, com. A	-32.3	-278	9.6
ex Laurel leaf oil, com. B	-32.6	-240	10.2
α -Terpinyl acetate synth. A	-33.4	-332	11.8
α -Terpinyl acetate synth. B	-32.8	-296	10.7

Contaminants affecting quality

The highly interconnected ecological system of our plants leads to the fact that it is almost impossible to state the total absence of contaminants in the supply chain for food and flavourings. Bio-accumulative compounds are usually assumed to be hydrophobic and fat-soluble if the octanol-water partition coefficient (K_{OW}) is higher than 100,000. Meanwhile it is known that even moderately hydrophobic compounds with K_{OW} between 100 and 100,000 can increase in concentration at each step in the food chain, a process known as bio-magnification. Bio-magnification of such a compound can occur in food webs that include humans and other air-breathing animals, even when it does not happen in food webs that are limited to fish and aquatic invertebrates. To bio-magnify in air-breathing animals, a compound is characterized by a high octanol-air partition coefficient (K_{OA}), and slow metabolism such as β -hexachlorocyclohexane (11). In addition contaminants like agricultural residues can arise from specific crops or can originate from packaging such as plasticizers. Certain food preparation methods can also give rise to contaminants such as furan or acrylamide. In general contaminants are undesired substances in the food chain, which do not represent an immediate health risk to consumers. A major concern is the risk of unexpected contaminants because of the potential damage to the image of brands when the occurrence is reported in the media. Therefore many authorities established institutions, which are responsible for risk analysis like the BfR (Bundesinstitut für Risikobewertung = Federal Institute for Risk Assessment) in Germany. According to Council Regulation EEC 315/93 Article 1 (12) the term contaminants is defined as “any raw material not intentionally added to food”. For a professional risk management of a contamination a series of typical properties of contaminants needs to be addressed (Table 6).

Table 6. List of typical properties for food contaminants.

Parameter	Typical property
Quantity	Trace levels < 100mg/kg
sensory quality	relevant in specific flavouring relevant in finished application
Purity	occurrence as single compound occurrence as mixture
Occurrence	non specific (e.g. phthalates) specific (e.g. 3-mono-chloro propandiol, 3-MCPD in soy sauce)

The risk assessment for contaminants can be conducted based on the failure mode and effect analysis (FMEA) (13). For the flavour industry the multiplicative combination of the severity of presence, the probability of occurrence and the detectability leads to calculated risk numbers which can be linked to action levels for adequate measures. This matrix needs to be continuously updated based on recent incident reports as well as state-of-the-art analytical capabilities.

Another aspect of the presence of contaminants is described by the subject of agricultural residues (AR). These compounds are used for a defined purpose in crop production such as pesticides in the production of citrus fruits. The AR analysis of citrus oils reveals several challenges for a reliable analytical procedure. The direct analysis of single-fold peel oils brings basically all applied analytical procedures close to the limit of detection. For electro spray ionization (ESI) in the HPLC-MS analysis of polar and semi-polar pesticides the injection of larger sample amounts suffers from a major ion suppression effect, which heavily affects the accuracy and the precision of quantification data (Figure 6).

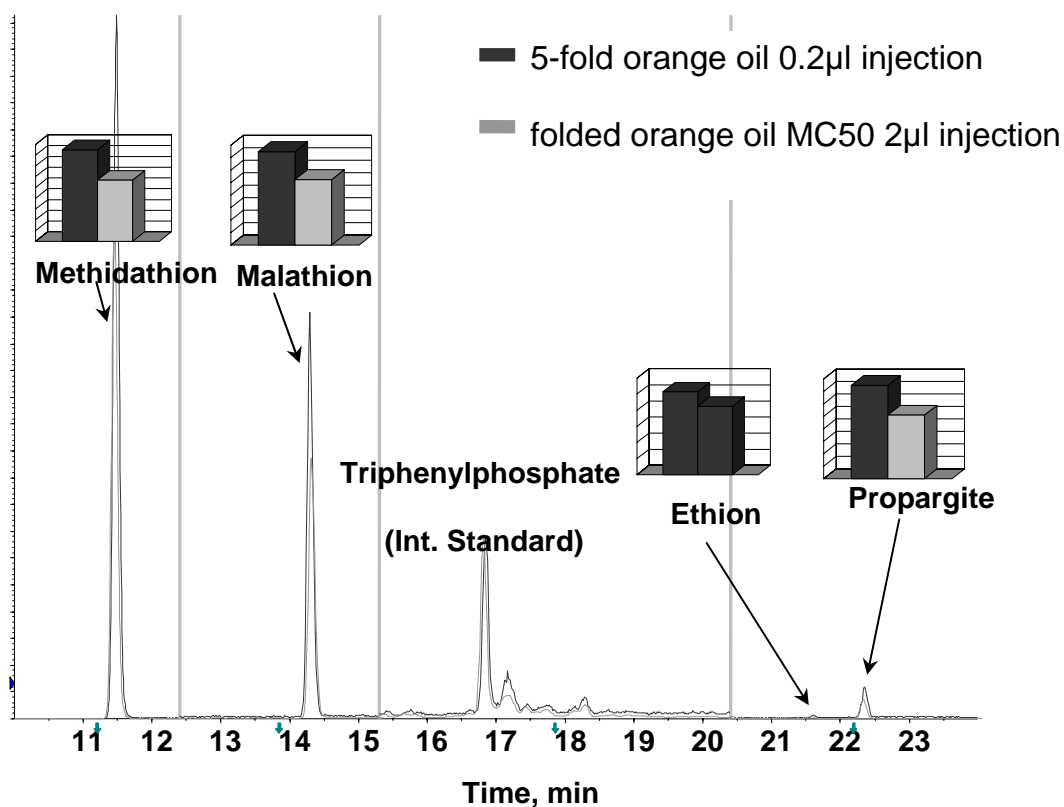


Figure 6. Ion suppression effect in electrospray ionization (ESI); signal response (peak area) of a 5-fold orange oil vs. a 50 fold multiconcentrated orange oil (MC50) with different injection volumes 0.2 µl and 2 µl.

For the correct qualitative identification of contaminants 2002/657/EC (16) requires at least 4 so-called identification points (IP) for the positive identification in order to ensure a correct analytical assignment at trace level (Table 7).

Table 7. Identification points in mass spectrometry (16).

MS technique	Points
LR-MS	1.0
LR-MS2 precursor ion	1.0
LR-MS2 transition products	1.5
HR-MS	2.0
HR-MS2 precursor ion	2.0
HR-MS2 transition products	2.5

Global specifications for flavourings

The process of establishing global specifications for flavouring raw materials and flavourings is basically facing three challenges: the enormous range of chemical classes, the complexity of physical and chemical properties and last but not least the history of the individual local and regional regulatory approaches. Modern food industry, however, is characterized by global development projects and cross-regional technology transfers. In this scenario standardisation a structured approach has key priority to achieve standardized specifications for flavourings and their respective raw materials. The classification of materials and the selection of test methods are embedded in a decision tree approach (Figure 7) in order to enable a systematic assignment of specifications for raw materials and flavourings.

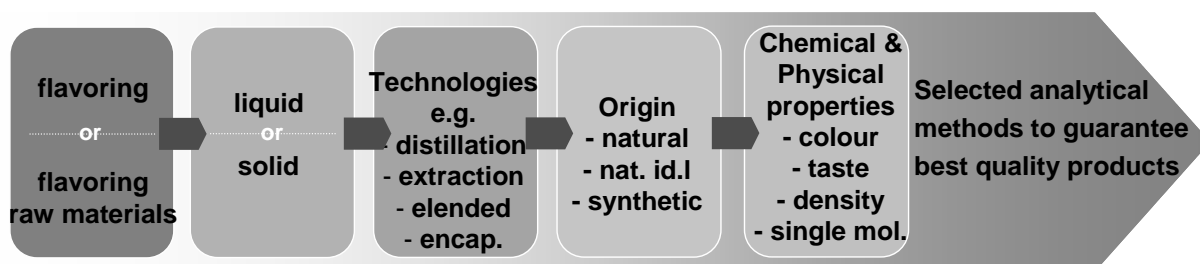


Figure 7. Decision tree approach for standardized global specification for flavour raw materials and finished flavourings.

A specification can technically be set up by three building blocks, which are a header, a set of parameters and respective limits or targets and additional information. Header information is very important to describe the subject by a common name but also by giving information such as synonyms, CAS numbers and inventory numbers. The set of parameters and limits build the core of the specification stating the physical, chemical, sensory and microbiological properties of the respective material. The generation of a specification is the process of selecting suitable parameters and assigning reasonable limits or target values. This process can be structured in three steps: Classification of the raw material, linkage of the raw material or raw material class to a test scope and application of limits or target values to the raw material. The selection of test methods, the so-called test scope has to be selected to cover a series of aspects, which is shown in (Table 8) (17).

Table 8. *Individual parameters of a test scope.*

Parameter	Example
Sensory properties	Odour, taste, colour, clarity, physical aspect
Microbiological properties	Total plate count, yeasts and moulds, coliforms, E. coli
Identity	Specific gravity, refractive index, IR spectroscopy
Purity	GC or HPLC
Stability/degradation	Peroxide value, acid value
Authenticity	Optical rotation, isotope ratio mass spectrometry, Deuterium NMR, HPLC
Contaminants	Specific trace analysis for compounds such as solvents or pesticides
Safety aspects	Bacillus cereus
Regulatory aspects	Permissibility in different regions

Based on a defined test scope for a class of materials the limits and targets are set for each individual material. Any test method has its limitations with regard to accuracy, precision, sensitivity, linearity, reproducibility and specificity. Many analytical methods can be described by these attributes, whereas microbiological and sensory methods cannot be validated the same way. Reasonable limits can be obtained by the review of existing data or based on material that represents the desired quality. Tolerances should be chosen with respect to the inherent variation and uncertainty of the test methods. Ideally the tolerances of an analytical parameter should not fall below six times standard variation (18). A specification, when finally generated, should basically describe the quality according to the criteria guaranteed high quality levels in production, reproduction of agreed test methods in a timely manner and respected variations or tolerances.

New challenges and new solutions

The use of nanoscale materials in food is a good example to describe the new challenges for food and flavour companies on different levels such as analytical quality control, food safety and performance analysis of ingredients. Based on the excellent success of nanoscale materials in non food material science, paint industry and technical chemistry various project teams are investigating the use of nanoscale materials in food packaging, coatings and in the combination with food processing aids. Nanoscale materials are characterized by a higher exposure factor to consumers per mass unit together with good olfactory transport and dermal penetration. In many cases nanoscale materials have new chemical and physical properties. Therefore analytical tools are needed to monitor migration and exposure. So far there is only limited set of methods to enrich, isolate and characterize nanoscale materials. At the same time existing natural nanoscale materials based on lactose, whey proteins, casein micelles or fat globules are getting more and more in the focus. Based on these facts the whole area of nanoscale technologies in food industry generates a massive work load, which needs to be addressed in the near future.

Acknowledgement

We are grateful to Ms Regina Ahlbrecht for her excellent work in editing this manuscript and to the management of Symrise for the strong support of all activities for quality improvement.

References

1. http://www.codexalimentarius.net/web/index_en.jsp.
2. Wolter C., Gessler A., Winterhalter P. (2008) *Flüssiges Obst* 3: 122-134.
3. Anlage Nr. 1b der *FruchtsaftV* (Fruchtsaft aus Fruchtsaftkonzentrat) vom 24. Mai 2004.
4. Stöllman U., Johansson F., Leufvén A. (1994) In *Shelf Life Evaluation of Foods* (Man C.M.D., Jones A.A., eds.), Chapman & Hall: Suffolk.
5. Barnekow R., Muche S., Ley J., Sabater C., Hilmer J.-M., Krammer G. (2007) In *Flavours and Fragrances – Chemistry, Bioprocessing and Sustainability*, Springer: Berlin, pp 457-488.
6. Krammer G.E., Weckerle B., Brennecke S., Weber B., Kindel G., Ley J., Hilmer J.-M., Reinders G., Stöckigt D., Hammerschmidt F.J., Ott F., Gatfield I., Schmidt C.O., Bertram H.J. (2006) *Mol. Nutr. Res.* 50: 345-350.
7. Mosandl A. (2007) In *Flavourings, Production, Composition, Applications, Regulations* (2nd edition), Ziegler H. (Ed.) Wiley-VCH: Weinheim, pp 664-697.
8. Schmidt H.-L., Werner R.A., Rossmann A., Mosandl A., Schreier P. (2007) In *Flavourings, Production, Composition, Applications, Regulations* (2nd edition), Ziegler H. (Ed.) Wiley-VCH: Weinheim, pp 602-663.
9. Kilic A., Hafizoglu H., Kollmannsberger H., Nitz S. (2004) *J. Agric. Food Chem.* 52: 1601-1606.
10. Hammerschmidt F.-J., Krammer G. (2007) In *Authentication of Food and Wine*, Ebeler S.E.; Takeoka G.R.; Winterhalter P. (Eds.), ACS Symposium Series 952, American Chemical Society: Washington DC, pp 87-108.
11. Kelly B.C., Ikonomou M.G., Blair J.D., Morin A.E., Gobas F.A.P.C. (2007) *Science* 317: 236.
12. Council Regulation (EEC) No 315/93 of 8 February 1993 laying down Community procedures for contaminants in food.
13. EN60812:2006 Analysis techniques for system reliability - *Procedure for failure mode and effect analysis* (FMEA), May 2006.
14. Gardner L.K., Lawrence G.D. (1993) *J. Agric. Food Chem.* 41: 693-695.
15. Halliwell B., Guttridge J.M.C. (1985) *Mol. Aspects Med* 8: 89-193.
16. 2002/657/EC Commission Decision of 12 August 2002 implementing Council Directive 96/23/EC concerning the performance of analytical methods and the interpretation of results.
17. Lösing G., Ebeling B., Förstner J., Althage R., Schmidt C.O., Krammer G.E. (2009) *Perfumer & Flavorist* 34(4): 30-36, 38-40, 42.
18. Handbuch Validierung in der Analytik, Stavros Kromidas, WILEY – VCH Verlag Germany 2000.

VANILLA BEAN QUALITY – A FLAVOUR INDUSTRY VIEW

K. GASSENMEIER and E. Binggeli

Givaudan Schweiz AG, Ueberlandstrasse 138, CH-8600 Switzerland

Abstract

Vanillin, vanillic acid, p-hydroxybenzaldehyde and p-hydroxybenzoic acid was quantified in more than 50 batches of vanilla beans from the crop 2006/2007 from Madagascar. The data were related to commercial quality criteria like size, colour and shape of the beans. Only 27% of all vanilla batches met the regulatory standard of the French equivalent definition, which requires 2 g Vanillin / 100 g cured bean. The ratio of the so called marker compounds were met by 55% of all samples. Strategies to bridge the gap between regulatory compliance and raw material market are discussed.

Introduction

Extracts of vanilla beans (*V. planifolia* and *V. tahitensis*) are of high commercial value and importance due to their specific organoleptic properties. In an effort to regulate quality (1) and prevent adulteration some analytical parameters of vanilla extracts are strictly regulated by authorities, giving minimum concentration of vanillin in standard vanilla extracts. Furthermore ratios of the marker compounds vanillin, vanillic acid, p-hydroxybenzoic acid and p-hydroxybenzaldehyde are set (2) and used as authenticity or quality parameters. These regulatory requirements are compared with the actual vanilla bean quality available on the market.

Experimental

All vanilla beans were obtained from Givaudan warehouse or as pre-shipment from suppliers. All beans were from Madagascar. The vanilla extracts were prepared following the French arrêté (3). Vanillin, vanillic acid, p-hydroxybenzoic acid and p-hydroxybenzaldehyde were quantified using a HPLC method described in (4).

Results

Vanillin content and commercial qualities. In commercial practice size, shape and colour are used as quality criteria for vanilla beans. The black beans are the highest grade and usually used in the retail market. The second quality is red beans, which are divided into split and non split. These subgroups are further classified by size. The red beans are used for extract preparation. Cuts are very small beans or broken material. An estimate for the production of the different grades from Madagascar is given in Table 1.

Table 1. Market share in percent of commercial grades of Madagascar beans.

Grade	Sub category	Share
Black		20%
Red non-split		30%
	Long (> 14 cm)	15%
	Mid (12 – 14 cm)	10%
	Short (< 12 cm)	5%
Red split		30%
	Long (> 14 cm)	15%
	Mid (12 – 14 cm)	10%
	Short (< 12 cm)	5%
Cuts		20%

The distribution of batches into vanillin concentration classes is shown in table 2. Most samples contain 1.2 to 2.2 g vanillin/100 g. Only 15 out of 55 batches show a vanillin content > 2g/100g. The average, minimum and maximum vanillin concentration of the commercial grades is displayed in table 3. The average over all samples was 1.76 g/100 g. The range for the black beans was 1.72 to 2.18, for red non split 1.38 to 2.45 and for red split quality 1.37 to 2.18. The average vanillin content decreased from black > red non split > red split > cuts. All qualities – except cuts - contain batches above and below 2 g/100g vanillin. The ratio of so called marker compounds vanillin, vanillic acid, p-hydroxybenzaldehyde and p-hydroxybenzoic acid are used as authenticity parameters. Average ratios for the different categories are displayed in table 4. Interestingly, with the exception of the cuts, all average ratios are within the expected ranges of the so-called ratio figures. However on a sample by sample and ratio by ratio view 45% of all samples do not meet at least one expected ratio. A more detailed discussion can be found in (4).

Table 2. Number of batches by concentration range

Vanillin range (g/100g)	# of Batches
0.8-1.0	1
1.0-1.2	1
1.2-1.4	6
1.4-1.6	10
1.6-1.8	13
1.8-2.0	9
2.0-2.2	11
2.2-2.4	3
2.4-2.6	1

Table 3. Vanillin concentration in g/100g related to bean quality.

Type	Vanillin in g/100g		
	Avg	Min	Max
Black	1.95	1.72	2.18
Red Non Split	1.82	1.38	2.45
Red Split	1.72	1.37	2.18
Cuts	1.13	0.86	1.36
All	1.76	0.86	2.45

Table 4. Average of ratios of marker compounds and number of samples, which are out of expected values by category.

	Expected Ratios	Black	Red Non Split	Red Split	Cuts	All
Vanillin / pHB Ald	10 - 20	14	17	17	17	17
Vanillin / pHB Acid	40 - 110	87	91	62	49	77
Vanillin / Vanillic acid	12 - 29	18	17	14	10	15
pHB Acid / pHB Ald	0.15 - 0.35	0.17	0.19	0.31	0.36	0.25
Vanillic acid / pHB Ald	0.53 - 1.50	0.81	1.04	1.3	1.82	1.19
% out of expected ratios		25	50	42	100	45

The influence of the size on vanillin content of red beans can be retrieved from table 5. Especially the non split beans show higher vanillin concentration with increasing size. In the group of the split beans this effect is not clear. For comparison the total potential of vanillin (vanillin and glucovanillin) in green beans by length is given. It appears that in smaller beans less glucovanillin is present. But even small green beans exhibit a potential of 3.3 g vanillin/100g.

Table 5. Vanillin content (g / 100g) in vanilla beans by size and shape.

	Short (< 12)	Mid (12 - 14)	Long (> 14)
Non Split	1.46	1.79	1.97
Split	1.64	1.76	1.72
Green*	3.3	4.8	5.3

* Sum of glucovanillin and vanillin, calculated on comparable dry matter.

Flavour profile and vanillin content. The vanilla extracts prepared from the beans were classified into 4 profile categories by an expert panel, and the average vanillin content of the categories calculated. The data are displayed in Table 6. The category with the best profile, described as balanced, good quality, beany notes showed an average vanillin content of 1.72 g/100g. In contrast the highest vanillin content of 2.00 g/100g was found in a category with a medium quality ranking. Its profile was dominated by strong vanillin notes, but resin and rum like notes were quite weak. Interestingly a good quality with a balanced profile and some phenolic aspects had less vanillin (1.43 g/100g) than the category with strong phenolic and woody off-notes (1.58 g/100g). Based on the data vanillin is not seen as a good indicator for the extract profile and the bean quality.

Table 6. *Extract profile and average vanillin concentration.*

Profile type	Average vanillin content in g/100g	Quality rating
Strong phenolic or woody	1.58	Negative
Balanced with some phenolic aspects	1.43	Good
Strong vanillin note, weak resin rum like notes	2.00	Medium
Balanced good quality, beany notes	1.72	Very good

Conclusion

Most of the Madagascar vanilla batches do not meet regulatory requirements set by some authorities in terms of vanillin content and so called ratios. The current classification of vanilla beans used in commercial practice like size, shape and colour are not reliable parameter to differentiate or select qualities according to vanillin content and profile. The industries quality parameters are focused on flavouring properties, cost effectiveness and regulatory compliance. Useful strategies are over folding, *i.e.* increasing the amount of beans per solvent volume to comply with regulatory requirements, optimisation of extraction technologies, analytical batch selection and development of industrial curing techniques. The regulatory requirements trigger the development of procedures, which *e.g.* use enzymes to release vanillin in high concentrations from green non cured vanilla beans (5, 6). This leads to high vanillin vanilla extracts, which, however, might be very poor in overall flavour. In the future, methods that encompass the sensory properties and purity of an extract would be preferred, although they pose huge challenges to the analytical chemist, because they require detailed knowledge of the minor compounds of vanilla extracts. In the dynamic field of vanilla, the concept of simple and restrictive analytical parameters should be reconsidered.

References

1. Republique francaise, Direction general de la concurrence, de la consommation et de la qualite et de la securite: note de service No 5387, 1988.
2. Republique francaise, Direction general de la concurrence, de la consommation et de la repression des fraudes (2003). Note d'information n 2003– 61. 2003
3. Method officielle de dosage de la vanilline, de l'aldehyde para-hydroxybenzoique, de l'acide vanilique, de l'acide para-hydroxybenzoique dans les gousses de vanille et les produit vanilles. Arrete du 11 juin 1987, parue au JORF, p3171.
4. Gassenmeier K., Riesen B., Magyar B. (2008) *Flavour Frag. J.* 23: 194-201.
5. Graves R.E., Hall R.L., Karas A.J.(1958) *Cured vanilla extract from green vanilla beans* , US Patent No. 2835591.
6. Takahashi M., Hirai H., Shiraishi S. (1998) *Manufacture of natural vanilla flavor by enzymatic treatment.* Japanese Patent No. 10316992, 1998.

ODOUR-ACTIVE COMPOUNDS OF UFA/CLA ENRICHED BUTTER AND CONVENTIONAL BUTTER DURING STORAGE

S. MALLIA^{1,2}, F. Escher², C. Hartl³, P. Schieberle³, and H. Schlichtherle-Cerny¹

¹ *Agroscope Liebefeld-Posieux Research Station ALP, 3003 Berne, Switzerland*

² *Institute of Food Science and Nutrition, Food Technology and Sensory Science, ETH Zurich, 8092 Zurich, Switzerland*

³ *Deutsche Forschungsanstalt für Lebensmittelchemie, Lichtenbergstrasse 4, 85748 Garching, Germany*

Abstract

Butter enriched in unsaturated fatty acids (UFA) and conjugated linoleic acid (CLA) and conventional butter were analysed for their odour profiles during cold storage at 6°C. The volatile compounds were extracted using headspace solid phase microextraction and solvent-assisted flavour evaporation and identified by gas chromatography-olfactometry and GC-mass spectrometry. Aroma extraction dilution assay was performed to identify the most potent odorants in UFA/CLA butter and in conventional butter. The quantification of the most potent odorants of UFA/CLA and conventional butters was performed using stable isotope dilution assays. Both, fresh UFA/CLA and fresh conventional samples had a very similar odour profile, characterized by fruity (methyl 2-methylbutanoate, 3-methylbutyl acetate, δ -decalactone) milky (2-nonanone), soapy (nonanal) and sulphury (dimethyl disulphide) notes. The storage significantly affected the concentrations of pentanal, heptanal, nonanal, δ -decalactone and butanoic acid, which significantly increased in stored UFA/CLA enriched butter. Some compounds, such as (*Z*)-3-hexenol and (*E*)-2-heptenal, with fatty notes, were identified only in the UFA/CLA enriched samples.

Introduction

It is desirable to increase the level of unsaturated fatty acids (UFA) and conjugated linoleic acid (CLA) in dairy products as a health benefit in human nutrition (1-2). On the other hand, the higher UFA/CLA content could maybe negatively affect the flavor of the dairy products since unsaturated lipids are more prone to auto-oxidation (3). The aim of the present investigation was to evaluate the oxidative stability of butter enriched in UFA and CLA in comparison to conventional butter, focusing on aroma compounds. The aroma profiles of the two butter types were analysed during storage and the most important odour-active compounds were quantified.

Experimental

UFA/CLA enriched butter and conventional butter were obtained from the milk of cows fed pasture and sunflower seeds, and pasture and corn silage, respectively. Butter samples kept under refrigerated conditions (6 °C) were analysed for their odour-active composition at 0 (fresh) and 6 weeks of storage. The odour compounds were extracted using head-space solid phase microextraction (HS-SPME) and solvent-assisted flavour evaporation (SAFE) coupled to gas chromatography mass

spectrometry/olfactometry (GC/MS/O). The volatiles were separated and identified as described by (4). The flavour dilution (FD)-factors of the odorants were determined by aroma extract dilution analysis (AEDA). The most potent odours were quantified by stable isotope dilution analysis (SIDA). Pentanal and heptanal were quantified using [5,6-²H₂]-hexanal (5). The following labelled standards were synthesized according to the procedures published in the reference given in parentheses: [8,9-²H₂]- δ -octalactone (6), [10,11-²H₂]- δ -decalactone, [12,13-²H₂]- δ -dodecalactone and [3,4-²H₂]-butanoic acid (7), [2,3-²H₂]-(*E,Z*)-2,6-nonadienal (8).

Results

The odour profiles of fresh UFA/CLA butter and fresh conventional butter obtained using SPME were both characterized by milky, soapy and sulphury notes, due in particular to 2-nonanone, nonanal and dimethyl disulphide, respectively (Table 1). (*Z*)-3-hexenol (oily, green) and 2-phenylethyl acetate (flower) were perceived only in fresh UFA/CLA enriched butter. After 6 weeks of storage, heptanal (fatty), 1-octen-3-one (mushroom-like), (*E*)-2-octenal (flower), nonanal (soapy), (*E,Z*)-2,6-nonadienal (cucumber-like), δ -decalactone (fruity) were more intensely perceived at the sniffing port, in UFA/CLA enriched butter. (*E*)-2-heptenal, with fatty/soapy odour, was found exclusively in UFA/CLA butter. Dimethyl disulphide disappeared during storage, as previously observed by (9).

Table 1. Selected odorants found by SPME in fresh and stored UFA/CLA enriched and conventional (CONV) butter.

Compound	Odour descriptor	LRI HP-5MS	Fresh		Stored butter	
			UFA/CLA	CONV	UFA/CLA	CONV
Dimethyl disulphide	Sulphur	742	++	+	nd	nd
Hexanal	Green	801	+	+	++	++
Butanoic acid	Cheesy	807	+	+	+++	++
(<i>Z</i>)-3-Hexenol	Oily, green	861	+	nd	nd	nd
Heptanal	Green/fatty	909	+	+	+++	++
(<i>E</i>)-2-Heptenal	Fatty/soapy	958	nd	nd	++	nd
1-Octen-3-one	Mushroom	986	+	+	+++	++
Octanal	Almond/fruity	1007	++	+	++	+
(<i>E</i>)-2-Octenal	Flower	1058	nd	nd	+++	++
2-Nonanone	Milky	1095	++	++	++	++
Nonanal	Soapy	1121	++	++	+++	++
(<i>E,Z</i>)-2,6-Nonadienal	Cucumber	1154	+	+	+++	++
2-Phenylethyl acetate	Flower	1257	++	nd	nd	nd
δ -Decalactone	Fruit	1522	+	+	+++	++

AEDA confirmed the results obtained by SPME and additionally found methyl-2-butanoate, 3-methylbutyl acetate, pentanal, decanal, (*E*- and (*Z*)-2-nonenal, δ -octalactone and δ -dodecalactone as impact odour compounds of the two kinds of butter (Table 2). The FD-factors increased in almost all the odour compounds after storage. 2-Phenyl acetate was detected exclusively in the fresh samples, whereas decanal only in stored samples. δ -Dodecalactone, δ -decalactone and (*E,Z*)-2,6-nonadienal had the highest FD-factor in both butter types, but especially in stored UFA/CLA enriched butter.

Table 2. Impact odour compounds (FD factor ≥ 8) in fresh and 6 weeks stored (6 °C) UFA/CLA enriched butter and conventional (CONV) butter.

Odorant	Odour quality	FD factor ^a					
		Fresh		Stored			
		LRI FFAP	LRI HP-5MS	UFA/C LA	CONV	UFA/CL A	CONV
Methyl 2-methyl butanoate	Fruit	1016	776	32	32	8	8
Pentanal	Fat, green	738	973	8	8	64	16
Hexanal	Green	1082	810	32	16	64	64
3-Methylbutyl acetate	Orange	1116	-	32	16	16	16
Heptanal	Soapy	1170	910	8	8	128	32
Octanal	Almond, fruit	1277	1007	8	4	8	4
Nonanal	Soapy, citrus	1385	1109	64	64	64	32
2-Nonanone	Milk	1402	1101	64	64	64	64
Decanal	Green	1486	1250	-	-	64	32
2-Phenylethyl acetate	Fruit	1810	1250	64	16	-	-
(Z)-2-Nonenal	Hay	1510	1148	4	4	64	32
(E)-2-Nonenal	Grass	1529	1163	8	4	64	32
(E,Z)-2,6-Nonadienal	Cucumber-like	1567	1154	32	16	128	64
Butanoic acid	Cheesy	1620	856	4	4	64	64
δ -Octalactone	Fruit	1923	1290	8	8	64	64
δ -Decalactone	Peach-like	2201	1469	32	16	128	64
δ -Dodecalactone	Peach-like	2420	1509	8	8	256	128

^a FD factor determined by 2 panellists. The FD factors between the 2 panellists differed not more than by a factor of 2.

To estimate the sensory contribution of the odorants to the odour of the butter samples, the odour activity values (OAVs) were calculated by dividing the concentrations of the odorants by their odour thresholds in sunflower oil. The OAVs of the odorants in the two fresh butter types were almost identical. Only heptanal and δ -decalactone had higher OAV in fresh UFA/CLA butter compared to that of fresh conventional butter (Table 3). After 6 weeks of storage, pentanal, heptanal, δ -decalactone and butanoic acid had the highest OAV in UFA/CLA enriched butter. In particular, δ -decalactone with an OAV= 18, was found the more prominent odour compound in stored UFA/CLA enriched butter.

Most of the odour-active compounds found in the butter samples originated from oxidation of unsaturated fatty acid and in particular, from linoleic acid (3).

However, the oxidation of CLA could also form odour compounds. The formation of odorants from CLA follows different chemical pathways. A radical oxidation mechanism with hydroperoxide formation is less probable with CLA, since more activation energy is required to separate the conjugated double bonds (10). The compounds might more probably be formed from CLA by a mechanism of 1,2 cycloaddition, which can lead to aldehydes, esters and lactones (10). However, further studies are required on the chemical oxidation pathways of CLA.

Table 3. Odour Thresholds, concentrations and OAVs of the major odorants of UFA/CLA enriched and conventional butter

Compound	Odour threshold ^a (µg/L)	Fresh				Stored			
		UFA/CLA (µg/kg)	OAV UFA/CLA	CONV (µg/kg)	OAV conv	UFA/CLA (µg/kg)	OAV UFA/CLA	CONV (µg/kg)	OAV conv
Pentanal	240	235	<1	64	<1	661	3	289	1
Heptanal	250	963	4	364	1	1703	7	1140	5
δ-Octa- lactone	120	114	<1	137	1	303	3	487	4
δ-Deca- lactone	260	2858	7	2061	5	7245	18	5293	13
δ-Dode- calactone	120	1314	11	1464	12	1491	12	1536	13
(E,Z)-2,6- Nonadienal	3.8	17	5	17	5	17	5	20	5
Butanoic acid	135	1606	12	1568	12	1885	14	1820	14

^a Odour thresholds calculated in sunflower oil by (11)

References

1. Ip C., Chin S.F., Scimeca J.A., Pariza M.W. (1991) *Cancer Res.* 51: 6118-6124.
2. Ip C., Banni S., Angioni E., Carta G., McGinley J., Thompson H., Barbano D., Bauman D. (1999) *J. Nutrition* 129: 2135-2142.
3. Grosch W. (1987) In *Autoxidation of unsaturated lipids* (Chan H.W.-S., ed.) Academic Press Inc., pp. 95-139.
4. Mallia S., Piccinali P., Rehberger B., Badertscher R., Escher F., Schlichtherle-Cerny H. (2008) *Int. Dairy J.* 18: 983-993.
5. Guth H., Grosch W. (1993) *Z. Lebensm. Unters. Forsch.* 196: 22-28.
6. Christlbauer M. (2005) *PhD Thesis*, Technical University of Munich
7. Schieberle P., Gassenmeier K., Guth H., Sen A., Grosch W. (1993) *Lebensm. Wiss. Technol.* 26: 347-353.
8. Guth H., Grosch W. (1990) *Lebensm. Wiss. Technol.* 23: 513-522.
9. Shooter D., Jayatissa N., Renner N. (1999) *J. Dairy Res.* 66: 115-123.
10. Yurawecz M.P., Delmonte P., Vogel T., Kramer J.K.G. (2003) In *Advances in Conjugated Linoleic Acid Research, Vol. 2* (Sébédio J., Christie W.W., Adlof R., eds.), AOCS Press, pp. 56-70.
11. Rychlik M., Schieberle P., Grosch W. (1998) Compilation of odor threshold, odor qualities and retention indices of key food odorants. *Deutsche Forschungsanstalt für Lebensmittelchemie and Institut für Lebensmittelchemie der Technischen Universität München*, Garching, Germany.

INFLUENCE OF ETHYLENE-BLOCKING ACTION, HARVEST MATURITY AND STORAGE DURATION ON AROMA PROFILE OF APPLES (ILDRØD PIGEON) DURING STORAGE

M. POPIELARZ¹, M.A. Petersen¹, and T.B. Toldam-Andersen²

¹ *Department of Food Science, Faculty of Life Sciences, University of Copenhagen, Rolighedsvej 30, DK-1958 Frederiksberg C*

² *Department of Agricultural Sciences, Faculty of Life Sciences, University of Copenhagen, Højbakkegård Allé 21, DK- 2630 Taastrup*

Abstract

Effects of the blocker of ethylene action 1-methylcyclopropene (1-MCP), maturity stage, and storage duration on apple aroma profile were investigated. 1-MCP acts as an effective ethylene receptor blocker and is newly registered in Denmark. Experiments were conducted using the popular Danish cultivar Ildrød Pigeon (IP). IP is a small-fruited, red coloured cultivar with a very characteristic aroma. It is harvested in mid-late September and sold as a traditional specialty at Christmas time. Aroma potential of IP has not been investigated yet. Therefore there is a great need to explore it also in connection to 1-MCP treatment. Results revealed a slight tendency of 1-MCP treatment to change the aroma profile at different storage duration. However, delay of 1-MCP application after harvest may have reduced the impact on volatile production.

Introduction

Aroma profile is one apple quality parameter which influences consumer purchase decision. Aroma of apples is a complex mixture of volatile compounds, with a typical profile for each different variety. It is known that many aroma compounds increase in concentration during apple ripening. The ripening process is initiated by the plant hormone ethylene, which plays an important regulatory role in aroma production during ripening (1). Therefore, chemicals which block ethylene action or production are also expected to influence apple aroma profile (1-3). One ethylene blocker is 1-MCP (SmartFresh, AgroFresh, Inc.), which binds to ethylene receptors and thus decreases quality changes caused by the ripening process (4). The Danish cultivar Ildrød Pigeon (IP) was chosen for this study. IP is very popular because of its taste and special aroma (5), and it is eaten especially during Christmas time.

In the current study apples were treated with 1-MCP with a one-week delay after harvest. In practice IP apples should be exposed to sun light after harvest to obtain fully red colour development. Consequently there is a question if 1-MCP should be used straight after or before light exposure, not to intervene into anthocyanin development as part of ripening processes. In this experiment delay of 1-MCP was decided to evaluate aroma profile, so far without exposure to sun light.

The main objective of the study was to determine the effects of apple maturity stage at harvest, 1-MCP treatment, and different storage durations on the aroma profile of IP apples.

Experimental

Apples were grown in the University of Copenhagen's experimental orchard 'Pometet'. Fruits were harvested twice in September 2007; at normal commercial harvest and two weeks later. In total, 10 samples were measured during the experiments. Each sample contained 12 apples.

After each harvest, 5 samples were transferred to cold storage (1.5°C) for one week. After a week in cold storage one sample was used for aroma analyses, two untreated samples were kept in cool storage (1°C) and two samples were treated with 1-MCP (after treatment kept in cool storage as untreated samples).

Treatment with 1-MCP was carried out by releasing 1-MCP gas into a box covered tightly by a plastic bag. A probe with 0.075 g 1-MCP was prepared for each box (one box of volume of 0,0072 m³). According to the producer AgroFresh Inc., in 1m³ the concentration of 1-MCP (0,14%) should be 1000ppb 1-MCP v/v in the air. The probe with 1-MCP was placed in the box together with a small ventilator to ensure adequate distribution of 1-MCP. The 1-MCP treatment lasted for 20 hours at 22°C. After treatment samples were transferred to small cold storage chambers as was done with the untreated samples.

Two samples from each harvest (one treated and one untreated) were stored until mid October – short storage and two samples until mid December (one treated and one untreated) – long storage. On the fifth remaining sample, aroma analysis were made a week after harvest (after a week in a cool storage) to assess starting aroma profile.

After removal from cool storage samples were kept for 5 days at room temperature (23°C) before aroma analysis. Volatile analyses were carried out on juice pressed from 12 apples from each sample and performed in triplicate. The aroma compounds were measured using dynamic headspace sampling and analysed on a Hewlett-Packard G1800A GC/MS. The aroma compounds were measured according to method of Petersen and al. (6). Peak areas were determined from single ion peak areas and used as relative measures of concentration of compounds. A total of 41 aroma compounds were chosen.

Aroma data were analysed by Principal Component Analysis using LatentiX (Version 1.0, Latent5, Denmark). The same PCA model was used to illustrate sample distribution based on aroma compounds and dependency on measured factors. Analyses of variance were carried out using InfoStat (*InfoStat versión 2008*. Grupo InfoStat, FCA, Universidad Nacional de Córdoba, Argentina). The Fisher Least Significant Difference at the $p \leq 0.05$ level was used.

Results

The 41 chosen aroma compounds belonged to 6 groups: acids (1 compound), aldehydes (9 compounds), alcohols (13 compounds), esters (14 compounds), terpene (1 compound), ketones (2 compounds) and phenylpropanoid (1 compound).

Earlier studies have shown that production of volatiles is reduced in apples treated with 1-MCP (1,2). This tendency was also detected in this investigation. ANOVA showed that compared with 1-MCP treated apples, untreated apples produced higher amounts of butanoic acid, propanal, butanal, 1-heptanol, propyl acetate, methyl 2-methylbutanoate, ethyl butanoate and estragole. This indicates that the untreated apples were riper. Accordingly, the PCA plot of PC1 vs. PC5 showed separation of apples treated and not treated with 1-MCP (Figure1) according to

aroma profiles. An incomplete separation can be partly explained by the timing of 1-MCP treatment, which was carried out one week after each harvest time. It is likely that the ethylene-mediated aroma-induction process had already started and 1-MCP was applied too late to inhibit it.

A significant difference in aroma production was detected between maturity stages. Apples from first and second harvest developed significantly different aroma profiles during storage. In the PCA plot in (Figure 2), the maturity stages are clearly separated.

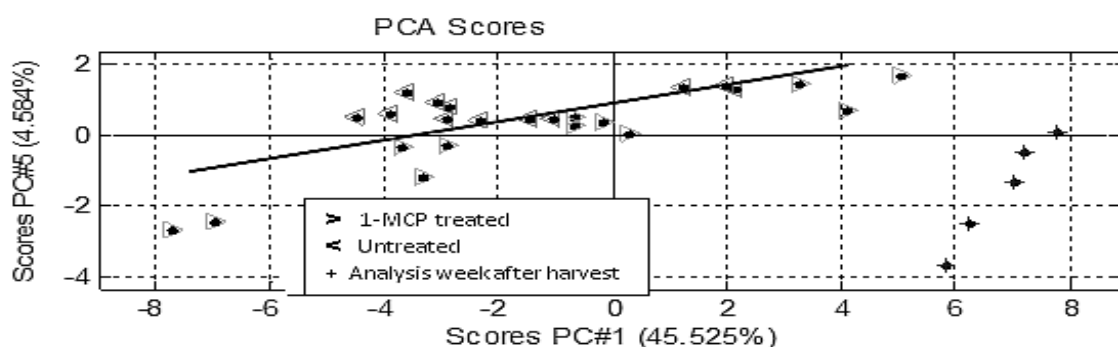


Figure 1. Scores plot PC1 vs PC5 represents PCA model for aroma production of apples treated and untreated with 1-MCP.

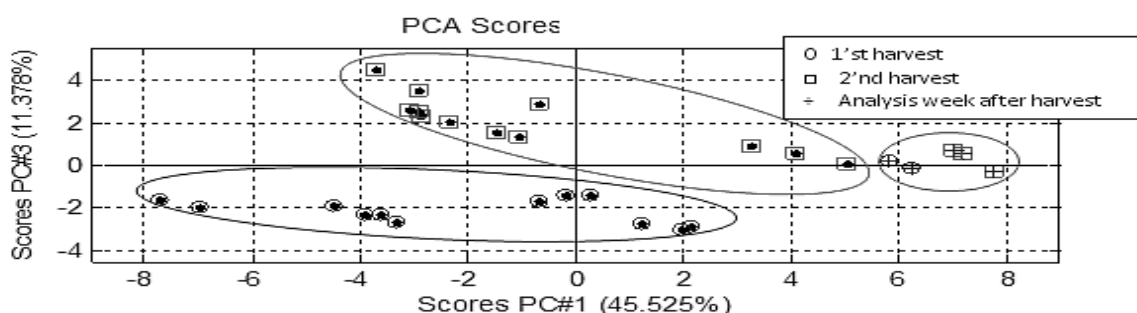


Figure 2. Scores plot PC1 vs PC3 presents PCA model for aroma production of apples from 1st and 2nd harvest (model includes treated and untreated samples).

Apples from first harvest (commercial maturity) had a relatively high concentration of the aldehydes hexanal, E-2-hexenal and (E,E)-2,4-hexadienal. By contrast, production of alcohols and esters was generally greater in apples harvested two weeks later. However, 2-methyl-1-propanol, 3-octanol, methyl acetate, ethyl acetate and hexyl formate were more abundant in the aroma profile of apples harvested at commercial maturity. The same was observed with estragole and (E,E)- α -farnesene. The distinct separation in PCA indicates that harvest time had an impact on apple aroma development during storage.

The duration of storage influenced the aroma profile of the apples notably. The 3 groups of different storage duration were clearly separated. Samples analysed one week after harvests had low amounts of aroma compounds. Only (E,E)-2,4-hexadienal, 2-hexen-1-ol and hexyl acetate were present in high amounts. However, the aroma profile changed substantially during further cold storage. In some studies it has been observed that concentrations of aldehydes and alcohols decrease with the time of storage, whereas ester production increases (2). Increases in acids, esters

and ketones were noted in the current study with IP apples. The measured ketones (2 compounds), the acid (butanoic acid) and the esters (14 compounds), except hexyl acetate, increased during the storage period. Hexyl acetate was at the highest concentration when measured one week after harvest.

The production of some of the alcohols and aldehydes increased during the short storage, after which production was quite stable. In contrast to this, (E)-2-hexenal, (E,E)-2,4-hexadienal and 2-hexen-1-ol declined in production. Those compounds had the highest concentration at the beginning of the experiments.

In conclusion, the results showed that harvest time (maturity stage) and storage period influenced production of volatiles in Ildrød Pigeon apples more than 1-MCP application. Apples treated with the ethylene blocker had decreased production of some aroma compounds. Apples picked at two different maturity stages two weeks apart developed different volatile profiles. Apples from the first harvest had a higher concentration of most aldehydes, the terpene (E,E)- α -farnesene and the phenylpropanoid estragole, but were low in some alcohols and esters. The aroma profile of IP apples one week after harvest was low in total volatiles, but production increased significantly during additional storage time, especially for esters and ketones.

References

1. Kondo S., Setha S., Rudell D.R., Buchanan D.A., Mattheis J.P. (2005) *Postharvest Biol. Tech.* 36: 61-68.
2. Lurie S., Pre-Aymard C., Ravid U., Larkov O., Fallik E. (2002) *J. Agric. Food Chem* 50: 4251-4256.
3. Ferenczi A., Song J., Tian M., Vlachonasios K., Dilley D., Beaudry R. (2006) *J.Amer.Soc.Hort.Sci.* 131: 691-701.
4. Fan X., Blankenship S.M., Mattheis J.P. (1999) *J. Amer.Soc.Hort.Sci.* 124: 690-695.
5. Ministeriet for Fødevarer, Landbrug og Fiskeri Danmarks JordbrugsForskning (2000), *Frugt- og bærsorter til haven* 131: 5.
6. Petersen M.A., Poll L., Toldam-Andersen T.B. (2007) In *Recent Highlights in Flavour Chemistry & Biology*, Proceedings of the 8th Wartburg Symposium, (Hofmann T., Meyerhof W., Schieberle P., eds.), pp 345-348.

CHANGES IN THE KEY ODOUR-ACTIVE COMPOUNDS AND SENSORY PROFILE OF CASHEW APPLE JUICE DURING PROCESSING

D.S. GARRUTI¹, H.V.V. Facundo¹, M.A. Souza Neto¹, and R. Wagner²

¹ *Embrapa Tropical Agroindustry, PO Box 3761, 60511-110, Fortaleza, Brazil*

² *Department of Food Science and Technology, Federal University of Santa Maria, RS, Brazil*

Abstract

Samples of cashew apple juice were collected in an industrial plant in order to monitor the juice key odour-active compounds at three different processing steps: extraction, pasteurisation and concentration. Volatile compounds were isolated by dynamic headspace technique and analysed by GC-MS and Osme GC-O method. Results were correlated to sensory descriptive data by multivariate analysis. Pasteurisation did not change very much the perception of cashew-like compounds, but did reduce compounds contributing to sweet, fruity, floral and green notes. Pasteurised cashew apple juice maintained fresh juice flavour intensities but a moderate cooked flavour. Evaporation, in its turn, drastically reduced key compounds while concentrated others, like occurred to a ketone, described as sickly sweet, and to a sulphur compound, yielding a juice characterized by cooked and sulphur flavours.

Introduction

The appeal of natural cashew apple (*Anacardium occidentale*, L.) juice is attributed to its high vitamin C content, averaging three to six times that of orange juice. Despite its high level of astringency, cashew apple shows good characteristics for industrialization owing to its fleshy pulp, soft peel, lack of seeds, high sugar content and strong exotic flavour. The volatiles composition of cashew apples from a specific genetic material (clone CCP76) was already assessed in a previous work (1) as well as the volatile profile of commercial cashew apple nectars (2). In the juice industry, concentration of fruit juice is necessary in order to reduce volume and stabilize the product, but many concentrated juices lack most of the aroma volatiles (3-5) which are lost or changed due to enzymatic activity, thermal influence and evaporation (6). The present study aimed to evaluate the changes in the odour-active compounds in cashew apple juice during a commercial juice concentration process and investigate how they influence its sensory properties.

Experimental

Materials. Cashew apple juice samples were withdrawn at three processing steps of a large scale Brazilian industrial plant, from the same batch: extraction, pasteurisation and concentration. Samples were stored at -18 °C prior analyses.

Volatiles collection and analysis. Volatiles from the headspace of cashew apple juice were swept by vacuum to a Porapak Q[®] trap for 2 h at room temperature and

eluted with 300 μ L dichloromethane (7). Compounds were separated on a CPWax 52CB column (50 m x 0.25 mm i.d. x 0.25 μ m, Varian) and identified from linear Retention Indices and EI mass spectra (NIST 05 MS Library Database).

GC-Olfactometry. The relative importance of each odour compound was evaluated by the Osme time intensity GC-O method (8). Sniffing was performed in duplicate, by four trained judges, who reported intensity using a 9 cm time-intensity scale (software SCDTI, Unicamp, Brazil) and descriptors for any detected odour. Guaiacol was added in every run as an internal odour standard.

Sensory analysis. The aroma and flavour profile was developed by descriptive analysis, in duplicate, by a panel of 8 trained judges.

Statistical analysis. Data were submitted to ANOVA and the most discriminative descriptors were selected for multivariate correlation (PLSR-2) as an exploratory analysis to describe the relationships between sensory (mean scores) and olfactometric data (mean intensity).

Results

A total of 93 volatile compounds were detected by FID in cashew apple juice samples, of which 50 were odour-active. Sensory panel also perceived another 22 compounds with very low threshold that were not detected by instrumental means and were labelled as small letters. Table 1 lists the main odoriferous compounds which presented odour intensity greater than 1 in at least one processing step.

Table 1. Main odour-active compounds in the cashew apple juice samples from industrial processing steps.

Peak n ^o	RI ^a	Compound	Odour description	Odour Intensity		
				Extr	Past	Conc
d	<1000	ND	fruity, sweet	4.29	2.40	2.05
e	<1000	ND	fruity, sweet	2.13	0.98	-
2	<1000	2-Butanone	cashew, fruity, fruit candy	1.88	2.98	-
4	<1000	5-Methyl-2-hexanone	cashew, sweet, fruit candy	1.54	3.48	0.61
g	<1000	ND	tutti-frutti, fruit candy	3.64	5.01	3.03
7	<1000	Ethyl propionate	cashew, sweet, fruit candy	4.35	1.74	2.26
12	<1000	NI	fruity, green	2.27	1.97	0.83
19	1038	Ethyl butyrate	fruity, sweet	3.24	2.72	-
21	1050	Ethyl 2-methylbutyrate	fruity, floral	1.44	2.37	-
23	1067	Ethyl isovalerate	cashew, fruity, fruit candy	1.67	3.67	0.66
h	1135	ND	fermented cashew, sweaty	4.13	4.56	-
37	1154	Ethyl crotonate	fruity, fruit candy	2.30	2.06	-
42	1178	Heptanal	plastic, glue	2.41	2.85	-
47	1207	3-Methyl-1-butanol	acid, herb, sweaty	1.41	1.52	-
i	1221	ND	green, metallic	2.85	2.76	-
51	1245	NI (sulphur compound)	butane gas, glue	-	-	1.63
54	1265	Isobutyl isovalerate	cashew, perfume, floral	1.26	-	0.83
58	1293	Ethyl 3-hexenoate	green	1.90	1.24	-
60	1312	(Z)-3-Hexen-1-ol	green, unripe fruit	3.62	3.91	-
65	1357	Allyl hexanoate	green, wax	2.44	2.81	-
l	1392	ND	perfume	2.17	-	-
70	1439	Ethyl octanoate	fruity, floral	1.80	0.88	-
76	1510	Benzaldehyde	acid, green	2.58	-	-
86	1650	2-Methyl butanoic acid	sweaty, fermented fruit	5.08	5.55	5.25
91	1996	NI (ketone)	sugar candy, sickly sweet	1.46	1.65	2.91

ND = not detected; NI = not identified.

The major odour-active compounds here detected were also found by other authors, with the same odour descriptions. Some examples are ethyl butyrate (1, 2), ethyl propionate (1), ethyl isovalerate (1, 2), benzaldehyde (1, 2), 2-methyl butanoic acid (1, 2) and (Z)-3-hexen-1-ol (1).

Most cashew-like compounds (2-butanone, 5-methyl-2-hexanone, ethyl isovalerate) increased their perception during processing until pasteurisation, possibly due to enzymatic activity, before heat treatment, over bounded compounds, increasing their concentration on the juice. Some contributing odorants (fruity, sweet, green) showed good stability; remaining unaltered or slightly decreasing after pasteurisation. On the other hand, Table 1 shows high losses of cashew-like perceptions, as well as for most contributors during concentration. Distinct behaviours were found for bad-smelling compounds: 2-methyl butanoic acid (sweaty, fermented) remained constant and a sulphur compound, which was not perceived in the unprocessed juice, showed up with moderate intensity. Compound labelled 91, a non-identified ketone with a sickly sweet smell, was concentrated during processing.

Sensory assessors developed a vocabulary of 7 aroma (cashew apple, sweet, fermented, artificial, acidic, green, floral) and 8 flavour descriptors (cashew, fermented, artificial, green, sulphurous, cooked fruit, and sweet and acid tastes) but only five showed significant difference among samples from various processing steps (Figure 1). The results of PLSR-2 carried out only with these five descriptors that could discriminate samples are in Figure 2, showing the multivariate relationships between sensory attributes and perception of odoriferous compounds. PC1 explained 79.2% of the samples variations, differentiating Concentration from the other samples. Concentrated juice was characterized by Acid and Sweet aroma, Cooked and Sulphur flavours while unprocessed juice (Extraction) and pasteurised sample showed higher Green aroma and Cashew flavour, typical fresh fruit sensory qualities.

Compound 91, described as sugar candy and sickly sweet, perceived in higher intensity in the concentrated juice, was associated to Cooked flavour and Sweet aroma whereas the unidentified sulphur compound 51 was related to the Sulphur flavour. Good news about concentration was that bad-odour compounds like heptanal (peak 42, plastic, glue) and peak h (fermented, sweaty) were probably lost during concentration, since they were not perceived in the concentrated juice. Also the smelly compound 2-methyl butanoic acid (peak 86, sweaty), the most intense odour rated by sensory panel, was not concentrated.

PC2 differentiated pasteurisation sample from the unprocessed juice, mainly due to volatile compounds. Extraction samples were characterized by higher perceptions of fruity and sweet compounds and ethyl propionate (peak 7, cashew-like), but pasteurised juice showed higher perceptions of three other cashew-like compounds (peaks 2, 4 and 23). However their volatile compositions yielded similar cashew flavour intensities for both samples. The biggest difference between them was that the sensory panel also perceived a moderate cooked flavour in the pasteurised sample.

In general, cashew apples odour-active volatile compounds showed good stability to initial industrial processing steps and pasteurisation, being the sensory properties of the processed (pasteurised) juice very similar to those of a fresh juice. Traditional concentration, however, had a great effect on cashew-like and contributing volatiles, resulting in a juice with acid aroma and cooked and sulphur flavours.

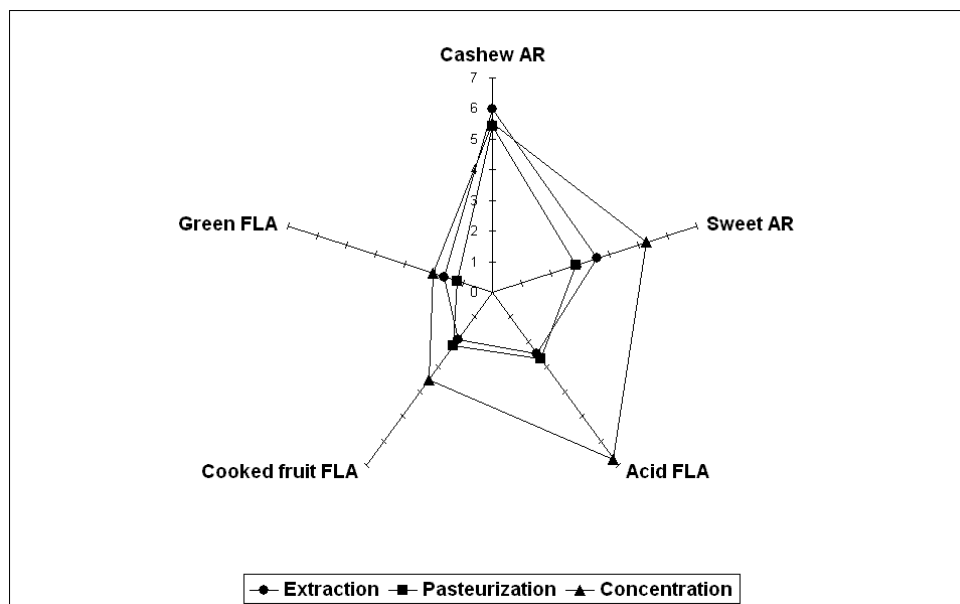


Figure 1. Flavour attributes of cashew apple juice which showed significant difference among different processing steps (AR = aroma; FLA = flavour).

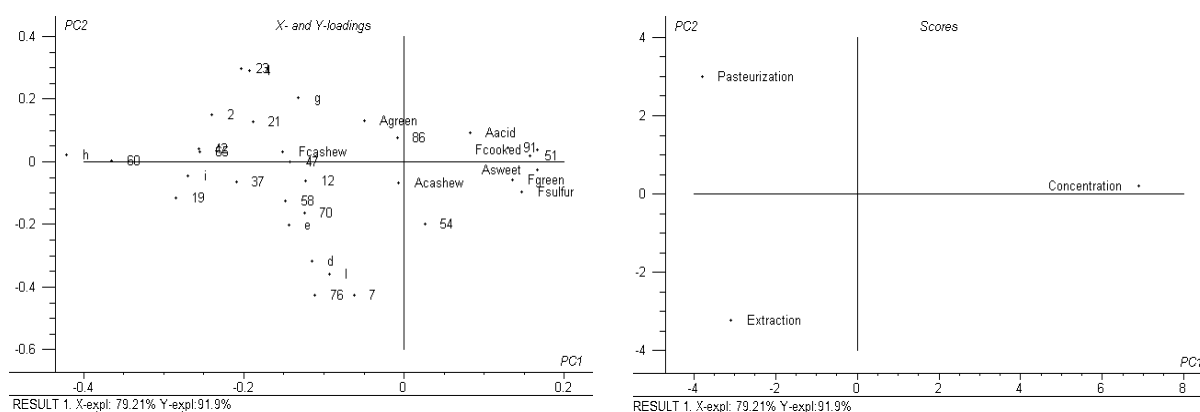


Figure 2. Scores (a) and Loadings (b) for PLS regression for the cashew apples juice samples from industrial processing steps.

References

- Garruti D.S., Franco M.R.B., Da Silva M.A.A.P., Janzantti N.S., Alves G. L. (2003) *J. Sci. Food Agric.* 83:1455-1462.
- Valim M.F., Rouseff R.L., Lin J. (2003) *J. Agric. Food Chem.* 51: 1010-1015.
- Varming C., Andersen M.L., Poll L. (2004) *J. Agric. Food Chem.* 52: 7628 -7636.
- Elss S., Preston C., Hertzog C., Heckel F., Richling E., Schreier P. (2005) *LWT- Food Sci. and Technol.* 38: 263-274.
- Steinhaus M., Bogen J., Schieberle P. (2006) In *Flavor Science: Recent Advances and Trends* (Bredie W.L.P., Peterson M.A., eds.); Elsevier Science B.V., pp 189-192.
- Poll L., Nielsen G.S., Varming C., Petersen M.A. (2006) In *Flavor Science: Recent Advances and Trends* (Bredie W.L.P., Peterson M.A., eds.); Elsevier Science B.V., pp 239-244.
- Franco M.R.B., Garruti D.S., Da Silva M.A.A.P. (1998) *Rev. Cubana Quim.* 10: 273–274.
- McDaniel M.R., Miranda-Lopes B.T., Watson M., Libbey L.M. (1990) In *Flavours and Off-flavours* (Charalambous G., ed.); Elsevier B.V., pp 23-36.

STRATEGIES FOR MINIMISING THE INFLUENCE OF THE BARLEY CROP YEAR ON BEER FLAVOUR STABILITY

A. STEPHAN and G. Stettner

Bitburger Braugruppe GmbH, Römermauer 3, 54634 Bitburg, Germany

Abstract

To avoid a forced generation of Strecker aldehydes and therefore less flavour stability in the bottled beer it has become necessary to develop strategies to reduce barley crop effects on the beer quality. One of these strategies is to influence the protein modification (Kolbach index) during the malting process. To this purpose, 4 selected malts with protein contents between 9.4 % and 11.8 % and soluble nitrogen amounts between 0.62 % and 0.77 % were processed in the pilot plant of Bitburger brewery in a 20 hl scale. Amino acids and corresponding Strecker aldehydes were monitored during beer production as well as in freshly bottled and 6-months stored beers, respectively. Furthermore, the analytical data were confirmed by sensory profile tests of the freshly and 6-months stored bottled beers. The final results show a significant correlation between protein modification and flavour stability of beer.

Introduction

The quality of malt as well as of the barley it is produced from is key parameters for beer flavour stability. Due to reduced acreage in Western Europe and poor harvests in the 2006 and 2007 crops, the actual availability of barley, especially spring barley, for brewing has substantially decreased. The 2007 barley crop shows protein contents between 11.0 % and 13.0 %, while former crops showed much lower contents between 9.0 % and 11.0 %. Without adjusting the malting process to achieve a lower Kolbach index, higher protein amounts in barley result in higher soluble nitrogen contents in the brewing malt. The latter leads to higher free amino acid amounts during beer production causing a forced generation of Strecker aldehydes and therefore less flavour stability in the bottled beer [1, 2, 3].

Keeping these facts in mind it has become necessary to develop strategies to reduce barley crop effects on beer flavour stability for example by influencing protein modification (Kolbach index) during the malting process.

Experimental

Materials. The trials were carried out in triplicate in a 20 hectolitre pilot plant at Bitburger brewery. A standard 2-mash decoction procedure (56°C/68.5°C/74°C) was used to produce Pilsener type beers from 300 kg barley malt, variety Scarlett. The four different malt specifications used for the trials are shown in Table 1. Worts were boiled 70 minutes at 100°C and fermented at 10.5°C.

Methods. Aldehydes were quantified after cold solvent extraction by using an accelerated approach described recently [4]. Amino acids were quantified by conventional method after derivatization with o-phthalaldehyde by fluorescence detection.

Sensory analysis. Beer samples were analysed by profile tests [5] after 6 months storage by at least 10 trained assessors in separate sensory cabins. The attributes fresh, papery, bread-like, sherry-like and overall aged were evaluated on a scale between 0 and 9.

Table 1. *Analysed qualities of the tested malts ordered according to Kolbach index (analytical methods based on Kongress wort by MEBAK [6]).*

		Malt 1	Malt 2	Malt 3	Malt 4	Malt 5
Humidity	%	5.5	4.9	4.9	5.0	4.4
Extract	%	80.6	82.3	83.0	82.4	83.1
pH		5.96	5.95	5.89	5.82	5.93
Boiled colour	EBC	4.9	3.9	5.5	6.2	7.4
Total protein	%	11.8	10.2	9.8	9.4	9.2
Soluble nitrogen	%	0.68	0.62	0.69	0.77	0.84
Kolbach index (KI)		36.1	38.2	44.5	51.1	56.4

$$\text{Kolbach index} = \frac{\text{soluble nitrogen [\%]} \times 6.25 \times 100}{\text{total protein [\%]}}$$

Results

The malts used for brewing trials were selected on the basis of their Kolbach indices (36.1 – 56.4). Total proteins varied from 9.2 to 11.8% and soluble nitrogen contents from 0.62 to 0.84% (Table 1). The varying amounts of amino acids released during the brew house process were equalized by fermentation and maturation, leading to almost the same aldehyde concentrations in freshly bottled beers [7]. Only after storage aldehyde generation corresponded to the values of the precursors (Table 2).

Table 2. *Free amino acid amounts [mg/L] after brew house process in cooled wort and Strecker aldehydes [$\mu\text{g/L}$] in beer after 6 months storage at 28°C (n=3)*

	Strecker aldehydes	KI 36 ^a	KI 38	KI 44	KI 51	KI 56
Wort	Methionine	29	30	38	44	53
	Leucine	101	118	148	175	228
	Phenylalanine	77	87	99	126	163
	Isoleucine	44	51	67	78	83
Stored beer	Methional	1.2	1.5	2.2	3.0	8.9
	3-Methylbutanal	5.6	5.8	10.9	12.1	17.2
	Phenylacetaldehyde	11.6	11.8	14.9	16.9	23.4
	2-Methylbutanal	3.0	3.3	7.0	7.8	8.8

^a Trials named by Kolbach index of malt analysis (KI 36 was performed with malt 1, KI 38 with malt 2 etc.)

Not only low soluble nitrogen amounts, but also moderate Kolbach indices resulted in significantly lower amounts of FAA. While the difference in soluble nitrogen amounts of the malts was in maximum 35%, the amounts of the Strecker aldehyde generating FAAs differed up to 90% in the cooled worts. It appears that the protein modification based on the malting process is much more important than the

resulting total soluble nitrogen amount. Obviously there is a remarkable variation in the generation of Strecker aldehydes from the FFAs. While FFAs differed between the trials in maximum by a factor of 2, the generation of Strecker aldehydes varied between a factor of 2 for phenylacetaldehyde and a factor of 7 for methional (Table 2).

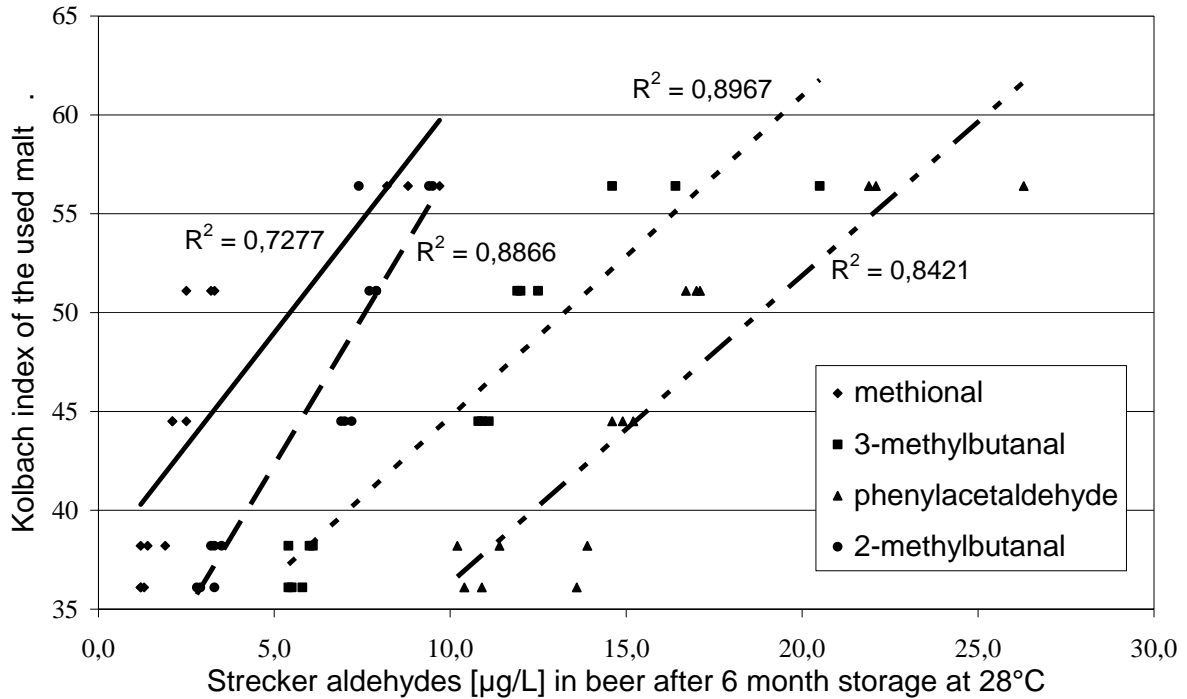


Figure 1. Correlation of Kolbach index and Strecker aldehyde concentration [µg/L].

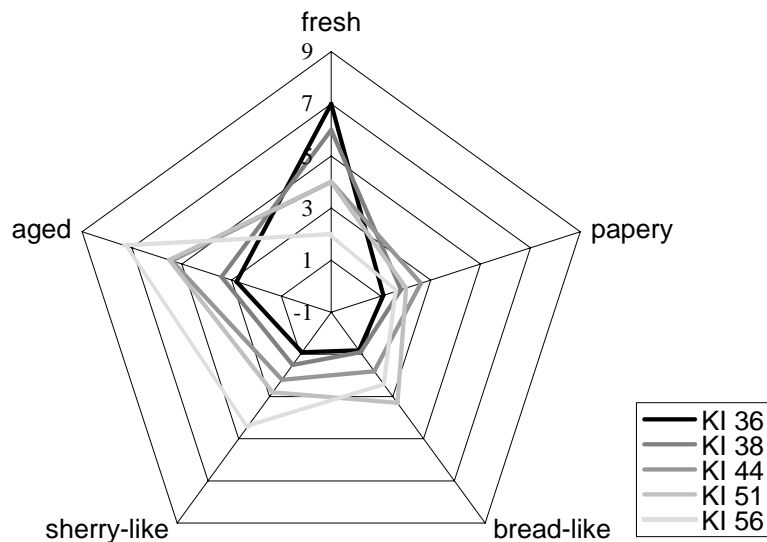


Figure 2. Results of the retronasal sensory evaluation of the 6 months stored samples (28°C).

The correlation of Kolbach index of malt analysis and corresponding Strecker aldehyde generation after storage is shown in Figure 1. The analysis of the Kolbach

index of the malt shipment samples permits a reliable prediction of Strecker aldehyde formation which is responsible for the aged sensory perception. The usefulness of the Kolbach index for taste stability prediction is confirmed by the sensory results of the stored beers (Figure 2). Increasing Kolbach indices resulted in stronger “aged” flavours after 6 month storage, especially with a more intense sherry note, whereas no sensory differences were perceived in the freshly bottled beers.

Conclusion

The use of malts with lower Kolbach indices led to reduced Strecker aldehyde generation in the final product and consequently to enhanced flavour stability. Especially barley crop years like 2007 with consistently high protein yields necessitate a reduced protein modification in the malting process to achieve high taste stability in the final product.

References

1. Schieberle P., Komarek D. (2002) In *Freshness and Shelf Life of Foods* (K.R. Cadwallader, H.P. Weenen, eds.), ACS, pp. 70-79.
2. Methner F.J., Fritsch H., Stephan A. (2003) In *Proceedings of the 29th EBC congress* (European Brewery Convention ed.), Fachverlag Hans Carl, pp. 732-739.
3. Stephan A., Fritsch H., Stettner G. (2006) In *Developments in Flavor Science 43* (Bredie, W., Petersen M., eds.), Elsevier, pp 265-268.
4. Stephan A., Sieren B., Weber T., Stettner G. (2008) In *Recent Highlights in Flavor Chemistry & Biology* (Hofmann T., Meyerhof W., Schieberle P., eds.), Deutsche Forschungsanstalt für Lebensmittelchemie, pp 328-331.
5. Fritsch H., Stephan A., Stettner G., Methner F.-J., Schieberle P. (2005) In *Proceedings of the 30th EBC congress* (European Brewery Convention ed.), Fachverlag Hans Carl, pp 886-893.
6. Anger H.M. (2006) Brautechnische Analysemethoden Band I, Selbstverlag der MEBAK.
7. Stephan A. , Kusche M., Stettner G. (2007) In *Proceedings of the 31th EBC congress* (European Brewery Convention ed.), Fachverlag Hans Carl, pp 220-225.

HS-SPME GC-MS ANALYSIS OF FRESH AND RECONSTITUTED ORANGE JUICES

A. DE WINNE and P. Dirinck

Laboratory for Flavour Research, Catholic Technical University Sint-Lieven, K.U. Leuven Association, Gebr. Desmetstraat 1, BE-9000 Gent, Belgium

Abstract

In this study, the volatile flavour components of freshly squeezed orange juices and commercial processed orange juices were investigated. The freshly squeezed oranges were obtained from three different orange brands. Sampling of the processed orange juices consisted of one refrigerated fresh juice and four reconstituted juices packed in Tetrabrik or glass. Aroma components of all juices were extracted with headspace-solid phase micro extraction followed by gas chromatography-mass spectrometry. Semi-quantitative data, obtained from GC-MS profiling were statistically treated by multivariate analysis. Principal Component Analysis clearly demonstrated differences between freshly squeezed, refrigerated fresh and reconstituted orange juices. The volatile composition of the juices was influenced by the type of processing and also by the packaging. The analytical results were related with a ranking test for six descriptors by a trained laboratory panel (n= 12). Good correlations were obtained between analytical and sensory data.

Introduction

Orange juice is one of the most appreciated drinks and it is accepted all over the world. Its fresh and uniquely delicate flavour is due to complex combinations of several odour components (1). There is still an important flavour difference between freshly squeezed orange juices and commercially processed orange drinks (2-5). The sensory quality is of great importance to the consumer and several studies have shown that the aroma composition changes during storage (6). Nisperos-Carriedo and Shaw (2) found the most important changes in volatile components in juices that were reconstituted from concentrates, packaged by aseptic means and stored at room temperature. Further more, the cultivars of "Valencia" oranges (2-4), Brazilian "Pera" (5) and Turkish "Kozan" oranges (7) have been investigated. Static and dynamic headspace analyses were often used to determine the volatiles in different orange juice samples and orange cultivars (2, 4). Recently, the HS-SPME sampling method combined with gas chromatography mass spectrometry was used for the qualitative and quantitative analyses of volatile compounds in the headspace of the orange juice (8, 9) and lemon varieties (10).

The aim of this study was to analyse the volatile components in three freshly squeezed juices (no packaging) and five packed orange juices (Tetrabrik or glass) and to relate the volatile composition to sensory differences. Differences in volatile composition among the different packaging systems were also demonstrated.

Experimental

Fruit juice samples. Sampling consisted of five different commercial orange juices and three freshly squeezed orange juices as presented in (Table 1). The freshly squeezed juices were obtained from three different orange brands and bought in local food stores.

Table 1. Evaluated fresh and processed orange juices.

Code	Type of juice	Type of packaging	Volume
BG	fresh	no	
CA	fresh	no	
PA	fresh	no	
TO	refrigerated fresh juice	Tetrabrik	1 l
MM	reconstituted with pulp	Tetrabrik	0,2 l
AS	reconstituted	Tetrabrik	1,5 l
GA	reconstituted with pulp	glass	1 l
LZ	reconstituted	glass	0,2 l

Sensory analysis. A ranking test with a panel of 12 panellists was performed comparing all processed orange juices with one of the freshly squeezed orange juice. The fresh juice (BG) was used as reference sample. Six descriptors were evaluated: aroma intensity, fresh flavour, sweetness, pulp, taste of water and bad aftertaste. Panel members were asked to organize the samples from low to high of the respective parameter.

Sample preparation. Isolation of the volatiles was performed by headspace-solid phase micro extraction (HS-SPME) with a 100 μ m PDMS fibre (Supelco®, USA). Aliquots of 10 ml of reconstituted or fresh orange juice were poured into 20 ml vials and sealed with PTFE lined caps. Prior to HS-SPME, samples were allowed to equilibrate at 60 °C under agitation for 15 min. The volatiles were extracted for 30 minutes at 60 °C.

Gas Chromatography-Mass Spectrometry (GC-MS) - Principal Component Analysis (PCA). A HP-6890N/5973 GC-MS system (Agilent Technologies®), with a PONA column (HP 50 m x 0,2 mm i.d., film thickness 0,50 μ m, Agilent Technologies®) was used under the following conditions: initial oven temperature was hold at 40 °C for 5 min., then programmed from 40 to 110 °C at 10 °C/min, from 110 to 180 °C at 2 °C/min, from 180 to 250 °C at 10 °C/min and finally maintained 6 min at 250 °C. Injection was performed in the splitless mode. The mass spectra were obtained by electron impact at 70eV. Identification of the volatiles was based on comparison of the spectra with the spectra of the Wiley library. Semi-quantitative determinations of the volatile components were calculated by relating the peak intensities to the intensity of nonane as internal standard and were expressed as μ g/l of juice. For interpretation of the semi-quantitative data of respectively the reconstituted and fresh orange juices and for visualization of the relationships between the different samples and their volatile composition, principal component analyses were performed using Unscrambler® 6.1 (Camo, Norway) statistical software.

Results and Discussion

The fresh orange sample BG was significantly evaluated as the sweetest sample with the freshest flavour, the highest level of pulp and with the lowest bad aftertaste. The reconstituted sample in glass GA had significantly lower fresh flavour, probably due to a bad aftertaste. Also the other sample packed in glass LZ scored low in freshness and in aroma intensity. Apart from the reference sample BG, the samples TO and AS scored high for fresh flavour and sweetness. The sample MM had the lowest amount of pulp.

Aroma profiles were obtained by HS-SPME-GC-MS. Especially aldehydes, esters and terpenes were identified. (Figure 1) illustrates a histogram of the sum of the concentrations ($\mu\text{g/l}$) of the identified monoterpene hydrocarbons quantified in all analysed fruit juices. The highest concentrations of monoterpenes were found in the juices GA and LZ, the reconstituted orange juices, packed in glass. These monoterpenes were more volatile and were probably better kept due to the glass packaging. In the Tetrabrik packaging, an important part of them was lost. The polyethylene liner of the package could absorb some of the flavour components. In relation with the sensory test, the samples GA and LZ were evaluated as samples with a less fresh taste. The higher level of monoterpene hydrocarbons in these samples probably added an undesirable character to the orange juice. According to Shaw (1), the essential oil of orange peel contains high levels of limonene and a high peel oil level could contribute to a bitter flavour. The juice GA had also a high α -pinene content, which could reflect addition of amounts of peel oil by processors.

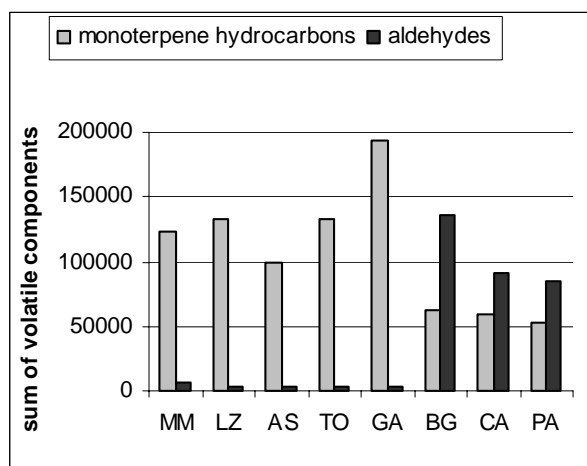


Figure 1. Histogram of the sum of concentrations of monoterpene hydrocarbons and aldehydes ($\mu\text{g/l}$ juice), in all orange juices

Variation in aldehyde content among the processed and fresh products is also shown in (Figure 1). Generally, the fresh orange juices showed higher aldehyde levels. Octanal and decanal were considered as important contributors to orange flavour (2, 7). Shaw (1) and Buettner and Schieberle (6) proved that the fruity ethyl butanoate and the citrus-like decanal were the most potent odorants in Valencia Late and Navel Oranges. In relation with the sensory test, the reference freshly squeezed sample BG was evaluated as the sample with the freshest taste.

Principal component analysis (PCA) of the HS-SPME-GC-MS profiles allowed a good classification between fresh orange juice and reconstituted orange juice (Figure 2). All freshly squeezed samples had a positive PC1-score (61%) and all processed samples had a negative PC1-score. Shaw et al. (3) showed with headspace GC-

technique that aseptically packaged reconstituted juice had a different profile. The refrigerated fresh orange juice TO had a strong positive PC2-score, the reconstituted orange juices had a negative PC2-score. In the reconstituted orange samples a good classification according to the packaging composition (Tetrabrik or glass) was obtained (not presented). The two orange juices packed in glass were located at the negative PC1-score. The reconstituted orange juice AS, was situated in the middle of the figure. From (Figure 2), one may conclude that the presence of the aldehydes (octanal, neral and geranial) and the esters (ethyl octanoate and ethyl decanoate) are very important for the flavour of a fresh orange juice. The HS-SPME-GC-MS-PCA approach explained the important sensory differences between processed orange juices and freshly squeezed orange juices. The sensory difference could be related to the absence of important aroma components such as aldehydes, and ethyl esters in the reconstituted orange juices.

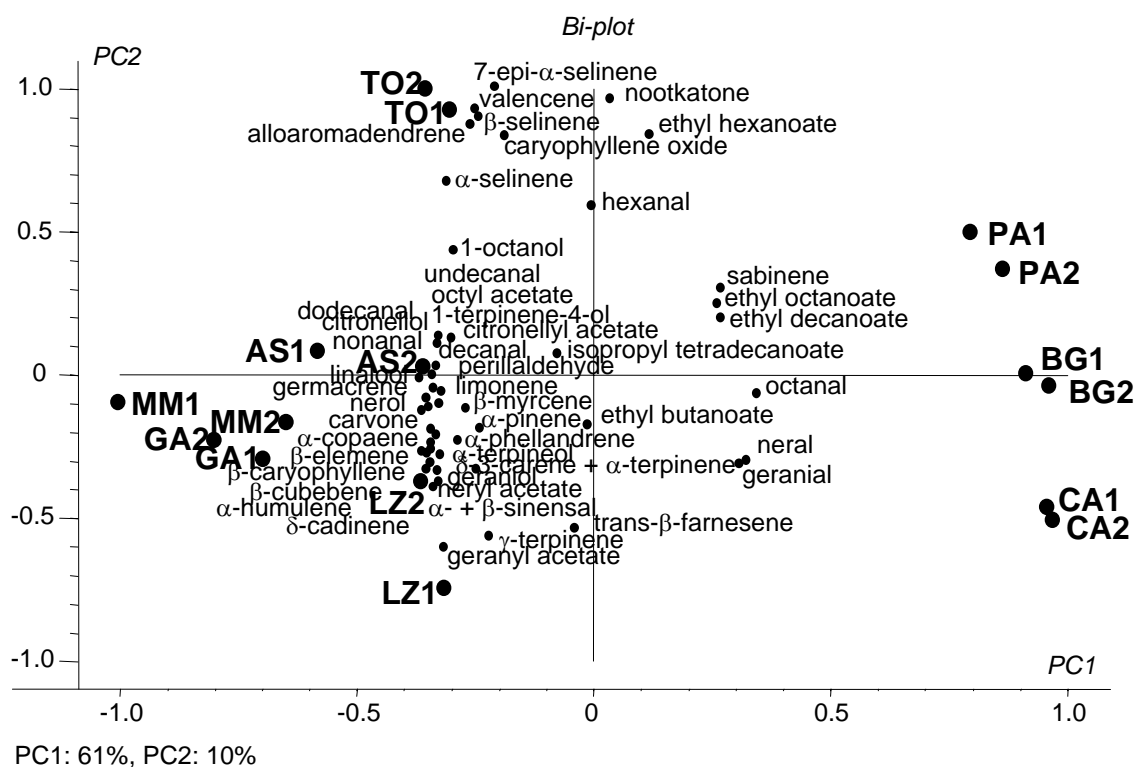


Figure 2. PCA bi-plot of the HS-SPME-GC-MS results of all orange juices.

References

1. Shaw P.E. (1991) In *Volatile Compounds in Foods and Beverages: Fruits II* (Maarse H., ed.), Marcel Dekker, pp 305-328.
2. Nisperos-Carriedo M.O., Shaw P.E. (1990) *J. Agric. Food Chem.* 38: 1048-1052.
3. Shaw P.E., Buslig B.S., Moshonas M.G. (1993) *J. Agric. Food Chem.* 41: 809-813.
4. Moshonas M.G., Shaw P.E. (1994) *J. Agric. Food Chem.* 42: 1525-1528.
5. Tønder D., Petersen M.A., Poll L., Olsen, C.E. (1998) *Food Chem.* 61: 223-229.
6. Buettner A., Schieberle P. (2001) *J. Agric. Food Chem.* 49: 2387-2394.
7. Selli S., Cabaroglu T., Canbas A. (2004) *J. Food Comp. Anal.* 17:789-796.
8. Jia M., Zhang Q.H., Min D.B. (1998) *J. Agric. Food Chem.* 46: 2744-2747.
9. Rega B., Fournier N., Nicklaus S., Guichard E. (2004) *J. Agric. Food Chem.* 52: 4204-4212.
10. Allegrone G., Belliardo F., Cabella P. (2006) *J. Agric. Food Chem.* 54: 1844-1848.

FATE OF POLYFUNCTIONAL THIOLS IN SAUTERNES WINES THROUGH AGEING

S. Bailly and S. COLLIN

Université catholique de Louvain, Unité de brasserie et des industries alimentaires, Croix du Sud, 2 bte 7, B-1348 Louvain-la-Neuve, Belgium

Abstract

Recent papers have revealed the importance of polyfunctional thiols in fresh Sauternes wines (1, 2), but very little is yet known about the fate of such compounds during aging in the bottle. Here it is shown that most polyfunctional thiols with roasted or citrus notes (3-sulfanylpropyl acetate, 2-sulfanylethyl acetate, 3-methyl-3-sulfanylbutanal, and 3-sulfanylheptanal) are degraded within a year upon bottle aging in a cellar. Only 3-sulfanylhexan-1-ol was still found in aged samples at concentrations above its threshold value. Most other key aromas previously found in the fresh noble rot wine are still present in aged samples: varietal aroma (α -terpineol), sotolon, fermentation alcohols (3-methylbutan-1-ol and 2-phenylethanol) and esters (ethyl butyrate, ethyl hexanoate and ethyl isovalerate), carbonyls (*trans*-non-2-enal and β -damascenone), and wood flavours (guaiacol, vanillin, eugenol, β -methyl- γ -octalactone and furaneol).

Introduction

Sauternes wines are traditional AOC French wines made from cv Sauvignon Blanc, Semillon, or Muscadelle grapes contaminated by noble rot (*Botrytis cinerea*). Recent papers have revealed the importance of polyfunctional thiols in fresh Sauternes wines (1,2). A few studies were dedicated to the fate of polyfunctional thiols during ageing in the bottle (3,4,5). In the present work, polyfunctional thiols were monitored through cellar aging of Sauternes wines.

Experimental

Wine samples. Sauternes wines samples were a kind gift from Château Guiraud, Sauternes, France. W-2002 sample was taken just after bottling (18 months of maturation in oak barrels, vintage 2002) and analysed after 1,5 and 3 years of storage in a wine cellar ($14^{\circ}\text{C} \pm 2^{\circ}\text{C}$).

XAD 2 and pHMB extraction procedures were used, according to Bailly *et al.* (1) and Lermusieau *et al.* (6).

Gas chromatography analyses with Olfactometric Detection (GC-O). 1 μL extract was analysed with a Chrompack CP9001 gas chromatograph equipped with a splitless injector maintained at 250°C ; the split vent was opened 0.5 min post-injection. Compounds were analysed using wall-coated open tubular apolar CP-Sil 5-CB (50m x 0.32 mm i.d., 1.2 μm film thickness) and polar FFAP (25m x 0.32 mm i.d., 0.3 μm film thickness) capillary columns. The carrier gas was nitrogen and pressure was fixed to 50 kPa (CP-Sil 5-CB) or 30 kPa (FFAP). The oven temperature was programmed to raise from 36°C to 85°C at $20^{\circ}\text{C}/\text{min}$, then to 145°C at $1^{\circ}\text{C}/\text{min}$, and

finally to 250°C at 3°C/min. Extracts were analysed by three panellists and complete AEDA was performed by two of them on CP-Sil 5-CB column. The extracts were diluted stepwise with diethyl ether (1+2 by volume). The dilution factor (FD) is defined as the dilution where the compound can still be detected.

Gas chromatography analyses with PFPD (GC-PFPD). 2 µL of pHMB extract was analysed on a ThermoFinnigan Trace GC 2000 gas chromatograph connected to a ThermoFinnigan Trace PFPD detector and equipped with a splitless injector maintained at 250°C; the split vent was opened 1 min post-injection. The carrier gas was helium at a flow rate of 1.7 mL/min. Compounds were analysed using an apolar CP-Sil5-CB capillary column as described above. The oven temperature was programmed to stay for 4 min at 40°C, and then raised from 40°C to 132°C at 2°C/min, then to 250°C at 10°C/min.

Results

In a previous work (1), we determined key odorants of two Sauternes wines by GC-O AEDA (7) applied to Amberlite XAD 2 resin extracts. This extraction method allowed recovery yields above 75%, except for small hydrophilic lactones such as sotolon. Various complementary techniques have been used to identify the odorants: co-injection of commercial standards or combinatorial synthesis products (8,9) on one or two capillary columns, GC-MS, GC-PFPD on pHMB extract, and odour description at the sniffing port (especially when no peak was available with the usual detectors).

Among the key odorants, α -terpineol (floral, musty orange with FD= 81-243) is a well-known grape constituent present in free or glycoside form. Fermentation modifies the aroma profile, with production of many alcohols, esters, and acids. Fusel alcohols such as 3-methylbutan-1-ol (alcohol, chocolate with FD= 243-729) and 2-phenylethanol (co-eluting with linalool ; rose, wine with FD= 243-729) are present in considerable amount. Fermentation ethyl esters are also produced (ethyl butyrate, acid fruit, liquor with FD= 81; ethyl hexanoate, syrup, acid fruit, green apple with FD= 27-243 ; ethyl isovalerate, red fruit with FD= 81-243), bringing some fruity aromas to the wine. A few unreduced carbonyls such as β -damascenone (stewed fruit, peach with FD= 81-243) and *trans*-non-2-enal (cardboard, rubber with FD= 9-243) show high dilution factor values. Among the key odorants, oak-derived flavours are also of prime importance. Guaiacol (wood, phenolic with FD= 81-243), eugenol (hay tree, dental with FD= 27-81), vanillin (vanilla, cake with FD= 9-81), β -methyl- γ -octalactone (sweet, coconut, butter with FD= 243) and γ -nonalactone (sweet, coconut with FD= 27-81) are genuine wood-extractable compounds (10). Furaneol (cotton candy with FD= 27-81) is one of the compounds responsible for the “toasty caramel” aroma. Finally, sotolon (caramel, curry with FD= 81-243) brings the sweetened aroma to botrytized wines. Also worth mentioning is the presence of many polyfunctional thiols: 3-sulfanylpropyl acetate (olive, bacon, plastic with FD= 27-81), 3-sulfanylhexan-1-ol (fruity, rhubarb with FD= 81-729), 3-sulfanylheptanal (fruity, lemon with FD= 81-2187), 2-(sulfanylmethyl)hexan-1-ol (unpleasant, floral with FD= 9-81), 3-methyl-3-sulfanylbutanal (petroleum-like with FD= 0-27), and 2-methylfuran-3-thiol (bacon-like with FD = 27-81). A synergistic effect is suspected between the two latter thiols.

As shown in Table 1, most varietal aromas, fermentation esters, and wood flavours previously found in fresh noble rot wines are still present in aged samples. On the other hand, most polyfunctional thiols with roasted or citrus notes (3-sulfanylpropyl acetate, 2-sulfanylethyl acetate, 3-methyl-3-sulfanylbutanal, 3-sulfanylheptanal) (Table 2) proved to be degraded within a year, upon of bottle aging in a cellar. Oxidation (thiol and/or aldehyde) and ester hydrolysis are most probably

the main phenomena responsible for this disappearance. The same profile has been observed in vintage 2003 still under investigation (data not shown).

Table 1. Evolution of varietal, fermentation, oak and noble rot key-odorants during the ageing in bottle of a 2002 Sauternes vintage. GC-O AEDA ($FD=3^{n-1}$ with n = number of dilutions before no detection) in XAD 2 extracts.

RI		Substance ^a	Odour	FD-factor		
CPSi5	FFAP			fresh	1.5 year	3 years
		Varietal aroma				
1179	1706	α -Terpineol (2-(4-methylcyclohex-3-en-1-yl)propan-2-ol)	Floral, musty orange	243	81	243
		Fermentation compounds				
707	1217	3-Methylbutan-1-ol	Alcohol, chocolate	243	81/243	729
770	969	Ethyl butyrate (ethyl butanoate)	Acid fruit, liquor	81	81	81
828	1114	Ethyl isovalerate (ethyl 3-methylbutanoate)	Red fruit	243	81	243
975	1241	Ethyl hexanoate	Syrup, acid fruit, green apple	243	81	81
1090	1921	2-Phenylethan-1-ol and Linalool (3,7-dimethylocta-1,6-dien-3-ol)*	Rose, wine	243	243	243
		Influence of oak maturation				
1025	1992	Furaneol (4-hydroxy-2,5-dimethylfuran-3(2H)-one)	Cotton candy	81	81	27
1063	1873	Guaiacol (2-methoxyphenol)	Wood, phenolic, spicy	81	243	27/81
1130	1497	<i>trans</i> -non-2-enal	Cardboard, rubber	9	27	27
1281	1968	β -Methyl- γ -octalactone	Sweet, cocoa, butter	243	243	729
1322	2032	γ -Nonalactone	Sweet, cocoa, butter	27	27	27
1337	1835	Eugenol (4-allyl-2-methoxyphenol)	Hay tree, dental	81	81	81
1360	2555	Vanillin (4-hydroxy-3-methoxybenzaldehyde)	Vanilla, cake	81	81	27
1368	1818	β -Damascenone	Stewed fruit, peach	81	81	243
		Botrytis cinerea or oxidation compound				
1068	2213	Sotolon (3-hydroxy-4,5-dimethylfuran-2(5H)-one)	Caramel, praline, curry	243	243	243

*: Co-elution of both compounds;

^a: Coincidence of GC retention indices, odours on two capillary columns (CP-Sil5-CB and FFAP-CB), and mass spectrometric data with those of pure compounds available.

Only 3-sulfanylhexasan-1-ol (grapefruit) proved to survive, suggesting the existence of a pool protected against oxidation. A concentration 50 times above its threshold value (60 ng/L (11)) is still measured in vintage 2002 after 3 years.

This work has also revealed two very interesting compounds which are generated through aging: abhexon (ethyl analogue of sotolon), never mentioned before in sweet wines, and raspberry ketone. Unfortunately, as previously shown for sotolon, the usual XAD-2 extraction does not allow very efficient recovery of hydrophilic molecules like abhexon. A modified protocol is therefore required to improve quantification of this spicy aroma in aged wine.

Table 2. Evolution of thiols during the ageing in bottle of a 2002 Sauternes vintage. GC-O AEDA ($FD=3^{n-1}$ with n = number of dilutions before no detection) in XAD2 extracts or IST equivalents ($\mu\text{g/L}$) from GC-PFPD on pHMB extracts.

RI		Substance	Odour	FD-factor			IST equivalents ($\mu\text{g/L}$)		
CPSil5	FFAP			1.5 fresh	3 year	3 years	1.5 fresh	3 year	3 years
845	1653	3-Methyl-3-sulfanylbutanal ^b	Petroleum, bacon	27	0	0			
845	1306	2-Methylfuran-3-thiol ^a	Petroleum, bacon	81	27	27			
884		2-Sulfanylethyl acetate ^a	Roasted	9	0	0	0.3	0	0
989	1565	3-Sulfanylpropyl acetate ^a	Olive, bacon, plastic	81	3	3	0.8	0	0
1096	1853	3-Sulfanylohexan-1-ol ^a	Fruity, rhubarb, grapefruit	81	81	729	4.5	3	3
1118	1659	3-Sulfanyloheptanal ^b	Fruity, lemon	2187	0	0			
1217	1985	2-(Sulfanylmethyl)-hexan-1-ol ^b	Unpleasant, floral	81	n.d.	n.d.			

a: Coincidence of GC retention indices, odours on two capillary columns (CP-Sil5-CB and FFAP-CB), and mass spectrometric data with those of pure compounds available;

b: Coincidence of GC retention indices and odours on two capillary columns (CP-Sil5-CB and FFAP-CB) with those of pure standards.

References

- Bailly S., Jerkovic V., Marchand-Brynaert J., Collin S. (2006) *J. Agric. Food Chem.* 54 : 7227-7234.
- Sarrazin E., Shinkaruk S., Tominaga T., Bennetau B., Frerot E., Dubourdieu D. (2007) *J. Agric. Food Chem.* 55 : 1437-1444.
- Murat M.L., Tominaga T., Saucier C., Glories Y., Dubourdieu D. (2003) *Am. J. Enol. Vitic.* 54 : 135-138.
- Tominaga T., Guimbertau G., Dubourdieu D. (2003) *J. Agric. Food Chem.* 51: 1016-1020.
- Tominaga T. (1998). *Thèse de l'Université de Bordeaux 2*.
- Lermusieau G., Bulens M., Collin S. (2001) *J. Agric. Food Chem.* 49(8): 3867-3874.
- Grosch W. (1994). *Flav. Fragr. J.* 9: 147-158.
- Vermeulen C., Collin S. (2002) *J. Agric. Food Chem.* 50 : 5654-5659.
- Vermeulen C., Pellaud J., Gijs L., Collin S. (2001). *J. Agric. Food Chem.* 49: 5445-5449.
- Jarauta I., Cacho J., Ferreira V. (2005) *J. Agric. Food Chem.* 53: 4166-4177.
- Tominaga T., Murat M-L., Dubourdieu D. (1998) *J. Agric. Food Chem.* 46: 1044-1048.

AROMATIC PROFILE OF OXIDISED RED WINES

M. AZNAR^{1,2}, T. Balboa¹, T. Arroyo¹, and J.M. Cabello¹

¹ *Departamento de Agroalimentación, IMIDRA, Finca “El Encín” A2 Km 38.2, Alcalá de Henares 28800, Madrid, Spain*

² *Departamento de Química Analítica, Centro Politécnico Superior de Ingenieros, C/Maria de Luna 3, Zaragoza 50018, Spain*

Abstract

Oxidative degradation of wine has negative effects on its aroma quality. White wines oxidation has been studied and the development of descriptors such as “cooked vegetables” or “honey-like” as well as the decrease of fresh and fruity aromas related to the variety has been linked to oxidation processes. The aim of this work was the study of the aromatic profile of 3 oxidised red wines and a non-oxidised wine by GC-Olfactometry (GC-O) and the relationship between olfactometric data with sensory analysis. Results showed that the decrease of fruity and flowery notes observed in the sensory analysis was linked to a decrease in compounds such as *cis*-3-hexenol, linalool or 2-phenylacetate in the GC-O. Even though typical white wine descriptors such as “cooked vegetables” or “honey-like” were found in the red oxidised wines, new descriptors with higher intensity were found such as “cognac-brandy-sherry” or “overripped fruit”, some compounds that increased their intensity in GC-O and could be linked to these aromas were methional, *trans*-2-octenal, decanal, dodecanal, homofuraneol, 2-methyl-3-furanthiol and some fusel alcohols

Introduction

Redox reactions are responsible for important changes in the wine's chemical composition. The “oxidative spoilage” comprises the loss of fruit and floral aromas, the development of off-flavours such as “honey-like”, “boiled-potato” or “farm-feed” and early yellowing or browning, which implies a loss of quality in the white wines (1,2). The aim of this work was the study of the aromatic profile of natural oxidised red wines and the relationship between sensory analysis and olfactometric data.

Experimental

Wines. One non-oxidised red wine (NOW1) and 3 natural oxidised wines (OW1, OW2, OW3) were selected on the basis of their aroma and oxidation level.

Analyses. The antioxidative capacity of the samples was checked by the Photochemoluminescence Photochem® method. Sensory analyses of the wines were performed by a trained panel; the panel was trained to identify the aroma of reference solutions with typical wine aromas. Two tasting cards were used, a general terms tasting card (Figure 1), designed in previous wine tastings by wine experts, and an oxidative terms tasting card (Figure 2) this card was prepared following the AFNOR (NFV-09_021) procedure For GC-Olfactometric analysis, extracts were obtained by dynamic headspace extraction (3). Olfactometry was carried out by 8 trained panellists. They evaluated the aroma description and intensity, the intensity

was measured by a 4-point category scale (0 = not detected; 1 = weak, hardly recognizable odour; 2 = clear but not intense odour and 3 = intense odour). Results were expressed as modified frequency percentage: $\%MF = (\%C \times \%I)^{1/2}$, which takes into account the percentage of citation (%C) and the intensity of the aroma detected (%I)

Results

Antioxidative capacity measurement. Antioxidative capacity of the non oxidised red wine (44.24 g/L of ascorbic acid equivalents) was around 10 times higher than that of the oxidised wines (OW1: 3.76, OW2: 4.60, OW3: 4.50 g/L of ascorbic acid equivalents).

Sensorial wine tasting. General terms tasting card (Figure 1): The average intensity of the terms “fruity”, “flowery”, “herbal”, “lactic-yeast” and “chemical” decreased during wine oxidation; while “spicy” and “phenolic” did not change and, obviously, “oxidation” and “off-flavours” terms increase. Oxidative terms tasting card (Figure 2): The terms more frequently used in oxidised wines were “very ripe fruit-raisin-overripe fruit”, “cognac-brandy-sherry” and “old/evolved wine” with frequencies of citation higher than 60%. Other terms such as “honey-molasses”, “varnish-paint-glue-resin-rubber-solvent” and “liquorice-curry” reached also values between 30 and 42%. Nevertheless, other terms with high importance in oxidised white wines (4), such as “cooked potatoes”, “hay-dry grass-straw” or “herbal-plant stem-tannin”, obtained frequency values below 20%, and for the last two terms the frequency of citation was even higher for the non-oxidised wines.

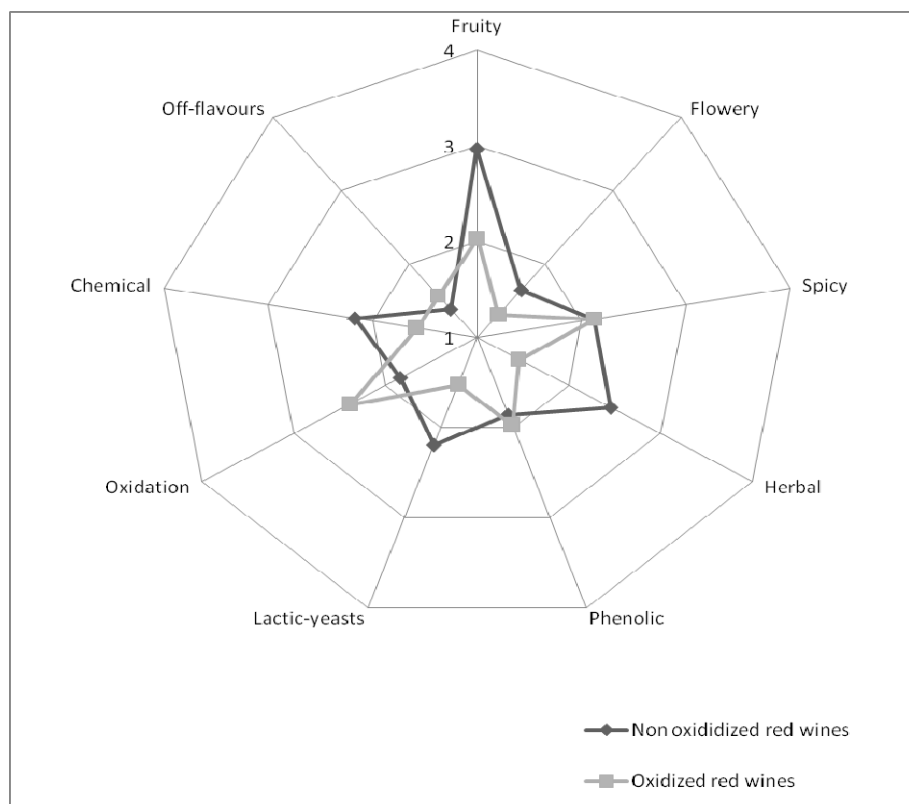


Figure 1. Citation frequency of oxidative terms for a non oxidised wine (NOW1) and 3 oxidised wines (OW1, OW2, OW3).

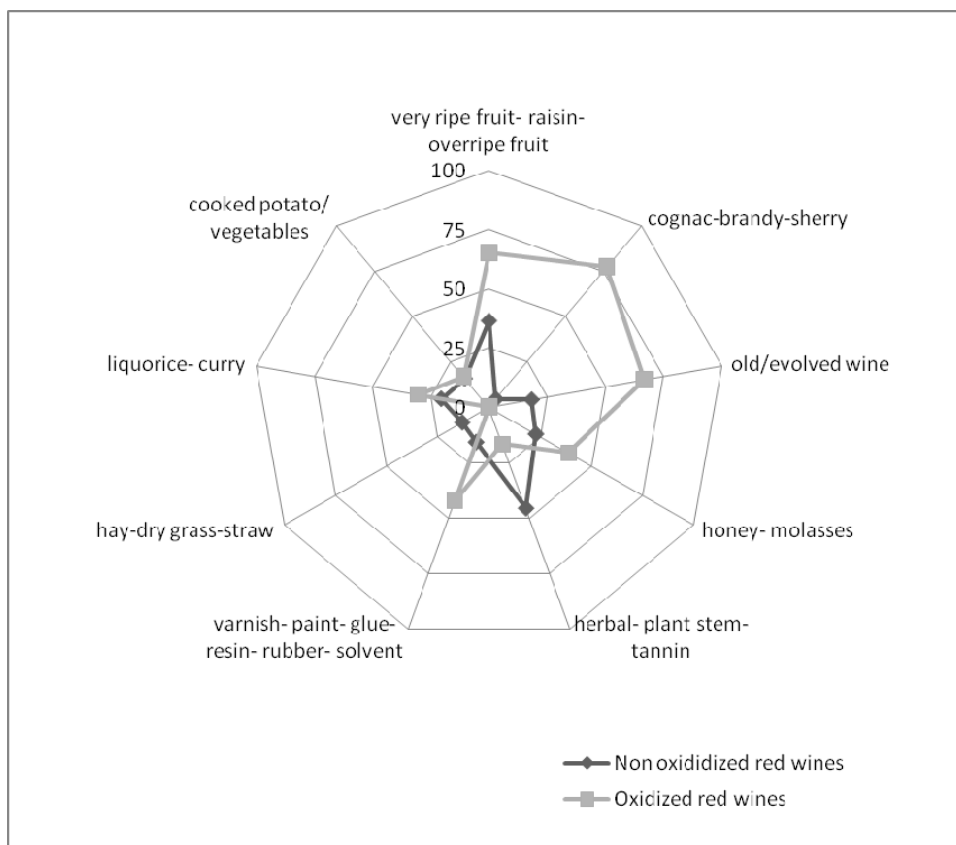


Figure 2. Intensity of general terms for a non oxidised wine (NOW1) and 3 oxidised wines (OW1, OW2, OW3).

GC-Olfactometric analysis. Results from GC-O (Table 1) showed the increase or decrease on the intensity of some volatiles whose aroma could be related to the differences found between non-oxidised and oxidised wines during the sensory analysis. It was observed that certain volatiles with fruity, herbal or flowery aromas such as *cis*-3-hexenol, linalool, 2-phenylethyl acetate or β -damascenone, had lower values in the oxidised wines, which explains the low values of these descriptors in the sensory analysis. Some volatiles with spicy or phenolic aromas such as eugenol, m-cresol or 2,6-dimethoxyphenol did not showed differences between oxidised and non-oxidised wines as it occurred in the sensory analysis. Nevertheless, guaiacol, 4-ethylphenol or isoeugenol showed lower %MF in the oxidised wines. Probably the aroma intensity of the first ones did not allow panellist to detect differences in these descriptors during the tasting. Finally, volatiles in italics were volatiles with oxidative related descriptions that showed higher %MF values in the oxidised wines. Among these volatiles we found compounds with cooked potatoes aromas, such as methional, compounds with chemical, dry, green, straw and solvent aromas, such as *trans*-2-octenal, decanal or dodecanal; compounds with sweet aromas, such as homofuraneol, ethyl-2-methyl pentanoate or ethyl-4-methyl pentanoate and compounds with “dense” aromas such as 2-methyl-3-furanthiol or some fusel alcohols. The high values of these volatiles in oxidised wines could be related to descriptors such as “cooked potatoes”, “varnish-paint-glue-resin-rubber-solvent” or “very ripe fruit-raisin-overripe fruit”.

Table 1. Kovats index (KI), aroma description and %MF values of some of the volatiles found during the GC-O analysis of a non oxidised wine (NOW1) and 3 oxidised wines (OW1, OW2, OW3).

KI	Descriptor	Compound	NOW	OW1	OW2	OW3
1144	fruity, anise	<i>ethyl 2-methylpentanoate</i> ^b	0	14	40	6
1196	fruity, anise	<i>ethyl 4-methylpentanoate</i> ^b	0	27	34	47
1356	hay, burnt	<i>2-methyl-3-furanthiol</i> ^d	0	18	47	35
1388	flowery, green	cis-3-hexenol	47	20	28	19
1427	chemical	<i>trans-2-octenal</i> ^b	0	0	68	11
1467	cereals, dirty grass	<i>methional</i> ^b	0	38	23	27
1508	chemical	<i>decanal</i> ^c	0	0	0	43
1559	fresh fruit, flowery	linalool ^a	23	0	13	11
1730	green, bitter almond	<i>dodecanal</i> ^d	0	22	7	17
1812	flowery, lilac	2-phenylethyl	34	27	27	19
1832	peach, baked apple	β -damascenone ^a	79	61	44	36
1882	veterinary, toasty	guaiacol ^b	48	28	31	6
2100	sweet, cake	<i>homofuraneol</i> ^b	0	20	43	0
2147	veterinary, bitumen, stable, wood	m-cresol ^a	31	29	29	11
2236	chemical, phenolic, bitumen, burnt	4-ethylphenol ^b	31	0	0	0
2308	species, incense	2,6-dimethoxyphenol ^b	19	0	7	17
2334	flowery, phenolic	isoeugenol ^b	30	18	7	18

^a Identification based on retention time, aroma and mass spectrum,

^b Identification based on retention time and aroma,

^c Identification based on aroma, mass spectrum and bibliography KI,

^d Identification based on aroma and bibliography KI

Volatiles in *italics* are those with descriptors related to oxidative degradation

Acknowledgments

This work has been funded by the Spanish INIA (Project RTA2005-00172); Spanish INIA PhD grant n°19 (BOE num. 208, 31/08/2006).

References

1. Silva Ferreira A., Oliveira C., Hogg T., Guedes de Pinho P. (2003) *J. Agr. Food Chem.* 51: 4668-4672.
2. Silva Ferreira A., Guedes de Pinho P., Rodrigues P., Hogg, T. (2002). *J. Agr. Food Chem.* 50: 5919-5924.
3. Campo E., Ferreira V., Cacho J. (2005) *J. Agr. Food Chem.* 53: 5682-5690.
4. Escudero A., Asensio E., Cacho J., Ferreira V. (2002) *Food Chem.* 77: 325-331.

INHIBITION OF LIGHT-INDUCED OFF-FLAVOUR DEVELOPMENT BY SINGLET OXYGEN QUENCHERS IN CLOUDY APPLE JUICE

M. HASHIZUME¹, M.H. Gordon², and D.S. Mottram²

¹ *Glico Dairy Products Co., Ltd., Institute for Technical Research, 2-14-1 Musashino, Akishima-shi, Tokyo, 1960021, Japan*

² *Department of Food Biosciences, University of Reading, Whiteknights, Reading, RG6 6AP, UK*

Abstract

Beverage companies sometimes receive reports that cloudy fruit juices have developed a “metallic flavour” when they are exposed to light, which results in consumer complaints. These degradations have been shown to be caused by photooxidation, in which singlet oxygen played an essential role. In the present study, aqueous antioxidants, such as crocin, crocetin, and norbixin, have been investigated. The development of seven off-flavour compounds was monitored in cloudy apple juices from concentrates stored in glass bottles under fluorescent light (3000 lx, 8 °C). It was found that crocin, known to be a singlet oxygen quencher and a food colouring additive, was effective in inhibiting the development of light-induced off-flavour.

Introduction

Cloudy apple juice develops a metallic flavour when it is exposed to light (1). Off-flavour induced by fluorescent lights in reconstituted cloudy apple juice was analysed by SPME-GC-MS and seven volatile compounds; pentanal, 2-methyl-1-penten-3-one, hexanal, 1-octen-3-one, (*E*)-2-heptenal, 6-methyl-5-hepten-2-one, and (*E*)-2-octenal, were found to increase significantly in the cloudy apple juice after light exposure and this could contribute to the off-flavour (2). The current approach to avoiding the development of light-induced off-flavour in beverages is through the choice of packaging materials. Opaque cans, bottles and aluminium-paper cartons inhibit photooxidation by protecting juice from light. In addition, glass bottles are impermeable to oxygen (3) and effective in inhibiting photooxidation in spite of light transparency. When the initial dissolved oxygen in cloudy apple juice is low and the headspace is small enough that little oxygen is present in the bottle, the formation of off-flavours in the juice is low because of the limited availability of oxygen (4). However, these approaches are relatively passive ways to inhibit off-flavour formation and the effect of other relevant factors should be studied. Singlet oxygen may play a role in the formation of lipid peroxides in the presence of light. Many compounds including synthetic and natural components are reported to act as singlet oxygen quenchers, but most are insoluble in water (e.g. canthaxanthin, β -carotene, lycopene, and zeaxanthin). Three singlet oxygen quenchers were chosen and their effect on the photooxidation of cloudy apple juice has been evaluated.

Experimental

Samples. Apple juice concentrates (40° Brix), to which ascorbic acid had been added for the inhibition of browning in juice, were reconstituted to 12° Brix. The samples were stored in glass bottles with 30% air headspace, exposed to 3000 lx fluorescent lights and kept at 8 °C for 40 h in a cold storage room. Simultaneously, equivalent samples were stored in the dark as a reference control. The singlet oxygen quenchers used in the study were water soluble and dissolved by adding them directly into the reconstituted apple juice.

Analysis of volatiles. Twenty grams of cloudy apple juice, an internal standard (750 ng bromobenzene) and a stirring bar were placed in a 40 mL vial and capped with a PTFE septum. Solid phase microextraction (SPME) was performed with a 75 µm carboxen/ polydimethylsiloxane (PDMS) fibre. The SPME fibre was exposed to the sample headspace at 35 °C for 45 min. Each sample was analysed in triplicate. A Hewlett-Packard 6890 Series GC coupled to a 5973 Series MSD was used for analysis. The column was a 60 m INNOWAX column (i.d. 0.25 mm, 0.25 µm, Agilent, Inc., USA). The oven temperature was kept at 40 °C for 2 min and programmed to increase at 4 °C per minute. The final temperature was 240 °C and was held for a further 10 min. The temperature of the injector was 250 °C. The GC Linear Retention Indices (LRI) of the isolated compounds were determined externally with a mixture of hydrocarbons (C6-C25) which were run under the same conditions. The relative peak areas of off-flavour compounds were estimated by comparing the peak areas in the selected ion chromatogram (m/z 44 for pentanal, m/z 69 for 2-methyl-1-penten-3-one, m/z 56 for hexanal, m/z 70 for 1-octen-3-one, m/z 83 for (*E*)-2-heptenal, m/z 108 for 6-methyl-5-hepten-2-one, and m/z 83 for (*E*)-2-octenal) with that of the internal standard (m/z 158), and the proportion of each compound (%) was calculated relative to the amount present in the light-exposed control after 40 h.

Results and Discussion

Crocin (crocetin di-gentiobiose ester) is one of the carotenoids extracted from Saffron (*Crocus sativus* L.). It is well soluble in water and can be commercially obtained as a chemical reagent (Sigma-Aldrich K.K., Japan). According to Manitto et al. (5), the rate constant for quenching singlet oxygen in water is $1.8 \times 10^9 \text{ M}^{-1}\text{s}^{-1}$. By adding crocin (25-250 mg/l) to the reconstituted apple juice, the formation of off-flavour compounds was reduced significantly compared to the light-exposed control (Figure 1). The apparent amounts of alkanals in the light-exposed crocin-added-sample (250 mg/l) were 74-80% of those in the control. However, the initially existing concentrations of pentanal and hexanal were 33% and 34%, respectively, and when this is taken into account the increased amounts following light-exposure were calculated to be approximately 41-47%. Therefore, the effect on these volatiles is similar to that of other lipid oxidation products (1-octen-3-one, (*E*)-2-heptenal, and (*E*)-2-octenal), since these 3 compounds were formed at approximately 49-55% of the concentration in the light-exposed control. However, the effect of crocin on the formation of 2-methyl-1-penten-3-one and 6-methyl-5-hepten-2-one was different. Although crocin inhibited their formation significantly when compared with the light-exposed control, the relative amounts were 69-78% of those in the control which was higher than those of the other off-flavour compounds.

Crocetin is also extracted from Saffron and obtained from Sigma-Aldrich Japan K.K. Its rate constant for quenching singlet oxygen in water is higher than that of crocin at $2.5\text{-}5.5 \times 10^9 \text{ M}^{-1}\text{s}^{-1}$ (5). It is less soluble than crocin and up to 100 mg/l crocetin could be dissolved (or suspended) in the juice. The addition of a low

concentration (25-50 mg/l) of crocetin resulted in increasing the formation of off-flavours except for pentanal, and it seems crocetin acted as a pro-oxidant.

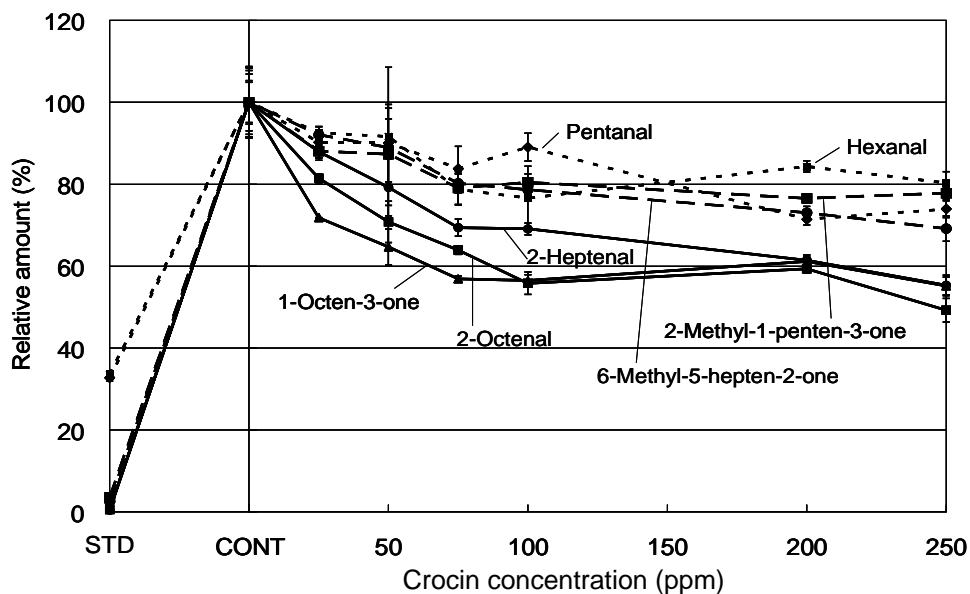


Figure 1. Relative amount (%) of off-flavour compounds in cloudy apple juice following the addition of crocetin in comparison with control juice. Relative amount is calculated with respect to the light-exposed control (CONT; equal to 100%), based on the comparison of peak area in the headspace using bromobenzene as an internal standard. Standard sample (STD) stored in the dark at 8 °C. Error bars show standard deviation from three replicate analyses.

Norbixin (9'-*cis*-6,6'-diapocarotene-6,6'-dioic acid) is extracted from the seeds of the annatto tree (*Bixa orellana*), and is a well-known colour additive for foods. The quenching rate constant in water is $2.3 \times 10^{10} \text{ M}^{-1}\text{s}^{-1}$ (6). The annatto extract was obtained from Saneigen FFI K.K. (Japan). The results with norbixin were similar to those of crocetin. Apparently it acts as a pro-oxidant for the lipid degradation and the formation of 6-methyl-5-hepten-2-one. The formation of hexanal was not changed significantly by the addition of norbixin.

Thus it has been shown that crocetin has a remarkable inhibitory effect on light-induced off-flavour development in cloudy apple juice. However, when crocetin was dissolved in cloudy apple juice, its colour became orange-yellowish and was obviously different from the natural appearance of apple juice. Therefore, it is not practical to use crocetin for inhibiting the photooxidation of cloudy apple juice. It was also shown that not all aqueous singlet oxygen quenchers were effective inhibitors. Further investigation into the mechanism seems necessary.

References

1. Hashizume M., Gordon H.M., Mottram D.S. (2006) In *Flavour Science: Recent Advances and Trends* (Bredie W.L.P., Petersen M.A., eds.); Elsevier Science B.V., pp 273-276.
2. Hashizume M., Gordon H.M., Mottram D.S. (2007) *J. Food Agric Chem.* 55: 9177-9182.
3. Karatapanis A.E., Badeka A.V., Riganakos K.A., Savvaidis I.N., Kontominas M.G. (2006) *Int. Dairy J.* 16: 750-761.
4. Hashizume M. (2007) *PhD Thesis*, University of Reading, UK.
5. Manitto P., Speranza G., Monti, D., Gramatica P. (1987) *Tetrahedron Lett.* 28: 4221-4224.
6. Speranza G., Manitto P., Monti D. (1990) *J. Photochem. Photobiol. B: Biol.* 8: 51-61.

EARTHY OFF-FLAVOUR IN WINE: EVALUATION OF REMEDIAL TREATMENTS FOR GEOSMIN CONTAMINATION

M.T. LISANTI, P. Piombino, A. Gambuti, A. Genovese, and L. Moio

Dipartimento di Scienza degli Alimenti - Università degli Studi di Napoli Federico II, via Università 100, 80055, Portici, Italy

Abstract

Seven treatments (activated charcoal, bentonite, PVPP, yeast walls, potassium caseinate, zeolite and grape seeds oil), were evaluated for their ability in decreasing the concentration of geosmin in red and white wine. The treatments were also evaluated for their effect on the concentration of sixteen aroma volatile compounds. In red wine, potassium caseinate and grape seeds oil were able to decrease the concentration of geosmin of 14 and 83%, respectively; while in white wine, deodorant charcoal and grape seeds oil decreased geosmin of 23 and 81%, respectively. The treatments resulted effective in decreasing geosmin, also decreased aroma volatile compounds with esters mostly decreased by all treatments. Only the treatment with grape seeds oil resulted potentially effective in decreasing earthy off-flavour both in red and in white wine.

Introduction

Wine aroma can be altered by the appearance of off-flavours. Among them, musty-earthly odours are particularly detrimental. Odours described as mushrooms, mouldy, camphoric, or earthy are observed in must made with rotten grapes, particularly when high rainfall and hail occur during the vintage. Geosmin (*trans*-1,10-dimethyl-*trans*-9-decalol), was identified as the responsible for a strong earthy odour in red and white wines although detected at low concentration (up to 400 ng/L), due to its extremely low olfactory perception threshold (10 ng/L in water, 60-65 ng/L in white wine, 80-90 ng/L in red wine (1, 2)). Geosmin origins from the metabolism of *Penicillium expansum* fungus in grapes pre-contaminated by *Botrytis cinerea* (3) and shows a great stability during alcoholic fermentation (4, 5). Even when great attention is paid during vine growing and grape vinification remedial treatments could be necessary. At present, no satisfactory means of removing geosmin from wine exist and no study has been published on this item. In this exploratory study seven treatments (deodorant activated charcoal, bentonite, PVPP, yeast walls, potassium caseinate, zeolite and grape seeds oil) were evaluated for their efficacy in decreasing the amount of geosmin in white and red wines. The effect of these treatments on several volatile compounds important for wine aroma was also evaluated.

Experimental

Wines. White wine (cv. Falanghina) and red wine (cv. Aglianico), both spiked with 360 ng/L of geosmin (Sigma, St. Louis, USA) were analysed. The wines were previously analysed for their concentration in geosmin, which resulted below the limit of quantification (0.020 µg/L).

Treatments. Seven treatments at the indicated doses were tested: deodorant charcoal (20 g/hL), polyvinyl polypyrrolidone (PVPP) (80 g/hL), zeolite (20 g/hL), bentonite (30 g/hL), potassium caseinate (50 g/hL), yeast walls (40 g/hL) and grape seeds oil (0.5 L/hL). Each treatment was performed in triplicate, for 14h at 20°C. After racking and filtration, each treatment replicate was analysed in duplicate.

Analysis of volatile fraction. Geosmin and the aroma volatile compounds were extracted by a three-step liquid-liquid extraction with n-pentane (1). The organic extracts were analysed by Gas Chromatography- Mass Spectrometry in Selective Ion Monitoring mode (GC/MS-SIM). Volatile compounds were quantified by interpolating relative peak area in the calibration graphs. The significance of differences between the mean data of each treatment and the respective untreated wine was assessed by a *t*-test ($\alpha= 0.05$) (Statgraphics plus 5.1).

Results

Table 1 reports the concentration of geosmin determined in the contaminated red and white wines, and in the same wines after the seven treatments. In a first phase of the experimentation deodorant charcoal, PVPP and zeolite, while in a second phase bentonite, grape seeds oil and K caseinate, were tested. In red wine, only grape seeds oil and K caseinate were able to decrease the concentration of geosmin, of 83 and 14%, respectively. In the first case, the final concentration was below the olfactory perception threshold reported in red wine (80 ng/L, (1)). In white wine, deodorant charcoal and grape seeds oil decreased geosmin contamination of 23 and 81%, respectively. Considering that the main difference in composition between red and white wine is a higher content of the former in polyphenols, principally flavonoids (6), the different efficacy of charcoal in red and white wine could be due to a competition between geosmin and red wine polyphenols for the adsorption sites, while the different behaviour of K caseinate could be explained by a “cooperative adsorption” between geosmin and red wine polyphenols, the adsorption of the latter making more available the hydrophobic sites of caseinate for geosmin.

Table 1. Effect of the treatments on geosmin concentration in red and white wine.

Red wine	Geosmin (ng/L)	NOU ^a	% dec ^b	White wine	Geosmin (ng/L)	NOU ^a	% dec ^b
red wine 1	355 ± 31	8,9		white wine 1	397 ± 76	9,9	
charcoal	367 ± 86	9,2	ns	charcoal	305 ± 25	7,6	23
PVPP	344 ± 4	8,6	ns	PVPP	413 ± 36	10,3	ns
zeolite	324 ± 25	8,1	ns	zeolite	468 ± 56	11,7	ns
red wine 2	323 ± 16	8,1		white wine 2	348 ± 24	8,7	
bentonite	284 ± 74	7,1	ns	bentonite	350 ± 31	8,7	ns
yeast walls	303 ± 52	7,6	ns	yeast walls	318 ± 40	8,0	ns
grape seeds oil	53 ± 5	1,3	83	grape seeds oil	65 ± 16	1,6	81
K caseinate	277 ± 22	6,9	14	K caseinate	330 ± 15	8,2	ns

^a Number of Odour Units (concentration/olfactory perception threshold in wine model solution (40 ng/L (2)), ^b Significant perceptual decreases ($\alpha= 0.05$) (ns= not significant).

The treatments that showed an efficacy in decreasing geosmin concentration also decreased the determined aroma volatile compounds. In red wine (Table 2), both grape seeds oil and K caseinate decreased the four determined esters (isoamyl acetate, ethyl hexanoate, ethyl octanoate and ethyl decanoate), responsible for fruity notes in wine. For both the treatments, esters were the most decreased volatile compounds, while alcohols were not decreased. Grape seeds oil also decreased all terpenols, responsible for floral olfactory notes, β -damascenone, 4-vinylguaiacol, and

4-vinylphenol. Besides esters, K caseinate decreased linalool and β -damascenone. It is interesting to underline that, even if grape seeds oil decreased a higher number of compounds respect to K caseinate, geosmin was the most decreased compound for the former but not for the latter.

Table 2. Effect of the treatments that reduced geosmin contamination in red wine on the concentration of aroma volatile compounds.

Compound	Red wine 2			Grape seeds oil			K caseinate		
	OPT ^a	Conc. ($\mu\text{g/L}$) ^b	NOU ^c	Conc. ($\mu\text{g/L}$) ^d	NOU ^c	% dec ^e	Conc. ($\mu\text{g/L}$) ^d	NOU ^c	% dec ^e
esters									
isoamyl acetate	30 ⁽⁷⁾	497,0 \pm 22,5	16,6	288,5 \pm 18,9	9,6	42	237,2 \pm 14,8	7,9	52
ethyl hexanoate	14 ⁽⁸⁾	117,6 \pm 22,9	8,4	<3.6	<0.26	>97	<3.6	<0.26	>97
ethyl octanoate	5 ⁽⁸⁾	177,8 \pm 25,9	35,6	<3.1	<0.62	>98	47,9 \pm 6,1	9,6	73
ethyl decanoate	200 ⁽⁸⁾	28,7 \pm 5,0	0,14	<0.99	<0.005	>97	4,2 \pm 1,1	0,02	85
alcohols									
3-methyl-1-butanol	30000 ⁽⁷⁾	373320,0 \pm 83746,5	12,4	273626,7 \pm 68334,6	9,1	ns	375658,3 \pm 46416,2	12,5	ns
1-hexanol	8000 ⁽⁷⁾	2828,0 \pm 584,0	0,35	2268,4 \pm 593,8	0,28	ns	2985,6 \pm 272,0	0,37	ns
(Z)-3-hexen-1-ol	400 ⁽⁷⁾	236,1 \pm 48,1	0,59	193,3 \pm 50,4	0,48	ns	262,3 \pm 20,4	0,66	ns
2-phenylethanol	10000 ⁽⁷⁾	98966,7 \pm 24572,9	9,9	71353,3 \pm 20860,8	7,1	ns	111418,3 \pm 12516,1	11,1	ns
terpenes									
linalool	15 ⁽⁷⁾	17,5 \pm 1,0	1,2	11,0 \pm 2,4	0,7	37	14,7 \pm 1,0	1,0	16
α -terpineol	250 ⁽⁸⁾	10,7 \pm 0,9	0,04	7,8 \pm 1,4	0,03	28	11,3 \pm 0,9	0,05	ns
geraniol	30 ⁽⁷⁾	18,2 \pm 0,8	0,61	13,4 \pm 1,3	0,45	27	18,4 \pm 1,0	0,61	ns
norisoprenoids									
β -damascenone	0.05 ⁽⁷⁾	0,9 \pm 0,1	17,3	0,4 \pm 0,0	7,4	57	0,7 \pm 0,0	14,5	16
phenols									
4-vinylguaiacol	130 ⁽⁹⁾	1,3 \pm 0,2	0,01	<0.8	<0.006	>39	1,1 \pm 0,3	0,01	ns
4-vinylphenol	180 ⁽⁹⁾	40,6 \pm 5,3	0,23	29,4 \pm 4,4	0,16	28	40,7 \pm 6,4	0,23	ns

^a Olfactory Perception Thresholds in wine model solution (references in brackets), ^b Mean of three extraction replicates, ^c Number of Odour Units (concentration/olfactory perception threshold), ^d Mean of six replicates (three treatment replicates, each extracted twice), ^e Significant perceptual decreases ($\alpha = 0.05$) (ns= not significant).

The calculation of NOU (concentration/olfactory perception threshold) represents a useful approach to evaluate the potential olfactory impact of geosmin, after the treatments. Considering the volatile compounds present in the untreated wine at concentration higher than olfactory threshold, the decrease of the olfactory impact of esters following grape seeds oil treatment resulted particularly high (Table 2). However, the olfactory impact of geosmin (Table 1) respect to that of the volatile compounds at concentration higher than olfactory threshold is much less important in the treated wine than in the untreated one. Following the treatment with K caseinate, the decrease of the olfactory impact of geosmin was lower than that of the olfactory impact of positive aroma compounds as isoamyl acetate, ethyl octanoate, linalool and β -damascenone; moreover ethyl hexanoate was decreased below its olfactory threshold. Considering these results, in spite of a decrease of the concentration of geosmin, its olfactory impact could result even increased.

Considering the treatments that reduced geosmin contamination in white wine (Table 3), deodorant charcoal significantly decreased all the determined volatile compounds, most of all esters. Grape seeds oil only decreased esters, terpenes and β -damascenone, while it did not decrease alcohols and vinylphenols.

Considering NOUs (Table 1,3), charcoal significantly decreased the olfactory impact of the volatile compounds having a positive olfactory impact in the untreated wine (NOU>1), and a potential masking effect on geosmin (isoamyl acetate, ethyl hexanoate, ethyl octanoate, β -damascenone), this result could determine, in spite of a decrease of geosmin concentration, a slight increase of earthy off-flavour.

Table 3. Effect of the treatments that reduced geosmin contamination in white wine on the concentration of aroma volatile compounds.

Compound	White wine 1					White wine 2					Grape seeds oil				
	OPT ^a	Conc. (µg/L) ^b	NOU ^c	Conc. (µg/L) ^d	NOU ^c % dec ^e	Conc. (µg/L) ^b	NOU ^c	Conc. (µg/L) ^d	NOU ^c % dec ^e	Conc. (µg/L) ^b	NOU ^c	Conc. (µg/L) ^d	NOU ^c % dec ^e		
esters															
isoamyl acetate	30 ⁽⁷⁾	846,9 ± 26,5	28,2	464,0 ± 36,8	15,5	45	886,5 ± 31,3	29,6	572,3 ± 68,8	19,1	35				
ethyl hexanoate	14 ⁽⁸⁾	191,8 ± 4,1	13,7	85,8 ± 11,9	6,1	55	1159,6 ± 65,4	82,8	61,8 ± 1,9	4,4	95				
ethyl octanoate	5 ⁽⁸⁾	382,4 ± 6,2	76,5	118,1 ± 14,6	23,6	69	1251,9 ± 62,6	250,4	80,4 ± 16,4	16,1	94				
ethyl decanoate	200 ⁽⁸⁾	84,3 ± 3,7	0,42	2,2 ± 0,1	0,01	97	180,7 ± 8,2	0,90	<0.99	<0.005	>99.5				
alcohols															
3-methyl-1-butanol	30000 ⁽⁷⁾	301753,3 ± 60889,9	10,1	235062,5 ± 9050,8	7,8	22	165436,7 ± 8337,8	5,5	189952,6 ± 39225,7	6,3	ns				
1-hexanol	8000 ⁽⁷⁾	1849,6 ± 305,4	0,23	1557,5 ± 78,3	0,19	16	1299,7 ± 79,9	0,16	1563,2 ± 292,0	0,20	ns				
(Z)-3-hexen-1-ol	400 ⁽⁷⁾	77,3 ± 6,0	0,19	70,8 ± 1,0	0,18	8	54,5 ± 2,8	0,14	70,3 ± 11,9	0,18	ns				
2-phenylethanol	10000 ⁽⁷⁾	71166,7 ± 16765,0	7,1	51090,9 ± 2681,1	5,1	28	33416,7 ± 1573,1	3,3	38446,9 ± 10087,0	3,8	ns				
terpenes															
linalool	15 ⁽⁷⁾	33,7 ± 1,8	2,2	25,8 ± 1,4	1,7	23	25,1 ± 0,8	1,7	15,7 ± 2,0	1,0	38				
α-terpineol	250 ⁽⁸⁾	9,6 ± 0,9	0,04	7,9 ± 0,5	0,03	18	20,9 ± 1,0	0,08	14,0 ± 2,2	0,06	33				
geraniol	30 ⁽⁷⁾	34,9 ± 1,5	1,2	28,0 ± 1,0	0,93	20	8,3 ± 0,7	0,28	5,6 ± 0,4	0,19	33				
norisoprenoids															
β-damascenone	0.05 ⁽⁷⁾	2,9 ± 0,2	57,1	2,1 ± 0,1	42,0	26	2,8 ± 0,1	55,8	0,9 ± 0,1	18,8	66				
phenols															
4-vinylguaiaicol	130 ⁽⁹⁾	320,2 ± 27,1	2,5	188,4 ± 9,4	1,4	41	377,1 ± 5,6	2,9	322,7 ± 81,2	2,5	ns				
4-vinylphenol	180 ⁽⁹⁾	129,2 ± 19,5	0,72	77,3 ± 3,7	0,43	40	117,9 ± 3,3	0,65	101,9 ± 22,8	0,57	ns				

^a Olfactory Perception Thresholds in wine model solution (references in brackets), ^b Mean of three extraction replicates, ^c Number of Odour Units (concentration/olfactory perception threshold), ^d Mean of six replicates (three treatment replicates, each extracted twice), ^e Significant perceptual decreases ($\alpha = 0.05$).

After the treatment of white wine with grape seeds oil, the olfactory impact of geosmin respect to that of esters, 2-phenylethanol, β-damascenone, 4-vinylguaiaicol, all positive compounds for white wine aroma, resulted decreased. As for the red wine, this result let to hypothesize an efficacy of oil in decreasing earthy off-flavour. However, further studies are necessary in order to evaluate the sensory effect as well as possible secondary effects of the treatment with grape seeds oil. The study of different doses and time of contact for those treatments that showed a potential efficacy in decreasing geosmin in wine is in progress.

References

1. Darriet P., Pons M., Lamy S., Dubourdiou D. (2000) *J. Agric. Food Chem.* 48: 4835-4838.
2. Darriet P., Lamy S., La Guerche S., Pons M., Dubourdiou D., Blancard D., Steliopoulos P., Mosandl A. (2001) *Eur. Food Res. Tech.* 213: 122-125.
3. La Guerche S., Chamont S., Blancard D., Dubourdiou D., Darriet P. (2005) *Antonie van Leeuw.* 88: 131-139.
4. La Guerche S., Dauphin B., Pons M, Blancard D, Darriet P (2006) *J. Agric. Food Chem.* 54: 9193-9200.
5. Darriet P, Pons M, Henry R, Dumont O, Findeling V, Cartolaro P, Calonnec A, Dubourdiou D (2002) *J. Agric. Food Chem.* 50: 3277-3282.
6. Singleton V.L., Noble A. (1976) In *Phenolics, Sulphur and Nitrogen Compounds in Food Flavors* (Charalambous G., Kantz, eds.); ACS, 26: 47-70.
7. Guth H. (1997) *J. Agric. Food Chem.* 45: 3027-3032.
8. Ferreira V., Lopez R., Cacho J.F. (2000) *J. Sci. Food Agric.* 80: 1659-1667.
9. Chatonnet P., Dubourdiou D., Boidron J.N. (1995) *J. Sci. Food Agric.* 62: 191-202.

IDENTIFYING AROMA COMPONENTS RESPONSIBLE FOR LIGHT-INDUCED OFF-FLAVOUR IN PASTEURISED MILK

M. MARTENS, M. Reekers, W. Timmermans, and C. Ponne

FrieslandCampina Corporate Research, Harderwijkerstraat 41006, 7418BA Deventer, The Netherlands

Abstract

Light exposure of pasteurised milk results in the formation of a typical off-flavour. Consumers can perceive this typical off-flavour even after a short light exposure time. We confirmed that light exposure of pasteurised milk results in the formation of a number of volatile components. Analysis of the volatile fraction of light exposed pasteurised milk (LEPM) by gas chromatography / fraction collection showed the presence of two fractions with a typical plastic and earthy odour. The components could be identified as 1-hexen-3-one and 1-octen-3-one, respectively. A quantitative analytical method, based on a derivatization step followed by GC/MS-NCI analysis, was developed. Addition of both components to fresh pasteurised milk (in concentrations as present in LEPM) followed by sensory analysis showed no significant differences with LEPM. This result proves that 1-octen-3-one and 1-hexen-3-one are the components responsible for the light-induced off-flavour in pasteurised milk. The threshold values for 1-hexen-3-one and 1-octen-3-one in pasteurised milk were determined to be 5 and 90 ng/L, respectively. The described analytical technique can be used to determine the sources of the off-flavour components and wavelengths, at which the components are formed.

Introduction

Consumer acceptance of a food is largely determined by flavour preliminary because flavour can be readily judged. Light induced off-flavour in milk is a well known milk flavour (1). This is an issue because packaging of foods in transparent (synthetic) materials is an ongoing trend. Light exposure of pasteurised milk results in the formation of a typical off-flavour that is described as earthy/plastic. Consumers are able to perceive this typical off-flavour even after short light exposure times. Aldehydes, ketones and volatile sulphur components are thought to play a role in light induced off flavours (2).

In recent literature (3) the changes in volatile aroma components in light exposed pasteurised milk were determined. In this study, we confirm these changes but also show that these components are not responsible for the observed light induced off-flavour. With additional flavour research we were able to identify the two components responsible for the typical light induced off-flavour in pasteurised milk.

Experimental

Light exposure. Samples were exposed to light in closed transparent glass bottles of 200 ml in a retail fridge (7°C, 4000 lux) or in a modified SUNTEST® (7°C, 50.000 lux).

GC/MS (sniffing). Dynamic headspace extraction was performed on 100 ml of milk (120 minutes, 38°C, 100 ml helium/min on Tenax-Carbosieve III). The Tubes were desorbed at 250°C and volatiles were trapped at -150°C. The components were separated by gas chromatography on a CP-Sil5CB column (30 m x 0.25 mm, d = 1 µm) and simultaneous detection was performed by mass spectrometry (scanning 30-200 m/z) and sniffing.

Quantification method. The used derivatisation step is described elsewhere (4). The derivatives of the components of interest and the internal standard (d₅-benzaldehyde) were analysed by GC/MS-NCI by selective monitoring of two abundant ions per component.

Sensory testing. A Quantitative Descriptive Analysis (QDA) panel (N= 12) was trained on the specific attributes light odour and light taste in pasteurised semi skimmed milk that was illuminated during different time intervals (0, 2, 4, 6, 8, 10 minutes at 50.000 lux). For the consumer test 58 randomly selected consumers were used.

Results and Discussion

In a triangle test consumers (N= 58) were asked to distinguish between light exposed (2, 4, 6, 8 and 10 minutes at 50.000 lux) and non-illuminated semi skimmed pasteurised milk. Consumers were able to detect a significant difference between non-illuminated milk and milk that is light exposed during 4 minutes at 50.000 lux. Most of the consumers describe the deviation of the light exposed samples as having a strong smell and bad taste.

GC/MS/sniffing analysis of non illuminated and light exposed milk resulted in a list of components that are formed during light exposure. In Table 1 these components and corresponding concentrations are presented. The components were identified based on injection of the pure standards and mass spectral comparison. However, addition of the components to non-illuminated milk in the concentrations as detected in light exposed milk did not result in the typical plastic/earthy off-flavour.

Table 1. Increase of volatile aroma components during light exposure of pasteurised semi-skimmed milk (4 h at 4000 lux).

Component	Non illuminated milk (µg/L)	Light exposed milk (µg/L)
Methanethiol	0.4	1.5
Pentanal	0.7	11.8
Dimethyldisulphide	0.02	0.11
Pentanol	2.5	47.8
Hexanal	1.38	4.26
Heptanal	0.54	1.74
Octanal	1.08	1.48
Nonenal	0.50	1.05

Since the typical earthy/plastic off-flavour was not detectable fractions of one minute were collected in cold water (1 ml, 4°C) at the end of the GC column and smelled. For the light exposed milk sample this resulted in two fractions that contain a typical plastic and mushroom smell. Using mass spectrometry and injection of the

pure standards the components were identified as 1-hexen-3-one and 1-octen-3-one, respectively.

To prove that these components are indeed the components responsible for the formation of light induced off-flavour a recombination experiment was carried out. For both components the concentration was determined in light exposed milk and non-illuminated milk. Both components were added to non-illuminated milk in the concentration as was determined in the light exposed milk sample and evaluated by a QDA panel. Since no significant differences were observed it can be concluded that addition of both components results in milk that has the typical light induced off-flavour.

The effect of addition of the individual components on the sensory properties and the threshold was determined. The results showed that a QDA panel can detect additions of 1-hexen-3-one and 1-octen-3-one in a concentration of 5 ng/L and 90 ng/L, respectively.

Table 2 shows the formation of 1-hexen-3-one and 1-octen-3-one in skimmed, semi-skimmed and full cream milk (natural fatty acid composition) after light exposure. It can be seen that the off-flavour formation is related to the fat content. In literature it is described that 1-octen-3-one can be formed by auto-oxidation of linoleic acid (5), a component that is present in milk fat.

Table 2. Formation of 1-hexen-3-one and 1-octen-3-one in different types of milk during 10 minutes light exposure (50.000 lux, 7°C).

Milk type	1-Hexen-3-one ($\mu\text{g/L} \pm \text{SD}$, N=2)	1-Octen-3-one ($\mu\text{g/L} \pm \text{SD}$, N=2)
Skimmed	Nd ^a	52 \pm 2
Skimmed light exposed	Nd ^a	199 \pm 1
Low fat	5 \pm 2	40 \pm 6
Low fat light exposed	41 \pm 4	259 \pm 31
Full cream	12 \pm 5	63 \pm 7
Full cream light exposed	85 \pm 7	435 \pm 6

^a Not detectable

In conclusion, we can say that consumers can pick up easily the light induced off-flavour in pasteurised semi skimmed milk. The components responsible for light induced off-flavour formation of semi-skimmed pasteurised milk were identified as 1-hexen-3-one and 1-octen-3-one. A method is described for measurement of these components at ng/L level. There are strong indications that fat plays an important role in the formation of both components. This knowledge opens the way to determine the sources of the off-flavour components and mechanisms of formation. This will help to develop new process and packaging concepts.

References

1. Thomas E.L. (1981) *J. Dairy Sci.* 64: 1023-1027.
2. Gaafar A.M., Gaber F.I. (1992). *Egyptian J. Dairy Sci.* 20: 111-115.
3. Karatapanis A.E., Badeka A.V., Riganakos K.A., Savvaidis I.N., Kontominas M.G. (2006). *Internat. Dairy J.* 16: 750-761.
4. Strassnig S., Wenzl T., Lankmayr P. (2000) *J. Chromatogr. A* 891: 267-273.
5. Belitz H.-D., Grosch W. (1999). "*Food Chemistry*", 2nd ed. Springer-Verlag: Heidelberg, Germany.

SENSORIAL ASPECTS OF “BRETT CHARACTER”: RE-EVALUATION OF THE OLFACTORY PERCEPTION THRESHOLD OF VOLATILE PHENOLS IN RED WINE

A. ROMANO, M.C. Perello, A. Lonvaud-Funel, G. de Revel

UMR 1219 Œnologie, Université de Bordeaux, INRA, ISVV; Faculté d'Œnologie, 351 Cours de la Libération, 33405 Talence, France

Abstract

Wine spoilage caused by the yeast *Brettanomyces bruxellensis* (sometimes referred to as “Brett character”) results in the production of several volatile compounds and a large spectrum of flavours and aromas. Ethylphenols are the best-known markers of this defect but ethylphenol contents of wines do not always match tasting notes. Sensory analysis was employed to demonstrate the complexity of “Brett character”. A masking effect of isobutyric acid and isovaleric acid on the detection of ethylphenols in wine was proven. This partly explained the poor correspondence between ethylphenol concentrations and presence of “Bretty” descriptors.

Introduction

Worldwide wine production has been significantly distressed by *Brettanomyces bruxellensis* spoilage [1]. The development of *B. bruxellensis* in wine entails the synthesis of ethylphenols (namely 4-ethylphenol and 4-ethylguaiacol). These compounds have a commonly used aggregate limit threshold of $400 \mu\text{g l}^{-1}$ [2]. This limit carries significant economic importance as winemakers have made it the basis for treating wines thought to be at risk of *B. bruxellensis* spoilage. In a previous study [3] we demonstrated that volatile phenol production in wine by *B. bruxellensis* is accompanied by the synthesis of organic acids (from C_3 to C_{10}) and short chain acid ethyl-esters (from C_2C_6 to C_2C_{10}). This work was aimed at ascertaining the influence of this metabolic activity on the development of Brett character and in particular on the perception of “Bretty” notes.

Experimental

All reagents and standards were of the highest available purity grade. A 2006 Bordeaux red wine was used for detection threshold calculation (pH 3.5, ethanol 12.2 % (v/v), total reducing sugars 2.0 g/l, volatile acidity 0.55 g/l expressed as acetic acid, total phenolics 49 expressed as absorbance at 280 nm, 4-ethylphenol + 4-ethylguaiacol 13 $\mu\text{g/l}$). All the other red wines (pH 3.4, ethanol 12.5-13.7 % (v/v), total reducing sugars 1.2-2.4 g/l, volatile acidity 0.51-0.84 g/l, 58-98 total phenolics) were commercial samples that originated from wineries throughout the Bordeaux region and belonged to the 2005 vintage. We chose the measurement of absorbance at 280 nm as a rapid method to estimate wine phenolic complexity [4].

Fifty-one red Bordeaux wines of the 2005 vintage were tasted with the aim of wine profiling for commercial purposes. Four professionals of the wine sector evaluated samples both orthonasally and retronasally and a list of freely perceived

descriptors was obtained for each wine. Samples were presented to the tasters employing tulip shaped tasting glasses.

Volatile phenols were determined by GC-MS analysis coupled to solid-phase micro-extraction (SPME) on polyacrylate fibres [3]. For carboxylic acid and ethyl ester determination 10-ml aliquots of wine were supplemented with 40 μ l of an internal standard solution (3-octanol at a concentration of 400 mg/l in water:ethanol 1:1 v/v). Samples were then extracted twice with diethylether:isohexane (1:1 v/v) and wine extracts were submitted to GC-FID analysis [5]. All analytical determinations were carried out in duplicate. Correlation coefficients among different variables were calculated by the general linear model. Calculations were performed employing Minitab statistical software (Minitab Inc., State College, PA).

Detection thresholds were calculated following ISO guidelines [6]. Six sets of three-alternative forced-choice (3-AFC) tests were performed. Each series contained one positive sample supplemented with ascending (17 - 34 - 68 - 137 - 275 - 550 μ g/l) concentrations of ethylphenols in a 10:1 concentration ratio of 4-ethylphenol and 4-ethylguaiacol.

Experimental data are interpolated on the basis of the equation (1). This expresses the probability of orthonasal detection (p) as a function of detection threshold (t). The parameter b is related to the slope of the curve. Detection threshold corresponds to a 0.5 probability of correct detection after correction for chance guessing (0.33 probability). Calculations were performed employing Excel software (Microsoft, Redmond, WA).

$$(1) \quad p = \frac{\frac{2}{3}}{1 + e^{b(1-x)}} + \frac{1}{3}$$

The panel consisted of 10 expert judges belonging to the laboratory staff. The judges were already trained in the perception of the sensory notes of 4-ethylphenol and 4-ethylguaiacol in wine but they were not informed about the purpose of the test. Samples were evaluated orthonasally and consisted in 4 ml wine aliquots presented within 20 ml screw capped bottles with 2 cm neck diameter. The wine samples were introduced into the bottles and these were capped at least one hour before the experiment in order to allow for equilibration. All tests were performed in a room equipped with individual tasting booths.

Results

“Bretty” notes and ethylphenol concentrations in commercial wines. Fifty-one Bordeaux red wines were profiled for commercial purposes. On the basis of the tasting notes samples were subdivided into three classes. “Heavily tainted” wines presented “Bretty” descriptors for all judges, in “mildly tainted” wines such descriptors were found by at least one judge and “non tainted” wines were virtually faultless. Wines were submitted to GC-MS analysis for volatile phenols. 4-ethylphenol and 4-ethylguaiacol were present in all samples with a 10:1 average concentration ratio, typical of Bordeaux wines. Vinylphenols were instead not detectable.

The correlation between sensory data and ethylphenol contents appeared to be very poor (Table 1). No significant differences were found in the average ethylphenol content of each class.

Table 1. Descriptive analysis and corresponding ethylphenol contents of commercial wines.

Sensory profile	Number of wines	4-Ethylphenol + 4-ethylguaiacol ($\mu\text{g/l}$)	
		Min-max	Average ^a
Heavily tainted	5	196-746	375 (223)
Mildly tainted	10	8-563	272 (201)
Non tainted	36	5-1370	403 (389)

^a standard deviation between brackets

Wine analysis for carboxylic acids and ethyl-esters. Twenty-six commercial wines (5 heavily tainted, 6 mildly tainted and 15 non tainted) were selected among the previously mentioned 51 and submitted to GC-FID analysis for carboxylic acids and ethyl-esters. A statistically significant correlation ($1-\alpha= 0.95$) could be evidenced between ethylphenols and isobutyric (iC4) and isovaleric (iC5) acids. All other carboxylic acids (from C3 to C10) and ethyl-esters (from C6 to C10) showed instead very poor correlations (Table 2). *B. bruxellensis* is presumably the only known species that produces ethylphenols in winemaking conditions. Our results indicate therefore that isobutyric acid and isovaleric acid are to be considered as important markers of Brett character.

Table 2. Concentration of carboxylic acids and ethyl-esters of some commercial wines (mg/l). Correlation coefficients (*r*) with ethylphenols are reported.

	C_3+C_4	iC ₄	iC ₅	C ₆	C ₈	C ₁₀	C ₂ C ₆	C ₂ C ₈	C ₂ C ₁₀
Min		1.34	1.87	0.63	0.51	0.21	0.07	0.10	0.18
Max	<0.1	4.67	6.73	1.92	2.22	1.36	0.48	0.50	0.67
Average ^a		2.62 (0.79)	3.49 (1.12)	1.02 (0.35)	0.82 (0.42)	0.45 (0.22)	0.31 (0.11)	0.27 (0.10)	0.42 (0.12)
<i>R</i>	n.a.	0.66 ^b	0.78 ^b	0.05	0.14	0.07	0.19	0.13	0.29

^a standard deviation between brackets; ^b significant at 99% confidence level

Calculation of ethylphenol detection thresholds. An aggregate detection threshold was measured in wine for the mixture 4-ethylphenol : 4-ethylguaiacol in a 10 : 1 concentration ratio. In a second experiment the detection threshold was calculated in a wine supplemented with 1 mg/l isobutyric acid and 1 mg/l isovaleric acid. In a preliminary trial we verified that “rancid” and “sweaty” olfactory notes typical of these compounds were not detectable at these concentrations.

The comparison between the two detection thresholds of the ethylphenols allowed us to ascertain that isobutyric acid and isovaleric acid do possess a masking effect with respect to these ethylphenols: in fact the detection threshold value was three times higher when wine was supplemented with the carboxylic acids (Figure 1). The calculated detection threshold for ethylphenols in wine was about four times lower than that reported in literature (Chatonnet *et al.*, 1992), but it must be reminded

this is easily influenced by wine complexity. The wine employed for detection threshold calculation, unlike the ones submitted to sensory profiling, was not barrel aged and its phenolic complexity was significantly below average, as indicated by the values of absorbance at 280 nm (experimental).

The results presented in this work demonstrate that some secondary metabolites other than volatile phenols have a sensory impact on the spoiled wine. This partly explains the poor correlation between sensory data and ethylphenol contents. Some incoherencies between sensory and analytical data could also be explained on the basis of the presence of other ethylphenols (e.g. 4-ethylcatechol) whose role in relation to “Brett character” has not been fully disclosed yet [7].

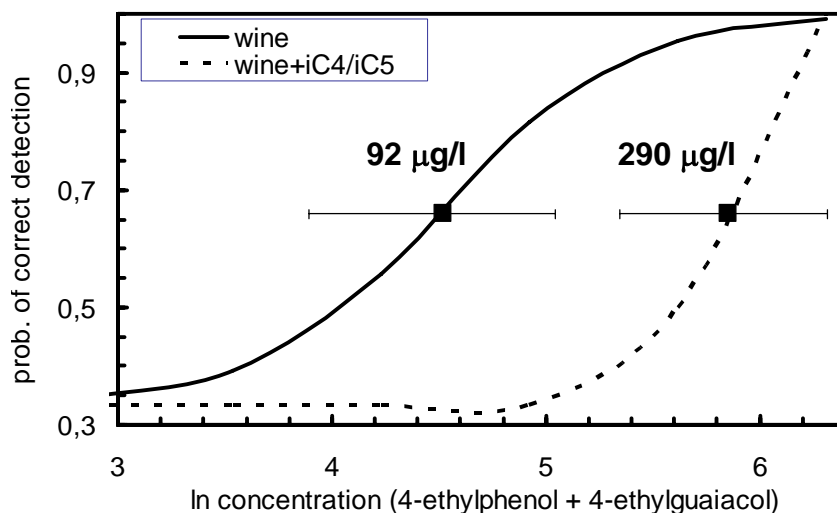


Figure 1. Orthonasal detection thresholds of 4-ethylphenol and 4-ethylguaiacol in a 10 : 1 concentration ratio. Threshold is calculated in a red Bordeaux wine and in the same wine supplemented with 1 mg/l isobutyric acid and 1 mg/l isovaleric acid. Error bars represent 95% confidence limits.

References

1. Loureiro V., Malfeito-Ferreira M. (2006) In *Food Spoilage Microorganisms* (de Blackburn C., ed.), Woodhead Publishing, Cambridge, pp 354-398.
2. Chatonnet P., Dubourdieu D., Boidron J.N., Pons M. (1992) *J. Sci. Food Agric.* 60:1 65-178.
3. Romano A., Perello M.C., de Revel G., Lonvaud-Funel A. (2008) *J. Appl. Microbiol.* 104: 1577-1585.
4. Somers T.C., Evans M.E. (1977) *J. Sci. Food Agric.* 28: 279-287.
5. Silva M.L., Malcata F.X., de Revel G. (1996) *J. Food Compos. Anal.* 9 : 72-80.
6. ISO 13301:2002 General guidance for measuring odour, flavour and taste detection thresholds by a three-alternative forced-choice (3-AFC) procedure. (http://www.iso.org/iso/iso_catalogue/catalogue_tc/catalogue_detail.htm?csnumber=36791)
7. Hesford F., Schneider K., Porret N.A., Gafner J. (2004) *Am. J. Enol. Viticult.* 55: 295A.

THE OLFACTOSCAN: *IN-VIVO* SCREENING FOR OFF-FLAVOUR SOLUTIONS

K.M.M. Burseg and C. DE JONG

NIZO food research B.V., Kernhemseweg 2, P.O. Box 20, 6710 BA Ede, The Netherlands

Abstract

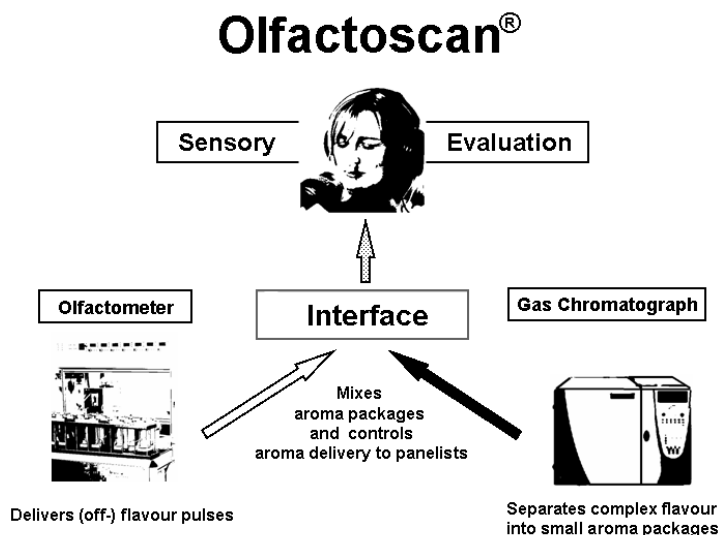
The Olfactoscan is a sensory screening technique that identifies suppressing or enhancing aroma interactions for flavour optimisation. It combines olfactometry and gas chromatography via a specially developed interface: the gas chromatograph generates aroma packages from a flavour mixture that are one by one mixed with a pulse from a specific odorant as produced by the olfactometer. Trained panellists evaluate the intensity of that particular odour in the presence of each aroma package of compounds generated after gas chromatographic separation. Aroma packages of compounds that suppress or enhance the perception of the specific odorant are further identified with mass spectrometry. The dynamic principle of the Olfactoscan allows a rapid sensory screening of a high number of compounds (>100) within a short time (15-20 min). As it represents a sensory screening method, interactions at receptors as well as higher levels (olfactory bulb, olfactory cortex) can be identified. Here, the Olfactoscan principle is described and an application example is given.

Introduction

The formation and presence of volatile off-flavours in foods and beverages is a widespread and costly problem for the food industry. It is often impossible to control or avoid the reactions ingredients undergo upon processing or storage (oxidation, enzymatic degradation etc.) that lead to the formation of certain off-flavours. If the removal of an off-flavour is not feasible other volatiles can be added that mask or suppress the perception of the off-flavour [1]. Odour masking or suppression is a phenomenon frequently observed in odorant mixtures and is the result of interactions of odorants for receptor binding sites [2-4]. Also, suppression mechanisms at higher levels such as the olfactory bulb or olfactory cortex have been suggested [5-8]. As a consequence, the mixture of odorants will be perceived as different from its individual compounds and the characteristic note of, for example, a certain off-flavour will be masked [10, 17]. This concept of off-flavour masking is of great interest for the food industry. However, predicting which odorants mask or suppress the perception of a selected off-flavour by means of trial-and-error methods is difficult and often time-consuming. Receptor interactions can be studied using *in-vitro* screening assays of (human) olfactory receptors [9-11]. However, these methods do not measure odorant interactions in the olfactory bulb or olfactory cortex and results cannot be translated directly into a sensorial percept. In this paper we present an *in-vivo* screening method, the Olfactoscan, which allows the rapid sensorial determination of masking and/or suppressing odour interactions.

Experimental

Olfactoscan. The Olfactoscan combines olfactometry (OM4, Burghart, Wedel, Germany) and gas chromatography (Trace GC, Thermo Scientific, Milan, Italy) making use of a specially developed interface. Off-flavour pulses are generated by an olfactometer and are, one by one, mixed with discrete odour-packages generated after gas chromatographic separation of a (defined) flavour mixture. Trained



panellists evaluate the perceived intensity of the off-flavour when mixed with each individual odour-package. Compounds that show masking or suppressing properties are identified and tested in a real food matrix. As this method is based on the sensorial evaluation of odour interactions, it includes masking as well as suppressing effects at all levels, namely at receptors, olfactory bulb as well as olfactory cortex.

Figure 1. The Olfactoscan combines olfactometry and gas chromatography to screen for natural off-flavour solutions.

Screening experiment. The Olfactoscan was validated by finding a masking compound for methional, a typical potato-like off-flavour in beverages [12-14]. Methional solutions in propylene glycol were prepared (3, 6, 9 µg/L) for the olfactometer experiments. Methional pulses (1000 ms) were created by sending an air flow (4 L/min) through the methional solutions. Between pulses, warm, humidified air (60 % RH, 40 °C) was delivered. The inter-stimulus interval was set to 20 s.

A solution of eight aroma compounds hexanal was prepared in methanol for separation with gas chromatography. The composition of this GC flavour mixture was ethyl butyrate (208 mg/L), hexanal (150 mg/L), limonene (142 mg/L), heptanal (142 mg/L), *cis*-4-heptenal (20 mg/L), octanal (110 mg/L), 2,6 dimethyl pyrazine (82 mg/L) and benzaldehyde (208 mg/L). The concentrations of the compounds were of the same perceived intensities as a 6 µg/L methional olfactometer pulse (evaluated by three trained panellists). A volume of 1 µl of the GC flavour mixture was injected (split less) into the GC equipped with a split less injector, Deans switch, FID and a fused silica capillary column (Heliflex AT-1000; 30 m x 0.25 mm x 0.25 µm; Alltech, USA). The compounds were separated making use of the following oven program: 60 °C to 120 °C at 10 °C/min, 120 °C to 220 °C at 40 °C/min. Eluting compounds were sent to the olfactometric port to be mixed with olfactometer pulses. This created a continuum of methional mixtures with changing GC compounds that was immediately sent into the nose of the panellist.

Panellists. A total of 16 panellists (age 28-52, one male) were recruited for the experiment who had participated in earlier experiments involving gas chromatography-olfactometry. Each panellist was trained in recognizing olfactometer

methional pulses (3–9 µg/L in propylene glycol) but also received a methional sample to familiarize him/herself at home with the odour. For the olfactoscan test, panellists first received a series of methional pulses (warming-up). They were then informed that they would receive a series of odour events that may or may not contain methional and were instructed to push a button if methional was recognized. Methional pulses were given in mixtures with the compounds of the GC flavour mixture as well as unmixed to verify that, if panellists did not recognize methional in a mixture, this was due to masking or suppression effects and not due to sensory fatigue. Each panellist evaluated each methional concentration in separate runs. For each run and concentration, it was counted how often methional was correctly identified if given in a mixture. Correct identifications were pooled and tested for statistical significance (paired comparison test, [15]).

Results and Discussion

The results of the screening experiment are shown in Table 1. A high number of panellists (> 10) identified methional if it was mixed with one of the compounds of GC flavour mixture. This was also observed upon reducing the methional concentration of the solution in the olfactometer from 9 to 3 µg/L. For octanal, however, the number of correct methional identifications decreased strongly with decreasing methional concentration. At 3 µg/L, methional was no longer perceivable if mixed with octanal. Subjects correctly identified the control pulses of unmixed methional (from a 3 µg/L solution; $p = 0.05$, data not shown) suggesting that if panellists failed to identify methional in a mixture it was due to masking or suppressing properties of the mixture compound rather than sensory fatigue.

Table 1. Results of the olfactoscan study with 16 panellists. The numbers represent how often methional (in three concentrations) was perceived when mixed with an odorant of the GC flavour mixture. Data for octanal indicated in **bold** shows that at 3 µg/L methional was no longer perceivable when mixed with octanal.

Methional	Ethyl butyrate	Hexanal	Limonene, Heptanal	<i>cis</i> -4-Heptenal	Octanal	2,6 Dimethyl pyrazine	Benzaldehyde
9 µg/L	15	14	13	15	9	13	11
6 µg/L	14	8	11	11	6	8	10
3 µg/L	10	11	6	11	0	13	13

As discussed earlier, odour interactions may occur at the receptor level (competition for olfactory receptor binding sites) or at higher (perceptual) levels such as the olfactory bulb or olfactory cortex. Olfactory receptors discriminate subtle differences in chemical structures of odorants although they tolerate other molecular features in the ligand-binding site [4, 11].

In this study, methional (3-(methylthio) propionaldehyde) was screened against other aldehydes such as hexanal, heptanal, octanal, *cis*-4-heptenal and benzaldehyde. At the concentrations studied, significant interactions were observed only between octanal and methional. This suggests highly specific competition for receptor binding sites between these compounds resulting in a non-additive receptor

code. As a consequence, the perceived mixture odour quality was different from the quality of methional (or octanal) if presented unmixed [16]. However, interactions at higher levels such as the olfactory bulb or olfactory cortex can also not be excluded. Overall, the study demonstrates the applicability of the Olfactoscan screening technique to identify targeted odorant-interactions such as the suppression of methional perception in mixtures with octanal. In this study, a validation mixture with known compounds was used. For scale-up experiments, the number of compounds and so the possibility to find odour interactions can be increased up to a hundred compounds.

The Olfactoscan is a sensory (*in-vivo*) screening technique that, for any given compound, can assist in finding masking but also synergistic odorant interactions at olfactory receptors as well as higher levels (olfactory bulb, olfactory cortex). The identified odour interactions may then be used in food, beverage or body-care applications to improve their aroma quality. This was successfully tested for the octanal-methional combination in orange juice (submitted for publication). A patent application for the Olfactoscan has been filed.

References

1. Luckow T., Sheehan V., Fitzgerald G., Delahunty C. (2006) *Appetite* 47: 315-323.
2. Oka Y., Nakamura A., Watanabe H., Touhara K. (2004) *Chem. Senses* 29: 815-822.
3. Kay L.M., Lowry C.A., Jacobs H.A. (2003) *Behav Neurosci* 117: 1108-1114.
4. Sanz G., Schlegel C., Pernellet J.C., Briand L. (2005) *Chem. Senses* 30: 69-80.
5. Wilson D.A. (2003) *J. Neurophysiol.* 90: 65-72.
6. Tabor R., Yaksi E., Weislogel J.M., Friedrich R.W. (2004) *J. Neurosci.* 24: 6611-6620.
7. Giraudet P., Berthommier F., Chaput M. (2002) *J. Neurophysiol.* 88: 829-838.
8. Wilson D.A., Stevenson R.J. (2003) *Trends Neurosci.* 26: 243-247.
9. Shirokova E., Schmiedeberg K., Bedner P., Niessen H., Willecke K., Raguse J.D., Meyerhof W., Krautwurst D. (2005) *J. Biol. Chem.* 280: 11807-11815.
10. Krautwurst D., Yau K. W., Reed R. R. (1998) *Cell* 95: 917-926.
11. Araneda R.C., Kini A.D., Firestein S. (2000) *Nat. Neurosci.* 3: 1248-1255.
12. Bezman Y., Rouseff R.L., Naim M. (2001) *J. Agric. Food Chem.* 49: 5425-5432.
13. Perpete, P. & Collin, S. (1999) *J. Agric. Food Chem.* 47:2374-2378.
14. Escudero A., Hernandez-Orte P., Cacho J., Ferreira V. (2000) *J. Agric. Food Chem.* 48: 4268-4272.
15. Meilgaard M.C., Carr, B.T. (1999) *Sensory evaluation techniques*. 3th edit., CRC Press, Boca Raton.
16. Parisot F. A., Satre E, Williams R.C., Kurtz A.J., Acree T.E. (2008) *Poster at 12th Weurman Symposium 2008*, Interlaken, Switzerland.

INFLUENCE OF MODIFIED ATMOSPHERE PACKAGING ON THE AROMA OF CHEESE

I. VAN LEUVEN, T. van Caelenberg, and P. Dirinck

Laboratory for Flavour Research, Catholic University College Ghent, K.U. Leuven Association, Gebr. Desmetstraat 1, BE-9000 Gent, Belgium

Abstract

In this study objective analytical techniques were used to measure the change in volatile composition of sliced, modified atmosphere packaged semi-hard cheese, with and without the rind, and to compare it to the volatile composition of an unpackaged cheese (as a whole block) during shelf life. The cheese samples were analysed by a combination of simultaneous steam distillation-extraction followed by gas chromatography-mass spectrometry. Analyses were performed on all cheese samples immediately after packaging and after 10 weeks of storage. Visualisation of the analytical results was performed by principal component analysis. Additionally, triangle tests were performed immediately after packaging and after 10 weeks of storage. The sensory results were in good accordance with the chemical-analytical results.

Introduction

Nowadays, for convenience reasons, there is an increasing market for packaging of food products in small portions. However, food producers want these products to have similar sensory properties as the products in the traditional distribution systems. Modified atmosphere packaging (MAP) extends the shelf life of cheese but flavour changes can be observed during preservation.

Cheese flavour is a very complex phenomenon. During ripening of cheese, several chemical and biochemical pathways of the main milk components - fat, casein and lactose - occur. The typical cheese aroma is the result of volatiles formed by lipolysis, proteolysis and metabolism of residual lactose, lactate and citrate (1 - 6). More than 600 volatile compounds have been identified in cheese (7). However, only a small fraction of these compounds are really responsible for cheese flavour. Fat, proteins, peptides, amino acids, volatile sulphur compounds, alcohols, aldehydes, ketones and volatile fatty acids are some of the classes of compounds that contribute to cheese flavour (8).

The aim of this study was to evaluate the change in volatile composition of MAP cheeses during shelf life by using chemical-analytical techniques and sensory tests. In previous studies (9, 10) SDE-GC-MS analysis was successfully used for the aroma characterisation of cheese.

Experimental

Cheese samples. A sliced, modified atmosphere packaged semi-hard cheese, with and without the rind and an unpackaged semi-hard cheese (as a whole block) was supplied by a Belgian cheese maker. The private label cheese samples were made

of the same batch of milk, had undergone a similar processing and were stored under the same temperature and light exposure conditions. The MAP cheeses were packaged under modified atmosphere conditions (70 % N₂ + 30 % CO₂). All samples were stored in a refrigerator at 4 °C until they were needed for analysis. The cheese samples were analysed by GC-MS and with a sensory panel immediately after packaging (t₀) and after 10 weeks of storage (t₁).

Simultaneous Steam Distillation-Extraction (SDE). For isolation of the cheese volatiles a sample of 50 g of blended cheese was suspended in 600 mL of water and was extracted in a simultaneous steam distillation-extraction apparatus (Alltech Associates, Inc., Lokeren, Belgium) using 60 mL of dichloromethane. For determination of the semi-quantitative volatile composition undecane was used as internal standard and was spiked to the solvent. After cooling to ambient temperature the combined dichloromethane fractions were concentrated to a final volume of 0.5 mL in a Kuderna-Danish concentrator (Alltech Associated Inc., Deerfield, Illinois, USA). For each cheese sample duplicate isolations of volatiles were performed (analysis 1 and 2).

Gas Chromatography-Mass Spectrometry (GC-MS). At the inlet of a HP 5890 gas chromatograph coupled to a HP 5971A MSD mass spectrometer (Agilent Technologies, Santa Clara, CA, USA) 1 µL of a cheese extract was injected on a DB-1MS capillary column (100 % dimethylpolysiloxane, L 60 m x I.D. 0.25 mm x 0.25 µm film thickness; J&W Scientific, Folsom, CA, USA). The GC-MS conditions were the same as described in (10). Identification of the cheese volatiles was tentatively made by comparing the mass spectra of the different volatiles with the mass spectra of a commercial Mass Spectral Library Wiley275 (J. Wiley & Sons LTD., Somerset, New Jersey, USA). Semi-quantitative data of the isolated aroma compounds were calculated by relating the peak area of the cheese volatile to the peak area of undecane. The concentrations of the volatiles were expressed as ng g⁻¹ of cheese.

Statistical analysis. Principal component analysis (PCA) was performed on the semi-quantitative aroma compositions of the cheese samples using the Unscrambler 6.1 (Camo, Oslo, Norway).

Triangle test. Triangle tests were performed in the sensory lab, using a trained panel of 15 assessors, immediately after packaging (t₀) and after 10 weeks of shelf life (t₁). For each triangle test the sum of the correct responses was calculated and compared with the sum needed for significant flavour difference ($p < 0.05$), which is 9 for 15 assignments.

Results

Triangle tests showed no significant differences between the unpackaged cheese and the packaged cheeses, with and without rind, immediately after packaging (t₀) because the sum of the correct responses was ≤ 9 ($n = 15$; $p < 0.05$). Significant differences were observed between the unpackaged cheese and the packaged cheeses, with and without rind, after 10 weeks of storage (t₁) because the sum of correct responses was > 9 ($n = 15$; $p < 0.05$).

The SDE-GC-MS profiling of the semi-hard cheeses resulted in the identification of 71 volatile components mostly formed by proteolysis, lipolysis and metabolism of residual lactose, lactate and citrate. All cheese volatiles were classified in different chemical classes: aldehydes, alcohols, ketones, volatile acids, ethyl esters, γ - and δ -lactones, sulphur compounds, and others (7 packaging volatiles). The packaging compounds, which were tentatively identified as branched-chain hydrocarbons, could

not precisely be identified because of the similarity of the mass spectra. From (Table 1) it was clear that the rind, the MA packaging and the shelf life had less influence on the amounts of aldehydes, ketones, volatile acids, lactones and sulphur compounds. Most differences were obtained for the concentrations of alcohols, ethyl esters and packaging compounds. The amount of alcohols and ethyl esters was clearly increased in the sliced, MAP cheese with rind at t1. The sum of the concentrations of the packaging volatiles was 2.5 times higher in the sliced, MAP cheese without rind compared to the sum of the concentrations obtained for the sliced, MAP cheese with rind.

Table 1. Sum of concentrations of the cheese volatiles classified in different classes

Class	Sum of concentrations (ng/g) ^a					
	unpacked-t0	sliced, MAP-t0 with rind	sliced, MAP-t0 without rind	unpacked-t1	sliced, MAP-t1 with rind	sliced, MAP-t1 without rind
Aldehydes	406.4 (0.1-7.8)	428.8 (0.0-7.4)	513.4 (0.0-17.0)	507.2 (0.3-14.0)	510.8 (0.0-59.0)	581.2 (1.1-60.0)
Alcohols	89.3 (0.0-3.7)	417.2 (0.0-91.0)	104.7 (0.0-2.6)	159.6 (0.0-16.0)	1040.4 (0.1-59.0)	132.5 (0.0-2.9)
Ketones	9631.0 (0.0-236.0)	9794.8 (0.1-159.0)	9832.4 (0.0-119.0)	9789.5 (0.1-43.0)	9133.3 (1.4-516.0)	10232.2 (2.0-193.0)
Volatile acids	24523.7 (1.0-379.0)	24960.3 (1.5-964.0)	28937.5 (3.4-940.0)	32147.9 (2.0-606.0)	31575.1 (0.0-489.0)	25961.6 (0.0-1056.0)
Ethyl esters	122.1 (0.0-5.0)	158.0 (0.0-17.7)	149.7 (0.0-6.2)	188.4 (0.0-6.1)	1025.4 (0.0-25.0)	146.2 (2.3-12.0)
Lactones	2722.5 (0.0-26.0)	2762.5 (3.2-96.0)	2922.8 (2.0-39.0)	2765.3 (0.0-78.0)	2637.6 (2.2-204.0)	2468.2 (1.1-68.0)
Sulphur compounds	17.9 (0.0-0.4)	17.9 (0.0-3.0)	16.1 (0.0-1.6)	19.6 (0.0-2.9)	35.8 (2.5-5.8)	30.8 (0.0-3.4)
Others	0.0	300.1 (0.7-50.0)	729.6 (5.5-54.0)	0.0	601.6 (0.1-79.0)	1504.8 (0.0-47.0)

^a Mean values of duplicate analyses (standard deviation range of the individual compounds)

To visualise the differences in the volatile composition of the analysed cheese samples during shelf life (t0 and t1) a PCA biplot of the semi-quantitative SDE-GC-MS concentrations of the alcohols, ethyl esters and packaging volatiles was made (Figure 1). There seemed to be no great difference in the volatile composition of all cheese samples immediately after packaging (t0). Only the MAP cheese without rind differed slightly from the other cheese samples as a result of the occurrence of higher levels of the packaging compounds. Less difference was observed for the aroma evolution of the unpackaged cheese during storage. This cheese sample was still situated at the negative PC1 axis at t1. A clear differentiation was made between the sliced, MAP cheese without rind and the sliced, MAP cheese with rind at t1. Sliced and MAP cheese without rind was characterised by packaging volatiles after 10 weeks of storage. Those packaging compounds, tentatively identified as branched-chain hydrocarbons, had no great impact on the sensory properties of the cheese. Sliced and MAP cheese with rind seemed to undergo a forced ripening process during shelf life due to the increase of concentration of ethyl esters (ethyl butanoate, ethyl hexanoate, ethyl octanoate, ethyl decanoate, ethyl dodecanoate, ethyl tetradecanoate, ethyl hexadecanoate) and alcohols (3-methylbutanol, 2-methylbutanol, 2-pentanol, 2-heptanol, 2-nonanol, 2-undecanol, 2-phenylethanol), mainly formed by alcoholic fermentation during anaerobic conditions of the MAP cheese during shelf life. Ethyl esters contribute to the 'floral' and 'fruity' note of cheese.

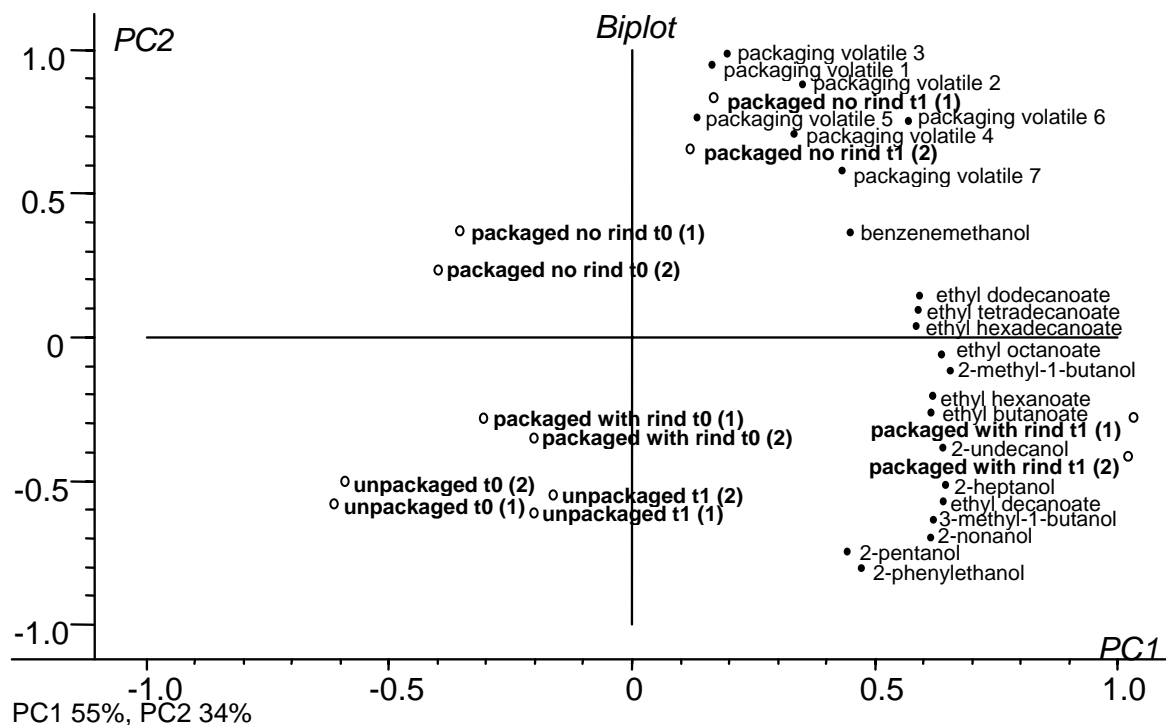


Figure 1. PCA biplot of the SDE-GC-MS concentrations of alcohols, ethyl esters and packaging volatiles of the unpackaged cheese and the sliced, MAP cheese, with and without rind, during shelf life (t0 and t1).

Summarising, clear differences in volatile composition between unpackaged and packaged cheeses under MAP conditions were observed, mainly due to the occurrence of compounds formed by alcoholic fermentation (ethyl esters and alcohols) and to the occurrence of packaging volatiles in the sliced and packaged cheeses. Triangle tests resulted in significant differences between the three cheese samples after 10 weeks of storage.

This work was supported by the Institute for the Promotion of Innovation by Science and Technology in Flanders (IWT-Flanders).

References

1. Dumont J.P., Adda J. (1979) In *Progress in flavour research* (Land D.G., Nursten H.E., eds.), Applied Science Publishers: London, pp 245-262.
2. Fox P.F., Singh T.K., McSweeney P.L.H. (1995) In *Chemistry of structure-function relationships in cheese* (Malin E.L., Tunick M.H., eds); Plenum Press: New York, pp 59-98.
3. Urbach G. (1997) *Internat. J. Dairy Technol.* 50: 79-89.
4. McSweeney P.L.H., Sousa M.J. (2000) *Lait* 80: 293-324.
5. Smit G., van Hylckama Vlieg J.E.T., Smit B.A., Ayad E.H.E., Engels W.J.M. (2002) *Austr. J. Dairy Technol.* 57: 61-68.
6. Marilley L., Casey M.G. (2004) *Int. J. Food Microbiol.* 90: 139-159.
7. Maarse H., Visscher C.A. (1989) In *Volatile compounds in food* (6th ed.), *Qualitative and quantitative data* (Vol 1). TNO-CIVO Food Analysis Institute, Zeist
8. Urbach G. (1993) *Int. Dairy. J.* 3: 389-422.
9. Dirinck P., De Winne A. (1999) *J. Chromatogr. A* 847: 203-208.
10. Van Leuven I., Van Caelenberg T., Dirinck P. (2008) *Int. Dairy. J.* 18: 790-800.

INTENSE ODORANTS OF CARDBOARD AND THEIR TRANSFER TO FOODS

Michael CZERNY

Fraunhofer-Institute for Process Engineering and Packaging, Giggenhauser Str. 35, D-85354 Freising

Abstract

The odour-active compounds of cardboard were identified by Aroma Extract Dilution Analysis and GC-MS identification experiments. Vanillin was detected with the highest odour intensity, followed by γ -nonalactone, (*E*)-2-nonenal, 2-methoxyphenol, δ -decalactone, and an unknown odorant. The strong odour intensities detected indicate that the odorants in cardboard are most likely present in high concentrations. Sensory analyses demonstrated that characteristic cardboard notes were transferred to sunflower oil exposed to moistened cardboard. This indicates that the liberation of odorants from cardboard as a result of improper production, handling, and storage can consequently cause off-flavours in packaged foods.

Introduction

Paper and cardboard materials are widely used for food packaging purposes, e.g. for sugar, salt, chocolate and confectionary products. Interactions of these packaging materials with the food products should be avoided because of a potential transference of odour-active volatiles into the food, causing off-flavours. Producers therefore aim at controlling the concentration of volatiles in their products (1) and try to manufacture papers and cardboards with low odour levels. Nevertheless, off-flavours have occurred sporadically in the past. Sources of the malodours can be inappropriate raw materials, chemical reactions and microbiological activities during processing, as well as the presence of contaminants in coatings used for printing (2,3,4).

Sensory panels and electronic noses have often been used to characterize cardboard odour and off-odours (5,6), but the chemical structures of the volatiles causing cardboard odour could not be established with these methods. The first successful approaches in identifying odorants in paper products were done by Leitner and Pfannhauser (7) and Ziegleder (8). They found several aldehydes, e.g. hexanal, octanal, nonanal, as odours-active compounds in cardboard samples by GC/olfactometry. Although they used sensory methods, the complete range of odorants may not have been screened due to limitations of the applied extraction methods. The aim of the present study was therefore to identify the whole set of odour-active compounds.

Experimental

The volatile compounds of cardboard (20 g, cut into squares, 5 x 5 mm), which was moistened with tap water (5 mL), were extracted with dichloromethane (200 mL) for 16 h at room temperature. The volatiles were isolated by Solvent Assisted Flavour

Evaporation (SAFE) distillation (9) and Aroma Extract Dilution Analysis (AEDA) was performed according to (10). The odour-active compounds were identified by comparing the odour quality, linear retention index (11) and mass spectrum (MS-EI) with the properties of the reference compounds.

Aroma Profile Analysis (APA) was performed according to (12). Odour transfer experiments were performed with the set-up detailed in (Figure 1). Cardboard squares (2 g) were placed in a glass flask (80 mL, flask 2) and moistened with tap water (1 mL). This flask was then placed in flask 1 (500 mL), containing sunflower oil (100 mL). Flask 1 was closed with a glass lid and stored for 2 days at room temperature in darkness. An additional glass flask (500 mL) was filled with sunflower oil (100 mL), closed with a lid, and stored in parallel, under the same conditions, as the control.

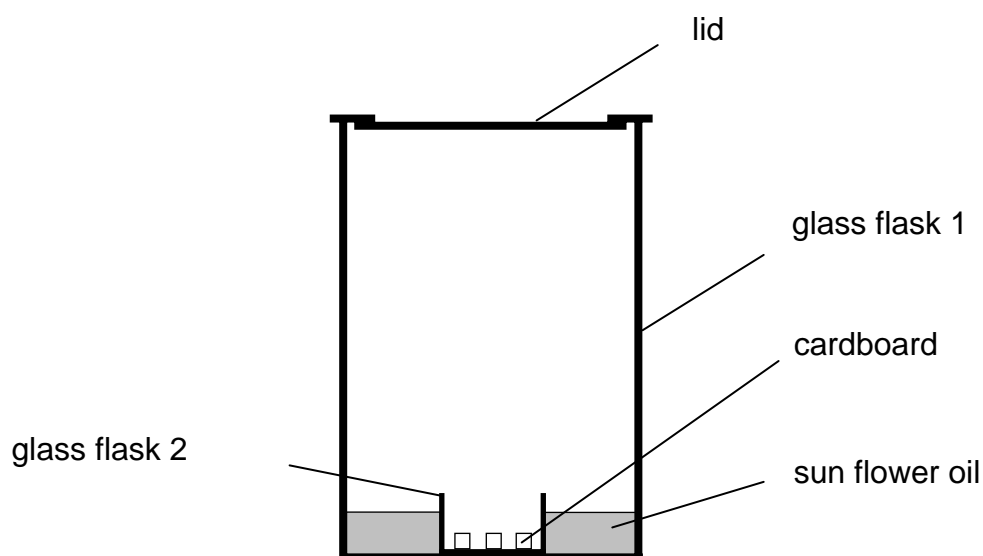


Figure 1. Set-up for odour transfer experiments.

Results

Initially, a cardboard sample was evaluated by APA. As detailed in (Figure 2), the attributes cardboard-like, woody, and musty were predominant. However, an off-flavour was detected following moistening of the cardboard. This malodour was caused by marked intensity increases of the aforementioned odour notes and the additional detection of a fatty and mouldy note (Figure 2). This sensory examination clearly demonstrated that cardboards can have a high potential to liberate unpleasant odours, especially when they are in contact with water.

To gain insight into the molecular reasons for the malodour, the volatiles were isolated from the moistened cardboard and their relative activities were estimated by AEDA. The highest intensity (FD- (flavour dilution-) factor 4096) was determined for the vanilla-like smelling vanillin (Table 1).

The following compounds were found as additional intense odorants within a FD-range of 128-512: γ -nonalactone (odour quality: coconut-like, sweet), (*E*)-2-nonenal (cardboard-like, fatty, green), 2-methoxyphenol (smoky, vanilla-like), δ -decalactone (coconut-like, sweet), 4-methylphenol (horse stable-like, faecal), *trans*-4,5-epoxy-(*E*)-2-decenal (metallic), 4-ethylphenol (musty, spicy, phenolic), and two unknown compounds with woody and coconut-like attributes. With the exception of (*E*)-2-nonenal (7), all compounds were identified as cardboard odorants for the first time.

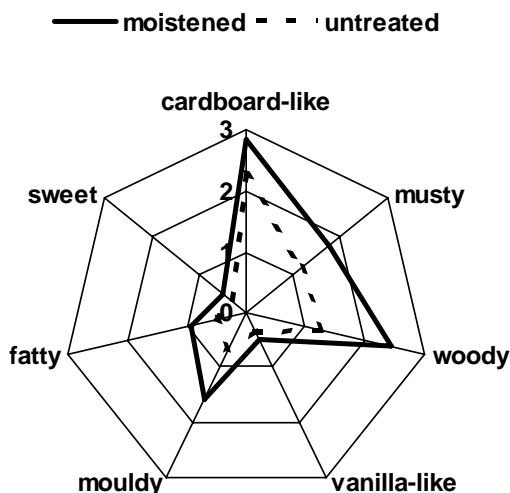


Figure 2. Aroma Profile Analyses of dry and moistened cardboard.

Table 1. Intense odorants in a cardboard sample identified by Aroma Extract Dilution Analysis^a and GC/MS experiments.

Odorant	Odour quality	RI ^b on		FD-factor ^c
		DB-FFAP	DB-5	
Vanillin	vanilla-like, sweet	2559	1396	4096
γ -Nonalactone	coconut-like, sweet	2014	1360	512
(<i>E</i>)-2-Nonenal	cardboard-like, fatty, green	1525	1157	512
Unknown	woody	2490	2012	512
2-Methoxyphenol	smoky, vanilla-like	1851	1086	256
δ -Decalactone	coconut-like, sweet	2185	1496	256
4-Methylphenol	horse stable-like, faecal	2077	1075	128
<i>trans</i> -4,5-Epoxy-(<i>E</i>)-2-decenal	metallic	1997	1382	128
4-Ethylphenol	musty, spicy, phenolic	2448	1432	128
Unknown	coconut-like	2448	1432	128

^a Compounds with FD-factors ≥ 128 are listed. ^b RI: linear retention index (11) on capillaries DB-FFAP and DB-5. ^c Flavour Dilution- (FD-) factor, determined by Aroma Extract Dilution Analysis (10).

The evaluated odorant pattern was well in agreement with the results of the APA. A comparison of both datasets indicates that the cardboard-like attribute was most probably generated by (*E*)-2-nonenal exhibiting this characteristic note. This correlation for the fatty note can also be assumed. The unknown odorant (FD 512, Table 1) and 4-ethylphenol were most likely responsible for the woody and musty quality, respectively.

In a further experiment, transfer of the malodour to foods was simulated by exposing sunflower oil to moistened cardboard using the set-up detailed in (Figure 1) (cf. "Experimental" section). An oil sample without cardboard exposure was also stored in parallel under the same conditions as a control. The sunflower oils were removed from the flask after two days and evaluated by APA. The results are illustrated in Figure 3. The control sample exhibited a fatty and oily note, which was

characteristic for sunflower oil. In contrast, the cardboard-exposed sunflower oil was affected with an off-flavour. The malodour was caused by the occurrence of cardboard-like, sweet, and woody notes, which had weak to medium intensities (Figure 3). The results indicate that odorants evaporated from the cardboard and diffused via air into the oil phase. It can be assumed that (*E*)-2-nonenal in particular is one of the important off-flavour odorants due to its characteristic odour attribute and the relatively high intensity of the cardboard-like note in sunflower oil.

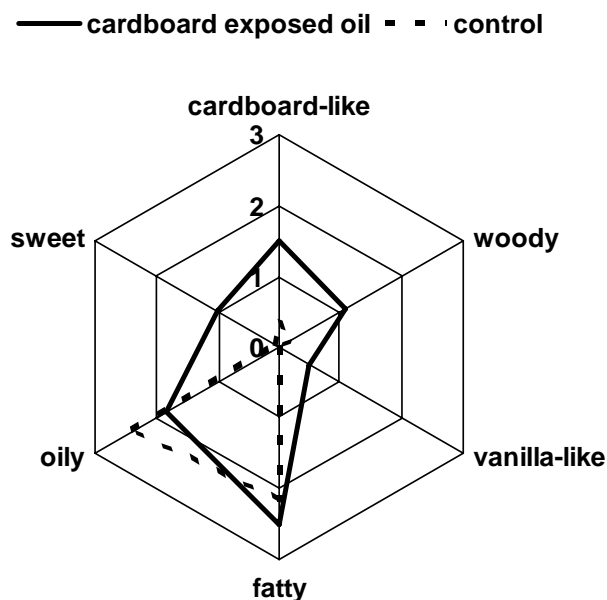


Figure 3. Aroma Profile Analyses of sunflower oil exposed to moistened cardboard, and an untreated sunflower oil sample (control).

In summary, the results suggest that cardboards contain the identified odorants most likely in high amounts due to their high FD-factors. In case of improper production, handling, and storage (e.g. moistening), cardboards can liberate odorants and cause off-flavours in packaged foods.

References

1. Ljungberg Willing B.I., Brundin A., Lundström I. (1998) *Packag. Technol. Sci.* 11: 59-67.
2. Lustenberger M., Ziegleder G., Betz G. (1994) *Wochenblatt für Papierfabrikation* 22: 899-902.
3. Ziegleder G., Stojacic E., Lustenberger M. (1995) *Packag. Technol. Sci.* 8: 219-228.
4. Tice P.A., Offen C.P. (1994) *Tappi Journal* 77: 149-154.
5. EN 1230-2:2002-04. *Paper and board intended to come in contact with foodstuffs.* Sensory analysis, part 2.
6. Forsgren G., Hakan F. (1999) *Nordic Pulp and Paper Research Journal* 14: 5-16.
7. Leitner E., Pfannhauser W. (2000) In *Frontiers of Flavour Science* (Schieberle P., Engel K.-H., eds.), German Research Center for Food Chemistry, Garching, Germany, pp 74-78.
8. Ziegleder G. (2001) *Packag. Technol. Sci.* 14:131-136.
9. Engel W., Bahr W., Schieberle P. (1999) *Eur. Food Res. Technol.* 209: 237-241.
10. Grosch, W. (2001) *Chem. Senses* 26:533-545.
11. van den Dool, H., Kratz, P.D. (1963) *J. Chromatog.* 11:463-471.
12. Scheidig, C., Czerny, M., Schieberle, P. (2007) *J. Agric. Food Chem.* 55:5768-5775.

Section 6

**Flavour Generation by
Thermal Processes**

EFFECT OF REACTION CONDITIONS ON THE GENERATION OF 4-HYDROXY-2,5-DIMETHYL-3(2H)-FURANONE FROM RHAMNOSE

T. DAVIDEK¹, S. Illmann^{1,2}, E. Gouézec¹, A. Rytz³, H.P. Schuchmann², and I. Blank¹

¹ Nestle Product Technology Centre Orbe, Nestec LTD., 1350 Orbe, Switzerland

² Food Process Engineering, Karlsruhe University, 76131 Karlsruhe, Germany

³ Nestlé Research Center, 1000 Lausanne 26, Switzerland

Abstract

The effect of various reaction parameters, including phosphate concentration (from 0.2 mol/kg to 1 mol/kg), rhamnose:lysine ratio (from 1:2 to 1:4) and reaction temperature (90°C to 120°C) and the effect of several amino acids (glycine, alanine, serine, threonine, proline, cysteine, lysine), on the kinetics of 4-hydroxy-2,5-dimethyl-3(2H)-furanone (HDMF) formation from rhamnose under aqueous conditions was assessed. Whereas all reaction parameters studied had some impact on the kinetics of HDMF formation, their impact on the maximum yield of HDMF was negligible. In general, the increase in phosphate concentration, in temperature or the decrease of rhamnose/lysine ratio resulted in shorter reaction times required to reach maximum yields of HDMF. Out of the amino acids tested Lysine was the most effective in generating of HDMF from rhamnose. Yields up to 50 mol% were obtained.

Introduction

4-Hydroxy-2,5-dimethyl-3(2H)-furanone (HDMF) is an important odorant of many fruits (e.g. pineapple), fermented foods (e.g. soy sauce) and thermally processed foods (e.g. roasted coffee) (1). This caramel-like, sweet and fruity smelling compound has first been isolated by Hodge *et al.* (2) from the reaction mixture of rhamnose and piperidine acetate. Since then, other studies have confirmed 6-deoxyhexoses as effective precursors of HDMF (3-6). However, literature data are rather fragmented and the conditions favouring the formation of HDMF from rhamnose are not completely understood. We have recently reported on yield optimization of HDMF from rhamnose under cooking conditions (aqueous system, 120°C) by systematically varying several reaction parameters including reaction time, pH, the presence of phosphate, concentration and ratio of reactants. Although this experimental design approach permitted to reach high yields of HDMF (~ 40 mol%) the optimisation of certain reaction parameters did not show any maxima and the yield of HDMF continued to increase through the whole experimental region covered (7). The aim of the present study was, therefore, to check if the yield of HDMF could be further improved by employing conditions not covered by the experimental design.

Experimental

The reaction mixtures were prepared by dissolving of corresponding quantities of rhamnose, monosodium dihydrogen phosphate and selected amino acids (Lys, Gly, Ala, Ser, Thr, Pro or Cys) in water. After adjustment of the pH (pH 7) with the solution of NaOH (0.1 mol/L), the reaction mixtures were adjusted to a total amount of 100 g

with water. The solutions were dispatched (a 5 mL) into Pyrex tubes (200 x 20 mm) and thermally treated (at 120°C, 110°C, 100°C or 90°C) in a silicone bath for a defined period of time. To stop the reaction, the samples were taken out of the oil bath and put directly into ice water. After cooling down, the reaction mixtures were spiked with ethylmaltol (internal standard), cleaned on SPE cartridge ENVI-Chrom P and analysed by gas chromatography - mass spectrometry (GC/MS) for HDMF as already described (7).

Results

In our recent study, the yield of HDMF from rhamnose was shown to increase with phosphate concentration in the range from 0 to 0.2 mol/kg and with decreasing rhamnose to lysine ratio in the range from 2:1 to 1:2 (7). The yield of HDMF might be therefore further increased by employing higher phosphate concentration or lower rhamnose:lysine ratios.

Effect of phosphate concentration. The kinetics of HDMF formation from rhamnose (in mol% as compared to rhamnose) in the presence of lysine and different levels of phosphate (pH 7) is shown on (Figure 1).

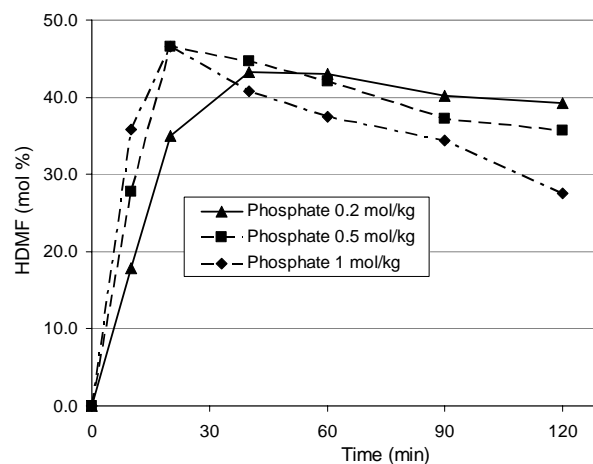


Figure 1. HDMF formation kinetics at different levels of phosphate (pH 7, rhamnose = 0.2 mol/kg, molar ratio Rha/Lys = 1:2, 120°C).

The increase of phosphate level from 0.2 mol/kg to 0.5 mol/kg or 1 mol/kg led to further increase of HDMF yield, however only at the early stages of the reaction. After reaching a maximum (about 47 mol% after 20 min) the yield started to decline and the final yield was lower as compared to that observed for medium phosphate level (0.2 mol/L). These data indicate that both the rate of HDMF formation and the rate of HDMF degradation increase with increasing phosphate concentration. The rapid degradation of rhamnose in the presence of high phosphate concentrations results in rapid cumulating of HDMF, however as soon as the rhamnose is exhausted the concentration of HDMF rapidly declines. Thus although a better HDMF yield is obtained when high levels of phosphate are employed (0.5 or 1 mol/kg) as compared to moderate concentrations (0.2 mol/kg), the reaction is more difficult to control (high risk of over-processing).

Effect of rhamnose to lysine ratio. The kinetics of HDMF formation from rhamnose in the presence of phosphate (0.2 mol/kg; pH 7) as affected by decreasing rhamnose to lysine ratio is shown in (Figure 2).

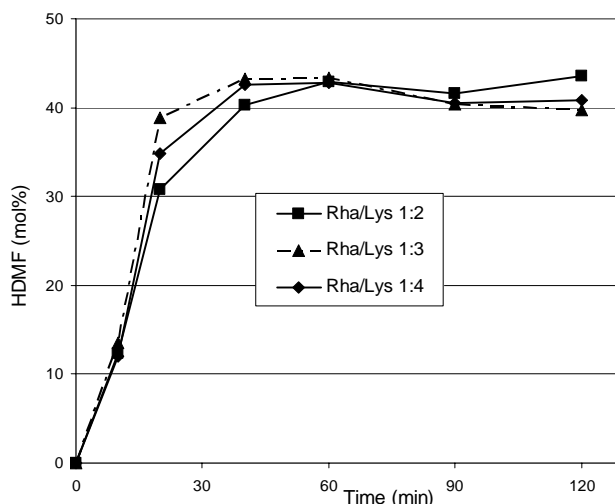


Figure 2. HDMF formation kinetics at different molar ratio rhamnose/lysine (phosphate = 0.2 mol/kg, pH 7, rhamnose = 0.2 mol/kg, 120°C).

The results indicate that decrease of the rhamnose to lysine ratio from 1:2 to 1:3 causes a moderate increase of HDMF yield, however only at the beginning of the reaction, thereafter the overall yields obtained are comparable. Further decrease of the rhamnose to lysine ratio to 1:4 is of no interest as the final HDMF yield was similar to those obtained at ratios 1:2 and 1:3 and the yields at the beginning of the reaction was lower as compared to ratio 1:3.

Effect of reaction temperature. To evaluate how the yield of HDMF is affected by the reaction temperature, the experiments were performed at 90°C, 100°C and 110°C, using the optimum reaction parameters leading to the highest HDMF yield at 120°C (0.2 mol/kg phosphate, pH 7, Rha/Lys = 1:2, 0.2 mol/kg rhamnose).

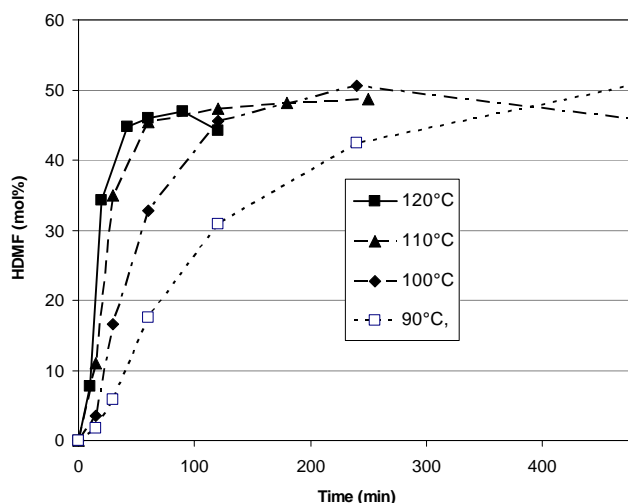


Figure 3. HDMF formation kinetics at different temperatures.

As illustrated in Figure 3, similar yields of HDMF were obtained at all temperatures studied, however the kinetics of the formation differed. Whereas a decrease of temperature from 120°C to 110°C did not change the kinetics significantly, further decrease led to significantly slower reaction kinetics. Therefore, the temperature range from 110°C to 120°C is of interest as this temperature permits

to obtain high yields of HDMF in short reaction time and the fluctuation of the reaction temperature does not affect significantly the time required to reach this high yields of HDMF.

Effect of amino acids. To evaluate whether the yield of HDMF from rhamnose is affected by the type of amino acid, six amino acids (Gly, Ala, Ser, Thr, Pro and Cys) were assessed and compared to lysine.

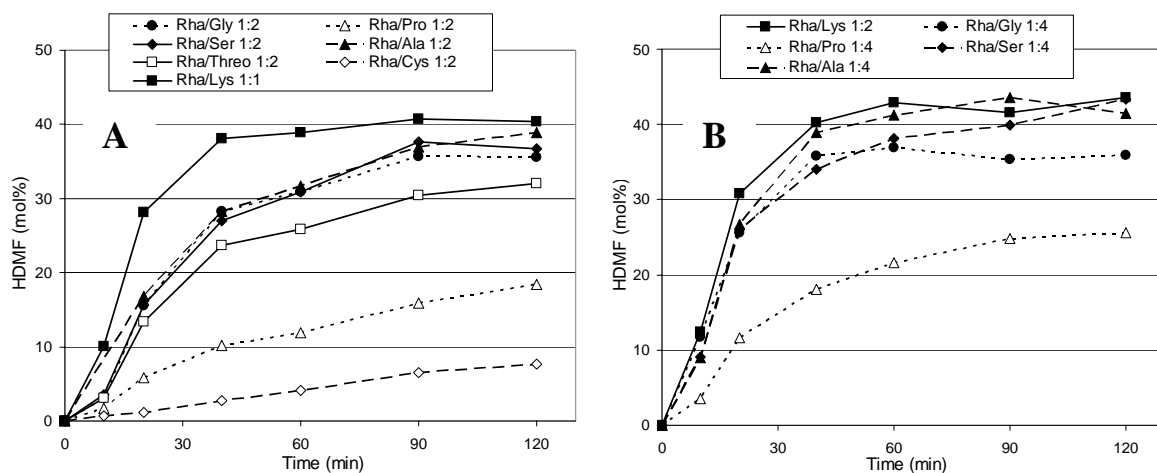


Figure 4. Effect of different amino acids on HDMF formation kinetics; A) Rha/NH₂ ratio = 1:2; B) Rha/NH₂ ratio = 1:4. (phosphate = 0.2 mol/kg, pH 7, rhamnose = 0.2 mol/kg, 120°C).

None of the amino acid tested was as efficient as lysine, especially at the beginning of the reaction (Figure 4A), when the molar ratio Rha/NH₂ 1:2 was used (it corresponds to Rha/Lys ratio 1:1). The yields obtained in the presence of Ala, Ser, Gly and Thr were about one third lower as compared to lysine. Much lower yields were obtained in the presence of proline and especially cysteine. Four amino acids were further tested at a concentration corresponding to molar ratio Rha/NH₂ 1:4. Similarly to lysine all four amino acid performed better when used in higher excess (Figure 4B) as compared to ratio Rha/NH₂ 1:2.

References

1. Zabetakis I., Gramshaw J.W., Robinson D.S. (1999) *Food Chem.* 65: 139-151.
2. Hodge J.E., Fisher B.E., Nelson E.C. (1963) *Am. Soc. Brewing Chemists Proc.* 163: 84-92.
3. Shaw P.E., Berry R.E. (1977) *J. Agric. Food Chem.* 25: 641-644.
4. Schieberle P. (1992) In *Flavour precursors-thermal and enzymatic conversion* (Teranishi R., Takeoka G.R., Güntert, M., Eds.), Washington, DC, pp.164-174.
5. Havela-Toledo E., Naim M., Zehavi U., Rouseff R.L. (1997) *J. Agric. Food Chem.* 45: 1314-1319.
6. Shaw J.J., Burris D., Ho C.-T. (1990) *Parfumer Flavorist* 15: 61-66.
7. Davidek T., Illmann S., Gouézec E., Rytz A, Schuchmann H.P., Blank I. (2009) *J. Agric. Food Chem.* 57: 2889-2895.

BASIC AND ACIDIC SUGARS AS FLAVOUR PRECURSORS IN THE MAILLARD REACTION

K. KRAEHENBUEHL¹, T. Davidek², S. Devaud¹, and Olivier Mauroux¹

¹ Nestlé Research Center, PO-Box, CH-1000 Lausanne 26, Switzerland

² Nestlé Product Technology Center, CH-1350 Orbe, Switzerland

Abstract

Charged and neutral sugars were reacted with cysteine in wet model systems using exactly the same reaction conditions. Degradation kinetics is significantly accelerated in acidic and basic monosaccharides as compared to neutral pentoses/hexoses. Browning levels and residual sugar values are not correlated. The acid and basic sugars studied generate very specific analytical volatile profiles. Aroma impact compounds and key intermediates leading to their formation such as enolones are formed in larger amounts especially from uronic and ketoaldonic acids. Decarboxylation is a key step preceding the formation of a majority of volatiles detected in these model systems. Charged sugars could potentially be applied in combination with neutral sugars glucose, xylose to fine tune sensory aroma profiles.

Introduction

Acidic and basic sugars have received relatively low attention as flavour precursors in the Maillard reaction as compared to neutral sugars (1) – (4). In the present work uronic and aldonic acids, aldosamine and neutral sugars were reacted with cysteine in wet model systems using exactly the same reaction conditions (Figure 1). Degradation reaction kinetics, relative analytical volatile profiles were compared. ¹³C labelling experiments were performed in order to obtain mechanistic information on the reaction pathways involved in the degradation of acidic sugars.

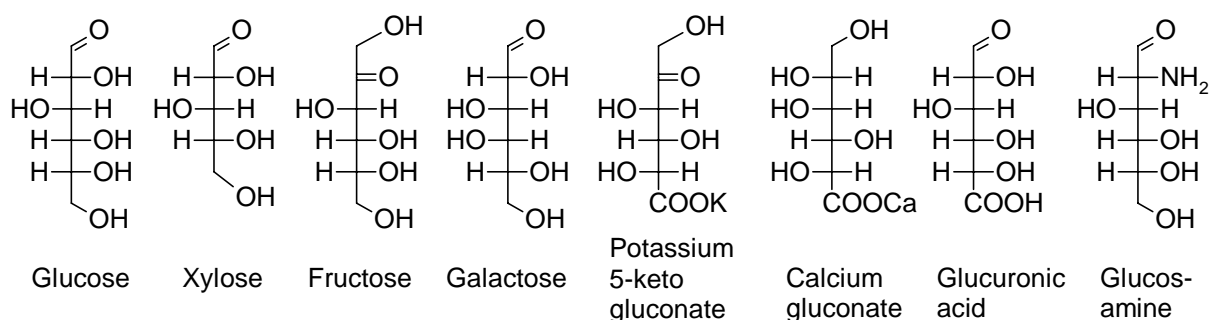


Figure 1. Neutral and charged monosaccharides studied.

Materials and Methods

Reaction. Monosaccharide (0.9mmol) and L-cysteine hydrochloride monohydrate (45mg, 0.25mmol) in 5mL phosphate buffer (200mM, pH 6.5) were heated at 125°C for 25min in a Pyrex tube sealed with a Teflon lined stopper (10cm x 1.5cm i.d.). The tube was cooled to room temperature on ice and aliquots were sampled for SPME-

GC-MS (2x0.5mL) and for HPAEC (0.1mL). The remaining solution was adjusted to pH 5.0 and extracted with Et₂O (3x10mL). The combined extracts were dried over anhydrous Na₂SO₄, filtered and distilled to 10mL with Vigreux column and further down to 200-300µL by microdistillation.

GC-MS analysis. This was performed on a GC 6890A coupled to an MSD 5973 (Agilent, Palo Alto, CA) using a DB-WAX column (30 m x 0.25 mm x 0.25 µm, J&W Scientific, Folsom, CA). The liquid organic extracts were analysed by splitless (0.5 µL) duplicate injection at 250°C with an oven temperature program: 25°C (2min), 40°C/min to 50°C (1min), 6°C/min to 240°C (15min). MS parameters: ion source, 280°C; electron impact, 70 eV; total ion current data treatment with Data analysis and Nestlé MS Database and Wiley spectral libraries. Peak identification was validated by comparison of retention indexes with tabulated values. Semi-quantitative comparison of model systems was based on relative peak areas of individual compounds after normalization by the weight of the concentrated organic extract.

HPAEC. Residual sugars were quantified using standard analytical conditions (5).

Results and Discussion

Residual sugars and browning. Neutral and charged sugars reacted under identical conditions (180mM, pH6.5, 125°C, 25 min sugar / cysteine molar ratio 4:1) result in clear differences in terms of browning and sugar degradation kinetics (Figure 2). Relative reactivity of neutral sugars is as previously described hexose < pentose. Compared to these well known monosaccharides, the acidic sugars with a carbonyl function (glucuronic acid and potassium 5-ketogluconate) show much faster degradation rates. Gluconic acid is quite stable under the same conditions. Decarboxylation is therefore not the only responsible of the fast reaction kinetics observed for some of the acidic sugars. Maillard reaction between carbonyl functions (aldehyde or ketone) and amino acid is playing a key role. Browning level and residual sugar values are not correlated. The browning order from light to dark as observed visually is: Calcium gluconate < xylose < glucose ~ galactose ~ fructose < glucuronic acid < potassium 5-ketogluconate < glucosamine. The fastest browning model is the aminosugar glucosamine although its sugar degradation level is fairly low with 20% only consumed. On the other hand the reaction of the neutral pentose xylose is virtually colourless although over 40% of the starting material has been consumed. Charged acidic sugars glucuronic acid and 5-ketogluconate presented an intermediate browning although their residual sugar levels were quite different with 43% (respectively 15%) sugar left. The sugar decrease is not directly linked to the formation of potent chromophores in these model systems.

Analytical volatile profiles. Major differences are observed in the profiles, specific volatiles are obtained for the charged sugars (Table 1). The number and total amount of volatiles formed in the charged sugar models is higher than with neutral monosaccharides. Maillard reaction kinetics is faster for these systems. All pyrazines and some sulphur compounds (thiazole, mercaptopropionic acid) are largely favoured in the glucosamine reaction. The acidic sugars show a rich profile with high levels of formic/acetic acids and key flavour intermediates (norfuranol, furaneol, dicarbonyl and hydroxycarbonyls). Nitrogen compounds (pyridines, pyrroles) are also significantly higher in the reactions with acidic sugars. Some of these volatiles are also found in xylose and fructose models but at much lower concentration. Gluconic acid has the poorest profile qualitatively and quantitatively. This is consistent with its low degradation level.

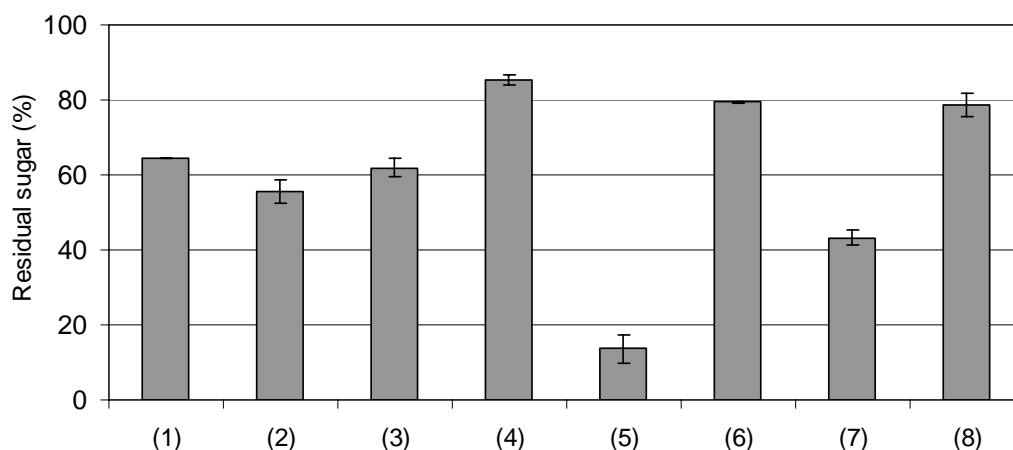


Figure 2. Residual sugar (% relative to initial) as determined by HPAEC after model reaction: (1) glucose, (2) xylose, (3) fructose, (4) galactose, (5) 5-ketoglucotate, (6) Ca-gluconate, (7) glucuronic acid, (8) glucosamine.

Table 1. Diethyl ether extract liquid injection GC-MS data - relative peak area compared to Glc-NH₂ model system (%). Sugar precursors: (1) glucose, (2) xylose, (3) fructose, (4) galactose, (5) 5-ketoglucotate, (6) Ca-gluconate, (7) glucuronic acid, (8) glucosamine.

Sugar precursor	(1)	(2)	(3)	(4)	(5)	(6)	(7)	(8)
Acetic acid	363	260	501	270	1604	21	430	100
Formic acid	305	228	421	370	25195	0	3911	100
1-Hydroxy-2-propanone	70	364	97	43	3046	1	950	100
1-Hydroxy-2-butanone	59	0	78	30	1519	141	83	100
3-Hydroxy-2-butanone	34	168	58	296	4432	390	430	100
2,3-Pentanedione	41	0	45	42	1042	20	0	100
Pyrazine	15	55	34	2	61	3	24	100
2-Methylpyrazine	0	0	1	0	13	0	1	100
2-Ethylpyrazine	2	6	83	1	59	0	10	100
2,3-Dimethylpyrazine	1	0	5	0	27	0	3	100
Pyridine	374	0	157	15	45	158	2459	100
3-Methylpyridine	27	202	72	0	1203	0	4513	100
2-Acetylpyrrole	107	12	142	69	162	3	81	100
1-H-Pyrrole-2-carboxaldehyde	8	36	40	25	226	0	209	100
2-Furaldehyde	35	305	55	204	1920	36	606	100
2-Furfuryl alcohol	23	14	131	329	430	13	53	100
Furaneol	25	0	25	8	783	0	13	100
Norfuraneol	129	1835	120	35	3573	8	33589	100
Thiazole	23	40	45	24	2156	13	79	100
2-Acetylthiazole	57	113	203	100	945	16	183	100
3-Mercaptopropionic acid	34	0	28	0	42	0	0	100
Tetrahydrothiophen-3-one	4	0	21	21	114	0	16	100
2-Carboxaldehydethiophene	4	8	7	3	196	4	27	100

Mechanistic hypotheses. Due to their specific structures the charged sugars studied in this work generate volatile profiles very different from those observed with neutral pentoses or hexoses. The accumulation of pyrazines and thiazoles in glucosamine reaction systems is easily explained by the presence of the additional amino group in the sugar. Enolone formation from acidic sugars is not straightforward to explain. One mechanistic hypothesis is shown in Figure 3. Norfuranol is observed in model systems with glucuronic acid and ketogluconate even in the absence of amino acid. It can be explained by elimination and decarboxylation of the sugar itself (path A). However, the amounts of enolones are significantly increased in the presence of an amino acid. Path B seems a plausible mechanistic hypothesis involving the amino acid as a catalyst. Elimination of the bulky amino group from the furanose form of the Schiff base (intermediate 2) should be favoured over water elimination from the corresponding intermediate 1 in path A. Model systems were also prepared with ketogluconic acid ^{13}C -labelled at the carbon in alpha position to the carboxylic acid C(2). The analysis of the corresponding volatiles shows that acetic acid formed in large amounts in this model system is not fragmented from the C1-C2 end of the molecule. It is most likely cleaved from the reducing end of the sugar (C5-C6). Hydroxypropanones and butanones do not incorporate the ^{13}C label either and are therefore formed from the C3 to C6 end. These results indicate that decarboxylation is a key step preceding the formation of a majority of volatiles detected in these model systems.

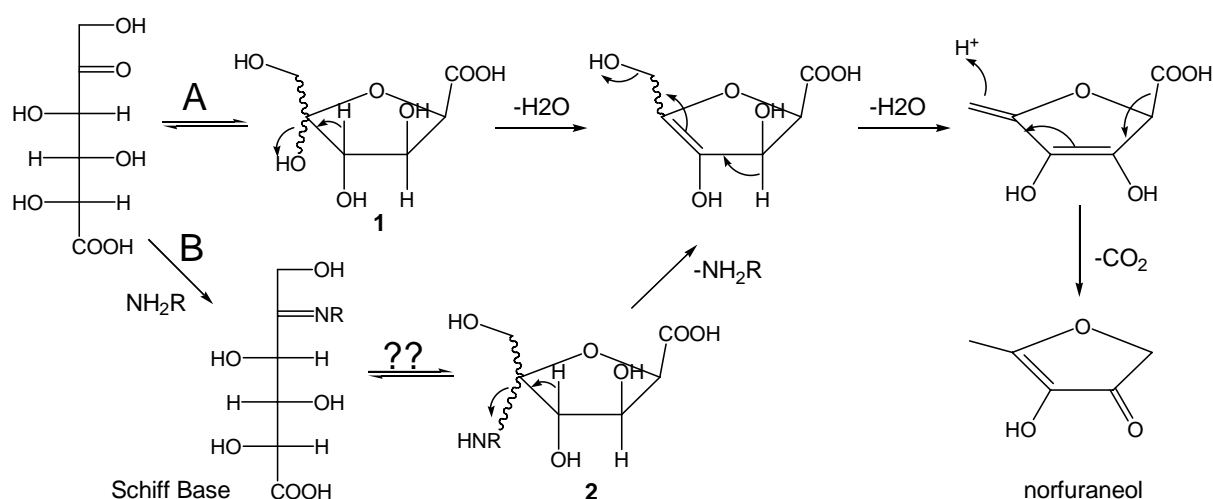


Figure 3. Mechanistic hypothesis for the formation of norfuranol from 5-ketogluconic acid.

References

1. Hashiba H. (1982) *Agric. Biol. Chem.* 46: 547-548.
2. Candiano G., Zetta L., Benfenati E., Icardi G., Queirolo C., Gusmano R., Ghiggeri G.M. (1990) In *Maillard React. Food Process., Hum. Nutr. Physiol.*, Ed. Birkhaeuser, Basel, Switz. 109-114.
3. Shu C.K., Bowman G.(1998) *J. Agric. Food Chem.* 46: 1129-1131.
4. Chen J., Ho C.T. (1998) *J. Agric. Food Chem.* 46: 1971-1974.
5. Davidek T., Clety N., Devaud S., Robert F., Blank I. (2003) *J. Agric. Food Chem.* 51: 7259-7265.

QUENCHING METHOD, MOISTURE CONTENT, AND AROMA STABILITY OF ROAST AND GROUND COFFEE

J. BAGGENSTOSS^{1,2} and F. Escher¹

¹ *Institute of Food Science and Nutrition, Swiss Federal Institute of Technology (ETH), Schmelzbergstrasse 9, 8092 Zürich, Switzerland*

² *Present Address: Nestlé PTC Orbe, Route de Chavornay, 1350 Orbe, Switzerland*

Abstract

Roasted coffee beans with different moisture content were ground and packaged under nitrogen and under normal atmosphere. The evolution of characteristic odorants was followed by means of headspace solid-phase microextraction coupled to gas chromatography–mass spectrometry. Under atmospheric storage conditions, decrease of dimethyl sulphide, 3-mercapto-3-methylbutyl formate, and *N*-methylpyrrole was accelerated in the coffee with highest water content. Storage under nitrogen atmosphere during 83 days at 37°C resulted in a considerable faster degradation of dimethyl sulphide, 3-mercapto-3-methylbutyl formate, *N*-methylpyrrole, 2-furfurylthiol, 2- and 3-methylbutanal, 2,3-butanedione, and 2,3-pentanedione with increasing moisture content. With both storage conditions, a large increase of dimethyl trisulphide concentration was observed; the increase being more pronounced in coffees with higher moisture content. This is a sign of faster thiol oxidation in roast and ground coffees with increased moisture content. The decrease in aroma stability is mainly attributed to a plasticising effect of water, which decreases the glass transition temperature of ground coffee and by this increases the mobility of reactants.

Introduction

Aroma stability of roasted coffee is very limited. It is supposed that aroma staling of coffee is mainly a result of degradation of important odorants such as methanethiol, 2-furfurylthiol, and Strecker aldehydes, rather than an effect of newly formed off-odorants (1, 2). Loss of aroma compounds is particularly fast if storage takes place under normal atmospheric conditions, and roast and ground coffee is especially susceptible to oxidation because of its increased surface and the short diffusion distance for the action of oxygen. Single sealed portions of roast and ground coffee increased in popularity recently and have gained high market share. High storage stability is expected in these coffees, particularly if grinding, degassing and packaging takes place under protective atmosphere. However, manufacturers tend to increase moisture content to the maximum allowed (5g / 100 g wb) although there is still little knowledge about the consequences of an increased water content on aroma deterioration in roast and ground coffee under protective atmosphere.

Experimental

Raw material, roasting, grinding, and storage conditions. Batches (45 kg) of Colombian *Coffea arabica* with initial water content of 10 g / 100 g wb were roasted

with a semi-fluidizing bed roaster CR-1250 from G. W. Barth Ltd. (Freiberg/Neckar, Germany). The coffees were roasted to an equal degree of roast, and roasting times were around 13.5 min. The roaster layout with separate roasting and cooling zones allowed the application of different quenching methods, *i.e.* air quenching, water quenching in the roasting zone, and water quenching in the cooling zone. By water quenching in the roasting zone only, it was possible to produce a water-quenched coffee without increasing its moisture content. The application of water in the cooling zone, however, resulted in an increased moisture content in the final product. Using the quenching methods mentioned above, four batches of coffee with identical degree of roast and differing water contents were produced (Table 1). Roasted coffees were packaged under nitrogen in polyethylene valve bags in portions of 1 kg as soon as the quenching process was completed. Colour and moisture content of the roasted coffees were determined as previously described (3).

Table 1. *Roasting trials with different quenching methods and resulting water contents.*

Batch	Quenching method	Water used in RZ ^a [L]	Water used in CZ ^b [L]	Moisture roasted coffee [g/100 g wb]	Colour [L*]
Q1	air	0	0	1.3	21.2
Q2	water (RZ) & air	5	0	1.4	21.2
Q3	air & water (CZ)	0	6	3.2	21.2
Q4	air & water (CZ)	0	8	6.5	21.5

^a roasting zone

^b cooling zone

After 24 h of equilibration time under nitrogen atmosphere at room temperature, the roasted coffee beans were ground and packaged. To prevent the contact of coffee with oxygen, the full operation was carried out under protective atmosphere. For this purpose, a disk mill (Bühler-Miag 4000, Bühler Ltd., Milano, Italy) was placed in a glove box with controlled nitrogen atmosphere (<1% O₂). Coffee beans were ground at level 3, then transferred to 100 g polyethylene valve bags, which were then heat sealed. The packaged coffee was stored at 37 °C during 83 days. In addition, open storage at normal atmosphere and 25 °C in the absence of light during 40 days was carried out.

Aroma analysis. Dimethyl sulphide, dimethyl trisulphide, 3-mercapto-3-methylbutyl formate, 2-furfurylthiol, 2-methylbutanal, 3-methylbutanal, hexanal, 2,3-butanedione, 2,3-pentanedione, N-methylpyrrole, and 2,3,5-trimethylpyrazine were sampled with headspace solid-phase microextraction (HS-SPME), analysed by GC-MS, and quantified by stable isotope dilution assay as described (3).

Results

Open storage of roast and ground coffee. Storage under normal atmospheric conditions leads to a very fast degradation of aroma compounds and the emergence of stale notes within a few days of storage (1, 4, 5). The evolution of some high volatile aroma compounds during open storage is displayed in Figure 1. While no differences with moisture content were observed for 2,3-butanedione, 2-furfurylthiol (not shown), 2- and 3-methylbutanal (not shown), 2,3-pentanedione (not shown), and 2,3,5-trimethylpyrazine (not shown); 3-mercapto-3-methylbutyl formate, dimethyl sulphide, and N-methylpyrrole (not shown) degraded faster in the coffee with highest

moisture content. Dimethyl trisulphide exhibited a large increase with increasing moisture content. A similar behaviour was observed in an earlier study on roasted coffee beans with different moisture contents (6), and the assumption was made that the fast increase in coffees with high moisture content was related to a faster oxidation of thiols.

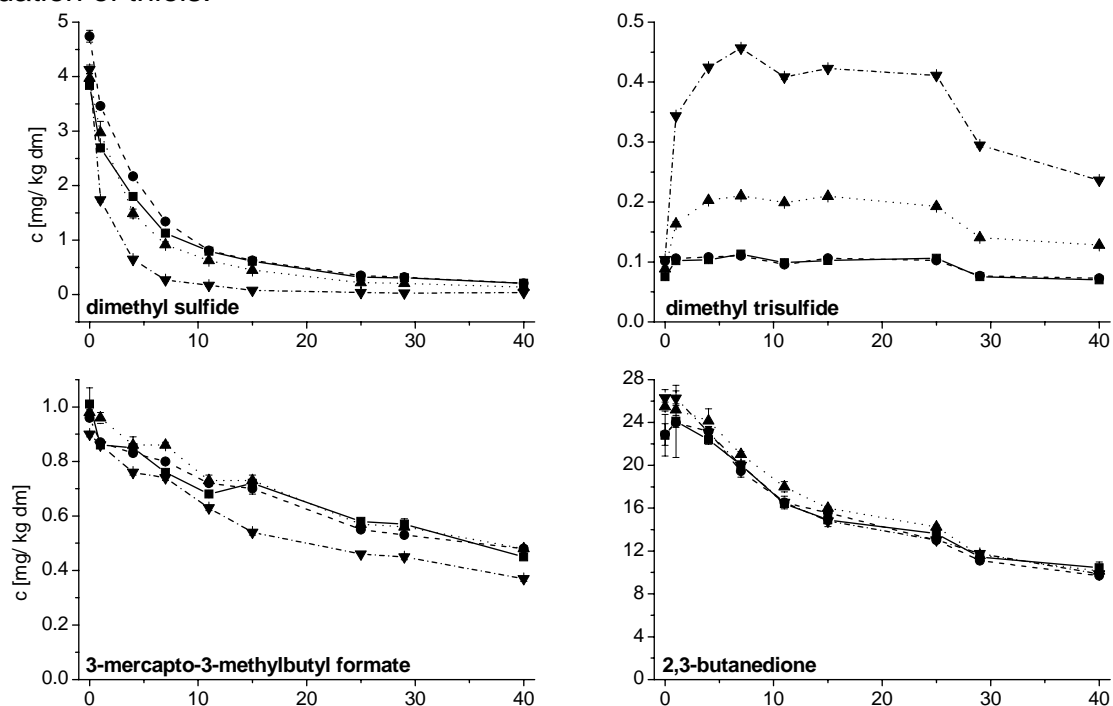


Figure 1. Alteration of selected aroma compounds during open storage of roast and ground coffee: air quenched (Q1, 1.3 g H₂O/ 100 g wb, ■), water quenched in roasting zone (Q2, 1.4 g H₂O/ 100 g wb, ●), water quenched in cooling zone (Q3, 3.2 g H₂O/ 100 g wb, ▲), water quenched in cooling zone (Q4, 6.5 g H₂O/ 100 g wb ▼).

Storage of roast and ground coffee under nitrogen atmosphere. Roast and ground coffee sealed in valve bags with an oxygen concentration lower than 1% was stored at 37 °C during 83 days. The increased storage temperature was chosen to shorten storage time. The impact of temperature on roast and ground coffee shelf-life was investigated by Cardelli and Labuza (7). The authors found a decrease in shelf-life of about 20% by increasing the storage temperature by 10 °C. The retention of aroma compounds after storage is displayed in Figure 2. Due to the better storage conditions, changes in the aroma profiles were slower, and differences in degradation rates with different moisture content were clearly visible.

Dimethyl sulphide, 2-furfurylthiol, 3-mercapto-3-methylbutyl formate, 2- and 3-methylbutanal, 2,3-butanedione, 2,3-pentanedione, and *N*-methylpyrrole exhibited considerable faster degradation with increased water content. Similar to the open stored samples, the increase of dimethyl trisulphide was more important with increasing moisture content. The concentration of 2,3,5-trimethylpyrazine remained practically constant during storage. The amount of hexanal, which is a secondary product of lipid oxidation, was more than doubled after 83 d of storage, but no differences with moisture content were observed. This is in agreement with data on water activities of roast and ground coffee at a moisture content between 2 and 5 g/ 100 g wb, which were specified as being between 0.1 and 0.5 (8, 9). According to Labuza (10), lipid oxidation is only slightly enhanced at these two water activity

values. The faster degradation reactions of odorants in coffees with high moisture content may be explained by the plasticizing effect of water, which reduces the glass transition temperature in amorphous solid systems (11). It was shown that a reduced glass transition temperature led to increased reaction rates in low moisture systems (11-14).

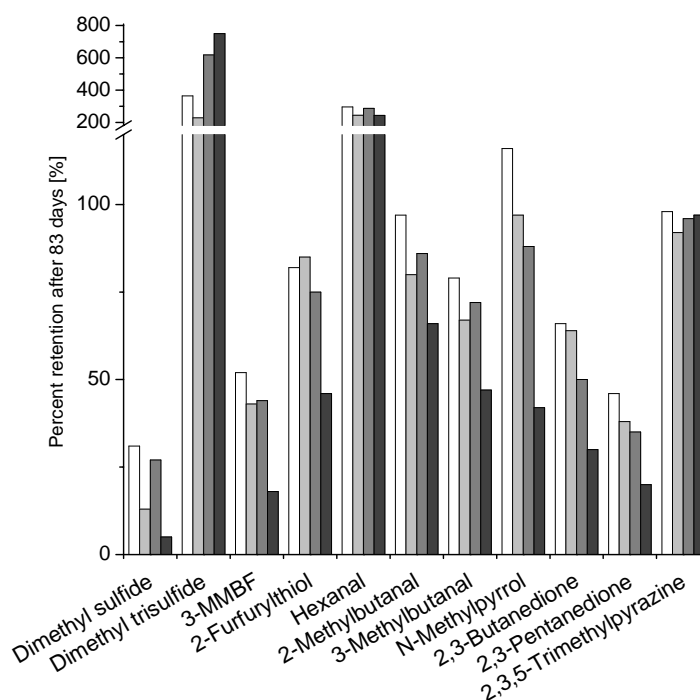


Figure 2. Percent retention (relative to $t = 0$ d) of aroma compounds during storage under nitrogen atmosphere at 37 °C. Air quenched (Q1, 1.3 g H₂O/ 100 g wb, □), water quenched in roasting zone (Q2, 1.4 g H₂O/ 100 g wb, ◻), water quenched in cooling zone (Q3, 3.2 g H₂O/ 100 g wb, ◼), water quenched in cooling zone (Q4, 6.5 g H₂O/ 100 g wb, ◼◼). 3-MMBF: 3-mercapto-3-methylbutyl formate.

References

1. Czerny M., Schieberle P. (2001) In *19th International Scientific Colloquium on Coffee*; Trieste, Italy.
2. Holscher W., Steinhart H. (1992) *Z. Lebensm-Unters Forsch.* 195: 33-38.
3. Baggenstoss J., Poisson L., Kaegi R., Escher F. (2008) *J. Agric. Food Chem.* 56: 5836-5846.
4. Clinton W.P. (1980) In *9th International Scientific Colloquium on Coffee*; London, UK.
5. Hinman D.C. (1991) In *14th International Scientific Colloquium on Coffee*; San Francisco, USA.
6. Baggenstoss J., Poisson L., Luethi R., Perren R., Escher F. (2007) *J. Agric. Food Chem.* 55: 6685-6691.
7. Cardelli C., Labuza T.P. (2001) *LWT-Food Sci. Technol.* 34: 273-278.
8. Cepeda E., de Lattiero R.O., San Jose M.J., Olazar M. (1999) *Int. J. Food Sci. Technol.* 34: 287-290.
9. Iglesias H.A., Chirife J. (1982) *Handbook of food sorption isotherms: water sorption parameters for food and food components*; Academic Press: New York.
10. Labuza T.P. (1971) *CRC Crit. Rev. Food Technol.* 2: 355-405.
11. Bell L.N. (1995) *Food Res. Int.* 28: 591-597.
12. Acevedo N., Schebor C., Buera M.P. (2006) *J. Food Eng.* 77:1108-1115.
13. Buera M.P., Karel M. (1995) *Food Chem.* 52: 167-173.
14. Karmas R., Buera M. P., Karel M. (1992) *J. Agric. Food Chem.* 40: 873-879.

COFFEE FLAVOUR MODULATION – REINFORCING THE FORMATION OF KEY ODORANTS WHILE MITIGATING UNDESIRABLE COMPOUNDS

L. POISSON¹, J. Kerler¹, Ch. Milo¹, F. Schmalzried^{1,2}, T. Davidek¹, and I. Blank¹

¹ Nestlé Product Technology Centre Orbe, Nestec LTD., CH-1350 Orbe, Switzerland

² University of Hohenheim, Institute for Food Chemistry, Stuttgart, Germany

Abstract

A combination of biomimetic in-bean experiments and spiking of green coffee beans with potential precursors was implemented to study formation pathways of several key odorants like 2-furfurylthiol (FFT) and alkylpyrazines during coffee roasting. Both labelled and unlabelled precursor molecules were used and the target analytes in the roasted coffee samples were analysed in terms of their isotope labelling pattern and their abundance. The biomimetic experiments elucidated that FFT is very likely not generated *via* 2-furaldehyde, which is in contrast to what was found in model studies. In addition, the incorporation of the arabinose C5-skeleton into FFT could not be confirmed, and our study showed that smaller arabinose fragments are integrated into the FFT molecule. In the second series of experiments, proposed pathways for the formation of alkylpyrazines were confirmed and the role of amino acids (e.g. alanine) was underpinned. In conclusion, the results of the biomimetic in-bean experiments emphasised the potential of this methodology for the verification of formation pathways in complex food systems like coffee. Furthermore, it represents a tool for the evaluation of options to modulate the aroma profile of roast and ground coffee.

Introduction

The formation of important coffee aroma compounds that belong to the group of thiols and pyrazines has been extensively studied in model systems under dry heating conditions (1-3). This has recently been extended to undesirable compounds such as furan (4, 5). In arabinose/cysteine model experiments, Tressl *et al.* (1) showed that 2-furfurylthiol (FFT) is formed via 3-deoxypentose and 2-furaldehyde while maintaining the intact carbon chain. Further experiments with polysaccharides isolated from green coffee and roasted in the presence of cysteine performed by Grosch (2) provided evidence that arabinogalactans are key precursors of FFT.

Amrani-Hemaimi *et al.* (3) showed in different model studies that C6 and C5 sugars (e.g. fructose, glucose or arabinose) are potential precursors for alkylpyrazines whose degradation compounds form key intermediates (*i.e.* α -amino-oxo compounds) through the Strecker reaction. In addition, alanine and glycine play a key role as they are integrated into the side chain of the alkylpyrazine molecule (3).

However, as it has been recently demonstrated for the formation of furan from ascorbic acid, the conclusions from model systems have to be taken with caution and cannot simply be extrapolated to complex food products (4). Hence, to study the importance of precursors for the formation of key aroma compounds during coffee roasting under real conditions, the so-called biomimetic in-bean experiments were developed. The idea of this approach is to make use of the green coffee beans as

'mini reactor' for model reactions, which allows a more realistic evaluation of potential precursors and provides very useful insight into formation pathways. The method involves the extraction of the green coffee by hot water, followed by the replacement of the solubilised fraction by a compounded equivalent. This biomimetic recombined extract (BRE) can be selectively omitted or fortified in particular precursors or, for mechanistic studies, labelled precursors may be incorporated. In addition, spiking of untreated green coffee beans with precursors or precursor groups represent another straightforward tool to studying the modulation of coffee flavour.

Coffee flavour modulation is an even more challenging task when aiming at optimisation of flavour generation and the mitigation of undesirable molecules such as furan, as both odorants and process contaminants were found to be formed from common precursors (4, 5). Therefore, our study aimed at verifying formation pathways of several key odorants such as FFT and alkylpyrazines in the coffee bean. In parallel, furan was monitored in order to identify strategies for its mitigation.

Experimental

Biomimetic in-bean experiments. Hot water extraction of green coffee beans. Green coffee beans were extracted with hot water as reported in the literature (6) using some modifications. 70 kg of green Arabica coffee beans (Colombia) were extracted consequently four times with demineralised water at 95 °C for a total of 2 h to obtain the water soluble substances. The extracts were collected and concentrated to a total solid content of approximately 27 %. After that, both the exhausted beans and the aqueous natural green bean extract were freeze-dried and stored at -40 °C until use.

Incorporation of biomimetic recombined extracts (BRE). The reconstituted green coffee extract (BRE, based on analytical results of the water soluble green coffee composition) was dissolved in demineralised water at 80 °C. 50 g of water were used for 125 g exhausted beans (EB) in order to guarantee a complete incorporation of the model solution into the coffee beans. The pH value of the compounded water soluble fraction was adjusted to 5.5 (corresponding to the pH of the natural extract) with a 16.5% w/w solution of KOH, and water exhausted green coffee beans were soaked with the BRE at 50 °C for at least 5 h. During soaking, the beans were gently stirred using a Rotavapor.

Omission experiments. BRE extracts with omission of potential precursors or precursor groups were reincorporated in the exhausted coffee beans as described before. The compounded extracts were omitted in all free sugars as well as all free amino acids.

Mechanistic studies. D-[U-¹³C₅]-arabinose (0.9 g) was added to the compounded model extract, which was omitted in all sugars, and incorporated into the water extracted, exhausted green beans. Additionally, green coffee beans were spiked with L-[3-¹³C]-alanine (0.48 g/150 g beans).

Spiking of precursor compounds. For the flavour modulation experiments, untreated green beans were fortified with equimolar amounts of different sugars such as glucose, arabinose (approximately 4 g of each sugar), or sucrose (about 50% of the natural amount in coffee), or amino acids like cysteine (0.45 g/150 g beans) or alanine (0.48 g/150 g beans). Each of the precursors was dissolved in 60 g demineralised water and green coffee beans (150 g) were soaked with the prepared solution for 2 h at 50 °C and for 2 h at room temperature. All treated green coffee samples were freeze-dried and then roasted at same conditions on a "Signum" rotating fluidized bed roaster (Neuhaus-Neotec, Germany) for 380 s at 236 °C.

Instrumental analysis. Quantification by Solid Phase Micro Extraction (SPME) combined with GC/MS. R&G coffee was suspended in hot water to obtain a slurry and after cooling spiked with defined quantities of labelled isotopes of the analytes. The prepared coffee suspensions were equilibrated (60 min, 20 °C) in the sealed vials and the aroma compounds were extracted from the headspace (10 min, 40 °C) using SPME (2 cm fibre coated with PDMS/DVB/Carboxen; Supelco). Aroma compounds were thermally desorbed in the injector port of the GC at 240 °C coupled to a mass spectrometer (Thermo DSQ). Separation of compounds was achieved on a polar silica thin-film capillary (Phenomenex ZB-Wax, 60 m × 0.25 mm; film thickness, 0.25 µm). Absolute concentrations are expressed as relative amounts compared to the reference set at 100 % (biomimetic recombined beans and green coffee).

Results and Discussion

2-Furfurylthiol (FFT). Milo *et al.* (6) reconfirmed previous work on models that FFT is mainly formed from water non-soluble precursors. In their biomimetic studies increased amounts of FFT were found in roasted coffee from water-extracted, exhausted beans. Indeed, the omission of all water soluble sugars in the biomimetic recombined green coffee resulted in significantly increased amounts of FFT, whereas 2-furaldehyde content was highly suppressed to less than 40% as compared to a fully reconstituted R&G coffee (BRE; see Figure 1A). Spiking experiments also did not show a relationship between the formation of FFT and 2-furaldehyde, as fortification of green beans with sucrose (50% of natural content) increased 2-furaldehyde amounts up to 160%, whereas concentrations of FFT considerably decreased (Fig. 1B). Hence, it seems that the formation of FFT during coffee roasting *via* 2-furaldehyde as intermediate compound is a minor pathway only. In addition, incorporation of D-[U-¹³C₅]-arabinose did not yield fully labelled FFT as it would be expected, but partially labelled FFT with ¹³C₁, ¹³C₂ and ¹³C₃-moieties (Figure 2). In line with these data, spiking of green coffee with arabinose did not result in increased amounts of FFT nor 2-furaldehyde, which confirms the conclusion of Milo *et al.* (6) that FFT is mainly formed from the non-water soluble fraction. In contrast, spiking experiment (Figure 1B) with cysteine resulted in enhanced FFT amounts, which shows an interesting avenue for coffee aroma modulation.

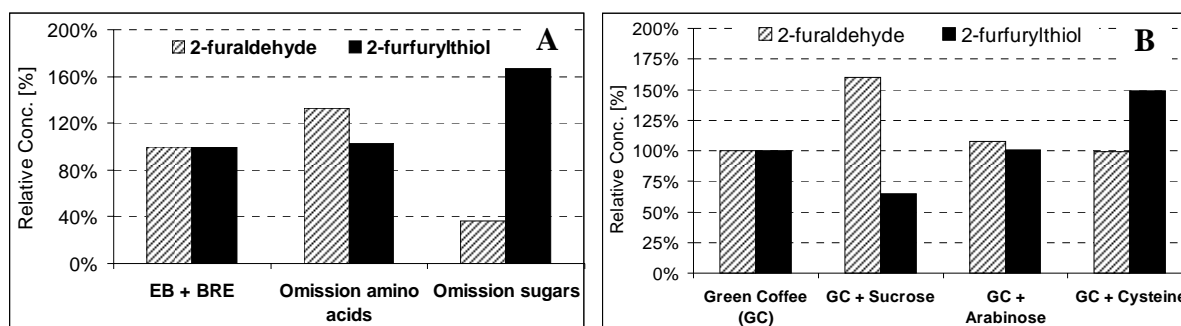


Figure 1. Omission experiments (A) as well as spiking of green coffee with sugars (equimolar amounts) and cysteine (B). Water exhausted beans (EB), biomimetic recombined extract (BRE).

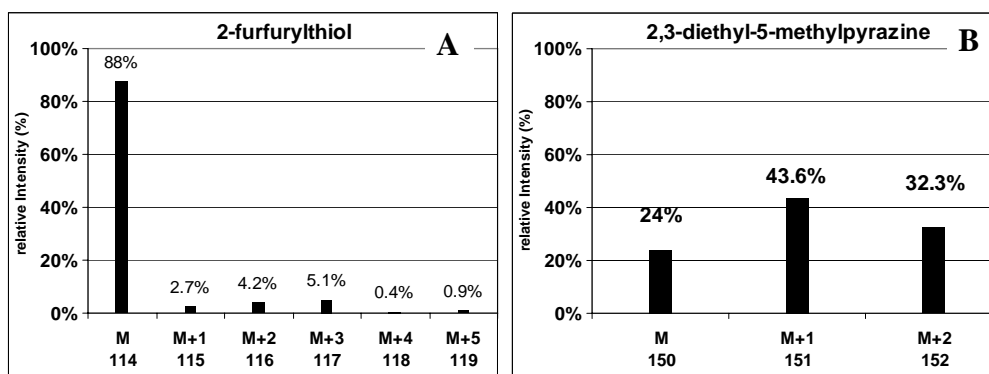


Figure 2. Incorporation of *D*-[U-¹³C₅]-arabinose (16% of natural content, A), and spiking with *L*-[3-¹³C]-alanine (B).

Pyrazines. Omission and spiking experiments confirmed the importance of free amino acids as precursors for the alkylpyrazines (Figure 3). Omission of all free amino acids decreased the amounts of 2-ethyl-3,5-dimethylpyrazine (EDMP) and 2,3-diethyl-5-methylpyrazine (DEMP) to 50% and even less than 25%, respectively, relative to the reference (BRE). As a confirmation of this result, spiking with alanine highly increased amounts of pyrazines, EDMP to almost 300% and DEMP up to more than 900%. All these results are further sustained by the spiking experiment with labelled alanine, which was efficiently incorporated into the side chain of the DEMP molecule (Figure 2B).

To study the impact of free sugars on pyrazine formation, recombined green coffee was omitted in all water-soluble sugars. This led to a considerable increase in contents of the two pyrazines (Figure 3A). Together with the fact that spiking of green beans with sucrose and arabinose had a suppressing effect on alkylpyrazine contents (Figure 3B), it can be stated that their generation involves the competition between bound and free sugars for the water extractable nitrogen source.

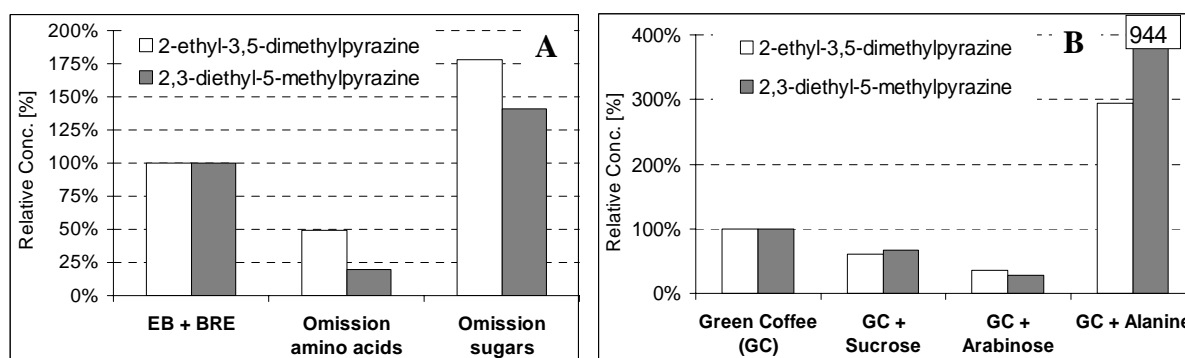


Figure 3. Omission experiments (A) and spiking of green coffee with sugars (equimolar amounts) and alanine (B).

Furan. Similar to the formation of FFT as shown in model studies (1, 2), Limacher *et al.* (5) reported that in arabinose model systems the major formation pathway of furan proceeds *via* 3-deoxyosone and 2-furaldehyde as key intermediates (4). Indeed, incorporation of *D*-[U-¹³C₅]-arabinose in green coffee beans (Figure 4B) verified the direct conversion of the carbon skeleton of arabinose into furan. The in-bean experiments, where green beans were spiked with different sugars, resulted in

arabinose having the highest potential in generating furan, followed by rhamnose and sucrose (Figure 4A).

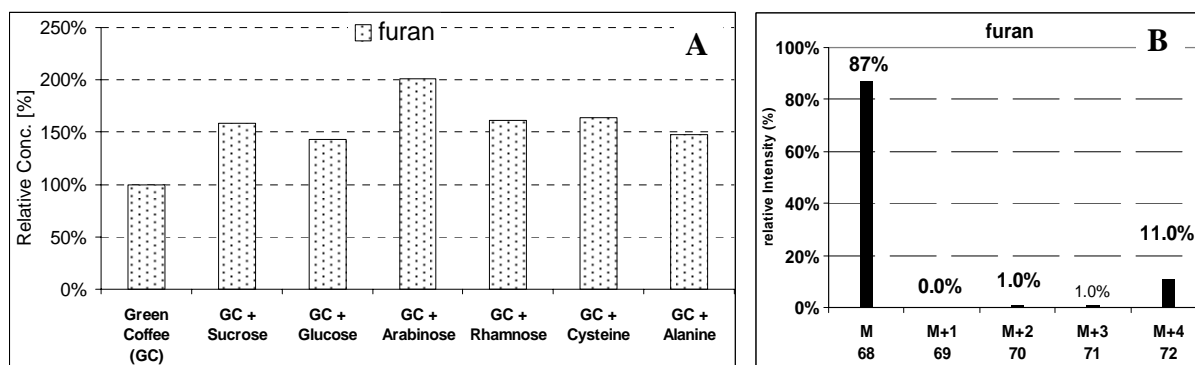


Figure 4. Spiking of green coffee with different sugars (equimolar amounts) and/or amino acids (A) and incorporation of D-[U-¹³C₅]-arabinose (16% of natural content) (B).

References

1. Tressl R., Helak B., Kersten E., Nittka C. (1993) In *Recent Dev. Flav. Fragrance Chem.* (Hopp, R., Mori, K., eds.), 3rd Proc. Int. Haarmann Reimer Symp., VCH: Weinheim, Germany, pp 167-181.
2. Grosch W. (1999) *18th Coll. Sci. Intern. Cafe*, pp 17-26.
3. Amrani-Hemaimi M., Cerny C., Fay L.B. (1995) *J. Agric. Food Chem.* 43: 2818-2822.
4. Limacher A., Kerler J., Conde-Petit B., Blank I. (2007) *Food Add. Contam.*, 24(Suppl. 1): 122-135.
5. Limacher A., Kerler J., Davidek T., Schmalzried F., Blank I. (2008) *J. Agric. Food Chem.* 56: 3639-3647.
6. Milo C., Badoud R., Fumeaux R., Bobillot S., Fleury Y., Huynh-Ba T. (2001) *19th Coll. Sci. Intern. Cafe*, pp 87-96.

STRUCTURES AND SENSORY ACTIVITY OF MOUTH-COATING TASTE COMPOUNDS FORMED BY ELLAGITANNIN TRANSFORMATION DURING OAK WOOD TOASTING USED IN BARREL MANUFACTURING

A. GLABASNIA and T. Hofmann

Chair of Food Chemistry and Molecular Sensory Science, Technische Universität München, Lise-Meitner-Str. 34, D-85354 Freising, Germany

Abstract

Aimed at investigating the chemical and sensory changes of ellagitannins during toasting of oak barrels, the native ellagitannins castalagin and vescalagin have been thermally treated in model systems after isolation from oak wood by means of gel permeation chromatography and HPLC. Depending on their stereochemistry at the C1 carbon atom of the glucose core, these astringent ellagitannins are degraded via different pathways into less mouth-coating taste compounds. These compounds then act as transient intermediates, which are further converted into deeply golden-brown coloured, melanoidin-type macromolecules. For example, the *S*-configured castalagin is oxidised to the previously not reported dehydrocastalagin, whereas the *R*-configured vescalagin, is converted into deoxyvescalagin, which means that both compounds show a complete different reaction pattern based on their stereochemistry.

Introduction

Wines and spirits such as whiskey are matured in toasted oak barrels for extended periods to give the beverages the desirable aroma, taste, and colour. Some of the native oak wood compounds are well characterised [1,2] and the toasting of oak wood is commonly known as one of the most important steps inducing the formation of taste and browning compounds by thermal degradation of wood constituents (e.g. ellagitannins). Nevertheless the structures of taste-active non-volatiles generated during oak wood toasting remain mainly unknown. Therefore, the chemical nature and sensory activity of reaction products produced in toasting model experiments were studied.

Experimental

Castalagin (**1**) and vescalagin (**2**) were extracted from oak wood chippings with 70% aqueous methanol and purified by means of gel permeation chromatography (GPC) using LH-20 material, followed by preparative RP-HPLC as described elsewhere [3]. The purified ellagitannins were placed in a glass vial and thermally treated in a lab oven for up to 60 min at 175°C. After cooling, the toasted samples were taken up in water and analysed by RP-HPLC/DAD. The formed degradation products were isolated by means of prep. HPLC and then identified by means of LC-MS/MS and 1D/2D-NMR experiments [4].

Results and Discussion

Samples of purified castalagin (**1**) and vescalagin (**2**) (Figure 1), isolated from oak wood chippings, were thermally treated at 175°C. After taking up the reaction mixture in water, the product profile of both reaction mixtures was monitored by means of HPLC-DAD. A “hump” of mouth-coating, brown coloured, melanoidin-type polymers (CP) was detected as well as ellagic acid (E), indicating a thermohydrolytic cleavage of the ellagitannins. In addition, individual major reaction products were produced upon toasting of **1** and **2** besides residual amounts of non-reacted ellagitannins as outlined in Figure 2. After isolation of **T1** and **T2** the following LC/MS/MS and 1D/2D NMR experiments interestingly showed that **1** was oxidized to the previously not reported dehydrocastalagin (**T1**) strongly depending on the stereochemistry. Its diastereomer **2**, just differing at the C1 carbon atom of the glucose core, is surprisingly converted into deoxyvescalagin (**T2**) (Figure 2). Similar results for this stereo-guided reaction pattern were found for the hydrolysis products castalin and vescalin, lacking the ellagic acid unit, as well as for the dimers roburin D (casta-configuration) and roburin A (vesca-configuration). These results prove that the C1 stereo chemistry is the key driver for the reaction upon thermal treatment regardless of the molecule size.

Comparison of both reaction mixtures revealed also major differences in their thermo-stability with **1** as the more stable isomer and **2** as an excellent precursor for mouth-coating polymers, being converted more rapidly and effectively into polymeric structures.

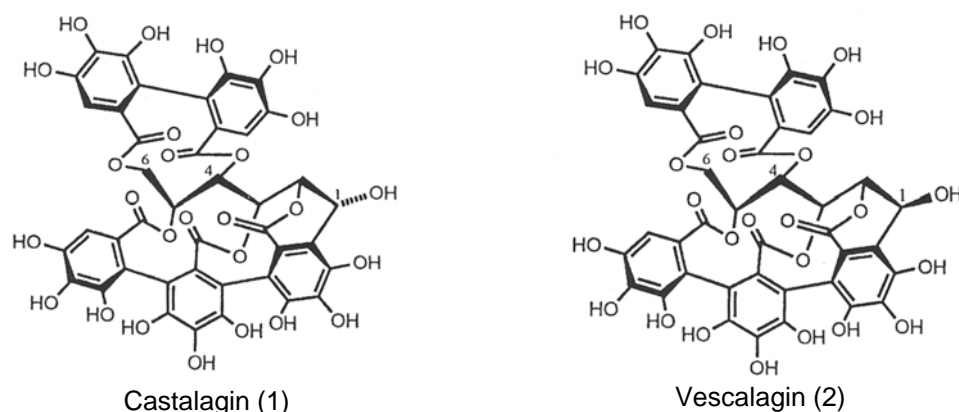


Figure 1. Structure of castalagin (1) and vescalagin (2).

In order to investigate the impact on the taste the sensory properties of the ellagitannin transformation products **T1** and **T2** were determined by means of an expert panel and compared to those of the native ellagitannins **1** and **2**. These sensory studies revealed taste thresholds for astringency of 1.1 µmol/L for both **1** and **2** whereas the thermal metabolites **T1** and **T2** were evaluated with somewhat higher thresholds of 4.4 and 3.3 µmol/L, respectively. The isolated polymers CP exhibited a mouth-coating oral sensation at a threshold concentration of 13.8 mg/L. As their oak-derived precursor ellagitannins **1** and **2** both imparted strong astringency at the low taste threshold of 0.9 mg/L each, it might be concluded that the toasting process is converting the highly astringent ellagitannins into less puckering, mouth-coating

substances. Thus this conversion might contribute to the balanced gustatory profile of oak-matured spirits (Table 1).

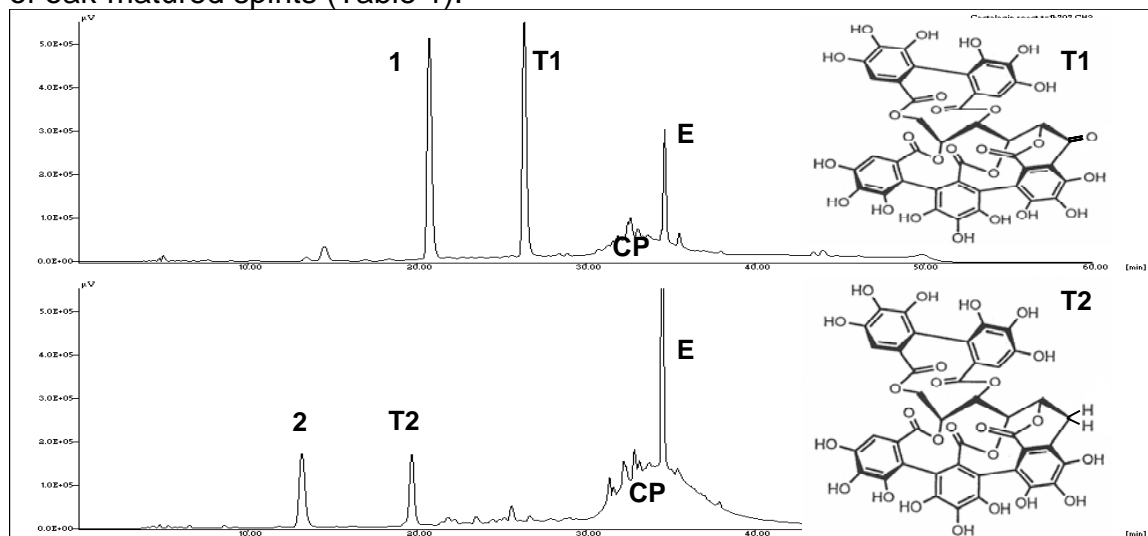


Figure 2. RP-HPLC chromatogram after thermal treatment of 1 and 2 (60 min, 180°C).

Table 1. Taste thresholds of native ellagitannins and their degradation products.

Compound	Threshold in $\mu\text{mol/L}$	Threshold in mg/L
Castalagin (1)	1.1	1.0
Vescalagin (2)	1.1	1.0
Dehydrocastalagin (T1)	4.4	4.1
Deoxyvescalagin (T2)	3.4	3.1
Polymeric hump	-	13.4

Based on quantitative model experiments (data not shown) the formation of the coloured oligomers might occur via two alternative pathways. On the one hand 1 and 2 are converted by oxidation respectively reduction into the transient intermediates T1 and T2 which then rapidly further undergo degradation to yield mouth-coating, melanoidin-type polymers. On the other hand castalagin and vescalagin, formed upon thermohydrolytic cleavage of ellagic acid from 1 and 2 and as such of low taste activity, were found as potential intermediates in polymer generation (Figure 3).

Conclusions

During oak wood toasting the astringent native ellagitannins are converted into less astringent metabolites. These metabolites were identified as transient intermediates of thermal transformation of ellagitannins into mouth-coating melanoidin-type polymers which contribute to the colour and balanced taste of oak matured beverages. These studies offer insights into the complex ellagitannin transformation chemistry and give some molecular explanation for the change of sensory-active non-volatiles in oak wood during toasting inducing the desired balanced, smooth taste of oak matured spirits.

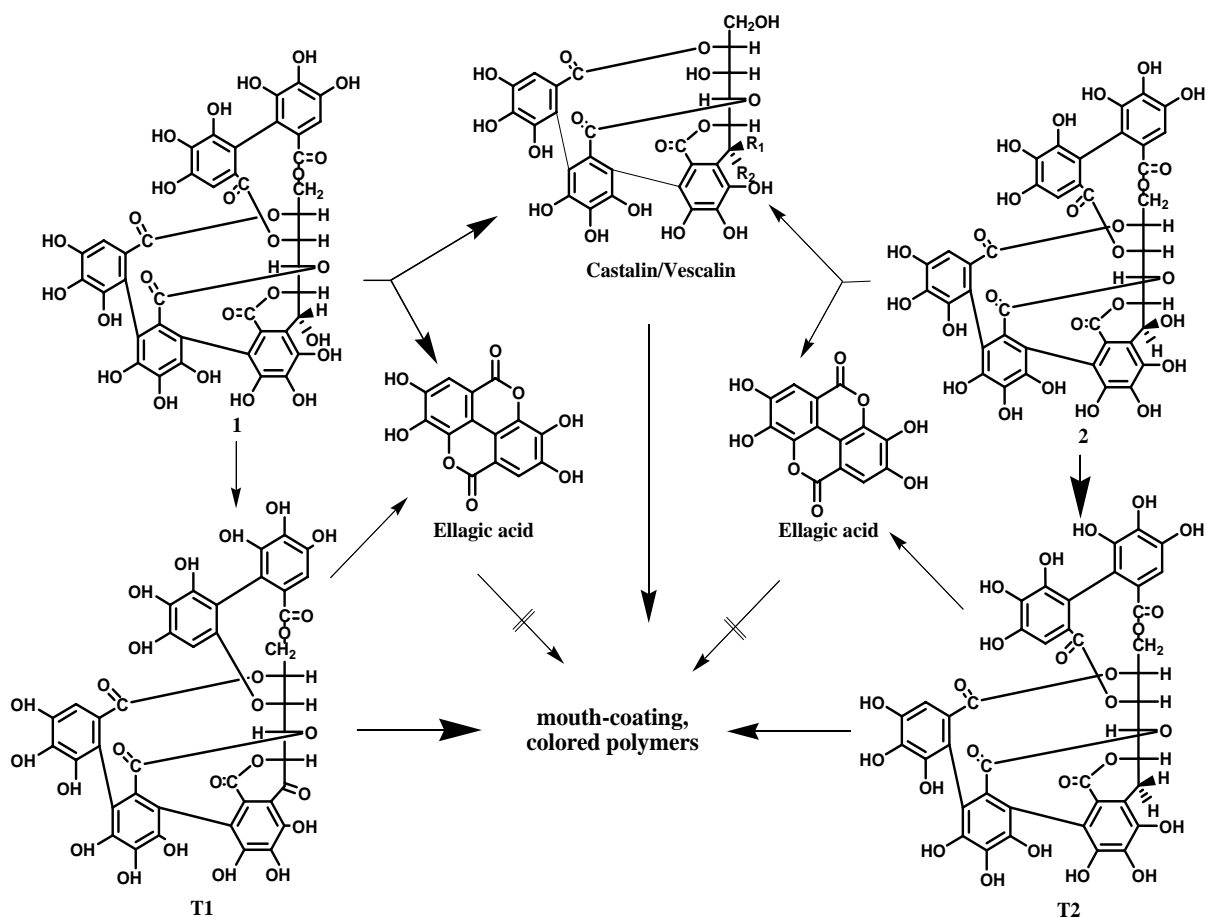


Figure 3. Degradation pathways of 1 and 2 upon thermal treatment.

References

1. Herve du Penhoat C., Michon V., Peng S., Viriot C., Scalbert A., Gage D., (1991) *J. Chem. Soc.*, 1653 ff.
2. Cadahia E., Varea S., Muñoz L, Fernandez de Simon B., Garcia-Vallejo M., (2001) *J. Agric. Food Chem.* 49 : 3677-3684.
3. Glabasnja A., Hofmann T. (2006) *J. Agric. Food Chem.* 54: 3380-3390.
4. Glabasnja A., Hofmann T. (2007) *J. Agric. Food Chem.* 55: 4109-4118.

MODELLING THE GENERATION OF FLAVOUR IN A REAL FOOD SYSTEM

D.P. BALAGIANNIS¹, J.K. Parker¹, D.L. Pyle¹, N. Desforges², and D.S. Mottram¹

¹ *Department of Food Biosciences, University of Reading, Whiteknights, Reading, RG6 6AP, United Kingdom*

² *Waltham Centre for Pet Nutrition, Waltham on the Wolds, Melton Mowbray, Leicestershire LE14 4RT, United Kingdom*

Abstract

Control of aroma generation during the Maillard reaction presents great scientific and industrial interest. Although there have been many studies conducted in simplified model systems, the results are difficult to apply to complex food systems where the structure of the matrix and the presence of other components can have a significant impact on the reaction. In such complex systems, some degree of qualitative control may be possible, but quantitative and predictive changes can only be achieved through the development of mathematical models based on reaction kinetics. In the work described here, an aqueous extract of raw defatted homogenised meat was chosen as a simplified food matrix for studying the kinetics of the Maillard reaction. Beef liver extract was prepared and cooked for different time intervals from 5 to 240 minutes at 130°C. Volatile analysis of the cooked samples was conducted using dynamic headspace extraction followed by GC-MS analysis. Free amino acid and sugar analyses were also performed. Volatiles identified included Strecker aldehydes, pyrazines and thiazoles. Multi-response kinetic modelling of the formation of 2- and 3-methylbutanal was carried out based on a simplified version of the Strecker degradation pathway.

Introduction

The Maillard reaction is the reaction between reducing sugars and amino compounds which is responsible for much of the generation of flavour compounds in cooked foods. It consists of many parallel and consecutive pathways, which render it very complex and difficult to control. Currently, it is possible to manipulate certain volatiles by altering the selected precursors, but these changes are qualitative and are likely to have an impact on the wider volatile profile. Quantification of such changes is complicated as many factors are involved, and requires the development of mathematical models based on the kinetics of the Maillard reaction.

Modelling is a process whereby a system of mathematical equations is generated in order to represent “reality” as accurately as possible. It is an iterative process (1) and comprises the following steps: generation of an initial hypothesis based on established reaction mechanisms, experimental design, modelling of data, model evaluation and criticism, and development of a new improved hypothesis on which to base further experiments. When the model is generated using data from several parts of the system simultaneously (reactants, intermediates, products), the process is called multi-response modelling. The aim of this work was to perform multi-response kinetic modelling of the Maillard reaction in a simplified meat system in

order to predict the level of key flavour compounds for a given set of process conditions.

Experimental

An aqueous extract of raw defatted homogenised meat was chosen for this study in order to obtain a more uniform heating profile than in meat tissue itself. It also removed the interference from lipids and simplified the extraction and analytical procedures. In this study, ox liver was used as the meat base. It was sliced, mixed with an equal quantity of deionised water and homogenised by blending it for 1 min (Megamix Cuisine Système 5100 automatic). The mix was then centrifuged for 20 min at 14000 rpm at 4°C and then the supernatant was filtered (Whatman filter number 3) under vacuum. Aliquots of the aqueous liver extract (20 ml) were sealed in 30 ml glass ampoules, immersed in an oil bath at 130°C and heated for different time intervals from 5 to 240 min. At least two replicates were prepared for each heating time. After heating, each ampoule was immersed in a coolant at -50°C to stop the reaction.

Dynamic headspace extraction was used for the extraction of the volatiles as described previously (2). Homogenised heated extract (5 g) and HPLC grade water (10 ml) were placed in a 250 ml conical flask with a Dreschel head and the volatiles were swept onto Tenax absorbent by nitrogen gas. The analysis of the compounds was performed on a Perkin-Elmer Clarus 500 GC-MS system (Perkin-Elmer, Beaconsfield, United Kingdom) coupled with an automated thermal desorption unit (Turbomatrix ATD). Quantification of the volatiles of interest was performed by generating calibration curves using the standard addition method.

The free amino acids were measured using the EZ-Faast amino acid derivatisation technique (Phenomenex, Torrance, CA). The initial sample size used was 0.5g, which was mixed with 0.01M HCl (10 ml). GC-MS analysis of the derivatised amino acids was performed on an Agilent 5975 system (Agilent, Palo Alto, CA) in electron impact mode (3). Sugar analysis was performed using a 8220i Dionex ion chromatography system (Dionex Corp., Sunnyvale, CA) (3). Standards of glucose, fructose, sucrose, ribose, maltose and mannose were used for quantification. Modelling was performed using Athena Visual Studio software (<http://athenavisual.com>).

Results

Many compounds were identified but, at this stage, only a few important flavour volatiles were selected for quantification and subsequent modelling. Compounds which were formed by the same reaction pathways showed similar trends with time. For example 3-methylbutanal and 2-methylbutanal were both formed very rapidly during the first 50 min, peaked and then showed a tendency to decrease over the remainder of the heating period (Figure 1a). Pyrazine and methylpyrazine both increased rapidly reaching a steady state, but a slightly different profile was obtained for a second group of pyrazines (2,5-dimethylpyrazine, ethylpyrazine and 2,3-dimethylpyrazine) which may be formed by a different mechanism. Likewise the thiazoles were split into two groups: thiazole and 4-methylthiazole generated similar profiles with respect to time, while 2-acetylthiazole and 2-propionylthiazole both followed another rate profile. This is an indication that different reaction mechanisms

are involved for each group, but within each group it should be possible to apply the same mathematical model.

(Figure 1b) shows the change in total free amino acids with time. There was a slight decrease over time, but two-thirds of the original amount still remained after 240 min suggesting that the amino acids were in excess. Glucose was the predominant sugar in the liver extract. It was consumed faster than the total amino acids (Figure 1b) and was 85% depleted by the end of the reaction, suggesting that glucose is a limiting precursor in this food system.

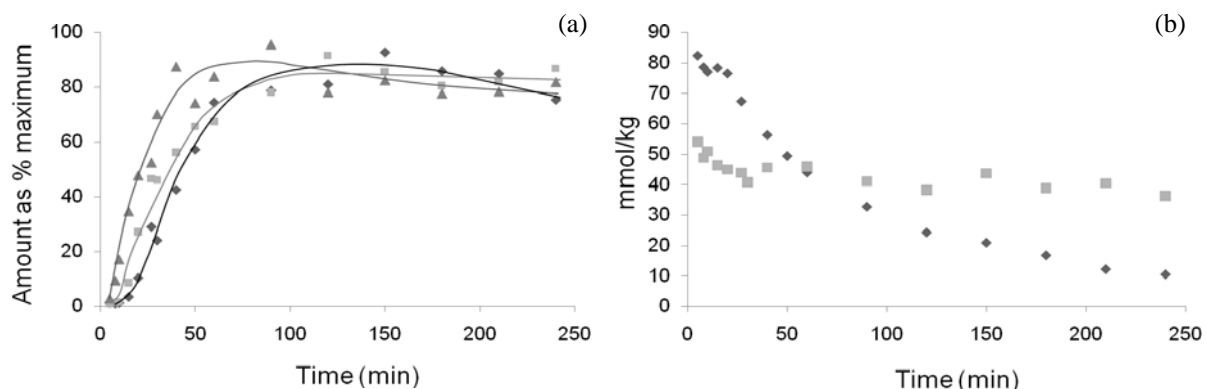


Figure 1: Trend for volatile and precursor compounds with time: (a) 3-methylbutanal (♦), pyrazine (■), 2-acetylthiazole (▲); (b) total amino acids (■), glucose (♦).

Modelling 3-methylbutanal and 2-methylbutanal. In order to model the formation of these Strecker aldehydes it was necessary to use a simplified version of the Strecker degradation pathway, an approach initially proposed by Wedzicha (4). This was achieved by using just one kinetically important intermediate (INT) which represents a group of rate-limiting intermediates likely to be those dicarbonyl compounds that are active in the Strecker degradation. It by-passes the short-lived intermediates which have minimal impact on the overall kinetics of the reaction. Thus, it was possible to propose a simplified chemical mechanism that described the formation of these compounds (Figure 2).

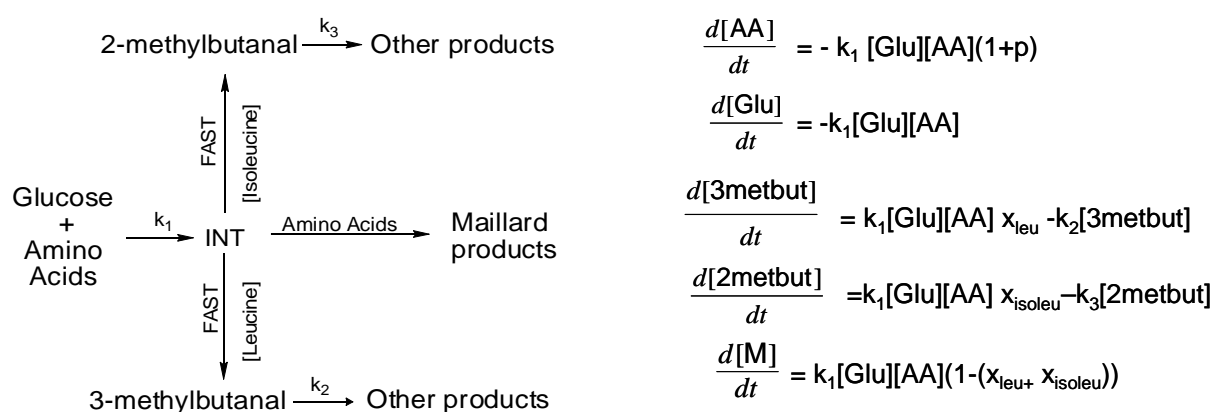


Figure 2. Mechanism of the formation of 3- and 2-methylbutanal and the corresponding set of differential equations.

By applying standard rate laws to this mechanism, a model was developed which comprised a set of ordinary differential equations. Six parameters were included among them; k_1 , k_2 and k_3 which are the reaction rate constants, p which accounts for

other amino acid reactions, and x_{Ileu} and x_{Isoleu} which represent the fraction of the respective amino acids which participate in the Strecker degradation. These parameters were estimated by using the software Athena Visual Studio, taking into account all the responses that had been determined experimentally (multi-response kinetic modelling). This led to the formation of a model which showed a good fit to the experimental data (Figure 3). However, further testing needs to be done in order to evaluate and validate it as a predictive tool.

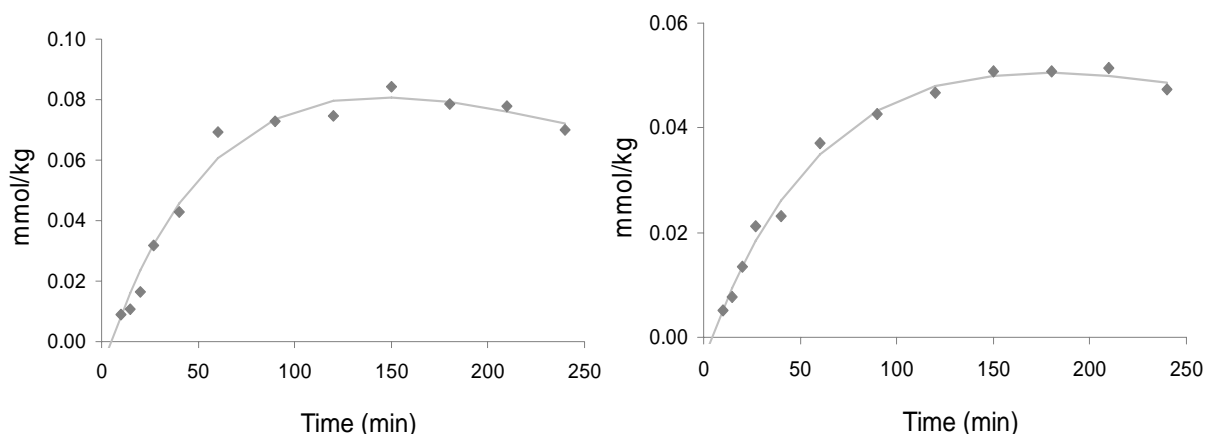


Figure 3. The model (line) shows good fit with the experimental values (points) for both (a) 3-methylbutanal and (b) 2-methylbutanal formation.

Conclusions

This preliminary experiment showed that modelling flavour formation in a complex food is possible and multi-response modelling appears to be a suitable technique for this purpose. When it was implemented for 2- and 3-methylbutanal, the model that was developed showed good fit to the experimental data.

This paper is dedicated to the late Professor Leo Pyle (1941-2008).

References

1. van Boekel M.A.J.S. (2000) *Czech J. Food Sci.* 18: 1-4.
2. Methven L., Tsoukka M., Oruna-Concha M.J., Parker J.K., Mottram D.S. (2007) *J. Agric. Food Chem.* 55: 1427-1436.
3. Elmore J.S., Koutsidis G., Dodson A.T., Mottram D.S., Wedzicha B.L. (2007) *J. Agric. Food Chem.* 53: 1286-1293.
4. Wedzicha B.L., Mottram D.S., Elmore J.S., Koutsidis G., Dodson A.T. (2005) In *Chemistry and Safety of Acrylamide in Food* (Freidman M., Mottram D.S., eds.), Advances in Experimental Medicine and Biology, Vol. 561, Springer: New York, pp 235-254.

FORMATION OF FLAVOUR PRECURSORS BY THE AMP PATHWAY IN CHICKEN MEAT

M. Aliani¹, J.T. Kennedy², C.W. McRoberts², and L.J. FARMER^{1,2}

¹ Queen's University Belfast, Belfast, UK

² Agri-Food and Biosciences Institute, Newforge Lane, Belfast, BT9 5PX, UK

Abstract

Ribose, a key flavour precursor in chicken meat, is believed to derive from the ATP breakdown pathway. This paper reports an investigation of this pathway. AMP, IMP, inosine and adenosine were added to chicken crude extract that had been dialysed against either phosphate or citrate buffer. Analyses were conducted to determine the quantities of key metabolites. These studies suggest that a number of pathways may contribute to the breakdown of AMP and its metabolites. Phosphate ions play a key role in determining the balance between these pathways.

Introduction

The volatile compounds responsible for meat flavours and odours develop during cooking by complex reactions between natural components in raw meat. In chicken, ribose has previously been shown to be of particular importance for flavour generation, with a much greater effect than ribose-5-phosphate or thiamine, when the natural concentrations of these compounds are taken into account (1). The generally accepted route of formation of ribose is via the breakdown of ATP to AMP and inosine to give ribose and hypoxanthine (2), as illustrated by the heavy arrows in (Figure 1). However, many other related pathways are known in living organisms and the enzymes classified (Figure 1). While information is available on these individual enzyme pathways, few studies have investigated the whole enzyme system. Amongst the few reports of these pathways in meat is that of Lee and Newbold (3) who presented evidence, using enzyme inhibitors, that, in ox muscle (*longissimus dorsi*), IMP was degraded to hypoxanthine by a pathway involving steps (d) and (f) rather than (d) and (e) (Figure 1). However, sugar concentrations were not reported.

Both IMP and inosine are present in chicken meat postmortem and only a small proportion appears to be converted to ribose (4). For optimum flavour generation it would be desirable to increase this conversion. Phosphate ions are important cofactors or products of several of these pathways (Figure 1) and it was expected that their presence or absence would inhibit some pathways and promote others.

This study was designed to test the effect of the presence or absence of key metabolites on the formation of sugars and nucleotides by the AMP breakdown pathway in a simple extract intended to mimic the whole chicken enzyme system.

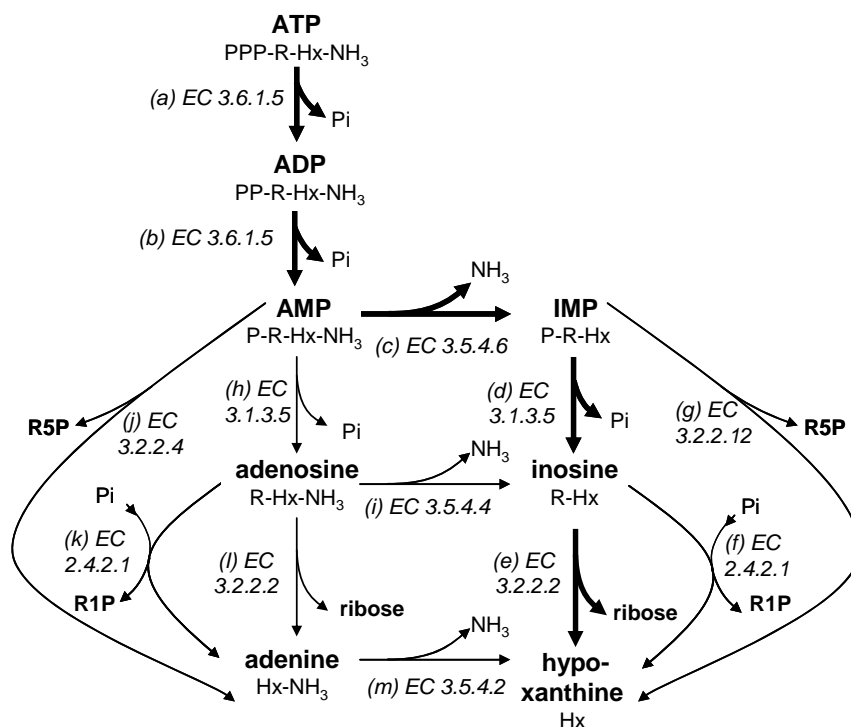


Figure 1. Known ATP breakdown pathways that may occur in chicken meat.

Experimental

Chicken breast meat without skin (10 kg, pH 5.98) was minced and mixed thoroughly, before taking a sample (750g). This sample was homogenized with 1500 ml KCl (0.16 M) for 3 minutes at 4 °C and the mixture centrifuged at 14,000 g at 4 °C for 30 minutes (Beckman centrifuge, UK). Two aliquots of the crude extract supernatant (650 ml) were dialysed against 10 liters of either phosphate or citrate buffer (0.1 M, pH 6.0). Phosphate buffer is one of the major buffering constituents of meat, and was used at a concentration to simulate the ionic strength and pH of meat, while citrate buffer was chosen to give the same ionic strength and pH, but an absence of phosphate ions. The dialyzed crude extracts (450 ml) were supplemented with a vitamin, co-factor and mineral solution (50 ml) to supply any essential cofactors that would have been lost through dialysis. Its composition was based on that of several commercial assay media (Sigma, Poole, UK) and comprised: riboflavin (0.1), thiamine (0.1), biotin (0.001), niacin (0.2), para-aminobenzoic acid (0.2), panthanoic acid (Ca²⁺) (0.1), pyridoxine HCl (0.2), pyridoxamine (0.08), folic acid (0.02), cobalamine (0.1), NADP (765.0), NAD (3.0), FMN (3.0), FAD (3.0) (mg L⁻¹ of mixture added); MgCl₂ 4H₂O (0.1), MgNO₃ (0.1) (mM of mixture added).

Two experiments were conducted. In Experiment 1, solutions of IMP, AMP, inosine and adenosine (6 µmol in 1 mL HPLC grade water) were added individually to 5 ml of dialyzed crude extract (against either phosphate or citrate buffer) in triplicate and incubated at 37 °C for 0, 5 or 18 hours. In Experiment 2, crude extract dialyzed against citrate buffer was used. IMP or inosine (20 µmol or 6 µmol, respectively, in 1 mL HPLC grade water) was added, with or without phosphate (600 µmol, in 1 mL HPLC grade water) to 5 ml of dialyzed crude extract to give a final volume of 7 mL. Samples were prepared in triplicate and incubated at 37 °C for 0 or 5 hours. All samples were treated with perchloric acid (15% v/v) and neutralised with KOH (6 M). Extracts were analysed by reverse phase HPLC (5) for nucleotides and

related compounds (Experiment 1) and by GC-MS, for sugars and sugar phosphates (Experiment 2), using a method adapted from that of Le Blanc and Ball (6).

Results and Discussion

Figures 2 and 3 show the effect of adding selected AMP metabolites into dialyzed chicken crude extract on the quantities of nucleoside-related compounds and sugars. Figure 2 shows that there was no large change in metabolite concentrations between 5 and 18h incubation, as would be consistent with exponential growth of microorganisms. Furthermore, the residual sugars in dialyzed (or non-dialyzed) crude extract, to which no metabolites had been added, did not show any decrease between 0 and 5 hours (data not shown). This gives confidence that the effects observed are largely due to the action of enzymes endogenous to the chicken muscle rather than due to microbial growth.

The simple extraction process and the inclusion of a range of minerals and cofactors aimed to ensure that the enzymes in this system remained active after extraction and dialysis. The conversion of metabolites observed in dialysed and undialysed extracts (data not shown) showed that the enzyme systems remained active. The different breakdown steps will be discussed in reverse order, as the later steps have a clear effect on the progress of those that precede them.

Inosine breakdown. The breakdown of inosine to form hypoxanthine is evidently very dependent on the presence of phosphate (Figure 2), with little breakdown occurring in citrate buffer. This suggests that the generally accepted pathway (e) may not be the most important pathway for the breakdown of inosine and that pathway (f), requiring phosphate and giving ribose-1-phosphate, may be more important. This agrees with the results reported by Lee and Newbold (3). Ribose-1-phosphate was sought using GC-MS; it was not detected but appeared to be labile under analysis, so its absence cannot be assumed.

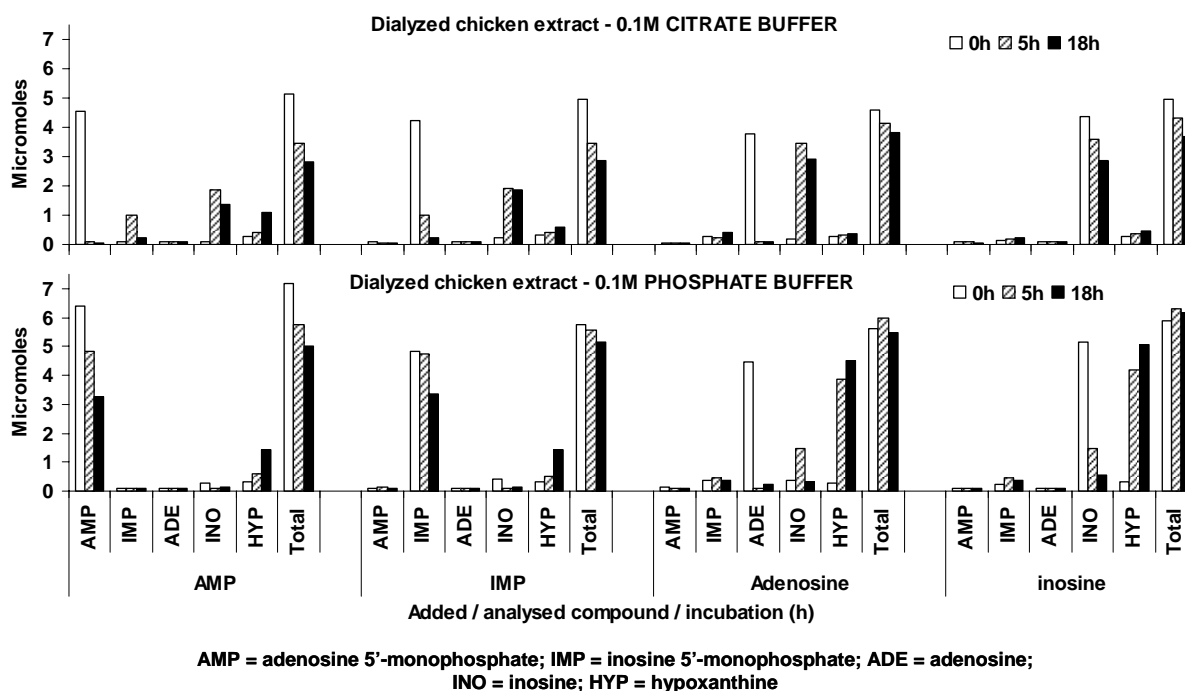
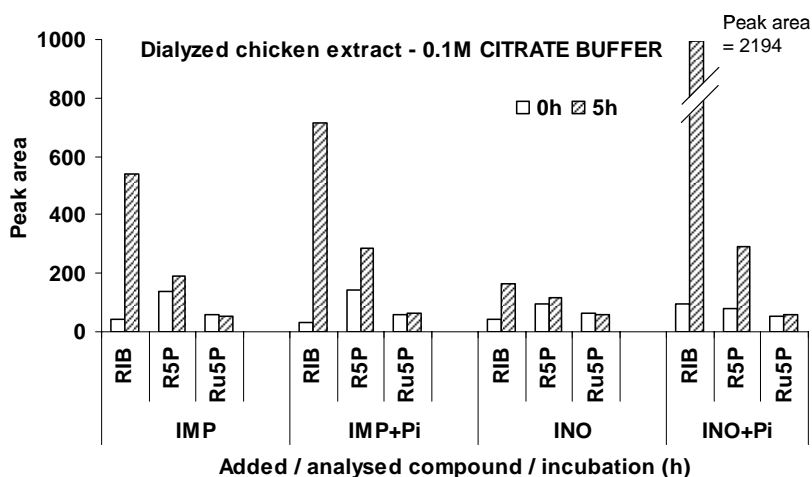


Figure 2. Effect of adding compounds (6 μ mol) to crude extract of chicken, dialyzed against citrate or phosphate buffer, on AMP metabolites.



IMP = inosine 5'-monophosphate; inos = inosine; RIB = ribose;
R5P = ribose-5-phosphate; Ru5P = ribulose-5-phosphate

Figure 3. Effect of adding IMP (20 μmol) or inosine (6 μmol), with and without phosphate (Pi), to crude extract of chicken, dialyzed against citrate buffer, on sugars.

Unexpectedly, both ribose and ribose-5-phosphate were increased with phosphate (Figure 3). The very large increase in ribose with added phosphate is difficult to explain as neither its breakdown from inosine nor its formation from ribose-1-phosphate would be expected to be enhanced by phosphate. The ribose-5-phosphate might be formed either by a reversal of pathway (d) to form IMP in the presence of phosphate (7), followed by pathway (g) to give ribose-5-phosphate and hypoxanthine, or by pathway (f) to give hypoxanthine and ribose-1-phosphate, which may then be converted to ribose-5-phosphate (8). Figure 2 indicates that only small quantities of IMP were formed on addition of inosine in the presence of phosphate (by a reversal of (d)), which agrees with the findings of Lee and Newbold (3). Thus, pathway (f) may be the more important breakdown route for inosine, despite the absence, as yet, of direct evidence for this.

IMP breakdown. The dephosphorylation of IMP to inosine (d) is inhibited, at least partially, by phosphate (Figure 2). However, again, the presence of phosphate caused more ribose and ribose-5-phosphate to be detected (Figure 3). The additional ribose-5-phosphate may be formed by (g), with IMP giving ribose-5-phosphate and hypoxanthine, or by the alternative pathway suggested for inosine breakdown. As expected, ribulose-5-phosphate, almost certainly formed by the pentose phosphate pathway, was unaffected in the presence or absence of phosphate.

Adenosine breakdown. Adenosine breaks down very readily to give inosine, presumably by pathway (i) in (Figure 1). This conversion is rapid, with addition of adenosine and inosine giving identical products at 5 and 18 hours. However, there is no direct evidence in the data reported in (Figure 2) that adenosine is formed from AMP by pathway (h), though it is possible that this could be due to rapid onward breakdown of adenosine to inosine. From the almost complete loss of added adenosine to inosine (in citrate) and hypoxanthine (in phosphate), it is likely that any adenosine present in chicken meat would be rapidly broken down to inosine.

AMP breakdown. In citrate buffer, AMP breaks down to give a small amount of IMP together with inosine and hypoxanthine (Figure 2). These pathways would appear to be fast. In contrast, in phosphate buffer, little of the AMP breaks down and

little IMP or inosine is detected. Nevertheless, hypoxanthine is formed. This may reflect the incomplete inhibition of pathways (h) / (d) by phosphate followed by rapid breakdown of inosine (and adenosine) to give hypoxanthine.

Role of phosphate. Dusek *et al.* (9) reported free phosphates as ca. 4500 mg “free P₂O₅”/kg in chicken breast. It may be calculated from this that the concentration of phosphates in the aqueous component of chicken (assuming a water content of 75%) is ca. 0.08M. These concentrations are only a little lower than in the phosphate buffer used in Experiments 1 and 2 (0.1 M). Thus, in chicken meat, it is likely that phosphate enhances the breakdown of inosine more than it inhibits its formation.

Conclusion

Evidence is provided that, whilst most of the accepted AMP breakdown pathways occur, additional pathways may also contribute to the breakdown of AMP and its metabolites to give ribose and related flavour precursors. Phosphate ions play a key role in determining the balance of activities of these pathways and of the products formed.

References

1. Aliani M., Farmer L.J. (2005) *J. Agric. Food Chem.* 53: 6455-6462.
2. Lawrie R.A. (1992) *Meat Science*, 5th Ed., Pergamon, Oxford.
3. Lee C.A., Newbold R.P. (1963) *Biochim. Biophys. Acta* 72: 349-352.
4. Aliani M., Farmer L.J. (2006) In *Flavour Science: Recent Advances and Trends* (Bredie W.L.P. Petersen M.A., eds), pp 329-334, Elsevier, Amsterdam.
5. Aliani M., Farmer L.J. (2005) *J. Agric. Food Chem.* 53: 6067-6072.
6. Leblanc D.J., Ball A.J.S. (1977) *Anal. Biochem.* 84: 574-578.
7. Tanaka N., Hasan Z., Hartog A.F., van Herk T., Wever R. (2003) *Org. Biomol. Chem.* 1: 3470-3470.
8. Camici M., Tozzi M.G., Ipata P.L. (2006) *J. Biochem. Biophys. Meth.* 68: 145-154.
9. Dusek M., Kvasnicka F., Lukaskova L., Kratka J. (2003) *Meat Sci.* 65: 765-769.

MEAT FLAVOUR GENERATION IN MAILLARD COMPLEX MODEL SYSTEMS

S.I.F.S. MARTINS, G.A. Desclaux, A. Leussink, E.A.E. Rosing, L. Jublot, and G. Smit

Unilever R&D (Unilever Food and Health Research Institute), Olivier van Noortlaan 120, PO Box 114, 3130 AC Vlaardingen, The Netherlands

Abstract

Meat flavour generation in Maillard complex model systems was studied. Mixtures of 3 amino acids and 2 sugars were studied at 3 concentration levels and 3 reaction times using a statistical factorial design. The selected systems tried to mimic the flavour composition in real food products containing both meat and tomato cooked together. Samples were compared by their thiol composition and sensorial profile. The used meat flavour generation marker was 2-methyl-3-furanthiol (MFT). It was observed that MFT formation was well correlated with cysteine and xylose as starting material as well as with the meaty sensory attribute. Synergetic effects seem to occur between glutamic acid and cysteine. In the presence of glutamic acid the sensorial profile changed from burnt, roasted meat to boiled meat, bouillon-like. Also the reaction kinetics of MFT generation changed in the presence of glutamic acid. We strongly believe that to study model systems with increased complexity will give results which can more reliably be translated to real food products.

Introduction

The formation of thiols, related to meat flavour, during the Maillard reaction has been known for decades (1). Besides thiamine, sulphur containing amino acids, such as cysteine, are known to be indispensable reaction precursors. In the presence of ribose or its less expensive isomer xylose, they participate in the Maillard reaction and Strecker degradation to form sulphur-containing compounds characteristic of meat odour (Figure 1). A number of which have been identified and reported in literature. Up-to-date, most studies focused on simple model systems, using only one sugar and one amino acid. Often those results are difficult to translate into real food products. The complex composition of real food products is expected to have a big impact on the reaction kinetics of the generated flavour compounds as well as on the final sensory profile (2). Farmer *et al.* (3) reported that the cysteine/ribose/lecithin reaction mixture had a much more pronounced “meaty, beefy” odour than a reaction mixture containing cysteine and ribose only. The aim of the present study was to better understand the impact of the system composition on the kinetics of known meat flavour generation markers. Also, to verify if the sensorial profile changed as a result. The selected systems’ composition tried to mimic meat flavour generation in real food products containing both meat and tomato cooked together.

Experimental

Meat flavour related complex model systems (more than one sugar and one amino acid) were studied using a statistical experimental design. Time and concentration

were the variable parameters, whereas pH and temperature were kept constant at 6 and 100°C, respectively, as shown in Table 1. The type of reactants was also a variable parameter, however in order to provide a minimum of meat flavour generation all systems had a minimum level of xylose and cysteine present. The studied systems were heated at 100°C in pyrophosphate buffer solution (50 mL, 0.2M, pH 6). D-Glucose (D-Glc), D-Xylose (D-Xyl), L-Cysteine (L-Cys), L-Glutamic acid (L-Glu), L-Glycine (L-Gly), 2-methyl-3-furanthiol (MFT), furfurylthiol (FFT) and bis(2-methyl-3-furanyl) disulfide (MFT-MFT) were purchased from Aldrich (Zwijndrecht, The Netherlands) and the respective stable-isotope labelled internal standard (labelling degree >98%) MFT* ([2H3] 2-methyl-3-furanthiol) and MFT*-MFT* ([2H6] bis(2-methyl-3-furanyl)disulphide) from AromaLAB AG (Munich, Germany). Prior to analysis by SPME GC-MS, 1% dithiothreitol (DTT) was added, enough to enable reducing conditions (reducing potential: -330 mM). Under these conditions the measured thiols were prevented from oxidation and/or liberated from already established sulphide bounds. Sensorial evaluation was done with an expert panel of 10 panellists. Common Flavour Language references were used. A standardised communication tool for sensory purposes developed by Unilever, International Flavour & Fragrances, Firmenich and Symrise.

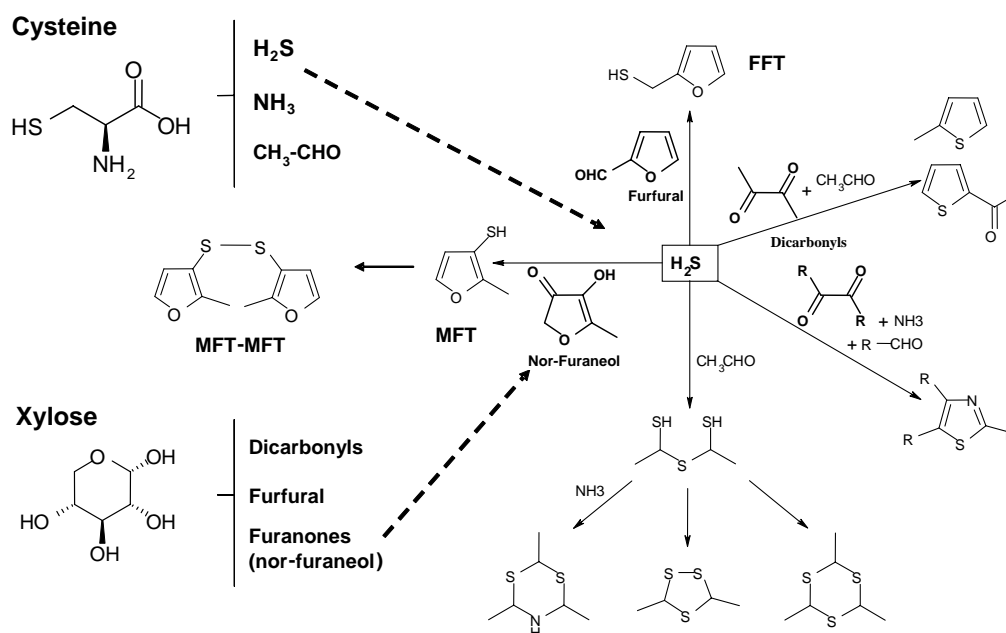


Figure 1. 2-Methyl-3-furanthiol (MFT), furfurylthiol (FFT) and bis(2-methyl-3-furanyl) disulphide (MFT-MFT), known meat aroma volatiles, formed by the reaction of cysteine with carbonyl compounds. Adapted from Mottram & Mottram (1).

Table 1. Complex model systems composition (%) heated at 100°C, pH 6.

Sample	D-Xyl	D-Glc	L-Cys	L-Gly	L-Glu	Time (h)
A	3	0	0.05	1.5	1.5	3
B	0.05	3.6	0.75	0	0	0.5
C	0.05	3.6	0.05	1.5	0	3
D	3	0	0.75	1.5	1.5	1.75
E	0.05	3.6	0.05	0	1.5	0.5
F	3	3.6	0.05	1.5	0	0.5
G	0.05	0	0.75	0	0	1.75
H	3	0	0.75	1.5	0	3

Results and Discussion

The use of cysteine in combination with a pentose is responsible for the formation of very potent sulphur-containing meat flavour compounds, such as 2-methyl-3-furanthiol (MFT), 2-furfurylthiol (FFT) and bis(2-methyl-3-furanyl) disulphide (MFT-MFT), as described in Figure 1. In aqueous solution it was observed that these compounds show considerable instability. MFT, in particular, was highly dependent on the reaction time and cysteine content. Similar results have been observed by Seeventer and co-workers (4). The signal intensity greatly increased with cysteine concentration, stabilising above cysteine concentration of 0.5% (results not shown). This led us to the hypothesis that the presence of cysteine, prevented MFT from oxidation and/or promoted its liberation from previously formed disulfide bonds by reducing them. As a result, MFT quantification was performed under reducing conditions by addition of dithiothreitol, which has similar reducing potential as cysteine. The measured concentration of MFT was therefore the total potential amount, even if some may have already been in the dimmer form.

The results showed that MFT formation increased when both cysteine and xylose increased simultaneously (Figure 2). This is in line with the reaction mechanism presented in Figure 1. However, the reaction kinetics of MFT generation seemed to be influenced by the increasing complexity of the system. For the same initial concentration of xylose and cysteine, the addition of glutamic acid reduced, by approximately half, the time required to generate the same amount of MFT (Figure 2, sample D vs sample H). Synergetic effects seem to occur between cysteine and glutamic acid. An extra experiment where system H is measured after 1.75 hours of reaction, with and without glycine, should be performed to support this conclusion. In line with the high levels of MFT, samples D & H were also the ones perceived as the meatiest as shown in Figure 3. However, in the presence of glutamic acid (sample D) the sensorial profile changed from burnt, roasted meat to boiled meat, bouillon-like.

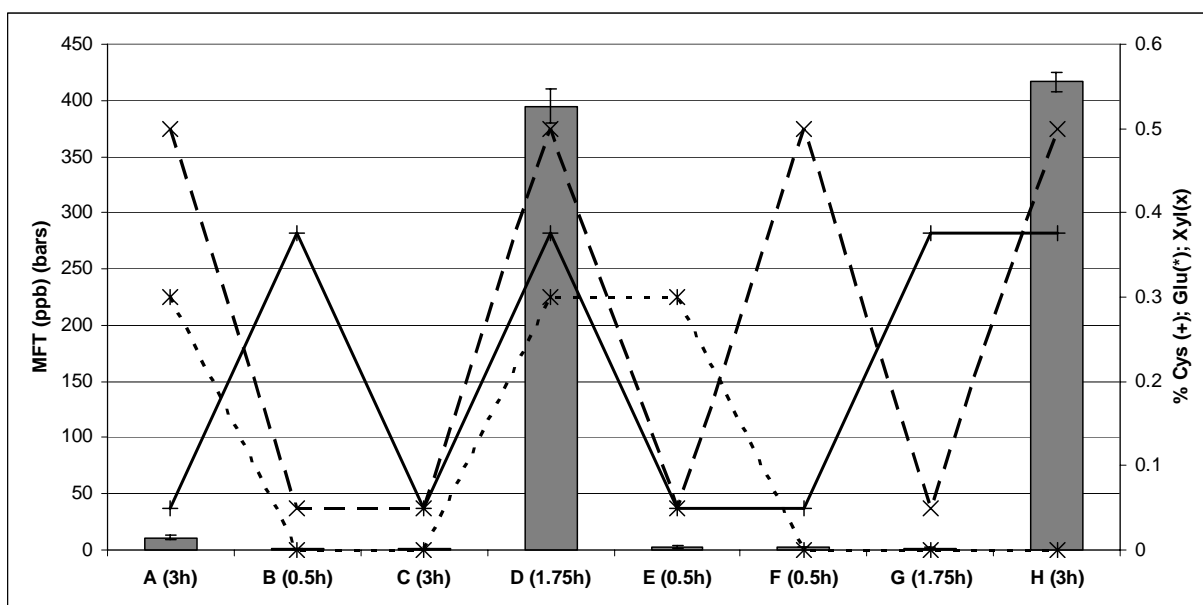


Figure 2. Complex model systems in an aqueous pyrophosphate buffer solution (0.2M, pH 6) heated at 100°C. 2-Methyl-3-furanthiol (MFT); L-Cysteine (Cys); L-Glutamic acid (Glu); D-Xylose (Xyl).

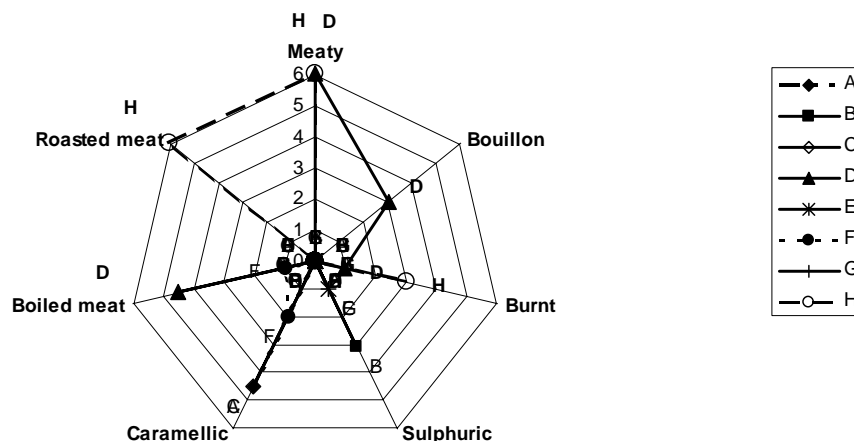


Figure 3. Sensorial evaluation of meat flavour complex model system samples. Samples A, B, C, D, E, F, G, H composition described in Table 1. An expert panel of 10 panellists and the Common Flavour Language references were used.

Synergetic effects seem to occur between glutamic acid and cysteine, with impact on the sensory profile. In home cooking, such as stewing of meat, tomato is often used. Tomato is known to be a rich source of glutamic acid. This kitchen practice gives the meat a more cooked note instead of a roasted note, which is in line with the obtained results. However, as mentioned above many other meaty compounds apart from MFT are also formed. Further validation of the present results would be necessary to verify if samples having highest MFT level are always the meatiest.

Conclusions

Some evidence has been given that studies in complex model systems give results which can more reliably be translated into real food products. The analytical data were well aligned with the sensorial evaluation. The samples rich in MFT were also the ones perceived as most meaty in the sensory evaluation. The alignment between analytical and sensorial results supported the hypothesis that providing reducing conditions, MFT could be used as a meat flavour reaction marker, to compare samples with different cysteine content. The increase in complexity, mainly in terms of amino acid content influenced the reaction kinetics. Synergetic effects seem to occur between glutamic acid and cysteine with an important impact on the sensory profile. Future work is still required to better understand the underlying reaction mechanism.

References

1. Mottram D.S., Mottram H.R. (2002) In *Heteroatomic Aroma Compounds* (G.A. Reineccius, T.A. Reineccius, eds.), Am. Chem. Soc., Washington, pp. 81-100.
2. van Boekel M.A.J.S. (2006). *Biotech. Adv.* 24: 230-233.
3. Farmer L.J., Mottram D.S., Whitfield F.B. (1989) *J. Sci. Food Agric.* 49: 347-368.
4. Seenventer P.B., Weenen H., Winkel C., Kerler J. (2001) *J. Agric. Food Chem.* 49: 4292-4295.

HYDROXYCINNAMIC ACID-MAILLARD REACTIONS: INSIGHTS INTO FLAVOUR DEVELOPMENT OF WHOLE GRAIN FOODS

D. Jiang and D.G. PETERSON

Department of Food Science, The Pennsylvania State University, 327 Food Science Building, University Park, PA 16802

Abstract

The flavour properties of cereal food products have been reported to be negatively influenced when formulated with whole grain versus refined flour. The objective of this study was to investigate the reactivity of the phenolic compounds in whole grain on the mechanisms of the Maillard reaction in low moisture high temperature simulated roast model systems. Using isotope labelling techniques, the hydroxycinnamic acids were reported to be reactive with key transient Maillard reaction products, such as hexose sugar fragments. The structure of one ferulic acid-Maillard reaction product was characterised by NMR and MS and identified as 6-(4-hydroxy-3-methoxyphenyl)-5-(hydroxymethyl)-8-oxabicyclo[3.2.1]-oct-3-en-2-one. Based on retrosynthesis, this reaction product was suggested to be generated by a [5+2] cycloaddition reaction between a dehydrated/cyclised degradation product of 3-deoxy-2-hexosulose and a decarboxylated ferulic acid. In summary, ferulic acid was reported to influence Maillard chemistry, a key mechanism of flavour generation.

Introduction

With the increasing scientific evidence supporting a positive connection between the consumption of whole grain foods and health promotion, the food industry has responded by reformulating traditionally refined flour based products into 'whole grain' foods. Although these whole grain products have a perceived health benefit among consumers, changes in the flavour properties can be viewed negatively and ultimately influence product choice. For example, Bakke and Vickers (1) reported people preferred refined bread to whole grain bread when both were made with equivalent ingredients (refined versus whole grain flour). The Maillard reaction is well known to be a key mechanism of flavour development in cereal based foods. We have previously reported that the hydroxycinnamic acids suppressed the generation of Maillard-type aroma compounds in a hard red spring whole wheat bread model system (2). In the current study, we investigate the reactivity of ferulic acid, the most abundant phenolic in wheat, on the mechanisms of the Maillard reaction to suggest how these food phenolics may alter flavour development of a whole grain food in comparison to a refined flour-based product.

Experimental

Model reaction systems. Five reaction mixtures, (a) glucose + glycine, (b) glucose + glycine + ferulic acid, (c) 1:1 $^{13}\text{C}_6$: $^{12}\text{C}_6$ Glucose + Glycine + Ferulic acid (d) Glucose + 1:1 $^{13}\text{C}_2$, ^{15}N : $^{13}\text{C}_2$, ^{14}N Gly + Ferulic acid and (e) 3-deoxy-2-hexosulose + ferulic acid; each at 3 mmol (except 3-deoxy-2-hexosulose was at 3 μmol) were heated in 15 g

quartz sand with 10% moisture for 15 min at 200°C. The reaction mixtures were extracted with methanol, further purified and concentrated by solid phase extraction for further analysis.

Liquid Chromatography/Mass Spectrometry (LC/MS). Samples were analysed in electrospray ionization (ESI) mode on a Shimadzu HPLC system (Shimadzu, Columbia, MD) equipped with a degasser (DGU-14A), two pumps (LC-10ADvp), an autosampler (SIL-10vp), and a Waters column heater (model TCM; Waters, Milford, MA) with an ultra aqueous C18 column (particle size 5 µm, 250 x 2 mm I.D.; Restek, Bellefonte, PA) interfaced to a Quattro Micro triple quadrupole mass spectrometer (Waters) as previously described (3). In brevity, the mobile phase consisted of a linear concentration gradient of two solvents (A and B). Solvent A was 0.1% formic acid and solvent B was methanol. The mobile phase consisted of a series of linear gradients of B in A starting at 10% B in A (0-2 min), increasing to 90% B in A (2-30 min), and then held at 90% for 5 min (30-35 min).

Nuclear Magnetic Resonance (NMR). The isolate was further fractionated by LC-MS (instrument configuration was the same as described above) utilizing the FractionLynx software (Waters Corp.) and a Waters Fraction Collector (III). The purified target analyte was freeze dried, dissolved in deuterated methanol and analysed by a Bruker DRX-400 NMR. The chemical shifts (δ values) were referenced to the ^1H or ^{13}C chemical shifts of the internal standard trimethylsilane. ^1H , ^{13}C , gradient selected ^1H - ^1H correlation spectroscopy (COSY), gradient selected heteronuclear multiple quantum coherence (HMQC), and gradient selected heteronuclear multiple bond coherence (HMBC) spectra were recorded at 400 MHz for ^1H and 100 MHz for ^{13}C . ^1H - ^1H COSY, HMBC, and HMQC two-dimensional (2D) NMR techniques were used to assign correlations between ^1H and ^{13}C signals.

Results

Food phenolics, such as the flavan-3-ols, have been previously reported to alter the mechanisms of Maillard-type flavour development in model and food systems (3-8). Based on a similar analytical approach utilized for the flavan-3-ols, the reactivity of hydroxycinnamic acids were investigated in simple glucose-glycine Maillard model systems. Figure 1 (top) illustrates the MS spectrum for an analyte with the predicted molecular weight of 276 that was only detected when ferulic acid was added to a glucose-glycine model reaction. To further define the composition of this reaction product, a CAMOLA reaction (9) where glucose was added as a 1:1 $^{12}\text{C}_6$ to $^{13}\text{C}_6$ glucose mixture as well as a AMMOLA reaction (5), glycine added as a 1:1 $^{13}\text{C}_2$, ^{15}N : $^{13}\text{C}_2$, ^{14}N glycine, were subsequently analysed. An MW+6 isotopomer for this compound with a MW of 276 was reported for the CAMOLA reaction (see Fig. 1 bottom) whereas no isotopomers were identified for the AMMOLA reaction. This indicated this unknown compound consisted of an intact C_6 sugar moiety but nothing from glycine. Because it is unlikely the C_6 sugar moiety would have a molecular weight of 276, a ferulic acid moiety was consisted a component of this analyte. Further fractionation/purification and NMR analysis of this unknown analyte revealed the molecular structure which is shown in Figure 2, or 6-(4-hydroxy-3-methoxyphenyl)-5-(hydroxymethyl)-8-oxabicyclo[3.2.1]-oct-3-en-2-one. Based on retrosynthesis, the suggested pathway for the formation for this compound is illustrated in Figure 3. The Maillard reaction product, 3-deoxy-2-hexosulose, was proposed to generate an oxypyrylium zwitterion by dehydration and cyclization which reacted with decarboxylated ferulic acid, by a less common [5+2] cycloaddition. For a

[5+2] cycloaddition reaction, a more electron rich dienophile would be more reactive (*i.e.* decarboxylated ferulic acid, 2-methoxy-4-vinylphenol). This reaction product could be easily generated by directly reacting 3-deoxy-2-hexosulose with either ferulic acid or 2-methoxy-4-vinylphenol. Interestingly, this cyclo-adduct compound was not generated by reacting glucose and ferulic acid but required glycine, suggesting only negligible amounts of 3-deoxy-2-hexosulose were generated via caramelisation reactions in these model systems.

The phenolic-Maillard interactions identified provide a new food chemistry reaction that may explain, in part, the lower flavour preference associated with whole grain foods. The negative flavour properties of whole grain foods have been previously related to the bitter taste properties of the phenolic compounds and perhaps due to increased generation of lipid oxidation products. However, phenolic induced changes in Maillard-type flavour development may also influence product acceptability. Additionally, the cyclo-adduct generated by our model phenolic-Maillard reactions (Figure 2) has been previously identified as a potential bioactive in ancient Chinese medicine thought to promote blood circulation (11). Related Maillard-phenolic reaction products may provide further insights into health benefits of whole grain foods and likewise strategies for process optimization of the product quality.

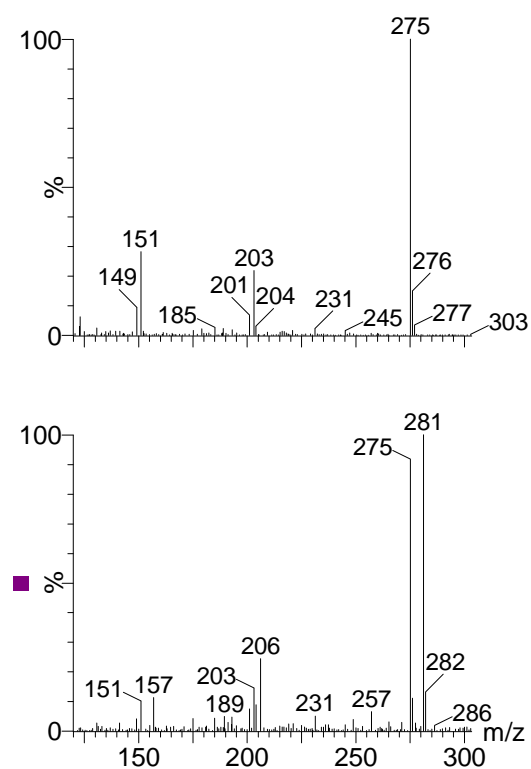


Figure 1. LC/MS-ESI (-ve ion mode) measured isotopomers of a select analyte (M-1, 275) from glucose + glycine + ferulic acid (top) and 1:1 $^{13}\text{C}_6$: $^{12}\text{C}_6$ glucose + glycine + ferulic acid (bottom); at equivalent retention time.

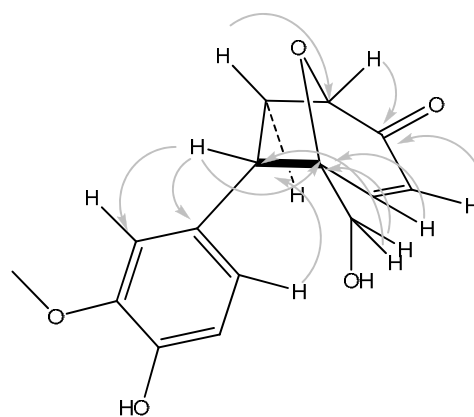


Figure 2. Structure of ferulic acid-Maillard adduct, M-1 of 275; illustrating significant HMBC correlations (\rightarrow).

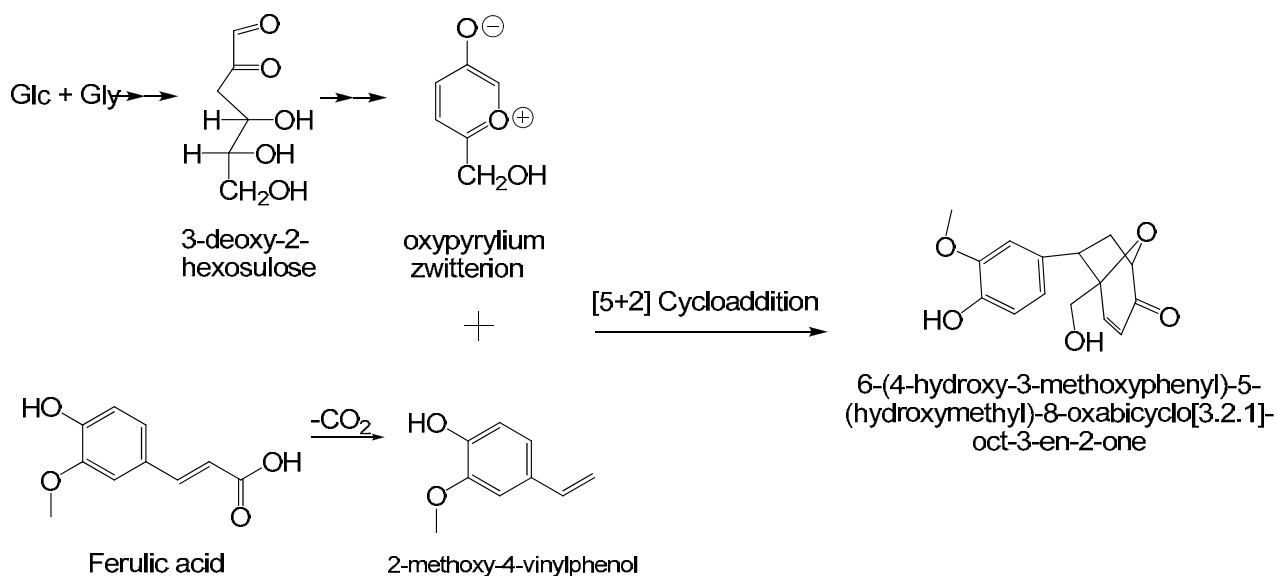


Figure 3. Proposed reaction mechanism for a select reaction product generated in a ferulic acid-Maillard model system; adapted from (10)

References

1. Bakke A., Vickers Z. (2007) *J. Food Sci.* 72: S473-S480.
2. Moskowitz M.R., Peterson D.G. In *234th American Chemical Society National Meeting Proceedings*, Boston, MA, August 19-23, 2007.
3. Totlani V., Peterson, D.G. (2007) *J. Agric. Food Chem.* 55: 414-420.
4. Totlani V., Peterson D.G. (2006) *J. Agric. Food Chem.* 54: 7311-7318.
5. Totlani V., Peterson, D.G. (2005) *J. Agric. Food Chem.* 53: 4130-4135.
6. Noda Y., Peterson D.G. (2007) *J. Agric. Food Chem.* 55: 3686-3691.
7. Schwambach S.L., Peterson D.G. (2006) *J. Agric. Food Chem.* 54: 502-508.
8. Colahan-Sederstrom P.M., Peterson D.G. (2005) *J. Agric. Food Chem.* 53: 389-402.
9. Schieberle P., Fischer R., Hofmann T. (2003) In *Flavour Research at the Dawn of the Twenty First Century*, pp. 447-452.
10. Jiang D., Peterson D.G. (2009) *J. Agric. Food Chem.* 57: 9932-9943.
11. Snider B.B., Grabowski J.F. (2006) *Tetrahedron*, 5171-5177.

CHANGES IN THE AROMA COMPONENTS OF PECANS DURING ROASTING

K.R. CADWALLADER, H. Kim, S. Puanggraphant, and Y. Lorjaroenphon

Department of Food Science and Human Nutrition, University of Illinois at Urbana-Champaign, 1302 W. Pennsylvania Avenue, Urbana, IL 61801, USA

Abstract

Volatile components formed during the roasting of pecan kernels originate mainly via lipid oxidation/degradation and Maillard/Strecker reactions. Of particular importance to the sweet and nutty aroma of roasted pecans are 2-acetyl-1-pyrroline, 2-propionyl-1-pyrroline, 4-hydroxy-2,5-dimethyl-3(2*H*)-furanone, 3-methylbutanal, 3-ethyl-2,5-dimethylpyrazine, 2-ethyl-3,5-dimethyl-pyrazine, 2,3-diethyl-5-methylpyrazine, 2-pentylpyridine, and 2-acetyltetrahydropyridine. Results from this study provide useful information to producers and end-users of pecan on the components that have the greatest impact on the aroma quality of this important tree nut.

Introduction

Tree nuts are appreciated worldwide and are used extensively in confectionary, bakery, culinary and other food product applications. Recent studies have demonstrated various nutritional and health benefits associated with consumption of tree nuts (1). Pecans (*Carya illinoensis*) are the only native tree nuts grown for commercial purposes in the US and rank number three worldwide behind almonds and walnuts, with about 90M metric tons of pecans produced annually. Only a few studies have been published on the volatile constituents of pecans (2-4). Our previous studies indicated the involvement of numerous thermally generated volatile compounds in the characteristic aroma of roasted pecan (5). The objective of the present study was to monitor the generation of selected potent odorants in pecan kernels during roasting.

Experimental

Roasting of pecans. Freshly shelled pecan kernels (halves; Stewart variety, 2007 season, Vienna, GA, USA) were roasted for 0, 10, 20 or 30 min) at 170 °C in a forced-air oven.

Extraction of volatile compounds. Ground sample (50 g), plus 12.5 g of NaCl and 10 µL of internal standard solution containing 2-methyl-3-heptanone (4.31 mg/mL of methanol), α -6-amylpyrone (0.81 mg/mL), 2,4,6-trimethylpyridine (1.21 mg/mL), 2-ethylbutanoic acid (1.50 mg/mL) and ethyl maltol (2.08 mg/mL) was extracted with diethyl ether (1 x 100 mL; 2 x 100 mL). The ether extract was subjected to solvent-assisted flavour evaporation (SAFE) and then separated into neutral, acidic and basic components. Extracts were concentrated to 200 µL prior to GC-MS analysis (6). Duplicate extractions were performed for each treatment.

GC-MS analysis. Analyses were performed using an Agilent 6890/5973N GC/MSD system (Palo Alto, CA, USA) in EI mode (70 eV). Each extract (1 µL) was

injected in the cool on-column mode. Neutral and acidic compounds were separated on a Stabilwax column (30 m length x 0.25 mm I.D x 0.25 μ m film, Restek, Bellefonte, PA, USA). Oven temperature was programmed from 40 to 225 °C at a rate of 4 °C/min with initial and final hold times of 5 and 20 min, respectively. Basic compounds were separated using a SAC-5 column (30 m length x 0.25 mm I.D x 0.25 μ m film, Supelco, Bellefonte, PA, USA). The GC oven was held at 40 for 5 min, ramped to 240 °C at 6 °C/min, and held at 240 °C for 20 min. Helium was used as a carrier gas at a constant flow of 1.0 mL/min.

Calibration procedures. For accurate quantification, response factors were determined using five-point standard curves. Recovery factors were determined using soybean oil (Crisco, Orrville, OH, USA) as a mimic matrix, which was then subjected to the above mentioned extraction procedures and GC-MS analyses.

Enantiomeric composition. Enantiomeric composition of selected lactones (nos. 9-11) were determined by GC-MS using an Inertcap Chiramix column (30 m length x 0.32 mm I.D x 0.32 μ m film, GL Science Inc., Tokyo, Japan). The oven was held at 120 °C for 2 min, ramped to 165 °C (held for 20 min) at a rate of 5 °C/min. Carrier gas (He) was set at a constant flow of 1.5 mL/min. MSD conditions were same as above, except SIM mode was used for detection of no. 9 (ions 97 and 68) and nos. 10 and 11 (ion 85).

Odour threshold determination. Orthonasal odour detection threshold for 6S-massoiolactone (Fleyrchem Inc., Middletown, NY, USA) was determined in fresh canola oil using ASTM procedure E679-91 (7).

Results

Concentrations for selected volatile constituents are given in (Table 1). Lipid (thermal) oxidation and Maillard/Strecker degradation reactions accounted for the formation of most of the predominant odorants in roasted pecan. Highest rate of formation for lipid-derived compounds occurred between 20 to 30 min, while Strecker aldehydes formed more rapidly between 10 and 20 min. Most of the other Maillard reaction volatiles formed at a steady rate between 10 and 30 min. Based on their relatively high odour-activity values (OAVs), odorants with green/rancid/fatty (e.g nos. 4-8, 20), coconut-like (no. 9), caramel (no. 13) and nutty/roasty (nos. 1, 14-19) notes were the main contributors to the overall aroma of roasted pecan (Figure 1).

Roasting caused great increases in some lipid-derived odorants, e.g, (*E,E*)-2,4-decadienal (no. 8) increased by > 20,000 fold after roasting for 30 min. Despite the large increases in the lipid-derived aldehydes, the OAVs for these compounds were only moderately high due to their relatively high odour detection thresholds in the lipid-based medium (pecan contains over 70% unsaturated lipid). The aroma of pecan, especially in its roasted form, might be influenced by presence of lactones (especially no. 9). Lactones have not been previously reported pecan and have been only rarely reported in other tree nuts (9). Among the lactones, the coconut-smelling massoiolactone increased by ~75 fold as a result of roasting (170 °C; 30 min). Surprisingly, its enantiomeric ratio (85% 6S: 15% 6R) was not affected by roasting (data not shown).

A number of N-containing heterocyclic volatiles were formed during roasting of pecan. The harsh/green smelling 2-pentyl pyridine (no. 20) may have been formed by the reaction of 2,4-decadienal (no. 8) with free ammonia liberated from amide groups of amino acids during roasting (10). Roasty/nutty odorants (nos. 14-19) appear to very important to the overall aroma of roasted pecan. In particular, 2-acetyl-1-

pyrroline (no. 14) and 2-propionyl-1-pyrroline (no. 15) had by far the highest OAVs among the compounds listed in Table 1. Both of these compounds have been previously reported as key odorants in various heated foods (11).

Table 1. Concentrations of selected volatile components of natural (raw) and roasted pecan kernels.

No.	Compound ^a	Roasting period (170 °C) (ng/g) ^b			
		raw	10 min	20 min	30 min
<i>Neutral compounds^c</i>					
1	2-methylbutanal [57]	15	99	833	1240
2	3-methylbutanal [58]	7.4	82	419	474
3	Phenylacetaldehyde [120]	19	117	309	336
4	Hexanal [56]	335	605	2630	7100
5	(<i>E</i>)-2-Nonenal [70]	13	26	113	342
6	(<i>E</i>)-2-Decenal [70]	12	110	742	3080
7	(<i>E</i>)-2-Undecenal [70]	3.3	132	991	3880
8	(<i>E,E</i>)-2,4-Decadienal [81]	0.4	124	1390	8150
9	6-Pentyl-5,6-dihydro-2 <i>H</i> -pyran-2-one (massoialactone) (85:15 6 <i>S</i> /6 <i>R</i> ratio) [97] ^d	94	598	4460	6960
10	γ -Nonalactone (racemic) [85] ^d	43	50	80	215
11	γ -Decalactone (racemic) [85] ^d	122	116	118	139
<i>Acidic compounds^e</i>					
12	3-Hydroxy-2-methyl-4-pyrone (maltol) [126]	-- ^f	208	211	500
13	4-Hydroxy-2,5-dimethyl-3(2 <i>H</i>)-furanone (HDMF) [128]	--	874	933	2450
<i>Basic compounds^g</i>					
14	2-Acetyl-1-pyrroline [83]	--	--	80	146
15	2-Propionyl-1-pyrroline [97]	--	--	40	66
16	2-Acetyltetrahydropyridine (sum of tautomers) [125]	--	--	6.9	81
17	3-Ethyl-2,5-dimethylpyrazine [135]	--	21	444	992
18	2-Ethyl-3,5-dimethylpyrazine [135]	--	0.5	9.8	20
19	2,3-Diethyl-5-methylpyrazine [150]	--	--	28	100
20	2-Pentylpyridine [93]	--	--	29.3	113

^a Numbers in brackets indicate mass ion used for quantitative analysis. ^b Average of duplicate determinations. ^c Determined against 2-methyl-3-heptanone (i.s.) unless otherwise noted. ^d Determined against 6- α -amylpyrone (i.s.). ^e Determined against ethyl maltol (i.s.). ^f Not detected. ^g Determined against 2,4,6-trimethylpyridine (i.s.).

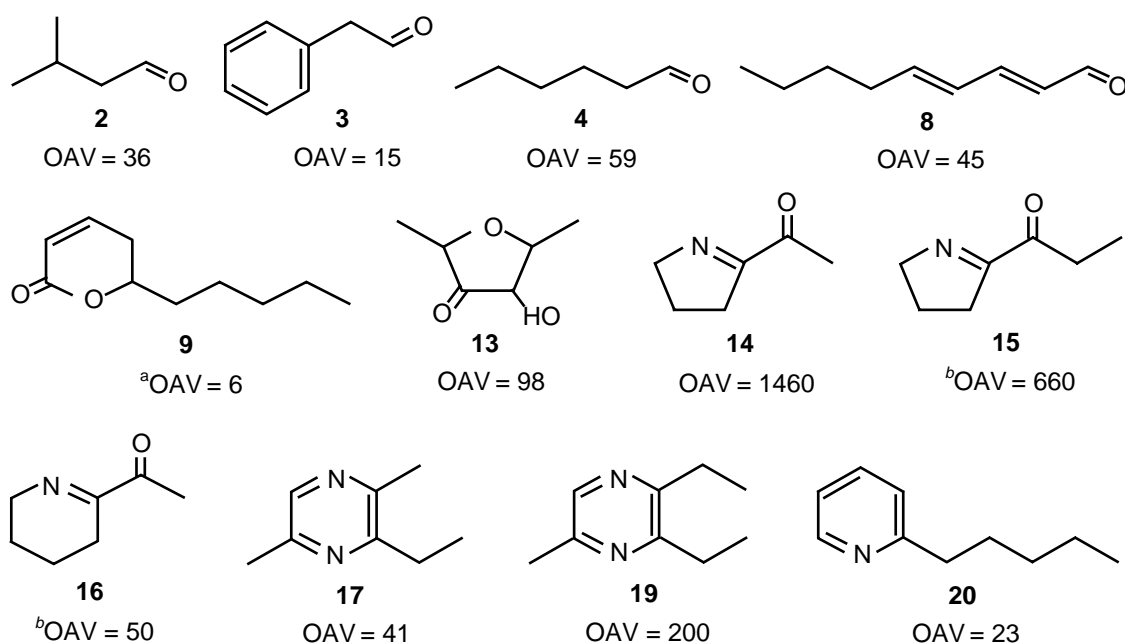


Figure 1. Structures and odour-activity values (OAVs) for selected volatile components of pecan kernels roasted at 170 °C for 30 min. [^aOAVs were calculated from odour detection threshold determined in canola oil (1100 ng/g for no. 9 in present study) or from published odour detection thresholds in oil or ^bwater (from 10).]

References

1. Mukuddem-Peterson J., Oosthuizen W., Jerling J.C. (2005) *J. Nutr.* 135: 2082-2089.
2. Horvat R.J., Senter S.D. (1980) *J. Am. Oil Chem. Soc.* 57: 111.
3. Mody N.V., Hedin P.A., Neel W.W. (1976) *J. Agric. Food Chem.* 24: 175-177.
4. Wang P.S., Odell G.V. (1972) *J. Agric. Food Chem.* 20: 206-210.
5. Puangraphant S. (2007) MS Thesis, University of Illinois, December 2007.
6. Rotsachakul P., Chaiseri S., Cadwallader, K.R. (2008) *J. Agric. Food Chem.* 56: 528-536.
7. ASTM. (1992) *Standard practice E 679-91, Determination of Odor and Taste Thresholds by a Forced-Choice Ascending Concentration Series Method of Limits*; American Society for Testing and Materials, Philadelphia, PA.
8. Rychlik M., Schieberle P., Grosch W. (1998). *Compilation of Odor Thresholds, Odor Qualities and Retention Indices of Key Food Odorants*; Deutsche Forschungsanstalt für Lebensmittelchemie and Institut für Lebensmittelchemie der Technischen Universität München, Garching, Germany.
9. Cadwallader K.R., Puangraphant S. (2008) In *Tree Nut Nutraceuticals and Phytochemicals*. (Alasalvar C., Shahidi F., eds.); Taylor and Francis, LLC (in press).
10. Kim Y-S, Hartman T.G., Ho C.-T. (1996) *J. Agric. Food Chem.* 44: 396-3908.
11. Hofmann T., Schieberle P. (1998) *J. Agric. Food Chem.* 46: 2721-2726.

AROMA COMPOUNDS IN FRENCH FRIES FROM THREE POTATO VARIETIES

J.S. ELMORE, J.A. Woolsgrove, D.K. Wang, A.T. Dodson, and D.S. Mottram

Department of Food Biosciences, University of Reading, Whiteknights, Reading RG6 6AP, UK

Abstract

Sugars and free amino acids were measured in three potato varieties widely available in the United Kingdom. French fries were cooked for 6, 9 and 12 min at 180 °C, and the effects of cooking time and variety on volatile composition were examined. Maillard reaction-derived aroma compounds increased as cooking time increased. Varieties Desiree and Maris Piper were relatively high in sugars and aroma compounds derived from sugars, e.g. 5-methylfurfural and dihydro-2-methyl-3[2H]-furanone, whereas variety King Edward was relatively high in free amino acids and their associated aroma compounds, such as pyrazines and Strecker aldehydes.

Introduction

Popular British potato varieties Desiree, King Edward and Maris Piper are available all year. They are picked in early autumn and then stored. To prevent sprouting, potatoes are either sprayed with a sprout suppressant or are stored at around 4 °C (1). However, at low temperatures, breakdown of starch to sugar causes the phenomenon of low temperature sweetening, resulting in increased browning on cooking. This is also associated with increased formation of acrylamide, a suspected carcinogen (2).

As part of a study to examine the effect of potato storage time on acrylamide formation in French fries, and the relationships between acrylamide formation, colour and aroma composition, we examined how the aroma compounds in French fries formed from the Maillard reaction are related to levels of free amino acids and sugars in the raw potato.

Experimental

Potatoes of the above three varieties were purchased pre-packed (2.5 kg bags) from three different supermarkets in February 2008, *i.e.* after approximately 5-6 months storage. French fries (300 g; 5-8 cm × 1 cm × 1 cm) were cooked in sunflower oil at 180°C for 6, 9 and 12 min. The cooked fries were blended with water (50g fries: 150 g water). Aroma volatiles were collected from 50 g of blended sample at 30 °C onto a Tenax TA trap, which was then heat-desorbed using a Perkin-Elmer ATD and analysed by GC-MS (DB-5MS column: 60 m × 0.32 mm, 1 µm film thickness; J & W) (3). Compounds were identified by comparing their mass spectra and linear retention indices with those of authentic compounds. Chromatographic peak areas of identified compounds were measured relative to that of 100 ng of 1,2-dichloro-benzene (DCB), which was added to the Tenax trap immediately after collection.

Table 1. Major Maillard reaction-derived compounds in French fries from three varieties of potato cooked at 180 °C for 6, 9 and 12 min ($n = 3$). Peak areas in a 50 g sample (French fries:water = 1:3) are measured relative to that of 100 ng of 1,2-dichlorobenzene internal standard (= 100)

Pea k No.	LRI	Compound	Desiree			Maris Piper			King Edward			std error	CT ^a	V ^b
			6 min	9 min	12 min	6 min	9 min	12 min	6 min	9 min	12 min			
1	501	acetone	6.3	7.0	10.9	4.9	4.7	10.3	8.0	6.5	5.8	0.6	ns	ns
2	557	2-methylpropanal	508	729	944	447	530	1100	737	894	1170	58.6	***	*
3	600	2,3-butanedione	6.3	11.2	12.1	6.2	10.1	18.5	6.8	8.9	12.4	1.0	**	ns
4	604	2-butanone	9.4	17.2	21.4	6.3	13.8	23.5	15.0	16.6	23.5	1.4	***	ns
5	653	3-methylbutanal	264	397	390	232	356	686	560	749	784	47.0	**	***
6	664	2-methylbutanal	1300	2000	2010	1310	1370	3150	1820	2530	2990	195	*	ns
7	694	2,3-pentanedione	6.46	14.9	20.3	5.54	14.0	32.0	8.34	12.4	19.9	1.84	***	ns
8	745	dimethyldisulphide	13.9	15.4	16.7	6.26	14.4	16.0	22.2	27.3	34.8	2.21	ns	**
9	739	2-methylpropanoic acid	5.13	13.1	14.2	1.07	4.66	24.7	8.71	10.2	8.26	1.78	*	ns
10	807	dihydro-2-methyl-3[2H]-furanone	1.08	4.65	10.6	0.04	2.50	8.81	1.35	3.01	6.44	0.70	***	*
11	824	methylpyrazine	16.1	31.2	41.7	5.62	27.4	49.1	37.6	52.3	86.4	5.32	***	**
12	826	3-methylbutanoic acid	2.46	6.75	4.42	0.69	3.85	8.50	6.25	6.90	4.31	0.68	ns	ns
13	831	furfural	8.20	21.0	34.5	1.65	10.0	32.8	3.87	9.19	12.2	2.92	**	ns
14	836	2-methylbutanoic acid	8.74	20.1	18.9	2.09	9.30	29.0	14.9	17.7	11.8	2.24	ns	ns
15	909	2-acetylfuran	2.73	5.44	10.0	0.09	1.70	4.20	1.78	2.95	5.02	0.68	**	**
16	913	2,6(and 2,5)-dimethylpyrazine	21.7	40.7	50.6	5.73	27.5	45.1	53.3	73.4	118	7.48	**	***
17	917	ethylpyrazine	3.65	7.24	13.4	1.29	8.72	16.3	9.75	17.8	31.4	2.11	**	**
18	962	5-methyl-2-furfural	1.72	5.97	14.2	0.03	1.65	5.82	0.85	1.88	5.35	1.04	**	*
19	999	2-ethyl-6-methylpyrazine 2-ethyl-3-methylpyrazine +	3.03	7.76	12.6	0.51	7.65	11.9	16.2	23.5	42.3	2.81	**	***
20	1003	trimethylpyrazine	4.11	9.22	12.2	0.70	7.87	12.6	15.3	21.9	40.8	2.61	**	***
21	1004	2-ethyl-5-methylpyrazine	3.99	8.40	11.0	0.61	6.68	8.50	9.08	13.3	27.5	1.71	**	**
22	1050	phenylacetaldehyde	7.10	11.6	11.3	2.12	7.70	11.1	10.2	14.6	21.8	1.31	**	**
23	1078	3-ethyl-2,5-dimethylpyrazine	3.92	8.57	11.5	0.29	6.47	8.57	18.4	25.4	49.2	3.35	**	***

^{a,b} Probability that there is a difference between means for (a) cooking time and (b) variety; ns, no significant difference between means ($p > 0.05$); * significant at the 5 % level; ** significant at the 1 % level; *** significant at the 0.1 % level.

Portions of the flesh of each raw potato sample were freeze-dried for precursor analysis. Free amino acids (excluding arginine) were measured using EZ-Faast for GC-MS (Phenomenex); sugars were measured by high-performance anion-exchange chromatography (Dionex) (4).

Results

Table 1 contains those compounds derived from the Maillard reaction, which were present in at least one sample, with a peak area of more than 5% of the peak area of the DCB standard. Of these compounds, 20 increased with cooking time, while none decreased, and 16 varied with variety. Three compounds, which could be formed by sugar breakdown alone, namely 2-acetylfuran, dihydro-2-methyl-3[2H]-furanone and 5-methylfurfural, were highest in Desiree, while many of the remaining Maillard-derived compounds were highest in King Edward, e.g. Strecker aldehydes and dimethyl disulfide, formed relatively early in the Maillard reaction, and alkylpyrazines, which are stable end-products (5).

Table 2 shows the levels of the key aroma and acrylamide precursors in the three varieties. King Edwards were relatively low in sugars and high in amino acids, Desiree were relatively high in sugars and amino acids, while Maris Piper were relatively high in sugars and low in amino acids. Desiree was much higher in asparagine than the other two varieties and has been shown to produce significantly more acrylamide in French fries than Maris Piper (2). As the potatoes had been stored, sugar levels were relatively high, compared with freshly-harvested potatoes, and the French fries obtained were golden brown in colour. It was noted that King Edwards from one supermarket were threefold higher in fructose and glucose, compared to those from the other two supermarkets (data not shown).

Table 2. Levels of key aroma and acrylamide precursors (mmol per kg dry weight) in 3 varieties of potato ($n=9$). Values in the same column with different letters are significantly different.

Variety	Glucose	Fructose	Total sugars	Asparagine	Total amino acids ^a
Desiree	32.4	29.7 (b)	68.4 (ab)	74.0 (b)	266.5 (b)
King Edward	28.5	23.2 (a)	56.4 (a)	33.8 (a)	257.9 (b)
Maris Piper	32.9	31.3 (b)	71.4 (b)	29.6 (a)	179.5 (a)

^a excluding arginine

A principal component analysis was performed on the statistically significant data, to visualise the relationships between precursors and aroma compounds (Figure 1). Sugar-derived aroma compounds were separated from the rest along principal component (PC) 1, and were associated with the sugars and varieties Desiree (DES) and Maris Piper (MP). Most of the remaining aroma compounds were clustered with King Edwards (KE) and the amino acids alanine, serine and glycine, which were separated from the other amino acids along PC 2. These amino acids have been shown to be important in the formation of low-molecular weight pyrazines (5), such as those in Table 1, which were highest in the French fries made from King Edwards.

As well as showing how cooking time can affect flavour formation in French fries, these results also show the effects of sugars and amino acids on aroma formation. As reducing sugars increase during potato storage, levels of sugar-derived

compounds, such as furfural, should become relatively more important in the aroma profile of the cooked French fries and may act as a predictor of acrylamide formation.

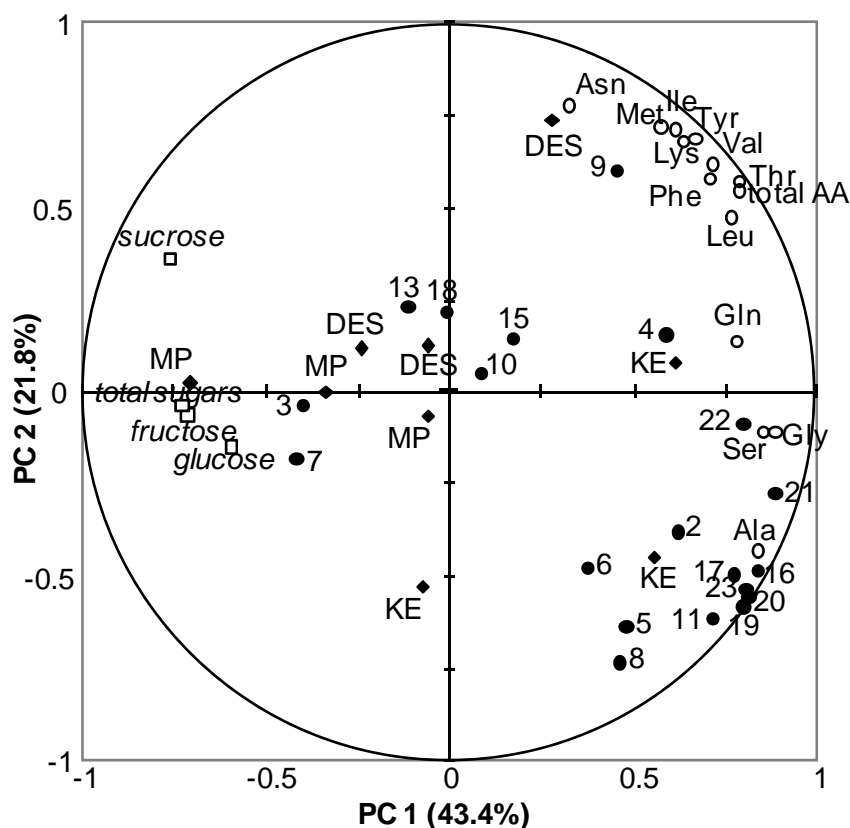


Figure 1. PCA plot showing relationships between aroma compounds and their precursors in French fries cooked for 9 min: ● aroma compound, ◆ potato variety, ○ amino acid, □ sugar.

References

1. Kumar D., Singh B.P., Kumar P. (2004) *Ann. Appl. Biol.* 145: 247-256.
2. Burch R.S., Trzesicka A., Clarke M., Elmore J.S., Briddon A., Matthews W., Webber N. (2008) *J. Sci. Food Agric.* 88: 989-995.
3. Methven L., Tsoukka M., Oruna-Concha M.J., Parker J.K., Mottram D.S. (2007) *J. Agric. Food Chem.* 55: 1427-1436.
4. Elmore J.S., Mottram D.S., Muttucumaru N., Dodson A.T., Parry M.A.J., Halford N.G. (2007) *J. Agric. Food Chem.* 55: 5363-5366.
5. Nursten H.E. (2005) *The Maillard Reaction: Chemistry, Biochemistry and Implications*; Royal Society of Chemistry.

UNDERSTANDING THE IMPACT OF CONCHING ON CHOCOLATE FLAVOUR USING A COMBINATION OF INSTRUMENTAL FLAVOUR ANALYSIS AND TASTING TECHNIQUES

A. Fischer, T. Abubaker, A. HÄSSELBARTH, and F. Ullrich

Kraft Foods R&D Inc., Bayerwaldstrasse 8, D-81737 Munich, Germany

Abstract

The present study discusses a linked analytical–sensory approach for the elucidation of chocolate flavour changes induced by conching. Using a bundle of different sample preparation techniques prior to instrumental analysis and extensive sensory testing, insights into the chocolate flavour development were obtained. A strong relationship between analytically measurable aroma profile, perceived sensory attribute intensity and texture development was observed. It was shown that conching reduces the concentration of most aroma compounds especially in the fat phase, whereas the aroma content in water-soluble material (sugar, protein) and in the insoluble material (cocoa solids) remains constant. Although the aroma concentration is overall clearly declining during conching, chocolate with high conching time is perceived as richer in chocolate flavour. It is concluded that improving texture properties enable a more balanced flavour perception. It is therefore highly important to optimise the texture formation process as a prerequisite to optimal aroma perception.

Introduction

Chocolate conching is known to be one of the key quality driving steps in chocolate manufacturing, which is still very time-consuming and energy-intensive. The initial dry conching phase is very important to decrease moisture and to improve rheology. It is also believed to be the most critical step for flavour development. The final liquid conching phase, initiated by lecithin and cocoa butter addition, is believed to be less critical for final chocolate quality.

In the present study we focus on the development of aroma properties which progress parallel to changes in texture (1-4). Special care has been taken to develop suitable analytical and sensory tools to track the analytically measurable development between different chocolate phases and the overall perceived sensory profile.

Experimental

Manufacturing of milk chocolate. For this study five milk chocolates (ingredients: sugar, milk powder, cocoa butter, cocoa flakes, lecithin as emulsifier) differing in the dry conching time (1 h, 2 h, 4 h, 10 h, 24 h; final temperature 75°C) were produced in a 6 kg Austin conche. All other production parameters were kept constant.

Sample preparation. In order to track the distribution of potent aroma compounds inside the various chocolate phases during conching a special preparation technique

has been set up. For that purpose, chocolate has been dissolved in water and centrifuged.

30 g of molten chocolate were dissolved in 70 g of warm water (50 °C). The pH of the slurry was adjusted to 4. After spiking the chocolate slurry with a set of different internal standard compounds the slurry was equilibrated by stirring for 30 minutes. Afterwards the slurry was separated into three phases by centrifugation (30000 g) at 4 °C for 45 minutes. The low temperature is required to form a solid fat phase which can be easily removed from the other phases and analysed.

Quantification of potent aroma compounds. The aroma compounds contained in the fat phase were quantified by thermodesorption-GC-MS analysis. The quantification of the aroma compounds in the water-soluble phase was conducted by GC-MS after solid phase extraction (SPE) (5). The aroma compounds remaining in the insoluble residual material were extracted with diethyl ether, purified by high vacuum distillation, concentrated and quantified by GC-MS. The aroma profiles in the entire, non separated chocolates were determined by thermodesorption-GC-MS analysis (6).

Sensory evaluation. Sensory evaluation of the milk chocolates was performed with a trained sensory panel (10 panellists) on solid chocolate and molten chocolate, respectively. The overall aroma intensity of the water-soluble phases was rated on a scale from 0 = no aroma perception until 6 = strong aroma perception. Also the intensity of the fat phases separated simply by centrifuging molten chocolate without addition of water was rated.

Results and Discussion

Quantification of potent aroma compounds in different phases. After phase separation the well-known potent aroma compounds of milk chocolate (7) were quantified in the separated fat by thermodesorption-GC-MS. As illustrated in Figure 1 the concentrations of most aroma compounds were reduced during conching.

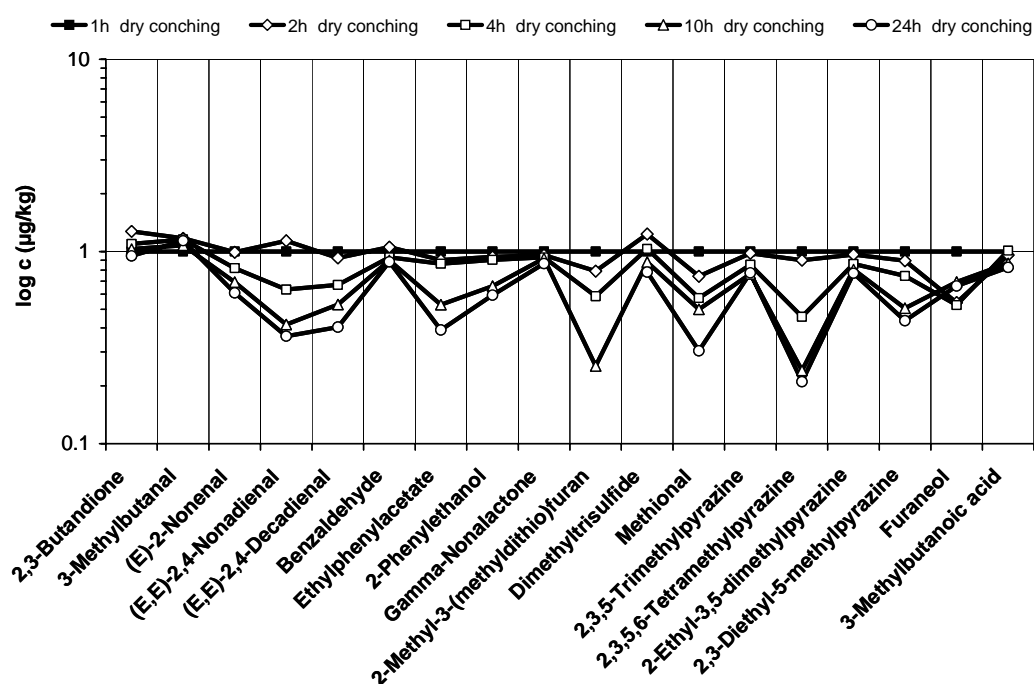


Figure 1. Relative concentration of aroma compounds in the separated fat phase developing with increasing time.

Contents of the fatty smelling aldehydes (E)-2-nonenal, (E,E)-2,4-nonadienal and (E,E)-2,4-decadienal and the honey-like smelling ethylphenylacetate and 2-phenylethanol were significantly reduced in fat by conching. Also, the pyrazines, which are very important for the overall chocolate aroma, and the sulphur compounds methional and 2-methyl-3-(methylthio)furan decreased with longer conching times.

In order to further differentiate potential binding sites the aroma dissolved in the water phase and the aroma remaining attached to the insoluble material were also quantified. It was found, that although the aroma concentration for many compounds is declining in the fat phase, the aroma profile of two latter phases is not changing (data not shown).

The quantitative results of the whole chocolate without preceding separation is dominated by the decrease in concentrations as observed in the fat phase of the respective chocolate.

In an additional experiment it was demonstrated that conching of non-deodorized cocoa butter alone (same conche, same times) is resulting in steeply declining aroma concentrations (data not shown). It is assumed that the reduction of aroma compounds during conching of chocolate is primarily caused by evaporation.

Sensory evaluation. In order to assess the impact of conching time on the aroma profile, the conching trials were accompanied by a trained sensory panel. For this purpose solid chocolate, molten chocolate, the separated fat phase from molten chocolate, and the water-soluble phase were evaluated. Sensory evaluation of the separated fat phase showed that the overall aroma intensity decreased with extended conching (Figure 2). This confirms the analytical results (Figure 1).

Chocolates with longer conching times were found to contain lower levels of analytically measurable aroma. This is supported by sensory results obtained in molten chocolate and in the separated fat phase. Sensory results obtained from solid chocolate, however, show an increase in perceived aroma intensity (Figure 2). It is concluded that improving texture properties enable a more balanced flavour perception. In other words the harsh and poorly melting chocolate texture, as obtained with short conching times, is believed to act like a masking effect for flavour perception. The sensory properties of the water-soluble phase are not changing with progressing conching time and are therefore in agreement with the analytical results.

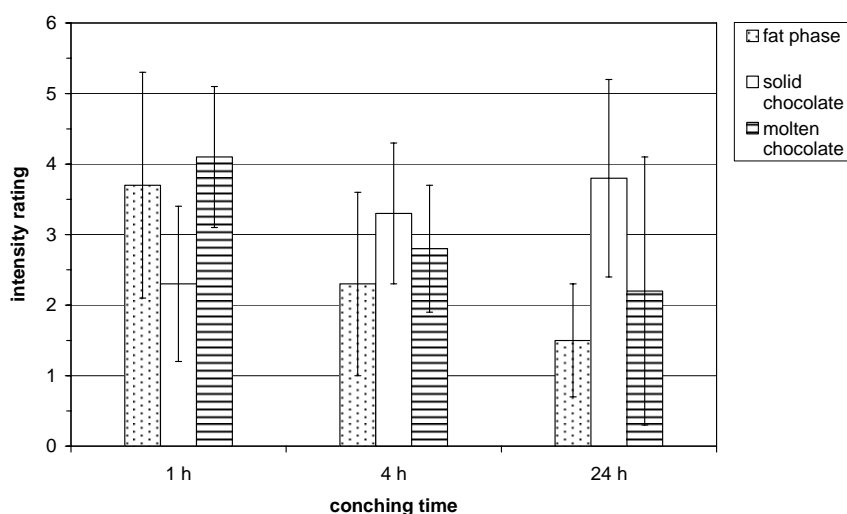


Figure 2. Development of overall aroma intensity with increasing conching time in solid chocolate, separated fat phase, and molten chocolate.

Since lower levels of aroma compounds lead to a lower perceived aroma intensity in molten chocolate, it is concluded that melting chocolate is removing the masking effect of a poorly conched chocolate and is also indicating that the aroma perception is driven by the aroma contained in the fat phase.

Conclusion

The total aroma contained in chocolate is distributed over three different chocolate phases (fat, water-soluble material, insoluble material). Conching is primarily affecting the aroma content in the fat phase. The aroma attached to water-soluble binding sites is found to be unaffected. Key driver for aroma perception, however, seems to be the aroma contained in the fat phase. Beside that, texture development during conching has a critical impact on a balanced perception of chocolate aroma.

References

1. Ziegleder G., Balimann G., Mikle H., Zaki H. (2003) *Süsswaren* 3: 14-16.
2. Ziegleder G., Balimann G., Mikle H., Zaki H. (2003) *Süsswaren* 4: 16-18.
3. Ziegleder G., Balimann G., Mikle H., Zaki H. (2003) *Süsswaren* 5: 14-16.
4. Counet C., Callemien D., Ouwerx C., Collin S. (2002) *J. Agric. Food Chem.* 50: 2385-2391.
5. Naef R., Jaquier A., Velluz A., Maurer B. (2006) *J. Agric. Food Chem.* 54: 9201-9205.
6. Pfnür P., Hässelbarth A., Schulze M., Ullrich F. (2003) In *Flavour Research at the Dawn of the Twenty-first Century* (Le Quéré J.L., Étievant P.X., eds.); Editions Tec & Doc, Londres-Paris-New York, pp 698-701.
7. Schnermann P., Schieberle P. (1997) *J. Agric. Food Chem.* 45: 867-872.

FLAVOUR EVOLUTION INVESTIGATIONS IN A TOBACCO GENE-TO-SMOKE PROJECT

F. FRAUENDORFER, M. Christlbauer, J.C. Hufnagel, J.-P. Schaller, A. Glabasnia, and F. Gadani

Philip Morris International R&D, Applied Research, Quai Jeanrenaud 56, 2000 Neuchâtel, Switzerland

Abstract

Tobacco undergoes several processing steps from harvest to consumption. The aim of this study was to follow the flavour evolution of oriental tobacco from green leaves to cured leaves to aerosol (smoke). Aerosol was generated by electrically heating tobacco, a novel approach which allows aerosol formation at lower temperatures compared to conventional combustion. Taste and aroma properties were assessed using a combined sensory and analytical approach. Gas Chromatography-Olfactometry and Aroma Extract Dilution Analysis indicated that aroma constituents in tobacco aerosol can be divided into three groups: 1) compounds already present in green leaves with high flavour dilution (FD) factors; 2) compounds formed mainly during curing; and 3) compounds formed during aerosol generation. Furthermore, several odorants with high FD factors in the green and cured tobacco leaves were not detected in the tobacco aerosol. Evaluation of taste and trigeminal properties by a trained sensory panel revealed only three different sensory attributes, namely irritation, astringency, and bitterness. While the intensity of both irritation and astringency was perceived to decrease from green tobacco leaves to tobacco aerosol, bitterness was perceived to be most intense in the tobacco aerosol. The results of the study clearly indicate that the plant material, the curing process, and the aerosol formation process all have an impact on the overall flavour properties of tobacco aerosol.

Introduction

From the time of harvest to that of consumption, the leaf of the tobacco plant (*Nicotiana tabacum*) undergoes several processing steps. Some of these steps involve biochemical and thermal transformations, which change the chemical composition and flavour properties. For the first time, the flavour development from green tobacco leaves to tobacco aerosol (smoke) has been assessed, using a combined sensory and analytical approach.

In this study, tobacco smoke was produced by applying a novel method. In conventional smoking articles, aerosol is generated by the combustion of cured tobacco leaves. One approach to developing innovative smoking products which may have the potential to reduce health risks associated with their use compared to conventional products is to apply lower temperatures to tobacco, e.g. by electrically heating the tobacco instead of burning it. These results in reduced yields of some smoke constituents and decreased activity in some standard toxicological tests (1).

Experimental

Materials. Oriental tobacco (*Basma xanthi*) from the same origin (Macedonia) and crop year (2007) was used for all experiments. Sample preparation was performed as indicated in Table 1.

Table 1. Sample preparation of green and cured tobacco leaves.

Sample Preparation & Methods	
Aroma	Taste
<ul style="list-style-type: none"> • Adding 100 mL CaCl₂ solution (4.5 mol/L) to 15 g* green (3 g* cured) grinded tobacco and stirring, cooled by ice bath (1h) • Extracting with 3 x 50 mL dichloromethane • Solvent Assisted Flavour Evaporation (SAFE) • Reducing volume using microdistillation equipment 	<ul style="list-style-type: none"> • Extracting 5 g grinded tobacco (cured and green) with 2 x 50 mL methanol and 1 x 50 mL water • Removing methanol (Rotavap) • Freeze drying • Redissolving in ethanol 50 % and diluting* with water (1:100)
<ul style="list-style-type: none"> • Aroma Extract Dilution Analysis (AEDA), using Gas Chromatography Mass Spectrometry Olfactometry (GC-MS-O) 	<ul style="list-style-type: none"> • Sensory evaluation with trained panel • Nicotine determination (LC-DAD)

* Weights and dilutions were adjusted based on dry weight

Smoking experiments. A schematic overview of the setup is shown in (Figure 1). Tobacco aerosol was produced by electrically heating a plug of cured tobacco (100 mg). A pump was adjusted to simulate realistic puffing conditions (puff frequency: 2 puffs/min; puff volume: 50 mL; puff duration: 2 s). The aerosol was condensed in a recently described cryogenic instrument (2). After the last puff, the trap was rinsed with solvent (dichloromethane for the aroma analysis and ethanol for the taste analysis) and the condensate was further processed in the same way as the leaf extracts (see Table 1).

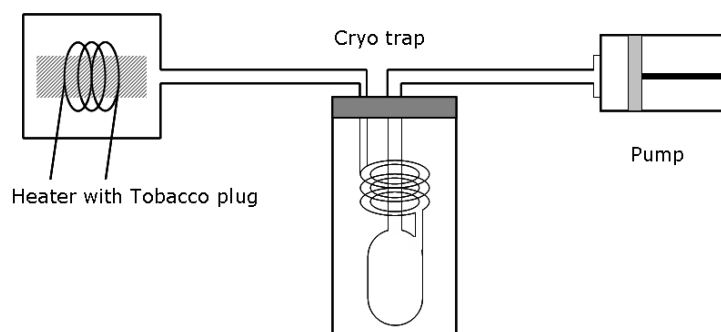


Figure 1. Aerosol formation and trapping.

Results and Discussion

Aroma. Gas Chromatography-Olfactometry revealed 48 aroma active regions for the green tobacco leaves, 62 for the cured tobacco leaves, and 49 for the tobacco aerosol. The compounds with the highest Flavour Dilution (FD) factors for each sample are given in (Table 2). Although the majority of the odorants are present at all three stages of tobacco processing, substantial differences were observed in the FD factors. In the green tobacco leaves, pyrazines such as 2-ethyl-3,5-dimethylpyrazine, and 2-isopropyl-3-methoxypyrazine, showed the highest FD factors. While these pyrazines were also dominant in the cured tobacco leaves, several other compounds, mostly with a carbonyl function, such as 2,3-butanedione, 2-methylbutanal, and phenylacetaldehyde, were also detected in high dilutions in the cured tobacco leaves.

In the tobacco aerosol, 2,3-butanedione was detected with the highest FD factor, followed by 2-/3-methylbutanoic acid, 2-ethyl-3,5-dimethylpyrazine, (E)- β -damascenone, 3-(methylthio)propionaldehyde, 2-acetyl-1-pyrroline, and 3-methylbutanal. Focusing on the origin of the aroma compound composition of the tobacco aerosol (smoke), the results of the AEDA indicate three sources:

- Compounds already present in green leaves with high FD factors, such as (E)- β -damascenone, 3-(methylthio)propionaldehyde, and 2-acetyl-1-pyrroline.
- Compounds formed mainly during the curing process, such as 2,3-butanedione, 2-methylbutanal, and 3-methylbutanal.
- Compounds formed mainly during aerosol formation (heating), such as 2-/3-methylbutanoic acid, 4-hydroxy-2,5-dimethyl-3(2H)-furanone, and some pyrazines.

Table 2. AEDA results of green and cured tobacco leaves and the corresponding tobacco aerosol.

Compound*	Odour quality	FD factor in tobacco		
		Aerosol	Cured	Green
Aroma compounds present in green tobacco				
2-ethyl-3,5-dimethylpyrazine	earthy	64	32	512
2-isopropyl-3-methoxypyrazine	bell pepper	< 1	512	256
propyl-2-methylbutanoate	fruity, elder	< 1	128	128
2-acetyl-1-pyrroline	popcorn	64	64	128
(E)- β -damascenone	cooked apple	64	128	64
2,6-dimethylphenol	plastic, phenolic	16	64	32
3-(methylthio)propionaldehyde	cooked potato	64	64	32
unknown (RI on OV 1701: 914)	geranium	< 1	8	32
(E,Z)-2,6-nonadienal	cucumber	4	8	16
1-hexen-3-one	metallic, rubber	1	32	16
3-methyl-2-buten-1-thiol	beer	16	32	16
unknown (RI on OV 1701: 1145)	earthy	< 1	4	16
unknown (RI on OV 1701: 872)	fatty	< 1	< 1	16
2-sec-butyl-3-methoxypyrazine	bell pepper	32	16	8
Aroma compounds formed mainly during curing				
2,3-butanedione	buttery	256	256	8
3-ethyl-2,5-dimethylpyrazine	earthy	2	128	8
2-methylbutanal	malty	32	64	1
1-octen-3-one	mushroom	2	64	8
(Z)-1,5-octadien-3-one	geranium	< 1	64	4
3-methylbutanal	malty	64	32	4
phenylacetaldehyde	honey	2	32	2
2-methyl-2-butanthiol	sulphury, herbaceous	< 1	32	4
hexanal	grassy	< 1	32	2
(E,E,Z)-2,4,6-nonatrienal	oat flakes	< 1	16	1
2-methylbutanol	malty, green	< 1	16	< 1
dimethyl trisulphide	cabbage	32	8	2
2-methoxyphenol	smoky	16	8	< 1
benzothiazole	phenolic	16	4	< 1
Aroma compounds formed mainly during aeroionisation				
2/3-methylbutanoic acid	sweaty	64	4	< 1
2-propanoyl-1-pyrroline	popcorn	32	2	1
2,3-diethyl-5-methylpyrazine	earthy	32	4	< 1
3-ethyl-2-methoxypyrazine	earthy, bell pepper	16	1	1
2-ethenyl-3,5-dimethylpyrazine	earthy	16	< 1	< 1
2-methyl-3-(methylthio)furan	meaty	16	2	< 1
4-hydroxy-2,5-dimethyl-3(2H)-furanone	caramel	16	< 1	< 1

* Identification was performed based on three criteria: Similarity of retention index (RI), similarity of mass spectra, and similarity of aroma quality with reference compound.

Beside the formation of odorants, it was also observed that several compounds present in the cured leaves were either not detected in the tobacco aerosol or were detected with much lower FD factors (e.g. (Z)-1,5-octadien-3-one, hexanal, and (E,E,Z)-2,4,6-nonatrienal). These constituents might be either degraded during the thermal treatment or simply not transferred from the heated tobacco to the tobacco aerosol.

Taste and Trigeminal Perception. Sensory assessment of the tobacco samples revealed only three orosensory qualities: bitterness, irritation, and astringency. The perceived intensity for astringency and irritation decreased with the processing of the tobacco, being highest in the green tobacco leaves and lowest in the tobacco aerosol (Figure 2). A possible explanation for the decreasing irritation might be the decreasing concentration of nicotine, a constituent which is known to cause irritation. In contrast to astringency and irritation, bitter taste was more pronounced in the tobacco aerosol than in the cured and green tobacco leaves.

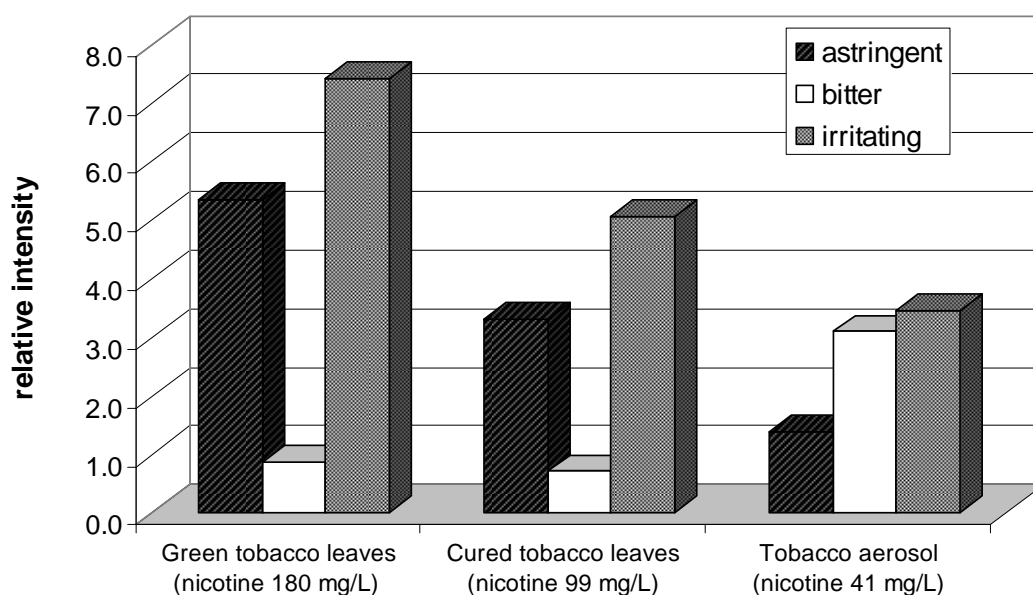


Figure 2. Sensory assessment of taste and trigeminal properties in green tobacco leaves, cured tobacco leaves, and tobacco aerosol.

As for the aroma properties, the results of the taste and trigeminal evaluation indicate that during heating and aerosol formation, some taste active compounds are formed (increasing bitterness), while others are decomposed or not aerosolized (decreasing astringency).

Acknowledgement

We would like to thank Sabine Fer for excellent laboratory assistance.

References

1. Patskan G., Reininghaus W. (2003) *J. Appl. Toxicol.* 23: 323-328.
2. Plata N., Hofer I., Roudier S., Schaller J.-P. (2006) *J. Aerosol Sci.* 37: 1871-1875.

Section 7

Flavour Generation by Bio-Mediated Processes

WHITE BIOTECHNOLOGY: SUSTAINABLE OPTIONS FOR THE GENERATION OF NATURAL VOLATILE FLAVOURS

R.G. BERGER

Institut für Lebensmittelchemie, Gottfried Wilhelm Leibniz Universität Hannover, Callinstrasse 5, D-30167 Hannover, Germany

Abstract

Microorganisms are regularly associated with food spoilage and dangerous diseases; thus, not only food scientists are afraid of them. However, numerous bacteria and fungi are essential to the empirical food biotechnologies (alcoholic, lactic, mixed fermentations); they form and transform, along efficient and selective enzymatically catalysed pathways, a variety of volatile flavours specific of the respective foods. Potent flavour forming microorganisms were selected in recent years, and concerted bioprocesses for the production of natural flavours were developed. Bioengineering provides technical aids to improve the yields, such as membrane aided and two-phase processes, fed-batch procedures, gas phase feeding, and efficient *in-situ* removal (ISRP) to avoid inhibitory product concentrations. Novel instruments from the toolbox of biochemistry and molecular biology, such as accelerated sequencing will help to establish “white biotechnology” as a viable and sustainable alternative for flavour production.

Sources and quality of flavours

The majority of industrial flavours is provided by higher plants from many different genera. These classical agricultural sources, however, depend on climate, season, soil and fertilisers; they are prone to microbial and insect infestation, contain trace concentrations of key compounds, and they may suffer from socio-political instabilities and uncertain supply from overseas. Important flavour plants such as *Citrus* or *Mentha* species have suffered from cold snaps or depleting soil. Altogether, these imponderabilities not only affect the market price, but also cause continuing problems of quality, such as contamination by pesticides and insecticides.

The production of volatile and non-volatile microbial flavours is typical of the empirical biotechnologies. The experience gathered with these processes has delivered the scientific basis for the selection of new flavour forming strains and for the development of aroma yielding processes on the industrial scale. Biocatalysts are distinguished by high selectivity and efficiency, and multi-step syntheses can be performed if intact cells with their in-built regeneration of enzymes and co-factors are used. More recently, other properties of bioprocesses have found attention: Bioprocesses are environmentally compatible; they run under mild physical conditions, use renewable substrates and do not accumulate problematic wastes (1). To round off the bundle of motives for the development of new bioprocesses the increasing concern about food quality should be mentioned. Many consumers equal food quality with the attribute “natural”, and fermentation processes with their long tradition seem to guarantee safe and high quality food. The fatal consequences of consuming, for example, products of alcoholic fermentation in excess are not in line

with the wide-spread risk estimation of the public and have not yet resulted in a more science based thinking of the average food consumer.

Which biocatalyst is best?

There exist three large domains of life, the *bacteria* (for example *Lactobacilli*, *Staphylococci*, *Streptococci*), the *archaea* (extremophiles and producers of methane), and the *eucarya* (plants, animals, fungi). Among the innumerable diversity of species and strains are autotrophic and heterotrophic, aerobic and anaerobic, photosynthetic, iron accumulating, and halophilic or thermophilic representatives. A concerted screening for flavour generating species, other than guided by the nose, appears impossible. However, more than eighty years after the first mentioning in literature, and as a result of more than twenty years of in-depth research in the field, the potential of numerous genera for the formation of volatile flavours is quite well known: The physiologically simple prokaryotic organisms form the appreciated fermentation flavours containing short-chain alcohols, biogenic amines, carbonyls and fatty acids, while yeasts form volatile alcohols and esters from the degradation of metabolites of primary pathways. Higher fungi show the largest potential for flavour formation; all kinds of volatiles including methyl ketones, lactones, phenols, phenylpropanoids, terpenes and terpenoids and more have been found (2-5). Many believe that we are currently looking at the proverbial tip of the iceberg, because every new screening reveals new flavour producers. Some of the volatile flavours, such as the constituents of fusel oil, are ubiquitous, others, such as raspberry ketone (6) or nootkatone (7), were found in few or even in one single species, and only when cultivated under specific conditions.

Use of enzymes

Microorganisms may as well be used as a sustainable source of enzymes, such as lipases, glycosidases or carbon-carbon coupling activities to perform single step reactions (8). There are perhaps 25,000 enzymes present in nature, but less than 100 are used on a larger industrial scale; most of them are hydrolases. Lipases, acidic glycoproteins active at the oil-water interface, catalyse not only the cleavage of different types of ester bonds, but also the reverse reaction (esterification), transesterification (ester plus alcohol), interesterification (ester plus acid) and acyl transfer onto various nucleophilics. The most prominent applications of lipolysis are flavour formation from milk fat and the reverse hydrolytic reaction of alcohol and acid to carboxylic esters with fruity notes. If stereochemically pure esters are aimed at, the kinetic resolution of racemic precursor mixtures is a solution: Lipases from *Penicillia*, *Rhizopus*, *Trichoderma* and from bacterial sources prefer, for example, (-)-menthyl esters and leave the (+)-form untouched. The particularly useful immobilised lipase of *Candida antarctica* esterified methyl-branched fatty acid chains to resolve, for example 4-methyloctanoic acid (9), while a porcine pancreatic lipase served the same purpose in an enantioselective transesterification reaction (Figure 1) (10).

With a special focus on wine, glycosidases were described to liberate aroma-active aglyca from their glycosidic precursors (11). Glycosidases from *Aspergilli* showed less inhibition by glucose, fructose, ethanol and low pH, and their application resulted in improved wine flavour, as was confirmed by sensory tests. The same approach worked with vanilla beans, birch bark (for the release of raspberry ketone),

milk (phenols) and cyanogenic glycosides (for example, for the release of benzaldehyde).

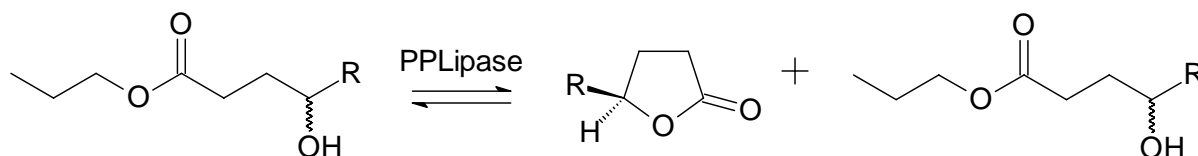


Figure 1. Formation of an (*S*)-lactone by selective transesterification of a racemic 4-hydroxyacid propyl ester.

More complicated is the application of oxidoreductases, as their action requires charge transfer in the form of two one-electron or two one-electron steps. As the electrons have to be supplied stoichiometrically by a second substrate, the success of such processes depends on an efficient regeneration of this co-substrate. This can be achieved by 1) using a second enzyme catalysing a second reaction in the reverse redox direction, and 2) by selecting enzymes which accept the same co-factor. The coupled reaction can be brought to completion, for example, by the production of a volatile product (cleavage of formic acid to H₂O and CO₂) which escapes from the reaction. This means in turn that enough co-factor will be available for the first, the desired reaction. A variant of this is crystallisation of the product of the coupled reaction to form an insoluble precipitate (Figure 2) (as reviewed in 12).

Among the oxidoreductases used for flavour generation are alcohol dehydrogenases, peroxidases including chloroperoxidase, lipoxygenases, amine oxidases and vanillyl alcohol oxidase (8). Basidiomycetes, the taxonomically most developed class, present a rich source of novel oxidoreductases and combine easy bioprocessing with complex metabolism. Most of the 200 edible mushrooms belong to one of the 16 orders of basidiomycetes rendering them well suitable for food applications. The first secretomes have been analysed using 2D-electrophoresis (13), and a large diversity of enzymes was revealed.

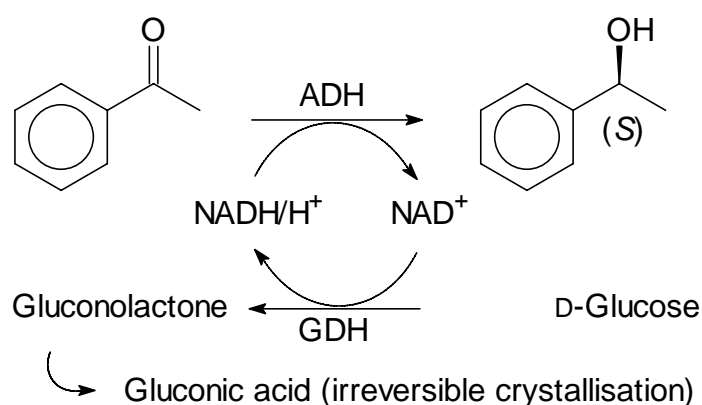


Figure 2. Regeneration of co-factors in a coupled dehydrogenase reactions.

One of them, a so-called versatile peroxidase of *Pleurotus eryngii*, catalysed the asymmetric cleavage of β -carotene and other tetraterpenoid structures to a volatile part (such as β -ionone from β -carotene) and a non-volatile apocarotenal (Figure 3;

Zelena *et al.*, this volume) (14,15). A plant counterpart of this enzyme was described recently (16).

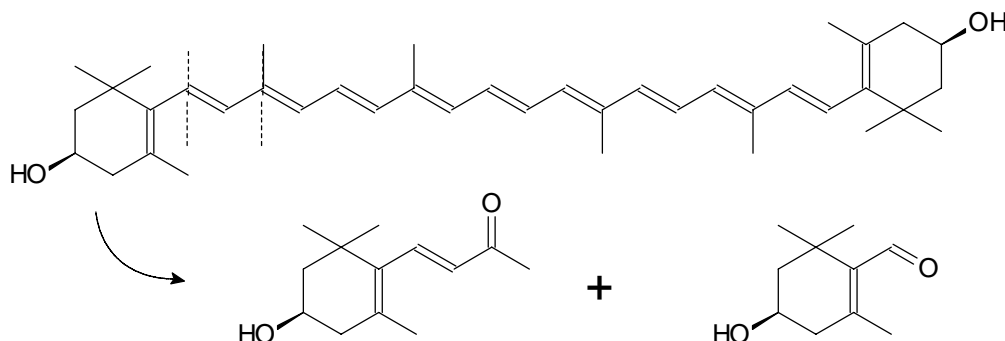


Figure 3. The so-called versatile peroxidase of *Pleurotus eryngii* cleaved zeaxanthin to 3-hydroxy- β -ionone and β -cyclocitral (Zelena *et al.*, this volume).

Genetic engineering

Once the sequence or partial sequence of an enzyme associated with flavour formation has been known, a few of the amino acids can be back translated into the DNA sequence. The complementary piece, if contacted with the genomic set of DNA of the respective cell, will hybridise only with the matching sequence. This primer is then elongated by adding a ligase and nucleotides in non-limiting concentration. The newly-formed double strand is then amplified using PCR to obtain material for sequencing. This piece of DNA represents the structural gene coding for the enzyme of interest. In a final step, the DNA is recombined with a larger DNA molecule ("vector") which is transferable into a heterologous host. The host cell reads and expresses the foreign genetic sequence as if it was its own. Several options exist to even over-express the new enzyme protein, thereby delivering the target biocatalyst in unlimited amount. Several food enzymes, such as rennin, are produced and used since many years without problems.

From the viewpoint of the human user the recombinant enzyme may work not well enough. A number of techniques, such as error-prone PCR, mutation strains, or saturation mutagenesis have been developed for the exchange of nucleotides. Heterologous over-expression of these "mutated genes" may yield thousand enzyme variants per day. Most of them are worse, but a few may show improved stereoselectivity, substrate specificity or else. These are mutated again, expressed, screened and amplified again in an iterative process. To cite an example from the flavour field, a vanillyl alcohol oxidase was shown to introduce a hydroxyl group into the side chain of 4-ethylphenol. The resulting (*R*)-1-(4'-hydroxyphenyl)-ethanol showed high enantiopurity. A so-called "double mutant" enzyme in which two amino acids were replaced showed the opposite stereochemistry and gave the pure (*S*)-enantiomer (17). In the course of such work a lot is learned about the correlations of enzyme structure and catalytic effect. Amino acids positioned next to the active site often govern the size and geometry of substrates accepted, while amino acids located far away from the catalytic events ("hot spots") may govern the folding of substructures required for the correct conformation of the catalytically active enzyme.

The fascinating options of genetic engineering continue to stimulate research efforts regardless of public resentments. *E. coli* engineered by using genes encoding feruloyl-CoA synthetase and feruloyl hydratase/aldolase from *Pseudomonas*

fluorescens produced 2.5 g of vanillin per L (18) Engineering volatile thiol release in *Saccharomyces cerevisiae* using vice versa an *Escherichia coli* gene encoding a tryptophanase with strong cysteine- β -lyase activity resulted in improved wine aroma (19). The (*E*)- β -caryophyllene synthase (OsTPS3) accounted for the major inducible volatile sesquiterpenes in rice (20); unwanted allelochemical side-effects were noted. In ripening strawberries differentially expressed genes and transcriptional factor domains were followed. Epimerase, carotene desaturase, zinc metabolism enzymes, and certain transcriptional factors were activated (21). It will be the next step to relate these enzymes with flavour metabolism which in turn opens possibilities for the concerted expression of key enzymes, be it in the aroma plant or in a heterologous host.

Whole cell systems

An intact microbial cell regenerates the enzyme chains, required cofactors and transporters and thus maintains a continuous flow of metabolites. However, from the preparation of the nutrients to the final down-streaming of product, all steps have to proceed under sterile conditions; moreover, unwanted metabolites may accumulate, and the desired product(s) as well as the substrate(s) may, even at low concentrations, inhibit the producer cell. It is the most important task of the bioengineer to set the biological, chemical and physical parameters of the process in a way that the above problems are minimised and the potential of the cells is fully exploited.

After the definition of the target compound an extended screening of microorganisms is usually the first step in setting up a new process. Previous experience with certain species or general biochemical information will aid in pre-selecting suitable species. As it was known, for example, that some basidiomycetes tolerated millimolar concentrations of monoterpene hydrocarbons, species were chosen from this class of fungi to perform biotransformations of limonene. *Pleurotus sapidus*, an edible relative of the oyster mushroom *Pleurotus ostreatus*, was found to convert exogenous (*R*)-(+)-limonene to all of the four carveols and to both carveones, but much better stereoselectivity was achieved using *Rhodococcus opacus* which formed *trans*-(+)-carveol and (*S*)-(+)-carvone, while the diastereomer *cis*-(+) carveol was amenable through *Fusarium proliferatum*, a phytopathogenic fungus. When (*S*)-(-)-limonene was the precursor, *trans*-(*S*)-carveol and (*R*)-(-)-carvone were formed with good stereopurity (22,23).

Obviously, this conventional trial-and-error approach is laborious and time-consuming. Genetic engineering would be the superior tool, as it implements the desired metabolic trait and, if functional expression can be achieved, directly results in a productive flavour forming cell culture. However, there is a major scientific obstacle: Although the chemistry of flavours is so well known most of the genes and enzymes involved in their biogenesis are not. A concerted modification of a producer cell would depend on the "knowledge and availability of genes that encode enzymes of key reactions" leading to volatile flavours (24).

Labelling studies are still rare. For example, stable isotope labelling was used to elucidate the catabolism of leucine to branched-chain fatty acids in *Staphylococcus xylosus*, an important starter culture in fermented meat (25), and in similar work deuterated intermediates of α -pinene oxide were used to confirm 3,4-dimethylpentenoid acid as a degradation product (26). In the same way the catabolism of phenylalanine was studied (27). Based on the fundamental biochemical

data established a process for the generation of gram per litre concentrations of 2-phenylethanol and 2-phenylethylacetate by baker's yeast was successfully developed (28). An extended labelling study was devoted to the synthesis of furanoterpenoids from monoterpenes containing a conjugated diene moiety (Krings *et al.*, this volume). A solubilised fraction of mycelium lyophilisates of several *Pleurotus* species converted deuterated β -myrcene or chemically related structures in an initial step, similar to a 2+4 cycloaddition of 1,3-dienes with dienophile $^1\text{O}_2$, to 1,4-endoperoxides. These were converted through the key intermediate α -(*Z*)-acaridiol to the respective furans, such as perillene and rose furan (29).

A great surprise for the biochemical community was the finding that two independent pathways to isopentenyl diphosphate exist. In plants monoterpenes are generated through the novel plastidial DXP/MEP (1-deoxy-D-xylulose/2-C-methyl-D-erythritol-4-phosphate) pathway, while sesquiterpenes are formed along both the classical cytosolic mevalonate and the novel pathway. As both pathways show different discrimination of ^{13}C , isotope analysis of linalool enantiomers in strawberry was able to show that the (*R*)-enantiomer was formed through the DXP/MEP pathway, whereas the opposite enantiomer was found labelled only after administration of [5,5- $^2\text{H}_2$]-mevalonic acid lactone (30). These results not only explain why mixtures of enantiomers are sometimes found in the cell, but will also help in mapping quantitative trait loci (QTL) responsible for flavour pathways (31). Genetic work in the field of isoprenoid metabolism has resulted in the cloning of a number of geranyl and farnesyl diphosphate cyclases (32-35). Recombinant over-expression in homologous and heterologous plant hosts, for example in tobacco or in *Arabidopsis*, has not always been successful, but transcript analysis or antibody testing have at least proven the principal feasibility.

Competitiveness of Bioprocesses

Looking at the variability and uncertainty introduced by the use of a biocatalyst, the viability of a bioprocess for flavour production has been questioned. A key parameter for both economic and environmental performance is biomass concentration, because the concentration of the effective catalyst governs overall reaction rate. Space-time-yields of commercial bioprocesses range from milligram to three-digit grams per litre and hour. An inverse double-log correlation of product concentration and sales price was found. A market price of a bioflavour of 100 to 500 \$ per kg would correspond with yields in the range from 100 milligrams to one gram per litre; although data from literature are patchy, many processes reported have beaten the one gram per litre threshold (Table 1). More than 100 single flavour constituents and complex flavour mixtures are commercial, among them volatile aliphatic and aromatic alcohols, such as fusel alcohols and cinnamyl alcohol, acids, and esters, such as 2-phenylethyl acetate, aldehydes, such as hexenals and vanillin, ketones, a series of 4- and 5-alkanolides, and some terpenoids.

White Biotechnology

The European Commission defines White Biotechnology as a modern version of biotechnology

"based on the use of renewable resources and clean production and less pollution and less energy intensive processes in biological systems, such as whole cells or enzymes, used as reagents or catalysts".

Table 1. Selected bioprocesses with yields higher than one gram per litre (1-5)^a.

Volatile Flavour Compound	Yield [g per L ⁻¹]	Time to max. Conc.
Isonovalal	400	2.5 h
Cinnamyl alcohol	166	
Acetaldehyde	130	4 h
2-/3-Methylbutanoic acid	80	65-92 h
2-Heptanone	60	
Isovaleraldehyde	40	7 h
Isopentyl hexanoate	30	6 h
2-Phenylethanol plus 2-phenylethyl acetate	26	30 h
Vanillin	18	50 h
Diacetyl	14	
4-Decanolide	11	55 h
2,5-Dimethylpyrazine	4	5 d
3-(Z)-Hexenol	4	
Jasmonic acid	1.5	11 d
Irones	1.2	3 d
2-Furfurylthiol	1	

^a typically maximum yield of process as specified by the authors

It is mainly these ecological and sustainability aspects that differentiate the novel term White Biotechnology from previous descriptions of biotechnology. The first severe effects of the depletion of fossil fuels are felt while this chapter is being written; therefore, there is good reason to believe that the development of alternative raw materials and energy-saving processes will be strongly stimulated in the future.

Enzyme technologies in the food industry would be more popular, if less complicated steps for enzyme isolation and purification would be available. Isoelectric foaming of microbial broths could close this gap for those enzymes which are bipolar enough to accumulate at the gas/liquid interface of a foam. Transport of fungal laccases and lipases in a few minutes with full retention of activity has been demonstrated. The foaming equipment is easily set up and does not require much process controls. Various options for foam breaking exist (36).

Biotechnology usually takes place in an aqueous environment; however, many flavour precursors, such as lipids, and the flavour products themselves are not well water soluble. Aqueous/organic two phase systems or pure organic phases (for enzymes) were shown to overcome the solubility problems (37). Some enzymes were also shown to work well in supercritical and ionic fluids, such as butyl-methylimidazolium hexafluorophosphate. The extended half-life of enzymes in the xenobiotic ionic liquids has attracted a lot of recent research, although the reasons for the improved stability remain somewhat unclear (38). Another unusual environment for an enzyme is the gas phase. Solubility limits and microbial contamination are excluded, and high diffusion coefficients can be observed at elevated temperature. This approach is obviously particularly well suited for reverse hydrolytic reactions, but has been extended recently to redox and C-C-coupling reactions (Figure 4) (39,40).

Cold recovery of flavour products using absorption or adsorption complies well with the characteristics of a white bioprocess. Progress has been made in the use of activated carbon. Principally a material difficult to desorb, electrically heated carbon

cloth could present a versatile solution for the future. A multi-layer cloth is placed into the outlet air stream of a bioreactor. After the capacity of the cloth is exhausted, a small stream of regeneration air is passed through the electrically heated cloth. This stream now contains the formerly adsorbed aroma compounds, from which they can be condensed, absorbed or otherwise concentrated for further application (41).

Future prospects

Of particular interest are currently rapid sequencing techniques. As the life sciences move towards a better understanding of living cells, the genetic information behind the metabolic events opens a direct access to manipulating the performance of an industrially used cellular system. Among several recent approaches is tip amplified atomic force microscopy with Raman spectrometry. The technique uses a silver coated nano-tip of an atomic force microscope to amplify the scattered light of a laser beam and gives a high lateral resolution of some nucleobases of a RNA single strand (42). As a result, genetic information will be provided with little effort, and this can in turn be applied to a better understanding of the flavour forming pathways, may they run in a genetically modified cell or in a wild strain.

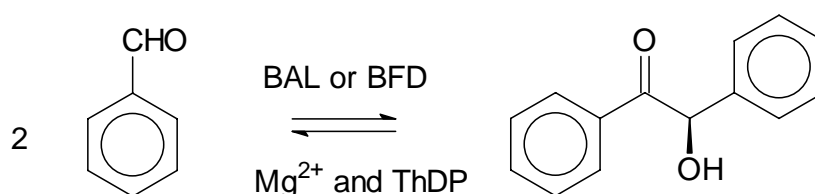


Figure 4. Gas/solid carboligation: Conversion of benzaldehyde to benzoin using thiamine diphosphate-dependent benzaldehyde lyase (BAL) or benzoylformate decarboxylase (BFD).

Acknowledgement

This work was in part supported by the Bundesministerium für Bildung und Forschung through the cluster program *Biokatalyse2021* (FKZ 0315172F).

References

1. Schrader J. (2007) In *Flavours and Fragrances – Chemistry, Bioprocessing and Sustainability* (Berger R.G., ed.), Springer: Heidelberg, pp 507-574.
2. Berger R.G. (1995) *Aroma Biotechnology*, Springer, Heidelberg.
3. Longo M.A., Sanroman M.A. (2006) *Food Technol. Biotechnol.* 44: 335-353.
4. Berger R.G. (2007) In *Modifying Flavour in Food* (Taylor A., Hort J., eds.), Woodhead Publishing: Cambridge, pp. 64-94.
5. Havkin-Frenkel D., Belanger F.C. (eds.) (2008) *Biotechnology in Flavor Production*, Wiley: Chichester.
6. Zorn H., Taupp D.E., Hülsdau B., Scheibner M., Fraatz M.A., Berger R.G. (2007) In *Recent Highlights in Flavor Chemistry and Biology* (Hofmann T., Meyerhof W., Schieberle P., eds.). DFA: München, 203-209.
7. Kaspera R., Krings U., Nanzad T., Berger R.G. (2005) *Appl. Microbiol. Biotechnol.* 67: 477-483.
8. Menzel M., Schreier P. (2007) *Flavours and Fragrances – Chemistry, Bioprocessing and Sustainability* (Berger R.G., ed.), Springer: Heidelberg, pp. 489-505.

9. Franssen M., Alessandrini L., Terraneo G. (2002) *Pure Appl. Chem.* 77: 273-277.
10. Lutz D., Huffer M., Gerlach D., Schreier P. (1992) In *Flavor Precursors: Thermal and Enzymatic Conversions*, ACS Symp. Ser. 490, (Teranishi R., Takeoka G.R., Güntert M., eds.) ACS: Washington, pp. 32-41.
11. Sarry J.-E., Gunata Z. (2004) *Food Chem.* 87: 509-521.
12. Nakamura K., Matsuda T. (2006) *Curr. Org. Chem.* 10: 1217-1246.
13. Zorn H., Peters T., Nimtz M., Berger R.G. (2005) *Proteomics* 5: 4832-4838.
14. Scheibner M., Hülsdau B., Zelena K., Nimtz M., de Boer L., Berger R.G., Zorn H. (2008) *Appl. Microbiol. Biotechnol.* 77: 1241-1250.
15. Uenojo M., Marostica Jr M.R., Pastore G.M. (2007) *Quimica Nova* 30: 616-622.
16. Vogel J.T., Tan B.-C., McCarty D.R., Klee H.J. (2008) *J. Biol. Chem.* 283: 11364-11373.
17. van den Heuvel R.H.H., Fraaije M.W., Ferrer M., Mattevi A., van Berkel W.J.H. (2000) *PNAS* 97: 9455-9460.
18. Barghini P., Di Gioia D., Fava F., Ruzzi M. (2007) *Microb. Cell Fact.* 6: 13-20
19. Swiegers J.H., Capone D.L., Pardon K.H., Eley G.M., Sefton M.A., Francis I.L., Pretorius I. S. (2007) *Yeast* 24: 561-574.
20. Cheng A.-X., Xiang C.-Y., Li J.-X., Yang C.-Q., Hu W.-L., Wang L.-J., Lou Y.-G., Chen X.-Y. (2007) *Phytochemistry* 68: 1632-1641.
21. Milella L., Lapelosa M., Greco I., Martelli G. (2006) *Acta Horticult.* 708 (Proc. Vth Intl. Strawberry Symp., 2004), pp 489-496.
22. Kaspera R., Krings U., Onken J., Berger, R.G. (2003) In *Frontiers of Flavour Science*, Proc. 10th Weurman Congress (Le Quére J.-L., Étievant P.X., eds.) Lavoisier Intercept: London, pp 397-400.
23. Kaspera R., Krings U., Pescheck M., Sell D., Schrader J., Berger R.G. (2005) *Z. Naturforsch.C*, 60c: 459-466.
24. Schwab W., Davidovich-Rikanati R., Lewinsohn E. (2008) *Plant J.* 54: 712-32.
25. Beck H. C., Hansen A. M., Lauritsen F.R. (2004) *J. Appl. Microbiol.* 96: 1185-1193.
26. Zorn H., Neuser F., Berger R.G. (2004) *J. Biotechnol.* 107: 255-263.
27. Wittmann C., Hans M., Bluemke W. (2002) *Yeast* 19: 1351-1363.
28. Etschmann M.M.W., Sell D., Schrader J. (2005) *Biotechnol. Bioeng.* 92: 624-634.
29. Krings U., Hapetta D., Berger R.G. (2008) *Appl. Microbiol. Biotechnol.* 78: 533-541.
30. Hampel D., Mosandl A., Wuest M. (2006) *J. Agric. Food Chem.* 54: 1473-1478.
31. Sevini F., Marino R., Grando M.S., Moser S., Versini G. (2004) *Acta Horticult.* 652 (Proc. 1st Intl. Symp. Grapevine Growing, Commerce and Research) 439-446.
32. El Tamer M.K., Smeets M., Holthuysen N., Lucker J., Tang A., Roozen J., Bouwmeester H.J., Voragen A.G.J. (2003) *J. Biotechnology* 106: 15-21.
33. Guterman I., Shalit M., Menda N., Piestun D., Dafny-Yelin M., Shalev G., Bar E., Davydov O., Ovadis M., Emanuel M., Wang J., Adam Z., Pichersky E., Lewinsohn E., Zamir D., Vainstein A., Weiss D. (2002) *Plant Cell* 14: 2325-2338.
34. Pechous S. W., Whitaker B. D. (2004) *Planta* 219: 84-94.
35. Sharon-Asa L., Shalit M., Frydman A., Bar E., Holland D., Or E., Lavi U., Lewinsohn E., Eyal Y. (2003) *Plant J.* 36: 664-674.
36. dos Prazeres J.N., Simiqueli A.P., Pastore G.M., Linke D., Zorn H., Nimtz M., Berger R.G. (2007) *Fresenius Environm. Bull.* 16: 1503-1508.
37. Cantone S., Hanefeld U., Basso A. (2007) *Green Chemistry* 9: 954-971.
38. Feher E., Major B., Belafi-bako K., Gubicza L. (2007) *Biochem. Soc. Trans.* 35: 1624-1627.
39. Trivedi A.H., Spiess A.C., Dausmann T., Buechs J. (2006) *Biotechnol. Prog.* 22: 454-458.
40. Mikolajek R., Spiess A.C., Pohl M., Lamare S., Buechs J. (2007) *ChemBioChem* 8: 1063-1070.
41. Chmiel H. (2007). *Pers. Commun.*
42. Bailo, E., Deckert, V. (2008). *Angew. Chemie* 120, 1682-1685.

BIOCONVERSION OF β -MYRCENE TO PERILLENE – METABOLITES, PATHWAYS, AND ENZYMES

U. KRINGS, S. Krügener, S. Rinne, and R.G. Berger

Zentrum Angewandte Chemie, Institut für Lebensmittelchemie, Gottfried Wilhelm Leibniz Universität Hannover, Callinstraße 5, D-30167 Hannover, Germany

Abstract

The conversion of β -myrcene by cells and lyophilisate of submerged cultured *Pleurotus ostreatus* is described. Based on deuterium-labelled β -myrcene and identified intermediates two different conversion pathways are proposed. The formation of α -(Z)-acaridiol is the rate limiting step of perillene formation by active cells. Thus, high yields of perillene can be achieved using *in-situ* product recovery in fed batch cultivation upon supplementation of α -(Z)-acaridiol. While active mycelium possesses an epoxidase activity, lyophilisate generates perillene along a novel dioxygenase catalysed pathway.

Introduction

One of the most challenging, but also potentially most rewarding fields of current biotechnology of flavours is the transformation of abundant terpene hydrocarbons to oxyfunctionalised terpenoid derivatives. Among microorganisms predominately fungi of the genus basidiomycetes were found to tolerate mmolar concentration of terpene hydrocarbons and to convert them to terpenoid flavours (1). Perillene (3-(4-methyl-3-pentenyl)-furan), an unusual furanoid monoterpene with a unique flowery citrus-like flavour, is an important sensory contributor to essential oils, such as rose, lavender, geranium and citrus (2). It is a minor constituent of the essential oil of Chinese basil (*Perilla frutescens*), Himalayan *Elsholtzia* species, and *Brugmansia candida* (*Solanaceae*); the natural flavour compound is commercially not available. Perillene was identified as a minor bioconversion product (up to 1 mg L⁻¹) exclusively in the culture liquid of a *Pleurotus* strain supplemented with β -myrcene (3). Work on β -myrcene metabolites, pathways derived thereof, and first results on separation and characterisation of the responsible enzymes are given.

Experimental

Fungus. *Pleurotus ostreatus* (DSMZ 1020) was obtained from the collection of the DSMZ, (Deutsche Sammlung von Mikroorganismen und Zellkulturen) Braunschweig, Germany.

Cultivation and precursor studies. Fungal cultures were grown agitated (24 °C, 150 rpm) in 200 mL of a glucose/asparagine/yeast extract medium (4, 5).

Isolation and purification of conversion products. A daily volume of 20 mL culture broth (medium and biomass) was separated from the mycelium by filtration (folded filter, 240 mm, Roth, Karlsruhe, Germany), completely transferred into a separatory funnel and extracted three times with 30 mL azeotropic pentane / Et₂O (1:1.12, v/v). The combined extracts were dried over dry sodium sulphate, concentrated (42 °C) to

a volume of 1 mL using a Vigreux column. n-Nonadecane (43.8 μg) was added as a standard. HRGC and HRGC-MS analyses were maintained as described elsewhere (5,6).

Separation of active enzyme fractions. Solubilised protein fractions of mycelium lyophilisates of *P. ostreatus* were concentrated and analysed using FPLC (Biologic Duo Flow Chromatography System, Bio-Rad). Separation was achieved either using size exclusion chromatography (Biorad Glass-Econo-Column, 240 mL, and 20 mM HEPES-Puffer (pH 5,5) with 0.1% cholic acid and 0.025% OBAS as the eluent, or hydrophobic interaction chromatography (OMEGA-Aminooctyl-Agarose, 5 mL, and 200 mM HEPES-Puffer (pH 5,5) with 5% glycerol, 0.1% cholic acid + 0.025% OBAS as the eluent.

Results and Discussion

A pathway starting from geraniol was postulated for the synthesis of perillene by the *Perilla* plant (Figure 1), but this could not be reproduced for liquid cultures of basidiomycetes (5-7). The presence of geraniol in pellet cultures of *P. ostreatus* did not yield any detectable accumulation of perillene, nor did the presence of geraniol, nerol or neral.

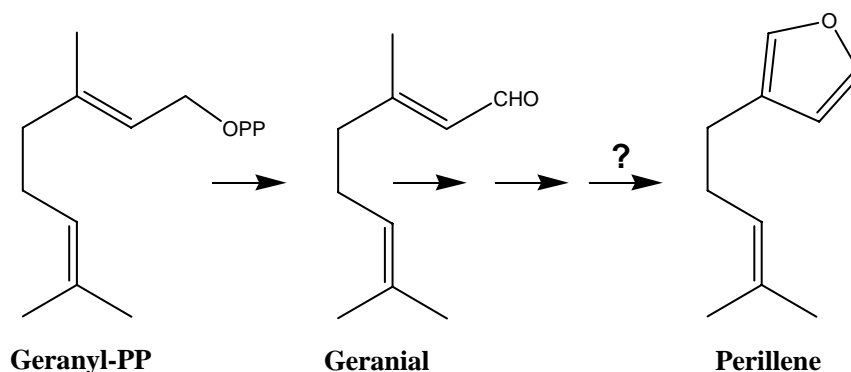


Figure 1. Hypothetical pathway of perillene formation with *Perilla frutescens* (7).

Using trideutero-labelled β -myrcene a reaction sequence starting with the enzymatic epoxidation of the 3,10-double bond of β -myrcene was found (6) (Figure 2). Reaction step 2 of Figure 2 was identified as being rate limiting. Fed-batch supplementation of α -(Z)-acaridiol to a bioreactor equipped with an adsorbent trap yielded almost quantitative conversion to perillene (80.3 mg L^{-1}) (8). However, most of the 3,10-myrcene epoxide generated on β -myrcene feeding was hydrolysed (chemically and enzyme catalysed) to the respective vicinal diol. A minor part of the epoxide was hydrolysed *via* the uncommon opening of the epoxide to the corresponding 1,4-diol, and this reaction was found to be catalysed by the L-asparagine present in the liquid culture medium.

To separate and characterise the P450 monooxygenases, which were assumed to introduce oxygen to β -myrcene to result in the respective epoxides, the mycelium of *P. ostreatus* was lyophilised, re-suspended, and the buffer submitted to size exclusion or hydrophobic interaction chromatography. Surprisingly, single fractions converting β -myrcene to perillene were found (Figure 3), which is contradictory to the mechanism of the intact cell (Figure 2), because at least one additional redox enzyme should be needed.

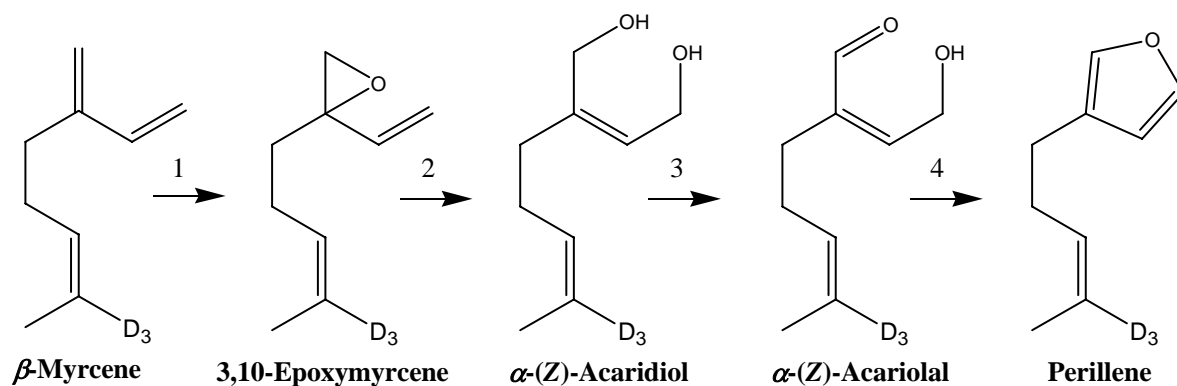


Figure 2. Confirmed perillene formation by *P. ostreatus* (6).

Besides the intracellular and membrane associated monooxygenase obviously a dioxygenase-type enzyme was made amenable through the lyophilisation step. The proposed intermediate endoperoxide of β -myrcene can be cleaved easily by a transition metal, for example $\text{Fe}^{2+/3+}$, catalysed reaction to the corresponding hydroxyl aldehyde which reacts to perillene by re-cyclisation and elimination of water (Figure 4). The fungal model system may contribute to a better understanding of plant pathways leading to furano-terpenoids (9,10). Further work will be focused on the purification, sequencing and characterisation of the dioxygenase-type enzyme.

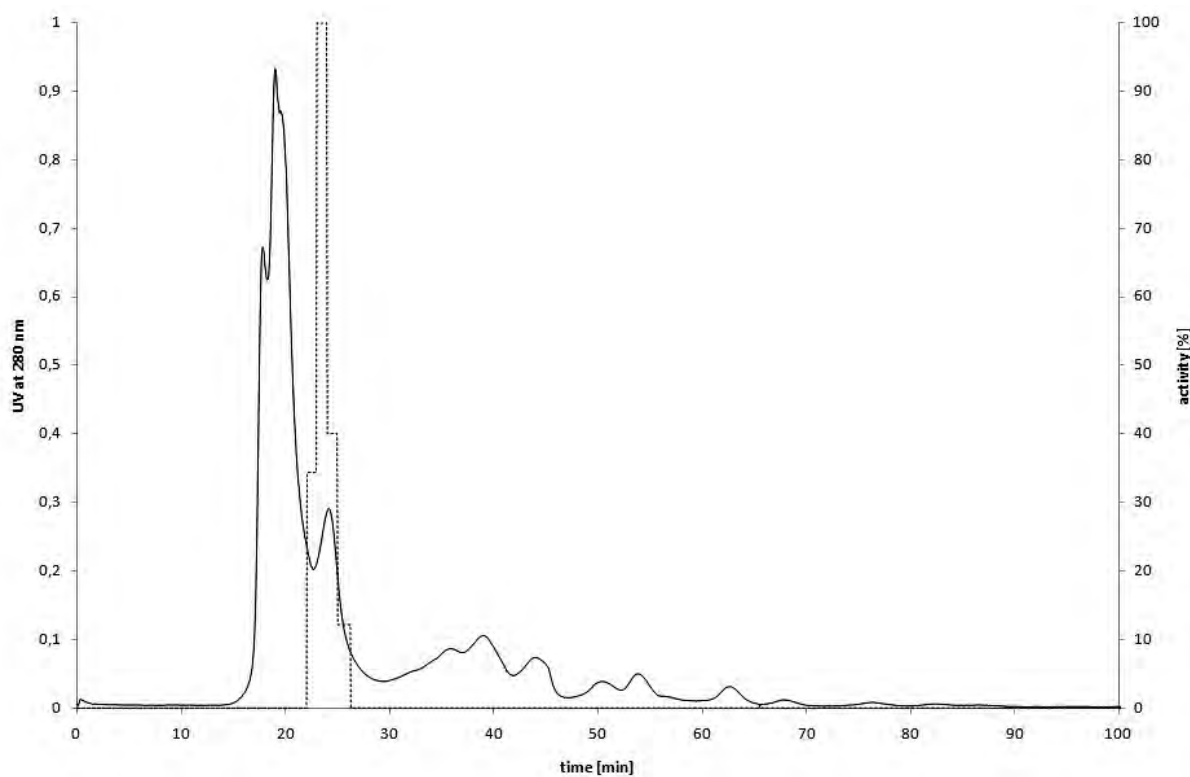


Figure 3. Gel chromatography of solubilised proteins of *P. ostreatus* lyophilisate: Total protein (-) and perillene formation (···) after β -myrcene supplementation. 100% of activity represents 18 mg L^{-1} of perillene.

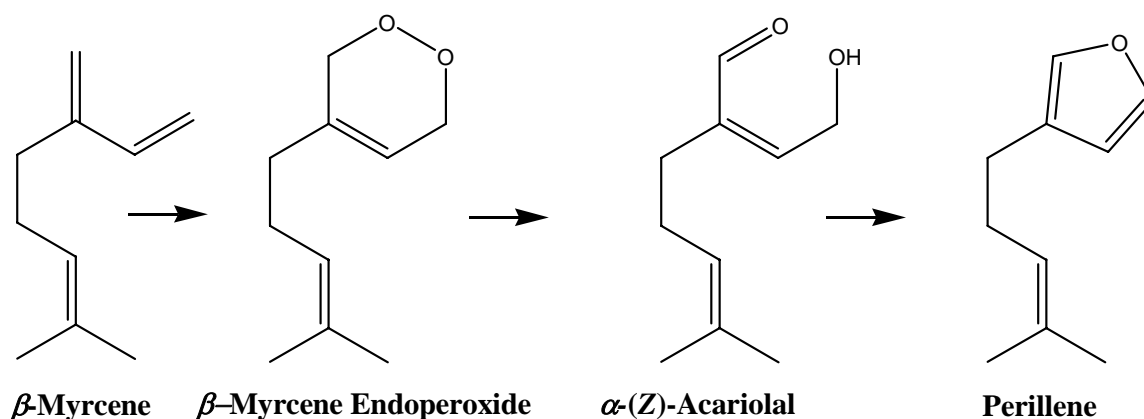


Figure 4. Postulated perillene formation with a purified enzyme fraction of *P. ostreatus*

Acknowledgement

We are grateful for a grant from the Deutsche Forschungsgemeinschaft (DFG KR 2958/1-1).

References

1. Schrader J. (2007). In *Flavour and Fragrances* (R.G. Berger, ed.) Springer-Verlag: Berlin, Heidelberg, pp 507-566.
2. Ohloff G. (1994) *Scent and Fragrances*. Springer-Verlag: Berlin, Germany.
3. Busmann D., Berger R.G. (1994) *J. Biotechnol.* 37: 39-43.
4. Onken, J., Berger R.G. (1999) *J. Biotechnol.* 69: 163-168.
5. Krings U., Hapetta D., Berger R.G. (2008) *Biocatal Biotransform.* 26: 288-295.
6. Krings U, Hapetta D., Berger, R.G. (2008) *Appl. Microbiol. Biotechnol.* 78: 533-541.
7. Yuba A., Yazaki K., Tabata M., Honda G., Croteau R. (1996) *Arch. Biochem. Biophys.* 21: 280-287.
8. Krings U., Berger R.G. (2008). *Biotechnol. Lett.* 26: 253-257.
9. Turner J.A, Herz W. (1977) *J. Org. Chem.* 42: 1900-1904.
10. Demole E., Demole C., Berthet D. (1973) *Helv. Chim. Acta* 56: 265-271.

BIOCATALYSIS BASED TRANSFORMATION OF VALENCENE INTO NOOTKATONE

M. DJURIS¹, V. Stefuca¹, M. Eghbaldar², P.v.d. Schaff²

¹ *Department of Chemical and Biochemical Engineering, Institute of Chemical and Environmental Engineering, Faculty of Chemical and Food Technology, Slovak University of Technology, Radlinského 9, SK-812 37 Bratislava, Slovakia*

² *Axxence Aromatic GmbH, Tackenweide 28, D-46446 Emmerich, Germany*

Abstract

Nootkatone (FEMA GRAS no. 3166) is a character impact flavour molecule which is vital in grapefruit flavours. In this work, the transformation of valencene into nootkatone using hydroperoxide of linoleic acid prepared by an enzyme catalysed reaction was conducted in aqueous solution at temperatures of 20, 40 and 60 °C and different pH in order to investigate their influence on the reaction course. The optimal pH value for the nootkatone formation rate at 60 °C was found to lie between pH of 6.0 and 7.0. Temperature of about 40 °C was obtained to be optimal from the point of view of the conversion to nootkatone. Maximum conversion obtained at optimum reaction conditions was 6 % and still shows an increasing trend.

Introduction

Nootkatone (FEMA GRAS no. 3166) is a character impact flavour molecule which is vital in grapefruit and other citrus flavours. Due to an increasing demand for natural flavours, several studies have been done on enzymatic or microbial conversion of natural valencene into nootkatone. Until now little attention was paid to biocatalytic transformation of valencene into nootkatone using a fatty acid hydroperoxide, although it does not require any metals. Muller et al. [1] described the preparation of a mixture of nootkatone and nootkatol by oxidation of valencene in an appropriate reaction medium in the presence of a hydroperoxide of an unsaturated fatty acid in an oxygen-containing atmosphere. It was reported [1] that the temperature may vary between 20 and 80 °C with an optimum temperature around 50 °C. The reaction could be carried out at pH between 5 and 10, and pH had influence on the chemical profile of the reaction product. The best yield of nootkatone was at pH values between 7.5 and 9.5. Lower pH values induced formation of a higher amount of nootkatol in the reaction mixture. In this work, the transformation of valencene into nootkatone as the major product, using hydroperoxides of linoleic acid (HPODs) prepared by an enzyme catalysed reaction was conducted at different temperatures and pH in order to investigate their influence on the reaction. Moreover, the influence of repeated HPODs addition to the reaction mixture on the conversion of valencene to nootkatone was investigated.

Experimental

Materials. Soybean lipoxygenase-1 (SBLOX-1) (Type I-B) (>50,000 units per mg of solids) was purchased from Sigma. Linoleic acid (>99 %), tetrasodium salt of xylenol

orange, cumene hydroperoxide, 2,6-di-*t*-butyl-4-methylphenol were purchased from Aldrich. All other chemicals were of analytical grade. Valencene (GC content 70 %), nootkatone (85 %), and γ -octalactone (99.6 %), were kindly supplied by Axxence Aromatic GmbH.

Preparation of HPODs. The HPODs were prepared by enzymatic dioxygenation of linoleic acid by SBLOX-1 in 0.1 M borate buffer, pH 10, in a jacketed glass reactor thermostated to 6 °C that was continuously intensively stirred under air.

Oxidation of valencene by HPODs. Oxidation of valencene in presence of the HPODs was investigated in a jacketed reactor under stirring and aeration. The reactions were conducted at 20, 40 and 60 °C at 50 mL of reaction mixture. The initial concentration of valencene was 31.4 mM and initial HPODs concentrations were 16.2 mM, 15.4, and 32.5 at 60, 40, and 20 °C, respectively. During reaction 0.75 ml of sample was periodically withdrawn and analysed by GC.

Measurements of the thermal stability of HPODs. HPODs concentration was measured in a 15 ml glass batch reactor with 8 ml of medium (solution of HPODs) at 6, 20, and 40 °C and 12 ml of medium at 60°C that was stirred at constant temperature. The initial HPODs concentrations were 6.32, 6.32, 6.75, and 80.2 mM at temperatures 6, 20, 40, and 60 °C, respectively.

HPOD assay. HPODs concentration was measured spectrophotometrically using the xylenol orange method [2]. Freshly diluted commercial cumene hydroperoxide was used for calibration of the xylenol orange reagent.

Analysis of reaction mixture. Samples withdrawn during valencene oxidation were extracted by diethyl ether and analyzed by gas chromatography using the Agilent Technologies 7890A GC System equipped with an Agilent Technologies HP-5 capillary column (length 30 m x 0.320 mm i.d., film thickness 0.25 μ m) and FID detector used at 300 °C.

Results

HPODs stability. Material balance of HPODs degradation was described in terms of a batch stirred tank reactor with ideal mixing:



The thermal HPODs degradation was described by first order kinetics:

$$c_{HPOD} = c_{HPOD0} \cdot e^{-k_d t} \quad (2)$$

Where c_{HPOD0} is the HPODs concentration at the beginning and k_d is first order reaction rate constant.

At 6 °C no HPODs degradation was noticed. Results of HPODs degradation at temperatures 20, 40 and 60 °C are shown in Figure 1. The first order kinetics was found to describe the HPODs degradation adequately. The dependence of obtained values of rate constants on temperature shown in Figure 2 was described in terms of the Arrhenius equation:

$$k_d = A \cdot \exp\left(-\frac{E_a}{RT}\right) \quad (3)$$

A is a pre-exponential factor and E_a is the activation energy, R is the gas constant, T is temperature. Parameters of the Arrhenius equation were obtained to be: $E_a = 98000 \pm 2200 \text{ J mol}^{-1}$, $A = 1.03 \cdot 10^{12} \text{ s}^{-1}$.

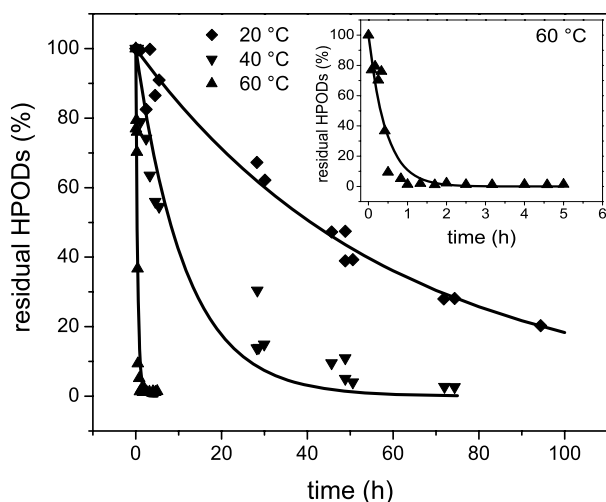


Figure 1. HPODs degradation at 20, 40, and 60 °C.

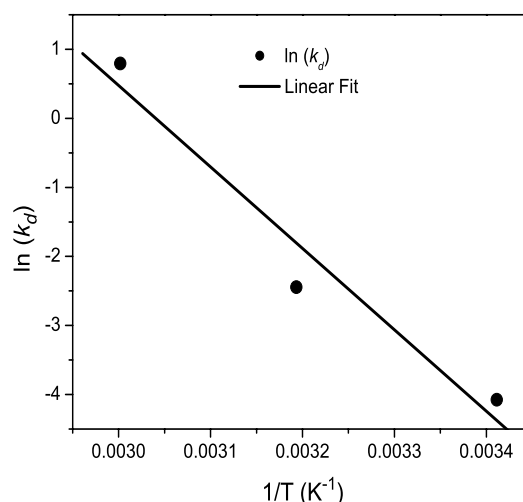


Figure 2. Temperature dependence of the first order rate constant of HPODs degradation.

Influence of pH on the rate of nootkatone production. The pH dependence of the nootkatone formation rate was evaluated from the reaction rate of nootkatone formation at the respective pH. The reaction rate of nootkatone formation was evaluated from maximum linear slope of the time-dependence of nootkatone formation at 60 °C. The pH optimum lies between 6 and 7.

Influence of repeated HPODs addition. Valencene oxidation at 60 °C under anaerobic conditions did not show nootkatone production confirming that molecular oxygen is needed, so all experiments were done at aerobic conditions. The obtained results are shown in Figures 3-5. It can be seen that parallel to the nootkatone production a nootkatone degradation occurs. For example, at 60 °C (Figure 3) the reaction of nootkatone degradation predominates the reaction of its production. Hence, additions of fresh HPODs to the reaction mixture accelerate the desired reaction rate, helping to obtain a positive nootkatone balance.

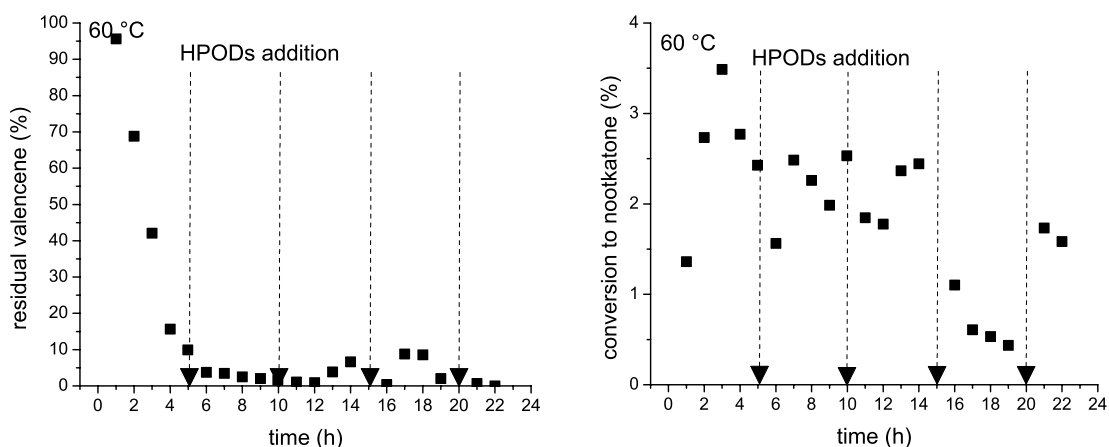


Figure 3. Valencene oxidation at 60 °C and pH 6.6. The initial valencene concentration – 31.4 mM, initial HPODs concentration - 16.2 mM. At marked times 10 ml of 16.2 mM HPODs were added.

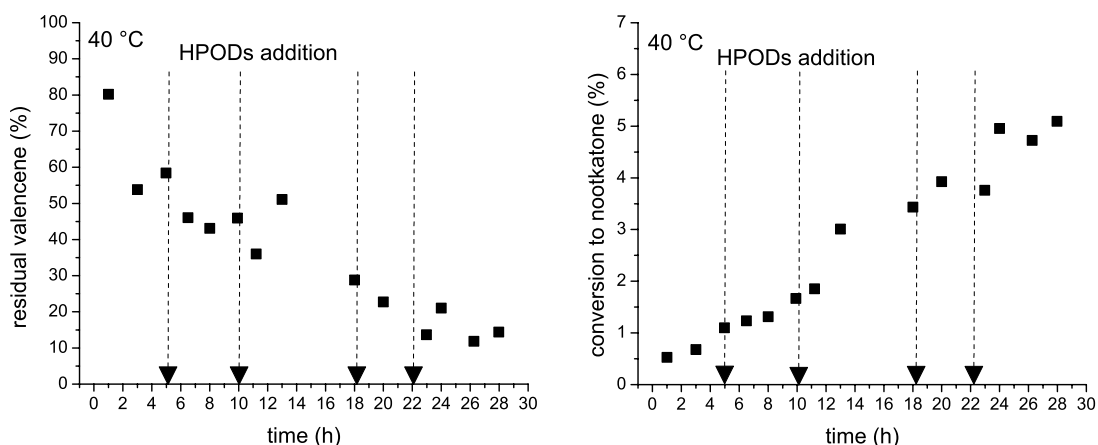


Figure 4. Valencene oxidation at 40 °C, pH= 6.6. The initial valencene concentration – 31.4 mM, initial HPODs concentration - 15.4 mM. At marked times 10 ml of 15.4 mM HPODs were added.

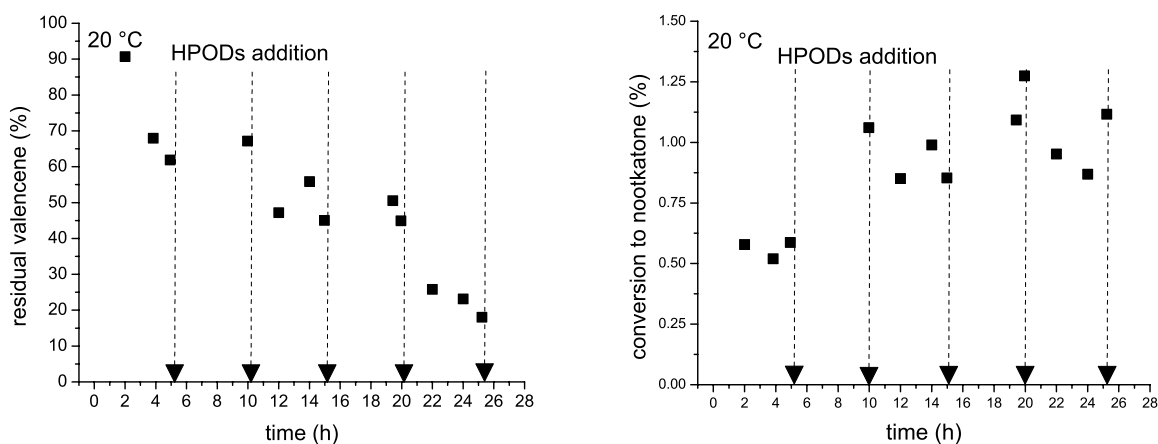


Figure 5. Valencene oxidation at 20 °C, pH= 6.6. The initial valencene concentration – 31.4 mM, initial HPODs concentration - 32.5 mM. At marked times 10 ml of 32.5 mM HPODs were added.

From the analysis of the valencene concentration during the reaction it is evident that the main part is not converted to nootkatone, while the majority of products of these degradation reactions were not detected by GC at given analysis conditions. Moreover, as it can be seen in Figures 3-5, the valencene degradation was faster at higher temperatures.

Comparing the yield of nootkatone in the first three hours at a temperature range of 20 to 60 °C, the best result was obtained at 60 °C. However, the temperature of 60 °C is not justified from the point of view of final conversion, even though the addition of fresh HPODs enables higher nootkatone production. Among the studied temperatures the best conversion is 6 % at 40 °C and still shows an increasing trend (Figure 4). Therefore the reaction at 40 °C is the best compromise between the rates of HPODs degradation, nootkatone production and valencene degradation.

References

1. Muller B., Dean C., Schmidt C., Kuhn J.-C. (1998) US Patent 5,847,226 (1998).
2. Jiang Z.-Y., Woollard A.C.S., Wolff S.P. (1991) *Lipids* 26: 853-856.

GENERATION OF NORISOPRENOID FLAVOURS FROM CAROTENOIDS BY FUNGAL PEROXIDASES

K. Zelena¹, B. Hardebusch¹, B. Hülsdau¹, R.G. Berger¹, and H. ZORN²

¹ *Leibniz Universität Hannover, Institut für Lebensmittelchemie, Callinstraße 5, D-30467 Hannover, Germany*

² *Justus-Liebig-Universität Gießen, Institut für Lebensmittelchemie und Lebensmittelbiotechnologie, Heinrich-Buff-Ring 58, D-35392 Gießen, Germany*

Abstract

Two extracellular enzymes (MsP1 and MsP2) from the culture supernatants of the basidiomycete *Marasmius scorodoni* ("garlic mushroom") are capable of carotenoid degradation. The encoding genes were cloned from genomic DNA and cDNA libraries, and databank homology searches identified MsP1 and MsP2 as members of the so-called "DyP-type" peroxidase family. Wild type enzymes and recombinant peroxidases expressed in *Saccharomyces cerevisiae* and *Escherichia coli* were employed for the release of norisoprenoids from terpenoid precursor molecules. Various carotenes, xanthophylls, and apocarotenals were subjected to the enzymatic degradation. Volatile breakdown products were characterized by GC-FID and GC-MS, while non-volatile reactions products were determined by means of HPLC-DAD and HPLC-MS. With the exception of lycopene, the respective C13 norisoprenoids proved to be the main volatile degradation products in each case.

Introduction

Numerous apocarotenoids are derived from the excentric cleavage of the polyene chains of carotenes and xanthophylls in various plant species. Many of these cleavage products (norisoprenoids) act as potent flavour compounds. As the occurrence of norisoprenoids, such as e.g. α - and β -ionone, in their producer plants is restricted to trace amounts, biotechnological processes copying natural carotenoid degradation have been envisaged. Only recently, two extracellular enzymes (MsP1 and MsP2) capable of carotenoid degradation have been purified from culture supernatants of the basidiomycete *Marasmius scorodoni* ("garlic mushroom"). The genes encoding MsP1 and MsP2 were cloned and sequenced from genomic DNA and cDNA libraries, and databank homology searches identified the enzymes as members of the so-called "DyP-type" peroxidase family (1, 2). In the present investigation, various carotenes, xanthophylls, and apocarotenals were subjected to the enzymatic degradation by wild type and recombinant MsP1 and MsP2, and volatile and non-volatile cleavage products were characterized.

Experimental

The *Marasmius scorodoni* strain (CBS 137.86) was obtained from the Dutch "Centraalbureau voor Schimmelcultures", Baarn. Production and purification of wild-type enzymes were performed as described in (2), and recombinant MsP2 was produced in cultures of *S. cerevisiae* and *E. coli* according to (3).

β -Apo-8'-carotenal was obtained from BASF (Ludwigshafen, Germany). Lycopene and zeaxanthin were donated from DSM (Delft, The Netherlands), and β -carotene and (+)- α -terpineol were purchased from Fluka (Seelze, Germany). Violaxanthin and neoxanthin were extracted from spinach, and purified by preparative HPLC (4). Lutein was released by saponification of marigold (*Tagetes erecta*) oleoresin and subsequently purified by HPLC as described previously (4). Substrate emulsions (0.01%) were prepared as described in (1). The biotransformation was performed in 15 mL sodium acetate buffer (50 mM, pH 5.0) for 60 min at 27 °C (150 rpm), and initiated by addition of enzyme preparation (12 mU) and 5 μ L of 20 mM H₂O₂ solution. For the blanks, the enzyme samples were heat inactivated (100 °C, 20 min) prior to the reaction. The degradation products were purified by SPE (Chromabond C₁₈, M & N, Düren, Germany), and identified by GC/MS by comparing their Kovats indices and mass spectra with published data. Quantification was performed by GF/FID using (+)- α -terpineol (1.42 mM) as an internal standard (1). After further purification of the extract by flash chromatography on silica 60 (60-200 mesh, Merck, Darmstadt, Germany), non-volatile breakdown products were determined by HPLC-DAD and HPLC-MS according to (5, 6).

Results

Six different carotenes and xanthophylls were subjected to the enzymatic degradation. All substrates were readily degraded within 60 min, and, with the exception of lycopene, the respective C₁₃ norisoprenoids proved to be the main volatile degradation products in each case (Fig. 1, Tab. 1).

Table 1. Volatile degradation products of carotenes and xanthophylls.

Substrate	Degradation product	Yield [mol%]	Kovats index	GC-MS [m/z]
β -Carotene	β -ionone	7.9	1911 ^a	192 (M ⁺⁺), 177 (100), 135, 107, 105
	β -ionone-5,6-epoxide	1.3	1964 ^a	208 (M ⁺⁺), 135, 124, 123 (100)
	dihydroactinidiolide	7.0	2321 ^a	180(M ⁺⁺), 137, 111 (100), 110, 109
	β -cyclocitral	1.5	1595 ^a	152 (M ⁺⁺), 137, 123, 109, 67 (100)
	2-hydroxy-2,6,6-trimethylcyclohexanone	2.5	1583 ^a	156 (M ⁺⁺), 128, 110, 95, 71 (100)
Lutein	3-hydroxy- α -ionone	11.0	1627 ^b	208 (M ⁺⁺), 147, 125, 124, 109 (100)
	3-hydroxy- β -ionone	6.3	1677 ^b	208 (M ⁺⁺), 193 (100), 175, 147, 131
	3-hydroxy- β -ionone	5.7	1677 ^b	208 (M ⁺⁺), 193 (100), 175, 147, 131
Zeaxanthin	3-hydroxy- β -cyclocitral	traces	2346 ^a	168 (M ⁺⁺), 135 (100), 121, 107, 91
Violaxanthin, neoxanthin	3-hydroxy- β -ionone-5,6-epoxide	6.9 6.8	1688 ^b	224 (M ⁺⁺), 125, 124, 123 (100), 109
	geranial	1.3	1269 ^b	152 (M ⁺⁺), 136, 121, 107, 69 (100)
Lycopene	6-methyl-5-heptene-2-one	7.2	1324 ^a	126 (M ⁺⁺), 111, 108 (100), 93, 71

^a CW 20 M, 30 m x 0.32 mm i.d., 0.25 μ m film thickness; ^b DB 5, 30 m x 0.32 mm i.d., 0.25 μ m

Expression of Multidisciplinary Flavour Science

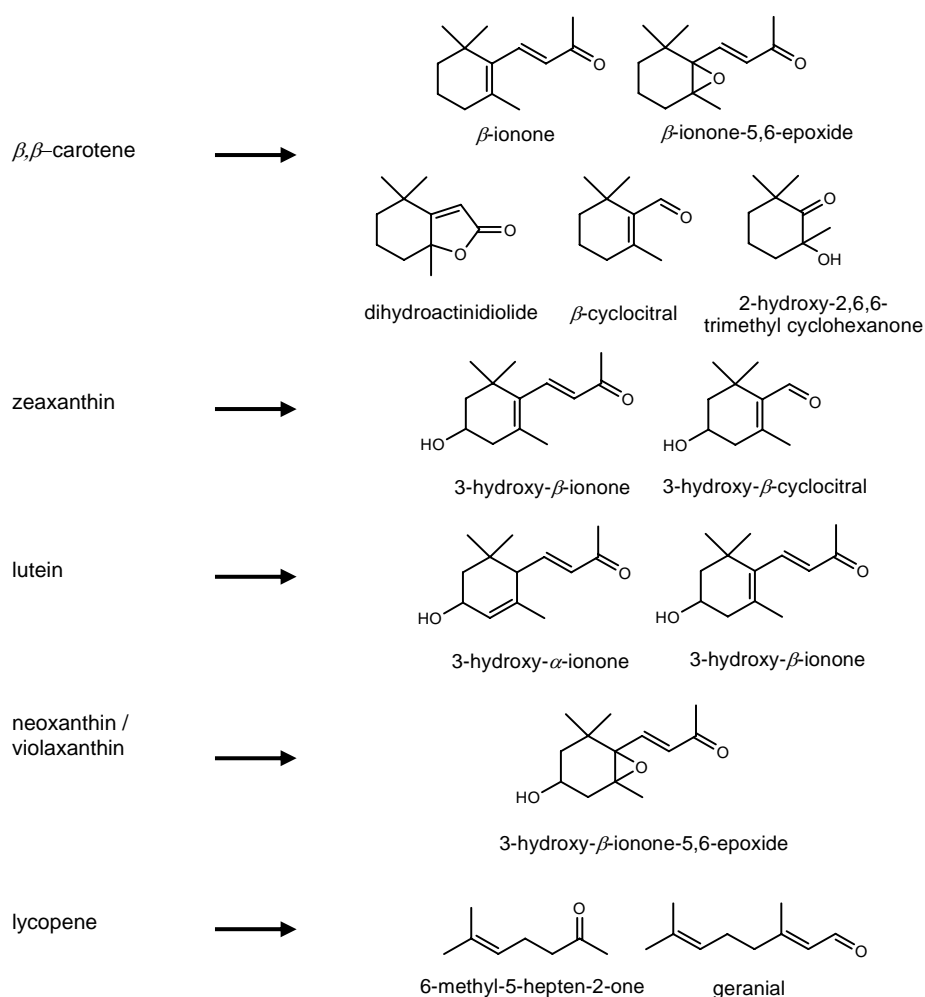


Figure 1. Norisoprenoid compounds released from carotenes and xanthophylls by MsP1 and MsP2 catalysis.

β -Apo-8'-carotenal was selected as a representative for non-tetraterpenoid carotenes. The spectrum of volatile cleavage products generated by peroxidase treatment was dominated by β -ionone, dihydroactinidiolide, and β -cyclocitral, and thus was comparable to that obtained with β -carotene as substrate. Non-volatile breakdown products of carotenes and xanthophylls were separated and tentatively identified on basis of their UV/VIS spectra and molecular masses by HPLC-DAD and HPLC-MS (Fig. 2, Tab. 2).

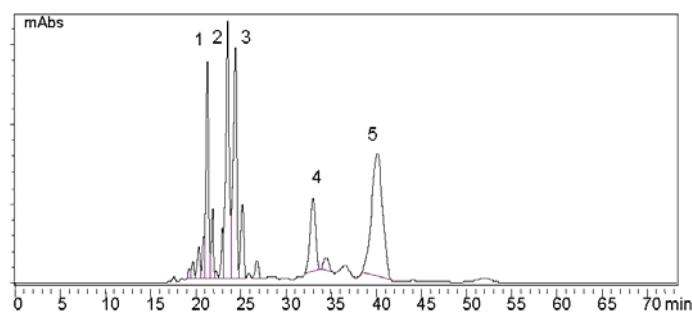


Figure 2. Enzymatic cleavage of β -carotene by extracellular enzymes of *M. scorodoni*; HPLC-MS chromatogram (1= β -apo-14'-carotenal; 2= β -apo-12'-carotenal; 3= β -apo-10'-carotenal; 4= β -carotene-monoepoxide; 5= β -carotene-5,6-epoxide).

Although the non-volatile carotenoid cleavage products listed above were detected in trace concentrations only, all of the carotenoids were readily degraded under the experimental conditions chosen. While the cleavage of zeaxanthin, lycopene, and neoxanthin amounted to about 30%, almost 60% of the β -carotene was degraded within 60 min under conditions.

Table 2. Non-volatile degradation products of carotenes and xanthophylls tentatively identified by HPLC-DAD and HPLC-MS analyses.

Substrate	Product retention time [min]	[M + H ⁺]	Tentative identification
β -Carotene	21.3	311	β -apo-14'-carotenal
	23.5	351	β -apo-12'-carotenal
	24.4	377	β -apo-10'-carotenal
	33.0	553	β -carotene-monoepoxide
	40.1	553	β carotene-5,6-epoxide
Lutein /	15.5	327	3-hydroxy-apo-14'-carotenal
	19.5	367	3-hydroxy-apo-12'-carotenal
zeaxanthin	20.8	393	3-hydroxy-apo-10'-carotenal
	23.5	433	3-hydroxy-apo-8'-carotenal
	40.9	585	lutein / zeaxanthin epoxide
Violaxanthin /	12.4	343	3-hydroxy- β -apo-14'-carotenal-5,6-epoxide
neoxanthin	16.5	383	3-hydroxy- β -apo-12'-carotenal-5,6-epoxide
	17.7	409	3-hydroxy- β -apo-10'-carotenal-5,6-epoxide

Conclusions and Outlook

The extracellular peroxidases MsP1 and MsP2 efficiently degraded carotenoids to norisoprenoid flavour compounds. The H₂O₂ required for the catalytic activity of the peroxidases may be supplemented or generated *in-situ* by addition of glucose and glucose oxidase. Apart from the production of "bioflavours", the novel enzymes could become interesting tools in detergents and food bleaching applications.

References

1. Zorn H., Langhoff S., Scheibner M., Berger R.G. (2003) *Appl. Microbiol. Biotechnol.* 62: 331-336.
2. Scheibner M., Hülsdau B., Zelena K., Nimtz M., de Boer L., Berger R.G., Zorn H. (2008) *Appl. Microbiol. Biotechnol.* 77: 1241-1250.
3. Zelena K., Zorn H., Berger R.G. (2009) *submitted for publication.*
4. Hardebusch B. (2006) Dissertation LU Hannover.
5. Mathieu S., Terrier N., Procureur J., Bigey Z. (2005) *J. Exp. Bot.* 56: 2721-2731.
6. Zorn H., Langhoff S., Scheibner M., Nimtz M., Berger R.G. (2003) *Biol. Chem.* 384: 1049-1056.

BIOTRANSFORMATIONS OF SECONDARY ALCOHOLS AND THEIR ESTERS: ENANTIOSELECTIVE ESTERIFICATION AND HYDROLYSIS

H. Strohmalm, S. Dold, K. Pendzialek, M. Weiher, and K.-H. ENGEL

Technische Universität München, Wissenschaftszentrum für Ernährung, Landnutzung und Umwelt, Lehrstuhl für Allgemeine Lebensmitteltechnologie, Am Forum 2, D-85350 Freising-Weihenstephan

Abstract

An efficient method to prepare optically pure esters of secondary alcohols via lipase-catalysed esterification is described. Starting from the racemic alcohols optically pure (*R*)-esters were obtained by esterification with enantioselective *Candida antarctica* lipase B as catalyst. The re-esterification of the remaining unreacted alcohol using lipase from *Candida cylindracea* yielded optically enriched (*S*)-esters. Purification via liquid solid chromatography led to high chemical purities of the prepared esters.

Introduction

Short-chain esters (acetates, butanoates, hexanoates and octanoates) of secondary alcohols (2-pentanol, 2-heptanol and 2-nonanol) are suitable for a differentiation of purple (*Passiflora edulis* Sims) and yellow (*Passiflora edulis* f. *flavicarpa*) passion fruits (1). Nearly optically pure (*R*)-enantiomers of these esters are characteristic volatiles of the purple variety and not detectable or present only in trace levels in the yellow fruits (2). Enzyme-catalysed kinetic resolutions, in which one enantiomer of a racemic substrate is selectively converted by the enzyme, are efficient methods to prepare optically pure substances (3). Hydrolases are among the most widely applied catalysts for this type of biotransformations. They catalyse esterifications in organic medium as well as hydrolyses under aqueous conditions.

Experimental

For the screening of enzymes and the determination of esterification rates, 200 μmol of 2-heptanol and 200 μmol of organic acid were diluted in 1 mL heptane. Hydrolyses were performed with 200 μmol of ester in 1 mL potassium phosphate buffer. The reactions were started by addition of 80 units of enzyme and carried out on a rotary shaker for 8 h at room temperature. For the monitoring of esterification rates aliquots (20 μL) taken after defined intervals were diluted in 1000 μL diethyl ether, for analysis of hydrolysis rates the aqueous aliquots were extracted with 1000 μL of a mixture of pentane and diethyl ether [1:1, v/v], dried over anhydrous sodium sulphate and analyzed by capillary gas chromatography (GC). Separations of the enantiomers of alcohols and esters were achieved on heptakis-(2,3-di-*O*-methyl-6-*tert*-butyldimethylsilyl)- β -cyclodextrin as stationary phase (40°C/2min//2°C/min) (4). Reaction rates and enantioselectivity were calculated on the basis of enantiomeric excesses (*ee*) of substrate and product according to (5).

Results

The screening of commercial lipases and esterases for the esterification of racemic 2-heptanol with butanoic acid revealed significant differences regarding reaction rate and enantioselectivity (Table 1).

Except for porcine liver esterase, the enzymes preferred the (*R*)-alcohol. Immobilised *Candida antarctica* lipase B (CALB imm.) showed the highest enantioselectivity as well as the highest conversion rate. On the other hand, the lipase from *Candida cylindracea* exhibited only slight preference for the (*R*)-alcohol.

Table 1. Screening of enzymes for kinetic resolution of racemic 2-heptanol via esterification with butanoic acid (after 8 h reaction at room temperature).

Enzymes	Supplier	Conversion (%)	ee _{alcohol} (%)	ee _{ester} (%)	E
Lipases					
<i>Candida antarctica</i> lip.B (imm.)	Sigma L-4777	46	84.9 (S)	100 (R)	>100
<i>Candida cylindracea</i>	Fluka 62316	22	2.7 (S)	9.6 (R)	1.2
Porcine pancreas	Sigma L-3126	0.3	0.3 (S)	85.3 (R)	>100
Esterases					
<i>Mucor miehei</i>	Fluka 46059	0.5	0.5 (S)	100 (R)	>100
Porcine liver	Fluka 46064	8	0.8 (R)	10.0 (S)	1.2

ee: enantiomeric excess; E: enantioselectivity, calculated according to (5)

Immobilised *Candida antarctica* lipase B (CALB imm.) was selected as biocatalyst for esterifications of racemic 2-heptanol and various short-chain organic acids in heptane and for hydrolyses of 2-heptyl esters in aqueous medium.

As shown in Figure 1, maximum esterification rates were achieved for all 2-heptyl esters after 2-4 hours. For the hydrolyses of the racemic esters, the maximum conversion rates decreased with increasing chain length of the substrates. In both organic and aqueous medium CALB imm. catalysed the selective reaction of the (*R*)-substrate.

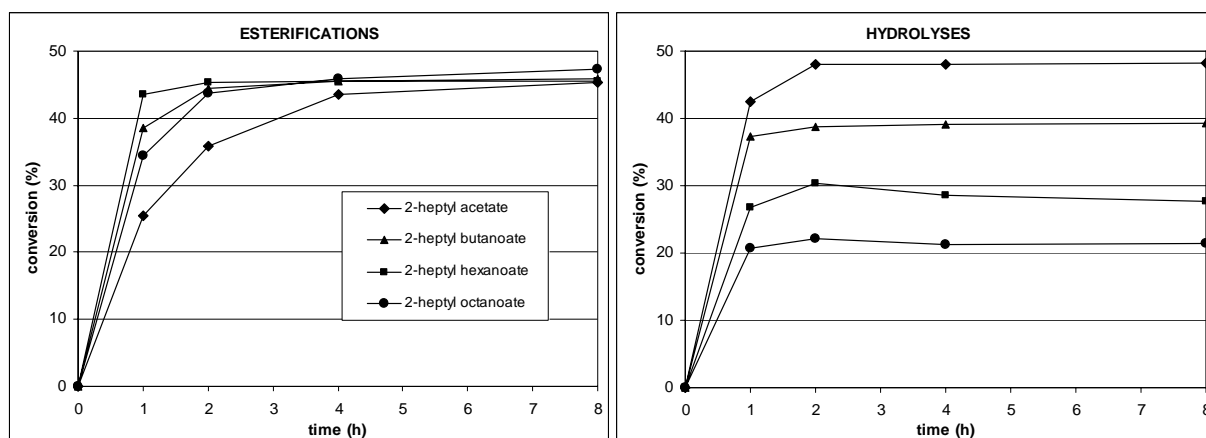


Figure 1. Reaction rates (%) determined for the CALB-catalysed synthesis and hydrolysis of 2-heptyl esters.

Figure 2 shows the capillary gas chromatographic separation of product ((*R*)-2-heptyl butanoate) and remaining substrate (2-heptanol: 92.5 % (*S*) : 7.5 % (*R*)) obtained by CALB-catalysed esterification of 2-heptanol.

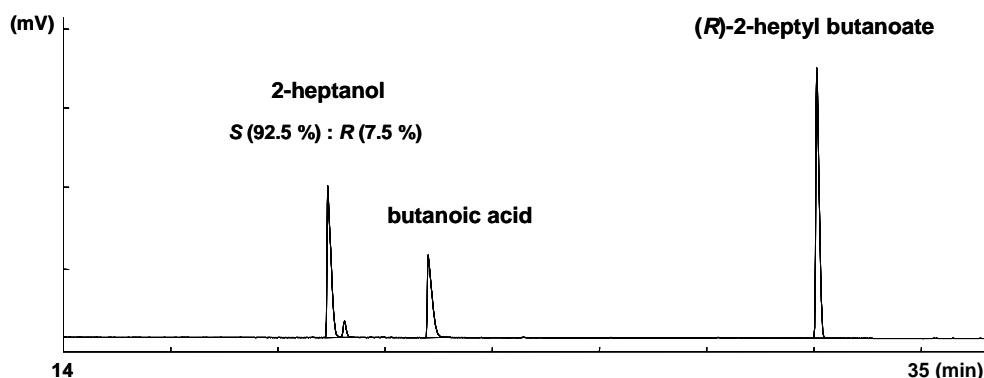


Figure 2. Enantioselective esterification of racemic 2-heptanol and butanoic acid with CALB *imm.* (8 h reaction). GC: heptakis(2,3-di-*O*-methyl-6-*tert*-butyl-dimethylsilyl)- β -cyclodextrin; 40°C/2min//2°C/min; GC-system see (2).

Figure 3 outlines the procedure developed for the preparation of optically pure (*R*)- and optically enriched (*S*)-esters of secondary alcohols.

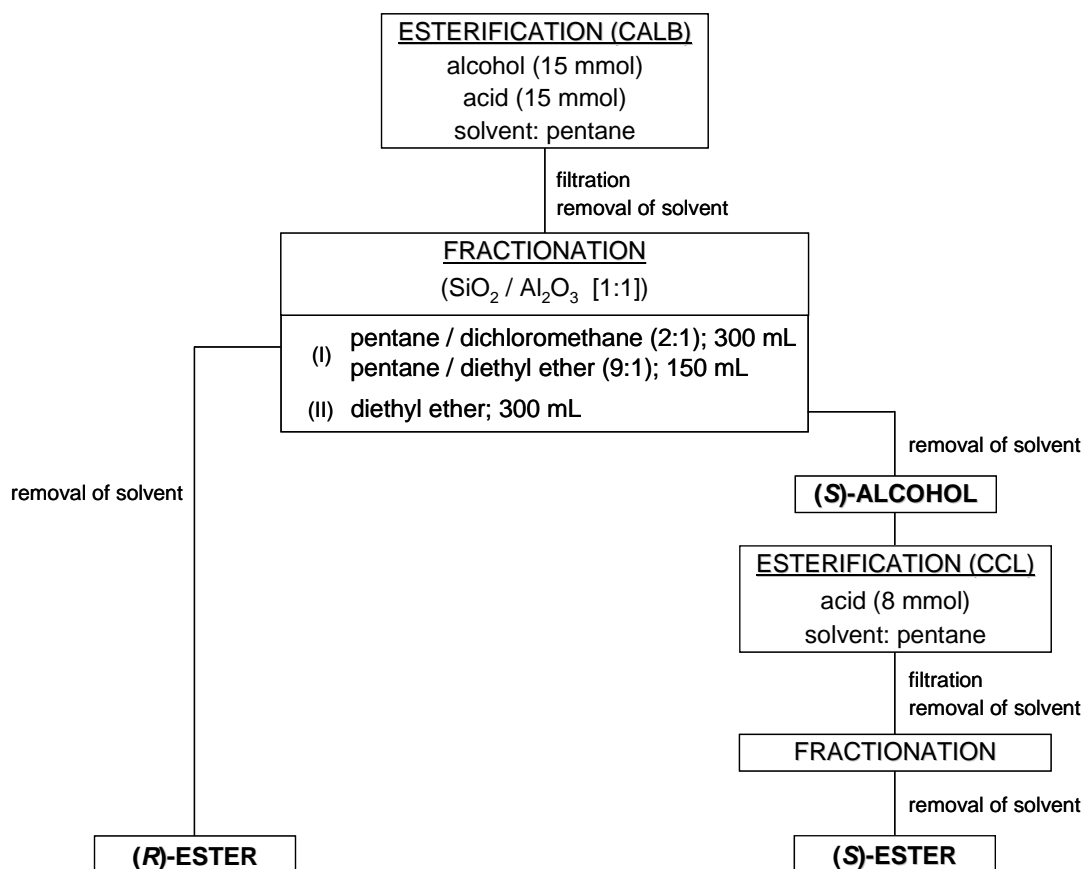


Figure 3. Preparation of optically pure / enriched esters of secondary alcohols via lipase-catalysed kinetic resolution.

After esterification of the racemic secondary alcohol using enantioselective CALB imm. as catalyst the obtained (*R*)-ester was separated from the non-esterified alcohol by fractionation using SiO₂/Al₂O₃ [1:1] as adsorbent. The remaining acid was removed by adsorption on Al₂O₃. After recovery of the unreacted alcohol and addition of an equimolar amount of acid the mixture was re-esterified with CCL. The (*S*)-ester was obtained by subsequent fractionation and removal of the solvent.

The yields, purities, enantiomeric excesses and optical rotations of the prepared 2-heptyl esters are listed in Table 2.

Table 2. Yields, purities, enantiomeric excesses (*ee*) and optical rotations [α]_D of the prepared (*R*)- and (*S*)-2-heptyl esters.

	<i>(R)</i> -Ester					<i>(S)</i> -Ester				
	Yield		Purity (GC)	Opt. purity (<i>ee</i>)	α_D	Yield		Purity (GC)	Opt. purity (<i>ee</i>)	α_D
2-Heptyl-	[g]	[mol%]	[%]	[%]	[°]	[g]	[mol%]	[%]	[%]	[°]
Acetate	0.96	40.3	99.5	> 99.9	- 6.46	0.26	11.1	99.8	85.3	+ 5.99
Butanoate	1.27	45.6	99.6	> 99.9	- 9.40	1.23	43.9	99.3	82.4	+ 7.49
Hexanoate	1.42	44.2	99.3	> 99.9	- 9.41	0.53	16.6	99.8	82.4	+ 7.76
Octanoate	1.57	43.2	99.2	> 99.9	- 8.88	1.46	40.1	99.2	82.8	+ 7.44

[α]_D determined with solutions (3g/100mL) in acetone [temperature: 23-24 °C]

Conclusions

The procedure developed for the preparation of the enantiomers of 2-alkyl esters starting from the racemic alcohols is based on the following steps:

- (i) Enantioselective esterification of the (*R*)-alcohols using *Candida antarctica* lipase B as biocatalyst.
- (ii) Separation of the product ((*R*)-alkyl ester) and the remaining substrate ((*S*)-alcohol) via liquid solid chromatography.
- (iii) Esterification of the remaining alcohol using the lipase from *Candida cylindracea*.

The described approach allows the preparation of optically pure (*R*)- and optically enriched (*S*)-esters with high chemical purities. The substances are currently being tested regarding their sensory properties.

References

1. Engel K.-H., Tressl R. (1983) *Chem. Mikrobiol. Technol. Lebensm.* 8: 33-39.
2. Strohmalm H., Dregus M., Wahl A., Engel K.-H. (2007) *J. Agric. Food Chem.* 55: 10339-10344.
3. Ghanem A., Aboul-Enein H. (2005) *Chirality* 17: 1-15.
4. Schmarr H.-G. (1992) Dissertation, Goethe Universität Frankfurt/Main, Germany.
5. Chen C.-S., Fujimoto Y., Girdaukas G., Sih C.J. (1982) *J. Am. Chem. Soc.* 104: 7294-7299.

INTEGRATED BIOPROCESS FOR THE PRODUCTION OF THE NATURAL ANTIMICROBIAL MONOTERPENE R-(+)-PERILLIC ACID WITH *P. PUTIDA*

M. Antonio Mirata and J. SCHRADER

DECHEMA e.V., Karl-Winnacker-Institut, Biochemical Engineering, P.O. Box 150104, D-60061 Frankfurt/Main, Germany

Abstract

Experiments investigating the effects of perillic acid on bioconversion activity and growth of *P. putida* showed that product inhibition limits the production of perillic acid in fed-batch bioreactor to about 65 mM. To overcome this drawback, an *in-situ* product recovery bioprocess with anion exchange resin was developed. By using an integrated fed-batch bioprocess, which was set up by coupling a bioreactor with a bypass *in-situ* recovery loop filled with anion exchange resin Amberlite IRA 410 Cl, perillic acid was extracted periodically from the broth and subsequently completely eluted from the resin with a mixture 60:40 (v/v) of ethanol and HCl 1M. This integrated bioprocess permitted to increase the final product concentration by 130 % to 150 mM after four days cultivation corresponding to a productivity of 37 mM/d.

Introduction

Perillic acid, an almost odourless monoterpenoic acid, has a strong growth-inhibitory effect on bacteria and moulds. In addition to its broad antimicrobial spectrum, perillic acid shows antiallergenic properties making the acid a promising natural alternative to conventional preservatives, such as formaldehyde derivatives, for application in the cosmetics and pharma industries (1, 2). Limonene, the natural precursor of perillic acid, is a low priced by-product of the citrus processing industry and thus an environmentally friendly and cheap starting material for perillic acid synthesis. Since the regioselective oxyfunctionalisation of a C10-hydrocarbon such as limonene is not trivial to chemistry and usually demands harmful reagents such as heavy metal catalysts, biotechnology may be an interesting alternative. The microbial transformation of limonene frequently results in a large number of different metabolic products (3). However, the solvent tolerant gram-negative bacterium *P. putida* DSM 12264 is able to oxidise (+)-limonene to (+)-perillic acid via perillyl alcohol and perillaldehyde as metabolic intermediates and high product concentrations in the g/L range can be obtained under conventional cultivation conditions (4, 5). Nevertheless, the maximum product concentration, which has been so far achieved in a fed-batch biotransformation, is limited to about 65 mM after 9 days due to growth-inhibitory effects of perillic acid (5). This work reports on the development of an *in-situ* product recovery method based on anion exchange resins in order to further raise the productivity of the biocatalytic process by reducing the impact of product inhibition.

Experimental

Chemicals. *S*-(-)-perillic acid (> 95 %), *R*-(+)-limonene (\geq 96 %), Amberlite IRA 410 Cl anion exchange resin, all reagents and solvents were purchased from Sigma-Aldrich, Germany.

Microorganism and media. *Pseudomonas putida* DSM 12264 (DSMZ, Braunschweig, Germany) was used. Terrific broth (TB) was used as complex medium for the growth inhibition assays and for the production of biomass. TB consisted of (in g/L): tryptone 12; yeast extract 24; glycerol 5; KH_2PO_4 2.3; K_2HPO_4 12.5; (pH 7). Phosphate buffer medium (0.1 M, pH 7) consisting of (in g/L) KH_2PO_4 5.2 and K_2HPO_4 10.7 and (in mM) glycerol 50 and limonene 150 was used for resting cells biotransformation assays. For all experiments investigating product inhibition effects, perillic acid concentration was adjusted in the media by adding respective aliquots of a highly concentrated alkaline perillic acid solution (403 mM, pH 10). E2 medium was used for limonene fed-batch biotransformations in the bioreactor, whose pre-cultures were prepared in LB medium (5).

Product inhibition during the bacterial growth and the biotransformation. To investigate the inhibitory effect of perillic acid on *P. putida* growth, cultivations were performed at different perillic acid concentrations between 0 and 119 mM in buffered TB medium to keep the pH at 7. The media (30 mL in 300 mL flasks) were inoculated with 5 % (v/v) of a pre-culture grown overnight in TB, and these cultures were incubated at 30°C, 240 rpm for 32 hours. For each perillic acid concentration, the maximum specific growth rate of the cultivation was determined by computer based differentiation of the growth curves using the software Origin (version 6.0, Microcal, USA) in order to estimate the perillic acid concentration above which cells do not grow by means of a linear mathematical model (6). To examine the action of perillic acid on *P. putida* limonene bioconversion, resting cell biotransformations were carried out with equal amounts of biocatalyst (1.1 g cdw/L; cdw: cell dry weight) but with increasing concentrations of perillic acid (0 mM to 30 mM). Biomass of *P. putida* was previously produced in 500 mL TB medium in 2 L Erlenmeyer flasks at 30°C, 240 rpm for 24 hours. The specific activity, which is expressed as Units (1U = 1 μmol perillic acid/min) per gram cdw, was determined by differentiation of the product formation kinetics (Origin, version 6.0, Microcal, USA).

Fed-batch biotransformation. The fed-batch biotransformation experiments with and without *in-situ* product recovery were carried out in 0.16 L culture volume with a FedBatchPro parallel fermentation system (DASGIP, Juelich, Germany), at 30°C. The dissolved oxygen concentration was kept above 60% saturation by adjustment of the stirring speed from 1000 rpm to maximum 2000 rpm. Air was supplied at a constant rate of 10 L/h to the reactor. The pH was maintained at 7.0 with 4 M NaOH. The culture was inoculated with 6% LB preculture ($\text{OD}_{600\text{nm}} = 7$), previously prepared by overnight cultivation in 100 mL Erlenmeyer flasks at 30°C and 240 rpm, in 0.15 L E2 medium containing 100 mM of glycerol, 150 mM of ammonium and 4% (240 mM) of limonene. Glycerol was fed to the culture at an average rate of 16 mM/h between day 0.5 and day 6, and each 24 hours 75 mM pure limonene was added to the culture. To prevent limitations of other nutrients, 1 mL/L trace elements, 1 mL/L 1 M magnesium sulphate and 70 mM ammonium were daily added to the culture between day 2 and day 5.

***In-situ* recovery of perillic acid in external loop and product purification.** *In-situ* recovery of perillic acid was performed by periodical recirculation of the culture at a flow rate of 3.6 L/h through a fluidized bed of anion exchange resin situated in an

external loop for 30 minutes per cycle when the perillic acid concentration approached 30 mM. A modified glass-chromatography column was used as fluidized bed column (15 mm inner diameter, length 220 mm, total volume 38 mL; purchased by Omnifit, Cambridge, England). The column was coupled between the bioreactor and the peristaltic pump (Ismatec, Glattburg, Switzerland) with Pharmed BPT tube (2.5 mm OD, 2.4 mm ID; Saint-Gobain, Vernet, France) and through the pump with Teflon tubing (4.3 mm OD, 2.9 mm ID; Hamilton, Bonaduz, Switzerland). The broth volume in the external recovery loop represented approximately 10% of the whole culture volume. The fluidized bed contained 20 g Amberlite IRA 410 Cl anion exchange resin. The bed of Amberlite IRA 410 Cl was aseptically changed with new resin (20 g) after the second and the third day from the start of the biotransformation. Each batch of resin loaded with perillic acid was successively eluted with 200 mL 1M HCl/ethanol (40:60 v/v) for 3.5 hours in a 500 mL shaking flask. To determine the additive perillic acid concentration during the integrated bioprocess, the quantification of the perillic acid content in the elution mixtures was performed by HPLC and was related to the reactor volume. This calculated concentration was added to the concentration of perillic acid found in the broth at the time when the recovery was performed. Afterwards, all elution mixtures containing perillic acid were collected and were filtered through a round filter paper (3 mm, diameter 15 cm; Whatman, England). The ethanol was evaporated in a rotary evaporator (55°C, 200 mbar) until appearance of white crystals in the aqueous 1M HCl solution. After vacuum filtration, the crystals of perillic acid were dried for 12 hours in a freeze dryer.

Analysis of perillic acid. For quantification of perillic acid, 1 mL of culture broth or 1 mL of elution agent was centrifuged at 14,500 g for 12 min and 10 μ L supernatant was analyzed by HPLC (Shimadzu) comprising LC 10AT pump, M10A diode array detector (at 220 nm), and Lichrospher RP8 5 μ 125 x 4 column (Phenomenex). The mobile phase was methanol / water 70:30 (v/v) containing 0.5 % 3M phosphoric acid, at 1 mL/min and 40 °C. Commercially available S(-)-perillic acid was used as external standards.

Results

Inhibitory effects of perillic acid on P. putida. Systematic investigations of the negative effect of increasing concentrations of perillic acid indicated that both growth and limonene biotransformation are inhibited by perillic acid. The maximum growth rate of non-transforming *P. putida* decreased linearly to complete inhibition at 165 mM perillic acid, while biotransformation of limonene with resting cells showed an exponential decrease of maximum specific activity from almost 8 U/g cdw without perillic acid to < 0.5 U/g cdw at > 25 mM perillic acid.

Fed-batch biotransformation. A fed-batch process was established to optimize the growth-associated production of perillic acid. A product concentration of 65 mM perillic acid was obtained with growing *P. putida* cells after 6 days (Figure 1) and with a maximum productivity of 27 mM/d during the first two days of cultivation. Product formation was not limited by glycerol, ammonium or limonene concentrations but by product inhibition at higher product concentrations.

Ion exchange-based in-situ product recovery fed-batch bioprocess. In order to avoid product inhibition during the limonene biotransformation and to enhance the production of perillic acid, an ion exchange-based *in-situ* product recovery fed-batch bioprocess was developed. Due to the dissociation behaviour of perillic acid (> 99 % dissociated form at pH 7) complete adsorption on anion exchange resins was

observed in preliminary experiments. The anion exchange resin did not influence cell integrity, composition of cultivation media or biotransformation pH (data not shown). By using an integrated fed-batch bioprocess, which was set up by coupling a bioreactor with a by-pass *in-situ* recovery loop containing a column filled with anion exchange resin Amberlite IRA 410 Cl (Figure 2), perillic acid was extracted periodically from the broth and subsequently completely eluted from the resin with a mixture 60:40 of ethanol and 1M HCl.

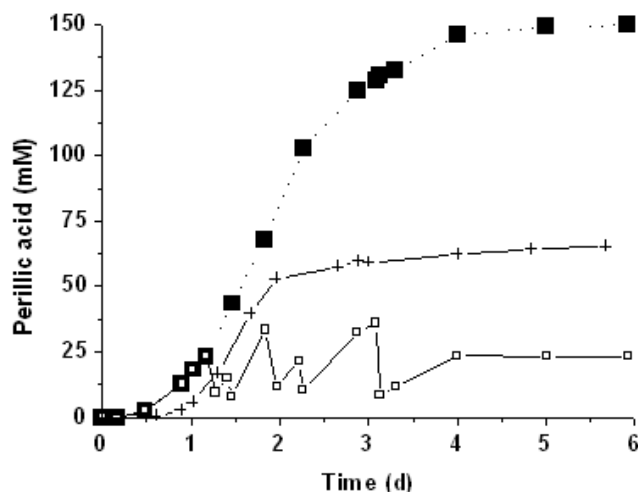


Figure 1. Comparison of perillic acid production kinetics with and without *in-situ* product removal. Perillic acid concentrations in the reactor during a conventional fed-batch biotransformation (+) and during an ISPR fed-batch biotransformation (□) as well as the resulting additive perillic acid concentration of the ISPR fed-batch biotransformation (■) are given.

Coupling a limonene fed-batch biotransformation process with an ion exchange-based *in-situ* product removal permitted to get a final additive perillic acid concentration of 150 mM after four days cultivation corresponding to a maximum productivity of 37 mM/d. Figure 1 shows the perillic acid concentration in the broth and the additive perillic acid concentration for the integrated bioprocess.

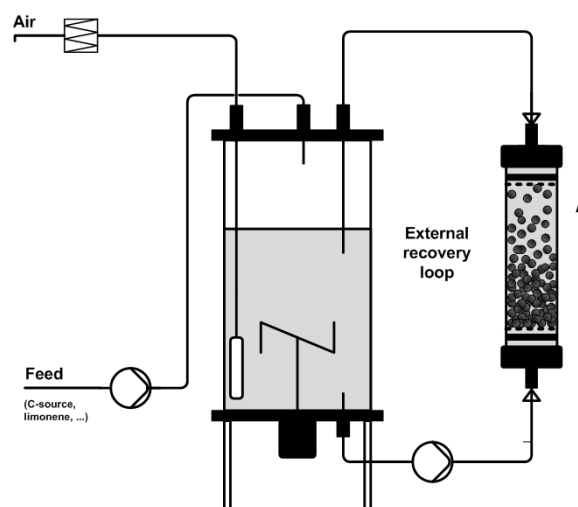


Figure 2. Scheme of the anion exchange-based *in-situ* product recovery fed-batch bioreactor for the production of perillic acid with *P. putida* DSM 12264.

Downstream processing based on an ethanolic distillation delivered a product with a purity of $\geq 92\%$ and with only negligible loss of $\leq 3\%$. Using an integrated fed-batch bioprocess, it was possible to overcome product inhibition derived limitations of the limonene biotransformation. A periodical extraction of perillic acid by an external recovery loop with anion exchange resin led to a 2.3-fold increase in overall final perillic acid concentration and a 1.4-fold increase in productivity compared to the conventional fed-batch bioprocess previously described (4, 5). To the authors' knowledge, the results reported in this work correspond to the highest final product concentration and productivity achieved by microbial monoterpene oxyfunctionalisation up to now.

References

1. Rieks A., Kähler M., Kirchner U., Wiggernhorn K., Kinzer M., Risch S. (2004) WO 2004076400.
2. Erdmann S.M., Merk H.F. (2003) *Hautarzt*, 54: 331-337.
3. Schrader J. (2007) In *Flavours and Fragrances* (Berger R.G., ed.); Springer, chapter 23, pp 507-574.
4. Speelmanns G., Bijlsma A., Eggink G. (1998) *Appl. Microbiol. Biotechnol.* 50: 538-544.
5. Mars A.E., Gorissen J.P.L., van den Beld I., Eggink G. (2001) *Appl. Microbiol. Biotechnol.* 56: 101-107.
6. Luong J.H.T. (1985) *Biotechnol. Bioeng.* 27:280-285.

LINALOOL BIOTRANSFORMATION WITH FUNGI

M.A. Mirata¹, M. Wüst², A. Mosandl³, und J. SCHRADER¹

¹ DEHEMA e.V., Karl-Winnacker-Institut, Biochemical Engineering, P.O. Box 150104; D-60061 Frankfurt/Main, Germany

² University of Applied Sciences Western Switzerland, Institut Life Technologies, Route du Rawyl 64, CH-1950 Sion 2, Switzerland

³ Institut für Lebensmittelchemie, Johann Wolfgang Goethe-Universität, Marie-Curie-Strasse 9, D-60439 Frankfurt/Main, Germany

Abstract

Different fungal strains were screened for their ability to convert linalool into valuable flavour compounds. *Aspergillus niger* DSM 821, *Botrytis cinerea* 5901/02 and *Botrytis cinerea* 02/FBII/2.1 produced isomers of lilac aldehyde and lilac alcohol via 8-hydroxylinalool as postulated intermediate. Linalool oxides and 8-hydroxylinalool accumulated as major products during fungal linalool biotransformations. Furanoid *trans*-(2*R*, 5*S*) and *cis*-(2*S*, 5*R*) linalool oxide as well as pyranoid *trans*-(2*R*, 5*S*) and *cis*-(2*S*, 5*S*) were identified as main stereoisomers, formed by epoxidation of (±)-linalool via the postulated key intermediates (3*S*, 6*S*)-6,7-epoxylinalool and (3*R*, 6*S*)-6,7-epoxylinalool. *Corynespora cassiicola* DSM 62475 was shown for the first time to stereospecifically produce 357 mg/L linalool oxides from linalool in just three days, corresponding to a productivity of 120 mg/L*d and a molar conversion yield close to 100 %.

Introduction

Lilac aldehyde and lilac alcohol have been described as characteristic minor components of *Syringa vulgaris* L. flowers. Recently biogenetic studies with stable isotope labelled precursors have shown that *S. vulgaris* L. converts linalool into lilac aldehydes and lilac alcohols (1, 2). Due to the evidence of a plant biosynthetic pathway we hypothesized that there are also other biological systems capable of transforming linalool into the desired lilac aroma compounds. Microorganisms, especially fungi, have been shown to be very versatile biocatalysts for the production of a wide range of flavour and fragrance compounds from cheap natural precursors such as terpenoids (3). Therefore, this work aimed at screening different fungi for their capacity to transform linalool to valuable products such as the aforementioned lilac compounds or linalool oxides. This included also the analysis of the stereoisomeric distribution of furanoid and pyranoid linalool oxides.

Experimental

The experimental details described in detail in (4). In the following the main procedures will be summarised.

Microorganisms, culture media, chemicals. *Botrytis cinerea* 5901/2, 5909/1, 92/lic/1, 97/4, 99/16/3, 00/II10.1, 02/FB II/2.1, and P10 (BLWG, Veitshöchheim, Germany); *Aspergillus niger* ATCC 16404, DSM 821, *Corynespora cassiicola* DSM

62475, *Penicillium digitatum* DSM 62840, *P. italicum* DSM 62846 (DSMZ, Braunschweig, Germany); *Geotrichum candidum* (HEVs, Sion, Switzerland); *P. digitatum* NRRL 1202 (ARS culture collection, Illinois, USA). *Saccharomyces cerevisiae* Ceppo 20, Zymaflor VL1, Uvaferm 228, SIHA Riesling n° 7 (E. Begerow GmbH & Co., Langenlonsheim, Germany). The strains were grown on malt extract agar (MEA) and biotransformation experiments were performed in malt yeast broth (MYB). (\pm)-Linalool (> 97 % (v/v)), (-)-linalool (> 98.5 % (v/v)), 1-octanol (> 99.5 % (v/v)), cis- and trans-furanoid linalool oxide (> 97 % (v/v), mixture of isomers) and tert-butyl methyl ether (MTBE) (> 99.8 % (v/v)) were purchased from Fluka, Germany. Lilac alcohol and lilac aldehyde stereoisomers, 8-hydroxylinalool and standards of cis- and trans-furanoid and pyranoid linalool oxide isomers were synthesized as described in (4).

Biotransformations. Screening experiments and linalool toxicity assays were performed in 40 mL SPME vials filled with 15 mL MYB. Linalool biotransformations with the selected strains using a feed strategy were carried out for 12 d in 2L Erlenmeyer flasks filled with 500 mL MYB. After the cultivation period, the cultures were analyzed by SPME as well as by organic phase extraction to characterize the linalool bioconversion products and to quantify 8-hydroxylinalool and linalool oxides, the stereoisomeric distribution of which was also established. To test the potential of a non-biological formation of the target compounds a blank experiment was performed in 100 mL MYB medium. The cultivation conditions, the amount of substrate used and the feed strategy have been described in (4).

Analytical methods. For identification of linalool bioconversion products 15 mL liquid culture was analyzed by GC/MS using a SPME headspace extraction (4). Lilac aldehydes and alcohols were identified by comparing their mass spectra and retention indices with those of the references. Other compounds were identified by NIST mass spectral library V 2.0. The concentrations of linalool, cis- and trans-furanoid linalool oxide, cis- and trans-pyranoid linalool oxide and 8-hydroxylinalool in the liquid cultures were determined using 1-octanol as internal standard. The stereoisomeric distribution of linalool oxides was determined by enantioselective GC. The dry biomass was determined with an infrared moisture analyzer (Sartorius, Germany). Glucose was analyzed enzymatically (Yellow Spring Instrument, USA).

Results

Detection of characteristic mass spectrum fragments of lilac aldehyde and lilac alcohol. Nineteen fungal strains were screened for their ability to convert (\pm)-linalool into lilac aldehyde and lilac alcohol isomers. The fungal strains were cultivated on a 15 ml scale 14 days in linalool-supplemented (30 mg/L) malt yeast broth. The culture headspace SPME-GC/MS was the analytical method used to detect the three characteristic fragments m/z 111, 153 (lilac aldehyde) and 155 (lilac alcohol) within the time window of the chemically synthesized references compounds. The positive strains were *A. niger* ATCC 16404 and DSM 821, *B. cinerea* 5901/2 and 02/FBII/2.1, *S. cerevisiae* Zymaflor VL1 and Uvaferm 228, and *C. cassiicola* DSM 62475.

Determination of linalool toxicity. The positive strains were cultivated with twelve increasing linalool concentrations (0 mg/L to 1000 mg/L). In order to acquire the maximum non-growth-inhibiting concentration of linalool in the culture media, toxicity curves were determined. All strains tested tolerated linalool in the range of 50 g/L to 200 mg/L. In the case of *B. cinerea* 5901/2 a linalool concentration of 150 mg/L was identified as the maximum value at which growth was still unhampered (4).

Biotransformation of linalool and identification of lilac aldehyde and lilac alcohol isomers. In subsequent experiments the selected strains were grown on 500 mL scale with sequential feeding of linalool and glucose to avoid toxic effects by the substrate and to enhance product formation. SPME GC/MS analysis and comparison with a non-biological blank experiment confirmed that *B. cinerea* 5901/2, *B. cinerea* 02/FBII/2.1 and *A. niger* DSM 821 are clearly positive strains to produce detectable amounts of lilac aldehyde and lilac alcohol isomers, as shown in Figure 1 with the GC/MS analysis of *B. cinerea* 5901/2.

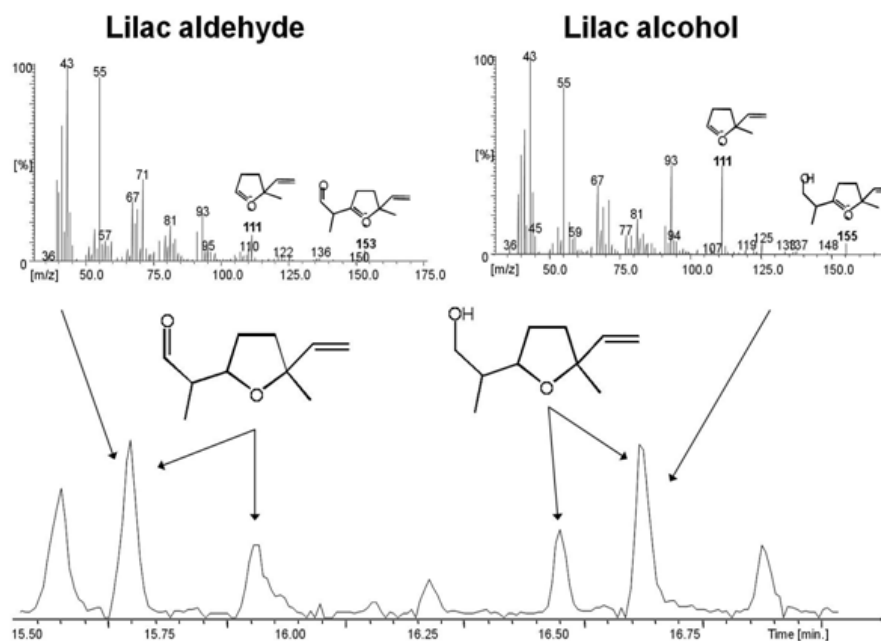


Figure 1. Fragment ion chromatogram (m/z 111) showing two lilac aldehyde and two lilac alcohol isomers produced by *B. cinerea* 5901/2. Exemplary mass spectra of lilac alcohol and lilac aldehyde are given. (Adapted with permission from *J. Agric. Food Chem.* 2008, 56, 3287-96. Copyright 2008 ACS).

Quantification of the major biotransformation products. Linalool oxide diastereoisomers and 8-hydroxylinalool turned out to be the major linalool biotransformation products of the aforementioned cultivation experiments. These compounds were quantified after fed-batch cultivation of *A. niger* ATCC 16404 and DSM 821, *B. cinerea* 5901/2 and 02/FBII/2.1, and *C. cassiicola* DSM 62475 to determine the molar conversion yield for the major products. *Aspergillus niger* DSM 821 (Fig. 2) converted almost 80 % of the substrate (323 mg/L) into a mixture of 252 mg/L of linalool oxides principally and 8-hydroxylinalool (37 mg/L) after 6 days of cultivation, while biotransformation of *A. niger* ATCC 16404 was less pronounced. *B. cinerea* 5901/2 converted 60 % of the given linalool (285 mg/L) into 167 mg/L 8-hydroxylinalool after 9 days cultivation (Fig. 2). However, *B. cinerea* 02/FBII/2.1 produced 116 mg/L of a mixture of linalool oxides and 8-hydroxylinalool with a conversion yield of 50 % from 230 mg/L linalool. With a conversion yield >96 % after only 3 days, corresponding to 357 mg/L of linalool oxides, *C. cassiicola* DSM 62475 (Fig. 2) turned out to be the most actively transforming strain. In contrast to *B. cinerea* 02/FBII/2.1 and *A. niger* ATCC 16404, this improved productivity can be explained by a faster growth of *C. cassiicola* DSM 62475, thereby leading to an enhanced biomass formation.

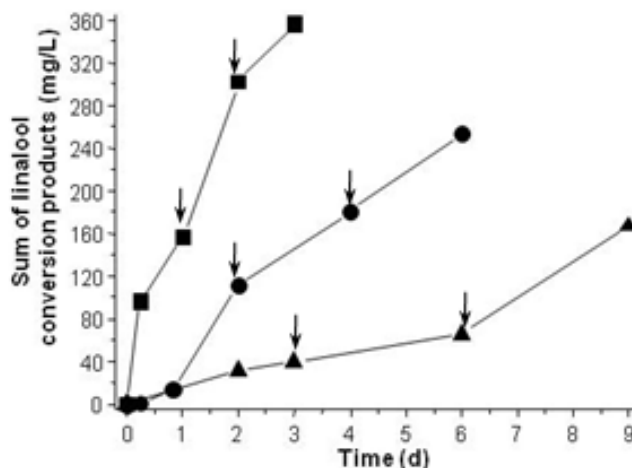


Figure 2. Product formation kinetics of linalool conversion by *A. niger* DSM 821 (●), *B. cinerea* 5901/2 (▲) and *C. cassiicola* DSM 62475 (■) with sequential feeding of linalool and glucose as indicated by the arrows (4). (Reproduced with permission from *J. Agric. Food Chem.* 2008, 56, 3287-96. Copyright 2008 ACS)

Stereoisomeric distribution of furanoid and pyranoid linalool oxides. The enantiomeric and diastereoisomeric distribution of linalool oxides produced by *A. niger* DSM 821, *B. cinerea* 02/FBII/2.1, and *C. cassiicola* DSM 62475 was analyzed by enantioselective GC (4). (Figure 3) shows that the stereoselective conversion of (R/S)-linalool by *A. niger* DSM 821, *B. cinerea* 02/FBII/2.1, and *C. cassiicola* DSM 62475 led to 5R-configured furanoid linalool oxides and 5S-configured pyranoid linalool oxides, both via 6S-configured epoxy linalool as the postulated intermediates, as previously described by Demyttenaere and Willemen (1998) (5).

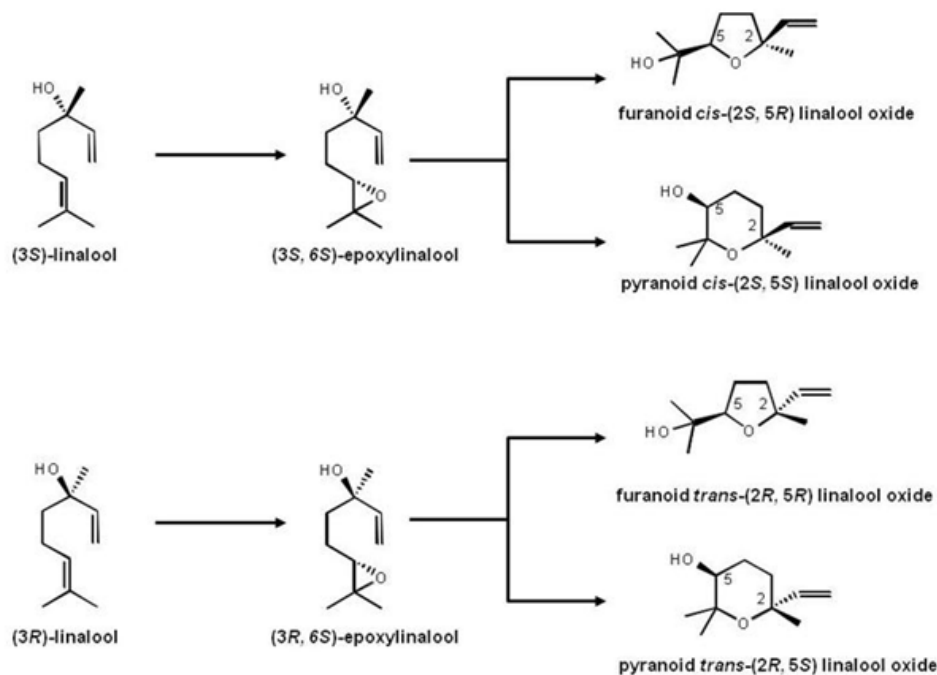


Figure 3. Stereoisomeric distribution of furanoid and pyranoid linalool oxide from conversion of (R/S)-linalool by fungi. (Adapted with permission from *J. Agric. Food Chem.* 2008, 56, 3287-96. Copyright 2008 ACS)

The production of lilac compounds from (\pm)-linalool by fungal-biotransformation, via 8-hydroxylinalool as postulated intermediate, as been demonstrated for the first time. Furthermore, the 6*S*-configured epoxy-linalool enantiomers are the postulated key intermediates for fungal production of linalool oxides. *C. cassiicola* DSM 62485 was identified as novel and highly efficient biocatalyst producing linalool oxides. Figure 4 summarises the linalool conversion pathways by fungi.

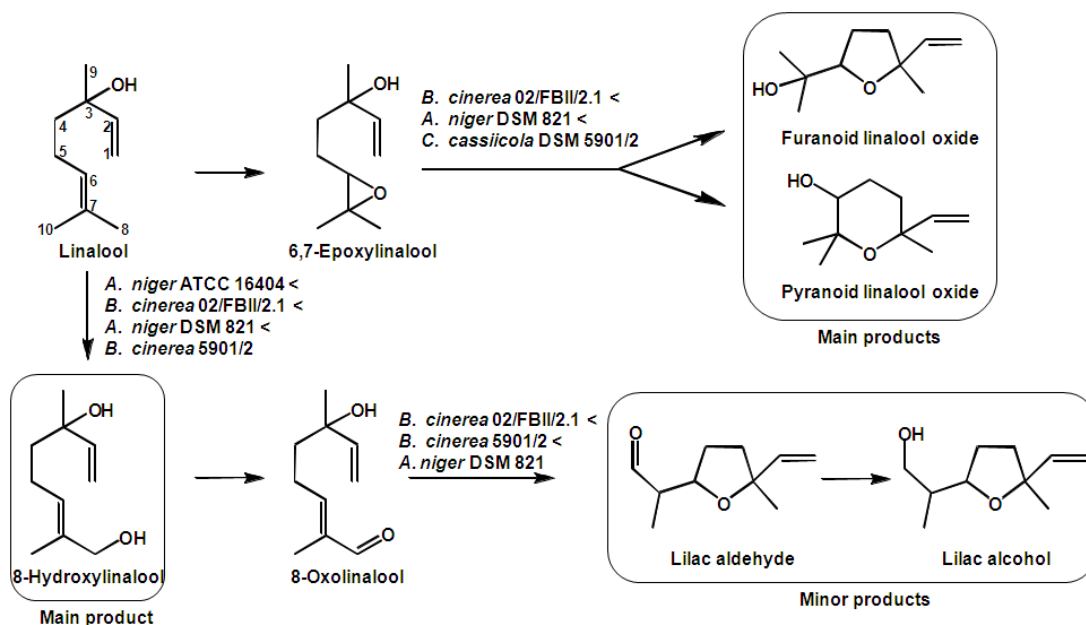


Figure 4. Postulated conversion of linalool to main and minor products by fungi ordered in ascending catalytic activity (4). (Reproduced with permission from *J. Agric. Food Chem.* 2008, 56, 3287-96. Copyright 2008 ACS)

References

1. Kreck M., Mosandl A. (2003) *J. Agric. Food Chem.* 51: 2722-2726.
2. Kreck M., Püschel S., Wüst M., Mosandl A. (2003) *J. Agric. Food Chem.* 51: 463-469.
3. Schrader J.; Berger R.G. (2001) In *Biotechnology* (Rehm H.-J., Reed G., eds.); Wiley-VCH, pp 377-383.
4. Mirata M.-A., Wüst M., Mosandl A., Schrader J. (2008) *J. Agric. Food Chem.* 56: 3287-3296.
5. Demyttenaere J.C.R., Willemen H.M. (1998) *Phytochem.* 47: 1029-1036.

PRODUCTION OF METHIONOL AND 3-(METHYLTHIO)-PROPYLACETATE WITH YEASTS

M.M.W. Etschmann¹, P. Koetter², W. Bluemke³, K.-D. Entian², and J. SCHRADER¹

¹ *DECHEMA e.V., Karl-Winnacker-Institut, Biochemical Engineering, Theodor-Heuss-Allee 25, 60486 Frankfurt/Main, Germany*

² *Institut of Molecular Biosciences, Frankfurt University, Max-von-Laue-Str. 9, 60438 Frankfurt/Main, Germany*

³ *Evonik Degussa GmbH, Rodenbacher Chaussee 4, 63457 Hanau-Wolfgang, Germany*

Abstract

The Ehrlich pathway, prevalent in yeast metabolism, converts amino acids to the corresponding higher alcohols which may be further transesterified to their acetate esters. High product concentrations can be achieved if the amino acid is the sole nitrogen source and present at high concentrations. The main conversion products of L-methionine are 3-(methylthio)-1-propanol (methionol) and 3-(methylthio)-propylacetate (3-MTPA), which both smell broth-like and reminiscent of meat and potatoes. Up to now there is no report about an industrially applied process for the production of natural methionol and 3-MTPA. Overexpression of the ATF1 gene under the control of a TDH3 promoter together with an optimization of the glucose feeding regime lead to product concentrations of 2.2 g L⁻¹ 3-MTPA plus 2.5 g L⁻¹ methionol. These are the highest concentrations reported up to now for the synthesis of these valuable aroma compounds.

Introduction

The aroma compounds 3-(methylthio)-1-propanol (methionol) and 3-(methylthio)-propylacetate (3-MTPA) both have a powerful odour reminiscent of soup, meat, onions and potatoes and are derived from the sulphur amino acid methionine [1]. Naturally they occur in many fruits, beer and malt whisky. In cheese they are important compounds of characteristic aroma profiles [2] whereas in beer and wine the methionine derivatives are considered as off-flavours [3].

The deliberate production of methionine derived flavours is rarely reported, and if so, mostly in the context of soy sauce production, as those flavours contribute essentially to the condiment's aroma [4].

The Ehrlich pathway, which plays an important role in the biological formation of methionine-derived flavours is prevalent in yeasts and is especially active if the amino acid is the sole nitrogen source for the organism. Figure 1 shows the reaction principle. The amino acid is transaminated and decarboxylated to the corresponding aldehyde which is then reduced to the higher alcohol. If alcohol acetyl transferase activity is present in the organism, the alcohol can be partially transesterified to the acetate ester.

In previous investigations with L-phenylalanine as the sole nitrogen source for yeast strains, rose-like flavour compounds had been produced very successfully. Maximum product concentrations of 26.5 g L⁻¹ 2-phenylethanol and 6.1 g L⁻¹ 2-

phenylethyl-acetate could be achieved by intensive optimization of bioprocessing parameters [5] [6] [7] [8].

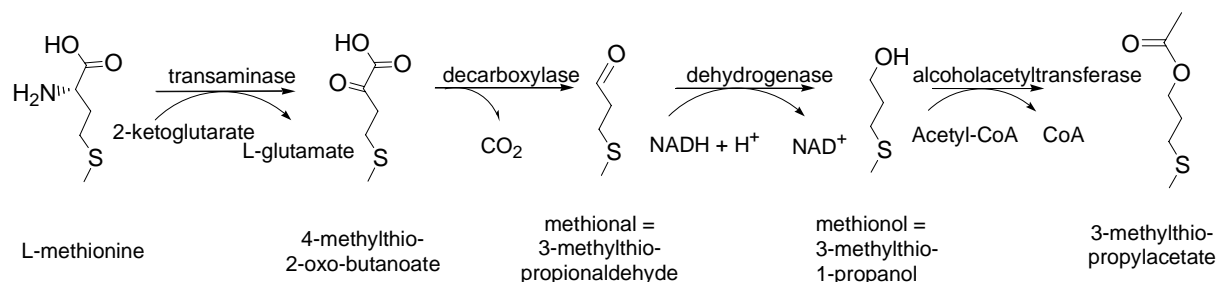


Figure 3 Ehrlich pathway with L-methionine as precursor, leading from the amino acid to the higher alcohol with subsequent esterification to the acetate.

In the present work metabolic engineering was applied in addition to the improvement of the bioprocess parameters for the cultivation of *S. cerevisiae* CEN.PK113-7D with L-methionine as nitrogen source. Overexpression of the *ATF1* gene coding for alcohol acetyl transferase 1 and adaptation of the glucose feed mode led to a considerably enhanced production of 3-MTPA. We therefore report for the first time the production of methionol and 3-(methylthio)-propylacetate on the grams per litre scale.

Experimental

For bioreactor and minireactor cultivations 20 g L⁻¹ L-methionine, 12.4 g L⁻¹ KH₂PO₄ and 1.6 g L⁻¹ K₂HPO₄ were sterilized in deionised water. After cooling an appropriate amount of autoclaved glucose solution as well as 0.04 L of a filter-sterilized vitamin and trace mineral concentrate [6] was added per litre of medium. Cultivations were carried out at 30°C either in a 2.4 L bioreactor KLF 2000 (Bioengineering, Wald, Switzerland) or in a Dasgip FedBatch Pro 4-fold parallel cultivation system (Dasgip GmbH, Juelich, Germany). Process conditions and analytical procedures can be found elsewhere [9] in detail.

Results

Inhibition studies for *S. cerevisiae* CEN.PK113-7D with externally added methionol and 3-MTPA showed that growth impairment becomes noticeable only at concentrations of about 5 g L⁻¹ and 2 g L⁻¹ 3-MTPA respectively. In preliminary shake flask cultivations of *S. cerevisiae* CEN.PK113-7D the glucose reservoir was depleted after about 18 hours and 1.5 g L⁻¹ methionol were synthesized during that time. As product inhibition effects were not to be expected at this concentration, measures for *in-situ* product removal were foregone for the time being. The acetate ester 3-MTPA was present, but at a concentration < 50 mg L⁻¹. By cultivation in a bioreactor carbon limitation was eliminated and process control improved. The process kinetics are given in Figure 2 and show that the formation of methionol started promptly and in a logarithmic fashion for the first 24 hours and shows association with the biomass formation. Both continued, albeit at a lower slope, until 64 hours. Apart from 6.2 g L⁻¹ cell dry weight and 46 g L⁻¹ ethanol, 3.5 g L⁻¹ methionol were obtained in this fed-batch process. This corresponds to a yield of 0.64 mol mol⁻¹ L-methionine and is

competitive with the only published bioprocess of industrial relevance whose product, however, is not methionol but its oxidation product 3-(methylthio)-propionic acid [10].

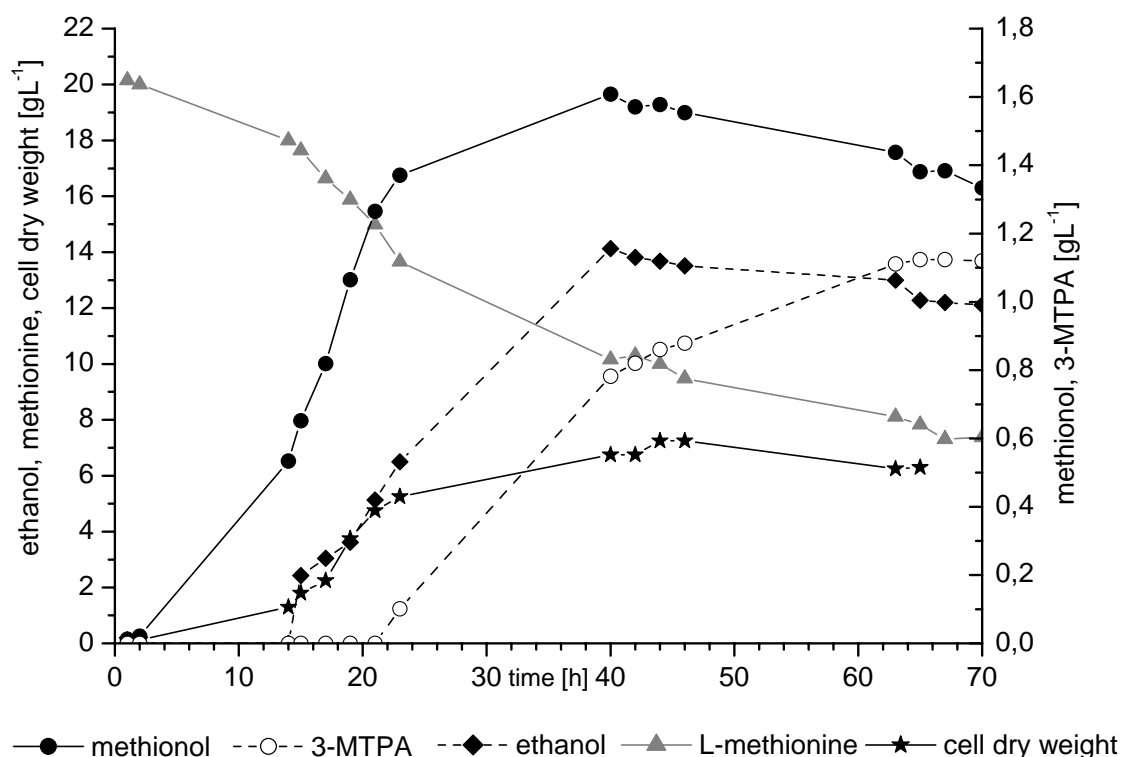


Figure 2. Bioprocess kinetics of the production of methionol with *S. cerevisiae* CEN.PK113-7D during batch cultivation in a 0.45 L bioreactor with 0.2 L working volume. Glucose was fed at a constant flow rate between $t=26$ h and 36 h. Reprint with kind permission of Springer [9].

Strain optimization by genetic engineering. The existence of 3-MTPA in the cultivation broth showed that *S. cerevisiae* CEN.PK113-7D features at least one of the two alcohol acetyl transferase genes ATF1 and ATF2. The overexpression of the alcohol acetyl transferase gene ATF1 had been successfully proven before in wine yeast [11] and sake yeast [12]. However, due to the physiological amino acid concentrations in both grape and rice mash, the product concentrations in the examples cited above were naturally low. With the present work we investigated whether the principle of ATF1 overexpression could be transferred to *S. cerevisiae* CEN.PK113-7D and the Ehrlich pathway harnessed for efficient methionol-type flavour production in media with high amino acid concentration.

For this, strain CEN.PK834-1C was constructed by substitution of the ATF1 promoter against the strong and constitutively expressed promoter of the TDH3 gene. The kanMX4-TDH3p cassette was genomically integrated by double homologous recombination. The correct integration of both recombination sites was analysed by diagnostic PCR. Using primer pairs ATF1-A1/K2 and TDH3-A7/ATF1-A2 for the PCR resulted in the expected PCR products of 639bp and 319bp, respectively (data not shown).

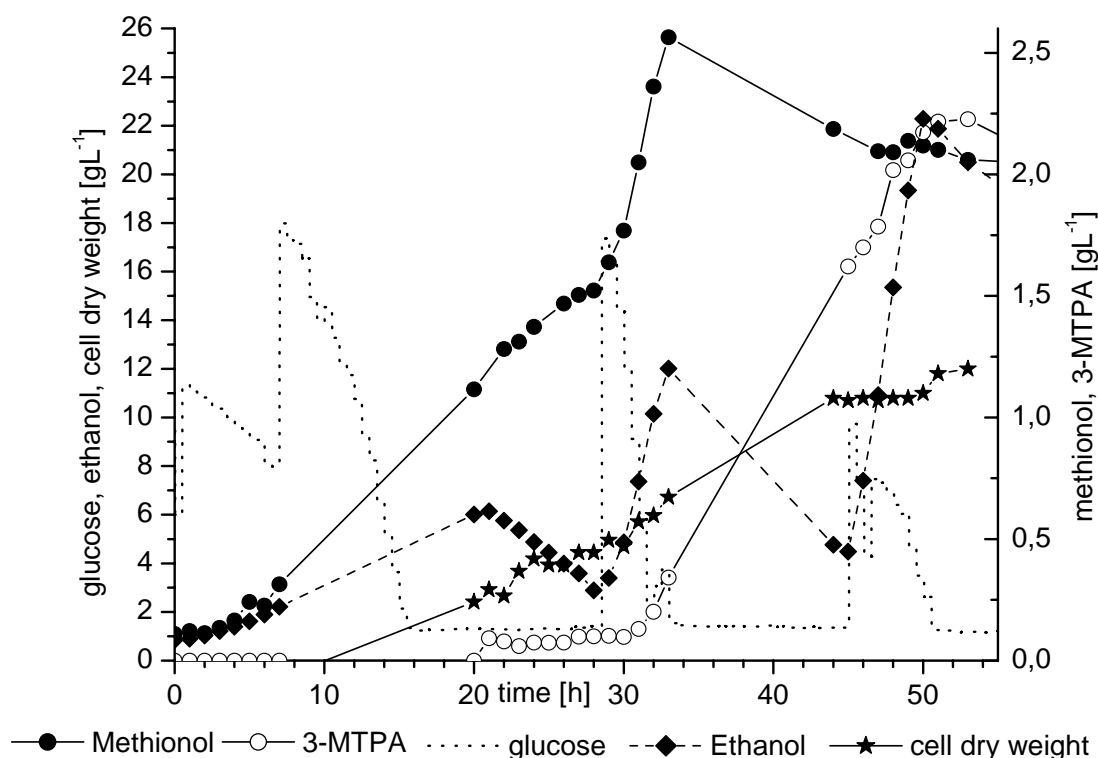


Figure 3. Bioprocess kinetics of *S. cerevisiae* CEN.PK834-1C in a bioreactor. Glucose was fed manually at $t=8$ h, 29 h, and 45 h. The glucose concentration in the reactor was monitored online. Reprint with kind permission of Springer [9].

To avoid excessive ethanol accumulation depletion of the glucose reservoir was endorsed and thus the yeast forced to use ethanol as energy source. Under these conditions 2.2 g L^{-1} 3-MTPA were obtained in addition to 2.5 g L^{-1} methionol with the *ATF1* overexpression mutant (Figure 3). Concentrations of these methionol-type flavour compounds as high as these have – to the authors' knowledge – not been cited in literature before.

The 3-MTPA formation did not set in before a methionol concentration of > 1.0 to 1.5 g L^{-1} in the supernatant had been reached, indicating that not only overexpression but also a critical precursor concentration is necessary to thrive on *Atf1* activity.

The shift from glucose as the sole carbon source to glucose and ethanol as alternate carbon sources caused a remarkable increase in product concentrations and yields $Y_{P/S}$ with CEN.PK834-1C compared to a bioreactor cultivation with a constant glucose concentration of $1\text{-}2 \text{ gL}^{-1}$ (data not shown). The positive effect of the alternate C-sources is not explicable so far, thus further experiments are necessary to elucidate this phenomenon. Ideally these should include analyses of the cellular metabolite pools and of key enzyme activities involved in product formation to gain a better understanding of the bioprocess kinetics.

References

1. Arctander S. (1969) *Perfume and Flavor Chemicals. Aroma Chemicals.* Published by the author. Montclair, NJ, USA.
2. Kagkli D.M., Tache R., Cogan T.M., Hill C., Casaregola S., Bonnarme P. (2006) *Appl Microbiol Biotechnol* 73: 434-42.
3. Landaud S., Helinck S., Bonnarme P. (2008) *Appl Microbiol Biotechnol* 77: 1191-205.
4. Aoki T., Uchida K. (1991) *Agric Biol Chem* 55: 2113-2116.
5. Etschmann M., Sell D., Schrader J. (2003) In *Flavour Research at the Dawn of the Twenty-first Century. Proceedings of the 10th Weurman Flavour Research Symposium* (J.L. Le Quéré, P.X. Étievant, eds.) Editions Tec&Doc: Paris, pp 385-388.
6. Etschmann M.M.W., Sell D., Schrader J. (2004) *J Mol Catal B: Enzym* 29: 187-193.
7. Etschmann M.M., Sell D., Schrader J. (2005) *Biotechnol Bioeng* 92: 624-634.
8. Etschmann M.M., Schrader J. (2006) *Appl Microbiol Biotechnol* 71: 440-443.
9. Etschmann M.M.W., Kötter P., Hauf J., Bluemke W., Entian K.-D., Schrader J. (2008) *Appl Microbiol Biotechnol* 80: 579-587.
10. Whitehead I.M., Ohleyer E. (1993) Microbial carboxylic acid production method, WO9308293
11. Lilly M., Lambrechts M.G., Pretorius I.S. (2000) *Appl Environ Microbiol* 66: 744-753.
12. Hirose I., Aritomi K., Hoshida H., Kashiwagi S., Nishizawa Y., Akada R. (2004) *Appl Microbiol Biotechnol* 65: 68-73.

β -GLUCOSIDASE PRODUCTION BY NON-SACCHAROMYCES YEASTS ISOLATED FROM VINEYARD

T. ARROYO¹, G. Cordero¹, A. Serrano¹, and E. Valero²

¹ *Agroalimentación, IMIDRA, El Encín. A-2 Km 38,200. Alcalá de Henares, 28800 Madrid, Spain*

² *Biología Molecular e Ingeniería Bioquímica. UPO, Sevilla, Spain*

Abstract

In order to select yeasts with biotechnological properties, 156 strains of non-*Saccharomyces* yeasts have been analysed. 83 were isolated in the vineyard under two forms of biological defence, organic culture and conventional culture. The others 73 strains came from the IMIDRA (Spain) collection. The strains have been studied under the point of view of their β -glycosidase activity. The yeasts that present this activity were genetically identified by PCR-RFLP of ITS region of chromosomal DNA. 29% of vineyard strains and 33% of the IMIDRA collection showed β -glucosidase activity under the assay conditions. The yeasts with high β -glucosidase activity were isolated from the vineyard under organic culture conditions.

Introduction

β -Glucosidase commercial enzyme is one of the most interesting glycosidases especially used for hydrolysis of glycoconjugated aroma precursors, in musts and wines (1). An alternative to the commercial enzymes could be the use of specific enzymes contained in yeasts forming part of the wine ecosystem. Non-*Saccharomyces* yeasts produce endogenous and exogenous enzymatic activities into microbial cells able to develop odorous compounds. Recent investigations about biodiversity of yeasts strains in French and Portugal vineyards showed a large proportion of non-*Saccharomyces* strains (2). In relation to these results the aim of this study was to investigate the β -glucosidase enzymatic activities of non-*Saccharomyces* strains isolated under different conditions of biological defence of the vineyard.

Experimental

Non-Saccharomyces strains and molecular identification. 96 grape samples were harvested in the Origin Appellation "Vinos de Madrid" during 2006 and 2007 campaigns, by two systems of biological defence, organic culture and conventional culture.

83 non-*Saccharomyces* yeasts of vineyard selected according to its ability to grow in a medium containing L-lysine and 73 non-*Saccharomyces* strains from IMIDRA yeasts collection (CLI): *Candida* (38), *Metschnikowia* (11), *Hanseniaspora* (1), *Hansenula* (2), *Kloeckera* (10), *Pichia* (7), *Rhodotorula* (4) was used in this study.

The molecular identification of yeast non-*Saccharomyces* was carried out with PCR amplification of the ITS ribosomal region. The PCR products were treated with the restriction endonucleases CfoI, Hae III and HinfI (3).

β-Glucosidase enzymatic activity. Test to study β-glucosidase enzymatic activity were carried out using plates containing medium with arbutin (Sigma) as substrate (yeast extract 0.3% w/v, malt extract 0.3 % w/v, meat-peptone 0.5% w/v, arbutin 0.5% w/v and YNB lys+ 0,67% w/v). After sterilization (121°C, 20 min) a sterile solution of ferric ammonium citrate (1% w/v) was added to the medium. The plates inoculated with 0.1 mL of the yeast to be tested, were incubated at 30° C for 5 days. Hydrolysis of arbutin by yeasts appeared as a dark brown colour in agar. 1mg/mL of an enzyme extracted from almonds (EC.3.2.1.21, Sigma, 5.2 U/mg solid) was used as a positive control. An activity scale from 0 (null) to 7 was elaborated in order the semiquantitative activity yeasts assessment.

Results

A vineyard of Arganda region (Origin Apellation “Vinos de Madrid”) was sampling in two harvest seasons (2006 and 2007). In total, 96 grape samples were collected, and 900 colonies was isolated from the initial population and spontaneous fermentation. When the L-lysine method was applied, 700 isolates were grouped under non-*Saccharomyces* yeasts. The large proportion of non-*Saccharomyces* strains founded in the vineyard probe the importance of this source like a non-*Saccharomyces* biodiversity reserve. In order to study the distribution of β-glucosidase activity in yeasts from vineyard and yeasts isolated in wines, 156 strains were taken, 83 were isolated in the vineyard under different conditions of defence biological, organic crop and conventional crop and 73 strains belonging to the IMIDRA yeasts collection. These strains were tested to obtain the restriction patterns of ITS ribosomal region. The ITS and the restriction fragments size of this studied strains are summarized in (Table 1). In base to this restriction fragments, the 83 isolates from vineyard were grouped under 13 different species of yeasts, types 1-13 in the Table. Although in the majority of cases, the PCR products from strains of the same species had identical molecular sizes, and species of the same genus had similar sizes for the amplified fragment, these PCR products showed a high degree of length variation, between 500 and 900 bp. The comparative study of this profiles which the profiles compiles in bibliography o database of reference collections has not been always possible. For this reason will be useful the use of classical method and other molecular techniques to recognize the genus and species of this patterns. The 56% of isolates investigated were strains type 1. In this case the PCR products and the amplified fragment of this type had showed the same size that the strain 1962 CECT (Spanish collection of type cultures), identified as *Kluyveromyces thermotolerans*. Types 2 and 6 are the second most abundant and each one represents no more than 8%. The 73 yeasts strains of IMIDRA collection previously identified to level of genus, corresponding to genus *Candida* (38), *Hanseniaspora* (1), *Hansenula* (2), *Kloeckera* (10), *Mestchnicowia* (11), *Pichia* (7), and *Rhodotorula* (4).

Table 1 shows also the results of β-glucosidase activity measured by using plates with arbutin. When the activity is present, the splitting of arbutin is observed by the dark brown colour by reaction of hydroxyquinone and ferric ammonium citrate. In order to establish a rapid semiquantitative method to measure the yeasts activity, an scale of colour (cream until dark brown) have been made increasing until seven times the enzyme extracted from almonds (EC.3.2.1.21, Sigma). The results showed that 29 % of vineyard strains present activity β-glucosidase in the assay conditions. All types of non-*Saccharomyces* species, except the type 8, were β-glucosidase positive. The types 3 and 13 were only isolates in vineyard in organic crop and the

Table 1. Origin, type/genus, ITS and RFLPs and activity control of the positive β -glucosidase strains. CLI= IMIDRA yeasts collection. A= Arganda, SM= San Martín, N= Navalcarnero. CV= Conventional culture. OC= Organic culture.

IMIDRA Collection	β -glucosidase Activity	Origin	Type/Genus sp	PCR-AP	RESTRICTION FRAGMENTS (RFLPs)		
				ITS	HaeIII	CfoI	HinfI
23A-9C	+++++++	CV	5	650	600	550	300
23A-3A	+++++++	CV	3	650	600	550	350
23A-6C	+++++++	CV	5	650	600	550	300
6 - 5A	+++++	OV	13	500	475	200+100	250+250
19A-1A	+++++	CV	6	450	400+150	300+250	300X2
19A-2A	+++++	CV	6	450	400+151	300+251	300X3
21A-5C	+++++	CV	5	650	600	550	300
6-2A	++++	OV	13	500	475	200+100	250+250
6 - 10A	++++	OV	13	500	475	200+100	250+250
23-2A	++++	CV	9	650	575	300	300X2
23-2C	++++	CV	12	800	800	300	350+200+175
24A-1A	++++	CV	7	375	375+300+100	200+100	200X2
23-3A	++++	CV	9	650	575	300	300X3
24A-2A	++++	CV	7	375	375+300+100	200+100	200X2
12A-1A	+++	CV	11	750	750	300+100	350+100
2 - 6C	+	OV	2	900	300+200+100	300+300	350
7-6B	+	OV	10	800	800	325+225+150	400+300
7-8B	+	OV	4	750	750	325	350+175+150
23-9C	+	CV	12	800	800	300	350+200+175
12A-7C	+	CV	2	900	300+200+100	300+300	350
3 - 4A	+/-	OV	1/ <i>Kluyveromyces thermotolerans</i>	700	310+215+90+90	315+285+95	355+345
10 - 10C	+/-	CV	1/ <i>Kluyveromyces thermotolerans</i>	700	310+215+90+90	315+285+95	355+435
CLI 1	+++++++	A	<i>Hansenula sp</i>	610	600	490	300
CLI 70	+++++	N	<i>Rhodotorula sp</i>	600	375+200	275+225+75	300+200
CLI 457	+++++	A	<i>Metschnikowia pulcherrima</i>	375	250+100	200+75	190
CLI 219	++++	A	<i>Metschnikowia pulcherrima</i>	400	375+250	190+75	190
CLI 50	++++	N	<i>Rhodotorula sp</i>	600	400+200	275+225+75	350+200
CLI 68	++++	N	<i>Metschnikowia pulcherrima</i>	400	250+75+50	190+75	190
CLI 460	++++	A	<i>Metschnikowia pulcherrima</i>	400	250+100	200+75	190
CLI 461	++++	A	<i>Metschnikowia pulcherrima</i>	375	250+100	200+75	190
CLI 463	++++	A	<i>Metschnikowia pulcherrima</i>	375	250+100	200+75	190
CLI 49	+++	N	<i>Rhodotorula sp</i>	600	400+200	275+225+75	350+200
CLI 560	++++	SM	<i>Metschnikowia pulcherrima</i>	375	275+100	190+75	200
CLI 72	+++	N	<i>Kloeckera sp</i>	750	700	300+100	300+190+175
CLI 903	++	EN	<i>Kloeckera apiculata</i>	750	700	300+100	300+200+190
CLI 458	+++	A	<i>Metschnikowia pulcherrima</i>	375	250+100	200+75	190
CLI 225	+++	A	<i>Kloeckera sp</i>	750	700	300+100	300+200+190
CLI 417	+++	A	<i>Hanseniospora sp</i>	-	-	-	-
CLI 3	++	A	<i>Kloeckera sp</i>	750	750	300	350
CLI 29	++	A	<i>Kloeckera sp</i>	-	-	-	-
CLI 31	++	A	<i>Kloeckera sp</i>	-	-	-	-
CLI 187	++	SM	<i>Kloeckera sp</i>	-	-	-	-
CLI 190	++	SM	<i>Kloeckera sp</i>	-	-	-	-
CLI 194	++	SM	<i>Kloeckera sp</i>	750	700	650+100	225+200+175
CLI 512	++	N	<i>Kloeckera</i>	750	300+100	300+100	300+200+190

types 5 and 11 were founded in conventional crop. The profile type 1 has presented a very weak activity and is present in both culture conditions. The 33% of the strains of IMIDRA collection have presented also β -glucosidase activity. Similar results were

founded in other studies about Spanish wines. In La Mancha region, the 25% of the non-*Saccharomyces* strains presented β -glucosidase activity (4). In sequence ascending the genus with the higher activity were: *Hansenula*, *Metschnikowia*, *Hanseniaspora*, *Kloeckera* and *Rhodotorula*. (Table 1) also shows the intensity of enzymatic activity. *Hansenula* and *Metschnikowia* have been the most actives with values between 4 and 6 times the value of the control activity. *Metschnikowia pulcherrima* was linked to the enzyme β -glucosidase in the studies carried out in La Mancha (4). Strains belonging to genus *Candida* and *Pichia* have not shown β -glucosidase activity in this study. Strauss et al. (5) detected null or some weak activity β -glucosidase activity in genus *Candida* when arbutin was used as substrate of enzyme. *Kloeckera* has a lower activity, 2 or 3 times the control value, *Hanseniaspora* and *Kloeckera* (anamorphic form of *Hanseniaspora*) are highly present in the first stages of the vinification, its can support at least 5 alcoholic degrees. The proportion of yeasts isolates in vineyard with enzymatic activity is similar in contrast with yeasts of wine. The results have shown that the types 3, 5 and 13 are 6 to 7 times more active than the control. This result to indicate that of vineyard present a high biodiversity of non-*Saccharomyces* yeasts with an important proportion of strains with β -glucosidase production. The distribution of this kind of yeast in the vineyard seems to be dependent of the sanitary treatments applied. The most active yeasts, types 3 and 13, have been isolates in organic conditions. We can conclude saying that the vineyard is an important source of non-*Saccharomyces* yeasts with a high β -glucosidase activity.

Acknowledgements.

This work was supported by INIA project RM2006-00012-00-00.

References

1. Rodríguez M.E., Lopes C., Valles S., Giraud M.R., Caballero A. (2007) *Enzyme Microb. Technol.* 41: 812-820.
2. Valero E.; Cambon B.; Schuller D.; Casal M., Dequin S. (2007) *FEMS Yeast Res.* 7: 317-329.
3. Esteve-Zarzoso B., Belloch C., Uruburu F., Querol A. (1999) *Internat. J. System. Bacteriol.* 49: 329-337.
4. Fernández M., Úbeda J.F., Briones A.I. (2000) *Internat. J. Food Microbiol.* 59: 29-36.
5. Strauss M.L.A., Jolly N.P., Lambrechts M.G., van Rensburg P. (2001) *J. Appl. Microbiol.* 91: 182-190.

ASSESSMENT OF AROMA OF CHOCOLATE PRODUCED FROM TWO GHANAIAN COCOA FERMENTATION TYPES

M. OWUSU¹, M.A. Petersen¹, and H. Heimdal²

¹ *Department of Food Science/Quality and Technology, Faculty of Life Sciences, University of Copenhagen; Rolighedsvej 30, DK-1958 Frederiksberg C, Denmark*

² *Toms Confectionery Group, Toms Alle 1, DK-2750, Ballerup, Denmark*

Abstract

Chocolates produced from two cocoa fermentation types (heap' and tray') were analysed by GC-MS and GC-O to identify and detect important odorants. The most important odour in both types of chocolate was identified as 2/3-methyl butanal with a cocoa/chocolate attribute. One odour described as grassy/lettuce and which seemed to be important for the aroma of both types of chocolates remained unidentified. Two acids, 3-methyl butanoic acid with an unpleasant blue cheese odour and acetic acid with a sharp, vinegar odour were also identified as key odorants in the two types of chocolates. Differences were identified in the types of odorants important in the two types of chocolate and these are expected to cause sensory differences between the two types of chocolate.

Introduction

The aroma of chocolate is one of its most important characteristics that determine quality. The fermentation of cocoa is critical for the formation of precursors that develops the characteristic chocolate aroma in roasted beans. The aroma and flavour of cocoa depends on the genotype of the cocoa tree that has produced the beans, the origin, and how the beans have been fermented (1, 2). Most Ghanaian farmers practise the traditional heap fermentation method (3). This is a method where upon breaking of the pod, the beans are piled on and covered by banana leaves. The heaps differ in size and may range from 20 to 1000 kg. Big heaps have to be turned once every 24-72 hours to achieve even fermentation but this is not adhered to by most Ghanaian farmers because of the tediousness involved (3). Another fermentation method developed by the Cocoa Research Institute of Ghana (CRIG) is the Tray system which involves fermenting the beans in 10 cm deep wooden trays. Eight to ten trays are stacked on top of each other and the top-most tray is covered with banana leaves. This method allows aeration of the fermenting mass without having to turn and ensures better and more even fermentation (3). Efforts are being made to encourage cocoa farmers in Ghana to adopt the tray system to improve the quality of fermented beans. This investigation aims to assess the chemical basis for differences between the aroma of chocolate produced from Ghanaian cocoa beans fermented by the above mentioned methods: heap and tray.

Experimental

Chocolate samples. Heap- and tray-fermented cocoa beans, grown and fermented in Ghana, were used for the manufacture of dark chocolate at Toms Confectionery

Group A/S, Denmark, using the same recipe. The ingredients used in the production of the dark chocolate were sugar, cocoa beans, cocoa butter and lecithin as emulsifier.

Dynamic headspace sampling and GC-MS. Dynamic headspace sampling using Tenax traps and thermal desorption is described in a lot of studies (4, 5). The technique was optimised by using 20 g of sample and purging with a nitrogen flow of 200 mL/min for 1 h at 30°C. The volatiles were analysed using GC-MS (4, 5).

GC-O. GC-O analysis was performed by three trained judges who evaluated both chocolates using the method described in (4).

Results

GC-MS identified 64 volatile aroma components in 'heap' chocolate and 58 in 'tray' chocolate. These included alcohols, acids, aldehydes, esters, furans, ketones, pyrazines, a pyrrole and a sulphur compound (Table 1). Although similar compounds have been reported by earlier workers in chocolate and other cocoa products, differences exist in the reported number of aroma compounds identified in these products. Cournet et al. 2004 identified more pyrazine-type compounds, for instance, in dark chocolate than was identified in the present study. Such differences may stem from the genotype of cocoa used, the fermentation/drying method and the manufacturing process. In the case of chocolate, the most important processes being the degree of roasting of the cocoa beans and conching of the chocolate and the ingredients used.

Peak areas of isoamylacetate, linalool and methyl phenyl acetate were significantly different ($p < 0.05$) for the two types of chocolate, whilst 2-acetylcyclopentanone, furfural, furfuryl alcohol, 1-(2-hydroxyphenyl)-ethanone and o-methoxyphenol were detected in only 'heap' chocolate.

Twenty-three odours were detected by GC-O analysis of 'heap' chocolates and 24 odours in 'tray' chocolates, three of them in each type of chocolate still unknown. Of these, 15 odours in 'heap' chocolate and 19 odours in 'tray' chocolate seemed important as they were detected by all three judges and these included one unknown with a grassy, lettuce attribute in both types of chocolates. The most important odorant, in both types of chocolate, based on the summed duration in minutes that the odorant was detected by the judges, was a peak described as having a chocolate or cocoa odour and identified as a non separable mixture of 2- and 3-methylbutanal. This has also been reported by some earlier workers (1, 2, 6).

Four odorants were detected as important in 'heap' chocolate alone whilst 7 odorants were detected as important in 'tray' chocolate alone. These odorants included pyrazines and the aldehydes, most of which are derived during the chocolate production process but others such as the alcohols and acids are products of fermentation which have persisted in the chocolate (7). The acids seemed rather abundant in both types of chocolate; 3-methyl butanoic acid, with an unpleasant blue cheese odour, and acetic acid with a sharp, vinegar odour, also seemed to be major contributors to the aroma of both types of chocolates. Linalool, detected as a key odorant in 'tray' chocolate alone is known to give a flowery tea-like odour to cocoa and is related to the fermentation method (7).

Differences in key odorants are expected to result in sensory differences between chocolate produced from heap- and tray-fermented cocoa beans. Further work is underway to do a sensory evaluation of the chocolates using a trained sensory panel to relate sensory measurements to instrumental measurements.

Table 1. Aroma components of chocolate produced from heap- and tray-fermented cocoa beans.

Compound	Identification ^a	Description of odour	Peak area ^b x10 ³	
			'heap'	'tray'
2/3-Methylbutanal	MS, GC-O, S	cocoa, chocolate	438	512
2,3-Butanedione	MS, GC-O, S	caramel, sweet	327	201
Hexanal	MS, S		59	86
Isoamylacetate	MS		388*	95*
2-Pentanol	MS, S		107	79
2-Heptanone	MS, S		88	64
Heptanal	MS, S		17	18
2/3-Methyl butanol	MS, S		45	26
2-Pentyl furan	MS, S		82	95
1-Pentanol	MS, S		94	53
Methylpyrazine	MS		48	35
3-Hydroxy-2-butanone	MS, GC-O	fruity	365	220
2-Octanone	MS		60	58
Octanal	MS, GC-O, S	orange, soapy	30	22
2,5-Dimethylpyrazine^d	MS, GC-O, S	earthy, mushroom	104	76
2,6-Dimethylpyrazine	MS		64	54
2-Decanol	MS		51	24
Ethylpyrazine^d	MS, GC-O	popcorn	22	16
2-Acetylcyclopentanone	MS		43	-
2,3-Dimethylpyrazine^c	MS, GC-O	popcorn, potato	61	37
Dimethyl trisulphide	MS, GC-O, S	unpleasant, sharp	12	10
2-Ethyl-6-methylpyrazine	MS		37	25
2-Nonanone	MS, GC-O, S	alcohol	72	43
Nonanal	MS, GC-O, S	fresh, fruity	120	113
2,3,5-Trimethylpyrazine	MS, GC-O	earthy, grass	388	166
Unknown 1	GC-O	sharp, liquorice	n.d.	n.d.
Unknown 2	GC-O	grass, lettuce	n.d.	n.d.
Ethyl octanoate	MS, S		29	26
Acetic acid	MS, GC-O, S	vinegar, sharp	3596	4686
Furfural	MS, S		37	-
2,5(or 6)-Dimethyl-3-ethylpyrazine	MS, GC-O, S	potato, earthy	35	21
Linalool oxide	MS, S		34	20
Tetramethylpyrazine	MS, GC-O	potato, earthy	2393	1042
2-Acetylfuran	MS, GC-O, S	sharp, rubber	26	14
2-Decanone	MS		9	23
Benzaldehyde^d	MS, GC-O, S	vegetable, grass	359	267
2,3,5-Trimethyl-6-ethylpyrazine^c	MS, GC-O	grass, paprika	39	14
Propanoic acid	MS, S		31	21
Linalool^d	MS, GC-O	flowery, fruity	16*	47*

Table 1. cont'd.

Compound	Identification ^a	Description odour	Peak area ^b x 10 ³	
			'heap'	'tray'
2-Methyl propanoic acid	MS		1135	518
1,3/2,3-Butanediol	MS		1945	1746
Dihydro-2(3H)-furanone	MS		79	55
Butanoic acid	MS, S		68	47
Phenylacetaldehyde^d	MS, GC-O	cocoa	132	121
1-Phenyl ethanone	MS, GC-O	flowery, sweet	137	70
Furfuryl alcohol^c	MS, GC-O, S	oat	14	-
3-Methyl butanoic acid	MS, GC-O, S	unpleasant, blue cheese	1453	912
3-Methyl-2-heptanone	MS		-	10
Benzyl acetate ^d	MS, GC-O, S	liquorice	14	9
Methyl phenylacetate	MS		29*	8*
Epoxylnalol	MS, GC-O	sweet, flowery	34	18
Ethyl phenylacetate	MS, GC-O, S	flowery, rose	133	255
1-(2-Hydroxyphenyl)-ethanone	MS		16	-
1-Phenylethanol	MS		44	19
Phenethyl acetate	MS, GC-O, S		775	667
1-Butanol-3-methyl benzoate	MS		214	93
Hexanoic acid^d	MS, GC-O, S	sharp, spicy	131	108
Butoxyethoxy ethylacetate	MS		31	32
o-Methoxyphenol	MS, S		53	-
Benzyl alcohol^c	MS		61	214
Unknown 3	GC-O	sweet, vanilla	n.d.	n.d.
2-Phenethyl alcohol	MS, GC-O, S	flowery, rose	881	324
2-Phenyl-2-butenal	MS		30	16
Heptanoic acid	MS, S		131	108
2-Acetylpyrrole	MS		63	59
Phenol	MS		71	28

^a Identification by (MS) mass spectra, (GC-O) Gas Chromatography-Olfactometry and S, standard compound; ^b mean of five replicates; ^c key odorant in 'heap' chocolate alone; ^d key odorant in 'tray' chocolate alone; * significant difference at p<0.05; n.d., not determined; -, not detected.

References

1. Counet C., Ouwerx C., Rosoux D., Collin S. (2004) *J. Agric. Food Chem.* 52: 6243-6249.
2. Bonvehi J. S. (2005) *Eur Food Res Technol* 221: 19-29.
3. Baker D.M., Tomlins K.I., Gay C. (1994) *Food Chemistry* 51: 425-431.
4. Nielsen G.S., Poll L. (2004) *J. Agric. Food Chem.* 52: 1642-1646.
5. Varming C., Petersen M.A., Poll, L. (2004) *J. Agric. Food Chem.* 52: 1647-1652.
6. Frauendorfer F., Schieberle P. (2006) *J. Agric. Food Chem.* 54: 5521-5529.
7. Gill M.S., Macleod A.J., Moreau M. (1984) *Phytochemistry* 23: 1937-1942.

AROMA FORMATION IN A CHEESE MODEL SYSTEM BY DIFFERENT LACTOBACILLUS HELVETICUS STRAINS

M.A. PETERSEN¹, H.T. Kristensen¹, M. Bakman², C. Varming¹, M.P. Jensen¹, and Y. Ardö¹

¹ Department of Food Science, Faculty of Life Sciences, University of Copenhagen, Rolighedsvej 30, DK-1958 Frederiksberg C, Denmark

² Arla Foods Innovation, Rørdrumvej 2, DK-8220 Brabrand, Denmark

Abstract

A model cheese system consisting of mild, young, normal-fat, semi-hard cheese, homogenised with water to a dry matter content of 40% was inoculated with six different *Lactobacillus helveticus* strains and ripened for four weeks. After ripening, considerable increases were seen in content of free amino acids. Furthermore, the strains effected formation of different aroma patterns, and it is concluded that the model system is sensitive and that the six *Lactobacillus helveticus* strains resulted in patterns of volatiles that are likely to be associated with different sensory characteristics.

Introduction

Traditionally, *Lactobacillus helveticus* was not used in semi-hard cheese production, but research has shown that these bacteria may be used to markedly increase amino acid release and to improve the sensory profile of low-fat semi-hard cheese (1). Their impact on aroma production in cheese is suspected to be strain dependent, and in this study six different strains of *Lactobacillus helveticus* were compared and evaluated using a cheese model system.

Experimental

From a screening using molecularbiological methods of a large number of *Lactobacillus helveticus* isolates from cheese, cultures and bacteria banks, strains with potentially different properties were selected (See Table 1). The strains were cultivated with 1% inoculation level in 8x20 ml MRS for 19 hours at 37°C. In the beginning of stationary phase the bacteria were harvested by centrifugation for 10 min at 4500 rpm (708 xg), 4°C (Sigma 3-10). The supernatant was removed and the pellet was diluted in 1 ml sterile water before use. The total number of bacteria was determined on MRS plates. A cheese model was made from mild, young (one week) normal-fat, semi-hard cheese, cut into pieces and homogenised with water to a dry matter content of approx. 40%. The cheese paste obtained was heated to 80°C to inactivate enzymes and unwanted bacteria and nisin was added to improve lysis of the *Lactobacillus* cells and as a preservative. The mixture was poured into sterile beakers with 100 g in each and the lid was closed immediately. After cooling to 40°C, *Lactobacillus helveticus* culture was added by stirring (each beaker was stirred app. 60 times) with sterile metal spoons in an aseptic bench, and the samples (100 g) were sprayed with natamycin to avoid growth of fungi. Finally the samples were

ripened for four weeks at 20°C. Reference samples of the model with no added *Lactobacillus* were incubated in parallel to assure absence of activities of unwanted microorganisms.

Table 1. Strains of *Lb. helveticus* used in the study.

Strain
<i>Lb. helveticus</i> CNRZ 32
<i>Lb. helveticus</i> CNRZ 303
<i>Lb. helveticus</i> ATCC 15009 (type strain)
<i>Lb. helveticus</i> LHC2
<i>Lb. helveticus</i> MI 2275 (Isolate from cheese culture)
<i>Lb. helveticus</i> MI 2359 (Isolate from cheese)

After 2 and 4 weeks of ripening, the samples were analysed for volatiles by dynamic headspace sampling and GC-MS (method modified after (2)). For determination of total amount of amino acids and of 12 specific amino acids, cheese samples were extracted with 6.0% 5-sulfosalicyl acid, derivatised with 6-aminoquinolyl-N hydroxysuccinimidyl carbamate (AQC), and analysed using RP-HPLC with scanning fluorescence detection (AccQTag).

Results

All the examined strains of *Lactobacillus helveticus* effected considerable increases in total concentrations of free amino acids (Table 2). Mainly the same amino acids increased in all the cheese models (data not shown), and for half of the 12 analysed amino acids (Leu, Ile Val, Phe, Pro and Lys) the increase was highest for cheese models with *Lactobacillus helveticus* ATCC 15009 and MI 2275, indicating higher lysis. The presence of the same aminopeptidase activities in all the examined strains was revealed. Amino acids are important flavours, but since they also are intermediates in aroma production, differences in overall flavour of the cheese models were still expected.

Table 2. Total content of amino acids.

<i>Lactobacillus helveticus</i> strain	mmol/kg
Control	4.8
CNRZ 32	17.9
LHC2	18.3
MI 2359 (from cheese)	18.8
CNRZ 303	19.3
ATCC 15009 (type strain)	19.8
MI 2275 (from cheese culture)	25.9

This was confirmed by (Figure 1). When type of strain was related to aroma pattern using PLS regression, a clear separation of most of the cheese models was obtained, thus demonstrating considerable impact of *Lactobacillus helveticus* on volatiles normally considered potentially important aroma compounds in cheese (3). This was obtained after 2 and 4 weeks of ripening in the model system used.

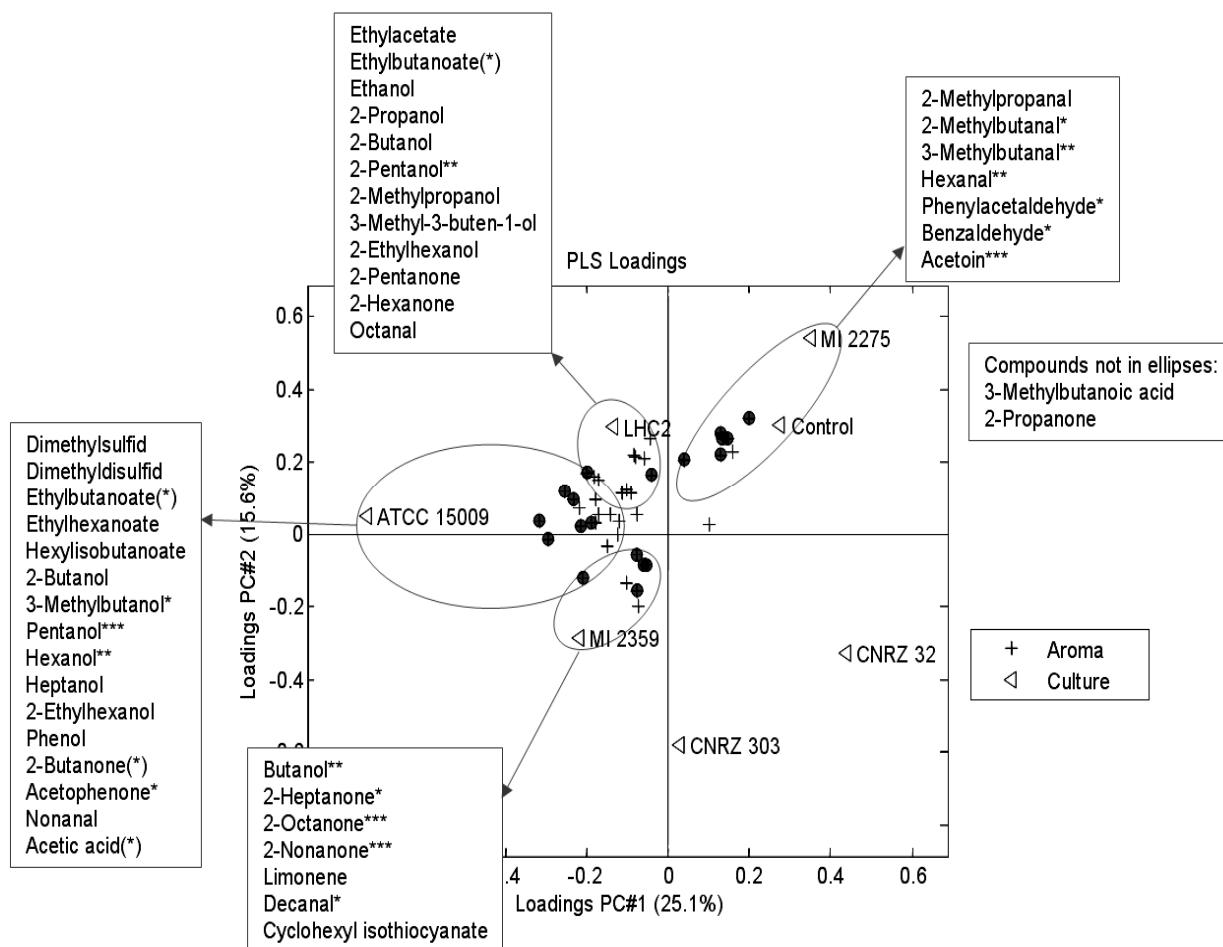


Figure 1. Loadings plot from a dummy PLS relating aroma data to strain. A red circle indicates a volatile compound where the concentration is significantly influenced by the culture (ANOVA). The boxes list compounds having higher concentration in the model and asterisks indicate significant influence of culture (ANOVA, *: $p < 0.05$; **: $p < 0.01$; *** $p < 0.001$).

Most compounds increased in concentration as compared to the control (however, phenylacetaldehyde, hexanal and 3-methylbutanal were lower than the control for all *Lactobacillus helveticus* strains except MI 2275 (data not shown)). The results indicate that MI 2275 has high capacity of amino acid catabolism since all the volatiles found in significantly higher amounts than in the control were possibly amino acid derived (Table 2) (3). The other strains had increased levels of mainly alcohols and also ketones derived from lipids (except 3-methylbutanol which is amino acid derived), indicating significant lipase/esterase activities. It should be noted that there was a characteristic difference for MI 2359, being the only strain with increased levels of several methyl ketones. Free fatty acids are the principal methyl ketone precursors through β -oxidation to β -keto acids (4) and the increased formation in the MI 2359 model could be a result of increased lipase activity.

It is concluded that the model system has a potential in screening experiments by achieving useful results about processes going on during cheese ripening within the short time of only 4 weeks. Furthermore, the six *Lactobacillus helveticus* strains tested had a clear effect on release of free amino acids and of volatiles that are likely

to be associated with different sensory characteristics. Cheese making experiments are needed to confirm the interesting effects in different cheese varieties.

Table 2. Volatiles present in significantly higher amounts in models with *Lb. helveticus* strains than in controls (ANOVA, $p < 0.05$). The strain CNRZ32 did not significantly increase the amount of any volatile component.

MI 2275	LHC2	ATCC	CNRZ 303	MI 2359
3-Methylbutanol		3-Methylbutanol		
2-Methylbutanal		Butanol	Butanol	Butanol
3-Methylbutanal	Pentanol	Pentanol		Pentanol
	Hexanol	Hexanol		Hexanol
		2-Butanone		Decanal
Benzaldehyde				2-Heptanone
Acetoin				2-Octanone
				2-Nonanone

Acknowledgment

The work was financially supported by the Danish Dairy Research Foundation and the Danish Directorate for Food, Fisheries and Agri Business

References

- Ardö Y., Larsson P.O., Månsson H.L., Hedenberg A. (1989) *Milchwissenschaft* 44: 485-490.
- Andersen C.M., Andersen L.T., Hansen A.M., Skibsted L.H., Petersen M.A. (2008) *J. Agric. Food Chem.* 56: 1611–1618.
- Ardö Y (2006) *Biotechnology Advances* 24: 238-242.
- Collins Y.F., McSweeney P.L.H., Wilkinson M.G. (2003) *Int. Dairy J.* 13: 841-866.

ODORANTS IN MILD AND TRADITIONAL ACIDIC YOGHURTS AS DETERMINED BY SPME-GC/O/MS

H. SCHLICHOTHERLE-CERNY, D. Oberholzer, und U. Zehntner

Agroscope Liebefeld-Posieux Research Station ALP, Schwarzenburgstrasse 161, CH-3003 Berne, Switzerland

Abstract

Yoghurt is one of the most widely consumed fermented milk products. For more than 50 years, volatile compounds have been intensely studied in many foods using gas chromatography-mass spectrometry (GC/MS). During the last decade many studies used also sensory techniques to identify aroma compounds in foods and beverages. A combination of instrumental and sensory methodologies, such as GC-olfactometry to investigate the aroma active compounds, however, was only rarely applied to yoghurt. Acetaldehyde, 2,3-butanedione, 2,3-pentanedione, 1-octen-3-one, 1-nonen-3-one and dimethyl sulphide were reported as character impact compounds of yoghurt. Some flavour compounds are already present in milk, such as dimethyl sulphide, 1-octen-3-one, acetic acid, and 2-phenylacetaldehyde. On the other hand, other key aroma compounds increase during fermentation, particularly acetaldehyde, 2,3-butanedione, 2,3-pentanedione, and methional.

Introduction

In order to obtain a specific desired aroma profile in fermented milk products the application of the appropriate strains is highly important. Their technological and sensory properties during and after fermentation are important criteria to select strains for culture development. In yoghurt, acetaldehyde with its typical "fresh" odour is a well-desired compound, especially in mild yoghurts which otherwise may risk to impart undesirably intense buttery and cheesy aroma notes associated with high concentrations of 2,3-butanedione, 2,3-pentanedione and butanoic acid, respectively. A typical yoghurt odour was correlated with the presence of the three key aroma compounds, acetaldehyde, 2,3-butanedione and 2,3-pentanedione. However, the pH value significantly influences the perception and intensity of aroma attributes (1-3).

The objective of the present study was to compare the volatile aroma compounds of a mild yoghurt containing selected *Lactobacillus (Lb.) delbrueckii* ssp. *bulgaricus* and *Streptococcus (S.) thermophilus* strains (J550) and a traditional acidic yoghurt produced using a commercial culture (Yo-Mix™ 621). The yoghurt samples have been fermented to pH 4.5 and 4.6, respectively and fermentation was stopped at these values. Solid-phase microextraction (SPME) and GC-MS combined with olfactometry allowed to identify acetaldehyde, 2,3-butanedione, 2,3-pentanedione, 1-octen-3-one, methional, benzaldehyde and several free short-chain fatty acids among other odorants in the two yoghurt samples. Differences for 2,3-butanedione, 2,3-pentanedione, acetaldehyde and free fatty acids were observed in the aroma profiles of the samples. The sensory perception and description of the samples obtained from four trained panellists using GC/O/MS also varied.

Experimental

Yoghurt manufacturing at pilot plant scale. Pasteurised milk (12 kg) containing 3 % of skimmed milk powder was incubated with the slow acidifying culture J550 (Agroscope Liebefeld-Posieux, Berne, Switzerland) at 45 °C to pH 4.5 or with a commercial reference culture for traditional acidic yoghurt (Yo-Mix™ 621, Danisco, Copenhagen, Denmark) at 42 °C to pH 4.6, respectively. Incubation with J550 took 5:20 h until pH 4.5 was reached; the incubation with the reference culture for traditional acidic yoghurt took 3:20 h. Then the yoghurt samples were cooled to 5 °C. In both yoghurt samples further acidification by microbial activity led to a decrease in pH value to 4.1 in the mild yoghurt and to pH 3.9 in the traditional acidic yoghurt sample. Culture J550 contained 3 strains of *Lb. bulgaricus* and of *Streptococcus thermophilus*, the exact composition of the reference culture was not specified.

Extraction and analysis of volatile compounds by GC/O/MS. The yoghurt samples were extracted and analysed using headspace SPME employing a 2 cm DVB/CAR/PDMS SPME-fibre (Supelco, Bellefonte, CA, USA). An Agilent 6890N/5973 GC-MS instrument (Agilent, Santa Clara, CA, USA) equipped with a CombiPAL autosampler (CTC Analytics, Zwingen, Switzerland) and a polar SolGelWax (SGE, Schmidlin, Neuheim, Switzerland) capillary column, 30 m × 0.25 mm × 0.25 µm film thickness, was used for the GC-MS analyses with flame ionisation detection (FID), mass selective detection and an olfactometric detector (ODP 2, Gerstel, Mühlheim, Germany) mounted in parallel by splitting the flow into three streams at the end of the capillary column. Helium was used as carrier gas at a constant flow of 1 mL/min. Extraction time for SPME was 45 min at 40 °C. The GC oven temperature was kept at 35 °C for 7 min, increased at 7 °C/min to 160 °C, and at 20 °C/min to 240 °C. The MS transfer line was set to 280 °C, the ODP transfer line to 240 °C. The GC/O analyses were carried out by four trained panellists. Mass spectra were obtained in the EI mode at 70 eV and a scan range from m/z 29-300. The volatiles were identified on the basis of the same GC linear retention indices (LRI) and mass spectra as the ones of authentic reference compounds.

Quantification of selected compounds. D- and L-isomers of lactic acid were determined enzymatically as described by (2), acetic and butanoic acid were analysed as ethyl esters after headspace derivatisation according to (4). 2,3-Butanedione and 2,3-pentanedione were quantified by stable isotope dilution analysis (SIDA) using known amounts of ¹³C₄-labelled 2,3-butanedione as internal standard. The labelled standard was synthesised according to (5). The ions m/z 86, 90 and 100 were used for quantification in the EI mode on an Optima-Wax capillary column, 30 m × 0.25 mm × 0.25 µm film thickness (Macherey-Nagel, Düren, Germany). The GC oven temperature was kept at 40 °C for 4 min, increased at 20 °C/min to 120 °C and then at 50 °C/min to 240 °C. The odour activity value (OAV) was calculated as quotient of concentration and odour threshold concentration. It indicates how many times an odorant is present above its odour threshold and allows to assess its aroma contribution.

Results

GC/O/MS analyses (Table 1) revealed the presence of known key aroma compounds (1-3) in both yoghurt samples, such as acetaldehyde, 2,3-butanedione and 2,3-pentanedione, as well as methional. The buttery, creamy odour of 2,3-butanedione was stronger perceived in mild yoghurt, whereas 2,3-pentanedione as well as the

pungent acetic acid were more intense in the traditional acidic sample. The sulphury dimethyl trisulphide and the mushroom-like and metallic smelling 1-octen-3-one were found only in mild yoghurt, the traditional acidic yoghurt revealed the corresponding alcohol 1-octen-3-ol.

Table 1. Selected odorants in mild and traditional acidic yoghurt detected by SPME GC/O/MS.

Odorant	Odour quality	Odour intensity ^a	
		Mild yoghurt	Traditional acidic yoghurt
Acetaldehyde	Fruity, acidic, fresh	+	+
2,3-Butanedione	Creamy, buttery	++	+
2,3-Pentanedione	Creamy, buttery	+	++
Methional	Cooked potato-like	+	+
Acetic acid	Pungent, acidic	+	++
Butanoic acid	Rancid, sweaty	+	+
1-Octen-3-one	Mushroom-like, metallic	+	-
1-Octen-3-ol	Mushroom-like	-	+
Dimethyl trisulphide	Garlic, sulphury	+	-

^a Odour intensities: ++ strong, + clear, - not perceived

Mild yoghurt contained less lactate and only the L- enantiomer most probably due to the activity of *S. thermophilus* (Figure 1), whereas the traditional acidic yoghurt revealed both, D- and L-lactate.

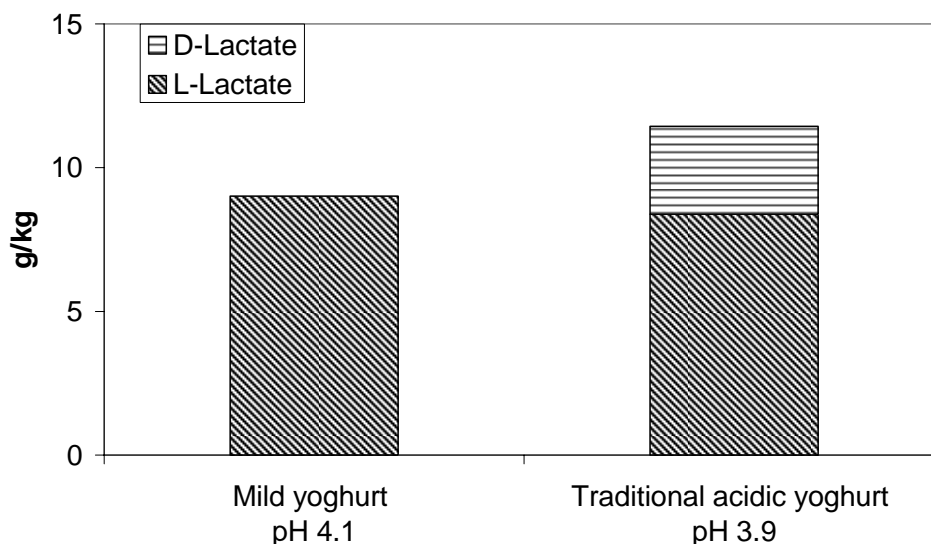


Figure 1. D- and L-lactate contents in mild and traditional acidic yoghurts.

Table 2 reveals a 1.7 fold higher concentration and an odour activity value (OAV) of 810 for 2,3-butanedione (diacetyl) compared to an OAV of 477 in traditional acidic yoghurt. The OAV for butanoic acid in mild yoghurt (176) is 2.3 fold higher than in traditional acidic yoghurt (77) and may play a decisive role of its creamy aroma, but may also impart a cheesy note. On the other hand, the acetic acid and 2,3-pentanedione concentrations of traditional acidic yoghurt exceed the ones found for

mild yoghurt by the factor of 1.5 and 1.8, respectively. These results confirm the GC/O findings shown in Table 1.

Table 2. Concentrations and odour activity values (OAV) of selected odorants in mild and traditional acidic yoghurt.

Odorant	Concentration $\mu\text{g}/\text{kg}$			OAV ^a	
	Odour threshold ^b	Mild	Traditional	Yoghurt	
		yoghurt J550	acidic yoghurt Yo-Mix™ 621	Mild J550	Acidic Yo-Mix™ 621
2,3-Butanedione	4	3239	1909	810	477
2,3-Pentanedione	30	205	370	7	12
Acetic acid	22000	54045	84070	2	4
Butanoic acid	50	8811	3862	176	77

^a Odour activity value, OAV, calculated as quotient of concentration and odour threshold concentration

^b Orthonasal odour threshold concentration determined in water according to (6)

Quantification of other key aroma compounds, such as acetaldehyde, methional, 2-methyltetrahydrothiophene-3-one and *E*-2-nonenal which were reported to increase during fermentation (1) will lead to a distinctive profiling of the single strains used to combine new starter cultures. Moreover, the fermentation process may be further defined as well by knowing the aroma formation capacity and odour contribution of the streptococci and lactobacilli. This knowledge may thus help to define optimal technological processes, such as the choice of fermentation temperature or the duration of fermentation needed to obtain a desired aroma profile.

Acknowledgement

We gratefully acknowledge H.P. Künzi for skillful technical assistance.

References

- Ott A., Fay L.B., Chaintreau A. (1997) *J. Agric. Food Chem.* 45: 850-858.
- Ott A., Germond J.E., Baumgartner M., Chaintreau A. (1999) *J. Agric. Food Chem.* 47: 2379-2385.
- Ott A., Hugi A., Baumgartner M., Chaintreau A. (2000) *J. Agric. Food Chem.* 48: 441-450.
- Mallia S., Piccinali P., Rehberger B., Badertscher R., Escher F., Schlichtherle-Cerny H. (2008) *Int. Dairy J.* 18: 983-993.
- Schieberle P., Hofmann T. (1997) *J. Agric. Food Chem.* 45: 227-232.
- Rychlik M., Schieberle P., Grosch W. (1998) *Compilation of Odour thresholds, odour qualities and retention indices of key food odorants*; Deutsche Forschungsanstalt für Lebensmittelchemie: Garching, pp 7-45.

FLAVOUR INGREDIENTS FROM FERMENTED DAIRY STREAMS

M.-L. Delabre and J.G. Bendall

Fonterra Research Centre, Dairy Farm Road, Private Bag 11029, Palmerston North, New Zealand

Abstract

Using a combination of enzyme and microbial fermentation technologies, dairy streams can be converted into complex flavour ingredients for food applications. The advantage of this process is faster and more controllable flavour development than in traditional food fermentations. The resulting flavour ingredients have a more diverse range of flavours, and better balance, than enzyme-modified cheeses (EMCs). For the consumer, these products can be labelled as 'all dairy' and are perceived as 'clean label'. Here we describe processes and flavours for two examples of dairy-derived flavour ingredients: (i) a milk fermentation that uses a selected combination of bacterial cultures to produce a savoury flavour ingredient; and (ii) the microbial fermentation of an enzymatically treated cheese to produce a flavour ingredient that contains complex sulphury notes that are reminiscent of surface-smear-ripened cheese.

Introduction

For food manufacturers to satisfy consumer preferences, products need natural ingredients as flavourings. Fermentation, in which microbial enzymes catalytically bio-transform foods, is a long-established natural method for providing foods with storage stability, as well as improving flavour. Enzyme-modified cheese (EMC) technology is one means by which a cheese slurry is incubated with various enzymes to generate flavours rapidly, and at a far greater intensity than would be the case for naturally ripened cheese (1). However, unlike naturally ripened cheese, which has an overall flavour arising from the balance of a wide variety of flavour compounds, EMC often contains mainly a single class of flavour compound (e.g. short-chain fatty acids) and so may suffer from a poor flavour balance. Our colleagues have developed flavour ingredients with better flavour balance, whereby dairy substrates are fermented using bacterial cultures in combination with additional enzyme treatments, while maintaining pH and temperature control (2, 3). Here we describe the process flow and components of two such flavour ingredients. The first example embodies a milk fermentation to produce an all-dairy savoury flavour ingredient (SFI). The second example embodies an all-dairy complex sulphury flavour ingredient (CSFI).

Experimental

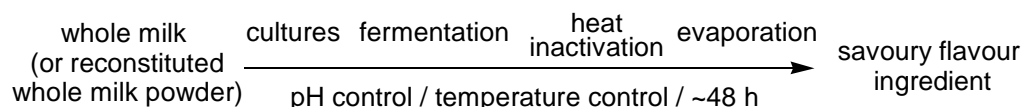
Production of flavour ingredients. For the SFI, made from whole milk (or reconstituted whole milk powder), unwanted organism growth during fermentation is prevented by controlled preheating (2). The preheated milk is then fermented with two distinct strains of bacteria for 48 h at controlled pH and temperature. For the CSFI, a cheese slurry is hydrolysed by a protease enzyme and is fermented for 100 h at controlled

pH and temperature (3). Heat inactivation terminates the fermentation for both examples. The SFI is either used as a paste or is dried to produce a powdered flavour product. The CSFI can be mixed with cheese curd to give a flavoured paste.

Identification of the important flavour compounds in the flavour ingredients. Known methods were used: to analyse L-glutamic (4), L-aspartic (4) and succinic (5) acids; to extract volatile aroma compounds (6); and for gas chromatography (GC) (7). For semi-quantitative analysis with GC–flame ionization detection, the CSFI was spiked with D₇-butyric acid as an internal standard. Unless otherwise stated, the retention time of each aroma compound was checked against that of an authentic standard - obtained either from a commercial source or from chemical synthesis. Potent odorants were screened using aroma extract dilution analysis (AEDA). The extract was sequentially diluted twofold, and the sniffing runs were repeated, until no odorants were detected. Each odorant's final dilution corresponds to the flavour dilution (FD) value. Methanethiol was identified separately using headspace solid-phase microextraction (SPME) with a carboxen fibre (75 µm coating, manual holder).

Results and Discussion

SFI Process. Fermentation of whole milk (or reconstituted whole milk powder) at controlled pH and temperature (see below) gives an SFI with an intense and very palatable savoury flavour. The final ingredient may be in the form of either a concentrated paste or a spray-dried powder.



SFI characteristics. The SFI has a complex savoury flavour and may comprise 0.5–5% of the final product, depending on the application. Taste compounds were deduced (Table 1).

Table 1. Putative taste compounds and their taste activity values (TAVs).

Taste compound	Concentration (mM) in 5% formulation	Taste threshold (mM)	TAV
succinic acid	15	0.4 ^a	37.50
L-glutamic acid	1.3	3.92 ^b	0.30
L-aspartic acid	0.02	4.00 ^b	0.001

^a Warmke, R., Belitz H.-D., and Grosch, W. (1996) *Z. Lebensm. Unters. Forsch.* 203: 230–235; ^b Haefeli, R.J., and Glaser, D. (1990) *Lebensm. Wiss. Technol.* 23: 523–527.

The principal taste compound of SFI was succinic acid with a *salty* character, similar to monosodium glutamate (8, 9), making reduced-salt applications possible.

CSFI process. The two-stage CSFI fermentation process (see below) includes both enzymatic and fermentation steps to give a flavour ingredient with a smear-ripened and savoury type of flavour much more rapidly than with traditional fermentation.

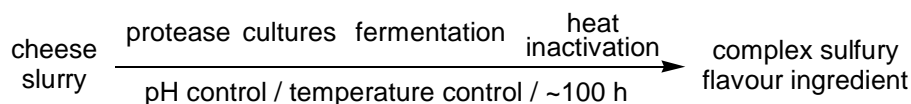


Table 2. Aroma compounds from the CSFI extract found by GC–olfactometry using AEDA.

RI ^a	Identity ^b	FD value	Conc. (µg/g)	Some descriptors	RI	Identity	FD value	Conc. (µg/g)	Some descriptors
935	ethyl 2-methylpropanoate	4	0.05	fruity	1650	acetophenone	4	0.05	rolled oats
970	pyruvaldehyde	32	trace	butter	1680	3-methylbutanoic acid	64	5	marmite
1005	methanesulphenic acid ^d	64	unseen	chives	1750	dimethyl tetrasulphide ^c	1	trace	cheesy
1030	ethyl butanoate	32	0.2	fruity	1795	4-methylpentanoic acid	16	50	rancid, sweaty
1055	ethyl 2-methylbutanoate	8	trace	fruity	1830	1,2,4-trithiolane ^c	4	trace	sweaty
1075	ethyl 3-methylbutanoate	16	trace	fruity	1845	hexanoic acid	8	7.5	sweet, sweaty
1095	4-methylpentanal	4	0.12	burnt, cheesy	1890	unknown	2	unseen	cooked
1100	dimethyl disulphide	8	80	cabbage-like	1915	phenylethanol	8	2	melted butter
1130	S-methyl thiopropanoate	16	0.05	cheesy	1955	benzothiazole	16	0.1	overcooked veges
1140	S-methyl thio-2-methylpropanoate	8	0.05	cheesy	2025	unknown	32	unseen	rancid
1165	2-methylbutyl acetate	16	0.1	banana	2070	octanoic acid	4	130	rancid
1190	ethyl 4-methylpentanoate	4	1.5	fruity	2095	1-phenylbut-2-en-1-one ^c	4	1.2	medicinal
1195	heptan-2-one	4	12	fruity	2100	<i>p</i> -cresol	32	0.8	urine
1195	S-methyl thiobutanoate	64	trace	rotten cheese	2150	nonanoic acid	16	1	toasted cheese
1225	S-methyl thio-3-methylbutanoate	8	trace	cheese	2185	dimethyl pentasulphide ^c	32	trace	burnt cheese
1305	2,4-dithiapentane	64	0.1	match-head	2255	δ-decalactone	8	5	coconut
1305	unknown	2	unseen	cheesy	2285	decanoic acid	8	130	soapy
1355	S-methyl thio-4-methylpentanoate	4	0.05	sulphurous	2305	dec-9-enoic acid	8	9	soapy
1385	dimethyl trisulphide	256	0.9	rotten drains	2395	γ-dodecalactone	16	0.6	peaches
1420	dimethyl thiosulphinate ^c	8	trace	sulphurous	2425	γ-dodec- <i>cis</i> -6-enolactone	16	0.1	peaches
1440	2-ethyl-3,5-dimethylpyrazine	16	0.1	rotten cheese	2420	1,2,4,6-tetrathiepane ^c	4	trace	toasty
1470	methional	8	trace	boiled potatoes	2455	δ-dodecalactone	4	1.2	sweet fruity
1485	2-(methylthio)ethanol ^c	16	0.2	cheese	2490	indole	8	0.1	faecal
1510	propanoic acid	2	0.2	sweaty	2505	γ-dodec- <i>cis</i> -6, <i>cis</i> -9-dienolactone	32	0.05	muesli
1535	dimethyl thiosulphonate ^c	8	trace	cheesy	2530	skatole	32	0.2	garden dirt
1565	ethyl 3-(methylthio)propanoate	4	trace	boiled noodles	2560	<i>N</i> -benzylidene phenylethylamine ^c	16	1	wet hessian
1600	2-methylpropanoic acid	16	0.2	cheesy	2600	phenylethyl acetamide ^c	64	1	wet cat hair
1610	undecan-2-one	16	10	cheesy	2640	phenylethyl formamide ^c	256	0.5	burnt wool
1630	butanoic acid	32	2	marmite					

^a Compounds are listed in order of their GC retention index, using an EC-1000 column. Retention indexes (RI) are included (based on *n*-alkanes). ^b Unless otherwise stated, each aroma compound was identified by comparing it with an authentic standard based on the following criteria: matching retention times on the same column; mass spectrum; descriptions of its aroma attribute. ^c An authentic standard was not available. Tentative identification was based on the mass spectrum. ^d The identification is speculative.

CSFI characteristics. The CSFI is a potent flavour ingredient that can be used in applications at 0.1% concentration. The majority of potent aroma compounds from the CSFI arise from degradation of the amino acids methionine, phenylalanine, leucine, isoleucine and valine. Sulphur compounds contribute particularly to the profile of flavour compounds (Table 2). Many of these are already known as cheese flavour compounds including: dimethyl disulphide, S-methyl thiopropanoate, S-methyl thiobutanoate, S-methyl thio-3-methylbutanoate, 2,4-dithiapentane and dimethyl trisulphide (10). Other known flavour compounds, not previously described in the cheese flavour literature (to the authors' knowledge), include: S-methyl thio-2-methylpropanoate and dimethyl tetrasulphide (11); dimethyl thiosulfinate and dimethyl thiosulfonate (12); and 1,2,4-trithiolane and 1,2,4,6-tetrathiepane (13). These, and other compounds listed in Table 2, have previously been seen only in a non-commercial Cheddar cheese that developed astonishingly intense flavours after maturation for 21 years (J.G. Bendall, unpublished results). AEDA revealed the presence of a potent odorant, with a chive character and a retention index of 1005, for which no peak was observed by GC–mass spectrometry. By the nature of its aroma character, this odorant is likely to be a sulphur-containing compound. Few sulphur-containing chemical structures with such a short retention time are possible, and other plausible sulphur-containing compounds were eliminated as candidates after checking their retention indexes against those of authentic standards. It is therefore speculated that the odorant may have been methanesulphenic acid (CH₃S-OH), which is known as an intermediate in the generation of other sulphur-containing flavour compounds from methionine (12).

By combining enzyme and microbial fermentation technologies, while maintaining pH and temperature control, dairy substrates can be fermented into 'clean label' flavour ingredients that contain succinic acid, which imparts a savoury taste, as well as a wide range of potent aroma compounds that can impart a more complex and balanced flavour than could otherwise be generated using EMC technology.

Acknowledgements

The authors thank: Vaughan Crow for providing the samples of flavour ingredients; Nicky Robertson, Emily Chen and Stephanie Harvey for succinate and amino acid analyses.

References

7. Kilkawley K.N., Wilkinson M.G., Fox P.F. (1998) *Int. Dairy J.* 8: 1–10.
8. Schlothauer R.C., Carroll T., Davey G.P., Chan J.R. (2004) US Patent 2004/1046600 A1.
9. Crow V.L., Hayes M., Curry B.J., Samal P.K.G., Schofield R., Holland R. (2005) US Patent 2005/0123646 A1.
10. Cohen S.A., Michaud D.P. (1993) *Anal. Biochem.* 211: 279–287.
11. Michal G., Beutler H.-O., Lang G., Gunter U. (1976) *Z. Anal. Chem.* 279: 137–138.
12. Bendall J.G. (2007) *J. Food Prot.* 70: 1037–1040.
13. Bendall J.G. (2001) *J. Agric. Food Chem.* 49: 4825–4832.
14. Velíšek J., Davídek J., Kubelka V., Thu T.T.B., Hajšlová J. (1978) *Nahrung* 22:735–743.
15. Rubico S.M., McDaniel M.R. (1992) *Chem. Senses* 17: 273–289.
16. Cuer A., Dauphin G., Kergomard A., Roger S., Dumont J.P., Adda J. (1979) *Lebensm. Wiss. Technol.* 12: 258–261.
17. Martin N., Neelz V., Spinnler H.-E. (2004) *Food Qual. Pref.* 15: 247–257.
18. Kubec R., Drhová V., Velíšek J. (1998) *J. Agric. Food Chem.* 46: 4334–4340.
19. Shieh J.-C., Sumimoto M. (1992) *Mokuzai Gakkaishi* 38: 1159–1167.

BIOSYNTHESIS OF VANILLIN VIA FERULIC ACID IN *VANILLA PLANIFOLIA*

O. NEGISHI¹ and Y. Negishi²

¹ Graduate School of Life and Environmental Sciences, University of Tsukuba, Tsukuba, Ibaraki 305-8572, Japan

² Institute of Nutrition Sciences, Kagawa Nutrition University, Sakado, Saitama 350-0288, Japan

Abstract

Several ¹⁴C-labelled precursors were fed to vanilla bean disks and their conversions to glucovanillin examined. The results showed radioactivities of 11%, 15%, 29% and 24% were incorporated into glucovanillin within 24 hr from ¹⁴C-labelled phenylalanine, 4-coumaric acid, ferulic acid and methionine, respectively. In the process of incorporation of methionine into glucovanillin, ¹⁴CH₃ of methionine was also trapped by unlabelled ferulic acid. However, ¹⁴C-labelled 4-hydroxybenzaldehyde and 4-hydroxybenzyl alcohol were not converted to glucovanillin. These results suggest that the synthetic pathway in *Vanilla planifolia* for vanillin is 4-coumaric acid → ferulic acid → vanillin → glucovanillin.

Introduction

Vanillin is accumulated as a glucoside in vanilla beans (*Vanilla planifolia*). The good aroma of vanilla is generated by “curing”, a fermentation process in which glucovanillin (vanillin glucoside) is hydrolyzed by glucosidase in vanilla bean. On the formation of vanillin in vanilla bean, Anwar (1) proposed that vanillin is synthesized from coniferin, a precursor of lignin, by shortening of the C₃ side chain and hydrolysis of glucoside, whereas Zenk (2) proposed that vanillin is formed from ferulic acid with shortening of the side chain by β-oxidation. Tokoro et al. (3) proposed a pathway to form glucovanillin from the glucoside of the 4-hydroxybenzyl alcohol after analysis of glucosides in green vanilla beans. Furthermore, Yazaki et al. (4) reported the existence of a non-oxidative reaction for shortening of the phenylpropanoid side-chain and the formation of 4-hydroxybenzaldehyde from 4-coumaric acid (C₆-C₃ compound) in cell free extract of *Lithospermum erythrorhizon* cell cultures. On the other hand, Podstolski et al. (5) also reported an enzyme involved in the reaction that converts 4-coumaric acid to 4-hydroxybenzaldehyde in tissue culture of vanilla. However, the complete biosynthetic pathway of vanillin from phenylpropanoids has not been demonstrated yet. In order to clarify the biosynthetic pathway for vanillin, we carried out pulse-chase experiments with ¹⁴C-labelled compounds in green vanilla beans.

Experimental

Radioisotopes. [U-¹⁴C]-L-Phenylalanine (Phe, 360 mCi/mmol), [U-¹⁴C]-L-tyrosine (360 mCi/mmol) and [methyl-¹⁴C]-L-methionine (Met, 54 mCi/mmol) were purchased

from Moravek Biochemicals, Inc., Brea, CA. [^{14}C]-Methyl iodide (7.6 mCi/mmol) was a product of DuPont, Boston, MA.

Syntheses of ^{14}C -precursors. [^{14}C]-4-Coumaric acid was prepared by the deamination of [^{14}C]-L-tyrosine with phenylalanine ammonia lyase (6). [^{14}C]-Ferulic acid was synthesized by the condensation between malonic acid and vanillin that was prepared by the methylation of 3,4-dihydroxybenzaldehyde with $^{14}\text{CH}_3\text{I}$ via the modification of 4-position by benzyl group (6, 7). [^{14}C]-4-Hydroxybenzaldehyde was prepared by the ozonolysis of [^{14}C]-4-coumaric acid with an ozone generator (DMO-10BDF, Ishimori Co. Ltd., Tokyo, Japan) (6). Furthermore, [^{14}C]-4-hydroxybenzyl alcohol was obtained by the reduction of [^{14}C]-4-hydroxybenzaldehyde with NaBH_4 (6). [^{14}C]-4-Coumaric acid (50 mCi/mmol), [^{14}C]-ferulic acid (7.6 mCi/mmol), [^{14}C]-4-hydroxybenzaldehyde (50 mCi/mmol), [^{14}C]-4-hydroxybenzyl alcohol (50 mCi/mmol), [^{14}C]-L-Phe (50 mCi/mmol), [^{14}C]-L-Met (54 mCi/mmol) were used as ^{14}C -precursors in the feeding experiments.

Feeding experiments. Green vanilla beans 6 months after pollination from Indonesia were washed with 0.02% chloramphenicol and cut into 2 cm length pieces (2 g). Subsequently, the 2 cm piece of green bean was further sliced into 2 mm lengths to form 10 disks, these disks were separately placed on a Petri dish. Each disk was fed 10 μl of ^{14}C -labelled compound (0.2 μCi) and incubated at 26°C under light conditions. After 1, 3, 6, 12 and 24 hr, sets of 10 disks each were frozen and stored at -80°C until the following extraction.

Extraction and separation of ^{14}C -labelled metabolites. Extraction of ^{14}C -labelled metabolites from ten disks of vanilla beans was carried out by homogenizing them with MeOH. After the separation of ^{14}C -labelled aglycones with ether from the MeOH extract, the remaining water solution was passed through an Amberlite XAD-2 column. The column was washed with water, followed by the elution of ^{14}C -labelled glucosides with MeOH. The solutions containing aglycones and glucosides were concentrated and lyophilized. Furthermore, 50% MeOH solutions of the lyophilized powders were used to analyse the metabolites by HPLC (TSK-gel ODS 80Ts, 5 μm , 250 \times 4.6 mm ID, Tosoh Corporation, Japan) (8). The flow rate was 0.6 ml/min and eluate was monitored at 280 nm. Furthermore, eluates were collected for every 1 min and their radioactivities were measured with a scintillation counter.

Results

Feeding experiments with several ^{14}C -compounds. ^{14}C -4-Coumaric acid (15%) and ^{14}C -ferulic acid (29%) were incorporated into glucovanillin within 24 hours (Figures 1-a, b). This suggests that ferulic acid is the precursor nearer to vanillin than 4-coumaric acid. During the early time of the feeding experiments the higher incorporations of ^{14}C into unknown compounds were observed. These unknown compounds from 4-coumaric acid and ferulic acid were shown to be their glucose esters (data not shown). ^{14}C -Labels from 4-hydroxybenzaldehyde distributed to 4-hydroxybenzyl alcohol and their glucosides (Figure 1-c). In addition, conversion of 4-hydroxybenzyl alcohol to its glucoside seems to be easy (Figure 1-d). However, ^{14}C -labelled 4-hydroxybenzaldehyde and 4-hydroxybenzyl alcohol were not converted to glucovanillin. ^{14}C from Phe was incorporated into 4-coumaric acid, ferulic acid, their glucose esters, vanillin and glucovanillin (11% within 24 hr) (Figure 1-e). In the ^{14}C -Met-feeding experiment to which unlabelled ferulic acid was added (Figure 1-g), the rate of conversion from Met to glucovanillin slowed (16% within 24 hr) when

compared to the control (24% within 24 hr) (Figure 1-f). The incorporation of much ^{14}C into ferulic acid was observed at 3 hr after feeding and into feruloyl glucose during the incubation times from 3 to 24 hrs. These results suggest ferulic acid is directly converted to vanillin, not via feruloyl glucose which decreased slowly. Slow conversion rates for glucose esters are also shown in (Figures 1-a, b and e).

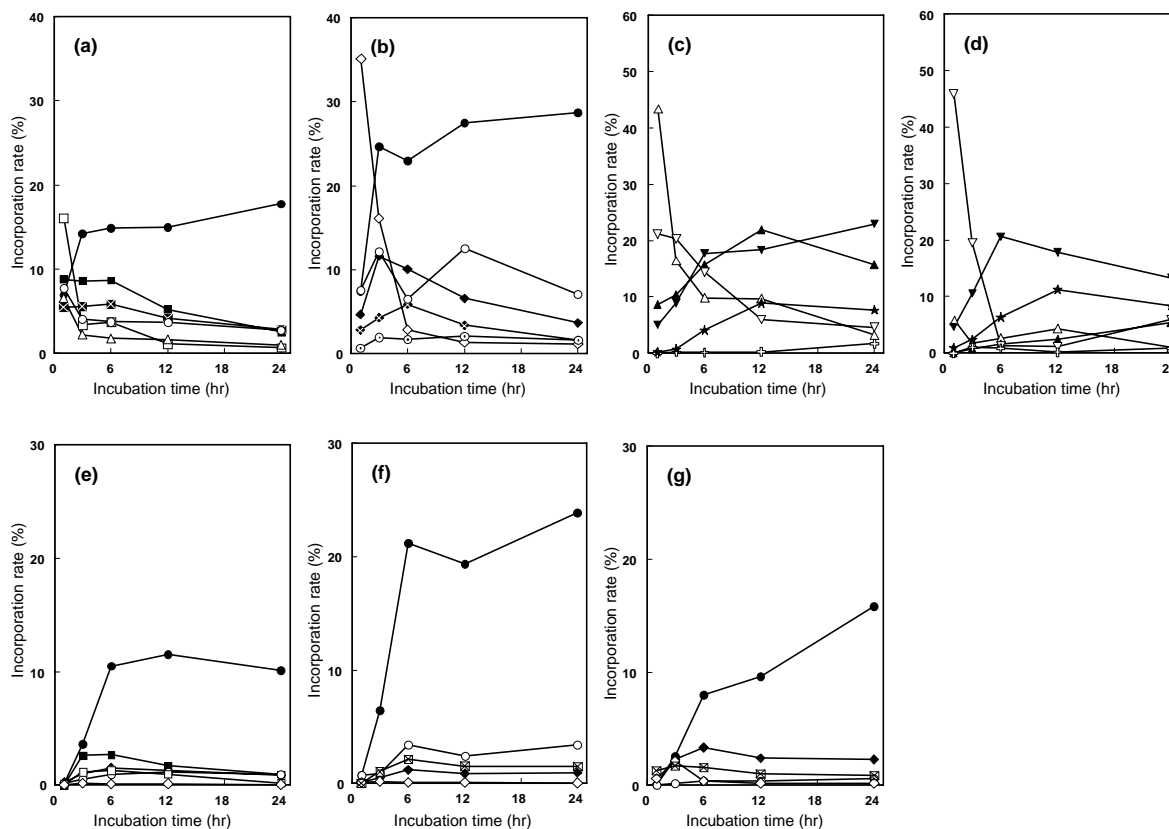
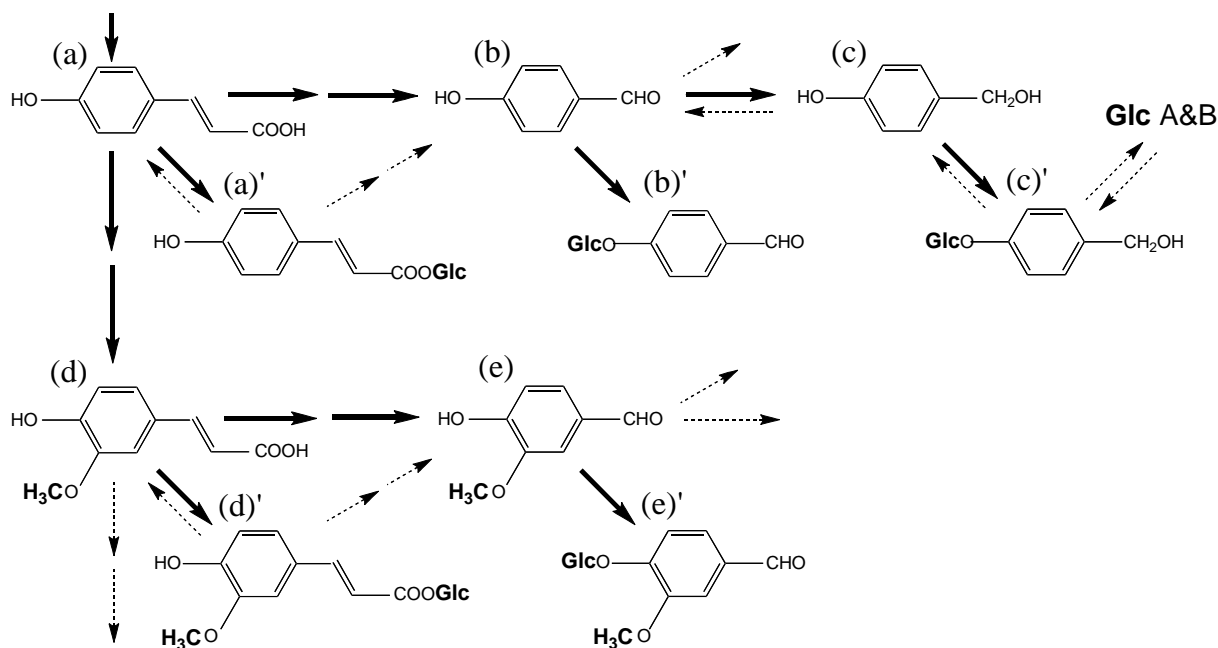


Figure 1. Feeding experiments with several ^{14}C -compounds. ^{14}C -4-Coumaric acid (a), ^{14}C -ferulic acid (b), ^{14}C -4-hydroxybenzaldehyde (c), ^{14}C -4-hydroxybezyl alcohol (d), ^{14}C -Phe (e), ^{14}C -Met (f) and ^{14}C -Met + cold ferulic acid (g) were fed to vanilla green bean disks. In the experiment of (g), $0.4 \mu\text{mol}$ of ferulic acid was added toward $2 \mu\text{Ci}$ of Met. \circ , vanillin; \bullet , glucovanillin; \odot , vanillyl alcohol glucoside; \square , 4-coumaric acid; \blacksquare , unknown-1 or 4-coumaroyl glucose (trans); \boxtimes , unknown-2 or 4-coumaroyl glucose (cis); \diamond , ferulic acid; \blacklozenge , unknown-3 or feruloyl glucose (trans); \blacklozenge , unknown-4 or feruloyl glucose (cis); \triangle , 4-hydroxybenzaldehyde; \blacktriangle , 4-hydroxybenzaldehyde glucoside; ∇ , 4-hydroxybezyl alcohol; \blacktriangledown , 4-hydroxybezyl alcohol glucoside; $+$, glucosides A & B (3); \star , unknown-5; \boxtimes , unknown-6; and \blacksquare in (e) and \blacklozenge in (f) and (g) show total 4-coumaroyl and feruloyl glucose, respectively. The decreases of ^{14}C -precursors in (e)-(g) were not determined.

Biosynthetic pathway for vanillin. Based on these results we propose that vanillin is synthesized via ferulic acid from phenylpropanoids (Scheme 1). Pathway from ferulic acid to vanillin can be supported by the existence of enzyme catalyzing the reaction in the cell-free extract. We have already detected the enzyme activity and the partial purification and characterization of the key enzyme are in progress.



Scheme 1. Proposed biosynthetic pathway for vanillin and related compounds from phenylpropanoids, and formation of their glucosides and glucose esters in *Vanilla planifolia*. (a) 4-coumaric acid; (b) 4-hydroxybenzaldehyde; (c) 4-hydroxybenzyl alcohol; (d) ferulic acid; (e) vanillin; and (a)' (b)' (c)' (d)' (e)' show the respective glucose esters or glucosides. Glc A&B are esters of tartaric acid and 2 molecules of (c)' (3).

References

1. Anwar M.H. (1963) *Anal. Chem.* 35: 1974-1976.
2. Zenk M.H. (1965) *Z. Pflanzenphysiol.* 53: 404-414.
3. Tokoro K., Kawahara S., Amano A., Kanisawa T., Indo M. (1990) In *Flavour Science and Technology* (Bessiere Y., Thomas A.F, eds.); Wiley, Chichester, Vol.73, pp 73-76.
4. Yazaki K., Heide L., Tabata M. (1991) *Phytochemistry* 30: 2233-2236.
5. Podstolski A., Havkin-Frenkel D., Malinowski J., Blount J.W., Kourteva G., Dixon R.A. (2002) *Phytochemistry* 61: 611-620.
6. Negishi O., Sugiura K., Negishi Y. (2009) *J. Agric. Food Chem* 57: 9956-9961.
7. Funk C., Brodelius P.E. (1990) *Plant Physiol.* 94: 95-101.
8. Negishi O., Ozawa T. (1996) *J. Chromatogr. A.* 756: 129-136.

DIVERSITY OF VOLATILE PATTERNS IN A GENE BANK COLLECTION OF PARSLEY (*PETROSELINUM CRISPUM* [MILL.] NYMAN)

D. ULRICH¹, H. Budahn¹, T. Struckmeyer¹, F. Marthe¹, H. Krüger¹, and U. Lohwasser²

¹ *Julius Kühn-Institute (JKI), Federal Research Centre for Cultivated Plants, Erwin-Baur-Straße 27, D-06484 Quedlinburg, Germany*

² *Leibniz Institute of Plant Genetics and Crop Plant Research (IPK), Corrensstr. 3, D-06466 Gatersleben, Germany*

Abstract

A collection of 219 accessions mostly provided by the German Gene Bank of the Leibniz Institute of Plant Genetics and Crop Plant Research in Gatersleben, Germany was cultivated in field. The patterns of volatile metabolites were determined effectively by a rapid, non-targeted analysis approach in leaf homogenates. The used method is a combination of an effective sample preparation and a non-targeted data processing. First results show that the investigated accessions belong to two different basic chemotypes. The two types differ mainly in volatiles deriving from the lipoxygenase pathway ((*Z*)-3-hexenal, (*E*)-2-hexenol), the phenylpropane compound apiol and minor terpenes like β -myrcene and γ -terpinene. The relationship of the volatile patterns to common essential oil analysis as well as properties like resistance and sensory quality (profile analysis and reference test) will be investigated in future.

Introduction

Parsley (*Petroselinum crispum* [Mill.] Nyman.) is widely used as a pot-herb, both fresh and dry. The essential oil is applied in food industry and as a fragrance in perfume manufacturing. The composition of volatile compounds of freshly harvested and dried parsley as well as the essential oil has been studied in the past (1). In contrast, the diversity of the volatile metabolites in different cultivars and accessions is widely unknown. Therefore a collection of 219 accessions mostly provided by the German Gene Bank of the Leibniz Institute of Plant Genetics and Crop Plant Research in Gatersleben, Germany was cultivated in field. The patterns of volatile metabolites were determined effectively by a rapid, non-targeted analysis approach in leaf homogenates. By this way in principle the area of all peaks of a chromatogram set above a threshold are detectable. Overlooking of unexpected substances caused by a high diversity of the volatile metabolites is prevented using this non-targeted method. In parallel molecular analysis using AFLP, SRAP, RAPD- and dpRAPD-markers were performed to discover the genetic relationship of the different accessions.

Experimental

Plant material. A collection of 219 accessions mostly provided by the German Gene Bank of the Leibniz Institute of Plant Genetics and Crop Plant Research in

Gatersleben, Germany was cultivated in field. The plant material was stored until analysis at -86 °C.

Sample preparation. After thawing 1 mass part of parsley and 3 volume parts of a 20 % (w/v) sodium chloride solution were homogenized for 1 minute in a Waring blender. The homogenate was filtered using gossamer. For each sample, four headspace vials containing 4 g solid NaCl for saturation were filled with a 10 ml aliquot of the supernatant, sealed with a magnetic crimp cap including septum.

Automated headspace-SPME-GC. 100- μ m-polydimethylsiloxane-fibre (Supelco, Bellefonte, PA, USA); equilibration time 10 min at 35 °C (300 rpm); extraction 15 min at 35 °C; desorption 2 min splitless and 3 min with split at 250 °C; GC Agilent Technologies 6890) equipped with MPS2 autosampler from Gerstel (Mühlheim, Germany) and FID; column HP INNOWax, 0.25 mm ID, 30 m length and 0.5 μ m film thickness; carrier gas hydrogen 1.1 ml/min; temperature programme 45 °C (5 min), from 45 to 210 °C at 5 K/min and 15 min at 200 °C. All samples were run in triplicate. The volatiles were identified by parallel running of mass spectrometric analysis (GC/MS) and by retention indices.

Marker analyses. DNA of the parsley genotypes was isolated according to Porebski (2). RAPD analysis followed the protocol of Williams (3), dpRAPD-analysis according to Budahn (4) and SRAP-analysis corresponding to Li (5). The amplification products were separated on denaturing PAAGE (Sequigene GT, BIO-RAD, 38 x 50 cm). Geles were silver stained according to Bassam (6). AFLP amplification followed Vos (7) and separation and detection using Licor 4300S. Clear and strong bands were recorded as 1/0 matrix. The distance analysis was realized with NTSYSpc (Exeter Software) in the UPGMA modus.

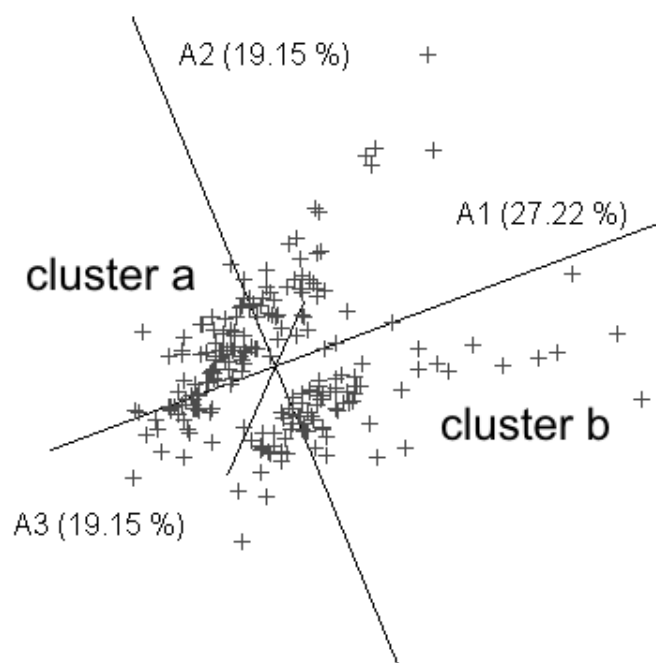


Figure 1. 3D-plot of a principal component analysis (PCA) of altogether 219 genotypes using 133 peaks. The visualization shows two clearly distinct clusters. Cluster **a** contains 132 genotypes and cluster **b** 87, respectively. Software: Statistika 7.1 by StatSoft.

Results

To prevent overlooking of qualitative changes (new compounds) a so called non-targeted or holistic analysis approach with pattern recognition of chromatograms was used (8,9,10). Data input for pattern recognition by the commercial software CHROMStat™ 2.6 were percentage reports (retention time/peak area data pairs). This kind of data processing consider all detectable peaks of an analysis set (in this experiment around 600) without peak allocation or identification. Using CHROMSTAT™, the chromatograms were divided into 133 time intervals, each of which represent a possible peak (substance) occurring in at least one chromatogram of the analysis set. A modified principal component analysis (PCA) was performed to visualize the results and check the reproducibility of GC analyses. Substance identification of genetically interesting peaks was done by parallel GC/MS runs of identical samples.

The results of analysis of volatile metabolites as well as the distance analysis based on molecular markers showed that the 219 genotypes split clearly into two groups. Regarding metabolites the two groups differ mainly in volatiles deriving from the lipoxygenase pathway ((*Z*)-3-hexenal, (*E*)-2-hexenal), the phenylpropane compound apiol and minor terpenes like β -myrcene and γ -terpinene. (*Z*)-3-hexenal (green-grassy) and β -myrcene (parsley-like) are known as character impact compounds of the typical parsley aroma (1). Also apiol is characterised by a parsley-like odour whereas γ -terpinene smells like wood, terpene and lemon. Root parsley genotypes clustered into the smaller group (cluster b) and all genotypes with curled leaves, except one, belong to the other group (cluster a). Genotypes with smooth leaves can be found in both groups. The allocation of genotypes to the two clusters shows only 10 mismatches (5 %) in comparison between the metabolomic and molecular marker data.

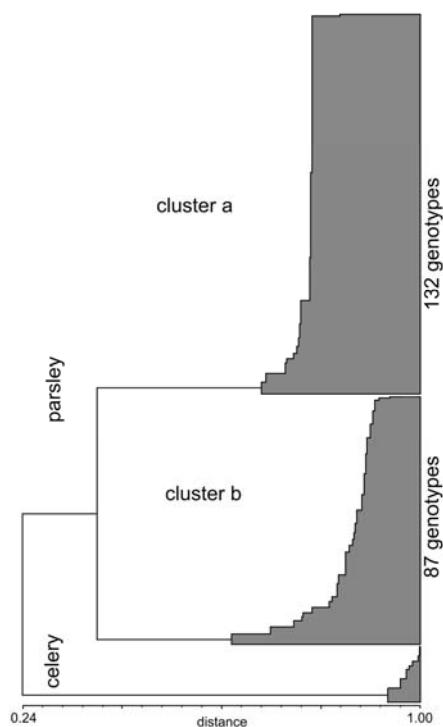


Figure 2. Analysis of genetic distance using AFLP, SRAP, RAPD and dpRAPD markers. For comparison celery was included to enhance the statistical power.

These results indicate that all investigated accessions split into two groups on the base of the lipoxygenase activity. The grouping does not correlate with leaf shape (curled or smooth) which is one of the most noticeable trait in parsley. The relationship of the volatile patterns with common essential oil analysis, properties like resistance and sensory quality (profile analysis and reference test) will be investigated in future

References

1. Masanetz C., Grosch, W. (1998) *Flav. Fragr. J.* 13: 115-124.
2. Porebski S.; Bailey L.G.; Baum B.R. (1997) *Plant Mol. Biol. Rep.* 15: 8-15.
3. Williams J.G.K.; Kubelik A.R., Livak K.J.; Tingey S.V. (1990) *Nucl. Acids Res.* 18: 6531-6535.
4. Budahn H.; Schrader O.; Peterka H. (2008) *Euphytica* 162: 117-128.
5. Li G., Quiros C.F. (2001) *Theor. Appl. Genet.* XX: 455-461.
6. Bassam B.J.; Caetano-Anolles G.; Gresshoff P.M. (1991) *Anal. Biochem.* 19: 80-83.
7. Vos P., Hogers R., Bleeker M., Reijans M., van de Lee T., Hornes M., Frijters A., Pot J., Peleman J., Kuiper M. (1995) *Nucleic Acids Res.* 23: 4407-4414.
8. Schulz I., Ulrich D., Fischer C. (2003) *Food* 47: 136–139.
9. Olbricht K., Grafe C., Weiss K., Ulrich D. (2008) *Plant Breeding* 127: 87-93.
10. Ulrich D. (2008) In *Fruit and vegetable flavour* (Brückner B., Wyllie S.G., eds.), Woodhead Publishing: Cambridge, England, pp 167-179.

ATMOSPHERIC CARBON DIOXIDE INDUCES CHANGES OF AROMA VOLATILES IN BRASSICACEAE

A. KRUMBEIN, M. Schreiner, H.-P. Kläring, and I. Schonhof

Institut für Gemüse- und Zierpflanzenbau Grossbeeren / Erfurt e.V., Theodor-Echtermeyer-Weg 1, D-14979 Grossbeeren, Germany

Abstract

Atmospheric carbon dioxide (CO₂) concentration is an environmental factor that is undergoing dramatic changes. The objective of the present study was to determine the effect of ambient (450 ppm) and elevated atmospheric CO₂ (880 ppm) on aroma volatiles in *Brassicaceae* using broccoli grown in a controlled greenhouse environment as an example. The higher CO₂ concentration seems to increase by up to 100% the biosynthesis of three fatty acid-derived C₇ aldehydes ((*E*)-2-heptenal, (*E,Z*)-2,4-heptadienal, (*E,E*)-2,4-heptadienal), two fatty acid-derived C₅ alcohols (1-penten-3-ol, (*Z*)-2-pentenol), and two amino acid-related nitriles (phenylpropanenitrile, 4-methylpentanenitrile). In contrast, the sulphur-containing compound 2-ethylthiophene and C₆ alcohol (*E*)-2-hexenol decreased. From the affected volatiles, (*E,Z*)-2,4-heptadienal, 1-penten-3-ol, and 2-ethylthiophene in particular may contribute to the flavour of broccoli.

Introduction

Atmospheric carbon dioxide (CO₂) concentration is an environmental factor that is undergoing dramatic changes, from 280 ppm in pre-industrial times to approximately 380 ppm at present (1). Climate simulations indicate a further ongoing increase in atmospheric CO₂ of up to twice today's concentration (2). Atmospheric CO₂ enrichment is known to significantly enhance the growth and development of plants, implying a potential for elevated levels of CO₂ to alter the concentrations of plant constituents (3). For example, elevated atmospheric CO₂ in comparison to ambient CO₂ concentration changed concentrations of carbon-based plant compounds such as aliphatic and indole glucosinolates in broccoli (4). However, at present, no information is available on the effect of elevated atmospheric CO₂ on aroma volatiles in *Brassica* vegetables, which strongly contribute to their flavour, and hence consumer acceptability. For this reason, the objective of the present study was to determine the effect of ambient and elevated atmospheric CO₂ on aroma volatiles in *Brassicaceae* using broccoli as an example.

Experimental

Plant material. Broccoli (*Brassica oleracea* var. *italica* Plenck) cv Marathon was grown in a controlled greenhouse environment in a block design with three replicates (4). 54 broccoli plants were used for each treatment and replicate, with each plant being grown in a soil-filled 40-liter container spaced 0.6 x 0.7 m from each other, resulting in a density of 2 plants m⁻². Plants at the three-leaf stage were exposed to two different atmospheric CO₂ concentrations at daytime: ambient atmospheric CO₂

(450 ppm) and elevated atmospheric CO₂ (880 ppm). Plants were grown at a daily mean temperature of 15.3°C and radiation at 10.04 mol m⁻² d⁻¹. A mixed sample of florets from each replicate consisting of five fully developed broccoli heads was taken for the analysis.

Dynamic headspace sampling and GC-MS. Fresh florets (300 g) were blended with 250 ml distilled water for 30 s and held for 180 s; 400 ml saturated calcium chloride solution was added to deactivate the enzymes of lipid oxidation, and the mixture was reblended for 10 s. An internal standard (2-octanone) was then added and the mixture was blended for another 10s. The mixture was placed in a 3 l flask containing a magnetic stirrer, and purified air (150 ml min⁻¹) was passed through the mixture and out of the flask through a Tenax trap (200 mg Tenax TA, 60-80 mesh). Isolation was carried out for 150 min, after which time the trap was removed and volatiles were extracted with 3 ml acetone and concentrated with nitrogen flux to a volume of 50 µl. The extracts were determined by GC-MS using the following instruments and parameters: HP5890 Series II plus MSD 5972A; splitless, injector temperature 250°C; Supelcowax 10 column 30 m x 0.25 mm i.d./0.25 µm; 1 ml helium min⁻¹; temperature program: 3 min at 40°C; from 40°C at 1°C min⁻¹ to 60°C, 2 min at 60°C; from 60°C at 5°C min⁻¹ to 180°C, 10 min at 180°C. The relative peak areas of the total ion chromatogram were normalised with the peak area of the internal standard.

Statistical analysis. The results were evaluated using Student's t-test (level of significance 5%).

Results

Using the dynamic headspace sampling technique and GC-MS, a total of 40 volatiles was identified in broccoli (5). Elevated atmospheric CO₂ seems to influence the biosynthesis of few fatty acid-derived aldehydes and alcohols, amino acid-related nitriles and a sulphur-containing compound. The higher CO₂ concentration led to an enhancement of up to 100% of the C₇ aldehydes (*E*)-2-heptenal, (*E,Z*)-2,4-heptadienal, and (*E,E*)-2,4-heptadienal (Figure 1), C₅ alcohols 1-penten-3-ol and (*Z*)-2-pentenol (Figure 2), and the two amino acid-related nitriles phenylpropanenitrile and 4-methylpentanenitrile (Figure 3).

The reason for the accumulation of amino acid and fatty acid derived volatiles could be the formation of a carbohydrate pool due to increased photosynthesis at higher CO₂ concentrations that forms the basis for the synthesis of further compounds, such as amino acids or fatty acids. In the Calvin-Benson cycle, carbon dioxide is bound to an acceptor (pentose phosphate ribulose-1,5-bisphosphate), which then undergoes carboxylation and further reduction to glyceraldehyde-3-phosphate (GAP) (6). The triose-phosphate GAP flows into a pool of carbohydrates with different carbon chain lengths (C₃-C₇), from which various substances like sugars and amino acids are synthesised (6). In contrast, the sulphur-containing compound 2-ethylthiophene (Figure 3) and the C₆ alcohol (*E*)-2-hexenol (Figure 2) decreased. Elevated carbon dioxide also affects aroma volatiles in strawberries (7); elevating the ambient CO₂ concentration (ambient + 300, and ambient + 600 ppm CO₂) resulted in an increase of furaneol, linalool and seven important esters, e.g. ethylhexanoate and ethylbutanoate, but in a decrease of the esters butyl acetate and methyl methanoate in strawberries. The authors claimed that the increase of soluble sugars in strawberries arising from elevated CO₂ treatment may result in an increase in the availability of precursors able to produce esters and furanones (7).

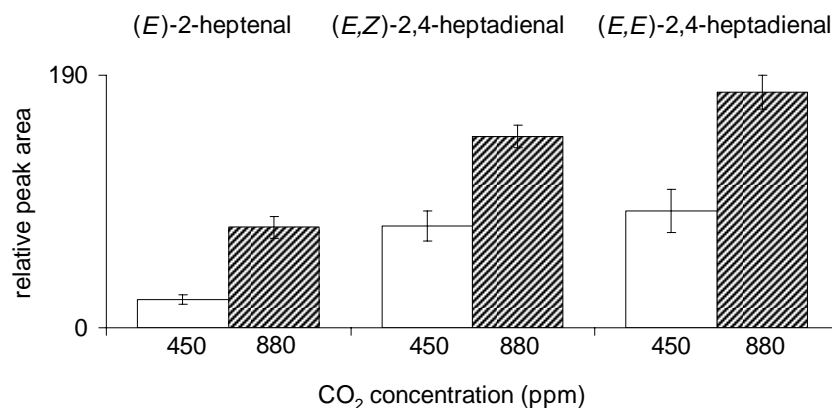


Figure 1. Relative peak area of C₇ aldehydes in broccoli florets grown at ambient CO₂ (450 ppm) or elevated CO₂ (880 ppm).

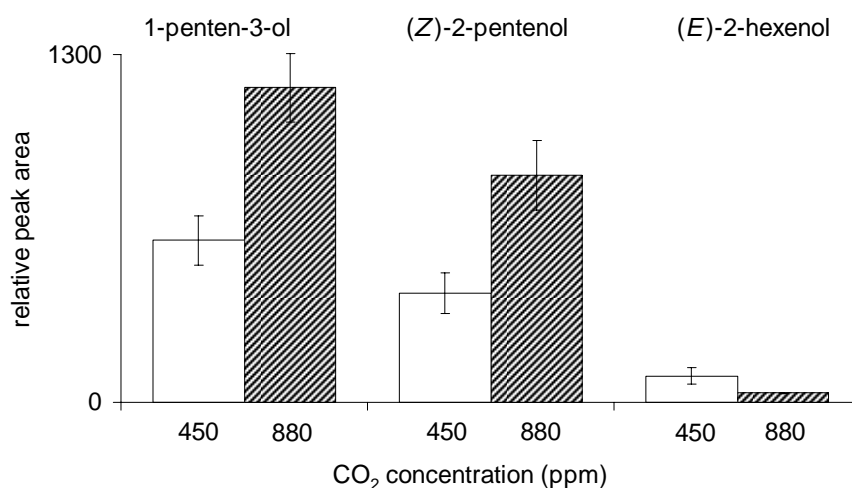


Figure 2. Relative peak area of C₅ and C₆ alcohols in broccoli florets grown at ambient CO₂ (450 ppm) or elevated CO₂ (880 ppm).

Regarding the aroma volatiles in broccoli that changed due to elevated atmospheric CO₂, (E,Z)-2,4-heptadienal, 1-penten-3-ol and 2-ethylthiophene in particular are odour active compounds with herbaceous, grassy and moldy odour notes, respectively (8).

Quantitative descriptive sensory analysis of different broccoli and cauliflower cultivars showed that (E,Z)-2,4-heptadienal and 1-penten-3-ol were closely associated with the sensory attribute “broccoli” in odour and flavour while 2-ethylthiophene was associated with the flavour attributes “leek” and “green/grassy” (8). Furthermore, together with the ascertained reduction of the bitter tasting indole glucosinolate content in broccoli grown at elevated atmospheric CO₂ (4), the changes in aroma volatiles probably contribute towards improved flavour. Whether the

investigated changes could influence consumer acceptance needs further detailed sensory analysis.

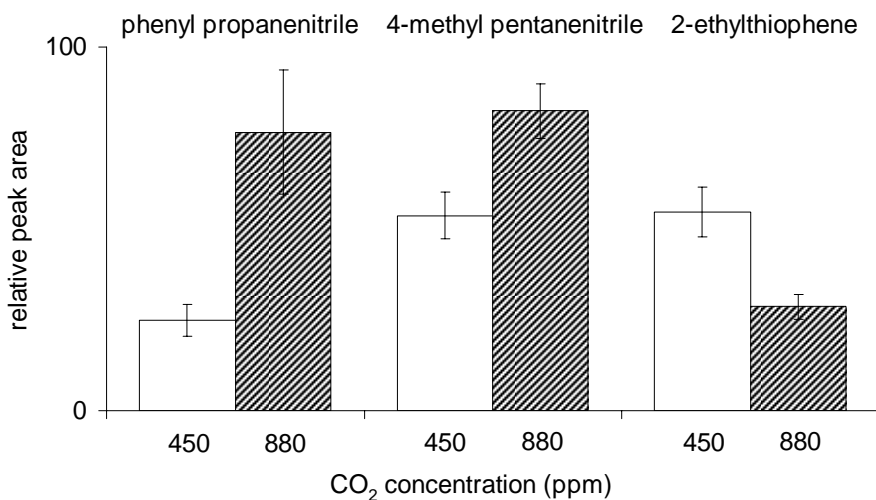


Figure 3. Relative peak area of nitriles and an S-containing compound in broccoli florets grown at ambient CO₂ (450 ppm) or elevated CO₂ (880 ppm).

References

1. Steffen W., Crutzen P.J., McNeill J.R. (2007) *AMBIO* 36: 614-621.
2. Gerber S., Joos F., Prentice I.C. (2004) *Global Change Biol.* 10: 1223-1239.
3. Idso S.B., Idso K.E. (2001) *Environ. Exp. Bot.* 45: 179-199.
4. Schonhof I., Kläring H.-P., Krumbein A., Schreiner M. (2007) *J. Chem. Ecol.* 33: 105-114.
5. Krumbein A., Hansen M., Hansen A.M. (1997) In *Flavour Perception, Aroma Evaluation* (H.-P. Kruse, M. Rothe, eds.); Eigenverlag Universität Potsdam, pp. 504-507.
6. Larcher W. (2003) *Physiological plant ecology*, Springer, Berlin Heidelberg New York.
7. Wang S.Y., Bunce J.A. (2004) *J. Sci. Food Agric.* 84: 1464-1468.
8. Krumbein A., Schonhof I., Brückner B. (2006) In *Flavour Science: Recent Advances and Trends* (W.L. Bredie, M.A. Petersen, eds.); Elsevier B.V.: Amsterdam, pp 342-345.

Section 8

Impact Aroma and Taste Molecules

IDENTIFICATION OF β -ALANYL DIPEPTIDES CONTRIBUTING TO THE THICK-SOUR, WHITE-MEATY OROSENSATION INDUCED BY CHICKEN BROTH

A. Dunkel and T. HOFMANN

Chair of Food Chemistry and Molecular Sensory Science, Technische Universität München, Lise-Meitner-Str. 34, 85354 Freising, Germany

Abstract

Mouthfulness enhancing peptides were identified in chicken broth by means of activity-guided, sequential fractionation including solvent extraction, ultrafiltration, gel permeation chromatography, HPLC, and HILIC, in combination with human psychophysical experiments. LC-MS/MS and 1D/2D-NMR studies on isolated fractions led to the characterization of taste modulating peptides such as β -alanyl-3-methyl-L-histidine (anserine), β -alanyl-L-histidine (carnosine), and the previously not reported β -alanyl-glycine. Quantitation of these peptides, followed by taste recombination and omission experiments confirmed the contribution of these peptides to the thick-sour and white-meaty orosensation induced by chicken broth.

Introduction

Due to its desirable white-meaty and thick-sour taste, chicken broth is frequently used as a base for savoury dishes in many countries all over the world. The knowledge on the odorous volatiles contributing to the smell of chicken broth is rather comprehensive and more than 450 aroma compounds were reported in literature (1). In contrast, only fragmentary data are available on the non-volatile constituents contributing to the attractive orosensory sensation induced by a freshly prepared chicken broth. Most literature studies report only on quantitative data of basic taste compounds such as, e.g. carbohydrates, amino acids, nucleotides, organic acids, and minerals (2-3), but neither activity-guided identification experiments targeting the thick-sour, white-meaty orosensation induced by chicken broth, nor recombinatory trials have been reported. In order to identify the key compounds evoking this thick-sour and white-meat-like impression upon consumption of chicken broth, we applied an activity-guided fractionation approach combined with the recently developed comparative taste dilution analysis (cTDA) (4) as a screening tool for the discovery of taste modulating compounds in foods.

Experimental

Chicken broth was prepared by heating 1 kg chicken including meat, bones, and skin in the presence of 1.5 L water at 90°C in a clay pot. After heating for 24 h, the solid parts of the chicken were removed and the remaining broth was used for sensory and chemical analysis. The experimental details on the sensory analysis, the procedures used for isolation and identification of the compounds inducing a thick-sour, white-meaty orosensation, as well as the quantitative data are reported elsewhere (5).

Results

Solvent extraction and ultrafiltration. To gain insight into the polarity of the compounds imparting the thick-sour, white-meaty orosensation, a chicken broth was extracted with pentane to remove the non-polar lipid fraction. After lyophilisation, the aqueous fraction was separated by a sequential ultrafiltration affording a high-molecular weight fraction (HMW; MW > 5 kDa), a medium molecular weight fraction (5 kDa > MW > 1 kDa), and a low-molecular weight fraction (LMW; MW < 1 kDa) (Figure 1). Sensory analysis revealed that the quantitatively predominating high molecular weight fractions were nearly tasteless and showed only a pronounced viscosity due to the presence of high amounts of gelatine. In contrast, the LMW compounds exhibiting a molecular weight below 1 kDa imparted the typical complex taste profile of chicken broth including the thick-sour, white-meaty orosensation.

Separation and identification of key taste compounds. In order to evaluate the participation of known taste-active compounds, ion chromatographic analysis and HPLC-MS/MS experiments led to the identification and quantitative determination of a total of 50 putative basic taste compounds including 25 amino acids, 5 carbohydrates, 12 nucleotides and nucleosides, 5 organic acids, 5 cations, 2 inorganic anions, as well as gelatine (5). Preparation of an aqueous basic taste recombinant (bTR) by dissolving all of the quantified substances in water in their natural concentrations, followed by sensory analysis demonstrated that the intensities of the basic taste qualities sour, bitter, sweet, salty, umami, as well as the viscosity matched those found for the authentic chicken broth. Interestingly, the thick-sour, white-meaty orosensation was perceived much more intensely in the chicken broth when compared to the tastant cocktail (5).

As the compounds inducing the thick-sour, white-meaty orosensation were not found to be present among the well-known basic taste compounds, the LMW fraction was separated by gel permeation chromatography (GPC) to give 7 fractions, which were freeze-dried, dissolved in the same volume of the bTR solution and evaluated for their taste modifying activity by means of cTDA (4, 5). GPC fraction A (Figure 1) was found to induce the thick-sour, white-meaty orosensation when added to the bTR solution, whereas an aqueous solution of this GPC fraction exhibited only a faint umami and slightly salty intrinsic taste (5). Interestingly, none of the other GPC fractions collected showed a similar sensory activity.

HPLC analysis of GPC fraction A using reversed-phase stationary phases did not allow a sufficient retention of the compounds, thus indicating a high polarity of these substances. However, a fast preliminary separation was achieved by means of a pentafluorophenylpropyl (PFPP) stationary phase (5) delivering several subfractions, amongst which only the late eluting fraction B (Figure 1) was found to impart the characteristic thick-sour, white-meaty orosensation when dissolved in the bTR solution. This active fraction was further separated by means of hydrophilic interaction liquid chromatography (HILIC) (5) to yield several subfractions which again were evaluated for inducing the thick-sour, white-meaty orosensation. Comparative sensory profile analysis of these HILIC fractions dissolved in the bTR solution enabled the localization of the taste modulating compounds in the major fraction C (Figure 1), whereas all the other HILIC fractions showed only low activity, or were inactive.

To identify the molecules inducing the thick-sour, white-meaty orosensation, fraction C was separated by re-chromatography and the subfractions analysed by means of LC-MS/MS as well as NMR experiments. Based on the spectroscopic data

and co-chromatography with commercial reference compounds, β -alanyl-*N*-methyl-L-histidine (L-anserine), β -alanyl-L-histidine (L-carnosine), as well as the previously not reported β -alanyl-glycine were identified as the taste modulating compounds in fraction III-8/5.

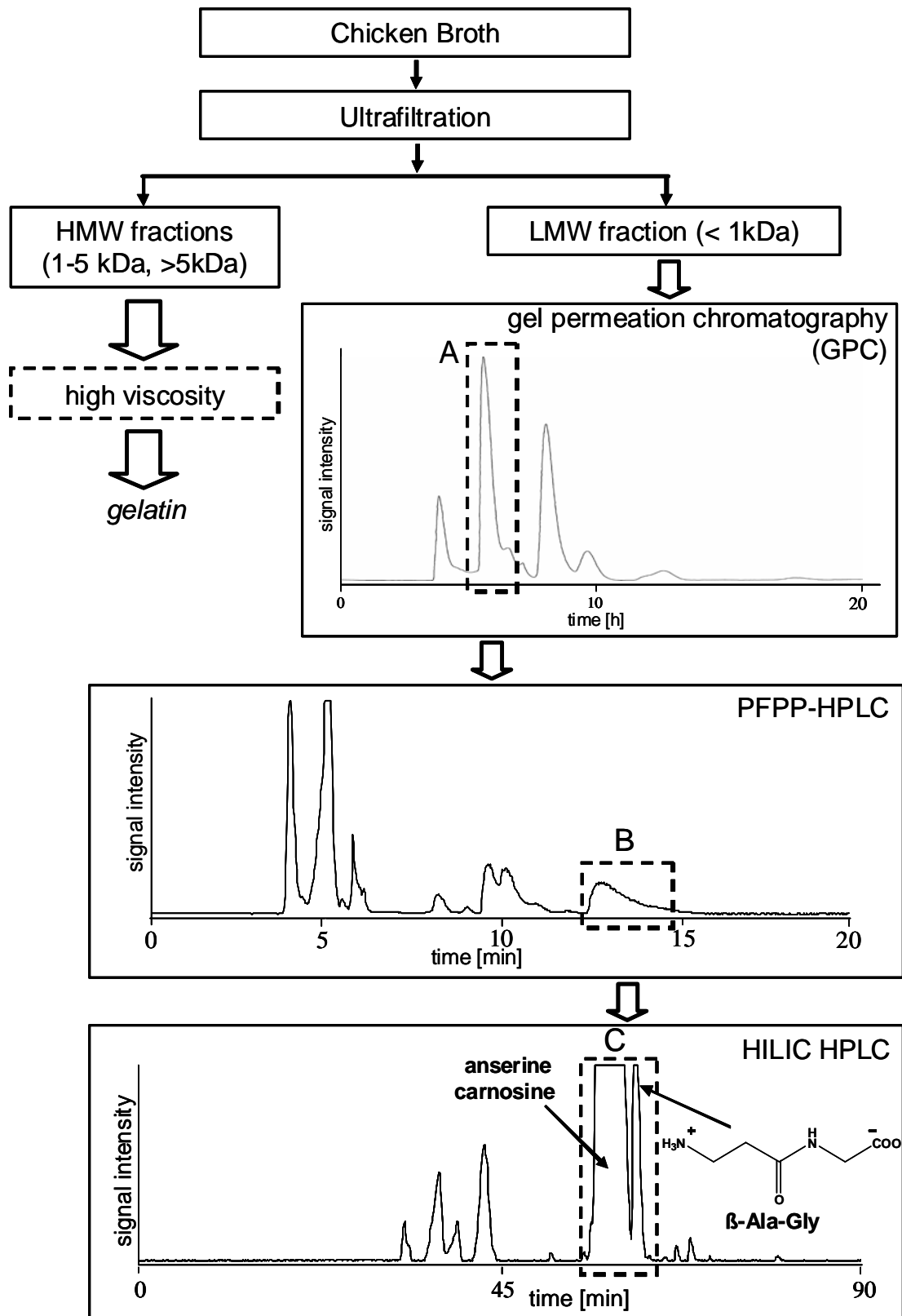


Figure 1. Flow-diagram depicting the activity-guided isolation of taste-modulating β -alanyl peptides from chicken broth.

Quantitation and recombination experiments. Quantitation of the identified β -alanyl dipeptides was performed by means of HILIC-HPLC coupled to an electrospray tandem mass spectrometer running in the multiple reaction monitoring (MRM) mode (5). Rather high concentrations were found for the three taste-modulating peptides, e.g. 1340 mg/L for L-anserine, 660 mg/L for L-carnosine, followed by 300 mg/L for the previously not reported β -alanyl-glycine.

In order to confirm the taste modulatory activity of these peptides, these peptides were dissolved in the up-mentioned amounts in the basic taste recombinant (bTR) to yield the total taste recombinant (tTR), which was then compared to the authentic chicken broth by means of taste profile analysis. To achieve this, the intensities of the taste qualities sweet, bitter, salty, umami, and sour as well as the viscosity and the thick-sour, white-meaty orosensation were judged on a linear scale from 0 (not detectable) to 5 (strongly detectable). As given in Table 1, the authentic chicken broth was characterised by an intense umami taste (4.0) and sourness (3.5), whereas bitterness and sweetness were not perceived at all. In addition, a rather high viscosity (3.5) and the thick-sour, white-meaty impression (4.0) was described by the sensory panel. The bTR solution containing the 50 basic taste compounds in their natural concentrations showed a good congruence for the basic taste qualities, but showed only low ratings for the typical thick-sour, white-meaty orosensation (1.5). Interestingly, spiking the bTR solution with the three β -alanyl dipeptides L-carnosine, L-anserine, and β -alanyl-glycine in their natural concentrations drastically enhanced the thick-sour, white-meaty impression, e.g. the intensity of this sensation in the tTR solution was evaluated with a value of 3.8 being close to the value found for the authentic chicken broth (Table 1). These data clearly demonstrate the key role of these peptides in evoking the thick-sour, white-meaty orosensation induced by chicken broth.

Table 1. Taste profile analysis of authentic chicken broth (CB), basic taste recombinant (bTR), and total taste recombinant (tTR) including L-carnosine, L-anserine, and β -alanyl-glycine.

Sample	Sweet	Bitter	Salty	Umami	Sour	Thick-sour, white-meaty sensation	Viscosity
CB	0	0	2.0	4.1	3.5	4.0	3.5
bTR	0	0	1.9	4.0	3.5	1.5	3.5
tTR	0	0	2.0	4.0	3.6	3.8	3.5

References

1. Chen C.-W., Ho C.-T. (1998) In *Flavor of meat, meat products and seafoods* (Shahidi, F., ed.); Blackie Academic and Professional, pp 84-100.
2. Fujimura S.; Koga H.; Takeda H.; Tone N.; Kadowaki M., Ishibashi T. (1996) *Anim. Sci. Technol.* 67: 423-429.
3. Kato H.; Nishimura T. (1987) In *Umami: A basic taste* (Kawamura Y; Kare M.R., eds); Marcel Dekker, pp 289-306.
4. Ottinger H.; Soldo T.; Hofmann T. (2003) *J. Agric. Food Chem.* 51: 1035-1041.
5. Dunkel A.; Hofmann T. (2009) *J. Agric. Food Chem.* 57: 9867-9877.

LC TASTE[®] AS A NOVEL TOOL FOR THE IDENTIFICATION OF FLAVOUR MODIFYING COMPOUNDS

K.V. Reichelt¹, R. Peter², M. Roloff², J.P. LEY², G.E. Krammer², and K.-H. Engel¹

¹ *Technische Universität München, Chair of General Food Technology, Am Forum 2, D-85350 Freising-Weihenstephan, Germany*

² *Symrise GmbH & Co. KG, Flavor & Nutrition, Research & Innovation, P.O. Box 1253, D-37601 Holzminden, Germany*

Abstract

LC Taste[®] methodology, which allows direct correlation between analytical data and online *in-vivo* sensory evaluation, was tested for the ability to identify taste modulating compounds from complex plant derived matrices. Tests were carried out using the known flavour modifying compounds homoeriodictyol (HED), sterubin and hesperetin either alone or in combination to evaluate their taste modifying effects after fractionation via high temperature liquid chromatography. In addition, fractions of Herba Santa methanolic extract, containing these three compounds was also tested. Bitter masking and sweet enhancing effects, respectively, were clearly detectable in the relevant fractions.

Introduction

Flavour and taste modification (bitter masking, sweet or salt enhancing, etc.) is currently an important topic for the food industry (1, 2). In many products the contents of salt and nutritive sweet carbohydrates have to be reduced which leads to a change in taste profile. Compounds such as polyphenols which are added to various types of foods providing health benefits often show bitter taste. These unwanted side effects are in most cases not tolerated by the consumer.

Flavour modifiers are commonly defined as substances which have no typical flavouring properties per se but which are able to modify the flavour profile of other flavouring substances. In combination with other flavouring substances and food ingredients these substances are able to modify the flavour profile of flavoured foods. This consequently leads to a modified perception of the foodstuff by panellists and consumers and is reflected in reproducible changes of flavour profiles in sensory (3).

In addition to the fact that these compounds have little or no intrinsic taste, but show their effects only in the presence of taste-active compounds, detection of taste modifiers in natural sources is frequently hindered by the complexity of plant extracts which makes the work laborious as well as time and cost intensive. Typical methods developed for the identification of flavour modifying compounds are taste dilution analysis (TDA), comparative taste dilution analysis (cTDA) or dose over threshold (DoT) analysis, which in general are rather time consuming (4, 5, 6).

To accelerate and to simplify the identification of novel taste modifying compounds from plant extracts, an extension of the known LC Taste[®] methodology (7, 8) was developed, which allows correlating data from real-time analysis and *in vivo* detection of relevant taste modifying compounds by a specially trained sensory panel (Figure 1).

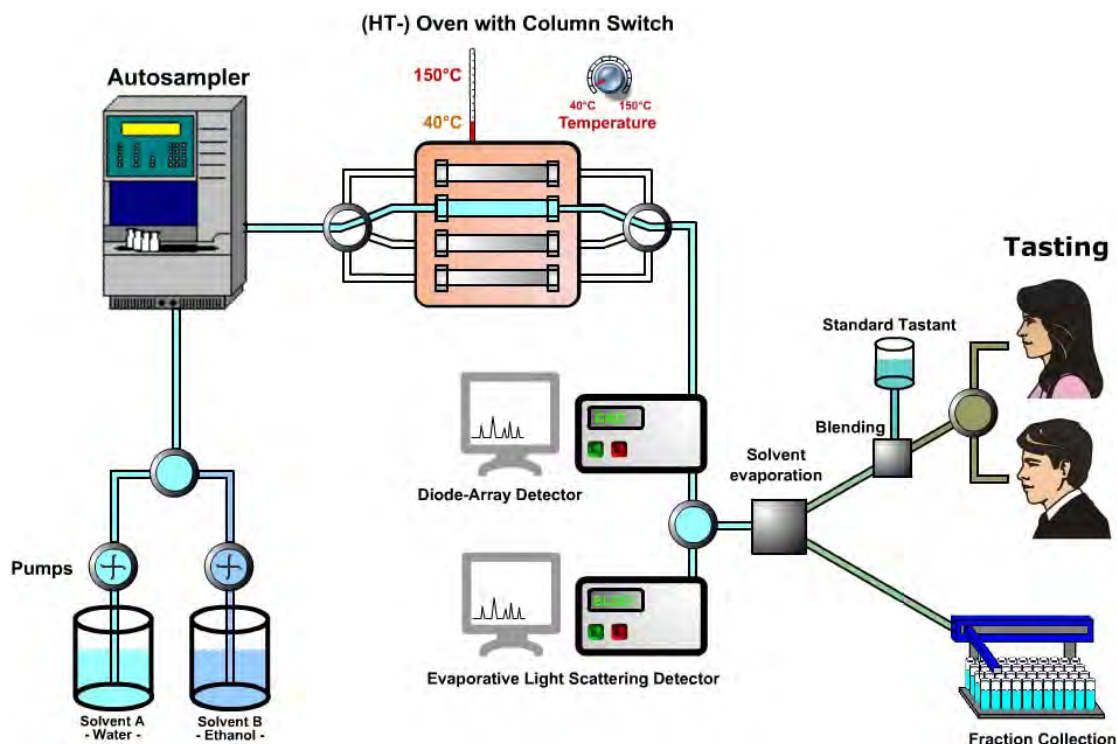


Figure 1. Schematic representation of LC Taste[®] device.

Experimental

Chemicals and extracts. Homoeriodictyol (HED) and sterubin were isolated according to (9). Hesperetin was purchased from Sigma (Steinheim, Germany). Dried *Eriodictyon californicum* leaves (500 g) were treated with 3.2 l of boiling water for one hour to break up the plant material. The plant material was filtered, dried and extracted 3 times with 2.0 l of methanol each for one hour. The resulting methanolic extract was evaporated to dryness (97.7 g).

High temperature high performance liquid chromatography (HTLC). The HPLC apparatus consisted of two pumps (SunChrom HPLC pump SunFlow 100; SunChrom, Friedrichsdorf, Germany), an injector (100 µl loop; Midas, Spark, AJ Emmen, The Netherlands), a column oven (Polaratherm Series 9000; Selerity Technologies Inc., Salt Lake City, Utah, USA), an ELSD detector (Sedex 85 LT-ELSD, Sedere, Alfortville, Cedex, France) and a diode array detector (SunChrom SpectraFlow, SunChrom, Friedrichsdorf, Germany), monitoring the effluent in a wavelength range between 200 nm and 400 nm. Separations were performed with a Hamilton PRP-1 reversed phase column (Hamilton Company, Reno, Nevada, USA) in a 250 x 10 mm semi-preparative scale with a particle size of 10 µm. After injection of the sample (100 µl full loop) the analysis was carried out at 120°C isotherm using a water/ethanol gradient with a flow rate of 3 ml/min to elute the compounds.

Sensory studies. Thresholds for basic tastes were determined with a panel of 12-16 specially trained, healthy persons without any reported taste disorders using sucrose, sodium chloride, citric acid, caffeine and mono sodium glutamate either as described in (10) or after fractionation via high temperature liquid chromatography. Masking and enhancing studies were done using paired comparison test method using water fractionated under the same conditions as a reference. Samples were blinded and coded and presented in randomized order.

Results

In order to determine the performance of both the novel LC Taste[®] technology and the panel, taste recognition thresholds for basic tastes were determined. There were no significant differences between LC Taste[®] and conventional determination of thresholds. Furthermore, known taste modifying compounds such as HED, sterubin (9) and hesperetin (11) (Figure 2) were subjected to HTLC, diluted 1:10 with standard solutions containing caffeine (500 ppm) and sucrose (5%), respectively, to yield final concentrations of 50 ppm each and evaluated sensorially by the dedicated panel to determine bitter masking and sweet enhancing effects of these compounds (Figure 3). As a comparison, water was fractionated under the same conditions, diluted with the test solutions as described above and presented to the panellists. Normalized modulation probability (NMP) factor of both samples, showing the presumption of a tested compound or fraction to have taste modulating effects was calculated as follows

$$\text{NMP} = (n_{\text{higher}} - n_{\text{lower}}) / n_{\text{total}}$$

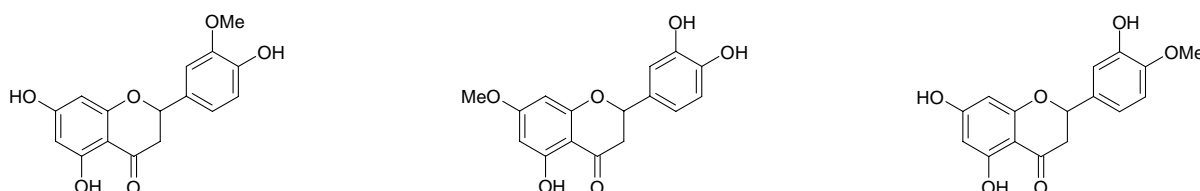


Figure 2. Chemical structures of homoeriodictyol (HED), sterubin & hesperetin from *Herba Santa* (*Eriodictyon californicum* (H. & A.) Torr., Hydrophyllaceae).

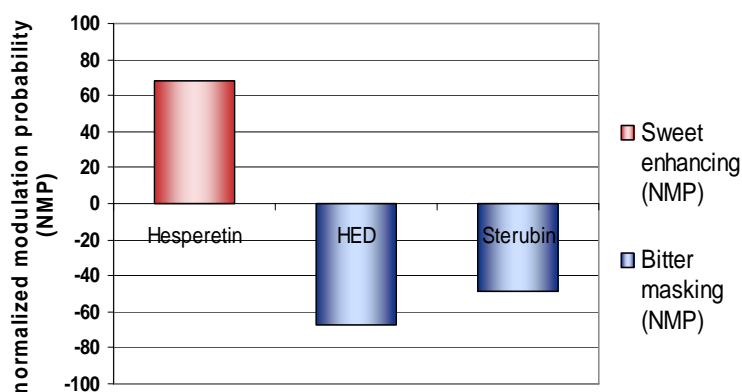


Figure 3. NMP-factors for hesperetin, HED (tested as sodium salt) and sterubin tested as single compounds (50 ppm each) on caffeine and sucrose solution after fractionation via LC Taste[®] ($n=15$).

A recombine from methanolic *Herba Santa* extract was prepared, containing the before tested compounds HED (80 ppm in final solution), hesperetin (20 ppm) and sterubin (40 ppm) and separated and fractionated via HTLC. The eluate was diluted 1:10 with the testing solutions containing sucrose or caffeine and evaluated by the sensory panel to determine the taste modulating properties of the recombine fractions in comparison to samples containing no test compound (Figure 4).

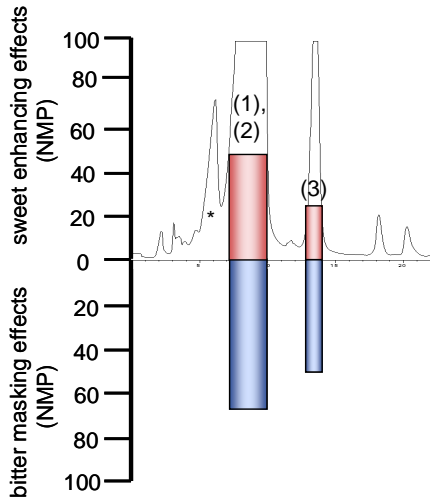


Figure 4. NMP-factors for hesperetin (1, 20 ppm), HED (2, 80 ppm; tested as sodium salt), and sterubin (3, 40 ppm) tested as recombine from Herba Santa extract on caffeine and sucrose solution after fractionation via LC Taste[®] (n= 15).

In addition, methanolic Herba Santa extract was separated via HTLC and fractionated. Selected fractions, including those containing HED, hesperetin and sterubin were diluted with testing solutions and evaluated sensorially by an expert panel (n= 8) to identify possible taste modulating effects (Figure 5). As described above, samples fractionated under the same conditions but containing no test compound served as reference samples.

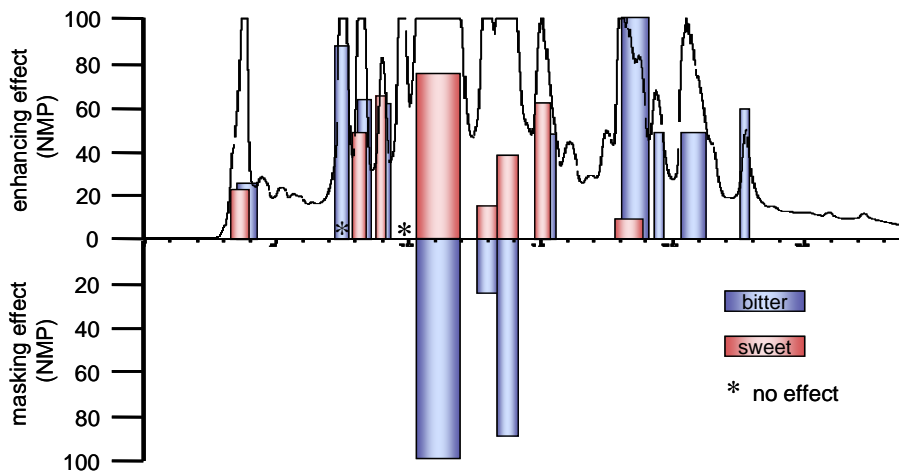


Figure 5. NMP-factors for selected peaks from Herba Santa extract tested on sucrose and caffeine solution after fractionation via LC Taste[®] (n= 8).

It was shown that the taste modulating effects of the tested single compounds HED, hesperetin and sterubin were detectable by sensory analysis using LC Taste[®]. The same effect was shown for a recombine of Herba Santa extract, containing the three compounds mentioned above. Herba Santa extract was separated and fractionated via HTLC under the same conditions. Selected peaks were tested for their taste modulating properties using sucrose and caffeine solution as test solution. Two fractions, containing the taste modulating compounds HED, hesperetin and sterubin clearly showed sweet enhancing and bitter masking effects, respectively. In

addition to this known active compounds, three other fractions showed interesting sweet enhancing effects. Several other fractions did not seem to reduce but to enhance bitterness. These fractions will be analysed in detail to know which compounds are responsible for these effects.

References

1. Ley J.P. (2008) *Chem. Percept.* 1: 58-77.
2. Ley J.P., Blings M., Paetz S., Kindel G., Freiherr K., Krammer G.E., Bertram H.-J. (2008) In *Sweetness and Sweeteners – Biology, Chemistry, and Psychophysics* (Weerasinghe D.K., DuBois G.E., eds.), American Chemical Society: Washington, DC, USA, 2008, pp 400-409.
3. Krammer G., personal communication.
4. Ottinger H., Soldo T., Hofmann T. (2003) *J. Agric. Food Chem.* 51: 1035-1041.
5. Soldo T., Hofmann T. (2005) *J. Agric. Food Chem.* 53: 9165-9171.
6. Scharbert S., Hofmann T. (2005) *J. Agric. Food Chem.* 53: 5377-5384.
7. Roloff M.; Erfurt H.; Kindel G.; Schmidt C.-O.; Krammer G.E. (2006) WO 2006/111476.
8. Krammer G. *et al.* (2006) In *Flavour Science: Recent Advances and Trends* (Bredie W.L.P., Petersen M.A., eds.), Elsevier: Amsterdam, Netherlands, pp 169-172.
9. Ley J.P.; Krammer G.; Reinders G.; Gatfield I.L.; Bertram H.-J. (2005) *J. Agric. Food Chem.* 53: 6061-6066.
10. Deutsches Institut für Normung, e.V. (2005) DIN 10959 Sensorische Prüfverfahren - Bestimmung der Geschmacksempfindlichkeit.
11. Ley J.P.; Kindel G.; Paetz S.; Riess T.; Haug M.; Schmidtman R.; Kammer G.E. (2007) WO 2007/014879.

STRUCTURAL ANALOGUES OF HISPOLON AS FLAVOUR MODIFIERS

J.P. LEY, S. Paetz, M. Blings, P. Hoffmann-Lücke, T. Riess, G.E. Krammer

Symrise GmbH & Co. KG, Flavor & Nutrition, Research & Innovation, P.O. Box 1253, D-37601 Holzminden, Germany

Abstract

Starting from the previous structure-activity relationships for bitter-masking molecules based on homoeriodictyol we have investigated into the promising class of hispolon (i.e. 1-(3,4-dihydroxyphenyl)-hex-1-en-3,5-dione) derivatives as well as dihydrochalcones. In contrast to the mostly bitter-sweet tasting phloridzin the only very weak sweet-tasting aglycon phloretin showed strong masking effects against different bitter compounds such as caffeine, salicin, and quinine. Besides their masking effects phloretin and some hispolon derivatives such as the 1-(3-hydroxy-4-methoxyphenyl)-hexan-3,5-dione ([2]-isogingerdione) show remarkably strong sweet enhancing properties

Introduction

Due to the increasing importance of healthier products, frequently ingredients are added which are good for health but poor in taste. On the other hand, some common ingredients such as sucrose or other bulk carbohydrates are used in reduced amounts or omitted totally to lower the caloric intake. Unfortunately, in most cases the taste of the products is sacrificed and therefore a high demand for flavour modifiers with low intrinsic taste such as bitter maskers (1) or umami or sweet taste enhancers (e.g. 2) has developed during the past years. Some potent new bitter masking molecules such as the 1-carboxymethyl-5-hydroxy-2-hydroxymethylpyridinium inner salt (3) and some derivatives related to the flavanone homoeriodictyol (Figure 1) (4) were developed: hydroxybenzoic acid vanillylamides (5), hydroxylated deoxybenzoins (6), and short chain gingerdiones (7) related to hispolon (8). Some of the latter derivatives showed additional sweet enhancing properties (9) without being sweet and may be used in flavours to increase preference for low-carbohydrate applications which occasionally contain also high-intensity sweeteners as well.

In the present study we have extended our previous structure-activity concepts (5, 9) starting from homoeriodictyol leading to several interesting relatives with new flavour modifying properties.

Experimental

Synthesis. Phloretin and Phloridzin were obtained from Kaden Biochemicals (Hamburg). All other chemicals were purchased from Sigma-Aldrich (Steinheim, Germany) or Acros Organics (Geel, Belgium). The syntheses of gingerdiones and dehydrogingerdiones were performed via condensation of the corresponding hydroxylated benzaldehydes with a boron complex of the acylacetone as described

earlier (6, 7). Dihydrochalcones were prepared starting using base catalyzed aldol condensation of the appropriately substituted and protected (as benzyl derivatives) acetophenones and benzaldehydes, respectively, by subsequent combined debenzylation and reduction of the intermediate chalcones by catalytic hydrogenation similar to the described procedures (e.g. 10). All compounds were verified by ^1H - and ^{13}C -NMR and LC-MS spectroscopic methods following to purification via flash chromatography up to 95 % (HPLC).

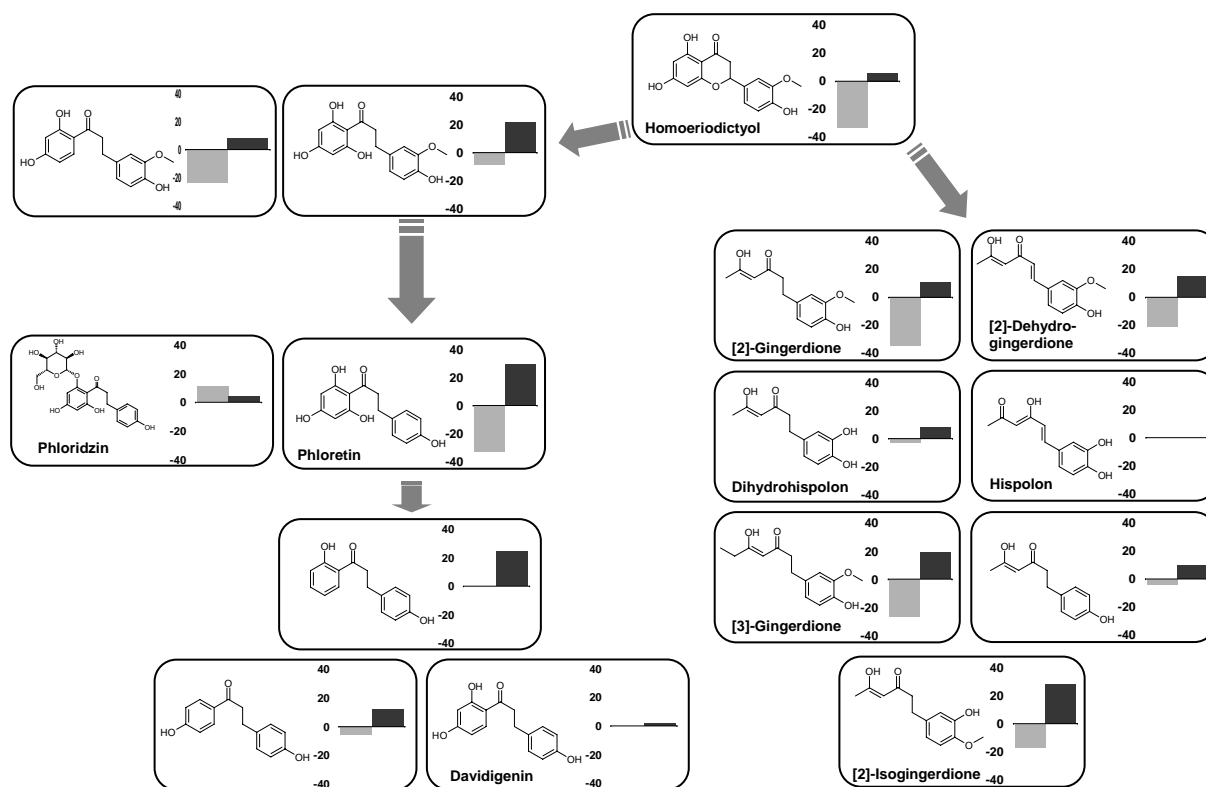


Figure 1. Sweet enhancing activity in a 5 % sucrose base (black) and bitter masking effect towards 500 ppm caffeine (gray) of various dihydrochalcones, gingerdiones, and dehydrogingerdiones related to homoeriodictyol.

Sensory studies. Masking and enhancing studies were done using the duo-comparison method with a panel of 12-16 trained, healthy persons without any reported taste disorder. Samples were blinded, coded and presented in randomized order. Panellist had to rate the intensity of the basic taste quality on a scale of 1 (nothing) to 10 (extremely strong). Modifying effects were calculated relative to the blind sample by $\text{modifying effect} = [\text{rating}(\text{test}) / \text{rating}(\text{blind})] - 1$.

Intrinsic sweetness was determined by comparing the blinded test concentrations to a series of dilutions of sucrose (0%, 0.25%, 0.5%, 0.75%, 1.0%, 1.5%, 2.0%, 3.0%, 4.0%, 5.0%).

The sweetness ratings of a series of dilutions of sucrose (0.25 % – 90 %) were determined using the 1-10 scale by the panel and the dose response plot was used to normalize the enhancing ratings into sucrose equivalents (SE) (7).

For the determination of synergistic effects, for each test compound-concentration the normalized SE of the 5 % sucrose solution was added to the intrinsic sweetness (expressed as SE) of the test compound at this concentration. The sum was

compared to the SE of the experimental sweetness of 5 % sucrose solution containing the test compound.

Results

Starting from the previously described structure-activity relationships (4, 5) we have investigated into the promising class of hispolon derivatives (7) as well as tasteless dihydrochalcones to find new taste modulating molecules (Figure 1). Besides their bitter masking effects (6) some hispolon derivatives and dihydrochalcones show remarkable sweet enhancing properties without being sweet. At higher concentrations, certain dihydrochalcones such as hesperetin dihydrochalcone and especially their glycosides (e.g. neohesperidin dihydrochalcone, NHDC) are already known as sweet molecules (10) but most of the aglycons we have synthesised and tested are generally tasteless. Phloretin, in contrast to the bitter-sweet tasting phloridzin, shows strong masking effects towards different bitter compounds such as caffeine, salicin, and quinine but not for the tested bitter peptide Leu-Trp (see Figure 2). Therefore, phloretin may be a valuable tool for elucidation of bitter receptor characterization.

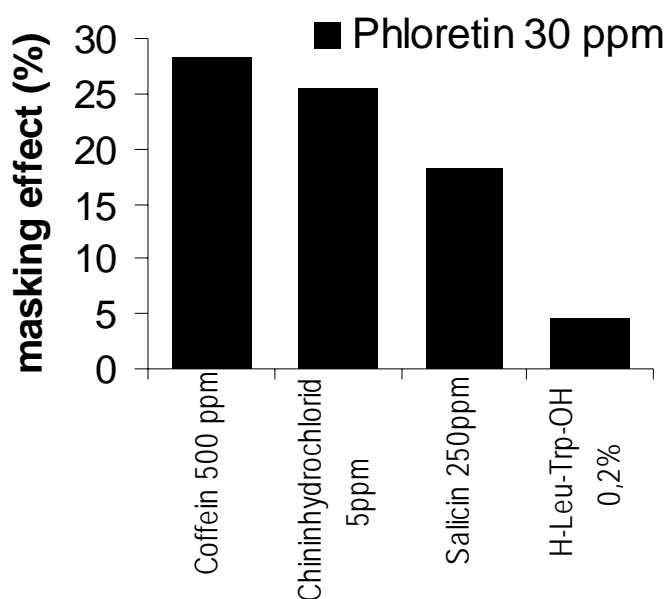


Figure 2. Masking activity of phloretin against different bitter compounds (relative expression).

Phloretin and [2]-isogingerdione exhibit both intrinsic sweetness near to or lower than 1% sucrose equivalent at 100 ppm (see Figure 3A, 3B) and show much higher sweet enhancing effects as expected by simple addition.

Thus, we conclude that the new flavour modifiers exhibit a clear synergistic effect which cannot be explained simply by competitive binding to one active site on the sweet receptor couple. Further studies considering the receptor level will be performed to elucidate the mechanism.

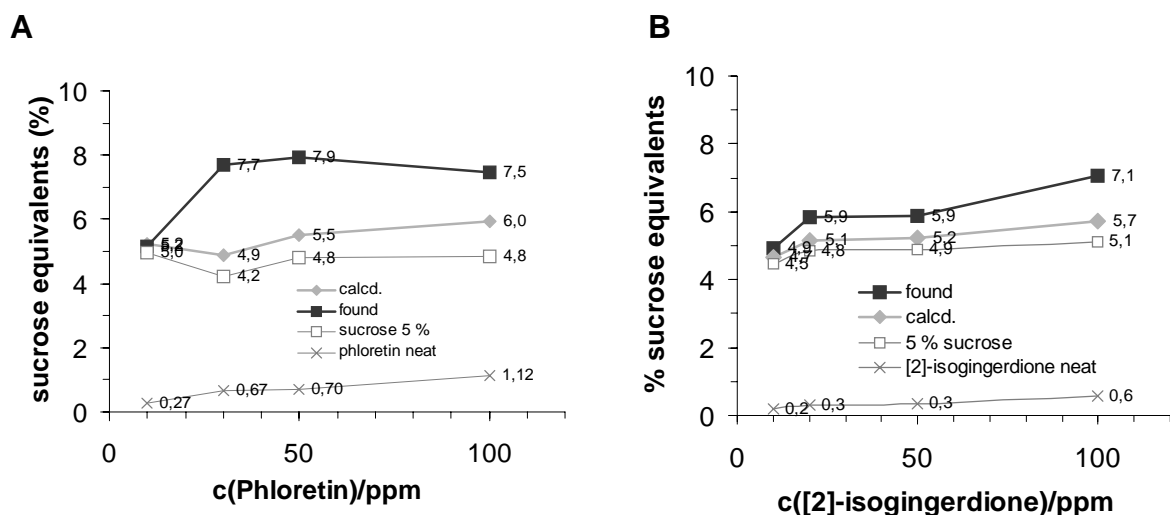


Figure 3. Comparison of intrinsic sweetness of neat phloretin (A) and neat [2]-isogingerdione (B) as well as calculated and found sweet intensities of sucrose/phloretin and sucrose/[2]-isogingerdione mixtures, respectively, normalized as sucrose % equivalents

References

- Ley J.P. (2008) *Chemosensory Perception* 1: 58-77.
- Soldo T., Blank I., Hofmann T. (2003) *Chem. Sens.* 28: 371-379.
- Soldo T., Hofmann T. (2005) *J. Agric. Food Chem.* 53: 9165-9171.
- Ley J.P., Krammer G., Reinders G., Gatfield I.L., Bertram H.-J. (2005) *J. Agric. Food Chem.* 53: 6061-6066.
- Ley J.P., Blings M., Paetz S., Krammer G.E., Bertram H.-J. (2006) *J. Agric. Food Chem.* 54: 8574-8579.
- Ley J.P., Kindel G., Paetz S., Krammer G. (2006) Symrise GmbH & Co. KG, WO 2006 106,023.
- Ley J.P., Paetz S., Blings M., Hoffmann-Lücke P., Bertram H.-J., Krammer G.E. (2008) *J. Agric. Food Chem.* 56: 6656-6664.
- Ali, N.A.A., Jansen, R., Pilgrim, H., Liberra, K., Lindequist, U. (1996) *Phytochemistry* 41: 927-929.
- Ley J.P., Blings M., Paetz S., Kindel G., Freiherr K., Krammer G.E., Bertram H.-J. (2008) In *Enhancers for sweet taste from the world of non-volatiles: polyphenols as taste modifiers* (Weerasinghe D.K., DuBois G.E., eds.), Oxford University Press: New York, USA, pp 400-409.
- DuBois G.E., Crosby G.A., Stephenson R.A. (1981) *J. Med. Chem.* 24: 408-428.

DIHYDROMALTOL (2,3-DIHYDRO-5-HYDROXY-6-METHYL-4H-PYRAN-4-ONE): IDENTIFICATION AS A POTENT AROMA COMPOUND IN RYAZHENKA KEFIR AND SENSORY EVALUATION

M. PREININGER, L. Gimelfarb, H.-C. Li, B. E. Dias, F. Fahmy, and J. White

Kraft Foods Technology Center, 801 Waukegan Road, Glenview, IL 60025, USA

Abstract

Dihydromaltol (DHM; 2,3-dihydro-5-hydroxy-6-methyl-4H-pyran-4-one) was identified as a novel potent aroma compound in a dairy product, Ryazhenka kefir, a Russian-style kefir made from cooked milk. Flavour impact of the structurally related caramelised smelling compounds, DHM, 2,5-dimethyl-4-hydroxy-3[2H]-furanone (DMHF; Furaneol[®]), 5-ethyl-4-hydroxy-2-methyl-3[2H]-furanone (EHMF; Homofuronol[®]) and maltol, was evaluated in various dairy samples by applying the odour activity value concept (OAV = concentration / odour threshold) using flavour thresholds. Besides DHM, also its novel homologue, dihydro-ethylmaltol (DHEM; 6-ethyl-2,3-dihydro-5-hydroxy-4H-pyran-4-one), was synthesised. DHEM has a caramelised odour but not been not found in nature, in contrast to its furanoid isomer, EHMF. Based on flavour thresholds in water, DHM (50-250 µg/kg) by itself was found to be approximately half as potent as DMHF but about 40-times more potent than maltol, and DHEM (10-100 µg/kg water) was found to be more potent than DHM.

Introduction

Ryazhenka kefir, a commercial, Russian-style kefir made from cultured cooked milk, has a rich, brown, creamy, cooked milk-like flavour. Because consumers desire “rich”, “creamy” flavour in dairy products, the objective of this study was to identify potent aroma compounds in Ryazhenka, and to estimate the flavour impact of selected, caramelised smelling cyclo-enolones in various liquid dairy products.

Experimental

Materials. “Ryazhenka Kefir - Cooked Cultured Milk” (3.8 % fat, live culture; Lifeway Foods Inc., IL, USA); Original Kefir (3.3 % fat; Lifeway); Evaporated Whole Milk (Carnation; Nestle Inc., USA); UHT whole milk (Gosners, UT, USA). UHT whole milk or Evaporated Whole Milk was inoculated with kefir (1 %) and incubated at 30 °C for 18 h. Cultured samples were heated (72 °C, 30 min) to inactivate cultures prior to analysis. Synthesised (Chemrise Inc.; Moscow, Russia) were 2,5-[¹³C₂]-dimethyl-4-hydroxy-3[2H]-furanone ([¹³C₂]-DMHF) (1), 5-[²H₃]-ethyl-4-hydroxy-2-methyl-3[2H]-furanone ([²H₃]-EHMF) (2), dihydromaltol (DHM; 2,3-dihydro-5-hydroxy-6-methyl-4H-pyran-4-one) and dihydro-ethylmaltol (DHEM; 6-ethyl-2,3-dihydro-5-hydroxy-4H-pyran-4-one) according to (3), starting with maltol or ethyl maltol, respectively. Chemical purity (>95 %) of DHM and DHEM was verified by ¹H-NMR and olfactory purity by GC/O. Flavour compound sources: DMHF (Furaneol[®]; Firmenich), EHMF (Homofuronol[®]; Givaudan), maltol (Phoenix Chemicals) and ethyl maltol (Citrus & Allied).

Isolation of volatiles. Similar to (4), dairy samples (25 g) were mixed with anhydrous sodium sulphate (~170 g). The resulting powder was placed in a glass vessel (3.5 x Ø11 cm) for purge-and-trap (P&T) sampling onto Tenax-TA[®] (180 mg), using nitrogen as purge gas channelled through the powder (60 °C, 70 ml/min, 90 min). For quantitation of cyclo-enolones, the liquid samples were spiked with the internal standards, [¹³C₂]-DMHF and [²H₃]-EHMF in ethanol, and equilibrated (5 °C) overnight before sample preparation for P&T.

GC/Olfactometry-Mass Spectrometry (GC/O-MS). After P&T, the volatiles of the dairy samples were thermo-desorbed (270 °C, 5 min) from the trap via a TDS-2 system (Gerstel; Germany) into a Cool Injection System (CIS4, Gerstel) for simultaneous GC/O-MS analysis (GC6890, Agilent Technologies, USA; ODP2, Gerstel; MSD5973, Agilent) using FFAP or DB5 capillaries (Agilent). Column temperature programming was similar to (3).

GC-MS quantitation. As in GC/O-MS, the volatiles were thermo-desorbed from traps via a TDS-3 into a CIS4 for quantitative analysis on a HP-FFAP capillary (30 m x 0.25 mm ID x 0.25 µm film; Agilent) coupled with an MSD5975 (Agilent) operated in EI-SCAN mode. For quantitation of dihydromaltol and maltol via [¹³C₂]-DMHF, and DMHF and EHMF via their corresponding isotope standards, the peak area of the extracted molecular ion trace of each compound was normalized based on its percentage versus its TIC peak area in a standard mixture that was analysed under the same conditions. No recovery factors were applied in quantitative calculation.

Results and Discussion

Using P&T-TDS-GCO/MS, three GC-sniffers found the caramelised smelling 2,3-dihydromaltol (DHM; Kováts RI_{FFAP}: 1876; RI_{DB-5}: 1092-1098) among the ten most intense odorants in Ryazhenka kefir, besides hexanoic acid, trans-4,5-epoxy-(E)-2-decenal, DMHF, butyric acid, (E)-2-nonenal, 2-acetyl-1-pyrroline, methional, dimethyltrisulphide and 1-octen-3-one (data not shown). DHM was found for the first time as a potent odorant in a dairy product, and its identity confirmed by same analysis of synthesised DHM. DHM and DMHF coelute on a DB-5 capillary and have very similar odour and mass spectrum, hence the use of FFAP for detection of DHM being crucial.

In order to evaluate and compare the flavour impact of selected, caramelised smelling cyclo-enolones (DHM, DMHF, EHMF, maltol) in various dairy samples, the odour activity value concept (OAV = concentration / odour threshold) (5) was applied, using flavour/taste thresholds in water. The flavour thresholds for DHM were determined as 50-250 µg/kg in water and skim milk (Table 1), thus DHM by itself being about half as potent as DMHF (30 µg/kg water) (6) but much more (~ 40x) potent than maltol (7,100-13,000 µg/kg water) (6, 7).

Dihydro-ethylmaltol (DHEM; RI_{FFAP}: 1901; RI_{DB-5 (J&W)}: 1166) was synthesised as a novel homologue of DHM. DHEM also has caramelised odour but has not been found in nature, in contrast to its furanoid isomer, EHMF. DHEM (MS-EI data): *m/z* 43 (10 %), 57 (100 %), 58 (36 %), 69 (4 %), 86 (17 %), 99 (3 %), 114 (2 %), 127 (2 %), 141 (5 %), 142 (83 %, MW), 143 (7 %). DHEM (¹H-NMR (CDCl₃) data): δ 1.69 ppm, 3H, tr.; δ 2.44 ppm, 2H, q.; δ 2.62 ppm, 2H, tr.; δ 4.33 ppm, 2H, tr.. The flavour threshold of DHEM (10-100 µg/kg water) was determined and is lower than that of DHM, similar to the difference between DMHF and EHMF (5 µg/kg water) (8). Other derivatives of DHM also have caramel aroma, except for the non-planar 2,2-dimethyl-DHM (9), confirming the structure-odour hypothesis of (10).

Table 1. Sensory threshold values ($\mu\text{g}/\text{kg}$) of dihydromaltol (DHM) and dihydro-ethylmaltol (DHEM) at 25 °C.

Threshold ($\mu\text{g}/\text{kg}$) for:	Dihydromaltol ^a	Dihydro-ethylmaltol ^b
Flavour in water	50 (3/6) ^c - 250 (6/6)	10 (4/5) - 100 (4/5)
fFlavour in skim milk	50 (3/7) - 250 (6/7)	n.d.
Flavour in 2 % milk	≤ 50 (7/7) (cooked milk like)	100 (2/3)
Odour in water	250 (3/6) - 1000 (4/6)	n.d.
Detection in water	25 (3/6) (milky mouthfeel; no aroma or flavour; 6/6)	n.d.

^a Matrix spiked with DHM at 25 (not for 2 % milk), 50, 250, 1000, 2000, 3000, 5000 and 10,000 $\mu\text{g}/\text{kg}$.

^b Matrix spiked with DHEM at 10, 100, 1000 and 12,000 $\mu\text{g}/\text{kg}$.

^c Ratio of panellists able to identify the spiked sample from the un-spiked matrix in comparison, starting with lowest spike concentration.

n.d. = not determined

Based on its highest OAVs (OAV: 18-56, Table 2) compared to the other enolones, DMHF is the dominant caramelised flavour impact compound in commercial Ryazhenka kefir made with cooked milk (No. 1, 2), in Ryazhenka grown on UHT-milk (No. 4-6) or on evaporated milk (No. 8, 9), and in evaporated milk (No. 7). However, DMHF has no or little flavour impact in UHT-milk (OAV: <1, No. 3), cream (OAV: <1, No. 12) or heated cream (80 °C for 8 h; OAV: 2, No. 13). DHM (OAV: 1-6) and EHMF (OAV: 1-18) have low to medium flavour impact in Ryazhenka samples (No. 1, 2, 4-6, 8, 9), but close to none in UHT-milk, evaporated milk, and cream (all OAV: <1). Only trace amounts of DHM (<10 $\mu\text{g}/\text{kg}$) were found in Original Kefir made commercially with pasteurized milk (No. 10) or grown on UHT-milk (No. 11). Maltol does not reach its flavour threshold in any of the measured liquid dairy samples, and therefore, has the lowest flavour impact among the analysed cyclo-enolones.

Based on GC/O data, DHM was reported as an important odorant in sweet bell pepper powder (11), was identified among the most odour active volatiles in barley malt (3), and was reported to contribute to the “toasty caramel” aroma of heated oak used in wine making (12). Among other volatile compounds, DHM was quantified in various wines (13) and its content monitored during aging of sweet fortified wines under aerobic and anaerobic conditions (14). Although the aroma impact of the measured wine volatiles was discussed using data similar to OAVs, sensory threshold data of DHM were not reported. In aqueous Maillard reaction models, DHM was identified from the reaction of D-glucose with L-phenylalanine under anaerobic boiling conditions (15). Using stable isotope labelled compounds in aqueous Maillard reaction models, a possible pathway has been suggested for the thermal generation of DHM from 2,3 dihydro-3,5-dihydroxy-6-methyl-4H-pyran-4-one (3-hydroxy-DHM), a Maillard reaction intermediate from hexoses (16).

Table 2. Concentration and Odour Activity Values (OAV) of potent caramelised smelling aroma compounds in dairy samples ¹.

No.	Sample	Concentration (µg/kg)				OAV = conc. / flavour threshold ²			
		Dihydro-maltol	DMHF	EHMF	Maltol	Dihydro-maltol	DMHF	EHMF	Maltol
1	RK1: "Ryazhenka Kefir"	746	1618	21	3312	3.0	54	4.2	0.3
2	RK2: "Ryazhenka Kefir"	574	781	<5	4576	2.3	26	<1	0.5
3	UHT-milk	<20	<20	<5	4831	<<1	<1	<1	0.5
4	RK3: UHT-milk fermented with RK1 inoculate	416	640	21	4995	1.7	21	4.2	0.5
5	RK4: UHT-milk fermented with RK1 inoculate (pH 4.1)	271	540	6	n.a.	1.1	18	1.2	n.a.
6	RK5: UHT-milk fermented with RK1 inoculate (pH 5.4)	217	574	8	n.a.	0.9	19	1.6	n.a.
7	Evaporated milk	25	526	<5	3671	<<1	18	<1	0.4
8	RK6: evaporated milk fermented with RK1 inoculate	1405	1404	56	7508	5.6	47	11	0.8
9	RK7: evaporated milk fermented with RK1 inoculate	1392	1677	88	5216	5.6	56	18	0.5
10	OK1: "Original Kefir"	8	n.a.	n.a.	n.a.	<<1	n.a.	n.a.	n.a.
11	OK2: UHT-milk fermented with OK1 inoculate	<10	79	<5	n.a.	<<1	2.6	<1	n.a.
12	Cream, fresh	<5	21	<5	12	<<1	0.7	<1	<<1
13	Cream, heated (80 °C for 8 h)	<5	55	<5	270	<<1	1.8	<1	<<1

¹ Aroma compounds quantified using internal standards, [¹³C₂]-DMHF and [²H₃]-EHMF (acronyms defined in text); no recovery factors applied.

² Flavour thresholds in water (see text): dihydromaltol (250 µg/kg; Table 1), Furaneol (30 µg/kg), EHMF (5 µg/kg); maltol (10,000 µg/kg).

n.a. = not analysed

References

1. Sen A., Schieberle P., Grosch W. (1991) *Lebensm. Wiss. Technol.* 24: 364-369.
2. Blank I., Fay L.B., Lakner F.J., Schlosser M. (1997) *J. Agric. Food Chem.* 45: 2642 -2648.
3. Fickert B., Schieberle P. (1998) *Nahrung / Food* 42: 371-375.
4. Buttery R.G., Takeoka G.R., Naim M., Rabinowitch H., Nam Y. (2001) *J. Agric. Food Chem.* 49: 4349-4351.
5. Grosch W. (2001) *Chem. Senses* 26: 533-545.
6. Pittet A., Rittersbacher P., Muralidhara R. (1970) *J. Agric. Food Chem.* 18: 929-933.
7. Leffingwell & Assoc. (1999) Odor Properties & Molecular Visualization - Burnt sugar, caramel & maple notes. <http://www.leffingwell.com/burnt.htm>.
8. Guth H. (1996) Habilitation script. Technical University, Munich-Garching, Germany.
9. Gelin S. (1975) *Tetrahedron Lett.* 48: 4255-4258.
10. Hodge J.E. (1967) In *Symposium on Foods. Chemistry and Physiology of Flavors* (Schultz H.W., Day E.A., Libbey L.M., eds.); AVI Publishing, Westport, Connecticut, pp 465-49
11. Zimmermann M., Schieberle P. (2000) *Eur Food Res Technol* 211: 175-180.
12. Cutzach I., Chatonnet P., Henry R., Pons M., Dubourdieu D. (1997) *J. Agric. Food Chem.* 45: 2217-2224.
13. Cutzach I., Chatonnet P., Henry R., Pons M., Dubourdieu D (1998) *J. Int. Sci. Vigne Vin* 32: 211-221.
14. Cutzach I., Chatonnet P., Dubourdieu D. (1999) *J. Agric. Food Chem.* 47: 2837-2846.
15. Mevissen L., Baltes W. (1983) *Z. Lebensm. Unters. Forsch.* 176: 206–207.
16. Kim M.O., Baltes W. (1996) *J. Agric. Food Chem.* 44: 282-289.

CHARACTERIZATION OF COMPOUNDS INVOLVED IN SPECIFIC FRUITY AROMAS OF RED WINES

B. Pineau¹, J.-C. BARBE^{1,2}, C. van Leeuwen², D. Dubourdieu¹, and Ph. Darriet¹

¹ *Institut des Sciences de la Vigne et du Vin - UMR 1219 Œnologie, Faculté d'Œnologie - 210, chemin de Leysotte - CS 50008 - 33882 VILLENAVE D'ORNON Cedex*

² *ENITA de Bordeaux - 1, Cours du général de Gaulle - CS 40201 - 33175 GRADIGNAN Cedex*

Abstract

Preparative HPLC method, which preserves wine aromas and isolates fruity characteristics in specific fractions, was applied to red wine aroma extracts. Various odour-active zones were detected in typical fractions. Aromatic compounds responsible for 18 of these zones were identified as various ethyl esters and acetates. In view of their olfactory thresholds, the concentrations of these compounds present had no direct impact on the fruity aroma of red wines. Nevertheless, an overall sensory effect was clearly established in red wine, leading to “red berry” or “black berry” nuances. Higher than average levels of ethyl propanoate, ethyl 2-methylpropanoate, and ethyl 2-methylbutanoate were involved in black-berry aromas, while higher concentrations of ethyl butanoate, ethyl hexanoate, ethyl octanoate, and ethyl 3-hydroxybutanoate conferred red-berry aromas. Interactions were also investigated between ethyl esters and β -damascenone or 3-mercaptohexan-1-ol, impacting the perception of ethyl propanoate and ethyl butanoate.

Introduction

Today, one of the major challenges in red wine production and research is to obtain typical red- and black-berry aromas, which have not yet been fully explained. Preparative High Pressure Liquid Chromatography (HPLC) methods have been recently developed (1), which could offer a way of isolating groups of volatiles, prior to Gas-Chromatography-Olfactometry (GC-O) analyses. The main goals of our study were, on the one hand, to determine how to apply this preparative HPLC method to the selection and characterization of the highly-specific red- and black-berry aromas of red Bordeaux wines and, on the other hand, to study the real impact of the compounds characterised using sensory reconstitution tests.

Experimental

Wine extraction for HPLC assays. 1 mL wine extract was obtained from 500 mL wine, extracted using 100 mL, 50 mL, and 50 mL dichloromethane.

Wine extraction for ester quantification. 250 μ L wine extract was obtained from 50 mL wine, spiked with 20 μ g octan-3-ol (internal standard) and extracted using 3 x 5 mL diethyl ether/pentane (1:1, v:v).

Gas Chromatography–Mass Spectrometry (GC-MS) and GC-O. A concentrate (2 μ L) was obtained with diethyl ether/pentane. For chromatographic conditions see (2).

Fruity fraction extraction. Fractions 17 to 21, blended and diluted in 35 mL distilled water, were extracted with the same method as the wine samples, but with 3 x 5 mL dichloromethane, producing a 200 µL final volume of extract.

Reversed Phase HPLC assays were performed using a Waters C18 column (30 cm x 3.9 mm i.d.). Chromatographic conditions were taken from (1). The 25 fractions obtained were then directly evaluated by three trained assessors.

De-aromatised red wine was prepared as described by Pineau *et al.* (3)

Sensory analyses were performed in black glasses, using triangle tests. Panel 1 consisted of Oenology students, who received weekly training sessions, whereas the winemakers and researchers from Bordeaux faculty of Oenology in panel 2 were all experienced in wine tasting.

On the one hand, sensory reconstitution tests were performed, using HPLC fruity fractions 19 to 21. In each test, two samples corresponded to an aromatically-neutral dry white wine (Muscadet wine) alone, while the third was spiked with HPLC fraction(s), added individually or blended together, to reproduce the initial concentrations in the original red wines. Simple olfaction was performed by panel 2 (11 participants) to detect the single sample. When detected, the intensity of its fruity aroma was evaluated on a 5-point scale.

Sensory reconstitution tests were performed, using pure esters, and two matrices: a dilute alcohol solution and a de-aromatised red wine (3). Each matrix was spiked with 12 esters, at the average concentrations found in red wines, to obtain 2 initial matrices (Table 1). Different test matrices were then prepared by adding again some of the above ethyl esters to the initial matrices, to reach their maximum concentrations found in red wines (Table 1).

The method consisted in comparing the initial matrices with each of the test matrices in triangle tests. In tests 4 and 9, participants who detected the test matrix were then asked to describe the fruity nuances in the sample by choosing 2 descriptors among the following: redcurrant, raspberry, strawberry, cherry, blackberry, and blackcurrant.

Table 1. Concentrations of 12 ethyl esters and acetates (µg/L) in initial and test matrices used for triangle sensory reconstitution tests.

	C2iC4	C2iC5	C2C4	C2C6	C2C8	2Me-C3C2	2Me-C4C2	3OH-C4C2	C3C2	C4C2	C6C2	C8C2
Initial matrix	65	935	1,5	7,4	0,2	16	2	534	13	208	386	358
TM - test 1	65	935	1,5	7,4	0,2	16	2	534	80	208	386	358
TM - test 2	65	935	1,5	7,4	0,2	40	2	534	13	208	386	358
TM - test 3	65	935	1,5	7,4	0,2	16	5	534	13	208	386	358
TM - test 4	65	935	1,5	7,4	0,2	40	5	534	80	208	386	358
TM - test 5	65	935	1,5	7,4	0,2	16	2	534	13	400	386	358
TM - test 6	65	935	1,5	7,4	0,2	16	2	534	13	208	700	358
TM - test 7	65	935	1,5	7,4	0,2	16	2	534	13	208	386	700
TM - test 8	65	935	1,5	7,4	0,2	16	2	900	13	208	386	358
TM - test 9	65	935	1,5	7,4	0,2	16	2	900	13	400	700	700

C2iC4: isobutyl acetate, C2iC5: isoamyl acetate, C2C4: butyl acetate, C2C6: hexyl acetate, C2C8: octyl acetate, 2MeC3C2: ethyl 2-methylpropanoate, 2MeC4C2: ethyl 2-methylbutanoate, 3OHC4C2: ethyl 3-hydroxy-butanoate, C3C2: ethyl propanoate, C4C2: ethyl butanoate, C6C2: ethyl hexanoate, C8C2: ethyl octanoate. TM: tested matrix.

Results

Applying preparative HPLC to a wine extract resulted in 25 fractions in diluted alcoholic media. It was thus possible to describe the aromatic characteristics of each fraction by direct olfaction. As evidenced by analyses performed on various red wines, fruity characteristics were kept from wines to fractions.

Moreover, the aromatic impact of each fraction was clearly demonstrated by reconstitution tests, with significant detection rates in each case. The simplest matrix led to the highest detection rates: 95% of the panel detected fractions 19 or 20 in diluted alcoholic solution, but only 60% in de-aromatised red wine. As shown in Figure 1, each fraction gave a clearly identified red-/black-berry aroma to a white wine with no intrinsic fruity aromas. The highest intensity was obtained when all 3 fractions were combined. The aromatic compounds in these fractions were thus shown to contribute to the fruity characteristics of red wines.

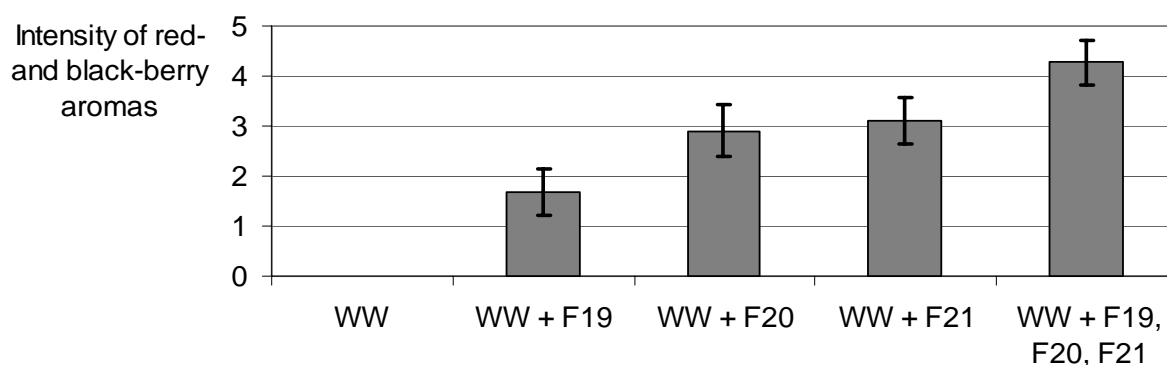


Figure 1. Intensity of the perception of specific red- and black-berry aromas in a white wine spiked with fruity fractions selected from fractionated red wine. WW: dry white wine, F19: fraction 19, F20: fraction 20, F21: fraction 21.

Globally, following fractionation of various red wines, red- and black-berry aromas were perceived in fractions 17 to 21. A blend of these characteristic fractions from each wine was analysed by GC-O. Using BPX-5 and BP-20 columns, 51 and 42 fruity odour-active zones were detected, respectively. The aromatic compounds responsible for 18 of the most intense odour-active zones were identified by GC-MS as various esters.

From quantification results, the concentration of each compound was considerably lower than its olfactory threshold, determined in a de-aromatised red wine, where esters had been eliminated by the evaporation process. Consequently, these compounds apparently had no direct impact on the fruity aroma of red wines. Nevertheless, each compound corresponded to an intense odour-active zone of fruity fraction extracts, confirming the phenomenon pointed out by Ferreira et al. (4). As the 18 compounds characterised belonged to the same chemical family, the possibility of indirect impact via perceptive interactions was considered.

Some Bordeaux wines, characterised by dominant jammy and black-berry aromas were shown to have the highest ethyl propanoate, ethyl 2-methylpropanoate, and ethyl 2-methylbutanoate levels. The results of sensory reconstitution tests, using pure esters, and studying the possibility of a correlation between these two observations, are presented in Table 2.

They showed globally excellent significant levels. Except for ethyl 2-methylbutanoate in diluted alcoholic solution, assessors systematically detected the

test matrices. Moreover, the highest detection rates were observed when all three compounds were added. When assessors were asked to describe the test matrices' fruity aroma, a majority selected two descriptors corresponding to black-berry aromas, as shown in Table 3.

Table 2. Detection percentage of test matrices following supplementation with ethyl propanoate, ethyl 2-methylbutanoate, and ethyl 3-methylbutanoate.

Additional supplementation	Test 1 C3C2	Test 2 2MeC3C2	Test 3 2MeC4C2	Test 4 C3C2 + 2MeC3C2 + 2MeC4C2
Model solution	72***	67***	44	78***
Model red wine	53*	60***	55**	55**

*: 5% significant level, **: 1% significant level, ***: 0.1% significant level. C3C2: ethyl propanoate, 2MeC3C2: ethyl 2-methylpropanoate, 2MeC4C2: ethyl 2-methylbutanoate.

Table 3. Descriptors selected to qualify the aromatic differences induced by supplementation with ethyl propanoate, ethyl 2-methylbutanoate, and ethyl 3-methylbutanoate (test 4).

Number of assessors	Dilute alcohol solution	Dearomatised red wine
Total	35	24
Selecting 2 "black-berry" descriptors	23	13
Selecting 1 "black-berry" and 1 "red-berry" descriptors	8	7
Selecting 2 "red-berry" descriptors	4	4

The same experiment was performed based on other wines, characterised by dominant red-berry and fresh-fruit aromas and which presented the highest ethyl butanoate, ethyl hexanoate, ethyl octanoate, and ethyl 3-hydroxybutanoate concentrations. As previously observed, the highest detection rates were obtained with the four ethyl esters spiked together. In this case, a large majority of participants selected two descriptors corresponding to red-berry aromas to characterise the aromatic differences perceived.

There were only very small differences in the concentrations of the 7 ethyl esters considered and, except for ethyl hexanoate, levels in the test matrices remained well below the individual olfactory thresholds. Thus, sensory reconstitution tests clearly established that very small variations in concentrations of certain ethyl esters were perceptible in a de-aromatised red wine and had an impact on its red- and black-berry aromas.

References

1. Aznar M., Lopez R., Cacho J.F., Ferreira V. (2001) *J. Agric. Food Chem.* 49: 2924-2929.
2. Sarrazin E., Dubourdieu D., Darriet Ph. (2007) *Food Chem.* 103: 536-545.
3. Pineau B., Barbe J.C., van Leeuwen C., Dubourdieu D. (2007) *J. Agric. Food Chem.* 55: 4103-4108.
4. Ferreira V., Lopez R., Escudero A., Cacho J. (1998) *J. Sci. Food Agric.* 77: 259-267.

ORIGINAL INDIRECT IDENTIFICATION OF 3-SULFANYLHEXAN-1-OL DIMER (3,3'-DISULFANEDIYLDIHEXAN-1-OL) IN SAUTERNES BOTRYTISED WINES

E. Sarrazin¹, S. Shinkaruk², C. Thibon³, P. Babin⁴, B. Bennetau⁴, T. Tominaga¹, and PH. DARRIET¹

¹ *Faculté d'Œnologie, Institut des Sciences de la Vigne et du Vin, UMR 1219, INRA, Université Bordeaux II, 351 cours de la Libération, F-33405 Talence Cedex, France*

² *Ecole Nationale d'Ingénieurs des Travaux Agricoles de Bordeaux, 1 cours du Général de Gaulle, CS 40201, F-33175 Gradignan Cedex, France*

³ *SARCO, BP 40, F-33015 Bordeaux Cedex, France*

⁴ *Institut des Sciences Moléculaires, Université Bordeaux 1, UMR 5802, CNRS, 351 cours de la Libération, F-33405 Talence Cedex, France*

Abstract

A four-step purification method was developed to isolate a citrus-reminiscent compound that seemed to be specific to Sauternes botrytised wines. Combining multidimensional gas chromatography coupled with mass spectrometry and sniffing detection, with exact mass measurement, the fragmentation pattern of the odorant and its elemental formula (C₆H₁₂OS) were determined. Based on these data, the unusual structure of 3-propyl-1,2-oxathiolane was identified and characterised for the first time. The specific occurrence of 3-propyl-1,2-oxathiolane in Sauternes wine extracts was demonstrated to be an indirect proof of the presence of 3-sulfanylhexasan-1-ol dimer (3,3'-disulfanediyldihexasan-1-ol). Although 3-sulfanylhexasan-1-ol has already been shown to undergo oxidative dimerisation in natural products, this mechanism has never been established in wine. The tentative identification of 3,3'-disulfanediyldihexasan-1-ol is thus decisive to enhance our understanding of the way 3-sulfanylhexasan-1-ol, a major wine odorant, evolves under mild oxidative conditions, such as wine ageing.

Introduction

Sauternes wine aroma has recently been studied by gas chromatography-olfactometry (GC-O) (1). Among the volatile compounds found in these specialty wines, six were reminiscent of citrus. Five were volatile thiols and have been identified as 3-sulfanylhexasan-1-ol, 4-methyl-4-sulfanylpentan-2-one, 3-sulfanylpentan-1-ol, 3-sulfanylheptan-1-ol and 2-methyl-3-sulfanylbutan-1-ol (2, 3). The last citrus zone did not correspond to a volatile thiol. As this odorant was not detected in dry white wines made from the same grape varieties (*i.e.* Semillon and Sauvignon blanc), it seemed to be specific to botrytised wines. However, it was detected by GC-sniffing using a 230 °C-injection mode, but not using a 45°C-injection mode. It was thus thought to be formed thermally in the injector from another compound that might be present specifically in botrytised wines. The aim of this research was to identify the citrus odorant, as well as to understand its thermal formation from botrytised wine extracts in the injector.

Experimental

Purification method. A 4.5 L sample of Sauternes wine was extracted with two successive additions of 600 mL of dichloromethane. The combined organic phases were washed with a 1 mM aqueous solution of sodium *p*-hydroxymercuribenzoate in 0.2 M Trizma[®] base [2-amino-2-(hydroxymethyl)-1,3-propanediol], pH 10 (2 x 120 mL for 10 min each time). The organic phase obtained was dried over anhydrous sodium sulphate and concentrated using a rotary evaporator to 2 mL. The concentrate was then purified by reverse-phase HPLC, using the method developed by Pineau *et al.* (4). The fractions with remarkable odours were extracted again with dichloromethane, as described by Pons *et al.* (5), and analysed by MDGC-MS-sniffing.

Heart-Cut Multidimensional Gas Chromatography-Olfactometry-Mass Spectrometry-Sniffing (MDGC-MS-sniffing). The MDGC separation was performed on two GC ovens, as described by Pons *et al.* (5). Preseparation was performed using a non polar SPB1 fused silica capillary column (30 m, 0.25 mm i.d., 0.25 µm film thickness). The second column was a BPX5, a BPX50 or a BPX70 (SGE, 50 m, 0.25 mm i.d., 1.0 µm film thickness). The Agilent 5973 MS detector was functioning in electronic impact (70 eV) or chemical ionization modes (CH₄ reactant). Mass spectra were taken over the *m/z* 40-300 range.

Synthesis of 3-propyl-1,2-oxathiolane. 3-Propyl-1,2-oxathiolane was synthesised from 3-sulfanylhexasan-1-ol using an optimized procedure similar to that proposed by Davis and Whitham (6). ¹H and ¹³C NMR spectra were recorded with a Bruker AC-300 FT (¹H: 300 MHz, ¹³C: 75 MHz), using TMS as an internal standard. Chemical shifts (δ) are expressed in ppm. NMR ¹H (CDCl₃) δ 0.93 (t, CH₃-8); 1.32 (m, 2H, CH₂-7); 1.35-1.87 (m, 2H, CH₂-6); 1.87 (m, 1H, CH-4b); 2.33 (m, 1H, CH-4a); 4.00 (m, 2H, CH₂-5); 4.14 (m, 1H, CH-S). NMR ¹³C (CDCl₃) δ 14.0 (CH₃-8); 22.5 (CH₂-7); 37.0 (CH₂-4); 38.5 (CH₂-6); 53.5 (CH-3); 75.1 (CH₂-5).

Results and Discussion

Identification of 3-propyl-1,2-oxathiolane. The volatile compounds from a total of 4.5 L Sauternes botrytised wine were isolated by liquid-liquid extraction with dichloromethane. Acidic compounds as well as volatile thiols were removed by washing the organic extract with an alkaline mercury solution. As the citrus compound could not be accurately identified from this extract by MDGC-MS-sniffing, a further purification step was undertaken to avoid coelution. This was performed by HPLC with a C₁₈ reversed-phase column and led to 25 fractions. The samples containing the citrus odorant were extracted again and analysed by MDGC-MS-sniffing. Combining MS detection on electronic impact and chemical ionization modes, the molecular mass of the citrus odorant was established as M = 132 ([M + H]⁺ = 133) (Figure 1). MDGC-MS-sniffing analysis was repeated for the same extract on BPX70 and BPX50 columns (oven II), confirming this result. Linear retention indices on these two capillaries were respectively 1592 and 1236.

Exact mass measurement was then used to determine the elemental formula as C₆H₁₂OS (132.0605 Da) on a Waters GCT Premier (Waters, Manchester, UK). Based on these data, the unusual structure of 3-propyl-1,2-oxathiolane was hypothesized. This compound was synthesised and its structure was fully characterised for the first time (¹H and ¹³C NMR, 2D NMR, IR). As mass spectrum and linear retention indices of the synthetic pure substance were identical to data obtained from wine samples, the identification of 3-propyl-1,2-oxathiolane was confirmed.

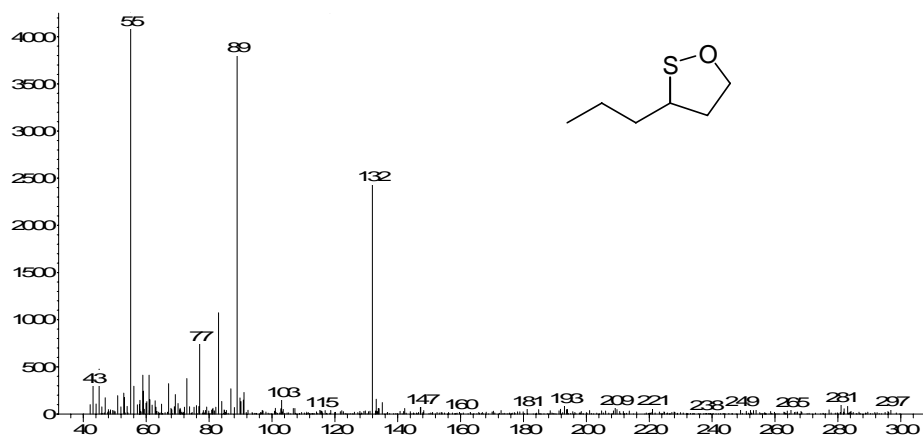


Figure 1. Mass spectrum and molecular structure of 3-propyl-1,2-oxathiolane.

Origin of 3-propyl-1,2-oxathiolane. One of Sauternes wine key-odorants is 3-sulfanylhexan-1-ol (**I**) (2, 3). This compound is also found in passion fruit where it is known to oxidize by dimerisation to form the disulfide (**II**) (7), which can then oxidize to the sultine (**III**) (8) (Figure 2). 3-propyl-1,2-oxathiolane (**IV**) was synthesised but was shown to be very unstable and to oxidize quickly to **III**. On the basis of the sulphur oxidation state, **IV** was thought to be an intermediary oxidizing product, and an hypothetical mechanism was suggested in agreement with the pathways already proposed for other kinds of organic sulphur-containing compounds (9, 10) (Figure 2).

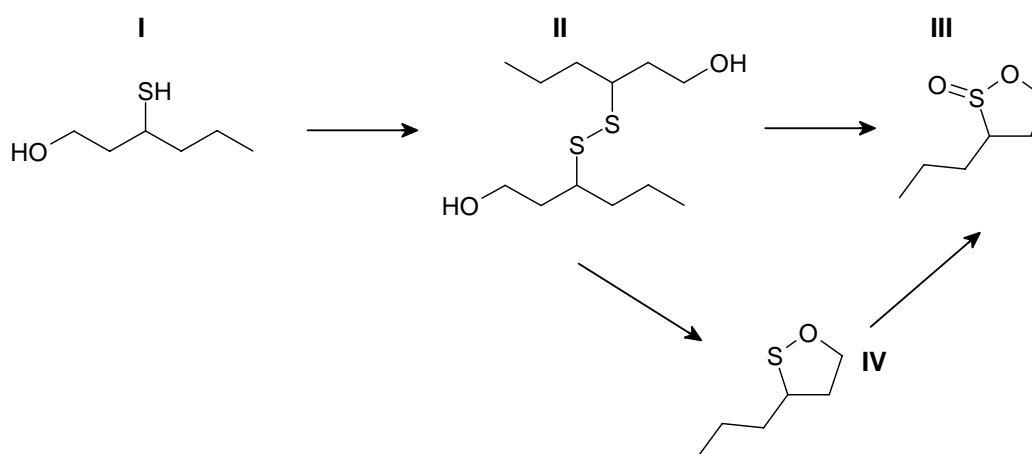


Figure 2. Oxidation pathway of 3-sulfanylhexan-1-ol. Origin of the unusual structure of 3-propyl-1,2-oxathiolane.

To validate this hypothesis, synthetic **II** and **III** were injected by GC-MS at 45°C and 230°C. As **IV** was only detected when **II** was injected at 230°C, the thermal formation of the oxathiolane **IV** from the disulfide **II** was confirmed. This oxidation pathway of 3-sulfanylhexan-1-ol is thus experimentally demonstrated for the first time. The same result was obtained for botrytised wine samples: the GC-sniffing analysis revealed the presence of the interesting compound only using a-230°C injection mode. As a consequence, the identification of 3-propyl-1,2-oxathiolane (**IV**) in Sauternes botrytised wines is an indirect evidence of the presence of the disulfide **II**. As far as we know, this dimer is tentatively identified in wine for the first time.

However, 3-propyl-1,2-oxathiolane was detected in Sauternes botrytised wines, but not in dry white wines made from the same grape varieties. Therefore, these results suggested a specific composition of botrytised wines which made possible the formation of the disulfide during wine ageing.

Conclusion

This research reported the tentative identification of 3-sulfanylhexas-1-ol disulfide (3,3'-disulfanediyldihexas-1-ol) in Sauternes botrytised wines. 3-Sulfanylhexas-1-ol has a high olfactory impact in botrytised wines. Therefore, it is challenging to extend our knowledge of its reactivity and stability, particularly under mild oxidative conditions, such as Sauternes wine ageing in oak barrels.

Acknowledgements

We thank Waters Corporation (Manchester, UK) for their kind help in high resolution mass spectrometry analysis.

References

1. Sarrazin E., Dubourdieu D., Darriet P. (2007) *Food Chem.* 103: 536-545.
2. Tominaga T., Baltenweck-Guyot R., Peyrot des Gachons C., Dubourdieu D. (2000) *Am. J. Enol. Vitic.* 51: 178-181.
3. Sarrazin E., Shinkaruk S., Tominaga T., Bennetau B., Frérot E., Dubourdieu D. (2007) *J. Agric. Food Chem.* 55: 1437-1444.
4. Pineau B., Barbe J.C., Dubourdieu D. (2009) In *Oeno 2007, 8^e Symposium International d'Œnologie* (Vigne & Vin Publications Internationales, ed., Bordeaux), pp 810.
5. Pons A., Lavigne V., Frérot E., Darriet P., Dubourdieu D. (2008) *J. Agric. Food Chem.* 56: 5285-5290.
6. Davis A.P., Whitham G.H. (1981) *J. Chem. Soc. - Chem. Comm.* 15: 741-742.
7. Werkhoff P., Güntert M., Krammer G., Sommer H., Kaulen J. (1998) *J. Agric. Food Chem.* 46: 1076-1093.
8. Yolka S., Duñach E., Loiseau M., Lizzani-Cuvelier L., Fellous R., Rochard S., Schippa C., George G. (2002) *Flav. Fragr. J.* 17: 425-431.
9. Givens E.N., Hamilton L. A. (1967) *J. Org. Chem.* 32: 2857-2860.
10. Doi J.T., Luehr G.W., Muster W.K. (1985) *J. Org. Chem.* 50: 5716-5719.

KEY ODORANTS OF THE TYPICAL AROMA OF SHERRY VINEGAR

R.M. CALLEJÓN¹, M.L. Morales¹, A.M. Troncoso¹, and A.C. Silva Ferreira²

¹ *Área de Nutrición y Bromatología, Facultad de Farmacia, Universidad de Sevilla. c/ P. García González nº 2, E- 41012, Sevilla, Spain*

² *Escola Superior de Biotecnologia, Universidade Católica Portuguesa. R. Dr. Antonio Bernardino de Almeida, 4200-072 Porto, Portugal*

Abstract

A representative Sherry vinegar was analysed by gas chromatography-olfactometry (GC-O). Two GC-O techniques were used targeting compounds with impact on the perceived quality of Sherry vinegar, i.e. detection frequency and aroma extract dilution analysis. A total of 108 aromatic notes were detected and 64 of them were identified. Diacetyl, isoamyl acetate, acetic acid, and sotolon reached the highest frequency and flavour dilution (FD) factors. Ethyl acetate accounted for the maximum frequency but had only a FD factor of 4. Similarity tests were performed between the Sherry vinegar and model solutions of all possible combinations of these compounds. The highest value from the similarity test was observed when diacetyl, ethyl acetate and sotolon were added simultaneously. The profile of this model solution and the representative Sherry vinegar showed a good similarity in the general aroma description, which emphasises the important contribution of these 3 compounds to the global aroma of this vinegar.

Introduction

There is a need for the characterization of the typical sensory properties of traditional products not only for the industrialization of food production, but also for laws on food safety and even for the development of innovative products. Sherry vinegar is one of the most renowned products of this type in the world. A minimum period of six months of aging in wood barrels is mandatory for these products. Its main characteristics are a high acetic degree (legally, a minimum of 7°) and a special flavour which resembles that of Sherry wine. The aroma composition of these vinegars has been studied by several authors (1, 2). However, systematic studies to indicate the odorants responsible for the characteristic bouquet of Sherry vinegar have not been reported up to now.

Targeting substances with large impact on the perceived quality of a food product represents one of the most challenging tasks in flavour research. The main difficulty is correlation between sensory and chemical data. Despite of controversial reports concerning the best suited technique for a given matrix, several methods using gas chromatography with olfactometry have been applied to the purpose of ranking substances by their respective impact on the overall aroma of a foodstuff (3, 4).

This work deals with the evaluation of “sensory quality” of Sherry wine vinegar and with the presentation of substances, which plays an important role on the perceived character of Sherry vinegars. We have used two gas chromatography-olfactometry (GC-O) techniques: aroma extract dilution analysis (AEDA) and frequency counting (FC) using simultaneously two exits on a customised “multipost”

sniffer ODO-II. They have been compared to define their respective discrimination ability.

Experimental

Vinegar sample. A representative 2 year-old vinegar (“Vinagre Reserva”, VR1) was selected by the sensory panel as being a Sherry vinegar “type”.

Chemical analysis. Major volatile compounds were determined by direct injection GC-Flame Ionization Detector (GC-FID) (5). A total of 52 minor compounds were determined by Headspace Sorptive Extraction-Gas Chromatography-Mass Spectrometry (HSSE-GC-MS) (6) and sotolon by Liquid-Liquid Extraction GC-MS (7).

Gas Chromatography-Olfactometry. Dichloromethane extracts of the VR1 sample were analysed by GC-O customised by Dr. Silva Ferreira’s group with two olfactory outlets in order to obtain simultaneous odour evaluations from multiple panellists (8).

Sensory analysis. Descriptive analysis (8) and similarity tests between VR1 and each aroma model solution were carried out (7). Aroma model solutions were prepared in a 7% (w/v) acetic acid solution by diluting the compounds, which reached the highest scores in GC-O, in the same concentrations found for the sample VR1.

Results

The GC-O study revealed the presence of 108 aromatic notes among which 64 could be described by the panellists. Table 1 shows compounds reaching high detection frequency in GC-O. Among them, a variety of odour-active regions, identified as ethyl acetate, diacetyl, isoamyl acetate, acetic acid, butyric acid, isovaleric acid and sotolon, reached the highest detection frequencies (100%). Good correlations were observed among the simultaneous AEDA ($r > 0.90$) carried out by two panellists. Only 19 odour compounds showed differences of more than one dilution factor. By sniffing serial dilutions, 26 odour-active compounds accounted for FD factors ≥ 256 . Nine of them could not be identified.

By comparing results obtained with the two techniques used in this study, detection frequency and AEDA, we can see that they agree in many cases. Hence, diacetyl, isoamyl acetate, acetic acid and sotolon, reached the maximum frequency and the highest FD factors, therefore, being potent odorants of Sherry vinegar. However, results were not in agreement for certain odorants ($r < 0.45$). For example, ethyl acetate displayed the highest frequency (9/9) but only a FD factor of 4. Various authors have critically compared the different GC-O methodologies, using either mixtures of references standards or real food systems (9) and discrepancies in results existed since they are based on different principles. Each of the GC-O methodologies has advantages and limitations. Hence, the use of both techniques allows more information to be obtained and reduces the errors when using just one of them.

Similarity tests between solutions and Sherry vinegar were performed to check the sensory impact of those compounds with a FD factor ≥ 512 and detected in all sniffing trials, i.e. diacetyl, isoamyl acetate and sotolon. In addition, ethyl acetate was also selected in spite of its low FD factor because it was detected in all sniffing trials. Moreover, it is one of the typical sensory attributes of Sherry vinegar used as descriptor in the descriptive sensory analysis chart for Sherry vinegars (10). The highest value from the similarity test was observed when diacetyl, ethyl acetate and sotolon were added simultaneously (Table 2).

Table 1. Detection frequency and AEDA of the odours of VR1 Sherry wine vinegar.

RI	Odour Quality	Odorant (tentative identification)*	Detection Frequency	FD1	FD2
1063	Glue	Ethyl acetate	9	2	4
1080	Strawberry	Ethyl isobutyrate	7	512	1024
1084	Butter	Diacetyl	9	4096	4096
1118	Cherry, strawberry	Butyl acetate	6	128	1024
1123	Banana, mulberry, strawberry	Isoamyl acetate	9	4096	4096
1422	Pungent	Acetic acid	9	1024	1024
1468	Mulberry, fruit, banana, strawberry	Unknown	8	1	2
1484	Boiled potato	Methional	7	4	4
1496	Strawberry, sweet	Unknown	8	8	16
1532	River water, vapour	Unknown	9	1	2
1557	Mulberry, fruit	Benzaldehyde	7	2	4
1563	Aspirin, mulberry	Ethyl nonanoate	8	128	256
1595	Cheese, feet	Isobutyric acid	8	64	128
1655	Burned, burned hair	Unknown	7	8	16
1661	Cheese, vomit	Butyric acid	9	256	256
1705	Cheese	Isovaleric acid	9	128	128
2054	Clove	Eugenol	8	2	2
2151	Flower, fruit, banana	Unknown	7	128	512
2201	Curry, liquorice, "oloroso sherry wine"	Sotolon	9	512	512
2255	Sweet-rancid, wood, liquor	Unknown	7	512	512
2360	Liquor, liquorice, sweet	Unknown	7	512	512

* Identification of odorants: Comparison of mass spectra, chromatographic retention index (RI) and odour description with experimental and literature data.

Table 2. Results obtained from sensorial analysis by comparison test.

Aroma Model Solutions	Similarity Value (SV)	Standard Deviation (SD)
a.s. + [1] + [2] + [4]	5.38	0.55
a.s. + [1] [2] + [3] + [4]	4.59	0.58
a.s. + [1] + [3] + [4]	4.57	0.58
a.s. + [2] + [3] + [4]	4.35	0.62
a.s. + [2] + [4]	4.11	0.58
a.s. + [3] + [4]	4.08	0.61
a.s. + [2] + [3]	3.57	0.55
a.s. + [1] + [4]	3.55	0.55
a.s. + [1] + [2]	3.25	0.62
a.s. + [1] + [2] + [3]	3.15	0.58
a.s. + [4]	2.76	0.58
a.s. + [2]	1.83	0.62
a.s. + [1] + [3]	1.79	0.62
a.s. + [1]	1.70	0.55
a.s. + [3]	1.54	0.58

a.s.: acetic acid solution (7 % v/v); [1] diacetyl, [2] ethyl acetate; [3] isoamyl acetate; [4] sotolon

The profile of this model solution and the representative Sherry vinegar showed similar intensities in the "sweet aroma", "pungent sensation" and "alcohol/liquor" descriptors, in addition to a good similarity in the "general impression" (Figure 1). This result emphasises the important contribution of these 3 molecules (diacetyl, ethyl acetate and sotolon) to the global aroma of this Sherry vinegar. Hence, they can be considered as key odorants of Sherry vinegar.

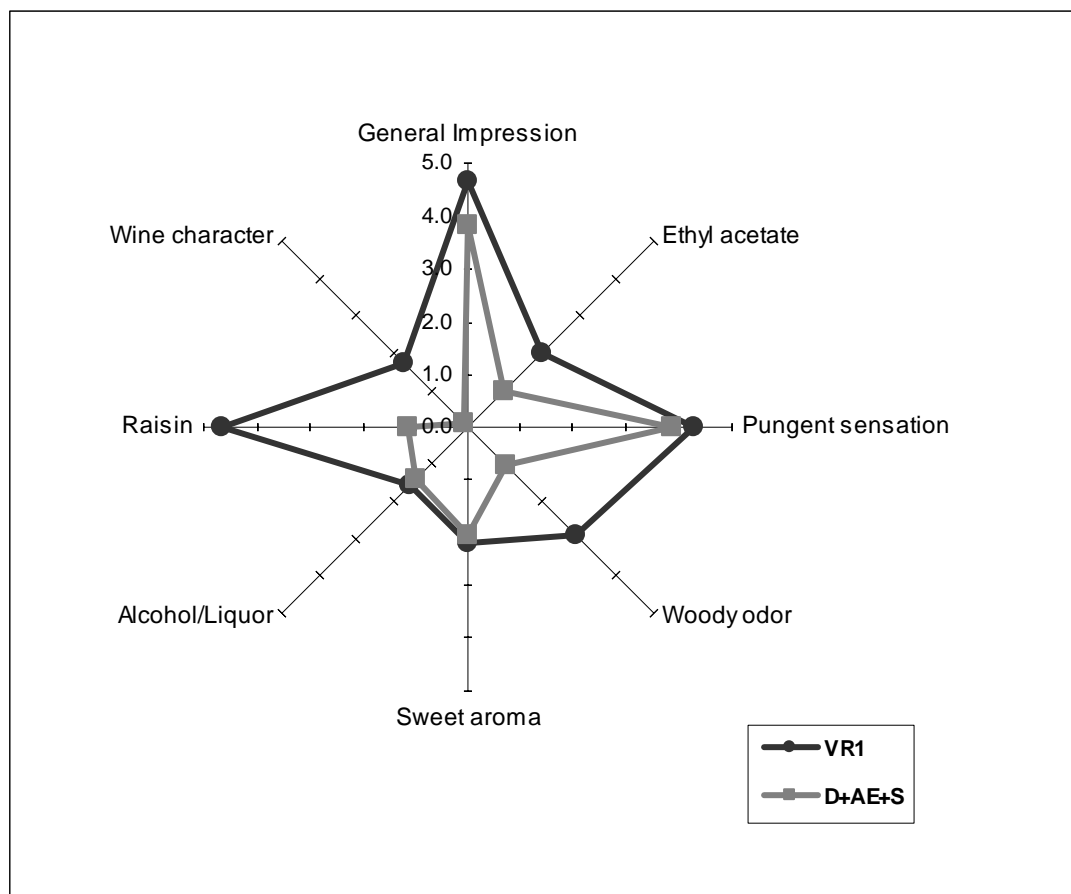


Figure 1. Flavour profiles of VR1 sample (black line) and aroma model (grey line).

References

1. Morales M.L., González G.A., Casas J.A., Troncoso A.M. (2001) *Eur. Food Res. Technol.* 212: 676-682.
2. Guerrero E.D., Natera R., Castro R., Barroso C.G. (2007) *J. Chromatogr. A* 1167: 18-26.
3. Campo E., Ferreira V., Escudero A., Marqués J.C., Cacho J. (2006) *Anal. Chim. Acta* 563: 180-187.
4. Silva Ferreira A.C., Hogg T., Guedes de Pinho P. (2003) *J. Agric. Food Chem.* 51: 1377-1381.
5. Morales M.L., Tesfaye W., García-Parrilla M.C., Casas J.A., Troncoso A.M. (2001) *J. Sci. Food Agric.* 81: 611-619.
6. Callejón R.M., Troncoso A.M., Morales M.L. (2008) *J. Chromatogr. A* 1204: 93-103.
7. Silva Ferreira A.C., Barbe J.C., Bertrand A. (2003) *J. Agric. Food Chem.* 51: 4356-4363.
8. Callejón R.M., Morales M.L., Troncoso A.M., Silva Ferreira A.C. (2008) *J. Agric. Food Chem.* 56: 6631-6639.
9. van Ruth S.M. (2004) *J. Chromatogr. A* 1054: 33-37.
10. Tesfaye W., García-Parrilla M.C., Troncoso A.M. (2002) *Sensory Studies* 17: 132-140.

NOVEL KEY AROMA COMPONENTS OF GALBANUM OIL

N. MIYAZAWA¹, A. Nakanishi¹, N. Tomita¹, Y. Ohkubo¹, S. Ishizaki¹, and T. Maeda²

¹ Technical Research Center, T. Hasegawa Co., Ltd., 335 Kariyado, Nakahara-ku, Kawasaki 211-0022, Japan

² Flavor Institute, T. Hasegawa Co., Ltd., 335 Kariyado, Nakahara-ku, Kawasaki 211-0022, Japan

Abstract

Considering the complexity and potency of the odour, galbanum oil was assumed to contain so far not identified compounds with high odour contribution. By gas chromatography-mass spectrometry-olfactometry analysis of galbanum oil, fruity-green-balsamic notes were detected at two different retention times. The mass spectra of the newly discovered notes were elucidated by conducting multidimensional gas chromatography-mass spectrometry-olfactometry (MD-GC-MS-O). By analysing the MS data, six chemical structures were proposed: (6*E*/*Z*,8*E*)-undeca-6,8,10-trien-2-one, (6*E*/*Z*,8*E*)-undeca-6,8,10-trien-3-one, and (6*E*/*Z*,8*E*)-undeca-6,8,10-trien-4-one. The compounds were then synthesised in an attempt to match the MS, retention indices, and odour qualities. The MD-GC-MS-O analyses of the candidate compounds led to the identification of the novel key aroma compounds, (6*Z*,8*E*)-undeca-6,8,10-trien-3-one and (6*Z*,8*E*)-undeca-6,8,10-trien-4-one, in galbanum oil. These compounds have fairly low thresholds in water of 0.010 ppb and 0.072 ppb, respectively.

Introduction

Galbanum oil is obtained by steam distillation of the resin of *Ferula galbaniflua* (Boissier et Buhse), a large Umbellifer plant that grows wild mainly in Iran, Turkey, Afghanistan, and neighbouring countries. The oil, a widely used ingredient in industry, has a powerful green odour with dry-woody, balsamic, and bark-like tonalities (1). In perfumery, the oil is used to confer green notes and augment fougère, chypre, and oriental notes. In flavouring, it contributes to the savoury notes of curries and sauces.

Galbanum oil is mainly composed of hydrocarbon monoterpenes (2) such as β -pinene, α -pinene, and Δ^3 -carene, but these components hardly contribute to the characteristic green notes. Instead, the tiny quantities of C11 hydrocarbons and methoxypyrazines present in the oil contribute most to the aroma (3). But the complexity and potency of the green odour could not solely be explained by the compounds identified so far. Therefore, we assumed that there were clearly other hidden key odorants that contribute to the total aroma. In this study we used GC-MS-O to discover these components in a commercially available galbanum oil from Iran.

Experimental

Iranian galbanum oil was purchased from Nihon SiberHegner (Tokyo, Japan). (6*E*/*Z*,8*E*)-Undeca-6,8,10-trien-2-one (**1**) (6*E*:6*Z* = 47:53), (6*E*/*Z*,8*E*)-undeca-6,8,10-

trien-4-one (**2**) ($6E:6Z = 46:54$) and ($6E/Z,8E$)-undeca-6,8,10-trien-3-one (**3**) ($6E:6Z = 50:50$) were synthesised in our laboratory (Figure 1).

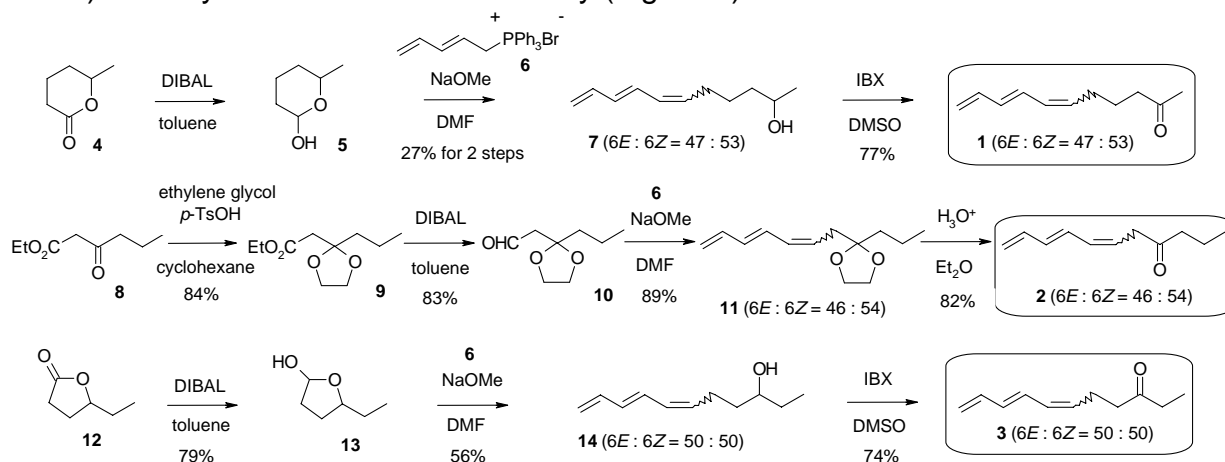


Figure 1. Syntheses of ($6E/Z,8E$)-undeca-6,8,10-trien-2-one (**1**), ($6E/Z,8E$)-undeca-6,8,10-trien-4-one (**2**) and ($6E/Z,8E$)-undeca-6,8,10-trien-3-one (**3**)

To concentrate the key aroma, commercial galbanum oil (950 g) was distilled to yield a distillate (103.2 g) which was confirmed to have the target odour of fruity-green-balsamic notes by GC-MS-O. Then silica gel chromatography was performed three times to yield a concentrated effluent (660 mg) having the target odour. Upon MD-GC-MS-O analysis of the concentrated effluent, the section of the chromatogram that was obtained via the first GC equipped with a polar column (TC-WAX) as containing the compound with the target odour was selectively injected to the second GC equipped with a nonpolar column (TC-1) and analysed by GC-MS-O.

The thresholds and odour qualities of synthesised ($6E/Z,8E$)-undeca-6,8,10-trienones were evaluated in water solutions of a mixture of ($6E$) and ($6Z$)-isomers by a trained panel.

Results

To identify the odour-active compounds, we analysed galbanum oil by GC-MS-O and detected characteristic odours at five different retention times on a TC-WAX column. We were able to identify four odour-active compounds of five characteristic odours by matching them with MS, retention indices (RIs), and odour qualities, as follows: ($3E,5Z$)-undeca-1,3,5-triene for the fruity and pineapple-like odour (RI= 1403), 2-isopropyl-3-methoxypyrazine for the earthy odour (RI= 1446), linalool for the fruity and floral odour (RI= 1550), and guaiacol for the medicinal odour (RI= 1863). For the fruity, green, and balsamic odour (RI= 1899), however, a low content of the odour-active compound and overlapping in the chromatogram with other compounds thwarted our attempt to obtain the MS. Therefore, we attempted to obtain the MS by concentrating the compound.

After thorough studies, we found that the target compound was fairly low in both volatility and polarity. By a combined method of distillation and repeated silica gel chromatography, we removed low-boiling compounds, hydrocarbon terpenes, oxygenated terpenes and polar compounds from commercial oil in sequence and finally obtained a concentrated effluent having the target odour, which was then analysed by MD-GC-MS-O. As a result, although we had presumed that the aroma would originate from only one compound, we were surprised to detect the target

fruity-green-balsamic odour at two different retention times (RI= 1316 and 1328) on the TC-1 column. We thus obtained the pure MS of two compounds, hereinafter referred to as “unknown A” and “unknown B”.

Two features of the unknowns suggested that the compounds were structural isomers: (i) their similar fruity-green-balsamic odour, and (ii) the correspondence of the molecular weight (MW) of 164. The fragment ions at m/z 43 and 71 of unknown A were characteristic of an acetyl group or a butyryl group, whereas the fragment ion at m/z 57 of unknown B was characteristic of a propionyl group. These data suggested that an oxygen atom was present in the molecules. The MW of the unknowns (164) minus that of an oxygen atom (16) plus that of two hydrogen atoms (2) is 150, exactly the same MW of (3*E*,5*Z*)-undeca-1,3,5-triene, one of the characteristic odour components of galbanum oil. Thus, we assumed that the chemical structures of the unknowns were oxygenated isomers of (3*E*,5*E*/*Z*)-undeca-1,3,5-triene, namely, (6*E*/*Z*,8*E*)-undeca-6,8,10-trien-2-one (**1**) or (6*E*/*Z*,8*E*)-undeca-6,8,10-trien-4-one (**2**) for unknown A and (6*E*/*Z*,8*E*)-undeca-6,8,10-trien-3-one (**3**) for unknown B.

The syntheses of the candidate compounds, (6*E*/*Z*,8*E*)-undeca-6,8,10-trien-2-one (**1**), (6*E*/*Z*,8*E*)-undeca-6,8,10-trien-4-one (**2**) and (6*E*/*Z*,8*E*)-undeca-6,8,10-trien-3-one (**3**), were accomplished by application of a Wittig reaction with the same phosphonium salt **6** (**4**) as the key step (Figure 1).

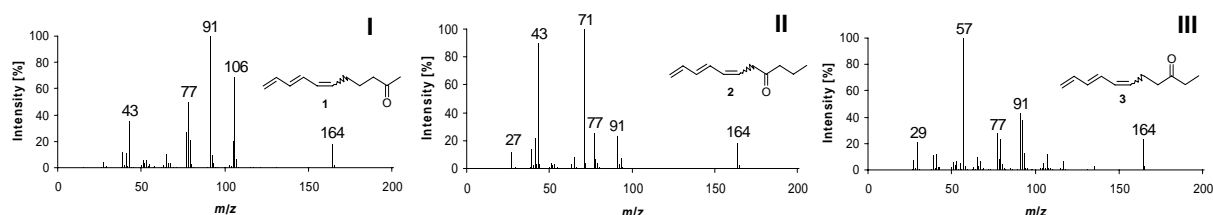


Figure 2. Mass spectra (MS-EI) of (I) (6*E*/*Z*,8*E*)-undeca-6,8,10-trien-2-one (**1**), (II) (6*E*/*Z*,8*E*)-undeca-6,8,10-trien-4-one (**2**) and (III) (6*E*/*Z*,8*E*)-undeca-6,8,10-trien-3-one (**3**).

Table 1. Retention indices of unknowns and (6*E*/*Z*,8*E*)-undeca-6,8,10-trienones on TC-WAX and TC-1 columns.

No.	Compound	RI on	
		TC-WAX	TC-1
	Unknown A	1899	1316
	Unknown B	1899	1328
1a	(6 <i>Z</i> ,8 <i>E</i>)-Undeca-6,8,10-trien-2-one	1913	1320
1b	(6 <i>E</i> ,8 <i>E</i>)-Undeca-6,8,10-trien-2-one	1947	1338
2a	(6 <i>Z</i> ,8 <i>E</i>)-Undeca-6,8,10-trien-4-one	1899	1316
2b	(6 <i>E</i> ,8 <i>E</i>)-Undeca-6,8,10-trien-4-one	1899	1328
3a	(6 <i>Z</i> ,8 <i>E</i>)-Undeca-6,8,10-trien-3-one	1899	1328
3b	(6 <i>E</i> ,8 <i>E</i>)-Undeca-6,8,10-trien-3-one	1924	1339

For confirmation, the synthesised compounds were analysed according to the same method used to analyse unknowns in galbanum oil. Although the odour of the ketone **1** was similar to that of unknown A, the MS and RI of the ketone **1** did not match those of unknown A. However, finally, we identified unknown A as (6*Z*,8*E*)-undeca-6,8,10-trien-4-one (**2a**), a novel compound in galbanum oil, by matching the

MS, RI, and odour quality. For unknown B, another candidate compound, (6*Z*,8*E*)-undeca-6,8,10-trien-3-one (**3a**), was also identified as a novel compound in galbanum oil by matching the MS, RI and odour quality (Figure 2, Table 1).

The odour qualities of newly synthesised (6*E*/*Z*,8*E*)-undeca-6,8,10-trienones were profiled similarly to each other as balsamic, green and woody notes. On the other hand, the thresholds which were evaluated by 30 panellists were surprisingly different, being 0.700 ppb for (6*E*/*Z*,8*E*)-undeca-6,8,10-trien-2-one (**1**), 0.072 ppb for (6*E*/*Z*,8*E*)-undeca-6,8,10-trien-4-one (**2**) and 0.010 ppb for (6*E*/*Z*,8*E*)-undeca-6,8,10-trien-3-one (**3**) (Table 2).

Table 2. Aroma profiles of newly synthesised (6*E*/*Z*,8*E*)-undeca-6,8,10-trienones.

No.	Compound	6 <i>E</i> : 6 <i>Z</i>	Odour quality	Threshold (ppb)
1	(6 <i>E</i> / <i>Z</i> ,8 <i>E</i>)-Undeca-6,8,10-trien-2-one	47 : 53	Balsamic, green, woody	0.700
2	(6 <i>E</i> / <i>Z</i> ,8 <i>E</i>)-Undeca-6,8,10-trien-4-one	46 : 54	Balsamic, green, woody	0.072
3	(6 <i>E</i> / <i>Z</i> ,8 <i>E</i>)-Undeca-6,8,10-trien-3-one	50 : 50	Balsamic, green, woody, earthy	0.010

In conclusion, we detected MS data of key components responsible for the fruity-green-balsamic notes in galbanum oil and proposed six chemical structures: (6*E*/*Z*,8*E*)-undeca-6,8,10-trien-2-one (**1**), (6*E*/*Z*,8*E*)-undeca-6,8,10-trien-4-one (**2**) and (6*E*/*Z*,8*E*)-undeca-6,8,10-trien-3-one (**3**). Next, we synthesised the candidate compounds, and identified two of them, (6*Z*,8*E*)-undeca-6,8,10-trien-4-one (**2a**) and (6*Z*,8*E*)-undeca-6,8,10-trien-3-one (**3a**), by matching MS, RIs, and odour qualities. We point out that the compounds (6*Z*,8*E*)-undeca-6,8,10-trien-4-one (**2a**) and (6*Z*,8*E*)-undeca-6,8,10-trien-3-one (**3a**) were identified for the first time solely in galbanum oil and not in other natural products.

References

1. Arctander S. (1960) In *Perfume and Flavor Materials of Natural Origin*; Elizabeth, pp. 256-258.
2. Lawrence B.M. (2007) *Perfum. Flavour.* 32: 49-51.
3. McAndrew B.A., Michalkiewicz D.M. (1988) In *Flavors and Fragrances: A World Perspective* (Lawrence, B. M., Mookherjee, B. D., Willis, B. J., eds.); Elsevier, pp 573-585.
4. Näf F.; Decorzant R.; Thommen W.; Willhalm B.; Ohloff G. (1975) *Helv. Chim. Acta* 58: 1016-1037.

AROMA VOLATILES OF MANGABA (*HANCORNIA SPECIOSA* GOMES)

L.C. Oliveira^{1,2}, F. Valim³, N. Narain², and R. ROUSEFF¹

¹ *University of Florida, Institute of Food and Agricultural Sciences, Citrus Research and Education Center, 700 Experiment Station Road, Lake Alfred, Florida 33850 USA*

² *Núcleo de Engenharia de Alimentos,, Universidade Federal de Sergipe, 49100-000 – São Cristóvão – SE. Brazil*

³ *Florida Department of Citrus, Scientific Research Department, 700 Experiment Station Road, Lake Alfred, Florida 33850, USA*

Abstract

Thirty-one volatiles have been identified in mangaba, an unusual tropical fruit from Brazil, puree headspace using SPME and GC-MS. There were 17 esters, six alcohols and three ketones, two alkanes and one aldehyde. The three largest peaks were esters (4-pentenyl acetate, isoamyl acetate and 3-methyl-2-butenyl acetate), accounting for over 58% of the total volatile peak area. Over 12 sulphur volatiles were observed using a sulphur specific, pulsed flame photometric detector (PFPD). Seven sulphur volatiles have been tentatively identified: hydrogen sulphide, methane thiol, sulphur dioxide, dimethyl sulphide, dimethyl disulfide, dimethyl trisulphide and methional. Of these, only two, methional and diethyl disulfide, appear to have aroma activity. The overall fruity, tropical aroma of mangaba puree is primarily due to the relatively large amount of isoamyl acetate and 4-pentenyl acetate but whose complexity is the result of the 15 additional esters.

Introduction

There is a growing trend in the juice and beverage industry to include exotic and natural fruit juices in newer beverage products. Mangaba is a relatively unknown tropical fruit native to the northeast region of Brazil where it has proliferated spontaneously in the uncultivated highlands (1). Fruits are yellow about the size of plums whose white, sweet, acid pulp has been described as having a “pleasant and strong flavour”. The fruit also was also thought to be good for digestion as well as an aide for people suffering from fever (2). Once the fruit ripens, it softens rapidly and becomes difficult to handle. The fruit is highly acid, pH 2.9 (3) and high in vitamin C (138-158 mg/100 g pulp) (4). One of the interesting characteristics of mangaba is that when eaten as a fresh ripe fruit or in the form of its products, it leaves a slight gummy residue in the mouth. Mangaba puree, nectar, and ice cream are commercially produced on a limited scale and greatly appreciated by the local population. There has been only one prior report on mangaba volatile composition and it employed aqueous distillation and solvent extraction (5).

The objective of this study was to characterise the aroma volatiles of mangaba (*Hancornia speciosa* Gomes) using sample preparation techniques less prone to produce artefacts (headspace SPME).

Experimental

Mangaba samples. Mangaba (*Hancornia speciosa* Gomes) consisted of frozen pulp samples purchased in Aracaju, Sergipe, Brazil, on April 2007. These samples consisted of pasteurized and quick frozen pulp, packed in 100g polyethylene bags which were immediately stored in a -18°C freezer and kept frozen until analysis.

SPME headspace procedures. Mangaba samples were diluted with distilled water (1:2) and 10 mL aliquots were transferred to 40 mL glass vials with screw caps and Teflon-coated septa containing a micro-stirring bar and placed on a water bath at 40°C. After equilibrating for 15 min, a Carboxen/DVB /PDMS SPME fibre (Supelco Co., Bellefonte, PA, USA) was exposed for 30 min. After exposure, the SPME apparatus was inserted into the GC and desorbed at 220 °C for 5 min.

GC-FID/PFPD. An Agilent 6890N GC (Palo Alto, CA) with FID and PFPD (OI Analytical Co., College Station, TX) detectors was used to detect sulphur volatiles. Separation was accomplished with a DB-wax column (30 m x 0.32 mm. i.d. x 0.5 µm, J&W Scientific; Folsom, CA). Helium carrier gas flow rate was 2 mL/min. Injector and FID detector temperatures were 220 °C and 290 °C, respectively. A 0.75 mm injector liner was employed to improve peak shape and chromatographic efficiency. Injections were splitless. PFPD detector temperature was 250 °C and sulphur gate time was 6-24.9 ms. Detector outputs were recorded and integrated using Chrom Perfect Software (Justice Innovations, NJ, USA).

GC-MS. Mass spectra were obtained using a Perkin Elmer Clarus500 (Shelton, CT, USA) gas chromatograph–mass spectrometer using a 60 m x 0.25 mm i.d. x 0.5 µm Stabilwax column (Restek). The injector temperature was 240°C and headspace volatiles were concentrated and introduced into the chromatograph via SPME. Helium was used as the carrier gas at 2 mL/min. The oven temperature program consisted of a single thermal gradient from 40 to 240 °C at 7 °C/min. The MS was set to scan from mass 25 to 300 at 5.0 scans/s in the positive electron impact mode. Ionization energy was set at 70 eV. NIST database was used for fragmentation spectrum identification.

Results

Comparison with earlier studies. The only previous study of mangaba volatiles (5) identified 32 volatiles from the mature fruit. In that study the fruit was macerated, mixed with water, hydrodistilled, using a Clevenger-type apparatus, for 3 h and then extracted with dichloromethane and analysed with GC-MS. No highly volatile compounds were reported because they were obscured by the dichloromethane peak. In contrast, the samples in this study were collected under much milder conditions. SPME was used to collect headspace volatiles from the Mangaba puree which had been diluted with water in the same way as the earlier study and warmed to 40 °C. Exposure time was only 30 min at 40 °C compared to 3 hours at 100 °C.

As shown in Table 1, 31 volatiles were identified in the present study. Although the number of volatiles was similar in both studies, there was little similarity in the specific compounds identified. The earlier study identified 11 alcohols, 10 esters, four aldehydes and four ketones. In contrast, the current study identified 17 esters, six alcohols, three ketones and one aldehyde. Only 9 of the 31 peaks identified in this study were also reported in the earlier study and have been italicized in Table 1 for comparison purposes. There are multiple reasons for these differences. The earlier study separated the volatiles using DB-5 column. The separation efficiency of a DB

five column versus a Wax column was also evaluated in this study. The Wax column was chosen over the DB-5 column as it provided superior resolution for the Mangaba volatiles. However, the primary reason for the major differences in these studies is due to the way the samples were prepared. The three hours of heating the highly acidic Mangaba purée at 100 °C undoubtedly altered its chemical composition through a combination of acid-catalyzed hydration, Maillard-type and thermal decomposition reactions.

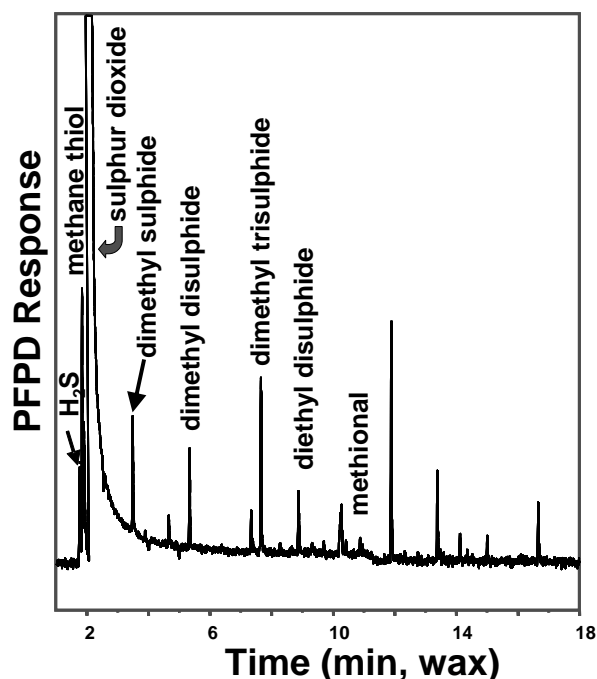
Table 1. *Mangaba volatiles identified from the combination of GC-MS LRI values (Wax) and fragmentation pattern matching. Perfect match = 1000.*

LRI	Ref.	Name ^a	Match	Area %	CAS No.
726	720	acetaldehyde	925	0.96	75-07-0
838	836	methyl acetate	970	1.72	79-20-9
898	902	ethyl acetate	950	7.54	141-78-6
946	949	ethanol	926	4.03	64-17-5
956	959	<i>2,4,5-trimethyl-1,3-dioxolane</i>	928	5.46	3299-32-9
996	999	<i>2,4,5-trimethyl-1,3-dioxolane</i>	882	0.52	3299-32-9
1050	1053	ethyl butyrate	905	0.31	105-54-4
1065	1068	ethyl 2-methylbutyrate	938	0.19	7452-79-1
1086	1089	<i>butyl acetate</i>	926	1.49	123-86-4
1097	1100	2-hexanone	895	0.29	591-78-6
1126	1129	methyl E-2-butenolate	909	0.19	623-43-8
1136	1139	isoamyl acetate	955	25.43	123-92-2
1153	1156	1-butanol	907	0.41	71-36-3
1171	1173	3-heptanone	928	0.58	106-35-4
1205	1209	methyl hexanoate	856	0.33	106-70-7
1211	1214	4-pentenyl acetate	918	26.19	1576-85-8
1215	1219	isoamyl alcohol	926	4.96	123-51-3
1233	1235	butyl butyrate	933	0.60	109-21-7
1247	1250	ethyl hexanoate	882	0.53	123-66-0
1263	1266	<i>3-methyl-3-buten-1-ol</i>	938	1.87	763-32-6
1270	1273	<i>3-methyl-2-butenyl acetate</i>	913	6.51	1191-16-8
1287	1290	<i>hexyl acetate</i>	896	0.57	142-92-7
1334	1338	E-3-hexenyl butyrate	848	0.39	53398-84-8
1363	1367	<i>1-hexanol</i>	891	0.21	111-27-3
1372	1375	3-methyl-3-butenyl isovalerate	897	0.15	54410-94-5
1411	1416	2-nonanone	880	0.24	821-55-6
1471	1475	acetic acid	968	2.13	64-19-7
1563	1558	<i>linalool</i>	827	0.10	78-70-6
1666	1671	<i>methyl benzoate</i>	952	0.99	93-58-3
1708	1714	<i>ethyl benzoate</i>	959	0.64	93-89-0
2487	2493	benzoic acid	912	1.86	65-85-0

^a Identified compounds in italics were also reported by Sampaio and Nogueira (5).

Headspace volatiles. As seen in Table 1, mangaba aroma volatiles consisted of 17 esters, 6 alcohols and 3 ketones. The fruit flavour enhancing acetaldehyde was the only aldehyde observed. The volatile profile of mangaba is dominated by two esters, isoamyl acetate and 4-pentenyl acetate which produced over half (52%) of the total volatile peak area. Isoamyl acetate is common to many fruits and possesses a “juicy fruit” aroma reminiscent of both banana and pear whereas 4-pentenyl acetate has a fruity, solvent-like aroma. Although no single aroma volatile could be

considered a mangaba character impact volatile, the overall sweet, fruity, tropical aroma was due to the balance of the remaining 15 esters, but especially isoamyl acetate and 4-pentenyl acetate. 2,4,5-Trimethyl-1,3-dioxolane has an oxygen heterocyclic structure and apparently occurs in two forms. It is found in other foods and beverages such as tequila, cupuacu (*Theobroma grandiflorum* Spreng.), blackberries (*Rubus laciniata* L.), and Turkish raki.



Mangaba sulphur volatiles. Sulphur volatiles have never been reported in mangaba fruit, but like many tropical fruits they are plentiful. The character impact compounds of many fruit are sulphur volatiles (6). However, not all fruit sulphur volatiles have aroma activity (7). Shown in Figure 1 is the sulphur chromatogram of the headspace from mangaba puree. The major sulphur volatile is sulphur dioxide followed by methane thiol and an unidentified volatile at 11.9 min. The other identified volatiles include: hydrogen sulphide, dimethyl sulphide, dimethyl disulphide, dimethyl trisulphide and methional. Of the seven identified volatiles, only two, methional and diethyl disulphide, appear to have aroma activity based on our experiences with these

compounds on this detector and preliminary GC-O results. Several remaining sulphur volatiles remain to be identified.

Figure 1. SPME headspace chromatogram of mangaba sulphur volatiles using a PFPD detector.

References

1. Narain N. (1990) In *Fruits of tropical and subtropical origin: Composition, properties and uses* (Nagy S., Shaw P. E., Wardowski W. F., eds), Florida Science Source, Lake Alfred, pp 159-165.
2. Texeira E. (1954) *Fruits from brazil*. Instituto Nacional do Livro, Rio de Janeiro, Brazil.
3. Trevas V.F., Freire G.S., Falcone E.G., Trevas I. P. (1971) Report of the section of agriculture and cattle-raising technology, research division and agriculture and cattle-raising experimentation, Convenio do Ministerio da Agricultura (Estado da Paraiba)/Suberintendencia do Desenvolvimento do Nordeste, pp. 105-184.
4. Granja M.L.B.B. (1985) Effect of preservation methods and storage time on the quality of umbu (*Spondias tuberosa* arr. Cam) and mangaba (*Hancornia speciosa* Muell), Joao Pessoa, Brazil, Universidade Federal da Parafba, M.Sc. Thesis.
5. Sampaio T. S., Nogueir, P.C.L. (2006) *Food Chem.* 95: 606-610.
6. Boelens M.H., van Gemert L.J. (1993) *Perfumer & Flavorist* 18(3): 29-39.
7. Perez-Cacho P.R., Mahattanatawee K., Smoot J.M., Rouseff, R. (2007) *J. Agric. Food Chem.* 55: 5761-5767.

CHEMICAL AND AROMA PROFILES OF DIFFERENT CULTIVARS OF YUZU (*CITRUS JUNOS* SIEB. EX TANAKA) ESSENTIAL OILS

M. SAWAMURA and N.T. Lan-Phi

Kochi University, B-200 Monobe, Nankoku, Kochi, 783-8502, Japan

Abstract

The cold-pressed peel oils of six different yuzu cultivars were investigated by instrumental and olfactory analysis. A total of sixty-nine compounds of the six samples were identified. Application of GC-olfactometry and aroma extract dilution analysis technique in three-fold stepwise dilution of the neat oil for all samples indicated eight odorants with the highest flavour dilution (FD) values. Those were limonene, α -pinene, α - and β -phellandrene, myrcene, γ -terpinene, (*E*)- β -farnesene and linalool. Among the six cultivars, 'Komatsu sadao' seemed to be the best cultivar in terms of aroma quality, showing the highest number of components having yuzu-like odour notes.

Introduction

Yuzu (*Citrus junos* Sieb. ex Tanaka) is the most popular among the 70 kinds of Japanese sour citrus fruits (1) with a strong characteristic aroma. Yuzu fruit and its juice have been traditionally used in making vinegar and easing. Yuzu essential oil is widely used in food, beverages, cosmetics, perfumery and aromatherapy. Recently, consumers have been attracted by yuzu flavour, and the demand for yuzu is increasing steeply. Yuzu is cultivated widely in Japan but the main producing area is Kochi which is approx. 50% of the total annual production. The characteristic aroma of yuzu among cultivars is said to be somewhat different. A vast number of studies on the volatile constituents of yuzu cold-pressed oil have been carried out (2-5). The defined cultivars, however, were not mentioned. In this study, the results of volatile compounds and aroma characteristics of the six yuzu cultivars will be presented.

Experimental

Materials. The six yuzu cultivars: 'Jimoto' (JIM); 'Komatsu Koichi' (KOK); 'Komatsu Sadao' (KOS); 'Kumon' (KUM); 'Nagano' (NAG) and 'Yasu' (YAS), were collected from the Kochi Fruit Experimental Station, Japan in November, 2005. The peel oil was extracted from the flavedo by cold-pressing method in our laboratory. Authentic compounds were purchased from Wako Pure Chemical Industries (Japan), Aldrich Chemical Co. (USA), Fluka Fine Chemicals (Switzerland), Nacalai Tesque Inc. (Japan) and Tokyo Kasei Kogyo Co. Ltd (Japan).

GC-MS condition. The composition analysis of the oil was carried out by using a gas chromatograph-mass spectrometer (GC-MS QP-5050A, Shimadzu, Kyoto) equipped with a polar DB-Wax column, 60 m \times 0.25 mm i.d., film thickness 0.25 μ m (J & W Scientific, Folsom, CA, USA), and a non-polar DB-1 column, 60 m \times 0.25 mm i.d., film thickness 0.25 μ m (J & W Scientific, Folsom, CA, USA). The column

temperature was programmed from 70°C (2 min hold) to 230°C (20 min hold) at 2°C/min. The injector and ion source temperature was 250°C. Nitrogen was the carrier gas at a flow rate of 0.8 ml/min. Mass spectra in the electron impact mode (MS-EI) was generated at 70 eV. An oil sample of 0.2 µl was injected in the split mode injection. Identification and quantitative determination were based on Retention Index (RI), mass spectra and co-injection with authentic standards if necessary.

GC-Olfactometry (GC-O) and Aroma Extract Dilution Analysis (AEDA). Samples were prepared by stepwise three-fold dilution with acetone. GC-O was performed by using gas chromatograph (GC-17A, Shimadzu) equipped with a DB-Wax wide-bore fused silica capillary column, 60 m × 0.53 mm i.d., film thickness 1 µm (J & W Scientific, Folsom, CA, USA) connected to a humidifier ODO II (SGE, Japan). The GC conditions were as given above for the GC-MS. An oil sample of 0.5 µl was injected. Nitrogen carrier gas flows at 3.5 ml/min. All dilutions were sniffed in triplicate until no odour was detected in the maximum diluted sample. The highest dilution at which an individual component could be detected was defined as the flavor dilution (FD) factor for that odorant.

Results

Identification of the volatile components. Sixty-nine compounds were identified, constituting about 98.5-99.6% of the entire volatile concentration. The volatile composition of the six yuzu oils (Table 1) was mostly summed up by eighteen monoterpenes. Among them, the most predominant was limonene (63.1-68.1%), followed by γ -terpinene (11.4-12.5%), β -phellandrene (4.6-5.4%), myrcene (3.0-3.2%) and α -pinene (2.3-2.7%). Bicyclo-germacrene was present in the greatest amount (1.5-2.0%) with respect to the other sesquiterpenes in most of the oils analysed. The two isomeric sesquiterpenes (*Z*)- and (*E*)- β -farnesene were also quantified, and the (*E*) isomer was predominant at a higher proportion of 0.9-1.3%. The presence of bicyclo-germacrene and (*E*)- β -farnesene in yuzu oil was previously reported at significant amount by Sawamura (2000). Germacrene is often identified in citrus oils such as in lime oil (7) and germacrene D was the significant constituent of Japanese yuzu oil (4). In this study, germacrene B and D accounted for 0.1-0.2% and 0.3-0.4%, respectively. Other sesquiterpenes such as δ -elemene (0.1-0.2%) and β -caryophyllene (0.3%) also commonly existed. Monoterpene and sesquiterpene alcohols were the minor component in these yuzu oils. Linalool (1.9-2.9 %) and α -terpineol (0.2-0.3%) were predominant as the former, while germacrene D-4-ol (0.3-0.4%) as the latter. Alcohol group (2.7-4.0%) was summed up most of the oxygenated content. The concentration of aldehydes in these samples was low compared to that of other groups identified. Six aldehydes were detected and their content ranged from trace to 0.1%. Octanal and nonanal, which play a remarkable role in some citrus fruits, were also determined at very low content. Other minor components including one ester, two ketones and two oxides were presented in a trace amount.

Characterisation of the odorants. The odour-active components of yuzu oils were determined on the basis of flavour dilution (FD) factor value resulted from GC-sniffing and AEDA. The data in (Table 2) showed that limonene, α -pinene, and α - and β -phellandrene had the highest FD value. The other odorant with high FD values were myrcene, linalool, (*E*)- β -farnesene and γ -terpinene. Among sesquiterpene hydrocarbons, *trans*- β -farnesene, germacrene D and bicyclo-germacrene were

having the highest FD factors. Two alcohols, linalool and α -terpineol were the odour-active compounds among the alcohols found in these yuzu oils. Octanal and decanal were represented odour-active components of aldehydes. Among characterised odorants, the compounds possesses yuzu-like note are often considered for its remarkable contribution in reconstruction of yuzu aroma model. Fifteen compounds of the six samples were described as having yuzu-like aroma. KOS seemed to be the best cultivar in terms of aroma quality, showing the highest number of components having yuzu-like odour notes. β -Elemene, β -caryophyllene, γ -elemene, α -muurolene, bicyclo-germacrene, δ -cadinene and germacrene B indicated yuzu-like odour and/or citrus-like note in at least four out of the six samples. Bicyclo-germacrene, however, little contributed to yuzu flavour as previously reported (8). There were no compounds showing yuzu-like odour in all samples.

Table 1. Volatile composition of the six cultivars of yuzu peel oils

Peak No.	Compound	RI		Relative concentration (%)					
		DB-Wax	DB1	JIM	KOK	KOS	KUM	NAG	YAS
1	α -pinene	1040	943	2.7	2.6	2.6	2.5	2.4	2.3
3	β -pinene	1126	980	1.1	1.1	1.0	1.0	1.0	0.9
4	sabinene	1135	977	0.5	0.5	0.5	0.5	0.5	0.4
6	myrcene	1171	991	3.2	3.1	3.0	3.0	3.1	3.0
7	α -phellandrene	1179	1006	0.9	0.8	0.9	0.9	0.8	0.7
9	α -terpinene	1193	1018	0.3	0.3	0.3	0.3	0.3	0.3
10	limonene	1222	1037	63.1	63.2	67.8	66.6	65.3	68.1
11	β -phellandrene	1229		5.4	5.1	5.3	5.2	4.8	4.6
13	γ -terpinene	1262	1061	12.5	12.1	11.4	11.5	12.3	11.6
15	<i>p</i> -cymene	1282	1021	0.6	0.6	0.4	0.5	0.4	0.4
16	terpinolene	1295	1088	0.7	0.7	0.6	0.6	0.7	0.6
25	δ -elemene	1479	1343	0.2	0.2	0.2	0.2	0.2	0.1
32	linalool	1555	1093	2.8	2.9	1.9	2.4	2.6	2.1
35	β -elemene	1597	1394	0.1	0.1	0.1	0.1	0.1	0.1
36	β -caryophyllene	1607	1425	0.3	0.3	0.3	0.3	0.3	0.3
43	(<i>E</i>)- β -farnesene	1671		1.3	1.1	0.9	0.9	1.2	0.9
44	α -humulene	1680	1459	0.1	0.1	0.1	0.1	0.1	0.1
45	α -terpineol	1706	1183	0.3	0.3	0.2	0.2	0.3	0.2
47	germacrene D	1719	1487	0.4	0.4	0.3	0.3	0.4	0.3
51	bicyclogermacrene	1746	1500	2.0	2.0	1.5	1.8	2.0	1.7
53	δ -cadinene	1766		0.1	0.1	0.1	0.1	0.1	0.1
58	germacrene B	1841		0.2	0.2	0.1	0.1	0.2	0.1
62	germacrene D-4-ol ^t	2063		0.4	0.4	0.3	0.4	0.4	0.4
66	thymol	2193	1280	0.3	0.2	0.2	0.2	0.2	0.2
	Aliphatics (1)			tr	nd	nd	tr	nd	tr
	Monoterpenes (18)			91.1	90.0	93.6	92.6	91.5	93.0
	Sesquiterpenes (23)			4.5	4.3	3.3	3.6	4.3	3.6
	Aldehydes (6)			0.1	0.1	tr	0.1	0.1	tr
	Alcohols (16)			3.9	4.0	2.7	3.4	3.7	3.0
	Esters and Ketones (3)			tr	tr	tr	tr	tr	tr
	Oxides (2)			tr	tr	nd	tr	tr	tr
	Total (69)			99.5	98.5	99.6	99.6	99.6	99.6

^t: Tentatively identified; tr: trace, peak area quantified less than 0.05%; nd: not detected. The values are means of triplicated analyses for each sample.

Table 2. FD values of the aroma active compounds of yuzu peel oils

Peak	Compound	$\log_3(\text{FD-factor})^a$					
		JIM	KOK	KOS	KUM	NAG	YAS
1	α -pinene	7	8	5	8	8	8
3	β -pinene	7	8	6	7	8	5
4	sabinene	7	7	6	8	7	4
6	myrcene	7	8	5	8	7	8
7	α -phellandrene	7	7	6	7	8	9
9	α -terpinene	6	6	5	7	7	5
10	limonene	8	7	7	9	8	7
11	β -phellandrene	7	7	9	8	7	6
13	γ -terpinene	7	7	8	6	7	7
15	<i>p</i> -cymene	6	4	4	8	4	5
16	terpinolene	7	5	4	9	5	6
17	octanal	4	5	4	7	4	4
25	δ -elemene	7	4	4	7	6	4
30	decanal	4	5	7	4	5	4
31	β -cubebene	5	6	6	5	6	5
32	linalool	7	8	6	7	8	7
35	β -elemene	4	4	7	5	4	4
36	β -caryophyllene	5	6	6	8	6	6
37	terpinen-4-ol	4	5	6	6	5	4
40	γ -elemene	4	4	7	4	4	5
43	(<i>E</i>)- β -farnesene	7	6	6	9	6	9
45	α -terpineol	6	5	6	6	6	7
47	germacrene D	6	7	6	6	6	8
51	bicyclogermacrene	6	7	5	8	6	9

^a: The base-3 logarithm of flavor dilution factor value on DB-Wax colour

Although the six cultivars investigated had essentially yuzu characteristic odour, some differences could differentiate one from the others.

References

1. Sawamura M. (2005) In *Fruits. Growth, Nutrition, and Quality* (Dris, R., ed.), WFL Publisher, pp 1-24.
2. Kusunose H., Sawamura M. (1980). *Nippon Shokuhin Kogyo Gakkaishi*. 27: 517-521.
3. Ohta H. (1983). *J. Chromatogr.* 268: 336-340.
4. Njoroge S.M., Ukeda H., Kusunose H., Sawamura M. (1994) *Flav. Fragr. J.* 9: 159-166.
5. Song H.S., Sawamura M., Ito T., Ukeda H. (1999) *Flav. Fragr. J.* 14: 383-389.
6. Ullrich F., Grosch W. (1987) *Z Lebensm Unters Forsch.* 184: 147-158.
7. Lan Phi, N.T., Minh Tu N.T., Nishiyama C., Sawamura M. (2006) In *Flavor Science: Recent Advances and Trends* (Bredie W.L.P., Petersen M.A., eds.), Elsevier, pp 193-196.
8. Song H.S., Sawamura M., Ito T., Kawashimo K., Ukeda H. (2000) *Flav. Fragr. J.* 15: 245-250.

VOLATILE COMPOUNDS AND AMINO ACIDS IN CHEESE POWDERS MADE FROM MATURED CHEESES

C. VARMING¹, T.K. Beck², M.A. Petersen¹, and Y. Ardö¹

¹ *Department of Food Science, University of Copenhagen, Rolighedsvej 30, 1958 Frederiksberg C, Denmark*

² *Lactosan A/S, Nordbakken 2, 5750 Ringe, Denmark*

Abstract

Three types of cheese powder made from well-matured cheeses were analysed for their content of volatile compounds and amino acids. The cheese powder types could be distinguished according to their amino acid and volatile compound profiles. The amino acids glutamic acid and GABA are likely to contribute directly to the taste of a food application.

Introduction

Cheese powder is used as a natural flavour ingredient in industrial applications such as biscuits, sauces, ready meals and processed cheese. In addition, cheese powders produced from well-matured cheeses have the potential to boost the cheese flavour of food products and may replace flavour enhancers such as sodium glutamate and yeast extract. Introductory sensory tests of three different cheese powders, made from well-matured cheeses, in tomato soup, showed that they influenced the flavour of tomato, cheese, sourness and richness, in three different ways. However, limited information is available regarding flavour constituents of cheese powder (1), hence the aim of the present study was to characterise the differences in composition of volatile compounds and amino acids in three types of cheese powders made from well-matured cheeses.

Experimental

Cheese powders. Three types of cheese powder based on minimum 50% smeared type cheese (eight samples), minimum 50% hard cheese (five samples) and minimum 50% Blue type cheese (two samples), respectively (Lactosan A/S, Ringe, Denmark) were made by melting and spray drying a mixture of well-matured cheeses. All cheese powders were produced at different days from recipes comprising between 5 and 13 assorted cheeses, with a variation between batches of the same cheese powder type depending on availability of cheeses on the market.

Dynamic headspace sampling and GC-MS analysis. Volatile compounds were isolated by dynamic headspace sampling on Tenax TA traps using 30 grams of cheese powder, 110 ml of water and 1.00 ml of internal standard (4-methyl-1-pentanol). The collected volatiles were thermally desorbed and analysed by GC-MS with a J & W Scientific DB-Wax column (1). Tentative identifications were carried out by probability-based matching with mass spectra in the G1035A Wiley library

(Hewlett-Packard). Calculations were based on peak areas divided by area of internal standard. The dynamic headspace samplings were performed in duplicate.

Amino acids with HPLC. Free amino acids were analysed by reversed phase HPLC. For primary amino groups derivatisation was made using *o*-phthaldialdehyde, and for the secondary amino group of proline, fluoroenylmethyl chloroformate was used (2).

Results

Using principal component analysis the three types of cheese powders could be distinguished according to their content of amino acids and volatile compounds (48% explained variation), however large variations occurred between batches within each cheese powder type (Figure 1).

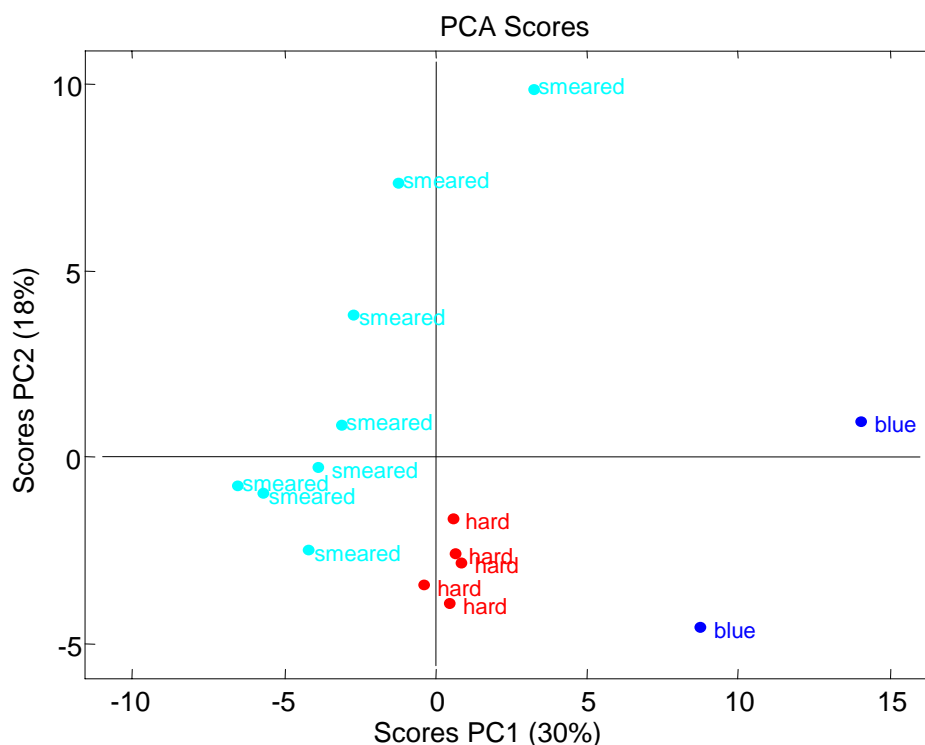


Figure 1. PCA scores plot of all amino acids and volatile compounds identified in the three types of cheese powder made from smeared, hard and blue type well-matured cheeses, respectively.

Of the 80 volatile compounds identified in the cheese powders (data not shown) 26 differed significantly between the cheese powder types (Table 1). The smeared type cheese powders had the significantly highest level of 2,5-dimethyl-5-trimethylpyrazine, as well as of dimethyl trisulphide and phenol that are characteristic compounds of smear ripened cheeses, and of which dimethyl trisulphide is expected to contribute to the aroma character of this cheese powder type (3). The hard type cheese powders had low to medium levels of most volatile compounds. The blue type cheese powders were characterised by the highest levels of most volatile compounds, including methyl ketones, esters and lactones, many of which are known compounds of blue cheese and are expected to contribute to the aroma characteristic of this cheese powder type (3). Similar results were obtained in (1).

Table 1. Average levels of volatile compounds (arbitrary units, peak areas divided by internal standard x1000) with significant different levels ($P < 0.05$) in the three types of cheese powder.

Volatile compound	Smearred type (n= 8)	Hard type (n= 5)	Blue type (n= 2)
Dimethyl trisulphide	89a ¹	31b	23b
Methyl propanethioate	3b	0b	93a
Octanal	19b	19b	34a
Decanal	33b	30b	96a
Diacetyl and 2-pentanone ²	301b	358b	569a
3-Penten-2-one	19ab	8b	32a
2-Hexanone and hexanal ²	104b	140ab	203a
2-Heptanone	473b	570b	3013a
2-Octanone	15b	18b	86a
2-Nonanone	227b	375b	2635a
8-Nonen-2-one	23b	44b	317a
2-Undecanone	19b	32b	279a
Ethyl acetate	23b	27b	124a
Methyl hexanoate	14b	21b	94a
Pentyl butanoate	32b	33b	101a
2-Methyl-butyl-hexanoate	11b	15b	043a
Methyl decanoate	2b	7b	42a
1-Butanol	9b	7b	23a
2-Heptanol	52b	75b	172a
2-Nonanol	13b	25b	79a
Phenol	246a	123b	46b
γ -Pentalactone	2b	3b	9a
γ -Hexalactone	1b	2b	43a
γ -Heptalactone	2b	5b	11a
2,5-Dimethyl-5-ethylpyrazine	11a	2b	0b
Trimethylbenzene	1b	6ab	9a

¹ Within each volatile compound values with different letters are significantly different.

² Co-eluting compounds.

The concentration of 16 of the 23 identified amino acids differed significantly between the three cheese powder types (Table 2). The content of leucine and glutamic acid were highest in all samples. Smearred cheese type and hard cheese type powders had the highest total content of free amino acids as well as of more of the individual amino acids, indicating that the cheeses used were more mature.

Especially glutamic acid but also aspartic acid are of interest due to their umami taste (4), however, they did not vary significantly between cheese powder types. Literature is contradictory about the taste sensation of the glutamic acid breakdown product γ -aminobutyric acid (GABA), which has been shown to contribute to sour and umami as well as astringent sensations. The taste characteristic and taste threshold of α -aminobutyric acid (AABA) has not been well established, but due to its structural resemblance with glutamic acid it may also be of importance.

GABA, glutamic acid, aspartic acid, alanine, leucine, methionine and isoleucine had taste activity values (TAV) > 1 in all the cheese powders (data not shown) (4); but considering the level of 2-6% cheese powder used in food applications, only

glutamic acid and GABA are likely to contribute directly to the taste. However, interactions between the amino acids and other constituents might affect their taste qualities and taste threshold levels.

Table 2. Average concentration of amino acids in the three types of cheese powder.

Amino acid	Concentration (mmol/kg)		
	Smearred type (n= 8)	Hard type (n= 5)	Blue type (n= 2)
Leu	45a ¹	39a	29b
Glu	37	36	28
Val	34a	29a	17b
Pro	32a	28a	17b
Ala	25a	19b	11c
GABA	24a	15b	1.9c
Lys	23	26	26
Ile	20a	18a	11b
Phe	18a	16a	11b
AABA	18a	10b	1.6c
Gly	14a	13a	6.4b
Met	10	8.4	8.0
Asp	8.1	11	10
His	5.7	6.7	6.2
Thr	5.5	7.1	5.3
Cit	5.5	5.3	4.8
Tyr	5.4b	5.9b	7.7a
Orn	5.3a	4.4ab	2.5b
Gln	5.2b	7.4a	8.8a
Ser	5.1b	8.5a	7.6a
Asn	2.7b	5.4a	5.4ab
Trp	2.3a	1.7b	2.1ab
Arg	0.4b	2.0a	3.6a
Total free amino acids	351a	323a	231b

¹ Within each amino acid values with different letters are significantly different ($P < 0.05$).

Sensory evaluations of the effects of the different types of the mature cheese powders applied in foods will be performed and the taste threshold value and taste properties of GABA and AABA should be further evaluated in order to determine their contribution to umami or other taste properties.

References

1. Varming C., Petersen M.A., Beck T.K., Ardö Y. (2008) In *Recent Highlights in Flavor Chemistry and Biology* (Hofmann T., Meyerhof W., Schieberle P., eds); Deutsche Forschungsanstalt für Lebensmittelchemie, pp 336-339.
2. Butikofer U., Ardö, Y. (1999) *Bulletin of the International Dairy Federation* 337: 24-32.
3. Curioni P.M.G., Bosset J.O. (2002) *Int. Dairy J.* 12: 959-984.
4. Rotzoll N., Dunkel A., Hofmann T. (2006) *J. Agric. Food Chem.* 54: 2705-2711.

FIRST IDENTIFICATION OF TWO POTENT THIOL COMPOUNDS IN RIPENED CHEESES

A. M. SOURABIÉ^{1,2}, S. Landaud², P. Bonnarme², A. Saint-Eve², and H-E. Spinnler²

¹ SAF-ISIS, Z.A. 40140 Soustons, France

² UMR INRA / AGROPARISTECH GMPA, CBAI, F-78850 Thiverval-Grignon, France

Abstract

Different methods of sample preparation followed by extractions with *p*-hydroxymercuribenzoate (*p*HMB) were used to investigate the occurrence of thiol compounds in ripened cheeses. The analysis of cheese extracts by GC coupled with PFPD, MS and olfactometry detections enabled the identification of ethyl 2-mercaptopropionate (ET2MP) and ethyl 3-mercaptopropionate (ET3MP) in Munster and Camembert cheeses. The average concentrations of ET3MP measured in Munster and Camembert cheeses were 3.88 and 1.67 µg/Kg respectively while ET2MP was only found in trace amounts in Munster cheese.

Introduction

It is nowadays well established that hundreds of compounds are involved in the overall cheese flavour. Among them, sulphur ones are of particular interest because of their very powerful odours and low perception thresholds. As reviewed by Molimard and Spinnler (1) there are lot of evidence that sulphur odorants like methanethiol, polysulphides and *S*-methyl thioesters play an important role in the flavour of cheese. Conversely, until now only little attention has been given to the possible occurrence of thiols in cheese. To date, apart from methanethiol, only one thiol compound was identified in Gouda cheese (5). The difficulty of carrying out thiols isolation in cheese is due to the complexity of its matrix and to the very low concentrations of such compounds which make them undetectable by the classic means. The objective of this study was to isolate new thiols in cheese using a method inspired from Tominaga et al. (2, 3). The method was considerably modified to overcome the problems related with the fat content and heterogeneity of cheese.

Experimental

Initial sample preparation. Several varieties of cheeses were used for this study due to their strong sulphur odour (6). The first step of preparation consisted in removing from the surface of each sample thin layers that were subsequently cut into small cubes. After addition of dichloromethane (DCM) the mixtures were stirred for 18 to 20 h. Then, the volatile thiols contained in the organic phases were extracted twice using a *p*HMB solution and purified on a strongly basic anion-exchanger column.

Extraction of thiols from the columns (6). The volatile thiols were released from the thiol-*p*HMB complexes by eluting an L-cysteine solution. The eluates were successively extracted by 4 and 3 mL of DCM and dried on anhydrous Na₂SO₄. They were finally concentrated under a nitrogen flux and 3 µL was injected in GC.

Identification and quantification of volatile thiols. The apparatus and analytical methods were recently depicted in (6). The volatile thiols were identified by comparing their retention times and their mass spectra in SCAN mode with those of the commercial references. The calculation of linear retention indices (RI_{MS} and RI_{PFPD}) and the quantification of volatile thiols were performed as previously described (6).

Determination of the olfactive perception threshold. Ascending forced-choice procedures were used to evaluate the odour threshold value of ET3MP in cream (6). The best estimated thresholds were calculated according to Meilgaard et al. (7).

Results

Thiols identification and quantification. Among the cheese samples analysed, thiols could only be identified in Munster brand “*Ermitage*” and Camembert brand “*Jean Vernier*” (6). The PFPD chromatogram of the Munster cheese extract shows numerous peaks. After a comparison of its PFPD retention time with that of a pure reference and GC-MS identification, a first peak ($RI_{MS}= 935$, $RI_{PFPD}= 1012$) was identified as ET2MP, a potent odorant found in cashew apple juice (8), strawberry oil (9) and wine (10). Following the same procedure, a second peak ($RI_{MS} = 1024$, $RI_{PFPD}= 1101$) was identified as ET3MP, a volatile previously reported in Concord grape (11) and wine (10). As presented in (Figure 1) its mass spectrum (Figure 1A) tightly matched up to that of the commercial reference (Figure 1B).

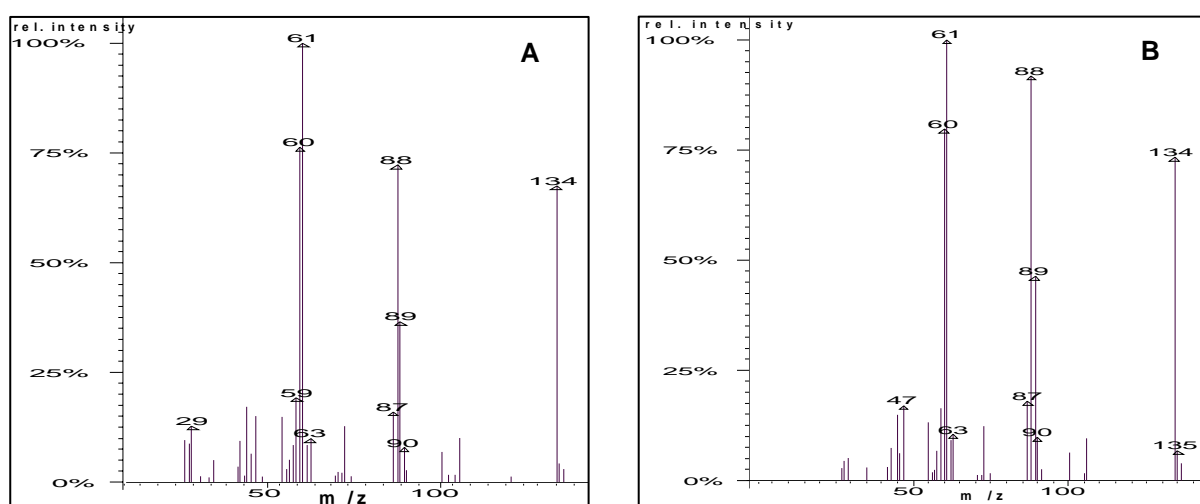


Figure 1. Mass spectra (MS/EI) of ET3MP detected in a final L-cysteine extract of Munster “*Ermitage*” (A) compared to that of its commercial analogue (B).

To our knowledge, this is the first report of the occurrence of these two thiol compounds in cheese. Moreover, an additional attribute for their identification was represented by their odour quality assessed by GC-O which was identical to those of the pure references at the same concentration. The average concentration for ET3MP in the surfaces of Munster and Camembert samples were $3.88 \pm 0.22 \mu\text{g/kg}$ and $1.67 \pm 0.19 \mu\text{g/kg}$ respectively while ET2MP was only found in trace amounts in Munster. As cheese aroma formation often begins by the surface before diffusion into the core, and given that thiols are more sensitive to oxidation on the surfaces, the concentrations of these thiols in the whole cheeses may be higher than those of the surfaces.

Hypothetical biosynthetic pathways. The metabolic routes leading to the formation of both ET2MP and ET3MP in cheese are not elucidated yet. However, it can be supposed that they could be similar to those described for other thiol compounds in wine and beer. Hence, their synthesis must be related to the microbial catabolism of amino acids, mainly alanine, cysteine and methionine which are present in caseins. Whatever the pathway, it is likely that 2- and 3-mercaptopropionate were formed before subsequent esterification with ethanol. First, alanine could be converted by an ammonia lyase to form acrylate that could subsequently react with hydrogen sulphur (H_2S) issued from cysteine to yield either ET2MP or ET3MP in a Markovnikov's type reaction (Figure 2). Moreover, alanine could undergo a dehydrogenation catalysed by an alanine dehydrogenase (EC 1.4.1.1) to produce pyruvate which finally yields 2-mercaptopropionate by a nucleophilic substitution with H_2S (Figure 2). Alternatively, pyruvate could be formed by glycolysis during cheese ripening.

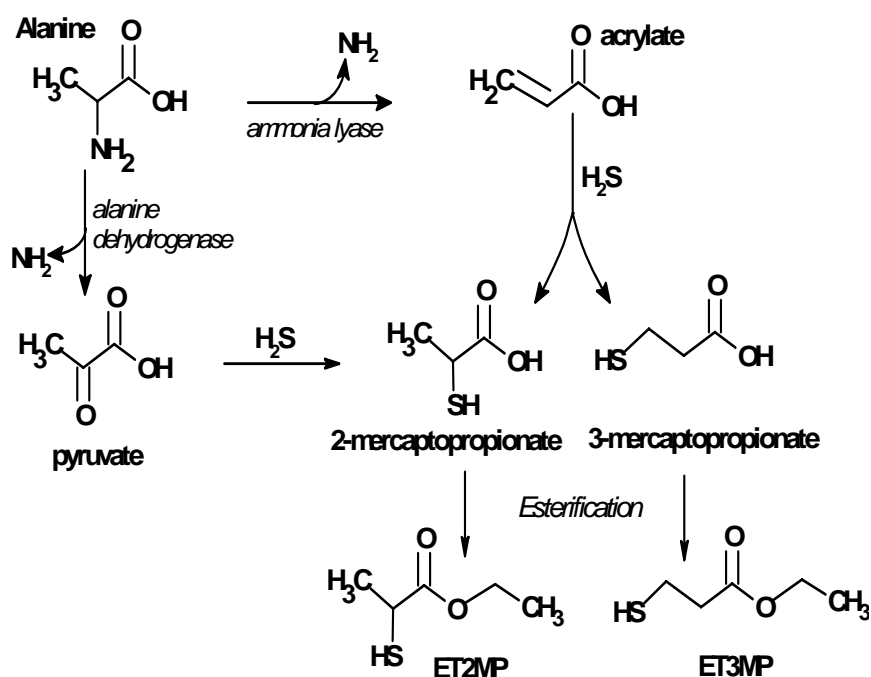


Figure 2. Hypothetical formation pathways of ET2MP and ET3MP.

Besides, as methionine can generate homocysteine by a methyl transfer, an additional route for ET3MP synthesis could be the Ehrlich degradation of this amino acid which is well-known to occur in fermented beverages and cheese (Figure 3).

Evaluation of the sensorial properties. Many odorous zones were identified by the judges during the olfactometric analysis of Munster and Camembert cheeses. Odour corresponding to the peak of ET2MP was described as “fruity, sulphur, animal, foxy, burnt and pungent” while the descriptors for the peak of ET3MP were “grapy, fruity, rhubarb, sulphur and empyreumatic”. The group perception threshold for ET3MP in fresh cream was 723 ppt, giving evidence of its very powerful odour. The presence of ET3MP in Munster and Camembert at concentrations above its perception threshold in cream suggests that it probably make a significant contribution to the aroma of these cheeses. Despite ET2MP was found in trace amounts, its detection by GC-O and its low perception threshold (500 ppt in wine model solution) (10) allows to assume that it must also contribute to the flavour of Munster.

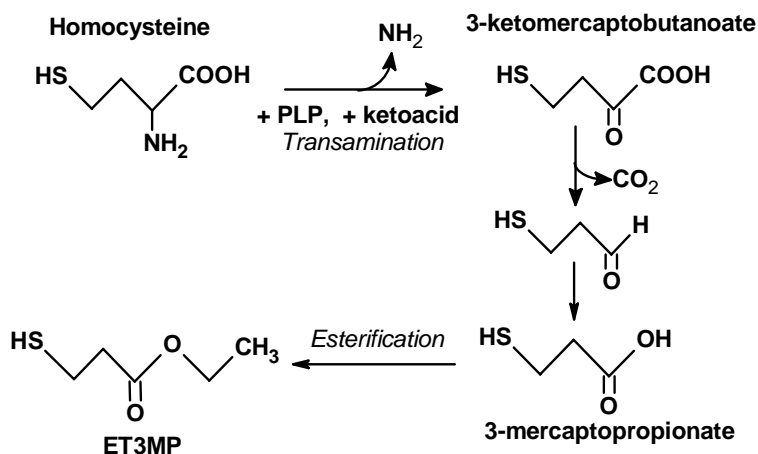


Figure 3. Proposed formation route of ET3MP via the Ehrlich pathway.

In this study we have demonstrated for the first time the unequivocal occurrence of two new thiols, ET2MP and ET3MP, in different cheese varieties. These promising results are a first step toward a better understanding of thiols contribution to cheese flavour. Nevertheless, further studies will be necessary to investigate their formation pathways in cheese.

Acknowledgment

This paper is dedicated to the late Dr. Takatoshi Tominaga who has greatly contributed to the knowledge of thiols isolation. Part of this work was supported by the EcoMet Program funded by ANR (Agence Nationale de la Recherche, France).

References

1. Molimard P., Spinnler H.E. (1996) *J. Dairy Sci.* 79: 169-184.
2. Tominaga T., Guimbertau G., Dubourdieu, D. (2003) *J. Agric. Food Chem.* 51: 1373-1376.
3. Tominaga T., Dubourdieu D. (2006) *J. Agric. Food Chem.* 54: 29-33.
4. Vermeulen C., Lejeune I., Tran T.T.H., Collin S. (2006) *J. Agric. Food Chem.* 54: 5061-5068.
5. Badings H.T., Stadhouders J., van Duin H. (1968) *J. Dairy Sci.* 51: 31-35.
6. Sourabié A.M.; Spinnler H.E.; Bonnarme P.; Saint-Eve A.; Landaud S. (2008) *J. Agric. Food Chem.* 56: 4674-4680.
7. Meilgaard M., Civille G.V., Carr B.T. (1991) In *Sensory Evaluation Techniques*. CRC Press: Boca Raton, pp 123-133.
8. Maciel M.L., Hansen T.J., Aldinger S.B., Labows J.N. (1986) *J. Agric. Food Chem.* 34: 923-927.
9. Teranishi R., Corse J.W., McFadden W.H., Black D.R., Morgan A.I. (1961) *J. Food Sci.* 28 :478-483.
10. Tominaga T., Guimbertau G., Dubourdieu D. (2003) *J. Agric. Food Chem.* 51: 1016-1020.
11. Kolor M.G. (1983) *J. Agric. Food Chem.* 31: 1125-1127.

CHEMICAL AND SENSORY ANALYSIS OF CYSTEINE-S-CONJUGATES AS FLAVOUR PRECURSORS

C. STARKENMANN, B. Le Calvé, Y. Niclass, I. Cayeux, S. Beccucci, and M. Troccaz

Firmenich SA, Corporate R&D Division, P.O. Box 239, CH-1211 Geneva 8, Switzerland

Abstract

The presence of cysteine-S-conjugates in a wide variety of natural products such as onion, garlic, asparagus, wine, and passion fruit has been described. These conjugates are flavour precursors that release volatile sulphur compounds upon the action of enzymes during fermentation or when food is cut. Through careful sensory analysis, we investigated the release of 3-sulfanylhexan-1-ol, 1-propane thiol, and 2-heptane thiol from their precursors S-[1-(2-hydroxyethyl)-1-butyl]-L-cysteine, S-propyl-L-cysteine, and S-(1-methylhexyl)-L-cysteine, respectively, in the mouth. This study demonstrated a clear time-delayed perception of volatile sulphur compounds when an odourless solution of cysteine-S-conjugate precursor was taken into the mouth. The transformation of cysteine-S-conjugate by mouth microflora such as *Fusobacterium nucleatum* was also demonstrated.

Introduction

(*R/S*)-3-Sulfanylhexan-1-ol **1** has been described as a key flavour odorant in passion fruit (1, 2), wine (3), *Ruta chalepensis* L. (4), *Persicaria odorata* (5), *Poncirus trifoliata* (L.) Raf. (6), human sweat (7), and yeast (8). 1-Propane thiol **2** is present in the *Alliums* genus and in some types of beers; 2-heptane thiol **3** is detected in red bell peppers (*Capsicum annuum*) (9). One biological precursor of (*R/S*)-3-sulfanylhexan-1-ol **1** appears to be a cysteine-S-conjugate (S-[1-(2-hydroxyethyl)butyl]-L-cysteine, also named S-(3-hexan-1-ol)-L-cysteine) **4**, identified for the first time in *Vitis vinifera* L. cv Sauvignon and later in passion fruit (10, 11) and bitter orange (6).

Here we describe the sensory characteristics of the mouth release of volatile organic sulphur compounds **1–3** from their purified cysteine-S-conjugates **4–6** in analogy to what happens with food systems. The role of mouth microflora and the interactions of saliva proteins with volatile sulphur compounds are also discussed.

Experimental

Cysteine-S-conjugates. S-[1-(2-Hydroxyethyl)-1-butyl]-L-cysteine **4** was prepared according to published methods (5, 12). S-Propyl-L-cysteine **5** was prepared according to reference (13) and S-(1-methylhexyl)-L-cysteine **6** was prepared according to reference (14). Detailed analytical procedures, as well as incubations with mouth microorganisms, are described in reference (14) (Figure 1).

Sensory methodology: Subjects. Thirty trained panellists from Firmenich S.A., Geneva, were asked to evaluate the perceived odour intensity.

Testing protocol. To avoid any fatigue or sensation overlap, subjects tasted only one sample per session. Each subject received a sample (30 mL) in a cup. Subjects

were asked to sequentially sip the entire sample into their mouth and to start a timer at the same time. They then spit out the sample after 5 s. They evaluated the time at which they started to perceive a sulphur flavour (T_{begin}), the maximum perceived sulphur intensity and its corresponding time (I_{max} and T_{max}), and finally the perceived sulphur intensity 3 min after sipping the sample ($I_{3 \text{ min}}$) or the time at which the sulphur intensity disappeared if it was less than 3 min after sipping (T_{end}). Each evaluation was rated on a linear scale from *not at all* to *very intense* (coded from 0 to 10). Tests were repeated twice to demonstrate repeatability of the sensory measurement (Table 1, Figure 2). T_{end} and $I_{3 \text{ min}}$ are averaged for the panel using the following rules. If the subject didn't perceive any odour before 3 mins, the data were recording as $I_{3 \text{ min}}$ is equal to 0 and T_{end} scored given by the subject (less than 180s). If the subject perceived always the odour after 3 mins, the data were recording as $I_{3 \text{ min}}$ scored given by the subject and T_{end} is equal to 180s. The results present the panel average for T_{end} and $I_{3 \text{ min}}$. Then the average is calculated for all the subjects.

Results

The (*R/S*)-3-sulfanylhexan-1-ol **1** (Figure 1) was tasted in plain water at 0.01 ppm, and this concentration was above the reported odour threshold of around 5–60 ng/L (15); therefore all subjects were able to detect the smell without ambiguity. (*R/S*)-3-Sulfanylhexan-1-ol **1** (free thiol) was perceived almost immediately at T_{begin} 5 (\pm 2) s and its maximum odour intensity was found to be at T_{max} 20 (\pm 4) s (Figure 2, Table 1). The cysteine-S-conjugate **4**, tasted at 1 ppm, was perceived at T_{begin} 12 (\pm 2) s; the rating of the maximum intensity (I_{max}) was the same, but T_{max} was shifted to 39 (\pm 8) s. Finally, the odour persisted over 163 (\pm 9) s (calculated panel average time), demonstrating a very long, lingering effect compared with **1**, which disappeared after 100 (\pm 12) s. The perceived sulphur intensity according to time is represented by (Figure 2) (panel average and confidence interval at 5%). The retronasal odour profiles of the combined cysteine-S-conjugate and free thiol were similar.

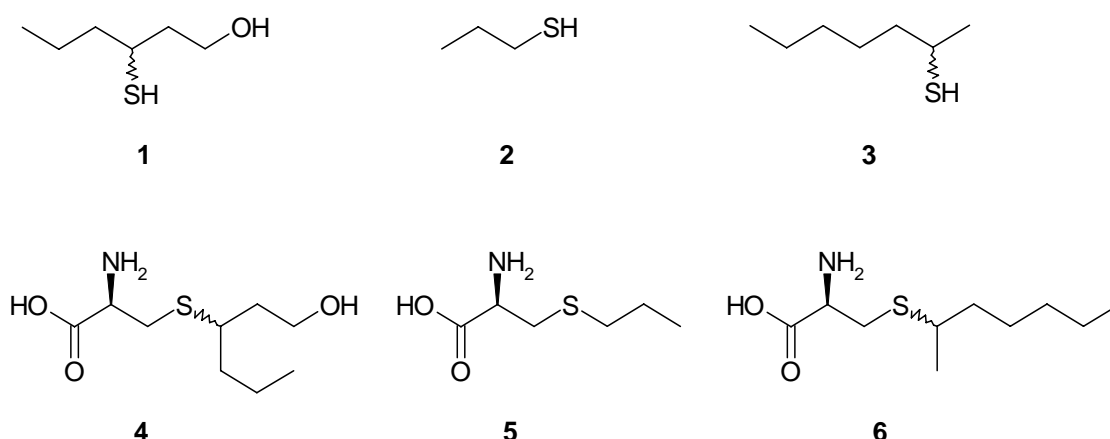


Figure 1. Structures of cysteine-S-conjugates and their corresponding free thiols.

To demonstrate this effect with a more hydrophobic thiol such as 1-propane thiol **2**, we selected the cysteine-S-conjugate **5**. The occurrence of **2** and **5** in onion and in *Allium* genus. (16) and the importance of 1-propane thiol **2** in many natural flavours (15) made **2** a very good candidate for this study. The same sensory test was organized. Results are summarized in Table 1. T_{max} appeared to be significantly shifted from 20 (\pm 4) s to 37 (\pm 7) s when **2** was liberated from **5**. The maximum

flavour intensity (I_{\max}) of **2** at 10 ppb (1.3×10^{-7} mole/L) was the same as the I_{\max} of cysteine-S-conjugate **5** at 20 ppm ($1.2 \cdot 10^{-4}$ mole/L). The T_{begin} values were not significantly different, but the long-lastingness in the mouth was significantly longer for the cysteine-S-conjugate.

Table 1. Time-intensity study. The subjects reported the time of sulphur perception onset (T_{begin}); the maximum perceived sulphur intensity on a linear scale from 1 to 10 and its corresponding time (I_{\max} and T_{\max}); and the perceived intensity 3 min after they had sipped the sample (I_{end}) or the time at which the sulphur intensity disappeared if it was earlier than 3 min (T_{end}). I_{end} and T_{end} are panel average: data in bold indicate significant differences at 5% (Student's t test) between the free thiols and their cysteine-S-conjugates.

Product	Conc (mg/L)	Conc (mole/L)	T_{begin} (s)	I_{\max}	T_{\max} (s)	I_{end}	T_{end} (s)
1	0.01	$7.50 \cdot 10^{-8}$	5	6.1	20	0.4	101
4	1	$4.50 \cdot 10^{-6}$	12	5.8	39	1.6	163
2	0.01	$1.30 \cdot 10^{-7}$	7	4.7	20	0.4	76
5	20	$1.20 \cdot 10^{-4}$	10	5.3	36	1.8	155
3	0.01	$7.60 \cdot 10^{-8}$	5	4.2	20	0.3	99
6	1	$4.50 \cdot 10^{-6}$	10	5.2	40	1.5	159

2-Heptane thiol **3** is a key odorant molecule in bell pepper (9) and its natural precursor **6** in bell pepper was recently identified (14). The Student's t test shows a significant difference for T_{begin} , when **3** was perceived from its corresponding conjugate **6**. The time to reach the maximum intensity (T_{\max}) was significantly longer when **3** was liberated from **6**, and the lingering effect was at least 1 min longer for **6** compared with **3** (Table 1).

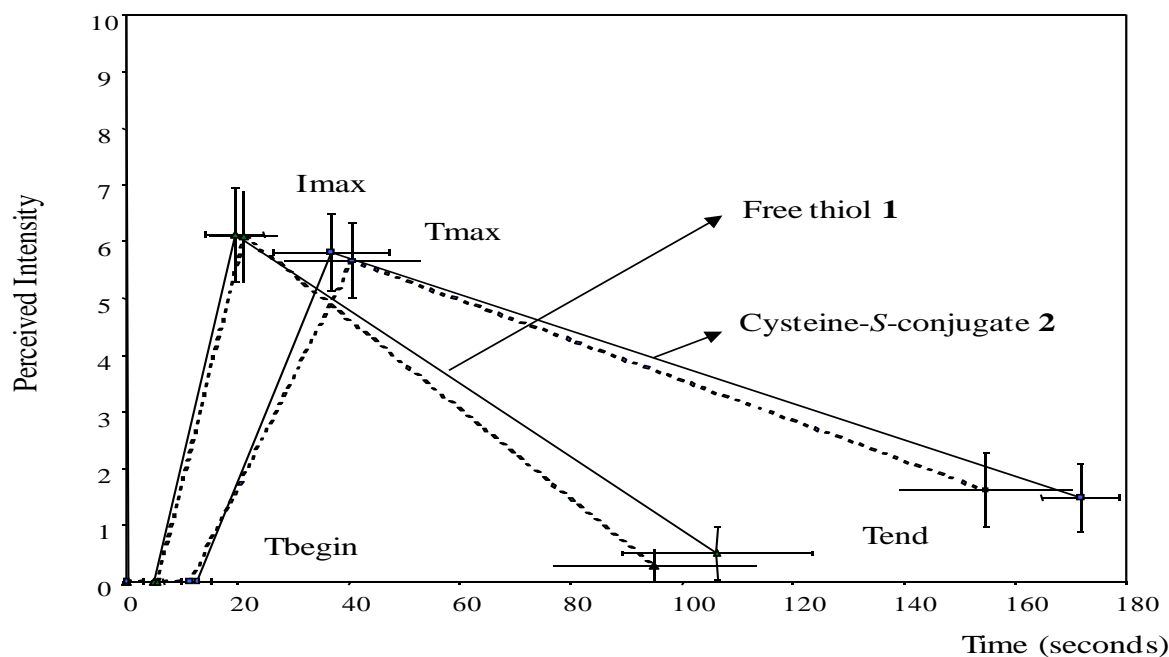


Figure 2. Compared perceived intensities over time of compound **1** tested in its free state and in the cysteine-S-conjugate form **4**. Dotted lines are repetitions of the panel. Bars represent errors around I , T .

The stability of **4** in sterile saliva was monitored by LC-MS and was found to be stable for 50 hours at room temperature, but **4** was completely consumed by crude saliva. The mouth microflora was cultivated and after selection of different bacterial populations, we were able to show that anaerobes (strict anaerobes, Gram negative) efficiently consumed the conjugate. Finally, because of the strong interaction of free thiols with saliva (14), the bio-generation of **1** from **4** was studied in water with anaerobic bacteria from mouth microflora known for the generation of mouth malodour: *Fusobacterium nucleatum* (17, 18). The dosage was monitored by HPLC and fluorescent detection after derivatization of **1** with Acrylodan™ (14). This analysis clearly demonstrated that the cysteine-S-conjugate **4**, at 1 mg/L in water at neutral pH, was stable after 40 hours at 22° C and that **1** was not formed, but in the presence of *F. nucleatum*, after 1 min, **4** was detected at 0.1 g/L, a concentration that is about five times above the odour threshold (14).

In conclusion, cysteine-S-conjugates are flavour precursors in the mouth because of the action of mouth microflora. The delayed release of the volatile thiol modulates the odour perception of some food. This result also explains, for example, the long-lasting odours of onion powders or Sauvignon White grapes in the mouth.

References

1. Engel K.H., Tressl R. (1991) *J. Agric. Food Chem.* 39: 2249–2252.
2. Werkhoff, P., Guntert M., Krammer G., Sommer H., Kaulen J. (1998) *J. Agric. Food Chem.* 46: 1076–1093.
3. Tominaga T., Furrer A., Robert H., Dubourdieu D. (1998) *Flav. Fragrance J.* 13: 159–162.
4. Escher S., Niclass Y., van de Waal M., Starkenmann C. (2006) *Chem. Biodivers.* 3: 943–947.
5. Starkenmann C., Luca L., Niclass Y., Praz E., Roguet D. (2006) *J. Agric. Food Chem.* 54: 3067–3071.
6. Starkenmann C., Niclass Y., Escher S. (2007) *J. Agric. Food Chem.* 55: 4511–4517.
7. Troccaz M., Starkenmann C., Niclass Y., van de Waal M., Clark A.J. (2004) *Chem. Biodivers.* 1: 1022–1035.
8. Kotseridis Y., Baumes R. (2000) *J. Agric. Food Chem.* 48: 400–406.
9. Simian H., Robert F., Blank I. (2004) *J. Agric. Food Chem.* 52: 306–310.
10. Tominaga T., Peyrot des Gachons C., Dubourdieu D. (1998) *J. Agric. Food Chem.* 46: 5215–5219.
11. Tominaga, T., Dubourdieu D. (2000) *J. Agric. Food Chem.* 48: 2874–2876.
12. Starkenmann C. (2003) *J. Agric. Food Chem.* 51: 7146–7155.
13. Tsuge K., Kataoka M., Seto Y. (2002) *J. Agric. Food Chem.* 50: 4445–4451.
14. Starkenmann C. Le Calve B., Niclass Y., Cayeux I., Beccucci S., Troccaz M. (2008) *J. Agric. Food Chem.* 56: 9575-9580.
15. Vermeulen C., Gijs L., Collin S. (2005) *Food Rev. Intern.* 21: 69–137.
16. Lancaster J.E., Boland, M.J. (1990) In *Onions and Allied Crops* (III ed.), pp 33–72.
17. Tsai C.C., Chou H.-H., Wu T.-L., Yang Y.-H., Ho K.-Y., Wu Y.-M., Ho Y.-P. (2008) *J. Periodont. Res.* 43: 186–193.
18. Kleinberg I., Westbay G. (1990) *Oral Biol. Med.* 1: 247–259.

GRAPE ODOURLESS PRECURSORS OF SOME RELEVANT WINE AROMAS

R. LOPEZ, N. Loscos, P. Hernández-Orte, J. Cacho, and V. Ferreira

Laboratory for Flavor Analysis and Enology, Department of Analytical Chemistry, Faculty of Science, University of Zaragoza, C/ Pedro Cerbuna, 12. 50009 Zaragoza, Spain

Abstract

The precursor extract obtained from different grape varieties (Chardonnay, Cabernet Sauvignon, Verdejo, Merlot, Tempranillo and Grenache) was fractionated on a reversed-phase HPLC system. A total of 15 fractions of 8 mL were collected. Each fraction was submitted to the following hydrolytical procedures: harsh acid hydrolysis, enzymatic hydrolysis and alcoholic fermentation. The released aroma compounds were extracted and analysed by GC-MS. Some aroma compounds were mainly found in two or more fractions, which indicates the presence of more than one precursor. In addition, in some cases, the aromas were formed in different extent depending on the treatment. The existence of a maximum of concentration of δ -octalactone in one of the fractions for enzymatic hydrolysis suggests the existence of a glycosidic precursor for this compound. However, δ -octalactone was formed in a different fraction only after fermentation, which suggests the existence of a second non-glycosidic precursor for this aroma. In the case of γ -nonalactone, the aroma was formed only after fermentation or acid hydrolysis, which suggests that the main precursor of this compound is not a glycosidic precursor.

Introduction

The chemistry of wine aroma precursors is extremely complex because there are hundreds of potential aroma precursors in grapes (glycosides, polyalcohols and some others) that only after many complex transformations form the aroma molecules. While the precursors of some relevant aroma compounds, such as linalool and β -damascenone, have been exhaustively studied, the precursors of many other relevant wine aroma molecules, such as aliphatic lactones, are barely known. The work presented here shows some preliminary results about the numbers and type of precursors of some wine aromas.

Experimental

Precursors were extracted following the procedure described by Loscos et al. (1) from different grape varieties (Chardonnay, Cabernet Sauvignon, Verdejo, Merlot, Tempranillo and Grenache). A mixture of the extracts of each variety (corresponding to 1.5Kg of grapes) was concentrated and then fractionated on a reversed-phase HPLC system equipped with a semipreparative C18 column. A total of 15 fractions were collected. Fractions (an aliquot of 800 μ L per fraction) were submitted to the following hydrolytical procedures: harsh acid hydrolysis, enzymatic hydrolysis and alcoholic fermentation. Norisoprenoids compounds were mainly studied by harsh acid

hydrolysis and SPME extraction. Harsh acid hydrolysis was carried out in citric acid buffer solution (0.2 M, 10% EtOH, pH 2.5, 100°C, 1h). Enzymatic hydrolysis was carried out in citrate/phosphate buffer (0.1 M / 0.2 M, pH 5) by incubating at 40°C for 16 h after addition of 12 mg of enzyme preparation AR-2000. Alcoholic fermentation was carried out in a synthetic media (30g/L of glucose, 0.9 g/L (NH₄)₂SO₄, 0.9 g/l (NH₄)₂HPO₄) and sterile conditions using Fermicru LVCB yeast strain. Aroma compounds released by enzymatic hydrolysis and alcoholic fermentation were extracted by SPE following the procedure described by Ibarz et al. (2). Released aroma compounds were determined by GC-MS under the conditions reported by Loscos et al. (1). For each kind of hydrolysis, a control sample without added precursors was analysed.

Results and discussion

According to the experimental procedure, the existence of a single precursor molecule for a given aroma compound, will be evidenced by the presence of the released aroma molecule in a single fraction. The hydrolysis more efficient at revealing the compound gives some additional clues about the nature of the precursor molecule.

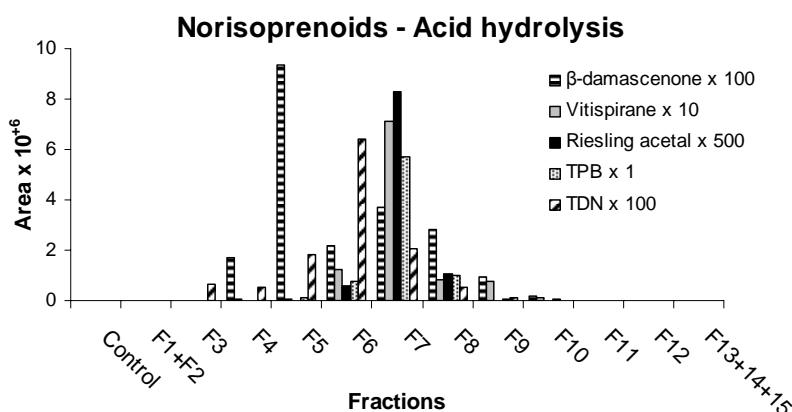


Figure 1. Area for the norisoprenoid compounds released by acid hydrolysis.

Some norisoprenoids are better revealed by acid hydrolysis (Figure 1). β-damascenone was found with maxima in fractions F5 and F7, indicating the presence at least of two precursors, which is in accordance with data reported by Winterhalter et al. (3). The presence of the β-damascenone in these two fractions was confirmed after enzymatic hydrolysis and alcoholic fermentation. On the other hand, Riesling acetal, vitispiranes, t-1-(2,36-trimethylphenyl)but-1,3-diene (TPB) and 1,1,6-trimethyl-1,2-dihydronaphthalene (TDN) were found in several fractions with a single maximum. Such broad chromatographic peak could be due to a deficient elution of a single aroma precursor, but it could be also the likely result of the presence of many similar precursor molecules. For example, TDN was clearly found in more than one fraction (F6 and F7) after enzymatic hydrolysis of the fractions, which indicates the presence of two precursors of different nature. Winterhalter et al. (3) described that at least three classes of precursors could exist for TDN and vitispiranes.

Among terpene compounds, linalool and α-terpineol (Figures 2 and 3) were found after alcoholic fermentation in almost all fractions in the same concentration, even in the control (synthetic must fermented without aroma precursor fraction). This could be due to the ability of yeast to synthesise de novo terpenes. However, after

enzymatic hydrolysis, linalool and α -terpineol were mainly found in one fraction, which indicates the presence of a glycosidic precursor for these compounds. In the case linalool, this glycosidic precursor seems to be slightly hydrolyzed during alcoholic fermentation. Some other non-glycosidic precursors for this aroma molecule should exist since the levels of linalool in fermentative hydrolysis show a relative maximum.

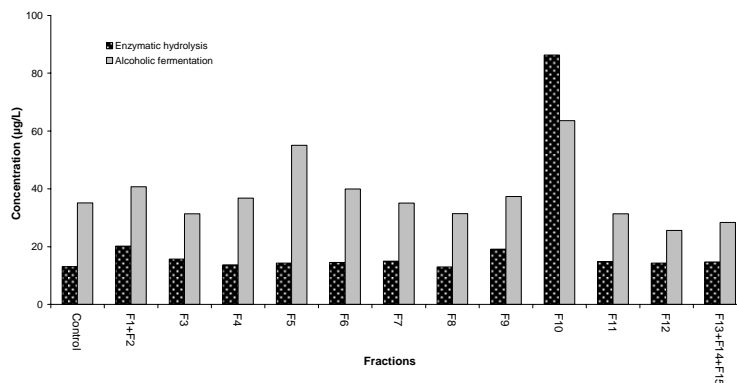


Figure 2. Concentration (referred to 800 μ L of fraction) of linalool after enzymatic hydrolysis and alcoholic fermentation.

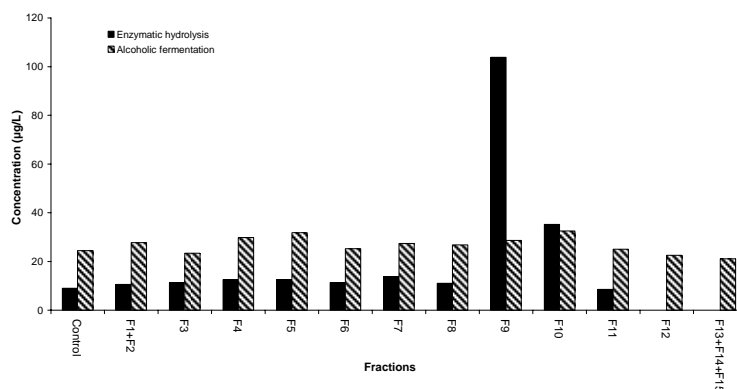


Figure 3. Concentration (referred to 800 μ L of fraction) of α -terpineol after enzymatic hydrolysis and alcoholic fermentation.

Among vanillin compounds, acetovanillone and ethyl vanillate (Figure 4) were mainly found in only one fraction after the three hydrolytical procedures. In the case of acetovanillone, the precursor, mainly present in fraction 5, was hydrolyzed more easily by enzymatic hydrolysis. However, no significant differences between the three hydrolytical procedures were observed for ethyl vanillate (mainly present in fraction 10).

The existence of a maximum of concentration of δ -octalactone in one of the fractions for enzymatic hydrolysis (Figure 5) suggests the existence of a glycosidic precursor for this compound. The structure of this compound could be similar to the glycosidic precursor of whisky lactone found in wood (4). In addition, δ -octalactone was formed in a different fraction after fermentation, which suggests the existence of a second non-glycosidic precursor for this aroma.

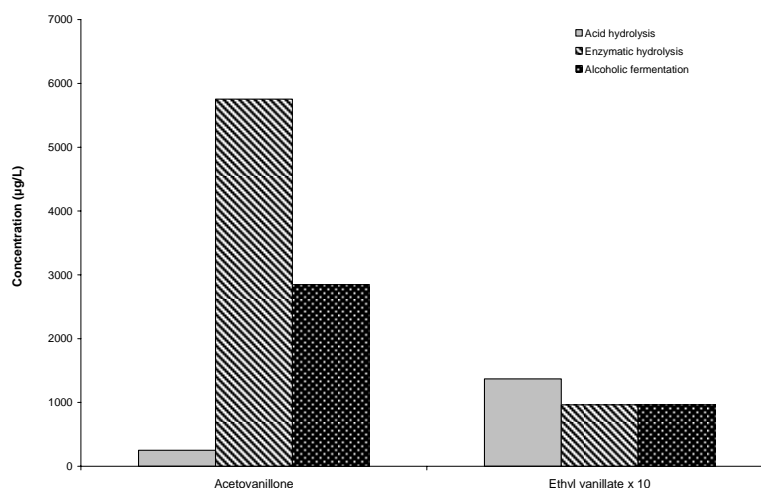


Figure 4. Concentration (referred to 800 µL of fraction) of acetovanillone and ethyl vanillate (multiplied by a factor 10) for the three hydrolytical procedures.

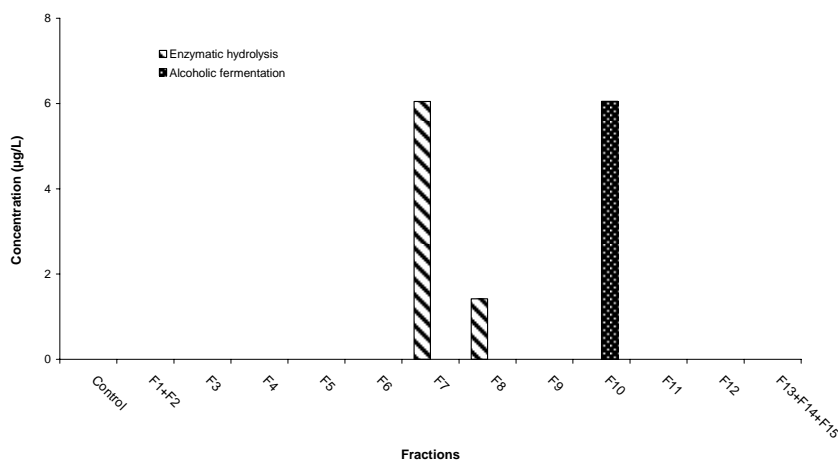


Figure 5. Concentration (referred to 800 µL of fraction) of δ-octalactone after enzymatic hydrolysis and alcoholic fermentation.

This work presents a preliminary study about the number of precursors of the main wine aroma compounds. Although similar studies have been carried out, it is the first time that the possible existence of two precursors of δ-octalactone (one of them, a glycosidic compound) is reported. Nevertheless, further studies must be carried out to clarify the structure of these aroma precursors.

References

1. Loscos N., Hernandez-Orte P., Cacho J., Ferreira V. (2007) *J. Agric. Food Chem.* 55: 6674-6684.
2. Ibarz M.J., Ferreira V., Hernandez-Orte P., Loscos N., Cacho J. (2006) *J. Chrom. A* 1116: 217-229.
3. Winterhalter P., Sefton M. A., Williams P. J. (1990) *Am. J. Enol. Vitic.* 41: 277-283.
4. Raunkjaer M., Pedersen D.S., Eelsey G.M., Sefton M.A., Skouroumounis G.K. (2001) *Tetrahedron Lett.* 42: 8717-8719.

IDENTIFICATION OF VOLATILE COMPOUNDS RESPONSIBLE FOR PRUNE AROMA IN PREMATURELY AGED RED WINES

A. PONS^{1,3}, V. Lavigne^{1,3}, E. Frérot², Ph. Darriet³, and D. Dubourdieu³

¹ *SEGUIN MOREAU SA, R&D Division, Z.I. Merpins, BP 94, 16103 Cognac, France*

² *Firmenich S.A., Corporate R&D Division, P.O. Box 239, CH-1211 Geneva 8, Switzerland*

³ *UMR 1219 Œnologie. Institut des Sciences de la Vigne et du Vin, Université Victor Segalen Bordeaux 2, 351 cours de la Liberation 33405 Talence cedex, France*

Abstract

The premature aging of red *Vitis vinifera* L. wines is mainly associated with the formation of an intense off-flavour reminiscent of prunes. The compounds responsible for this deterioration in red wine flavour have not previously been identified. Sensory descriptive analysis associated with a gas chromatography – olfactometry technique was first performed to find characteristic odoriferous zones aged red wines with or without a marked prune aroma. Afterwards, high pressure liquid chromatography, gas chromatography and multidimensional gas chromatography coupled with mass spectrometry were used to identify the odorants reminiscent of prunes in prematurely-aged red wines. Three compounds were detected with a strong odour of prunes; γ -nonalactone, β -damascenone and 3-methyl-2,4-nonanedione. The perception threshold of this β -diketone in a model hydroalcoholic solution is 16 ng/L. Identified for the first time in aged red wines, this very powerful volatile compound was also suggested to produce the characteristic prune aroma of prematurely aged red wines.

Introduction

The reputation of famous red Bordeaux wines is strongly associated with their aging potential. Indeed, these wines conserve the flavour nuances of young wines while developing specific varietal nuances. However, this ideal aging does not occur in every wine. Premature aging or untypical aging is a well-known phenomenon in white wines [1]. Premature-aging aroma phenomena may also reflect the defective aging of red wines. Prematurely-aged red wines develop several aromatic nuances reminiscent of prunes and figs. In our experience of red wine tasting, the presence of these overriding odours affects the quality and subtlety of the wine flavour and may shorten its shelf life. Despite their importance for the wine industry, the chemical compounds responsible for these off-flavours were not previously known. The main goal of this research was to identify key aroma compounds in prematurely-aged red wines with an intense prune aroma.

Experimental

Wine samples. Red wines used in this study were from several origins (Bordeaux, Burgundy, and Valdepeñas) and vintages (from 1949 to 2004), prematurely-aged or not.

Wine extraction. Procedure 1 (standard extraction procedure). Red wines (100 mL) were extracted three times with pentane/dichloromethane (1/1, v/v; 3 x 10 mL). The organic layer was dried over Na₂SO₄, and then concentrated to 0.5 mL under nitrogen flow (approximately 100 mL/min).

Procedure 2 (specific to the identification of prune aroma). Red wine (1.5 L) with a marked prune aroma was extracted with pentane/dichloromethane (1/1, v/v; 3 x 160 mL). The resulting organic phases obtained in 10 runs were mixed, dried over Na₂SO₄, and concentrated to 300 mL by distilling the solvent with a Rotavapor system. The organic phase was treated three times with an aqueous Trizma base (Fluka, St Quentin Fallavier, France) buffer (0.1 M; pH 10, 50 mL). Then, the organic extract containing neutral and basic compounds was dried over Na₂SO₄ and concentrated to 2 mL under nitrogen flow.

Capillary Gas Chromatography – Olfactometry (GC-O). The analysis was carried out alternately by two operators on a HP5890 series II (Agilent Technologies, Palo Alto, CA) coupled with olfactory detection using ODO-1 installation (Scientific Glass Engineering (SGE), Ringwood, Australia). A 2 µL sample of the extract (procedure 1) was introduced onto a polar BP20 capillary column or a SPB1 capillary column. The injector was set at 230 °C. Oven temperature was initially set at 45 °C for 1 min, then raised to 240 °C at 3 °C/min and held at that temperature for 20 min.

Heart-cut Multidimensional Gas Chromatography- Olfactometry – Mass Spectrometry (MDGC–O-MS). *General set-up of the system.* The MDGC separations were performed on three capillary columns with different stationary phases or film thicknesses on two GC ovens: Oven I was a Hewlett Packard 5890 series II, while Oven II was an Agilent 6890 coupled with a 5973 quadrupole mass spectrometer. The outlet of the precolumn was connected to a sniff port (ODO I) to determine odour retention time in this configuration and to the second column, via a Gerstel MCS 2 multicolumn switching system.

MDGC conditions for wine extract analysis. The injector temperature was set at 230 °C. The sample was transferred from the pre-column to the main column via the MCS (Gerstel, Germany) system at a defined cut time. Pre-separation was performed using a nonpolar SPB1 fused silica capillary column (30 m, 0.25 mm i.d., 0.25 µm). The second column was a 50 m x 0,25 i.d. x 0.25 µm BP20 (SGE, France). The electron energy for the EI mass spectra was 70 eV and CI was initiated using methane as the reactant gas.

High Pressure Liquid Chromatography (HPLC) Purification. Chromatographic conditions. The procedure was based on the method described by Pons [2]. The HPLC fractionation of wine was accomplished with a HPLC Waters (Milford, MA). The column used was a Novapak C18 (3.9 x 318 mm, 4 µm). The chromatographic conditions included a flow rate of 0.5 mL/min and an injection volume of 270 µL. The linear program gradient involved Phase A, water and Phase B, ethanol; 0 % B reaching 100 % B in 50 minutes. An automated fraction collector (Bio Rad, France) was connected to the end of the column to collect 1 mL of the eluted solvent every 2 minutes. The HPLC eluate was recovered in 25 separate fractions, evaluated for their smell as described below. The fractions with remarkable odours were re-extracted and analysed.

Flavour fraction re-extraction. The alcohol content of the fractions eluted by HPLC was adjusted to 12 % (v/v). Then, the solution was extracted three times with 0.5 mL pentane/dichloromethane mixture (1/1, v/v). The solvent extract was concentrated under nitrogen to 200 µL and used for GC-O analysis, as well as for further purification by multidimensional GC coupled with olfactometry and MS.

Results and Discussion

The most important descriptors related to the oxidative character of aged red wines were identified by a trained panel. The terms selected were: "prunes", "figs", and "overripe fruit". GC-O analysis of wine extracts revealed the odour zones corresponding to the wine flavours. The main odoriferous zones reminiscent of prune in wine extract are listed in Table 1. The three odoriferous zones perceived by GC-O as strongly reminiscence of prematurely-aged red wine aroma were: OZ1, OZ2, and OZ3. OZ1 had a strong prune odour. Surprisingly, this odour was detected at two retention times with different intensities on a nonpolar capillary column (SPB1). Odoriferous zones OZ2 and OZ3 were more similar to dried fruit.

Table 1. Identifying the odour-active regions in the red wine extracts with prematurely-aged aromas.

Odoriferous zones	Odour descriptors ^a	BP20 ^b	SPB1 ^c	Compound identified	Identification methods ^d
OZ1	Prune ^e ,	1742	1213 (1296)	MND	HPLC-MDGC-MS, RI, RC
OZ2	Dried fruit, apple sauce ^e	1841	1369	β -damascenone	GC-MS, RI, RC
OZ3	Overripe peach ^e	2041	1325	γ -nonalactone	GC-MS, RI, RC

^a Odour descriptors generated by the two assessors during GC-O. ^b Retention index (LRI) of odour peak on a BP20 column by GC-O. ^c Retention index of odour peak on an SPB1 column by GC-O. LRI of minor peak resulting from the keto-enol equilibrium of the compound is given in brackets. ^d Compounds were identified on the basis of hyphenated HPLC-MDGC-MS or GC-MS techniques by comparing their mass spectra and retention indices (RI) with reference databases and their odours with reference compounds (RC).

Using GC-MS with chemical standards, it was possible to identify the molecules corresponding to the following retention indices: OZ2, β -damascenone ($RI_{polar}=1841$, $RI_{nonpolar}=1369$) and OZ3, γ -nonalactone, ($RI_{polar}=2041$, $RI_{nonpolar}=1325$). β -damascenone is a widespread powerful flavouring compound in nature [3, 4]. It has been previously identified in young wines of different origins [5], as well as aged red wines [6]. γ -Nonalactone has been identified in many different wines [7]. Concentrations are higher in old red wines [8] and red wines aged in oak barrels [9].

Identification of 3-methyl-2,4-nonanedione (MND) in prematurely-aged red wine. The volatiles from a total of 15 L prematurely-aged red wine were isolated by liquid-liquid extraction (*procedure 2*). Acidic compounds were removed by washing the organic extract with Trizma base buffer (pH 10). At this point, the application of MDGC to the organic wine extract is a logical step forward in analyzing such complex samples. The first-dimension chromatogram obtained from a wine extract (*procedure 2*) is complex, as seen in Figure 1A, which also shows the transferred section, corresponding to the prune odour retention window. The second dimension chromatogram (Figure 1B) had two peaks (peak 1 and peak 2) at the retention time of prune odour. However, the mass spectrum for these peaks indicated co-elution of other compounds and it was impossible to obtain a clear mass spectrum. So, in our case, the MDGC-MS method was not capable of identifying a trace compound from a quasi-crude red wine extract. A further purification step was necessary to avoid co-elution. HPLC chromatography with a C18 reversed-phase column was used to

divide the organic wine extract into 25 fractions. Fraction 18 was smelled of prunes and was then re-extracted and analysed by MDGC (Figure 1C). Based on MS (EI) data and also MS (CI, CH₄) spectra, which indicated a molecular mass $M = 170$ ($[M + H]^+ = 171$), the peak corresponding to the odoriferous zone (Figure 1C) was identified as 3-methyl-2,4-nonanedione. This compound was first mentioned by Guth and Grosch as an off-flavour in reversed soybean oil [10]. To the best of our knowledge, this is the first time that this very powerful compound has been identified in wine.

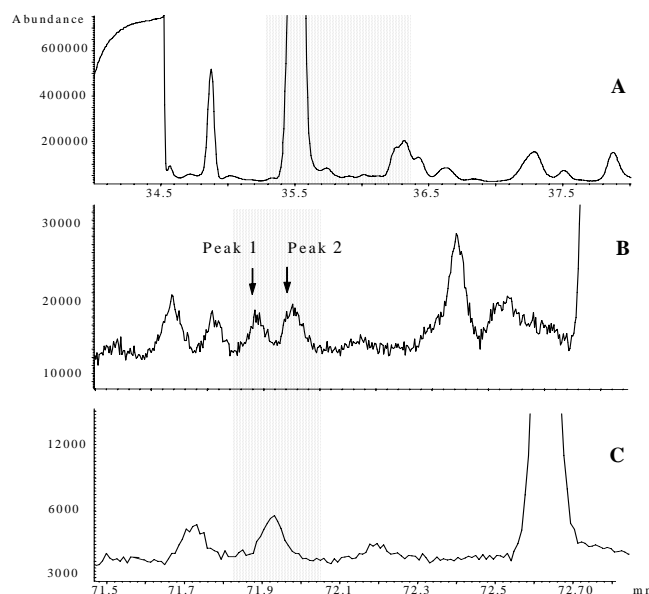


Figure 1. Example of a GC-MS (A), MDGC-MS (B) and HPLC-MDGC-MS (C) separation of an organic red wine extract.

Odour Characteristics of MND. The odour threshold of MND was first reported by Guth [10] in air (0.007 to 0.0014 ng/L). In our research, the perception threshold of MND in wine model solution, determined by a well-trained panel of 40 persons, was found to be 16 ng/L. MND has a strong anise, hay-like odour. These descriptors may depend on its concentration. Indeed, at low concentrations, MND smells different from the pure compound and is rather reminiscent of prematurely-aged red wine. In small amounts (100 ng/L), it has a minty flavour, at 1 µg/L it is reminiscent of anise, fruit kernels, and prunes, whereas at 10 µg/L its flavour is mainly described as anise.

References

1. Lavigne-Cruège V., Dubourdieu D. (2002) In *13th International Enology Symposium* (Trogus H., Gafner J., Sutterlin., eds), International Association of Enology: Montpellier, France, pp 331-347.
2. Pons A., Lavigne V., Frérot E., Darriet P., Dubourdieu D. (2008) *J. Agric. Food Chem.* 56: 5285-5290.
3. Kotseridis Y., Baumes R. L., Skouroumounis G. K. (1999) *J. Chromatogr. A* 849: 245-254.
4. Acree T., Braell P., Butts M. (1981) *J. Agric. Food. Chem.* 29: 688-690.
5. Ferreira V., Cacho R.L. (2000) *J. Sci. Food. Agric.* 80: 1659-1667.
6. Aznar M., Lopez R., Cacho J., Ferreira V. (2001) *J. Agric. Food. Chem.* 48: 2924-2929.
7. Sarrazin E., Dubourdieu D., Darriet P. (2007) *Food Chem.* 103: 536-545.
8. Pons A. (2006) Recherches sur l'arôme de vieillissement défectueux des vins, PhD Thesis, Université Victor Segalen Bordeaux II, Bordeaux.
9. Cerdan T.G., Goni D.T., Azpilicueta C.A., (2004) *J. Food Eng.* 65: 349-356.
10. Guth H., Grosch W. (1989) *Fat Sci. Technol.* 91: 225-230.

QUANTIFICATION OF DIMETHYL TETRASULPHIDE IN ONIONS BY A NEWLY DEVELOPED STABLE ISOTOPE DILUTION ASSAY

M. GRANVOGL and P. Schieberle

Lehrstuhl für Lebensmittelchemie der Technischen Universität München, Lichtenbergstr. 4, 85748 Garching, Germany

Abstract

It is well-known that predominantly volatile sulphur compounds contribute to the flavour of onions and other *Allium* varieties. Therefore, a stable isotope dilution assay was developed for the quantification of dimethyl tetrasulphide using gas chromatography/mass spectrometry and newly synthesised [²H₆]-dimethyl tetrasulphide as internal standard. Application of the recently developed method on onions (*Allium cepa* L.) revealed amounts of 2.4 µg/kg in cooked onions, whereas 34.9 µg/kg were found in deep-fried onions.

Introduction

Sulphur containing aroma compounds, which are formed during cutting by a very fast enzymatic degradation of cysteine sulphoxides followed by a cascade of chemical reactions, predominantly contribute to the aroma of raw onions (1-2). After disruption of the intact cell structure, the enzyme alliinase (located in the vacuole) is enabled to get into contact with these substrates (cytoplasm). Depending on the precursor structures (trans-*S*-(1-propenyl)-L-cysteine sulphoxide (isoalliin), *S*-propyl-L-cysteine sulphoxide (propiin), *S*-methyl-L-cysteine sulphoxide (methiin), *S*-ethyl-L-cysteine sulphoxide (ethiin), *S*-allyl-L-cysteine sulphoxide (alliin)), different primary reaction products (e.g., alk(en)yl thiosulphinates, alk(en)yl thiosulphonates, cepaenes) are built. However, the chemistry of onion volatiles is much more complex because significant changes in the spectrum of the volatiles occur during processing, e.g. cooking (3) or deep-frying, resulting in a lot of new compounds like thiophenes or zwiebelanes as well as di-, tri-, and tetrasulphides (4), which can be formed by decomposition reactions followed by disproportionation and insertion reactions.

Because stable isotope dilution assays have been proven to be a potent tool for the quantification of, in particular, minor compounds like flavourings in food (5), the purpose of the present study was (i) to develop a new stable isotope dilution assay for dimethyl tetrasulphide (DMTS) and (ii) to determine its concentrations in cooked and deep-fried onions.

Experimental

Synthesis (6). Potassium hydroxide (1.0 g) was dispersed and suspended in tetrahydrofuran (14 mL; containing 0.2 % of water). Then, dispersed sulphur (128 mg, 0.5 mmol) and, after 5 min, [²H₃]-methyl iodide (285 mg, 2 mmol; dissolved in tetrahydrofuran (water content 0.2 %)) was added. After a further 2 h of stirring, the mixture was filtered, the solvent was evaporated (50 °C, 380 mbar), and diethyl ether (5 mL) was added to the residue. This solution was washed twice with hydrochloric

acid (0.02 mol/L; total volume 10 mL), dried over anhydrous sodium sulphate, and the solvent was evaporated (30 °C, 600 mbar) to about 1 mL. For further clean-up, an aliquot (0.5 mL) was applied onto a water-cooled column packed with a slurry of silica gel in n-pentane (10 g; silica gel 60, 0.063-0.200 mm). Chromatography was performed using n-pentane (80 mL; 3 mL/min) as eluant. The solvent was evaporated (30 °C, 600 mbar) to about 2 mL leading to a solution containing DMTS as major product beside minor amounts of dimethyl trisulphide and dimethyl pentasulphide. For further purification, aliquots (3 µL) were injected into a GC-oven (FFAP fused silica capillary column, 30 m x 0.32 mm i.d.; 0.25 µm film thickness; J&W Scientific, Folsom, CA) coupled to a preparative fraction collector (PFC; Gerstel, Mülheim/Ruhr, Germany) resulting in the pure labelled standard [²H₆]-dimethyl tetrasulphide ([²H₆]-DMTS; yield 67 %).

Intactly cooked onions. One whole, peeled onion (approximately 150 g) was cooked for 20 min in a pressure cooker. After cooling, the sample was homogenised using an Ultraturrax and [²H₆]-DMTS (0.5 µg), dissolved in dichloromethane, was added and stirred for 50 min in a closed vessel. After addition of further dichloromethane (200 mL), the sample was stirred for another 50 min. The mixture was centrifuged, and, after decanting off the solvent, the extraction was repeated twice (total volume 200 mL). The further work-up as well as the quantification of DMTS was performed by means of two-dimensional GC-MS as described recently (7).

Deep-fried onions. Onions (100 g) were finely sliced and immediately deep-fried at 150 °C for 165 s in a chip pan using 5 kg of palm butter. After deep-frying, the surplus palm butter was removed from the deep-fried onions using a paper towel. The material was frozen in liquid nitrogen, and, after addition of anhydrous sodium sulphate (100 g), the sample was homogenised in a blender. After addition of [²H₆]-DMTS (3.0 µg), the material was extracted twice with diethyl ether (total volume 300 mL) for a total time of 2 h. The volatiles were isolated as described above for the cooked onions.

Odour threshold determination. The odour threshold values in tap water or sunflower oil, respectively, were determined using triangle tests as described in (8).

Results

Isotopomers of aroma compounds containing a 100 % stable isotope label are often not commercially available. Hence, the first step in the development of a stable isotope dilution assay is the synthesis of the respective isotopomer. For this purpose, a position in the target molecule has to be chosen for labelling, which is not eliminated during mass spectrometry. Therefore, the isotopically labelled standard [²H₆]-DMTS was synthesised.

The mass spectrum of unlabelled DMTS is shown in (Figure 1A). The symmetric fragment of the tetrasulphide (m/z 79) was monitored as base peak and the molecular ion (m/z 158) was obtained with second highest intensity. Besides these fragments, the unlabelled compound also showed a signal at m/z 160 resulting from the isotopic mass pattern of sulphur (roughly four percent per sulphur atom). In the mass spectrum of the newly synthesised isotopomer [²H₆]-DMTS (Figure 1B), the molecular ion at m/z 164 was observed, confirming the expected incorporation of six deuterium atoms into the target molecule. The symmetric mass fragment consequently showed the labelling resulting from the remaining threefold labelled methyl group.

The amounts of DMTS in cooked as well as in deep-fried onions were determined by GC-MS using a response curve. As example, the mass chromatogram obtained for the quantification of DMTS in a yellow cooked onion sample is illustrated in (Figure 2).

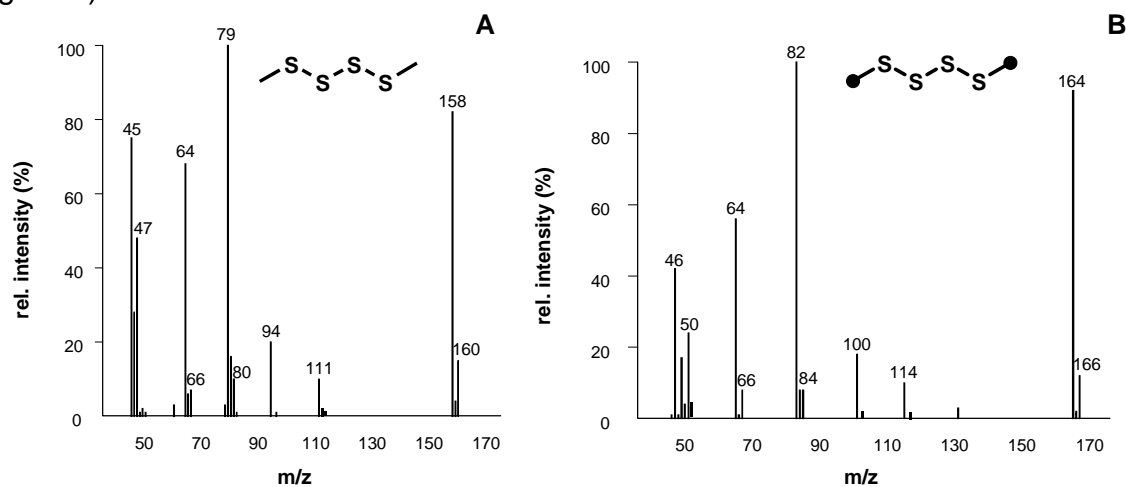


Figure 1. Mass spectra (MS/EI) of DMTS (A) and $[^2\text{H}_6]$ -DMTS (B). ● deuterium labelling at this carbon atom.

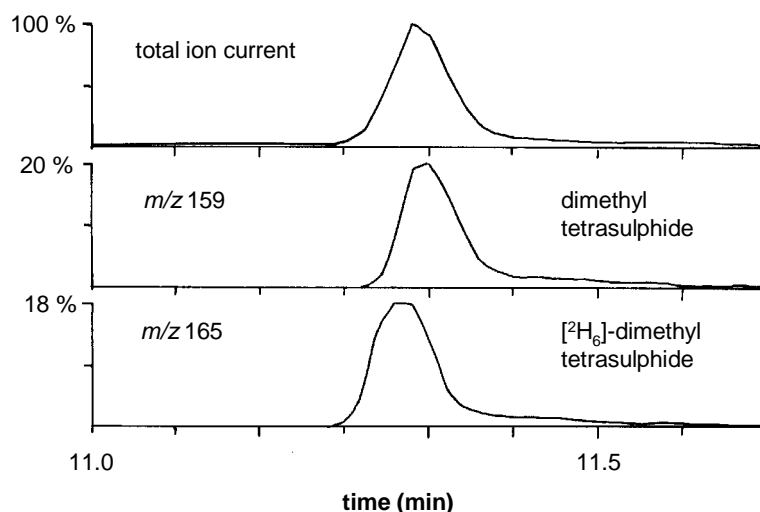


Figure 2. Mass chromatogram (CI) obtained during DMTS quantification in a yellow onion sample. m/z 159: DMTS (analyte); m/z 165: $[^2\text{H}_6]$ -DMTS (standard).

The varying DMTS amounts in cooked and deep-fried onions (Table 1) can be explained by the different temperature profiles occurring during heat-processing. At the beginning of the cooking process, the temperature within the onions is much lower in comparison to the frying conditions. Thus, the alliinase (temp. optimum: 34–40 °C) could be active for a longer time during cooking of the entire bulb whereas the enzyme should be inactivated immediately during frying of the finely sliced onions.

Odour activity values (OAV; ratio of concentration to odour threshold) are a helpful tool to estimate the contribution of a single odorant to a given aroma. A calculation of the odour threshold of DMTS revealed a recognition threshold of 0.02 $\mu\text{g/L}$ in water as well as of 1.8 $\mu\text{g/L}$ in sunflower oil, respectively (Table 1). These values were determined in two different matrices to simulate the corresponding food, in detail the “aqueous” cooked onions and the “fatty” deep-fried onions (fat content

approximately 58 %). A calculation of the OAV's of DMTS in the different onions suggested that this compound should undoubtedly contribute to the aroma of cooked and deep-fried onions, because its concentration was 19-fold and 120-fold, respectively, above its corresponding odour threshold (Table 1).

Table 1. Concentrations, odour thresholds (water and sunflower oil), and resulting odour activity values (OAV) of cooked and deep-fried onions.

	Concentration ($\mu\text{g}/\text{kg}$) ^a	Recognition threshold ($\mu\text{g}/\text{L}$) ^b	OAV ^c
Cooked onions	2.4 (1.6- 2.9)	0.02	120
Deep-fried onions	34.9 (28.1-37.1)	1.8	19

^a Mean values of sextuplicates (concentration range). ^b Recognition threshold for cooked onions based on tap water as matrix and for deep-fried onions on sunflower oil, respectively.

^c Odour activity values were calculated by dividing the concentrations of DMTS by its corresponding recognition threshold.

Application of the OAV concept on the results obtained during the quantification of DMTS in different processed onions showed the importance of this tool in the flavour chemistry of onions and in food in general. Regarding only the analysed concentrations of the tetrasulphide, the contribution to the overall aroma of cooked as well as of deep-fried onions could be misjudged. The concentration of the analyte was determined about 15 times higher in the deep-fried onions compared to the concentration obtained for the cooked onions primarily pointing to a greater influence of the tetrasulphide on the deep-fried onion aroma. However, considering the calculated OAVs, a reversal of the significance of the tetrasulphide to the corresponding flavour perception could be clearly demonstrated. Due to the 90-fold higher recognition threshold of DMTS in sunflower oil in comparison to the threshold in tap water, a 6.3-fold higher OAV resulted for DMTS in cooked onions. Therefore, only by combination of the determined concentration and the recognition threshold, a reasonable estimation of the contribution of DMTS to the overall aroma of processed onions could be achieved. Furthermore, the importance of the correct choice of the food simulating matrix for the threshold determination and, therefore, for a correct conclusion could be shown.

In summary, precise quantitative data for the potent odorant DMTS eliciting an intense cabbage-like aroma were achieved by means of a newly developed stable isotope dilution assay. The contribution of DMTS to the aroma of cooked and deep-fried onions could be correctly estimated only with the OAV concept. Further, the influence of different heat-processing steps on the generation of varying amounts of a single odorant in onions could be shown.

References

1. Block E. (1992) *Angew. Chemie* 104: 1158-1203.
2. Carson J.F. (1987) *Food Rev. Int.* 3: 71-103.
3. Tokitomo Y. (1995) *Nippon Shokuhin Kagaku Kogaku Kaishi* 42: 279-287.
4. Griffiths G., Trueman L., Crowther T., Thomas B., Smith B. (2002) *Phytother. Res.* 16: 603-615.
5. Hofmann T., Schieberle P., Grosch W. (1996) *J. Agric. Food Chem.* 44: 251-255.
6. Morel G., Marchand E., Foucaud A. (1980) *Synthesis* 11: 918-921.
7. Granvogl M., Christlbauer M., Schieberle P. (2004) *J. Agric. Food Chem.* 52: 2797-2802.
8. Czerny M., Christlbauer M., Christlbauer M., Fischer A., Granvogl M., Hammer, M., Hartl C., Hernandez N.M., Schieberle P. (2008) *Eur. Food Res. Technol.* 228: 265-273.

NOVEL ESTERS IN THAI GREEN CHILLI

J.S. ELMORE¹, S. Srisajjalertwaja², A.T. Dodson¹, A. Apichartsarangkoon², and D.S. Mottram¹

¹ *Department of Food Biosciences, University of Reading, Whiteknights, Reading RG6 6AP, UK*

² *Department of Food Science and Technology, Chiang Mai University, Chiangmai 50100, Thailand*

Abstract

The volatile compositions of fresh and baked Thai green chillis were examined. Some rarely-reported esters, derived from 3-methyl-1-butanol and 4-methyl-1-pentanol, were present at high levels, particularly in lightly baked chillis. The mass spectral data of some of these esters are reported for the first time. In addition, some tentatively-identified esters, derived from the same medium chain fatty acids that make up the side-chains of pungent capsaicins, are reported for the first time.

Introduction

Green chilli paste (nam phrik noom) is a traditional Northern Thai dip with a unique flavour, which is popular throughout Thailand. Its major ingredients are baked chilli, baked shallot, garlic and fish sauce. The chilli used is a variety of *Capsicum annum* Linn., known in Thailand as phrik noom (Jak Ka Pat variety).

Here we compare the headspace volatiles of fresh phrik noom with those of samples baked at 210 °C for 5 or 25 min, the latter cooking time appropriate for Thai green chilli paste.

Experimental

Chopped green chilli samples (5 g) were placed in a 40 ml glass vial and the headspace extracted at 35°C for 45 min by SPME, using a 50/30µm DVB/Carboxen on PDMS fibre. Extracts were analysed by GC-MS (HP5972 MSD with 5890 GC) using a VF-5MS column (60 m × 0.25 mm, 0.25 µm film thickness; Varian). The fibre was desorbed at 250 °C for 3 min. Initial oven temperature was 40 °C (2 min) rising to 250 °C at 4 °C min⁻¹. Carrier gas was helium at 144.8 kPa, and the mass spectrometer scanned from *m/z* 400 to *m/z* 29 at 2.05 scans per second.

Compounds were identified by comparing their mass spectra with spectra in databases (1,2) and by comparing their linear retention indices with those of reference compounds or literature values where available. To confirm tentative identifications, esters of 3-methyl-1-butanol and 4-methyl-1-pentanol were prepared by refluxing the appropriate alcohol and acid, the alcohol in excess, under acidic conditions for 1 hour. They were analysed by GC-MS in split mode (20:1) under the same conditions as for the chilli extracts, except that the mass spectrometer scanned from *m/z* 250 to *m/z* 10 at 3.09 scans per second. Three samples were analysed for each treatment.

Results

Several interesting changes occurred to the volatiles of Thai green chillis when they were cooked. Odour-potent sulphur-containing compounds rapidly disappeared and were absent from extracts of the cooked chilli. 2-Isobutyl-3-methoxypyrazine, regarded as an important constituent of chilli aroma (3), also disappeared on cooking, along with methyl salicylate. Terpenes and sesquiterpenes were relatively unaffected by heating, while long-chain alkanes and alkenes, probably of little sensory importance, increased as a proportion of the total volatiles.

Along with the aforementioned compounds, the chillis contained several unusual esters, in particular two interesting sets of 3-methyl-1-butyl and 4-methyl-1-pentyl esters, the relative amounts of which are shown in Table 1, along with their mass spectra. The esters were usually present at the highest percentage in the samples baked for 5 min. Most of these esters have been reported previously in a steam-distilled extract of tabasco peppers (*Capsicum frutescens*) (4). Apart from this one paper, the compounds in Table 1 containing 4-methylpentyl groups have not been reported in foods. 3-Methyl-1-butanol and 4-methyl-1-pentanol were present in the uncooked chilli but rapidly disappeared on cooking. 4-Methylpentyl butanoate, pentanoate and hexanoate are in the NIST library (1) but their spectra were quite different from those we obtained.

The capsaicinoids, which are responsible for the pungency of chilli peppers, are a series of vanillylamides of branched fatty acids. The three most common capsaicinoids in *Capsicum* species including Thai chilli, are capsaicin, dihydrocapsaicin and nordihydrocapsaicin (5), which are formed from 8-methyl-6-nonenoic acid, 8-methylnonanoic acid and 7-methyloctanoic acid, respectively. Seven esters were present in the fresh and lightly cooked chillis, which were tentatively identified as esters of these three acids. These compounds do not appear to have been reported in food before. The relative amounts of these compounds are shown in (Table 2), along with other compounds of interest, which were present at relatively high levels in the aroma volatiles of one or more of the samples.

In conclusion, a number of methyl-branched esters have been found in Thai green chilli at relatively high levels, which have not been previously reported in foods and may have interesting sensory properties. Some of these compounds disappear on heating, while others increase substantially. These changes, which occur, even in mild cooking, will have a considerable effect on the aroma of Thai green chilli.

References

1. NIST/EPA/NIH Mass Spectral Library (2005) National Institute of Standards and Technology, Gaithersburg, MD.
2. Adams R.P. (2007) *Identification of Essential Oil Components by Gas Chromatography/Mass Spectrometry* (4th Edn.), Allured.
3. Mazida M.M., Salleh M.M., Osman H., (2005) *J. Food Compos. Anal.* 18: 427-437.
4. Haymon L. W., Aurand L.W. (1971) *J. Agric. Food Chem.* 19: 1131-1134.
5. Kozukue N., Han J.S., Kozukue E., Lee S.J., Kim J.A., Lee K.R., Levin C.E., Friedman M. (2005) *J. Agric. Food Chem.* 53: 9172-9181.

Table 1. 3-Methyl-1-butyl and 4-methyl-1-pentyl esters in fresh and baked (5 and 25 min at 210 °C) Thai green chilli, as a percentage of the total aroma extract (mean values, n= 3).

ESTER	LRI ^a	fresh	5 min	25 min	Mass spectral data <i>m/z</i> (% intensity) ^b
<i>3-methyl-1-butyl</i>					
2-methylpropanoate	1013	<0.10	0.19	<0.10	NIST library
butanoate	1056	<0.10	0.11	<0.10	NIST library
2-methylbutanoate	1101	0.46	1.20	0.94	NIST library
3-methylbutanoate	1109	0.29	0.27	<0.10	NIST library
pentanoate	1155	<0.10	0.17	0.88	NIST library
4-methylpentanoate	1218	<0.10	0.48	0.45	70 , 43(78), 41(43), 55(41), 71(38), 99(32), 81(22), 29(20), 39(16), 42(14), 117(12)
hexanoate	1253	<0.10	<0.10	<0.10	NIST library
<i>4-methyl-1-pentyl</i>					
2-methylpropanoate	1112	0.22	2.72	2.31	43 , 89(65), 71(48), 56(46), 84(36), 41(33), 69(26), 42(11), 55(10), 57(10), 39(8), 129(7)
butanoate	1157	<0.10	1.03	<0.10	43 , 41(75), 71(58), 89(56), 56(38), 39(29), 84(27), 69(25), 42(24), 55(16), 85(9), 129(9)
2-methylbutanoate	1201	1.92	12.08	7.75	103 , 57(86), 85(67), 43(66), 56(56), 84(53), 41(43), 69(29), 29(18), 55(15), 39(10), 143(5)
3-methylbutanoate	1207	1.18	4.00	2.40	85 , 103(84), 56(77), 43(72), 57(64), 84(60), 41(49), 69(33), 42(17), 55(14), 29(12), 143(8)
pentanoate	1254	0.18	2.62	2.30	85 , 103(97), 56(87), 43(61), 84(61), 57(60), 41(47), 69(35), 55(21), 29(19), 42(15), 143(11)
4-methylpentanoate	1315	0.93	4.02	4.56	43 , 117(87), 56(81), 84(69), 99(51), 41(45), 69(38), 85(36), 81(34), 55(27), 101(14), 157(10)
hexanoate	1351	0.30	0.41	0.48	43 , 117(100), 56(83), 84(74), 99(64), 41(42), 69(38), 85(27), 71(26), 55(23), 57(15), 157(9)

^a Linear retention index on a VF5-MS column^b Base peak in bold

Table 2. Selected compounds in fresh and baked (5 and 25 min at 210 °C) Thai green chilli, as a percentage of the total aroma extract (mean values, n= 3). Compounds in italics are tentatively identified, using mass spectral library data or spectral interpretation.

LRI ^a	Compound	Fresh	5 min	25 min
<600	ethanol	12.1	nd ^b	nd
606	ethyl acetate	2.27	nd	nd
654	3-methylbutanal	1.32	<0.10	nd
663	2-methylbutanal	0.84	nd	nd
685	1-penten-3-one	1.34	<0.10	nd
695	<i>allyl methyl sulfide</i>	3.50	nd	nd
734	3-methyl-1-butanol	0.62	nd	nd
741	dimethyl disulfide	0.77	<0.10	0.19
765	1-pentanol	1.17	nd	nd
836	4-methyl-1-pentanol	2.07	nd	nd
859	diallyl sulfide	0.84	nd	nd
990	2-pentylfuran	1.17	<0.10	0.39
996	ethyl hexanoate	0.77	nd	nd
1045	<i>cis-β-ocimene</i>	0.33	1.15	0.44
1136	pentyl 2-methylbutanoate	0.09	0.69	0.17
1140	(<i>Z</i>)-3-hexen-1-ol 2-methylpropanoate	nd	0.31	nd
1142	pentyl 3-methylbutanoate	<0.10	0.27	nd
1154	hexyl 2-methylpropanoate	<0.10	1.06	0.78
1178	2-methoxy-3-isobutylpyrazine	2.10	0.36	nd
1201	methyl salicylate	7.63	nd	nd
1244	hexyl 3-methylbutanoate	0.10	<0.10	0.17
1257	<i>7-methyloctanoic acid ethyl ester</i>	0.56	nd	nd
1337	<i>8-methyl-6-nonenoic acid ethyl ester</i>	2.45	nd	nd
1356	<i>8-methylnonanoic acid ethyl ester</i>	0.96	nd	nd
1361	<i>2-methyltridecane</i>	10.4	16.9	14.8
1400	tetradecane	1.11	2.20	1.77
1442	<i>α-pentadecene</i>	2.38	5.18	2.81
1460	<i>2-methyltetradecane</i>	3.17	8.98	6.83
1469	<i>α-himachalene</i>	1.53	1.93	0.88
1500	<i>γ-himachalene</i> + pentadecane	6.12	11.1	6.94
1503	<i>an unknown MW 204 sesquiterpene</i>	1.12	1.47	0.95
1560	<i>2-methylpentadecane</i>	0.85	2.78	1.96
1588	<i>8-methyl-6-nonenoic acid 3-methylbutyl ester</i>	<0.10	0.61	nd
1600	hexadecane	0.45	1.35	1.09
1607	<i>8-methylnonanoic acid 3-methylbutyl ester</i>	nd	0.30	nd
1662	<i>2-methylhexadecane</i>	0.40	0.95	0.75
1681	<i>pentadecanal</i>	0.10	1.48	1.11
1687	<i>8-methyl-6-nonenoic acid 4-methylpentyl ester</i>	nd	0.64	nd
1700	heptadecane	0.42	0.93	1.51
1706	<i>8-methylnonanoic acid 4-methylpentyl ester</i>	nd	0.52	nd

^a Linear retention index on a VF5-MS column^b Not detected (<0.01%)

VOLATILE COMPOUNDS IMPORTANT TO THE AROMA OF ITALIAN TYPE SALAMI: ASSESSMENT BY OSME AND DETECTION FREQUENCY TECHNIQUES

R. WAGNER¹; M.A.A.P. da Silva²; M.R.B. Franco¹

¹ *Departament of Food Science, State University of Campinas*

² *Departament of Food and Nutrition, State University of Campinas, P.O.Box. 6121, Campinas-SP, Brazil*

Abstract

The aim of this research was to determine the odoriferous importance of the volatile compounds present in Italian type dry-fermented sausages produced in Brazil. Volatile compounds were isolated by dynamic headspace technique and analysed by GC-FID and GC-MS. Their odoriferous importance was assessed by two olfactometric techniques, OSME and Frequency of Odour Detection. Among the most important volatile compounds pointed out by both techniques were the 1-octen-3-ol (described as legume broth odour-like), guaiacol (smoke), 1-octen-3-one (mould), 2- and 3-methylbutanoic acids, (cheese), ethyl 2-methylbutanoate, ethyl butanoate, propyl acetate, ethyl 3-methylbutanoate and methylpropyl acetate (fruity notes) and diallyldisulphide (garlic). While alcohol was the most abundant class of compounds present in the salami isolated, GC-Olfactometry revealed that the most important contributors for the product's odour were esters, sulphides, aldehydes, terpenes and phenols, followed by ketones and alcohols.

Introduction

In Brazil, the production of dry-fermented sausages, also known as salami is gaining economic importance in the country's meat market, which in 2007 corresponded to US\$ 11.3 billions. In spite of its economic potential in the Brazil, there are only two researches concerning the volatile profiles of Brazilian dry-fermented sausages (1,2); and neither of them assessed the odoriferous importance of the volatiles present in the samples. Thus, the aim of the present study was to determine the odoriferous importance of the volatile compounds present in Italian type dry-fermented sausages produced in Brazil, using GC-OSME (3) and Frequency of Odour Detection techniques (4).

Experimental

Selection of the samples. Ninety six habitual consumers of salami, evaluated six of the most consumed brands of salami in Brazil, rating through a 9-point hedonic scale (1= disliked extremely, 9= liked extremely) how much they liked or disliked the samples aroma. Following, the volatile profile of the brand showing the most acceptable aroma was determined as described bellow. This was an Italian type salami with pork and beef meat, loin pork fat and addition of white wine, smoke aroma, garlic, white and black pepper among other spices, milk powder and other essential ingredients. It obtained an average acceptability of 7.6 among the

consumers; 63.5% of the subjects reported they liked the aroma of this sample between “liked very much and liked extremely”; and only 7.3% of the consumers stated they did not like it.

Preparation of the samples. Five samples of the salami brand described above, all produced in the same batch, were minced and homogenized in a domestic grinder. An aliquot of 60 g was further transferred to the trapping system described below (n=3).

Isolation and identification of volatile compounds. The headspace volatile compounds of the grinded sample were swept by vacuum (100 mm of Hg) to a Porapak Q[®] trap for 3 h 26 min at 40 °C, in accordance with the methodology developed by Franco and Rodriguez-Amaya (5), and modified by Wagner (6). A highly representative extract of the original salami aroma was obtained after elution of the trap with dichloromethane (6). The volatile compounds were separated on a DB-Wax fused capillary column (30 m x 0.25 mm id, 0.5 µm film) in a Shimadzu model 17A gas chromatograph. The splitless mode injector and flame ionisation detector were maintained at 250 °C. Helium was the carrier gas at a flow rate of 1.0 mL.min⁻¹. The oven temperature was set at 35 °C, held for 5 min, programmed to 80 °C (2 °C.min⁻¹) and then to 200 °C (4 °C.min⁻¹). The volatile compounds were identified in a Shimadzu model QP-5000 mass spectrometer. Co-injection of the sample with a standard mixture of paraffin homologues (C6-C24) allowed the calculation of the volatiles Kovats indices. Identification was made by matching the volatiles mass spectra with published data (NIST 98), and also by comparison of experimental and theoretical Kovats indices. Finally, the mass spectra of pure standards were obtained, allowing the positive identification of volatiles that matched the standards retention indices and mass spectra.

Osme GC-Olfactometry. Four selected and trained judges evaluated the GC effluents using Osme methodology (3). Subjects rated the intensity of the stimuli using a time-intensity approach (0= none, 9= extreme). The judges also provided verbal descriptions of the odour quality of each stimulus. Only odoriferous stimuli (peaks) reported at least twice by at least two of the four judges were computed for the generation of the “consensus aromagram”, which was obtained by averaging each stimulus odour intensity and area across judges and replications.

FD GC-Olfactometry. Using the Frequency of Odour Detection technique (FD) (4), 11 untrained subjects evaluated the GC effluents, reporting the presence of odour stimuli. Subjects used the software SCDTI to report the initial and final time of each stimulus perception. The final aromagram of frequency detection was generated from the sum of each stimulus detected by the panel members. Judges also provided a verbal description of each stimulus odour quality.

Results and Discussion

One hundred and four of the one hundred and seventeen volatiles detected by the FID in the salami isolate were identified; among all the compounds, alcohols was the major chemical class, corresponding 49.3%, followed by the terpenes (23.5%) and esters (18.3%). The predominant volatiles in the Brazilian salami were propanol (22.3%), 2-butanol (21.1%), ethyl butanoate (5.8%), 3-methylbutanol (4.2%), limonene (4.0%), sabinene (3.8%), β-pinene (3.4%), 3-carene+diallylsulfide (2.8%), ethyl propanoate (2.6%), propyl acetate (2.4%) β-caryophyllene (2.1%), ethyl hexanoate (1.6%), α-pinene (1.5%), ethyl 3-methylbutanoate (1.1%), diallyldisulphide (0.8%) and 4-terpineol+γ-valerolactone (0.7%). The same compounds, but at

different proportions, were found in Italian type salami from other countries (7,8); this difference can be attributed to the use of different ingredients, raw materials, processes, among others. Overall, 86 regions of odour (odour peaks) were perceived in the GC effluents by the trained judges using Osme and/or the untrained subjects using FD techniques.

Table 1. *Odoriferous volatiles identified in Brazilian salami Italian type, their respective odour intensities (Osme) and frequency of detection in the GC effluent and odour description.*

I ^a	F ^b	KI-MS ^c	Compound	Odour descriptors
7.91	11	967*	Nd	garlic, gas, spice
5.65	9	1472	1-octen-3-ol	legume pottage, baked potatoes
5.51	10	1879	guaiacol	smoked, hospital, chemical
4.73	10	1309	1-octen-3-one	mould, brush, mushroom
4.58	8	1687	3-methylbutanoic acid + 2-methylbutanoic acid	dirty socks, cheese, fermented
4.53	11	1062	ethyl 2-methylbutanoate	fruity, berries fruits
4.48	11	1048	ethyl butanoate	fruity, floral, sweet
4.41	11	<1000	propyl acetate	fruity, orange, sweet
4.19	9	1487	diallyldisulphide	garlic, fermented, spice
4.12	11	1079	ethyl 3-methylbutanoate	fruity, cheese, stink bug
4.10	9	<1000	methylpropyl acetate	sweet, fruity, butter
3.94	4	1090	hexanal	grass, green, brush
3.86	11	1472	(E)2-octenal	sweet, fruity, stink bug
3.72	8	1284	terpinolene + methylallyldisulphide	spice, garlic, pungent
3.52	5	1593	dimethylsulfoxide	garlic, spice
3.34	10	1975	p-cresol	smoked, fresh, chemical
3.30	3	1397	2-nonanone	grass, green, pungent
3.26	10	1567	linalool	papaya, floral, perfume
2.91	8	1226	3-methylbutanol	fermented, cheese, rotten fruit
2.49	9	1246	ethyl hexanoate	fruity, sweet, berries fruits
2.41	6	1457	Ni	plastic, wood, hospital
2.38	9	1147	ethyl valerate	fruity, sweet, floral
2.29	9	2049	1,4-dimethoxy-2-methylbenzene	clove, mentholated, green
2.28	5	1210	1,8-cineol	mentholated, eucalyptus, green
2.15	5	1545	(E)2-nonenal	peanut, wax
2.14	7	1439	2-cyclohexen-1-one	grain, coffee, fermented
2.09	--	1071	2,3-pentanedione	cheese, fruity

^a Odours intensities by Osme; ^b Frequency of odours detection; ^c Experimental Kovats indices; *GC-Olfactometric Kovats index; Nd = undetected by GC/MS; Ni = unidentified compound.

Table 1 shows the identity and odour quality of all volatiles classified as highly or moderately important to the salami aroma in accordance with Osme or FD techniques. Compounds whose intensities range from 4 to 7.9 by Osme, or showing frequency of detection by at least 9 judges by the FD technique, indicate volatiles possessing the highest odoriferous impact for the salami aroma. On the other hand, compounds showing intensities ranging from 2.0 to 4.0, or showing frequency of detection by at least 5 judges, indicate volatiles possessing moderate odoriferous

importance. The remaining compounds were considered of low importance for the salami aroma of this sample. The first compound in Table 1, not detected by MS, represents the highest aroma impact volatile present in the sample (intensity = 7.91). It was described as garlic, gas and spice and, in accordance with Schmidt & Berger (9), the garlic aroma is usually characterised by sulphur compounds. In fact, in the present study the sulphur compounds diallyldisulphide, methylallyldisulphide and dimethylsulfoxide were also described as garlic aroma and classified as important volatiles for the salami aroma (Table 1). Diallyldisulphide was considered one of the most important contributor to the aroma of several types of salami when evaluated by the olfactometric technique AEDA (8); it usually originates from garlic.

Eight esters were identified as important contributors to the salami aroma. Since these compounds possess fruity-like smell, they probably suppress undesirable odour notes in the sample, such as rancid; consequently, they might be desirable compounds in the salami and might be responsible for the highest acceptability of the tested sample among the consumers. Possibly, these esters originated from the action of microbial esterases over alcohols and acids present in the salami (9,10). Volatiles most likely generated from the auto-oxidation and β -oxidation of unsaturated free fat acids were also identified as compounds of high aroma impact (Table 1), such as 1-octen-3-ol, 1-octen-3-one, hexanal, (E)-2-octenal, 2-nonanone and (E)-2-nonenal. The compounds 3-methylbutanol, 3- and 2-methylbutanoic acids, contributed to the fermented aroma notes of the salami (Table 1), and probably were originated from catabolism of branched-chain amino acids by microbial degradation (10).

Conclusion

This work pointed out the most important volatile compounds contributors for the Brazilian salami aroma of a sample considered of a high acceptability by consumers. Overall, these results may aid the Brazilian industry to improve the sensory quality of its salami.

Acknowledgements

The authors thanks CNPq, Brazil, for the financial support.

References

1. Campos R.M.L., Hierro E., Ordóñez J.A., Bertol T.M., Terra N.N., De La Hoz L. (2007) *Food Chem.* 103: 1159-1167.
2. Antoni I. (2005) Tese (doutorado) Faculdade de Engenharia de Alimentos, Universidade Estadual de Campinas, Campinas – SP.
3. Da Silva M.A.A.P., Lundahl D.S., McDaniel M.R., (1994) In *Trends in Flavour Research*. (Maarse H., van der Heij D. G., eds.), Elsevier Science, pp 191-209.
4. Le Guen S., Prost C., Demaimay M. (2000) *J. Agric. Food Chem.* 48: 1307-1314.
5. Franco M.R.B., Rodriguez-Amaya D. B. (1983) *J. Sci. Food Agr.* 34: 293-299.
6. Wagner R. (2008) Tese (doutorado) Faculdade de Engenharia de Alimentos, Universidade Estadual de Campinas, Campinas – SP.
7. Marco A., Navarro J.L., Flores M. (2007) *J. Agric. Food Chem.* 55: 3058-3065.
8. Schmidt S., Berger R.G. (1998) *Lebensm. Wiss Technol.* 31: 559-567.
9. Stahnke L.H. (1994) *Meat Sci.* 38: 39-54.
10. Montel M.C., Masson F., Talon R. (1998) *Meat Sci.* 49: 111-123.

AROMA COMPOUNDS IN ELEVEN EDIBLE MUSHROOM SPECIES: RELATIONSHIP BETWEEN VOLATILE PROFILE AND SENSORIAL CHARACTERISTICS

P. Guedes de Pinho¹, B. Ribeiro¹, R.F. Gonçalves¹, P. Baptista², P. Valentão¹, R.M. Seabra¹, P.B. Andrade¹

¹ REQUIMTE/Serviço de Farmacognosia, Faculdade de Farmácia da Universidade do Porto, R. Aníbal Cunha 164, 4050-047 Porto, Portugal

² CIMO/Escola Superior Agrária, Instituto Politécnico de Bragança, Campus de Sta Apolónia, Apartado 1172, 5301-855 Bragança, Portugal

Abstract

Volatile and semi-volatile components of 11 wild edible mushrooms, *Suillus bellini*, *Suillus luteus*, *Suillus granulatus*, *Tricholomopsis rutilans*, *Hygrophorus agathosmus*, *Amanita rubescens*, *Russula cyanoxantha*, *Boletus edulis*, *Tricholoma equestre*, *Fistulina hepatica* and *Cantharellus cibarius*, were determined by headspace solid-phase microextraction and by liquid extraction combined with gas chromatography-mass spectrometry. 51 volatiles were formally identified, based on commercial references, and the 13 others were tentatively identified. Using sensorial analysis, the descriptors “mushroom-like”, “farm-feed”, “floral”, “honey-like”, “hay-herb” and “nutty” were obtained. A correlation between sensory descriptors and volatiles was observed by applying multivariate analysis (principal component analysis and agglomerative hierarchic cluster analysis) to the sensorial and chemical data. The studied edible mushrooms can be divided in three groups. One of them is rich in C8 derivatives, such as 3-octanol, 1-octen-3-ol, trans-2-octen-1-ol, 3-octanone and 1-octen-3-one; another one is rich in terpenic volatile compounds; and the last one is rich in methional. The presence and contents of these compounds give a considerable contribution to the sensory characteristics of the analysed species.

Introduction

Wild edible mushrooms are consumed a lot in many countries as a food. Their culinary and commercial value is mainly due to their organoleptic properties such as their aroma. The aroma of each mushroom species is very characteristic, which determines the distinction between them (1). Among the diverse volatile compounds, a series of aliphatic eight carbon (C8) components, such as 1-octen-3-ol, 2-octen-1-ol, 3-octanol, 1-octanol, 1-octen-3-one, and 3-octanone, have been reported to be the major contributors to the characteristic mushroom flavour. 1-octen-3-ol, described as “mushroom-like flavour” and “raw mushroom” is considered to be the main responsible for the characteristic flavour of most of the edible mushroom species (2). Despite the high consumption of mushrooms, few studies concern their aroma.

In this work, different volatile extraction techniques were used in order to get a complete screening of volatile and semi-volatile compounds of all eleven wild edible mushrooms. HS-SPME technique was used into the headspace of the mushroom and the less volatile compounds were obtained using organic solvents. Finally, a

relationship between the contents of the identified volatiles and the sensorial descriptors was established.

Experimental

Samples. Samples of eleven different wild edible mushroom species (*Suillus bellini*, *Suillus luteus*, *Suillus granulatus*, *Tricholomopsis rutilans*, *Hygrophorus agathosmus*, *Amanita rubescens*, *Russula cyanoxantha*, *Boletus edulis*, *Tricholoma equestre*, *Fistulina hepatica* and *Cantharellus cibarius*) were collected in Trás-os-Montes region.

Sensorial studies. A panel composed by seven people was engaged in sensorial determinations. For the descriptors selection, 0.5 g of each mushroom powder were putted into an empty 15 mL vial, which was immediately sealed with a PTFE-silicone septa and put in a magnetic plate at 600 r.p.m. for 10 min, at 45 °C. The AFNOR procedure was used to select the most important descriptors (3).

Chemical extraction. 25 mg of each mushroom powder were analysed by HS-SPME (4), for dichloromethane (DCM) extraction, approximately 200 mg of each mushroom powder were used according to (5).

Gas Chromatography - Mass Spectrometry analysis. HS-SPME and dichloromethane extracts were analysed using a Varian CP-3800 gas chromatograph (USA) with a VARIAN Saturn 4000 mass selective detector (USA) and a Saturn GC/MS workstation software 6.8 (4). Identification of compounds was achieved by i) comparing the mass spectra present in the NIST 05 MS Library Database, ii) the Kovats indices and/or iii) by comparisons of the mass spectrum obtained from the sample and those from pure standards injected in the same conditions.

Peak areas were determined by re-constructed FullScan chromatogram using for each compound some specific ions (quantification ions, Table1). The relative area of each peak (%) was determined, considering 100% de sum of all identified peaks.

Statistical analysis. Principal component analysis (PCA) and Agglomerative hierarchic cluster analysis (dendogram) (AHC) were carried out using XLSTAT 2007.5 software.

Results

Sensory results. The descriptors selected were “farm-feed” (28%), “mushroom-like” (24%), “floral”(18%), “honey-like”(8%), “nutty”(8%), “hay-herb”(7%) and 7% corresponded to other descriptors which were discarded. The evaluation of the analysed mushroom species showed several differences among their sensory profiles. Using PCA with a total variance of 75.8% (F1 and F2 axes), the 11 mushroom species can be divided in three groups. The one with “floral” and “honey” descriptors includes *S. granulatus* and *S. luteus*; the second group, presenting “hay-herb”, “nutty” and “mushroom-like” notes is composed by *A. rubescens*, *C. cibarius*, *S. bellini*, *T. equestre*; and finally the species characterized by “farm-feed” are *H. agathosmus*, *T. rutilans*, *R. cyanoxantha*, *B. edulis*, *F. hepatica*.

Aroma composition. HS-SPME and dichloromethane extractions allowed the identification of 64 volatile compounds in the analysed mushroom species (Table 1). These include a total of 5 volatile acids, 8 non volatile acids, 7 esters, 9 alcohols, 7 aldehydes, 7 ketones, 11 terpenes, 1 volatile phenol, 2 lactones and 7 other compounds. Thirteen compounds were tentatively identified and fifty one were identified by comparison of the Kovats index and the MS spectrum of the pure

chemical standard. In some cases the same extracts and standards were injected on two different polarity columns. Among the volatile acids there are 5 fatty acids (myristoleic, palmitoleic, stearic, linoleic and oleic acids) and 3 others: benzoic, cinnamic and phenylacetic acids. *H. agathosmus* presented the highest percentage of myristoleic, palmitoleic, oleic and cinnamic acids. On the other hand, the species that contained the highest esters percentage – *T. rutilans* and *F. hepatica* – correspond to the ones that presented the lowest percentage of non volatile acids. *S. bellini* was identified as the richest species in alcohols, which are considered to be the main odorants of the “mushroom-like” aroma (2). Among these compounds, *C. cibarius* presented the highest percentage of 1-octen-3-ol, while *A. rubescens* was the one with the highest amount of 3-octanol. *T. equestre* also had a considerable percentage of these two compounds. Statistical results showed that these alcohols have higher correlations with the “nutty” descriptor than with the “mushroom-like” aroma ($r=0.897$ and $r=0.537$, respectively). *T. equestre* and *S. luteus* presented the highest levels of aldehydes. Benzaldehyde and phenylacetaldehyde were identified in all of the species. Phenylacetaldehyde is considered to be responsible for “honey” notes (2), *S. luteus* was the specie presenting the highest levels of this aldehyde. *B. edulis* was the richest specie in methional. This compound has a very low olfactive perception limit and its descriptor is “boiled potato” (6). This descriptor was not used by the panel for these mushroom species; however, this species was described with notes of “farm-feed”. A very high correlation between methional and “farm-feed” descriptor has been found ($r= 0.791$), the presence of this compound can explain its aroma characteristics (6, 7), methional has been recently identified in pine-mushroom specie (7).

Among the identified ketones, two different groups emerge: one is constituted by 3-octanone and 1-octen-3-one, while the other one is composed by volatile norisoprenoids, such as β -ionone, 6-methyl-5-hepten-2-one, *trans*-geranylacetone, (*E,E*)-farnesylacetone. These odour-active substances are known to be oxidative by-product or degradation products derived from carotenoids (8, 9). These 4 compounds have never been identified in mushrooms. The *trans*-geranylacetone and the (*E,E*)-farnesylacetone are present in higher levels in the *S. bellini*, *S. granulatus* and *S. luteus* mushroom species, it seems that these compounds can be markers of this mushroom genus. *A. rubescens* was the specie that present the highest contents of 3-octanone, while *C. cibarius* contains the highest amount of 1-octen-3-one. *S. bellini*, *S. granulatus* and *S. luteus*, were the richest species in norisoprenoid compounds. Several terpene compounds have been identified in fresh wild mushrooms before (10), however the *trans*-nerolidol, eucalyptol, menthol and 1,4-cineole have not been found in mushroom species (Table1).

Using an Agglomerative Hierarchic Cluster Analysis (HCA) the eleven studied species were divided in three groups: group 1 was composed by *S. bellini*, *A. rubescens*, *T. equestre* and *C. cibarius*; group 2 comprised *T. rutilans*, *H. agathosmus* and *B. edulis*; and group 3 included *S. luteus*, *S. granulatus*, *R. cyanoxantha* and *F. hepatica*. As far as we know, this work is the first approach to the volatile characterization of these edible mushroom species. The employment of two extraction techniques combined with GC-MS permitted the identification of a large number of compounds in all the studied species. It was possible to distinguish groups of wild edible mushroom species based in their odour properties and their aroma chemical composition.

Table 1. Relative percentage (%) of some of the 64 volatile compounds of mushroom species using HS-SPME and by DCM extraction.

Compound	Kovats index	Quantification Ions (m/z)	Samples (RA%)											Method
			A. rubescens	B. edulis	C. cibarius	F. hepatica	H. agathosmus	R. cyanoxantha	S. bellini	S. granulatus	S. luteus	T. equestre	T. rutifans	
<i>trans</i> -2-Hexen-1-ol ^{a,c}	814	57;82	nd	nd	33.1	nd	75.4	nd	100	nd	nd	nd	nd	HS-SPME
1-Hexanol ^{a,c}	841	56;69	nd	12.3	100	4.1	32.9	nd	29.8	21	nd	19.1	8.8	HS-SPME
Methional ^{a,c}	858	76;104	nd	100	nd	nd	nd	nd	nd	8	19	nd	nd	HS-SPME
α -Pinene ^{a,b}	948	93	63.6	11.2	4.9	6.7	13.1	31.9	15.8	9.1	100	10.2	13.3	HS-SPME
1-Octen-3-one ^{a,c}	956	55;97	15.7	8.9	100	nd	nd	nd	nd	nd	13	nd	nd	HS-SPME
6-Methyl-5-hepten-2-one ^{a,b}	962	93	nd	nd	nd	nd	nd	13.3	100	nd	40.6	nd	nd	HS-SPME
3-Octanone ^{a,c}	970	43;99	100	nd	nd	nd	nd	nd	nd	nd	nd	nd	nd	HS-SPME
β -Pinene ^{a,b}	978	93	18.1	nd	nd	21.3	32.8	nd	71.4	100	26.5	nd	nd	HS-SPME
3-Octanol ^{a,c}	979	55;83	100	nd	nd	nd	nd	nd	nd	nd	0.1	nd	nd	HS-SPME
1-Octen-3-ol ^{a,c}	998	57;99	17.4	31	100	1.6	64.4	16.4	40.3	4.9	nd	58.8	35.5	HS-SPME
1,4-Cyneole ^{a,b}	1012	111	nd	nd	nd	nd	nd	3.1	nd	100	1.4	nd	1.3	HS-SPME
Limonene ^{a,c}	1018	67	11.4	2.6	3.3	6.1	4.1	20.8	2.7	14.5	100	1.5	8.4	HS-SPME
Eucalyptol ^{a,c}	1059	93	48.6	29.3	39.9	74.6	45.4	42	26.7	63.9	nd	16.6	100	HS-SPME
Phenylacetaldehyde ^{a,c}	1081	91	7.3	2.2	1.5	12.3	5.5	16.2	3.5	30.6	100	19.4	4.2	HS-SPME
<i>trans</i> -2-Octen-1-ol ^{a,c}	1064	57;81;95	20.7	nd	nd	3.2	nd	20.6	100	2.2	nd	81.2	82.7	HS-SPME
Linalool ^{a,c}	1082	93	17	1	nd	1.6	4	22	18.7	100	25.2	nd	nd	HS-SPME
2-Phenylethanol ^{a,c}	1091	91	6.6	18.4	1.6	30.8	9.6	13.8	3.8	100	25.9	40.5	7.2	HS-SPME
Menthol ^{a,c}	1164	81	7.7	31	78.5	21.2	21.4	18.9	100	31.3	8.1	22.7	16.2	HS-SPME
α -Terpineol ^{a,c}	1175	59;121	nd	nd	nd	21.7	nd	100	nd	63.1	50.7	nd	nd	HS-SPME
<i>trans</i> -Geranylacetone ^{a,c}	1383	107	nd	4.5	nd	5.1	7.3	7.3	41.9	100	65.4	2.6	nd	DCM
β -Ionone ^{a,c}	1457	177	nd	59	nd	nd	79.1	nd	37.7	nd	100	87.1	17.4	HS-SPME
<i>trans</i> -Nerolidol ^{a,c}	1564	93	nd	nd	nd	nd	nd	nd	11.3	84.8	100	nd	nd	HS-SPME
Farnesylacetone ^{a,b}	1902	69	nd	nd	nd	nd	nd	nd	57.1	100	98.4	nd	nd	DCM

^aMS, identified by NIST05; ^bRI, identified by retention indices; ^cS, identified by comparison with reference compound; 100: highest area obtained; RA (%): relative areas in percentage; nd: not detected

References

1. Cronin D. A., Wada S. (1971) *J. Sci. Food Agric.* 22: 477-479.
2. Cho, I. H.; Kim S.-Y.; Choi, H.-K.; Kim, Y.-S. (2006) *J. Agric. Food Chem.* 54: 6332-6335
3. AFNOR NFV09-021. Recueil de normes françaises, contrôle de la qualité des produits alimentaires, analyse sensorielle, AFNOR, ISBN2-12-190843-9, 1991, (4^a edition).
4. Guedes de Pinho, P.; Ribeiro, B.; Gonçalves, R. F.; Baptista, P.; Valentão, P.; Seabra, R. M.; Andrade, P. B. (2008) *J. Agric. Food Chem.* 56: 1704-1712.
5. Silva Ferreira, A. C., Guedes de Pinho, P. (2003) *J. Food Science* 68: 2817-2820.
6. Soares da Costa M., Gonçalves C., Ferreira A., Ibsen C. Guedes de Pinho P., Silva Ferreira A. C. (2004) *J. Agric. Food Chem.* 52: 7911-7917.
7. Cho I. H., Lee S. M., Kim S. Y., Choi H. K., Kim K. O., Kim Y. S. (2007) *J. Agric. Food Chem.* 55: 2323-2328
8. Cole, E. R.; Kapur, N. S. (1957) *J. Food Sci.* 8: 360-365.
9. Silva Ferreira A. C., Guedes de Pinho P. (2004) *Anal. Chim. Acta.* 513: 169-176.
10. Breheret S., Talou T. (1997) *J. Agric. Food Chem.* 45: 831-836.

DEVELOPMENT OF HIGH IMPACT SULPHUR CHEMICALS FOR MUSHROOM FLAVOURS

H. COLSTEE, M. van der Ster, L. Braamer, C. Niedevelde, and C. Merlier

I.F.F. (Nederland) B.V., Zevenheuvelenweg 60, P.O.Box 5021, 5004 EA Tilburg, The Netherlands

Abstract

Novel hydrogen sulphide and methyl mercaptan adducts of 1-octen-3-one have been synthesised. Among others 1-mercapto-3-octanone, 1-methylthio-3-octanone, the corresponding alcohols as well as a number of esters thereof have been made available for sensory evaluation. Sensory showed that with the exception of 1-mercapto-3-octanol, none of the prepared compounds show interesting mushroom characteristics. However 1-methylthio-3-octanyl acetate shows interesting vegetable melon and cucumber notes, while 1-methylthio-3-octanyl butyrate could be used as an ingredient in savoury applications.

Introduction

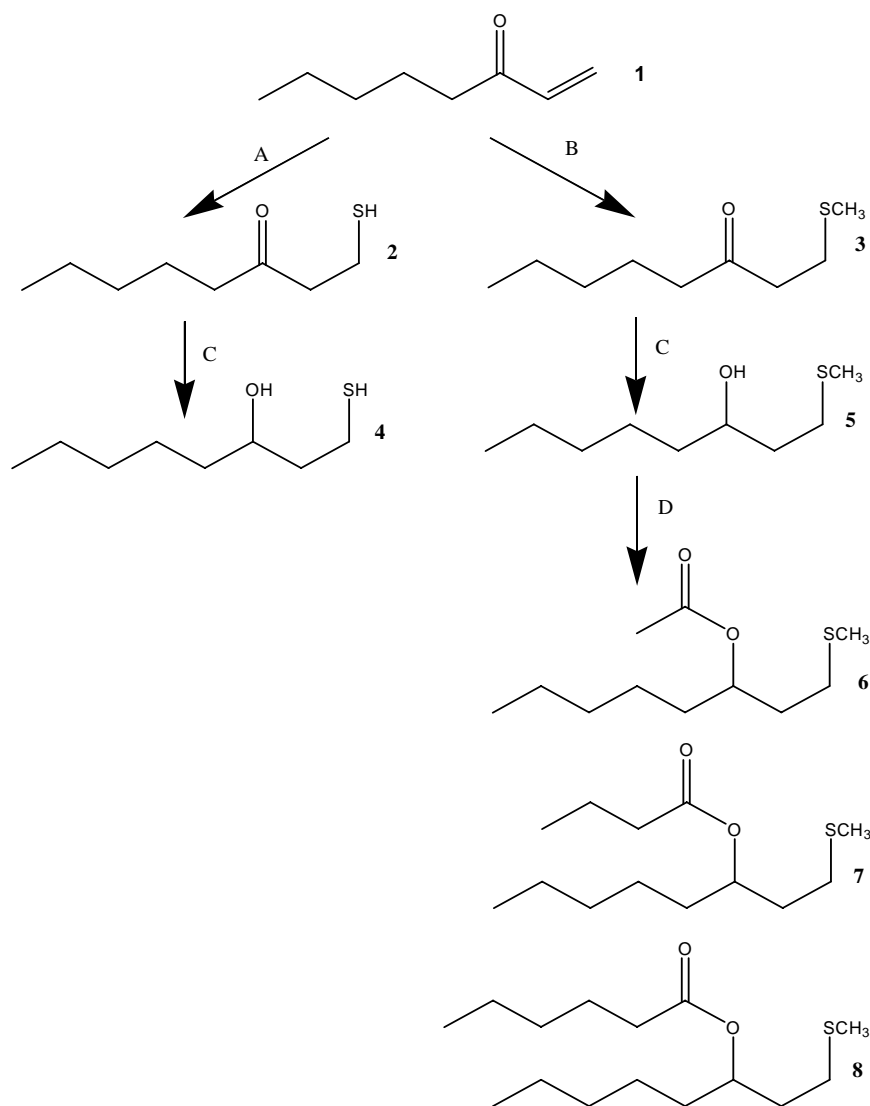
Mercapto and methylthio containing sulphur compounds are known flavour components. Among others 3-methylthiohexanal is found in tomato paste (1), 3-methylthiobutanol in potato (2), 3-mercaptohexanol and 3-methylthiohexylacetate in passion fruit (3) and 1-methylthio-2-butanone in coffee (4). Since 1-octen-3-one, hydrogen sulphide and methyl mercaptan occur in mushroom the sulphur adducts of 1-octen-3-one have been synthesised to see whether these compounds contribute to an improved mushroom taste. Esters of mercapto and methylthio containing flavouring substances are known also (3). Therefore a number of novel esters of 1-mercapto-3-octanol and 1-methylthio-3-octanol were synthesised for sensory evaluation also. The Michael addition of sulphur to α - β unsaturated aldehydes and ketones is a well known pathway for the formation of organic sulphur compounds in nature. This chemical scheme has been used as the basis for the synthesis of the sulphur containing ketones. The reduction of the ketones was done using sodium borohydride, a well described pathway for the synthesis of alcohols. For the ester preparation the well known route using corresponding acid chlorides catalysed by pyridine was chosen.

Experimental

Reagents. All chemicals were purchased on the global market.

Chemistry. The addition of hydrogen sulphide [A] and methylmercaptan [B] was done in ethanol, catalysed by piperidine. The reaction was performed in an autoclave at 25°C for 4 hours. The crude products (2 and 3) were washed to neutral and fractionated at reduced pressure. The corresponding alcohols (4 and 5) were prepared by reduction of products 2 and 3 using sodium borohydride [C]. The crude product was purified by fractional distillation at reduced pressure. Three esters (6-8) were prepared by the reaction of 1-methylthio-3-octanol (5) with the corresponding

acid chlorides, catalysed by pyridine [D]. The crude esters were purified by fractional distillation at reduced pressure followed by column chromatography to remove traces of the unreacted 1-methylthio-3-octanol.



Scheme 1. Synthesis pathway.

Product purification. Products were purified by combination of fractional distillation and column chromatography. Purity was checked additionally by GC-sniff.

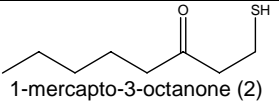
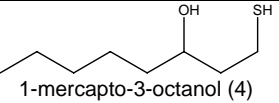
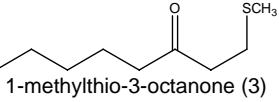
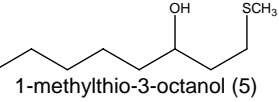
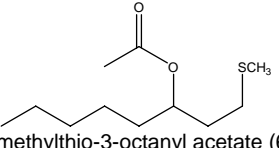
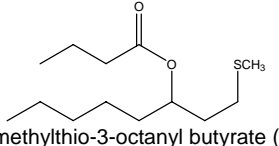
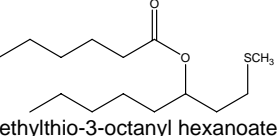
Analysis. Samples were analysed by means of gas-liquid chromatography (GLC-FID) using CP-sil 5-CB [15m x 0.15mm x 0.15um] and CP-wax 52-CB [15m x 0.15 mm x 0.12um] type columns. The structures of compounds were identified by GC-MS using a CP-sil 5-CB column [50m x 0.25mm x 0.25um].

Results

Prepared compounds and evaluation results. The prepared compounds have been evaluated by tasting in water by an expert panel. The results are summarized in table 1. Only 1-mercapto-3-octanol and 1-methylthio-3-octanyl acetate show some mushroom taste, although not characteristic enough to be used in mushroom

flavours. The acetate and butyrate esters of 1-methylthio-3-octanol show interesting characteristic notes for use in vegetable and savoury flavours.

Table 1. Evaluation and MS data of prepared compounds.

Compound	Evaluation level (ppm) in water	Taste descriptors	MS data, m/z (%)
 1-mercapto-3-octanone (2)	0.5	Sulphury, plastic, berry	43(100),61(81),71(71),41(46), 55(36), 99(34), 47(25), 89(13), 127(12),142(5), 160(2)
 1-mercapto-3-octanol (4)	0.5	Sulphur, sweet mushroom, onion, bell pepper, tomato	55(100),87(93),41(56),101(52), 47(44),115(29),144(5),128(4), 162(1)
 1-methylthio-3-octanone (3)	5	Oxidized citrus, tomato vine, vegetable peel, blue cheese	75(100),61(74),71(65),43(63), 99(45),55(38),103(37), 174(29) , 83(27),127(20)
 1-methylthio-3-octanol (5)	10	Oxidized citrus, tropical, green	72(100),61(96),43(41),55(40), 57(39),85(33),99(29),87(25), 143(19), 176(14)
 1-methylthio-3-octanyl acetate (6)	10	Green, melon, cucumber, slightly mushroom	43(100),87(82),61(66),69(46), 81(41),110(38),158(28),143(24), 129(6), 218(5)
 1-methylthio-3-octanyl butyrate (7)	3	Yeasty, cheesy, goat-like, garlic	87(100),43(84),61(76),69(72), 71(70),110(58),81(53),158(47), 143(37), 246(4)
 1-methylthio-3-octanyl hexanoate (8)	2	Yeasty, cognac	87(100),61(84),69(81),43(68), 110(61),143(50),158(44), 274(1)

Conclusion

None of the prepared compounds were found to add flavour that contributed to an improved mushroom taste although some of them showed interesting characteristics. Unfortunately, with the exception of 1-methylthio-3-octanone, none of the compounds were “found in nature yet”, which limit their use.

References

1. Buttery R.G., Teranishi R., Flath R.A, Ling L.C. (1990) *J.Agric. Food Chem.* 38: 792-795.
2. Carlin J.T., Ho C.-T., Chang S.S., Velluz A., Pickenhagen W. (1990) *Lebensm. Wiss. Technol.* 23: 276.
3. Engel K. -H., Tressel R. (1991) *J.Agric. Food Chem.* 39:2249-2252.
4. Stoll M., Winter M., Gautschi F., Flament I., Willhalm B. (1967) *Helv.Chim.Acta* 50: 628-694.

2-ACETYL-2-THIAZOLINE, A NEW CHARACTER IMPACT VOLATILE IN JASMINE RICE

K. MAHATTANATAWEE¹ and R. L. Rouseff²

¹ Department of Food Technology, Faculty of Science, Siam University, Bangkok 10163, Thailand

² University of Florida, IFAS, Citrus Research and Education Center, Lake Alfred, FL USA

Abstract

The fragrant Thai Jasmine rice or Khao Dawk Mali 105 (KDML) is one of the most popular fragrant rice cultivars. Thai jasmine rice volatiles were investigated using headspace SPME, GC-O, GC-PFPD (pulsed flame photometric detection) and GC-MS. Two GC-O peaks were described as cooked jasmine rice among the 23 aroma peaks observed. One of them was the previously reported 2-acetyl-1-pyrroline (2-AP). The primary objective of this study was to identify the second character impact volatile. This second aroma peak was examined using GC-O, PFPD using both polar and non-polar GC columns. GC-O and PFPD retention characteristics from the rice matched that of authentic 2-acetyl-2-thiazoline (2-AT). The identification was confirmed using GC-MS by comparing both mass spectra and retention values of 2-AT standards and sample. This is the first time 2-AT has been identified as character impact volatile in cooked jasmine rice. However, the aroma intensity of 2-AT was always less than that of 2-AP.

Introduction

Rice (*Oryza sativa* L.) is a major dietary component of people in many countries. Fragrant rice cultivars are considered more desirable and of higher quality primarily due to their pleasing aroma compared to many cultivars with little aroma. There are at least three major scented cultivars, Basmati, Thai, and Azucena. 2-Acetyl-1-pyrroline (2-AP) was the first reported character impact volatile in fragrant rice (1). Thai Jasmine rice such as Khao Dawk Mali 105 (KDML) is one of the more popular fragrant rice cultivars because its pleasant aroma and soft texture after cooking. More than 155 volatile compounds have been reported in rice (2,3). 2-AP has been reported as the sole character impact volatile in fragrance rice (4). 2-AP is also responsible for the characteristic aroma of white bread, pandan (*Pandanus amaryllifolius*) leaves and bread flowers (*Vallais glabra*) (5). The purpose of this study was to determine if there were additional character impact volatiles in Jasmine rice.

Experimental

Headspace sampling. Static headspace solid phase micro extraction, HS SPME, was used to collect and concentrate rice volatiles. The cooked rice was prepared by adding 5 g of rice and 5 g of water into a 40 mL glass vial, loosely sealing with a Teflon-coated septum and cooked in rice cooker for 18 minutes. The cooked rice sample was equilibrated at 40°C for 15 min in a water bath and a 2 cm 50/30 µm

divinylbenzene/Carboxen/-polydimethylsiloxane (DVB/Carboxen/PDMS) Stable Flex fibre (Supelco, Bellefonte, PA) was exposed to the cooked rice volatiles for 30 min. The sorbed rice volatiles were introduced into the GC injector where they were thermally desorbed.

Gas Chromatography-FID/Olfactometry. Chromatography was performed using an Agilent 6890N GC (Agilent Technologies, USA) equipped with a sniffing port. Samples were run separately on DB-Wax and ZB-5 columns. Oven temperature was programmed from 40 to 240°C at 7°C/min. Helium was the carrier gas at flow rate of 2.0 mL/min. Injector and detector temperature were 220 °C and 275 °C, respectively. Injections were splitless. Two trained assessors evaluated each sample in duplicate on both ZB-5 and DB-Wax columns. Intensities of all odour-active compounds of each GC-O run were normalized and averaged.

Gas Chromatography-PFPD. Sulphur-compounds were detected using a Pulsed Flame Photometric Detector (PFPD) in the square root mode (Model 5380, OI Analytical Co., College Station, TX) coupled to a HP-5890 Series II GC. Separation was accomplished using two different capillary columns as described above. GC conditions were the same as in the GC-O studies. Identification of sulphur volatiles was confirmed by matching LRI values from authentic standards on both columns.

Gas Chromatography-Mass spectrum. Identities of odour-active compounds were confirmed using gas chromatography-mass spectroscopy (GC-MS). Analyses were performed using a Perkin-Elmer Clarus 500 quadrupole mass spectrometer equipped with Turbo Mass software, v5.4, (Perkin-Elmer, Shelton, CT) and an RTX-5 capillary column (Restek; column length = 60 m, inner diameter = 0.25 mm, film thickness = 0.50 µm). Mass spectra matches were made by comparison of NIST 2005 v2.0 standard spectra (NIST, Gaithersburg, MD). Only those compounds with spectral fit values ≥ 800 were considered positive identifications. Authentic standards were used to confirm GC-MS identifications.

Results

There have been at least three studies in which rice volatiles were examined for aroma activity (68). Over 50 volatiles were reported to have aroma activity between these three studies. Interestingly, there were only seven volatiles which were common to all three studies and only nine volatiles which were common to at least two of the studies. Twenty three aroma active peaks were detected (Figure 1, Table 1) and 21 have been identified. Seven of these 21 had been previously identified by Buttery (6) and included 2-acetyl-1-pyrroline, (E,E)-2,4-decadienal, hexanal, (E)-2-nonenal, octanal, decanal and 4-vinylguaiaicol. The other previously identified aroma volatiles are denoted by superscripts in Table 1. Two volatiles in Table 1 were described as “cooked jasmine rice”. One was the previously reported 2-acetyl-1-pyrroline (1). The second character impact volatile was also observed by GC-PFPD (Figure 2). Retention characteristics matched that of authentic 2-acetyl-2-thiazoline (2-AT). The identification was conclusively confirmed using GC-MS and comparing the mass spectrum between 2-AT standard and sample.

As seen from the aroma intensity values in Table 1, the aroma intensity of 2-AT in cooked jasmine rice was only about $\frac{1}{4}$ as intense as the major character impact compound 2-AP. 2-AT was first identified in beef broth (9) and has been reported in other foods, but this is the first time 2-AT is reported in cooked jasmine rice.

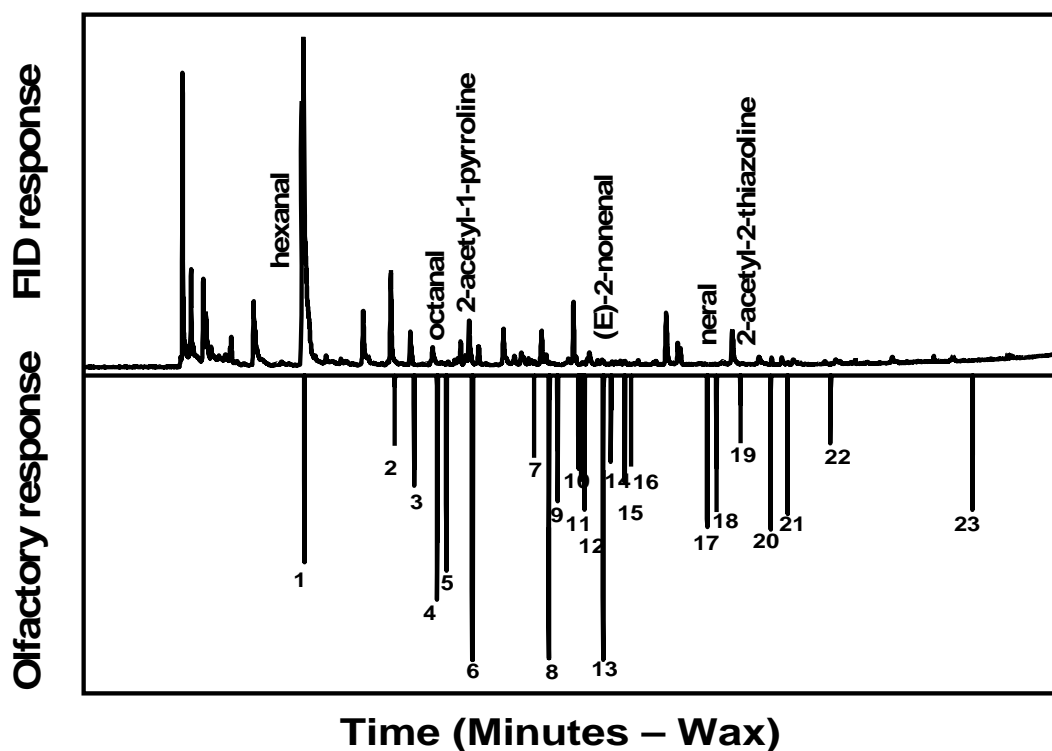


Figure 1. Aroma active volatiles in cooked jasmine rice detected by olfactometry (numbers in figure correspond to those in Table 1)

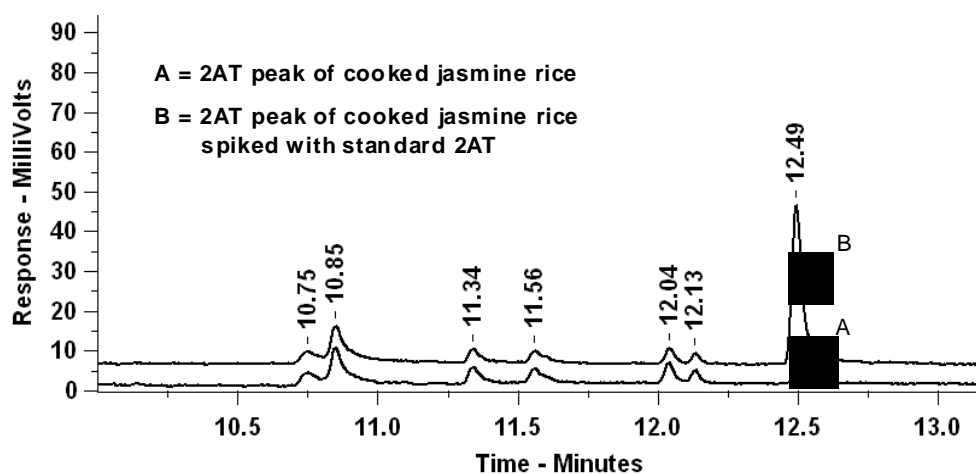


Figure 2. 2-AT detected in cooked jasmine rice volatiles by GC-PFPD (A) and rice sample spiked with standard 2-AT (B).

Table 1. Tentative identification of aroma active volatiles in cooked jasmine rice.

Peak no.	Identification	Descriptors	LRI-GC-O		Aroma intensity
			DBwax	DB5	
1	Hexanal ^{a,b,c}	green	1073	798	6.8
2	Unknown	minty	1221	ND	2.6
3	Ethyl hexanoate	sweet fruity	1252	ND	3.9
4	Octanal ^{a,b,c}	citrus-like	1286	999	7.7
5	1-Octen-3-one ^b	mushroom	1300	980	6.7
6	2-Acetyl-1-pyrroline ^{a,b,c}	cooked jasmine rice	1338	924	10.0
7	(E)-2-Octenal ^c	fatty	1430	1062	2.9
8	Methional ^b	cooked potato	1451	912	9.7
9	1-Octen-3-ol ^c	mushroom	1464	980	4.4
10	Unknown	musty, moldy	1495	ND	3.2
11	Decanal ^{a,b,c}	fatty metallic	1500	1202	3.7
12	(Z)-2-Nonenal ^b	metallic	1504	1149	4.6
13	(E)-2-Nonenal ^{a,b,c}	metallic	1533	1161	10.0
14	Linalool	sweet, floral	1545	1100	2.9
15	1-Octanol ^c	fatty, metallic	1567	1062	3.7
16	(E,Z)-2,6-Nonadienal ^b	soapy, fatty	1576	1157	3.4
17	(E,E)-2,4 Nonadienal ^b	soapy, fatty	1700	1218	5.4
18	Neral	minty, citrus-like	1715	1245	4.7
19	2-Acetyl-2-thiazoline	cooked jasmine rice	1756	1109	2.3
20	(E,E)-2,4-Decadienal ^{a,b,c}	fatty	1808	1318	5.3
21	β -Damascenone	sweet honey	1838	1395	4.9
22	2-Phenylethanol ^b	sweet floral	1913	1106	2.4
23	4-Vinyl guaicol ^{a,b,c}	clove-like	2187	1327	4.7

a= reported by (6), b= reported by (7), c= reported by (8).

Acknowledgement

This study was supported in part by the Thailand Research Fund (TRF) Thailand, and the University of Florida, USA.

References

1. Buttery R.G., Ling L.C., Juliano B. (1982) *Chem. Ind. (London)* 23: 958-959.
2. Maga J.A. (1984) *J. Agric. Food Chem.* 32: 964-970.
3. Tsugita T. (1986) *Food Rev. Inter.* 1: 497-520.
4. Widjaja R., Craske J. D., Wootton M. (1996) *J. Sci. Food Agric.* 70: 151-161.
5. Wongpornchai S., Sriseadka T., Choonvisase S. (2003) *J. Agric. Food Chem.* 51: 457-462.
6. Buttery R.G., Turnbaugh J.G., Ling L. C. (1988) *J. Agric. Food Chem.* 36: 1006-1009.
7. Jezussek M., Juliano B.O., Schieberle P. (2002) *J. Agric. Food Chem.* 50: 1101-1105.
8. Yang D.S., Shewfelt R.L., Lee K.-S., Kays S.J. (2008) *J. Agric. Food Chem.* 56: 2780-2787.
9. Tonsbeek C.H., Copier H., Plancken A.J. (1971) *J. Agric. Food Chem.* 19: 1014-1016.

IMPACT FLAVOUR COMPOUNDS IN COOKED RICE CULTIVARS FROM THE CAMARGUE AREA (FRANCE)

I. Maraval¹, C. Mestres¹, K. Pemin²⁻⁴, F. Ribeyre¹, R. Boulanger¹, E. Guichard²⁻⁴, Z. GUNATA⁵

¹ UMR Qualisud, CIRAD, 73 Rue J.F. Breton, Montpellier F-34398 France

² INRA, UMR1129 FLAVIC, F-21000 Dijon, France

³ ENESAD, UMR1129 FLAVIC, F-21000 Dijon, France

⁴ Université de Bourgogne, UMR1129 FLAVIC, F-21000 Dijon, France

⁵ UMR Qualisud, Université de Montpellier II, place E. Bataillon, 34095 Montpellier Cedex 5, France

Abstract

Rice from two scented (Aychade, Fidji) and one nonscented (Ruille) cultivars from Camargue area (France) together with one Asian scented rice (Thai) were cooked and volatile compounds were extracted by dichloromethane/pentane (1:2, v/v) solvent mixture. 40 odorous compounds were noticed during GC-O analysis of the organic extracts, amongst which oct-1-en-3-one and 2-acetyl-1-pyrroline were almost constantly perceived. Hierarchical cluster analysis (HCA) of perceived odours enabled to distinguish the groups of rice cultivars. 60 compounds were identified and quantified by GC-MS. New odour-active components of cooked rice were detected for the first time including oct-3-en-2-one, 2-methylpropanoic acid, γ -decalactone and δ -decalactone. A principal component analysis (PCA) differentiated scented cultivars from a non-scented one and scented rice cultivars from Camargue from Thai sample.

Introduction

Scented rice is highly appreciated in Asian diet by its specific aroma. Its consumption has tendency to increase in North America and Europe including France. New scented cultivars suitable to temperate climate have been developed in the Camargue, a traditional rice cultivation area in the south of France [1]. 2-acetyl-1-pyrroline (2AP) developing a roasty popcorn-like odour, was reported as an important contributor to the scented character of cooked rice [2-5]. However, other volatile compounds, such as aldehydes, volatile phenols, and sulphur- and nitrogen-based compounds were considered as contributors to the overall cooked aroma of scented rice [6,7]. In the present study the flavour compounds of cooked rice from two scented (Aychade and Fidji) rice cultivars from the Camargue area were compared with those of a well-known Asian scented rice cultivar (Thai) through GC-O and GC-MS analyses [8,9]. Additionally one non-scented rice cultivar (Ruille) from the Camargue area has been subject of the study.

Experimental

Rice Samples. Aychade, Fidji and Ruille were harvested in 2006 in the Camargue area. Thai was purchased as milled grain in a French supermarket.

Extraction of flavour compounds and representativeness of the organic extracts. Rice (5 g) was cooked with mineral water (10 mL) in open steam for 20 min. After

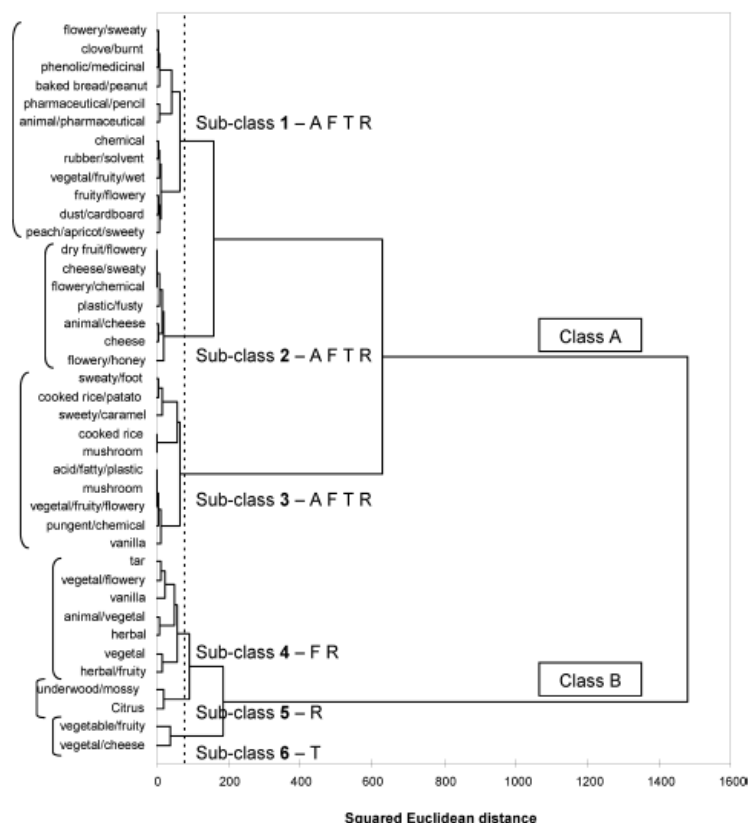
resting for 10 min, the freshly cooked rice was frozen under liquid nitrogen followed by the addition of 30 g of anhydrous sodium sulphate. The ensemble was ground to flour under liquid nitrogen and extracted with 100 mL of organic solvent or organic solvent mixtures: dichloromethane, dichloromethane/pentane (1:2, v/v), ether, and ether/pentane (1:1, v/v). The organic extracts were concentrated to ca. 0.5 mL through a Vigreux column and a Kuderna-Danish concentrator fitted with a Snyder column (Jezussek et al. [6]). The representativeness of the organic extracts was estimated by sensory analysis. Panellists were asked to note the similarity between the odour of the organic extracts and the freshly cooked rice. More details are reported elsewhere [10].

GC-O and GC-MS Analysis. The dichloromethane/pentane (1:2, v/v) organic extracts from four cooked rice were analysed by GC-O with odour detection frequency method. Semi-quantification of volatiles were performed by GC-MS analysis using 2,4,6- trimethylpyridine as internal standard [10]

Statistical treatment. HCA was performed with XL-STAT Prov.7 (Addinsoft), PCA with Statistica v.7.1 (StatSoft).

Results and discussion

Representativeness of the Organic Extracts. Higher similarity values with the reference (cooked rice) were obtained with dichloromethane and dichloromethane / pentane (1:2, v/v) extracts. Dichloromethane/pentane (1:2, v/v) mixture was chosen for further work because of its lower temperature for the evaporation.



GC-O results. 40 odorous compounds have been detected by GC-O, among which 2 showed high detection frequency in the 4 cultivars: 2-Acetyl-1-pyrroline (2AP, cooked rice attribute) and oct-1-en-3-one (mushroom attribute).

Hierarchical cluster analysis (HCA) of odorous compounds enabled to distinguish the groups of rice cultivars. Class (A) includes odours detected at similar frequency of detection for the 4 rice. Class (B) reports odours detected by frequency of detection which differed between cultivars (Figure 1).

Figure 1. HCA dendrogram of aroma attributes obtained from the four cooked rice cultivars (from A. Aychade, F. Fidji, T. Thai, R. Ruille, reprinted with permission from J. Agric. Food Chem, 2008, 56, 5291-5298. Copyright 2008 American Chemical Society).

GC-MS Analysis. 60 compounds have been identified and quantified by GC-MS analysis. 4 of them have been detected for the first time in cooked rice: oct-3-en-2-one, 2-methylpropanoic acid, γ -decalactone and δ -decalactone. As expected, the level of 2AP was higher in the scented cultivars than in the non-scented one.

Principal component analysis (PCA) treatment enabled to separate Camargue cultivars from Thai sample and scented cultivars from non-scented one (Figure 2). Fatty acids and cinnamic acids derived volatile compounds, such as (*E,Z*)-deca-2,4-dienal, hexanal and 4-vinylphenol, 2-methoxy-4-vinylphenol highly contributed to the discrimination of cultivars.

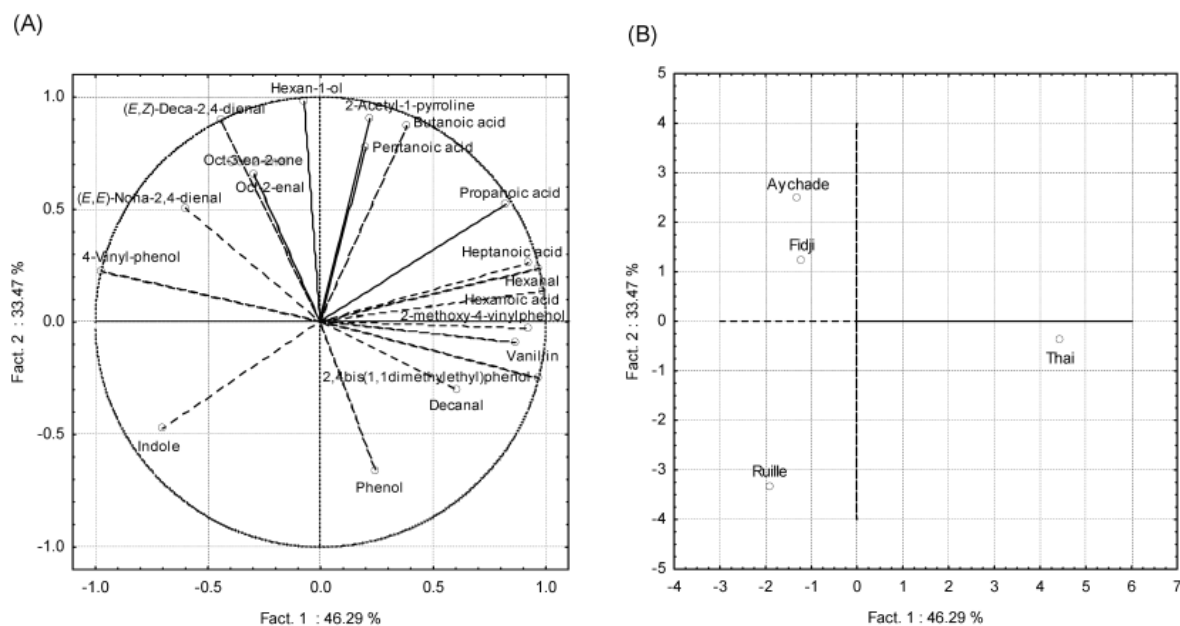


Figure 2. Bi-plot of variables scores (A) and rice loadings (B) on the first two axes of the principal component analysis (Reprinted with permission from *J. Agric. Food Chem*, 2008, 56, 5291-5298. Copyright 2008 American Chemical Society).

The odour active values (OAV) of the volatiles were calculated to have some view with regard to the contribution of volatiles to cooked rice flavour (Table 1).

Table 1. Odour-active values (OAV) of volatiles in the four cooked rice cultivars. (Reprinted with permission of ACS from *J. Agric. Food Chem*, 2008, 56, 5291).

compounds	odour threshold ($\mu\text{g/L}$) ^a	OAV ^b			
		Aychade	Fidji	Thai	Ruille
2-Acetyl-1-pyrroline	0.10	2150.00	2640.00	1860.00	nd
(<i>E,Z</i>)-Deca-2,4-dienal	0.07	2328.57	1671.43	357.14	257.14
2-Methoxy-4-vinylphenol	3.00	124.33	84.67	187.67	10.,67
4-Vinyl-phenol	10 .00	112.70	107.90	nd	96.20
(<i>E,E</i>)-Nona-2,4-dienal	0.09	74.43	33.21	19.23	38.52
Decanal	2 .00	46.00	30.50	53.50	46.00
Hexanal	5.00	13.94	12.27	24.39	8.47
Vanillin	20.00	13.00	6.95	19.95	11.10
Oct-2-enal	3.00	16.00	nd	nd	nd
Indole	140.00	1.80	0.77	0.49	2.61
Butanoic acid	240.00	1.38	0.91	1.15	0.44

^a Odour threshold values in water obtained from the literature. ^b The odour unit values were obtained by dividing the concentration of the odorant compound in the cooked rice by its odour threshold in water. nd: not determined since the concentration was below the detection limit of quantification (< 2 $\mu\text{g/L}$).

11 Compounds displayed OAVs greater than 1. The OAV for 2AP was very high in scented rice cultivars confirming its role in the flavour of these products. The second highest OAV was obtained with (*E,Z*)-deca-2,4-dienal. The scented cultivars from Camargue were distinguished by OAV of this compound in the same magnitude as the OAV of 2AP. Hence this aldehyde may play a significant role on the global aroma of scented Camargue cultivars. It is mainly formed upon auto-oxidation of linoleic acid. One can suppose the occurrence of the higher levels of linoleic acids in Camargue scented cultivars. The level of this acid in rice was supposed to correlate negatively with ripening temperature [11]. This may be reason of the lower levels of (*E,Z*)-deca-2,4-dienal in Thai cultivar. Two volatile phenols, 2-methoxy-4-vinylphenol and 4-vinylphenol showed high OAVs. Their formation from decarboxylation of putative cinnamic acid precursors is well documented [12,13]. Surprisingly 4-vinylphenol was not detected in Thai sample. This may be related to the compositional differences in cinnamic acids among rice cultivars [14].

In conclusion, organic extracts of cooked scented rice from Camargue cultivars (Aychade and Fidji), displayed aroma profile close to that of a well-known scented cultivar, Thai. However, quantitative differences were noticed for the levels of some flavour compounds, issued from the degradation of lipids and cinnamic acids, between scented Camargue cultivars and Thai one. Cultivar effect but also the growing and storage conditions could take part in these differences.

References

1. Clément G., Audebert A., Roques S., Maraval I., Mestres C., Gay F. (2007) In *Proceeding of the 4th international temperate rice conference*, pp. 180-181, Novara, Italy.
2. Buttery R.G., Ling L.C., Juliano, B.O. (1982) *Chem. Ind.*, 958-959.
3. Buttery R.G., Ling L.C., Juliano B.O., Turnbaugh J.G. (1983) *J. Agric. Food Chem.* 31: 823-826.
4. Paule C.M., Powers J.J. (1989) *J. Food Sci.* 54: 343-346.
5. Petrov M., Danzart M., Giampaoli P., Faure J., Richard H. (1996) *Sci. Aliments* 16: 347-360.
6. Jezussek M., Juliano B.O., Schieberle, P. (2002) *J. Agric. Food Chem.* 50: 1101-1105.
7. Buttery R.G., Turnbaugh J.G., Ling, L.C. (1988) *J. Agric. Food Chem.* 36: 1006-1009.
8. Etievant P.X., Moio L., Guichard E., Langlois D., Leschaeve I., Schlich P., Chambellant E. (1994) In *Trends in Flavor Research* (Maarse D.G., ed.), pp 179-190, Elsevier, Amsterdam.
9. Escudero A., Hernandez-Orte P., Cacho J., Ferreira, V. (2000) *J. Agric. Food Chem.* 48: 4268-4272.
10. Maraval I., Mestres C., Pernin K., Ribeyre F., Boulanger R., Guichard E., Gunata Z. (2008) *J. Agric. Food Chem.* 56: 5291-5298.
11. Taira H., Taira H.K.F. (1979) *Jpn. J. Crop Sci.* 48: 371-377.
12. Maga J.A. (1984) *J. Agric. Food Chem.* 32: 964-970.
13. Goodner K.L., Jella P., Rouseff, R.L. (2000) *J. Agric. Food Chem.* 48: 2882-2886.
14. Chung I.M., Ahn J.K., Yun S.J. (2001) *Can. J. Plant Sci.* 81: 815-819.

SPICE UP YOUR LIFE – THE ROTUNDONE STORY

C. Wood^{1,2}, T.E. Siebert¹, M. Parker¹, D.L. Capone¹, G.M. Elsey¹, A.P. Pollnitz¹, M. Eggers³, M. Meier³, T. Vössing⁵, S. Widder³, G. KRAMMER⁴, M.A. Sefton¹, and M.J. Herderich¹

¹ *The Australian Wine Research Institute (AWRI), PO Box 197, Glen Osmond (Adelaide), SA 5064, Australia*

² *School of Agriculture, Pontificia Universidad Católica de Chile, Casilla 306 Correo 22, Santiago, Chile*

³ *Symrise Scent & Care Division, Mühlenfeldstr. 1, D-37603 Holzminden, Germany*

⁴ *Symrise Flavor & Nutrition Division, Mühlenfeldstr. 1, D-37603 Holzminden, Germany*

Abstract

A spicy, 'black pepper' aroma is important to some high quality Australian Shiraz (Syrah) red wines. An interesting sesquiterpene, rotundone, was identified for the first time by gas chromatography-mass spectrometry-olfactometry as an important aroma impact compound in a variety of food products and specific wines. This study confirmed that rotundone is mainly responsible for the peppery characters in Shiraz grapes and red wine (and to a lesser extent in wine from other varieties). Furthermore rotundone was also found in much higher amounts in other common herbs and spices. In particular, rotundone was identified, for the first time, in extracts of peppercorns (*Piper nigrum*) where it was found in the highest concentration, and is the only odorant thus far detected in that spice with an obvious pepper-like aroma. The aroma detection threshold for rotundone was 16 ng/L in red wine and 8 ng/L in water. While most of the sensory panellists were sensitive to rotundone, approximately 20% could not detect this compound at the highest concentration tested (4000 ng/L). Thus, the sensory experience of two consumers enjoying the same glass of Shiraz wine or sharing the same meal seasoned with pepper might be very different.

Introduction

Identification of the compounds responsible for the distinctive aroma and flavour of food products and beverages can be a challenging task, as many key odorants are often present in parts per trillion (ng/kg) concentrations only (1-6). A spicy, 'black pepper' aroma is important to some high quality Australian Shiraz (Syrah) red wines (7,8) and we set out to find the compound(s) responsible for this distinctive aroma. This task led us to identify an obscure sesquiterpene, rotundone (9-11), by gas chromatography-mass spectrometry-olfactometry (GC-MS-O) as a hitherto unrecognised important aroma impact compound in a variety of food products (12). Figure 1 shows the mass spectrum of rotundone C₁₅H₂₂O.

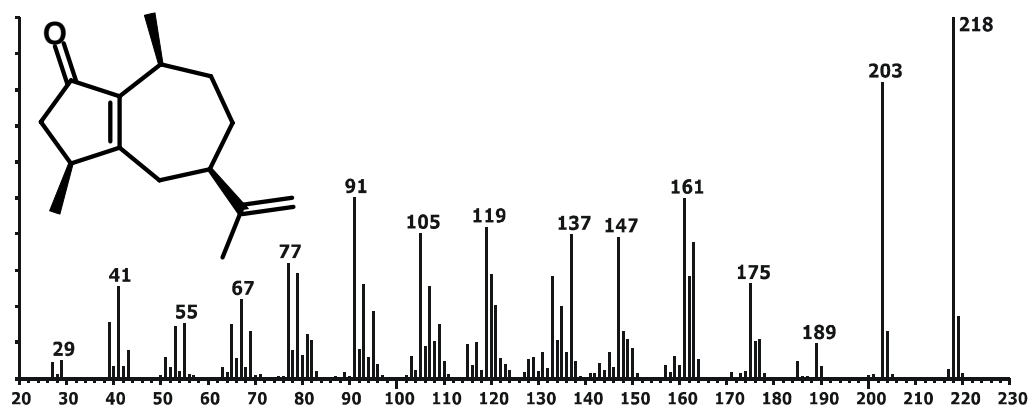


Figure 1. Mass spectrum of (-)-rotundone.

Results

After synthesis of rotundone for reference purposes as reported by us in a recent publication (12) we developed a dedicated analytical method using stable isotope dilution analysis with d_5 -rotundone to provide quantitative data with the required precision (13). By GC-MS we confirmed that not only is rotundone responsible for the peppery characters in Shiraz grapes and red wine (and to a lesser extent in wine from other varieties), but that it can also be found in much higher amounts in other common herbs and spices. In particular, rotundone was identified, for the first time, in extracts of peppercorns (*Piper nigrum*) where it was found in the highest concentration, and is the only odorant thus far detected in that spice with an obvious pepper-like aroma. Table 1 summarises the occurrence of rotundone in various plants and plant products. In grapes, rotundone concentrations ranged from 10 to 620 ng/kg; environmental effects which yet have to be fully characterized led to significant variation between individual vineyard sites and growing seasons (Table 2).

Table 1. Concentration of rotundone in various plants and plant products.

Sample	Rotundone concentration ($\mu\text{g}/\text{kg}$, mean of duplicate extraction and analysis)
White pepper (<i>Piper nigrum</i>)	2025
Black pepper (<i>Piper nigrum</i>)	1200
Wine (<i>Vitis vinifera</i>)	0.15
Grapes (<i>Vitis vinifera</i>)	0.62
Marjoram (<i>Origanum majorana</i>)	208
Geranium (<i>Pelargonium alchemilloides</i>)	25
Nut grass (<i>Cyperus rotundus</i>)	920
Rosemary (<i>Rosmarinus officinalis</i>)	86
Saltbush (<i>Atriplex cinerea</i>)	37
Basil (<i>Ocimum basilicum</i>)	4
Thyme (<i>Thymus vulgaris</i>)	5
Oregano (<i>Origanum vulgare</i>)	1

Table 2. Concentration of rotundone (ng/kg) in Shiraz grapes from six Australian vineyards over two vintages (2002 and 2003). 2002 was widely regarded as being a more 'peppery' year than 2003 for Shiraz grapes in many wine regions in Australia.

Sample	Rotundone concentration (ng/kg)	
	2002	2003
Vineyard A	10	82
Vineyard B	25	31
Vineyard C	76	38
Vineyard D	133	61
Vineyard E	486	117
Vineyard F	619	76

The aroma detection threshold for rotundone was determined according to ASTM method E 679-79 as best estimate threshold of 16 ng/L in red wine and 8 ng/L in water. While most of the 47 sensory panellists were very or moderately sensitive to rotundone, approximately 20% could not detect this compound at the highest concentration tested (4000 ng/L). The variation in individual sensitivity to rotundone suggests that the way wine containing this compound is assessed by consumers or wine judges could vary substantially from one person to another. The observation that a sizable group of people are not very sensitive or completely anosmic might explain why the sensory relevance of rotundone had been overlooked for so many years.

References

1. Bayonove C., Cordonnier R., Dubois, P. (1975) *Comptes Rendus Académie des Sciences Paris Série D* 281: 75–78.
2. Harris R.L.N., Lacey M.J., Brown W.V., Allen M.S. (1987) *Vitis* 26: 201–207.
3. Pollnitz A.P., Pardon K.H., Liacopoulos D., Skouroumounis G.K., Sefton M.A. (1996) *Aust. J. Grape Wine Res.* 2: 184-190.
4. Guth H. (1997) *J. Agric. Food Chem.* 45: 3022–3026.
5. Tominaga T., Furrer A., Henry R., Dubourdiu D. (1998). *Flav. Frag. J.* 13:159–162.
6. Tominaga T., Darriet P., Dubourdiu D. (1987) *Vitis* 35: 207–210.
7. Parker M., Pollnitz A.P., Cozzolino D., Francis I.L., Herderich M.J. (2007) *J. Agric. Food Chem.* 55: 5948-5955.
8. Iland, P., Gago P. (2002) *Australian Wine: Styles and Tastes*. Patrick Iland Wine Promotions, Adelaide, Australia.
9. Kapadia V.H., Naik V.G., Wadia M.S., Dev S. (1967) *Tetrahedron Lett.* 47: 4661-4667.
10. Ishihara M., Tsuneya T., Uneyama K. (1991) *Phytochem.* 30: 3343–3347.
11. Ishihara M., Tsuneya T., Uneyama K. (1993) *J. Essent. Oil Res.* 5: 283-289.
12. Wood C., Siebert T.E., Parker M., Capone D.L., Elsey G.M., Pollnitz A.P., Eggers M., Meier M., Vössing T., Widder S., Krammer G., Sefton M.A., Herderich M. (2008) *J. Agric. Food Chem.* 56: 3745-3748.
13. Siebert T.E., Wood C., Elsey G.M., Pollnitz A.P. (2008) *J. Agric. Food Chem.* 56: 3745-3748.

THE INFLUENCE OF CHEMICAL STRUCTURE ON ODOUR QUALITIES AND ODOUR POTENCIES IN CHLORO-ORGANIC SUBSTANCES

A. Strube, A. BUETTNER

Fraunhofer-Institute for Process Engineering and Packaging (IVV), Giggenhauser Str. 35, D-85354 Freising, Germany

Abstract

The musty 'cork taint' off-flavour is widespread in stored food products and packaging materials. Several candidate compounds attributed to this off-flavour, being described with earthy musty odours, have been identified, including geosmin, 2-methylisoborneol, 3-isobutyl-2-methoxypyrazine, 3-isopropyl-2-methoxypyrazine and different chloroanisoles. However, because of the low odour threshold concentrations of many of these analytes, their identification is often difficult by conventional analytical methods. In the present study, the odour qualities and odour thresholds in air of nineteen chloroanisoles were evaluated using gas chromatography-olfactometry. Analytical characterization of the substances was based on retention indices according to Kovats, as well as mass spectrometry. Odour threshold concentrations and characteristic odour qualities were found to be dependent on the chemical structures of these compounds.

Introduction

The musty 'cork taint' off-flavour is widespread in stored food products and packaging materials. Chloroanisoles are primary candidates attributed to this off-flavour and have been reportedly identified in wine (1), drinking water (2), corn and wheat (3), sake and fish (4), and cork stoppers (5). However, due to the low odour thresholds of some of these compounds they are often difficult to analyse by standard means, e.g. large volume extraction gas chromatography mass spectrometry (GC-MS) (1) or multiple headspace solid phase micro-extraction (SPME) GC-MS (6).

This study presents an evaluation of the odour qualities and odour thresholds in air of chloroanisoles using GC-olfactometry (GC-O). The GC-O method is particularly useful for odour assessments because it enables possible impurity interferences from the analytical standards used to be excluded from the analysis. The influence of molecular structure on odour character is discussed in relation to odour activity.

Experimental

Chemicals. The following chemicals, listed with their respective purities, were used: 3-Chloroanisole 99 %, 4-chloroanisole 95%, 2-chloroanisole 98 %, 2,6-dichloroanisole 99 %, 3,5-dichloroanisole 99 %, 3,4-dichloroanisole 95 %, 2,5-dichloroanisole 95 %, 2,4-dichloroanisole 95 %, 2,3,6-trichloroanisole 98 %, 2,3-dichloroanisole 95 %, 2,3,5,6-tetrachloroanisole 95 %, 2,3,4,6-tetrachloroanisole 99 %, 2,4,5-trichloroanisole 99 %, 3,4,5-trichloroanisole 99.5 %, 2,3,5-trichloroanisole 95 %, 2,3,4,5-tetrachloroanisole 95 %, and pentachloroanisole 99 % (Promochem,

Wesel, Germany); 2,3,4-trichloroanisole 99.9 % (Riedel-de-Haen, Seelze, Germany); 2,4,6-trichloroanisole 99 % (Sigma Aldrich, Steinheim, Germany). All compounds were freshly distilled prior to analysis. Chemical and sensory purities were checked by high resolution (HR) GC-O as well as HRGC-MS.

HRGC-O. Known amounts of (*E*)-2-decenal and target chloro-organic substances in dichloromethane were analysed by HRGC-O. HRGC was performed with a helium GC (Carlo Erba, Dreieich, Germany) using the following capillaries: DB-FFAP (30 m × 0.32 mm fused silica capillary, free fatty acid phase FFAP, 0.25 µm; Chrompack, Mühlheim, Germany) and DB-5 (30 m × 0.32 mm fused silica capillary DB-5, 1.5 µm; J & W Scientific, Fisons Instruments). Application of the samples into the GC system was performed at 40 °C using the cool-on-column technique. After 2 min, the temperature of the oven was raised at 10 °C/min to 240 °C and held for 5 min. The flow rate of the helium carrier gas was 2.5 ml/min. At the end of the capillary the effluent was split into a sniffing port and a flame ionisation detector (FID), or alternatively a MS, using two deactivated but uncoated fused silica capillaries (100 cm × 0.32 mm). The FID and the sniffing port were held at 300 °C and 250 °C, respectively.

Sensory evaluation. Panellists. Five trained volunteers (four female, one male) from the Fraunhofer IVV Institute (Freising, Germany), exhibiting no known illness at the time of examination. Prior to participation in the experiments, panellists were tested for their olfactory functions during weekly training sessions with selected supra-threshold aroma solutions. Subjective aroma perception was normal throughout the training and at the time of the experiments, as tested with a defined set of aroma substances and an internally developed flavour language.

Flavour language. The flavour language was developed by five trained panellists of the sensory panel. The panellists had to describe the odour character of each substance by GC-O three times at different concentrations. The results were discussed in the group after each session. The attributes with nominations of at least 70 % of all summarized mentions of the three sessions were selected for the flavour language.

Odour threshold concentration (OTC). The OTCs in air were determined as previously described by Ulrich *et al.* (7). The odour thresholds were evaluated by five trained panellists of the sensory panel. Anosmias, if any, were recorded and were not taken into consideration for threshold determinations.

Results

The chemosensory data in Table 1 mirrors the influence of molecular structure on odour qualities and OTCs of chloroanisoles, with a broad range of OTCs in air ranging from 5 pg/l to 470 ng/l. Compounds with by far the lowest OTCs were 2,4,6-trichloroanisole and 2,3,4,6-tetrachloroanisole with OTCs of 5 and 10 pg/l air, respectively, followed by 2,3,6-trichloroanisoles (30 pg/l air) and 2,6-dichloroanisole with 600 pg/l air. OTCs in the lower ng/l air range were 4-chloroanisole (2.9 ng/l air), 2,3,5- and 2,4,5-trichloroanisole (1.7 and 5.1 ng/l air, respectively), 2,3,5,6-tetrachloroanisole (3.91 ng/l air), 2,3,4,5-tetrachloroanisole (5.7 ng/l air) and pentachloroanisole with 2.2 ng/l air.

Generally, 2,6-substitution correlated with the highest odour intensities while 3- and 3,5-substitution had a low activity impact. The other substitution patterns such as 2,4- and 2,5-substitution exhibited average to low odour intensities. The medicinal odour character prevailed in mono- and di-substituted compounds while the musty

cork taint increased with higher substitution. During sniffing analysis it became evident that an adaptation effect was pronounced for several substances such as 2,4,6-TCA and 2,6-DCA (8).

Table 1. *Odour qualities and odour threshold concentrations (OTCs) of the chloroanisoles*

Odorant	Odour quality ^a	OTC in air (ng/l) ^{bc}	Retention index ^d on		
			DB 5	DB- FFAP	DB- 1701
2-Chloroanisole	medicinal	14.33	1133	1673	1238
3-Chloroanisole	medicinal, sweet	34.45	1109	1590	1193
4-Chloroanisole	medicinal	2.90	1117	1617	1208
2,3-Dichloroanisole	medicinal	16.80	1345	1976	1465
2,4-Dichloroanisole	medicinal	18.53	1305	1894	1415
2,5-Dichloroanisole	corky	44.40	1296	1883	1404
2,6-Dichloroanisole	corky, medicinal	0.60	1319	1697	1302
3,4-Dichloroanisole	medicinal	17.63	1313	1881	1418
3,5-Dichloroanisole	corky	467.38	1268	1765	1354
2,3,4-Trichloroanisole	medicinal	30.38	1543	2240	1678
2,3,5-Trichloroanisole	medicinal	1.77	1481	2109	1595
2,3,6-Trichloroanisole	corky, leather-like	0.03	1406	1921	1485
2,4,5-Trichloroanisole	corky	5.10	1482	2095	1592
2,4,6-Trichloroanisole	corky, musty	0.005	1359	1800	1423
3,4,5-Trichloroanisole	corky	32.89	1493	2094	1602
2,3,4,5-Tetrachloroanisole	corky	5.74	1700	2411	1830
2,3,4,6-Tetrachloroanisole	corky	0.01	1567	2070	1645
2,3,5,6-Tetrachloroanisole	corky	3.91	1564	2067	1642
Pentachloroanisole	corky	2.19	1775	2319	1854

^a Odour quality as perceived at the sniffing port.

^b Odour thresholds in air, determined as described in (7)

^c Mean value of four measuring points.

^d Retention index according to Kovats (9)

Discussion

Previous aroma quality assessments of chloroanisoles have used the paired comparison technique. In this technique, solutions spiked with different chloroanisoles were each compared with a boiled odour-free water sample and the panellists were asked to identify the sample containing the chloroanisole, and to describe the odour quality. Based on this technique the compounds 2,3,4,5-tetrachloroanisole, 2,3,6-trichloroanisole and 2,4,6-trichloroanisole were all described as musty, 2,3,4,5-tetrachloroanisole and 2,3,5,6-tetrachloroanisole as musty and solvent-like, 2,4,5-trichloroanisole as medicinal, and 2,4,5-trichloroanisole as having a sweet odour character. The monochloroanisoles were described as medicinal, sweet and solvent-like (9).

In these assessments, however, determinations of chloroanisole odour qualities and intensities were performed in aqueous solutions. Therefore, since odour thresholds in water are influenced by factors such as volatility and polarity, the

absolute odour intensities as functions of the chemical structure could not be evaluated. Furthermore, data might have been biased due to impurities present in the evaluated samples. This assumption agrees with our investigation in which GC-O analysis of several chloroanisole references indicated contamination of these standards with traces of other highly potent chloroanisole-odorants such as 2,4,6-trichloroanisole. The GC-O method is therefore particularly useful since it allows isolation of the target analyte for direct olfactory assessment without the risk of unknown interference effects from impurity compounds.

References

1. Sanvicens N., Moore J.E., Guelbault, G.G., Marco M.P. (2006) *J. Agric. Food Chem.* 54: 9176-9183.
2. Piriou P., Malleret L., Bruchet A. (2001) *Wat Sci Technol.* 1: 11-18.
3. Seitz L.M., Ram M.S. (2000) *J. Agric. Food Chem.* 48: 4279-4289.
4. Miki A., Isogai A., Utsunomiya H. (2005) *J. Biosci Bioeng.* 100: 178-183.
5. Ezquerro O., Garrido-Lopez A., Tena M.T. (2006) *J. Chrom A.* 1102: 18-24.
6. Ezquerro O., Tena M.T. (2005) *J. Chrom A.* 1068: 201-208.
7. Ullrich F., Grosch W. (1987) *Z. Lebensm. Unters. Forsch.* 184: 277-282.
8. Griffiths N.M. (1974) *Chem Sens Flav.* 1: 187-195.
9. van den Dool H., Kratz P. (1963) *J. Chrom.* 11: 463-471.

AROMA ANALYSIS OF SEA BUCKTHORN BERRIES BY SENSORY EVALUATION, HEADSPACE SPME AND GC-OLFACTOMETRY

S. LUNDÉN, K. Tiitinen, and H. Kallio

Department of Biochemistry and Food Chemistry, University of Turku, 20014 Turku, Finland

Abstract

The effect of different volatile compounds on the orthonasal odour of sea buckthorn (*Hippophaë rhamnoides* L.) berries was studied with berries of four different origins. The differences between samples in odour quality were significant in most descriptors. The wild strain of ssp. *sinensis* origin differed the most from the other samples in odour quality: The intensity of fermented odour was stronger, it was the least pungent and type of sweetness was mellow. A total of 74 volatile compounds were identified from the headspace of sea buckthorn berries. The most numerous compounds found were esters such as ethyl hexanoate, 3-methylbutyl 3-methylbutanoate and ethyl 2-methylbutanoate. The number of volatile compounds was higher in the wild strain of ssp. *sinensis* compared to other samples. Gas chromatography-olfactometry analysis showed also differences between the samples in the descriptions of the odour. The odour of the compounds separated by GC was described with terms referring to fruits, such as sweet, strawberry, pineapple and apple, but also such as solvent and mushroom like.

Introduction

Sea buckthorn (*Hippophaë rhamnoides* L.) berries have a unique, strong flavour and high acidity. The aroma is mild but characteristic. The flavour of sea buckthorn is typically described as sour, bitter and astringent [1, 2]. The high nutritional value and health effects of the berries have made sea buckthorn cultivation and research more interesting. However, there is only a limited number of studies on sensory properties of the berries and mostly concerning flavour and taste properties. However, from the consumer point of view the sensory quality is equally important as the nutritional value. Berries of different origin have reported to vary in both nutritional and sensory properties [2, 3]. The aim of this study was to examine if the origin of the berry effect on the orthonasal odour of sea buckthorn and what are the volatile aroma compounds causing the differences in the odour between the samples.

Experimental

Berries of two varieties of ssp. *mongolica* origin, 'Avgustinka' and 'Trofimovskaja', one of ssp. *caucasica* x ssp. *rhamnoides*, 'Raisa', and a wild type of ssp. *sinensis* were investigated. Frozen berries were analysed after thawing and crushing. The sensory properties of sea buckthorn aroma were investigated with trained sensory panel (n=12) by generic descriptive analysis. The sensory descriptors were created during the training sessions and the samples were evaluated based on intensities of the total, green, fermented and pungent odour and the type of sweet odour from

fresh to mellow. The volatile compounds were isolated by headspace solid phase micro extraction and analysed with gas chromatograph coupled to a mass selective detector. RH-5MS+ column (LabAlliance, USA) was used in the analysis. Volatile compounds were identified based on mass spectrum library (Wiley 229), identical mass spectrum and retention time of reference compounds and comparing to earlier results by Tiitinen et al. [2]. Relative concentrations were calculated dividing the peak area with internal standard (methyl butanoate) peak area and multiplying the ratio with internal standard concentration. Gas chromatography-olfactometry was used to investigate which of the isolated compounds were sensed orthonasally and how were they described. GC program for olfactory analysis was similar to volatile compounds analysis but FID was used as the detector (column DB-5MS, J&W Scientific, USA).

Results

There were significant differences between samples in all of the sensory descriptors evaluated except green odour (Figure 1). The wild type of ssp. *sinensis* differed the most from the other samples: The intensity of fermented odour was stronger, it was least pungent and type of sweetness was mellower in this sample compared to others. There were not any significant differences between the two varieties of ssp. *mongolica* origin.

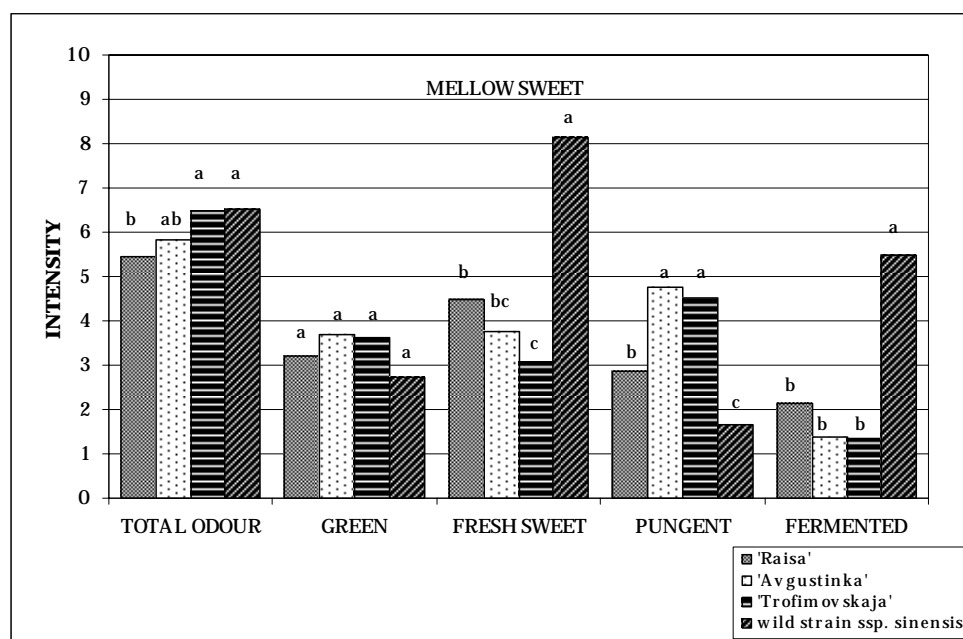


Figure 1. Mean intensities of aroma attributes in sea buckthorn samples ($n=36$). Significant differences between samples are marked a-c ($p<0.05$).

A total of 74 volatile compounds were identified and a total of 91 compounds were detected in the headspace of the sea buckthorn berries. The most numerous compounds found were esters such as ethyl hexanoate, 3-methylbutyl 3-methylbutanoate and ethyl 2-methylbutanoate (Table 1). The number of volatile compounds was higher in the wild strain of ssp. *sinensis* origin than in other samples and numerous compounds were detected only from the wild strain of ssp. *sinensis* origin. These were ketones, such as 2-butanone, and branched esters, e.g. 2-methylpropyl 3-methylbutanoate.

Table 1. Mean ($n=3$) relative concentrations of most abundant volatile compounds in sea buckthorn samples from GC-MS analysis and descriptions from the GC-O analysis. TRO, 'Trofimovskaja', AUG, 'Avgustinka', RAI, 'Raisa', WSS, wild strain of *ssp. sinensis* origin.

Peak no.	Compound	AUG	WSS	RAI	TRO	Description
2	Ethanol	60.8	19.9	36.6	69.9	solvent, pungent
12	Ethyl 2-methylbutanoate	108.7	28.9	133.6	326.3	sweet, strawberry
13	Ethyl 3-methylbutanoate	610.4	45.9	261.0	443.4	sweet, fruity
26	Propyl 2-methylbutanoate	nd	8.7	3.1	5.0	sweet, berrylike
35	2-Methylpropyl 2-methylbutanoate	nd	309.4	nd	nd	mushroom, solvent
38	2-Methylpropyl 3-methylbutanoate	nd	685.8	nd	nd	mushroom, fertiliser
39	Ethyl hexanoate	723.7	50.0	977.0	1692.5	fruity, berrylike
43	3-Methylbutyl 2-methylpropanoate	18.4	321.2	nd	19.6	
58	2-Methylbutyl 2-methylbutanoate	nd	603.9	nd	nd	
59	3-Methylbutyl 3-methylbutanoate	1370.2	1516.8	2.7	213.9	fermented, spoiled, compost
68	Ethyl benzoate	70.7	5.3	112.8	277.7	sweet, plastic, artificial
73	Ethyl octanoate	93.3	8.5	249.1	382.0	coconut, synthetic
79	3-Methylbutyl hexanoate	267.7	16.1	1.0	121.1	
89	3-Methylbutyl benzoate	95.8	5.1	2.2	140.9	pungent, sour

nd: not detected

Gas chromatography-olfactometry analysis showed also differences between the samples in the descriptors of the odour and the percentage of perceptions (Figure 2). The odour of the compounds separated by GC was described with terms referring to fruits, such as sweet, strawberry, pineapple and apple like, but also such as solvent and mushroom like (Table 1).

Partial least-squares regression (PLS2) analysis was used to investigate relations between sensory attributes and volatile compounds (Figure 3). Higher amount of ethanol (2) correlates with higher intensity of pungent odour and is also related to two samples of *ssp. mongolica* origin. Propyl 2-methylbutanoate (26) correlates with fermented odour and is related to the sample of wild strain *ssp. sinensis*. Results of GC-O analysis support these findings. Ethanol is described as solvent and pungent like and the highest percentage of perceptions is for the sample of *ssp. mongolica* origin. Compounds described as mushroom and fertiliser like or fermented are most abundant and are also only or most often perceived in wild strain of *ssp. sinensis* origin.

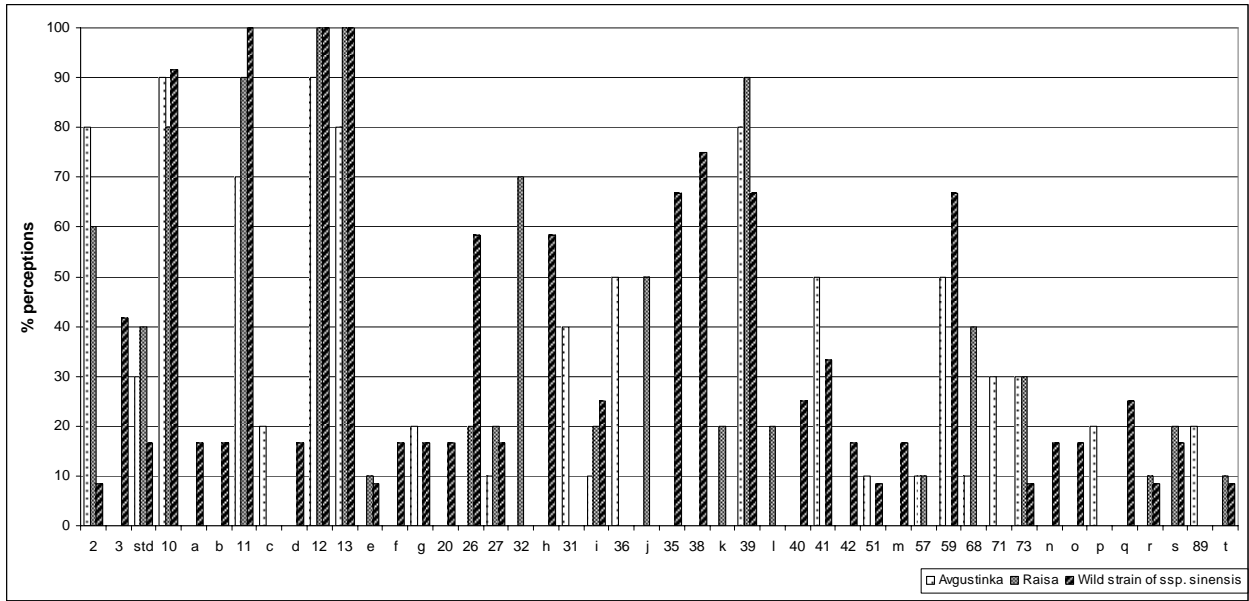


Figure 2. Aromagram of the GC-O analysis of sea buckthorn samples. Numbering refers to Table 1. Unidentified perceptions are marked a-l.

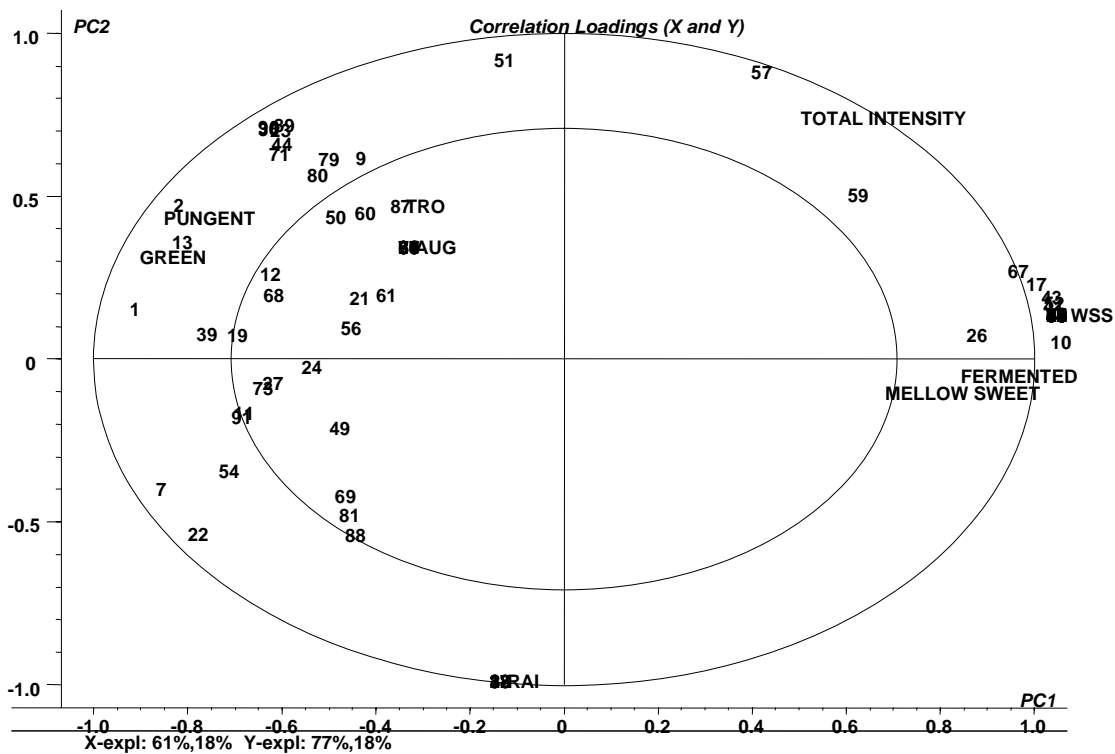


Figure 3. PLS2 plot of the relation between sensory properties and volatile compounds. Numbers refer to Table 1.

References

1. Tang X., Kälviäinen N., Tuorila H. (2001) *Lebensm – Wiss Technol* 34: 102-110.
2. Kallio H., Yang B., Peippo P. (2002) *J. Agric. Food Chem.* 50: 6136-6142.
3. Tiitinen K., Hakala M., Kallio H. (2005) *J. Agric. Food Chem.* 53: 1692-1699.

THE ANALYSIS OF VOLATILES AND NON-VOLATILES IN YERBA MATÉ TEA (*ILEX PARAGUARIENSIS*)

N.C. DA COSTA¹, Y. Yang¹, J. Kowalczyk¹, and M.L. Poulsen²

¹ *International Flavors & Fragrances Inc., 1515 Highway 36, Union Beach, New Jersey 07735, USA*

² *International Flavors & Fragrances Inc., Placa Luiz Domingos Sillos, 01, Distrito Industrial do Una, Taubaté, SP12071-001 Brazil*

Abstract

Yerba maté is technically a herbal tea consumed in several countries in South America and reputed to have health benefits. The aged maté is the most prized for consumption. Aged maté was extracted via two techniques and the volatiles compared qualitatively and by relative quantitation using GC and GC-MS. In addition, quantitation of non-volatiles such as amino acids, organic acids and sugars by liquid chromatography are presented.

Introduction

Yerba maté (18 months aged) from Brazil was supplied for in depth analysis. The maté was extracted by liquid/liquid extraction (1) and simultaneous steam distillation extraction respectively. GC-MS analysis of both extracts detected over 320 volatile and semi-volatile components of which many have been reported previously (2-4). However select compounds are presented which provide a link between volatiles and non-volatiles, including breakdown products from chlorogenic acid. Maté is known to contain several classes of non-volatiles such as purines, chlorogenic acid and its analogues, flavanoids, saponins, amongst others (5). Non-volatile work was conducted on free amino acids, organic acids and sugars content.

Experimental

Sample preparation. Liquid/liquid extraction was performed by steeping 150g of mate in 1L of hot water for 8-10 minutes at 70-80°C. The solution was rapidly cooled in an ice bath, filtered into a separatory funnel and twice extracted with 150mL of dichloromethane. The combined extracts were dried, filtered and reduced to a volume of 1mL using a solvent evaporation system. Steam distillation-extraction was performed by using a Likens-Nickerson apparatus. Approximately 150g of yerba maté was added to 2.5L of distilled water and steam distilled into 150mL of dichloromethane over 3hours. The procedure was repeated and the combined extracts were treated as previously described.

GC & GC-MS. The extracts were analysed using an HP6890 gas chromatograph with OV-1 capillary column (50m x 0.32mm i.d., 0.5 µm film thickness, Restek) in split ratio 40:1 and splitless modes. Temperature program from 40°C to 270°C at a rate of 2°C/min with a holding time at 270°C of 10 minutes. For the polar phase, HP6890 gas chromatograph with split/splitless injection and a CPwax capillary column (50m x 0.32mm i.d., 0.3µm film thickness, Restek) using the same injection and detection

techniques. Temperature program was from 60°C held for 10 minutes, ramped at 2°C/min to a final temperature of 220°C and held for 20 minutes. For GC-MS the chromatographic conditions were the same as described for GC analysis. Autospec high resolution, double-focusing, magnetic sector instrument. Identification was using standard retention data and in-house and commercial MS libraries.

Non-volatiles. Yerba maté sample (3.0g) was extracted with boiling water for 10 mins. The samples were filtered prior to LC analysis. Free Amino acids, LC-MS: Finnigan Surveyor system/ LXQ-34000, Column: TSK-Gel Amide 80 (250 x 4.6 mm) SSN K0302-83H, Amino acids AAS18 standards (Sigma). Free Organic acids, HPLC-UV Agilent Technologies 1100LC Column: BIO-RAD 300x7 Amines XPX-87H, UV 210 nm, standards (Sigma). Free Sugars, HPLC-UV Agilent Technologies 1100LC Column: Prevail carbohydrate ES (250 x 4.6 mm), 5µm, ELSD detector, standards (Sigma).

Results

Comparison of liquid/liquid (Figure 1.) and steam distillation (Figure 2.) extracts for a “tea” show that while the former gives more representative concentrations for volatile components it is harder to identify trace components due to the dominating caffeine peak. With the steam distillation extract there is much more detail to be gained as water soluble caffeine is greatly reduced. However many other polar components are also reduced or missing. Thus these two extraction techniques are complimentary for the analysis of a “tea”. Note that steam distillation artefacts are in theory minimized by the fact that the tea is already thermally treated in preparation.

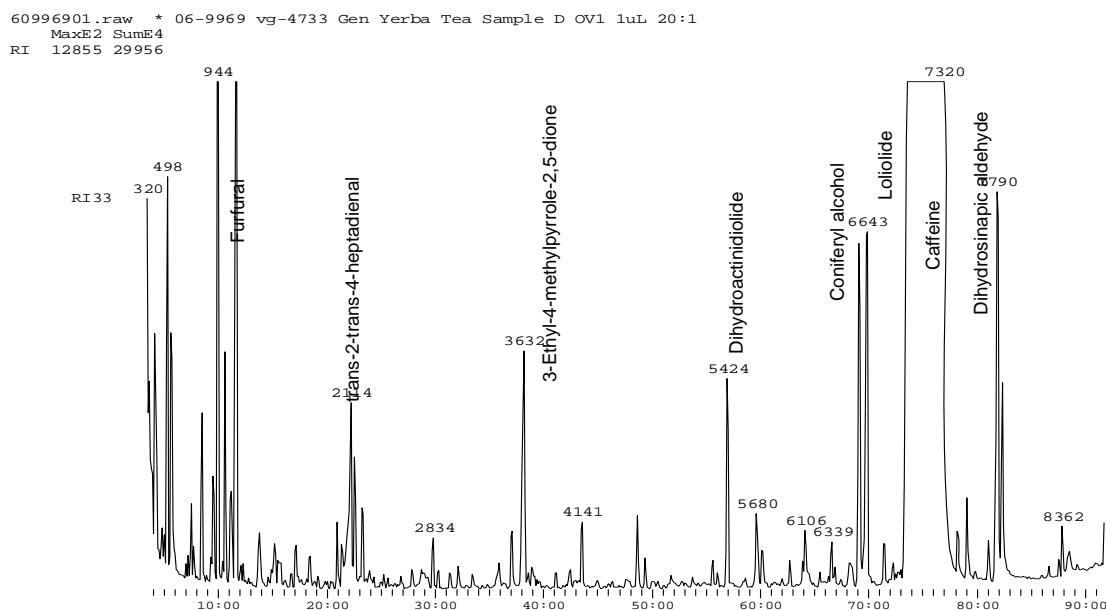


Figure 1. Liquid/liquid extract of 18 month old maté.

Expression of Multidisciplinary Flavour Science

61340901.raw * 06-13409 vg-5062 Gen Mate D Steam Distilled OVI 1uL 40:1
MaxE1 SumE3
RI 35598 98313

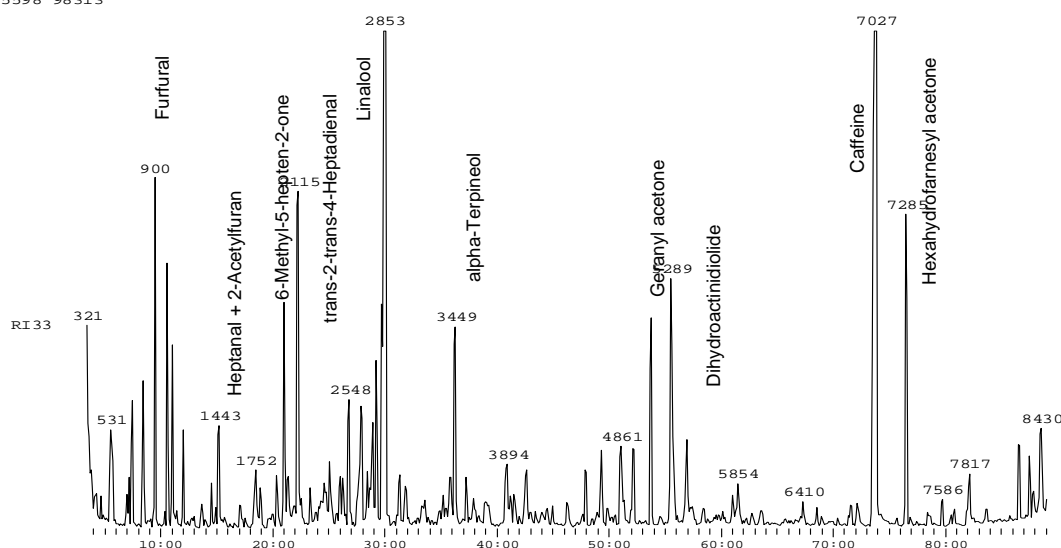


Figure 2. Steam distillate extract of 18 month old maté.

Table 1. Volatile components in yerba mate.

Compound	Retention Index (Kovats)	Relative peak area	
		Liquid/liquid	Steam distillate
Furfural	800	0.38	26.15
Heptanal	878	0.00	8.48
2-Acetylfuran	880	0.19	7.89
6-Methyl-5-heptenone	963	0.17	31.71
trans-2-trans-4-Heptadienal	981	0.29	48.20
Linalool	1085	0.09	53.76
alpha-Terpineol	1177	0.00	14.99
3-Ethyl-4-methyl-1H-pyrrole-2,5-dione*	1192	1.60	3.27
4-Methyl-3-vinyl-1H-pyrrole-2,5-dione*	1210	0.48	0.00
Geranyl acetone	1430	0.66	18.25
Dihydroactinidiolide	1495	1.28	3.66
Coniferyl aldehyde*	1672	0.41	0.00
Coniferyl alcohol*	1688	5.98	0.00
Loliolide*	1698	3.30	0.00
Theobromine	1777	63.66	0.26
Caffeine	1789	883.72	8.58
Hexahydrofarnesyl acetone	1798	0.00	3.78
Sinapic aldehyde*	1915	1.08	0.00
Dihydrosinapic aldehyde*	1933	7.65	0.00
Hexadecanoic acid*	1943	4.12	0.12

Select volatiles are presented in (Table 1). Note that molecules new to the analysis of maté are denoted with *. Clearly seen are break down products from chlorogenic acid such as the coniferyl alcohol, coniferyl aldehyde and sinapic aldehyde and dihydrosinapic aldehyde. The dominating caffeine peak in the liquid/liquid extract suppresses all other components. In contrast the steam distillation extract has reduced these water soluble and polar components revealing more trace volatiles.

Table 2. Free Amino, Organic acids & Sugars in 18 month aged Yerba maté.

Amino acid	Concentration %	Organic acid	Concentration %
Glutamic acid	0.17	Citric acid	1.69
Phenylalanine	0.01	Malic acid	0.30
Methionine	n.d.	Oxalic acid	0.18
Tyrosine	0.00	Quinic acid	1.62
Valine	0.00		
Proline	0.13	<u>Sugar</u>	<u>Concentration %</u>
Threonine	0.02	Fructose	0.60
Serine	0.02	Glucose	0.98
Leucine	0.00	Sucrose	4.96
Iso-Leucine	0.01		
Tryptophan	n.d.		
Glutamine	n.d.		
Asparagine	n.d.		

From the non-volatile analytical work (Table 2) it was established that with aging of the maté there is an increase in sugars such as sucrose. Free glutamic acid and proline were the most significant amino acids and citric and quinic the most significant organic acids detected. The latter from chlorogenic acid break down.

References

1. Jacques R.A., dos Santos Freitas L., Peres V.F., Dariva C., de Oliveira J.V., Caramão E.B. (2006) *J. Sep. Sci.* 29: 2780-2784.
2. Kawakami M., Kobayashi A. (1991) *J. Agric. Food Chem.* 39: 1275-1279.
3. Lozano P.R., Cadwallader K.R., de Mejia E.G. (2007) In *Chemistry and Flavour*, Tunick M.H., de Mejia E.G. (eds.), ACS: Washington D.C, p143-50.
4. Machado C.C.B., Bastos D.H.M., Janzantti N.S., Fascanali R., Marques M.O.M., Franco M.R.B. (2007) *Quim. Nova.* 30: 513-518.
5. Heck C.I., De Mejia E.G. (2007) *J. Food Sci.* 72: R138-151.

CIGARETTE SMOKE: GC-OLFACTOMETRY ANALYSES USING TWO COMPUTER PROGRAMS

V.M.E. COTTE¹, S.K. Prasad¹, P.H.W. Wan¹, R.S.T. Linforth², and A.J. Taylor²

¹ *British American Tobacco, R&D, Regents Park Road, Southampton, SO15 8TL, UK*

² *Division of Food Sciences, University of Nottingham, Loughborough, LE12 5RD, UK*

Abstract

The aroma quality of cigarette smoke is an important characteristic for smokers. It is therefore important to understand and identify the key aroma compounds in tobacco smoke. GC-Olfactometry and Nasal Impact Frequency were used to analyse the smoke from ten different tobacco types and blends. The smoke from one puff of each was trapped onto a cooled mini-pad with subsequent thermal desorption. This study had the objectives of a) training panellists on odour recognition, b) automating the recording of odours detected and aromagram construction, c) developing a sample preparation (one 'fresh' puff analysed) and d) providing a list of key aromas identified. Six common aromas were found in the smoke of ten cigarette samples and were identified as diacetyl, 2,5-dimethylfuran, 2- and 4-picoline, 2,5-dimethyl pyrazine and trimethyl benzene.

Introduction

The aroma profile of tobacco smoke is an important quality factor for consumers and the researcher / product developer, to understand and improve tobacco products with optimised flavour release. To date, only a few studies on the analysis of tobacco smoke using Gas Chromatography-Olfactometry (GC-O) were available for review (1-4). However, none of these articles described in detail the nature and character of tobacco smoke aroma. Critical reviews on GC-O methods provide a strong support towards the frequency method being faster, simpler and more repeatable than dilution or intensity methods (5,6). However, no automatic data recording and processing methods for Nasal Impact Frequency (NIF) were available in the public domain at the time of this study. Some software is available (7,8), but these do not offer an automated process of combining individual aromagrams.

Since tobacco smoke is a very complex and dynamic system, where aerosols are also formed, cold trapping for single puff chemical analysis has been used (9). Therefore, it was decided to collect only one puff trapped onto a cooled mini-pad, with Direct Thermal Desorption (DTD) analysis of smoke aroma compounds to minimise potential ageing artefacts. Therefore, the main aims of the study were:

1. To develop software to increase the throughput of odour data processing,
2. To develop a sample preparation to analyse 'fresh' smoke samples using DTD,
3. To identify key aromas in tobacco smoke from varying tobacco types.

Experimental

Materials. The ten cigarette samples included six single tobacco types: Burley (BU), Flue Cured (FC), Maryland (MA), Oriental (OR), Stems (ST), Expanded (ET) (corresponding to the building blocks of a commercial US Blend (USB) cigarette), three blends (one blend without casings and without top flavour (B1); one blend with casings but without top flavours (B2); one blend with casings and with top flavours (B3)) and one commercial sample (CO) used as a tobacco blend reference (USB Light).

Improved methods for processing GC-Olfactometry data. Odour recognition training. Odour recognition training was conducted using 18 different odour categories (not shown) and using a pool of 20 panellists.

Methods for recording and processing aroma detection. The start time, end time, duration and a description of eluting odours were recorded during GC-O assessments using a first computer program (Figure 1). The second computer program enabled rapid construction of aromagrams from the raw data produced by the first program. As shown in (Figure 2), the second program displays nine panels gathered in one window on the computer screen. The raw odour data can be selected (panel 2) and plotted into aromagrams in a few seconds (panels 4 and 8). The NIF values and a list of descriptors are also generated automatically (panels 5 and 6 respectively). Both computer programs were built in-house using C++.

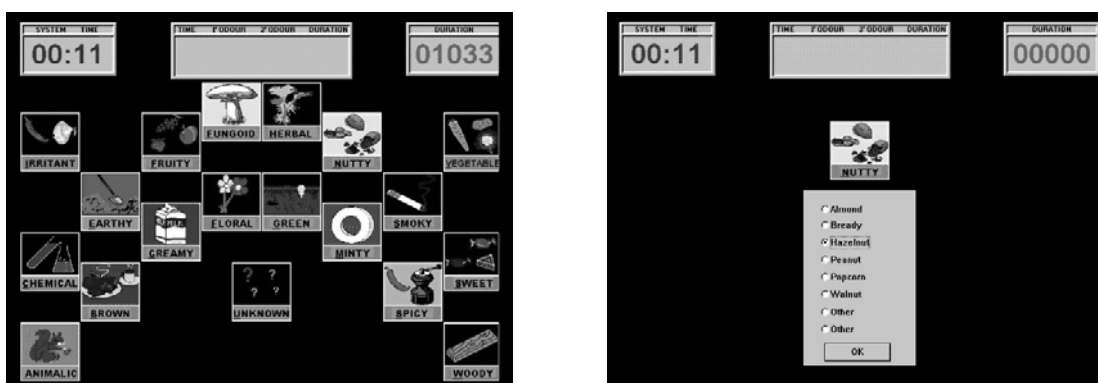


Figure 1. Sequence of odour recording software. Screens 1 and 2 (not shown) have icons clicked to determine odour on and off respectively. Screens 3 and 4 (shown above) show icons to identify odour description (point and click using the computer mouse).

Methods for Direct Thermal Desorption – Gas Chromatography (DTD-GC). Sample preparation. Glass tubes from Gerstel, Germany held a mini-pad of 4 mm diameter (Cambridge Filter Pad). The tubes were fitted between a single port smoking machine (Model RM1, Borgwaldt, Hamburg, Germany) and a cigarette pad holder. The mini-pad was cooled at -60°C . The third puff was trapped onto the cryo-cooled mini-pad. The third puff is considered more representative than the lighting or post-lighting puff.

DTD -GC -Olfactometry (DTD-GC-O) and DTD-GC-Mass Spectrometry (MS). The smoke trapped onto the mini-pad was desorbed in a Thermal Desorption System TDS2 (Gerstel); from -50°C to 37°C and cryo-focused into a Cold Injection System CIS4 (Gerstel); GC (HP6890); Column: non polar; Detectors: FID and ODP2 (Gerstel). The smoke of the ten cigarette types was evaluated ten times using the in-

house computer program (Figure 1). For DTD-GC-MS, HP 5973 (MSD) was used. The identification of odour-active compounds was performed by comparing their mass spectra with those from the MS library database (Wiley). Their corresponding odour descriptions were compared with those described in the FRM 98 database (10).

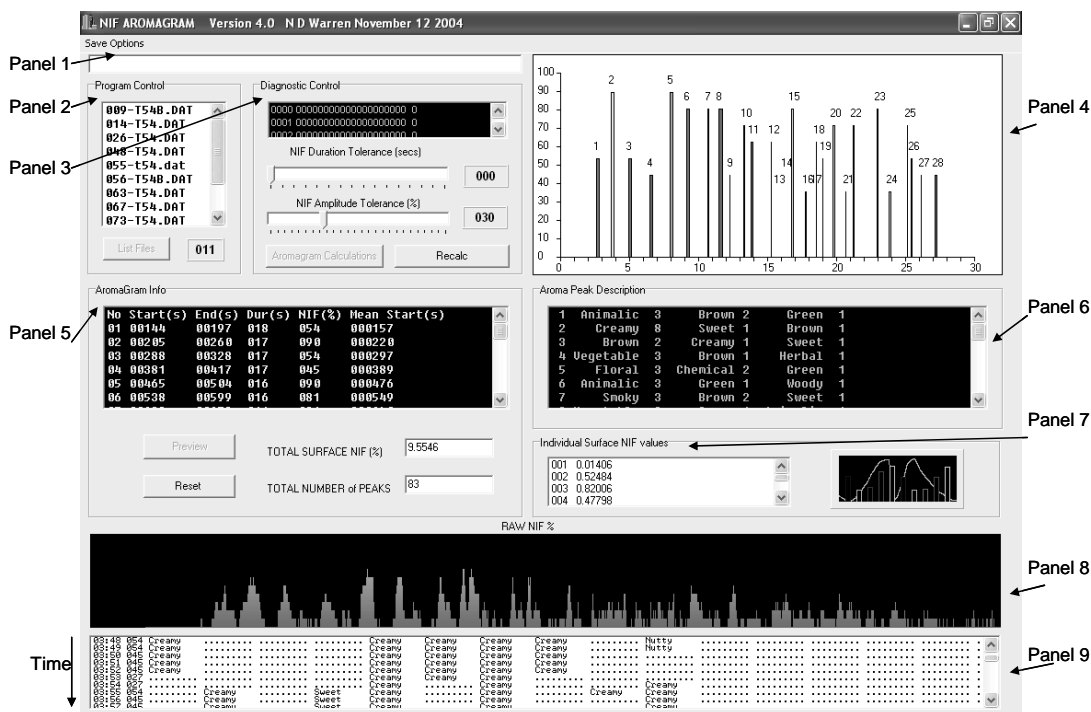


Figure 2. NIF aromagram plotting software. Panel 5: list of times (s) and NIF values (%), Panel 6: key odour descriptors; Panel 8: aromagram.

Results

GC-O and GC-MS results. 228 compounds were identified by MS (matching spectra) and 15 to 21 odours above a NIF value of 40% were detected in the ten cigarette samples. Six common aromas were found in all ten cigarette samples (Compounds 2, 4-8 in Table 1). They were characterised using three methods: matching spectra, retention indices from authentic standards and matching flavour descriptors (10).

Conclusions

The goal of this study was to provide insight into the nature of the key aroma compounds in cigarette smoke. This insight will help in cigarette design to optimise flavour release for consumers. The development of the Direct Thermal Desorption DTD-GC-O technique has been essential to the analysis of the smoke aroma compounds in this study. The main challenge for this part of the work was in preparing smoke samples that would be as 'fresh' as possible owing to the inherent dynamism of the smoke aerosol. In summary, this study has:

1. established one suitable method to prepare 'fresh' smoke samples by DTD,
 2. developed two software programs to process odour data more efficiently,
 3. provided a list of key aroma compounds in the smoke of ten cigarette types
- This list was then used to select ions for nose-space analysis of smoke in subsequent studies using APCI-MS (11).

Table 1. Tobacco smoke aromas found in ten cigarette analysed by DTD-GC-O.

	RI ^a	Odour ^b	Identification ^c	NIF (%)									
				FC	MA	OR	ST	ET	BU	B1	B2	B3	CO
1	~475	animalic/sulphur	n.a. ^d	80	72	0	80	80	55	90	80	54	40
2	594	creamy	diacetyl ^{e,f,g}	90	72	50	80	100	88	90	70	90	90
3	627	brown/fruity	isovaleraldehyde ^{e,f,g}	60	0	40	60	60	77	70	80	54	70
4	690	green/chemical	2,5-dimethyl furan ^{e,f,g}	100	54	60	80	100	77	80	90	90	80
5	826	animalic/green	2-picoline ^{e,f,g}	80	63	40	60	60	77	60	50	81	40
6	880	animalic/brown	4-picoline ^{e,f,g}	70	45	70	40	50	55	50	60	81	100
7	914	nutty/brown	2,5-dimethyl pyrazine ^{e,f,g}	100	72	90	50	90	100	70	80	81	40
8	980	fungoid/animalic	trimethyl benzene ^e	60	54	80	70	80	44	80	70	63	40
9	1025	earthy/green	C ₁₀ terpene ^e	0	63	40	0	40	66	80	0	63	50
10	1094	smoky/green	guaiacol ^{e,f,g}	60	63	80	0	90	77	70	60	100	70
11	1140	green/fruity	n.a. ^d	70	0	70	0	50	66	50	60	90	50
12	1155	green/floral	keto-isophorone ^e	50	72	60	40	50	66	50	50	0	0
13	1191	brown/smoky	n.a. ^d	70	63	80	60	60	88	0	60	72	40
14	1215	green	n.a. ^d	0	0	60	40	0	88	0	60	0	0
15	1250	fungoid/green	n.a. ^d	0	54	50	60	0	44	0	50	72	60
16	1304	fruity/animalic	indole ^{e,f,g}	0	54	50	50	40	44	0	0	81	50
17	1405	floral/animalic	skatole ^{e,f,g}	0	54	60	40	0	0	50	50	100	60

^a Retention Index on non-polar column Rtx-5MS. ^b Odour description from GC-O analyses. ^c Identification: not available^d, matching Mass Spectra^e, aroma description^f, RI from authentic standards^g

Acknowledgements

The authors acknowledge Nigel Warren, British American Tobacco, Southampton, for his support on authoring the two computer programmes.

References

1. Taylor H.J., Winter D.B., Miranda E.J.F., da Silva J.R.P. (1999) *Beitrage zur Tabakforschung International* 18: 175-187.
2. Honma Y., Higashi N., Shimoda M., Hayakawa I. (2004) *Nippon Nogeikagaku Kaishi* 78: 572-574.
3. Higashi N., Shikata H., Shimoda M., Hayakawa I. (2004) *Beitrage zur Tabakforschung International* 21: 32-39.
4. Bazemore R., Harrison C., Greenberg M. (2006) *J. Agric. Food Chem.* 54, 497-501.
5. Pollien P., Ott A., Montignon F., Baumgartner M., Muñoz-Box R., Chaintreau, A. (1997) *J. Agric. Food Chem.* 45, 2630-2637.
6. Delahunty C.M., Eyres G., Dufour J.-P. (2006) *J. Sep. Sci.* 29: 2107-2125.
7. Acree T.E., Barnard J. (1994) In *Trends in Flavour Research* (Maarse H., van der Heij D. G., eds.), Elsevier Science B.V., pp 211-220.
8. Mottay P. (2004) In *Handbook of Flavor Characterisation: Sensory analysis, Chemistry and Physiology* (Deibler K.D., Delwiche J., eds), pp 277-284.
9. Dube M.F., Green C.R. (1982) *Rec. Adv. Tob. Sci.* 8: 42-102.
10. BACIS (1997) FRM 98 Database of Flavour (Raw) Materials. Boelens Aroma Chemical Information Services (BACIS), Huizen, The Netherlands.
11. Cotte, V.M.E., Prasad, S.K., Wan, P.H.W., Linforth, R.S.T., Taylor, A.J. (2008) In *Recent Highlights in Flavor Chemistry and Biology* (T. Hofmann, W. Meyerhof & P. Schieberle, eds), pp 39-47.

Section 9

**Targeted and Holistic Approaches
in Flavour Analysis**

OPPORTUNITIES FOR FLAVOUR ANALYSIS THROUGH HYPHENATION

P.J. MARRIOTT¹, G.T. Eyres^{1,2}, and J.-P. Dufour²

¹ *School of Applied Sciences, RMIT University, GPO Box 2487V, Melbourne, Victoria 3001, Australia*

² *Department of Food Science, University of Otago, PO Box 56, Dunedin 9054, New Zealand*

Abstract

The advances in chemical and flavour knowledge that can be made through improved separation and identification capabilities cannot be underestimated. In this paper, we explore a number of new integrated methods that we have recently introduced that permit improved resolution and separation power for a range of analytical studies. These focus on multidimensional gas chromatography, comprehensive two-dimensional gas chromatography (GC), olfactometry, mass spectrometry and nuclear magnetic resonance spectroscopy. The overriding aim is to provide technical solutions that employ the best possible separation of compounds. Better separation of compounds allows tools such as olfactometry, mass spectrometry, nuclear magnetic resonance spectroscopy, and other detectors to provide much better characterisation of separated chemical species. We demonstrate various novel strategies that provide the necessary separation power, integrated with specific detection steps. Case studies in the areas such as sensory-directed identification of a woody odorant in hop essential oil, correlation of compound identifications in coriander leaf, and development of new preparative capabilities in multidimensional GC with nuclear magnetic resonance spectroscopy.

Introduction

The role, implementation and use of multidimensional gas chromatography (MDGC) is now well established (1,2). MDGC has a long history although the promise and widespread application of MDGC remains unfulfilled (3). What driving force developed MDGC, even in the early days of capillary GC? The elegance of linking two or more columns in a hyphenated arrangement demanded investigation, just to see how it might benefit the technology. At the other extreme is the recognition that a single column GC solution is simply inadequate to provide the analytical answers that an analyst seeks. In this context, we have little solution other than to resort to multiple separation dimensions. Fetterolf and Yost (4) then Kidwell and Riggs (5) presented discussion on the informing power of hyphenated analytical separations with mass spectrometry (MS). A single GC column has an informing power of about 500-600 (i.e. can separate 500-600 peaks (compounds) in a single analysis). Complex sample have a high likelihood of multiple peak overlaps, and according to Davis and Giddings (6-8) may demand multidimensional separations. Electron induced ionisation GC/MS increases informing power to about 6.6×10^6 due to the discrimination of the MS dimension; MS is able to provide considerable identification

power due to the use of library matching. GC/MS-MS further extends informing power to an amazing 6.6×10^9 , due to the selectivity of the second MS dimension.

Similarly, GC can provide significantly more resolving power by selecting small zones of eluting peaks from a first column, then separate them on a second (orthogonal) column, by choice of different polarity phases. Consider selection of a complex group of peaks eluting within a zone equivalent to 10 peaks wide (about 1 min of effluent, possibly comprising 50 overlapping peaks). Applying this to a 2D column with a peak capacity of 500, should allow separation of each sampled peak. But can we develop a method that can do this with one injection, in real time? The 2D column cannot provide a capacity of 500, within a 1 min analysis time (in a manner that could permit the next fraction from the 1D column, and every subsequent fraction thereafter).

An elegant analysis that almost demands MDGC, is that of enantioselective analysis. The most logical approach is to use an achiral 1D column, followed by an enantioselective 2D ($e\text{-}^2D$) column. A narrow zone of effluent from 1D containing the target enantiomers is passed it to the second, $e\text{-}^2D$ column, for complete chiral separation. Ideally, the two fully resolved enantiomers will be completely resolved from any matrix compounds transferred with the enantiomeric compounds (9). Use of an $e\text{-}^1D$ column is not appropriate; a wider transfer effluent zone that encompass the two resolved enantiomers will capture more matrix compounds which have to be resolved from the enantiomers.

Two methods most closely achieve the rapid sequential 2D analysis for all compounds in a sample. Our first approach is based on a method called rapid targeted MDGC, which selects contiguous zones of effluent from a first column (10,11). About 1 min of effluent from the 1D column is collected in a device we call a longitudinally modulated cryogenic system (LMCS). The cryotrap is moved away from the cooled zone to release components to the 2D column. A peak capacity of 40+ peaks in a 1 min sampled zone is realised (the re-injection band is negligibly narrow; a fast 0.1 mm ID 2D column of about 5+ m long generates very fast 2D analysis). The second is to use comprehensive 2D GC (GC \times GC) (12,13). Here, a much shorter, narrow bore 2D column (ca 1 m long; 0.1 μm ID), and a modulator (we use the LMCS for this) performs a repetitive “collect – pulse” operation from the 1D to 2D column. A number of modulations arise for each 1D peak, according to the modulation ratio M_R selected (14), and each modulation (2D separation) should ideally be completed within the same timeframe as the modulation period. A further method that involves multiple trapping elements (15) each separately eluted through a conventional column, or to different detectors, is not a rapid method.

Using advanced separations for essential oil samples

Targeted MDGC has been not used for many applications to date, but included alleged allergens in personal products (16), where the problem is isolation of small amounts of allergen in the presence of large amounts of matrix materials. For terpenes and related compounds, the similarity of MS library matches makes positive identification difficult. With better resolution we can achieve better analysis certainty.

GC \times GC has been used for analysis of a broad range of essential oils. In a typical application, we used GC \times GC/TOFMS to compare volatile headspace compounds in a variety of pepper and related aromas (17). Other applications have been reported in the review series by Adahchour *et al.* (18,19) such as ginger, hops, sandalwood, wine, and these works are an excellent overview of the technology of GC \times GC.

Incorporation of olfactometry with GC×GC and MDGC

Olfactory analysis using GC (GC-O) is commonly used to determine odour activity of individual compounds in a mixture. Well-established procedures can be used for assessing odour quality and relative importance of odour-active compounds eluting from the GC (20). The overall aroma of a sample is a convoluted combination of many interacting odorants. The individual separated molecules in GC-O will present their own odour signatures. It is difficult to determine the recombined odour simply from individual separated compound(s), due to complex interactions and physiological effects (i.e. threshold, volatility, receptor biology). Odour assessment is more complex than might be acknowledged by the above comment. Combining I values, MS and odour profiling is a powerful multidimensional strategy. Where peak overlaps arise, precisely allocation of the olfactory result to analytical data (e.g. assignment of chemical structure to an aroma compound) is difficult. Inadequate resolution leads to uncertainty of compound identity, and is an opportunity for application of multidimensional separation technologies. Recent research serves to demonstrate the capabilities of some new techniques available to chromatographers.

Begnaud and Chaintreau (21) described the development of an arrangement that quantitatively trapped compounds within a capillary column loop, isolated them on-line from preceding and following peaks, and introduced the target region into the 2D column for effective resolution from interfering matrix compounds (Figure 1A). This allows both MS and/or olfactory analysis. A small split flow ($\sim 10\%$) to a monitor detector achieves correct timing to ensure target trapping in the loop which must be sufficiently cool to retain the trapped compounds of the target region. The storage loop operates in two ways (Figure 1B). The first is a reverse direction loop through the cryotrap (Fig 1B(i)). The second (Fig 1B(ii)) as originally proposed, passes the loop through the same direction as the incoming strand. The former arrangement allows smaller loop size, with fewer movements of the cryotrap to permit the solute to enter, be trapped then remobilised into the second dimension.

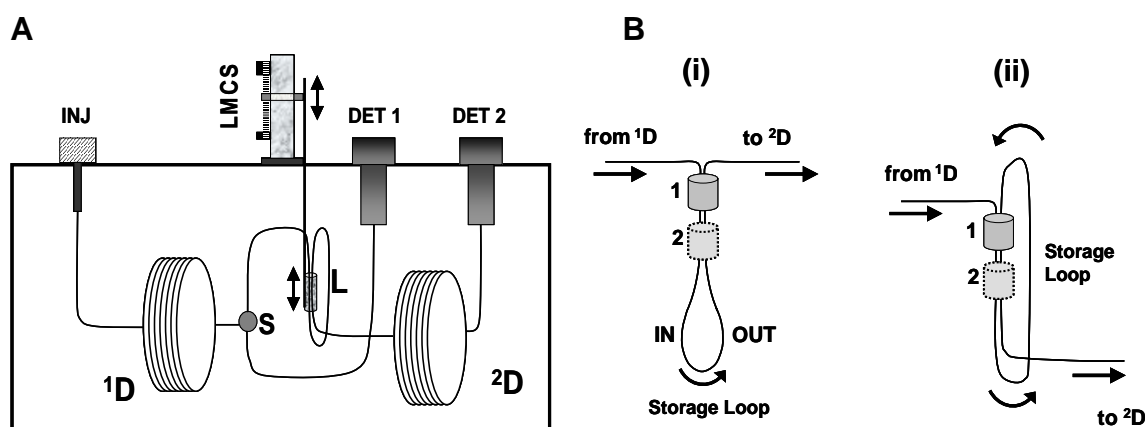


Figure 1. (A) Schematic diagram of a 'double cool-strand loop modulator' incorporating a looped column (L) through a longitudinally modulated cryogenic system (LMCS). Target regions can be selected, sampled and passed to the second dimension (2D). The union (S) allows a small flow to pass to the first detector (DET 1) to allow precise selection of the target region. (B) Two different arrangements for the looped column modulator.

A common approach to implementing MDGC is via a micro-fluidic pressure-balanced Deans switch system, (Figure 2). ¹D column eluate is directed to a monitor detector; when a target region elutes from the ¹D column, flow is diverted to the start of the ²D column (see Marriott (22)). A cryotrapping device incorporated into the system, to cryo-focus the heartcut analyte band at the head of the second column, would be a preferred option, particularly for short, thin-film columns, to maximise performance.

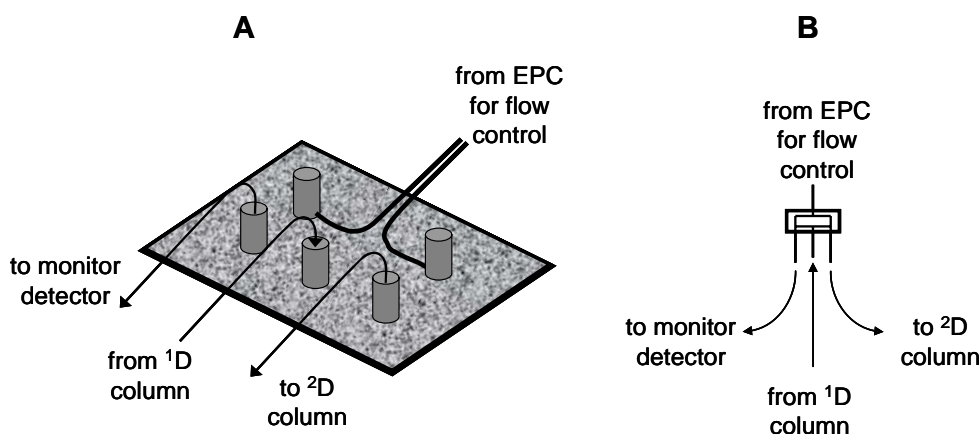


Figure 2. (A) Schematic diagram of the physical design of a Deans switch system. (B) is the representation of the Deans switch used in Figure 4.

A second case study incorporates GCxGC with GC-O for coriander leaf volatiles (23). Coriander character-impact odorants were located by CharmAnalysis™ aroma profiling in GC-O. The GCxGC distribution of components permitted identification of series of related compounds. Each series (*E*-2-alken-1-ols; alkanols; *E*-2-alkenals; *Z*-2-alkenals; *Z*-4-alkenals; alkanals; alkanes) forms an approximate linear relationship within the 2D space, confirmed by using GCxGC-time-of-flight mass spectrometry (TOFMS) (Figure 3). Such plots allow prediction of individual compound locations, and confirms of their presence. I values, MS and reference compound injection were variously used for identification.

This study did not employ GCxGC-O to evaluate odour activity, although this group has investigated this approach, finding that the 'modulation' process can enhance the perception of volatile aroma compounds concentrated by the cryotrapping step. But it is difficult for the assessor to assign specific peaks. Other researchers (24) claimed olfactory detection can reliably be used with GCxGC, demonstrating identification of many compounds; this is yet to be confirmed. Further study focused on essential oils from four hop varieties, and the presence of a potent 'spicy, woody, cedarwood' odour (25). The following summarises our hyphenated method progression:

(i) GC-O located the odour-active region. The GC had considerable complexity in this region (oxygenated sesquiterpenes). GC/MS analysis could not adequately identify a single component responsible for the odour perception. Peak overlap prevented olfactory (CharmAnalysis™) response correlation with particular peak abundances.

(ii) GCxGC analysis quantitatively separated the target region, revealing up to 13 resolved components. It was possible to compare relative peak abundances in GCxGC analysis of eight samples of hop oils, with the CharmAnalysis™ results; in this case, a greater %Charm value could be correlated with a specific peak increase

in the oil extract ($R^2 = 0.95$). However this still is inadequate for providing confirmatory evidence that the suspected peak is correctly assigned to the odour.

(iii) MDGC and selecting the appropriate zone allowed the target region to be passed to the 2D column, with separation of all the peaks. Each peak was submitted to olfactory assessment. The woody odour was tentatively assigned to 14-hydroxy- β -caryophyllene by its mass spectrum and retention index acquired with GCxGC/TOFMS.

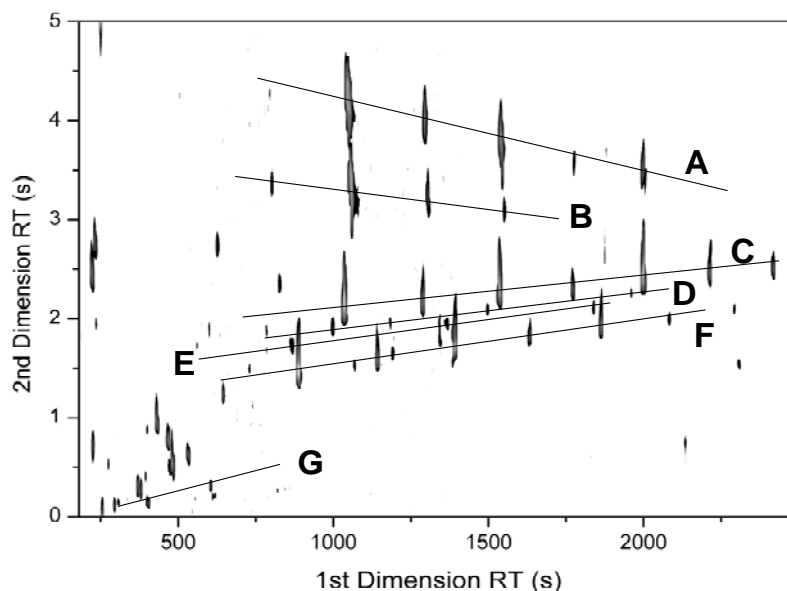


Figure 3. GCxGC analysis of Coriander oil. Series of compounds identified were (using GCxGC-TOFMS analysis). A: E-2-alken-1-ols; B: alkanols; C: E-2-alkenals; D: Z-2-alkenals; E: Z-4-alkenals; F: alkanals; and G: alkanes.

Development of micro-prep capillary MDGC with MS and NMR spectroscopy

MDGC is usually best accomplished with MS detection, which works best with well resolved peaks with a single peak entering the detector. Overlapping peaks can still be analysed (background subtraction, deconvolution, or quantified by selected ion monitoring using identified unique ions); none of these techniques are necessary with pure GC peaks, achieved by using MDGC. With pure peaks there should be no limitation to the detection tools that can be on-line or off-line hyphenated with GC. We must consider: (i) can detection be directly hyphenated with MDGC? (ii) what procedure can deliver the separated solute to the spectroscopic system? (iii) what is the relative sensitivity needed to provide adequate detection of target molecules?

For (i), on-line hyphenation requires compatibility with the separation step, for real-time data acquisition. Some methods cannot accomplish this; others may have suitable sensitivity for GC hyphenation, but the interface may be unwieldy. Therefore, we resort to situation (ii). We pioneered a Deans switch device to direct flow and selected compound to a FID or a cryotrap at the end of the LMCS-MDGC system (26). Point (iii) is a critical consideration if there is a significant mismatch between the amount of solute that can be reliably injected into the MDGC system, and sensitivity of detection. The latter is normally the limiting step (of lower sensitivity) so multiple injections/trappings of solute is required, and/or overloading of the MDGC system. A pure isolated compound from the MDGC system then allows any spectroscopic method for its identification. The focus is on chemical identification, since once

identified and the pure spectra obtained, this can be added to a database (e.g. MS, or I values) for identification in other samples. Collected residue can be analysed by MS, GC/MS, GCxGC (to get retention position in 2D space), FTIR, high-resolution MS, or optical methods. Wilkins *et al.* were early adopters of MDGC with simultaneous detection, such as MS and FTIR (27).

Our recent work (26) demonstrated such an approach, integrating a novel approach for MDGC, with cryotrapping and off-line NMR spectroscopy, initially presented for qualitative separation of geraniol from a region where many compounds coeluted on the ¹D column. Geraniol was collected by using a Deans switch at outlet of the MDGC, cutting the single component to an external cryotrap (Figure 4). The system operates automatically, apart from manual elution of the cryotrap tube into an NMR tube. Automatic injection and multiple sample repetitions (up to 100) can accumulate sufficient solute (~ 78 µg) to perform ¹H NMR in both 1D and 2D modes. NMR identification, supported by MS information, makes absolute structural configuration possible. Geraniol was chosen to demonstrate our approach, and a 'blind' study of randomly selected compounds is now needed.

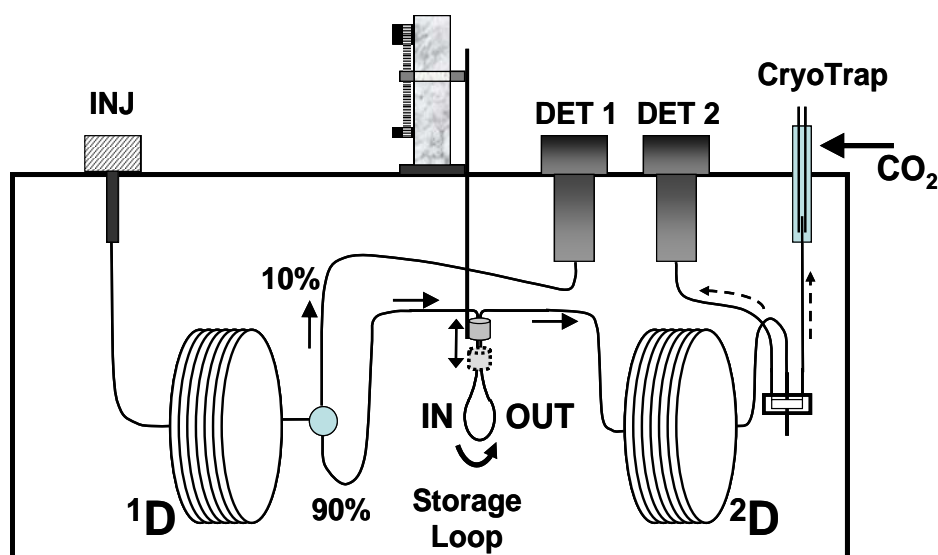


Figure 4. Procedure developed for MDGC with NMR. DET 1 provides a monitor signal for the total sample. The looped LMCS cryo-system selects specific target regions, to facilitate separation of the target zone on the ²D column. The Deans switch diverts the target (geraniol) to an external cryotrap, to collect the trapped geraniol for subsequent NMR analysis.

Figure 5 demonstrates the method for isolation of geraniol from a complex mixture of essential oils. Geraniol is completely resolved from the matrix components, allowing collection of pure component from a complex sample, and analysis by NMR – but any desired spectroscopic technique may be used.

Conclusions

Hyphenated analysis for flavour monitoring, detection and discovery is a very robust, continually advancing, topic. For volatile compounds, GC/MS is used reliably, often providing the answer demanded by the analyst. It is increasingly recognised that complex samples require more than a single column separation. The power of MS is often insufficient to provide unambiguous measurement for grossly overlapping

compounds. We must resort to higher peak capacity or MDGC methods. Various new approaches have been introduced in our laboratory to address the above limitations.

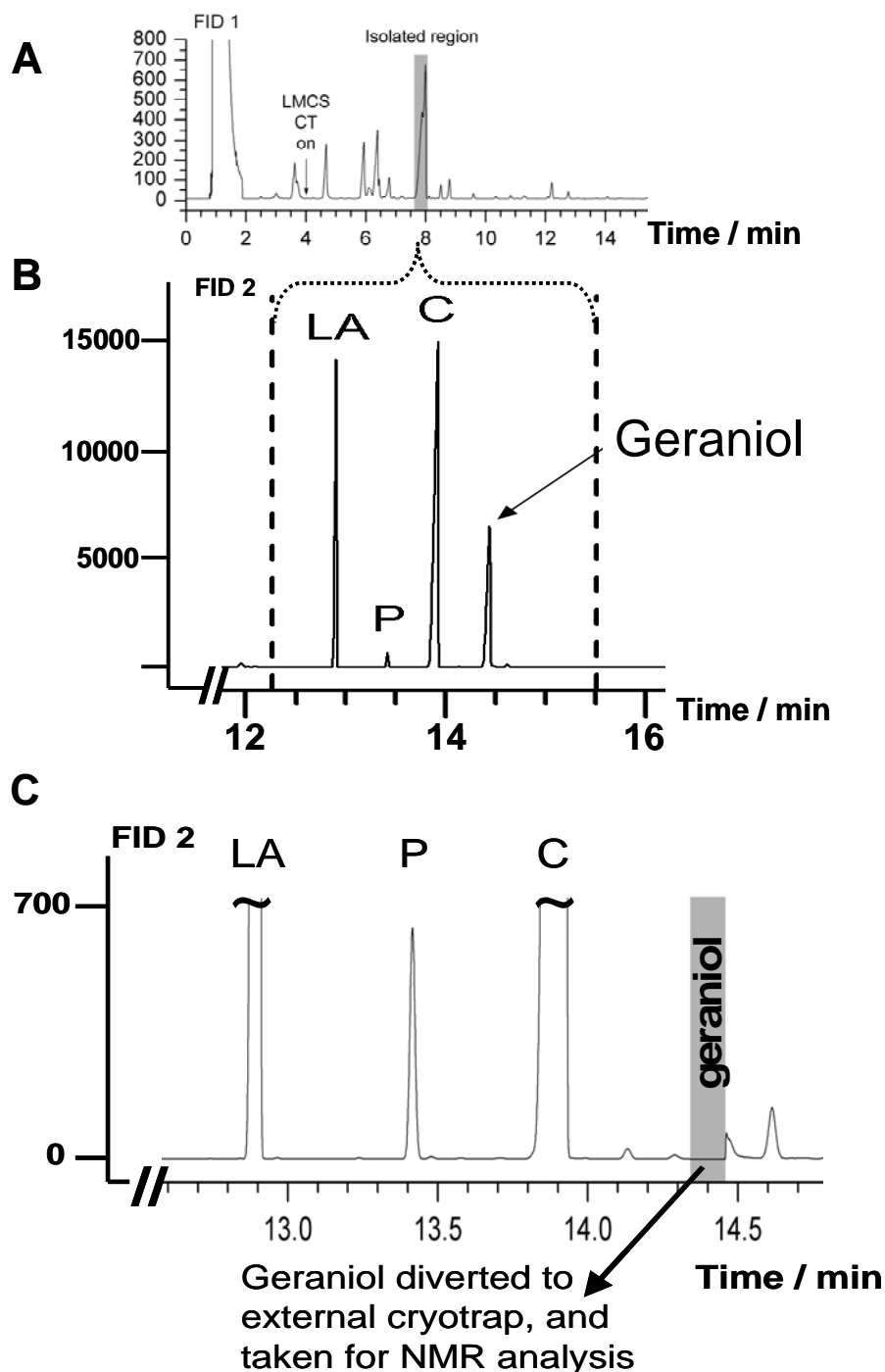


Figure 5. Data acquired for the system shown in (Figure 4) (A). FID 1 monitors the 1D result, to indicate the appropriate target sampling region. (B) Both preceding and following zones are resolved from the target region, shown in expanded format. FID 2 is the result for the target region. (C) Geraniol is diverted to the external cryotrap. Compounds are identified as follows: linalyl acetate (LA), pulegone (P), carvone (C).

We maximise resolution and improve capabilities for detection. Case studies include coriander leaf oil showing trends in chemical class retention in GCxGC, analysis of

hop oils with woody character by using GC-O correlated with GCxGC data, and finally MDGC-O. A new study demonstrated the power of a micro-scale MDGC separation method, with a loop modulator and a micro-fluidic Deans switch to isolate a pure geraniol component, followed by NMR analysis. Truly, the methods utilising multidimensional separations and hyphenation with advanced spectroscopic procedures will permit many new and exciting future studies for flavours.

Acknowledgements

The authors wish to thank Dr Matthew Klee, Agilent Technologies, for provision of the Deans switch devices. Mr Paul Morrison's deft abilities at implementing multidimensional systems are greatly appreciated.

References

1. Cortes H. (ed.) (1990) *Multidimensional Chromatography: Techniques and Applications*, Marcel Dekker: New York, NY.
2. Mondello L., Lewis A.C., Bartle K.D. (eds.) (2002) *Multidimensional Chromatography*, John Wiley & Sons Ltd: Chichester, England.
3. Bertsch W. (1999) *J. High Resol. Chromatogr.* 22: 647-665.
4. Fetterolf D.D., Yost R.A. (1984) *Int. J. Mass Spectrom. Ion Proc.* 62: 33-49.
5. Kidwell D.A., Riggs L.A. (2004) *For. Sci. Int.* 145: 85-96.
6. Davis J.M., Giddings J.C. (1983) *Anal. Chem.* 55: 418-424.
7. Giddings J.C. (1995) *J. Chromatogr. A* 703: 3-15.
8. Davis J.M., Samuel C. (2000) *J. High Resolut. Chromatogr.* 23: 235-44.
9. Mondello L., Catalfamo M., Dugo G., Dugo P. (1998) *J. Chromatogr. Sci.* 36: 201-209.
10. Dunn M.S., Marriott P.J., Shellie R.A., Morrison P.D. (2003) *Anal. Chem.* 75: 5532-5538.
11. Dunn M.S., Vulic N., Shellie R.A., Whitehead S., Morrison P., Marriott P.J. (2006) *J. Chromatogr. A* 1130: 122-129.
12. Marriott P.J., Kinghorn R.M. (1997) *Anal. Chem.* 69: 2582- 2588.
13. Marriott P., Shellie R. (2002), *Trends Anal. Chem.* 21: 573-583.
14. Khummueng W., Harynuk J., Marriott P.J. (2006) *Anal. Chem.* 78: 4578-4587.
15. Krock K.A., Ragunathan N., Wilkins C.L. (1993) *J. Chromatogr.* 645: 153-159.
16. Dunn M.S., Shellie R.A., Morrison P.D., Marriott P.J. (2004) *J. Chromatogr. A* 1056: 163-169.
17. Cardeal Z.L., Gomes da Silva M.D.R., Marriott P.J. (2006) *Rapid Commun. Mass Spectrom.* 20: 2823-2836.
18. Adahchour M., Beens J., Vreuls R.J.J., Brinkman U.A.Th. (2006) *Trends Anal. Chem.* 25: 438-454, 540-553, 726-741, 821-840.
19. Adahchour M., Beens J., Brinkman U.A.Th. (2008) *J. Chromatogr. A* 1186: 67-108.
20. Delahunty C.M., Eyres G., Dufour J.-P. (2006) *J. Sep. Sci.* 29: 2107-2125.
21. Begnaud F., Chaintreau A. (2005) *J. Chromatogr. A* 1071: 13-20.
22. Marriott P.J., Mitrevski B. (2009) in Press, LC-GC Europe.
23. Eyres G.T., Dufour J.-P., Hallifax G., Sotheeswaran S., Marriott P.J. (2005) *J. Sep. Sci.* 28: 1061-1074.
24. d'Acampora Zellner B., Casilli A., Dugo P., Dugo G., Mondello L. (2007) *J. Chromatogr. A* 1141: 279-286.
25. Eyres G.T., Marriott P.J., Dufour J.-P. (2007) *J. Ag. Food Chem.* 55: 6252-6261.
26. Eyres G.T., Urban S., Morrison P.D., Dufour J.-P., Marriott P.J. (2008) *Anal. Chem.* 80: 6293-6299.
27. Wilkins C.L., Giss G.N., Brissey G.M., Steiner S. (1981) *Anal. Chem.* 53: 113-117.

TWO-DIMENSIONAL GC AND NITROGEN CHEMILUMINESCENCE DETECTION TO ANALYSE VOLATILE N-COMPOUNDS IN WINE WITH AND WITHOUT OFF-FLAVOUR

D. RAUHUT, B. Beisert, S. Fritsch, and H. Kürbel

Forschungsanstalt Geisenheim / Geisenheim Research Center, Fachgebiet Mikrobiologie und Biochemie / Section Microbiology and Biochemistry, Von-Lade-Straße 1, D-65366 Geisenheim

Abstract

The occurrence of 2-aminoacetophenone (2-AAP), indicator substance for atypical aging in wine, and other volatile nitrogen compounds such as indole, skatole, anthranilic acid methyl and ethyl ester, which are suspected to contribute to this off-flavour, was studied in wine with and without aroma defect. Current analytical methods were optimised using solid supported liquid-liquid-extraction and two-dimensional gas chromatography combined with a nitrogen chemoluminescence detector. Wine with a distinct atypical aging note had increased levels of 2-AAP ($>0.6 \mu\text{g L}^{-1}$ 2-AAP), while no increase of other *N*-compounds was observed.

Introduction

An increase of off-flavours developed in wine during the aging process in the last two decades due to global climate change and stress conditions in the course of the vegetation period of vines [1-6]. 2-AAP (odour threshold value $0.7 \mu\text{g L}^{-1}$) was identified as key compound in white and rosé wine for this atypical aging (ATA) off-flavour [1]. Various attributes describing ATA flavour notes such as acacia blossom, naphthalene-like, and furniture polish point out that apart from 2-AAP probably other volatile compounds are involved [1-6]. Therefore, it is assumed that the different attributes to describe ATA in wine are related to an increase of other specific nitrogen *N*-compounds such as indole, skatole, anthranilic acid methyl (ASME) and ethyl (ASEE) ester, and others.

The extraction of the *N*-compounds was optimised by solid supported liquid-liquid-extraction (SLE). Two-dimensional gas chromatography (GC-GC) in connection with a nitrogen chemoluminescence detector (NCD) was applied for the qualitative and quantitative analysis of *N*-compounds in wine with and without ATA [7]. The use of two-dimensional gas chromatography to analyse 2-AAP and other *N*-substances was necessary to avoid problems due to matrix effects and co-eluting compounds that were already described [1, 7, 8].

Experimental

Materials. 2-AAP was purchased from Acros Organics (Geel, Belgium); ASME and ASEE, 2-methylindole (2-Mel) and 5-methylindole (5-Mel) were obtained from Aldrich (Steinheim, Germany); indole and skatole were purchased from Fluka (Buchs, Switzerland); n-pentane was obtained from Carl Roth (Karlsruhe, Germany) and the Chem ElutTM extraction cartridges from Varian (Darmstadt, Germany).

Sample preparation. For sample preparation the two internal standards 2-methylindole ($c = 3 \mu\text{g L}^{-1}$) and 5-methylindole ($c = 1 \mu\text{g L}^{-1}$) were added to 20 mL of wine. 5-Mel was used for quantification and 2-Mel as control standard. The wine was then added to the dry Chem Elut™ extraction cartridges (V (solid support) = 20 ml). Thereby the aqueous sample was adsorbed and distributed into a thin layer over the packed material of the extraction cartridges. After 10 min of adsorption time 20 mL of n-pentane were given onto the cartridges. While the solvent ran through the cartridges the analytes were extracted from the aqueous film. For better extraction efficiency and recovery, elution was repeated with another aliquot of n-pentane [9]. The collected extracts were concentrated to about 50 μL for analysis.

Analysis by LVI-GC-GC-NCD. Analysis was carried out with large volume injection (LVI) followed by GC-GC-NCD. 10 μL of the extract were injected into a DB-1 capillary column (J & W Scientific, Agilent Technologies, Palo Alto, USA; 60 m x 0.32 mm x 1.0 μm) installed on the first gas chromatograph (Agilent Series 6890, Agilent Technologies, Palo Alto, USA) equipped with a MPS 2 autosampler (Gerstel, Mülheim, Germany) coupled with a Cooled Injection System CIS 4 (Gerstel, Mülheim, Germany) operating in solvent vent mode (0 °C, 12 °C s^{-1} to 280 °C, hold for 3 min). Helium was used as carrier gas at constant flow rate (1.2 mL min^{-1}). The temperature of the first GC was programmed from 60 °C (hold for 1 min) to 230 °C (hold for 72 min) at a rate of 10 °C min^{-1} . A flame ionisation detector (FID) was used as monitor detector.

When passing through the DB-1 column, which acted as a pre-column, the GC fraction from 18 to 20.5 min was cut out at a Multi Column Switching System MCS (Gerstel, Mülheim, Germany) programmed with a pressure rate of 0.6 kPa min^{-1} and the fraction transferred to the second GC. The temperature of the transfer line was kept at 240 °C during the whole time of analysis.

At the second GC (Agilent Series 6890, Agilent Technologies, Palo Alto, USA) separation took place at a DB-WAX capillary column (J & W Scientific, Agilent Technologies, Palo Alto, USA; 60 m x 0.32 mm x 0.25 μm). The oven was programmed from 60 °C (hold for 25 min) to 150 °C at a rate of 5 °C min^{-1} , then up to 205 °C at a rate of 1.5 °C min^{-1} and finally up to 230 °C (hold for 8 min) at a rate of 10 °C min^{-1} . Column flow was set to 1.2 mL min^{-1} .

Temperature of the pyrolysis oven of the NCD (Antek Series 7090 Nitrogen Detector, PAC, Houston, USA) was set to 950 °C with a furnace vacuum of 140 Torr. Oxygen flow was at 10 mL min^{-1} and ozone flow at 25 mL min^{-1} respectively with a vacuum in the detector chamber of 13 Torr. Chemiluminescence was detected in a range of 600 to 900 nm.

Results

The extraction of *N*-containing analytes from wine was optimised by the use of SLE instead of liquid-liquid-extraction or SPE (solid phase extraction). SLE simplified and sped up the sample preparation. Figure 1 indicates a chromatogram of a wine, which was spiked with *N*-compounds. The application of SLE in combination with the chosen solvent avoided emulsions, an overloaded chromatogram and problems due to matrix effects.

Linear calibration was obtained for all *N*-components. The calibration graph for 2-AAP ($n= 5$ for each measured concentration) is taken as an example and presented in Figure 2. The ratio of the areas of the two internal standards (2-Mel : 5-Mel) was used for control. The average value of all ratios measured during the calibration

phase was 1.1 with a standard deviation of ± 0.1 (relative standard deviation (RSD) 10 %).

The results of five different extracts and analysis from the same sparkling wine (mean $1.4 \mu\text{g L}^{-1}$) led to a standard deviation of ± 0.06 and 4.1 % was calculated for the RSD.

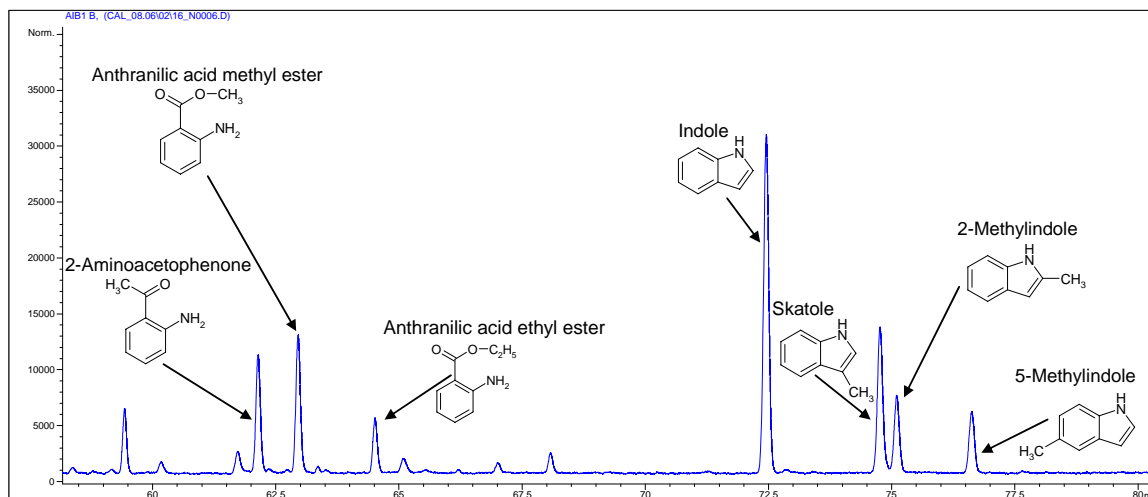


Figure 1. Chromatogram of a wine spiked with *N*-compounds ($2 \mu\text{g L}^{-1}$ 2-AAP, $2 \mu\text{g L}^{-1}$ ASME, $2 \mu\text{g L}^{-1}$ ASEE, $3.6 \mu\text{g L}^{-1}$ indole, $2 \mu\text{g L}^{-1}$ skatole, internal standards: $3 \mu\text{g L}^{-1}$ 2-Mel, $1 \mu\text{g L}^{-1}$ 5-Mel).

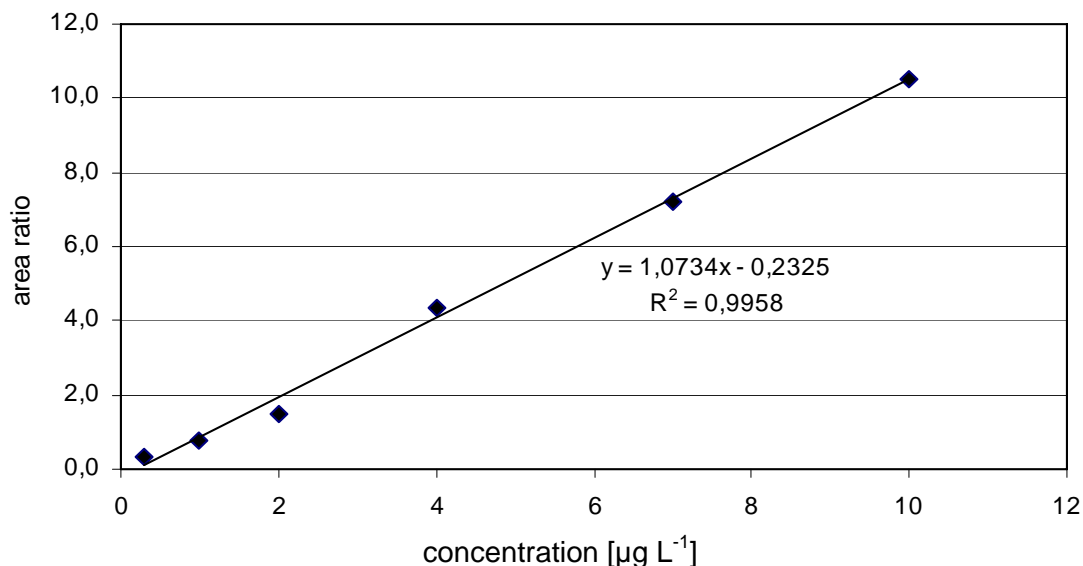


Figure 2. Calibration graph of 2-AAP.

The concentrations of different *N*-compounds in wine with and without ATA are demonstrated with a selection of analysed wines in (Table 1). It is obvious that all wines with an ATA off-flavour had concentrations of 2-AAP over the threshold value. The other four measured *N*-compounds showed no increased levels.

Table 1. Concentration of different N-compounds in wine with and without ATA off-flavour.

Wine Sample	2-AAP [$\mu\text{g L}^{-1}$]	ASME [$\mu\text{g L}^{-1}$]	ASEE [$\mu\text{g L}^{-1}$]	Indole [$\mu\text{g L}^{-1}$]	Skatole [$\mu\text{g L}^{-1}$]	ATA off-flavour
1983 Riesling Spätlese Rheingau	0.8	0.4	0.9	0.3	0.4	yes
1985 Riesling QbA. Rheingau	0.6	2.3	1.0	nd	nd	no
1990 Riesling QbA. Rheingau	1.3	1.2	rd	rd	nd	yes
1990 Riesling Kab nett Rheingau I	0.3	nd	0.5	0.2	0.3	no
1990 Riesling Kab nett Rheingau II	0.1	0.4	0.4	rd	0.2	no
1990 Riesling Spätlese Rheingau I	0.2	1.2	0.6	rd	nd	no
1990 Riesling Spätlese Rheingau II	0.7	nd	1.4	rd	nd	yes
1998 Blanc de Noir Palatinate	1.4	0.3	rd	rd	nd	yes
2004 Müller-Thurgau Rheingau I	1.2	0.3	0.3	0.3	0.1	yes
2004 Müller-Thurgau Rheingau II	2.1	0.4	0.3	0.2	nd	yes
2004 Müller-Thurgau Rheingau III	1.0	0.3	tr	0.4	0.1	yes
2004 Müller-Thurgau Rheingau IV	1.0	0.2	rd	0.4	0.1	yes
2004 Müller-Thurgau Rheingau V	1.7	0.1	rd	0.3	0.1	yes
2007 Pinot gris Palatinate	nd	nd	rd	0.9	nd	no

nd: not detected; tr: traces

The developed analytical method is an appropriate tool to analyse 2-AAP and other N-compounds like ASME, ASEE, indole and skatole without interference of the matrix in wine and sparkling wine and can be used for ongoing studies in this research field.

References

1. Rapp A., Versini G., Ullemeyer, H. (1993) *Vitis* 32: 61-62.
2. Rapp A., Versini G. (1997) *Vitic. Enol. Sci.* 51: 193-203.
3. Köhler H. *et al.* (1996) *Rebe & Wein*: 7: 213-218.
4. Köhler H.-J. *et al.* (2001) In *Deutsches Weinbau-Jahrbuch*, 52. Jhg. Waldkircher Verlag, pp 219-228.
5. Hühn T. *et al.* (2000) In *Deutsches Weinbau-Jahrbuch*, 51. Jhg. Waldkircher Verlag, pp 229-236.
6. Hoenicke K., Simat T.J., Steinhart H., Christoph N., Gessner M., Kohler H.-J. (2002) *Anal. Chim. Acta* 458: 29-37.
7. Rauhut D., Kuerbel H., Fischer S., Beisert B. (2007) In *Recent Highlights in Flavour Chemistry & Biology, Proceedings of the 8th Wartburg Symposium, Deutsche Forschungsanstalt für Lebensmittelchemie*, pp 314-318.
8. Schmarr H.-G., Ganss S., Sang W., Potouridis T. (2007) *J. Chromatogr. A* 1150: 78-84.
9. Instructions manual Chem ElutTM extraction cartridges 16-255-1 10/05.

A FAST AND SIMPLE PROCEDURE FOR THE SELECTIVE ISOLATION OF POLYFUNCTIONAL MERCAPTANS IN A MICRO SOLID PHASE EXTRACTION CARTRIDGE

L. MATEO-VIVARACHO, J. Cacho, and V. Ferreira

Laboratory for Flavour Analysis and Enology. Analytical Chemistry, Faculty of Sciences, University of Zaragoza, 50009, Spain

Abstract

Commonly used strategies for the analysis of polyfunctional mercaptans, make use of the complexing properties of the thiol group to certain forms of mercury. Because of the fact that p-hydroxymercury benzoate salt (p-OHHgB) is strongly retained in some neutral polymeric resins, a new solid phase method (SPE) method based on the extraction-isolation of mercaptans by forming complex with p-OHHgB has been developed. A micro-SPE LiChrolut-EN cartridge previously imbibed in a solution of p-OHHgB can retain the mercaptans contained in more than 100 mL of wine. Although originally the method was devised as just a qualitative screening procedure, it has shown a more than acceptable analytical behaviour. The method has been applied to the determination of some key polyfunctional mercaptans of wine and coffee, reaching detection limits in the ng L^{-1} level. The major advantage of the method is that it is fast and sample manipulation is kept minimal.

Introduction

Volatile thiols such as 2-methyl-3-furanthiol (MF), 2-furfurylthiol (FFT), 4-mercapto-4-methyl-2-pentanone (MP), 3-mercaptohexylacetate (MHA) and 3-mercaptohexanol (MH), are very strong-smelling molecules that play an outstanding role on the aroma of numerous foods such as coffee [1], meat [2], onions [3], green tea [4] and wine [5]. Although the contribution of polyfunctional mercaptans to the sensory characteristics of some wines is very important, there are just a few reports on methods for their analytical determination. The most commonly used strategies for the analysis of these compounds, leaving aside the recently proposed methods based on derivatisation of thiols with 2,3,4,5,6-pentafluorobenzyl bromide [6], make use of the complexing properties of the thiol group.

Some authors use a selective extraction of thiols from an organic solution with an aqueous solution of p-OHHgB [7,8], while other authors use mercury covalently bonded to a certain resin or sorbent [9]. The use of aqueous solutions of p-OHHgB in order to obtain a selective enrichment of mercaptans is an appealing idea; nevertheless, because of the fact that p-OHHgB salt is strongly retained in some neutral polymeric resins, a SPE method based on the extraction-isolation of mercaptans by forming complex with p-OHHgB inside the cartridge has been developed. According to this, the main goals of the present work are to study the different variables affecting the isolation of polyfunctional thiols in a micro-SPE cartridge of just 20 mg of LiChrolut-EN resins previously imbibed in a solution of p-OHHgB.

Experimental

Method. 20 mg LiChrolut-EN solid phase extraction cartridge are prepared in 1 mL standard polypropylene SPE reservoirs. The cartridges are conditioned and rinsed with 1 mL of a 0.1 M in TRIS solution, pH 7.2. Then, 1 mL of a 2 mM in p-OHHgB solution in TRIS 0.1 M, pH 7.2, is poured into the cartridge. Once the p-OHHgB is fixed in the bed, 100 mL of wine, spiked with 1-heptanethiol, 4-methoxy- α -toluenethiol, 4-methoxy-2-methylbutan-2-thiol and 3-mercapto-3-methyl-butyl-formate as internal and surrogate standards, are percolated through the cartridge. After this, the cartridge is rinsed with 5 mL of an aqueous solution containing 40 % methanol (v/v) and 5 g L⁻¹ of tartaric acid buffered at pH 3. After this, non polar impurities are removed from the cartridge by rinsing with 6 mL of pentane. Before elution, the bed is dried with a N₂ stream. Complexes formed in the cartridge are eluted with 600 μ L of dichloromethane 100 mM in 1,4-dithioerythritol. The extract is washed with 5 mL water and transferred to a 2 mL vial containing a small amount of anhydrous Na₂SO₄. After adding the chromatographic internal standard, 20 μ L of this extract are injected and analysed by GC-quad-MS in the conditions described below.

Gas chromatography-mass spectrometry. Apparatus: Shimadzu QP-2010 GC with a quadrupole mass spectrometric detection system. Injector: Optic 3 from ATAS-GL (Veldhoven, The Netherlands); injection conditions: 20 μ L of extract are injected in a packed liner for large volume injection. The initial temperature of the injector is 55 °C and after 17 s it is heated at 5 °C s⁻¹ up to 250 °C. The carrier gas is He, flowing through the column initially at 0.6 mL min⁻¹. 17 s after the injection the flow is increased to 1.8 mL min⁻¹ for 3 min. After this period it is fixed at 1 mL min⁻¹. The split valve is opened the 1st 17 seconds of analysis, closed the 3 following min, and opened again for the rest of the analysis. The column is a DB-WAXETR from J&W Scientific, 60 m x 0.25 mm I.D., with 0.25 μ m film thickness. The column initial temperature is 45 °C for 2 min, heated to 110 °C at 5 °C min⁻¹, then to 230 °C at 9 °C min⁻¹ and finally to 250 °C at 15 °C min⁻¹; remaining at that temperature for 15 min. The ion source used is the Electronic Impact one at 220 °C; the interface was kept at 240 °C. The analytes and internal standards ions are acquired in Single Ion Monitoring (SIM) at 0.30 s⁻¹/point.

Calibration. Four different wines (two white wines, a young red wine and an aged red wine) were spiked with different masses of the analytes (four replicated levels plus the unspiked sample) and analysed according to the proposed procedure. The peak areas obtained in the corresponding ionic chromatograms were normalized by those of the internal standards (3-mercapto-3-methyl-butyl-formate for MF and MH, 4-methoxy-2-methylbutan-2-thiol for MP and MHA, 1-heptanethiol for FFT). With the data, a calibration graph was calculated for each sample.

Method development and validation. The amount of p-OHHgB fixed in the cartridge was measured by SS-GFAAS (Solid Sampling-Graphite Furnace Atomic Absorption Spectrometry). Rupture curves for the Hg loaded in the cartridge were made and mercury losses during the load and washing-up steps were studied. Leaving aside the measurement of Hg, different wine sample volumes (50-250 mL), washing up polar solutions (aqueous solutions of TRIS, tartaric, acetic or phosphoric acids at different pHs values) and non polar and washing up volumes (5-15 mL) were checked to ensure a 100 % extraction of the analytes and a large removal of interfering compounds.

Results

The first aim of this work has been the study of the selective retention of polyfunctional mercaptans in a micro-SPE cartridge containing organomercury salts. A thorough investigation about how to fix p-OHHgB on different polymeric sorbents has been developed and the specific retention properties of these materials, packed in micro-SPE format have been applied to develop a suitable method for the quantification of these compounds in wine. The amount of Hg-salt fixed in different beds (Bond Elut ENV from Varian and LiChrolut EN from Merck) was measured by SS-GFAAS according to the method described by M. Resano *et al.* [10]. At pH 10 there wasn't any retention of the Hg-salts in the sorbents and the best results were achieved by loading the mercury in TRIS 0.1 M at pH 7.2. This result made us think that only the neutral or mono charged forms of p-OHHgB are effectively retained by the sorbent and that the divalent form present at higher pHs is not retained, which should be taken into account in the method development.

LiChrolut EN resins were particularly efficient at retaining p-OHHgB at neutral pH, and the beds containing the Hg-salt can efficiently work as "affinity"-microcolumns to mercaptans, retaining some of the advantages of these kinds of polymeric sorbents. The retention of sulphur compounds is based on the specific binding to Hg, and the elution can take place well by the cleavage of the S-Hg bond by the addition of large amounts of a competitive mercaptan, or by the elution of the complex at high pHs. This fact makes it possible to obtain nearly infinite breakthrough volumes for mercaptans with more than 5 carbon atoms, as long as the pH is kept low; furthermore, satisfactory breakthrough volumes are obtained for smaller sulphur compounds. The proposed procedure was applied to wine. At the natural acid pH of wines, it was demonstrated that the breakthrough of mercaptans was higher than 100 mL for a micro-SPE cartridge containing only 20 mg of sorbent. Different rinsing solutions and volumes were studied and, at the same time, different amounts of the Hg present in the bed were assayed as can be seen in Figure 1.

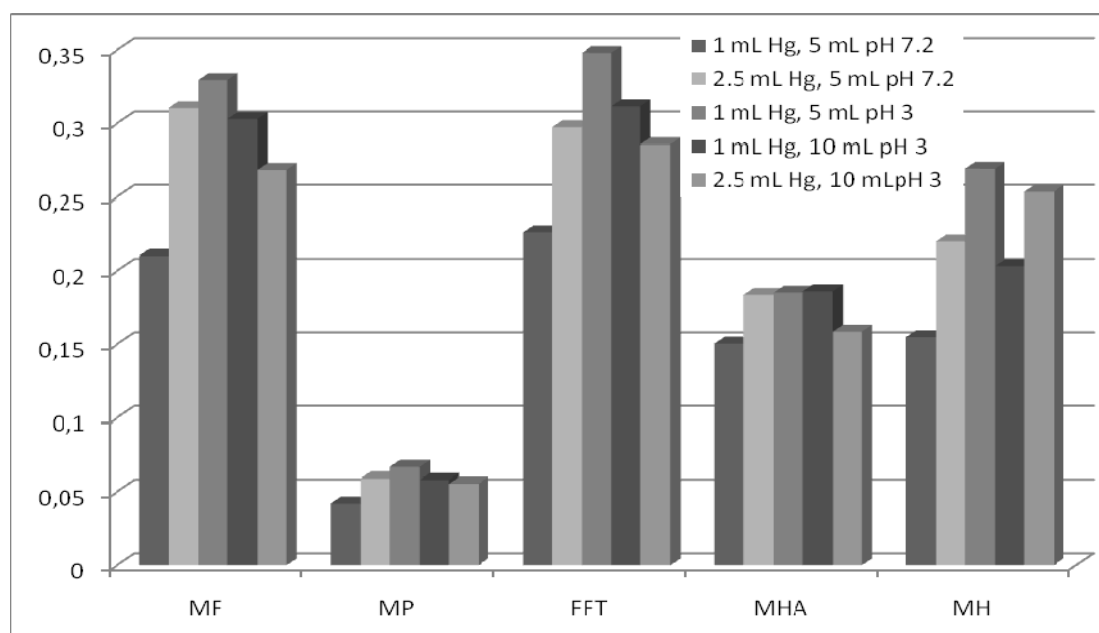


Figure 1. Influence of the amount of p-OHHgB loaded in the cartridge and effect of the pH and the volume of the polar washing-up solution.

The result of these assays showed, as expected, that the higher the pH of the washing up solution, the higher the losses of analytes although interfering fatty acids are removed more efficiently. The best results were obtained when the Hg-salt is loaded from 1 mL of a 2 mM in p-OHHgB solution and when the rinsing is carried out with 5 mL of a pH 3 solution with 40 % methanol.

The versatility of this technique has been demonstrated both concentrating light mercaptans present in aqueous solutions and developing a specific isolation method for polyfunctional mercaptans in wine. Analytical properties of such method can be seen in Table 1.

Table 1. Method linearity and detection limits (LD).

Analyte	RSD %	LD (ng L ⁻¹)	Average slope ^a	Average ^a R ²	Calibrated range (ng L ⁻¹)
MF	9.0	12.0	0.000281±7.00x10 ⁻⁶	0.9901	0-500
FFT	6.5	1.5	0.0267±6.38x10 ⁻³	0.9989	0-50
MP	12.3	1.5	0.000872±1.27x10 ⁻⁴	0.9978	0-50
MHA	8.5	5.0	0.00537±9.12x10 ⁻⁴	0.9988	0-500
MH	7.8	13.0	0.00217±4.49 x10 ⁻⁴	0.9967	0-1000

Data are peak areas normalized by that of the corresponding internal standard.

^a Average of 4 slopes calculated in four independent experiments in 4 different wines (n=5).

The proposed strategy is a competitive alternative for the fast and simple qualitative isolation of mercaptans from liquid matrixes and it can also be successfully applied to the development of quantitative procedures. As a demonstration (Table 1), the method has been applied to the determination of key polyfunctional mercaptans in wine, reaching detection limits in the ng L⁻¹ level and acceptable repeatability and linearity (0.990 < R² < 0.999). The major advantage of the method is that it is fast and sample manipulation is kept minimal.

References

1. Semmelroch P., Grosch W. (1995) *Food Sci. Technol.* 28: 310-313.
2. Kersch R., Grosch W. (1998) *J. Agric. Food Chem.* 46: 1954-1958.
3. Granvogl M., Christlbauer M., Schieberle P. (2004) *J. Agric. Food Chem.* 52: 2797-2802.
4. Kumazawa K., Kubota K., Masuda H. (2005) *J. Agric. Food Chem.* 53: 5390-5396.
5. Tominaga T., Dubourdieu D. (2006) *J. Agric. Food Chem.* 54: 29-33.
6. Mateo-Vivaracho L., Cacho J., Ferreira V. (2008). *J. Chromatogr. A* 1185: 9-18.
7. Darriet P., Tominaga T., Lavigne V., Boidron J.-N., Dubourdieu, D. (1995) *Flav. Fragr. J.* 10: 385-392.
8. Ferreira V., Ortin N., Cacho J. F. (2007) *J. Chromatogr. A* 1143: 190-198.
9. Schneider R., Kotseridis Y., Ray J.L., Augier C., Baumes R. (2003) *J. Agric. Food Chem.* 51: 3243-3248.
10. Resano M., Garcia-Ruiz E., Aramendia M., Belarra M.A. (2005) *J. Anal. Atom. Spectr.* 20: 1374-1380.

SOLID-PHASE EXTRACTION AS A ROUTINE METHOD FOR COMPARING KEY AROMA COMPOUNDS IN FRUITS

J.K. PARKER¹, E. Tsormpatsidis², J.S. Elmore¹, A.Wagstaffe², and D.S. Mottram¹

¹ Department of Food Biosciences, University of Reading, Whiteknights, Reading, RG6 6AP, UK

² School of Biological Sciences, University of Reading, Whiteknights, Reading, RG6 6AP, UK

Abstract

In some fruits, particularly strawberries, pineapples and melons, polar furans such as 2,5-dimethyl-4-hydroxy-3(2*H*)-furanone are known to be extremely important in defining the aroma. However, the techniques which are used routinely for volatile analysis tend to discriminate against such small polar compounds. In this study, solid phase extraction has been used to study the aroma profile of both strawberries and melons. The profile of a cultivated strawberry (*Fragaria x ananassa* L., cv. Elsanta) was compared to that of a cross between a cultivated and a wild strawberry (*Fragaria x ananassa* L., cv. Mara des Bois). Significant differences were found between the two cultivars. 2,5-Dimethyl-4-hydroxy-3(2*H*)-furanone and 2,5-dimethyl-4-methoxy-3(2*H*)-furanone were significantly higher in the wild cultivar. The same method was used to carry out a preliminary comparison of two varieties of musk melon (*Cucumis melo* L.): a new acidic cultivar was compared to a standard Galia melon. 4-Hydroxy-5-methyl-3(2*H*)-furanone was detected in both cultivars and trace amounts of 2,5-dimethyl-4-hydroxy-3(2*H*)-furanone were detected in the new cultivar.

Introduction

The odour active components of strawberries have been studied for many years using a number of extraction techniques. Although esters are known to be very important in strawberry aroma, Schieberle (1) showed using aroma extract dilution analysis (AEDA) that 2,5-dimethyl-4-hydroxy-3(2*H*)-furanone had the highest dilution factor, followed by butanoic acid, acetic acid and 3-hexenal, while 2,5-dimethyl-4-methoxy-3(2*H*)-furanone had the lowest dilution factor of the 15 volatiles quoted. Jetti (3), however, studied ten strawberry genotypes and showed that the levels of 2,5-dimethyl-4-methoxy-3(2*H*)-furanone varied considerably across the set. In those where it was present, the odour-activity values (OAV) were very high – up to 100 times greater than any other volatile component analysed. These two furanones are clearly extremely important in the aroma of fresh strawberries. In this study, a relatively rapid solid phase extraction (SPE) method, which retains semi-polar compounds such as furanones, has been used to compare the levels of these furanones, and other semi-polar compounds, in two strawberry cultivars.

The flavour of musk melons has also received much attention. Schieberle (4) showed using AEDA that esters and C6 aldehydes were the primary odorants in melons, but other authors stress the importance of C9 compounds (5) and sulphur-compounds (6) in imparting characteristic melon notes. However, Hayata (6) reported that in addition to thioesters and C9 compounds, a number of caramel-like odours

were amongst those with high odour dilution factors, one of which was identified as 2,5-dimethyl-4-hydroxy-3(2*H*)-furanone. In this paper, SPE has been used to compare the levels of 2,5-dimethyl-4-hydroxy-3(2*H*)-furanone and other semi-polar compounds present in two cultivars of musk melons. A novel acidic cultivar, which is described as “fresh and zesty” has recently emerged on the UK market. This was compared to a standard Galia melon.

Experimental

Preparation of strawberry extract. Strawberries were grown in polytunnels at the School of Biological Sciences Laboratories Field Unit, Shinfield, Reading, UK. Both varieties were grown under identical conditions using a standard commercial nutrient solution applied through a drip irrigation system. Strawberries were collected from eight Elsanta plants and from eight Mara des Bois plants. They were harvested early in the morning from the same flowering date and position on the truss for each plant. Undamaged strawberries (~200 g), were homogenized using a hand held blender and an aliquot of the homogenized purée (25 g) was placed in a centrifuge tube and shaken on a Vortex mixer for 1 minute. The tubes were then centrifuged for 20 minutes at 10,000 rpm at 4°C and the mixture was then filtered under vacuum through 5cm Buchi funnels. Following filtration, 0.05 ml of a solution of 3-chlorophenol (1 mg/ml in 10% MeOH/water) was added to the filtrate as an internal standard.

Preparation of melon extract. Three of the novel acidic melons and three standard Galia melons were obtained locally. Portions of skinned, deseeded melon (100 g) were chopped and blended in a food processor. Aliquots (30 g) were centrifuged, filtered as above and 0.1 ml of the internal standard added.

Solid Phase Extraction (SPE). Phenomenex Strata-X 33 µm tubes (12 ml) were used for the extraction. Strata-X is a functionalised polymer of styrene-divinylbenzene with a relatively high surface compared to standard reverse phase polymers. It has a range of different retention mechanisms (hydrophobic, hydrophilic and π - π interactions) which make it particularly suited to recovering a wide range of compounds. The tubes were conditioned with 10 ml each of MeOH and HPLC grade water. The filtered fruit extracts were applied to the tubes which were then washed twice with 10 ml water, dried on a vacuum manifold for 45 min and eluted using 10 ml of methyl acetate. The final extract was concentrated to 2 ml under a stream of nitrogen. Volatile identification was performed using a Hewlett-Packard 6890/5975 GC-MS equipped with an autosampler. A DB Wax column (30 m, 0.25 mm i.d., 0.25 µm film thickness, Agilent, UK) was used for separation of volatiles.

Results

Comparison of strawberry cultivars. The volatile components of cultivated strawberries and wild strawberries are well defined (1, 2). Over 50 peaks were found in the SPE extract, many of which are still unconfirmed or unknown. Twelve compounds were selected for semi-quantification (Table 1), all of which showed significant differences between the two cultivars. The Mara des Bois had significantly higher levels of a number of volatiles, in particular the two furanones (2,5-dimethyl-4-hydroxy-3(2*H*)-furanone and 2,5-dimethyl-4-methoxy-3(2*H*)-furanone) which make an important contribution to strawberry aroma. Elsanta had significantly higher levels of 2-hexenal, γ -decalactone and linalool. The absolute concentration of 2,5-dimethyl-4-

hydroxy-3(2*H*)-furanone was calculated using a five point calibration curve, each point being determined in triplicate. This gave values of 23 mg/kg and 50 mg/kg for Elsanta and Mara des Bois respectively, taking into account recovery rates of 70% (determined experimentally using 10ml of an aqueous solution (100 µg/ml)).

Table 1. Comparison of the polar compounds found in two cultivars of strawberry

Compound	LRI ^a	ID ^b	Elsanta ^c (n=8)	Mara des Bois (n=8) ^d	Sig ^e
2-Hexenal	1193	A	2.2 ^f	0.7	***
Methyl 3-hydroxybutanoate	1445	A	nd	1.0	***
Linalool	1524	B	0.2	nd	***
2-Methylpropanoic acid	1533	A	0.4	1.6	***
2,5-Dimethyl- 4-methoxy-3(2 <i>H</i>)furanone	1554	A	0.7	3.5	***
Butanoic acid	1589	B	7.7	5.0	*
2-Methylbutanoic acid	1634	A	2.0	1.5	*
2,5-Dimethyl-4-hydroxy-3(2 <i>H</i>)furanone	1980	A	3.8	8.0	***
Nerolidol	2006	B	0.2	0.1	*
γ-Decalactone	2094	A	1.3	nd	***
γ-Dodecalactone	2320	B	0.05	0.1	***
<i>trans</i> -Cinnamic acid	>2500		9.6	22	***

^a LRI on a DBWax column, ^b LRI compared with: A authentic standard, B literature value, ^c *Fragaria x ananassa* L., cv. Elsanta, ^d *Fragaria x ananassa* L., cv. Mara des Bois, ^e Significance from T-test where *** (p < 5%), ** (p < 1%), * (p < 0.1%) and ns = not significant, ^f Amount (mg/kg) using response factor of 1, nd = not detected

Comparison of melon cultivars. Fourteen compounds were selected for semi-quantitation (Table 2). 4-Hydroxy-5-methyl-3(2*H*)-furanone was detected in both cultivars and trace amounts of 2,5-dimethyl-4-hydroxy-3(2*H*)-furanone were found in the new variety. Both furanones were identified by three assessors when the SPE extract was used for preliminary GC-Olfactometry analysis. They were described as having a strong caramel/candyfloss type note and were the major aromas reported in the extract. Absolute amounts of the two furanones were determined using calibration curves and recovery studies. Although 2,5-dimethyl-4-hydroxy-3(2*H*)-furanone was only present in the new cultivar at 0.1 mg/kg, this is 100 times higher than the reported odour threshold (0.001 mg/kg) (8). 4-Hydroxy-5-methyl-3(2*H*)-furanone was present at 8 mg/kg and 15 mg/kg for the Galia and the new cultivar respectively, which is within the range of odour thresholds quoted (2-23 mg/kg) (8).

Another set of compounds which dominated the chromatogram of the new cultivar was a group of acetates and diacetates. These have been found in melon previously (7), and have relatively high odour thresholds so they may not have an organoleptic impact. However, the different amounts of 3-(methylthio)propyl acetate and 3,6-nonadienol may be important in characterising the aromas of the two cultivars. Further work is being carried out.

Table 2. Comparison of the polar compounds found in two cultivars of melon.

Compound	LRI ^a	ID ^b	Galia (n= 3)	New Cultivar (n= 3)	Sig ^c
<i>Furanones</i>					
2,5-Dimethyl-4-hydroxy-3(2 <i>H</i>)-furanone	2000	A	nd	0.02 ^d	**
4-Hydroxy-5-methyl-3(2 <i>H</i>)-furanone	2060	A	1.7	3.3	ns
<i>Acetates</i>					
2,3-Butanediol diacetate (1)	1462	A	0.03	1.0	ns
1,2-Propanediol diacetate	1483	B	0.26	0.2	ns
2,3-Butanediol diacetate (2)	1496	A	0.03	0.6	ns
1,2-Ethandiol diacetate	1513	B	0.07	0.4	*
2,3-Butanediol monoacetate (1)	1531	B	0.02	0.06	ns
2,3-Butanediol monoacetate (2)	1544	B	0.03	0.2	ns
3-(Methylthio)propyl acetate	1594	A	nd	0.3	***
Phenylethyl acetate	1775	A	nd	1.1	***
Benzyl acetate	1689	A	0.09	3.1	*
<i>Alcohols</i>					
(<i>E,Z</i>)-3,6-Nonadienol	1716	B	0.3	0.01	**
Benzyl alcohol	1828	B	0.9	0.3	ns
Phenylethyl alcohol	1865	B	0.1	0.1	ns

^a LRI on a DBWax column, ^b LRI compared with: A authentic standard, B literature value, ^c Significance from T-test where *** (p < 5%), ** (p < 1%), * (p < 0.1%) and ns = not significant, ^d Amount (mg/kg) using response factor of 1, nd = not detected

References

1. Schieberle P., Hofmann T. (1997) *J. Agric. Food Chem.* 45: 227-232.
2. Ulrich D., Rapp A., Hoberg E. (1995) *Z. Lebensm. Unters.-Forsch.* 200: 217-220.
3. Jetti R.R., Yang E., Kurnianta A., Finn C., Qian M.C. (2007) *J. Food Sci.* 72: S487-S496.
4. Schieberle P., Ofner S., Grosch W. (1990) *J. Food Sci.* 55: 193-195.
5. Wylie S.G., Leach D.N. (1992) *J. Agric. Food Chem.* 40: 253-256.
6. Hayata Y., Sakamoto T., Manebrat M., Li X., Kozuka H., Sakamoto K. (2003) *J. Agric. Food Chem.* 51: 3415-3418.
7. Wylie S.G., Leach D.N. (1990) *J. Agric. Food Chem.* 38: 2042-2044.
8. Rychlik M., Schieberle P., Grosch W. Compilation of Odor Thresholds, Odor Qualities and Retention Indices of Key Food Odorants, Deutsche Forschungsanstalt für Lebensmittelchemie and Institut für Lebensmittelchemie der Technischen Universität München.

DESIGN OF AN ARTIFICIAL CRUSHING FINGER DEVICE FOR RAPID EVALUATION OF ESSENTIAL OILS FROM AROMATIC PLANTS LEAVES

C. EL KALAMOUNI^{1,2}, C. Raynaud^{1,2}, and T. Talou^{1,2}

¹ LCA Université de Toulouse ; INP ; LCA (Laboratoire de Chimie AgroIndustrielle); ENSIACET, 4 Allées Emile Monso, F-31029 Toulouse, France

² INRA (Laboratoire de Chimie AgroIndustrielle) ; F-31029 Toulouse, France

Abstract

A special designed apparatus based on “Scratch' n Sniff” concept was developed for copying the crushing of aromatic plants leaves between fingers. The so-called Crushing Finger Device (CFD) was equipped with a TENAX trap for a rapid analysis of emitted volatiles by GC-MS. The CFD efficiency was presently evaluated by comparison of chromatographic profiles obtained with crushed, uncrushed leaves and essential oil of costmary (*Tanacetum Balsamita*) fresh leaves, chosen as model plant.

Introduction

A decade ago, several treks (NEBLINA, TASTETREK) were performed by companies of aromatic industry sector both in South-America and West-Africa in order to investigate the aromatic potentialities of rare exotic plants for novel flavours and fragrances formulations. As Midi-Pyrenees region (Southwest of France) has a rich and unvalorised wild vegetal heritage, especially for aromatic and medicinal plants, the MIPAROM Trek was conducted in order to collect and analyse various regional medieval (aka forgotten) aromatic plants, e.g. *Achillea millefolium*, *Tanacetum balsamita*, *Agastache foeniculum*, *Meum athamanticum*, *Chrysantemum balsamita*, *Myrris odorata*, *Calamintha gradiflora*. As a consequence of a global bibliographical survey study based on historical books, library archived documents and computerized data banks, a list of 20 regional plants to be investigated has been precised [1]. But as such plants being rare or their harvesting problematic as they were protected, sampling could be limiting. We have developed a strategic approach based either on the use of a specific/high effective sampling system with a classic detection or a classic sampling with a specific/ultra sensitive detection. If this last methodology was based on the coupling of SPME to Comprehensive GC (GCxGC-TOFMS) (current works) the first ones was based on a self designed apparatus [2], allowing to copy the crushing of leaves between fingers used by farmers or flavourists to sensorially evaluate the odour of aromatic plants. The so-called Crushing Finger Device (CFD) was based on a modified artificial mouth and has the objective to perform a rapid evaluation of essential oil content with only a couple of leaves through a controlled Dynamic HeadSpace (DHS) concentration of volatiles emitted by crushed fresh leaves. In the present paper we report the comparison of the chromatographic profiles of essential oil of leaves of our model plant, costmary (*Tanacetum Balsamita*), with the ones obtained with leaves without crushing (DHS) and with leaves processed by CFD-DHS.

Experimental

Materials. Costmary (*Tanacetum Balsamita*) plants using in the present study were collected at their optimum biological stage in Midi-Pyrenees area (south West France) in April-May 2008.

Dynamic HeadSpace with crushing (CFD/DHS). Two or three entire fresh leaves of costmary corresponding to 500mg were placed in the glass cell of the CFD thermostated at 25°C. A flow of purified nitrogen (100 ml/min) passed through the leaves for 5 min to trap the volatiles into a TENAX TA trap positioned at the top of the device. The crushing of leaves was set up by a motorized Teflon piston having transverse and rotative movements. 4 replicates were performed

Dynamic HeadSpace without crushing (DHS). The CFD piston was removed from the device and fresh leaves were carefully placed without damaging tissues. Operating conditions were applied as described before with 3 replicates performed.

Isolation of essential oil (EO). 100g of the aerial part of fresh costmary plants was hydrodistilled for 3h at 100°C by using a Clevenger-type apparatus in order to obtain essential oils. 4 replicates were performed.

Gas chromatographic analysis. Volatile analysis (EO) were performed with a Hewlett Packard 5890 SERIES II gas chromatograph equipped with FID and an Agilent 5973 Network GC-MS. (DHS, DHS/CFD) analysis were performed with a Perkin Elmer Clarus 500 GC-MS-FID equipped with a TurboMatrix TD thermodesorber. A fused-silica DB5 (0.25mm x 30m, 0.25µm film thickness) was used throughout this study. Temperature program used was: 30°C for 5min, then 5°C/min up to 200°C and 10 min isotherm at 200°C. γ-Terpinene was used as standard to estimate the concentration of volatiles compounds in CFD in µg/kg of dried material. Identification of volatiles was based on comparison of their retention times with those of authentic samples (calculated RI based on n-hydrocarbons series kit) and on computerized matching with commercial mass spectra data bank (NIST 2005 and WILEY) and Adams library [3].

Results

The composition of the yellow coloured essential oil obtained with a yield of 0,53% on a dry weight basis, was conform to literature [4-8] while thujone (cis and trans isomers) and 1,8-cineole were the main identified volatiles (Table 1). *trans*-Thujone was reported as the main compound of both essential oil (63.3%) and emitted volatiles from uncrushed (82.5%) and crushed ones (67.7%). The yield of emitted volatiles by fresh costmary leaves was by increasing order: CFD / DHS >> DHS.

The consequence of the crushing of the leaves by CFD was the explosion of the vesicles of storage of essential oil and the release of the main volatile compounds of the plant in atmosphere. The comparison of the GC-profiles of crushed leaves (Figure 1A) *versus* leaves without crushing (Figure 1B) showed an increase of number of top notes compounds (4 to 20). The major volatiles emitted during the crushing of leaves were 3-methylhexanal (0.3%), α-thujene (0.2%), α-pinene (0.7%), β-terpinene (2.4%), β-pinene (0.4%), 1,8-cineole (21%), γ-terpinene (0.5%), p-mentha-1,4(8)-diene (0.2%) and *cis*-thujone (3.3%). In case of essential oil, the minor compounds reported were 1,8-cineole (27.5%), γ-terpinene (0.1%), *cis*-thujone (4.2%), terpineol-4 (0.6%), germacrene D(0.9%), bicyclo-germacrene (0.1%), α-terpineol (0.2%), and β-eudesmol (0.4%) and could be assimilated to back notes components generated during hydrodistillation.

Table 1. Volatile compositions of essential oil, uncrushed and crushed fresh leaves of *Tanacetum balsamita*

Peak	Volatile Compound	RI (DB-5)	EO (n=4) %	DHS (n=3) %	CFD (n=4) %	CFD [c] µg/kg/5min	CFD [c] SD %
1	Hexanal, 3-methyl	738			0.3	0.5	11
2	1-Butanol, 2-methyl	742			0.1	0.2	23
3	1-Octen	791			0.4	0.5	15
4	3-Hexen-1-ol	857			0.3	0.4	34
5	1-Butanol, 3methyl-acetate	879			0.1	0.1	17
6	α-Thujene	926			0.2	0.1	23
7	α-Pinene	933		0.6	0.7	0.9	12
8	bicyclo[3.1.0]Hex-2-ene, 4-methylene-1-(1-methylethyl)	944			0.1	0.1	18
9	Camphene	950			0.1	0.2	7
10	β-Terpinene	973		1.7	2.4	3.7	26
11	β-Pinene	978		1.5	0.4	0.5	9
12	cis-Pinene-3-ol	989			0.1	0.3	25
13	3-Hexen-1-ol, acetate	1004			0.4	0.3	22
14	NI	1012			0.2	0.6	21
15	o-Cymene	1017			0.4	0.5	18
16	p-Pymene	1023	tr				
17	1,8-Cineole	1031	27.5	12.6	21	21.3	4
18	γ-Terpinene	1057	0.1		0.5	0.6	13
19	N.I.	1071	0.3				
20	N.I.	1072			0.2		
21	p-Mentha-1,4(8)-diene	1086			0.2	0.2	19
22	Butanoic acid, 2-methyl-3 ethylbutylester	1100			0.2	0.3	49
23	cis-Thujone	1107	4.2	1.1	3.3	4.9	9
24	trans-Thujone	1121	63.3	82.5	67.7	103.8	27
25	4-Terpineol	1166	0.6				
26	α-Terpineol	1185	0.2				
27	Sabinyl acetate	1282	tr				
28	Germacrene-D	1476	0.9				
29	bicyclo-Germacrene	1489	0.1				
30	β-Eudesmol	1650	0.4				

tr : Trace (<0,1%), NI : unidentified

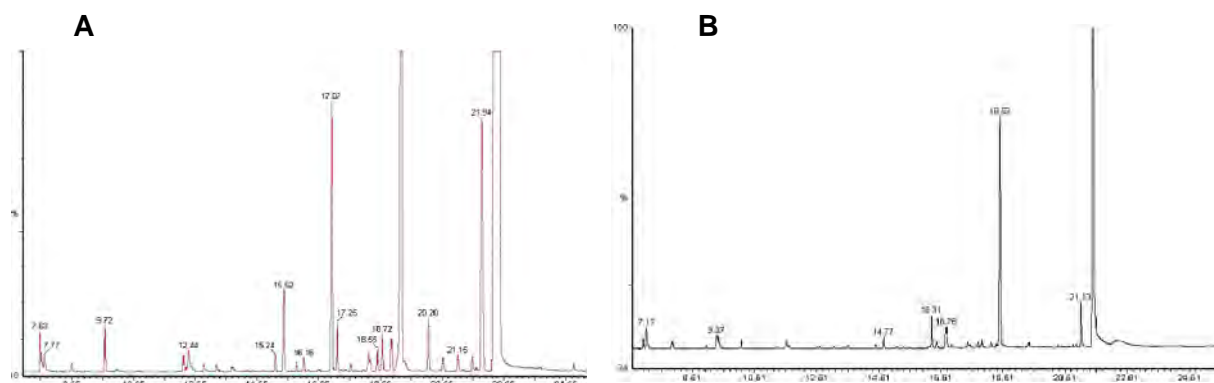


Figure 1. CFD/DHS-GC profile of crushed leaves (A) and DHS-GC profile of uncrushed leaves (B)

These preliminary results showed that GC profiles of essential oil (Figure 2) and volatiles emitted from crushed leaves (Figure 1A) by using the CFD had similarities for top and heart notes (*cis*-, *trans*-thujone and 1,8-cineol as major constituents) but also differences, especially for back notes components due to the extraction technique used (hydrodistillation vs dynamic headspace).

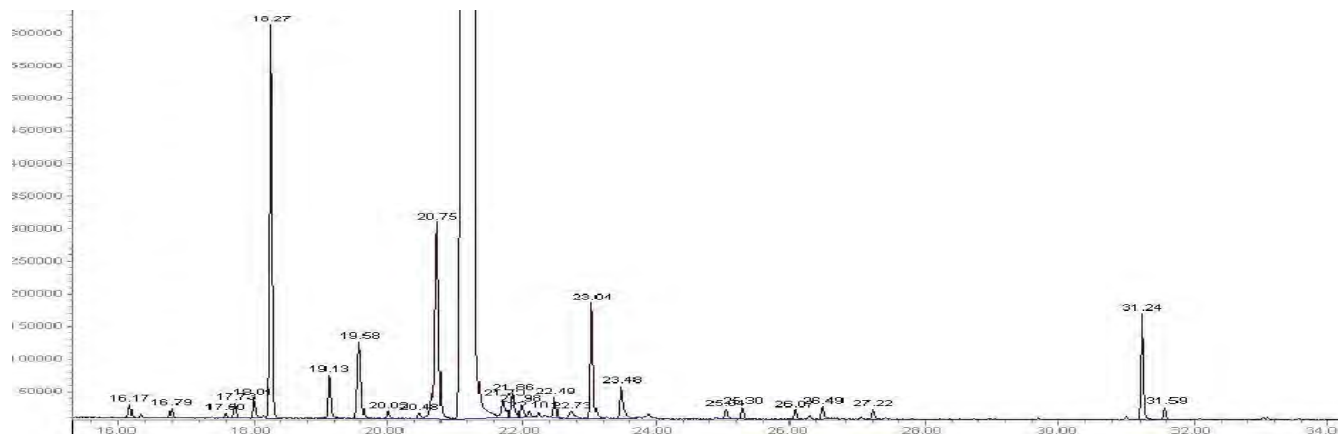


Figure 2. GC profile of Essential Oil of *Tanacetum balsamita*.

The coupling CFD/DHS, demonstrated the potential for rapid evaluation of essential oils from aromatic plant leaves. Indeed, this novel system allowed having a representative finger-print of fresh plant volatiles with similar top and heart notes than the essential oils (qualitatively and quantitatively). Comparison of results obtained with fresh costmary leaves by CFD/DHS-GC/MS vs SPME-GCxGC/TOFMS is in progress. The generalization of its use with various medieval aromatic plants from Midi-Pyrénées is suggested. Coupling of CFD/DHS and CFD/SPME with Fast-GC and GC-O for quality control and aroma key compounds identification purposes is being carried out.

References

1. El Kalamouni C. INP Toulouse *Doctorate Thesis*, in progress.
2. Talou T., El Kalamouni C. and Raynaud C. (2008) *Rapid evaluation of essential oil quality based on instrumentalized crushed fresh leaves volatiles assessment*. French Patent trading.
3. Adams R.P. (2001) *Identification of Essential Oils Components by Gas Chromatography/Quadrupole Mass Spectroscopy*. Allured Publishing Corporation, Carol Stream, IL.
4. Voigt R.F., Rogers C.H., Fischer E.B. (1938) *J. Am. Phar. Ass.*, 27: 643-654.
5. Bylaite E., Venskutonis R., Roozen J., Posthumus M. (2000) *J. Agric. Food Chem.* 48: 2409-2414.
6. Gallori S., Flamini G., Bilia A., Morelli I., Landini A., Vincieri F. (2001) *J. Agric. Food Chem.* 49: 5907-5910.
7. Monfared A., Davarani S., Rustaiyan A., Masoudi S. (2002) *J. Ess.Oil Res.* 14: 1-2.
8. Baser K.H.C., Demirci B., Tabanca N., Ozek T., Goren N. (2001) *Flav. Frag. J.* 16: 195-200.

ANALYSIS OF LIMITED SUBSTANCES IN COMPLEX FLAVOURINGS BY DIRECT THERMAL DESORPTION AND MULTIDIMENSIONAL GAS CHROMATOGRAPHY - MASS SPECTROMETRY

C. IBÀÑEZ and J. Solà

LUCTA S.A., Fragrances, Flavours & Feed Additives, P.O.Box 1112, 08080, Barcelona, Spain

Abstract

A direct thermal desorption and analysis by multidimensional gas chromatography mass spectrometry / flame ionisation detection method was investigated to extract and quantify some substances restricted by legislation, in complex hydrosoluble viscous flavourings. Direct thermal desorption gave better recoveries than solvent extractions while reducing the labour involved, and also decreased manipulation errors, emulsion formation and environmental hazards from solvents. Deans-type multidimensional gas chromatography using Agilent's capillary flow technology permitted us to obtain adequate separations and good peak shapes from previously overlapping or distorted peaks, using heart cut techniques and peak cryofocusing. We achieved optimisation of different operational parameters including the injection system and the temperatures for desorption and cryofocusing. An authentic tea flavouring sample was analysed using the optimised methods. Advantages and drawbacks of the system were evaluated.

Introduction

The analysis of some trace level substances restricted by legislation, including pyridine, diethylenglycol monoethyl ether (carbitol), menthyl formate, sorbic acid, benzoic acid, BHT and BHA present at the ppm level in complex hydrosoluble viscous flavourings is limited by the difficulties of typical lengthy and tedious solvent extractions (1). Emulsion formation and poor recoveries for carbitol, and, to some extent, for BHT, BHA, and sorbic acid have been observed. Furthermore, peak overlapping and distortion for carbitol and menthyl formate have occurred due to their proximity to the large menthol peak. In this latter case, overlapping peaks were obtained even with use of columns of different polarities.

To overcome all these problems, we examined the use of direct thermal desorption and analysis by multidimensional gas chromatography mass spectrometry / flame ionisation detection (DTD-MDGC-MS/FID) (2, 3) to better extract and quantify the substances mentioned above.

Experimental

Reagents. The following reagents were obtained from the indicated sources: carbitol (CAS 111-90-0) from Dow Chemical Ibérica; menthyl formate (CAS 2230-90-2) and tea flavour from Lucta; BHT (CAS 128-37-0) and BHA (CAS 25013-16-5) from Impex Química; sorbic acid (CAS 110-44-1) and benzoic acid (CAS 65-85-0) from Merck; and ethanol and pyridine from Panreac.

Chromatographic conditions. All analyses were performed with an Agilent 6890 single oven chromatography system equipped with a Gerstel *MPS2* Multipurpose Automatic Sampler, a Gerstel thermal desorption unit (*TDU*) and a Gerstel cooled injection system (*CIS4*). Sample detection was performed by flame ionisation detector (*FID*) and a mass selective detector (*MSD 5973*). Helium was used as the carrier gas. Separations were performed by capillary columns, with the first column being an *HP-FFAP* (50m x 0.32 mm x 0.50 µm) and the second being an *HP-1ms* (30m x 0.25 mm x 0.25 µm).

For separations, the desorption program was 30 °C (1 min) to 250 °C at a rate of 90 °C/min (10 min); desorption flow was 50 ml/min, at a pressure of 103 kPa. The injector temperature was programmed at a rate of 12 °C/s from -50 °C (liquid N₂ cooled) to 250 °C, (3 min), (glass wool packed insert.) A splitless time of 2 min was used, with a post-split flow of 84 ml/min. The *FID* temperature was set at 250 °C, with air flow at 450 ml/min, hydrogen flow at 40 ml/min, and make up nitrogen at 45 ml/min. The mass detector was operated at 70 eV, with the quadrupole operated at 150 °C, the ion source at 230 °C, and the auxiliary transfer line at 250 °C.

The following oven temperature programs were used: program 1, 100 °C initially, heating at 5 °C/min to 198 °C, 0 min, then cooled to 60 °C at 23 °C/min; program 2, 60 °C initially, heated at 4 °C/min to 101 °C, 0 min, then heating to 230 °C at 15 °C/min, held for 15 min.

The first column pressure was programmed as follows: 209.8 kPa to 310 kPa at 5.1 kPa/min, 0 min to 0 kPa at 51.7 kPa/min, 34.37 min. Post pressure: 69.5 kPa. The second column pressure was also programmed, as follows: 171.4 kPa to 255.3 kPa at 4.3 kPa/min, 3 min, to 122 kPa at 44.4 kPa/min, 34.44 min.

In these analyses, we also used a Deans-type *MDGC* system using Agilent Capillary Flow Technology. For peak refocusing within the second column, we used an in-house constructed liquid N₂ cooled cryofocusing system.

Results

To optimise some instrumental parameters, we conducted initial trials by injecting an ethanol standard solution (10 ppm) of each test substance into a glass wool plug in the *TDU* glass insert and using only the *HP-FFAP* column and the *FID* detector.

The *CIS4* cryogenic injector temperature was tested between 0 °C and -110 °C to collect the volatiles desorbed from the *TDU*. An optimum temperature of -50 °C gave the least peak distortion and the maximum peak area.

To optimise the sample desorption temperature, we used only the *MSD* detector. Test samples were desorbed in this case from glass cups placed into the *TDU* glass insert. We found that *SIM* methods were superior when tea flavourings spiked with the standard solutions were injected, and the products were easier to separate from interferences.

After testing a range of temperatures from 200 °C and 300 °C, 250°C was selected because good recoveries were achieved when two consecutive injections were made from the same glass cup (> 97% for all components). A temperature of 200 °C gave the worst recoveries and 300 °C gave no improvement in recoveries, but the possibility of degradation increased.

Finally, memory effects were checked by sampling a standard solution into glass wool or in a glass cup into the *TDU* glass liner. The use of glass cups gave better results for all components except for acids.

Once these optimised conditions were established, we addressed interference problems (Figure 1) with peak overlap of pyridine, menthyl formate, and carbitol with tea flavouring components (5 mg of tea flavouring were desorbed in a glass cup). SIM did not improve these results.

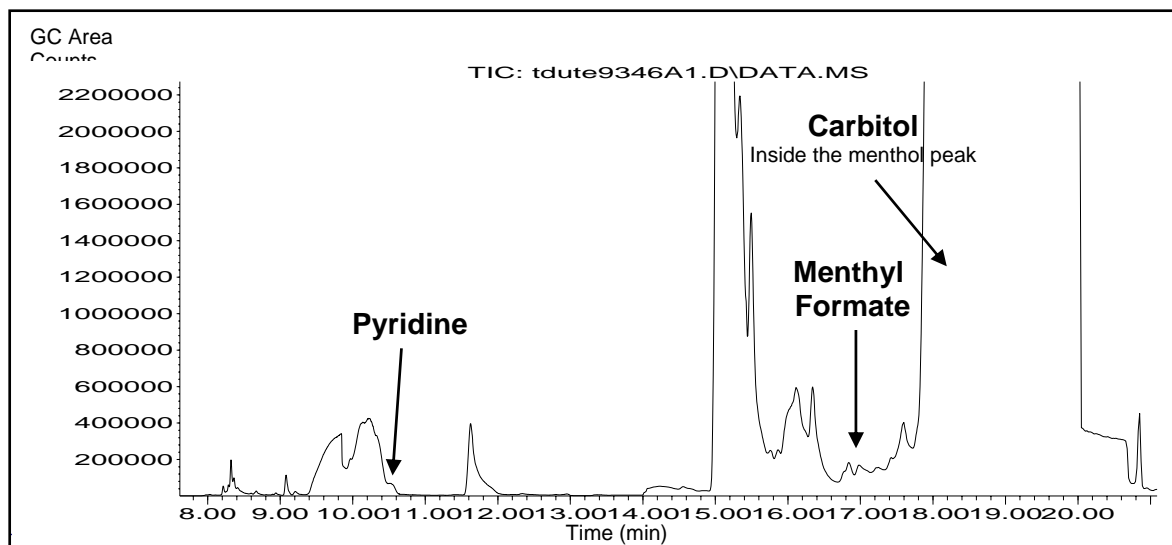


Figure 1. Separation of tea flavour components, 5 mg desorbed from a glass cup, using the original method, 100 °C initially, heating at 5 °C/min to 230 °C, with only the FFAP column.

For these unresolved peaks, MDGC was applied using a single oven. Cutting windows were selected and these three peaks were transferred to a second HP-1ms column, cryo-focused together with liquid nitrogen in the first coil of the second column, and reanalysed on this column, lowering the oven temperature and starting a second different oven program within the same oven. This cryofocusing system was constructed in house: the first coil of the second column was introduced into a narrow Teflon tube while liquid nitrogen flowed into it through a valve controlled by the chromatograph computer.

As we worked in constant flow mode, pressure increased with the oven temperature heating ramp. To maintain the ratios of pressures necessary to obtain adequate heart cuttings, we also programmed the pressures of the first and second column.

In this way, clear cuts and good peak shapes were obtained (Figure 2), giving quantitative results for all restricted components spiked in tea flavour comparable with a solvent extraction, as determined by external standards, except for benzoic acid which desorption concentration was found higher than the extraction one. Some thermal degradation of natural extracts present in the tea flavouring was suspected. Acidic water was used to dissolve the hydrophobic tea flavour and diethyl ether was used as the organic solvent.

The three products that were heart cut in the second analysis were the same three that eluted earlier. During our attempts to analyse the six restricted substances in a single run, we had to maintain the liquid nitrogen for an excessive time and this caused oven temperature fluctuation incompatible with the analysis.

Therefore, we will need to perform two additional studies to analyse all products under the same conditions, one without heart cutting for BHT, sorbic acid, benzoic acid, and BHA, and other with heart cutting for carbitol, menthyl formate, and

pyridine. Further studies will be required to achieve quantitative determinations of all substances in a single run. We also intend to improve the cryofocusing design at the beginning of the second column to use less liquid nitrogen to prevent temperature oven fluctuations. Future work will focus on the improvement of desorption of flavour volatiles and the prevention of the possible formation of thermally degraded products.

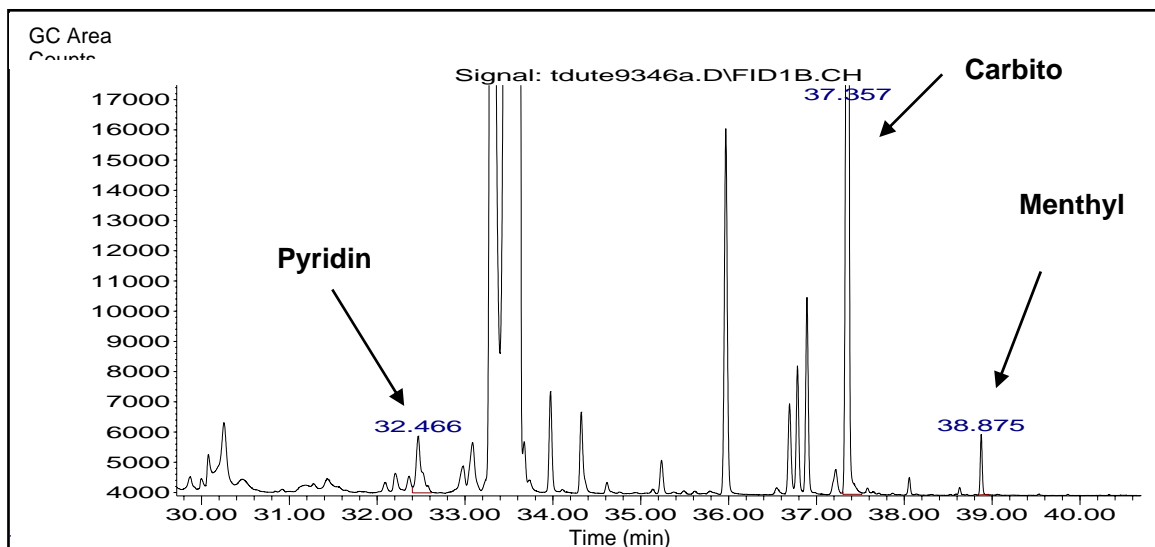


Figure 2. Separation of tea flavour components using the new MDGC method with FFAP/HP1ms columns and the FID detector. Conditions as outlined in the experimental section.

References

1. Ibáñez C. (1990) In *Proceedings of 5^a Jornadas de Análisis Instrumental*, Expoquimia, Barcelona, Spain.
2. Butrym E.D., Manura J.J. (1998) In *Flavor Profile Determination of Rice Samples Using Short Path Thermal Desorption GC Methods*, Application Note #71, Scientific Instrument Services, Ringoes, N.J., USA.
3. Grimm C.G., Lloyd S.W., Miller J.A., Spanier A.M. (2001) In *Flavor, Fragrance and Odor Analysis* (R. Marsili, ed.), *Food Science and Technology*, Vol. 115, CRC Press: London, pp 59-81.

CRITICAL PARAMETERS IN THE PERFORMANCE OF A DYNAMIC PURGING SYSTEM FOR THE PRODUCTION OF EXTRACTS FOR GAS CHROMATOGRAPHY-OLFACTOMETRY

F. San Juan, A. ESCUDERO, J. Cacho, and V. Ferreira

Laboratory for Flavour Analysis and Enology. Aragón Institute of Engineering Research (I3A), Department of Analytical Chemistry, Faculty of Sciences, University of Zaragoza, 50009 Zaragoza, Spain

Abstract

In this work the performance of a purge and trap system previously used for wine aroma screening has been evaluated. The evaluation consisted on a comparison between the odour intensities of selected odorants in the glass and the gas chromatography-olfactometry intensities of those odorants in the extracts obtained with the purging system. Results showed that the odour intensities of some polar and heavy compounds were undervalued by gas chromatography-olfactometry. A thorough research directed to identify the causes of such biases concluded that the physical design of the system is critical and the temperature of the olfactometric port is also a major concern in the detection of polar and heavy compounds. Furthermore, the elution of compounds from the trap (composed of LiChrolut EN resins) is critical and is greatly improved if it is slow, and the solvent is enriched with a polar modifier (methanol), and also the sorbent is carefully dried before elution. Finally, the solvent of the matrix (ethanol in the case of wine) must be introduced in the humidifier, since the odour perception of some odorants is critically affected by its presence.

Introduction

Gas Chromatography-Olfactometry (GC-O) is a powerful aroma-screening technique which, appropriately used, can provide a quite accurate idea of the odorants that are most relevant in the ortho or retronasal odour perception of a food product (1, 2). Ideally, the extract for GC-O should represent as close as possible the composition of the vapours reaching the pituitary during the consumption of the product. This makes that, a priori; dynamic headspace techniques should be preferred. However, several concerns about the performance of these techniques explain why most researchers keep on using total extraction techniques for screening purposes.

Experimental

Chemicals. Tartaric acid was of analytical quality, and it was supplied by Panreac Química SA (Barcelona, Spain). Lichrolut EN resins were from Merck (Darmstadt, Germany). Methanol was of HPLC quality from Lab-Scan (Dublin, Republic of Ireland) and dichloromethane was from Fischer (Leicester, U.K.), absolute ethanol was from Riedel de Haën (Seelze, Germany). Pure references compounds were supplied by Aldrich (Gillingham, U.K.), Sigma (St. Louis, MO), Fluka (Buchs, Switzerland) Poly Sciences (Niles, IL), and Lancaster (Strasbourg, France). The synthetic wine was water with 10% ethanol, 5 g/L of tartaric and pH 3, 2.

Preparation of extracts (3). The volatiles of synthetic wine enriched with 19 compounds were collected using a purge-and-trap system. The trap was formed by a standard polypropylene SPE tube packed with 400 mg of Lichrolut EN resins. The bed was washed with 20 mL of dichloromethane and dried by letting air pass through. The tube was placed on the top of a bubbler flask containing 80 mL of synthetic wine. It was continuously stirred with a magnetic stir bar and kept at a constant temperature of 37°C by immersion in a water bath. A controlled stream of nitrogen (100 mL/min) was passed through the sample during 200 min. Volatile synthetic wine constituents released in the headspace were trapped in the cartridge containing the sorbent and were further eluted with 3,2 mL of dichloromethane. The extract was kept at -30°C for 2h to eliminate any water content by freezing and further decantation. After this, the extract was concentrated under a stream of pure N₂ to a final volume of 200 µL.

GC-Olfactometry. Sniffings were carried out at constant pressure (linear velocity 30 cm.s⁻¹) on Thermo Quest Trace (Rodano, Italy) equipped with a FID and a sniffing port (ODO-1 from SGE, Ringwood, Australia) connected by a flow splitter to the column exit. The column was a DB-WAX from J&W (Folsom, US) 30 m x 0.32 mm x 0.5 µm. Temperature program: 35°C (1min), 5°C/min, 210°C. Injector and detector were both kept at 250°C. One microliter of solution was injected in a splitless mode, the splitless time being 1 min. The study performed five trained judges (4 women and 1 man, mean age 30 years). The judges were sniffing during whole run time without interruption. All judges were asked to measure the overall intensity of each odour using a 0-3 scale (1= weak, 2= clear but not intense, 3= intense odour) with seven possible scores (half values allowed). Panel intensities were calculated either as arithmetic mean of the measurements.

Sensory analyses. The same panel and the same scale of GC-O were utilised. All the orthonasal tests were carried out with tulip glasses containing 25 mL of synthetic wine enriched with a single analyte.

Results

An elution study of the resins Lichrolut EN was performed with the heaviest and most polar compounds. The elution speed and a percentage of methanol were critic to increase the recovery up to 100% (Table 1).

The recovery of the compounds was improved in case of drop by drop elution and dichlorometane with 5% methanol as solvent. The effect was very strong for ethyl lactate, furaneol, sotolon and methyl vanillate (Table 1).

The temperature of the olfactometric port is also a major concern in the detection of polar and heavy compounds. There were problems with methyl vanillate retention index. The olfactometric and FID detection time were not similar if the olfactometric port temperature was not high. There were condensation problems with the polar and heavy compounds.

An indication of an amplifying effect of ethanol on the perceived odour intensity was discovered in previous GC-O experiments (4). In a study (5) we tested twelve volatiles belonging to various chemical classes to confirm this phenomenon, by putting 10% and 20% hydroalcoholic solution into the humidifier of the sniffing port.

Several physical designs for the system were eventually thought. The liquid-gas transfer for the heaviest and most polar compounds has been considered as critical. Furthermore these compounds can be captured by the walls of the purge and trap system. We have also tried with a retronasal aroma simulator (6), glasses simulator

or respiration cycles. Good results have been reached with the design 2. The two designs are shown Figure 1.

Table 1. Elution data of Lichrolut EN resins.

Compound	Elution % with dichloromethane (DCM)	Elution % if SLOW and DCM-5% METHANOL
Isobutanol	75,2	132,4
Ethyl lactate	39,2	104,7
Methional	53,2	123,3
Methionol	55,0	95,2
Furaneol	0,0	98,1
Sotolon	0,0	122,4
2, 4, 6-trichlorophenol	58,4	103,0
2, 3, 6-trichlorophenol	50,4	103,5
Indole	79,7	101,6
Skatole	79,6	102,4
2, 4, 5-trichlorophenol	60,6	100,6
2, 3, 4-trichlorophenol	69,9	102,2
Methyl vanillate	34,5	126,7

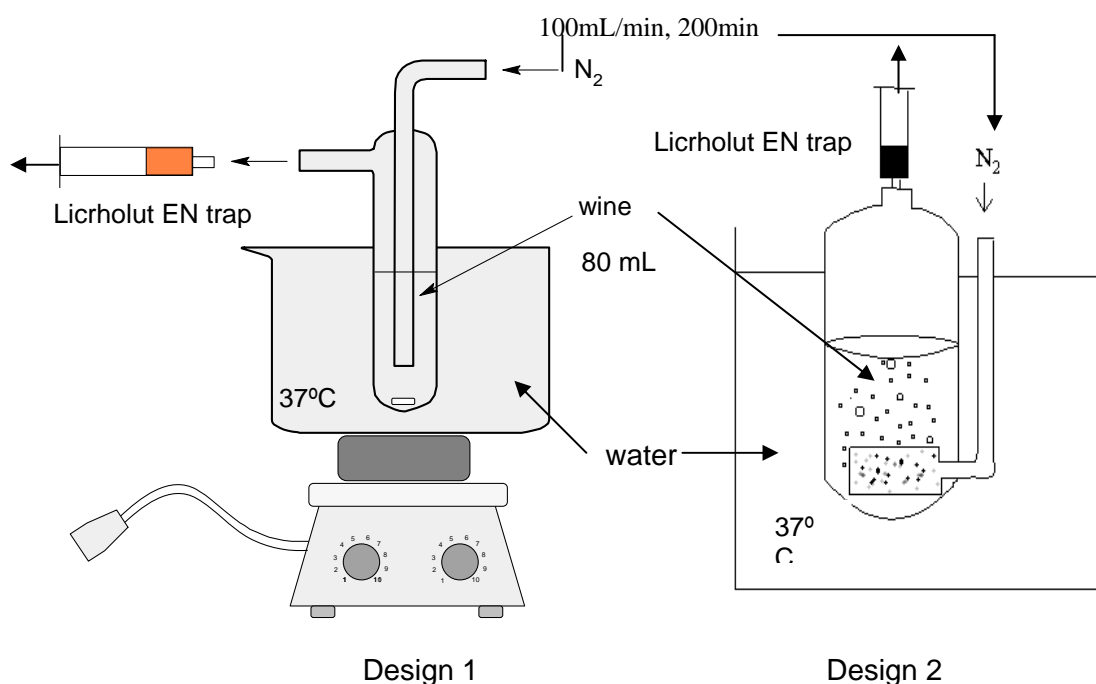


Figure 1. Calibrated dynamic purging systems. Design 1 is initial HS-SPE system (3). In design 2, the volatiles have a more direct way between sample and trap (less surface that competes for volatiles).

In order to calibrate the system, the orthonasal intensity tasted in cup from a synthetic wine enriched in one compound was compared with the olfactometric intensity of the extract obtained by HS-SPE. The data are shown in Table 2. The positive values show the compounds being smelled more olfactometrically than in cup. They are apolar compounds. The compounds with a value near of 0 (positive or

negative) are compounds whose assessment by the used system is correct. The negative values show the compound being smelled less olfactometrically than in cup. They are ethyl lactate, methionol, furaneol, sotolon and 2, 3, 4, 6-tetrachlorophenol; in design 1. Odour intensities of some polar and heavy compounds were undervalued by HS-SPE-GC-O in design 1. Good results have been reached with design 2.

Table 2. Comparison of designs. Differences between the intensity determined by GC-O and the intensity smelled orthonasally in a cup containing a synthetic wine enriched with a compound at the same concentration than the synthetic wine analysed by HS-SPE-GC-O.

	Design 1	Design 2
Ethyl 2-methylbutyrate	1.00	0.67
Isobutanol	- 0.20	0.08
Ethyl lactate	- 1.30	- 0.08
Methional	0.40	0.17
Decanal	0.75	1.33
Linalool	1.00	1.08
Methionol	- 1.25	0.67
Furaneol	- 1.30	- 0.50
Eugenol	- 0.25	0.83
Sotolon	- 2.00	- 0.17
2,4,6-trichlorophenol	- 0.30	- 0.25
2,3,6-trichlorophenol	0.10	0.50
Indole	- 0.30	1.08
Skatole	0.90	1.50
2,4,5-trichlorophenol	- 0.40	- 0.33
Methyl vanillate	0.08	0.25

References

1. Grosch W. (2001) *Chem. Senses* 26: 533-545.
2. Ferreira V., Pet'ka J., Aznar M., Cacho J. (2003) *J. Chromatogr.* 1002: 169-178.
3. Campo E., Ferreira V., Escudero A., Cacho J. (2005) *J. Agric. Food Chem.* 53: 5682-5690.
4. Pet'ka J., Cacho J., Ferreira V. (2003) In *7ème Symposium International d'Onologie*, Bordeaux.
5. Pet'ka J., Sádecka J., Escudero A., Kukurová K., Ferreira V. (2009) In *Expression of Multidisciplinary Flavour Science - XII Weurman Flavour Research Symposium* (Blank I, Wüst M., Yeretian C, eds.), Zurich University: Zurich, pp 553-556.
6. Roberts D.D., Acree T.E. (1995) *J. Agric. Food Chem.* 43: 2179-2186.

FURANEOL[®] AND MESIFURAN IN STRAWBERRIES – AN ANALYTICAL CHALLENGE

B. SIEGMUND, K. Bagdonaite, and E. Leitner

Graz University of Technology, Institute of Food Chemistry and Technology, Petersgasse 12/II, A8010 Graz, Austria

Abstract

2,5-Dimethyl-4-hydroxy-3(2*H*)-furanone (Furaneol[®]) and 2,5-dimethyl-4-methoxy-3(2*H*)-furanone (mesifuran) are very important flavour compounds in various types of foods, as for example in strawberries. Due to the chemical and physical properties, resulting in a high affinity to the strawberry matrix especially of Furaneol[®], the analysis is rather complex. It was the aim of this study to compare different extraction methods (i.e. headspace- as well as direct immersion-solid phase microextraction and solid phase extraction) and to develop a sensitive and reproducible analytical method for the quantitative determination of the two compounds. Solid phase extraction after aqueous extraction of the analytes from the strawberry matrix on a polymeric reversed phase matrix turned out to be the method of choice. With this method, Furaneol[®] as well as mesifuran can be easily extracted from the strawberries with high reproducibility and sufficient sensitivity. Quantitative determination is performed by using gas chromatography on a polar analytical column.

Introduction

2,5-Dimethyl-4-hydroxy-3(2*H*)-furanone (Furaneol[®], DMHF) and 2,5-dimethyl-4-methoxy-3(2*H*)-furanone (mesifuran, DMMF) (Figure 1) are very important natural flavour compounds in various fruits. Furaneol[®] is for example considered to be an impact compound for strawberry flavour.

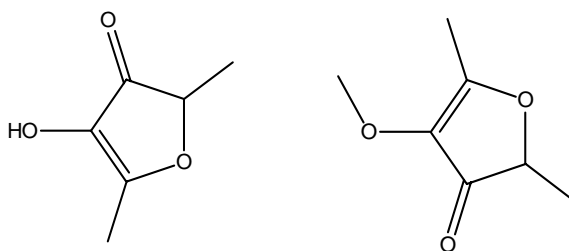


Figure 1. Chemical structures of Furaneol[®] and mesifuran.

Both compounds show very low odour threshold values (thresholds in water $4 \cdot 10^{-5}$ mg kg⁻¹ for Furaneol[®]; $3 \cdot 10^{-5}$ mg kg⁻¹ for mesifuran). Performing sensory evaluation, Furaneol[®] is described as caramel, burnt sugar-like and mesifuran as a smell similar to fermented fruit, and earthy-moldy (the descriptors were given by our trained sensory test panel from aqueous solutions of the compounds). For strawberries, very large differences in concentrations have been reported for both compounds (0-37 mg

kg⁻¹ for Furaneol[®] (1, 2, 8) and 0-23 mg kg⁻¹ for mesifuran (3, 4, 8)). Reasons for these variations in concentrations may be found for example in different strawberry varieties, or differing ripening stages of the fruits.

Regarding the facts that both compounds are thermally instable and that both show varying stability depending on the pH value (5, 6) in combination with the high affinity of Furaneol[®] to the strawberry matrix based on its pronounced polarity, the large variations in concentrations reported for strawberries might also be due to parameters used for the extraction and the subsequent analysis, respectively. As a consequence, we aimed to develop a sensitive and highly reproducible analytical method for the quantitative determination of Furaneol[®] and mesifuran from the strawberry matrix. Three different analytical approaches were chosen: (i) headspace solid phase microextraction (SPME), (ii) direct immersion SPME, (iii) solid phase extraction (SPE). The evaluation of the methods was mainly based on the ability to extract both compounds simultaneously, as well as on parameters like reproducibility, selectivity and sensitivity to the target compounds.

Experimental

Headspace SPME. 0.5 g, 2.0 g or 5.0 g of homogenized strawberries were transferred into a 20 mL headspace vial. For the sample development differing amounts (0.5 g or 2.0 g) of either NaCl or Na₂SO₄ were added. 1,2,3-Trichloropropane (50 µg kg⁻¹) was added as internal standard. The sample was stirred thoroughly using a glass coated magnetic stirrer. After 5 minutes equilibrium time, headspace sampling was performed over a period of 30 min at a sampling temperature of 45°C or 65°C using a DVB/CarboxenTM/PDMS fibre (2 cm stable flex). After sampling, the SPME fibre was immediately transferred into the GC-injection port for thermodesorption (injector temperature: 270°C). The fibre was kept in the injector for 10 minutes. The GC separation was performed on an HP5 column (column dimensions 30 m x 0.25 mm x 1.0 µm). The detection was performed by mass spectrometry in the scan mode as well as in the selected ion mode (*m/z* 128 and 85 for Furaneol[®], *m/z* 142 and 71 for mesifuran).

Direct immersion SPME. Experiments for the direct immersion SPME were performed from aqueous solutions (sample amount 10 mL) containing about 1 mg L⁻¹ per compound. Different SPME fibres (i.e. PEG, PDMS/DVB, PUA, PDMS, PA, CarboxenTM/PDMS, DVB/CarboxenTM/PDMS) were investigated with respect to their ability to enrich Furaneol[®] and mesifuran equally reproducibly. The fibres were immersed into the aqueous solution which was stirred at room temperature for 20 min. Afterwards, thermodesorption was performed in the injection port of the GC at 250°C or 270°C (injector temperature was depending on the used fibre material). The influence of NaCl-addition on the yields and the reproducibility was investigated (addition of 4 g NaCl per 10 mL aqueous sample). The GC separation was performed on an HP Innowax (column dimensions 30 m x 0.25 mm x 0.5 µm). The detection was performed via mass spectrometry in the scan mode as well as in the selected ion mode (*m/z* 128 and 85 for Furaneol[®], *m/z* 142 and 71 for mesifuran).

Solid phase extraction (SPE). 1.0 g of homogenized strawberries was mixed thoroughly with 50 mL buffer solution (potassium tartrate with tartaric acid; pH ~3.5). Maltol (5 µg absolute) was added to the extract as internal standard. After centrifugation, an aliquot of 10 mL was transferred onto the SPE cartridge (Strata X, polymeric reversed phase, particle size 33 µm, 500 mg/3 mL; Phenomenex). The SPE cartridge was conditioned with 5 mL methanol and 5 mL deionised water prior to

use. The elution of the analytes was performed with acetone (1 mL was discarded, 2 mL were collected). After centrifugation, the eluent was injected directly into the GC. The GC separation was performed on a DB Wax (column dimensions 30 m x 0.32 mm x 0.25 μ m), the detection was performed by FID. The identity of the compounds was confirmed by GC-MS analyses.

Results and Discussion

Headspace SPME. Headspace SPME is a well suitable method for the determination of volatile compounds from various food matrices. This was shown several times in literature. In our studies concerning the flavour of strawberries, headspace SPME is also used in order to gain 'aroma profiles' of the investigated fruits. Analyzing these profiles, it turned out that mainly for the determination of Furaneol[®], but also for mesifuran, the used parameters did neither yield in sufficient recoveries nor high reproducibilities for the two compounds. In order to enhance the performance of the method, several parameters were modified: (i) the sample amount was varied (0.5 g, 2.0 g, 5.0 g), (ii) different sampling temperatures were chosen (45°C, 65°C), (iii) different types of salt were added in different amounts. The results showed that none of the taken actions could increase the performance of the extraction with regard to the furanoid compounds. While other volatile compounds like various esters or aldehydes can be determined with high reproducibility, the two compounds of interest, especially Furaneol[®], could not be determined neither with sufficient yields, nor with high reproducibility using headspace SPME.

Direct immersion SPME. Based on the results obtained from headspace SPME, we concluded that the high affinity of Furaneol[®] based on its high polarity could be the reason for the bad reproducibility obtained in headspace analysis. As a consequence, we moved to direct immersion SPME, in order to avoid the transfer of Furaneol[®] and mesifuran from the sample matrix into the headspace. Method development was started with aqueous solutions of Furaneol[®] and mesifuran. Seven different SPME fibre types were investigated. The only fibre that enriched Furaneol[®] as well as mesifuran in reasonable amounts was a DVB/Carboxen[™]/PDMS fibre (2 cm stable flex). The addition of NaCl – in order to increase the extraction yield – led to a drastic decrease in the extraction yield for Furaneol[®], whereas the yields for mesifuran increased. In addition, the reproducibilities even from the aqueous solutions were very poor for either compound. Due to those problems, which already arose in the aqueous solution without the presence of any further fruit components, we did not follow this way any further.

Solid phase extraction (SPE). The group of V. Ferreira recently showed a quantitative way for the enrichment of Furaneol[®] from wine using SPE on chemically modified reversed phase material (styrene-DVB) (7). For the extraction of Furaneol[®] and mesifuran from the strawberry matrix, we modified the procedure that was described in (7). The analytes were extracted out of the strawberries with a tartaric acid buffer at the pH of the strawberry matrix (pH 3.5). Maltol was added to the system as internal standard to control the procedure. After centrifugation, an aliquot of the extract was directly transferred onto the preconditioned SPE cartridge. Amongst various polar solvents that were tested for the elution of the analytes, acetone showed the best performance for this task. This fairly simple method shows high linearity (for Furaneol[®] as well as for mesifuran from 0.25 to 200 mg kg⁻¹ strawberries), high recoveries of the analytes (95-110%) as well as high

reproducibility. The quantitative procedure was fully validated within this concentration range.

Based on these results, we selected the solid phase extraction as the method of choice for the extraction of Furaneol[®] and mesifuran out of the strawberry matrix. To demonstrate the applicability of the method to the strawberry matrix, Table 1 shows Furaneol[®] and mesifuran concentrations of different strawberries varieties determined by this method. For future studies, this method will be used to determine the influence of various external parameters on the flavour formation in the strawberry plant and the fruit.

Table 1. *Furaneol[®] and mesifuran concentrations in different strawberry varieties.*

Strawberry variety	Furaneol [®] conc. [mg kg ⁻¹]	Mesifuran conc. [mg kg ⁻¹]
Elsanta	30.7	7.3
Senga Sengana	17.4	5.9
Antea	24.3	4.8
Woodland strawberry (<i>Fragaria vesca</i>)	22.4	4.7

Acknowledgement

This work was supported by the Austrian Research Promotion Fund (FFG) and by Grünewald.

References

1. Ménager I., Jost M., Aubert C. (2004) *J. Agric. Food Chem.* 52: 1248-1254.
2. Lavid N., Schwab W., Kafkas E., Koch-Dean M., Bar E., Larkov O., Ravid U., Lewinsohn E. (2002) *J. Agric. Food Chem.* 50: 4025-4030.
3. Larsen M., Poll L. (1995) *Z. Lebensm. Forsch. Unters.* 201: 275-277.
4. Douillard C., Guichard E. (1990) *J. Sci. Food Agric.* 50: 517-531
5. Hirvi T., Honkanen E., Pyysalo T. (1980) *Lebensm. Wiss.. Technol.* 13: 324-325.
6. Shu C.K., Mookherjee B.D., Ho C.T. (1985) *J. Agric. Food Chem.* 33: 446-448.
7. Ferreira V., Jarauta I., López R., Cacho J. (2003) *J. Chrom. A* 1010: 95-103.
8. Pérez A.G., Olías R., Sanz C., Olías J.M. (1996) *J. Agric. Food Chem.* 44: 3620-3624.

ABSOLUTE STEREOCHEMISTRY OF FLAVOUR RELATED 2-SUBSTITUTED-3(2*H*)-FURANONES, 2,5-DIMETHYL-4-HYDROXY-3(2*H*)-FURANONE AND ANALOGUES

M. Emura¹, Y. YAGUCHI¹, D. Sugimoto¹, A. Nakahashi², N. Miura², K. Monde²

¹ Corporate Research & Development Division, TAKASAGO International Corporation, 4-11, 1-Chome, Nishi-Yawata, Hiratsuka city, Kanagawa 254-0073, Japan

² Laboratory of Advanced Chemical Biology, Graduate School of Advanced Life Science, Frontier Research Center for Post-genome Science and Technology, Hokkaido University, Kita 21, Nishi 11, Sapporo 001-0021, Japan

Abstract

Optical resolution of flavour related 2-substituted-3(2*H*)-furanone derivatives such as 2,5-dimethyl-4-hydroxy-3(2*H*)-furanone (DMHF) (1) and 2,5-dimethyl-4-methoxy-3(2*H*)-furanone (DMMF) (2) were accomplished using enantioselective carbon dioxide supercritical fluid chromatography. Absolute configurations of 1 and 2 were clarified as (*R*)-(+)-1, (*S*)-(-)-1, (*R*)-(+)-2 and (*S*)-(-)-2 by the vibrational circular dichroism technique as well as chemical relay reactions. Odour evaluation of each enantiomer revealed relationships between their configurations and their odour activities. (*R*)-(+) isomers represent intensive burnt caramel odour characteristics.

Introduction

2-Substituted-3(2*H*)-furanones such as DMHF (1), DMMF (2) and 2(or 5)-ethyl-4-hydroxy-5(or 2)-methyl-3(2*H*)-furanone (EHMF) (3a, 3b) have been found in many fruits and foods. These furanones are known to play an important role in flavour because of extremely low threshold value and their burnt sugar sweet odour characteristics.

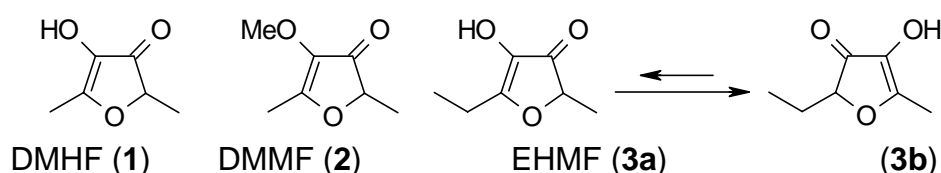


Figure 1. Chemical structures of 2-substituted-3(2*H*)-furanones.

Until now, only the optical rotation of 1 and 2 have been reported using an enzyme-catalyzed synthesis [1] or an enantioselective chromatography [2,3]. However, the absolute stereochemistry of these 2-substituted-3(2*H*)-furanones have not been reported over 40 years since their discovery [4,5], due to the racemisation through keto-enol tautomerism of its unique structure. Any of previously existing method could not allow solving this challenging theme. Recently we reported an efficient optical resolution method to prepare both enantiomers using enantioselective CO₂ supercritical fluid chromatography (SFC) for varieties of flavour chemicals [6].

Moreover, the vibrational circular dichroism (VCD) method coupled with computational *ab initio* quantum chemistry has been developed for the determination of absolute stereochemistry as a non-empirical method [7,8]. Consequently, we planned to apply enantioselective SFC as well as VCD technique in order to elucidate the absolute stereochemistry of these 2-substituted-3(2*H*)-furanones.

Experimental

CO₂ SFC system (Jasco corp.) with CHIRALPAK[®] IA (20 x 250 mm: DAICEL Chemical) using 2-propanol as an entrainer was used for preparative optical resolutions of 1 and 2. VCD spectra were measured on a Bomem/BioTools Chiral*ir* spectrometer. All spectra were recorded for 1 h at a resolution of 8 cm⁻¹ under an ambient temperature. Samples were dissolved in CCl₄ and then placed in a 100 μm CaF₂ cell. Chiral GC (5890GC: Hewlett-Packard) and chiral MDGC/MS (MDGC-2010: Shimadzu corp.) equipped Chirasildex-CB column (Varian Inc.) was used for the analyses of enantiomeric ratios.

Results

Optical Resolution of furanones. Enantioselective CO₂ SFC gave extremely fine separations for 1 and 2 (Figure 2). Approximately 30 mg of each enantiomer of them were isolated through multiple injections. The enantiomeric ratio was determined by chiral GC. During isolation operation and evaporation of solvent, no racemisation has observed.



Figure 2. Optical Resolution by Enantioselective CO₂ SFC.

Table 1. Optical Rotation Values of Isolated 1 and 2.

Compound	Optical Rotation Value [α] _D ²⁰	e.e.
(+)-1	+172° (c = 0.472, CCl ₄)	80%
(-)-1	-153° (c = 0.526, CCl ₄)	82%
(+)-2	+148° (c = 0.324, CCl ₄)	94%
(-)-2	-188° (c = 0.262, CCl ₄)	91%

VCD measurement of furanones. The IR and VCD spectra of each enantiomer of 1 and 2 were measured. Unfortunately, 1 was decomposed during measurement because of its low stability in CDCl₃ and CCl₄, whereas enantiomers of its methyl ether 2 showed entirely opposite VCD signals. The IR and VCD spectra of 2 were theoretically calculated based on the density functional theory at the B3PW91/6-

31G(d,p) level of theory. Conformational analysis offered a sole stable conformer for 2 in which the methoxy group was rotated (Figure 3). After harmonic vibrational analysis, simulated absorption and VCD spectra were obtained by using convolution with Lorentzian functions. All of the calculations were conducted with Gaussian03 program code. The observed VCD spectrum of (+)-2 was essentially identical to the calculated spectrum of (R)-2 (Figure 4), while IR spectra of them were almost superimposed. Therefore, (+)-2 was shown to have an R configuration (Figure 5).

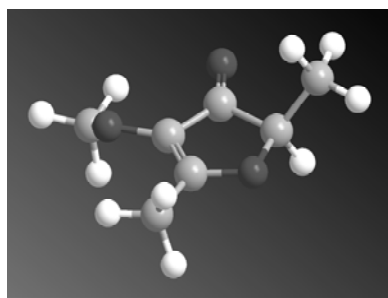


Figure 3

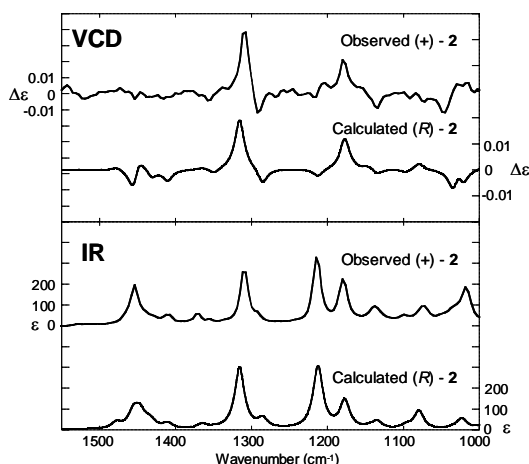


Figure 4

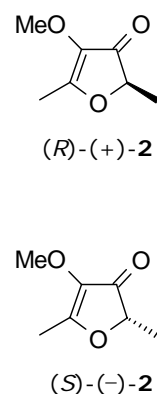
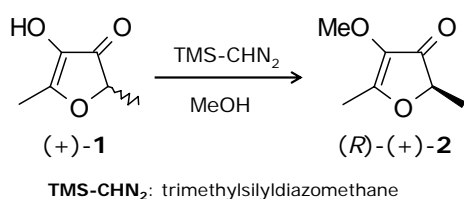


Figure 5

Determination of Absolute Configuration of DMHF (1). According to determination of absolute configuration of 2, derivatization from 1 to 2 was attempted. The careful trimethylsilyldiazomethane treatment of (+) and (-)-1 to prevent racemisation afforded a successful transformation into optically active 2 (Scheme 1). The methyl ether derivative from (+)-1 were completely identified as (R)-(+)-2 using chiral MDGC/MS. Meanwhile, (-)-1 was *vice versa* (Figure 6). The absolute configuration and optical rotation of 1 was confirmed as (R)-(+)-1 and (S)-(-)-1 [9], respectively (Figure 7).



Scheme 1

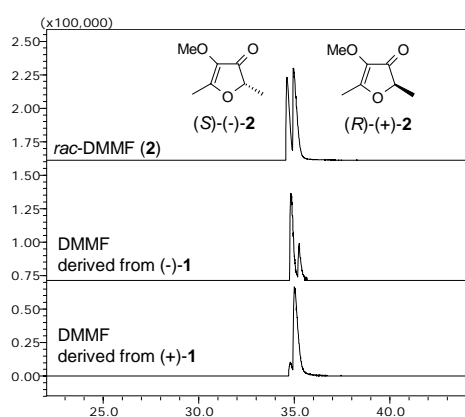


Figure 6

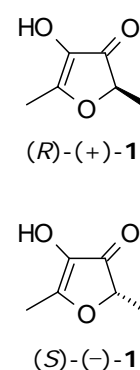


Figure 7

Odour Evaluation of DMHF (1) and DMMF (2). Odour evaluation of each enantiomer was performed under ethyl acetate solution with smelling strip. It is found that (R)-(+)-1 isomers have a burnt caramel note which represents odour characteristic of 2-substituted-3(2H)-furanones (Figure 8).

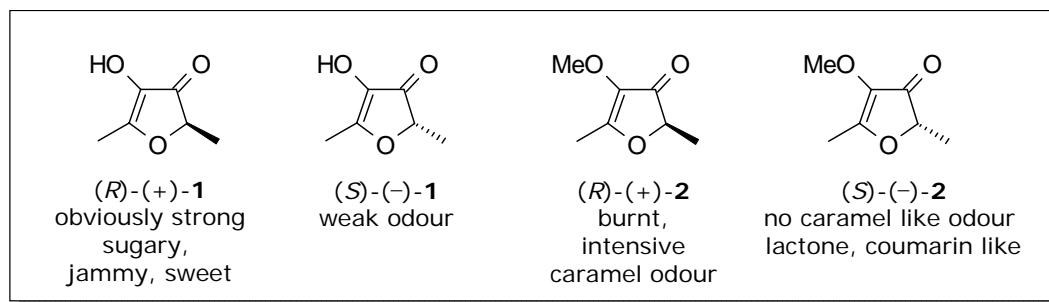


Figure 8. Odour Characteristics of Optically Active 2-Substituted-3(2H)-furanones.

Conclusion

In this study, we have accomplished for the first time to unveil the absolute stereochemistry of 1 and 2. Moreover, the structure-activity relationship study between the absolute configuration and their odour characteristics was revealed. The VCD method can be applied to various flavour compounds which absolute chemistry has been unclear.

Acknowledgments

We thank Prof. S.-I. Nishimura, Dr. T. Taniguchi at Hokkaido University and Mr. Y. Kawakami at TAKASAGO International Corporation for their valuable suggestions. This work was supported in part by a grant-in-aid for scientific research (Grants 20310127) from the Ministry of Education, Science, Sports, and Culture of Japan. A. N. gratefully acknowledges a fellowship from the Japan Society of the Promotion of Science.

References

- Suzuki N., Nozaki M. (1996) Abstracts of Papers, the 40th Symposium on the Chemistry of Terpenes, Essential Oils, and Aromatics, pp.
- Bruce G., Dietrich A., Mosandl A. (1995) *Z. Lebensm. Unters. Forsch.* 201: 249-252.
- Fischer N., Hammerschmidt F.J. (1992) *Chem. Microbiol. Technol. Lebensm.* 14: 141-148.
- Willhalm B., Stoll M., Thomas A.F. (1965) *Chem. Ind. London* 38:1629-1630.
- Rodin J.O., Himel C.M., Silverstein R.M., Leeper R.W., Gortner W.A. (1965) *J. Food Sci.* 30:280-285.
- Sugimoto D., Yaguchi Y., Kasuga H., Okajima S., Emura M. (2008) In *Recent Highlights in Flavor Chemistry & Biology: Proceedings of the 8th Wartburg Symposium* (Hofmann T., Meyerhof W., Schieberle P., eds.) *Deutsche Forschungsanstalt für Lebensmittelchemie*, Germany, pp.340-344.
- Freedman T.B., Cao X., Dukor R.K., Nafie L.A. (2003) *Chirality* 15: 743-758.
- Taniguchi T., Miura N., Nishimura S.I., Monde K. (2004) *Mol. Nutr. Food Res.* 48: 246-254.
- Yaguchi Y., Nakahashi A., Sugimoto D., Miura N., Sugimoto D., Monde K., Makoto E. (2008) *Org. Lett.* 10: 4883-4885.

HYDROPHOBIC INTERACTIONS BETWEEN AROMA COMPOUNDS AND β -LACTOGLOBULIN USING NMR AND A FLUORESCENT PROBE

L. Tavel¹, C. Moreau¹, E. Li-Chan², and E. GUICHARD¹

¹ UMR 1129 FLAVIC, ENESAD, INRA, Université de Bourgogne, 17, rue Sully, BP 86510, 21065 Dijon Cedex, France

² Food Science graduate program, the University of British Columbia, 2205 East Mall, Vancouver, British Columbia, Canada V6T 1Z4

Abstract

β -Lactoglobulin (bLg) is known to interact with aroma compounds affecting their release, and hence, their perception. bLg, composed of two hydrophobic binding sites, was used as a simple model food protein to investigate binding mechanisms as a function of ligand nature. Indeed, binding of small ligands to bLg sites is often selective, although some ligands bind to both sites. Interactions between bLg and one ketone, β -ionone, and one phenol, guaiacol were investigated by combining two techniques: 2D Nuclear Magnetic Resonance for binding site location, and fluorescence using the 6-propionyl-2-(*N,N*-dimethylamino)naphthalene (PRODAN) probe for surface hydrophobicity determination. While β -ionone may preferentially bind onto protein surface and compete with PRODAN for the same binding sites, guaiacol affected the chemical shifts of residues located at the entrance of the central cavity and does not prevent PRODAN from binding.

Introduction

Many aroma compounds are known to bind with proteins, and elucidating these binding interactions is a key in a better knowledge of flavour perception mechanisms [1]. β -Lactoglobulin (bLg), belonging to the lipocalin family, was used as a model food protein. bLg, a globular protein of 18.3 kDa, is composed of eight antiparallel β strands, labelled β -A to β -H, folded to form a central calyx. Attached to the calyx is a three-turn α helix which is followed by an extra β strand, β -I. Numerous studies have investigated interactions between bLg and small ligands, and indicate the existence of two binding sites: (i) one internal site, the central cavity, within the hydrophobic calyx, and (ii) one external site on the outer surface of bLg in a groove between β strands and α helix (Figure 1). Previous works showed different binding sites on bLg for aroma compounds as a function of their chemical class, and emphasized the importance of hydrophobic interactions [2].

In the present study, binding sites location by Nuclear Magnetic Resonance (NMR) spectroscopy [3] was combined with determination of protein surface hydrophobicity by fluorescence spectroscopy using a hydrophobic probe [4]. We focused on two aroma compounds, one ketone, β -ionone, and one phenol, guaiacol to investigate the impact of the nature of ligand on binding mechanisms.

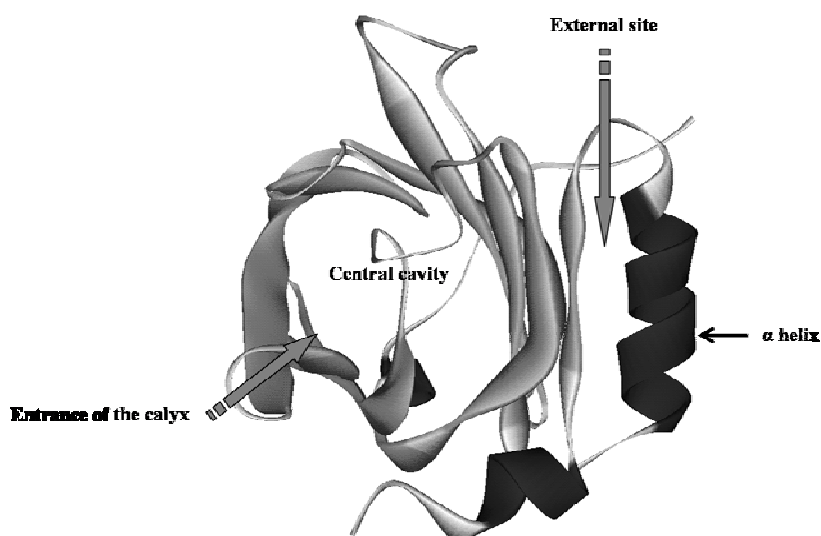


Figure 1. Secondary structure of bLg variant A at pH 2.6 obtained from PDB [5].

Experimental

Sample preparation. Bovine bLg variant A (purity $\geq 90\%$), provided by INRA Jouy-en-Josas, was dissolved in 12 mM NaCl pH adjusted to 2.65 (± 0.05) with and without β -ionone or guaiacol (Sigma Aldrich). As shown in Table 1, the bLg solutions were prepared at defined concentrations for NMR spectroscopy, while a range of concentrations was prepared for determination of surface hydrophobicity through binding of the fluorescent probe 6-propionyl-2-(dimethylamino)naphthalene (PRODAN) (Molecular Probes) Under these conditions, the protein is in its native monomeric state.

Table 1. Experimental conditions of NMR and fluorescence analyses.

Ligand	K_B (M^{-1})	Concentrations (μM) for NMR analysis		Concentrations (μM) for fluorescence analysis	
		Ligand	bLg	Ligand	bLg
β -Ionone	19143 ^a	500	250	11-54	22-109
Guaiacol	245 ^b	5000	1000	11-54	1200-6000

^a from [6], ^b from [7]

2D NMR experiments. 2D (1H , 1H) NMR TOCSY-Watergate spectra of solutions in 90% H_2O /10% D_2O (v/v) were recorded at 37°C on a Bruker Avance DRX 500 MHz NMR spectrometer as previously described [3]. NMR spectra were acquired and processed with Topspin 1.3 software.

Hydrophobicity measurements. The fluorescent probe PRODAN was added at a final concentration of 0.15 μM to protein solutions with or without an aroma compound. Surface hydrophobicity (S_0) values of protein were determined according to the method of Alizadeh-Pasdar and Li-Chan (2000) [4]. The relative fluorescence intensity (RFI) of samples was measured on a Shimadzu RF-5301 (Shimadzu Corp., Kyoto, Japan) spectrofluorometer at room temperature, with excitation and emission slit widths set at 5 nm and 3 nm, respectively. Emission scans were collected between 400 and 650 nm, at excitation wavelength of 365 nm. Preliminary

measurements verified that each aroma compound had no fluorescence in this range nor affected that of PRODAN. Data were analysed by an analysis of variance (ANOVA) procedure ($P \leq 0.05$).

Results and Discussion

2D NMR experiments. The NH-CH α region of the 2D NMR TOCSY-Watergate spectrum of bLg (reflecting the coupling between amide proton NH and C α -bonded protons CH α) is a fingerprint of the protein amino acid sequence. The chemical shifts (δ_{NH} , δ_{CH}) in ppm of 140 amino acid residues of bLg were assigned with an experimental error of ± 0.014 ppm based on the literature [8]. Ligand binding sites were determined through the chemical shift changes of amino acids involved in binding. Different amino acid residues were affected by the presence of β -ionone or guaiacol (Table 2). The addition of β -ionone induced chemical shift changes of the residues Ile12, Asp28, Ile29, Glu51, Ala80, Asp129 and Ala132. The residues Asp129 and Ala132 belong to α helix which may indicate preferential binding onto the protein surface in the external site. The presence of guaiacol affected the chemical shifts of Asp28, Asn63, and Gln68 with Asn63 and Gln68 being located at the entrance of the central cavity in ligand binding.

Table 2. Protein residues undergoing significant chemical shift changes with the presence of β -ionone or guaiacol.

Ligand	Residue	$\Delta\delta_{\text{NH}}$ (ppm)	$\Delta\delta_{\text{CH}\alpha}$ (ppm)	bLg structure
β -ionone	Ile12	0,027	0,000	N-terminal
	Asp28	0,041	0,000	loop AB
	Ile29	0,028	-0,055	loop AB
	Glu51	-0,027	0,000	loop BC
	Ala80	-0,027	0,055	strand β -E
	Asp129	0,027	0,000	α helix
	Ala132	-0,055	0,000	α helix
Guaiacol	Asp28	0,041	0,000	loop AB
	Asn63	0,000	0,041	loop CD
	Gln68	0,000	0,027	strand β -D

Hydrophobicity measurements. Surface hydrophobicity (S_0) values of bLg were determined through changes in fluorescence upon binding of PRODAN to protein hydrophobic regions in absence or presence of an aroma compound (Figure 2). The presence of β -ionone decreased S_0 value indicating that some PRODAN binding sites are no longer accessible to the probe. Combined with NMR results, the fluorescence data suggest competitions between β -ionone and PRODAN for common external binding sites and evidence of hydrophobic interactions between β -ionone and bLg. In contrast, no change of S_0 was induced by the presence of guaiacol, implying that guaiacol and PRODAN may have different binding sites. However, the hypothesis of common binding sites is not to be ruled out. Indeed, considering the low affinity of guaiacol for bLg ($K_B = 245 \text{ M}^{-1}$) determined previously by affinity chromatography [7], a displacement of guaiacol by PRODAN within bLg central cavity is conceivable.

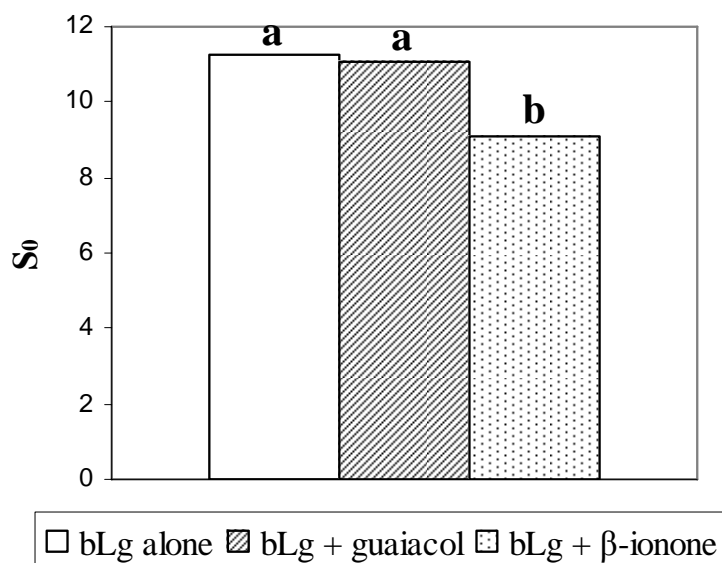


Figure 2. Surface hydrophobicity (S_0) of bLg measured for samples of bLg in absence or presence of an aroma compound. Bars show mean values of duplicate determinations, and the different letters (a-b) represent significant ($P \leq 0.05$) differences in S_0 values.

Conclusion

The determination of protein surface hydrophobicity in absence or presence of an aroma compound by PRODAN fluorescence in conjunction with binding site location by NMR provided useful information on the influence of ligand nature in binding mechanisms. Competition studies between aroma compounds using fluorescence and determination of binding site of PRODAN are currently in progress for a better understanding of the impact of the nature of aroma compounds on their interactions with bLg.

References

1. Guichard E. (2002) *Food Rev. Int.* 18: 49-70.
2. Tromelin A., Guichard E. (2004) *Qsar Comb. Sci.* 23: 214-233.
3. Moreau C., Tavel L., Le Quéré J.L., Guichard E. (2006) In *Flavour Science: Recent Advances and Trends Developments in Food Science.* (Bredie W.L.P., Petersen M.A., eds.), Elsevier: Oxford, pp 425-428.
4. Alizadeh-Pasdar N., Li-Chan E.C.Y. (2000) *J. Agric. Food Chem.* 48: 328-334.
5. Uhrinova S., Smith M.H., Jameson G.B., Uhrin D., Sawyer L., Barlow P.N. (2000) *Biochemistry* 39: 3565-3574.
6. Sostman K., Guichard E. (1998) *Food Chem.* 62: 509-513.
7. Reiners J., Nicklaus S., Guichard E. (2000) *Lait* 80: 347-360.
8. Uhrinova S., Uhrin D., Denton H., Smith M., Sawyer L., Barlow P.N. (1998) *J. Biomolecular NMR* 12: 89-107.

GAS CHROMATOGRAPHY-PEDESTAL OLFACTOMETER

F.A. Parisot¹, E. Satre², R.C. Williams³, A.J. Kurtz³, and T.E. Acree³

¹ *University of Burgundy - ENSBANA, Dijon, France*

² *University of Burgundy - ENSBANA, Dijon, France*

³ *Food Science & Technology, Cornell University, Geneva NY 14456, USA*

Abstract

Gas chromatography (GC) can deliver odorants as a pure dose to an olfactometer where its odour properties (quality and intensity) can be studied independent of other odours. Adding an odour to the olfactometer air before combining it with the GC effluent creates an odour pedestal upon which an odorant eluting from the GC can be studied to provide insight into mixture perception. This paper describes the development and testing of a gas chromatography - pedestal olfactometer (GC-PO). A constant pedestal composition was generated when the dynamic headspace released from polyethylene glycol solutions in a pedestal generator (PG) was combined using computer controlled valves with the humidified air from a gas chromatograph-olfactometer. To keep the solvent at the interface in equilibrium with the remainder of the solution it was stirred with a magnetic stirrer. Hexanal, octanal and decanal were used to test the performance and stability of the pedestal. Using gas chromatography-mass spectrometry and two methods of sampling the pedestal stimulus, the dynamics of the GC-PO were studied. The concentrations of the volatiles released in the GC-PO were linear, constant and could be turned on and off without any detectable background or residual odour.

Introduction

The pedestal olfactometer (PO) is the same, in principle, as the pedestal experiments used to study visual and auditory images in which a brief stimulus pulse (called the figure) is added to a steady-state stimulus (called the ground or pedestal). In 1992 Cain and Polak described the application of pedestal experiments to the study of olfaction: "A potential procedure could entail steady-state adaptation to one odorant and superposition of a second of different quality during test trials. Participants would need to detect the superposed stimulus. Similarity of odour quality, loss of sensitivity to the test odorant via cross-adaptation, and masking of the test stimulus could all come into play to make it more difficult to detect against the background." (1). In 2003 Hattori *et al.* described a GC-PO in which the pedestal is the headspace of green tea to study green tea odour impact compounds (2); a similar system using orange juice headspace was described by de Jong (3) to study masking of taints. As shown in Figure 1 the GC-PO described here uses a PG that relies on the release of odorants dissolved in polyethylene glycol (PEG). Varying odorant concentration in the PEG produces predictable pedestal compositions, and programming the valves delivers these pedestals at precise times for predictable durations.

Experimental

GC-PO Design. Odour perceptions of binary mixtures of hexanal (green) and octanal (citrus) are elemental exhibiting no emergent qualia: just green and citrus (4, 5). In order to study the perceptual experience of odour mixtures in greater detail GC-O air supplies were modified to produce an odour pedestal composed of square wave pulses of uniformly dosed air. These pulses were software controlled to be any duration greater than 1 min and occur anytime during the GC-PO run. Below is a description of the initial design and testing of the odour pedestal that will be used for GC-PO. In order to study the perceptual experience of odour mixtures in greater detail, GC-O air supplies were modified to produce an odour pedestal composed of square wave pulses of uniformly dosed air. These pulses were software controlled to be of any duration greater than 1 min and occur anytime during the GC-PO run. Figure 1-a. (top) shows a schematic of the D2000 air supply (DATU, Inc.) used to purify and humidify the airflow. Figure 1-a (bottom) shows the pedestal generator used to deliver a constant background odour (pedestal) to a GC-O output (2).

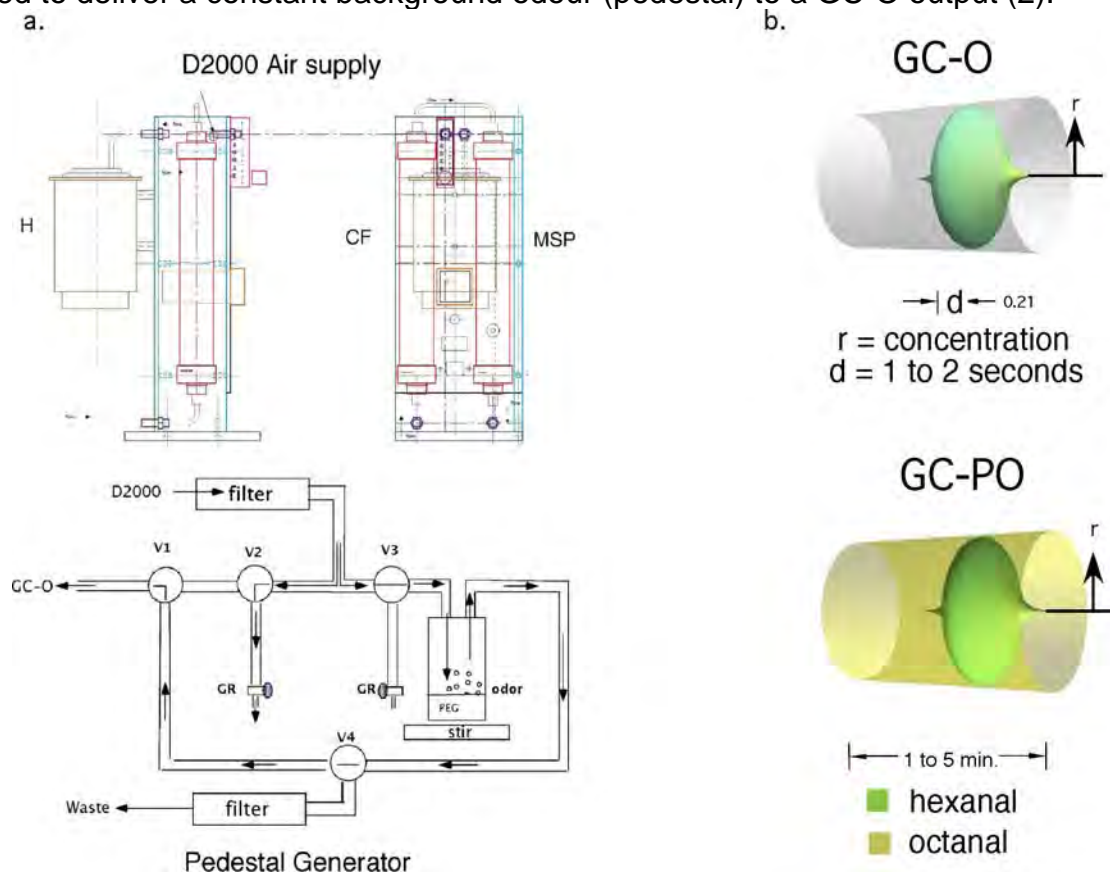


Figure 1. a. Top air purifier and humidifier (H), carbon filter (CF), molecular sieve pre-dryer (MSP). Bottom pedestal generator (PEG), the software controlled valves (V) and pressure balancing needle valves (GR). b. Graphic comparison between GC-O and GC-PO. On the left is a typical GC-O humidified air stream containing an idealized hexanal GC peak (green coded) being carried along in the olfactometry air. The concentration of the GC peak is Gaussian with a band width of 1 or 2 seconds. Below the olfactometry background air is coded yellow to indicate a uniform octanal concentration in the background air (pedestal) of a GC-PO experiment.

The valves (V) are operated with software-controlled actuators using an Arduino controller, driver and C program. The generator tank is filled with PEG containing the pedestal odour. A magnetic stir bar is rotated at about 250 rpm to create a mass transfer within the PEG that is greater than the rate at which odours cross the interface without disturbing the interface size and shape. Airflow was 5 L/min. The system operates by first producing a dynamic release of odorant in a bypass mode to a filter. The system then switches to a GC-PO mode for the time it takes an odorant to elute from the GC. Figure-ground experiments can be designed using mixtures in the pedestal generator as a ground, but only one odorant at a time can be tested as a figure (6,7).

Results and Discussion

Is olfactory processing of odorant mixtures elemental or configural (8-11), i.e. is odorant mixture processing combinatorial or competitive (12-13)? The GC-PO prototype described here was designed to study these questions. As shown in Figure 2-a the GC-PO produced a pedestal with a stable concentration with in 2 min. that remained stable for at least 15 min. for all three compounds tested. Figure 2-b shows that varying the concentration of hexanal, octanal and decanal in the PG solution produced precise linear concentrations in the pedestal air delivered to the GC-O. Preliminary studies show that a pedestal composed of octanal at a moderate concentration (0.04% v/v) can be sniffed at a rate of 1.5 sniffs/sec (mouth closed) for 10 to 15 seconds without changes in character or intensity. After 15 sec. intensity declines but odour character remains constant, while after a minute or more the subject becomes completely adapted to the pedestal odorants. Programming the GC-PO to produce pedestals composed of octanal (0.04% v/v) starting 10 sec before a GC-O injection of hexanal eluted and lasting 30 sec. yielded a clear stable octanal aroma followed by hexanal and octanal aromas that changed rapidly during the 2 sec elution time of the hexanal. Anecdotally the pedestal after the elution of hexanal was much weaker and exhibited a quale different from but related to the quale it exhibited initially.

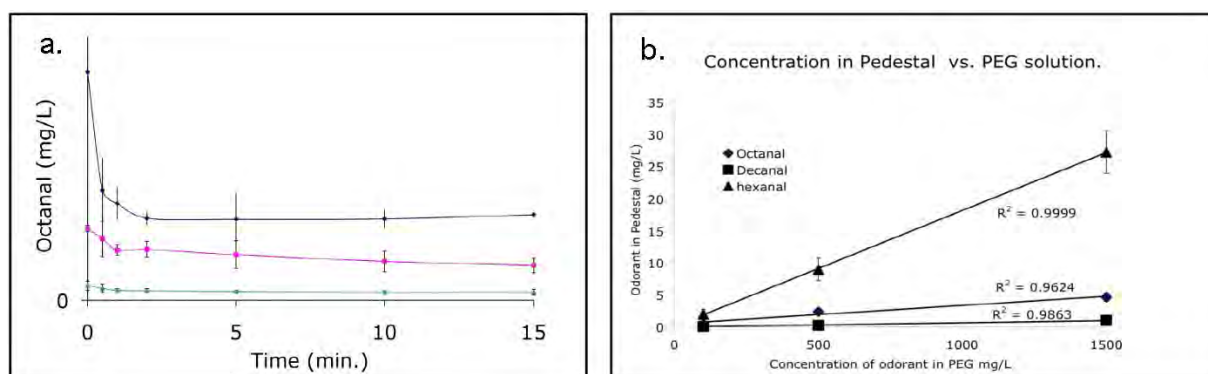


Figure 2. a. Variation in the pedestal generator output was less than the standard error in the concentration of the odorant measured by GCMS using Tedlag bag sampling between 1 and 15 min. The same results were obtained for both hexanal and decanal. Figure 2-b shows that the pedestal concentration is a linear function of the concentration in the PEG of the pedestal generator for hexanal, octanal, and decanal over the concentration ranges these compounds produce odour.

Next, protocols must be developed to quantify the phenomena revealed by the GC-PO. Beyond the obvious dilution analysis of the eluted odorants with and without a pedestal measures of the elemental and configural behaviour of the eluting compounds needs to be demonstrated with appropriate experimental designs. Using pedestals composed of multiple odorants would also provide insights into the perception of real food odours.

References

1. Cain W.S., Polak E.H. (1992) *Chem. Senses* 17: 481-491.
2. Hattori S., Takagaki H., Fujimori T. (2003) *Food Sci. Technol. Res.* 9: 350-352.
3. Burseg K., de Jong C. (2008) The Olfactoscan®: In-vivo screening for off-flavour solutions. Weurman, Interlaken Switzerland.
4. Cain W.S., Drexler M. (1971) *Annals of NY Acad. Sci.*: 427-439.
5. Laing D.G., Willcox M.E. (1983) *Chem. Senses* 7: 249-264.
6. Kadohisa M., Wilson, D.A. (2006) *J. Neurophysiol.* 95: 1888-1896.
7. Kurtz A.J., Lawless H. T., Acree T.E. (2008) Reference Matching of Dissimilar Binary Odor Mixtures. *Chemsens. Perception* (in preparation)
8. Laing D.G., Willcox M.E. (1983) *Chem. Senses* 7: 249-264.
9. Goyert H.F., Frank M.E., Gent J.F., Hettinger T.P. (2007) *Brain Res. Bullet.* 72: 1-9.
10. Zou Z., Buck L.-B. (2006) Combinatorial effects of odorant mixes in olfactory cortex. *Science* (Washington D C).
11. Gottfried J.A., Winston J.S., Dolan R.J. (2006) *Neuron* 49: 467-479.
12. Jinks A., Laing, D.G., Hutchinson I.A.N., Oram N. (1998) *Ann NY Acad Sci* 855: 834-836.
13. Kay L.M., Crk T., Thorngate J. (2005) *Behav. Neurosci.* 119: 726-733.

IMPROVEMENT OF SENSITIVITY IN QUANTITATIVE GC-OLFACTOMETRIC MEASUREMENTS

J. PEŤKA¹, J. Sádecká², A. Escudero³, K. Kukurová², and V. Ferreira³

¹ *Akras Flavours, Wiener Neudorf, Austria*

² *Food Research Institute, Bratislava, Slovakia*

³ *University of Zaragoza, Zaragoza, Spain*

Abstract

Indication of amplifying effect of ethanol on the perceived odour intensity was discovered in previous GC-O experiments. In this study we tested twelve volatiles belonging to various chemical classes to confirm this phenomenon. Two hydroalcoholic solutions and pure water were consecutively put into the humidifier of a GC-O system. Dichloromethane solution containing the tested volatiles at supraliminal concentrations was injected in a GC-O system. Two independent panels measured intensities of the twelve olfactory percepts at the chosen ethanol levels. Panellists of one panel were directed to sniff one minute around the expected retention time only, while the panellists of the second panel were sniffing incessantly during the whole analytical run. Significant amplifying effect of ethanol was observed in ten cases for the target-oriented first panel. Continuous aspiration of ethanol vapours caused, however, a decrease of average intensity for most of the selected volatiles in the case of the second panel.

Introduction

In a previous study (1) we investigated correlations between the outcomes of sensory tests of single flavour compounds dissolved in a wine-like medium and the results of GC-Olfactometry performed on their mixture. Unexpected forms of the dose-response functions of decanal and eugenol raised questions, which were tried to solve, under other means, by putting 10% hydroalcoholic solution into the humidifier of the sniffing port. New measurements focused on these two compounds showed that ethanol increased their odour intensity in the whole concentration range, i.e. at the peri-threshold level too. This means, obviously, that using hydroalcoholic solution in humidifier instead of water could enhance sensitivity of the sense of smell. Accordingly, it could make both qualitative and quantitative measurements of odours more reliable. In current study we extended the previous experimental design with additional hydroalcoholic solution and we tested higher number of volatile organic compounds as well. Furthermore, we tested a hypothesis of general amplifying effect of ethanol for all GC-O analyses, i.e. for those running during the whole analytical time uninterrupted too.

Experimental

Chemicals. All chemicals were gifts from Bedoukian Research Inc. (Danbury, US), except of dichloromethane, which was purchased from Merck (Darmstadt, Germany). They were dissolved in dichloromethane (twice rectified before use) at concentrations

given in (Table 1). Both panels were sniffing the same mixture, physically, to ensure same conditions.

GC-Olfactometry. Panel 1: Sniffings were carried out at constant pressure (linear velocity 34.5 cm.s^{-1} , measured at $143 \text{ }^{\circ}\text{C}$) on HP 5890 II (Palo Alto, US) equipped with a flame ionization detector (FID) and a sniffing port ODP 2 (Gerstel, Mülheim an der Ruhr, Germany). The column was a DB-WAX from J&W (Folsom, US) $30 \text{ m} \times 0.32 \text{ mm} \times 0.5 \text{ }\mu\text{m}$. Temperature program: $35 \text{ }^{\circ}\text{C}$ (1min), $5 \text{ }^{\circ}\text{C.min}^{-1}$, $210 \text{ }^{\circ}\text{C}$. Injector and detector were both kept at $230 \text{ }^{\circ}\text{C}$. One microliter of solution was injected in a splitless mode, the splitless time being 1 min. The study performed seven trained judges (5 women and 2 men, mean age 36 years). The judges were instructed to start sniffing one minute before the expected retention time.

Panel 2: Analytical conditions were the same, except of the gas chromatograph, which was Thermo Quest Trace (Rodano, Italy) equipped with a FID and a sniffing port (ODO-1 from SGE, Ringwood, Australia) connected by a flow splitter to the column exit. The study performed five trained judges (4 women and 1 man, mean age 30 years). The judges were sniffing during whole run time without interruption.

All judges were asked to measure the overall intensity of each odour using a 0-3 scale with seven possible scores (half values allowed). The sniffings were done using Latin square design to randomize the effect of different ethanol levels. Fresh solutions were used for each panellist. Panel intensities were calculated either as arithmetic mean of the measurements (in the following text named as *mean* panel intensities), or as a median of the same (*median* panel intensities).

Results

Different results were obtained depending on the methodology of the GC-O experiment. When the judges started to sniff short time before the expected retention time, *mean* panel intensity of ten compounds increased with rising concentration of ethanol in a humidifier (Table 1). The exceptions were ethyl butanoate, whose panel intensity dropped rapidly with 20% of ethanol in the humidifier, and 3-methyl-1-butanol, whose panel intensity was oscillating around 0.7. The progress of *median* panel intensities perfectly matched *mean* panel intensities; just in the case of 3-methyl-1-butanol they showed a rapid drop of intensity right after putting 10% hydroalcoholic solution into the humidifier.

The results of a panel smelling the mixture uninterruptedly were different. Increase of *mean* panel intensity with introduction of 10% hydroalcoholic solution into the humidifier was observed only for α -ionone and γ -octalactone (Table 2). For 20% hydroalcoholic solution the *mean* panel intensity increased comparing with 10% solution only in the case of α -ionone. In contrast, for eight compounds the intensity decreased with the first increase of ethanol content.

Suppression was, however, much less clear when median was used for calculation of panel intensity: only the panel intensity of decanal decreased when 10% of ethanol was added to the humidifier (we might speculate about 3-methyl-1-butanol too, whose concentration was under the threshold of the second panel, knowing the results of the first panel). *Median* panel intensity of the remaining odours stayed unchanged (but for many at zero level) or increased after introduction of hydroalcoholic solution in the humidifier (2-methylbutanoic acid, γ -octalactone, α -ionone). Further increase of ethanol content, however, caused decrease of some median panel intensities (methionol, γ -octalactone).

Table 1. Panel intensities of twelve compounds produced by the first group of judges at three levels of ethanol in a humidifier. Concentration (c) is in ppm.

Compound	c	Mean			Standard deviation			Median		
		0%	10%	20%	0%	10%	20%	0%	10%	20%
Ethyl butanoate	0.01	0.64	0.57	0.29	1.07	0.89	0.39	0.50	0.50	0.00
cis-3-Hexenal	0.05	1.18	1.29	1.50	0.35	0.64	0.71	1.00	1.25	1.75
2-Heptanone	9	1.46	1.82	2.04	0.86	0.93	0.85	1.50	2.00	2.00
3-Met-1-butanol	0.6	0.68	0.71	0.68	0.72	1.16	1.06	0.50	0.00	0.25
Decanal	1	1.32	2.04	2.14	0.70	1.01	1.05	1.25	2.25	2.25
Linalool	0.1	0.96	1.32	1.57	0.67	1.18	0.83	1.00	1.00	1.50
Acetylpyrazine	0.08	1.14	1.54	1.71	0.76	1.08	0.76	1.00	1.50	1.75
2-Met.but. acid	4	0.82	1.68	1.50	0.81	1.30	1.32	0.50	2.00	1.25
Methionol	1	2.11	2.54	2.57	0.72	0.42	0.43	1.75	2.50	2.75
α -Ionone	1	1.46	1.61	2.07	0.81	0.91	0.97	1.50	1.25	2.25
γ -Octalactone	0.08	1.07	1.79	1.89	0.80	0.89	0.78	1.00	2.00	2.00
Eugenol	0.2	0.75	0.86	1.14	0.72	0.75	0.96	0.50	0.75	1.25

Table 2. Panel intensities of twelve compounds produced by the second group of judges at three levels of ethanol in a humidifier.

Compound	Mean			Standard deviation			Median		
	0%	10%	20%	0%	10%	20%	0%	10%	20%
Ethyl butanoate	0.40	0.40	0.00	0.65	0.65	0.00	0.00	0.00	0.00
cis-3-Hexenal	1.30	1.20	1.30	0.91	0.76	0.84	1.50	1.50	1.50
2-Heptanone	1.40	1.10	1.10	0.42	1.02	0.65	1.50	1.50	1.50
3-Met-1-butanol	0.00	0.00	0.00	0.00	0.00	0.00	0.00	0.00	0.00
Decanal	1.00	0.40	0.20	0.94	0.65	0.45	1.50	0.00	0.00
Linalool	0.70	0.30	0.40	0.97	0.45	0.65	0.00	0.00	0.00
Acetylpyrazine	0.30	0.20	0.00	0.45	0.45	0.00	0.00	0.00	0.00
2-Met.but. acid	0.70	0.70	0.80	0.97	0.45	0.76	0.00	1.00	1.00
Methionol	0.90	0.70	0.70	0.89	0.67	0.84	1.00	1.00	0.50
α -Ionone	0.40	0.50	0.70	0.55	0.50	0.45	0.00	0.50	1.00
γ -Octalactone	1.10	1.60	0.50	0.55	0.42	0.87	1.00	1.50	0.00
Eugenol	2.10	1.80	2.00	0.22	0.27	0.35	2.00	2.00	2.00

The usefulness the current results depends on the aim of a GC-O study. If one needs to quantify specific odours by GC-O (2,3), it would be of great benefit to check, if their intensity increases with rising content of ethanol in the humidifier. This could considerably enhance confidence in identifying the odours, yet increasing the sensitivity of the method. Using hydroalcoholic solutions seems to act unfavourably for the classical, incessant GC-O design. Furthermore, one needs to keep in mind that the panellists are exposed to ethanol vapours for relatively long time.

The deep effect of ethanol on perception of volatiles has been, to our knowledge, observed for the first time by Williams (4,5). Ethanol altered the flavour of alcoholic beverages and gave the products persistency and body. It had a mellowing and suppressing effect on the aroma and altered the acid sugar balance. In his later work (5) Williams found out however, that small quantity of ethanol enhanced intensity of

cider aroma. LeBerre *et al.* (6) also reported synergistic effect of ethanol on odour intensity of isoamyl acetate and whisky lactone. Fischer and Berger (7) reported that dealcoholisation of wine led to reduction of its fruitiness, while the vegetative, musty and sweaty odours increased. In contrast, Guth (8) reported increase of fruity character while reducing the content of ethanol in Gewürztraminer wines. Obviously, we are discussing sensory data and these findings only confirm that individual responses may vary quite a lot.

At higher ethanol levels in water (such as in wines or distillates) are the volatiles better dissolved and their partition towards headspace decreases (6;8,9), mainly for more polar compounds (6;9). In the case of our GC-O setup, however, a quick mixing of vapours in the sniffing funnel was taking place, without a direct influence of water. To our knowledge only Guth performed a study fully comparable with ours (8), where he observed increase of odour thresholds in air (measured with olfactometer) after simultaneous introduction of ethanol vapours for three esters including ethyl butyrate, and three alcohols including 3-methyl-1-butanol. His results corroborate the results of our first panel (which was using a sniffing method comparable to that of an olfactometer), as only for these two compounds we observed decrease of mean panel intensity with rising ethanol concentration.

Our results may suggest that ethanol is competing with alcohols and esters on perceptive receptor level, diminishing the ability to differentiate new odour from the background. On the contrary, for the remaining groups of compounds ethanol may act as a contrast-forming, focusing factor. Ethanol might also help to accumulate the odorants in the lipid-rich perireceptor mucosa of the *regio olfactoria*, similarly to its activity in hydroalcoholic solutions (6;8,9), and herewith promote activation of a wider array of olfactory receptors, possibly by temporal integration (10,11).

References

1. Pet'ka J., Cacho J., Ferreira V. (2003) In *Oenologie2003: 7ème Symposium International d'Onologie* (Lonvaud-Funel, A., ed.); Lavoisier, pp. 563-565.
2. Pollien P., Fay L.B., Baumgartner M., Chaintreau A. (1999) *Anal. Chem.* 71: 5391-5397.
3. Ferreira V., Pet'ka J., Aznar M., Cacho J. (2003) *J. Chrom.* 1002: 169-178.
4. Williams A.A. (1972) *Flav. Ind.* 3: 604-607.
5. Williams A.A., Rosser P.R. (1981) *Chem. Senses* 6: 149-153.
6. Le Berre E., Atanasova B., Langlois D., Etiévant P., Thomas-Danguin T. (2007) *Food Qual. Pref.* 18: 901-908.
7. Fischer U., Berger R.G. (1996) In *4th International symposium on cool climate viticulture and enology* (Henick-Kling T.; Wolf T.E., Harkness E.M., eds.); Communications Services, pp. VII-13 - VII-17.
8. Guth H., Sies A. (2002) In *Eleventh Australian Wine Industry Technical Conference*; Winetitles, pp. 128-139.
9. Tsachaki M., Aznar M., Linforth R.S.T., Taylor A. (2006) In *Flavour Science: Recent Advances and Trends* (Bredie W.L.P., Petersen M.A., eds.); Elsevier, pp. 441-444.
10. Wise P.M., Toczydlowski S.E., Wysocki C.J. (2007) *Toxicol. Sci.* 99: 254-259.
11. Kurtz D.B., Zhao K., Hornung D.E., Scherer P. (2004) *Chem. Sens.* 29: 763-773.

NUMBER OF PANELLISTS OR NUMBER OF REPLICATES – HOW TO RECEIVE MOST INFORMATION FROM A GC-O-MS STUDY

A. SCHÄFER, M.D. Aaslyng, and L. Meinert

Danish Meat Research Institute, Maglegaardsvej 2, DK-4000 Roskilde, Denmark

Abstract

In a detection frequency analysis, a high number of panellists is necessary. As well-trained panellists can be difficult to recruit it can be of interest to use the same panellists in replicates of the same samples. To gain more information about the samples the variation is required to be between samples and not between individual panellists. This study shows that for samples with a low content of odour-active compounds, the variation is often between samples and not between panellists. In this case, when using the same panellist several times, the amount of information about the sample still increases. In samples with a higher content of odour active compounds, the variation is more often between panellists. In this case, using the same panellist in replicate does not increase the amount of information about the sample.

Introduction

GC-O analysis has been used for many years to gain knowledge of individual volatiles contributing to the aroma of, for example, foods (1-4). Using a GC equipped with two sniff ports in combination with a MS detector, it is possible to use two panellists to detect the aroma compounds and at the same time identify the compounds. When two panellists sniff the same sample at the same time, it is possible to discriminate between sample variation and panellist variation. To gain more information by using replicates of the same panellists the variation in detection is required to be between samples and not between panellists. The aim was to investigate the effect of replicates when using four panellists in a GC-O-MS analysis.

Experimental

Three grams of pork were heated in a conical flask for 7 min at either 150°C or 250°C. The volatiles were sampled by dynamic headspace at 50°C for 10 min purging with 60 ml N₂. Desorption of volatiles was performed thermally using an ATD400 (Automatic thermal desorber, Perkin Elmer, Bucks, UK). The trap was thermally desorbed at 250°C for 10 min. Volatile aroma compounds were cryo-focused onto the cold trap in the ATD400 at -30°C with a flow of 20 ml/min. Desorption from the cold trap was performed at 250°C for 5 min with a helium flow at 10 ml/min and an outlet split ratio of 1:10. Separation and identification were performed by gas chromatography/mass spectrometry (GC/MS, Agilent Technologies, Palo Alto, USA). Separation was performed with a DB5MS column (30 m, 0,25 mm I.D., 1 µm film thickness, J&W Scientific, USA) using an oven programme starting at 40°C for 5 min, rising 10°C/min to 310°C and holding for 5 min. The carrier gas was helium at a head pressure of 7.8 psi. The mass selective

detector was operated in SCAN mode with an energy voltage of 70 eV and an emission current of 35 μ A. Scanning was done from 33 m/z to 350 m/z. Compounds were tentatively identified using NIST/EPA/NIH Mass Spectral Database. The GC was equipped with two ODP2 sniffing ports from GERSTEL. The panellists were trained in the sniffing technique using artificial standards and real samples. Four panellists sniffed the samples with two panellists assessing each sample simultaneously. All four panellists assessed the samples twice with a new partner each time.

Results

For the samples heated at 150°C, 21 odour-active areas were detected by the panellists (Table 1). 10 compounds were tentatively identified in these areas.

Table 1. Aroma compounds in pork heated at 150°C detected by GC-O and tentatively identified by GC-MS.

No	KI	Compound ^{*1} Panellist	Replicate 1		Replicate 2		Replicate 3		Replicate 4		DF ^{*2}
			P1	P2	P3	P4	P2	P4	P3	P1	
1	<600	Sulphur dioxide	X		X	X		X	X		5
2	<600	Ethanol	X	X	X	X	X	X	X	X	8
3	<600	2-Methylpropanal	X	X	X	X	X	X	X		7
4	<600	2,3-Butanedione/ 2-Butanone	X	X	X	X	X	X	X	X	8
5	649	3-Methyl-butanal	X	X	X	X	X	X	X	X	8
6	659	2-Methyl-butanal		X	X			X	X	X	5
7	700	Heptane/ 2,3- Pentanedione	X	X	X	X		X			5
8	803	Hexanal	X	X		X	X	X	X	X	7
9	831		X	X		X			X	X	5
10	875		X	X	X	X	X	X	X	X	8
11	910		X	X		X	X	X		X	6
12	916		X	X	X	X		X	X		6
13	930		X	X	X	X	X	X	X	X	8
14	987		X	X	X	X	X	X	X	X	8
15	1035		X			X				X	3
16	1069		X		X	X	X	X			5
17	1101	Undecane	X	X	X	X	X	X	X	X	8
18	1107	Nonanal	X	X				X		X	4
19	1121		X	X	X		X	X			5
20	1168		X	X	X			X			4
21	1295		X	X	X						3

*¹ Tentatively identified by NIST and KI *² Detection frequency

Seven of the areas were detected by all panellists in both samples (no. 1, 4, 5, 10, 13, 14, 17). Two of the areas were only missed by one panellist in one of the samples (no. 3, 8). In eight of the areas, the compounds were not detected by any of the panellists in at least one sample (no. 7, 9, 15, 16, 18, 19, 20, 21). In these cases, the same panellist can be used for repeated sniffing and still increase the amount of information of the sample. In five odour-active areas (no. 1, 11, 15, 18, 21) at least

one panellist missed the odour in both samples. In these cases, the panellist might have a high odour threshold against the compounds, and using the same panellist in replicate does not increase the amount of information.

For the samples heated to 250°C, 28 odour-active areas were detected by the panellist (Table 2). Twenty of the compounds were tentatively identified.

Table 2. Aroma compounds in pork heated at 250°C detected by GC-O and tentatively identified by GC-MS.

No	KI	Compound ¹ Panellist	Replicate 1		Replicate 2		Replicate 3		Replicate 4		DF ²
			P1	P2	P3	P4	P2	P4	P3	P1	
1	<600	Sulphur Dioxide	X	X	X	X	X		X	X	7
2	<600	Triethylamine	X	X	X	X	X	X	X	X	8
3	<600	2-Methyl propanal	X	X	X	X	X	X	X	X	8
4	<600	2,3-Butanedione/ 2-Butanone	X	X	X	X	X	X	X	X	8
5	649	3-Methylbutanal	X	X	X	X	X	X	X	X	8
6	659	2-Methylbutanal	X	X		X		X		X	5
7	700	2,3-Pentanedione	X	X	X	X	X	X	X	X	8
8	721		X	X		X		X	X	X	6
9	726		X			X	X	X			5
10	783	2-Methylthiophene	X	X	X	X	X		X	X	7
11	798			X		X	X			X	5
12	803	Hexanal	X		X	X		X	X	X	6
13	817	2-Methylpyridine	X	X			X	X	X	X	6
14	827	Methylpyrazine	X	X	X	X	X	X	X	X	8
15	856	3-Furanmethanol	X	X		X	X	X			5
16	875		X	X	X	X	X	X	X	X	8
17	886		X	X	X	X		X	X		6
18	904	Heptanal	X	X	X		X	X	X	X	7
19	912/ 917	1-(2-Furanyl)- ethanone /	X	X	X	X	X	X	X	X	8
20	920/ 922	2,5-Dimethylpyrazine 2-Ethylpyrazine/ 2,3-Dimethylpyrazine	X				X	X	X		4
21	930		X	X	X	X	X	X	X	X	8
22	965	3-Ethylpyrazine		X	X	X	X		X	X	6
23	982	Dimethyl trisulphide	X	X	X	X	X	X	X	X	8
24	1006/ 1035	2-Ethyl-6-methyl- pyrazine / 2,3,5- Trimethylpyrazine	X	X	X	X	X	X	X	X	8
25	1069		X	X	X	X	X	X	X	X	8
26	1081/ 1088	3-Ethyl-2,5-pyrazine 2-Ethyl-3,5- dimethylpyrazine	X		X	X		X	X	X	6
27	1107	Nonanal	X	X	X	X	X		X	X	7
28	1129		X	X			X	X			4

¹ Tentatively identified by NIST and KI. ² Detection frequency.

In twelve of the areas, all panellists detected the odour in both samples (no. 2, 3, 4, 5, 7, 14, 16, 19, 21, 23, 24, 25) while in four of the areas, only one panellist missed the odour in one sample (no. 1, 10, 18, 27). In five areas, the same panellist missed

the odour in both samples (no. 6, 11, 12, 15, 26, 28). Four of these were the same panellist (P3). Only in four areas the odour was missed by both panellists in at least one sample (no. 13, 15, 20, 28). In the rest of the areas, different panellists missed the odour in different samples. In these cases, the same panellist can be used several times and still increase the amount of information of the samples (Table 3).

It is often difficult to recruit enough well-trained panellists for a detection frequency analysis. Sometimes, it is necessary for the same panellist to sniff several times instead of increasing the number of panellists. This requires that the variation in detection primarily is a variation between samples and not between panellists. If the variation is between panellists, a replicate using the same panellists will not increase the amount of information in the study.

Table 3. Summary of the number of odour-active areas detected in the samples.

	DF 8 ¹	DF 7	Missed by both panellist in a run	Missed in both runs by one panellist	Total number of odour active areas
150°C	7	2	8	4	21
250°C	12	4	4	5	28
Implication	Using same panellist twice ok	Using same panellist twice ok	Using same panellist twice ok	No extra information by using same panellist twice	

¹ Detection frequency

In this study, the samples heated to 150°C represent samples with a lower content of odour active compounds compared to samples heated to 250°C. In samples with a low concentration of odour-active compounds, the main reason for a lower detection frequency was variation between samples and not between panellists. In this case, the panellists can sniff in replicates without missing information about the odour-active areas. In the samples with a higher concentration of odour-active compounds, a lower detection frequency was often caused by a panellist who could not detect the odour in any of the samples. In this case, a higher number of panellists would increase the amount of information instead of using the same panellists twice.

References

1. Moon Y.S., Cliff M.A., Li-Chan E.C.Y. (2006) *Food Research Intern.* 39: 294-308.
2. Cerny C.; Grosch W. (1992) *Z. Lebensm. Unters. Forsch.* 194: 322-325.
3. Pollien P., Ott A.; Montigon F., Baumgartner M., Munoz-Box R., Chaintreau A. (1997) *J. Agric. Food Chem.* 45: 2630-2637.
4. Aaslyng M.D., Schäfer A. (2008) *Eur. Food Res. Technol.* 226: 937–948.

ANALYTICAL METHOD FOR IDENTIFICATION OF ODOUR-ACTIVE COMPOUNDS IN POLYOLEFINS

H. Hopfer, N. Haar, E. LEITNER

Institute of Food Chemistry and Technology, Graz University of Technology, Petersgasse 12/2, 8010 Graz, Austria

Abstract

A method for identification of odour-active compounds in polyolefins (namely polyethylene PE and polypropylene PP) is described. A combination of simultaneous distillation/extraction and fractionation on silica gel solid phase cartridges is needed (a) for enrichment of odour-active compounds in extract and (b) separation of odour-active substances heavily interfered by non-polar, non-odorous volatiles like alkanes and alkenes. Evaluation of odour-intensity and odour-activity is facilitated by using a combination of detection frequency (surface of nasal impact frequency) and aroma extract dilution analysis carried out by 6 trained panellists using GC-O. Identification of odour-active compounds is made by either GC-MS and/or comparison of retention indices and odour impression with pure substances.

Introduction

Plastic materials are a significant economic factor in Europe as 25% of 2006 worldwide produced 246 Mio. tonnes are produced here. Polyolefins – polyethylene PE and polypropylene PP- account for about 25 Mio tonnes mainly used in Packaging, Building & Construction and Automotive [1].

Due to increased consumer awareness and more restrict legislation plastic producers need to know what compounds are present within their products. Especially low molecular weight compounds such as odour-active substances are of interest. Presently, plastic producers measurement of odour by the use of sensory panel is of little use for product development as no information is obtained about single odorous substances and their concentrations. Knowledge about odorous compounds coming from plastics is mostly related to specific problems such as odour/flavour alteration of packaged goods [2]. Literature about odour-active compounds in polyolefins is for most cases dealing with PE, especially in packaging applications. Some publications can be found dealing with identification of odorous compounds in PE [3-5]. All authors report of carbonyls (alkanals, 2-alkenals and 1-alken-3-ones with chain length between 6 and 11 C-atoms) as major odour contributors coming from thermal oxidation processes. Sanders *et al.* [5] identified 8-Nonenal as a major contributor to the odour of a PE packaging with a sensory threshold at sub-ppb levels. Normal concentrations of carbonyls are in the lower µg/kg range, and can increase drastically under extreme thermal treatment up to 100mg/kg as reported by Bravo [3]. In case of PP, oxidation products and odorous compounds related to oxidation should be similar to PE. Nevertheless, intramolecular hydrogen transfer reactions due to presence of methyl groups as side chains should take place as described in [6]. The aim of this ongoing work is to obtain qualitative

and quantitative information about odour-active compounds in various PE and PP samples.

Experimental

Sample preparation and working-up procedure. Using Simultaneous Steam Distillation/Extraction (SDE) adapted from Veith [7], an n-pentane extract of polyolefin sample is obtained and used for further analysis. Samples are extracted fivefold with Internal Standard (IS, 20µg/kg sample) with one blank to monitor the whole preparation process. Preliminary tests showed that SDE does not contribute to additional thermal stress of the sample as processing and conveying temperatures can reach up to 290°C for PE. In comparison to simple solvent extraction SDE extracts only volatiles. Compared to normal static headspace (e.g. VDA 277) with sample amount up to 2g, SDE is able to work with much more sample amount. The extract is fractionated on silica gel SPE cartridges in three fractions using n-pentane, diethylether and mixtures of both respectively, followed by GC-MS analysis.

Detection Frequency – Aroma Extract Dilution Analysis (GC-SNIF-AEDA) [4, 9-10]. Evaluation of odour-active substances was accomplished by 6 trained panellists (5 females, 1 male, aged 25-45). All panellists are members of the in-house sensory panel and specially trained for odour evaluation and description. Each sample is sniffed in one run by a single panellist until odour-active substances are eluted. Maximum three runs per person and day are carried out. Dilutions (1:100 and 1:1000 if necessary) are evaluated by three and, one judge, respectively. A combination of Detection Frequency adapted from [4, 9] and Aroma Extract Dilution Analysis (AEDA) adapted from [10] has been developed. All obtained olfactory chromatograms are graphically overlaid and normalized. Compounds with SNIF-values of 80% and 100% for the pure extracts and all compounds detected by one judge in the diluted samples are used for identification. The identification of odour-active compounds is made by comparison of experimental and literature Kováts Retention Indices (RI) [8] with values from institute's own RI database. The validation was carried out by GC-O of pure standard solutions or GC-MS if concentrations are high enough. Pre-tests showed that comparison with reference databases is best when RIs are calculated at starting time of odour impression. This is of enormous influence for highly odour-active compounds eluting long time where RI spans over 50 indices. A substance was taken into account if the database value did not differ from the experimental value more than ± 5 .

Results

In Figure 1 separation of non-odorous, non-polar volatiles from mid-polar, odour-active compounds by fractionation on silica gel SPE cartridges is shown. Concentration of fraction 1 is 7 times less than that of fraction 2 due to more solvent eluting. Homologous series of n-aldehydes from C₇-C₁₂ in the concentration range of IS (20µg/kg) and above can be found in fraction 2 which would have been heavily interfered by linear and branched alkanes and alkenes without fractionation (n-alkanes from C₅-C₁₄ are marked in fraction 1).

In Figure 2, a SNIF chromatogram with corresponding FID chromatogram of crude extract is shown. Nearly all odour-active compounds elute between 700 and 1500 RI. For the shown PP sample 10 odour-active compounds are detected by all judges in the crude extract and further three are detected by 80% of the judges. For

the diluted samples (1:100) 9 compounds could still be detected by all judges and for the 1:1000 diluted sample 6 major odour drivers remained.

In Table 1 a summary of identified odour-active compounds in the PP sample from Figure 2 is shown. All compounds still detectable in the 1:1000 diluted sample are carbonyls (heptanal, octanal, 1-nonen-3-one, 6-nonenal, (E)-2-nonenal and decanal) and correspond well with the literature [3-5]. In the 1:100 diluted sample a Maillard product typically found in proline-containing foods like basmati rice [11] (2-acetyl-1-pyrroline) could be identified by 100% of the judges. Pure sample was synthesized (11) and used for reference GC-O. Origin of this product is still unknown as nitrogen-containing precursors are usually absent in plastics. Different explanations for the formation of 2-acetyl-1-pyrroline in polyolefins are postulated and currently under investigation.

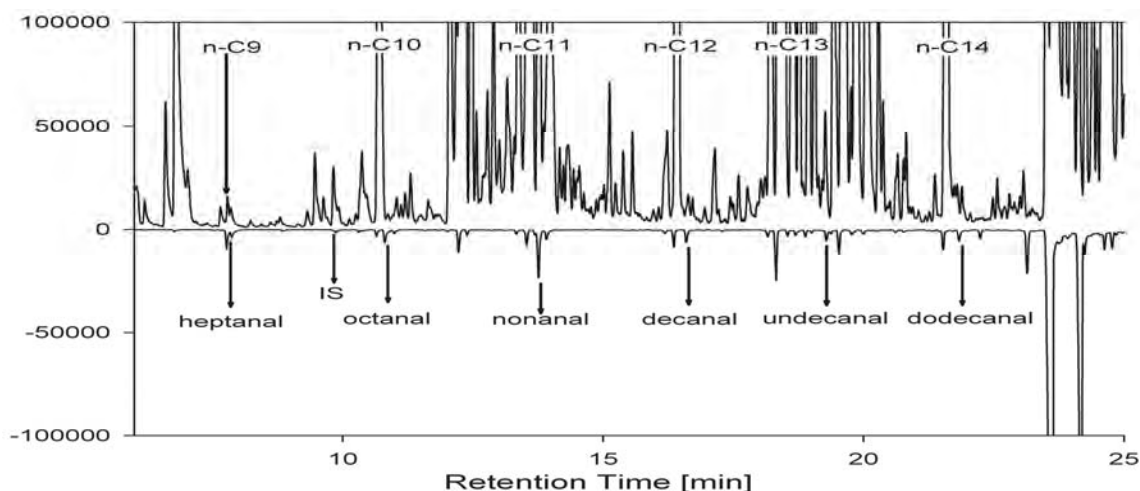


Figure 1. Total ion chromatogram (TIC) of PP fraction 1 (top) and fraction 2 (bottom) with marked homologous series of *n*-alkanes and *n*-alkanals.

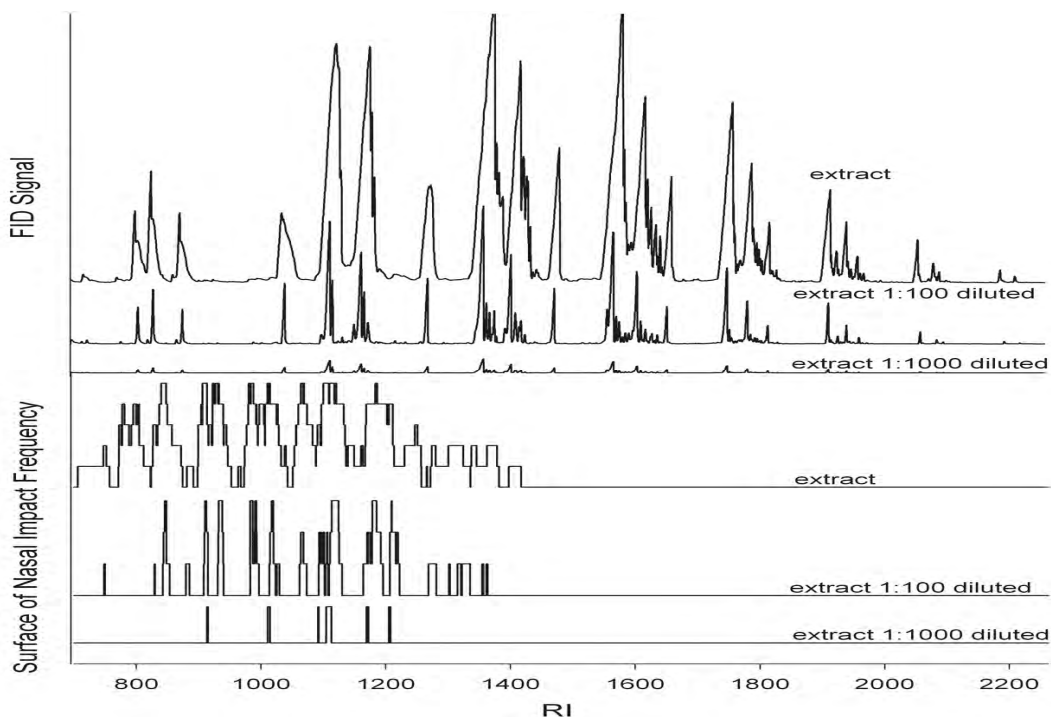


Figure 2. Detection frequency diagrams (SNIF diagrams) with corresponding FID signal for a PP extract, pure and in 1:100 and 1:1000 dilution.

Table 1. List of identified odour-active compounds in a PP sample.

Compound	RI(HP-5)	Detection [SNIF %]*	Identified**	Odour description
1-Hexen-3-one	773.6	100% I	a	plastic, glue, green
Hexanal	796.4	100% I	a	fresh, green apple, grass
(Z)-2-Hexenal	838.6	100% I + II	a	roasty, green, plastic, burnt
Heptanal	905.4	100% I + II + III	b [57µg/kg]	fatty, orange, aldehyde
2-Acetylpyrroline	926	80% I + 100% II	a	roasty, basmati, popcorn
Unknown	978	100% I + II		waxy, candle-wax, roasty
1-Octen-3-one	986.1	100% I + II	a	mushroom
Octanal	1008.6	100% I + II + III	b [73µg/kg]	orange, citrus, soapy, plastic
(E)-2-Octenal	1059.1	100% I + II	a	fatty, plastic, pungent, roasty
1-Nonen-3-one	1089.5	40% I + 100% II + III	a	mushroom
(E)-6-Nonenal/ 8-Nonenal/ (Z)-6-Nonenal/ Nonanal	1095.1/ 1099.3/ 1101.2/ 1104.6	100% I + II + III	a and b: Nonanal [232µg/kg]	(burnt) plastic, waxy, stink bug, green, fatty, soapy, goat, washing powder
(E)-2-Nonenal	1165.8	80% I + 100% II + III	a	cucumber, green, fatty, PE
Decanal	1203.1	40% I + 100% II + III	b [64µg/kg]	green, fatty, burnt plastic
(E)-2-Decenal	1269.1	20% I + 66% II	a	fresh, green, fatty, aldehyde
Undecanal	1298.5	20% I + 33% II	b [51µg/kg]	soapy, flowery, fatty, rancid
(E)-2-Undecenal	1356.9	20% I + 66% II	a	stink bug, dusty, green, fatty

* I: detection in pure extract, II: detection in 1:100 dilution, III: detection in 1:1000 dilution

** a: pure standard sniffing, b: MS identification and quantification by IS

Conclusion

The proposed sample preparation scheme is able to identify and quantify odour-active compounds in polyolefins. Among the found substances mainly carbonyls are detected with the lowest thresholds and highest odour-activity, respectively, for those with 8 or 9 C-atoms. This corresponds with investigations conducted on homologous series of aliphatic aldehydes (12). Additionally, a typical Maillard-product (2-acetyl-1-pyrroline) was successfully identified, its origin is still unclear and under further investigation.

References

1. Plastics Europe Association of plastics manufacturer (2008).
2. Lau O.W., Wong S.K. (2000) *J. Chromatogr. A* 882: 255-270.
3. Bravo A., Hotchkiss J.H., Acree T.E. (1992) *J. Agric. Food Chem.* 40: 1881-1885.
4. Linssen J.P.H., Janssens J.L.G.M., Roozen J.P., Posthumus M.A. (1993) *Food Chem.* 46: 367-371.
5. Sanders R.A., Zyzak D.V., Morsch T.R., Zimmerman S.P., Searles P.M., Srothers M.A., Eberhart B.L., Woo A.K. (2005) *J. Agric. Food Chem.* 53: 1713-1716.
6. Hoff A., Jacobsson S. (1982) *J. Appl. Polym. Sci.* 27: 2539-2551.
7. Veith G.D., Kiyus L.M. (1977) *Bull. Environ. Contam. Toxicol.* 17: 631-636.
8. Farkas, P., Le Quére J.L., Maarse H., Kovác M. (1994) In *Trends in Flavour Research* (Maarse H., van der Heij D.G., eds.), Elsevier Science: Amsterdam, pp145-149.
9. Pollien P., Ott A., Montigon F., Baumgartner M., Munoz-Box R., Chaintreau A. (1997) *J. Agric. Food Chem.* 45: 2630-2637.
10. Ullrich F., Grosch W. (1987) *Z. Lebensm. Unters. Forsch.* 184: 277-282.
11. BATTERY R.G., Ling L.C., Bienvenido O.J., Turnbaugh J.G. (1983) *J. Agric. Food Chem.* 31: 823-826.
12. Schnabel K.O., Belitz H.D., von Ranson C. (1992) *Z. Lebensm. Unters. Forsch.* 195: 515-522.

ASSESSMENT OF CIDERS TYPICALITY CHARACTERISATION THROUGH ODORANT VOLATILE COMPOUNDS

A. VILLIERE, G. Arvisenet, C. Prost, and T. Sérot

Laboratoire de biochimie alimentaire, Equipe Arôme, ENITIAA, UMR GEPEA CNRS 6144, Rue de la Géraudière, BP 82225, 44322 Nantes Cedex 3, France

Abstract

The aim of this work was to identify the compounds responsible for the typicality of ciders. In a first step, a method was developed to provide representative aromatic extracts of ciders. Then volatile compounds responsible for the odorant perception of three different ciders were analysed by gas chromatography, olfactometry, and mass spectrometry.

Introduction

Apple cider is an alcoholic beverage obtained by fermentation of apple must. The volatile compounds of apple and apple juice have been extensively studied over the last decades. However, there is little information about odorant volatile compounds of apple cider. Gas chromatography/olfactometry (GC/O) analysis is a powerful tool to determine key compounds of food aroma. The odour of the studied extract has to be close to that of the food used for extraction. This odour similarity is not obvious since different classes of compounds are preferentially extracted according to the chosen method. Therefore prior to GC/O analysis, a comparison of the odour of the food with the corresponding extract should be made. The objective of this work was to develop a representative extraction method to analyse volatile compounds of ciders and to examine those responsible for the odorant perception of different ciders. Only solvent-free extraction methods were tested in order to avoid undesirable odour of solvent and odours developed when heating to eliminate this solvent.

Experimental

Chemicals and materials. A commercial cider purchased in a supermarket was used for the development of a representative extraction method. Study of aroma compounds was conducted on three ciders selected among several according to their different organoleptic properties: a sweet cider from Normandy, a brut cider from the pays d'Auge and a pear cider. Discriminating tests allowed verifying that ciders were perceived differently by a panel of 36 naïve judges. Ciders were stored at -80°C until analyses in 125 mL brown flasks sealed with Teflon/rubber screw caps. Prior to analyses, vials were put at 37.5°C for 1h. Chemical standards ($p \geq 98\%$) used for mass spectra identification of odorant compounds were purchased from Aldrich (St Quentin Fallavier, France).

Choice of a representative extraction method. For all extractions, 20 mL of cider were sampled except when otherwise mentioned. For static headspace extraction, vials (60 mL) containing the cider were sealed using Teflon/Silicone septa plastic caps (Varian, France). After equilibration at 37.5°C for 1 h, 250 μL of headspace was

withdrawn using gastight syringe and injected into the injection port of the gas chromatograph (GC).

Headspace SPME (HS SPME) extractions were conducted with DVB/CAR/PDMS, CAR/PDMS and PDMS fibres (Supelco, Inc., Bellefonte, PA). Each sample was introduced in a 60 mL vial and equilibrated at 37.5°C in a thermostatic bath for 30 min under stirring. Then the fibre was introduced in the headspace for 10 min before being inserted into the injection port of the GC. Same fibres and procedure were used for aroma extraction by liquid SPME except that 60 mL of cider were placed in the 60 mL vial and the fibre was immersed in the cider.

Headspace purge and trap was conducted with a concentrator (model LSC 2000; Teckmar Inc., Cincinnati, OH) equipped with a capillary interface, for cryofocusing, connected to the GC. Cider was introduced into a flask (50 mL) containing a stir bar. Temperature was maintained at 37.5 °C with a heating ring and the headspace of the sample was purged with helium during 5 min at 60 mL min⁻¹. Volatile compounds extracted were swept into a Tenax trap at room temperature. After trap desorption, volatiles were cryo-focused at -40 °C using carbon dioxide and thermally desorbed at 200 °C for 2 min to be transferred into the column. Same procedure was applied for bubbling purge and trap except that 60 mL of cider was introduced in the flask and the sample was bubbled with helium during 5 min.

Recovery of the extracts and evaluation of the extracts representativeness. Extracts were analysed on a Varian Star 3400 GC (Varian, Palo Alto, CA) equipped with a DB Wax column (30 m length, 0.32 mm internal diameter, 0.5 µm film thickness, J&W Scientific, Folsom, CA). Detector temperature was set at 260°C and oven temperature program was set from 50 °C (5 min) to 150 °C at 5 °C.min⁻¹ and from 150 °C to 250 °C (7 min) at 10 °C.min⁻¹. Helium was used as carrier gas at 2 mL.min⁻¹ flow rate. The GC effluent was split 1:1 between the FID (T: 250 °C), to control the chromatographic pattern of the extract, and a 100mL glass syringe (1).

Twelve trained judges were asked to evaluate, on a 10 cm-scale, the proximity between the odour of each extract collected in the syringes and the original cider odour (representativeness). The reference (right anchor of the scale) corresponded to 0.05 mL of the original cider in a syringe. A hidden reference, containing 0.05 mL of the original cider, was also presented with the extracts. All syringes were foil-wrapped to prevent judges from seeing if they contained cider or gaseous extracts. Results are the means of the 12 judges' evaluations.

GC/O/MS analysis of 3 discriminated ciders. The GC/O system consisted of a 6890N GC (Hewlett-Packard Co., Palo Alto, CA) equipped with a FID, a mass detector (5973-Network), and a sniffing port ODP2 (Gerstel, Baltimore, MD). The GC effluent was split 1:1:1 between the FID, the mass detector and the sniffing port.

Extracts obtained from the three ciders were injected into a DB Wax column (30 m length, 0.32 mm internal diameter, 0.5 µm film thickness, J&W Scientific) and volatile compounds were separated according to chromatographic conditions similar to those described above except for flow rate of helium (3 mL.min⁻¹) and oven temperature program: 50 °C (2 min) to 80 °C at 3 °C.min⁻¹, from 80 °C to 105 °C at 5 °C.min⁻¹ and from 105 °C to 240 °C (1 min) at 10 °C.min⁻¹. Mass spectra were recorded in electron impact mode (70 eV) between 33 and 300 *m/z* mass range at a scan rate of 2.7 scan sec⁻¹. Compounds identification was based on a comparison of mass spectra with those of MS spectra database (Wiley 6) and of standard molecules injected in the same conditions. Coincidence of odour description by judges and literature data could be used to confirm identification of odorant compounds. Olfactometry tests were conducted with 10 trained judges. GC effluent

was carried to the sniffing port using deactivated capillary column heated at 200 °C and supplied with humidified air at 40 °C. Judges were asked to assign odour descriptor to each odorant area detected. Results were expressed in frequency detection. Only odorant areas perceived by at least 3 judges were considered.

Results

Representativeness of the extracts. Representativeness scores of the extracts obtained by the different methods ranged from 2.5/10 for the extracts obtained by liquid SPME with a PDMS fibre, to 6.5/10 for those obtained by HS SPME with a CAR/PDMS fibre (Table 1).

Table 1. Representativeness mean scores of the extracts - Letters represented results of multiple comparison of means test.

Extraction method	Representativeness mean score
Liquid SPME PDMS fibre	2.5 ^e
Headspace purge and trap	2.9 ^{de}
Bubbling purge and trap	3.8 ^{cde}
Liquid SPME Car/PDMS fibre	3.9 ^{cde}
Liquid SPME DVB/Car/PDMS fibre	4.4 ^{cde}
Headspace SPME DVB/CAR/PDMS fibre	4.5 ^{cd}
Headspace SPME PDMS fibre	4.9 ^{bc}
Headspace SPME CAR/PDMS fibre	6.5 ^{ab}
Hidden reference	8.5 ^a

The extract obtained by HS SPME with a CAR/PDMS fibre was the most representative of the original cider odour. Multiple comparisons of means showed that no difference was perceived between the odour of this extract and the odour of the hidden reference, contrary to other extracts. Therefore, these extraction conditions were applied to investigate the aroma typicality of discriminated ciders.

Olfactometric analyses of 3 discriminated ciders. More than 100 volatiles were detected in the ciders whereas only 50 were detected in previous studies (2, 3). A majority of them was esters (~60) and alcohols (~20).

43 odorant areas (OA) were pointed by judges in the sweet cider from Normandy and 24 in the pays d'Auge and pear ciders (Figure 1). These OA were either associated with a single volatile compound or with several coeluted volatile compounds.

15 OA, among the most potent ones, were common to the 3 ciders (numbered 1 to 15). However, their detection frequency differed from a cider to another. 7 OA were associated to esters (1, 3-5, 7, 10, 13), and were described with fruity or sweet notes. The others were described as floral, green, earthy or metallic.

Few OA were characteristic of only one cider. Six were found in the sweet cider from Normandy. There were associated with ethanal (fruity), 1-pentanol (fruity, sweet), heptyl acetate (metallic, earthy), hexyl butanoate (cocoa) and hexyl hexanoate (sweet) and one OA (rancid) could not be associated with a chromatographic peak. Two OA were detected only in the extract from the pear cider and were associated to ethyl crotonate (sweet) and β -citronellol (floral, fruity). No specific OA was found in the cider from the pays d'Auge. These results suggest that ciders odorant characteristics could be linked to both the OA specific to a cider and the proportions of major OA common to all ciders.

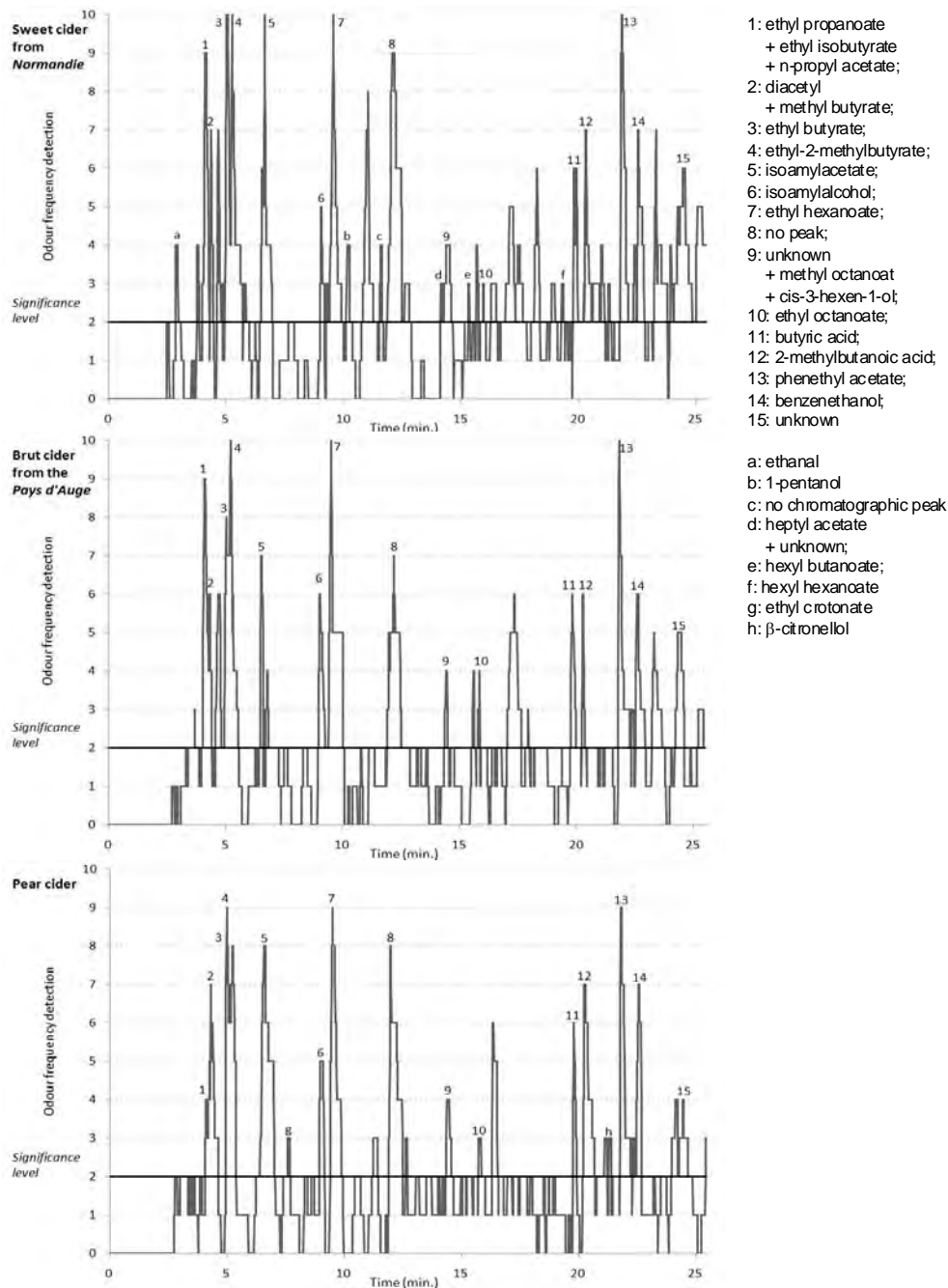


Figure 1. Olfactometric pattern of 3 discriminated ciders: a sweet cider from Normandy, a brut cider from the pays d'Auge and a pear cider.

Conclusion

These results provide elements to understand the origin of the typicality of ciders. Further studies, with a larger selection of ciders, will now be necessary to confirm if these aromatic profiles can explain ciders odorant typicality. Then a connection with the soil and the know-how of a region would be interesting to investigate.

References

1. Rannou C., Vanzeveren E., Le Bail A., Prost C. (2006) *Ind. céréales* 146: 16-18.
2. Le Quere J.M., Husson F., Renard C., Primault J. (2006) *LWT-Food Sci Technol.* 39: 1033-1044.
3. Xu Y., Fan W., Qian M.C. (2007) *J. Agr. Food Chem.* 55: 3051-3057.

QUANTITATION OF SULPHUR AROMA COMPOUNDS IN MAILLARD MODEL REACTION SYSTEMS OF DIFFERENT COMPOSITION

L. JUBLOT, E.A.E Rosing, L. v.d. Blom, G. Desclaux, S.I.F.S. Martins, A.M. Batenburg, and G. Smit

Unilever R&D (Unilever Food and Health Research Institute); Olivier van Noortlaan 120, PO Box 114, 3130 AC Vlaardingen, The Netherlands

Abstract

The development of a SPME-GCMS method aimed to quantify 2-methyl-3-furanthiol (MFT), furfurylthiol (FFT) and bis(2-methyl-3-furanyl) disulphide (MFT-MFT) in model reaction systems of various amino acid and sugar composition is presented. However, the concentration of cysteine was demonstrated to have a major impact on the thiol stability and the partition of sulphur species between thiols and their disulfides forms. The impact of cysteine was only partially compensated by stable isotopic labelled standards. We concluded that thiol and disulfide compounds can not be simultaneously measured reliably in model reaction systems containing an undefined cysteine concentration via analytical methods based on partition.

Introduction

Thiol compounds such as 2-methyl-3-furanthiol (MFT) and 2-furfurylthiol (FFT) exhibit very potent meat aroma characters. The analysis of these two thiols is complicated due to their instability, in particular their ability to oxidise into disulfides like MFT-MFT or FFT-FFT (1), also displaying meaty characters. To understand the impact of composition of the starting material and thermal condition on the formation of such meaty aroma compounds, an analytical method, allowing the quantification of targeted sulphur compounds in food matrices of different composition was desired. A method based on SPME-GCxGC-TOFMS was selected as a good compromise between sensitivity, automation, minimal sample preparation. Also, SPME-GCMS has already been reported for thiols and disulfides quantification (2). The experiments to validate the method were performed on GC-MS and are reported in this paper.

Experimental

MFT, FFT, and MFT-MFT were purchased from Aldrich (Zwijndrecht, The Netherlands) and the respective stable-isotope labelled internal standard (labelling degree >98%) MFT* ($[^2\text{H}_3]$ 2-methyl-3-furanthiol) and MFT*-MFT* ($[^2\text{H}_6]$ bis(2-methyl-3-furanyl)disulphide) from AromaLAB AG (Munich, Germany). These chemicals were spiked either in a pyrophosphate buffer (pH 6) or in a sulphur free model reaction system composed of glutamate (0.3%), glycine (2.5%), xylose (0.5%), glucose (0.5%) and fructose (0.5%) reacted at 100°C under reflux for 2 hours in the same buffer.

Analysis were performed via SPME-GC-MS, using 30 min absorption time at 60°C on a PDMS fibre (100µm coating) desorbed at 230°C in a Trace GC (Thermo).

Separation was performed with a Restek DB5 (30m x 0.25mm x 0.5 μ m film thickness) coupled to a 70 eV EI-trace DSQ MS (Thermo) operated in SIM mode.

Results and discussion

The chemical pathway of MFT and FFT formation is known to originate from the reaction of the sulphur amino acid cysteine with pentose (3). The sulfhydryl group of cysteine is a very strong reducing agent used frequently to prevent enzyme inactivation, by breaking disulfide bridges formed via oxidation. Since cysteine is a precursor of MFT and FFT, it is likely to be not fully degraded at the end of our thermal conditions (100°C for maximum 3 hours) and could exhibit an antioxidant activity influencing the equilibrium of sulphur species between their thiol and disulfide form.

To assess this hypothesis, various cysteine concentrations up to 1% were added into a sulphur-free reacted model system, in which standards of MFT and FFT (100 ppb) were spiked. A similar experiment was also performed with the addition of MFT-MFT (100 ppb), and the combined results are presented in Figure 1. For the thiol species, the signal intensity greatly increased with cysteine concentration, stabilising above cysteine concentration of 0.5%. The disulfide behaved in an opposite manner, with the signal intensity dropping dramatically between 0 and 0.25% cysteine and remained low and stable with increasing cysteine concentrations.

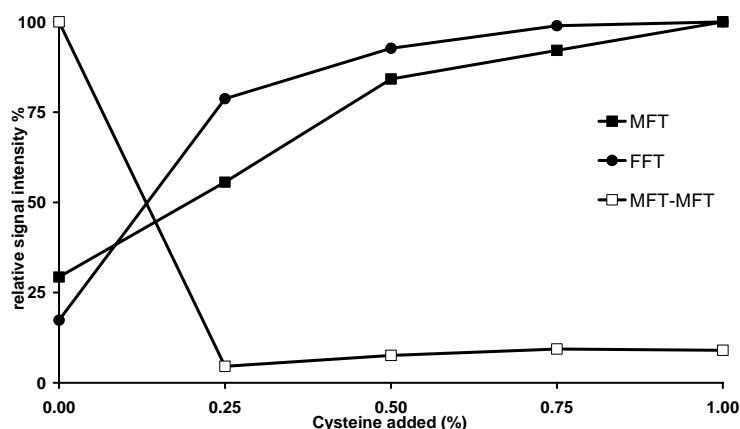


Figure 1. Influence of addition of Cysteine to the signal intensity of standard MFT, FFT and MFT-MFT spiked into a sulphur-free reacted model system. (MFT and FFT were measured in a separate experiment than MFT-MFT).

The result in Figure 1 shows that the reducing activity of cysteine influences the equilibrium between thiols and their disulfide forms. Moreover cysteine has also been shown to impact the stability of thiols over time (1), and its stabilising effect was studied (4). Using similar experimental conditions as in Figure 1, the effect of cysteine (0.1 and 0.4%) on MFT and FFT stability was monitored over 28 hours at room temperature and at 4°C with 0.4% cysteine. The results are presented in Figure 2. The samples kept at room temperature showed that a higher cysteine concentration improved the stability of MFT and FFT over time. A further improvement was obtained by keeping the sample at 4°C, although none of the conditions used here were sufficient to stop totally the degradation of MFT and FFT. To ensure reliable analytical results, it is important to select conditions where as little thiol degradation as possible occurs.

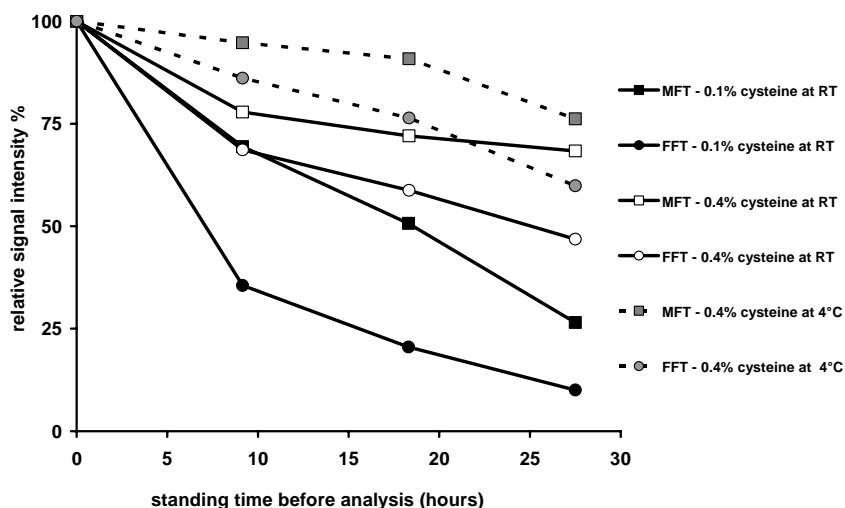


Figure 2. Decrease of spiked standard of MFT and FFT over time at added cysteine concentration of 0.1 and 0.4% into a sulphur-free reacted model system, kept either at room temperature (RT) or at cold temperature 4°C.

Beside cysteine; the composition of the model reaction system also influences the headspace concentration of MFT and FFT. This was demonstrated by spiking MFT and FFT into aliquots of a sulphur free model reaction systems, collected at regular interval during heating at 100°C, to simulate compositional changes. In such experiment (data presented in the poster), the signal intensity of MFT and FFT declined in a significant manner as the reaction time increased. For instance, the signal intensity of MFT after 60 minutes was only 15% of the intensity measured at the start of the reaction.

A consequence from Figure 1, Figure 2 and this last experiment is that quantification of MFT and FFT is not possible with external calibration in model reaction systems using a partition method like SPME. The use of stable-isotope labelled internal standard MFT* and MFT*-MFT* was attempted to compensate for the matrix effect and the effect of cysteine. Calibration lines for MFT and MFT-MFT in buffer were determined between 0 and 10 ng/g relative to their labelled internal MFT* and MFT*-MFT* (7 ng/g), using 0 and 0.2% cysteine. In the case of MFT-MFT, the calibration lines obtained are presented in Figure 3.

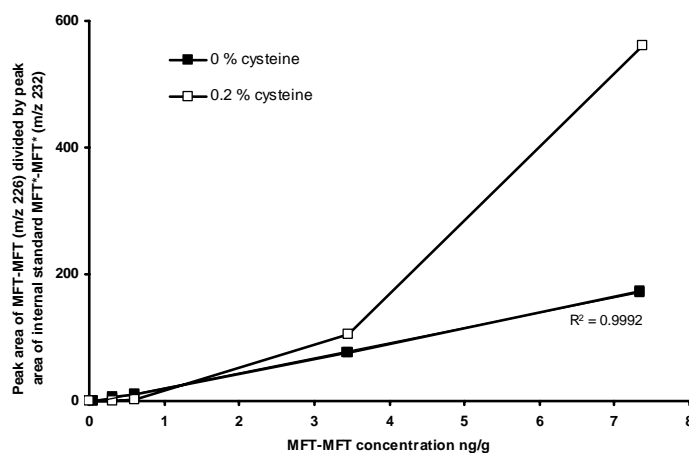


Figure 3. Calibration lines for MFT-MFT with the use of 7ng/g deuterated labelled internal standard (MFT*-MFT*) in buffer solution with two cysteine concentrations.

MFT-MFT behaved linearly in the absence of cysteine, but drifted severely from linearity at 0.2% cysteine. An examination to understand this loss of linearity showed that the peak area of MFT*-MFT* decreased with an increased concentration of MFT-MFT. This was explained by the formation of an increasing amount of a single substituted labelled species MFT-MFT*, as a result of an exchange of deuterated MFT* between the labelled and non labelled standard of MFT-MFT. Such result is in accordance with the cysteine effect observed in (Figure 1) and shows the dynamic nature of the equilibrium between MFT and its dimmer. Similar limitations to the application of labelled internal standards were reported to quantify mercaptans in wine (6). The consequence is that MFT* and MFT*-MFT* can not be used together for quantification in a single analysis via a partition technique if the cysteine concentration is not known.

Conclusion

The aim of this work was to develop an analytical method based on SPME-GC-MS capable of quantifying thiols and disulfides in Maillard systems of different composition. However, the method development has revealed that without prior knowledge of the cysteine concentration such quantification was not possible. The reducing activity of cysteine had a strong influence on the stability over time of thiol and governed the equilibrium of sulphur species between their thiol and disulfide forms. The use of stable-isotope labelled internal standards proved of limited contribution as they also reacted in an uncontrolled manner.

In the light on these results, quantification of thiols and disulfides generated from thermal reaction in a model reaction system was questioned as the concentrations of thiol and disulfide measured at the end of a reaction are greatly influenced by the redox state in each sample. A solution to suppress such effect would be to control the redox state of the sample and totally reduce disulfides into their thiols form, using a reducing agent such as Dithiothreitol (DTT). Doing so, the total potential thiol concentration formed via thermal generation would be measured rather than the actual thiol concentration in a sample. Such analysis would simplify thiol analysis resulting in more stable and reliable thiols measurements. The development of such analytical method to quantify total potential thiol concentration formed via thermal generation would be reported in a later stage.

References

1. Hofmann T., Schieberle P., Grosch W. (1996) *J. Agric. Food Chem.* 44: 251-255.
2. Mestres M., Marti M., Busto O., Guasch J. (1999) *J. Chrom. A* 849: 293-297.
3. Hofmann T., Schieberle P. (1995) *J. Agric. Food Chem.* 43: 2187-2194.
4. van Seeventer P.B., Weenen H., Winkel C., Kerler J. (2001) *J. Agric. Food Chem.* 49: 4292-4295.
5. Hofmann T., Schieberle P. (2002) *J. Agric. Food Chem.* 50: 319-326.
6. Mateo-Vivaracho L., Cacho J., Ferreira V. (2008) *J. Chrom. A* 1185: 9-18.

FLAVOUR METABOLOMICS: HOLISTIC VERSUS TARGETED APPROACHES IN FLAVOUR RESEARCH

R.C.H. DE VOS^{1,2,3}, Y. Tikunov^{1,2}, A.G. Bovy^{1,2}, and R.D. Hall^{1,2,3}

¹ *Plant Research International, P.O. Box 16, 6700 AA Wageningen, The Netherlands*

² *Centre for BioSystems Genomics, P.O. Box 98, 6700 AB Wageningen, The Netherlands*

³ *Netherlands Metabolomics Centre, Einsteinweg 55, 2333 CC Leiden, The Netherlands*

Abstract

Metabolomics refers to the large-scale and simultaneous (multi-parallel) analysis of up to hundreds of small molecules and their derived chemical features, present in extracts from samples of any biological origin, including human, animals, bacteria and plants or their products. Metabolomics techniques are progressively being more frequently applied in many different research areas, including pharmacology, microbiology, plant biology and the food sciences. Depending on the class of compounds of primary interest, different analytical platforms are nowadays in use in metabolomics research, although in the majority of cases use is made of mass spectrometry and/or nuclear magnetic resonance as metabolite detector. The parallel development of dedicated data processing and alignment software offers new possibilities for essentially untargeted metabolomics approaches in which all analytical information is taken into account. Compared to conventional analyses which are focussed on a limited set of compounds of primary interest, metabolomics approaches, together with sophisticated data processing tools, enable a more holistic and unbiased comparison of samples. This can help us to identify and understand those (bio)chemical processes and metabolites that are, for example, key for a specific flavour, fragrance or any other quality-related feature of food and industrial products.

Introduction to metabolomics

This workshop aimed to introduce and discuss metabolomics as a potential tool in flavour research, paying special attention to the pros and cons of holistic untargeted metabolomics versus the more traditional dedicated analyses of flavour compounds. After an introduction to metabolomics and data processing presented by the first author of this paper, recent examples of metabolomics approaches in flavour research area were discussed by Dr. Yury Tikunov from Plant Research International (tomato flavour research), Dr. Detlef Ulrich from Julius Kühn Institute (flavour breeding in strawberry and apple), Dr. Nijssen from TNO (sensory quality of food products) and Dr. Wulfert from University of Nottingham (dynamics of cooking reaction products). The general conclusion was that the potential of holistic metabolomics in flavour research is high within the restrictions of extractability, stability and dynamic range inherent to large-scale metabolite analyses.

Metabolomics is the latest –omics technology, geared towards providing an essentially unbiased, comprehensive qualitative and quantitative overview of the metabolites present in an organism (1). In both plant and human research, metabolomics is a rapidly developing technology, which will provide us with exceptionally rich data on the biochemical composition of materials under investigation. The latest separation and analytical techniques are being applied and modified to this purpose. Generally, Mass Spectrometry (MS) preceded by LC (liquid chromatography) or GC (gas chromatography) for the initial separation of compounds, and Nuclear Magnetic Resonance (NMR) are used for large-scale detection of compounds present in, mostly crude, extracts (1-2). In flavour research, both GC-(TOF)MS, for the analyses of natural volatiles or derivatised non-volatile compounds, and LCMS and/or NMR, for the analyses of non-volatile compounds, can be applied. As metabolomics aims to detect and provide information on a large number of compounds, a broad overview of the biochemical composition of extracts and differences between samples can be obtained. Detailed protocols for experimental design, sample preparation, metabolite extraction and reproducible detection have been described for the different platforms, e.g. GC-TOF MS of polar metabolites (3,4), ¹H-NMR profiling of primary metabolites (5), GC-MS of natural volatiles (6) and LC-MS of semi-polar compounds in aqueous-alcohol extracts (7).

Generally, metabolomics can be sub-divided into targeted and untargeted approaches. In the targeted approach, the aim is to detect and accurately quantify a specific, pre-determined set of known compounds, making use of authentic standards or reference compounds. In principle, targeted metabolomics approaches are no different from conventional dedicated methods as already used in analytical chemistry for decades. However, in metabolomics the general objective is to simultaneously analyse as many metabolites as possible. Examples of such (large-scale) targeted metabolomics approaches are the GC-(TOF)MS analyses of natural volatiles from plants organs like Petunia flowers (8) and strawberry fruits (9,10) and the GC-TOF MS analysis of metabolites involved in central cell metabolism using derivatised polar extracts from plants (11,12) or microbes (13). Likewise, targeted metabolomics based on LCMS has frequently been employed, e.g. to screen for specific classes of metabolites (e.g. 14,15).

Provided that suitable reference compounds are available for identification and quantification, targeted metabolomics approaches can provide relevant data and precise concentrations for a range of metabolites from different compound classes. In fact, GC-TOF MS-based profiling of derivatised polar metabolites is the most frequently used metabolomics approach, and a large number of reference compounds is available from a range of chemical suppliers. Dedicated software tools for automated processing and identification of GC(-TOF) MS spectral peaks are provided by the instrument suppliers, have been developed in-house or are available as freeware. For instance, a processing tool called TagFinder, enabling large-scale extraction and alignment of mass features and matching obtained mass spectra and retention indexes to compound libraries, has recently been published (16). However, the (commercial) availability of authentic standards is still a bottleneck, specifically for the large number of plant secondary metabolites. In practice, the majority of compounds detected in crude plant extracts or sample headspace is still unknown, i.e. they are completely novel or have not yet been unambiguously identified. In addition, our current knowledge of biological systems or complex chemical reactions is mostly very limited, which principally restricts targeted metabolomics approaches to those compounds or (bio)chemical reactions that are already known or predicted.

Therefore, an untargeted metabolomics approach that takes into account the information of both known and unknown compounds is essentially more comprehensive and can therefore be more successful in selecting metabolites that play a key role in specific biochemical processes, flavour characteristics, quality traits, or any other aspect of specific interest, irrespective of whether they have already been identified or not (7, 17). This approach is also called metabolic fingerprinting or untargeted metabolic profiling, referring to high throughput qualitative screening of the metabolic composition of an organism, tissue or extract (1). Untargeted metabolomics aims to gather information on as many metabolites as possible in each extract analysed and currently is the approach providing us with the most holistic view of the (bio)chemical composition of any sample. Generally, no attempt is initially made to identify the metabolites detected. All steps from sample preparation, separation and detection should thus be rapid and as simple as is feasible, to prevent as much as possible, potential loss and variation in extraction and detection of the unknowns. To enhance the chance of finding relevant compounds, any extraction and detection methods applied should at least be sufficient to reproducibly analyse compounds that are of primary interest to the research question, as 'non-targeted' metabolomics does certainly not imply 'non-hypothesis' research.

Untargeted metabolomics approaches based on MS have been made possible only recently (17-20), through the development of dedicated software for unbiased peak picking and mass signal alignment. In contrast to targeted approaches, which use specific mass traces to integrate and quantify known chromatographic peaks, in the untargeted approach metabolite recognition is not the primary goal and all analytical information present in the profiles in which all information is taken into account. A number of software tools for essentially untargeted processing GC-MS and/or LC-MS data are nowadays available as freeware from the internet, like MetAlign (7, 17-18, 20) and XCMS (19); or as commercial software packages from instrument suppliers (e.g. Markerlynx from Waters) and dedicated companies (e.g. ChromStat from ANALYT); or as tools developed in-house. All these tools enable automated peak detection and alignment of detected mass signals across samples, within user-defined settings. At the authors' laboratory, the Metalign software tool (free to download from www.metalign.nl) has been developed in close collaboration with Dr. Arjen Lommen (Institute of Food Safety, Wageningen, The Netherlands) and is nowadays routinely used for unbiased processing of all GC-(TOF)MS and LC-MS datasets. For instance, Metalign has been successfully used for plants to process and align up to 400 data files from LC-QTOF MS analysis (7, 18) and more than 200 data files from GC-MS (17) as well as GC-TOF MS analyses (Y. Tikunov, unpublished results). Generally, the raw data is first transformed into coordinates on the basis of mass, retention time, and signal amplitude. The specific mass-retention features are then aligned across all samples, resulting in a large data set of intensity for each mass signal x all samples. The latest version of Metalign is able to handle both accurate mass metabolomics data, such as those from LC-QTOF MS, LC-Orbitrap FTMS and GC-TOF MS, as well as nominal GC(TOF)MS or LCMS data (20).

Using untargeted metabolomics approaches, more than 20,000 mass signals can be extracted from LC-QTOF MS profiles and over 60,000 from GCMS profiles, depending on the type and amount of samples. Obviously, since mass spectrometers generate series of redundant mass signals per metabolite, in the form of ion fragments, adducts and isotopes thereof, the actual numbers of detected metabolites

are much smaller than the number of detected peaks. Mass signals derived from the same metabolite can easily be recognized by the fact, for example, that their intensities are highly correlated with each other across all samples and have similar retention times. These characteristics can be used to remove metabolite signal redundancy and to construct unique mass spectral clusters. For example, Tikunov *et al.* (17) described a so-called Metabolomics Mass Spectral Reconstruction (MMSR) method, in which the Metalign output of nearly 20,000 individual mass signals, derived from untargeted headspace profiling of tomato fruits, could be clustered into 322 different volatile compounds. Likewise, LC-QTOF MS analyses and subsequent untargeted mass signal extraction by XCMS and chromatographic correlation-based deconvolution revealed the presence of at least 180 different metabolites in Arabidopsis seeds (21). Thus, both GCMS- and LCMS-based untargeted approaches can provide information on the relative abundance of several hundreds of compounds, both known and as yet unknown.

To deal with the usually large amount of data resulting from an untargeted metabolomics experiment, appropriate data-processing is essential in deducing meaningful information from the dataset. By applying statistical and/or multivariate analysis tools mass signals (or clustered signals) that, for example, are differential between samples, chemical reactions or correlate with a specific flavour trait, can be selected. These selected signals are thus of major interest to identify, since at least some level of identification of metabolites is essential to understand the biological processes or (bio)chemical reactions underlying the observed changes or correlations. In LCMS, exact mass measurement is a powerful analytical tool to elucidate the exact elemental formulae of compounds detected. Possible compound candidates with a specific elemental formula can be deduced from several extensive metabolite databases freely accessible on the internet, such as the Human Metabolome Database (www.hmdb.ca), Japanese Metabolite database (www.metabolome.jp) and ChemSpider (www.chemspider.com). Candidate structures need to be confirmed with authentic standards, or further verified as far as possible by MS/MS or MSⁿ-fragmentation patterns together with any other structural information, e.g. UV/Vis absorbance spectra which is available (7). In GCMS, the mass spectrum and retention index of detected compounds are generally used to match and annotate compounds. Using the MMSR approach described above, Tikunov *et al.* (17) were able to identify putatively, based on a high hit of their mass spectra with the NIST library, about 100 out of the 322 volatiles. Obviously, for unambiguous identification of unknown metabolites and chemical features, purification or chemical synthesis followed by NMR structure elucidation is still needed. Nevertheless, by first selecting signals or metabolites, detected by untargeted GC(TOF)MS- or LCMS-based metabolic profiling, that are significantly linked to a specific flavour or other important quality trait, these often time-consuming activities can be restricted to relevant features only.

In principle, both targeted and untargeted metabolomics can be applied with all analytical platforms, including LC-MS, GC-MS and NMR. The major difference between targeted and untargeted comparative metabolomics approaches is the moment of identification of analytical signals: in the targeted approach the group(s) of metabolites under study are *a priori* known to the researcher and sample comparison is based on these identified compounds only. In the untargeted approach, no specific groups are chosen and all signals detected are taken into account. Compound identification is thus postponed to after selecting those signals that are found to be significant for the specific research question (Figure 1). Clearly, both approaches

have pros and cons. The main benefit of untargeted approaches is the more holistic view obtained of the differences in the metabolite composition between samples or extracts, thereby decreasing the chance of missing key metabolite(s). On the other hand, due to the processing of all analytical information present, the untargeted approach may come up with compounds that are (as yet) completely unknown and therefore not directly useful for the specific research question. If the researcher already knows what specific metabolites are key to his/her research question, an optimized targeted approach will be most successful and straight-forward. If the metabolites of interest are as yet unknown, then an untargeted approach will certainly provide a more comprehensive view of the sample extract and thereby increases the chance of finding new markers or providing novel insight into (bio)chemical pathways.

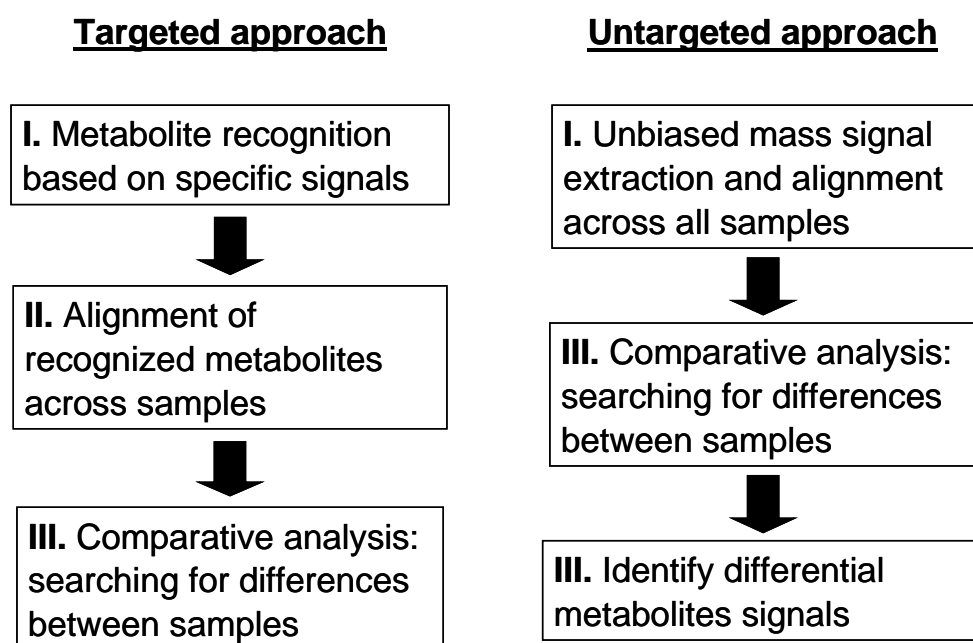


Figure 1. Targeted versus untargeted metabolomics. In the targeted approach, the data analyses is based on known metabolites only, while in the untargeted approach all metabolite signals from both known and unknown compounds are taken into account.

Examples of metabolomics applications in flavour research

Four researchers currently working on flavour metabolomics and participating in the XIIth Weurman Flavour Research Symposium, were asked to present some of their work and to discuss some pros and cons of untargeted “holistic” metabolomics. A short summary of these presentations will be presented below. For further details about these examples, the reader is referred to the specific contributions of these researchers elsewhere in this Proceedings book and/or their scientific publications.

The first two speakers provided examples of the potency of untargeted metabolomics approaches in research on the biosynthesis of flavour compounds in plants and fruits. These presentations showed that metabolomics is increasingly being applied in plant breeding, in order to find molecular markers for specific flavour characteristics, which can be used in plant breeding programs directed towards improved crop plants.

Dr. Yury Tikunov from Plant Research International, Wageningen, The Netherlands, showed an example of large-scale untargeted metabolomics in tomato fruit flavour research, using both GC-MS, GC-TOF MS and LC-MS platforms. Hundreds of GC-MS and LC-MS chromatograms obtained from different tomato cultivars were processed using Metalign software, and the resulting dataset was reduced to individual metabolites using mass-retention time clusters (MMSR method, 17). By applying multivariate analyses and correlation analyses tools, they were able to identify novel biochemical pathways leading to the production of key volatiles correlating to specific sensory characteristics of tomato fruit. The genetics behind these differential biochemical pathways is currently being investigated, in order to help tomato breeders to produce fruits with preferred and improved taste characteristics.

Dr. Detlef Ulrich from Julius Kühn-Institute, Quedlinburg, Germany, presented 3 examples from their volatile metabolomics research in strawberries, apples, and parsley in the context of plant breeding. They use ChromStat software to process the GC-MS chromatograms in an untargeted manner. The first example was on headspace volatiles from the progeny of a strawberry crossing population. The second example was on volatile screening of a large series of parsley genotypes, which, according to their volatile profiles, could be clustered into two main groups independent of leaf curling. The third and last example was on volatiles from apple fruit, again using the progeny from a specific cross. Having screened these genotypes, Dr. Ulrich and co-workers now aim to find genetic markers linked to specific volatile profiles, in order to assist plant breeding efforts.

The next two speakers showed examples of using metabolomics in research in the field of food processing, including quality of food products and reaction occurring during food processing.

Dr. Ben Nijssen from TNO Quality of Life, Zeist, The Netherlands, illustrated several cases of metabolomics in relation to processed food, including the origin of wines, stability of bottled beer, quality of cognac, bitterness of dairy products and quality of tomato dressing and sauces. The platforms they mostly apply in their research are based on GC-MS, GC-TOFMS and LC-MS. For data processing they developed their own specific deconvolution software. Using appropriate multivariate and statistical tools to couple the untargeted metabolomics profiles to sensory scores, in most cases they were able to identify key compounds responsible for the sensory quality of the food products.

Dr. Florian Wulfert from the Division of Food Sciences of Nottingham University, England, presented two case studies, where metabolomics was used to analyse instant drinks upon storage using GC-MS and modelling of Maillard reactions using APCI-MS. To obtain optimal information out of their raw data files, Dr. Wulfert and co-workers developed their own pre-processing software for untargeted metabolomics and specific chemometrics tools for studying time-effects. In the first case study, their untargeted metabolomics approach was able to pinpoint the major compounds and chemical reactions taking place in complex instant drink mixtures upon storage. In the second case study, they set up an experimental cooking device for the on-line analysis of volatiles, based on APCI-MS, in order to understand and control chemical reactions taking place upon cooking and to design better food products. By cooking starch-based samples, they were able to identify and follow reactive intermediates and end-products generated in these samples as a result of Maillard reactions.

Conclusions

These examples presented during the Metabolomics workshop at the XIIth Weurman Flavour Research Symposium, indicate that metabolomics approaches, either targeted or non-targeted, are already implemented and integrated in flavour research at different sites. Apart from the case studies described above, several lectures and posters presented during the Symposium indicate that metabolomics is being increasingly employed as a tool in flavour research. We also refer to, for instance, presentations by Dr. Skov (University Copenhagen, Denmark), Dr. van Hylckama-Vlieg (NIZO Food Research, Ede, The Netherlands) and Dr. Lindinger (Nestlé Research Centre, Lausanne, Switzerland). Clearly, metabolomics approaches are nowadays used not only by universities and research institutes, but also by several private industries dealing with flavour research.

Analogous to the increasing interest in applying metabolomics in many related research areas, including food processing (22), plant breeding (18) and microbiology (23), it is expected that the number of applications in flavour research will further increase. Improvements in both software and hardware, including tools used in flavour research, will even further increase our metabolite profiling capacity (24). For instance, improved compound separation systems, such as UPLC and GCxGC, will increase the number of detectable compounds. In addition, improved compound ionization systems and new mass detectors with higher sensitivity and extended linearity without compromising in scanning rate and mass resolution, will enable accurate detection of larger numbers of compounds. Together with the rapid development of freely available metabolite databases, it is foreseen that the numbers of unknown compounds in untargeted metabolic profiles will decrease gradually.

Acknowledgements

This work was financed by the EU Framework 6 programme project META-PHOR (2006-FOOD-CT-036220). RCHdeV, YT, AGB and RDH acknowledge additional financing from the Centre for Biosystems Genomics, and RCHdeV and RDH also from The Netherlands Metabolomics Centre, both initiatives under the auspices of the Netherlands Genomics Initiative.

References

1. Hall R.D. (2006) *New Phytologist* 169: 453-468.
2. Saito K., Dixon R., Willmitzer L. (Eds.) (2006) *Plant Metabolomics*. Springer-Verlag, Heidelberg, Germany.
3. Liscic J., Schauer N., Kopka J., Willmitzer L., Fernie A.R. (2006) *Nature Protocols* 1: 1-10.
4. Fiehn O., Wohlgemuth G., Scholz M., Kind T., Lee D.Y., Lu Y., Moon S., Nikolau N. (2008) *Plant J.* 53: 691-704.
5. Ward J.L., Harris C., Lewis J., Beale M. H. (2003) *Phytochemistry* 62: 949-957.
6. Tikunov Y, Verstappen F.W.A., Hall R.D. (2006) In *Metabolomics: Methods and Protocols* (W. Weckwerth, ed.). Humana Press, Totowa, New Jersey.
7. De Vos R.C.H., Moco S., Lommen A., Keurentjes J.J., Bino R.J., Hall R.D. (2007) *Nature Protocols* 2: 778-791.
8. Verdonk J.C., De Vos R.C.H., Verhoeven H.A., Haring M.A., Van Tunen A.J., Schuurink R.C. (2003) *Phytochemistry* 62: 997-1008.

9. Aharoni A., Keizer L.C.P., Bouwmeester H.J., Sun Z., Alvarez H.M., Verhoeven H.A., Blaas J., Van Houwelingen A.M.M.L., De Vos R.C.H., Van der Voet H., Jansen R.C., Guis M., Mol J., Davis R.W., Schena M., Van Tunen A.J., O'Connell A.P. (2000) *Plant Cell* 12: 647-661.
10. Olbricht K., Ulrich D., Grafe C. (2008) *Plant Breeding* 127: 87-93.
11. Fiehn O., Kopka J., Dörmann P., Altmann T., Trethewey R.N., Willmitzer L. (2000) *Nature Biotechnol.* 18: 1157-1161.
12. Schauer N., Semel Y., Balbo I., Steinfath M., Repsilber B., Selbig J., Pleban T., Zamir D., Fernie A.R. (2008) *Plant Cell* 20: 509-523.
13. Humston E., Dombek K.M., Hoggard J.C., Young E.T., Synovec R.E. (2008) *Anal. Chem.* 80: 8002-8011.
14. Huhman D.V., Sumner L.W. (2002) *Phytochemistry* 59: 347-360.
15. Jander G., Norris S.R., Joshi V., Fraga M., Rugg A., Yu S., Li L., Last R.L. (2004) *Plant J.* 39: 465-475.
16. Luedemann A., Strassburg K., Erban A., Kopka J. (2008) *Bioinformatics* 24: 732-737.
17. Tikunov Y., Lommen A., De Vos R.C.H., Verhoeven H.A., Bino R.J., Hall R.D., Lindhout P., Bovy A.G. (2005) *Plant Physiol.* 139: 1125-1137.
18. Keurentjes J.J., Fu J., De Vos R.C.H., Lommen A., Hall R.D., Bino R.J., van der Plas L.H., Jansen R.C., Vreugdenhil D., Koornneef M. (2006) *Nature Genetics* 3: 842-849.
19. Smith C.A., Want E.J., O'Maille G., Abagyan R. & Siuzdak G. (2006) *Anal. Chem.* 78: 779-787.
20. Lommen A. (2009) *Anal. Chem.* 81: 3079-3086.
21. Böttcher C., von Roepenack-Lahaye E., Schmidt J., Schmotz C., Neumann S., Scheel D., Clemens S. (2008) *Plant Physiol.* 147:2107-20.
22. Capanoglu E., Beekwilder J., Boyacioglu D., Hall R.D., De Vos R.C.H. (2008) *J. Agric. Food Chem.* 56: 964-973.
23. Van der Werf M.J., Verkamp K.M., Muilwijk B., Coulier L., Hankemeier T. (2007) *Anal. Chem.* 370: 17-25.
24. Moco S., Bino R.J., De Vos R.C.H., Vervoort J. (2007) *Trends in Anal. Chem.* 26: 855-866.

COFFEE CHEMOMETRICS AS A NEW CONCEPT: UNTARGETED METABOLIC PROFILING OF COFFEE

C. LINDINGER¹, R.C.H. de Vos², C. Lambot³, P. Pollien¹, A. Rytz¹, E. Voirol-Baliguet¹, R. Fumeaux¹, F. Robert¹, C. Yeretjian⁴, and I. Blank⁵

¹ Nestlé Research Center, Vers-chez-les-Blanc, 1000 Lausanne 26, Switzerland

² Plant Research International, 6700 AA Wageningen, The Netherlands

³ Nestlé Centre R&D Tours, Avenue Gustave Eiffel, 37097 Tours, France

⁴ Zurich University for Applied Sciences, Department Life Sciences and Facility Management, Institute for Chemistry & Biological Chemistry, 8820 Wädenswil, Switzerland

⁵ Nestlé Product Technology Center, 1350 Orbe, Switzerland

Abstract

Considerable work has been devoted in the last decades to the identification and quantification of key aroma-active compounds in coffee as well as their precursors. The aim of this work was to demonstrate the applicability of a data-driven holistic method rather than a targeted chemical study. As an illustrative example, coffees at different roast degrees were analysed with a range of instrumental techniques (LC-MS, GC-MS, PTR-MS) and evaluated by a sensory panel. This allowed identifying correlations between chemical markers and sensory qualities and developing a deeper understanding on reaction mechanisms involved in coffee aroma formation.

Introduction

Already in the early 1970s, chemometrics led to the development of statistical methods to treat multivariate data sets obtained by chemical analysis (1,2), in parallel to the design of optimized measurement strategies. Most of the theories developed at that time are still used when dealing with multiple and multivariate datasets, even though today's computers allow the treatment of much larger volumes of data. The application of "omics" approaches to monitor metabolites in the human body related to various diseases accelerated the development of statistical and instrumental techniques. Minimalistic approaches, such as principal component analysis (PCA) and partial least squares (PLS) and their extensions to orthogonal-PLS (OPLS), hierarchical PCA, PLS and OPLS, with the aim to reduce a multidimensional space to a lower dimensional planes, are regularly used to investigate complex problems. A main advantage of "data driven" methods is that they are not based on fundamental chemical theories and can therefore be applied to reproducible unbiased data.

The application of chemometrics to coffee is interesting because of its complexity, e.g. the formation of coffee flavour during roasting, but also due to the success of chemometrics in linking quality differences to aroma compounds and precursors. The range of datasets that can be included in such studies is large and may encompass genetic fingerprints, agricultural information, meteorological data during bean maturation, chemical fingerprints and sensory profiles. Some of these data can directly be compared between samples (e.g. the number of days of sunshine or the growing region) while others need to be pre-processed. In particular, GC and LC data need to be pre-processed in such a way that peaks are recognized

and aligned to compensate for shifts in retention time. A fully targeted approach requires that all compounds be identified before applying multivariate analysis. An untargeted approach overcomes these limitations but requires a more sophisticated pre-processing of the data including baseline correction, peak picking, alignment and centrotyping of raw data sets. As a consequence, time consuming identification can be focused on characteristic markers selected by multivariate statistics.

Experimental

To relate differences in chemical composition to cup quality, 65 coffee varieties grown in well defined conditions were evaluated by ten trained coffee panellists. Chemical data of volatile compounds was obtained by GC-TOF-MS/PTR-MS (Tenax desorption) and online PTR-MS measurements of roast and ground (R&G) coffee, prepared with an espresso machine. Volatiles released from coffee extracts within a sampling cell were analysed by online PTR-MS and trapped during two minutes on a Tenax trap for desorption on column using an automatic thermal desorption unit (4). Online PTR-MS data were interpreted by combining the GC-PTR-MS datasets with GC-MS (3). Thus, the various molecular contributions to single PTR-MS ion signals can be quantified and traced over time. Non-volatile compounds of extracts of green, slightly roasted and dark roasted coffees were analysed with LC-MS and GC-TOF-MS (after MSTFA derivatization) (6). For LC-MS measurements, 20 mg of powder from beans were weighed in 10 ml glass tubes and dissolved in 3 ml pure water and 75% methanol (containing 0.1% formic acid), respectively, by vortexing and sonication for 15 min. After centrifugation, the extracts were filtered through 0.2 µm PTFE filters, and directly used for LC-PDA-QTOF-MS analyses in ESI positive mode (6). For GC-TOF-MS measurements, 20 mg were weighed and extracted with pure water (80°C) in addition of an internal standard (Ribitol; Sigma, cat. no. 488-81-3). After stirring (10 min at 70°C in a thermomixer at 950 r.p.m.) the sample was centrifuged (10 min at 11000 g) and 750 µL chloroform (-20°C) added to the supernatant. The upper clear water phase (15 µL) was taken, dried in a vacuum concentrator and used for on-line MSTFA derivatization and GC-TOF MS analysis.

LC-MS and GC-TOF-MS raw data were processed by using the Metalign software (www.metalign.nl). The software includes base line correction, peak picking respecting a limitation in signal to noise ratio and alignment of the detected peaks through all samples by an algorithm which compensates for slight shifts in retention time. Due to the ionization induced fragmentation by electron impact in GC-MS, single compounds are represented by an average of 10 mass signals. To reduce the data volume and eliminate redundant information a “centrotyping” program, similar to that reported in Ref. (5), was applied. This program correlates the intensity profiles of individual mass signals across all samples within a predefined retention time window which can be adjusted according to the shifts in retention time caused by the limitation of instrumental accuracy. Mass signals that correlate are clustered and expressed as single centrotypes since they are expected to belong to one and the same compound (Figure 1). This reduces the data volume without loss of information, since the fragmentation pattern of each centrotypes is stored. Hence, this information can be used for identification via comparison with databases.

Cluster analysis and correlation maps were obtained to visualize correlations between sensory data, volatile compounds and non volatile compounds. Correlation maps help identifying groups of related centrotypes and show their interrelation.

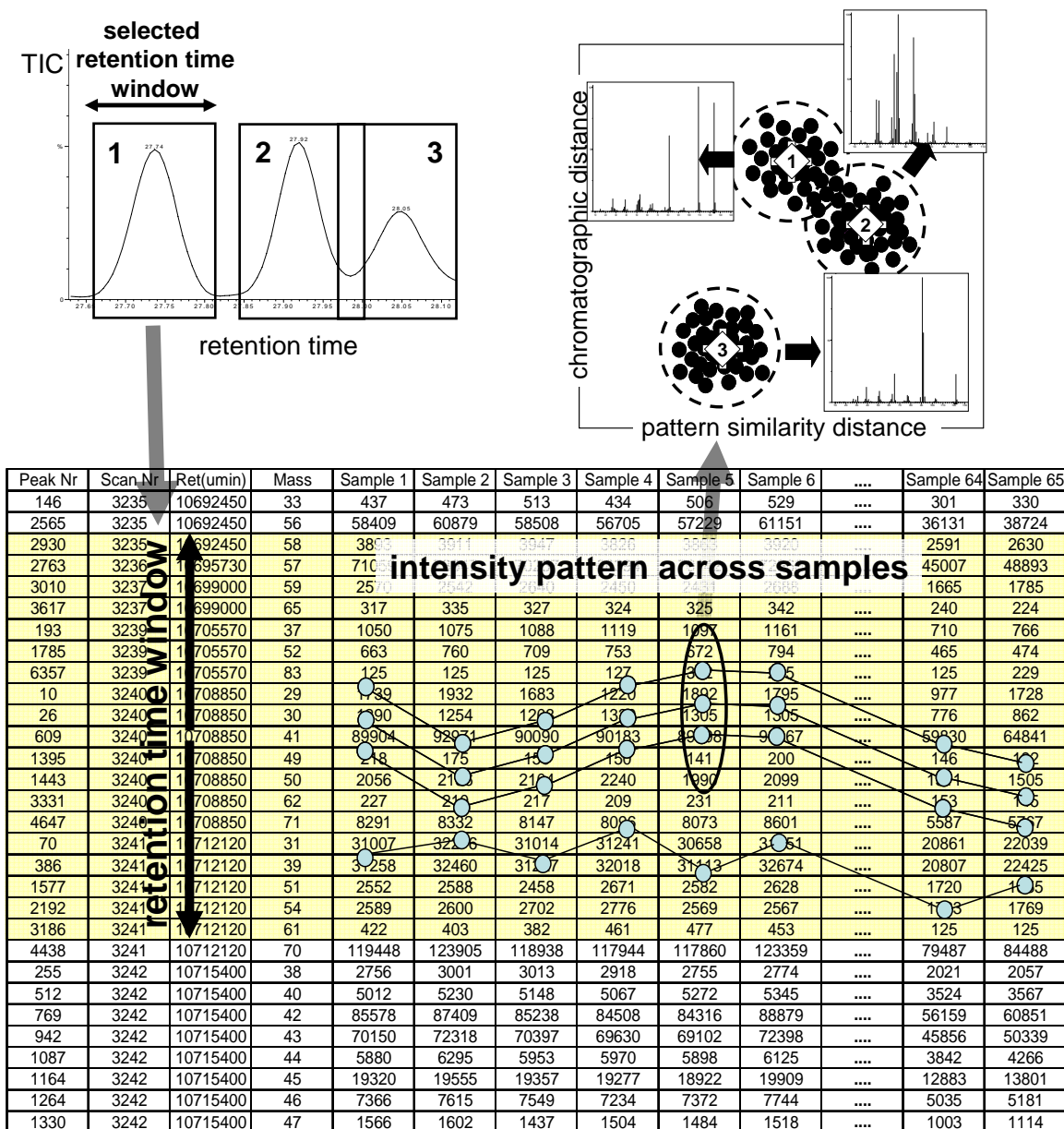


Figure 1. Example of eluted peaks selected within a defined retention time window. Three mass peaks correlate strongly through all samples and therefore most probably belong to the same compound. A fourth mass peak intensity shows a different pattern and therefore belongs to another compound.

Results and Discussion

A large set of markers were aligned through all samples applying the Metalign program to GC and LC data. Further reduction of the data using a centrotpe program helped remove redundant information, improving the readability and accuracy of correlation maps and multivariate analysis. This approach allowed comparing the differences in concentration of more than 200 volatile and 500 non-volatile compounds. The fragmentation patterns of individual compounds allowed identifying more than 150 volatile compounds. The identification of non-volatile compounds was focused on key correlations, where cluster analysis and correlation maps showed to be useful when investigating correlations between volatile

compounds their precursors and sensory profiles. The obtained datasets allowed developing a sensory predictive model which goes beyond the one already published (4), mainly by increasing the number of compounds included in the model (data not shown).

While the approach works for most of the compounds, volatile pyrazines were challenging to be differentiated by the automatic pre-processing and needed frequent manual intervention to avoid misalignment. However, the network of pyrazines was highly correlated (Figure 2) when analyzing the corresponding GC-TOF-MS correlation map.

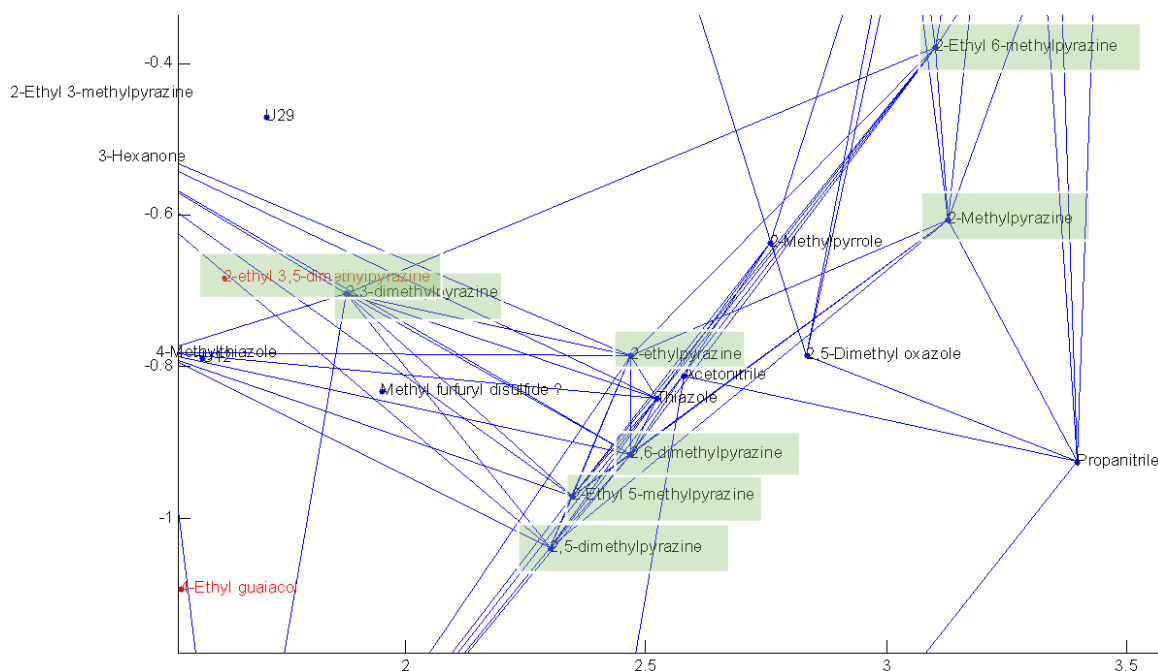


Figure 2. Correlation map: This network shows a series of pyrazines that are highly correlated (blue lines indicate a correlation higher 0.9).

By investigating changes in the chemical composition of volatiles and non-volatiles and testing their impact on predicted or evaluated sensory profiles, a robust method was developed to identify coffee varieties with the highest potential of in-cup quality.

References

1. Sharaf M.A., Illman D.L., Kowalski B.R. (1986) *Chemometrics, Chemical Analysis Series Vol. 82*: Wiley, New York.
2. Otto M. (2007) *Chemometrics, Statistics and Computer Application in Analytical Chemistry*: Wiley, Weinheim.
3. Lindinger C., Pollien P., Ali S., Yeretian C., Blank I., Mark T. (2005) *Anal. Chem.* 77: 4117-4124.
4. Lindinger C., Labbe D., Pollien P., Rytz A., Juillerat M.A., Yeretian C., Blank I. (2008) *Anal. Chem.* 80: 1574-1581.
5. Tikunov Y., Lommen A., de Vos R.C.H., Verhoeven H.A., Bino R.J., Hall R.D., Bovy A.G. (2005) *Plant Physiology* 139: 1125-1137.
6. de Vos R.C.H., Moco S., Lommen A., Keurentjes J.J.B., Bino R.J., Hall, R.D. (2007) *Nature Protocols* 2(4), 791.

MASS SPECTROMETRY-BASED ELECTRONIC NOSE CLASSIFICATION OF COMMERCIAL COFFEE BLENDS

I. DIRINCK, A. De Winne, I. Van Leuven, and P. Dirinck

Laboratory for Flavour Research, Catholic University College Ghent, K.U.Leuven Association, Gebr. Desmetstraat 1, BE-9000 Gent, Belgium

Abstract

In this study a combination of automated headspace-solid phase microextraction, mass fingerprinting and pattern recognition techniques (MS-nose) was used for fast classification and measuring the distinctiveness of commercial coffee blends. For evaluation of the system ten Nespresso[®] coffee blends were considered as an ideal sampling set. The MS-nose approach was compared to sensory difference testing by means of triangle tests and to classical analytical aroma characterisation using headspace-solid phase microextraction-gas chromatography-mass spectrometry. Good correlations between analytical and sensory data were obtained, indicating that mass spectrometry-based electronic nose technology can be used for fast digital odour characterisation of commercial coffee blends.

Introduction

An important challenge for aroma and food science is the development of fast analytical procedures for classification of food products in good accordance with sensory panel data. Electronic nose systems (e-nose) seemed to be an ideal approach when introduced a few decades ago. These systems analyse a sensor array response to a complete aroma, without separation of the components, and use pattern recognition software for data processing and correlation with sensory data. Although numerous commercial systems have been introduced and were claimed to be able to replace time-intensive sensory panels, solid-state sensor arrays have not generally lived up to expectations. Problems with drift, instability due to water vapour or carbon dioxide, need for frequent calibration, sensor poisoning and poor sensor-to-sensor and instrument-to-instrument reproducibility are some of the major problems (1).

Recently a new generation of e-nose systems, based on mass fingerprinting and considered more compatible with the basic knowledge of aroma chemists concerning the complexity and specificity of odour perception and the relation with food flavour, was introduced. Already several applications in the food field have been described (e.g. garlic flavouring in tomato sauce (2), wine (3), barrel ageing in oak of spirits (4)). In our research group a sample preparation autosampler for isolation of aroma compounds using headspace-solid phase microextraction (HS-SPME) with a quadrupole mass spectrometer as a sensing system in combination with pattern recognition software was used as a mass spectrometry-based electronic nose (MS-nose). This hyphenated HS-SPME-MS-nose configuration was already successfully applied on coffee powders for objective measurement of different parameters influencing roasted coffee flavour (e.g. classification of roasted coffee powders produced from green beans of different geographical origins, evaluation of the

difference between fast industrial and slow artisanal roasting processes and evaluation of packaging systems (5)). Also classification of wines from thematic comparisons was in good accordance with sensory analyses by oenologists (6). To differentiate the system from the conventional 'e-nose' systems, based on gas sensors, we indicated the combination of mass fingerprinting and pattern recognition techniques as 'MS-nose' system.

Experimental

Coffee samples. The samples consisted of 10 coffee powders (Nespresso®), commercialised in capsules and to be prepared using a Nespresso® coffee machine (Nestlé Nespresso SA). Ten Nespresso® blends were studied: Arpeggio, Cappricio, Cosi, Decaffeinato Intenso, Finezzo, Livanto, Ristretto, Roma, Vivalto and Volluto. For sampling 2 g of coffee powder was taken after homogenisation of two Nespresso® cups.

MS-nose analysis. The MS-nose configuration consisted of a fully automated sample preparation unit (Multi-PurposeSampler® or MPS-2®; Gerstel®, Mülheim an der Ruhr, Germany), a 6890/5973 GC-MS system (Agilent Technologies®, Palo Alto, CA) and a workstation with data acquisition software (Agilent Technologies®, Palo Alto, CA) and Pirouette® pattern recognition software for on-line data processing (Infometrix®, Woodinville, WA). This highly flexible system could be used in two modes: GC-MS mode and MS-nose mode. Helium was used as carrier gas (1 ml min⁻¹) and in the MS-nose mode the GC column was continuously held at 250 °C. Injector and transfer lines were maintained at 250 °C and 280 °C, respectively. The total ion current (70 eV) was recorded in the mass range from 40-230 amu (scan mode) using a solvent delay of 2 min and a run time of 5 min. For each of the six replicates ($n = 6$) of the different coffee blends a total mass spectrum was generated and converted by the software to a composite mass fingerprint, which could be easily imported into the Pirouette® pattern recognition software. Pirouette® allowed on-line exploratory data analysis by means of principal component analysis (PCA) and classification analysis by means of classification algorithms, such as soft independent modelling of class analogy (SIMCA).

GC-MS profiling. For GC-MS profiling the cross-linked methyl silicone column (HP-PONA, 50 m x 0.20 mm I.D., 0.5 µm film thickness, Agilent Technologies®) was programmed: 40 °C (5 min) to 160 °C at 3 °C/min, from 160 °C to 220 °C at 5 °C/min, held 3 min. Identification of coffee volatiles was performed by comparison with the mass spectra of the Wiley® 275.L library and a self-made mass spectral library. Semi-quantitative data of the coffee volatiles were obtained by relating the peak areas of the volatiles to the peak area of the internal standard nonane. Off-line principal component analysis (PCA) was performed using The Unscrambler® 6.1 (CAMO Software®, Oslo, Norway) statistical software.

Aroma isolation with HS-SPME. For both approaches isolation of the volatiles from the coffee powders was performed automatically with an autosampler, equipped with a headspace-solid phase microextraction unit, according the following conditions: 2-g samples of roasted and ground coffee blend were hermetically sealed in 20-ml vials and incubated for 5 min at 80 °C in the thermostated agitator of the MPS-2®. In the case of GC-MS profiling, a solution of the internal standard nonane was added to the vials. Sorption of coffee aroma compounds was performed for 11 min on a polydimethylsiloxane (PDMS) fibre (100 µm) (Supelco®, Bellefonte, PA). Thermal desorption temperature was set at 250 °C for 3 min.

Sensory analysis. In order to validate the MS-nose method for classification of coffee blends in good relation with sensory perception, five triangle tests were performed between coffee blends that were more or less related in the fast mass fingerprinting approach. For that purpose coffee brews (55 g/l) were prepared with Evian® water (90°C) under strictly standardised conditions using a French press (Bodum®, Triengen, Switzerland) and served at 50-60°C in individual assessment booths and subjected to a triangle test with a trained sensory panel ($n= 12$).

Results

In figure 1 a 3D-principal component analysis (PCA) score plot of the MS-nose data of 10 Nespresso® coffee blends is presented and it was clear that the replicates of the different blends were clustered after elimination of some outliers. The principal component analysis (PCA) also showed that Decaffeinato Intenso was clearly differentiated from all other coffee powders. Furthermore, visual inspection of the PCA score plot showed that some of the blends had similar mass fingerprints and were clustered: a) Arpeggio, Ristretto and Vivalto and b) Roma and Volluto. It was decided to perform GC-MS profiling on six coffee blends: Arpeggio, Livanto, Finezzo, Volluto, Capriccio and Cosi. Off-line PCA of the semi-quantitative volatile composition obtained by GC-MS profiling showed a similar biplot (not presented here) as with fast MS-nose technology. The biplot visualised the similarities between the coffee blends and the relation with their volatile composition. A good accordance between both MS-nose and GC-MS classifications was demonstrated.

The results of the triangle tests performed on five pairs of coffee blends were also indicated in Figure 1, showing that the flavour of the coffee brews of Arpeggio-Ristretto, Arpeggio-Vivalto, Volluto-Roma and Capriccio-Livanto could not be significantly differentiated, while the difference between Arpeggio and Cosi was highly significant. It could be stated that the results of mass fingerprinting were in good accordance with the sensory approach by means of triangle tests.

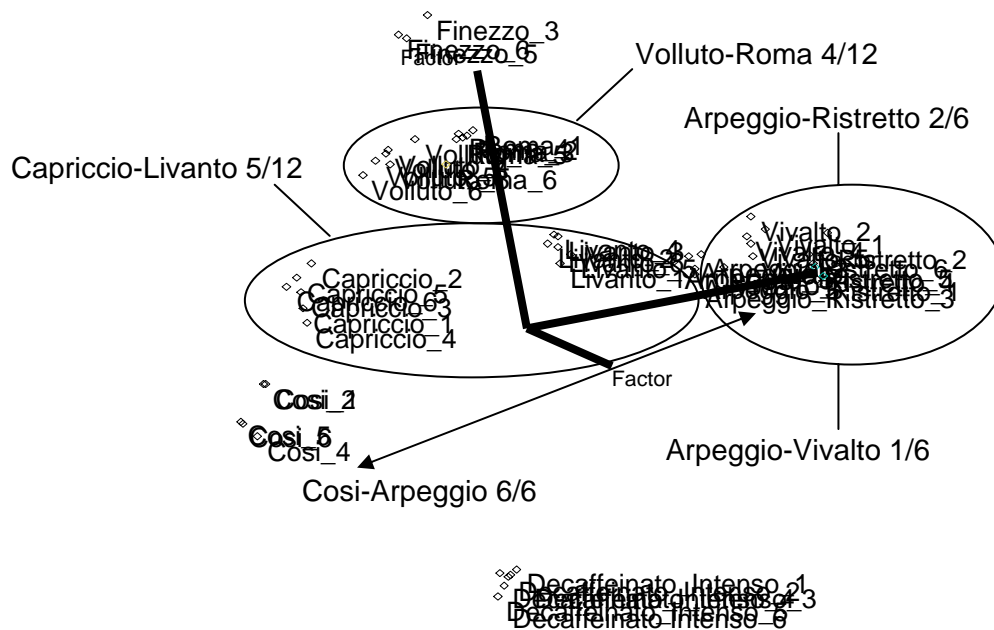


Figure 1. 3D-PCA score plot of the HS-SPME-MS-nose data of ten Nespresso® coffee powders ($n= 6$), together with the results of the triangle tests.

The results of on-line statistical evaluation of the mass fingerprints by means of Soft Independent Modelling of Class Analogy (SIMCA), a classification algorithm, were presented in (Table 1). The advantage of SIMCA is that interclass distances (IDs) between all objects were obtained, describing quantitatively the similarity or dissimilarity of the different blends. Interclass distances (IDs) varied between 3.7 and 21.9. It is generally accepted that samples can be differentiated when interclass distances (IDs) are higher than 4.

MS-nose technology is a valuable fast screening method for classification of coffee blends in relation to their flavour characters. According to SIMCA analysis all Nespresso® coffee blends could be analytically differentiated and, with the exception of Cosi-Capriccio, had interclass differences larger than 4. However, from the triangle tests it was clear that several of the blends could not be distinguished by sensory analysis. In comparison to GC-MS profiling there was a 15- to 20-fold gain in time. MS-nose technology can also be used for fast evaluation of all kind of parameters influencing the aroma of coffee powders.

Table 1. SIMCA interclass distances (IDs) of 10 Nespresso® coffee powders, obtained by HS-SPME-MS-nose analysis.

	Arpeggi	Cosi	Finezzo	Vivalto	Volluto	Capricci	Decaff	Livanto	Ristretto	Roma
Arpeggio	0.0	14.9	7.6	4.5	9.9	11.8	11.2	5.3	5.7	9.5
Cosi	14.9	0.0	10.3	19.6	10.0	3.7	8.4	11.9	21.6	13.6
Finezzo	7.6	10.3	0.0	9.6	4.0	7.5	12.5	6.1	11.2	4.0
Vivalto	4.5	19.6	9.6	0.0	14.7	16.3	14.7	9.9	5.9	16.8
Volluto	9.9	10.0	4.0	14.7	0.0	6.2	12.6	6.4	17.1	4.2
Capriccio	11.8	3.7	7.5	16.3	6.2	0.0	8.8	8.4	18.1	8.9
Decaff	11.2	8.4	12.5	14.7	12.6	8.8	0.0	10.1	15.6	14.1
Livanto	5.3	11.9	6.1	9.9	6.4	8.4	10.1	0.0	11.0	5.3
Ristretto	5.7	21.6	11.2	5.9	17.1	18.1	15.6	11.0	0.0	19.1
Roma	9.5	13.6	4.0	16.8	4.2	8.9	14.1	5.3	19.1	0.0

Acknowledgments

This work was supported by the Institute for the Promotion of Innovation by Science and Technology in Flanders.

References

1. Marsili R. (2002) In *Flavor, Fragrance and Odor Analysis* (Marsili, R., ed.); Marcel Dekker, pp 349-374.
2. Dittmann B., Zimmermann B., Engelen C., Jany G., Nitz S. (2000) *J. Agric. Food Chem.* 48: 2887-2892.
3. Martí M.P., Busto O., Guasch J. (2004) *J. Chromatogr. A* 1057: 211-217.
4. Martí M.P., Pino J., Boque R., Busto O., Guasch J. (2005) *Anal. Bioanal. Chem.* 382: 440-443.
5. Dirinck I., Van Leuven I., Dirinck P. (2005) In *State-of-the-Art in Flavour Chemistry and Biology* (Hofmann, T., Rothe, M., Schieberle, P., eds.), Deutsche Forschungsgemeinschaft für Lebensmittelchemie: Garching, pp 98-106.
6. Dirinck P., Dirinck I., van Leuven I. (2007) In *Food Quality, an Issue of Molecule-Based Science* (This H., Eklund T., eds.), *Société Française de Chimie*, pp 129-138.

FOOD PAIRING FROM THE PERSPECTIVE OF THE 'VOLATILE COMPOUNDS IN FOOD' DATABASE

M. KORT, B. Nijssen, K. van Ingen-Visscher, and J. Donders

TNO Quality of Life, Utrechtseweg 48, 3704 HE, Zeist, The Netherlands

Abstract

The database 'Volatile Compounds in Food' started in 1963. In the edition released in November 2007, a 'compare' function is offered as a new option. The database is used to evaluate the food pairing theory: if the major volatile molecules of two foods are the same, they might taste (and smell) nice when the foods are eaten together. With a sensory test it was proved whether the hypothesis of food pairing is valid. Seven different ingredients were mixed in all combinations. It was tested whether the score for the two combined ingredients was higher than the average score for the two separate ingredients. On basis of this experiment the food pairing theory can be rejected.

Introduction

Database. The late Dr Weurman started the database 'Volatile Compounds in Food' (VCF). He wanted to show that many different food products contain the same volatile compounds. From the very start he felt that this database could be of use to many other scientists in the field of flavour research. The database became first commercially available in the form of books and with the introduction of computers in the form of disks. Since 2000 researchers can consult the database sitting at their desk via Internet [1] on a subscription basis. New software is still being further developed to offer scientists more possibilities in making use of this new technology. In the edition released in November 2007, a 'compare' function offers the options to find the compounds in A **AND** in B, in A **OR** in B, in A **AND NOT** in B, in B **AND NOT** in A. This 'compare' function is one of the possibilities Dr Weurman had in mind.

Food pairing theory. Based on the fact that aroma of foods is so important for the way we perceive them, a hypothesis can be put forward: if the major volatile molecules of two foods are the same, they might taste (and smell) nice when the foods are eaten together. The concept was first appreciated by Benzi. He got the idea that jasmine and pork liver, which both contain indole, might work well together; it proved to be true.

Flavour pairing has most been described for the combination of wines with food products. In fact, almost every wine label gives menu suggestions. Heston Blumenthal is top chef of the restaurant The Fat Duck in Berkshire (England), which offers very exotic dishes. Examples of successful combinations of ingredients he made, based on the food pairing theory, are described in articles in the Guardian [2]. Bernard Lahousse and Lieven de Couverex from Belgium also are supporters of the flavour pairing theory. They are making a list of 250 food products, each with its main flavour components. The similarity between a certain product and others are shown graphically (Figure 1) on their Internet site [3]. The more flavours food products have in common, the shorter is the distance between the food products.

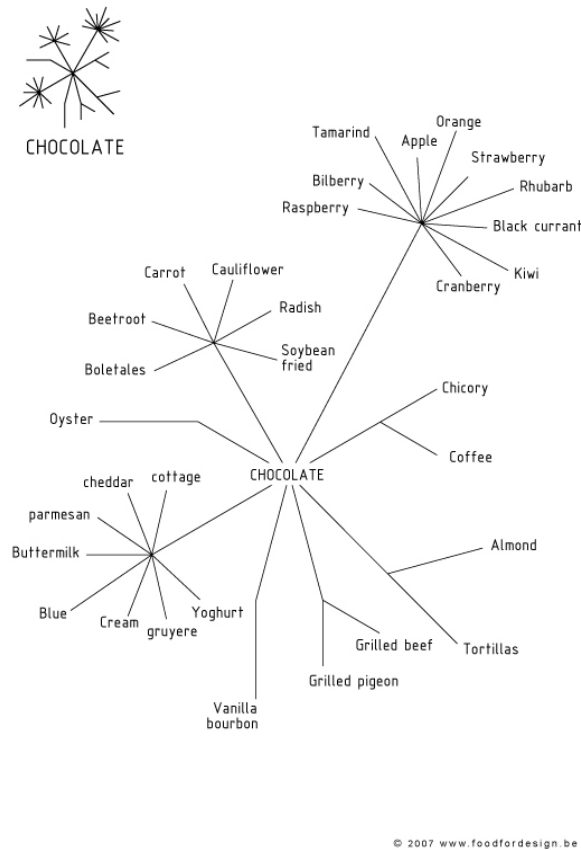


Figure 1. Tree for chocolate.

The theory was elaborated with the hypothesis that one can reconstruct, for example, a flavour from basil without using any basil. This can be done as follows. Search for a combination of other food products with one containing linalool (e.g. coriander), and one oestragol (e/g tarragon), and so on. That way you can reconstruct basil by combining coriander, tarragon, cloves and laurel. Blumenthal and Lahousse use the food pairing theory as a tool to inspire. The craftsmanship and experience of a chef is still needed to translate this inspiration into a good recipe.

Experimental

Three students from the Junior College of Utrecht developed a basic approach to prove whether the hypothesis of food pairing is valid [4]. The experiment was set up as follows. A panel of 50 students were asked to evaluate the taste of 7 ingredients. These ingredients were evaluated as such and as combinations of two ingredients. When the score for the two combined ingredients was higher than the average score for the two separate ingredients, the combination was accepted as successful. According to food pairing theory, this should be the case when the two ingredients share some characteristic flavour compounds.

The following ingredients were used in all their combinations: pear, tomato, potato, chocolate, beef, cauliflower and anise. Beef, potato and cauliflower were cooked first and then cooled. Each combination was mixed to a puree. In a separate experiment the best ratio to which the two ingredients should be mixed was determined. In the best ratio the taste of both ingredients should be recognizable. A panel of 8 persons were used for this experiment. These persons were not used in the other evaluations.

The panel members involved in the sensory test were not informed about the ingredients used. During the panel session they were blindfolded. The samples were offered on a spoon by a panel leader. The evaluations were spread over three days. After every sample the panel member had to drink water and eat a cracker. The order in which the samples were offered was varied per panellist. Scores were given in a range from 1 (awful) to 7 (very nice).

Results

Table 1 shows the actual scores (averaged over all persons) for the individual ingredients and the average scores for the combinations calculated from the two combined ingredients. Table 2 shows the actual scores (averaged over all persons) for the individual ingredients and their combinations. The combinations with a score higher than the calculated average score are highlighted. To determine whether a higher appreciation can be considered as significant, another approach was used. It was determined how often the combination of two ingredients was scored higher than the average calculated score. According to a one-tailed standard nominal distribution the taste is nicer than expected when the percentage of panel members with a higher score is above ca. 60 %. This proved to be the case for 5 combinations: anise-chocolate (97.2 %), cauliflower-pear (85.3 %), cauliflower-chocolate (83.3 %), potato-pear (79.4 %), cauliflower-potato (73.5 %). These are also combinations with a higher actual score according to Table 2.

Table 1. Actual scores for individual ingredients and calculated average scores for combinations.

	Pear	Tomato	Potato	Chocolate	Beef	Cauliflower	Anise
Pear	3.7						
Tomato	2.8	2.0					
Potato	2.8	1.9	1.8				
Chocolate	3.6	2.8	2.7	3.6			
Beef	2.8	2.0	1.9	2.8	2.0		
Cauliflower	2.5	1.7	1.6	2.4	1.7	1.3	
Anise	3.2	2.4	2.3	3.1	2.3	2.0	2.7

Table 2. Actual scores for individual ingredients and their combinations.

	Pear	Tomato	Potato	Chocolate	Beef	Cauliflower	Anise
Pear	3.7						
Tomato	2.8	2.0					
Potato	3.4	1.5	1.8				
Chocolate	2.6	1.2	2.5	3.6			
Beef	2.5	1.9	2.2	2.1	2.0		
Cauliflower	3.2	1.7	2.0	4.0	1.7	1.3	
Anise	3.5	2.0	2.4	3.8	2.3	2.0	2.7

The validity of food pairing theory was evaluated by the students together with the flavour experts of TNO. The absolute numbers of common compounds for all ingredient combinations were extracted from the VCF database (Table 3) and their common characteristic compounds were determined on the basis of experiences of TNO (Table 4). From Table 4 it can be concluded that food pairing theory is not valid when based on the principles of this experiment.

Table 3. Absolute number of common compounds for all ingredient combinations.

	Pear	Tomato	Potato	Cocoa	Beef	Cauliflower	Anise
Pear	85						
Tomato	25	392					
Potato	9	66	97				
Chocolate	25	157	52	557			
Beef	15	145	97	154	488		
Cauliflower	5	34	23	26	28	48	
Anise	1	15	5	13	2	1	44

Table 4. Percentage of common characteristic compounds. Highlighted are the successful combinations according to the sensory evaluation.

	Pear	Tomato	Potato	Cocoa	Beef	Cauliflower	Anise
Pear							
Tomato	16						
Potato	3	42					
Chocolate	2	43	33				
Beef	0	21	34	24			
Cauliflower	0	21	20	15	17		
Anise	0	11	6	7	0	0	

Discussion

The discrepancy between the supporters of the food pairing theory and the results of the sensory test is striking. The sensory test can be commented in several ways. In the first place, the circumstances under which the panel members had to evaluate the samples (blindfolded) and the way the products were served (cold puree) will not be found in practice. Furthermore, the assumption that 'the combination of two ingredients is considered successful when the score for the combination is higher than the average of the scores of the separate ingredients' can be debated. Nevertheless, this sensory test can be considered as an attempt to test food pairing theory in an objective way.

The way cooks use food pairing theory is almost the opposite of the basis of the sensory test. They do not use a panel or statistics. The combination of ingredients is given a nice appearance to influence the eater. The portions of ingredients are balanced to the preference of the cook and, last but not least, more ingredients are used to improve overall taste. We do not want to discourage playing with food pairing theory. This was just an attempt to discuss the theory in a scientific way.

References

1. Nijssen B., van Ingen K., Donders J. (2008) *Volatile Compounds in Food*, version 10.1.1, www.vcf-online.nl.
2. Blumenthal H., recipes, www.guardian.co.uk/weekend/story.
3. Lahousse B., de Couvreur L., Food for Design, www.foodpairing.be.
4. Janssens K., Darweesh S., Jansen M. (2008) Thesis: Over smaak valt niet te twisten? (Can one dispute about taste?), Junior College Utrecht.

Authors Index	Pages		
Aaslyng, Margit D.	557	Buhr, Katja	165
Abubaker, Tahira	309	Burgering, Maurits J.M.	41
Acree, Terry E.	63, 549	Burseg, Kerstin M.M.	249
Akuzawa, Ryoza	125	Busch, Johanneke	47
Aliani, Michel	288	Bushell, Mia C.	84
Andrade, Paula B.	467	Büttner , Andrea	95
Andriot, Isabelle	177	Cabello , Juan M.	231
Antenucci, Robert N.	154	Cacho, Juan	447, 517, 533
Apichartsarangkoon, Arunee	459	Cadwallader, Keith R.	301
Appendino, Giovanni	16	Callejón, Raquel M.	419
Ardö, Ylva	367,435	Capone, Dimitra L.	483
Arfa, Afef Ben	181	Cayeux, Isabelle	55, 443
Arroyo, Teresa	231,359	Chalier, Pascale	181, 185
Arvisenet, Gaëlle	169, 565	Chiralt, Amparo	147
Atlan, Samuel	109	Christlbauer, Monika	313
Aznar, Margarita	231	Collin, Sonia	227
Babin, Pierre	415	Colstee, Hans	472
Baer, Sebastian	76	Cordero, G.	359
Bagdonaite, Kristina	537	Cotte, V.M.E.	498
Baggenstoss, Juerg	271	Counet-Kersch, Christine	113
Bailly, Sabine	227	Czerny, Michael	257
Bakman, Mette	367	Da Costa, Neil C.	494
Balagiannis, Dimitrios P.	284	Da Silva, Maria A.A.P. Da	463
Balboa, Tania	231	Dall Aaslyng, Margit	133
Baptista, Paula	467	Darriet, Philippe	72, 411, 415, 451
Barbe, Jean-Christophe	411	Davidek, Tomas	263, 267, 275
Batenburg, A. Max	51, 569	de Graaf, Cees	41
Beccucci, Sabine	443	de Pinho, P. Guedes	467
Beck, Tove K.	435	de Revel, Gilles	245
Behrens, Maik	16, 20	de Vos, Ric C.H.	573, 581
Beisert, Beate	513	Debeaufort, Frédéric	143, 147
Bendall, Justin G.	375	Delabre, Marie-Laure	375
Bennetau, Bernard	415	Déléris, Isabelle	105, 109, 157, 173
Berger, Ralf G.	319, 328, 336	Demgensky, Stefanie	24
Bernadi, E	161	Derks, Eduard P.P.A.	88
Binggeli, Eva	203	Desclaux, Guillaume A.	293, 569
Blancher, Guillaume	154	Desforges, Neil	284
Blank, Imre	263, 275, 581	Devaud, Stéphanie	267
Blings, Maria	402	Dias, Benjamin E.	406
Bluemke, Wilfried	354	Dirinck, Inge	585
Boelrijk, Alexandra EM	41	Dirinck, Patrick	223, 253, 585
Bonnarme, Pascal	439	Djuris, Martina	332
Borysik, Antoni	33	Dodson, Andrew T.	305, 459
Boulanger, Renaud	479	Dold, Susanne	340
Bovy, Arnaud G.	573	Donders, Jan	589
Braamer, Lesly	472	Dubourdieu, Denis	411, 451
Brennecke, Stefan	191	Due Nielsen, Kenneth	151
Breslin, Paul	13	Dufour, Jean-Pierre	504
Briand, Loïc	29	Dunkel, Andreas	24, 393
Brockhoff, Anne	16	Eggers, Marcus	483
Budahn, H	383	Eghbaldar, Mohammed	332
Buettner, Andrea	486	El Kalamouni, Chaker	525
Bufe, Bernd	16	Elmore, J. Stephen	305, 459, 521

Else, Gordon M.	483	Hartl, E	207
Emura, Makoto	541	Hashizume, Midori	235
Engel, Karl-Heinz	397, 340	Hasselbarth, Alexander	309
Entian, Karl-Dieter	354	Heilig, Andrej	165
Escher, Felix	207, 271	Heimdal, Hanne	363
Escudero, Ana	533, 553	Herderich, Markus J.	483
Espinosa-Diaz, Marian	154	Hernández-Orte, Purificación	447
Etschmann, Maria W.	354	Hettinga, Anneke	113
Eyres, Graham T.	504	Hinrichs, Jörg	165
Fabra, Maria Jose	143, 147	Hoffmann-Lücke, Petra	402
Facundo, Heliofábia V.D. V.	215	Hofmann, Thomas	24, 280, 393
Fahmy, Farid	406	Holt, Alicia	139
Farmer, Linda J.	288	Hopfer, Helene	561
Ferreira, A.C. Silva	419	Hucher, N	161
Ferreira, Vicente	447, 517, 533, 553	Hufnagel, Jan Carlos	313
Fillonneau, Catherine	169	Hülsdau, Bärbel	336
Fischer, Anja	309	Ibáñez, Carlos	529
Flores, Mónica	129	Illmann, Silke	263
Förstner, Jan	191	Ingen-Visscher, Katja V.	589
Franco, Maria Regina B.	463	Ishizaki, Susumu	423
Frauendorfer, Felix	313	Issanchou, Sylvie	80
Frérot, Eric	451	Jaouen, I	161
Fritsch Stefanie	513	Jensen, Marie P.	367
Fumeaux, René	581	Jensen, Oliver E.	33
Gadani, Ferruccio	313	Jiang, Deshou	297
Gallagher, Michelle	59	Jong, Catrienus D.	249
Gambuti, Angelita	238	Jublot, Lionel	293, 569
Garruti, Deborah D. S.	215	Kallio, Heikki	490
Gassenmeier, Klaus	203	Kennedy, James T.	288
Genovese, Alessandro	238	Kennedy, Orla B.	84
Gierczynski, Isabelle	117	Kerler, Josef	275
Gimelfarb, Ludmilla	406	Kim, Hun	301
Glabasnia, Anneke	313	Kläring, Hans-Peter	387
Glabasnia, Arne	280	Knoop, Janine	47
Goichon, Hélène	55	Koetter, Peter	354
Gonçalves, Rui F.	467	Köhlhofer, Bernd	165
Gontard, Nathalie	181	Kort, Miriam	589
Gordon, Michael H.	235	Kowalczyk, Jerry	494
Gosney, Margot A.	84	Kraehenbuehl, Karin	267
Gouézec, Elisabeth	263	Krammer, Gerhard	191, 397, 402, 483
Granvogl, Michael	455	Kreutzmann, Stine	151
Gray, Lauren	84	Krings, Ulrich	328
Grisel, Michel	161	Kristensen, Helle T.	367
Grua-Priol, Joëlle	169	Krügener, Sven	328
Guessasma, Sofiane	121	Krüger, H.	383
Guichard, Elisabeth	29, 109, 117, 177 479, 545	Krumbein, Angelika	387
Guillard, Valérie	181	Kuhn, Christina	16
Gunata, Ziya	479	Kukurová, Kristína	553
Haar, Nina	561	Kürbel, Helmut	513
Hall, Robert D.	573	Kurtz, Anne J.	63, 549
Hamaguchi, Takashi	59	Labouré, Hélène	117
Hambleton, Alicia	143, 147	Lambot, Charles	581
Hammerschmidt, Franz-Josef	191	Lan Phi, Nguyen T.	431
Hardebusch, Björn	336	Laudaud, Sophie	439
		Landrieu, Eric	51

Langhans, Wolfgang	37	Morales, Lourdes M.	419
Lauverjat, Clémentine	105	Moreau, Céline	545
Lavigne, Valérie	451	Morin-Audebrand, Léri	80
Lawless, Harry T.	63	Mosandl, Armin	349
Le Calvé, Bénédicte	55, 443	Mottram, Donald S.	84, 235, 284, 305 459, 521
Le-Bail, Alain	169	Moutounet, Michel	185
Leeuwen, Cornelis V.	411	Nakahashi, Atsufumi	541
Leitner, Erich	537, 561	Nakanishi, Akira	423
Leussink, Annelies	293	Narain, Narendra	427
Leuven, Isabelle V.	585	Negishi, Osamu	379
Ley, Jakob P.	397, 402	Negishi, Yukiko	379
Li, Hui-Chen	406	Neto, Manoel A. D. S.	215
Li-Chan, Eunice C. Y.	545	Niclass, Yvan	443
Lindinger, Christian	581	Niedeveld, Cor	472
Linthorpe, Robert S.T.	101, 498	Niehues Birch, Anja	133
Lisanti, Maria T.	238	Nijssen, Ben	589
Lohwasser, U.	383	Norio Miyazawa	423
Lonvaud-Funel, Aline	245	Oberholzer, David	371
Lopez, Ricardo	447	Odake, Sachiko	125
Lorjaroenphon, Yaowapa	301	Oeseburg, Loes	113
Loscos, Natalia	447	Ohkubo, Yasutaka	423
Lösing, Gerd	191	Olivares, Alicia	129
Lubbers, Samuel	177	Oliveira, Lilia C.	427
Lundén, Saara	490	Osthaus, Jörg	191
Luyten, Hannemieke	113	Owusu, Margaret	363
Maeda, Tomoko	423	Paetz, Susanne	402
Magnan, Céline	105	Parisot, Fanny A.	549
Mahattanatawee, Kanjana	475	Parker, Jane K.	284, 521
Malhiac, Catherine	161	Parker, Mango	483
Mallia, Silvia	207	Pendzialek, Kathrin	340
Maraval, Isabelle	479	Perello, Marie Claire	245
Marriott, Philip J.	504	Pernin, Karine	479
Martens, Marty	242	Pernollet, Jean-Claude	29
Marthe, F.	383	Peter, Regina	397
Martins, Sara I.F.S.	293, 569	Petersen, Mikael A.	211, 363, 367, 435
Mateo-Vivaracho, Laura	517	Peterson, Devin G.	139, 297
Matumoto, Katsuyuki	59	Petka, Ján	553
Mauroux, Olivier	267	Peychès-Bach, Aurélie	185
McRoberts, Colin W.	288	Peyron, Stéphane	185
Meier, Lars	191	Pineau, Bénédicte	411
Meier, Manfred	483	Piombino, Paola	238
Meinert, Lene	133	Poinot, Pauline	169
Merabtine, Yacine	177	Poisson, Luigi	275
Merlier, Carolien	472	Pollien, Philippe	581
Mestres, Christian	479	Pollnitz, Alan P.	483
Methven, Lisa	84	Ponne, Carina	113, 242
Meyerhof, Wolfgang	3, 16, 20, 24	Pons, Alexandre	451
Meynier, Anne	157	Popielarz, Marta	211
Minert, Lene	557	Potineni, Rajesh V.	139, 154
Mirata, Marco-Antonio	344, 349	Poulsen, Mauricio L.	494
Miura, Nobuaki	541	Prasad, S. K.	498
Miura, Takayuki	125	Preininger, Martin	406
Miyazawa, Toshio	59	Preti, George	59
Moio, Luigi	238	Prost, Carole	169, 565
Monde, Kenji	541		

Puangraphant, Sirima	301	Sourabié, Alain M.	439
Pyle, D. Leo	284	Spinnler, Henri-Eric	439
Rauhut, Doris	513	Srisajjalertwaja, Siriwan	459
Raynaud, Christine	525	Stähler, Frauke	24
Reekers, Marc	242	Staint-Eve, Anne	439
Reichelt, Katharina V.	397	Starkenmann, Christian	443
Reichling, Claudia	20	Stefuca, Vladimir	332
Ribeiro, Bárbara	467	Steinhaus, Martin	76
Ribeyres, Fabienne	479	Stephan, Andreas	219
Riedel, Katja	24	Ster, Marc V.D.	472
Riess, Thomas	402	Stettner, Georg	219
Rinne, Sascha	328	Støier, Susanne	133
Robert, Fabien	581	Strohalm, Henk	340
Roloff, Michael	397	Strube, Andrea	486
Romano, Andrea	245	Struckmeyer, T.	383
Roozen, Jacques P.	125	Sugimoto, Daisuke	541
Rosing, Ed .A.E.	293, 569	Sulmont-Rossé, Claire	80, 117
Rouseff, Russell L.	427, 475	Talens, Pau	147
Ruijschop, Rianne Maj	41	Talou, Thierry	525
Rytz, Andreas	263, 581	Tarrega, Amparo	121
Sádecká, Jana	553	Täubert, Alexander	24
Saint-Eve, Anne	105, 109, 117, 157	Tavel, Laurette	545
Salles, Christian	121	Taylor, Andrew J.	33, 101, 498
San Juan, Felipe	533	Thibon, Cécile	415
Sandell, Mari	13	Tiitinen, Katja	490
Sanz, Guenhaël	29	Tikunov, Yury	573
Sarrazin, Elise	72, 415	Timmermans, Wim	242
Satre, Emeline	549	Toldam-Andersen, Torben B.	211
Savary, G	161	Tominaga, Takatoshi	72, 415
Sawamura, Masayoshi	431	Tomita, Naomi	423
Schäfer, Annette	133, 557	Tournier, Carole	47, 117
Schaft, Peter V. D.	332	Trautzsch, Stephan	191
Schaller, Jean-Pierre	313	Tréléa, Ioan Cristian	105, 109, 173
Schieberle, Peter	76, 165, 207, 455	Troccez, Myriam	443
Schlichtherle-Cerny, Hedwig	207, 371	Tromelin, Anne	29, 177
Schmalzried, Frank	275	Troncoso, Ana M.	419
Schmidt, Claus Oliver	191	Tsormpatsidis, Evangelos	521
Schönhof, Ilona	387	Ullrich, Frank	309
Schrader, Jens	344, 349, 354	Ulrich, Detlef	383
Schreiner, Monika	387	Valentão, Patrícia	467
Schuchmann, Heike P.	263	Valero, E.	359
Scott, David J.	33	Valim, Filomena	427
Seabra, Rosa M.	467	Van Caelenberg, Tim	253
Sefton, Mark A.	483	van der Velden, Rob	51
Sémon, Etienne	109, 117, 121	van Doorn, Rudi	88
Sérot, Thierry	565	van Leuven, Isabelle	253
Serrano, A.	359	van Ruth, Saskia	125
Shinkaruk, Svitlana	415	Varming, Camilla	367, 435
Siebert, Tracey E.	483	van den Blom, Leon	569
Siegmund, Barbara	537	Villiere, Angélique	565
Smit, Gerrit	47, 51, 293, 569	Voilley, Andrée	143, 147
Solé, Josep	529	Voirol-Baliguet, Elisabeth	581
Sostmann, Kai	154	Vössing, Tobias	483
Souchon, Isabelle	105, 109, 117, 157	Wagner, Roger	215, 463
	173	Wagstaffe, Alexandra	521

Wan, P.H.W.	498
Wang, Deng K.	305
Weber, Berthold	191
Weckerle, Bernhard	191
Weiher, Marcel	340
Wesselink, Wilma	113
Westerterp-Planteng, Margriet S.	41
White, James	406
Widder, Sabine	483
Williams, Robert C.	549
Winne, Ann D.	223, 585
Wise, Paul M.	59
Wittlake, Rüdiger	191
Wood, Claudia	483
Woolsgrove, Jodie A.	305
Wulfert, Florian	33
Wüst, Matthias	349
Yaguchi, Yoshihiro	541
Yang, Ying	494
Yeretjian, Chahan	581
Yven, Claude	121
Zehntner, Ulrich	371
Zelena, Kateryna	336
Zhang, Xiaomei	154
Zorn, Holger	336
Zouid, Imen	173

A

absolute configuration.....	541
acacia gum.....	161
α -(Z)-acariadiol.....	328
2-acetyl-1-pyrroline.....	475
2-acetyl-2-thiazoline.....	475
acidic/basic monosaccharides.....	267
acidity.....	151
acidulants.....	139
acrylamide.....	305
active packaging.....	181
adsorbents.....	238
AEDA (aroma extract dilution analysis).....	419
aerosol formation.....	313
agonist.....	29
β -alanylglycine.....	393
alignment software.....	573
alkylpyrazines.....	275
Allium species.....	455
2-aminoacetophenone (2-AAP).....	513
AMP (adenosin mono-phosphate).....	288
Anacardium occidentale.....	215
analytical-sensory correlation.....	223, 309, 467
anion exchange resin.....	344
anserine.....	393
antimicrobial agent.....	181
antioxidant.....	129
antioxidative capacity.....	231
APCI-MS.....	41, 101, 109, 117, 121, 139, 151
apparent diffusion.....	173
appetite.....	37, 41
apple (juice).....	76, 211, 235
aroma barrier.....	143
aroma composition.....	371
aroma compound binding sites.....	545
aroma compounds.....	109, 423
aroma defect.....	513
aroma diffusion.....	161
aroma formation.....	367
aroma intensity.....	117
aroma interactions.....	249
aroma permeability.....	147
aroma profile.....	387
aroma quality.....	301
aroma release.....	129, 139, 154, 157, 165, 173
aroma screening.....	533
aroma stability.....	271
aroma.....	41, 51, 143, 242, 313, 359, 419, 431, 451, 483, 494
aromagram.....	498
asparagine.....	305
Aspergillus niger.....	349
atmospheric storage.....	271
atypical aging.....	513
authenticity.....	191

B

basidiomycete.....	336
beef liver.....	284
beer quality.....	219
binary mixtures.....	63
biodiversity.....	383
bioengineering.....	319
biomimetic in-bean experiments.....	275
bioprocessing.....	319
biotransformation.....	332, 349
biphasic structure.....	173
bis(2-methyl-3-furanyl) disulphide (MFT-MFT)....	569
bitter masking.....	402
bitter taste receptor.....	16

Expression of Multidisciplinary Flavour Science

bitter taste.....	20
bitterness.....	3, 13
Botrytis cinerea.....	349
botrytised wine.....	72, 415
bottle aging.....	227
Brassica oleracea.....	387
Brassicaceae.....	387
bread.....	169
breath analysis.....	139, 151
breath flow.....	95, 101
brett character.....	245
Brettanomyces bruxellensis.....	245
broccoli.....	387
broth-like flavour.....	354
burnt caramel-like.....	541
butter.....	207
C	
¹⁴ C-labelled precursors.....	379
calcium imaging.....	16, 20
Camembert cheese.....	439
CAMOLA.....	297
Candida antarctica.....	340
Candida cylindracea.....	340
Candida strain.....	359
Capsicum annuum.....	459
carbon dioxide.....	55, 387
carboxylic acid.....	59
cardboard off-flavour.....	257
carnosine.....	393
carotenoid degradation.....	336
carvacrol.....	181
Carya illinoensis.....	301
cashew apple juice.....	215
castalagin.....	280
cereal products.....	297
charged sugars.....	267
cheese (powder).....	105, 113, 253, 367, 435
chemical markers.....	581
chemical structure.....	486
chemometrics.....	581
chewing (simulator).....	95, 105, 117, 121
chewing gum.....	101, 151, 154
chicken (broth).....	288, 393
chloroanisoles.....	486
chocolate flavour.....	309
chocolate.....	363
cider.....	565
cigarette smoke.....	498
Citrus junos.....	431
cocoa fermentation.....	363
coffee.....	68, 517, 581, 585
conching.....	309
conjugated linoleic acid (CLA).....	207
consumer(s) (behaviour).....	51, 80
contaminants.....	191
cooked rice aroma.....	479
cooking.....	305
Corynespora cassicola.....	349
costmary.....	525
4-coumaric acid.....	379
crocetin.....	235
crocin.....	235
crushing finger device.....	525
Cucumis melo L.....	521
curing process.....	313
custard dessert.....	117
cysteine-S-conjugates.....	443
cysteine.....	267, 293, 569

D

dairy gels.....	173
dairy matrix.....	165
dairy streams.....	375
data-driven.....	581
database.....	589
Deans-type multidimensional GC.....	529
degradation kinetics.....	267
(E)- β -damascenone.....	76
deoxigenase.....	328
detection frequency (analysis).....	479, 557, 561
detection threshold.....	165
diet.....	37
difference tests.....	80
diffusion (coefficient).....	105, 157
digital odour characterisation.....	585
dihydro-ethylmaltol.....	406
dihydrochalcones.....	402
dihydromaltol.....	406
2,5-dimethyl-4-hydroxy-3[2H]-furanone.....	406, 521, 537, 541
2,5-dimethyl-4-methoxy-3[2H]-furanone.....	537, 541
dimethyldisulphide.....	133
dimethyltetrasulphide.....	455
DOSY-NMR.....	161
dry-fermented sausages.....	463
dynamic headspace.....	525
dynamic purging system.....	533

E

earthy off-flavour.....	238
edible films.....	143
Ehrlich pathway.....	354
elderly consumers.....	84
ellagitannins.....	280
emulsion-based films.....	143, 147
emulsion.....	173
emulsions stability.....	161
ENaC.....	3, 24
encapsulation.....	143, 154
enzyme-modified cheese.....	375
enzymes.....	319
epoxidase.....	328
Eriodictyon californicum.....	397
Escherichia coli.....	336
essential oil(s).....	431, 525
(R)-esters.....	340
esters.....	185
esters of 3-methyl-1-butanol.....	459
esters of 4-methyl-1-pentanol.....	459
ethanol.....	185, 553
ethyl 3-mercaptopropionate.....	439
ethyl esters.....	411
5-ethyl-4-hydroxy-2-methyl-3[2H]-furanone.....	406
ethylene-blocker.....	211
ethylphenol.....	245
EXOM.....	113

F

factorial design.....	293
fat content.....	173
fatty acid hydroperoxide.....	332
fed-batch bioprocess.....	344
fermentation.....	371, 447
fermented sausage.....	129
Ferula galbaniflua.....	423
ferulic acid.....	297, 379
filtration.....	238
flavour formation.....	301
flavour modifiers.....	402
flavour optimization.....	249

Expression of Multidisciplinary Flavour Science

flavour precursors.....	443
flavour release.....	121, 133, 151
flavour retention.....	161
flavour stability.....	219
flavour stimuli.....	37
flavour-ingredient interactions.....	139
flavour.....	288, 332, 406
flavourings.....	529
flour.....	169
food breakdown.....	121
food discrimination.....	80
food intake.....	41
food matrix.....	121
food memory.....	80
food pairing theory.....	589
formation kinetics.....	263
formation pathways.....	275
<i>Fragaria x ananassa</i> L.....	521
french fries.....	305
fruity flavours.....	411
fungi.....	349
furaneol [®]	537
2-furfurylthiol (FFT).....	275, 569
<i>Fusobacterium nucleatum</i>	443

G

G protein-coupled receptors.....	16, 20
GABA.....	435
galbanum oil.....	423
gas chromatography (GC).....	504, 549
gas chromatography-olfactometry (GC-O).....	215, 231, 419, 431, 463, 475, 479, 486, 490, 498, 533, 557, 561, 565
gastrointestinal.....	37
genetics.....	3
geosmin.....	238
<i>Geotrichum candidum</i>	349
Gestalt.....	63
gingerdiones.....	402
glucomannan jelly.....	125
β -glucosidase.....	359
glucosinolate.....	13
glucovanillin.....	379
glutamic acid.....	293, 435
glycosidic flavour precursors.....	447
grape.....	447
green coffee.....	275
gustation.....	3
gustatory system.....	16
gustometer.....	47

H

<i>Hancornia speciosa</i>	427
<i>Hanseniaspora</i> strain.....	359
<i>Hansenula</i> strain.....	359
hard candy.....	139
headspace.....	490
health (benefits).....	37, 494
heap- and tray-fermented cocoa beans.....	363
hebra santa.....	397
hedonic values.....	76
2-heptanethiol.....	443
heterologous expression.....	16, 20
hexanal.....	133
1-hexen-3-one.....	242
hierarchical cluster analysis.....	479
high-in-taste-pulse.....	47
hispolon derivatives.....	402
holistic.....	573, 581
homoeriodictyol.....	397
hop essential oil.....	504
HPLC fractionation.....	411

hTAS2R38.....	13
human olfactory receptors.....	29
human.....	59
humidifier.....	533
hydrolysis.....	447
4-hydroxy-2,5-dimethyl-3[2H]-furanone (HDMF).....	263
hydroxycinnamic acids.....	297
hyphenation.....	504

I

IMIDRA collection.....	359
IMP.....	288
in silico model.....	16
in vivo monitoring.....	95
in vivo release.....	109
in-mouth aroma release.....	109
in-mouth mechanisms.....	121
in-nose measurements.....	105
in-situ product recovery (ISPR).....	344
in-vivo analysis.....	154
in-vivo aroma release.....	113, 117
in-vivo sensory evaluation.....	397
interaction.....	59
inulin.....	169
iota-carrageenan.....	143, 147, 177
isoamyl acetate.....	427
isothiocyanate (-N=C=S).....	3
isotope dilution assay.....	455, 569
isotope labelling.....	297
jasmine rice.....	475

JK

kefir.....	406
ketoaldonic acid.....	267
key odorants.....	207, 475
kinetic release.....	181
Kloeckera strain.....	359
Kolbach index.....	219

L

L-arginine.....	24
labelled precursors.....	275
Lactobacillus bulgaricus.....	371
Lactobacillus helveticus.....	367
β -lactoglobulin.....	545
LC Taste®.....	397
light-induced off-flavour.....	235, 242
lilac alcohol.....	349
lilac aldehyde.....	349
limonene.....	344
linalool (oxide).....	349
lipase-catalysed esterification.....	340
lipoxygenase-1.....	332
low-fat.....	113, 165
lysine.....	263

M

Maillard flavour formation.....	305
Maillard reaction.....	263, 284, 293, 297, 301
malt.....	219
maltol.....	406
mangaba.....	427
maple lactone.....	59
Marasmius scorodoni.....	336
mass fingerprinting.....	585
mass transfer.....	33, 105
mass transport.....	147
mastication.....	125
maximum intensity.....	105, 154
meat flavour.....	293
meat.....	288

Expression of Multidisciplinary Flavour Science

mechanistic modelling.....	173
mercaptans.....	517
1-mercapto-3-octanol.....	472
1-mercapto-3-octanone.....	472
2-mercaptopropionate.....	439
mesifuran.....	537
metabolomics.....	573
metallic flavour.....	235
3-methyl-2,4-nonanedione.....	451
2-methyl-3-furanthiol (MFT).....	293, 569
2/3-methylbutanal.....	363
3-methylbutanoic acid.....	363
1-methylcyclopropene.....	211
3-(methylthio)-1-propanol (methionol).....	354
1-methylthio-3-octanyl acetate.....	472
1-methylthio-3-octanyl butyrate.....	472
3-(methylthio)-propylacetate.....	354
Metschnikowia strain.....	359
microbial fermentation.....	375
microorganisms.....	319
milk fat.....	157
mixture perception.....	549
model cheese.....	121
modelling.....	33, 109
modified atmosphere packaging.....	253
moisture content.....	271
molecular marker.....	383
molecular mobility.....	161
molecular modelling.....	29
moromi.....	68
mouth microflora.....	443
mouth model.....	125, 129
mouth-coating.....	280
mouthfullness.....	393
MS-nose.....	151, 585
MS.....	573
MsP1.....	336
MsP2.....	336
multi-response kinetic modelling.....	284
multi-sensory interactions.....	51
multidimensional GC-MS.....	529
multidimensional GC.....	504
multivariate analysis.....	223, 467
Munster cheese.....	439
mushroom.....	467, 472
musk melon.....	521
β -myrcene.....	328

N

N-glycosylation.....	20
nasal breath.....	101
nasal cavity.....	109
nasal impact frequency.....	498
natural flavours.....	319
Nespresso®.....	585
Nicotiana tabacum.....	313
nitrogen atmosphere.....	271
non-Saccharomyces.....	359
nootkatone.....	332
norbixin.....	235
norisoprenoids.....	336
nuclear magnetic resonance (NMR).....	545, 573
number of panellists.....	557
nutrition.....	3
nutritional quality.....	169

O

oak barrel toasting.....	280
obesity.....	37
1-octene-3-one.....	242

Expression of Multidisciplinary Flavour Science

odorants.....	29, 177
odour binding protein (OBP).....	33
odour frequency detection.....	463
odour impact.....	463
odour intensity.....	553
odour quality.....	486, 490
odour threshold.....	486
odour transport.....	33
odour-mixture perception.....	63
odour.....	169
off-flavour.....	249, 513
olfaction.....	59
olfactometer.....	41, 249
olfactometry.....	406, 411, 504, 549
olfactory percept.....	553
Olfactoscan.....	249
on-line breath analysis.....	95
oral breath.....	101
oral cavity.....	95, 101
oral nutritional supplements.....	84
oral parameters.....	121
orange juice.....	223
organic extract.....	479
OSME.....	215, 463
oxidative dimerisation.....	411
oxidised red wines.....	231

P

packaged food.....	257
packaging.....	223
palatinose™.....	84
partition coefficient.....	105, 185
pasteurisation.....	215
pasteurised milk.....	242
pattern recognition.....	585
PCA-biplots.....	88
PCA.....	151, 211, 223, 435
PCR/RFLP.....	359
peak cryofocusing.....	529
pectin.....	177
pedestal experiment.....	549
Penicillium digitatum.....	349
Penicillium italicum.....	349
4-pentenyl acetate.....	427
peppery notes.....	483
peptides.....	393
perception.....	157
perillene.....	328
perillic acid.....	344
permeability.....	143
Petroselinum crispum.....	383
phase ratio variation.....	161
phosphate.....	263, 288
photooxidation.....	235
physicochemistry.....	109
physiology.....	109
phytase.....	169
Pichia strain.....	359
Piper nigrum.....	483
plant volatile.....	383
Pleurotus ostreatus.....	328
PLS (regression).....	215, 367
polyethylene (PE) (film).....	185, 561
polyfunctional thiols.....	227, 517
polyolefins.....	561
polypropylene (PP).....	561
polysaccharides.....	177
potato.....	305
precursors.....	288
predictive model.....	284

Expression of Multidisciplinary Flavour Science

premature aging.....	451
processing.....	215, 223
PRODAN fluorescence.....	545
1-propanethiol.....	443
3-propyl-1,2-oxothiolane.....	415
pruny off-flavour.....	451
<i>Pseudomonas putida</i>	344
psychometric functions.....	59
psychophysics.....	59
PTR-MS.....	105, 154, 165

Q

3D-QSAR.....	29
QSPR.....	177
quale.....	63
quality (markers).....	191, 203, 573
quantitation.....	207, 455, 537
quantitative GC-O.....	553
quantitative structure-property relationships.....	177

R

racemic alcohols.....	340
rapid evaluation.....	525
rate constant.....	33
reaction kinetics.....	293
receptor.....	3, 13
recombinant peroxidase.....	336
red wine.....	245, 411, 451
regulatory.....	203
replicates.....	557
representative aroma extract.....	565
retention-release.....	177
retro-nasal release.....	41
retronasal aroma release.....	125
retrosynthesis.....	297
rhamnose.....	263
<i>Rhodotorula</i> strain.....	359
ribose.....	288
ripened cheese.....	439
roasted coffee.....	271
roasted pecan kernels.....	301
rotundone.....	483

S

<i>Saccharomyces cerevisiae</i>	336, 349
saliva.....	129, 133
salivation.....	95
salt reduction.....	47, 51
salt taste.....	24
salt.....	51, 105
saltiness.....	47, 51
satiation.....	41
Sauternes (wine).....	72, 227, 415
savoury flavour ingredient.....	375
screening.....	517
sea buckthorn.....	490
sensory (descriptive) analysis.....	88, 215, 231, 257
sensory evaluation.....	76
sensory interactions.....	55
sensory perception.....	80
sensory profiling.....	151
sensory properties.....	105
sensory quality.....	581
sensory reconstitution test.....	411
sensory screening.....	249
sensory typicality.....	72
serial dilution sensory analysis.....	68
shelf life.....	253
sherry vinegar.....	419
smoke.....	313
sodium caseinate.....	147

Expression of Multidisciplinary Flavour Science

sodium channel.....	24
sodium.....	47
solid phase extraction (SPE).....	517, 521
sotolon.....	51, 419
soup.....	47, 51
sourness.....	55
soy protein.....	181
soy sauce.....	68
sparkling intensity.....	55
sparse-PCA.....	88
specifications.....	191
spectroscopic detection.....	504
spice.....	483
spoilage.....	245
stability.....	191
stereospecific oxidation.....	280
storage.....	211, 219, 253
strawberry.....	521, 537
Strecker aldehydes.....	219, 284
Strecker degradation.....	301
Streptococcus thermophilus.....	371
3-sulfanylhexan-1-ol.....	227, 443
sulphur volatiles.....	427
sunflower oil.....	165
surface hydrophobicity.....	545
surface nasal impact frequency (SNIF).....	561
swallowing.....	95, 101, 113
sweet enhancing.....	402
sweet(ness).....	3, 84, 151, 154
synergy.....	59
synthesis.....	472

T

T1R.....	3
T2R.....	3
Tanacetum balsamita.....	525
TAS1R.....	3
TAS2R.....	3, 20
taste perception.....	47
taste receptors.....	37
taste recombination.....	393
taste.....	3, 313, 435, 494
texture (properties).....	113, 117, 157, 309
Thai green chilli.....	459
thiol oxidation.....	271
thiol stability.....	569
thiourea compounds.....	13
tobacco.....	313
trigeminal.....	55
trimethylpyrazine.....	133
trimethyltrisulphide.....	271
tropical juice.....	215
two-dimensional GC.....	504
typicality.....	565

U

umami.....	3
(6Z,8E)-undeca-6, 8, 10-trien-3-one.....	423
(6Z,8E)-undeca-6, 8, 10-trien-4-one.....	423
unsaturated fatty acid (UFA).....	207
untargeted (approach).....	573, 581
uronic acid.....	267

V

V. planifolia.....	203
V. tahitensis.....	203
valencene.....	332
vanilla (beans).....	203, 379
Vanilla planifolia.....	379
vanillic acid.....	203
vanillin.....	203, 257, 379

Expression of Multidisciplinary Flavour Science

vegetables.....	13
vescalagin.....	280
vibrational circular dichroism.....	541
vineyard.....	359
viscosity.....	117, 157
volatile compounds.....	157, 169, 435, 463, 589

W

white biotechnology.....	319
whole grain flour.....	297
wine.....	238, 483, 513, 517, 533
woody odorant.....	504
xylose.....	293

XYZ

yeast.....	354
yerba maté.....	494
yogurt.....	109, 117, 157, 165, 371
yuzu.....	431

The Weurman Flavour Research Symposium, one of the most renowned international meetings on flavour science, takes place every 3 years in Europe. Participants from academia and industry from all five continents meet to discuss advances and trends in flavour science in an informal and open atmosphere. In July 2008, the 12th Weurman Flavour Research Symposium was organized in Interlaken, Switzerland. About 230 participants from 34 countries contributed with 177 lectures and posters to the wealth of flavour-related knowledge. The contributions were grouped in 8 sessions, i.e. biology, retention & release, psychophysics, quality, thermal generation, bioflavors, impact molecules, and analytics. Emerging topics were discussed in 3 workshops dealing with flavour and health, in-vivo flavour research, and flavour metabolomics. Highlights of the 12th Weurman symposium were published in a special issue of the Journal of Agricultural and Food Chemistry in 2009. This 12th Weurman Flavour Research Symposium has been the most impressive *Expression of Multidisciplinary Flavour Science*. It has offered an excellent forum for passionate exchange on traditional as well as emerging fields of flavour science. We believe that these proceedings will fructify and propel the development of flavour science and become an important reference to the field. Enjoy!



Imre BLANK received his PhD in Food Chemistry from the Technical University of Munich, Germany. After a 2 years assignment as research scientist at the German Food Research Institute of Food Chemistry in Garching he joined in 1991 the Nestle Research Centre (NRC) in Lausanne, Switzerland. In NRC he held various research and R&D management positions with focus on flavour science and Maillard chemistry. In 2005 he moved to the Nestle Product Technology Centre in Orbe as head of the Science & Nutrition department. His current research activities comprise coffee chemistry, flavour generation, and mechanistic aspects of the Maillard reaction cascade. Since 2009, he is lecturer at the Institute of Food Chemistry, Technical University of Munich.



Matthias WÜST received his PhD in Food Chemistry from the University of Frankfurt/Main, Germany. After a post-doc at the Institute of Biological Chemistry (IBC) of the Washington State University as a Feodor-Lynen-Fellow of the Alexander von Humboldt-Foundation he joined the Institute of Food Chemistry of the University of Frankfurt/Main as a research associate and lecturer in Instrumental Food Analysis. In 2003 he moved to the University of Applied Sciences of Western Switzerland in Sion where he was appointed as Professor in Food Chemistry. In 2009 he moved to the University of Bonn, Germany, where he actually holds the position of Professor in Bioanalytics/Food Chemistry at the Institute of Nutrition and Food Sciences (IEL). His current research is focused on the analysis and biosynthesis of terpenoids.



Chahan YERETZIAN received his PhD in Chemistry from the University of Bern, Switzerland. A post-doc at the University of California, Los Angeles (UCLA), and a subsequently Alexander von Humboldt Junior Award for a 2-year position at the Technical University of Munich, complemented his academic education. In 1995 he joined the Nestlé Research Center in Lausanne, Switzerland, where he held various research and R&D management positions, mainly in the product categories Coffee and Culinary. In 2007 he joined the Corporate Communication Department of Nestlé Nespresso, developing communication platforms on the science of coffee. Since 2008, he holds the position of head of the analytical technology group at the Institute of Chemistry and Biological Chemistry (ICBC) of the Zurich University of Applied Sciences. His current research is focused on the science and technology of coffee, and the development of novel on-line analytics for volatiles.